Monograph

Effective Work Functions of the Elements

Database, Most probable value, Previously recommended value, Polycrystalline thermionic contrast, Change at critical temperature, Anisotropic dependence sequence, Particle size dependence

Hiroyuki Kawano[1]

Faculty of Science, Ehime University, Bunkyo 2-5, Matsuyama 790-8577, Japan

As a token of deep gratitude, I would like to dedicate this monograph to my supervisors during my student days at Kyoto University and also to my family as follows:

Dr. Nobuji Sasaki (Professor Emeritus, Kyoto University)

Dr. Kumasaburou Kodera (Professor Emeritus, Kyoto University)

Shigeru Kawano, Fumiko Kawano, Shigeharu Kawano, Emiko Kawano,

Yuki Kawano, Katsuhiko Suzuki, Eriko Suzuki,

Hiroshi Yokoo, Yuriko Yokoo, Miyuu Yokoo

ARTICLE INFO

ABSTRACT

As a much-enriched supplement to the previous review paper entitled the "Effective work functions for ionic and electronic emissions from mono- and polycrystalline surfaces" [Prog. Surf. Sci. 83 (2008) 1–165], the present monograph summarizes a comprehensive and up-to-date database in Table 1, which includes more than ten thousands of experimental and theoretical data accumulated mainly during the last half century on the work functions (ϕ^+, ϕ^e and ϕ^-) effective for positive-ionic, electronic and negative-ionic emissions from mono- and polycrystalline surfaces of 88 kinds of chemical elements ($_1$H–$_{99}$Es), and also which includes the main experimental condition and method employed for each sample specimen (bulk or film) together with 490 footnotes. From the above database originating from 4461 references published to date in the fields of both physics and chemistry, the most probable values of ϕ^+, ϕ^e and ϕ^- for substantially clean surfaces are statistically estimated for about 600 surface species of mono- and polycrystals. The values recommended for ϕ^e together with ϕ^+ and ϕ^- in Table 2 are much more abundant in both surface species and data amount, and also they may be more

Monocrystallization degree governing work function
Annealing temperature dependent work function value
Methodologically dependent work function study
Gordy–Thomas equation
Hensley's equation
Anisotropy dependent work function sequence
Smoluchowski rule
Anisotropic surface energy correlative work function examination
Anisotropic melting point correlated work function evaluation
Wigner–Seitz radius dependent work function values
Solid–liquid phase transitional work function change
Allotropic transformational work function change
Bulgers orientation relationship
Magnetic transitional work function change
Metastable metal film work function
Metastable film thickness dependent Curie temperature
Superconductive transformational work function change
Particle size dependent work function

reliable and convenient than those in popular handbooks and reviews consulted widely still today by great many workers, because the latter is based on less-plentiful data on ϕ^e published generally before ~1980 and also because it covers no value recommended for ϕ^+ and ϕ^-.

Consequently, Table 1 may be more advantageous as the latest and most abundant database on work functions (especially ϕ^e) for quickly referring to a variety of data obtained under specified conditions. Comparison of the most probable values of ϕ^e recommended for each surface species between this article and other literatures listed in Tables 2 and 3 indicates that consideration of the recent work function data accumulated particularly during the last ~40 years is very important for correct analysis of these surface phenomena or processes concerned with either work function or its changes.

On the basis of our simple model about the work function of polycrystal consisting of a number of patchy faces (1–i) having each a fractional area (F_i) and a local work function (ϕ_i), its values of both ϕ^+ and ϕ^e are theoretically calculated and also critically compared with a plenty of experimental data. In addition, the "polycrystalline thermionic work function contrast" ($\Delta\phi^* \equiv \phi^+ - \phi^e$) well-known as the thermionic peculiarity inherent in every polycrystal is carefully analyzed as a function of the degree of monocrystallization (δ_m) corresponding to the largest (F_m) among F_i's (Tables 4–6 and Fig. 1), thereby yielding the conclusions as follows: (1) $\Delta\phi^* \simeq$ const (>0) holds for the generally called "polycrystalline" surfaces (usually $\delta_m <$ 50%), (2) $\Delta\phi^*$ ranges from ~0.3 eV (Pt) to 0.7 eV (Nb) depending upon the polycrystalline surface species, (3) in the case of the "submonocrystal" (50 < δ_m < 100%) tentatively named here, $\Delta\phi^*$ decreases parabolically down to zero as δ_m increases from ~50% up to 100% (monocrystal), (4) $\Delta\phi^* = 0.0$ eV applies to a clean and smooth monocrystalline surface ($\delta_m \approx$ 100%) alone, (5) regarding negative ion emission, on the other hand, our theoretical prediction of $\Delta\phi^{**} \equiv \phi^- - \phi^e = 0.0$ eV is experimentally verified to hold for any surface species under any surface conditions (Table 7), (6) every polycrystal (usually, $\delta_m <$ 50%) may be concluded in general to have a unique value of ϕ^e characteristic of its species with little dependence upon δ_m, (7) this conclusion affords us first a sound basis for supporting theoretically the experimental fact (Table 2) that every species of polycrystal has a nearly constant value of ϕ^e as well as ϕ^+ (usually within the uncertainty of ±0.1 eV) depending little upon the difference in the surface components (F_i and ϕ_i) among specimens so long as $\delta_m <$ 50%, (8) on the contrary to polycrystal ($\delta_m <$ 50%), any submonocrystal (50 < δ_m < 100%) has such an anomaly that it does not possess the unique value of work function characteristic of the surface species itself, because its ϕ^e as well as ϕ^+ changes considerably depending upon δ_m, (9) consequently, submonocrystal must be taken as another type (category) different from both poly- and monocrystals, (10) in this way, δ_m acts as the *key* factor mainly governing the work functions in the different mode between poly- and submonocrystals with δ_m lower and higher than the "critical point" of 50%, respectively, (11) on the contrary to δ_m, ϕ_m belonging to δ_m has a differential effect on both ϕ^+ and ϕ^e, but their values remain nearly constant so long as $\delta_m <$ 50% and, thus interestingly, (12) the complicate governance of ϕ^+ and ϕ^e by both δ_m and ϕ_m and also the anomaly of submonocrystal (cf. (8) above) observed first by our theoretical analysis may be considered as a new contribution to the work function studies developed to date.

Together with brief comments and experimental conditions, typical data on ϕ^e and/or ϕ^+ are summarized from the various aspects of (1) examination of the work function dependence upon the surface atom density of low-Miller-index monocrystals of typical metals such as Al, Ni, W and Re (Table 8), (2) demonstration of the above dependence usually called the "anisotropic work function dependence sequences" of both $\phi^e(110) > \phi^e(100) > \phi^e(111)$ and $\phi^+(110) > \phi^+(100) > \phi^+(111)$ for various bcc-metals (e.g., Nb, Mo, Ta and W) exactly obeying the Smoluchowski rule (Table 9), (3) substantiation of both $\phi^e(111) > \phi^e(100) > \phi^e(110)$ for a variety of fcc-metals (except Al and Pb) and $\phi^+(111) > \phi^+(100) > \phi^+(110)$ for Ni strictly following the above rule (Table 10), (4) verification of the quantitative relations between work function and surface energy and also melting point of the three low index planes of several metals (typically, Ni), (5) examination of the work function change ($\Delta\phi^e$) due to allotropic transformation from α to β or β to γ phase (Table 11) together with a concise outline of the Burgers orientation relationship, (6) evaluation of $\Delta\phi^e$ due to liquefying (Table 12), (7) estimation of $\Delta\phi^e$ due to transformation from ferro- to paramagnetic state (Table 13) in addition to a brief description of the Curie point dependence upon metastable metal film thickness above one monolayer, (8) estimation of $\Delta\phi^e$ due to transition from normal to superconducting state (Table 14), (9) study of the work function dependence on the Wigner–Seitz radius and also comparison between its theoretical values (by Kohn) and experimental data (Fig. 2), (10) inspection of the annealing effect on work function for layers or films, (11) verification of the coincidence of work function values among different experimental methods, and (12) inquisition of the work function dependence upon the size of fine particles (~20–100 Å in radius) studied by theory and experiment.

Contents

1. Introduction

The work function (ϕ) of a solid surface is the minimum energy necessary for an electron to transfer from the Fermi level to field-free space, and it is one of the important factors governing the electronic and ionic emissions from any surfaces by any means. Typically, positive-ionic, electronic and negative-ionic emissions from a patchy surface by various mechanisms (processes) are strongly dependent upon the effective work functions of ϕ^+, ϕ^e and ϕ^-, respectively, and they are evaluated theoretically from Eqs. (1)–(3) [1351].

$$\phi^+ = kT \ln[\Sigma F_i \exp(\phi_i/kT)], \tag{1}$$

$$\phi^e = -kT \ln[\Sigma F_i \exp(-\phi_i/kT)], \tag{2}$$

$$\phi^- = -kT \ln[\Sigma F_i \exp(-\phi_i/kT)]. \tag{3}$$

Here, F_i is the fractional surface area of the patch site (i) having the local work function (ϕ_i), where the total of ΣF_i is unity. All of the three above are the mean work functions weighted statistically according to the tendencies that positive ions (M^+) are *predominantly* emitted from high work function sites but that negative ions (X^-) and electrons (e^-) are done so from the sites of low ϕ_i. This predominance has a very important role in governing (determining) mainly the effective work functions of a patchy surface having various values of ϕ_i's and F_i's. Namely, ϕ_m belonging to F_m ($\equiv \delta_m$), the latter of which is named here the "degree of monocrystallization" correspondent to the largest among F_i's, has the "differential effect" upon both ϕ^+ and ϕ^e according to the condition whether ϕ_m is relatively higher or lower than the others among ϕ_i's, as will be demonstrated later (Section 4.4).

Such a theoretical prediction as mentioned just above is supported experimentally by a typical example of a Na/W system [85], as clearly shown in Fig. 20 [1351]. Of course, both ϕ^+ and ϕ^e of a patchy surface are generally different from the *simple* average given by

$$\phi^a = \Sigma F_i \phi_i. \tag{4}$$

Needless to say, ϕ^a is not weighted statistically according to the predominance mentioned just above. Consequently, the inequality of $\phi^+ > \phi^a > \phi^e$ always holds for any patchy surfaces, and it is to clean and smooth monocrystalline ones ($\delta_m = 100\%$) alone that the equality of $\phi^+ = \phi^a = \phi^e$ is applicable, as will be demonstrated in Section 4. On the contrary, it is reported for an actual specimen of polycrystalline W (F_i = 46.3%-(310), 18.9%-(110), 15.5%-(112), 14.0%-(100) and 5.4%-(111) oriented) that $\phi^a = 4.59 \approx 4.6$ eV calculated from Eq. (4) is taken as ϕ^e and also that the value ($\phi^a = \phi^e = 5.6$ eV) is considered to agree well with $\phi^e = 4.8 \pm 0.05$ eV determined for the same specimen by field emission [489] (for further information, see W(D) in Table 6 to be given later in Section 4.2). Regarding an imaginary specimen of W consisting of the four (100)–(112) faces with each 25% fractional area, ϕ^+ is theoretically estimated to be 4.51 eV [3843], which is much smaller than $\phi^a = 4.74$ eV to be evaluated from Eq. (4) and also than $\phi^+ = 5.12$ eV done so from Eq. (1) [3844]. Again, this result of $\phi^+ = 4.51$ eV $< \phi^a = 4.74$ eV also is not well consistent with our theoretical prediction (for detail, see Footnote 295 in Table 1).

Eqs. (1)–(3) are theoretically derived according to our simple model of thermal stimulation (thermal ionic and electronic emissions) [281]. However, the work functions to be thus calculated for a given species are generally expected to agree either well or fairly with those determined experimentally by any other methods without depending upon any of the emission mechanisms (processes) such as ion bombardment (secondary ion emission), electron impact (electron-stimulated ion desorption), fast-atom incidence (fast or cold surface ionization), photon irradiation (photoelectron and photoion emissions), very high electric voltage application (field-electron and -ion emissions) and so on [1351]. The progress achieved up to ~1980 for the studies of thermal positive ionic and electronic emissions is outlined or summarized in several books [14–17] and review articles [2,18–22]. Both of the features and data on the emissions studied mainly after ~1980 are summarized together with experimental conditions in Sections 2 and 3 [1351]. For other emissions due to various mechanisms, a brief information may be obtained from several books [13,615,1354,2829].

Since the work function (ϕ^e) is very important in many fields of pure and applied physics and chemistry and also since it is necessary to know the accurate or most probable value of ϕ^e as the universal (or material) constant characteristic of each of the essentially clean mono- and polycrystalline surface species of the chemical elements, many handbooks [10–12,1352–1354,1358,1359,4137,4191,4318] and reviews [13,488,1045,1312,1355–1357] are published to summarize the recommended or selected values of ϕ^e for a variety of surface species. Especially, both Michaelson [1045,1355] and Fomenko [10,12,1354] have made a valuable contribution to compiling critically the work function data on various poly- and monocrystalline surfaces. However, their publications don't include any work function data published after ~1980. In addition, their contents summarized for monocrystals are not sufficiently abundant in both surface species and work function data themselves, compared with those generally expected today in many fields of science and technology. Consequently, many workers may feel inconvenience in finding the accurate or reliable values of work function of various surface species, especially of monocrystalline ones interested in quite many workers. Typically, a theoretical study published in 2003 [4130] states that any experimental data for α-Fe(110) are not available for comparison with the theoretical value of 4.73 eV calculated by the authors themselves [4130], although many experimental data of 4.72–5.32 eV determined for α-Fe(110) by PE, CPD or FE [e.g., 530,1273,2035] were already published in 1971−2000 (see Table 1 to be shown later). For another example published in 2008 [4131], $\phi^e = 4.94$ eV for Cu(111) and 5.03 eV for β-Co(111) are cited from Table 2 in our previous review (in 2008) [1351] and from a theoretical article (in 2007) [2910], respectively, because any data on the latter are not included in any of the reviews and books published in 1949−2008 [1351], in contrast to this article tabulating seven data on β-Co(111) (4.93–5.76 eV [e.g., 229,2068,3192] published in 1992−2008) in Table 1. Similarly in an experimental study reported for

Pr in 1998 [4263], it is stated that ϕ^e has not yet been experimentally determined for Pr. But, several articles [2011,4066,4251,4253] published already in 1974–1982 include ϕ^e = 2.6–2.67 eV for Pr measured by FE or CPD (see Table 1), the data of which are slightly larger than 2.50 eV done by IP of Pr-clusters [4263] (see Result (18) in Section 11.3 about clusters).

The recent or present situation exemplified above suggests that a new and enriched handbook on work function should be widely distributed among all of the workers active in the fields of pure and applied surface sciences so as to be ready for consulting the recent data on work function and also for easily finding the most probable value of any surface species of chemical elements under study. From this point of view, the present author has tried to compile Table 1 covering the up-to-date and abundant work function data on a vast number of surface species of almost all the chemical elements and also to make up Table 2 recommending the most probable value of each species. Both of the tables may be very effective for filling up such a great blank in work function data as found in many handbooks and also for covering a very long absence from compiling new data during the last several tens of years since ~1980.

As will be shown later in Tables 2 and 3 and also discussed concretely in Section 3.2, some of the recommended or selected values [typically, 12,1045,1354,1358] don't seem to be very accurate or reliable enough to be fully acceptable today, mainly because many of them are usually based on the meager or scanty data published entirely before ~1980. Nevertheless, many of the preferable values of work function (ϕ^e) [1045], for example, have long been often and widely cited still to date by total 1935 groups of workers at present (May 2017) [4158] since the progressive review was published by Michaelson [1045] in 1977. In addition, many publications [typically, 1045,1352,1353,1355,1356,1358,1359] don't include any data on ϕ^+ and $\Delta\phi^*$. Consequently, they seem to be scarcely suitable enough in general for analyzing correctly these data on positive ion emission from polycrystals, although such emission or positive surface ionization (PSI) has long been employed widely as a very convenient technique for various purposes such as positive ion beam production, atomic and molecular beam detection, isotopic ratio determination, ionization potential measurement, analysis of surface state and processes, and so on [2,4–7,15,16,18,19,21,22]. Even a recent publication such as CRC Handbook (97th Ed. in 2016−2017) [1358] is entirely based on the data published before ~1980, similarly with those (82nd−96th editions in 2001−2015) [e.g., 11,1359]. Consequently, some of the work function values recommended in the above publications don't seem to be fully accurate or reliable enough to be straight or undoubtedly acceptable today. Typically for Cu(100), ϕ^e = 5.10 eV [358] cited in CRC Handbooks (1997−2017) [typically, 1358,4318] deviates considerably from our value of 4.58 ± 0.06 eV to be recommended in Table 2 and also from 4.59 ± 0.03 eV [953,2006] considered to be most reliable at present. Such a deviation as ranging from ~0.2 to 1.0 eV is found also for many other surface species, as will be demonstrated later in Section 3.2 and Table 3.

Recently (2015) after ~35 years' absence since ~1980, Derry et al. [4088] have published a compact review on clean monocrystalline metal surface work function, where the recommended values are based on these experimental data about 45 species of low-Miller-index surfaces for 15 kinds of very familiar metals without including much data achieved by theory for a variety of surface species of various elements. Consequently, it seems to be still confidently expected to publish such a comprehensive article on both experimental and theoretical work function data as covering not only low- but also high-Miller-index surfaces together with polycrystalline ones for more than several tens of quite many chemical elements interested generally in physics and chemistry.

It must be kept in mind that (1) the generally called "work function (ϕ)" appearing in usual publications [e.g., 1045,1352,1358] means $\phi = \phi^e$ unless otherwise stated, (2) the equality of $\phi^+ = \phi^e = \phi^- = \phi^a = \phi$ holds for clean and smooth monocrystalline surfaces alone, (3) the partial inequality of $\phi^+ > \phi^a > \phi^e = \phi^- = \phi$ conforms to these cases other than the case (2) mentioned just above and, hence, the relation of $\phi^+ - \phi^e \equiv \Delta\phi^* > 0$ applies always to both polycrystalline surfaces ($\delta_m < 50\%$) and non-clean and/or non-smooth monocrystalline ones ($\delta_m = 100\%$) in addition to the tentatively named "submonocrystalline" ones ($50 < \delta_m < 100\%$) to be fully explained later (Sections 4.3–4.5) and (4) $\phi^e = \phi^- = \phi$ is applicable to any surface species under any conditions irrespective of the degrees in both surface contamination and irregularity [1351]. Much data on $\Delta\phi^* > 0$ will be listed in Tables 4 and 5 based on both theory and experiment.

In principle, work function is generally expected to be the universal constant for each of the "clean and smooth" monocrystalline surface species. In practice, however, its data are found to scatter in a wide range (typically, ~4.1–5.2 eV for W(100), see Table 1) among different specimens or workers for the same surface species of actual "monocrystals". In other words, the degree of deviation from ideal surface conditions is different more or less among the actual specimens under study. This difference is usually due to such causes that the degrees of both surface contamination and defects and also of heteroatom density are different among the monocrystalline specimens under study and also that the extents of error in both measurement and data-processing are not identical among the corresponding workers. As one more cause, we can not deny the possibility that some of the specimens under study are somewhat less than 100% in the degree of monocrystallization (δ_m), as will be discussed later in Section 4. Especially in the case of a polycrystalline species consisting of patchy faces having F_i and ϕ_i, on the other hand, δ_m (largest among F_i's) also may be attributable as an additional cause to the difference in ϕ^e among various specimens. Typically for "submonocrystalline" tungsten ($50 < \delta_m < 100\%$), ϕ^e is 4.87 ± 0.06 eV at $\delta_m = 80\%$, while ϕ^e of the usually called "polycrystalline" tungsten ($\delta_m < 50\%$) remains nearly constant at 4.52 ± 0.10 eV with little dependence upon δ_m so long as $\delta_m < 50\%$, as will be demonstrated in Table 6 and Section 4. There, the anomaly of the former quite different from the latter is described thoroughly.

In the case of theoretical calculation, much larger scattering (typically, ~3.7–7.8 eV for W(100), see Table 1) is found for any monocrystalline surface species among different authors. This is probably because some of the theoretical models themselves are not yet fully perfect or reasonable and/or because some of their selections of numerical values of the parameters governing work function are neither adequate nor suitable.

Such a present situation outlined above suggests powerfully that much work function data accumulated to date by using various methods should be collected from not only regular publications in a variety of scientific fields but also special reports, conference proceedings and doctoral theses as many as possible and also that the abundant data coming from such a broad survey should be

examined carefully, in order to estimate accurately the most probable values of ϕ^e as well as ϕ^+ and ϕ^- for a large number of the mono- and polycrystalline surface species which are widely interested in theoretical and/or experimental researches by many workers.

From the above aspect, the present author has already published a comprehensive review paper [1351], where many of the work function data published to ∼2005 are tabulated and also examined carefully to estimate the most reliable value of work function for each of mono- and polycrystalline surfaces of popular elements together with several compounds. Regarding the chemical elements, however, the previous review includes the work function data for only 18 kinds of elements, and it involves the best estimate of the work function value for 74 surface species alone, thereby strongly indicating that a new article about the work function database enriched in both quality and quantity should be published in order to estimate the most probable values of work function for much more surface species of most of the solid and liquid elements in the periodic table.

The above viewpoint has made the present author to prepare this new article, which is intended mainly (1) to summarize comprehensively a larger amount (more than ten thousands) of theoretical and experimental work function data published to date, (2) to estimate accurately the most probable values of work functions (ϕ^e, ϕ^+ and ϕ^-) for both mono- and polycrystalline surfaces of almost all the solid elements and also for some of the liquid ones so long as the work function data are available today, (3) to determine correctly the polycrystalline thermionic contrasts ($\Delta\phi^* \equiv \phi^+ - \phi^e$ and $\Delta\phi^{**} \equiv \phi^- - \phi^e$), (4) to reveal clearly the *key* factor of δ_m governing mainly the work functions of both poly- and submonocrystals, (5) to examine carefully the anisotropic work function dependence upon surface atom density for the three low-Miller-index planes of both bcc- and fcc-monocrystals, (6) to epitomize concisely the work function dependence upon the Wigner–Seitz radius together with a comparison between theory and experiment, (7) to inspect closely the work function changes caused by allotropic, magnetic, superconductive and solid–liquid transitions according to the temperature variation around each critical point, (8) to outline briefly the work function and Curie point of metastable metal films and also (9) to explicate fully the work function dependence upon the size of fine particles.

Together with the specified condition and method employed for each work function measurement, the database on ϕ^e, ϕ^+ and ϕ^- to be summarized later for mono-, submono- and polycrystalline surfaces in Table 1 may be useful for quickly surveying more than ten thousands of sample systems (bulk or film) employed to date for a variety of work function studies by theory and experiment. As will be shown in Table 2 together with the literature values either recommended or selected previously by other authors [12,1045,1354,1358] and also by the present author [1351], many of the most probable values estimated from the above database (Table 1) may be citable or consultable as probably the most accurate and reliable reference data, nowadays at least, on ϕ^e, ϕ^+ and/or ϕ^- for general studies on work function and related subjects, and also many of them thus recommended for monocrystalline surfaces may be useful at present as the most reliable sources of local work function (ϕ_i) to be employable in Eqs. (1)–(3). The general reliability of our most probable values of ϕ^e to be listed in Table 2 is examined objectively by comparison with those recommended by others [12,1045,1354,1358]. In addition, the work function difference between the former and the latter will be discussed considerably in Section 3.2, and also the distribution of the difference ranging from 0.05 to 1.0 eV between the two will be summarized in Table 3.

For better understanding the polycrystalline thermionic contrast ($\Delta\phi^* \equiv \phi^+ - \phi^e$) dependent upon the degree of surface inhomogeneity in work function over the entire surface area, many experimental data are summarized for 32 surface species in Tables 4 and 5, clearly showing that clean and smooth monocrystalline surfaces alone stand upon $\Delta\phi^* = 0.0$ eV and also that polycrystalline ones have $\Delta\phi^* \approx 0.3 - 0.7$ eV, dependent upon the polycrystalline species. These data on $\Delta\phi^*$ may be helpful for analyzing correctly these positive ion emission data obtained for polycrystalline surface systems, where ϕ^e is not available in general for an accurate or reliable analysis of the latter data (see Section 4.1).

In order to clarify the problem how the work function of a patchy surface is governed by both local work function (ϕ_i) and its fractional surface area (F_i), some of the typical examples for calculating both ϕ^+ and ϕ^e from Eqs. (1) and (2) are summarized for W together with $\Delta\phi^*$ in Table 6. In addition, the quantitative relation between the contrast ($\Delta\phi^*$) and the maximum value ($\delta_m \equiv F_m$) among the various areas (F_i's) will be shown in Fig. 1 (see Section 4.3).

To examine closely the theoretical prediction that $\Delta\phi^{**} \equiv \phi^- - \phi^e \approx 0$ always holds without depending upon both surface species and condition, all of the experimental data available today are summarized for several elements in Table 7, which suggests strongly that $\Delta\phi^{**} = 0.0$ eV fitly applies to any mono-, submono- and polycrystals even when their surfaces are neither atomically clean nor flat (smooth), in contrast to $\Delta\phi^* = 0.0$ eV applicable only to those surfaces homogeneous in work function over the entire area.

From the viewpoint of the Smoluchowski rule [1040] concerning the relationship between surface-atom density and work function for monocrystalline surfaces of the three low-Miller-index orientations, the anisotropic sequences of both $\phi^e(110) > \phi^e(100) > \phi^e(111)$ for various bcc-metals and also $\phi^e(111) > \phi^e(100) > \phi^e(110)$ for fcc-ones are examined by using many experimental and theoretical data listed in Tables 8–10, fairly indicating that more than half of the respective data on Al and Pb (both fcc) alone does not satisfy the latter sequence (mentioned just above) in contrast to many other fcc-metals (Table 10). It cannot be emphasized enough that $\phi^+(hkl)$ is first reported here for both bcc-metals (Nb, Mo, Ta and W) and fcc-one (Ni) to follow faithfully the above rule.

To investigate the work function changes ($\Delta\phi^e$) due to allotropic, magnetic, superconductive and solid–liquid transitions, experimental data of many or several surface species are summarized in Tables 11–14, indicating that quite many of the surface species have $|\Delta\phi^e| < 0.1$ eV. In addition, the peculiarity of metastable metal films is outlined together with typical data on work function and Curie point depending upon film thickness. Finally, work function dependence upon the size of fine particles will be summarized together with comparison between theory and experiment in Section 11.

2. Database

The present author believes it very important to estimate the most probable work function values of many mono- and polycrystalline surfaces and also to solve the problem how the work function of an actual surface depends upon the specimen and/or condition employed by each individual group of workers. From this viewpoint, he has tried to do best for obtaining work function data as much as possible since ~2000 and also for inspecting both experimental condition and surface processing employed by each group of workers. In consequence, he has managed to summarize theoretical and experimental work function data based on 4461 references published to date in various fields of not only physics but also chemistry, as shown in Table 1. It contains the data for about 600 surface species of 88 kinds of chemical elements ($_1$H–$_{99}$Es) and also does the main conditions (residual gas pressure and surface temperature) and method together with 490 footnotes in order to provide further information about specimen preparation, surface treatment, data processing, etc. Such description may be very helpful to judging the questions whether the surface under study is substantially clean and/or whether the sample layers are essentially uniform over the entire surface area, in addition to resolving the problem how ϕ^e changes depending upon the degree of monocrystallization (δ_m) correspondent to the largest among the patchy surface areas (F_i's) for the poly- or submonocrystalline specimen having various values of local work function (ϕ_i's).

Table 1 consists of the nine columns to be explained concisely below, where the main points of experimental conditions are entered in Columns 2–5. In addition, several subjects and topics related to the items present in some of the columns will be outlined together with brief discussions.

Table 1
Theoretical and experimental data on the effective work functions (ϕ^+ or ϕ^- and ϕ^e) determined for various surfaces under the conditions specified herein. The value of ϕ^- is given with a superscript of N in the column of ϕ^+. Each of the recommended values herein is compared with that selected or recommended by other workers in Table 2.

Surface	Beam	Ion	P_r (Torr)	T (K)	ϕ^+ (eV)	ϕ^e (eV)	Meth.	Refs.
				1. Hydrogen H				
fcc								
H(100)	–	–	–	–	–	3.73	TC	[231]
H(110)	–	–	–	–	–	3.75	TC	[231]
H(111)	–	–	–	–	–	3.80	TC	[231]
H	–	–	–	–	–	3.77	TC	[1924]
H	–	–	–	–	–	3.84	TC	[231]
H	–	–	–	–	–	3.86	TC	[231]
H	–	–	–	–	–	4.0	TC	[944]
H	–	–	–	–	–	4.0	TC	[2648]
H	–	–	–	–	–	4.41	TC	[1924]
H	–	–	–	–	–	4.67	TC	[2648]
H	–	–	–	–	–	5.25	TC	[1955]
Recommended	–	–	–	–	–	**3.89 ± 0.09**	–	–
				3. Lithium Li				
bcc								
Li(100)	–	–	–	–	–	2.310	TC	[2947]
Li(100)	–	–	–	–	–	2.40	TC	[475][3]
Li(100)	–	–	–	–	–	2.61	TC	[1159,1980,3067]
Li(100)	–	–	–	–	–	2.9	TC	[474]
Li(100)	–	–	–	–	–	2.92	TC	[231]
Li(100)	–	–	–	–	–	2.93	TC	[1595]
Li(100)	–	–	–	–	–	2.96	TC	[1595]
Li(100)	–	–	–	–	–	2.96	TC	[4461][490]
Li(100)	–	–	–	–	–	2.986	TC	[4091]
Li(100)	–	–	–	–	–	3.0	TC	[474]
Li(100)	–	–	–	–	–	3.00	TC	[1095]
Li(100)	–	–	–	–	–	3.02	TC	[2427]
Li(100)	–	–	–	–	–	3.03	TC	[553]
Li(100)	–	–	–	–	–	3.03	TC	[637,2418]
Li(100)	–	–	–	–	–	3.037	TC	[2432]
Li(100)	–	–	–	–	–	3.04	TC	[3467]
Li(100)	–	–	–	–	–	3.05	TC	[1595]
Li(100)	–	–	–	–	–	3.06	TC	[637,2418]
Li(100)	–	–	–	–	–	3.09	TC	[1595]
Li(100)	–	–	–	–	–	3.1	TC	[474]
Li(100)	–	–	–	–	–	3.10	TC	[478]

(*continued on next page*)

Table 1 (*continued*)

Surface	Beam	Ion	P_r (Torr)	T (K)	ϕ^+ (eV)	ϕ^e (eV)	Meth.	Refs.
Li(100)	–	–	–	–	–	3.10	TC	[321]
Li(100)	–	–	–	–	–	3.11	TC	[3478]
Li(100)	–	–	–	–	–	3.11	TC	[1595]
Li(100)	–	–	–	–	–	3.11	TC	[711]
Li(100)	–	–	–	–	–	3.135	TC	[4460][490]
Li(100)	–	–	–	–	–	3.15	TC	[334]
Li(100)	–	–	–	–	–	3.20	TC	[3478]
Li(100)	–	–	–	–	–	3.25	TC	[476]
Li(100)	–	–	–	–	–	3.26	TC	[711]
Li(100)	–	–	–	–	–	3.27	TC	[1237]
Li(100)	–	–	–	–	–	3.28	TC	[1595]
Li(100)	–	–	–	–	–	3.28	TC	[3814]
Li(100)	–	–	–	–	–	3.30	TC	[475]
Li(100)	–	–	–	–	–	3.30	TC	[1030]
Li(100)	–	–	–	–	–	3.32	TC	[555]
Li(100)	–	–	–	–	–	3.32	TC	[556]
Li(100)	–	–	–	–	–	3.36	TC	[637]
Li(100)	–	–	–	–	–	3.39	TC	[476]
Li(100)	–	–	–	–	–	3.4	TC	[1088]
Li(100)	–	–	–	–	–	3.47	TC	[1030]
Li(100)	–	–	–	–	–	3.56	TC	[472]
Li(100)	–	–	–	–	–	3.60	TC	[1557]
Li(100)	–	–	–	–	–	3.70	TC	[1414]
Li(100)	–	–	–	–	–	3.71	TC	[1414]
Recommended	–	–	–	–	–	**3.12 ± 0.03**	–	–
Li(110)	–	–	–	–	–	2.31	TC	[2835]
Li(110)	–	–	–	–	–	2.40	TC	[475]
Li(110)	–	–	–	–	–	2.45	TC	[593]
Li(110)	–	–	–	–	–	2.479	TC	[2947]
Li(110)	–	–	–	–	–	2.75	TC	[3712]
Li(110)	–	–	–	–	–	2.78	TC	[1159,1980,3067]
Li(110)	–	–	–	–	–	2.90	TC	[3713]
Li(110)	–	–	–	–	–	2.96	TC	[3693]
Li(110)	–	–	–	–	–	3.00	TC	[1095]
Li(110)	–	–	–	–	–	3.09	TC	[231]
Li(110)	–	–	–	–	–	3.10	TC	[2835]
Li(110)/W(110)[1]	Li	–	?	~300	–	3.11 ± 0.05	CPD	[3361]
Li(110)/Mo(110)[1]	Li	–	?	~300	–	3.11 ± 0.05	CPD	[3361]
Li(110)	–	–	–	–	–	3.12	TC	[3692]
Li(110)	–	–	–	–	–	3.18	TC	[711]
Li(110)	–	–	–	–	–	3.18	TC	[4461][490]
Li(110)	–	–	–	–	–	3.22 ± 0.01*	TC	[4440]
Li(110)	–	–	–	–	–	3.221	TC	[4091]
Li(110)	–	–	–	–	–	3.25	TC	[1086]
Li(110)	–	–	–	–	–	3.26	TC	[2427]
Li(110)	–	–	–	–	–	3.27	TC	[553]
Li(110)	–	–	–	–	–	3.286	TC	[2432]
Li(110)	–	–	–	–	–	3.31	TC	[476,711]
Li(110)	–	–	–	–	–	3.32	TC	[3467]
Li(110)	–	–	–	–	–	3.33	TC	[334]
Li(110)	–	–	–	–	–	3.35	TC	[1734]
Li(110)	–	–	–	–	–	3.359	TC	[4460][490]
Li(110)	–	–	–	–	–	3.37	TC	[1086]
Li(110)	–	–	–	–	–	3.40	TC	[637]
Li(110)	–	–	–	–	–	3.43	TC	[637,2418]
Li(110)	–	–	–	–	–	3.43	TC	[3814]
Li(110)	–	–	–	–	–	3.44	TC	[476]
Li(110)	–	–	–	–	–	3.45	TC	[1734]
Li(110)	–	–	–	–	–	3.46	TC	[637,2418]
Li(110)	–	–	–	–	–	3.5	TC	[1086,1088]
Li(110)	–	–	–	–	–	3.54	TC	[1237]
Li(110)	–	–	–	–	–	3.55	TC	[475]
Li(110)	–	–	–	–	–	3.55	TC	[555]
Li(110)	–	–	–	–	–	3.55	TC	[556]
Li(110)	–	–	–	–	–	3.58	TC	[1030]
Li(110)	–	–	–	–	–	3.6	TC	[3137]
Li(110)	–	–	–	–	–	3.6	TC	[1086,1088]
Li(110)	–	–	–	–	–	3.61	TC	[321]
Li(110)	–	–	–	–	–	3.61	TC	[2402]

Table 1 (*continued*)

Surface	Beam	Ion	P_r (Torr)	T (K)	ϕ^+ (eV)	ϕ^e (eV)	Meth.	Refs.
Li(110)	–	–	–	–	–	3.63	TC	[555]
Li(110)	–	–	–	–	–	3.63	TC	[1086]
Li(110)	–	–	–	–	–	3.66	TC	[1086]
Li(110)	–	–	–	–	–	3.75	TC	[1086]
Li(110)	–	–	–	–	–	3.77	TC	[472]
Li(110)	–	–	–	–	–	3.78	TC	[1086]
Li(110)	–	–	–	–	–	3.87	TC	[1030,1089]
Li(110)	–	–	–	–	–	3.91	TC	[1089]
Li(110)	–	–	–	–	–	3.92	TC	[1087]
Li(110)	–	–	–	–	–	3.93	TC	[3713]
Li(110)	–	–	–	–	–	3.99	TC	[3693]
Li(110)	–	–	–	–	–	4.05	TC	[1089]
Li(110)	–	–	–	–	–	4.24	TC	[3692]
Recommended	–	–	–	–	–	**3.37 ± 0.05**	–	–
Li(111)	–	–	–	–	–	2.30	TC	[475]
Li(111)	–	–	–	–	–	2.35	TC	[593]
Li(111)	–	–	–	–	–	2.58	TC	[1159,1980,3067]
Li(111)	–	–	–	–	–	2.6	TC	[4461][490]
Li(111)	–	–	–	–	–	2.746	TC	[4091]
Li(111)	–	–	–	–	–	2.90	TC	[231]
Li(111)	–	–	–	–	–	2.90	TC	[1095]
Li(111)	–	–	–	–	–	2.925	TC	[4460][490]
Li(111)	–	–	–	–	–	2.93	TC	[553]
Li(111)	–	–	–	–	–	2.94	TC	[3467]
Li(111)	–	–	–	–	–	2.96	TC	[711]
Li(111)	–	–	–	–	–	2.97	TC	[321]
Li(111)	–	–	–	–	–	3.09	TC	[637,2418]
Li(111)	–	–	–	–	–	3.12	TC	[476,711]
Li(111)	–	–	–	–	–	3.12	TC	[637,2418]
Li(111)	–	–	–	–	–	3.13	TC	[1237]
Li(111)	–	–	–	–	–	3.13	TC	[556]
Li(111)	–	–	–	–	–	3.15	TC	[3814]
Li(111)	–	–	–	–	–	3.16	TC	[1030]
Li(111)	–	–	–	–	–	3.19	TC	[555]
Li(111)	–	–	–	–	–	3.2	TC	[1088]
Li(111)	–	–	–	–	–	3.20	TC	[1030]
Li(111)	–	–	–	–	–	3.25	TC	[475]
Li(111)	–	–	–	–	–	3.26	TC	[476]
Li(111)	–	–	–	–	–	3.42	TC	[472]
Li(111)	–	–	–	–	–	3.44	TC	[637]
Li(111)	–	–	–	–	–	3.58	TC	[1557]
Recommended	–	–	–	–	–	**3.04 ± 0.08**	–	–
Li(112)	–	–	–	–	–	3.30	TC	[321]
Li/W	Li	–	?	~300	–	1.84	PE	[2206]
Li/Si(100)	Li	–	8×10^{-11}	360	–	2.1*	CPD	[2414]
Li	–	–	–	–	–	2.1	TC	[2845]
Li/Si(100)	Li	–	$<1 \times 10^{-10}$	133, ~300	–	2.1*	PE	[2057]
Li	–	–	–	–	–	2.19	TC	[3725]
Li/Cu(100)	–	–	–	–	–	2.2*	TC	[3205]
Li/Si(100)[n]	Li	–	$<1 \times 10^{-10}$	~300	–	2.22 ± 0.05*	PE	[3935]
Li$_n$(n → ∞)[389]	–	–	–	–	–	2.25	TC	[4262]
Li/?	Li	–	?	?	–	2.28	?	[3785]
Li/Si(100)	Li	–	8×10^{-11}	360	–	2.3*	CPD	[2414]
Li/Ru(001)	Li	–	4×10^{-11}	200	–	2.3 ± 0.1*	CPD	[3606]
Li/glass	Li	–	?	~300	–	2.32 ± 0.03[2]	CPD	[349]
Li/Si(100)	Li	–	$<8 \times 10^{-11}$	~300	–	2.36*	PE	[2278]
Li/Si(100)	Li	–	$<2 \times 10^{-10}$	~300	–	2.36 ± 0.16*	PE	[2412]
Li/Si(100)	Li	–	$<3 \times 10^{-10}$	~300	–	2.38*	CPD	[1929]
Li/Si(100)[n]	Li	–	8×10^{-11}	360–500	–	2.4*	CPD	[1874]
Li/Si(111)[n]	Li	–	8×10^{-10}	~300	–	2.4	CPD	[2736]
Li/Cu(110)	Li	–	5×10^{-11}	140	–	2.4 ± 0.1	PE	[3454]
Li/Pt(111)	–	–	–	–	–	2.400	TC	[3245]
Li/Ni	Li	–	$<10^{-9}$	77	–	2.42	CPD	[2139,3698]
Li/?	Li	–	?	~300	–	2.42	PE	[3027]
Li	–	–	–	–	–	2.45	TC	[1744]
Li/Ni(110)	Li	–	8×10^{-11}	150	–	2.47*	CPD	[3219]
Li/graphene	–	–	–	–	–	2.49	TC	[4079]

Table 1 (*continued*)

Surface	Beam	Ion	P_r (Torr)	T (K)	ϕ^+ (eV)	ϕ^e (eV)	Meth.	Refs.
Li/Ni	Li	–	$<10^{-9}$	77	–	2.49	CPD	[3128]
Li/glass	Li	–	?	~300	–	2.49 ± 0.02[2]	CPD	[1374]
Li/Si(100)[p]	Li	–	8×10^{-11}	380–525	–	2.5*	CPD	[1874]
Li	–	–	–	–	–	2.5	TC	[3558]
Li/W	Li	–	$(<10^{-10})$	77	–	2.5	FE	[2711]
Li/Na/Cu(100)	Li	–	$\leq 1 \times 10^{-10}$	180	–	2.5	PE	[2678]
Li/Si(100)	–	–	–	–	–	2.5 ± 0.1*	TC	[3647]
Li	–	–	–	–	–	2.50*	TC	[1955]
Li	–	–	–	–	–	2.51	TC	[1571]
Li	–	–	–	–	–	2.52	TC	[1571]
Li/Cu(100)	Li	–	$\sim 10^{-10}$	~300	–	2.52 ± 0.08*	PE	[3297]
Li/Ni(110)	Li	–	8×10^{-11}	~300	–	2.53*	CPD	[3219]
Li/Si(100)[422]	Li	–	2×10^{-10}	~300	–	2.53	CPD	[4016]
Li/steel	Li	–	$\sim 10^{-10}$	~300–400	–	2.54 ± 0.02	PE	[4298,4299]
Li/Si(100)	Li	–	$<3 \times 10^{-10}$	~300	–	2.58*	CPD	[1929]
Li/Si(111)	Li	–	5×10^{-10}	~300	–	2.6	CPD	[2485]
Li/MgO(100)	Li	–	1×10^{-10}	~300	–	2.6	CPD	[1942]
Li/Si(100)	–	–	–	–	–	2.6*	TC	[732,4068]
Li/glass	Li	–	$\leq 10^{-7}$	~300	–	2.6	PE	[3253]
Li/Ru(001)	Li	–	$\leq 2 \times 10^{-10}$	100	–	2.6*	PE	[344]
Li	–	–	–	–	–	2.60	TC	[3477]
Li	–	–	–	–	–	2.63	TC	[3477]
Li	–	–	$\sim 10^{-10}$	~300	–	2.64 ± 0.02	PE	[4298,4315]
Li/Ru(001)	–	–	–	–	–	2.68	TC	[346]
Li/Ru(001)	Li	–	$\leq 2 \times 10^{-10}$	100	–	2.7*	PE	[344]
Li/Mo	Li	–	$\leq 3 \times 10^{-7}$	~300	–	2.7	PE	[1433]
Li/W(111)	Li	–	$(\leq 10^{-11})$	77	–	2.7	FE	[1977]
Li/W(110)	Li	–	?	5 (100)	–	2.7	CPD	[2387]
Li/Si(111)	Li	–	$<2 \times 10^{-11}$	90	–	2.7 ± 0.1*	PE	[3487]
Li/W(110)[39]	Li	–	$(\leq 10^{-10})$	77	–	2.75	FE	[1974]
Li/W(111)[39]	Li	–	$(\leq 10^{-10})$	77	–	2.75	FE	[1974]
Li/W(112)[39]	Li	–	$(\leq 10^{-10})$	77	–	2.75	FE	[1974]
Li/Ru(001)	Li	–	4×10^{-11}	~100–200	–	2.8	CPD	[1875,2285]
Li/Mo(112)	Li	–	$(\leq 10^{-11})$	77	–	2.8	CPD	[2027]
Li/Mo(110)	Li	–	?	77 (100)	–	2.8	CPD	[2387]
Li/Ni(100)	Li	–	$\leq 3 \times 10^{-10}$	~300	–	2.8	CPD	[936]
Li/Ir	Li	–	$\leq 10^{-4}$ (Li)	~700–1200	–	2.80	TE	[169]
Li/W(111)[39]	Li	–	$(\leq 10^{-10})$	77	–	2.80*	FE	[1974]
Li/Ge(100)	Li	–	$<1 \times 10^{-10}$	78	–	2.80*	FE	[4081]
Li/Ru(001)	–	–	–	–	–	2.86	TC	[346]
Li	–	–	–	0	–	2.86	TC	[4419]
Li/Ag(111)	Li	–	1×10^{-10}	~300	–	2.86*	CPD	[2866,2873]
Li/Ni(110)	Li	–	8×10^{-11}	150	–	2.87	CPD	[3219]
Li	–	–	–	–	–	2.87	TC	[3312]
Li/W(110)[39]	Li	–	$(\leq 10^{-10})$	77	–	2.87*	FE	[1974]
Li/Ge(111)	Li	–	$<1 \times 10^{-10}$	78	–	2.87*	FE	[4081]
Li(fp)	–	–	?	453	–	2.88	PE	[4256]
Li/W(112)[39]	Li	–	$(\leq 10^{-11})$	77	–	2.88 ± 0.02	CPD	[380]
Li/Ge(100)	Li	–	$\leq 10^{-10}$	~300	–	2.88 ± 0.08*	FE	[3936]
Li/W(110)	Li	–	$(\leq 10^{-11})$	77	–	2.9	FE	[1977]
Li/W(112)	Li	–	$(\leq 10^{-11})$	77	–	2.9	FE	[1977]
Li/C$_{60}$/Ni(110)	Li	–	8×10^{-11}	~300	–	2.9	CPD	[696]
Li	–	–	–	–	–	2.9	TC	[706]
Li/W(100)	Li	–	$(<10^{-11})$	~300	–	2.9	CPD	[2034,3976]
Li/W(111)	Li	–	$\sim 10^{-11}$	~300	–	2.9	CPD	[2535]
Li/W(112)	Li	–	$(\leq 10^{-11})$	~300	–	2.9	CPD	[259,380]
Li/W(110)	Li	–	$(\leq 10^{-11})$	77	–	2.9	FE	[259]
Li/W(111)	Li	–	$(\leq 10^{-11})$	~300	–	2.9	CPD	[259]
Li/W(110)	Li	–	$(\leq 10^{-11})$	5	–	2.9	CPD	[2387]
Li/Mo(110)	Li	–	$(\leq 10^{-11})$	77	–	2.9	CPD	[2387]
Li/Si(100)	Li	–	$<2 \times 10^{-11}$	~300	–	2.9*	PE	[2283]
Li/Ta(112)	Li	–	$(\leq 10^{-11})$	77, ~300	–	2.9	CPD	[2662]
Li/Si(100)	–	–	–	–	–	2.9 ± 0.1*	TC	[3647]
Li/Ge(111)	Li	–	$\leq 10^{-10}$	~300	–	2.90 ± 0.09*	FE	[3936]
Li/W(112)[39]	Li	–	$(\leq 10^{-11})$	77	–	2.91 ± 0.03	FE	[380]
Li	–	–	–	–	–	2.92	TC	[298]
Li/W(111)	Li	–	$\sim 10^{-9}$	77	–	2.92	FE	[363]
Li/W(112)[39]	Li	–	$(\leq 10^{-11})$	~300	–	2.93	CPD	[380,3341]
Li/W(112)[39]	Li	–	$(\leq 10^{-10})$	77	–	2.93*	FE	[1974]
Li/Ni(110)	Li	–	8×10^{-11}	~300	–	2.93	CPD	[3219]

Table 1 (*continued*)

Surface	Beam	Ion	P_r (Torr)	T (K)	ϕ^+ (eV)	ϕ^e (eV)	Meth.	Refs.
Li(fp)[42]	–	–	?	?	–	2.93 ± 0.05	PE	[3482]
Li(fp)	–	–	?	77	–	2.94	PE	[4256]
Li/W	Li	–	~10⁻⁹	77	–	2.94	FE	[363]
Li/W(112)	Li	–	(≤10⁻¹¹)	~300	–	2.94	CPD	[380]
Li(cluster)	–	–	–	–	–	2.95	TC	[3479]
Li/Pt(100)	–	–	–	–	–	2.96	TC	[3168]
Li/Au(100)	–	–	–	–	–	2.96	TC	[3168]
Li/Mo(110)	–	–	–	–	–	2.990	TC	[4046]
Li/Ni(110)	Li	–	≤8 × 10⁻¹¹	~300	–	3.0	CPD	[696]
Li/Si(111)	Li	–	?	~300	–	3.0*	?	[1716]
Li/Re	Li	–	~10⁻⁹	77	–	3.05	FE	[363]
Li/sapphire	Li	–	~10⁻⁹	78	–	3.05	PE	[1512]
Li/W(100)	Li	–	~10⁻⁹	77	–	3.06	FE	[363]
Li	–	–	–	–	–	3.07	TC	[231]
Li/Re(2111)	Li	–	~10⁻⁹	77	–	3.09	FE	[363]
Li/W(100)	Li	–	(<10⁻¹¹)	~300	–	3.1	CPD	[259]
Li/W(110)	Li	–	(<10⁻¹¹)	~300	–	3.1	CPD	[259]
Li/W(110)	Li	–	(<10⁻¹¹)	77	–	3.1	CPD	[259]
Li/Pt	Li	–	~10⁻¹⁰	~300	–	3.1	CPD	[437]
Li	–	–	–	–	–	3.10	TC	[1066]
Li	–	–	–	–	–	3.10	TC	[3467]
Li/W(011)	Li	–	(≤10⁻¹¹)	77	–	3.10	CPD	[2500]
Li/W(011)	Li	–	(≤10⁻¹¹)	77 (250)	–	3.10	CPD	[2500]
Li	–	–	–	–	–	3.11	TC	[521]
Li/W(112)	Li	–	~10⁻⁹	77	–	3.12	FE	[363]
Li/Pt(100)	–	–	–	–	–	3.154	TC	[3245]
Li	–	–	–	–	–	3.18	TC	[231]
Li/W(110)	Li	–	~10⁻⁹	77	–	3.19*	FE	[363]
Li/Mo(112)	–	–	–	–	–	3.2	TC	[468]
Li	–	–	–	–	–	3.21	TC	[1924]
Li_n(n → ∞)[389]	–	–	–	–	–	3.21	TC	[4262]
Li/Re(2112)	Li	–	~10⁻⁹	77	–	3.21*	FE	[363]
Li/Al(111)	Li	–	?	~300	–	3.22	CPD	[734]
Li/Re(2110)	Li	–	~10⁻⁹	77	–	3.24	FE	[363]
Li	–	–	–	–	–	3.24	TC	[4101]
Li	–	–	–	–	–	3.24	TC	[2427]
Li/Ru(0001)	Li	–	?	~300	–	3.3	PE	[4020]
Li	–	–	–	–	–	3.3	TC	[3558]
Li/W(110)	–	–	–	–	–	3.30	TC	[531]
Li	–	–	–	–	–	3.31	TC	[2629]
Li	–	–	–	–	–	3.32	TC	[3312]
Li	–	–	–	–	–	3.32	TC	[1613]
Li	–	–	–	–	–	3.33	TC	[1924]
Li	–	–	–	–	–	3.33	TC	[2061]
Li/Re(1011)	Li	–	~10⁻⁹	77	–	3.33*	FE	[363]
Li/W(100)	–	–	–	–	–	3.34	TC	[531]
Li/W(111)	–	–	–	–	–	3.34	TC	[531]
Li	–	–	–	–	–	3.36	TC	[553,2427]
Li	–	–	–	–	–	3.36	TC	[3477]
Li	–	–	–	–	–	3.36	TC	[3168]
Li	–	–	–	–	–	3.37	TC[3]	[475,519,2474]
Li	–	–	–	–	–	3.39	TC	[3220]
Li/W(112)	–	–	–	–	–	3.40	TC	[531]
Li	–	–	–	–	–	3.43	TC	[230]
Li	–	–	–	–	–	3.44	TC	[3467]
Li	–	–	–	–	–	3.45	TC	[738]
Li/Ru(001)	–	–	–	–	–	3.51	TC	[346]
Li	–	–	–	–	–	3.52	TC	[1571]
Li	–	–	–	–	–	3.53	TC	[1582]
Li	–	–	–	–	–	3.56	TC	[1167]
Li	–	–	–	–	–	3.58	TC	[1578,1582]
Li	–	–	–	–	–	3.60	TC	[1167]
Li	–	–	–	–	–	3.61	TC	[1167]
Li	–	–	–	–	–	3.63	TC	[1167]
Li	–	–	–	–	–	3.75	TC	[2382]
Li/Ru(001)	–	–	–	–	–	3.89	TC	[346]
Li/Pt(110)	–	–	–	–	–	4.004	TC	[3245]
Li	–	–	–	–	–	4.08	TC	[2629]
Recommended	–	–	–	–	–	**2.90 ± 0.03**[469]	–	–

Table 1 (*continued*)

Surface	Beam	Ion	P_r (Torr)	T (K)	ϕ^+ (eV)	ϕ^e (eV)	Meth.	Refs.
				4. Beryllium Be				
hcp ($\alpha, T < 800$ **K**)								
Be(0001)	–	–	–	–	–	4.7	TC	[3150]
Be(0001)	–	–	–	–	–	4.95	TC	[4427]
Be(0001)/mica[4]	Be	–	~10^{-10}	~300	–	4.98 ± 0.10	PE	[2009]
Be(0001)	–	–	?	77	–	5.0	PE	[2998]
Be(0001)	–	–	–	–	–	5.0 ± 0.1	TC	[3514]
Be(0001)	–	–	–	–	–	5.02 ± 0.05	TC	[3242]
Be(0001)/glass[4]	Be	–	?	~300	–	5.08 ± 0.08	CPD	[1782]
Be(0001)	–	–	–	–	–	5.1 ± 0.1	TC	[3514]
Be(0001)	–	–	<5×10^{-11}	~300	–	5.10 ± 0.02	PE	[2025]
Be(0001)	–	–	–	–	–	5.23	TC	[4417]
Be(0001)	–	–	–	–	–	5.25 ± 0.04	TC	[720]
Be(0001)	–	–	–	–	–	5.29	TC	[4004]
Be(0001)	–	–	–	–	–	5.3	TC	[1711]
Be(0001)	–	–	–	–	–	5.32	TC	[4461][490]
Be(0001)	–	–	–	–	–	5.321	TC	[4460][490]
Be(0001)	–	–	–	–	–	5.35	TC	[1734]
Be(0001)	–	–	–	–	–	5.36	TC	[3481]
Be(0001)	–	–	–	–	–	5.4	TC	[1704]
Be(0001)	–	–	–	–	–	5.45	TC	[4004]
Be(0001)	–	–	–	–	–	5.54	TC	[1925,1927,3200]
Be(0001)	–	–	–	–	–	5.556	TC	[4460][490]
Be(0001)	–	–	–	–	–	5.57	TC	[3481]
Be(0001)	–	–	–	–	–	5.61	TC	[4005]
Be(0001)	–	–	–	–	–	5.62	TC	[334]
Be(0001)	–	–	–	–	–	6.83	TC	[321]
Recommended	–	–	–	–	–	**5.27 ± 0.11**	–	–
Be(1010)	–	–	–	–	–	4.48	TC	[4461][490]
Be(1010)/W(110)	Be	–	<1×10^{-10}	~300	–	4.6	CPD	[3122]
Be(1010)	–	–	–	–	–	4.6 ± 0.1*	TC	[4442]
Be(1010)	–	–	–	–	–	4.644	TC	[4461][490]
Be(1010)	–	–	–	–	–	4.71	TC	[4004]
Be(1011)	–	–	–	–	–	5.03	TC	[4004]
Be(1011)	–	–	–	–	–	5.23	TC	[4004]
Be(1012)	–	–	–	–	–	4.81	TC	[4004]
Be(1012)	–	–	–	–	–	5.04	TC	[4004]
Be(1013)	–	–	–	–	–	4.46	TC	[4004]
Be(1013)	–	–	–	–	–	4.73	TC	[4004]
Be(1121)	–	–	–	–	–	4.58	TC	[4004]
Be(1121)	–	–	–	–	–	4.82	TC	[4004]
Be(1122)	–	–	–	–	–	4.81	TC	[4004]
Be(1122)	–	–	–	–	–	4.94	TC	[4004]
Be(1123)	–	–	–	–	–	4.25	TC	[4004]
Be(1123)	–	–	–	–	–	4.42	TC	[4004]
Be(1124)	–	–	–	–	–	5.72	TC	[321]
Be(2130)	–	–	–	–	–	4.17	TC	[4004]
Be(2130)	–	–	–	–	–	4.38	TC	[4004]
Be(3140)	–	–	–	–	–	4.23	TC	[4004]
Be(3140)	–	–	–	–	–	4.55	TC	[4004]
Be/W	Be	–	~10^{-10}	~300 (1070)	–	2.5	FE	[1784]
Be$_{45}$(cluster)	–	–	–	–	–	2.94	TC	[2657]
Be/W	Be	–	~10^{-7}	~300 (1070)	–	3.0	FE	[1784]
Be	–	–	?	~300	–	3.10	CPD	[2297]
Be	–	–	–	–	–	3.11	TC	[2493]
Be$_{45}$(cluster)	–	–	–	–	–	3.16	TC	[2657]
Be	–	–	–	–	–	3.17	TC	[2493]

Table 1 (*continued*)

Surface	Beam	Ion	P_r (Torr)	T (K)	ϕ^+ (eV)	ϕ^e (eV)	Meth.	Refs.
Be	–	–	?	?	–	3.17	PE	[3027]
Be(wire)	–	–	$<2 \times 10^{-9}$	~1100–1250	–	3.22 ± 0.08	TE	[2241]
Be/W(111)	Be	–	?	?	–	3.27 ± 0.13	FE	[1803]
Be	–	–	?	293	–	3.28	PE	[3028]
Be	–	–	–	–	–	3.50	TC	[1569]
Be	–	–	–	–	–	3.51	TC	[1571]
Be(block)	–	–	? (Cs)	~900–1600	–	367	TE	[3413]
Be(block)	–	–	~10^{-9}	~900–1200	–	3.67 ± 0.03	TE	[179]
Be	–	–	?	~300	–	3.7	PE	[2090]
Be	–	–	–	–	–	3.75	TC	[521]
Be	–	–	–	–	–	3.8	TC	[1955]
Be	–	–	–	–	–	3.80	TC	[2639]
Be/Al$_2$O$_3$/Al^{390}	Be	–	?	~300	–	3.89	CPD	[3057]
Be/Al$_2$O$_3$/Al^{390}	Be	–	?	~300	–	3.905 ± 0.05	CPD	[3057]
Be	–	–	$<8 \times 10^{-10}$	~300	–	3.92	CPD	[2657,2666,3286]
Be/metal	Be	–	?	~300	–	3.92	PE	[2561]
Be	–	–	–	–	–	3.93	TC	[1569]
Be	–	–	5×10^{-11}	~300	–	3.95	CPD	[3289]
Be/W	Be	–	?	~300 (≤850)	–	4.0 ± 0.1	FE	[1798]
Be	–	–	–	–	–	4.04	TC	[1744]
Be/Al$_2$O$_3$/Al^{390}	Be	–	?	~300	–	4.04 ± 0.06*	CPD	[3057]
Be/W	Be	–	?	~300	–	4.1	CPD	[2577]
Be/W(110)	Be	–	~10^{-10}	~300 (~850)	–	4.1	FE	[2837]
Be$_{33}$(cluster)	–	–	–	–	–	4.11	TC	[2657]
Be	–	–	–	–	–	4.21	TC	[738]
Be/GaAs	Be	–	?	?	–	4.26	?	[3054]
Be	–	–	–	0	–	4.30	TC	[4419]
Be	–	–	–	–	–	4.35	TC	[2629]
Be	–	–	–	–	–	4.39	TC	[1976]
Be/W	Be	–	~10^{-10}	~300 (~850)	–	4.4	FE	[2837]
Be$_{33}$(cluster)	–	–	–	–	–	4.41	TC	[2657]
Be$_{45}$(cluster)	–	–	–	–	–	4.43	TC	[2666,3790]
Be$_\infty$(cluster)	–	–	–	–	–	4.5	TC	[2365]
Be/W	Be	–	≤2×10^{-9}	~300	–	4.53	CPD	[3530]
Be	–	–	–	–	–	4.62	TC	[1613]
Be$_{45}$(cluster)	–	–	–	–	–	4.62	TC	[2666,3790]
Be/W(110)	Be	–	2×10^{-10}	300, 600	–	4.75	CPD	[3550]
Be/Mo(112)	Be	–	~10^{-11}	5{~300}	–	4.77*	CPD	[4450]
Be	–	–	–	–	–	4.79	TC	[1571]
Be	–	–	–	–	–	4.8	TC	[944]
Be/W	Be	–	?	?	–	4.8 ± 0.05	FE	[3937]
Be	–	–	–	–	–	4.80	TC	[1569]
Be/Mo(110)	Be	–	~10^{-11}	~300	–	4.82*	CPD	[4450]
Be/W(100)	Be	–	2×10^{-10}	~300	–	4.86 ± 0.03*	CPD	[3550]
Be/W(100)	Be	–	?	~300	–	4.90	CPD	[3981]
Be	–	–	–	–	–	4.91	TC	[298]
Be	–	–	–	–	–	4.97	TC	[1564]
Be/mica^4	Be	–	~10^{-10}	~300	–	4.98 ± 0.10	PE	[2009]
Be/W	Be	–	$<10^{-8}$	~300	–	~5.0	FE	[2308]
Be/W(112)	Be	–	$<5 \times 10^{-11}$	~300	–	5.00*	CPD	[1700]
Be	–	–	–	–	–	5.04	TC	[1564]
Be$_{19}$(cluster)	–	–	–	–	–	5.04	TC	[2657]
Be/glass^4	Be	–	?	~300	–	5.08 ± 0.08	CPD	[1782]
Be	–	–	–	–	–	5.11	TC	[1569]
Be	–	–	–	–	–	5.11 ± 0.06	TC	[3366]
Be	–	–	–	–	–	5.19	TC	[3729]
Be/W(111)	Be	–	~10^{-10}	~300 (~850)	–	5.3	FE	[2837]
Be$_{19}$(cluster)	–	–	–	–	–	5.35	TC	[2657]
Be	–	–	–	–	–	5.35 ± 0.16	TC	[1577]
Be	–	–	–	–	–	5.37	TC	[2629]
Be	–	–	–	–	–	5.39	TC	[1578,3458]
Be/W(112)	Be	–	1×10^{-10}	~300	–	5.6	CPD	[3117]
Be/W(112)	Be	–	~10^{-10}	~300 (~850)	–	6.0	FE	[2837]
Recommended	–	–	–	–	–	**4.28 ± 0.13**	–	–

Hexagonal (β, $T > 800$ K for bulk)

Be	–	–	?	?	–	3.66	TE	[3410]
Be	–	–	≤10^{-9}	~900–1200	–	3.665 ± 0.03	TE	[650]
Be	–	–	? (Cs)	~1200–1600	–	3.67	TE	[3413]
Be	–	–	≤1×10^{-9}	~900–1250	–	3.67 ± 0.03	TE	[179,3413]

Table 1 (*continued*)

Surface	Beam	Ion	P_r (Torr)	T (K)	ϕ^+ (eV)	ϕ^e (eV)	Meth.	Refs.
Be/W(100)	Be	–	2×10^{-10}	1200	–	4.56 ± 0.03*	CPD	[3550]
Be/W(100)	Be	–	2×10^{-10}	1170	–	4.59 ± 0.03*	CPD	[3550]
Be/W(110)	Be	–	2×10^{-10}	1000	–	4.65	CPD	[3550]
Be/W(110)	Be	–	2×10^{-10}	800	–	4.69	CPD	[3550]
Be/W(100)	Be	–	2×10^{-10}	1000	–	4.87 ± 0.03*	CPD	[3550]
Recommended	–	–	–	–	–	**4.2 ± 0.5**	–	–

5. Boron B

Surface	Beam	Ion	P_r (Torr)	T (K)	ϕ^+ (eV)	ϕ^e (eV)	Meth.	Refs.
B(mono)[391]	–	–	?	?	–	3.8 ± 0.1	TE	[1415]
B(mono)[391]	–	–	?	~300	–	4.3 ± 0.1	PE	[1415]
B(mono)[391]	–	–	$\sim 10^{-9}$	~300	–	4.30 ± 0.05	PE	[3100]
B(mono)	–	–	$\leq 3 \times 10^{-10}$	~1300–2400	–	4.45	TE	[1397]
B(hexagonal)	–	–	–	–	–	3.64	TC	[1571]
B(graphitic)	–	–	–	–	–	3.88	TC	[1571]
B[479]	–	–	–	–	–	4.09	TC	[4359]
B	–	–	–	–	–	4.10	TC	[1744]
B	–	–	–	–	–	4.11	TC	[4358]
B	–	–	–	–	–	4.16	TC	[4358,4439]
B	–	–	$<2 \times 10^{-6}$	1550–1855	–	4.38	TE	[3431]
B	–	–	–	–	–	4.44	TC	[298]
B/W[392]	–	–	–	–	–	4.5	TC	[913,4344]
B/W[392]	B	–	?	?	–	4.5	FE	[3503]
B/Ta	B_2H_6	–	$<3 \times 10^{-8}$	~300 (1000)	–	4.5 ± 0.1	PE	[1371]
B(nanowire)	–	–	–	–	–	4.52	TC	[4411]
B(graphitic)	–	–	–	–	–	4.66	TC	[1571]
B	–	–	–	–	–	4.77	TC	[1901]
B[479]	–	–	–	–	–	4.89	TC	[4359]
B	–	–	–	–	–	4.9	TC	[1955]
B/W	B	–	2×10^{-10}	?	–	5	FE	[2772]
B/W	B	–	2×10^{-10}	1230	–	5.1	FE	[2376]
B/Mo(110)	B	–	2×10^{-10}	~300 (~900)	–	5.3	CPD	[2698]
B[479]	–	–	–	–	–	5.39	TC	[4359]
B/Mo(110)[252]	B	–	2×10^{-10}	~300	–	5.8	CPD	[2698,2700,3655, 3963,4271]
B/La/Mo(110)[252]	B	–	2×10^{-10}	~300	–	5.8	CPD	[2700]
B/Gd/Mo(110)[252]	B	–	2×10^{-10}	~300	–	5.8	CPD	[2700]
Recommended	–	–	–	–	–	**4.50 ± 0.09**	–	–

6. Carbon C

Diamond (Diamond Structure)

Surface	Beam	Ion	P_r (Torr)	T (K)	ϕ^+ (eV)	ϕ^e (eV)	Meth.	Refs.
C(100)[B5]	–	–	$\sim 10^{-8}$	~300	–	2.9	FE	[2751]
C(100)[B5]	–	–	$\sim 10^{-8}$	~300	–	3.6	FE	[2751]
C(100)[B]	–	–	$<2 \times 10^{-10}$	~300	–	3.85 ± 0.2	CPD	[224]
C(100)[N]	–	–	1×10^{-11}	~300	–	4.7	PE	[1830]
C(100)[B]	–	–	$<2 \times 10^{-10}$	~300 (~1000)	–	4.75 ± 0.2	CPD	[224]
C(100)	–	–	–	–	–	5.04	TC	[3485]
C(100)[B6]	–	–	1×10^{-11}	~300	–	5.3	PE	[1830]
C(100)	–	–	–	–	–	5.5	TC	[2884]
C(100)	–	–	–	–	–	5.54	TC	[2758,2759]
C(100)[B6]	–	–	1×10^{-11}	~300	–	5.7	PE	[1830]
C(100)[B]	–	–	$\sim 10^{-10}$	~300	–	6.00	PE	[1829]
Recommended	–	–	–	–	–	**5.0 ± 0.6**	–	–
C(111)/Mo[7]	–	–	5×10^{-8}	~300	–	3.2	PE	[544,4059]
C(111)/Mo[8]	–	–	5×10^{-8}	~300	–	3.2	PE	[1205]
C(111)/Mo[8]	–	–	5×10^{-8}	~300	–	3.3	PE	[1205]
C(111)/Mo[8]	–	–	5×10^{-8}	~300	–	3.4	FE	[1205]
C(111)/Mo[8]	–	–	5×10^{-8}	~300	–	3.5	FE	[1205]
C(111)/Mo[8]	–	–	5×10^{-8}	~300	–	3.8	FE	[1205]
C(111)/Mo[8]	–	–	5×10^{-8}	~300	–	3.8	PE	[1205]
C(111)/Mo[7]	–	–	5×10^{-8}	~300	–	4.8	PE	[544,4059]
C(111)[B]	–	–	$\sim 10^{-10}$	~300 (1400)	–	4.85	CPD	[3597,3598]
C(111)[B]	–	–	$\sim 10^{-10}$	~300	–	4.97 ± 0.07	CPD	[1733,1736,3598]
C(111)/Mo[7]	–	–	5×10^{-8}	~300	–	5.1	PE	[544,4059]
C(111)	I_2	I_2^-	5×10^{-10}	723	5.4^N	–	NSI	[3771]
C(111)	–	–	$\sim 10^{-10}$	~300	–	5.5 ± 0.05	PE	[2131]
C(111)[B]	–	–	1×10^{-11}	~300	–	5.6	PE	[1830]

Table 1 (*continued*)

Surface	Beam	Ion	P_r (Torr)	T (K)	ϕ^+ (eV)	ϕ^e (eV)	Meth.	Refs.
C(111)	–	–	$\sim 10^{-8}$	~ 300	–	5.96	PE	[3434]
C(111)	–	–	6×10^{-4}	~ 300	–	6.1	PE	[3434]
C(111)	–	–	–	–	–	7 ± 0.7	TC	[2213]
Recommended	–	–	–	–	–	**5.4 ± 0.5**	–	–
C(112)	–	–	–	–	–	5.17	TC	[1627]

Polycrystalline Diamond or Diamond-like-Carbon

Surface	Beam	Ion	P_r (Torr)	T (K)	ϕ^+ (eV)	ϕ^e (eV)	Meth.	Refs.
C/Si(100)	CH_4, N_2	–	1×10^{-7}	500	–	1.5–4.5	FE	[3489]
C/Mo/Si	C	–	$< 10^{-5}$	~ 300 (670)	–	1.51	FE	[1726]
C/Si(100)	CH_4, N_2	–	1×10^{-7}	~ 300	–	1.7–5.4	FE	[3489]
C/W	C^+	–	$< 10^{-10}$	~ 300	–	2	FE	[2904]
C/Si(nw)/Si	CH_4, Ar	–	?	~ 300 (673)	–	2.23	FE	[3305]
C^p/Mo[480]	PH_3, CH_4	–	?	$\sim 700\{\sim 1200\}$	–	2.3	TE	[4371]
C/Si(nw)/Si	CH_4, Ar	–	?	~ 300 (673)	–	3.43	FE	[3305]
C/Si[9]	–	–	$\sim 10^{-9}$	~ 300	–	3.7	FE	[3568]
C/Mo[9]	–	–	$\sim 10^{-9}$	~ 300	–	3.7	FE	[3568]
C/Si	CH_4, H_2	–	$\sim 10^{-6}$	?	–	3.9	TE	[4286]
C/W[10]	–	–	$< 10^{-8}$	~ 300	–	4.1	FE	[2230]
C/Si	CH_4, N_2	–	1×10^{-7}	~ 300	–	4.1 ± 0.1	FE	[3489]
C/Mo,Ta	CH_4, H_2	–	?	~ 300 (~ 2300)	–	4.15 ± 0.05	FE	[2682]
C/cnt	CH_4, H_2	–	$\sim 10^{-6}$	~ 1200–1350	–	4.26	TE	[4286,4287]
C^B/W(100)	CH_4, B_2H_6	–	$\sim 10^{-8}$	1362{1100}	–	4.57	TE	[3015]
C/Mo,Ta	CH_4, H_2	–	?	~ 1500–1700	–	4.75 ± 0.05	TE	[2682]
C/Si(100)	?	–	$\leq 10^{-8}$	~ 300	–	4.9	PE	[2060]
C/Si	C^+	–	4×10^{-9}	~ 300	–	4.9 ± 0.1	CPD	[297]
C/Si	CH_4, H_2	–	?	~ 300 (?)	–	4.98	FE	[3742]
C/Si/Si(111)	CH_4, H_2	–	$\leq 10^{-9}$	~ 300 (~ 900)	–	5.0	FE	[2527]
C/Si	–	–	–	–	–	≥ 5.1	TC	[3299]
C/Si(mono)	CH_4, H_2	–	4×10^{-9}	~ 300 (?)	–	5.19 ± 0.1	PE	[699]
C/Mo	CH_4, H_2	–	$< 10^{-9}$	~ 300 (~ 1200)	–	5.2	FE	[3649]
C/Si(100)[29]	CH_4, H_2	–	$\leq 10^{-10}$	~ 300 (≥ 1200)	–	5.2 ± 0.2	FE	[698]
C/Si(100)[29]	CH_4, H_2	–	$\leq 10^{-10}$	~ 300 (≥ 1200)	–	5.6 ± 0.2	FE	[698,3620]
C/Si(100)[p]	CH_4, H_2	–	$\leq 10^{-10}$	~ 300 (≥ 1200)	–	6 ± 0.3	FE	[2066]
C(natural)	–	–	$\sim 10^{-8}$	~ 300	–	6.02 ± 0.1	PE	[3411]
C/Si(100)	CH_4, H_2	–	$\leq 10^{-10}$	~ 300 (≥ 1200)	–	6.3 ± 0.3	FE	[3620]
C/Si[9]	–	–	$\sim 10^{-9}$	~ 300	–	7.1	FE	[3568]
C/Mo[9]	–	–	$\sim 10^{-9}$	~ 300	–	7.1	FE	[3568]
Recommended	–	–	–	–	–	**4.6 ± 0.6**	–	–

Monocrystalline Graphite[488]

Surface	Beam	Ion	P_r (Torr)	T (K)	ϕ^+ (eV)	ϕ^e (eV)	Meth.	Refs.
C(0001)	–	–	–	–	–	3.6	TC	[1573]
C(0001)	–	–	–	–	–	4.1	TC	[1573]
C(0001)	–	–	–	–	–	4.44	TC	[1174]
C(0001)	–	–	4×10^{-11}	~ 300	–	4.5	PE	[4415]
C(0001)	–	–	–	–	–	4.65 ± 0.20[11]	TC	[1174]
C(0001)	–	–	2×10^{-10}	95	–	4.7	CPD	[525]
C(0001)	–	–	$\sim 10^{-10}$	~ 300	–	4.7 ± 0.1	PE	[236]
C(0001)	–	–	–	–	–	5.23	TC	[1174]
C(0001)	–	–	–	–	–	6.36	TC	[1503]
C(0001)	–	–	–	–	–	6.62	TC	[1503]
C(0001)	–	–	–	–	–	10.1	TC	[1503]
Recommended	–	–	–	–	–	**4.6 ± 0.3**	–	–
C(mono)	–	–	?	?	–	3.93[12]	FE	[2581]
C(mono)	–	–	$\leq 1 \times 10^{-10}$	~ 300	–	4.45	CPD	[286,450,537,665,839]
C(mono)	–	–	2×10^{-10}	~ 300	–	4.6	PE	[289,2653]
C(mono)	–	–	?	~ 300	–	4.60	PE	[1094]
C(mono)	–	–	$\sim 10^{-10}$	~ 300	–	4.7	PE	[235]
C(mono)	–	–	$\sim 10^{-10}$	~ 300 (1800)	–	4.7 ± 0.2	PE	[2508]

Highly Oriented Pyrolytic Graphite (HOPG)[488]

Surface	Beam	Ion	P_r (Torr)	T (K)	ϕ^+ (eV)	ϕ^e (eV)	Meth.	Refs.
C(HOPG)	–	–	$< 10^{-10}$	~ 300	–	4.4	PE	[284,1441]
C(HOPG)	–	–	4×10^{-10}	~ 300	–	4.4	PE	[4001]
C(HOPG)/C	?	–	$\sim 10^{-8}$	~ 2000–2400	–	4.4 ± 0.2	TE	[631]
C(HOPG)	–	–	?	~ 300	–	4.45	PE	[4437]
C(HOPG)	–	–	?	~ 300	–	4.475 ± 0.005	CPD	[287]
C(HOPG)	–	–	?	~ 300	–	4.5	FE	[622]
C(HOPG)	–	–	?	~ 300	–	4.5	PE	[4430]

Table 1 (*continued*)

Surface	Beam	Ion	P_r (Torr)	T (K)	ϕ^+ (eV)	ϕ^e (eV)	Meth.	Refs.
C(HOPG)	–	–	6×10^{-11}	~300	–	4.5 ± 0.1	PE	[632]
C(HOPG)	–	–	1×10^{-10}	~300	–	4.50 ± 0.05	PE	[3666]
C(HOPG)[170]	Cs	Cs^+	$\leq 6 \times 10^{-9}$	~1200–1500	4.51 ± 0.15*	(4.58 ± 0.02)	PSI	[1049]
C(HOPG)	–	–	$\leq 6 \times 10^{-9}$	~1200–1500	(4.65 ± 0.10)	4.58 ± 0.02	TE	[112,524,1049]
C(HOPG)	–	–	1×10^{-9}	~300	–	4.6	PE	[289,2653]
C(HOPG)	–	–	?	90	–	4.6	PE	[1620]
C(HOPG)	–	–	?	~300	–	4.6 ± 0.03	CPD	[4422]
C(HOPG)[170]	Cs	Cs^+	$\leq 6 \times 10^{-9}$	~1200–1500	4.60 ± 0.11*	(4.58 ± 0.02)	PSI	[112,524,1049]
C(HOPG)	Cs	Cs^+	$\leq 6 \times 10^{-9}$	~1200–1500	4.62 ± 0.17*	(4.58 ± 0.02)	PSI	[1049]
C(HOPG)	–	–	4×10^{-11}	~300	–	4.65	PE	[292]
C(HOPG)	–	–	2×10^{-11}	~300	–	4.67	CPD	[4279]
C(HOPG)	Cs	Cs^+	$\leq 6 \times 10^{-9}$	~1200–1500	4.69 ± 0.19*	(4.58 ± 0.02)	PSI	[1049]
C(HOPG)	–	–	?	~300	–	4.7	PE	[293]
C(HOPG)	–	–	$<10^{-9}$	~300	–	4.7	PE	[234,294]
C(HOPG)	–	–	1×10^{-9}	~300	–	4.7	PE	[2784]
C(HOPG)[13]	–	–	$<10^{-10}$	~300	–	4.7	CPD	[3215]
C(HOPG)	–	–	$\sim 10^{-10}$	~300	–	4.7 ± 0.1	PE	[526]
C(HOPG)	–	–	?	~300	–	4.79	PE	[4278]
C(HOPG)	–	–	?	~300	–	4.80	PE	[1166,3061]
C(HOPG)	–	–	–	–	–	4.81	TC	[296]
C(HOPG)	Cs	Cs^+	$\leq 6 \times 10^{-9}$	~1200–1500	4.82 ± 0.14*	(4.58 ± 0.02)	PSI	[1049]
C(HOPG)[13]	–	–	$<10^{-10}$	~300	–	5.0	CPD	[3215]
C(HOPG)	–	–	?	~300	–	5.0	CPD	[1600]
Recommended	–	–	–	–	**4.65 ± 0.12**	**4.66 ± 0.05**	–	–

Graphitic Carbon Film (not Carbidic)[443,452]

Surface	Beam	Ion	P_r (Torr)	T (K)	ϕ^+ (eV)	ϕ^e (eV)	Meth.	Refs.
C/Co(0001)	–	–	–	–	–	3.32	TC	[2423]
C/Mo	C_2H_2	–	$<10^{-10}$	~300 (558)	–	3.5*	FE	[2674]
C/Ni	C_{60}	C_{60}^-	5×10^{-10}	850–950	$3.5–4.0^N$	–	NSI	[3772,3773,3775]
C/Pt(210)	CO	–	$\sim 10^{-11}$	~300 (850)	–	3.6	FE	[453]
C/W	?	–	?	~300 (?)	–	~3.6	CPD	[3767]
C/Ni(111)	–	–	–	–	–	3.60	TC	[2423]
C/Ru(0001)	–	–	–	–	–	3.7	TC	[542]
C/TaC(111)[393]	C_2H_4	–	$<2 \times 10^{-10}$	~300 (1570)	–	3.7 ± 0.1	PE	[290]
C/Pt	C_2H_2	–	$\sim 10^{-9}$	~300 (1270)	–	3.75 ± 0.15	FE	[539,673]
C/Ni	C_{60}	C_{60}^-	5×10^{-10}	850–950	$3.9–4.4^{*N}$	–	NSI	[3772,3773]
C/Si[14]	–	–	?	~300 (770)	–	4.0 ± 0.15	PE	[1611]
C/Re	C_6H_6	–	2×10^{-9}	~300 (2140)	–	4.1	CPD	[407]
C/Ru(0001)	–	–	–	–	–	4.1	TC	[542]
C/Re–C(5%)	–	–	?	~300 (2200)	–	4.1 ± 0.1*	CPD	[2840]
C/Ru(001)	C_2H_4	–	2×10^{-10}	82 (>800)	–	4.2*	CPD	[455]
C/TaC(111)[393]	C_2H_4	–	$<2 \times 10^{-10}$	~300 (1270)	–	4.2 ± 0.1	PE	[290]
C/Ir	Cs	Cs^+	3×10^{-7}	~1200–1300	4.2 ± 0.1	(4.5 ± 0.1)	PSI	[1290]
C/Si[14]	–	–	?	~300	–	4.2 ± 0.15	PE	[1611]
C/Ni(111)	CO	–	$\sim 10^{-10}$	~300 (~560)	–	4.3	PE	[313]
C/Si[14]	–	–	?	~300	–	4.3 ± 0.1	PE	[1611]
C/Ni	CH_4, H_2	–	?	~300 (953)	–	4.3 ± 0.3	CPD	[1211]
C/Re(1010)	C_6H_6	–	$\sim 10^{-10}$	~1350–1750	(4.30 ± 0.05)	4.30 ± 0.05	TE	[4458]
C/Re(1010)	Na	Na^+	$\sim 10^{-10}$	~1150–1750	4.30 ± 0.05	(4.30 ± 0.05)	PSI	[4458]
C/Ir	CH_4	–	? (CH_4)	~1200–1800	(4.6 ± 0.1)	4.4	TE	[107]
C/Pt	C_2H_2	–	1×10^{-6}	1150–1750	(4.4^N)	4.4	TE	[675]
C/Pt	UF_6	UF_6^-	1×10^{-6}	1000	4.4^N	(4.4)	NSI	[675]
C/Pt–W(8%)	UF_6	UF_6^-	1×10^{-6}	1000	4.4^N	–	NSI	[675]
C/V(100)	–	–	–	–	–	4.4	TC	[1617]
C/graphite	?	–	$\sim 10^{-8}$	~1700–2100	–	4.4 ± 0.2	TE	[631]
C/Re[15]	C_6H_6	–	2×10^{-9}	~300 (<1900)	–	4.4 ± 0.3	CPD	[407,408]
C/Pt[338]	Cs	Cs^+	2×10^{-7}	~1400–2000	4.40 ± 0.03*	–	PSI	[50]
C/Pt–W(8%)[16]	K	K^+	?	1290	4.42	–	PSI	[1299]
C/Ir(111)	K	K^+	$<1 \times 10^{-9}$	~800–2000	4.44	–	PSI	[252]
C/Mo(100)	C_6H_6	–	$<10^{-10}$	~300 (1600)	–	4.45	CPD	[324,527]
C/Re(1010)	C_n, C_6H_6	–	1×10^{-10}	~300 (1600)	–	4.45	CPD	[286,537,665,839]
C/Ir(111)	Na	Na^+	$<5 \times 10^{-10}$	1600	4.45	–	PSI	[410]
C/Ir(111)	K	K^+	$<5 \times 10^{-10}$	1600	4.45	–	PSI	[409,411–413]
C/Ir(111)	C_n, C_6H_6	–	$<5 \times 10^{-10}$	~1600	–	4.45	TE	[3277]
C/Pt(111)	C_6H_6	–	$<10^{-10}$	~300 (1200)	–	4.45	CPD	[527,857,889]
C/Pt–W(8%)[170]	K	K^+	?	950–1100	4.46 ± 0.09	–	PSI	[397]
C/Ir	C_6H_6	–	$\leq 5 \times 10^{-6}$	1650–1900	–	4.47*	TE	[3751]
C/Pt[338]	K	K^+	2×10^{-7}	~1300–2000	4.48 ± 0.01*	–	PSI	[50]
C/Pt–W(8%)[341]	K	K^+	?	950–1100	4.48 ± 0.08	–	PSI	[397]
C/Pt–W(8%)	K	K^+	2×10^{-7}	~1200–1700	4.49 ± 0.01	–	PSI	[1285]

Table 1 (*continued*)

Surface	Beam	Ion	P_r (Torr)	T (K)	ϕ^+ (eV)	ϕ^e (eV)	Meth.	Refs.
C/Pt[338]	Rb	Rb$^+$	2×10^{-7}	~1200–2000	4.49 ± 0.01*	–	PSI	[50]
C/Pt[338]	K	K$^+$	2×10^{-7}	~1300–2000	4.49 ± 0.01	–	PSI	[1285]
C/Ir(111)	C_6H_6	–	≤8×10^{-9}	? (1700)	(4.5)	4.5	TE	[168]
C/Ir(111)	Ba	Ba$^+$	≤8×10^{-9}	?	4.5	(4.5)	PSI	[168]
C/Ir(111)	In	In$^+$	≤8×10^{-9}	?	4.5	(4.5)	PSI	[168]
C/Ru(0001)	C_2H_2	–	~10^{-11}	~300 (870)	–	4.5	PE	[542]
C/W	?	–	<5×10^{-9}	~300 (?)	–	4.5	FE	[288]
C/Ir(111)	In	In$^+$	≤8×10^{-10}	~1200–1600	4.5 ± 0.1	–	PSI	[105,3292,3546, 3547,3551,3783, 3784]
C/Ir	C_2H_4	–	3×10^{-7}	~1100–1200	(4.2 ± 0.1)	4.5 ± 0.1	TE	[1290]
C/Pt–W(8%)	C_4H_{10}	–	2×10^{-6}	1250–1770	(4.50 ± 0.05)	4.50 ± 0.02	TE	[108]
C/Pt–W(8%)	K	K$^+$	2×10^{-6}	~900–1700	4.50 ± 0.05	(4.50 ± 0.02)	PSI	[108]
C/Pt–W(8%)	Rb	Rb$^+$	?	1230	4.50 ± 0.09*	–	PSI	[737]
C/Pt–W(8%)	K	K$^+$	?	1230	4.51 ± 0.05*	–	PSI	[737]
C/Pt–W(8%)	Na	Na$^+$	≤3×10^{-7}	~1100–2150	4.54	–	PSI	[136]
C/Pt–W(8%)	C_4H_{10}	–	5×10^{-7}	~1500 (1750)	(4.58 ± 0.03)	4.54 ± 0.06	TE	[676]
C/Pt	Cs	Cs$^+$	≤6×10^{-9}	~1400–1600	4.55	–	PSI	[98]
C/Ir(111)	In	In$^+$	≤8×10^{-10}	?	4.55	–	PSI	[105]
C/Pt	C	–	?	~1200–1900	–	4.55	TE	[857]
C/Pt–W(8%)	K	K$^+$	2×10^{-6}	~900–1700	4.55 ± 0.07	(4.63 ± 0.06)	PSI	[108]
C/Pt	C_2H_4	–	4×10^{-9}	~1400–1650	–	4.57	TE	[1295]
C/Pt–W(8%)	Na	Na$^+$	5×10^{-7}	~900–1500	4.58 ± 0.03	(4.54 ± 0.06)	PSI	[676]
C/Ir	K	K$^+$	? (CH$_4$)	~1200–2000	4.6 ± 0.1	(4.4)	PSI	[107]
C/?	C	–	?	?	–	4.6 ± 0.2	?	[2640]
C/Pt–W(8%)	C_4H_{10}	–	2×10^{-6}	1250–1770	(4.55 ± 0.07)	4.63 ± 0.06	TE	[108]
C/quartz	C	–	?	~300	–	4.67 ± 0.12*	PE	[762]
C/Fe–Cu	C_2H_2	–	~10^{-8}	1109 (873)	–	4.7	TE	[764]
C/W	C	–	<3×10^{-10}	77 (~1000)	–	4.7 ± 0.05	FE	[663,4015]
C/Re	C_6H_6	–	~10^{-5}	<1800	–	4.7 ± 0.1	TE	[3753]
C/Rh	CsCl	Cs$^+$	<10^{-8}	~1000–1500	4.7 ± 0.1	–	PSI	[647]
C/Mo[17]	–	–	<10^{-9}	1650–1950	–	4.71 ± 0.18	TE	[791]
C/Mo[17]	–	–	<10^{-9}	1650–1950	–	4.73 ± 0.20	TE	[791]
C/Au(110)	C	–	?	~300 {~500}	–	4.74	CPD	[4404]
C/Au(110)	–	–	–	–	–	4.76	TC	[4404]
C/Al–Mg[18]	C	–	?	~300	–	4.79	PE	[2743]
C/Ir(111)	C	–	7×10^{-9}	1615–1785	(4.8)	4.8	TE	[103]
C/Ir(111)	Cs	Cs$^+$	7×10^{-9}	1685	4.8	(4.8)	PSI	[103]
C/Ir(111)	In	In$^+$	7×10^{-9}	1685	4.8	(4.8)	PSI	[103]
C/W	C_4H_{10}	–	?	1470–1810	–	4.8	TE	[237,295]
C/Re[415]	Cs	Cs$^+$	<10^{-8}	~700~1800	4.94*	–	PSI	[3753]
C/Ni	CH$_4$, H$_2$	–	?	~300 (~1300)	–	5	FE	[2802]
C/Si	CH$_4$, H$_2$	–	?	~300 (~1300)	–	5	FE	[2802]
C/Ir(111)	C	–	?	~300	–	5	CPD	[3858]
C/Fe(110)	C_2H_2	–	1×10^{-10}	~300 (550)	–	5.0	PE	[1541]
C/Mo	C	–	~10^{-8}	~300	–	5.0 ± 0.1	CPD	[299,2958]
C/Ag/Mo	C	–	~10^{-8}	~300	–	5.0 ± 0.1	CPD	[299]
C/Si	–	–	~10^{-10}	~300	–	5.0 ± 0.1	PE	[1738]
C/Si(100)[p]	C	–	≤10^{-10}	~300	–	5.0 ± 0.2	PE	[2066]
C/Pt(111)	CH$_4$, H$_2$	–	~10^{-10}	~300 (~600)	–	5.1	CPD	[3650]
C/Si(mono)	?	–	4×10^{-9}	~300 (?)	–	5.19 ± 0.1	PE	[699]
C/Al–Mg[18]	C	–	?	~300	–	5.32	PE	[2743]
C/Pt(111)	C_6H_6, etc.	–	?	~300 (~500)	–	5.4*	CPD	[1425]
C/Ni(100)	CO	–	<5×10^{-10}	~300 (~450)	–	5.7	CPD	[1790]
C/Re	UF$_4$	U$^+$	<1×10^{-8}	~2400–2700	5.84 ± 0.16	–	PSI	[276]
C/Fe(100)[427]	–	–	–	–	–	6.3*	TC	[4026]
Recommended	–	–	–	–	**4.50 ± 0.04**	**4.47 ± 0.05**	–	–
Recommended	–	–	–	–	**4.4 ± 0.1[N]**	–	–	–
Polycrystalline Graphite[488]								
C(filament)	–	–	<10^{-6}	?	–	3.41	TE	[2919]
C	–	–	–	–	–	3.54	TC	[1796]
C(tip)/W	–	–	5×10^{-9}	~300 (3655)	–	3.8	FE	[3607]
C(filament)	–	–	?	?	–	3.94	TE	[2456]
C(filament)	–	–	?	?	–	4.1	TE	[2459]
C(filament)	–	–	<5×10^{-8}	?	–	4.1	TE	[1482]
C	–	–	? (Ba)	~1100–1400	–	4.30	TE	[1773]
C(filament)	–	–	?	~1700–2200	–	4.34	TE	[115]
C(filament)	–	–	<10^{-5}	~1350–2100	–	4.35 ± 0.06	TE	[114]
C	–	–	~10^{-8}	~300	–	4.38 ± 0.01	PE	[760]

Table 1 (*continued*)

Surface	Beam	Ion	P_r (Torr)	T (K)	ϕ^+ (eV)	ϕ^e (eV)	Meth.	Refs.
C(rod)	–	–	?	0^E	–	4.39	TE	[113]
C	–	–	?	~1500 (~2800)	–	4.4	TE	[761]
C	–	–	?	?	–	4.4	TE	[3402]
C	–	–	?	?	–	4.4	TE	[3599]
C(ribbon)	–	–	3×10^{-7}	~1500–2200	(4.45 ± 0.08)	4.40 ± 0.02	TE	[71]
C(vitreous)	–	–	~10^{-10}	~300	–	4.42	CPD	[1516]
C(filament)	–	–	<10^{-6}	≤1610	–	4.44	TE	[285]
C(ribbon)	In	In$^+$	3×10^{-7}	1660–2310	4.44 ± 0.08	(4.40 ± 0.02)	PSI	[71]
C(ribbon)	K	K$^+$	3×10^{-7}	~1500–2000	4.46 ± 0.02	(4.40 ± 0.02)	PSI	[71]
C	–	–	?	?	–	4.5	TE	[2360]
C(filament)	–	–	?	?	–	4.55	TE	[2457]
C(rod)	–	–	?	~1300–2200	–	4.56	TE	[113]
C(filament)	–	–	?	≤2335	–	4.59	TE	[285]
C	–	–	2×10^{-9}	~300	–	4.6	PE	[1165,3225]
C(disk)	–	–	?	~300	–	4.6	CPD	[4175]
C[393]	–	–	<2×10^{-10}	~300	–	4.6 ± 0.1	PE	[290]
C(ribbon)	N$_2^+$	CN$^-$	<1×10^{-10}	1070–1290	4.6 ± 0.2^N	–	NSI	[617]
C(filament)	–	–	?	≤2125	–	4.61	TE	[285]
C(chamber)	–	–	?	0^E	–	4.62	TE	[1460]
C(chamber)	–	–	<10^{-5}	~1500–1650	–	4.62 ± 0.02	TE	[633,2303]
C	–	–	2×10^{-9}	~300	–	4.65 ± 0.05	PE	[291]
C	–	–	–	–	–	4.7	TC	[765]
C	–	–	<10^{-9}	~300	–	4.7	PE	[1894]
C	–	–	?	~300	–	4.72	PE	[2080]
C(vitreous)	–	–	~10^{-6}–10^{-8}	~300	–	4.75	PE	[1894]
C(tip)	–	–	1.8×10^{-7}	~300	–	4.8 ± 0.3	FE	[4445]
C	–	–	<10^{-6}	~300	–	4.81	PE	[2919]
C/SnO$_2$	–	–	?	~300	–	4.81	PE	[4453]
C	–	–	–	–	–	4.81[19]	TC	[296]
C	–	–	?	?	–	4.83	TE	[2569]
C	–	–	?	?	–	4.84	TE	[1462]
C(rod, etc.)	–	–	?	?	–	4.85 ± 0.05	TE, etc.	[238]
C(colloidal)/glass	–	–	<10^{-9}	~300	–	4.85 ± 0.08	CPD	[766]
C	–	–	–	–	–	4.91	TC	[767]
C	–	–	–	–	–	5.0	TC	[298]
C	–	–	?	~300	–	5.0	CPD	[3994]
C	–	–	–	–	–	5.23[19]	TC	[296]
C	–	–	–	~300	–	5.8, 5.85[20]	PE	[1735]
Recommended	–	–	–	–	**4.45 ± 0.05**	**4.63 ± 0.06**	–	–
Recommended	–	–	–	–	**4.6 ± 0.2^N**	–	–	–
Graphene[401,462,468,471,483,489]								
C/Pd(111)	–	–	–	–	–	4.03–4.738	TC	[4308]
C/Ni	C$_2$H$_2$	–	<2×10^{-8}	~300 (1113)	–	4.15 ± 0.05	CPD	[4438]
C/Cu	CH$_4$, H$_2$	–	5×10^{-10}	~300 (~1220)	–	4.25 ± 0.10	PE	[4243,4245]
C	–	–	–	–	–	4.26	TC	[4126]
C/Pd(111)	CH$_4$, Ar	–	?	~300 (~1200)	–	4.3 ± 0.1	CPD	[4282]
C/SiC(0001)	–	–	–	–	–	4.33	TC	[4409]
C	–	–	–	–	–	4.38	TC	[4079]
C/SiO$_2$/Si	–	–	?	~300	–	4.4	PE	[4376]
C/Pd(111)	CH$_4$, Ar	–	<1×10^{-10}	~300 (~1200)	–	4.42–4.49	CPD	[4308]
C	–	–	–	–	–	4.43	TC	[4451]
C(zigzag)	–	–	–	–	–	4.46	TC	[4360]
C[455]	–	–	–	–	–	4.48	TC	[3240]
C	–	–	–	–	–	4.48[468]	TC	[4174,4284]
C	–	–	–	–	–	4.60	CT	[4359]
C[439]	–	–	–	–	–	4.5	TC	[4105]
C/Cu	–	–	?	~300	–	4.5	CPD	[4103]
C	–	–	–	–	–	4.50	TC	[4127]
C	–	–	–	–	–	4.53	TC	[1168]
C/SiC	–	–	?	~300 (?)	–	4.55 ± 0.02	CPD	[4443]
C/SiO$_2$/Si	–	–	?	~300	–	4.56 ± 0.04	PE	[4129]
C/SiO$_2$/Si[442]	–	–	?	~300	–	4.57 ± 0.05	CPD	[4128]
C	–	–	–	–	–	4.58	TC	[4426]
C	–	–	–	–	–	4.60	CT	[4359]
C/HfO$_2$/Si	–	–	5×10^{-10}	~300	–	4.62 ± 0.08	PE	[4285]
C/Cu–Ni[417]	C$_2$H$_2$, etc	–	?	~300{~1500}	–	4.63–4.79	CPD	[3996]
C(sheet)	–	–	–	–	–	4.66	TC	[891]
C/Cu[417]	?	–	?	~300 (?)	–	4.67–4.78	CPD	[3996]
C(sheet)	–	–	–	–	–	4.68	TC	[2557]

Table 1 (*continued*)

Surface	Beam	Ion	P_r (Torr)	T (K)	ϕ^+ (eV)	ϕ^e (eV)	Meth.	Refs.
C/SiO$_2$/Si[442]	–	–	?	~300	–	4.69 ± 0.05	CPD	[4128]
C/Re(1010)	Na	Na$^+$	~10^{-10}	?	4.7 ± 0.05	–	PSI	[4458]
C	–	–	–	–	–	4.73[21]	TC	[767]
C/?	–	–	?	~1200	–	4.74 ± 0.04	TE	[4283]
C/Cu(111)	–	–	–	–	–	4.77	TC	[4402]
C	–	–	–	–	–	4.80	TC	[1743]
C/SiO$_x$//Si(100)[418]	?	–	?	~300 (?)	–	4.81 ± 0.06	CPD	[3997]
C	–	–	–	–	–	4.84[21]	TC	[767]
C/Cu[418]	CH$_4$	–	?	~300{1308}	–	4.92 ± 0.06	CPD	[3997]
C/Ir(111)	–	–	–	–	–	4.96	TC	[4219]
C(isolated)	–	–	–	–	–	5.11	TC	[4409]
C(ribbon)	–	–	–	–	–	6.30	TC	[3008]
Recommended	–	–	–	–	–	**4.67 ± 0.11**	–	–
Carbon Fullerene[433,454]								
C$_{60}$(111)/GeS(001)[394]	C$_{60}$	–	2 × 10^{-10}	~300{450}	–	4.7	PE	[457]
C$_{60}$(111)/GeS(001)[394]	C$_{60}$	–	2 × 10^{-10}	~300{450}	–	4.74 ± 0.03	PE	[543]
C$_{60}$(111)/GeS(001)[394]	C$_{60}$	–	2 × 10^{-10}	~300{450}	–	4.83 ± 0.05	PE	[543]
C$_{60}$/Ag[395]	C$_{60}$	–	≤1 × 10^{-10}	~300	–	4.46	CPD	[2198]
C$_{60}$/Au[395]	C$_{60}$	–	≤1 × 10^{-10}	~300	–	4.47	CPD	[2198]
C$_{60}$/Au(111)	C$_{60}$	–	?	~300	–	4.53	CPD	[4449]
C$_{60}$/Cu[395]	C$_{60}$	–	≤1 × 10^{-10}	~300	–	4.59	CPD	[2198]
C$_{60}$/Ag[395]	C$_{60}$	–	≤1 × 10^{-10}	~300	–	4.60	CPD	[2198]
C$_{60}$/Au[395]	C$_{60}$	–	≤1 × 10^{-10}	~300	–	4.62	CPD	[2198]
C$_{60}$/Ag(111)	C$_{60}$	–	1 × 10^{-10}	~300 (520)	–	4.63 ± 0.10	PE	[1195]
C$_{60}$/Au(111)	C$_{60}$	–	1 × 10^{-10}	~300 (570)	–	4.7	PE	[1070]
C$_{60}$/Al	C$_{60}$	–	~10^{-10}	~300	–	4.7 ± 0.1	PE	[1220]
C$_{60}$/Au/Si^n	C$_{60}$	–	?	~300	–	4.70 ± 0.01	CPD	[3228]
C$_{60}$/Cu[395]	C$_{60}$	–	≤1 × 10^{-10}	~300	–	4.72	CPD	[2198]
C$_{60}$/Rh(111)	C$_{60}$	–	1 × 10^{-10}	~300	–	4.80 ± 0.03	PE	[568,2282]
C$_{60}$/Au(110)[396]	C$_{60}$	–	?	?	–	4.82 ± 0.05	?	[3002,3006]
C$_{60}$/Cu(111)[22]	–	–	–	–	–	4.85*	TC	[233]
C$_{60}$/Cu	C$_{60}$	–	?	~300	–	4.85 ± 0.05	PE	[3178]
C$_{60}$/Cu(111)[396]	C$_{60}$	–	<2 × 10^{-10}	~300 (570)	–	4.86	PE	[316]
C$_{60}$/Au(110)	C$_{60}$	–	?	~300 (700)	–	4.9	CPD	[1144]
C$_{60}$/Cu(111)	C$_{60}$	–	4 × 10^{-11}	~300	–	4.9	PE	[4415]
C$_{60}$/Ag(110)	C$_{60}$	–	?	~300 (700)	–	4.92	CPD	[1144]
C$_{60}$/Ni(111)	C$_{60}$	–	<2 × 10^{-10}	~300 (570)	–	4.93	PE	[316]
C$_{60}$/Au(111)[22]	–	–	–	–	–	4.94	TC	[233]
C$_{60}$/Ag(111)[22]	–	–	–	–	–	4.96	TC	[233]
C$_{60}$/Au(111)[22]	–	–	–	–	–	4.96	TC	[233]
C$_{60}$/Ag(111)[22]	–	–	–	–	–	4.99	TC	[233]
C$_{60}$/W	C$_{60}$	–	≤10^{-9}	~300	–	5	FE	[3717]
C$_{60}$/Cr/C(HOPG)	C$_{60}$	–	1 × 10^{-10}	~300	–	5.0	PE	[2794]
C$_{60}$/Rh(111)[23,396]	C$_{60}$	–	6 × 10^{-11}	~300 (≤700)	–	5.05	CPD	[1007]
C$_{60}$/Cu(100)	C$_{60}$	–	?	~300	–	5.06	CPD	[4449]
C$_{60}$/Cu(111)	–	–	–	–	–	5.15	TC	[3486]
C$_{60}$/Al(111)[396]	C$_{60}$	–	~10^{-10}	~300{620}	–	5.15 ± 0.05	PE	[458,2681,2683]
C$_{60}$/Ag(111)	C$_{60}$	–	?	~300	–	5.19	CPD	[4449]
C$_{60}$/Al(110)[396]	C$_{60}$	–	~10^{-10}	~300{620}	–	5.25 ± 0.05	PE	[458,2681,2683]
C$_{60}$/Ta(110)[396]	C$_{60}$	–	?	~300	–	5.4	PE	[460]
C$_{60}$/Ni(110)	C$_{60}$	–	8 × 10^{-11}	~300{650}	–	5.61	CPD	[459,696]
C$_{60}$/Pt(111)[397]	C$_{60}$	–	4 × 10^{-11}	100 (900)	–	5.7	PE	[697]
C$_{60}$	–	–	–	–	–	5.74	TC	[3486]
C$_{60}$ (fine cryst.)	C$_{60}$	–	?	~300	–	6.5	PE	[1166,3061]
C$_{60}$/W	C$_{60}$	–	<1 × 10^{-10}	298, 370	–	11.7 ± 0.5	FE	[2520]
Recommended	–	–	–	–	–	**4.87 ± 0.06**	–	–
Single-Walled Carbon Nanotube[28,402,481]								
C(zigzag)	–	–	–	–	–	3.07–5.25	TC	[1743]
C(chiral)	–	–	–	–	–	3.47–4.92	TC	[1743]
C(armchair)	–	–	–	–	–	3.67–5.01	TC	[1743]
C/Si(100)	CH$_4$,H$_2$	–	≤10^{-10}	~300{1200}	–	3.7 ± 0.3	FE	[1171]
C/Ag/Ti/Cr/Si	–	–	<2 × 10^{-7}	~300 (?)	–	4.21	FE	[2201]
C(quartz)	–	–	?	~300 (~1200)	–	4.31	PE	[2446]
C(open ended)	–	–	–	–	–	4.47	TC	[1740]
C/Ni/W	C$_2$H$_2$	–	<5 × 10^{-8}	~300{870}	–	4.5	FE	[2288]
C(armchair)[455]	–	–	–	–	–	4.5	TC	[3240]
C[24]	–	–	–	–	–	4.5 ± 0.1	TC	[1168]

Table 1 (*continued*)

Surface	Beam	Ion	P_r (Torr)	T (K)	ϕ^+ (eV)	ϕ^e (eV)	Meth.	Refs.
C(chiral)[455]	–	–	–	–	–	4.5–5.5	TC	[3240]
C(zigzag)[455]	–	–	–	–	–	4.5–5.9	TC	[3240]
C/Si(111)[25]	–	–	$\sim10^{-10}$	~300	–	4.62 ± 0.06	PE	[3246]
C	–	–	–	–	–	4.64	TC	[1877]
C($d \geq 1$ nm)	–	–	–	–	–	4.69 ± 0.01	TC	[1169]
C(flake)	–	–	8×10^{-10}	~300	–	4.7	PE	[3229]
C/SiO$_2$	? (CVD)	–	1×10^{-10}	$\sim300\{1200\}$	–	4.7	PE	[3233]
C($d \rightarrow \infty$)[21]	–	–	–	–	–	4.73	TC	[767]
C/Si	? (CVD)	–	?	$\sim300\{\sim1200\}$	–	4.73	PE	[1172]
C	–	–	–	–	–	4.73	TC	[4446]
C(metallic)	–	–	–	–	–	4.73 ± 0.03	TC	[767]
C/W	–	–	$<3 \times 10^{-9}$	$\sim300\ (\sim1300)$	–	4.76	FE	[546]
C(capped)	–	–	–	–	–	4.78	TC	[1740]
C/ITO	–	–	$<10^{-10}$	~300	–	4.8	PE	[284]
C/GaAs	–	–	2×10^{-9}	~300 (?)	–	4.8	PE	[291,1165]
C/W	–	–	?	~300	–	4.8	FE	[3572]
C/SiO$_2$/Si	? (CVD)	–	1×10^{-7}	~1800–2100	–	4.8 ± 0.1	TE	[2555]
C/glass	–	–	?	~300	–	4.83	PE	[3795]
C($d \rightarrow \infty$)[21]	–	–	–	–	–	4.84	TC	[767]
C(mouth)[27]	–	–	–	–	–	4.86	TC	[3570]
C/ITO	–	–	?	~300	–	4.86	PE	[3795]
C/Si(111)[25]	–	–	$\sim10^{-10}$	~300	–	4.86 ± 0.10	CPD	[3246]
C/W	–	–	$<3 \times 10^{-9}$	$\sim300\ (\sim1300)$	–	4.88	FE	[546]
C	–	–	–	–	–	4.89	TC	[3787]
C/Si(111)[26]	–	–	$\sim10^{-10}$	~300	–	4.94 ± 0.07	CPD	[3246]
C(mouth)[27]	–	–	–	–	–	4.95	TC	[3570]
C/Si(111)[25]	–	–	$\sim10^{-10}$	~300	–	4.97 ± 0.07	CPD	[3246]
C/Si(111)[26]	–	–	$\sim10^{-10}$	~300	–	5.01 ± 0.17	CPD	[3246]
C(bundle)	–	–	–	–	–	5.02 ± 0.05	TC	[767]
C/?	–	–	?	~300	–	5.05	PE	[1166,3061]
C(capped)	–	–	–	–	–	5.05	TC	[2918,3682]
C (5,5)[28]	–	–	–	–	–	5.08	TC	[3570]
C(rope)/Pt	–	–	5×10^{-9}	~300	–	5.1	FE	[547]
C/?	–	–	?	~300	–	5.10	PE	[3061]
C/ITO	–	–	? (air)	~300	–	5.19	PE	[3795]
C(bundle)	–	–	–	–	–	5.2–5.4	TC	[3239]
C(neighbor)[27]	–	–	–	–	–	5.20	TC	[3570]
C/glass	–	–	? (air)	~300	–	5.24	PE	[3795]
C(neighbor)[27]	–	–	–	–	–	5.25	TC	[3570]
C(bundle)	–	–	–	–	–	5.3	TC	[3239]
C(armchair)	–	–	–	–	–	5.46 ± 0.02	TC	[548]
C(zigzag)	–	–	–	–	–	5.60 ± 0.03	TC	[548]
Recommended	–	–	–	–	–	**4.78 ± 0.06**	–	–
Multi-Walled Carbon Nanotube[402,481]								
C(yarn)[470]	–	–	?	~2000–2100	–	3.9	TE	[4307]
C(yarn)[470]	–	–	?	~2100–2200	–	4.1	TE	[4307]
C/glass	–	–	?	~300	–	4.18 ± 0.09	PE	[4003]
C/?	?	–	$\sim10^{-6}$	~300	–	4.2	FE	[1724]
C(pentagon)/Ta[30]	–	–	5×10^{-10}	~300	–	4.2–4.3	FE	[3942]
C/ITO	–	–	$<10^{-10}$	$\sim300\ (\sim470)$	–	4.3	PE	[284,1441]
C/W	? (CVD)	–	1×10^{-9}	$\sim300\{?\}$	–	4.3 ± 0.1	FE	[2546]
C/Si[31]	? (CVD)	–	8×10^{-10}	$\sim300\{\sim570\}$	–	4.4	PE	[3223,3225]
C	–	–	–	–	–	4.51–5.23	TC	[3240]
C(armchair)	–	–	–	–	–	4.53–4.54	TC	[3240]
C(zigzag)	–	–	–	–	–	4.53–4.99	TC	[3240]
C/Si[31]	? (CVD)	–	8×10^{-10}	$\sim300\ (\sim570)$	–	4.6	PE	[3223]
C/W	? (CVD)	–	1×10^{-9}	~600–1400	–	4.6 ± 0.7	TE	[2546]
C(yarn)	–	–	4×10^{-8}	1500–2200	–	4.60 ± 0.04	TE	[1092,4306]
C(powder)	–	–	?	~300	–	4.61 ± 0.03	PE	[4003]
C/W	? (CVD)	–	$\sim10^{-7}$	~300	–	4.61 ± 0.09	CPD	[1208]
C($r > 1$ nm)	–	–	–	–	–	4.63 ± 0.02	TC	[1169]
C/?[32]	?	–	?	~300	–	4.7 ± 0.1	FE	[545]
C/W	? (CVD)	–	1×10^{-9}	~300–720	–	4.7 ± 0.4	FE	[2546]
C/SiO$_2$/Si	? (CVD)	–	1×10^{-7}	~1800–2100	–	4.85 ± 0.03	TE	[2555]
C/Si(100)	CH$_4$, H$_2$	–	$\leq10^{-10}$	$\sim300\ (\sim1200)$	–	4.85 ± 0.2	PE	[1171]
C/Si(100)^p	CH$_4$, H$_2$	–	$\leq10^{-10}$	$\sim300\ (\geq1220)$	–	4.9	FE	[2066]

Table 1 (*continued*)

Surface	Beam	Ion	P_r (Torr)	T (K)	ϕ^+ (eV)	ϕ^e (eV)	Meth.	Refs.
C/?	–	–	?	~300	–	4.95	PE	[1166,3061]
C/Si(100)[403]	CH$_4$, H$_2$	–	<10^{-9}	~300{~1200}	–	~5	FE	[3649]
C/Si(100)	CH$_4$, H$_2$	–	≤10^{-10}	~300{~1200}	–	5 ± 0.3	FE	[1171]
C/W	?	–	2 × 10^{-10}	770 (970)	–	5.0	FE	[1840]
C/SiO$_2$	? (CVD)	–	2 × 10^{-10}	~300{1000}	–	5.1 ± 0.2	FE	[1837,3601]
C/Si(100)[403]	CH$_4$, H$_2$	–	~10^{-8}	~300{~1200}	–	5.3 ± 0.2	FE	[698,2425,3943]
C/epoxy	–	–	~10^{-6}	~300	–	5.4	FE	[1728]
C/SiO$_2$	? (CVD)	–	~10^{-10}	~300 (?)	–	5.4	FE	[3601]
C/?[32]	?	–	?	~300 (?)	–	5.6	FE	[545]
C/?[33]	?	–	?	~300	–	5.7	PE	[1735]
C/?[33]	?	–	?	~300	–	5.75	PE	[1735]
C/W[34]	–	–	≤2 × 10^{-11}	~300 (1000)	–	7.3 ± 0.7	FE	[1170]
Recommended	–	–	–	–	–	**4.63 ± 0.04**	–	–
Conical Carbon Nanotube[467]								
C/graphite	CH$_4$, H$_2$	–	~10^{-7}	~1300–1400	–	4.1–4.7	TE	[4280,4286]
C/Pt	CH$_4$, H$_2$	–	~10^{-7}	~1400–1500	–	4.2	TE	[4280,4286]
C/Pt	CH$_4$, H$_2$	–	~10^{-8}	~300 (?)	–	4.5	PE	[4280,4286]

11. Sodium Na

bcc

Surface	Beam	Ion	P_r (Torr)	T (K)	ϕ^+ (eV)	ϕ^e (eV)	Meth.	Refs.
Na(100)	–	–	–	–	–	2.355	TC	[2947]
Na(100)	–	–	–	–	–	2.38	TC	[1254]
Na(100)	–	–	–	–	–	2.40	TC	[1159,3067]
Na(100)	–	–	–	–	–	2.45	TC	[1556]
Na(100)	–	–	–	–	–	2.58	TC	[231]
Na(100)	–	–	–	–	–	2.60	TC	[3467]
Na(100)	–	–	–	–	–	2.638	TC	[4091]
Na(100)	–	–	–	–	–	2.65	TC	[2427]
Na(100)	–	–	–	–	–	2.66	TC	[553]
Na(100)	–	–	–	–	–	2.66	TC	[3477]
Na(100)	–	–	–	–	–	2.69	TC	[4222]
Na(100)	–	–	–	–	–	2.7	TC	[2851]
Na(100)	–	–	–	–	–	2.7	TC	[763]
Na(100)	–	–	–	–	–	2.71	TC	[1408]
Na(100)	–	–	–	–	–	2.75	TC	[475]
Na(100)	–	–	–	–	–	2.76	TC	[334]
Na(100)	–	–	–	–	–	2.77	TC	[711]
Na(100)	–	–	–	–	–	2.80	TC	[1557]
Na(100)	–	–	–	–	–	2.80	TC	[721]
Na(100)	–	–	–	–	–	2.83	TC	[3477]
Na(100)	–	–	–	–	–	2.83	TC	[1553]
Na(100)	–	–	–	–	–	2.84	TC	[556]
Na(100)	–	–	–	–	–	2.86	TC	[473]
Na(100)	–	–	–	–	–	2.88	TC	[555]
Na(100)	–	–	–	–	–	2.88	TC	[1030]
Na(100)	–	–	–	–	–	2.89	TC	[3814]
Na(100)	–	–	–	–	–	2.9	TC	[1088]
Na(100)[43]	–	–	–	–	–	2.9	TC	[2222]
Na(100)	–	–	–	–	–	2.93	TC	[476]
Na(100)	–	–	–	–	–	2.94	TC	[711]
Na(100)	–	–	–	–	–	2.95	TC	[321]
Na(100)	–	–	–	–	–	3.0	TC	[1088]
Na(100)	–	–	–	–	–	3.03	TC	[554]
Na(100)	–	–	–	–	–	3.04	TC	[476]
Na(100)	–	–	–	–	–	3.07	TC	[1030]
Na(100)	–	–	–	–	–	3.08	TC	[472]
Na(100)	–	–	–	–	–	3.27	TC	[1095]
Recommended	–	–	–	–	–	**2.80 ± 0.04**	–	–
Na(110)	–	–	–	–	–	2.01	TC	[3379]
Na(110)	–	–	–	–	–	2.18	TC	[3379]
Na(110)	–	–	–	–	–	2.25	TC	[3379]
Na(110)	–	–	–	–	–	2.464	TC	[2947]
Na(110)	–	–	–	–	–	2.52	TC	[1159,3067]
Na(110)	–	–	–	–	–	2.59	TC	[2685]
Na(110)	–	–	–	–	–	2.7	TC	[1556]

Table 1 (*continued*)

Surface	Beam	Ion	P_r (Torr)	T (K)	ϕ^+ (eV)	ϕ^e (eV)	Meth.	Refs.
Na(110)	–	–	–	–	–	2.75	TC	[231]
Na(110)	–	–	–	–	–	2.76	TC	[3467]
Na(110)	–	–	–	–	–	2.839	TC	[4069]
Na(110)	–	–	–	–	–	2.839	TC	[4091]
Na(110)	–	–	–	–	–	2.85	TC	[2427]
Na(110)	–	–	–	–	–	2.86	TC	[4222]
Na(110)	–	–	–	–	–	2.87	TC	[3477]
Na(110)	–	–	–	–	–	2.87	TC	[2835]
Na(110)	–	–	–	–	–	2.88	TC	[553]
Na(110)	–	–	–	–	–	2.9	TC	[3137]
Na(110)	–	–	–	–	–	2.9	TC	[2851]
Na(110)	–	–	–	–	–	2.9	TC	[1086]
Na(110)/Ni(100)[35]	Na	–	$\sim 10^{-11}$	173	–	2.90 ± 0.10	CPD	[1417]
Na(110)	–	–	–	–	–	2.91	TC	[711]
Na(110)	–	–	–	–	–	2.93	TC	[1086]
Na(110)	–	–	–	–	–	2.93	TC	[2835]
Na(110)	–	–	–	–	–	2.94	TC	[334]
Na(110)	–	–	–	–	–	2.94	TC	[1921]
Na(110)	–	–	–	–	–	3.0	TC	[1734]
Na(110)	–	–	–	–	–	3.00	TC	[473]
Na(110)	–	–	–	–	–	3.00	TC	[3477]
Na(110)	–	–	–	–	–	3.00	TC	[721]
Na(110)	–	–	–	–	–	3.04	TC	[3814]
Na(110)	–	–	–	–	–	3.06	TC	[476,711]
Na(110)	–	–	–	–	–	3.06	TC	[1086]
Na(110)	–	–	–	–	–	3.08	TC	[1030]
Na(110)	–	–	–	–	–	3.1	TC	[763]
Na(110)	–	–	–	–	–	3.1	TC	[1088]
Na(110)	–	–	–	–	–	3.1	TC	[2395]
Na(110)	–	–	–	–	–	3.10	TC	[475]
Na(110)	–	–	–	–	–	3.11	TC	[555]
Na(110)	–	–	–	–	–	3.11	TC	[2402]
Na(110)	–	–	–	–	–	3.13	TC	[556]
Na(110)	–	–	–	–	–	3.15	TC	[593]
Na(110)	–	–	–	–	–	3.16	TC	[476]
Na(110)	–	–	–	–	–	3.22	TC	[3379]
Na(110)	–	–	–	–	–	3.22	TC	[3712]
Na(110)	–	–	–	–	–	3.22	TC	[472,554]
Na(110)	–	–	–	–	–	3.3	TC	[1088]
Na(110)	–	–	–	–	–	3.3	TC	[1086]
Na(110)	–	–	–	–	–	3.32	TC	[1086]
Na(110)	–	–	–	–	–	3.33	TC	[1030,1089]
Na(110)	–	–	–	–	–	3.36	TC	[1087]
Na(110)	–	–	–	–	–	3.39	TC	[1086]
Na(110)	–	–	–	–	–	3.40	TC	[1089]
Na(110)	–	–	–	–	–	3.43	TC	[3713]
Na(110)	–	–	–	–	–	3.44	TC	[3713]
Na(110)	–	–	–	–	–	3.44	TC	[321]
Na(110)	–	–	–	–	–	3.44	TC	[3693]
Na(110)	–	–	–	–	–	3.46	TC	[3693]
Na(110)	–	–	–	–	–	3.49	TC	[1089]
Na(110)	–	–	–	–	–	3.61	TC	[3692]
Na(110)	–	–	–	–	–	3.62	TC	[1095]
Na(110)	–	–	–	–	–	3.64	TC	[3692]
Na(110)	–	–	–	–	–	5.93	TC	[3622]
Recommended	–	–	–	–	–	**$\underline{3.05 \pm 0.04}$**	–	–
Na(111)	–	–	–	–	–	2.26	TC	[3477]
Na(111)	–	–	–	–	–	2.39	TC	[1159,3067]
Na(111)	–	–	–	–	–	2.48	TC	[3477]
Na(111)	–	–	–	–	–	2.54	TC	[231]
Na(111)	–	–	–	–	–	2.56	TC	[711]
Na(111)	–	–	–	–	–	2.57	TC	[3467]
Na(111)	–	–	–	–	–	2.585	TC	[4091]
Na(111)	–	–	–	–	–	2.59	TC	[553]
Na(111)	–	–	–	–	–	2.6	TC	[2851]
Na(111)	–	–	–	–	–	2.60	TC	[1557]
Na(111)	–	–	–	–	–	2.63	TC	[4222]
Na(111)	–	–	–	–	–	2.65	TC	[475]
Na(111)	–	–	–	–	–	2.7	TC	[1088]

Table 1 (*continued*)

Surface	Beam	Ion	P_r (Torr)	T (K)	ϕ^+ (eV)	ϕ^e (eV)	Meth.	Refs.
Na(111)	–	–	–	–	–	2.70	TC	[593]
Na(111)	–	–	–	–	–	2.71	TC	[473]
Na(111)	–	–	–	–	–	2.72	TC	[3814]
Na(111)	–	–	–	–	–	2.73	TC	[476,711]
Na(111)	–	–	–	–	–	2.75	TC	[1553]
Na(111)	–	–	–	–	–	2.75	TC	[1030]
Na(111)	–	–	–	–	–	2.76	TC	[555]
Na(111)	–	–	–	–	–	2.76	TC	[556]
Na(111)	–	–	–	–	–	2.79	TC	[721]
Na(111)	–	–	–	–	–	2.79	TC	[1030]
Na(111)	–	–	–	–	–	2.8	TC	[1088]
Na(111)	–	–	–	–	–	2.82	TC	[472,554]
Na(111)	–	–	–	–	–	2.83	TC	[321]
Na(111)	–	–	–	–	–	2.85	TC	[476]
Na(111)	–	–	–	–	–	3.17	TC	[1095]
Recommended	–	–	–	–	–	**2.68 ± 0.06**	–	–
Na(112)	–	–	–	–	–	3.14	TC	[321]
Na	–	–	–	–	–	1.55	TC	[2704]
Na	–	–	?	~300	–	1.60	CPD	[2297]
Na/Si(100)	Na	–	1×10^{-10}	~300	–	1.7*	CPD	[3294]
Na/Si(100)	Na	–	2×10^{-10}	~300	–	1.7*	PE	[1727]
Na/Si(100)	Na	–	$\sim 10^{-11}$	~300	–	1.7*	PE	[2277]
Na/Si(100)	Na	–	$< 6 \times 10^{-11}$	~300	–	1.7*	CPD	[2433]
Na	–	–	–	~300	–	1.8	TC	[3737]
Na	–	–	–	–	–	1.82	TC	[2456]
Na/Rh(111)	–	–	–	–	–	1.869	TC	[4008]
Na/Si(100)	Na	–	1×10^{-10}	~300	–	1.9*	CPD	[3294]
Na/Si(100)	–	–	–	–	–	1.9*	TC	[2413]
Na/?	Na	–	?	~300	–	1.9 ± 0.1	PE	[3258]
Na/?	Na	–	?	~300	–	1.95 ± 0.02	PE	[3258]
Na/?	Na	–	?	~300	–	1.97 ± 0.03	PE	[3260]
Na/Rh(111)	–	–	–	–	–	1.987	TC	[4008]
Na/TiO$_2$(110)	Na	–	5×10^{-11}	~300	–	2.0	PE	[2787]
NaTiO$_2$/(110)	–	–	–	–	–	2.0*	TC	[3833]
Na/Cs	–	–	–	–	–	2.0*	TC	[3984]
Na/Si(100)	–	–	–	–	–	2.0*	TC	[2406]
Na/W(100)	Na	–	?	~300	–	2.0	PE	[1697]
Na/?	Na	–	?	~300	–	2.01 ± 0.03	PE	[3260]
Na/W	Na	–	?	~300	–	2.04*	CPD	[1459]
Na	–	–	–	–	–	2.05	TC	[1150]
Na/Si(100)	Na	–	1×10^{-10}	~300 (450)	–	2.06*	CPD	[3294]
Na/Ge(100)	Na	–	$< 1 \times 10^{-10}$	~300	–	2.1*	CPD	[2753]
Na/Si(111)	–	–	–	–	–	2.1	TC	[2731]
Na/Pt	Na	–	?	~300	–	2.1	PE	[2206]
Na	–	–	–	–	–	2.11	TC	[1951]
Na/W	Na	–	?	380	–	2.11 ± 0.05	FE	[3062]
Na/W	Na	–	?	80	–	2.14*	CPD	[3746]
Na	–	–	–	–	–	2.15	TC	[3725]
Na/Ge(001)	–	–	–	–	–	2.168	TC	[3499]
Na/Ag(100)	Na	–	1×10^{-10}	150	–	2.2	PE	[2038]
Na/Si(100)	Na	–	1×10^{-10}	293	–	2.2*	PE	[2184]
Na/W	Na	–	?	~300	–	2.2	FE	[3062]
Na/Ru(0001)	Na	–	6×10^{-11}	50	–	2.2*	CPD	[2188]
Na/TiO$_2$(110)	Na	–	8×10^{-11}	~300	–	2.2	PE	[3188]
Na/Ge(111)	Na	–	$\sim 10^{-10}$	~300	–	2.2	CPD	[2948]
Na/W	Na	–	$\sim 10^{-6}$	~300	–	2.25	PE	[3934]
Na/?	Na	–	?	~300	–	2.26	CPD	[2808]
Na/Si(100)	Na	–	1×10^{-10}	~300 (450)	–	2.26	CPD	[3294]
Na/W(111)	Na	–	(<10^{-10})	77	–	2.26	FE	[2323]
Na/metal	Na	–	$\leq 10^{-7}$	~300	–	2.27	PE	[1765]
Na/glass	Na	–	$\leq 3 \times 10^{-11}$	195	–	2.27 ± 0.01	PE	[2615]
Na/glass	Na	–	$\sim 2 \times 10^{-8}$	~300	–	2.28	PE	[2564]
Na/Ni	Na	–	$< 10^{-9}$	77	–	2.28	CPD	[2139,3128,3698]
Na/Ge(111)	Na$^+$	–	1×10^{-10}	~300	–	2.28	CPD	[3423]
Na	–	–	–	–	–	2.28	TC	[3637]
Na/quartz	Na	–	$\sim 10^{-10}$	~300	–	2.28 ± 0.08	PE	[1999]
Na/Si(111)	Na$^+$	–	1×10^{-10}	~300	–	2.29	CPD	[3423]
Na/glass	Na	–	?	~300	–	2.29	PE	[2561]

Table 1 (*continued*)

Surface	Beam	Ion	P_r (Torr)	T (K)	ϕ^+ (eV)	ϕ^e (eV)	Meth.	Refs.
Na/Ru(0001)	Na	–	3×10^{-10}	~300	–	2.29	CPD	[1824]
Na/Ge(111)	Na	–	?	~300	–	2.3	CPD	[2812,2813]
Na/Ge(111)	Na	–	2×10^{-10}	~300	–	2.3*	PE	[3648]
Na/W(112)	Na	–	$(<10^{-10})$	77	–	2.3	FE	[2323]
Na/quartz	Na	–	$\sim10^{-10}$	90	–	2.3	PE	[2605]
Na/Si(111)	–	–	–	–	–	2.3*	TC	[3962]
Na/Si(100)	Na	–	?	295	–	2.3	PE	[2174]
Na/Rh(100)	Na	–	?	~300	–	2.3	PE	[2158]
Na/Si(111)	Na	–	$<1 \times 10^{-11}$	~300	–	2.3*	CPD	[3484]
Na/Y	Na	–	2×10^{-10}	~300	–	2.3 ± 0.1	PE	[1813]
Na/Sc	Na	–	2×10^{-10}	~300	–	2.3 ± 0.1	PE	[1813]
Na/?	Na	–	?	~300	–	2.3 ± 0.1	PE	[3258]
Na/Cu, Ag	Na	–	5×10^{-9}	~300	–	2.3 ± 0.1	PE	[3081]
$Na_n(n \to \infty)$	–	–	?	~300	–	2.30	IP	[4200]
Na	–	–	–	–	–	2.30	TC	[3728]
Na	–	–	–	–	–	2.30	TC	[1744]
Na/glass	Na	–	$\leq10^{-7}$	~300	–	2.30	PE	[1765]
Na/W(100)	Na	–	$(<10^{-10})$	77	–	2.32	FE	[2323]
Na/?	Na	–	?	77	–	2.33 ± 0.05	PE	[2945]
Na/glass	Na	–	$\leq3 \times 10^{-11}$	195	–	2.34 ± 0.01	PE	[2615]
Na	–	–	–	–	–	2.35	TC	[1458]
Na/Ge(001)	–	–	–	–	–	2.353	TC	[3499,3500]
Na	–	–	–	–	–	2.36	TC	[3352]
Na/Re(1122)	Na	–	$<2 \times 10^{-9}$	~300	–	2.36	FE	[811]
Na/Mo	Na	–	$\sim10^{-10}$	293	–	2.36 ± 0.02	PE[36]	[3336,3337]
Na/quartz	Na	–	?	~300	–	2.36 ± 0.02	PE	[1988]
Na/glass	Na	–	$\leq3 \times 10^{-11}$	77	–	2.37 ± 0.01	PE	[2615]
Na	–	–	$\sim10^{-9}$	298	–	2.38 ± 0.02	PE	[2612,2613,4208]
Na	–	–	$\sim10^{-9}$	370	–	2.39 ± 0.02	PE	[4241,4314]
Na/Ni(110)	Na	–	?	>360	–	2.4*	PE	[2665]
Na/Si(111)	Na	–	$<4 \times 10^{-11}$	~300	–	2.4*	CPD	[2894]
Na/W(110)	Na	–	$\sim10^{-10}$	~300	–	2.4	PE	[2775,3768,3769]
Na/Si(111)	Na	–	4×10^{-11}	~300	–	2.4*	CPD	[3471]
Na	–	–	–	–	–	2.4*	TC	[1955]
Na/Mg(0001)	–	–	–	–	–	2.4*	TC	[2438]
Na/Cu(110)	Na	–	5×10^{-11}	140	–	2.4 ± 0.1	PE	[3454]
Na/Al/glass	Na	–	$<10^{-8}$	~300	–	2.40	PE	[1457]
Na/Mo	Na	–	4×10^{-10}	80	–	2.40 ± 0.03	PE[37]	[3336]
Na	–	–	$\sim10^{-9}$	183	–	2.41	PE	[2612,2613]
Na/Mo	Na	–	$\sim10^{-10}$	80 (293)	–	2.41	PE	[3337]
Na/graphene	–	–	–	–	–	2.42	TC	[4079]
Na/Re	Na	–	$<2 \times 10^{-9}$	~300	–	2.45	FE	[811]
Na/W(110)	Na	–	$(<10^{-12})$	~300	–	2.45	CPD	[1084]
Na/Cu(100)	Na	–	$\leq1 \times 10^{-10}$	180	–	2.45	PE	[2678]
Na/Si(111)	Na	–	$<6 \times 10^{-11}$	~300	–	2.45*	CPD	[2433]
Na/Mo	Na	–	4×10^{-10}	80 (293)	–	2.45 ± 0.04	PE[36]	[3336]
Na/Mo	Na	–	4×10^{-10}	80	–	2.45 ± 0.05	PE[37]	[3336]
Na/Si(111)	Na	–	$<5 \times 10^{-10}$	~300	–	2.46	PE	[2795]
Na/quartz	Na	–	?	~300	–	2.46	PE	[4300]
Na/Ta(110)	Na+	–	$\sim10^{-10}$	~300	–	2.46	CPD	[506]
Na/Ge(100)	Na	–	$<1 \times 10^{-10}$	77–120	–	2.46*	FE	[1550,3170]
Na/Ge(100)	–	–	–	–	–	2.46*	TC	[4042]
Na/?	Na	–	?	?	–	2.46	?	[3785]
Na/Al(100)	–	–	–	–	–	2.46 ± 0.10	TC	[1036]
Na/Ge(001)	–	–	–	–	–	2.475	TC	[3499]
Na/Al(111)	–	–	–	–	–	2.48	TC	[1594]
Na/Ge(111)	Na	–	$<1 \times 10^{-10}$	77–120	–	2.48*	FE	[1550,3170]
Na(fp, $r \to \infty$)[460]	–	–	?	~300	–	2.48*	IP	[4198]
Na(fp, $r \to \infty$)[460]	–	–	?	~300	–	2.49*	IP	[4198]
Na/TiO₂(441)	Na	–	5×10^{-11}	~300	–	2.5	PE	[2787]
Na/Ge(111)	Na	–	$<2 \times 10^{-10}$	100	–	2.5*	PE	[2421]
Na/Si(111)	Na	–	$<1 \times 10^{-10}$	130	–	2.5	PE	[1839]
Na/Si(100)	Na	–	1×10^{-10}	100	–	2.5*	PE	[2184]
Na/Si(100)	–	–	–	–	–	2.5*	TC	[2406]
Na/W(112)	Na	–	$<5 \times 10^{-11}$	~300	–	2.5	CPD	[1666]
Na	–	–	–	–	–	2.5	TC	[2845]
Na/W(112)	Na	–	$(\leq10^{-11})$	77	–	2.5	CPD	[2611]
Na/W(100)	–	–	–	–	–	2.5	TC	[1443]
Na/Li/Cu(100)	Na	–	$\leq1 \times 10^{-10}$	180	–	2.5	PE	[2678]
Na/Al(100)	–	–	–	–	–	2.51 ± 0.10	TC	[1576]

Table 1 (*continued*)

Surface	Beam	Ion	P_r (Torr)	T (K)	ϕ^+ (eV)	ϕ^e (eV)	Meth.	Refs.
Na(fp, $r \to \infty$)	–	–	?	~300	–	2.52 ± 0.04	IP	[2383,4148]
Na/Si(mono)	Na	–	5×10^{-10}	~300	–	2.53*	AI[38]	[1103]
Na/Re(1112)	Na	–	$<2 \times 10^{-9}$	~300	–	2.54	FE	[811]
Na/Ru(0001)	Na	–	?	~300	–	2.54	PE	[4020]
Na	–	–	–	–	–	2.55	TC	[1066]
Na/Al(111)	Na	–	?	~100 (150)	–	2.55	CPD	[2654]
Na/W(111)	Na	–	$<2 \times 10^{-9}$	~300	–	2.55	FE	[811]
Na(nanowire)[453]	–	–	–	–	–	2.55 ± 0.05*	TC	[4178]
Na$_n$($n \to \infty$)[40]	–	–	–	–	–	2.56	TC	[2171]
Na/W(110)	Na	–	$(<10^{-10})$	77	–	2.57	FE	[2323]
Na/Cu(111)	Na	–	5×10^{-11}	~300	–	2.57	PE	[969]
Na/W(110)	Na	–	$(<10^{-12})$	77	–	2.58	CPD	[1084]
Na/W(110)	Na	–	$(<10^{-12})$	77{300}	–	2.58	CPD	[1084]
Na	–	–	–	–	–	2.58	TC	[478]
Na/Cu(110)	Na	–	$<5 \times 10^{-10}$	~300	–	2.58	PE	[3182]
Na/Co(0001)	Na	–	5×10^{-11}	~300	–	2.58 ± 0.03	PE	[1926]
Na	–	–	–	–	–	2.59	TC	[3312]
Na/Mo	Na	–	5×10^{-10}	~300	–	2.59	AI	[4027]
Na	–	–	–	–	–	2.59	TC	[4031]
Na/Si(111)	Na	–	?	~300	–	2.6*	CPD	[1585]
Na/Ru(001)	Na$^+$	–	?	~300	–	2.6*	CPD	[2391]
Na/Ni(110)	Na	–	?	~100	–	2.6*	PE	[2665]
Na/Al(111)	Na	–	$~10^{-10}$	~300	–	2.6	CPD	[2833]
Na/Al(111)	–	–	–	–	–	2.6	TC	[2223]
Na/Ni(111)	Na	–	$<5 \times 10^{-10}$	~300	–	2.6	PE	[2183]
Na/Cu(110)	Na	–	$<5 \times 10^{-10}$	~300	–	2.6	PE	[2183]
Na/Cu(111)	Na	–	$<5 \times 10^{-10}$	~300	–	2.6	PE	[2183]
Na/W(112)	Na	–	$(\leq 10^{-11})$	300, 400	–	2.6	CPD	[2611]
Na/W	Na	–	$<2 \times 10^{-9}$	~300	–	2.6	FE	[811]
Na/Ni(100)	Na	–	8×10^{-11}	~300	–	2.6*	CPD	[3807]
Na/W(112)	Na	–	$<2 \times 10^{-9}$	~300	–	2.6	FE	[811]
Na/Cu(110)	Na	–	$<3 \times 10^{-10}$	~300 (370)	–	2.6*	PE	[2529]
Na	–	–	–	–	–	2.60	TC	[3312]
Na	–	–	–	–	–	2.61	TC	[298]
Na/Al	Na	–	5×10^{-10}	~300	–	2.61*	AI[38]	[1103]
Na	–	–	–	–	–	2.62	TC	[3467]
Na	–	–	–	–	–	2.62	TC	[4150]
Na/Cs/Pt[38]	Na	–	4×10^{-10}	20	–	2.62	AI[38]	[3496]
Na	–	–	–	–	–	2.63	TC	[2382]
Na	–	–	–	–	–	2.63	TC	[4031]
Na/Ni(111)	Na	–	$~10^{-11}$	~300	–	2.64*	PE	[3185]
Na/Cu(111)	Na	–	$~10^{-11}$	~300	–	2.64*	PE	[3185]
Na/Pt	Na	–	5×10^{-10}	~300	–	2.65	AI	[4027]
Na$_n$(fp)	–	–	?	423	–	2.65	PE	[4256]
Na/Cu(111)	Na	–	$~10^{-11}$	~300	–	2.66*	PE	[3183]
Na/Mg	Na	–	5×10^{-10}	~300	–	2.67*	AI[38]	[1103]
Na/graphite	–	–	–	–	–	2.67*	TC	[1843]
Na/W(110)	Na	–	$<2 \times 10^{-9}$	~300	–	2.68	FE	[811]
Na$_n$($n \to \infty$)[40]	–	–	?	110 ± 20	–	2.68	PE	[2171]
Na/Fe(110)	Na	–	5×10^{-11}	~300	–	2.69 ± 0.03	PE	[1926]
Na	–	–	–	–	–	2.7	TC	[2439]
Na/W	Na	–	~430 (Na)	~1900	–	2.7	TE	[1443]
Na/C(HOPG)	Na	–	?	40	–	2.7*	PE	[1618]
Na/Cu(111)[227]	Na	–	1×10^{-10}	~300	–	2.7*	CPD	[2495,2496]
Na/Ni(100)	Na	–	1×10^{-11}	~300	–	2.7*	CPD	[1413]
Na/Ni(100)	Na	–	$~10^{-10}$	~300	–	2.7*	CPD	[1992]
Na/Ni(110)	Na	–	$~10^{-10}$	~300	–	2.7*	CPD	[1992]
Na/Ni(100)	–	–	–	–	–	2.7	TC	[509]
Na/Al(100)	Na	–	$~10^{-10}$	~300	–	2.7*	CPD	[2833]
Na/Si(100)	Na	–	?	100	–	2.7	PE	[2174]
Na/Cu(100)	Na	–	?	~300	–	2.7	PE	[3451]
Na/Ru(001)	Na	–	?	~300	–	2.7*	CPD	[2984]
Na/Ni(111)	Na	–	$<3 \times 10^{-10}$	~300	–	2.7*	PE	[2177]
Na/Cu(111)	Na	–	$<3 \times 10^{-10}$	~300	–	2.7*	PE	[2177]
Na/Si(100)	Na	–	?	70	–	2.7	PE	[2178]
Na/Cu(110)	Na	–	?	?	–	2.7*	?	[3702]
Na/W(110)	Na	–	$<2 \times 10^{-11}$	~300	–	2.7	CPD	[2658]
Na/Al[38]	Na	–	?	~300	–	2.70*	AI	[3789]
Na$_n$($n \to \infty$)	–	–	?	~300	–	2.71	IP, TC	[4197]
Na/Cu(111)	–	–	–	–	–	2.73	TC	[1246]

Table 1 (*continued*)

Surface	Beam	Ion	P_r (Torr)	T (K)	ϕ^+ (eV)	ϕ^e (eV)	Meth.	Refs.
Na$_n$(n → ∞)	–	–	–	–	–	2.75	TC	[4193]
Na(r → ∞)[41]	–	–	–	–	–	2.75	TC	[2860]
Na/quartz	Na	–	~10^{-11}	77	–	2.75	PE	[3424]
Na	–	–	–	–	–	2.75	TC	[477]
Na/C(0001)	Na	–	2×10^{-10}	95	–	2.75	CPD	[525]
Na/Re(1120)	Na	–	<2×10^{-9}	~300	–	2.75	FE	[811]
Na(fp)[42]	–	–	?	?	–	2.75 ± 0.05	PE	[3482]
Na/Y	Na	–	?	~300	–	2.75 ± 0.1	PE	[1691]
Na/W(100)	Na	–	<2×10^{-9}	~300	–	2.76	FE	[811]
Na/Mo(112)	Na	–	(≤10^{-11})	77	–	2.76	CPD	[2030]
Na/graphite	–	–	–	–	–	2.77*	TC	[1843]
Na	–	–	–	–	–	2.77	TC	[3208]
Na/Cu(111)	Na	–	~5×10^{-11}	~300	–	2.77 ± 0.03	PE	[1922,1926]
Na	–	–	–	–	–	2.78	TC	[3477]
Na(cluster)	–	–	–	–	–	2.78	TC	[3479]
Na	–	–	–	–	–	2.78	TC	[1901]
Na/Cr[38]	Na	–	5×10^{-10}	~300	–	2.79	AI[38]	[1103,4027]
Na/Al(100)	Na	–	1×10^{-10}	100	–	2.8	CPD	[2875]
Na/Al(111)[43]	–	–	–	–	–	2.8	TC	[2222]
Na/Si(100)	–	–	–	–	–	2.8*	TC	[2406]
Na/Al(111)	Na	–	~10^{-11}	100 (240)	–	2.8*	CPD	[3296]
Na	–	–	–	–	–	2.8	TC	[706]
Na/Ti	Na	–	?	~300	–	2.8 ± 0.1	PE	[1691]
Na/Al[38]	Na	–	?	~300	–	2.80*	AI	[3789]
Na$_n$(n → ∞)[44]	–	–	~10^{-6}	~300	–	2.81	IP	[2053]
Na	–	–	–	–	–	2.81	TC	[231]
Na/Cu	Na	–	5×10^{-10}	~300	–	2.81	AI	[4027]
Na	–	–	–	–	–	2.83	TC	[231]
Na	–	–	–	–	–	2.84	TC	[2493]
Na	–	–	–	–	–	2.84	TC	[3467]
Na/Al(111)	Na	–	?	140, ~300	–	2.85	CPD	[734]
Na	–	–	–	–	–	2.85	TC	[738]
Na/Au(100)	Na	–	~10^{-11}	130, ~300	–	2.87	CPD	[2746]
Na	–	–	–	–	–	2.88	TC	[477]
Na/Pt(100)	–	–	–	–	–	2.88	TC	[3168]
Na/Au(100)	–	–	–	–	–	2.88	TC	[3168]
Na$_n$(n → ∞)	–	–	–	–	–	2.89	TC	[4254]
Na/Ni(111)	–	–	–	–	–	2.9*	TC	[2177]
Na/NbC(111)	Na	–	~1×10^{-10}	~300	–	2.9	PE	[2799]
Na/Al(100)	–	–	–	–	–	2.9	TC	[3149]
Na/Al(111)	Na	–	~5×10^{-10}	~300	–	2.9*	CPD	[2748]
Na/Ni(111)	Na	–	~10^{-10}	~300	–	2.9*	CPD	[1992]
Na/Al(001)	–	–	–	–	–	2.9	TC	[1711]
Na/metal	–	–	–	–	–	2.9	TC	[2195]
Na/Cu(111)	Na	–	<1×10^{-10}	~300	–	2.9*	CPD	[3295]
Na	–	–	–	–	–	2.90	TC	[477]
Na$_n$(n → ∞)	–	–	?	~300	–	2.90	TC	[4197]
Na	–	–	–	–	–	2.91	TC	[2061]
Na	–	–	–	–	–	2.91	TC	[1924,4035,4036]
Na	–	–	–	–	–	2.91	TC	[477]
Na	–	–	–	–	–	2.92	TC	[477]
Na	–	–	–	–	–	2.92	TC	[2427]
Na	–	–	–	–	–	2.92	TC	[1924,3208,4035]
Na	–	–	–	–	–	2.93	TC	[1613]
Na	–	–	–	–	–	2.93	TC	[4101]
Na/Re(1011)	Na	–	<2×10^{-9}	~300	–	2.93	FE	[811]
Na	–	–	–	–	–	2.93	TC	[521]
Na	–	–	–	–	–	2.93	TC	[3628]
Na	–	–	–	–	–	2.93	TC	[4431]
Na	–	–	–	–	–	2.94	TC	[3477]
Na	–	–	–	–	–	2.94	TC	[553,2427]
Na	–	–	–	186	–	2.949	TC	[2419]
Na	–	–	–	–	–	2.97	TC	[2493]
Na	–	–	–	–	–	2.98	TC	[2629]

Table 1 (*continued*)

Surface	Beam	Ion	P_r (Torr)	T (K)	ϕ^+ (eV)	ϕ^e (eV)	Meth.	Refs.
Na	–	–	–	0	–	2.983	TC	[2419]
Na/Al(111)	–	–	–	–	–	3.02	TC	[1594]
Na	–	–	–	–	–	3.06	TC[3]	[475,519,2474]
Na	–	–	–	–	–	3.06	TC	[3168]
Na/C(100)	–	–	–	–	–	3.1*	TC	[2759]
Na/Si(111)	Na	–	<4 × 10⁻¹¹	~300	–	3.1*	CPD	[3947]
Na	–	–	–	–	–	3.1	TC	[944]
Na/Al(111)	–	–	–	–	–	3.11	TC	[3158]
Na	–	–	–	–	–	3.16	TC	[1578]
Na	–	–	–	–	–	3.17	TC	[230]
Na/C(HOPG)	Na	–	?	90	–	3.2	PE	[1618]
Na/ZrC(100)	Na	–	?	~300	–	3.4	PE	[2798]
Na/quartz	Na	–	?	~300	–	3.45 ± 0.04	PE	[1988]
Na/Ta(110)	–	–	–	–	–	3.51	TC	[2538]
Recommended	–	–	–	–	–	**2.54 ± 0.03**	–	–

Liquid (*T* > 371 K)

Surface	Beam	Ion	P_r (Torr)	T (K)	ϕ^+ (eV)	ϕ^e (eV)	Meth.	Refs.
Na	–	–	~10⁻⁸	371	–	2.38	PE	[4208]
Na	–	–	~10⁻⁹	372	–	2.39	PE	[4241]
Na	–	–	–	371	–	2.924	TC	[2419]

12. Magnesium Mg

hcp

Surface	Beam	Ion	P_r (Torr)	T (K)	ϕ^+ (eV)	ϕ^e (eV)	Meth.	Refs.
Mg(0001)	–	–	–	–	–	3.0	TC	[3137]
Mg(0001)	–	–	–	–	–	3.2	TC	[1215]
Mg(0001)	–	–	–	–	–	3.3	TC	[1215]
Mg(0001)	–	–	–	–	–	3.4	TC	[1215]
Mg(0001)	–	–	–	–	–	3.44	TC	[231]
Mg(0001)	–	–	–	–	–	3.58	TC	[3467]
Mg(0001)[45]	–	–	5 × 10⁻¹¹	100–150	–	3.65	CPD	[3174]
Mg(0001)	–	–	–	–	–	3.65	TC	[1179]
Mg(0001)	–	–	–	–	–	3.66	TC	[3004]
Mg(0001)	–	–	–	–	–	3.69	TC	[2427]
Mg(0001)	–	–	–	–	–	3.69	TC	[1699]
Mg(0001)	–	–	–	–	–	3.69	TC	[1028]
Mg(0001)	–	–	–	–	–	3.7	TC	[1704,1711]
Mg(0001)	–	–	–	–	–	3.705	TC	[4460][490]
Mg(0001)	–	–	–	–	–	3.71	TC	[4417]
Mg(0001)	–	–	–	–	–	3.71	TC	[553]
Mg(0001)	–	–	–	–	–	3.718 ± 0.009	TC	[2556]
Mg(0001)	–	–	–	–	–	3.72	TC	[3234]
Mg(0001)	–	–	–	–	–	3.72	TC	[343]
Mg(0001)	–	–	–	–	–	3.72	TC	[4326]
Mg(0001)	–	–	–	–	–	3.74	TC	[4215]
Mg(0001)[46]	–	–	–	–	–	3.75 ± 0.05*	TC	[2552]
Mg(0001)	–	–	–	–	–	3.76	TC	[3481]
Mg(0001)	–	–	–	–	–	3.76	TC	[4004]
Mg(0001)	–	–	–	–	–	3.80	TC	[1179]
Mg(0001)	–	–	–	–	–	3.83	TC	[1028,1179]
Mg(0001)	–	–	1 × 10⁻¹⁰	~300	–	3.84 ± 0.02	PE	[2135]
Mg(0001)	–	–	–	–	–	3.86	TC	[334]
Mg(0001)	–	–	–	–	–	3.87	TC	[4005]
Mg(0001)	–	–	–	–	–	3.88	TC	[3481]
Mg(0001)	–	–	–	–	–	3.88	TC	[1030,1089]
Mg(0001)	–	–	–	–	–	3.89	TC	[4004]
Mg(0001)	–	–	–	–	–	3.9	TC	[2851]
Mg(0001)	–	–	–	–	–	4.0	TC	[2851]
Mg(0001)	–	–	–	–	–	4.0	TC	[2400]
Mg(0001)	–	–	–	–	–	4.00	TC	[1089]
Mg(0001)	–	–	–	–	–	4.01	TC	[1030]
Mg(0001)	–	–	–	–	–	4.05	TC	[475]
Mg(0001)	–	–	–	–	–	4.06	TC	[3004]
Mg(0001)	–	–	–	–	–	4.10	TC	[593]
Mg(0001)	–	–	–	–	–	4.18	TC	[556]
Mg(0001)	–	–	–	–	–	4.2	TC	[1088]
Mg(0001)	–	–	–	–	–	4.20	TC	[1089]
Mg(0001)	–	–	–	–	–	4.38	TC	[1087]
Recommended	–	–	–	–	–	**3.79 ± 0.07**	–	–

Table 1 (*continued*)

Surface	Beam	Ion	P_r (Torr)	T (K)	ϕ^+ (eV)	ϕ^e (eV)	Meth.	Refs.
Mg(1010)	–	–	–	–	–	3.39	TC	[4461][490]
Mg(1010)	–	–	–	–	–	3.64	TC	[4004]
Mg(1010)	–	–	–	–	–	3.652	TC	[4460][490]
Mg(1010)	–	–	–	–	–	3.76	TC	[4004]
Mg(1010)	–	–	–	–	–	3.79	TC	[4005]
Mg(0111)	–	–	–	–	–	3.70	TC	[4004]
Mg(0111)	–	–	–	–	–	3.88	TC	[4004]
Mg(0112)	–	–	–	–	–	3.63	TC	[4004]
Mg(0112)	–	–	–	–	–	3.74	TC	[4004]
Mg(0113)	–	–	–	–	–	3.58	TC	[4004]
Mg(0113)	–	–	–	–	–	3.66	TC	[4004]
Mg(1121)	–	–	–	–	–	3.56	TC	[4004]
Mg(1121)	–	–	–	–	–	3.68	TC	[4004]
Mg(1122)	–	–	–	–	–	3.67	TC	[4004]
Mg(1122)	–	–	–	–	–	3.80	TC	[4004]
Mg(1123)	–	–	–	–	–	3.53	TC	[4004]
Mg(1123)	–	–	–	–	–	3.68	TC	[4004]
Mg(2130)	–	–	–	–	–	3.49	TC	[4004]
Mg(2130)	–	–	–	–	–	3.72	TC	[4004]
Mg(3140)	–	–	–	–	–	3.48	TC	[4004]
Mg(3140)	–	–	–	–	–	3.68	TC	[4004]
Mg/glass	–	–	?	~300	–	>2.4	PE	[4010]
Mg	–	–	–	–	–	2.7	TC	[2456]
Mg	–	–	?	~300	–	<3.0	PE	[2295]
Mg	–	–	–	–	–	3.1	TC	[1955]
Mg/ins/Al[47]	Mg	–	?	~300	–	3.10 ± 0.09	CPD	[2028]
Mg	–	–	–	–	–	3.15	TC	[1744]
Mg/SiO₂/Si	Mg	–	?	~300 (570)	–	3.19	PE	[2355]
Mg	–	–	~7 × 10⁻⁹	~300	–	3.25	PE	[2001]
Mg	–	–	–	–	–	3.33	TC	[521]
Mg	–	–	–	–	–	3.34	TC	[231]
Mg	–	–	–	0	–	3.34	TC	[4419]
Mg/SiO₂/Si(100)	Mg	–	?	~300	–	3.45[48]	PE	[1442]
Mg	–	–	–	–	–	3.46	TC	[1924]
Mg	–	–	–	–	–	3.48	TC	[3467]
Mg	–	–	–	–	–	3.5	TC	[944]
Mg	–	–	1 × 10⁻⁵	~300	–	3.53	CPD	[1883]
Mg	–	–	–	–	–	3.54	TC	[231]
Mg	–	–	–	–	–	3.54	TC	[2427]
Mg	–	–	?	~300	–	3.55	CPD	[1883]
Mg[240]	–	–	?	~300	–	3.58*	CPD	[1367]
Mg	–	–	?	~300	–	3.58	CPD	[2297]
Mg	–	–	–	–	–	3.58	TC	[3467]
Mg/Al₂O₃/Si(100)	Mg	–	?	~300	–	3.6[48]	PE	[1442]
Mg/Mo(112)	Mg	–	?	?	–	3.6	CPD	[2404,2407]
Mg	–	–	?	~300	–	3.60*	CPD	[3621]
Mg/Mo	Mg	–	?	~300	–	3.60 ± 0.02	PE	[1635]
Mg/Ta	Mg	–	?	~300	–	3.60 ± 0.02	PE	[1635]
Mg/glass	Mg	–	?	~300	–	3.60 ± 0.02	PE	[1635]
Mg/glass[49]	Mg	–	?	~300	–	3.61 ± 0.03	CPD	[1368]
Mg/?	Mg	–	?	~300	–	3.63	PE	[1639]
Mg	–	–	–	–	–	3.65	TC	[2704]
Mg/glass[50]	Mg	–	?	~300	–	3.65 ± 0.05	CPD	[1368]
Mg	–	–	–	–	–	3.66	TC[3]	[475,2474]
Mg/quartz[51]	Mg	–	1 × 10⁻⁶	~300	–	3.66	PE	[1968,1973]
Mg	–	–	–	–	–	3.66	TC	[2629]
Mg	–	–	–	–	–	3.66	TC	[4418]
Mg/TiO₂(100)	Mg	–	?	~300	–	3.66	PE	[1612]
Mg/glass	Mg	–	?	~300	–	3.67 ± 0.02	PE	[1640]
Mg/glass	Mg	–	?	~300	–	3.68	PE	[2561]
Mg	–	–	<3 × 10⁻¹¹	~300	–	3.68 ± 0.15	AI	[4055]

Table 1 (*continued*)

Surface	Beam	Ion	P_r (Torr)	T (K)	ϕ^+ (eV)	ϕ^e (eV)	Meth.	Refs.
Mg/glass[88]	Mg	–	$<10^{-9}$	~300{77}	–	3.7	CPD	[1526]
Mg/Mo(112)	Mg	–	?	~300	–	3.7	CPD	[2409]
Mg	–	–	–	–	–	3.7	TC	[1993]
Mg	–	–	–	–	–	3.70	TC	[1066]
Mg	–	–	–	–	–	3.70	TC	[738]
Mg	–	–	5×10^{-10}	~300	–	3.72	PE	[594]
Mg/Cr	Mg	–	5×10^{-10}	~300	–	3.72	AI[38]	[1103]
Mg	–	–	–	–	–	3.75	TC	[3729]
Mg	–	–	–	–	–	3.75	TC	[1613]
Mg/W[244]	Mg	–	$\leq 2 \times 10^{-9}$	~300, ~900	–	3.76	CPD	[3530]
Mg	–	–	–	–	–	3.77	TC	[298]
Mg	–	–	–	–	–	3.77	TC	[1924]
Mg/glass[49,50]	Mg	–	?	~300	–	3.78	CPD	[1368]
Mg/W	Mg	–	$\leq 2 \times 10^{-9}$	~300	–	3.78	CPD	[3530]
Mg/Ni	Mg	–	?	~300	–	3.79	PE	[1640]
Mg	–	–	–	–	–	3.8	TC	[706]
Mg/W(112)	Mg	–	$(\leq 10^{-11})$	77	–	3.8	CPD	[2635]
Mg[38]	–	–	?	~300	–	3.80*	AI	[3789]
Mg	–	–	–	–	–	3.82	TC	[553,2427]
Mg	–	–	–	–	–	3.82	TC	[3477]
Mg	–	–	–	–	–	3.84	TC	[3477]
Mg/Au(100)	–	–	–	–	–	3.87	TC	[4326]
Mg	–	–	–	–	–	3.99	TC	[1578]
Mg/Si	–	–	–	–	–	4.08	TC	[1653]
Mg/Si	–	–	–	–	–	4.11	TC	[1653]
Mg/Re(1010)	Mg	–	$(<10^{-11})$	77 (~300)	–	4.11	CPD	[4275]
Mg/GaP	–	–	–	–	–	4.14	TC	[1653]
Mg/ZrO$_2$/Si(100)	Mg	–	?	~300	–	4.15[48]	PE	[1442]
Mg	–	–	–	–	–	4.18	TC	[1976]
Mg/GaP	–	–	–	–	–	4.25	TC	[1653]
Mg(foil)	–	–	$<1 \times 10^{-10}$	~300	–	4.3 ± 0.2	PE	[3584]
Recommended	–	–	–	–	–	**3.65 ± 0.05**	–	–

13. Aluminium Al

fcc

Surface	Beam	Ion	P_r (Torr)	T (K)	ϕ^+ (eV)	ϕ^e (eV)	Meth.	Refs.
Al(100)	–	–	–	–	–	3.22	TC	[2697]
Al(100)	–	–	–	–	–	3.36	TC	[3638]
Al(100)	–	–	?	~300	–	3.38 ± 0.07	PE	[239]
Al(100)	–	–	–	–	–	3.62	TC	[231]
Al(100)	–	–	–	–	–	3.63	TC	[3467]
Al(100)	–	–	–	–	–	3.71	TC	[473]
Al(100)	–	–	–	–	–	3.77	TC	[553]
Al(100)	–	–	–	–	–	3.780	TC	[560,2432]
Al(100)	–	–	–	–	–	3.782	TC	[1626]
Al(100)	–	–	–	–	–	3.8	TC	[2982]
Al(100)	–	–	–	–	–	3.805	TC	[1626]
Al(100)	–	–	–	–	–	3.806	TC	[2914]
Al(100)	–	–	–	–	–	3.83	TC	[476]
Al(100)	–	–	–	–	–	3.831	TC	[1626]
Al(100)	–	–	–	–	–	3.87	TC	[3004]
Al(100)	–	–	?	–	–	3.9	TC	[1088]
Al(100)	–	–	–	–	–	3.92	TC	[1159,3067]
Al(100)/Ge(100)[52]	–	–	–	–	–	3.94	TC	[3949]
Al(100)	–	–	–	–	–	4.00	TC	[321]
Al(100)	–	–	–	–	–	4.06	TC	[476]
Al(100)	–	–	–	–	–	4.1	TC	[2851]
Al(100)	–	–	–	–	–	4.1 ± 0.3	TC	[1568]
Al(100)	–	–	–	–	–	4.16	TC	[1030]
Al(100)	–	–	–	–	–	4.175 ± 0.052	TC	[2352]
Al(100)	–	–	–	–	–	4.20	TC	[475]
Al(100)/Al(100)[53]	Al	–	$\sim 10^{-10}$	~300 (~520)	–	4.20 ± 0.03	PE	[612]
Al(100)/KCl(100)	Al	–	$\sim 10^{-10}$	~300 (~520)	–	4.20 ± 0.03*	PE	[612]
Al(100)	–	–	–	–	–	4.21	TC	[2548]
Al(100)	–	–	–	–	–	4.22	TC	[1921]
Al(100)	–	–	–	–	–	4.227	TC	[2523]
Al(100)	–	–	–	–	–	4.24	TC	[1175]
Al(100)	–	–	–	–	–	4.25	TC	[593]
Al(100)	–	–	–	–	–	4.25	TC	[556]
Al(100)	–	–	–	–	–	4.255	TC	[4460][490]

Table 1 (*continued*)

Surface	Beam	Ion	P_r (Torr)	T (K)	ϕ^+ (eV)	ϕ^e (eV)	Meth.	Refs.
Al(100)	–	–	–	–	–	4.259	TC	[1175]
Al(100)	–	–	–	–	–	4.27	TC	[555,715]
Al(100)	–	–	–	–	–	4.27	TC	[3004]
Al(100)	–	–	–	–	–	4.27	TC	[4233]
Al(100)	–	–	–	–	–	4.27	TC	[4401]
Al(100)	–	–	–	–	–	4.27 ± 0.01	TC	[3241]
Al(100)	–	–	–	–	–	4.28	TC	[3241]
Al(100)	–	–	–	–	–	4.29	TC	[4233]
Al(100)	–	–	–	–	–	4.29	TC	[4357]
Al(100)	–	–	1×10^{-10}	~300	–	4.29	PE	[1572]
Al(100)	–	–	–	–	–	4.30	TC	[1030]
Al(100)	–	–	–	–	–	4.30	TC	[4087,4410]
Al(100)	–	–	–	–	–	4.30	TC	[1435]
Al(100)	–	–	–	–	–	4.32	TC	[4434]
Al(100)	–	–	–	–	–	4.35	TC	[1936]
Al(100)	–	–	–	–	–	4.36	TC	[1943]
Al(100)	–	–	–	–	–	4.38	TC	[1943]
Al(100)	–	–	–	–	–	4.38	TC	[561,721,1936, 4398]
Al(100)	–	–	–	–	–	4.39	TC	[3595]
Al(100)	–	–	–	–	–	4.39	TC	[2065,3485]
Al(100)	–	–	–	–	–	4.39	TC	[1936]
Al(100)	–	–	–	–	–	4.4	TC	[2905]
Al(100)	–	–	–	–	–	4.40	TC	[1936]
Al(100)	–	–	–	–	–	4.40	TC	[2065,2067]
Al(100)	–	–	–	–	–	4.41	TC	[557]
Al(100)	–	–	$<10^{-10}$	~300	–	4.41 ± 0.03	PE	[241]
Al(100)	–	–	–	–	–	4.42	TC	[482,721,4398]
Al(100)	–	–	–	–	–	4.42 ± 0.04	TC	[719]
Al(100)	–	–	–	–	–	4.43	TC	[4117]
Al(100)	–	–	–	–	–	4.432 ± 0.004	TC	[720]
Al(100)	–	–	–	–	–	4.45	TC	[1557]
Al(100)	–	–	–	–	–	4.46	TC	[716]
Al(100)	–	–	–	–	–	4.46	TC	[1943]
Al(100)	–	–	–	–	–	4.46	TC	[716]
Al(100)	–	–	–	–	–	4.46 ± 0.03	TC	[1935]
Al(100)	–	–	–	–	–	4.49	TC	[244]
Al(100)	–	–	–	–	–	4.50	TC	[3203]
Al(100)	–	–	–	–	–	4.50	TC	[714,984]
Al(100)	–	–	–	–	–	4.505	TC	[481]
Al(100)	–	–	–	–	–	4.51	TC	[1821]
Al(100)	–	–	–	–	–	4.51 ± 0.03	TC	[717,718]
Al(100)	–	–	–	–	–	4.53	TC	[1002]
Al(100)	–	–	–	–	–	4.54	TC	[240,2221]
Al(100)	–	–	–	–	–	4.56	TC	[1943]
Al(100)	–	–	–	–	–	4.59	TC	[1259]
Al(100)	–	–	–	–	–	4.63	TC	[240,714,984]
Al(100)	–	–	–	–	–	4.67	TC	[245,3149]
Al(100)	–	–	–	–	–	4.69	TC	[1563]
Al(100)	–	–	–	–	–	4.69	TC	[2697]
Al(100)	–	–	–	–	–	4.7	TC	[1088]
Al(100)	–	–	–	–	–	4.7	TC	[1711,1734]
Al(100)	–	–	–	–	–	4.7	TC	[3149,3156]
Al(100)	–	–	–	–	–	4.7 ± 0.1	TC	[713]
Al(100)	–	–	–	–	–	4.82	TC	[3339]
Al(100)	–	–	–	–	–	4.82	TC	[1871]
Al(100)	–	–	–	–	–	4.85	TC	[3477]
Al(100)	–	–	–	–	–	4.86	TC	[2697]
Al(100)	–	–	–	–	–	4.90	TC	[1095]
Al(100)	–	–	–	–	–	5.07 ± 0.10	TC	[1576]
Al(100)	–	–	–	–	–	5.24	TC	[3477]
Al(100)	–	–	–	–	–	5.45 ± 0.1	TC	[1036]
Recommended	–	–	–	–	–	**4.28 ± 0.05**	–	–
Al(110)	–	–	–	–	–	2.83	TC	[2697]
Al(110)	–	–	–	–	–	3.59	TC	[553]
Al(110)	–	–	–	–	–	3.60	TC	[473]
Al(110)	–	–	–	–	–	3.642	TC	[1626]
Al(110)	–	–	–	–	–	3.643	TC	[1626,2914]
Al(110)	–	–	–	–	–	3.65	TC	[475]

Table 1 (*continued*)

Surface	Beam	Ion	P_r (Torr)	T (K)	ϕ^+ (eV)	ϕ^e (eV)	Meth.	Refs.
Al(110)	–	–	–	–	–	3.7	TC	[2851]
Al(110)	–	–	–	–	–	3.7	TC	[2982]
Al(110)	–	–	–	–	–	3.70	TC	[593]
Al(110)	–	–	–	–	–	3.73	TC	[1159,3067]
Al(110)	–	–	–	–	–	3.76	TC	[321]
Al(110)	–	–	–	–	–	3.8	TC	[1088]
Al(110)	–	–	?	~300	–	3.80	PE	[239]
Al(110)	–	–	–	–	–	3.81	TC	[231]
Al(110)	–	–	–	–	–	3.82	TC	[3467]
Al(110)	–	–	–	–	–	3.85	TC	[1435]
Al(110)	–	–	–	–	–	3.87	TC	[3004]
Al(110)	–	–	–	–	–	3.88	TC	[555]
Al(110)	–	–	–	–	–	3.88	TC	[3004]
Al(110)	–	–	–	–	–	3.89	TC	[715]
Al(110)	–	–	–	–	–	3.89	TC	[1030]
Al(110)	–	–	–	–	–	3.92	TC	[4401]
Al(110)	–	–	–	–	–	3.95	TC	[1030]
Al(110)	–	–	–	–	–	3.97	TC	[474]
Al(110)	–	–	–	–	–	3.97	TC	[1563]
Al(110)	–	–	–	–	–	4.02	TC	[556]
Al(110)	–	–	–	–	–	4.06	TC	[4233]
Al(110)/Al(110)[53]	Al	–	~10^{-10}	~300 (~520)	–	4.06 ± 0.03	PE	[612]
Al(110)	–	–	–	–	–	4.07	TC	[474]
Al(110)	–	–	–	–	–	4.07	TC	[1175]
Al(110)	–	–	–	–	–	4.09	TC	[4087,4410]
Al(110)	–	–	–	–	–	4.10	TC	[476]
Al(110)	–	–	–	–	–	4.11	TC	[4233]
Al(110)	–	–	–	–	–	4.12	TC	[559]
Al(110)	–	–	–	–	–	4.14	TC	[559]
Al(110)	–	–	–	–	–	4.15	TC	[474]
Al(110)	–	–	–	–	–	4.19	TC	[1943]
Al(110)	–	–	–	–	–	4.2	TC	[2905]
Al(110)	–	–	–	–	–	4.20	TC	[557]
Al(110)	–	–	–	–	–	4.20	TC	[1212]
Al(110)	–	–	–	–	–	4.20	TC	[1943]
Al(110)	–	–	–	–	–	4.21	TC	[2548]
Al(110)	–	–	–	–	–	4.21 ± 0.04	TC	[719]
Al(110)	–	–	–	–	–	4.22	TC	[557]
Al(110)	–	–	–	–	–	4.22	TC	[1213]
Al(110)	–	–	–	–	–	4.25	TC	[3203]
Al(110)	–	–	–	–	–	4.26	TC	[1943]
Al(110)	–	–	–	–	–	4.28	TC	[476]
Al(110)	–	–	–	–	–	4.28	TC	[4117]
Al(110)	–	–	<10^{-10}	~300	–	4.28 ± 0.02	PE	[241,242]
Al(110)	–	–	–	–	–	4.29	TC	[721,4398]
Al(110)	–	–	–	–	–	4.30	TC	[561,721,4398]
Al(110)	–	–	–	–	–	4.30	TC	[2697]
Al(110)	–	–	–	–	–	4.32 ± 0.03	TC	[247,718]
Al(110)	–	–	–	–	–	4.35	TC	[1095]
Al(110)	–	–	~10^{-10}	~300	–	4.35 ± 0.05	PE	[458,2681]
Al(110)	–	–	–	–	–	4.36	TC	[1943]
Al(110)	–	–	–	–	–	4.44	TC	[3477]
Al(110)	–	–	–	–	–	4.47	TC	[2697]
Al(110)	–	–	–	–	–	4.5	TC	[1088]
Al(110)	–	–	–	–	–	4.5	TC	[1214]
Al(110)	–	–	–	–	–	4.83	TC	[248]
Al(110)	–	–	–	–	–	4.91	TC	[3477]
Recommended	–	–	–	–	–	**4.05 ± 0.06**	–	–
Al(111)	–	–	?	~300	–	3.11 ± 0.10	PE	[239]
Al(111)	–	–	–	–	–	3.13	TC	[2697]
Al(111)	–	–	–	–	–	3.47	TC	[1030,1089]
Al(111)	–	–	–	–	–	3.48	TC	[476]
Al(111)	–	–	–	–	–	3.53	TC	[1089]
Al(111)	–	–	–	–	–	3.6	TC	[3137]
Al(111)	–	–	–	–	–	3.6	TC	[1086]
Al(111)	–	–	–	–	–	3.7	TC	[1176,1216]
Al(111)	–	–	–	–	–	3.7	TC	[1011,1215]
Al(111)	–	–	–	–	–	3.72	TC	[231]
Al(111)	–	–	–	–	–	3.73	TC	[476]

Table 1 (*continued*)

Surface	Beam	Ion	P_r (Torr)	T (K)	ϕ^+ (eV)	ϕ^e (eV)	Meth.	Refs.
Al(111)	–	–	–	–	–	3.73	TC	[3467]
Al(111)	–	–	–	–	–	3.77	TC	[473]
Al(111)	–	–	–	–	–	3.78	TC	[3491]
Al(111)	–	–	–	–	–	3.79	TC	[1086]
Al(111)	–	–	–	–	–	3.8	TC	[1011,1215]
Al(111)	–	–	–	–	–	3.8	TC	[2222,2223]
Al(111)	–	–	–	–	–	3.83	TC	[1089]
Al(111)[54]	–	–	–	–	–	3.83–4.59	TC	[1101]
Al(111)	–	–	–	–	–	3.86	TC	[3004]
Al(111)	–	–	–	–	–	3.87	TC	[1042]
Al(111)	–	–	–	–	–	3.87	TC	[1086]
Al(111)	–	–	–	–	–	3.87	TC	[3158]
Al(111)	–	–	–	–	–	3.9	TC	[2982]
Al(111)	–	–	–	–	–	3.92	TC	[1030]
Al(111)	–	–	–	–	–	4.0	TC	[1086,1088]
Al(111)	–	–	–	–	–	4.0	TC	[1011,1215]
Al(111)	–	–	–	–	–	4.02	TC	[4087,4410]
Al(111)	–	–	–	–	–	4.04	TC	[1028,1179]
Al(111)	–	–	–	–	–	4.05	TC	[475]
Al(111)	–	–	–	–	–	4.05	TC	[4233]
Al(111)	–	–	–	–	–	4.059	TC	[1626]
Al(111)	–	–	–	–	–	4.06	TC	[1175]
Al(111)	–	–	–	–	–	4.07	TC	[3220]
Al(111)	–	–	–	–	–	4.08	TC	[4233]
Al(111)	–	–	–	–	–	4.08	TC	[2427]
Al(111)	–	–	–	–	–	4.08	TC	[4215]
Al(111)	–	–	–	–	–	4.085	TC	[735]
Al(111)	–	–	–	–	–	4.09	TC	[343]
Al(111)	–	–	–	–	–	4.09	TC	[553,1177]
Al(111)	–	–	–	–	–	4.092	TC	[735]
Al(111)	–	–	–	–	–	4.094	TC	[735]
Al(111)	–	–	–	–	–	4.096	TC	[560,2432]
Al(111)	–	–	–	–	–	4.1	TC	[1011,1215]
Al(111)	–	–	–	–	–	4.1	TC	[1088,2851]
Al(111)	–	–	–	–	–	4.10	TC	[1011]
Al(111)	–	–	–	–	–	4.117	TC	[1626,2914]
Al(111)	–	–	–	–	–	4.12	TC	[1159,3067]
Al(111)	–	–	–	–	–	4.12	TC	[1176]
Al(111)	–	–	–	–	–	4.12	TC	[1086,2844]
Al(111)	–	–	–	–	–	4.12	TC	[4029,4255]
Al(111)	–	–	–	–	–	4.13	TC	[2444]
Al(111)	–	–	–	–	–	4.15	TC	[2844]
Al(111)	–	–	–	–	–	4.16	TC	[2444]
Al(111)	–	–	–	–	–	4.17	TC	[1943]
Al(111)	–	–	–	–	–	4.17	TC	[3004]
Al(111)	–	–	–	–	–	4.17	TC	[1178]
Al(111)	–	–	–	–	–	4.18	TC	[555,715]
Al(111)	–	–	–	–	–	4.18	TC	[2402]
Al(111)	–	–	–	–	–	4.18	TC	[1921]
Al(111)	–	–	–	–	–	4.18	TC	[1943]
Al(111)/Ru(0001)[57]	Al	–	8×10^{-11}	~300	–	4.18 ± 0.06*	CPD	[301]
Al(111)	–	–	–	–	–	4.181	TC	[1626]
Al(111)	–	–	–	–	–	4.19	TC	[557]
Al(111)	–	–	–	–	–	4.19	TC	[1179]
Al(111)	–	–	–	–	–	4.19	TC	[1435]
Al(111)	–	–	–	–	–	4.2	TC	[2400]
Al(111)	–	–	–	–	–	4.2	TC	[2851]
Al(111)	–	–	–	–	–	4.2	TC	[734]
Al(111)	–	–	–	–	–	4.2	TC	[1011,1215]
Al(111)	–	–	–	–	–	4.20	TC	[3491]
Al(111)	–	–	5×10^{-11}	~300	–	4.20 ± 0.05	PE	[1915]
Al(111)	–	–	–	–	–	4.21	TC	[3491]
Al(111)	–	–	–	–	–	4.21	TC	[2548]
Al(111)	–	–	–	–	–	4.21	TC	[1028,1179]
Al(111)	–	–	–	–	–	4.22	TC	[1086]
Al(111)	–	–	–	–	–	4.22	TC	[1943]
Al(111)	–	–	–	–	–	4.22	TC	[4174,4284]
Al(111)	–	–	–	–	–	4.23	TC	[482,721,4398]
Al(111)	–	–	–	–	–	4.238	TC	[2523]
Al(111)	–	–	–	–	–	4.24	TC	[3175]

Table 1 (*continued*)

Surface	Beam	Ion	P_r (Torr)	T (K)	ϕ^+ (eV)	ϕ^e (eV)	Meth.	Refs.
Al(111)	–	–	$<10^{-10}$	~300	–	4.24 ± 0.02	PE	[241,242]
Al(111)	–	–	–	–	–	4.24 ± 0.04	TC	[1101]
Al(111)	–	–	–	–	–	4.25	TC	[561,721,4398]
Al(111)	–	–	–	–	–	4.25	TC	[3203]
Al(111)	–	–	?	100	–	4.25	CPD	[2654]
Al(111)	–	–	–	–	–	4.25	TC	[2685]
Al(111)/Ru(0001)[57]	Al	–	8×10^{-11}	~300	–	4.25*	CPD	[301,2417]
Al(111)	–	–	~10^{-10}	~300	–	4.25 ± 0.05	PE	[458,2681]
Al(111)	–	–	–	–	–	4.26	TC	[248]
Al(111)	–	–	–	–	–	4.26	TC	[1086]
Al(111)	–	–	–	~20–300	–	4.26	TC	[4310]
Al(111)/Al(111)[53]	Al	–	~10^{-10}	~300 (~520)	–	4.26 ± 0.03	PE	[612]
Al(111)	–	–	–	–	–	4.26 ± <0.1	TC	[1559]
Al(111)	–	–	–	–	–	4.27	TC	[556]
Al(111)	–	–	–	–	–	4.275	TC	[1096,2377]
Al(111)	–	–	–	–	–	4.28	TC	[2636]
Al(111)/quartz	Al	–	~10^{-10}	~300 (~520)	–	4.28 ± 0.01	PE	[612]
Al(111)	–	–	1×10^{-10}	~300	–	4.29	PE	[1572]
Al(111)/quartz[55]	Al	–	~10^{-9}	~300 (623)	–	4.29	PE	[3313]
Al(111)	–	–	~10^{-11}	~300	–	4.29 ± 0.02	PE	[1217,1598]
Al(111)	–	–	$<10^{-10}$	~300	–	4.3	PE	[249]
Al(111)	–	–	–	–	–	4.3	TC	[1011]
Al(111)	–	–	–	–	–	4.3	TC	[1176,1216]
Al(111)	–	–	–	–	–	4.3	TC	[2905]
Al(111)	–	–	?	20, 40	–	4.3	PE	[1688,2642]
Al(111)	–	–	?	?	–	4.30	?	[1218]
Al(111)	–	–	–	–	–	4.31	TC	[1011]
Al(111)	–	–	–	–	–	4.31	TC	[4401]
Al(111)/quartz[55]	Al	–	~10^{-9}	~300	–	4.31	PE	[3313]
Al(111)	–	–	–	–	–	4.31 ± 0.03	TC	[718]
Al(111)	–	–	–	–	–	4.32	TC	[321]
Al(111)	–	–	–	–	–	4.32	TC	[1943]
Al(111)	–	–	–	–	–	4.32	TC	[1594]
Al(111)	–	–	–	–	–	4.33	TC	[4117]
Al(111)	–	–	–	–	–	4.34	TC	[1011]
Al(111)	–	–	8×10^{-11}	90	–	4.36	PE	[250]
Al(111)	–	–	–	–	–	4.36	TC	[1557]
Al(111)	–	–	–	–	–	4.37	TC	[474]
Al(111)	–	–	–	–	–	4.38	TC	[1086]
Al(111)	–	–	1×10^{-10}	90, 300	–	4.38 ± 0.02	PE	[566]
Al(111)	–	–	–	–	–	4.39	TC	[1592,1594]
Al(111)/Ag(111)[56]	Al	–	$\leq 5 \times 10^{-10}$	150, 300	–	4.4	CPD	[2888]
Al(111)	–	–	–	–	–	4.4	TC	[1011]
Al(111)	–	–	–	–	–	4.4	TC	[1097]
Al(111)	–	–	–	–	–	4.40	TC	[1734]
Al(111)/Ru(0001)[57]	Al	–	8×10^{-11}	~300	–	4.41*	CPD	[301,2417]
Al(111)	–	–	–	–	–	4.43	TC	[1011]
Al(111)	–	–	?	?	–	4.48	?	[3661]
Al(111)	–	–	–	–	–	4.48 ± 0.08*	TC	[474]
Al(111)	–	–	–	–	–	4.49	TC	[1098]
Al(111)	–	–	–	–	–	4.491	TC	[481]
Al(111)	–	–	–	–	–	4.5	TC	[1011]
Al(111)	–	–	–	–	–	4.52	TC	[474]
Al(111)	–	–	~10^{-11}	40	–	4.53	PE	[1219]
Al(111)	–	–	–	–	–	4.53	TC	[1011]
Al(111)	–	–	–	–	–	4.54	TC	[334]
Al(111)	–	–	–	–	–	4.545	TC	[1096]
Al(111)	–	–	–	–	–	4.55	TC	[2636]
Al(111)	–	–	–	–	–	4.55 ± 0.05	TC	[558]
Al(111)	–	–	–	–	–	4.56	TC	[1594]
Al(111)	–	–	–	–	–	4.56	TC	[474]
Al(111)	–	–	–	–	–	4.60	TC	[2697]
Al(111)	–	–	–	–	–	4.62	TC	[1099]
Al(111)	–	–	–	–	–	4.7	TC	[1011]
Al(111)	–	–	–	–	–	4.7	TC	[1001,1097,3441]
Al(111)	–	–	–	–	–	4.74	TC	[1011]
Al(111)	–	–	–	–	–	4.75	TC	[1095]
Al(111)	–	–	–	–	–	4.77	TC	[2697]
Al(111)	–	–	–	–	–	4.81	TC	[1563]
Al(111)	–	–	–	–	–	4.82	TC	[1259]

Table 1 (*continued*)

Surface	Beam	Ion	P_r (Torr)	T (K)	ϕ^+ (eV)	ϕ^e (eV)	Meth.	Refs.
Al(111)	–	–	–	–	–	4.90	TC	[1087]
Al(111)	–	–	–	–	–	4.99	TC	[3477]
Al(111)	–	–	–	–	–	5.2	TC	[1100]
Al(111)	–	–	–	–	–	5.35	TC	[3477]
Al(111)	–	–	–	–	–	5.4	TC	[3441]
Recommended	–	–	–	–	–	**4.24 ± 0.04**	–	–
Al	–	–	–	–	–	2.62	TC	[3080]
Al	–	–	–	–	–	2.87	TC	[1436]
Al	–	–	?	~300	–	2.98	PE	[2460]
Al	–	–	–	–	–	3.0	TC	[2456]
Al	–	–	–	–	–	3.08	TC	[1436]
Al/?	Al	–	?	~300	–	3.15	CPD	[2708]
Al[130]	–	–	–	–	–	3.194	TC	[2887]
Al/Si(110)	Al	–	~10^{-11}	~300	–	3.2 ± 0.2	FE	[2394]
Al	–	–	?	~300	–	3.23	CPD	[2539]
Al(fp)[130]	–	–	–	–	–	3.233	TC	[2887]
Al	–	–	~10^{-8}	~300	–	3.26	PE	[3315]
Al(fp)[130]	–	–	–	–	–	3.269	TC	[2887]
Al	–	–	?	~300	–	3.38	CPD	[2297]
Al	–	–	?	~300	–	3.41*	CPD	[3621]
Al	–	–	6×10^{-3}	~300	–	3.43 ± 0.10	PE	[2079,2080]
Al	–	–	–	–	–	3.44	TC	[738]
Al/quartz[51]	Al	–	~10^{-5}	~300	–	3.47	PE	[1973]
Al/Si(111)	–	–	–	–	–	3.5	TC	[1679]
Al	–	–	?	~300	–	3.58	PE	[4278]
Al	–	–	–	–	–	3.62	TC	[231]
Al	–	–	–	–	–	3.64	TC	[521]
Al	–	–	–	–	–	3.65	TC	[477]
Al	–	–	–	–	–	3.66	TC	[1066]
Al	–	–	?	~300	–	3.70	PE	[239]
Al	–	–	–	–	–	3.73	TC	[3467]
Al	–	–	–	–	–	3.74	TC	[477,1924,4035, 4036]
Al	–	–	–	–	–	3.77	TC	[2427]
Al/quartz	–	–	~10^{-5}	~300	–	3.78	PE	[1973]
Al	–	–	–	–	–	3.79	TC	[1436]
Al	–	–	–	–	–	3.8*	TC	[1955]
Al	–	–	–	–	–	3.80	TC	[2949]
Al	–	–	–	–	–	3.815	TC	[2523]
Al	–	–	–	–	–	3.83	TC	[231]
Al	–	–	–	–	–	3.83	TC	[3467]
Al	–	–	–	–	–	3.87	TC[3]	[475]
Al	–	–	–	–	–	3.88	TC	[2474]
Al	–	–	1×10^{-5}	~300	–	3.88	CPD	[1883]
Al/Al$_2$O$_3$/Si(100)	Al	–	?	~300	–	3.9[48]	PE	[1442]
Al	–	–	–	–	–	3.93	TC	[230]
Al	–	–	–	–	–	3.99	TC	[4419]
Al/glass	Al	–	~10^{-6}–10^{-8}	~300	–	4.0	PE	[1894]
Al	–	–	~10^{-10}	~300	–	4.0 ± 0.1	PE	[1220]
Al	–	–	–	–	–	4.00	TC	[1901]
Al/Ag(110)	Al	–	<4×10^{-11}	~300	–	4.04*	PE	[3466]
Al/Si$_3$N$_4$	Al	–	?	?	–	4.06	?	[3519,3520]
Al/glass	Al	–	<10^{-8}	~300	–	4.08	PE	[1457]
Al/Pd/Ta(110)[398]	Al	–	8×10^{-11}	~300	–	4.1	PE	[2271]
Al	–	–	?	~300	–	4.1	PE	[1412]
Al/quartz[102]	Al	–	≤10^{-8}	4.2	–	4.1 ± 0.2	CPD	[1686]
Al	–	–	~10^{-7}	~300	–	4.12	CPD	[3513]
Al	–	–	–	–	–	4.12	TC	[477]
Al/SiO$_2$/Si	Al	–	?	~300 (570)	–	4.13	PE	[2355]
Al/SiO$_2$	Al	–	?	?	–	4.14	?	[3519,3520]
Al	–	–	–	–	–	4.14	TC	[2629]
Al	–	–	5×10^{-10}	~300	–	4.15	PE	[594]
Al/GaP	–	–	–	–	–	4.15	TC	[1653]
Al/Si(100)	–	–	–	–	–	4.15	TC	[3485]
Al/Pd(001)	Al	–	5×10^{-11}	325	–	4.15	CPD	[3206,3209]
Al/glass	Al	–	<1×10^{-9}	~300	–	4.15 ± 0.05	CPD	[655]
Al(nanowire)[453]	–	–	–	–	–	4.15 ± 0.05*	TC	[4178]
Al	–	–	–	–	–	4.16	TC	[2005]
Al	–	–	~10^{-9}	~300	–	4.16	PE	[3212]

Table 1 (*continued*)

Surface	Beam	Ion	P_r (Torr)	T (K)	ϕ^+ (eV)	ϕ^e (eV)	Meth.	Refs.
Al	–	–	–	–	–	4.17	TC	[477]
Al/Si(111)	Al	–	5×10^{-11}	~300	–	4.17 ± 0.05	CPD	[613,636]
Al/glass[59]	Al	–	5×10^{-11}	~300	–	4.17 ± 0.07	CPD	[1071,2100]
Al	–	–	–	–	–	4.18	TC	[3637]
Al	–	–	–	–	–	4.19	TC	[3264,3265,3267]
Al/W(111)	Al	–	$<1 \times 10^{-10}$	~300	–	4.19*	FE	[2616]
Al/glass	Al	–	$\leq 10^{-8}$	~300	–	4.19 ± 0.03	CPD	[349]
Al	–	–	–	–	–	4.2	TC	[706]
Al	–	–	–	–	–	4.2	TC	[4031]
Al	–	–	–	–	–	4.2	TC	[944]
Al/quartz	–	–	?	~300	–	4.2	PE	[4281]
Al/quartz	Al	–	$\leq 10^{-8}$	293	–	4.2 ± 0.2	CPD	[1686]
Al/quartz	Al	–	$\leq 10^{-8}$	135	–	4.2 ± 0.2	CPD	[1686]
Al[102]	–	–	$\leq 10^{-8}$	5	–	4.20	FE	[1686]
Al	–	–	$\leq 10^{-8}$	77	–	4.20	FE	[1686]
Al/glass	Al	–	?	90	–	4.20 ± 0.02	PE	[3031]
Al/glass	Al	–	?	~300	–	4.20 ± 0.02	PE	[3031]
Al/W	Al	–	$\sim 10^{-10}$	~300 (≤800)	–	4.20 ± 0.05	FE	[2715]
Al/glass	Al	–	$\sim 10^{-8}$	~300	–	4.20 ± 0.05	CPD	[133]
Al/glass	Al	–	5×10^{-11}	~300	–	4.20 ± 0.07	CPD	[1071]
Al/SiO$_2$	Al	–	?	~300	–	4.208	CPD	[1221]
Al/W	Al	–	$<1 \times 10^{-10}$	~300	–	4.21 ± 0.04	FE	[2616]
Al	–	–	–	–	–	4.22	TC	[1399]
Al	–	–	?	~300	–	4.22 ± 0.04*	CPD	[3867]
Al/glass	Al	–	5×10^{-11}	~300	–	4.22 ± 0.06	CPD	[1071]
Al	–	–	–	–	–	4.24	TC	[477,1924,4035]
Al$_n$(n → ∞)[459]	–	–	?	~300	–	4.25	TC	[4194,4197]
Al	–	–	?	?	–	4.25	?	[1535]
Al/ZrO$_2$/Si(100)	Al	–	?	~300	–	4.25[48]	PE	[1442]
Al	–	–	–	–	–	4.25	TC	[2439]
Al	–	–	–	–	–	4.25	TC	[4031]
Al	–	–	?	~300	–	4.25	PE	[3249]
Al/W	Al	–	$\leq 5 \times 10^{-8}$	~300	–	4.25 ± 0.05	CPD	[690]
Al/quartz	Al	–	$<1 \times 10^{-9}$	~300	–	4.25 ± 0.10	CPD	[655]
Al	–	–	$<3 \times 10^{-11}$	~300	–	4.25 ± 0.15	AI	[4055]
Al	–	–	–	466.5	–	4.259	TC	[2419]
Al/GaP	–	–	–	–	–	4.26	TC	[1653]
Al/quartz	Al	–	$<5 \times 10^{-10}$	293	–	4.26	PE	[1102]
Al/Mo(011)	Al	–	$\leq 2 \times 10^{-10}$	~300	–	4.26	CPD	[2655]
Al/Al$_2$O$_3$/Mo(011)	Al	–	$\leq 2 \times 10^{-10}$	~300	–	4.26	CPD	[2655]
Al/MgO/Mo(011)	Al	–	$\leq 2 \times 10^{-10}$	~300	–	4.26	CPD	[2655]
Al/quartz	Al	–	$\leq 5 \times 10^{-10}$	78	–	4.26 ± 0.01	PE	[435]
Al/Si	Al	–	$<6 \times 10^{-9}$	~300	–	4.26 ± 0.02	FE	[1540]
Al/Ta(110)[398]	Al	–	8×10^{-11}	~300	–	4.27	PE	[2271]
Al	–	–	–	–	–	4.27	TC	[553,2427]
Al	–	–	–	–	–	4.27	TC	[3477]
Al/quartz	Al	–	$<2 \times 10^{-9}$	~300	–	4.27 ± 0.02	PE	[725,1498]
Al	–	–	–	0	–	4.276	TC	[2419]
Al	–	–	–	–	–	4.28	TC	[3220]
Al$_n$(n → ∞)	–	–	–	–	–	4.28	TC	[4193]
Al$_{2000}$(z → 0)[60]	–	–	?	~300	–	4.28 ± 0.03	IP	[2199]
Al$_{32000}$(z → 0)[60]	–	–	?	~300	–	4.28 ± 0.03	IP	[2199]
Al/quartz[55]	Al	–	$\sim 10^{-9}$	~300 (623)	–	4.29	PE	[3313]
Al/quartz	Al	–	$<5 \times 10^{-10}$	293 (618)	–	4.29	PE	[1102]
Al/quartz	Al	–	$<5 \times 10^{-10}$	78 (293)	–	4.29 ± 0.01	PE	[435]
Al/quartz	Al	–	$<5 \times 10^{-10}$	78 (550)	–	4.29 ± 0.01	PE	[435]
Al/glass	Al	–	5×10^{-11}	~300	–	4.29 ± 0.09*	CPD	[1071]
Al	–	–	–	–	–	4.292	TC	[2649]
Al	–	–	–	–	–	4.3	TC	[1173]
Al/?	Al	–	$\sim 10^{-5}$	~300	–	4.3	CPD	[1376]
Al[58]	–	–	?	~300	–	4.3	CPD	[2550]
Al/Mo	Al	–	7×10^{-11}	~300	–	4.3	PE	[2226]
Al	–	–	–	–	–	4.3	TC	[1993]
Al	–	–	–	–	–	4.30	TC	[2914]
Al	–	–	$<3 \times 10^{-9}$	~300	–	4.30	CPD	[1180]
Al/quartz	Al	–	$\leq 5 \times 10^{-10}$	293 (~550)	–	4.30	PE	[435]
Al	–	–	–	–	–	4.30	TC	[1626,4431]
Al/quartz[55]	Al	–	$\sim 10^{-9}$	~300	–	4.31	PE	[3313]
Al/Si(001)	–	–	–	–	–	4.317	TC	[1941]
Al/Si(111)	Al	–	2×10^{-10}	~300	–	4.32 ± 0.1	PE	[2623]

Table 1 (*continued*)

Surface	Beam	Ion	P_r (Torr)	T (K)	ϕ^+ (eV)	ϕ^e (eV)	Meth.	Refs.
$Al_{32-95}(\infty)$	–	–	?	230	–	4.338	IP	[4192]
Al/W(001)	Al	–	$<1 \times 10^{-10}$	~300	–	4.34*	FE	[2616]
Al/Al	Al	–	?	~300	–	4.34	PE	[3250]
Al	–	–	–	–	–	4.34	TC	[298]
$Al_{32-95}(\infty)$	–	–	?	65	–	4.349	IP	[4192]
Al	–	–	–	–	–	4.35	TC	[1976]
Al/SiO_2	Al	–	?	~300	–	4.353	CPD	[1221]
Al/glass	Al	–	?	~300	–	4.36	PE	[1948]
Al/W(111)	Al	–	$<1 \times 10^{-10}$	~300	–	4.36	FE	[2616]
Al_{32000}[449]	–	–	–	–	–	4.36 ± 0.03*	TC	[2199]
Al	–	–	–	–	–	4.37	TC	[1613]
Al/Si	–	–	–	–	–	4.39	TC	[1653]
Al/Ag(110)	Al	–	$<4 \times 10^{-11}$	~300	–	4.40	PE	[3466]
Al/Si	–	–	–	–	–	4.42	TC	[1653]
Al/Si(111)	Al	–	$<5 \times 10^{-10}$	~300	–	4.45	PE	[1694]
Al/Mo(110)	Al	–	$<3 \times 10^{-10}$	~300	–	4.50	CPD	[2403]
Al_{2000}[449]	–	–	–	–	–	4.51 ± 0.03*	TC	[2199]
Al/W(001)	Al	–	$<1 \times 10^{-10}$	~300	–	4.65	FE	[2616]
Al/Si(111)	–	–	–	–	–	4.70 ± 0.1	TC	[3549,3740]
Al[61]	–	–	?	~300–600	–	4.75 ± 0.22	PE	[1222]
Al/Si(111)	Cs, Li	Cs^+	?	~300	4.8*	–	CPD	[1342]
Al[61]	–	–	?	~300–600	–	4.90 ± 0.06	PE	[1222]
Al	Cs	Cs^+	?	~300	4.96*	–	CPD	[611]
Recommended	–	–	–	–	**4.9 ± 0.1**	**4.26 ± 0.03**	–	–

Liquid ($T \geq 933$ K)

Surface	Beam	Ion	P_r (Torr)	T (K)	ϕ^+ (eV)	ϕ^e (eV)	Meth.	Refs.
Al	–	–	–	–	–	4.241	TC	[2419]

14. Silicon Si

Diamond Structure

Surface	Beam	Ion	P_r (Torr)	T (K)	ϕ^+ (eV)	ϕ^e (eV)	Meth.	Refs.
Si(100)	–	–	–	–	–	4.33	TC	[2521,2525]
Si(100)	–	–	–	–	–	4.36	TC	[2521]
Si(100)p	–	–	$\leq 10^{-9}$	300E	–	4.41*[62]	TE	[1225]
Si(100)[65]	–	–	–	~300	–	4.47*	TC	[2097]
Si(100)n	–	–	?	~300 (?)	–	4.5	PE	[2242]
Si(100)n	–	–	7×10^{-9}	~1200–1500	(4.54–4.84)	4.53 ± 0.1	TE	[74]
Si(100)n[64]	K	K^+	7×10^{-9}	~900–1550	4.54 ± 0.2	(4.53 ± 0.1)	PSI	[74]
Si(100)n	–	–	?	~300	–	4.6	PE	[2059]
Si(100)p	–	–	3×10^{-11}	~300	–	4.6	PE	[1872]
Si(100)n[64]	Li	Li^+	7×10^{-9}	~1050–1550	4.60 ± 0.03	(4.53 ± 0.1)	PSI	[74]
Si(100)	–	–	–	–	–	4.604	TC	[1941]
Si(100)n	–	–	?	~300 (1170)	–	4.7	PE	[768]
Si(100)n[64]	Na	Na^+	7×10^{-9}	~1000–1550	4.70 ± 0.02	(4.53 ± 0.1)	PSI	[74]
Si(100)	–	–	–	–	–	4.712	TC	[4460][490]
Si(100)n	–	–	4×10^{-11}	200	–	4.72 ± 0.05	CPD	[880]
Si(100)n[63]	Li	Li^+	7×10^{-9}	~1050–1550	4.74 ± 0.05	(4.53 ± 0.1)	PSI	[74]
Si(100)	–	–	–	–	–	4.79	TC	[4461][490]
Si(100)p	–	–	5×10^{-11}	~300	–	4.8	PE	[1868,1869,3605]
Si(100)p	–	–	$<10^{-9}$	~300 (773)	–	4.81	CPD	[116]
Si(100)n[63]	Tl	Tl^+	7×10^{-9}	~950–1550	4.81 ± 0.03	(4.53 ± 0.1)	PSI	[74]
Si(100)n[64]	Tl	Tl^+	7×10^{-9}	~950–1550	4.81 ± 0.07	(4.53 ± 0.1)	PSI	[74]
Si(100)p	–	–	$<10^{-9}$	~300 (773)	–	4.82	CPD	[116,1771]
Si(100)/W(110)	Si	–	?	~300	–	4.83	PE	[3448]
Si(100)p	–	–	$\leq 10^{-9}$	1330–1500	–	4.83 ± 0.03	TE	[1225]
Si(100)n[63]	Na	Na^+	7×10^{-9}	~1000–1550	4.84 ± 0.03	(4.53 ± 0.1)	PSI	[74]
Si(100)n[63]	K	K^+	7×10^{-9}	~900–1550	≥4.84	(4.53 ± 0.1)	PSI	[74]
Si(100)	–	–	1×10^{-10}	~300	–	4.85	PE	[2972]
Si(100)p	–	–	?	~300	–	4.85	TCS	[4050,4177]
Si(100)	–	–	2×10^{-10}	~300	–	4.85	FE	[275,440]
Si(100)	–	–	$\sim 10^{-10}$	200	–	4.85	CPD	[302]
Si(100)n	–	–	$\sim 10^{-11}$	~300	–	4.85 ± 0.1	PE	[2130]
Si(100)	–	–	–	–	–	4.859	TC	[3498,3501]
Si(100)[65]	–	–	–	1000	–	4.86*	TC	[2097]
Si(100)n	–	–	5×10^{-11}	~300	–	4.87	PE	[2150]
Si(100)p	–	–	–	–	–	4.876	TC	[4179]
Si(100)	–	–	–	–	–	4.9	TC	[1223]
Si(100)	–	–	5×10^{-11}	~300	–	4.9	PE	[1224]
Si(100)p	–	–	$<1 \times 10^{-10}$	~300	–	4.9	PE	[3177,3187,3189, 3191]

Table 1 (*continued*)

Surface	Beam	Ion	P_r (Torr)	T (K)	ϕ^+ (eV)	ϕ^e (eV)	Meth.	Refs.
Si(100)[n]	–	–	?	70 (1200)	–	4.9*	PE	[2178]
Si(100)	–	–	3×10^{-11}	~300	–	4.9 ± 0.1	PE	[2951]
Si(100)	–	–	–	–	–	4.9 ± 0.1	TC	[2680]
Si(100)[p]	–	–	2×10^{-10}	~300	–	4.91	FE	[1387]
Si(100)[p]	–	–	$\leq 10^{-9}$	~300 (1550)	–	4.91 ± 0.05	CPD	[1225]
Si(100)[n]	–	–	$\sim 10^{-10}$	~300 (~1200)	–	4.92	PE	[4125]
Si(100)[p]	–	–	$<10^{-9}$	~300	–	4.92 ± 0.02	CPD	[116,1771]
Si(100)[p]	–	–	$<10^{-9}$	~300 (1350)	–	4.96	CPD	[116]
Si(100)[n]	–	–	4×10^{-11}	~300	–	4.96	CPD	[1861]
Si(100)[p]	–	–	$\sim 10^{-10}$	~300	–	5.05 ± 0.05	PE	[1851]
Si(100)	–	–	–	–	–	5.1	TC	[3362]
Si(100)	–	–	$<1 \times 10^{-10}$	~300 (1120)	–	5.11 ± 0.03	PE	[1491,3950]
Si(100)[65]	–	–	–	1500	–	5.14*	TC	[2097]
Si(100)	–	–	–	–	–	5.12	TC	[2067,3485]
Recommended	**–**	**–**	**–**	**–**	**4.72 ± 0.10**	**4.82 ± 0.05**	**–**	**–**
Si(110)[p70]	–	–	?	1250–1400	–	3.17 ± 0.05	TE	[1500]
Si(110)[p434]	Na	Na$^+$	$\leq 5 \times 10^{-7}$	1000	3.32	(3.40)	PSI	[1472]
Si(110)[p434]	K	K$^+$	$\leq 5 \times 10^{-7}$	1000	3.32	(3.40)	PSI	[1472]
Si(110)[p434]	–	–	$\leq 5 \times 10^{-7}$	1000	(3.32)	3.40	TE	[1472]
Si(110)[n70]	–	–	?	1250–1400	–	3.76 ± 0.05	TE	[1500]
Si(110)[p70]	–	–	?	1400–1625	–	4.12 ± 0.05	TE	[1500]
Si(110)[p]	–	–	$\sim 10^{-9}$	1265–1500	–	4.12 ± 0.05	TE	[635]
Si(110)[p434]	Na	Na$^+$	$<5 \times 10^{-7}$	1600	4.14	(4.70)	PSI	[1472]
Si(110)[p434]	K	K$^+$	$<5 \times 10^{-7}$	1600	4.14	(4.70)	PSI	[1472]
Si(110)[n70]	–	–	?	1400–1625	–	4.14 ± 0.05	TE	[1500]
Si(110)[p434]	–	–	$\leq 5 \times 10^{-7}$	1300	(4.31)	4.31	TE	[1472]
Si(110)[p434]	Na	Na$^+$	$\leq 5 \times 10^{-7}$	1300	4.31	(4.31)	PSI	[1472]
Si(110)[p434]	K	K$^+$	$\leq 5 \times 10^{-7}$	1300	4.31	(4.31)	PSI	[1472]
Si(110)[p434]	Na	Na$^+$	$\leq 5 \times 10^{-7}$	1600	4.38	(4.70)	PSI	[1472]
Si(110)[p434]	K	K$^+$	$\leq 5 \times 10^{-7}$	1600	4.38	(4.70)	PSI	[1472]
Si(110)[p434]	Na	Na$^+$	$\leq 5 \times 10^{-7}$	1500–1600	4.38 ± 0.01	(4.69 ± 0.01)	PSI	[1472]
Si(110)[p434]	K	K$^+$	$\leq 5 \times 10^{-7}$	1500–1600	4.38 ± 0.01	(4.69 ± 0.01)	PSI	[1472]
Si(110)[p]	–	–	$\leq 10^{-9}$	~300	–	4.41*	TE	[1225]
Si(110)[65]	–	–	–	300	–	4.47*	TC	[2097]
Si(110)[p434]	–	–	$\leq 5 \times 10^{-7}$	1500–1600	(4.38 ± 0.01)	4.69 ± 0.01	TE	[1472]
Si(110)[p434]	–	–	$\leq 5 \times 10^{-7}$	1600	(4.38)	4.70	TE	[1472]
Si(110)[p]	–	–	$<10^{-9}$	~300 (773)	–	4.70	CPD	[116,1771]
Si(110)	–	–	$<1 \times 10^{-10}$	~300 (1120)	–	4.73 ± 0.03	PE	[1491,3950]
Si(110)[n]	–	–	$\leq 2 \times 10^{-10}$	~300	–	4.75 ± 0.01	PE	[3184]
Si(110)[p]	–	–	$<10^{-9}$	~300 (1350)	–	4.85	CPD	[116]
Si(110)[65]	–	–	–	1000	–	4.86*	TC	[2097]
Si(110)[p]	–	–	$\leq 10^{-9}$	1300–1600	–	4.87 ± 0.06	TE	[1225]
Si(110)[p]	–	–	$<10^{-9}$	~300	–	4.89 ± 0.02	CPD	[116,1771]
Si(110)[p]	–	–	$<10^{-9}$	~300 (1350)	–	4.91	CPD	[116]
Si(110)[65]	–	–	–	1500	–	5.14*	TC	[2097]
Recommended	**–**	**–**	**–**	**–**	**4.36 ± 0.03**	**4.44 ± 0.24**	**–**	**–**
Si(111)[p432]	–	–	?	~1100–1150	–	3.2	TE	[3540]
Si(111)	–	–	–	–	–	4.0	TC	[1679,2219]
Si(111)[n66]	–	–	$\leq 1 \times 10^{-7}$	1340–1600	(4.86–4.90)	4.04 ± 0.05	TE	[72]
Si(111)[p66]	–	–	$\sim 10^{-9}$	1265–1500	–	4.05 ± 0.04	TE	[635]
Si(111)[p66]	–	–	1×10^{-7}	~1300–1600	(4.84, 4.86)	4.07 ± 0.05	TE	[73]
Si(111)	–	–	?	1080–1600	–	4.1 ± 0.1	TE	[1662]
Si(111)[n]	–	–	?	~300	–	4.15	CPD	[4368]
Si(111)[p432]	–	–	?	~1150–1450	–	4.2	TE	[3540]
Si(111)	–	–	?	>1300	–	4.20	TE	[1510]
Si(111)	–	–	4×10^{-10}	~300	–	4.40 ± 0.05	PE	[1181,1227]
Si(111)	–	–	–	–	–	4.44	TC	[2688]
Si(111)[n64]	K	K$^+$	7×10^{-9}	850–1550	4.44 ± 0.1	(4.55 ± 0.1)	PSI	[74]
Si(111)[n67]	–	–	$<5 \times 10^{-11}$	60	–	4.5	PE	[2893]
Si(111)	–	–	–	–	–	4.5	TC	[300]
Si(111)	–	–	5×10^{-11}	~300	–	4.50	PE	[2865,3461]
Si(111)	–	–	$<5 \times 10^{-11}$	~300	–	4.50 ± 0.02	PE	[3109]
Si(111)	–	–	2×10^{-10}	?	(5.00, 5.23)	4.51 ± 0.05	TE	[75]
Si(111)[p]	–	–	?	~300	–	4.52	PE	[1229]
Si(111)	–	–	4×10^{-10}	~300	–	4.52 ± 0.03	PE	[1552]
Si(111)	–	–	$<4 \times 10^{-10}$	400	–	4.53	PE	[3708]
Si(111)	–	–	$\leq 4 \times 10^{-11}$	~300	–	4.53	PE	[1429,1430,2733]
Si(111)[p]	–	–	1×10^{-10}	~300 (1000)	–	4.55 ± 0.1	PE	[118]

Table 1 (*continued*)

Surface	Beam	Ion	P_r (Torr)	T (K)	ϕ^+ (eV)	ϕ^e (eV)	Meth.	Refs.
Si(111)	–	–	2×10^{-10}	?	(4.81 ± 0.05)	4.55 ± 0.05	TE	[75]
Si(111)	–	–	1×10^{-10}	~300 (?)	–	4.55 ± 0.1	PE	[118]
Si(111)[n]	–	–	7×10^{-9}	~1200–1500	(4.44–4.99)	4.55 ± 0.1	TE	[74]
Si(111)[n68]	–	–	$<3 \times 10^{-11}$	~300 (550)	–	4.56 ± 0.02	PE	[1228]
Si(111)[p]	–	–	2×10^{-10}	?	(4.76 ± 0.05)	4.58 ± 0.05	TE	[75]
Si(111)[n]	–	–	2×10^{-10}	?	(4.78 ± 0.05)	4.59 ± 0.05	TE	[75]
Si(111)	–	–	2×10^{-11}	~300	–	4.595	PE	[3196]
Si(111)[n]	–	–	3×10^{-10}	~300	–	4.6	CPD	[1959]
Si(111)	–	–	$<5 \times 10^{-10}$	~300	–	4.6	PE	[2795]
Si(111)	–	–	1×10^{-10}	298	–	4.6	PE	[1900,1906]
Si(111)	–	–	$\sim10^{-10}$	~300	–	4.60	PE	[2972]
Si(111)	–	–	$<1 \times 10^{-10}$	~300 (1100)	–	4.60 ± 0.03	PE	[1491,3950]
Si(111)[p]	–	–	$<4 \times 10^{-10}$	~300	–	4.60	PE	[3282]
Si(111)[p69]	–	–	1×10^{-10}	~300 (1000)	–	4.60 ± 0.13	CPD	[118]
Si(111)[p69]	–	–	1×10^{-10}	~300 (?)	–	4.60 ± 0.13	CPD	[118]
Si(111)[p,n]	–	–	$<10^{-9}$	1335	–	4.62	CPD	[119]
Si(111)[n]	–	–	5×10^{-11}	~300	–	4.63	PE	[2150]
Si(111)[n]	Na	Na$^+$	2×10^{-10}	?	4.63 ± 0.05	(4.59 ± 0.05)	PSI	[75]
Si(111)	–	–	–	–	–	4.64	TC	[4461][490]
Si(111)[n67]	–	–	3×10^{-11}	60	–	4.65	PE	[2660]
Si(111)[n]	–	–	$<4 \times 10^{-10}$	~300	–	4.65	PE	[3282]
Si(111)[p]	–	–	$<10^{-9}$	~300 (773)	–	4.66	CPD	[116]
Si(111)[n]	–	–	?	~300	–	4.66 ± 0.05	PE	[2776]
Si(111)	–	–	–	–	–	4.667	TC	[4460][490]
Si(111)[p]	–	–	$<10^{-9}$	~300 (773)	–	4.67	CPD	[116,1771]
Si(111)[n63]	K	K$^+$	7×10^{-9}	~850–1550	4.69 ± 0.1	(4.55 ± 0.1)	PSI	[74]
Si(111)[p]	–	–	3×10^{-10}	~300	–	4.7	CPD	[1959]
Si(111)[p,n]	–	–	5×10^{-11}	~300	–	4.7	PE	[2623,2625]
Si(111)	–	–	3×10^{-11}	~300	–	4.7 ± 0.1	PE	[2951]
Si(111)	–	–	–	–	–	4.71	TC	[2444]
Si(111)[p,n]	–	–	$<10^{-9}$	1638	–	4.72	CPD	[119]
Si(111)[p]	–	–	$\sim10^{-10}$	~300 (1550)	–	4.72	PE	[902]
Si(111)	–	–	$\sim10^{-10}$	~300	–	4.72	CPD	[3696]
Si(111)[n425]	–	–	$<10^{-10}$	~300	–	4.73 ± 0.07	CPD	[117,118]
Si(111)[n425]	–	–	$<10^{-10}$	~300	–	4.73 ± 0.07	PE	[117,118]
Si(111)[n68]	–	–	$<3 \times 10^{-11}$	~300 (800)	–	4.74 ± 0.02	PE	[1228]
Si(111)[p]	–	–	$\sim10^{-10}$	~300	–	4.74 ± 0.03	PE	[1851]
Si(111)[p]	–	–	$\leq10^{-9}$	~300 (1550)	–	4.74 ± 0.05	CPD	[1225,1387]
Si(111)[n63]	Li	Li$^+$	7×10^{-9}	~1000–1550	4.75 ± 0.03	(4.55 ± 0.1)	PSI	[74]
Si(111)[p]	–	–	$<10^{-9}$	~300	–	4.76	CPD	[116]
Si(111)[n]	–	–	$\sim10^{-10}$	~300	–	4.76	PE	[1388]
Si(111)[n]	–	–	5×10^{-10}	~300	–	4.76 ± 0.03	CPD	[3043]
Si(111)[p]	Na	Na$^+$	2×10^{-10}	?	4.76 ± 0.05	(4.58 ± 0.05)	PSI	[75]
Si(111)[p]	–	–	$<10^{-9}$	~300	–	4.77 ± 0.02	CPD	[116,1771]
Si(111)[p]	–	–	$\sim10^{-10}$	~300 (1600)	–	4.77 ± 0.05	PE	[1384]
Si(111)[n]	Na	Na$^+$	2×10^{-10}	?	4.78 ± 0.05	(4.59 ± 0.05)	PSI	[75]
Si(111)[n426]	–	–	$\sim10^{-10}$	~300	–	$4.79 \pm 0.02^*$	PE	[1889]
Si(111)[n64]	Tl	Tl$^+$	7×10^{-9}	~900–1550	4.79 ± 0.03	(4.55 ± 0.1)	PSI	[74]
Si(111)	–	–	3×10^{-11}	~300	–	4.8 ± 0.1	PE	[2951]
Si(111)	–	–	–	–	–	4.8	TC	[2731]
Si(111)	–	–	$\sim10^{-10}$	130	–	4.8	PE	[1817]
Si(111)[p]	K	K$^+$	?	1280	4.80	(4.1 ± 0.1)	PSI	[272]
Si(111)[n]	–	–	$<10^{-10}$	~300	–	4.80 ± 0.03	CPD	[117]
Si(111)[n66]	–	–	$\leq1 \times 10^{-7}$	1340–1600	(4.86–4.90)	$4.80 \pm 0.04^*$	TE	[72]
Si(111)[n64]	Na	Na$^+$	7×10^{-9}	~850–1550	4.80 ± 0.04	(4.55 ± 0.1)	PSI	[74]
Si(111)[n63]	Na	Na$^+$	7×10^{-9}	~850–1550	4.81 ± 0.02	(4.55 ± 0.1)	PSI	[74]
Si(111)	Na	Na$^+$	2×10^{-10}	?	4.81 ± 0.05	(4.55 ± 0.05)	PSI	[75]
Si(111)	–	–	–	–	–	4.811	TC	[4460][490]
Si(111)	–	–	1×10^{-10}	~300	–	4.82	PE	[1226]
Si(111)[n−p425]	–	–	$<10^{-10}$	~300	–	4.83	CPD	[117]
Si(111)	–	–	$\sim10^{-10}$	~300	–	4.83	PE	[3696]
Si(111)[p]	–	–	$<8 \times 10^{-11}$	~300 (1030)	–	4.83	CPD	[301]
Si(111)[p]	–	–	$\leq8 \times 10^{-11}$	~300	–	4.83	PE	[1904]
Si(111)[n68]	–	–	$<3 \times 10^{-11}$	~300	–	4.83 ± 0.02	PE	[1228]
Si(111)[p410]	–	–	$\leq1 \times 10^{-7}$	~1300–1600	(4.85–4.88)	$4.83 \pm 0.04^*$	TE	[73]
Si(111)[p]	–	–	$\sim10^{-10}$	~300	–	4.83 ± 0.05	CPD	[1396,1971]
Si(111)[p]	–	–	1×10^{-10}	~300	–	4.83 ± 0.07	CPD	[117]
Si(111)[n64]	Li	Li$^+$	7×10^{-9}	~1000–1550	4.84 ± 0.03	(4.55 ± 0.1)	PSI	[74]
Si(111)[n]	Na	Na$^+$	2×10^{-10}	?	4.84 ± 0.05	–	PSI	[75]
Si(111)[p66]	–	–	1×10^{-7}	1490–1510	(4.88 ± 0.10)	4.84 ± 0.14	CPD	[73]

Table 1 (*continued*)

Surface	Beam	Ion	P_r (Torr)	T (K)	ϕ^+ (eV)	ϕ^e (eV)	Meth.	Refs.
Si(111)[p]	–	–	?	~300	–	4.85	PE	[1229,3719]
Si(111)[p]	–	–	$<5 \times 10^{-11}$	~300	–	4.85 ± 0.02	PE	[2019,3109,3699]
Si(111)[p]	–	–	$<10^{-10}$	~300	–	4.85 ± 0.03	CPD	[117]
Si(111)	–	–	$\sim10^{-10}$	~300	–	4.85 ± 0.04	PE	[2151]
Si(111)[n]	–	–	5×10^{-11}	~300	–	4.85 ± 0.05	CPD	[613,636,3270]
Si(111)[p66]	Cs	Cs^{+}	1×10^{-7}	~1100–1600	4.85 ± 0.08	(4.86 ± 0.11)	PSI	[73]
Si(111)[p]	–	–	8×10^{-11}	~300 (1080)	–	4.850 ± 0.030	CPD	[301]
Si(111)	–	–	1×10^{-10}	~300	–	4.86	PE	[1551,3281]
Si(111)[n]	Li	Li^{+}	$\leq1 \times 10^{-7}$	1150–1620	4.86 ± 0.07	(4.04 ± 0.05)	PSI	[72]
Si(111)[p66]	–	–	1×10^{-7}	1490–1510	(4.85 ± 0.08)	4.86 ± 0.11	CPD	[73]
Si(111)	–	–	$<4 \times 10^{-10}$	~300	–	4.87	PE	[1566,3279]
Si(111)[n–p]	–	–	5×10^{-11}	~300	–	4.87 ± 0.02	PE	[1230,3589,3819]
Si(111)[n]	Na	Na^{+}	$\leq1 \times 10^{-7}$	1150–1620	4.87 ± 0.03	(4.04 ± 0.05)	PSI	[72]
Si(111)	–	–	$<5 \times 10^{-10}$	~300	–	4.88	PE	[1694]
Si(111)[p66]	Cs	Cs^{+}	1×10^{-7}	~1100–1600	4.88 ± 0.10	(4.84 ± 0.14)	PSI	[73]
Si(111)	–	–	–	–	–	4.889	TC	[4425]
Si(111)[n]	–	–	?	~300	–	4.89	PE	[2752]
Si(111)[p424]	–	–	1×10^{-10}	~300	–	4.9	PE	[1226]
Si(111)[n]	Cs	Cs^{+}	2×10^{-10}	~300	4.9 ± 0.1*	–	CPD	[609]
Si(111)[p]	–	–	$\sim10^{-10}$	~300	–	4.90	PE	[1388]
Si(111)[n]	In	In[+]	$\leq1 \times 10^{-7}$	1290–1620	4.90 ± 0.10	(4.04 ± 0.05)	PSI	[72]
Si(111)	–	–	–	–	–	4.902	TC	[4424]
Si(111)[p]	–	–	$<10^{-10}$	~300	–	4.92 ± 0.07	CPD	[117]
Si(111)[p]	–	–	$<10^{-10}$	~300	–	4.92 ± 0.07	PE	[117]
Si(111)[p426]	–	–	$\sim10^{-10}$	~300	–	4.97 ± 0.02*	PE	[1889]
Si(111)[n63]	Tl	Tl[+]	7×10^{-9}	~900–1550	4.99 ± 0.05	(4.55 ± 0.1)	PSI	[74]
Si(111)[n424]	–	–	1×10^{-10}	~300	–	5.0	PE	[1226]
Si(111)/W(100)	Si	–	$<5 \times 10^{-10}$	298 (613)	–	5.0	CPD	[355]
Si(111)	Na	Na^{+}	2×10^{-10}	?	5.00 ± 0.05	(4.51)	PSI	[75]
Si(111)[p67]	–	–	3×10^{-11}	~300	–	5.05	PE	[2660]
Si(111)[n67]	–	–	3×10^{-11}	~300	–	5.05	PE	[2660]
Si(111)[p]	Na	Na^{+}	?	1280	5.05	(4.1 ± 0.1)	PSI	[272]
Si(111)	–	–	–	–	–	5.05 ± 0.1	TC	[3549,3740]
Si(111)[p]	Na	Na^{+}	?	1380	5.06	(4.1 ± 0.1)	PSI	[272]
Si(111)[p]	–	–	2×10^{-10}	~300	–	5.10	PE	[1971]
Si(111)[p]	–	–	$<10^{-10}$	~300	–	5.15 ± 0.08	PE	[117]
Si(111)	–	–	$<5 \times 10^{-9}$	~300	–	5.18	PE	[3714]
Si(111)[p424]	–	–	1×10^{-10}	~300	–	5.2	PE	[1226]
Si(111)	Li	Li^{+}	2×10^{-10}	?	5.23 ± 0.05	(4.51 ± 0.05)	PSI	[75]
Si(111)[p67]	–	–	$<5 \times 10^{-11}$	60	–	5.4	PE	[2893]
Si(111)[p,n]	–	–	$<10^{-10}$	~300	–	5.4	PE	[3333]
Si(111)[p67]	–	–	3×10^{-11}	60	–	5.56	PE	[2660]
Si(111)	–	–	–	–	–	5.92	TC	[3151]
Si(111)	–	–	–	–	–	6.45	TC	[3151]
Recommended	–	–	–	–	**4.83 ± 0.07**	**4.86 ± 0.09**	–	–
Si(112)[p70]	–	–	?	~1250–1400	–	3.86 ± 0.05	TE	[1500]
Si(112)[n70]	–	–	?	~1250–1400	–	3.92 ± 0.05	TE	[1500]
Si(112)[p70]	–	–	?	~1400–1625	–	4.10 ± 0.05	TE	[1500]
Si(112)[p]	–	–	$\sim10^{-9}$	1265–1500	–	4.22 ± 0.05	TE	[635]
Si(112)[n70]	–	–	?	~1400–1625	–	4.4 ± 0.1	TE	[1500]
Si(112)	–	–	–	–	–	5.11	TC	[1627]
Recommended	–	–	–	–	–	**4.1 ± 0.2**	–	–
Si(541)[p70]	–	–	?	~1250–1400	–	3.67 ± 0.05	TE	[1500]
Si(541)[n70]	–	–	?	~1250–1400	–	3.74 ± 0.05	TE	[1500]
Si(541)[p70]	–	–	?	~1400–1625	–	4.17 ± 0.05	TE	[1500]
Si(541)[n70]	–	–	?	~1400–1625	–	4.3 ± 0.1	TE	[1500]
Recommended	–	–	–	–	–	**4.0 ± 0.3**	–	–
Si(???)	–	–	? (Cs)	~1300	–	3.9	TE	[1468]
Si(???)	–	–	$\leq3 \times 10^{-10}$	~1300–1700	–	3.96	TE	[1397]
Si(???)	–	–	?	~1200–1300	–	4.0	TE	[1468]
Si(???)	–	–	5×10^{-10}	~300	–	4.88	AI[38]	[1103]
Si/Mo(100)	Si	–	$<1 \times 10^{-10}$	295	–	3.2	FE	[1675]
Si/Mo(112)	Si	–	$<1 \times 10^{-10}$	295	–	3.4	FE	[1675]
Si	–	–	?	~1250–1700	–	3.59 ± 0.1	TE	[113]
Si	–	–	?	?	–	3.6	TE	[3402]
Si/Mo	Si	–	6×10^{-11}	~300 (1000)	–	3.81	FE	[3343]

Table 1 (*continued*)

Surface	Beam	Ion	P_r (Torr)	T (K)	ϕ^+ (eV)	ϕ^e (eV)	Meth.	Refs.
Si/W(100)	Si	–	$<3 \times 10^{-10}$	295	–	3.91	FE	[1671]
Si/W(111)	Si	–	$<3 \times 10^{-10}$	295	–	3.98	FE	[1671]
Si	–	–	$\sim10^{-10}$	?	–	4.0–4.3	TE	[1478]
Si	–	–	?	$\sim$1373–1623	–	4.02 ± 0.02	TE	[1308]
Si(nanowire)[71]	–	–	?	$\sim$300	–	4.13	PE	[2200]
Si[p]	–	–	?	$\sim$300	–	4.13 ± 0.05	CPD	[1309]
Si/Ba/W(110)[72]	Si	–	$<5 \times 10^{-10}$	$\sim$300	–	4.2–4.6	FE	[2013]
Si/W(112)	Si	–	$<3 \times 10^{-10}$	295	–	4.21	FE	[1671]
Si/Mo	Si	–	$<1 \times 10^{-10}$	295	–	4.23	FE	[1675]
Si/W(100)	Si	–	$<1 \times 10^{-10}$	295	–	4.26	FE	[1671]
Si	–	–	$\sim10^{-9}$	1265–1500	–	4.30 ± 0.03	TE	[635]
Si	–	–	–	–	–	4.35	TC	[298]
Si	–	–	?	$\sim$300	–	4.37–4.67	PE	[3609]
Si	–	–	–	–	–	4.4	TC	[1955]
Si/Si(111)[73]	Si	–	$\sim10^{-11}$	77	–	4.4 ± 0.1	PE	[2822]
Si[n][441]	–	–	–	–	–	4.42–4.63	TC	[4119]
Si[p]	–	–	$<2 \times 10^{-6}$	523	–	4.5	CPD	[1310]
Si[n]	–	–	$<2 \times 10^{-6}$	523	–	4.5	CPD	[1310]
Si[n]	–	–	?	$\sim$300	–	4.5 ± 0.1	CPD	[1600]
Si	–	–	–	–	–	4.56	TC	[1901]
Si[p]	–	–	$<2 \times 10^{-6}$	1023	–	4.6	CPD	[1310]
Si[n]	–	–	$<2 \times 10^{-6}$	1023	–	4.6	CPD	[1310]
Si	–	–	$<10^{-10}$	?	–	4.6	TE	[1492]
Si/W[76]	Si	–	2×10^{-10}	77 ($\leq$640)	–	4.6	FE	[2248]
Si/W(111)	Si	–	$<1 \times 10^{-10}$	295	–	4.66	FE	[1671]
Si/Mo	Si	–	$<1 \times 10^{-10}$	295	–	4.7	FE	[1675]
Si/W(110)	Si	–	$\leq5 \times 10^{-10}$	$\sim$300	–	4.7	FE	[2013]
Si/Ta(100)	Si	–	$<5 \times 10^{-11}$	$\sim$300	–	4.7	CPD	[3776]
Si/W[74]	–	–	–	–	–	4.7	TC	[913,4344]
Si/CoSi$_2$(111)	Si	–	?	$\sim$300	–	4.70 ± 0.05	PE	[2169]
Si/Co/CoSi$_2$(111)[75]	Si	–	?	$\sim$300	–	4.70 ± 0.05	PE	[2169]
Si/W[74]	Si	–	$<1 \times 10^{-10}$	295	–	4.72 ± 0.05	FE	[1231]
Si/W	Si	–	5×10^{-11}	$\sim$300 ($\leq$950)	–	4.77	FE	[3094]
Si/W[76]	Si	–	2×10^{-10}	77 ($\leq$525)	–	4.78 ± 0.06*	FE	[2248]
Si(amorphized)	–	–	$<3 \times 10^{-11}$	$\sim$300	–	478 ± 0.15	AI	[4055]
Si/W	Si	–	$<5 \times 10^{-10}$	298	–	4.8	CPD	[355]
Si	–	–	–	–	–	4.8	TC	[1993]
Si/W(110)	Si	–	$<1 \times 10^{-9}$	293	–	4.80	CPD	[1520]
Si[p](porous)	–	–	$<5 \times 10^{-9}$	$\sim$300	–	4.80–5.70	CPD	[1602]
Si/Si/W	Si	–	5×10^{-11}	$\sim$300 ($\leq$950)	–	4.82	FE	[3094]
Si/W(100)	Si	–	$\leq5 \times 10^{-10}$	298	–	4.82	CPD	[355]
Si/W(110)	Si	–	?	$\sim$300	–	4.83	PE	[3448]
Si[n][465]	–	–	5×10^{-11}	$\sim$300	–	4.85	CPD	[613]
Si	–	–	5×10^{-10}	$\sim$300	–	4.88	AI[38]	[1103]
Si/W(111)	Si	–	$\sim10^{-10}$	$\sim$300	–	4.9	FE	[818]
Si/W(100)	Si	–	?	$\sim$300	–	4.9	FE	[1438]
Si/W(111)	Si	–	$<1 \times 10^{-10}$	295	–	4.94	FE	[1671,2350]
Si	–	–	–	–	–	5.0	TC	[706]
Si/W(111)	Si	–	$\sim10^{-10}$	$\sim$300	–	5.0 ± 0.1	FE	[2713]
Si/W(116)	Si	–	$\sim10^{-10}$	$\sim$300	–	5.0 ± 0.1	FE	[2713]
Si/W(012)	Si	–	$\sim10^{-10}$	$\sim$300	–	5.0 ± 0.1	FE	[2713]
Si/W(013)	Si	–	$\sim10^{-10}$	$\sim$300	–	5.0 ± 0.1	FE	[2713]
Si/W	Si	–	$<3 \times 10^{-10}$	77	–	5.0 ± 0.1	FE	[4015]
Si/W(100)	Si	–	$<1 \times 10^{-10}$	295	–	5.01	FE	[1671,2350]
Si/W(100)	Si	–	$\sim10^{-10}$	613	–	5.02	CPD	[355]
Si[p][441]	–	–	–	–	–	5.03–5.10	TC	[4119]
Si/W(110)	Si	–	$<1 \times 10^{-10}$	295	–	5.06	FE	[1671]
Si	–	–	–	–	–	5.08	TC	[1744]
Si/W	Si	–	$\leq10^{-10}$	$\sim$300	–	5.1 ± 0.1	FE	[2712]
Si	Cs	Cs$^+$	?	$\sim$300	5.14*	–	CPD	[611]
Si/W(116)	Si	–	$<1 \times 10^{-10}$	295	–	5.15	FE	[1671,2350]
Si/Mo(112)	Si	–	$<1 \times 10^{-10}$	295	–	5.17	FE	[1675]
Si	–	–	–	–	–	5.17	TC	[4285]
Si/W(112)	Si	–	$<1 \times 10^{-10}$	295	–	5.30	FE	[1671,2350]
Si/Mo(100)	Si	–	$<1 \times 10^{-10}$	295	–	5.37	FE	[1675]
Si/W(112)	Si	–	$<1 \times 10^{-10}$	295	–	5.40	FE	[1671]
Si(tip)	–	–	$\sim10^{-10}$	$\sim$300	–	5.46	FE	[3072]
Si/W(113)	Si	–	$<1 \times 10^{-10}$	295	–	5.82	FE	[1671,2350]
Si/W(110)	Si	–	$<1 \times 10^{-10}$	295	–	5.82	FE	[1671,2350]

Table 1 (*continued*)

Surface	Beam	Ion	P_r (Torr)	T (K)	ϕ^+ (eV)	ϕ^e (eV)	Meth.	Refs.
Si/W(110)	Si	–	$<1 \times 10^{-10}$	295	–	5.90	FE	[1671]
Recommended	–	–	–	–	–	**4.65 ± 0.09**	–	–

15. Phosphorus P

P(111)	–	–	$\sim3 \times 10^{-10}$	~300	–	<1.34	CPD	[1681]
P(111)	–	–	$\sim3 \times 10^{-10}$	~300	–	1.41	CPD	[1681]
P	–	–	–	0	–	3.4–4.1	TC	[3034]
P	–	–	–	–	–	4.9	TC	[1905]
P	–	–	–	–	–	5.04	TC	[1901]
P	–	–	–	–	–	5.1	TC	[1955]
P/Fe(100)[427]	–	–	–	–	–	5.1*	TC	[4026]
Recommended	–	–	–	–	–	**5.0 ± 0.1**	–	–

16. Sulfur S

Film or Bulk (*α*, Rhombic, *T* < 370 K)

Surface	Beam	Ion	P_r (Torr)	T (K)	ϕ^+ (eV)	ϕ^e (eV)	Meth.	Refs.
S	–	–	–	0	–	3.9–4.5	TC	[3034]
S/Fe(110)	–	–	–	–	–	4.44	TC	[3236]
S/Fe(110)	–	–	–	–	–	4.66	TC	[3946,4337]
S/Fe(100)	–	–	–	–	–	4.71	TC	[4009]
S/Fe(110)[77]	–	–	–	–	–	4.98	TC	[4313]
S/Fe(110)[77]	–	–	–	–	–	4.999	TC	[4313]
S/Fe(100)[423]	–	–	–	–	–	5.0*	TC	[4019]
S/Ni	S_2	–	$\leq1 \times 10^{-10}$	77	–	5.0	FE	[1560]
S/Ni	S_2	–	$\leq1 \times 10^{-10}$	77 (530)	–	5.0	FE	[1560]
S/Si(100)	S_2	–	$<10^{-10}$	~300	–	5.0 ± 0.2*	CPD	[2890–2892]
S/Cu(111)	S_2	–	?	~470–870	–	5.067 ± 0.010	CPD	[948]
S/Cu(110)	S_2	–	?	~470–870	–	5.070 ± 0.010	CPD	[948]
S/Cu(210)	S_2	–	?	~470–870	–	5.075 ± 0.010	CPD	[948]
S/Cu(113)	S_2	–	?	~470–870	–	5.078 ± 0.010	CPD	[948]
S/Fe(110)[77]	–	–	–	–	–	5.08	TC	[4313]
S/Cu(112)	S_2	–	?	~470–870	–	5.083 ± 0.010	CPD	[948]
S/Ag(111)	S_2	–	?	~300	–	5.1*	CPD	[3118]
S/W	S_2	–	$<5 \times 10^{-10}$	~300 (≤770)	–	5.1	FE	[1524]
S/Ni	S_2	–	$<10^{-11}$	77	–	5.1	FE	[4017]
S/W(100)	S_2	–	$<2 \times 10^{-10}$	~300	–	5.1	CPD	[2854]
S/W(100)	S_2	–	$<2 \times 10^{-10}$	~300 (900)	–	5.1	CPD	[2854]
S/W(100)	H_2S	–	$<1 \times 10^{-10}$	~300 (900)	–	5.1	PE	[2669]
S/Ru(0001)	–	–	–	–	–	5.16	TC	[2554]
S/Cu(100)	S_2	–	?	~470–870	–	5.161 ± 0.010	CPD	[948]
S/Fe(110)	S_2	–	$\sim1 \times 10^{-10}$	~300 (1070)	–	5.2	PE	[1541]
S/W(310)	S_2	–	$\sim1 \times 10^{-10}$	~300 (570)	–	5.2	FE	[3438]
S/Fe(100)	–	–	–	–	–	5.2	TC	[1104]
S/Si(100)	–	–	–	–	–	5.2*	TC	[2062]
S/Mo(100)	H_2S	–	?	~300 (970)	–	5.2*	CPD	[3660]
S/Ru(001)	H_2S	–	$<2 \times 10^{-10}$	350	–	5.2 ± 0.2	PE	[2374]
S/Pd(111)[79]	S_2	–	?	550	–	5.20*	CPD	[2877]
S/Fe(100)[78]	–	–	2×10^{-9}	315 (970)	–	5.21 ± 0.03	PE	[565,3311]
S/Pd(111)[79]	S_2	–	?	~300	–	5.25*	CPD	[2877]
S/Fe(100)[78]	–	–	2×10^{-9}	315 (970)	–	5.26	PE	[565,3311]
S/Ni(110)	H_2S	–	$<1 \times 10^{-10}$	~300 (≥1070)	–	5.29	CPD	[1110]
S/W	S_2	–	0.1 (S_2)	~2200	–	5.3	TE	[394]
S/Fe(100)	–	–	–	–	–	5.3	TC	[1104]
S/Si(100)[n]	S_2	–	$\sim10^{-10}$	~300	–	5.30	PE	[4125]
S/Fe(100)	–	–	–	–	–	5.31	TC	[1708,1710]
S/Pd(111)[79]	S_2	–	?	100	–	5.31*	CPD	[2877]
S/Fe(100)	S_2	–	$<8 \times 10^{-11}$	673	–	5.33 ± 0.05*	CPD	[4324]
S/W(100)	S_2	–	$\sim1 \times 10^{-10}$	~300 (570)	–	5.4	FE	[3438]
S/W(111)	S_2	–	$\sim1 \times 10^{-10}$	~300 (570)	–	5.4	FE	[3438]
S/Ni(111)	H_2S	–	$<5 \times 10^{-10}$	~300 (~450)	–	5.4*	CPD	[1790]
S/Rh(100)	–	–	–	–	–	5.4 ± <0.2	TC	[1909]
S/Fe(100)	S_2	–	$<8 \times 10^{-11}$	~300	–	5.40 ± 0.05	CPD	[4324]
S/Ni(100)	H_2S	–	$<5 \times 10^{-10}$	~300 (~450)	–	5.45 ± 0.10*	CPD	[1790]
S/Fe(100)	–	–	–	–	–	5.47 ± 0.05*	TC	[4009]
S/W	S_2	–	$<5 \times 10^{-10}$	~300	–	5.5	FE	[1524]
S/W(110)	S_2	–	$<2 \times 10^{-10}$	~300	–	5.5	CPD	[2856]
S/W(110)	S_2	–	$<2 \times 10^{-10}$	~900	–	5.5	CPD	[2856]

Table 1 (*continued*)

Surface	Beam	Ion	P_r (Torr)	T (K)	ϕ^+ (eV)	ϕ^e (eV)	Meth.	Refs.
S/W	S_2	–	~10^{-5} (S_2)	~1700	–	5.5	TE	[394]
S/Fe(100)[427]	–	–	–	–	–	5.5	TC	[1104,4026]
S/Ni(100)	S_2	–	<10^{-10}	~300	–	5.5*	CPD	[2889]
S/Ni(100)	?	–	?	?	–	5.5 ± 0.1*	?	[3355]
S/Mo(100)	H_2S	–	≤10^{-5} (H_2S)	1450	–	5.5 ± 0.1	TE	[784]
S/Cu(111)	–	–	–	–	–	5.53*	TC	[2699]
S/Mo(100)	–	–	–	–	–	5.6	TC	[3457]
S/Ni(100)	?	–	?	?	–	5.6 ± 0.1*	?	[3355]
S/Ni(100)	–	–	–	–	–	5.65	TC	[1918]
S/Ni(111)	H_2S	–	<1×10^{-10}	~300 (≥1070)	–	5.65	CPD	[1110]
S/Ta(112)	–	–	<2×10^{-9}	~1300–1500	–	5.7	TE	[802]
S/Ni(100)	–	–	–	–	–	5.7 ± 0.1*	TC	[2976]
S	–	–	–	–	–	5.7 ± 0.1	TC	[1905]
S/Ni(100)	H_2S	–	<1×10^{-10}	~300 (≥1070)	–	5.73	CPD	[1110]
S	–	–	–	–	–	5.74	TC	[1901]
S/Fe(100)[423]	–	–	–	–	–	5.8*	TC	[4019]
S/Rh(111)	S_2	–	~10^{-10}	~300	–	6.0*	CPD	[1910]
S	–	–	–	–	–	6.0	TC	[1955]
S	–	–	–	–	–	6.02	TC	[3512]
S/W(110)	S_2	–	~1×10^{-10}	~300 (570)	–	6.2	FE	[3438]
S/Ag(111)	–	–	–	–	–	6.25*	TC	[2699]
S/Fe(100)[423]	–	–	–	–	–	6.5*	TC	[4019]
Recommended	–	–	–	–	–	**5.31 ± 0.08**	–	–

19. Potassium K

bcc

Surface	Beam	Ion	P_r (Torr)	T (K)	ϕ^+ (eV)	ϕ^e (eV)	Meth.	Refs.
K(100)	–	–	–	–	–	2.03	TC	[1254]
K(100)	–	–	–	–	–	2.21	TC	[231]
K(100)	–	–	–	–	–	2.214	TC	[2947]
K(100)	–	–	–	–	–	2.224	TC	[4091]
K(100)	–	–	–	–	–	2.25	TC	[2427]
K(100)	–	–	–	–	–	2.25	TC	[1159,3067]
K(100)	–	–	–	–	–	2.26	TC	[3467]
K(100)	–	–	–	–	–	2.27	TC	[553]
K(100)/KF(100)[80]	K	–	<5×10^{-10}	0^E	–	2.33 ± 0.05	PE	[2946]
K(100)	–	–	–	–	–	2.34	TC	[334]
K(100)	–	–	–	–	–	2.39	TC	[1547]
K(100)	–	–	–	–	–	2.40	TC	[475]
K(100)	–	–	–	–	–	2.43	TC	[711]
K(100)	–	–	–	–	–	2.49	TC	[321]
K(100)	–	–	–	–	–	2.50	TC	[1557]
K(100)	–	–	–	–	–	2.51	TC	[1030]
K(100)	–	–	–	–	–	2.55	TC	[3814]
K(100)	–	–	–	–	–	2.59	TC	[472]
K(100)	–	–	–	–	–	2.60	TC	[711]
K(100)	–	–	–	–	–	2.60	TC	[476]
K(100)	–	–	–	–	–	2.68	TC	[476]
K(100)	–	–	–	–	–	2.7	TC	[1088]
K(100)	–	–	–	–	–	2.71	TC	[1030]
K(100)	–	–	–	–	–	2.8	TC	[763]
K(100)	–	–	–	–	–	2.80	TC	[1095]
Recommended	–	–	–	–	–	**2.47 ± 0.04**	–	–
K(110)	–	–	–	–	–	2.13	TC	[2685]
K(110)	–	–	–	–	–	2.278	TC	[2947]
K(110)	–	–	–	–	–	2.35	TC	[1159,3067]
K(110)	–	–	–	–	–	2.37	TC	[231]
K(110)	–	–	–	–	–	2.372	TC	[4091]
K(110)	–	–	–	–	–	2.38	TC	[334,3179]
K(110)/glass	K	–	<5×10^{-9}	286–330	–	2.39 ± 0.01	PE	[2476]
K(110)/NaCl(100)[80]	K	–	<5×10^{-10}	0^E	–	2.41 ± 0.05	PE	[2946]
K(110)	–	–	–	–	–	2.42	TC	[2427]
K(110)	–	–	–	–	–	2.43	TC	[3467]
K(110)	–	–	–	–	–	2.44	TC	[553]
K(110)	–	–	–	–	–	2.57	TC	[1086]
K(110)	–	–	–	–	–	2.58	TC	[711]
K(110)	–	–	–	–	–	2.64	TC	[2835]
K(110)	–	–	–	–	–	2.7	TC	[1088]
K(110)	–	–	–	–	–	2.7	TC	[3137]

Table 1 (*continued*)

Surface	Beam	Ion	P_r (Torr)	T (K)	ϕ^+ (eV)	ϕ^e (eV)	Meth.	Refs.
K(110)	–	–	–	–	–	2.7	TC	[1086]
K(110)	–	–	–	–	–	2.72	TC	[1030]
K(110)	–	–	–	–	–	2.74	TC	[1086]
K(110)	–	–	–	–	–	2.74	TC	[2402]
K(110)	–	–	–	–	–	2.75	TC	[476,711]
K(110)	–	–	–	–	–	2.75	TC	[475]
K(110)	–	–	–	–	–	2.75	TC	[2835]
K(110)	–	–	–	–	–	2.76	TC	[472]
K(110)	–	–	–	–	–	2.790	TC	[4069]
K(110)	–	–	–	–	–	2.80	TC	[593]
K(110)	–	–	–	–	–	2.82	TC	[476]
K(110)	–	–	–	–	–	2.83	TC	[1087]
K(110)	–	–	–	–	–	2.84	TC	[3693]
K(110)	–	–	–	–	–	2.86	TC	[3713]
K(110)	–	–	–	–	–	2.9	TC	[1088]
K(110)	–	–	–	–	–	2.9	TC	[1086]
K(110)	–	–	–	–	–	2.90	TC	[321]
K(110)	–	–	–	–	–	2.94	TC	[1086]
K(110)	–	–	–	–	–	2.95	TC	[1086]
K(110)	–	–	–	–	–	2.96	TC	[3814]
K(110)	–	–	–	–	–	2.97	TC	[3692]
K(110)	–	–	–	–	–	3.01	TC	[1030,1089]
K(110)	–	–	–	–	–	3.02	TC	[3693]
K(110)	–	–	–	–	–	3.03	TC	[3712]
K(110)	–	–	–	–	–	3.03	TC	[3713]
K(110)	–	–	–	–	–	3.06	TC	[1089]
K(110)	–	–	–	–	–	3.07	TC	[1086]
K(110)	–	–	–	–	–	3.09	TC	[1086]
K(110)	–	–	–	–	–	3.10	TC	[1089]
K(110)	–	–	–	–	–	3.15	TC	[1095]
K(110)	–	–	–	–	–	3.15	TC	[3692]
K(110)	–	–	–	–	–	3.2	TC	[763]
K(110)	–	–	–	–	–	5.14	TC	[3622]
Recommended	–	–	–	–	–	**2.74 ± 0.04**	–	–
K(111)/Au/Si(111)[419]	K	–	~10^{-10}	~300	–	2.0	PE	[3999]
K(111)	–	–	–	–	–	2.17	TC	[231]
K(111)	–	–	–	–	–	2.18	TC	[4091]
K(111)	–	–	–	–	–	2.19	TC	[553]
K(111)	–	–	–	–	–	2.21	TC	[3467]
K(111)	–	–	–	–	–	2.21	TC	[711]
K(111)	–	–	–	–	–	2.24	TC	[1159,3067]
K(111)	–	–	–	–	–	2.35	TC	[475]
K(111)	–	–	–	–	–	2.38	TC	[476,711]
K(111)	–	–	–	–	–	2.39	TC	[1030]
K(111)	–	–	–	–	–	2.39	TC	[321]
K(111)	–	–	–	–	–	2.40	TC	[593]
K(111)	–	–	–	–	–	2.40	TC	[3814]
K(111)	–	–	–	–	–	2.42	TC	[472]
K(111)	–	–	–	–	–	2.45	TC	[1030]
K(111)	–	–	–	–	–	2.47	TC	[1557]
K(111)	–	–	–	–	–	2.48	TC	[476]
K(111)	–	–	–	–	–	2.5	TC	[1088]
K(111)/C$_{12}$/Au/ Si(111)[419]	K	–	~10^{-10}	~300	–	2.66	PE	[3999]
K(111)	–	–	–	–	–	2.75	TC	[1095]
Recommended	–	–	–	–	–	**2.39 ± 0.02**	–	–
K(112)	–	–	–	–	–	2.65	TC	[321]
K	–	–	–	–	–	1.05	TC	[2704]
K/NiO(100)	K	–	<1×10^{-10}	~300	–	1.3 ± 0.2	CPD	[2401]
K/Si(100)	–	–	–	–	–	1.4*	TC	[2406]
K/Si(100)	K	–	<4×10^{-11}	~300	–	1.4*	PE	[3709]
K/Si(100)	–	–	–	–	–	1.5*	TC	[3665]
K/Ge(100)	K$^+$	–	1×10^{-10}	~300	–	1.5	CPD	[3423]
K/Si(100)	K	–	~10^{-11}	295	–	1.5*	PE	[2274,2276]
K/Si(100)	K	–	<3×10^{-10}	~300	–	1.50*	CPD	[1929]
K/Si(100)	K	–	<6×10^{-11}	~300	–	1.57*	CPD	[2433]
K/Si(111)[221]	K	–	~10^{-9}	~300	–	1.6*	PE	[1823]

Table 1 (*continued*)

Surface	Beam	Ion	P_r (Torr)	T (K)	ϕ^+ (eV)	ϕ^e (eV)	Meth.	Refs.
K/Pt	K	–	?	~300	–	1.6	PE	[2206]
K/Si(100)	K	–	?	~300	–	1.6*	PE	[2994]
K/Si(111)	K	–	~10^{-11}	~300	–	1.6*	PE	[3685]
K	–	–	–	~300	–	1.6	TC	[3737]
K/Cu(100)	–	–	–	–	–	1.6*	TC	[3810]
K/Si(100)	K	–	5×10^{-11}	~300	–	1.6	PE	[1868,1869]
K/Si(100)	K	–	3×10^{-11}	~300	–	1.6	PE	[1872]
K	–	–	?	~300	–	1.60	CPD	[2297]
K/Pt	K	–	1×10^{-8}	273	–	1.61	CPD	[2083]
K/W	K	–	?	~300	–	1.66*	CPD	[1459]
K/Si(100)	K	–	$\leq 1 \times 10^{-10}$	~300	–	1.7	PE	[3191]
K/TiO$_2$(110)	K	–	4×10^{-11}	~300	–	1.70	PE	[2192]
K/Si(100)	K	–	$<3 \times 10^{-10}$	~300	–	1.70*	CPD	[1929]
K/Si(100)	–	–	–	–	–	1.75*	TC	[2399]
K/Si(100)	K	–	$<10^{-10}$	~300	–	1.75*	CPD	[2885]
K/Pt(111)	K	–	?	95	–	1.8	PE	[859]
K/Si(100)	K	–	?	~300	–	1.8*	PE	[2741]
K/Pt(111)	K	–	8×10^{-11}	~300	–	1.8	PE	[427,1584,2863]
K/W(100)	K	–	?	~300	–	1.8	PE	[1697]
K/TiO$_2$(110)	K	–	8×10^{-11}	~300	–	1.8	PE	[3188]
K/W(110)	K	–	$\leq 1 \times 10^{-10}$	~300	–	1.8	PE	[3191]
K/Si(111)	K	–	2×10^{-11}	~300	–	1.8	PE	[3196]
K/Si(111)	K	–	3×10^{-11}	~300	–	1.8*	CPD	[3470]
K/Si(111)	K	–	$<8 \times 10^{-11}$	~300	–	1.8*	PE	[2991]
K/Si(111)	K	–	4×10^{-10}	~300	–	1.8*	CPD	[2781]
K/Si(100)	K	–	5×10^{-11}	273	–	1.8*	PE	[2882]
K/Si(111)	K	–	?	~300	–	1.8*	CPD	[1587]
K/Si(100)	–	–	–	–	–	1.8*	TC	[2339]
K/Si(111)	K$^+$	–	1×10^{-10}	~300	–	1.80	CPD	[3423]
K/Ge(111)	K$^+$	–	1×10^{-10}	~300	–	1.82	CPD	[3422,3423]
K/Pt(111)	K	–	1×10^{-10}	~300	–	1.9	PE	[3989]
K/Si(100)	K	–	2×10^{-10}	~300	–	1.9*	CPD	[2785]
K/Si(100)	K	–	$<8 \times 10^{-11}$	250 (~300)	–	1.9*	PE	[2677]
K/Pt(111)	K	–	~10^{-10}	~300	–	1.9	PE	[1565]
K/Pt(111)	K	–	$\leq 1 \times 10^{-10}$	~300	–	1.9	PE	[3191]
K/W(110)	K	–	?	78 (400)	–	1.9	FE	[267,3818]
K/Si(111)	K	–	5×10^{-11}	~300	–	1.9*	PE	[3464,3465]
K/Rh(111)	–	–	–	–	–	1.925	TC	[4008]
K/W	K	–	?	375	–	1.95	FE	[3859]
K/Si(111)	K	–	$<6 \times 10^{-11}$	~300	–	1.96*	CPD	[2433]
K/TiO$_2$(110)	K	–	4×10^{-11}	~300	–	1.97	PE	[2192]
K/Au/Si(111)[419]	K	–	~10^{-10}	~300	–	2.0	PE	[3999]
K/Ni	K	–	~1×10^{-10}	78 (242)	–	2.0	FE	[1570]
K/Pd(111)	K	–	$<10^{-10}$	100 (450)	–	2.0	PE	[3817]
K/W(110)[81]	–	–	–	–	–	2.0	TC	[267,3818]
K/Si(100)	K	–	?	~300	–	2.0*	PE	[2741]
K/Co	K	–	?	320	–	2.0*	PE	[3373]
K/Pt(111)	K	–	2×10^{-10}	~300	–	2.0	PE	[3455]
K/ZrC(111)	K	–	$<4 \times 10^{-10}$	~300	–	2.0	PE	[2800]
K/Si(100)	–	–	–	–	–	2.0*	TC	[2224]
K/?	K	–	?	?	–	2.0	PE	[2231]
K/W(100)	K$^+$	–	~10^{-10}	~300	–	2.01	CPD	[506]
K	–	–	–	–	–	2.03	TC	[1254]
K/Pt	K	–	1×10^{-8}	195	–	2.03	CPD	[2083]
K/Ag(111)	K	–	4×10^{-10}	100	–	2.04	PE	[1579,2988]
K	–	–	–	–	–	2.05	TC	[1150]
K/W(110)[82]	K	–	$<1 \times 10^{-11}$	78	–	2.05*	FE	[373]
K	–	–	–	–	–	2.07	TC	[4031]
K/W(111)	K	–	~3×10^{-9}	~300	–	2.08	FE	[2766]
K	–	–	–	–	–	2.09	TC	[1951]
K	–	–	–	0	–	2.09	TC	[4419]
K/W(111)	K	–	?	78 (400)	–	2.1	FE	[267]
K/W(112)	K	–	?	78 (400)	–	2.1	FE	[267]
K/W	K	–	?	78 (400)	–	2.1	FE	[267]
K/NbC(100)	K	–	$<5 \times 10^{-10}$	~300	–	2.1	PE	[2796,2797]
K/W(111)	–	–	–	–	–	2.1	TC	[509]
K/Fe(110)	–	–	–	–	–	2.1*	TC	[3663]
K/Cu(110)	K	–	?	~300	–	2.1	PE	[1242]
K/Si(100)	K	–	4×10^{-10}	~300	–	2.1*	CPD	[2781]
K/Ag(100)	K	–	?	~300	–	2.10	PE	[2740]

Table 1 (*continued*)

Surface	Beam	Ion	P_r (Torr)	T (K)	ϕ^+ (eV)	ϕ^e (eV)	Meth.	Refs.
K/Ag(111)	K	–	1×10^{-10}	~300	–	2.10	CPD	[2867]
K	–	–	–	–	–	2.11	TC	[1066]
K/Cu(100)	K	–	1×10^{-11}	123	–	2.11 ± 0.02	PE	[3900]
K/W(100)	K	–	3×10^{-9}	~300	–	2.12	FE	[2766]
K/Ag	K	–	?	20, 80	–	2.12	PE	[3028]
K/Ag/glass[83]	K	–	$<10^{-8}$	~300	–	2.12	CPD	[1456]
K/Cu(119)	K	–	1×10^{-11}	123	–	2.12 ± 0.02*	PE	[3900]
K	–	–	–	–	–	2.13	TC	[4031]
K/quartz	K	–	?	82	–	2.137 ± 0.003	PE	[1961]
K/W(112)	–	–	–	–	–	2.14*	TC	[2978]
K/Mo	K	–	$<1 \times 10^{-11}$	78	–	2.14	FE	[648]
K/Ge(100)	K	–	$<1 \times 10^{-10}$	78	–	2.14	FE	[1550,3164]
K/Rh(111)	–	–	–	–	–	2.149	TC	[4008]
K/W	K	–	$<10^{-11}$	78	–	2.15	FE	[267]
K/W(111)	K	–	$<1 \times 10^{-11}$	78	–	2.15 ± 0.05	FE	[373]
K/W	K	–	?	~300	–	2.15 ± 0.05	PE	[3797]
K/Ag/glass[83]	K	–	$<10^{-8}$	~300	–	2.16	CPD	[1456]
K/Ge(111)	K	–	$<1 \times 10^{-10}$	78	–	2.16	FE	[1550,3164]
K/GaAs(110)	K	–	$<1 \times 10^{-10}$	~300	–	2.16	CPD	[2793]
K/Ag(100)	K	–	8×10^{-11}	125–150	–	2.17	CPD	[2790]
K/Ag/glass[83]	K	–	$<10^{-8}$	~300	–	2.17 ± 0.05*	CPD	[1456]
K/quartz	K	–	?	206	–	2.177 ± 0.004	PE	[1960,1961]
K/W	K	–	3×10^{-9}	~300	–	2.18	FE	[2766]
K(fp)	–	–	?	279	–	2.18	PE	[4256]
K/Re	K	–	$<10^{-10}$	~300	–	2.18 ± 0.05	FE	[1800]
K	–	–	–	–	–	2.2	TC	[1955]
K/Si(100)	K	–	?	200	–	2.2	CPD	[2783]
K/W	K	–	?	295	–	2.2	FE	[3859]
K/Si(100)[422]	K	–	2×10^{-10}	~300	–	2.2	CPD	[4016]
K/Mg(0001)	–	–	–	–	–	2.2	TC	[2438]
K/Al(100)	K	–	1×10^{-10}	100	–	2.2	CPD	[2875]
K/W	K	–	$(<10^{-10})$	77	–	2.2	FE	[2709]
K/Ru(001)	K	–	?	~300	–	2.2*	CPD	[2984]
K/quartz	K	–	$\sim 10^{-10}$	90	–	2.2	PE	[2605]
K/C/Fe–Cu	K	–	$\sim 10^{-8}$	873–973	–	2.2	TE	[764]
K/Rh(111)	K	–	1×10^{-10}	~300	–	2.2	PE	[568,2282]
K/Fe(110)	K	–	1×10^{-10}	~300	–	2.2	PE	[1232]
K/TiO$_2$(100)	K	–	4×10^{-11}	~300	–	2.2 ± 0.1	PE	[1717]
K/Cu(100)	K	–	$<5 \times 10^{-11}$	120	–	2.2 ± 0.1*	CPD	[1819]
K/C(100)	K	–	$<2 \times 10^{-10}$	90, 300	–	2.2 ± 0.2*	CPD	[2197]
K/Ta(111)	K	–	$<1 \times 10^{-11}$	78	–	2.20	FE	[648]
K/Mo(100)	K	–	$<1 \times 10^{-11}$	78	–	2.20	FE	[648]
K/W	K	–	$<1 \times 10^{-11}$	78	–	2.20	FE	[373]
K/Ru(0001)	K	–	3×10^{-10}	295	–	2.20	CPD	[1822]
K	–	–	–	–	–	2.20	TC	[3725]
K/Ni	K	–	$\leq 4 \times 10^{-7}$	~300	–	2.20	PE	[1765]
K	–	–	–	–	–	2.21	TC	[3728]
K/W(112)	K	–	$\sim 3 \times 10^{-9}$	~300	–	2.21	FE	[2766]
K/W(100)	K	–	?	78	–	2.21	CPD	[3981]
K/quartz	K	–	?	~300	–	2.216 ± 0.004	PE	[1960,1961]
K/Ni	K	–	$<10^{-9}$	77	–	2.24	CPD	[2139,3128,3698]
K/W	K	–	$<5 \times 10^{-8}$	77 (400)	–	2.24	FE	[267,269]
K/Ag/glass	K	–	$\sim 10^{-8}$	~80	–	2.24	PE	[1452]
K/Ag/glass[83]	K	–	$<10^{-8}$	~300	–	2.24	CPD	[1456]
K/?	K	–	?	?	–	2.24	?	[3785]
K/W(112)	–	–	–	–	–	2.25	TC	[267]
K/Ru(001)	K	–	1×10^{-10}	100	–	2.25	PE	[529]
K/Pd(100)	K	–	?	80	–	2.25	PE	[3176]
K/Ru(1010)	K	–	3×10^{-10}	430	–	2.25	CPD	[2161]
K/Mo(112)	K	–	$<1 \times 10^{-11}$	78	–	2.25	FE	[648]
K/glass	K	–	$\sim 10^{-9}$	82	–	2.25	PE	[2576]
K/Ta	K	–	$<1 \times 10^{-11}$	78	–	2.26	FE	[648]
K/Si(100)	K	–	1×10^{-10}	70	–	2.26	PE	[2190]
K	–	–	?	~300	–	2.26	PE	[2614]
K/Re(001)	K	–	2×10^{-10}	100	–	2.26	CPD	[513,3378]
K/Si(100)	K	–	5×10^{-11}	60, 273	–	2.26	PE	[1715]
K/Ta(110)	K$^+$	–	$\sim 10^{-10}$	~300	–	2.26	CPD	[506]
K	–	–	10^{-9}	298	–	2.26	PE	[2612–2614]
K/Pt	K	–	2×10^{-6}	~300	–	2.26 ± 0.02	PE	[2562]
K/Cu(111)	K	–	5×10^{-11}	~300	–	2.26 ± 0.03	PE	[1926]

Table 1 (*continued*)

Surface	Beam	Ion	P_r (Torr)	T (K)	ϕ^+ (eV)	ϕ^e (eV)	Meth.	Refs.
K	–	–	$\sim 10^{-9}$	335	–	2.27	PE	[4241]
K/metal	K	–	$\leq 4 \times 10^{-7}$	~300	–	2.27 ± 0.03	PE	[1765]
K/W(112)	K	–	$<1 \times 10^{-11}$	78	–	2.27 ± 0.05	FE	[373]
K	–	–	–	–	–	2.28	TC	[3477]
K	–	–	–	–	–	2.28	TC	[3352]
K(cluster)	–	–	–	–	–	2.28	TC	[3479]
K	–	–	–	–	–	2.28	TC	[4150]
$K_n (n \to \infty)$	–	–	?	~300	–	2.28	IP	[4161]
K(fp)[42]	–	–	?	?	–	2.28 ± 0.05	PE	[3482]
K/Pt(111)	K	–	$<3 \times 10^{-10}$	~300	–	2.29	PE	[2529]
K	–	–	$\sim 10^{-9}$	183	–	2.29	PE	[2612,2613]
K	–	–	–	–	–	2.29	TC	[3312]
$K_n (n \to \infty)$	–	–	–	–	–	2.29	TC	[4244]
K/graphite[464]	–	–	–	–	–	2.29*	TC	[4211]
$K_n (n \to \infty)$	–	–	?	195–395	–	2.29	PE	[4227]
K[156]	–	–	$<10^{-8}$	298	–	2.29 ± 0.03	PE	[2470,4208]
K/glass	K	–	$\leq 5 \times 10^{-9}$	298	–	2.29 ± 0.015	PE	[2476]
K/W	K	–	?	4.2, 21	–	2.3	FE	[3065]
K/Ni(111)	K	–	5×10^{-11}	120	–	2.3*	CPD	[3806]
K/Mo(112)	–	–	–	–	–	2.3	TC	[509]
K	–	–	–	–	–	2.3	TC	[706]
K/?	K	–	$<8 \times 10^{-11}$	77	–	2.3	PE	[3675]
K/Ni(100)	K	–	2×10^{-10}	120	–	2.3	PE	[2505]
K/Si(100)[422]	K	–	2×10^{-10}	~300	–	2.3*	CPD	[4016]
K/Al(111)	–	–	–	–	–	2.3	TC	[2223]
K/Fe(111)	K	–	$<10^{-10}$	~300	–	2.3*	CPD	[1865,2497]
K/Au(100)	K	–	$\sim 10^{-10}$	130, 300	–	2.3	CPD	[3202]
K/Ru(001)	K	–	5×10^{-11}	80	–	2.3	CPD	[1815]
K/Re(1010)	K	–	$\leq 10^{-11}$	77	–	2.3	CPD	[2503]
K	–	–	–	–	–	2.3	TC	[1993]
K/Rh(100)	K	–	$<1 \times 10^{-10}$	100	–	2.3	CPD	[3456]
K/Cu(110)	K	–	5×10^{-11}	140	–	2.3 ± 0.1	PE	[3454]
K/Cu, Ag	K	–	2×10^{-8}	~300	–	2.3 ± 0.1	PE	[3081]
K/C(0001)	K	–	3×10^{-10}	83–160	–	2.3 ± 0.1	CPD	[2801][488]
K/Ta(100)	K	–	$<1 \times 10^{-11}$	78	–	2.30	FE	[648]
K/Ta(112)	K	–	$<1 \times 10^{-11}$	78	–	2.30	FE	[648]
K	–	–	–	–	–	2.30	TC	[3467]
$K_n (n \to \infty)$	–	–	?	~300	–	2.30	IP,TC	[4197]
$K_n (n \to \infty)$	–	–	–	–	–	2.30	TC	[4244]
K/Pt	K	–	1×10^{-8}	85	–	2.30	CPD	[2083]
K/Mo	K	–	$\sim 10^{-10}$	~300	–	2.30 ± 0.02	PE	[3337]
K/Fe(110)	K	–	5×10^{-11}	~300	–	2.32 ± 0.03	PE	[1926]
K	–	–	–	–	–	2.33	TC	[298]
K/W(100)	K	–	$<1 \times 10^{-11}$	78	–	2.34	FE	[373]
K/graphite	–	–	–	–	–	2.35*	TC	[1843]
K/NbC(111)	K	–	$\leq 1 \times 10^{-10}$	~300	–	2.35	PE	[2797]
K/graphite[464]	–	–	–	–	–	2.36	TC	[4211]
K/Au(100)	K	–	$\sim 10^{-11}$	130, 300	–	2.37	CPD	[2746]
K/Mo	K	–	$\sim 10^{-10}$	80 (293)	–	2.38	PE	[3337]
K	–	–	–	–	–	2.38	TC	[3312]
K	–	–	–	–	–	2.38	TC	[4031]
K/Mo(112)	K	–	$(\leq 10^{-11})$	77	–	2.38	CPD	[2031]
K/glass	K	–	$\leq 3 \times 10^{-11}$	77	–	2.38 ± 0.01	PE	[2615]
K/glass	K	–	$\sim 10^{-10}$	77	–	2.39 ± 0.01	PE	[1481,1489]
K/Si(111)	K	–	3×10^{-10}	90	–	2.4*	PE	[2801]
K/Cu(111)	K	–	3×10^{-10}	90	–	2.4*	PE	[2801]
K/Au(111)	K	–	?	~300	–	2.4	PE	[1297]
K/cnt/Al_2O_3	K	–	5×10^{-8}	~300 (340)	–	2.4	PE	[4373]
K/Ni	K	–	$\sim 1 \times 10^{-10}$	78 (242)	–	2.4*	FE	[1570]
K/Re(1010)	K	–	$(\leq 1 \times 10^{-10})$	~300	–	2.4	CPD	[2490]
K/Ni(100)	K	–	?	20	–	2.4*	PE	[3662]
K/Ni(100)	K	–	?	20 (150)	–	2.4*	PE	[3662]
K/Ag(111)	K	–	1×10^{-10}	≤ 300	–	2.4	CPD	[1907]
K/Cu(100)	K	–	?	110	–	2.4*	PE	[3155]
K/Ta(100)	–	–	–	–	–	2.4	TC	[509]
K/Al(111)	K	–	?	100	–	2.4*	PE	[3629]
K/Si(100)ⁿ	K	–	8×10^{-11}	55, 273	–	2.4	PE	[2668]
K/Ru(001)	K	–	$<2 \times 10^{-10}$	85	–	2.4	CPD	[2176]
K/Cu(111)	K	–	$\sim 10^{-11}$	~300	–	2.4*	PE	[1825]
K/Ru(001)	K	–	$\sim 1 \times 10^{-10}$	85	–	2.4	CPD	[1818]

Table 1 (*continued*)

Surface	Beam	Ion	P_r (Torr)	T (K)	ϕ^+ (eV)	ϕ^e (eV)	Meth.	Refs.
K/Rh(111)	K	–	$\leq 5 \times 10^{-10}$	45	–	2.4	PE	[1128]
K/Pd(100)	K	–	$<2 \times 10^{-10}$	250	–	2.4*	CPD	[1574]
K/Ru(001)	K	–	4×10^{-11}	120	–	2.4*	PE	[2886]
K/Ru(001)[84]	K	–	$<8 \times 10^{-11}$	130	–	2.4	PE	[528]
K/Rh(111)	K	–	1×10^{-10}	50 (845)	–	2.4	PE	[1204]
K/W	K	–	$<1 \times 10^{-11}$	78	–	2.4 ± 0.05	FE	[373]
K/Ni(100)	K	–	$\sim 10^{-10}$	~ 300	–	2.4 ± 0.1*	CPD	[1411]
K/Si(100)	–	–	–	–	–	2.4 ± 0.2*	TC	[1702]
K/Cu(111)	K	–	$<5 \times 10^{-10}$	~ 300	–	2.40	CPD	[2517,3459]
K/W(100)	K	–	?	78	–	2.40	FE	[373]
K/Mo(111)	K	–	$<1 \times 10^{-11}$	78	–	2.40	FE	[648]
K(fp, $r \to \infty$)[460]	–	–	?	~ 300	–	2.40*	IP	[4198]
K/glass	K	–	$\leq 3 \times 10^{-11}$	195	–	2.40 ± 0.01	PE	[2615]
K	–	–	–	–	–	2.42	TC	[4441]
K/glass	K	–	$\leq 3 \times 10^{-11}$	195	–	2.43 ± 0.01	PE	[2615]
K/Cu(111)	K	–	$<8 \times 10^{-11}$	90–100	–	2.44	CPD	[2191]
K	–	–	–	–	–	2.45	TC	[231]
K/C(0001)[85]	K	–	$<2 \times 10^{-10}$	83	–	2.45 ± 0.15	PE	[2193]
K/W(112)	K	–	?	78	–	2.48	CPD	[658]
K	–	–	–	–	–	2.48	TC	[2061]
K	–	–	–	–	–	2.49	TC	[1924]
K/Ta(110)	–	–	–	–	–	2.5*	TC	[3663]
K/C(0001)[85]	K	–	$\sim 10^{-10}$	83	–	2.5*	PE	[1725]
K/Si(111)	K	–	5×10^{-11}	77	–	2.5*	PE	[3465]
K/Au(100)	K	–	$\sim 10^{-10}$	100	–	2.5	CPD	[3173]
K/Au(100)	K	–	$\sim 8 \times 10^{-10}$	~ 300	–	2.5*	CPD	[2792]
K/Ni(100)	K	–	$\sim 1 \times 10^{-11}$	~ 300	–	2.5*	CPD	[1413]
K/Cu(111)	K	–	3×10^{-10}	85, 160	–	2.5*	PE	[2801]
K/Re(1010)	K	–	$(\leq 1 \times 10^{-10})$	245	–	2.5	CPD	[2490]
K/W(112)	K	–	$(<10^{-11})$	245	–	2.5	CPD	[658]
K	–	–	–	–	–	2.50	TC	[553,2427]
K	–	–	–	–	–	2.50	TC	[3477]
K(fp, $r \to \infty$)[460]	–	–	?	~ 300	–	2.50*	IP	[4198]
K/Mo(110)	K	–	$<1 \times 10^{-11}$	78	–	2.50	FE	[648]
K	–	–	–	–	–	2.51	TC	[231]
$K_n(n \to \infty)$	–	–	?	?	–	2.52	IP	[4227]
K	–	–	–	–	–	2.53	TC	[1924]
K/W(110)	K	–	$\sim 3 \times 10^{-9}$	~ 300	–	2.54	FE	[2766]
K/Fe(100)	K	–	?	~ 300	–	2.55	PE	[1709]
K	–	–	–	–	–	2.55	TC	[738]
K/W(110)[82]	K	–	$<1 \times 10^{-11}$	78	–	2.55 ± 0.05	FE	[373]
K	–	–	–	–	–	2.56	TC	[3467]
K	–	–	–	–	–	2.56	TC	[2427]
K	–	–	–	–	–	2.58	TC	[1901]
K	–	–	–	–	–	2.58	TC	[4101]
K/Si(111)	K	–	5×10^{-11}	77	–	2.6*	PE	[3465]
K/Ag(111)	K	–	$<1 \times 10^{-10}$	~ 300	–	2.6	CPD	[1426]
K/Si(100)	K	–	8×10^{-10}	~ 300	–	2.6*	CPD	[3278]
K/Ag(111)	K	–	?	100	–	2.6*	CPD	[3569]
K	–	–	–	–	–	2.6	TC	[2845]
K/Co(0001)	K	–	$\sim 10^{-10}$	200	–	2.6 ± 0.3	PE	[3381]
K/Ta(110)	K	–	$<1 \times 10^{-11}$	78	–	2.60	FE	[648]
K/Al(111)	K	–	?	140	–	2.61	CPD	[734]
K/Al(111)	K	–	?	~ 300	–	2.61	CPD	[734]
K	–	–	–	–	–	2.62	TC	[1613]
K	–	–	–	–	–	2.62	TC	[2382]
K/graphite	–	–	–	–	–	2.63*	TC	[1843]
K/W	K	–	? (K)	~ 750–950	–	2.65	TE	[2292]
K/Cu(332)	K	–	$<2 \times 10^{-10}$	95	–	2.65*	PE	[1604]
K/C_{12}/Au/Si(111)[419]	K	–	$\sim 10^{-10}$	~ 300	–	2.66	PE	[3999]
K/Cu(100)	K	–	$<5 \times 10^{-10}$	~ 300	–	2.67*	CPD	[1431]
K	–	–	–	–	–	2.67	TC	[1578]
K	–	–	–	–	–	2.68	TC	[2629]
K	–	–	–	–	–	2.69	TC	[767]
K/Au(001)	K	–	$\sim 8 \times 10^{-10}$	~ 100	–	2.7*	CPD	[2792]
K/Pt(111)	K	–	1×10^{-11}	~ 300 (>500)	–	2.7	FE	[3227]
K	–	–	–	–	–	2.74	TC[3]	[475,519,2474]
K	–	–	–	–	–	2.74	TC	[230]
K	–	–	–	–	–	2.76	TC	[521]
K	–	–	–	–	–	2.76	TC	[3628]

Table 1 (*continued*)

Surface	Beam	Ion	P_r (Torr)	T (K)	ϕ^+ (eV)	ϕ^e (eV)	Meth.	Refs.
K	–	–	–	–	–	2.8	TC	[944]
K/Ni(100)	K	–	?	40	–	2.8 ± 0.1*	?	[2047]
K/graphite	K	–	4×10^{-10}	90	–	<2.9 ± 0.2	CPD	[2185]
K/Si(111)	–	–	–	–	–	2.9	TC	[300]
K/cnt[86]	K	–	8×10^{-10}	~300	–	3.3	PE	[3229]
K	–	–	–	–	–	3.30	TC	[2629]
K/C(100)	–	–	–	–	–	3.62*	TC	[2759]
K	–	–	–	–	–	3.71	TC	[3080]
K/cnt	K	–	$<2 \times 10^{-7}$	?	–	3.99	FE	[2201]
Recommended	–	–	–	–	–	**2.29 ± 0.02**	–	–
Liquid ($T > 337$ K)								
K	–	–	$\sim 10^{-9}$	338	–	2.27	PE	[4241]
K	–	–	$\leq 5 \times 10^{-9}$	338	–	2.30 ± 0.015	PE	[2476]
K[156]	–	–	$<10^{-8}$	338	–	2.30 ± 0.03	PE	[2470]

20. Calcium Ca

Surface	Beam	Ion	P_r (Torr)	T (K)	ϕ^+ (eV)	ϕ^e (eV)	Meth.	Refs.
fcc (α, $T < 523$ K)								
Ca(100)	–	–	–	–	–	2.55	TC	[1254]
Ca(100)	–	–	–	–	–	2.758	TC	[4091]
Ca(100)	–	–	–	–	–	2.87	TC	[4222]
Ca(100)	–	–	–	–	–	2.9	TC	[3653]
Ca(100)	–	–	–	–	–	2.9	TC	[1711]
Ca(100)	–	–	–	–	–	2.94	TC	[231]
Ca(100)	–	–	–	–	–	2.97	TC	[3467]
Ca(100)	–	–	–	–	–	3.38	TC	[476]
Ca(100)	–	–	–	–	–	3.52	TC	[476]
Ca(100)	–	–	–	–	–	3.57	TC	[1030]
Ca(100)	–	–	–	–	–	3.96	TC	[1030]
Ca(100)	–	–	–	–	–	4.09	TC	[321]
Recommended	–	–	–	–	–	**3.4 ± 0.4**	–	–
Ca(110)	–	–	–	–	–	2.813	TC	[4091]
Ca(110)	–	–	–	–	–	2.83	TC	[4222]
Ca(110)	–	–	–	–	–	2.92	TC	[231]
Ca(110)	–	–	–	–	–	2.92	TC	[3467]
Ca(110)	–	–	–	–	–	3.20	TC	[1030]
Ca(110)	–	–	–	–	–	3.29	TC	[476]
Ca(110)	–	–	–	–	–	3.41	TC	[476]
Ca(110)	–	–	–	–	–	3.43	TC	[1030]
Ca(110)	–	–	–	–	–	3.84	TC	[321]
Recommended	–	–	–	–	–	**3.3 ± 0.3**	–	–
Ca(111)	–	–	–	–	–	2.86	TC	[334,3179]
Ca(111)	–	–	–	–	–	2.936	TC	[4091]
Ca(111)	–	–	–	–	–	2.98	TC	[4215]
Ca(111)	–	–	–	–	–	2.98	TC	[4222]
Ca(111)	–	–	–	–	–	3.10	TC	[231]
Ca(111)	–	–	–	–	–	3.14	TC	[3467]
Ca(111)	–	–	–	–	–	3.26	TC	[2427]
Ca(111)	–	–	–	–	–	3.35	TC	[476]
Ca(111)	–	–	–	–	–	3.4	TC	[1711]
Ca(111)	–	–	–	–	–	3.4	TC	[3653]
Ca(111)	–	–	–	–	–	3.49	TC	[476]
Ca(111)	–	–	–	–	–	3.68	TC	[1030,1089]
Ca(111)	–	–	–	–	–	3.70	TC	[1030]
Ca(111)	–	–	–	–	–	3.76	TC	[1089]
Ca(111)	–	–	–	–	–	3.91	TC	[1089]
Ca(111)	–	–	–	–	–	4.40	TC	[321]
Recommended	–	–	–	–	–	**3.5 ± 0.2**	–	–
bcc (γ, $T > 723$ K)								
Ca(100)	–	–	–	–	–	3.52	TC	[321]
Ca(110)	–	–	–	–	–	2.84	TC	[334]
Ca(110)	–	–	–	–	–	4.09	TC	[321]

Table 1 (*continued*)

Surface	Beam	Ion	P_r (Torr)	T (K)	ϕ^+ (eV)	ϕ^e (eV)	Meth.	Refs.
Ca(111)	–	–	–	–	–	3.37	TC	[321]
Ca(112)	–	–	–	–	–	3.75	TC	[321]
fcc (α, T < 523 K for bulk)								
Ca	–	–	–	–	–	2.1	TC	[2845]
Ca/silica[87]	Ca	–	~10^{-11}	~300	–	2.2	PE	[1418]
Ca/?	Ca	–	<10^{-6}	?	–	2.24	TE	[2919]
Ca[174]	–	–	–	0^E	–	2.24	TC	[1747]
Ca	–	–	–	–	–	2.35	TC	[1744]
Ca/W	Ca	–	≤1 × 10^{-9}	~300 (670)	–	2.4	FE	[2587]
Ca/?	Ca	–	?	~300	–	2.42	PE	[3027]
Ca	–	–	–	–	–	2.50	TC	[2704]
Ca	–	–	–	–	–	2.53	TC	[3476]
Ca	–	–	–	–	–	2.55	TC	[1254]
Ca/silica[87]	Ca	–	~10^{-11}	~300	–	2.55	PE	[1418]
Ca	–	–	–	–	–	2.6	TC	[1955]
Ca	–	–	–	–	–	2.64	TC	[3476]
Ca/glass	Ca	–	?	~300	–	2.66	PE	[2924]
Ca	–	–	?	298	–	2.66 ± 0.07	PE	[3394]
Ca/Ir	Ca	–	≤1 × 10^{-9}	~300 (770)	–	2.7 ± 0.1	FE	[2587]
Ca	–	–	–	–	–	2.70	TC	[1066]
Ca/glass	Ca	–	?	298	–	2.706 ± 0.004	PE	[2232]
Ca	–	–	–	–	–	2.75	TC	[3318]
Ca/W	Ca	–	<2 × 10^{-9}	~300	–	2.75 ± 0.05	FE	[1687]
Ca	–	–	~10^{-6}	298	–	2.76	PE	[3389,3394]
Ca	–	–	–	–	–	2.78	TC	[298]
Ca	–	–	–	–	–	2.80	TC	[2949]
Ca/W[244]	Ca	–	≤2 × 10^{-9}	~900	–	2.84	CPD	[3530]
Ca	–	–	–	–	–	2.87	TC	[4418]
Ca/quartz	Ca	–	<5 × 10^{-10}	~300	–	2.87 ± 0.06	PE	[1997,1998,2024]
Ca/graphite	Ca	–	~10^{-9}	~300	–	2.89	CPD	[2957]
Ca/Mo	Ca	–	~10^{-9}	~300	–	2.89	CPD	[2957]
Ca	–	–	–	–	–	2.9	TC	[1993]
Ca/Cu(100)	Ca	–	~1 × 10^{-11}	110, 300	–	2.9	CPD	[2997]
Ca/Cu	Ca	–	<2 × 10^{-9}	~300	–	2.9	PE	[2332]
Ca/?	Ca	–	<8 × 10^{-11}	~300	–	2.9 ± 0.1	CPD	[3868]
Ca/W[244]	Ca	–	≤2 × 10^{-9}	~300	–	2.90	CPD	[3530]
Ca	–	–	–	–	–	2.91	TC	[3476]
Ca/Re	Ca	–	<8 × 10^{-11}	~300	–	2.92	CPD	[342]
Ca/graphite	Ca	–	~10^{-9}	~300	–	2.95	CPD	[2957]
Ca/silica[87]	Ca	–	~10^{-11}	~300	–	2.98 ± 0.05	PE	[1418]
Ca/glass[88]	Ca	–	<10^{-9}	~300{77}	–	3.0	CPD	[1526]
Ca/Ir	Ca	–	≤1 × 10^{-9}	~300 (770)	–	3.0 ± 0.1	FE	[2587]
Ca	–	–	–	–	–	3.00	TC	[3931]
Ca	–	–	–	–	–	3.01	TC	[3467]
Ca/quartz	Ca	–	~10^{-9}	~300	–	3.06	CPD	[2957]
Ca/graphite	Ca	–	~10^{-9}	~300	–	3.06	CPD	[2957]
Ca	–	–	?	~300	–	3.08	PE	[2080]
Ca	–	–	–	–	–	3.08	TC	[231]
Ca/W	Ca	–	~2 × 10^{-9}	~300	–	3.1	CPD	[3259]
Ca/Pt	Ca	–	?	~1200	–	3.1	TE	[4266]
Ca	–	–	–	–	–	3.1	TC	[706]
Ca	–	–	–	–	–	3.11	TC	[521]
Ca	–	–	–	–	–	3.13	TC	[3729]
Ca/Mo[89]	Ca$^+$	–	<1 × 10^{-9}	~300	–	3.13	PE	[2211]
Ca	–	–	–	–	–	3.15	TC	[1578]
Ca	–	–	–	–	–	3.19	TC	[231]
Ca	–	–	–	–	–	3.2	TC	[3030]
Ca/Ni	Ca	–	?	~300	–	3.20	PE	[2922]
Ca/Ta	Ca	–	~10^{-7}	~300	–	3.21	PE	[2463]
Ca	–	–	–	–	–	3.24	TC	[3467]
Ca/Mo[89]	Ca$^+$	–	<1 × 10^{-9}	~300	–	3.26	PE	[2211]
Ca	–	–	–	–	–	3.28	TC	[1613]
Ca	–	–	–	–	–	3.30	TC	[2629]
Ca	–	–	?	~300	–	3.33	CPD	[2297]
Ca	–	–	–	–	–	3.39	TC	[2474]
Ca/quartz	Ca	–	5 × 10^{-10}	~300	–	3.7 ± 0.3	PE	[2003,2008]
Recommended	–	–	–	–	–	**2.91 ± 0.03**	–	–

Table 1 (*continued*)

Surface	Beam	Ion	P_r (Torr)	T (K)	ϕ^+ (eV)	ϕ^e (eV)	Meth.	Refs.
				21. Scandium Sc[399]				
hcp (α, $T < 1660$ K)								
Sc(0001)	–	–	–	–	–	2.1	TC	[1090]
Sc(0001)	–	–	–	–	–	3.39	TC	[4461][490]
Sc(0001)	–	–	–	–	–	3.556	TC	[4460][490]
Sc(0001)	–	–	–	–	–	3.74	TC	[229,334,3179]
Sc(0001)/W(110)[90]	Sc	–	$\leq 1 \times 10^{-9}$	~300	–	3.8	CPD	[1982]
Sc(0001)	–	–	–	–	–	3.81	TC	[4005]
Sc(0001)	–	–	–	–	–	4.81	TC	[321]
Sc(1010)	–	–	–	–	–	3.10	TC	[4005]
Sc(1010)	–	–	–	–	–	3.35	TC	[4461][490]
Sc(1010)	–	–	–	–	–	3.563	TC	[4460][490]
Sc(1010)	–	–	–	–	–	3.772	TC	[4460][490]
Sc(1010)	–	–	–	–	–	4.60	TC	[321]
Sc(1124)	–	–	–	–	–	4.03	TC	[321]
fcc (β, $T > 1660$ K)								
Sc(100)	–	–	–	–	–	4.39	TC	[321]
Sc(110)	–	–	–	–	–	4.13	TC	[321]
Sc(111)	–	–	–	–	–	3.84	TC	[229,334]
Sc(111)	–	–	–	–	–	4.73	TC	[321]
hcp (α, $T < 1660$ K for bulk)								
Sc/W[91]	Sc	–	1×10^{-10}	~300 (≤ 1300)	–	2.8	FE	[1811]
Sc/W[91]	Sc	–	1×10^{-10}	~300 (≤ 1300)	–	2.9	FE	[1811]
Sc	–	–	–	–	–	2.9	TC	[1744]
Sc/W(100)	–	–	–	–	–	3.0	TC	[4258]
Sc/W	Sc	–	$\leq 7 \times 10^{-8}$	~300	–	3.0	FE	[1804]
Sc/Mo	Sc	–	$\leq 7 \times 10^{-8}$	~300	–	3.1	FE	[1804]
Sc/W(111)	Sc	–	($<10^{-10}$)	77	–	3.1 ± 0.1	FE	[3323]
Sc	–	–	–	–	–	3.15	TC	[3318]
Sc/W(111)	Sc	–	$\leq 10^{-8}$	~1100–1150	–	3.17 ± 0.03	TE	[2337]
Sc/W(111)	Sc	–	$\sim 10^{-9}$	~300	–	3.2	FE	[2011]
Sc[379]	–	–	–	–	–	3.2	TC	[1955]
Sc/W(100)	Sc	–	1×10^{-9}	~300	–	3.2	CPD	[1985]
Sc	–	–	–	–	–	3.23	TC	[1956]
Sc(foil)[255]	–	–	$<10^{-7}$	1300	–	3.23	TE	[3071]
Sc/W(112)	Sc	–	?	~300	–	3.26	CPD	[4011]
Sc	–	–	? (N_2)	~300	–	3.28 ± 0.02	CPD	[4066]
Sc	–	–	–	–	–	3.29	TC	[3476]
Sc[160]	–	–	–	–	–	3.3	TC	[1355]
Sc/W	Sc	–	1×10^{-9}	~300	–	3.3	CPD	[3617,4447]
Sc/Nb	Sc	–	$\leq 10^{-8}$	~1000–1150	–	3.3 ± 0.03	TE	[2359]
Sc/Ta	Sc	–	$\leq 10^{-8}$	~1000–1150	–	3.3 ± 0.03	TE	[2359]
Sc/Ru	Sc	–	$\leq 10^{-8}$	~1000–1150	–	3.3 ± 0.03	TE	[2359]
Sc/Os	Sc	–	$\leq 10^{-8}$	~1000–1150	–	3.3 ± 0.03	TE	[2359]
Sc/Ir	Sc	–	$\leq 10^{-8}$	~1000–1150	–	3.3 ± 0.03	TE	[2359]
Sc/Nb(110)	Sc	–	$\leq 10^{-8}$	~1000–1150	–	3.3 ± 0.03	TE	[2359]
Sc/W(100)	Sc	–	($<10^{-10}$)	77	–	3.3 ± 0.1	FE	[3323]
Sc	–	–	–	–	–	3.30*	TC	[1955]
Sc/Re	Sc	–	$\leq 10^{-8}$	~1000–1150	–	3.32 ± 0.03	TE	[2359]
Sc	–	–	–	–	–	3.33	TC	[1066]
Sc/Mo	Sc	–	$\leq 10^{-8}$	~1000–1150	–	3.34 ± 0.03	TE	[2359]
Sc/W	Sc	–	$\leq 10^{-8}$	~1000–1150	–	3.34 ± 0.03	TE	[2359]
Sc/W(100)	Sc	–	$\sim 10^{-10}$	~300 (≤ 1070)	–	3.36	CPD	[2528]
Sc	–	–	–	–	–	3.39	TC	[3476]
Sc	–	–	–	–	–	3.4	TC	[3318]
Sc/Re–Sc(9%)[92]	–	–	?	1200	–	3.4	TE	[1979]
Sc/Nb(100)	Sc	–	$\leq 10^{-8}$	~1000–1150	–	3.4 ± 0.03	TE	[2359]
Sc	–	–	2×10^{-10}	~300	–	3.4 ± 0.1	PE	[1813]
Sc	–	–	?	1200	–	3.45	TE	[1979]
Sc	–	–	–	–	–	3.5	TC	[706]
Sc/W(121)	Sc	–	($<10^{-10}$)	77	–	3.5 ± 0.1	FE	[3323]
Sc/quartz	Sc	–	$\sim 10^{-10}$	~300	–	3.5 ± 0.15	PE	[304]
Sc	–	–	–	–	–	3.53	TC	[298]
Sc/W(100)	Sc	–	$\leq 10^{-8}$	~1000–1150	–	3.56 ± 0.03	TE	[2337,2359]

Table 1 (*continued*)

Surface	Beam	Ion	P_r (Torr)	T (K)	ϕ^+ (eV)	ϕ^e (eV)	Meth.	Refs.
Sc	–	–	–	–	–	3.6	TC	[1993]
Sc	–	–	~10^{-9}	<1660	–	3.62	TE	[4356]
Sc/W(112)	Sc	–	?	~300 (~600)	–	3.60	CPD	[4011]
Sc/W(110)	Sc	–	≤10^{-8}	~1000–1150	–	3.62 ± 0.03	TE	[2337,2359]
Sc/W(110)	Sc	–	(<10^{-10})	~300	–	3.66*	CPD	[3329]
Sc	–	–	–	–	–	3.71	TC	[3476]
Sc	–	–	–	–	–	3.9	TC	[944]
Sc	–	–	?	~300	–	4.2	CPD	[2202]
Recommended	–	–	–	–	–	**3.33 ± 0.04**	–	–

fcc (β, $T > 1660$ K for bulk)

Surface	Beam	Ion	P_r (Torr)	T (K)	ϕ^+ (eV)	ϕ^e (eV)	Meth.	Refs.
Sc	–	–	–	–	–	3.44	TC	[1066]
Sc	–	–	~10^{-9}	>1660	–	3.46	TE	[4356]

22. Titanium Ti

hcp (α, $T < 1155$ K)

Surface	Beam	Ion	P_r (Torr)	T (K)	ϕ^+ (eV)	ϕ^e (eV)	Meth.	Refs.
Ti(0001)	–	–	–	–	–	3.8	TC	[1090,1899]
Ti(0001)/W(110)[93]	Ti	–	<10^{-11}	~300 (~650)	–	4.10	FE	[2196]
Ti(0001)	–	–	–	–	–	4.25	TC	[4417]
Ti(0001)	–	–	–	–	–	4.29	TC	[1980]
Ti(0001)	–	–	–	–	–	4.38	TC	[4087,4410]
Ti(0001)	–	–	–	–	–	4.38	TC	[1179]
Ti(0001)	–	–	–	–	–	4.40	TC	[1028,1179]
Ti(0001)	–	–	–	–	–	4.42	TC	[894]
Ti(0001)	–	–	–	–	–	4.45	TC	[2553]
Ti(0001)	–	–	–	–	–	4.51	TC	[4032,4086]
Ti(0001)	–	–	–	–	–	4.54	TC	[1179]
Ti(0001)	–	–	–	–	–	4.56	TC	[4284]
Ti(0001)	–	–	<10^{-10}	~300	–	4.58 ± 0.05	FE	[2258]
Ti(0001)	–	–	–	–	–	4.59	TC	[229,334]
Ti(0001)	–	–	?	~300	–	4.6 ± 0.2	PE	[3627]
Ti(0001)	–	–	4 × 10^{-11}	~300	–	4.60 ± 0.1	PE	[1902]
Ti(0001)	–	–	–	–	–	4.63	TC	[4032]
Ti(0001)	–	–	–	–	–	4.64	TC	[892]
Ti(0001)	–	–	–	–	–	4.66	TC	[1028,1179]
Ti(0001)/W(110)	Ti	–	(<5 × 10^{-11})	~300 (~900)	–	4.7 ± 0.1	CPD	[4234]
Ti(0001)	–	–	–	–	–	4.72	TC	[4005]
Ti(0001)	–	–	–	–	–	4.75	TC	[893]
Ti(0001)/glass[94]	Ti	–	?	~300	–	5.0	CPD	[2378]
Ti(0001)	–	–	–	–	–	5.00	TC	[321]
Recommended	–	–	–	–	–	**4.53 ± 0.10**	–	–
Ti(1010)	–	–	–	–	–	3.63	TC	[4005]
Ti(1010)	–	–	–	–	–	4.13	TC	[1980]
Ti(1010)/O=Ti[95]	Ti	–	?	~300	–	4.15	CPD	[2378]
Ti(1010)	–	–	–	–	–	4.78	TC	[321]
Ti(1011)/O=Ti[95]	Ti	–	?	~300	–	4.75	CPD	[2378]
Ti(1124)	–	–	–	–	–	4.18	TC	[321]

bcc (β, $T > 1155$ K)

Surface	Beam	Ion	P_r (Torr)	T (K)	ϕ^+ (eV)	ϕ^e (eV)	Meth.	Refs.
Ti(100)	–	–	–	–	–	3.94	TC	[321]
Ti(110)	–	–	–	–	–	4.57	TC	[321]
Ti(111)	–	–	–	–	–	3.76	TC	[321]
Ti(112)	–	–	–	–	–	4.18	TC	[321]

hcp (α, $T < 1155$ K for bulk)

Surface	Beam	Ion	P_r (Torr)	T (K)	ϕ^+ (eV)	ϕ^e (eV)	Meth.	Refs.
Ti	–	–	–	–	–	2.4	TC	[2456]
Ti/Ag	Ti	–	1 × 10^{-7}	~300	–	2.7–3.9	CPD	[1785]
Ti/Au	Ti	–	1 × 10^{-6}	~300	–	3.0–4.2	CPD	[1785]
Ti/W(016)[96]	Ti	–	<8 × 10^{-11}	~300	–	3.03	FE	[3222]
Ti	–	–	<10^{-3}	~300	–	3.10 ± 0.07	PE	[2571]
Ti/W	Ti	–	<8 × 10^{-11}	~300	–	3.18	FE	[3222]
Ti/W(116)	Ti	–	~10^{-10}	~300	–	3.47	FE	[4237]

Table 1 (*continued*)

Surface	Beam	Ion	P_r (Torr)	T (K)	ϕ^+ (eV)	ϕ^e (eV)	Meth.	Refs.
Ti/W(012)	Ti	–	$\leq 10^{-10}$	~300	–	3.5	FE	[3327]
Ti/W	Ti	–	$<8 \times 10^{-10}$	78 (≤1100)	–	3.50	FE	[1731]
Ti/W(111)[96]	Ti	–	$<8 \times 10^{-11}$	~300	–	3.50	FE	[3222]
Ti	–	–	–	–	–	3.51	TC	[3476]
Ti/W(011)[96]	Ti	–	$<8 \times 10^{-11}$	~300	–	3.52	FE	[3222]
Ti/glass	Ti	–	$<10^{-9}$	77–90	–	3.52	PE	[2096,3052,3053]
Ti/Ni	Ti	–	?	~300	–	3.55 ± 0.05	PE	[2617]
Ti/glass	Ti	–	$<10^{-9}$	293 (383)	–	3.57	PE	[3052]
Ti/Ge(111)	Ti	–	$\leq 10^{-9}$	~300	–	3.6	FE	[1496]
Ti/W	Ti	–	$\leq 10^{-10}$	~300	–	3.6	FE	[3327,3334]
Ti/W(110)	–	–	–	–	–	3.6*	TC	[2975]
Ti	–	–	–	–	–	3.61	TC	[3476]
Ti/W(023)	Ti	–	$\sim 10^{-10}$	~300	–	3.65	FE	[4237]
Ti/W	Ti	–	$\leq 10^{-10}$	~300	–	3.65 ± 0.06	FE	[3545]
Ti/W(112)	Ti	–	$\sim 10^{-10}$	~300	–	3.66	FE	[4237]
Ti/W(111)	Ti	–	$\leq 10^{-10}$	~300	–	3.7	FE	[3327]
Ti/W(100)	Ti	–	?	<1600	–	3.7	FE	[1438]
Ti/Au	Ti	–	2×10^{-9}	~300	–	3.7–4.7	CPD	[1785]
Ti/W(100)	Ti	–	$<10^{-10}$	800–1100	–	3.70 ± 0.05	FE	[4014]
Ti	–	–	10–12 (Ar)	~300	–	3.72	PE	[1652,4236]
Ti	–	–	–	0	–	3.72	TC	[339]
Ti	Cs	Cs⁺	? (Cs)	~1000	3.74*	(3.75)	PSI	[650]
Ti	–	–	? (Cs)	~1000–1100	(3.74*)	3.75	TE	[650]
Ti/W(001)[96]	Ti	–	$<8 \times 10^{-11}$	~300	–	3.75	FE	[3222]
Ti	–	–	$\leq 1 \times 10^{-9}$	1115	–	3.76	TE	[179]
Ti	–	–	$\leq 10^{-7}$	900–1170	–	3.77–5.5	TE	[2810]
Ti	–	–	–	–	–	3.78	TC	[3318]
Ti/SiO₂	Ti	–	?	~300	–	3.8	PE	[2899]
Ti/W(111)	Ti	–	$\leq 1 \times 10^{-10}$	77	–	3.8	FE	[2372]
Ti/glass	Ti	–	6×10^{-10}	293 (383)	–	3.81	PE	[3053]
Ti	–	–	–	–	–	3.81	TC	[1066]
Ti	–	–	3×10^{-11}	77	–	3.81	FE	[2424]
Ti	–	–	?	~300	–	3.82 ± 0.02	CPD	[2544]
Ti/W(100)	Ti	–	?	<1600	–	3.82 ± 0.05*	FE	[1438]
Ti	–	–	–	–	–	3.83	TC	[3318]
Ti/W(110)	Ti	–	$<5 \times 10^{-10}$	~300	–	3.85 ± 0.03	CPD	[1863]
Ti/W(100)	Ti	–	2×10^{-9}	~1550–1800	–	3.85 ± 0.04	TE	[2461]
Ti/glass	Ti	–	$<10^{-9}$	90 (383)	–	3.87	PE	[2096]
Ti	–	–	–	–	–	3.87	TC	[1901]
Ti	–	–	–	–	–	3.88	TC	[2005]
Ti/W(001)[97]	Ti	–	$\sim 10^{-10}$	293	–	3.88 ± 0.09	FE	[1404]
Ti/W(110)	Ti	–	$\leq 1 \times 10^{-10}$	77	–	3.9	FE	[2372]
Ti/W(112)	Ti	–	$\leq 1 \times 10^{-10}$	77	–	3.9	FE	[2372]
Ti/W	Ti	–	$\leq 7 \times 10^{-8}$	~300	–	3.9	FE	[1804]
Ti/Mo(110)	Ti	–	$\sim 10^{-10}$	~300	–	3.9	CPD	[3679]
Ti/W	Ti	–	$\sim 10^{-9}$	293 (900)	–	3.9	FE	[3738]
Ti	–	–	–	–	–	3.9	TC	[1993]
Ti	–	–	?	?	–	3.9	TE	[3402]
Ti/SiO₂	Ti	–	?	~300 (670)	–	3.9 ± 0.1	PE	[2899]
Ti/glass	Ti	–	?	~300	–	3.95	PE	[3027]
Ti/W(111)[98]	Ti	–	$\sim 10^{-11}$	~300 (600)	–	3.95	PE	[2194]
Ti/W(112)[96]	Ti	–	$<8 \times 10^{-11}$	~300	–	3.95	FE	[3222]
Ti	–	–	$\sim 10^{-6}$	~300	–	3.95	PE	[3027]
Ti/W[99]	Ti	–	5×10^{-11}	~300	–	3.95	FE	[1522]
Ti	–	–	–	–	–	3.95	TC	[2949]
Ti	–	–	$<2 \times 10^{-10}$	~300	–	3.96 ± 0.04	CPD	[1898]
Ti	–	–	–	–	–	3.98	TC	[3476]
Ti	–	–	–	–	–	4.0	TC	[2583]
Ti	–	–	–	–	–	4.0	TC	[1955]
Ti/Ag	Ti	–	1×10^{-7}	~300	–	4.0–4.6	CPD	[1785]
Ti	–	–	–	–	–	4.00	TC	[3637]
Ti/Re(1010)[97]	Ti	–	$\sim 10^{-10}$	293	–	4.00 ± 0.05	FE	[1404]
Ti	–	–	?	~300	–	4.07	PE	[4278]
Ti	–	–	–	–	–	4.09	TC	[1744]
Ti	–	–	3×10^{-11}	77	–	4.1	FE	[2424]
Ti	–	–	–	–	–	4.1	TC	[706]
Ti	–	–	–	–	–	4.10	TC	[3264,3265,3267]
Ti	–	–	$\sim 10^{-8}$	~1400–1700	–	4.10	TE	[4221]
Ti	–	–	1×10^{-9}	~300	–	4.13	CPD	[1252]
Ti	–	–	?	~300	–	4.14	CPD	[2297]

Table 1 (*continued*)

Surface	Beam	Ion	P_r (Torr)	T (K)	ϕ^+ (eV)	ϕ^e (eV)	Meth.	Refs.
Ti/TiI$_4$/W	–	–	?	~300 (?)	–	4.17	PE	[2927]
Ti/Au	Ti	–	2×10^{-9}	~300	–	4.2–5.6	CPD	[1785]
Ti	–	–	–	0	–	4.22	TC	[4419]
Ti	–	–	?	~300	–	4.23	CPD	[3338]
Ti/W(110)	Ti	–	($<5 \times 10^{-11}$)	~300	–	4.25	CPD	[4234]
Ti	–	–	$\leq 1 \times 10^{-9}$	1113	–	4.26	TE	[179]
Ti	–	–	2×10^{-10}	~300	–	4.33	PE	[1814]
Ti/quartz	Ti	–	~10^{-10}	~300	–	4.33 ± 0.1	PE	[304]
Ti/Si$_3$N$_4$	–	–	–	–	–	4.36	TC	[3517]
Ti	–	–	–	–	–	4.36	TC	[298]
Ti	–	–	$\leq 1 \times 10^{-9}$	1156	–	4.36	TE	[179]
Ti	–	–	$<10^{-3}$	~300	–	4.36 ± 0.04	PE	[2571]
Ti/W(110)	Ti	–	$\leq 10^{-10}$	~300	–	4.4	FE	[2372]
Ti	–	–	–	–	–	4.4	TC	[944]
Ti	–	–	$<10^{-3}$	~300	–	4.45 ± 0.05	PE	[2571]
Ti/O=Ti[95]	Ti	–	?	~300	–	4.60	CPD	[2378]
Ti/glass[94]	Ti	–	?	~300	–	4.76	CPD	[2378]
Recommended	–	–	–	–	–	**3.87 ± 0.05**	–	–

bcc (β, $T > 1155$ K for bulk)

Surface	Beam	Ion	P_r (Torr)	T (K)	ϕ^+ (eV)	ϕ^e (eV)	Meth.	Refs.
Ti	–	–	$\leq 10^{-9}$	~1100–1600	–	3.5–4.4	TE	[124]
Ti	–	–	$\leq 10^{-9}$	~1100–1600	–	3.55–4.25	TE	[650]
Ti/W(111)[98]	Ti	–	~10^{-11}	~300 (1100)	–	3.6	PE	[2194]
Ti/W[99]	Ti	–	5×10^{-11}	~300 (1100)	–	3.65	FE	[1522]
Ti/W(001)[97]	Ti	–	~10^{-10}	293 (1300)	–	3.65 ± 0.05	FE	[1404,1405]
Ti	–	–	? (Cs)	~1100–1400	–	3.7	TE	[650,3413]
Ti	–	–	~10^{-9}	1115–1537	–	3.76 ± 0.03	TE	[179]
Ti/graphite	Ti	–	$<10^{-5}$	1370–1510	–	3.95 ± 0.02	TE	[769,2304]
Ti	–	–	~10^{-8}	~1200–1600	–	4.00 ± 0.05	TE	[1775,1776]
Ti	–	–	3×10^{-9}	~1000–1430	–	4.1	TE	[159]
Ti	–	–	~10^{-9}	~1000–1450	–	4.10	TE	[1773]
Ti	–	–	$\leq 1 \times 10^{-9}$	1253–1585	–	4.23 ± 0.06*	TE	[179]
Ti	–	–	$\leq 1 \times 10^{-9}$	1156–1585	–	4.32 ± 0.08*	TE	[179]
Recommended	–	–	–	–	–	**3.93 ± 0.16**	–	–

23. Vanadium V

bcc

Surface	Beam	Ion	P_r (Torr)	T (K)	ϕ^+ (eV)	ϕ^e (eV)	Meth.	Refs.
V(100)	–	–	–	–	–	3.66	TC	[4412]
V(100)	–	–	–	–	–	3.7	TC	[1617]
V(100)	–	–	–	–	–	3.88	TC	[321]
V(100)	–	–	–	–	–	3.93	TC	[2437]
V(100)	–	–	~10^{-10}	~300	–	3.95	CPD	[3641]
V(100)	–	–	–	–	–	4.068	TC	[4460][490]
V(100)	–	–	~10^{-11}	~300	–	4.1 ± 0.1	PE	[2428,3371]
V(100)	–	–	$<8 \times 10^{-11}$	~300	–	4.10 ± 0.05	PE	[3380]
V(100)[100]	–	–	–	–	–	4.19 ± 0.02	TC	[3671]
V(100)	–	–	–	–	–	4.2	TC	[3615]
V(100)	–	–	–	–	–	4.28	TC	[1980,3067]
V(100)	–	–	–	–	–	4.29	TC	[2548]
V(100)	–	–	–	–	–	4.3	TC	[3615]
V(100)	–	–	~10^{-11}	~300	–	4.3 ± 0.1	PE	[3371,3372,3374, 3375]
V(100)	–	–	2×10^{-11}	250	–	4.3 ± 0.15	PE	[3368,3374]
V(100)	–	–	?	?	–	4.46	TE	[3695]
V(100)[195]	–	–	–	–	–	4.56	TC	[1876]
V(100)	–	–	–	–	–	4.57	TC	[229]
Recommended	–	–	–	–	–	**4.27 ± 0.05**	–	–
V(110)	–	–	–	–	–	4.52	TC	[321]
V(110)	–	–	$<8 \times 10^{-11}$	~300	–	4.65 ± 0.08	PE	[2428]
V(110)	–	–	–	–	–	4.96	TC	[2548]
V(110)	–	–	–	–	–	4.97	TC	[1980,3067]
V(110)	–	–	?	?	–	5.00	TE	[3695]
V(110)	–	–	–	–	–	5.017	TC	[4460][490]
V(110)	–	–	–	–	–	5.12	TC	[229,334]
V(110)	–	–	–	–	–	5.13	TC	[3179]
Recommended	–	–	–	–	–	**5.04 ± 0.07**	–	–

Table 1 (*continued*)

Surface	Beam	Ion	P_r (Torr)	T (K)	ϕ^+ (eV)	ϕ^e (eV)	Meth.	Refs.
V(111)	–	–	–	–	–	3.72	TC	[321]
V(111)	–	–	–	–	–	4.10	TC	[2548]
V(111)	–	–	–	–	–	4.11	TC	[1980,3067]
V(111)	–	–	?	?	–	4.19	TE	[3695]
V(112)	–	–	–	–	–	4.13	TC	[321]
V(112)	–	–	–	–	–	4.50	TC	[1980,3067]
V(116)	–	–	?	?	–	3.95	TE	[3695]
V(116)	–	–	–	–	–	4.11	TC	[1980,3067]
V/quartz[101]	V	–	$\leq 10^{-8}$	15	–	2.9 ± 0.2	CPD	[1686]
V/quartz	V	–	$\leq 10^{-8}$	293	–	3.0 ± 0.2	CPD	[1686]
V/quartz[101]	V	–	$\leq 10^{-8}$	4.2	–	3.1 ± 0.2	CPD	[1686]
$V_n(n \to \infty)$	–	–	–	–	–	3.68 ± 0.10	TC	[4261]
V	–	–	–	–	–	3.7	TC	[1744]
V[101]	–	–	$\leq 10^{-8}$	4.2–15	–	3.77	FE	[1686]
V	–	–	?	0^E	–	3.77	PE	[3027]
V/W(110)	V	–	$\sim 10^{-11}$	~300	–	3.8	CPD	[2430]
V/W(012)	V	–	$< 1 \times 10^{-10}$	~300	–	$3.81 \pm \leq 0.06$	FE	[1529]
V/Mo(110)	V	–	$\leq 2 \times 10^{-10}$	77	–	3.85	CPD	[328]
V/W(023)	V	–	$< 1 \times 10^{-10}$	~300	–	$3.86 \pm \leq 0.06$	FE	[1529]
V/W(111)	V	–	$< 1 \times 10^{-10}$	~300	–	$3.88 \pm \leq 0.06$	FE	[1529]
V	–	–	–	–	–	3.89	TC	[3476]
V	–	–	–	–	–	3.9	TC	[706]
V/TiO$_2$(110)	–	–	–	–	–	3.9*	TC	[4074]
V	–	–	–	–	–	3.94	TC	[3476]
V	–	–	–	–	–	4.0	TC	[3928]
V/W(112)	V	–	$< 1 \times 10^{-10}$	~300	–	$4.01 \pm \leq 0.06$	FE	[1529]
V/W	V	–	1×10^{-10}	77, 300 (~1300)	–	4.02	FE	[4018]
V	–	–	–	–	–	4.03	TC	[1901]
V	–	–	?	~300	–	4.08 ± 0.02	CPD	[2544]
V/W	V	–	1×10^{-10}	77, 300 (~1300)	–	4.08 ± 0.03*	FE	[4018]
V/TiO$_2$(110)	V	–	1×10^{-10}	~300	–	4.1	PE	[3564]
V	–	–	–	–	–	4.10	TC	[3318]
V/graphite	V	–	$< 10^{-5}$	1410–1540	–	4.12 ± 0.02	TE	[769,2304]
V	–	–	–	–	–	4.15	TC	[1066]
V	–	–	$< 2 \times 10^{-10}$	~300	–	4.17 ± 0.04	CPD	[1898]
V	–	–	–	–	–	4.18	TC	[3318]
V/W(110)	V	–	$< 1 \times 10^{-10}$	~300	–	4.19*	FE	[1529]
V	–	–	–	–	–	4.2	TC	[1993]
V	–	–	1×10^{-10}	~300	–	4.2	PE	[3564]
V/Ag(001)	V	–	2×10^{-10}	30	–	4.25 ± 0.05	PE	[3154,4377]
V/quartz	V	–	$\sim 10^{-10}$	~300	–	4.3 ± 0.1	PE	[304]
V	–	–	1×10^{-9}	~300	–	4.30	CPD	[1252]
V	–	–	–	–	–	4.32	TC	[298]
V	–	–	–	–	–	4.33	TC	[2949]
V	–	–	–	–	–	4.37	TC	[3476]
V/W(110)	–	–	$< 1 \times 10^{-10}$	~300	–	$4.42 \pm \leq 0.06$	FE	[1529]
V	–	–	?	~300	–	4.44	CPD	[2297]
V	–	–	–	–	–	4.44	TC	[3264,3265,3267]
V/Mo(110)	V	–	$\leq 2 \times 10^{-10}$	~300	–	4.54	CPD	[328]
V/Mo(110)	V	–	$\leq 2 \times 10^{-10}$	700	–	4.71	CPD	[328]
V	–	–	–	–	–	5.1	TC	[944]
Recommended	–	–	–	–	–	**4.10 ± 0.05**	–	–

24. Chromium Cr

bcc

Surface	Beam	Ion	P_r (Torr)	T (K)	ϕ^+ (eV)	ϕ^e (eV)	Meth.	Refs.
Cr(100)	–	–	–	–	–	3.710 ± 0.005	TC	[2805]
Cr(100)	–	–	–	–	–	3.88	TC	[2818]
Cr(100)	–	–	–	–	–	3.90	TC	[321]
Cr(100)[103]	–	–	5×10^{-10}	~300	–	3.90 ± 0.1	PE	[2870,3951]
Cr(100)/W(100)	Cr	–	5×10^{-10}	~300 (1700)	–	4.0 ± 0.1	CPD	[1488]
Cr(100)	–	–	–	–	–	4.05	TC	[1911,1912]
Cr(100)/Au(100)[103]	Cr	–	5×10^{-10}	~300	–	4.05 ± 0.1	PE	[3951]
Cr(100)	–	–	–	–	–	4.06	TC	[2805]

Table 1 (*continued*)

Surface	Beam	Ion	P_r (Torr)	T (K)	ϕ^+ (eV)	ϕ^e (eV)	Meth.	Refs.
Cr(100)	–	–	?	~300	–	4.10 ± 0.05	PE	[2638]
Cr(100)	–	–	–	–	–	4.25	TC	[1911]
Cr(100)	–	–	–	–	–	4.27	TC	[4034]
Cr(100)	–	–	–	–	–	4.40	TC	[1912]
Cr(100)	–	–	–	–	–	4.46	TC	[1011]
Cr(100)	–	–	~10^{-10}	~300	–	4.46 ± 0.06	CPD	[3445,3446]
Cr(100)	–	–	–	–	–	4.48	TC	[1011]
Cr(100)	–	–	–	–	–	4.50	TC	[2701]
Cr(100)	–	–	–	–	–	4.51	TC	[1011]
Cr(100)	–	–	–	–	–	4.57	TC	[1159]
Cr(100)	–	–	–	–	–	4.57	TC	[2701]
Cr(100)	–	–	–	–	–	4.58	TC	[229]
Cr(100)	–	–	–	–	–	4.60	TC	[1011]
Cr(100)	–	–	–	–	–	4.93	TC	[1011]
Cr(100)	–	–	–	–	–	4.94	TC	[229]
Recommended	–	–	–	–	–	**4.43 ± 0.14**	–	–
Cr(110)	–	–	–	–	–	4.44	TC	[4034]
Cr(110)	–	–	–	–	–	4.44	TC	[2685]
Cr(110)	–	–	–	–	–	4.53	TC	[321]
Cr(110)	–	–	–	–	–	4.70	TC	[2818]
Cr(110)	–	–	–	–	–	4.81	TC	[4421]
Cr(110)	–	–	(≤10^{-11})	~300	–	4.85	CPD	[2380]
Cr(110)/W(110)	Cr	–	~10^{-11}	~300 (~700)	–	4.9	CPD	[4260]
Cr(110)/Au(111)	Cr	–	≤5 × 10^{-10}	~300 (>670)	–	5.0	CPD	[3266]
Cr(110)/Ir(111)	Cr	–	≤5 × 10^{-10}	~300 (>670)	–	5.00 ± 0.04	CPD	[3266]
Cr(110)	–	–	–	–	–	5.08	TC	[1159]
Cr(110)/Nb(110)	Cr	–	~10^{-11}	~300 (~700)	–	5.2	CPD	[4260]
Cr(110)	–	–	–	–	–	5.30	TC	[229]
Cr(110)	–	–	–	–	–	5.45	TC	[229,334]
Recommended	–	–	–	–	–	**4.99 ± 0.19**	–	–
Cr(111)	–	–	–	–	–	3.72	TC	[321]
Cr(111)	–	–	–	–	–	3.78	TC	[4034]
Cr(111)	–	–	–	–	–	3.88	TC	[2818]
Cr(112)	–	–	–	–	–	4.05	TC	[2818]
Cr(112)	–	–	–	–	–	4.15	TC	[321]
Cr(116)	–	–	–	–	–	3.75	TC	[2818]
Cr(210)	–	–	–	–	–	4.15	TC	[2805]
Cr	–	–	? (Cs)	~1000–1400	–	3.57	TE	[650,3413]
Cr/ins/Al[47]	Cr	–	?	~300	–	3.71 ± 0.07	CPD	[2028]
Cr/W(100)	Cr	–	≤5 × 10^{-10}	293 (~900)	–	3.8 ± 0.1	FE	[1494,1515]
Cr/W(100)	Cr	–	5 × 10^{-10}	~300 (1200)	–	3.8 ± 0.1	CPD	[1488]
Cr	–	–	?	~300	–	3.88 ± 0.04	CPD	[2544]
Cr	–	–	?	?	–	3.89	TE	[3410]
Cr/W	Cr	–	≤7 × 10^{-8}	~300	–	3.9	FE	[1804]
Cr	–	–	≤1 × 10^{-9}	~1100–1400	–	3.90 ± 0.04	TE	[179,3413]
Cr	–	–	≤10^{-9}	~1050–1450	–	3.90 ± 0.05	TE	[650]
Cr/W	Cr	–	≤7 × 10^{-8}	~300	–	4.0	FE	[1804]
Cr/W(110)	–	–	–	–	–	4.0*	TC	[3001]
Cr/W(100)	Cr	–	5 × 10^{-10}	~300 (1700)	–	4.0 ± 0.1	CPD	[1488]
Cr/W(111)	Cr	–	?	77	–	4.07*	FE	[4250]
Cr$_n$(n → ∞)	–	–	–	–	–	4.07 ± 0.14	TC	[4261]
Cr/W(110)	Cr	–	<1 × 10^{-10}	100	–	4.1*	CPD	[1580]
Cr/W	Cr	–	1 × 10^{-9}	~300	–	4.10 ± 0.08	FE	[2618]
Cr/W(112)	Cr	–	?	77	–	4.10*	FE	[4250]
Cr/SiO$_2$/Si	Cr	–	?	~300 (570)	–	4.18	PE	[2355]
Cr	–	–	–	–	–	4.18	TC	[3476]
Cr/glass	Cr	–	~4 × 10^{-10}	77–90	–	4.19	PE	[2096,3053]
Cr/Ta(111)	Cr	–	~10^{-9}	~300	–	4.2 ± 0.1	FE	[1786,1789]
Cr	–	–	–	–	–	4.22	TC	[3476]
Cr	–	–	–	–	–	4.3	TC	[706]
Cr	–	–	–	–	–	4.3	TC	[3318]
Cr/Mo(110)	Cr	–	~10^{-10}	~300	–	4.3	CPD	[3679]
Cr	–	–	?	~300	–	4.34	PE	[2924]
Cr	–	–	–	–	–	4.38	TC	[1399]

Table 1 (*continued*)

Surface	Beam	Ion	P_r (Torr)	T (K)	ϕ^+ (eV)	ϕ^e (eV)	Meth.	Refs.
Cr	–	–	?	~300	–	4.38	CPD	[2297]
Cr	–	–	–	–	–	4.4	TC	[1993]
Cr/quartz	Cr	–	≤5 × 10⁻⁹	~300	–	4.4	PE	[2309]
Cr	–	–	–	–	–	4.40	TC	[3264,3265,3267]
Cr/glass	Cr	–	2 × 10⁻¹⁰	293 (373)	–	4.40	PE	[3053]
Cr	–	–	–	–	–	4.40	TC	[3637]
Cr	–	–	–	–	–	4.42	TC	[1066]
Cr	–	–	–	–	–	4.44	TC	[4031]
Cr/glass	Cr	–	?	77 (373)	–	4.44	PE	[2096]
Cr/glass	Cr	–	4 × 10⁻¹⁰	293 (378)	–	4.48	PE	[3053]
Cr	–	–	–	–	–	4.49	TC	[3318]
Cr/quartz	Cr	–	~10⁻¹⁰	~300	–	4.5 ± 0.15	PE	[304]
Cr	–	–	–	–	–	4.51	TC	[298]
Cr/ins/Al⁴⁷	Cr	–	?	~300	–	4.51 ± 0.09	CPD	[2028]
Cr	–	–	–	–	–	4.56	TC	[2949]
Cr/W(110)	Cr	–	(≤10⁻¹¹)	~300	–	4.56	CPD	[2380]
Cr	–	–	5 × 10⁻¹⁰	~300	–	4.57	AI³⁸	[4027]
Cr	–	–	–	–	–	4.57	TC	[4031]
Cr/graphite	Cr	–	<10⁻⁵	~1450–1620	–	4.58 ± 0.02	TE	[769,2304]
Cr	–	–	?	?	–	4.6	TE	[3402]
Cr/?	Cr	–	~10⁻⁵	~300	–	4.6	CPD	[1376]
Cr/Au/glass¹⁰⁴	Cr	–	?	~300	–	4.6	CPD	[3207]
Cr/Ni	Cr	–	?	~300	–	4.6 ± 0.1*	CPD	[3592]
Cr	–	–	2 × 10⁻⁸	~1000–1500	–	4.60	TE	[3400]
Cr/W(110)	Cr	–	~10⁻¹¹	~300	–	4.65	CPD	[4260]
Cr	–	–	–	–	–	4.68	TC	[3476]
Cr/Cu	Cr	–	<1 × 10⁻⁹	80	–	4.68	PE	[2472]
Cr	–	–	?	~80	–	4.7	CPD	[2294]
Cr/W(110)	Cr	–	<1 × 10⁻¹⁰	100 (1100)	–	4.8*	CPD	[1580]
Cr/Au/glass¹⁰⁴	Cr	–	?	~300	–	4.8*	CPD	[3207]
Cr	–	–	–	–	–	4.8	TC	[944]
Cr/W(110)	Cr	–	3 × 10⁻⁹	722	–	4.8	FE	[1615]
Cr	–	–	1 × 10⁻¹⁰	100	–	4.80 ± <0.1	PE	[672]
Cr/Au(100)¹⁰⁵	Cr	–	~10⁻¹¹	~300	–	4.87	PE	[3557]
Cr	–	–	–	–	–	4.88	TC	[1744]
Cr/W(110)	Cr	–	3 × 10⁻⁹	?	–	4.9	FE	[1616]
Cr/Au(111)	Cr	–	≤5 × 10⁻¹⁰	~300	–	4.9	CPD	[3266]
Cr/Ir(111)	Cr	–	≤5 × 10⁻¹⁰	~300	–	4.9	CPD	[3266]
Cr/W(110)	Cr	–	3 × 10⁻⁹	~300	–	5.0	FE	[1615]
Cr	–	–	<2 × 10⁻¹⁰	~300	–	5.05 ± 0.04	CPD	[1898]
Cr	–	–	–	–	–	5.2	TC	[3179]
Cr/Fe/Cr(110)	Cr	–	–	–	–	5.45	TC	[3010]
Cr/W	Cr	–	?	~300	–	7.4	FE	[2225]
Recommended	–	–	–	–	–	**4.38 ± 0.04**	–	–

25. Manganese Mn

fcc (γ, T = 1352–1407 K)

Mn(100)	–	–	–	–	–	4.58	TC	[463]
Mn(100)	–	–	–	–	–	4.97	TC	[321]
Mn(100)	–	–	–	–	–	5.37	TC	[229]
Mn(100)	–	–	–	–	–	5.55	TC	[463]
Mn(100)	–	–	–	–	–	5.76	TC	[229]
Mn(110)	–	–	–	–	–	4.67	TC	[321]
Mn(111)	–	–	–	–	–	5.18	TC	[229]
Mn(111)	–	–	–	–	–	5.36	TC	[321]
Mn(111)	–	–	–	–	–	5.45	TC	[229,334]

bcc (δ, T > 1407 K)

Mn(100)	–	–	–	–	–	4.27	TC	[321]
Mn(100)	–	–	–	–	–	4.90	TC	[229]
Mn(100)	–	–	–	–	–	5.31	TC	[229]
Mn(110)	–	–	–	–	–	4.97	TC	[321]
Mn(110)	–	–	–	–	–	5.34	TC	[229]
Mn(110)	–	–	–	–	–	5.69	TC	[229]

Table 1 (*continued*)

Surface	Beam	Ion	P_r (Torr)	T (K)	ϕ^+ (eV)	ϕ^e (eV)	Meth.	Refs.
Mn(111)	–	–	–	–	–	4.09	TC	[321]
Mn(112)	–	–	–	–	–	4.57	TC	[321]
Cubic (α–β, $T < 1079$ K for bulk)								
Mn	–	–	–	–	–	3.0	TC	[1744]
Mn$_n$(n → ∞)	–	–	5×10^{-4}	77	–	3.1	IP	[4264]
Mn/steel	Mn	–	$<2 \times 10^{-10}$	~300 (?)	–	3.54 ± 0.04	CPD	[1898]
Mn/ins/Al[108]	Mn	–	?	~300	–	3.60 ± 0.04	CPD	[2028]
Mn	–	–	?	~300	–	3.70 ± 0.04	CPD	[2544]
Mn$_n$(n → ∞)	–	–	–	–	–	3.74 ± 0.13	TC	[4261]
Mn	–	–	?	~300	–	3.76	PE	[3027]
Mn	–	–	–	–	–	3.76	TC	[3637]
Mn	–	–	–	–	–	3.8	TC	[2583]
Mn/glass	Mn	–	$<10^{-9}$	90	–	3.82	PE	[2096,3052,3053]
Mn/Cu(111)[106]	Mn	–	4×10^{-11}	~300	–	3.9	CPD	[3710]
Mn	–	–	–	–	–	3.90	TC	[3264,3265,3267]
Mn/glass	Mn	–	8×10^{-10}	293 (373)	–	4.06	PE	[3053]
Mn/glass	Mn	–	$<10^{-9}$	90 (373)	–	4.08	PE	[2096,3052]
Mn/glass	Mn	–	6×10^{-10}	293	–	4.1	PE	[3053]
Mn/quartz	Mn	–	$\sim10^{-10}$	~300	–	4.1 ± 0.2	PE	[304]
Mn	–	–	–	–	–	4.10	TC	[4418]
Mn	–	–	?	~300	–	4.14	CPD	[2297]
Mn/Cu(100)[107]	Mn	–	1×10^{-8}	293	–	4.2 ± 0.1	PE	[1554]
Mn/silica	Mn	–	$<2 \times 10^{-10}$	290	–	4.24 ± 0.02	PE	[923,2113]
Mn	–	–	–	–	–	4.27	TC	[3476]
Mn	–	–	–	–	–	4.37	TC	[298]
Mn	–	–	–	–	–	4.4	TC	[706]
Mn/ins/Al[108]	Mn	–	?	~300	–	4.40 ± 0.07*	CPD	[2028]
Mn	–	–	–	–	–	4.44	TC	[3318]
Mn	–	–	–	–	–	4.46	TC	[3476]
Mn	–	–	–	–	–	4.52	TC	[3318]
Mn	–	–	–	–	–	4.7	TC	[3928]
Mn	–	–	–	–	–	4.88	TC	[3476]
Mn	–	–	–	–	–	5.1	TC	[944]
Recommended	–	–	–	–	–	**4.08 ± 0.11**	–	–
fcc (γ, $T = 1352$–1407 K for bulk)								
Mn	–	–	–	–	–	4.28	TC	[3318]
Mn	–	–	–	–	–	4.34	TC	[3318]
bcc (δ, $T > 1407$ K for bulk)								
Mn/graphite	Mn	–	$<10^{-6}$	~1400–1500	–	3.83 ± 0.02	TE	[769,2304]

26. Iron Fe

Surface	Beam	Ion	P_r (Torr)	T (K)	ϕ^+ (eV)	ϕ^e (eV)	Meth.	Refs.
bcc (α, $T < 1042$ K)[407]								
Fe(100)[109]	–	–	–	–	–	3.7	TC	[2901]
Fe(100)	–	–	–	–	–	3.80	TC	[3946]
Fe(100)	–	–	–	–	–	3.85	TC	[4222]
Fe(100)	–	–	–	–	–	3.85	TC	[4374]
Fe(100)	–	–	–	–	–	3.86	TC	[4218]
Fe(100)	–	–	–	–	–	3.87	TC	[1625]
Fe(100)	–	–	–	–	–	3.88	TC	[4009]
Fe(100)[109]	–	–	–	–	–	3.9	TC	[2901]
Fe(100)	–	–	–	–	–	3.90	TC	[1623]
Fe(100)	–	–	–	–	–	3.91	TC	[1619]
Fe(100)	–	–	–	–	–	3.91	TC	[1625]
Fe(100)	–	–	–	–	–	3.94	TC	[4019]
Fe(100)	–	–	–	–	–	4.06	TC	[2911]
Fe(100)[110]	–	–	$<8 \times 10^{-10}$	77	–	4.17 ± 0.03	CPD	[920,3044]
Fe(100)[109]	–	–	?	~300	–	4.24	PE	[2901]
Fe(100)[110]	–	–	$<8 \times 10^{-10}$	77	–	4.24 ± 0.02	CPD	[920]
Fe(100)	–	–	–	–	–	4.29	TC	[549,1105]
Fe(100)	–	–	–	–	–	4.30	TC	[463]
Fe(100)	–	–	–	–	–	4.35	TC	[2777,3614]
Fe(100)	–	–	$<1 \times 10^{-10}$	~300 (1070)	–	4.4	PE	[919]
Fe(100)	–	–	–	–	–	4.4	TC	[2157]
Fe(100)	–	–	–	–	–	4.45	TC	[1708,1710]

Table 1 (*continued*)

Surface	Beam	Ion	P_r (Torr)	T (K)	ϕ^+ (eV)	ϕ^e (eV)	Meth.	Refs.
Fe(100)	–	–	–	–	–	4.47	TC	[1105]
Fe(100)	–	–	–	–	–	4.50	TC	[229,317]
Fe(100)	–	–	–	–	–	4.55	TC	[321]
Fe(100)	–	–	–	–	–	4.57	TC	[1105]
Fe(100)	–	–	–	–	–	4.586	TC	[4337]
Fe(100)	–	–	–	–	–	4.6	TC	[2650]
Fe(100)	–	–	5×10^{-10}	~300	–	4.64 ± 0.03	PE	[3310]
Fe(100)	–	–	$\leq 5 \times 10^{-11}$	~300	–	4.65 ± 0.05	PE	[1607]
Fe(100)	–	–	2×10^{-9}	~300 (720)	–	4.66 ± 0.02	PE	[3311]
Fe(100)	–	–	$\sim 10^{-9}$	~300 (720)	–	4.67 ± 0.03	PE	[921]
Fe(100)	–	–	?	~300	–	4.7	PE	[1709]
Fe(100)	–	–	$< 5 \times 10^{-11}$	~300	–	4.70 ± 0.05	PE	[1831]
Fe(100)	–	–	2×10^{-9}	~300 (820)	–	4.75 ± 0.03	PE	[565]
Fe(100)	–	–	–	–	–	4.77	TC	[1106,4386]
Fe(100)	–	–	–	–	–	4.78	TC	[461]
Fe(100)	–	–	1×10^{-9}	~300	–	4.88 ± 0.07	PE	[564,1107]
Fe(100)	–	–	?	98	–	4.9	PE	[3988]
Fe(100)	–	–	1×10^{-10}	~300	–	5.0	PE	[1531]
Fe(100)	–	–	–	–	–	5.01	TC	[1703]
Recommended	–	–	–	–	–	**4.64 ± 0.05**	–	–
Fe(110)	–	–	–	–	–	4.71	TC	[3761]
Fe(110)/Cu(100)	Fe	–	?	100	–	4.72	PE	[1273]
Fe(110)	–	–	–	–	–	4.73	TC	[4121]
Fe(110)	–	–	–	–	–	4.73	TC	[4130]
Fe(110)	–	–	–	–	–	4.75	TC	[1625]
Fe(110)	–	–	–	–	–	4.76	TC	[1625]
Fe(110)	–	–	–	–	–	4.77	TC	[4120]
Fe(110)	–	–	–	–	–	4.80	TC	[1623]
Fe(110)	–	–	–	–	–	4.81	TC	[1619]
Fe(110)	–	–	–	–	–	4.82	TC	[1619]
Fe(110)	–	–	–	–	–	4.84	TC	[3226]
Fe(110)	–	–	–	–	–	4.86	TC	[2911]
Fe(110)	–	–	–	–	–	4.86	TC	[3236]
Fe(110)/W(110)	Fe	–	?	~300	–	4.98	CPD	[2035]
Fe(110)/W(110)	Fe	–	?	100	–	5.02 ± 0.04	PE	[1273]
Fe(110)	–	–	1×10^{-10}	~300	–	5.05	PE	[1182,1232,1541, 2342]
Fe(110)/W(110)	Fe	–	?	~300 (800)	–	5.1	CPD	[4231]
Fe(110)	–	–	5×10^{-9}	~300	–	5.12	PE	[1107]
Fe(110)	–	–	–	–	–	5.12	TC	[4222]
Fe(110)	–	–	5×10^{-11}	~300	–	5.12 ± 0.06	PE	[922,969]
Fe(110)	–	–	–	–	–	5.16	TC	[334]
Fe(110)	–	–	–	–	–	5.21	TC	[229,317]
Fe(110)	–	–	–	–	–	5.30	TC	[321]
Fe(110)	–	–	–	–	–	5.30	TC	[2745]
Fe(110)/W(110)	Fe	–	3×10^{-10}	~300 (≤1100)	–	5.32 ± 0.02	FE	[530]
Fe(110)	–	–	–	–	–	5.45	TC	[3179]
Recommended	–	–	–	–	–	**4.99 ± 0.04**	–	–
Fe(111)	–	–	–	–	–	3.81	TC	[4222]
Fe(111)	–	–	–	–	–	3.89	TC	[1625]
Fe(111)	–	–	–	–	–	3.90	TC	[1619,1623]
Fe(111)	–	–	–	–	–	3.91	TC	[1619]
Fe(111)	–	–	–	–	–	3.95	TC	[1625]
Fe(111)	–	–	–	–	–	4.35	TC	[321]
Fe(111)	–	–	–	–	–	4.44	TC	[462]
Fe(111)	–	–	$\sim 10^{-9}$	~300 (720)	–	4.81 ± 0.02	PE	[487]
Recommended	–	–	–	–	–	**4.4 ± 0.3**	–	–
Fe(210)	–	–	–	–	–	4.20	TC	[1625]
Fe(210)	–	–	–	–	–	4.27	TC	[1625]
Fe(211)	–	–	–	–	–	4.06	TC	[1625]
Fe(211)	–	–	–	–	–	4.12	TC	[1625]
Fe(211)	–	–	–	–	–	4.85	TC	[321]
Fe(310)	–	–	–	–	–	3.95	TC	[1625]
Fe(310)	–	–	–	–	–	4.05	TC	[1625]

Table 1 (*continued*)

Surface	Beam	Ion	P_r (Torr)	T (K)	ϕ^+ (eV)	ϕ^e (eV)	Meth.	Refs.
Fe(321)	–	–	–	–	–	4.27	TC	[1625]
Fe(321)	–	–	–	–	–	4.32	TC	[1625]
bcc ($\alpha - \beta$, $T < 1179$ K)								
Fe(100)	–	–	–	–	–	4.5 ± 0.3	TC	[1104]
bcc (β, $T = 1042–1179$ K)								
Fe(100)	–	–	–	–	–	4.07	TC	[463]
Fe(100)[427]	–	–	–	–	–	4.2	TC	[1104]
Fe(100)	–	–	–	–	–	4.77	TC	[1106,2650]
Fe(100)	–	–	–	–	–	4.86	TC	[549]
Fe(100)	–	–	–	–	–	5.06	TC	[229]
Fe(110)	–	–	–	–	–	5.78	TC	[229,334]
Fe(111)	–	–	–	–	–	4.81	TC	[462]
fcc (γ, $T = 1179–1674$ K)								
Fe(100)	–	–	–	–	–	4.53	TC	[463]
Fe(100)	–	–	–	–	–	4.86	TC	[549,1105,2777, 3614]
Fe(100)	–	–	–	–	–	5.00	TC	[1914]
Fe(100)	–	–	–	–	–	5.1	TC	[2650]
Fe(100)	–	–	–	–	–	5.28	TC	[321]
Fe(100)	–	–	–	–	–	5.3	TC	[1916,2650]
Fe(100)	–	–	–	–	–	5.45	TC	[1913]
Fe(100)	–	–	–	–	–	5.55	TC	[229]
Recommended	–	–	–	–	–	**5.28 ± 0.19**	–	–
Fe(110)	–	–	–	–	–	4.97	TC	[321]
Fe(111)	–	–	–	–	–	5.54	TC	[229,334]
Fe(111)	–	–	–	–	–	5.70	TC	[321]
fcc (metastable, $T < 1042$ K)[114,407]								
Fe(100)/Cu(100)[412]	Fe	–	?	~300	–	4.62	PE	[2673]
Fe(100)/Cu(100)[412]	Fe	–	?	~300 (500)	–	4.67	PE	[2673]
Fe(100)/Cu(100)	Fe	–	?	~300 (460)	–	4.95 ± 0.05	PE	[2650]
Fe(100)/Cu(100)	–	–	–	–	–	5.10	TC	[1914]
Fe(100)/Cu(100)	Fe	–	?	~300	–	5.4	PE	[1913,4386]
Fe(100)/Cu(100)	–	–	–	–	–	5.4	TC	[1914]
Fe(100)/Cu(100)	–	–	–	–	–	5.48	TC	[1913,4386]
Fe(100)/Cu(100)	Fe	–	?	~300	–	5.5 ± 0.1	PE	[1913,4386]
Fe(100)/Cu(100)	–	–	–	–	–	5.58	TC	[1913,4386]
Fe(100)/Cu(100)	–	–	–	–	–	5.6	TC	[1916]
Recommended	–	–	–	–	–	**5.38 ± 0.22**	–	–
bcc (α, $T < 1042$ K for bulk)								
Fe	–	–	–	–	–	3.7	TC	[2456]
Fe/quartz[51]	Fe	–	~10^{-5}	~300	–	3.86	PE	[1973]
Fe	–	–	~10^{-6}	~300	–	3.91	PE	[3389,3394]
Fe	–	–	?	~300	–	3.92 ± 0.02	PE	[3388,3394]
Fe/silica	Fe	–	~10^{-8}	~300	–	4.0	PE	[2010]
Fe/glass	Fe	–	<1×10^{-10}	78	–	4.06	PE	[414]
Fe	–	–	?	~300	–	4.06 ± 0.01	CPD	[2544]
Fe/glass[369]	Fe	–	~10^{-10}	77	–	4.10 ± 0.02	PE	[2132,2133,2147]
Fe/glass	Fe	–	<10^{-9}	90	–	4.11	PE	[1957]
Fe/glass	Fe	–	2×10^{-10}	273	–	4.12	PE	[2096,3053]
Fe/glass	Fe	–	<10^{-9}	273	–	4.12	PE	[2307,3048]
Fe/glass	Fe	–	~10^{-10}	77	–	4.13	PE	[3052]
Fe	–	–	?	~300	–	4.16*	CPD	[3621]
Fe/glass	Fe	–	<10^{-9}	90	–	4.16	PE	[2763,3046]
Fe/glass	Fe	–	~10^{-8}	~300	–	4.16 ± 0.02	CPD	[13,349]
Fe/glass	Fe	–	~10^{-8}	~300	–	4.17 ± 0.03	CPD	[133]
Fe/Ag(100)	Fe	–	?	?	–	4.2	?	[1696]
Fe/W	Fe	–	~10^{-10}	~300	–	4.2	FE	[2369]
Fe	–	–	<10^{-6}	~300	–	4.2	PE	[2919]
Fe/W(110)	–	–	–	–	–	4.20	TC	[1270]
Fe	K	K$^+$	~10^{-9}	~700–1100	4.24	–	PSI	[2115]
Fe/W	–	–	?	?	–	4.25	FE	[3346]

Table 1 (*continued*)

Surface	Beam	Ion	P_r (Torr)	T (K)	ϕ^+ (eV)	ϕ^e (eV)	Meth.	Refs.
Fe/W(110)	–	–	–	–	–	4.26	TC	[1270]
Fe/W(100)	Fe	–	$<2 \times 10^{-10}$	~300	–	4.27	FE	[2257]
Fe/W(100)	Fe	–	$<2 \times 10^{-10}$	~600	–	4.27	FE	[2257]
Fe	–	–	6×10^{-3}	~300	–	4.30 ± 0.06	PE	[2079,2080]
Fe/W(111)	–	–	–	–	–	4.31	TC	[1270]
Fe/W(112)	–	–	3×10^{-10}	~300 (900)	–	4.31 ± 0.02	FE	[530]
Fe/W(111)	–	–	–	–	–	4.33	TC	[1270]
Fe/Ta(111)	Fe	–	$<1 \times 10^{-10}$	~300	–	4.35	CPD	[3302]
Fe/W(100)	Fe	–	$<5 \times 10^{-11}$	~300	–	4.35	CPD	[2035]
Fe/glass	Fe	–	$<1 \times 10^{-10}$	78 (293)	–	4.36	PE	[414]
Fe/glass	Fe	–	?	77	–	4.38	PE	[3075]
Fe/glass	Fe	–	$<10^{-10}$	77 (323)	–	4.38 ± 0.02	PE	[2147]
Fe	–	–	?	~300	–	4.40	CPD	[2297]
Fe	–	–	?	~300	–	4.40	PE	[4278]
Fe	–	–	–	–	–	4.40	TC	[1885]
Fe/glass[369]	Fe	–	$\sim 10^{-10}$	77 (323)	–	4.40	PE	[2133]
Fe/W(111)	Fe	–	$<5 \times 10^{-11}$	~300	–	4.40*	CPD	[2429]
Fe/glass	Fe	–	?	273	–	4.42	PE	[3075]
Fe	–	–	–	–	–	4.43	TC	[4031]
Fe/W(100)	Fe	–	3×10^{-10}	~300 (900)	–	4.43 ± 0.02	FE	[530]
Fe/W(110)	Fe	–	?	90	–	4.47	CPD	[2754]
Fe/W(100)	–	–	–	–	–	4.49	TC	[1270]
Fe	–	–	–	–	–	4.49	TC	[3476]
Fe/TiO$_2$(001)	Fe	–	$\sim 10^{-10}$	~300	–	4.5	CPD	[1567]
Fe	–	–	–	–	–	4.5	TC	[706]
Fe/Au(001)	–	–	–	–	–	4.5	TC	[1719]
Fe/W(110)	Fe	–	?	90	–	4.5	CPD	[2755]
Fe/Ag(001)	Fe	–	2×10^{-10}	30	–	4.5 ± 0.05	PE	[3145,4377]
Fe/quartz	Fe	–	$\sim 10^{-10}$	~300	–	4.5 ± 0.15	PE	[304]
Fe	–	–	–	–	–	4.51	TC	[2005]
Fe	–	–	–	–	–	4.51	TC	[1399]
Fe	–	–	–	–	–	4.52	TC	[1645]
Fe/W(100)	–	–	–	–	–	4.53	TC	[1270]
Fe	–	–	–	–	–	4.53	TC	[3318]
Fe	–	–	–	–	–	4.53	TC	[3476]
Fe	–	–	–	–	–	4.56	TC	[4031]
Fe/glass	Fe	–	$<10^{-9}$	273 (393)	–	4.56	PE	[2307]
Fe/W(110)	–	–	–	–	–	4.57	TC	[1270]
Fe/glass	Fe	–	$<10^{-9}$	90 (393)	–	4.57	PE	[3048]
Fe/W(116)	Fe	–	3×10^{-10}	~300 (900)	–	4.57 ± 0.03	FE	[530]
Fe/Si(111)	Fe	–	5×10^{-9}	~300	–	4.58 ± 0.05	CPD	[3270]
Fe	–	–	–	–	–	4.6	TC	[2583]
Fe	–	–	$\sim 10^{-7}$	~300 (750)	–	4.6 ± 0.03	CPD	[2346]
Fe/glass	Fe	–	2×10^{-10}	293 (393)	–	4.60	PE	[3052,3053]
Fe	–	–	?	~300	–	4.60	PE	[2924]
Fe	–	–	–	–	–	4.61	TC	[298]
Fe/glass	Fe	–	$<10^{-9}$	90 (393)	–	4.63	PE	[2096]
Fe	–	–	?	~300	–	4.63	PE	[2924]
Fe/W(111)	Fe	–	3×10^{-10}	~300 (900)	–	4.63 ± 0.02	FE	[530]
Fe	–	–	–	0	–	4.64	TC	[4419]
Fe	–	–	–	–	–	4.65	TC	[3352]
Fe	–	–	–	–	–	4.65	TC	[3264,3265,3267]
Fe[406]	–	–	$\sim 10^{-8}$	870	–	4.65 ± 0.01	PE	[305]
Fe/glass	Fe	–	3×10^{-10}	90 (393)	–	4.66	PE	[3053]
Fe/W(110)	Fe	–	?	90 (150)	–	4.66	CPD	[2754]
Fe/?	?	–	$\sim 10^{-6}$	~300	–	4.68	PE	[3027]
Fe	–	–	$\sim 10^{-10}$	~300	–	4.68	CPD	[3131]
Fe	–	–	–	–	–	4.68	TC	[3637]
Fe/W(111)	Fe	–	$<5 \times 10^{-11}$	~300	–	4.68	CPD	[2035]
Fe/W(111)	–	–	–	–	–	4.69	TC	[1270]
Fe/?	Fe	–	2×10^{-10}	4.2 (400)	–	4.7	PE	[1506]
Fe/glass	Fe	–	$<10^{-8}$	78	–	4.7 ± 0.02	CPD	[1646]
Fe/steel	Fe	–	$\sim 10^{-10}$	4.2	–	4.7 ± 0.1	PE	[1410]
Fe[406]	–	–	$\sim 10^{-8}$	~300	–	4.70 ± 0.01	PE	[305]
Fe/glass	Fe	–	$<10^{-9}$	90 (373)	–	4.71	PE	[2763,3046,3052]
Fe/W(112)	Fe	–	$<5 \times 10^{-11}$	~300	–	4.71	CPD	[2035]
Fe	–	–	1×10^{-8}	~300	–	4.71 ± 0.02	PE	[306]
Fe/silica	Fe	–	$<2 \times 10^{-10}$	290	–	4.71 ± 0.02	PE	[923,2113,2114]
Fe/glass	Fe	–	$<10^{-9}$	293 (373)	–	4.72	PE	[1957,3046]
Fe/W(110)	Fe	–	?	90 (600)	–	4.72	CPD	[2754]

Table 1 (*continued*)

Surface	Beam	Ion	P_r (Torr)	T (K)	ϕ^+ (eV)	ϕ^e (eV)	Meth.	Refs.
Fe	–	–	$\sim10^{-8}$	~300	–	4.72 ± 0.07	PE	[1630]
Fe/W(110)	–	–	–	–	–	4.73	TC	[531]
Fe	–	–	?	~300	–	4.74	PE	[2464]
Fe	–	–	$\sim10^{-7}$	~300 (≤1070)	–	4.75 ± 0.08	CPD	[2346]
Fe/W(110)	Fe	–	?	90 (175, 250)	–	4.76	CPD	[2754]
Fe/W(100)	–	–	–	–	–	4.77	TC	[1270]
Fe	–	–	–	–	–	4.77	TC	[2949]
Fe	–	–	1×10^{-8}	~300	–	4.77	PE	[306]
Fe/W(110)	Fe	–	?	90 (~300)	–	4.77	CPD	[2754]
Fe	–	–	1×10^{-8}	~300	–	4.77 ± 0.02	PE	[306]
Fe/Al(001)	–	–	–	–	–	4.79	TC	[3003]
Fe/W	Fe	–	3×10^{-10}	~300 (900)	–	4.8	FE	[530]
Fe	–	–	–	–	–	4.8	TC	[944]
Fe/W(110)	Fe	–	$\sim10^{-11}$	~300	–	4.8	CPD	[2430]
Fe	–	–	$\sim10^{-8}$	~300	–	4.8 ± 0.05	CPD	[1542]
Fe	–	–	$\sim10^{-9}$	~300 (≤1070)	–	4.80 ± 0.04	CPD	[2346]
Fe	–	–	$<10^{-9}$	~300	–	4.81	PE	[307]
Fe	–	–	$<2 \times 10^{-10}$	~300	–	4.85 ± 0.04	CPD	[1898]
Fe/W(111)	–	–	–	–	–	4.86	TC	[531]
Fe/?	Fe	–	$\sim10^{-5}$	~300	–	4.9	CPD	[1376]
Fe/W(110)	Fe	–	?	~300	–	4.9	CPD	[2755]
Fe/W(110)	Fe	–	?	~300 (600)	–	4.9	CPD	[2755]
Fe/W(100)	–	–	–	–	–	4.92	TC	[531]
Fe	–	–	–	–	–	4.92	TC	[1066]
Fe	–	–	6×10^{-9}	~300	–	4.95	PE	[1139]
Fe/W(110)	Fe	–	$<5 \times 10^{-11}$	~300	–	4.98	CPD	[2035]
Fe	–	–	–	–	–	5.00	TC	[3476]
Fe/W(112)	–	–	–	–	–	5.05	TC	[531]
Fe/Mo(110)	Fe	–	3×10^{-11}	500	–	5.07	CPD	[3293]
Fe/Mo(110)	Fe	–	3×10^{-11}	~300	–	5.09	CPD	[3293]
Fe/W(110)	Fe	–	3×10^{-10}	~300 (900)	–	5.32 ± 0.02	FE	[530]
Recommended	–	–	–	–	–	**4.55 ± 0.05**	–	–

bcc (β, $T = 1042$–1179 K for bulk)

Surface	Beam	Ion	P_r (Torr)	T (K)	ϕ^+ (eV)	ϕ^e (eV)	Meth.	Refs.
Fe	–	–	$\leq1 \times 10^{-9}$	~1100–1160	–	4.33	TE	[179]
Fe	–	–	–	–	–	4.44	TC	[3318]
Fe	–	–	–	–	–	4.45	TC	[3318]
Fe	–	–	3×10^{-8}	1120–1180	–	4.48 ± 0.06	TE	[310]
Fe	Na	Na$^+$	$\sim10^{-9}$	1180	4.49[112]	–	PSI	[303]
Fe	K	K$^+$	$\sim10^{-9}$	1180	4.49[112]	–	PSI	[303]
Fe[406]	–	–	$\sim10^{-8}$	1125	–	4.62 ± 0.01	PE	[305]
Fe	–	–	3×10^{-8}	1120–1180	–	4.64 ± 0.06*	TE	[310]
Fe[113]	–	–	$<10^{-6}$	1110–1170	–	4.77	TE	[3024]
Recommended	–	–	–	–	–	**4.52 ± 0.17**	–	–

bcc–fcc (β–γ, $T = 1042$–1674 K for bulk)

Surface	Beam	Ion	P_r (Torr)	T (K)	ϕ^+ (eV)	ϕ^e (eV)	Meth.	Refs.
Fe[111]	–	Na$^+$	5×10^{-9} (O_2)	~1050–1350	3.6 ± 0.1	(4.0 ± 0.1)	PSI	[277]
Fe[111]	–	K$^+$	5×10^{-9} (O_2)	~1050–1350	3.8 ± 0.1	(4.0 ± 0.1)	PSI	[277]
Fe	–	–	5×10^{-9} (O_2)	~1050–1350	(3.6–4.3)	4.0 ± 0.1	TE	[277,2115]
Fe	–	–	$\sim10^{-9}$	~1100–1300	(4.4 ± 0.2)	4.0 ± 0.2	TE	[308]
Fe	–	–	$\sim10^{-9}$	~1100–1300	–	4.3	TE	[309]
Fe[111]	–	K$^+$	5×10^{-9} (O_2)	~1050–1350	4.3 ± 0.1*	(4.0 ± 0.1)	PSI	[277]
Fe	Na	Na$^+$	$\sim10^{-9}$	~1050–1350	4.4 ± 0.2	(4.0 ± 0.2)	PSI	[308]

fcc (γ, $T = 1179$–1674 K for bulk)

Surface	Beam	Ion	P_r (Torr)	T (K)	ϕ^+ (eV)	ϕ^e (eV)	Meth.	Refs.
Fe	–	–	?	~1300–1500	–	4.04	TE	[1762]
Fe[473]	–	–	3×10^{-8}	1180–1250	–	4.21 ± 0.05	TE	[310]
Fe	–	–	1×10^{-9}	1205–1494	–	4.28 ± 0.06	TE	[179]
Fe/graphite	Fe	–	$<10^{-5}$	~1400–1600	–	4.31 ± 0.02	TE	[769,2304]
Fe	–	–	$\leq1 \times 10^{-9}$	~1200–1550	–	4.47 ± 0.09	TE	[179,3413]
Fe	–	–	$\leq10^{-9}$	?	–	4.5	TE	[650]
Fe	–	–	$\leq1 \times 10^{-9}$	1240–1510	–	4.50 ± 0.05	TE	[179]
Fe	–	–	$\leq1 \times 10^{-9}$	1283–1492	–	4.52 ± 0.04	TE	[179]
Fe	Na	Na$^+$	$\sim10^{-9}$	1183	4.55[112]	–	PSI	[303]
Fe	K	K$^+$	$\sim10^{-9}$	1183	4.55[112]	–	PSI	[303]
Fe	–	–	$\leq1 \times 10^{-9}$	1350–1494	–	4.55 ± 0.06	TE	[179]
Fe	–	–	?	?	–	4.6	TE	[3402]
Fe[473]	–	–	3×10^{-8}	1180–1250	–	4.66 ± 0.05*	TE	[310]

Table 1 (*continued*)

Surface	Beam	Ion	P_r (Torr)	T (K)	ϕ^+ (eV)	ϕ^e (eV)	Meth.	Refs.
Fe[406]	–	–	$\sim 10^{-8}$	1243	–	4.68 ± 0.01	PE	[305]
Fe[113]	–	–	$< 10^{-6}$	1170–1230	–	4.77	TE	[3024]
Recommended	–	–	–	–	–	**4.54 ± 0.05**	–	–
bcc (δ, $T > 1674$ K for bulk)								
Fe/graphite	Fe	–	?	1643–1763	–	4.76	TE	[2568]
Fe	–	–	?	1780–1850	–	4.76	TE	[2608]
fcc (metastable, $T < 1042$ K)[114]								
Fe/Cu(100)	Fe	–	$\sim 10^{-10}$	~ 300 (400)	–	4.46	PE	[2175]
Fe/Cu(100)	Fe	–	$\sim 10^{-10}$	~ 300	–	4.59	PE	[2175]
Fe/Cu(100)	Fe	–	?	30	–	4.7 ± 0.1	PE	[2878,4377]
Fe/Cu(100)	–	–	–	–	–	5.09	TC	[3654]

27. Cobalt Co

Surface	Beam	Ion	P_r (Torr)	T (K)	ϕ^+ (eV)	ϕ^e (eV)	Meth.	Refs.
hcp (α, $T < 695$ K for bulk)[474]								
Co(0001)	–	–	–	–	–	5.00	TC	[2910]
Co(0001)	–	–	$< 2 \times 10^{-10}$	~ 300	–	5.1 ± 0.1	PE	[2036]
Co(0001)	–	–	–	–	–	5.18	TC	[2423]
Co(0001)	–	–	?	?	–	5.2	PE	[2173]
Co(0001)	–	–	4×10^{-11}	100–300	–	5.2*	PE	[2141]
Co(0001)	–	–	5×10^{-11}	~ 300	–	5.20 ± 0.03	PE	[922,969]
Co(0001)[115]	–	–	$< 4 \times 10^{-10}$	~ 300	–	5.264	CPD	[3192,3193]
Co(0001)/Mo(110)	Co	–	$< 6 \times 10^{-11}$	~ 300	–	5.45	CPD	[3293]
Co(0001)	–	–	–	–	–	5.48	TC	[334]
Co(0001)	–	–	–	–	–	5.53	TC	[229,317]
Co(0001)	–	–	$\leq 5 \times 10^{-10}$	160–300	–	5.55 ± 0.20	PE	[2537,3381,3633]
Co(0001)	–	–	–	–	–	5.62	TC	[4005]
Co(0001)	–	–	–	–	–	5.69	TC	[463]
Co(0001)	–	–	–	–	–	5.75	TC	[321]
Co(0001)	–	–	–	–	–	5.80	TC	[463]
Co(0001)	–	–	–	–	–	5.81	TC	[229,334]
Recommended	–	–	–	–	–	**5.30 ± 0.18**	–	–
Co(1010)	–	–	–	–	–	5.50	TC	[321]
Co(1011)	–	–	$< 4 \times 10^{-10}$	300	–	5.250	CPD	[3193]
Co(1120)	–	–	4×10^{-11}	100–300	–	4.1*	PE	[2141]
Co(1124)	–	–	–	–	–	4.83	TC	[321]
fcc (β, $T > 695$ K for bulk)[474]								
Co(100)	–	–	–	–	–	5.047	TC	[2510]
Co(100)	–	–	–	–	–	5.174	TC	[2510]
Co(100)	–	–	–	–	–	5.25	TC	[321]
Co(100)	–	–	–	–	–	5.52	TC	[229,317]
Co(100)	–	–	–	–	–	5.83	TC	[229]
Recommended	–	–	–	–	–	**5.25 ± 0.17**	–	–
Co(110)	–	–	–	–	–	4.95	TC	[321]
Co(111)	–	–	–	–	–	4.93	TC	[2068]
Co(111)	–	–	–	–	–	5.03	TC	[2910]
Co(111)	–	–	–	–	–	5.05	TC	[4421]
Co(111)[115]	–	–	$< 4 \times 10^{-10}$	$\sim 300^E$	–	5.266	CPD	[3192]
Co(111)	–	–	–	–	–	5.44	TC	[4174,4284]
Co(111)	–	–	–	–	–	5.55	TC	[229,317]
Co(111)	–	–	–	–	–	5.68	TC	[321]
Co(111)	–	–	–	–	–	5.76	TC	[229,334]
Recommended	–	–	–	–	–	**5.39 ± 0.23**	–	–
bcc (metastable phase, $T < 695$ K)[428]								
Co(100)/GaAs(110)	–	–	–	–	–	4.66[430]	TC	[4023]
Co(100)/GaAs(110)	–	–	–	–	–	4.75[430]	TC	[4023]
Co(100)/GaAs(110)	–	–	–	–	–	5.10[429]	TC	[4023]
Co(100)/GaAs(110)	–	–	–	–	–	5.20[430]	TC	[4023]
Co(100)/GaAs(110)	–	–	–	–	–	5.55[429]	TC	[4023]

Table 1 (*continued*)

Surface	Beam	Ion	P_r (Torr)	T (K)	ϕ^+ (eV)	ϕ^e (eV)	Meth.	Refs.
fcc (metastable phase, $T < 695$ K)								
Co(100)/Cu(100)[412]	Co	–	?	~300	–	4.72	PE	[2673]
hcp (α, $T < 695$ K for bulk)[474]								
Co	–	–	~10^{-6}	~300	–	3.90 ± 0.02	PE	[3389,3394]
Co	–	–	?	~300	–	3.92	PE	[3388]
Co/glass	Co	–	<10^{-8}	78	–	4.1 ± 0.02	CPD	[1646]
Co[116]	–	–	≤3 × 10^{-8}	~300 (1120)	–	4.12 ± 0.04	PE	[1631,1632]
Co	–	–	–	–	–	4.16	TC	[1399]
Co	–	–	–	–	–	4.2*	TC	[1955]
Co	–	–	?	~300	–	4.21	CPD	[2297]
Co	–	–	?	~300	–	4.25	CPD	[2469]
Co	–	–	?	~300	–	4.27 ± 0.01	CPD	[2544]
Co	–	–	~10^{-6}(Ar)	293	–	4.35 ± 0.02	CPD	[3977]
Co/W	Co	–	?	?	–	4.4	FE	[3346]
Co/W(100)	Co	–	1 × 10^{-10}	100 (1100)	–	4.4*	CPD	[2270]
Co/?[117]	Co	–	2 × 10^{-10}	4.2	–	4.4 ± 0.1	PE	[1506]
Co	–	–	–	–	–	4.41	TC	[3476]
Co/glass	Co	–	<10^{-10}	77	–	4.426	PE	[2136]
Co/glass	Co	–	<10^{-10}	77	–	4.43 ± 0.02	PE	[2132,2147]
Co/glass[369]	Co	–	~10^{-10}	77	–	4.44	PE	[2133]
Co	–	–	–	–	–	4.47	TC	[2005]
Co	–	–	–	–	–	4.48	TC	[3318]
Co/?	Co	–	5 × 10^{-9}	~300	–	4.5	PE	[3506]
Co	–	–	–	–	–	4.53	TC	[3476]
Co/glass	Co	–	<10^{-10}	77 (196)	–	4.54 ± 0.02	PE	[2147]
Co/glass	Co	–	<10^{-10}	77 (273)	–	4.544	PE	[2136]
Co	–	–	–	–	–	4.56	TC	[3318]
Co/glass	Co	–	2 × 10^{-10}	293	–	4.59	PE	[3053]
Co	–	–	–	–	–	4.60	TC	[3637]
Co/glass	Co	–	<10^{-9}	90	–	4.60	PE	[2096,3052,3053]
Co/glass	Co	–	2 × 10^{-10}	90	–	4.61	PE	[3053]
Co/glass	Co	–	<10^{-10}	77 (273)	–	4.63 ± 0.02	PE	[2147]
Co	–	–	–	–	–	4.7	TC	[706]
Co/Pt(110)	Co	–	~8 × 10^{-11}	100	–	4.7 ± 0.1	PE	[1923]
Co	–	–	–	–	–	4.70	TC	[3264,3265,3267]
Co	–	–	–	–	–	4.70	TC	[3352]
Co/W(110)	–	–	–	–	–	4.72	TC	[531]
Co/CoSi$_2$(111)	Co	–	?	~300	–	4.75	PE	[2872]
Co/glass	Co	–	<10^{-10}	77 (478)	–	4.82 ± 0.02	PE	[2147]
Co/glass	Co	–	<10^{-10}	77 (≤478)	–	4.83 ± 0.01	PE	[2136]
Co/Si(111)[118]	Co	–	4 × 10^{-11}	~300	–	4.86 ± 0.05	PE	[2451]
Co	–	–	–	–	–	4.87	TC	[2949]
Co/silica	Co	–	<2 × 10^{-10}	290	–	4.89 ± 0.04	PE	[923,2113,2114]
Co/?[117]	Co	–	2 × 10^{-10}	400	–	4.9 ± 0.1	PE	[1506]
Co/glass[369]	Co	–	~10^{-10}	77 (323)	–	4.91	PE	[2133]
Co	–	–	<2 × 10^{-10}	~300	–	4.92 ± 0.04	CPD	[1898]
Co[119]	–	–	<4 × 10^{-10}	663	–	4.923	CPD	[1148]
Co/Pt(111)	–	–	–	–	–	4.94	TC	[4024]
Co/glass	Co	–	2 × 10^{-10}	293 (393)	–	4.95	PE	[3053]
Co/CoSi$_2$(111)	Co	–	?	~300	–	4.95 ± 0.05	PE	[2169]
Co	–	–	–	–	–	4.96	TC	[3476]
Co[119]	–	–	<4 × 10^{-10}	300	–	4.960	CPD	[1148,3193]
Co/glass	Co	–	<10^{-9}	293 (393)	–	4.97	PE	[2096,3052]
Co	–	–	~10^{-10}	300	–	4.97	CPD	[3153]
Co/Si(111)	Co	–	<5 × 10^{-9}	~300	–	4.97 ± 0.05	CPD	[3270]
Co$_n$($n \to \infty$)	–	–	–	–	–	4.98 ± 0.09	TC	[4261]
Co/Pd(111)	Co	–	<3 × 10^{-10}	~300	–	5.0	PE	[3645]
Co/W(110)	Co	–	1 × 10^{-10}	100	–	5.0*	CPD	[2270]
Co	–	–	–	–	–	5.0	TC	[944]
Co/quartz	Co	–	~10^{-10}	~300	–	5.0 ± 0.1	PE	[304]
Co/glass	Co	–	2 × 10^{-10}	293 (393)	–	5.00	PE	[3053]
Co	–	–	–	–	–	5.00	TC	[298]
Co/Pd(111)	–	–	–	–	–	5.00	TC	[4024]
Co/glass	Co	–	?	77 (≤373)	–	5.05 ± 0.15	PE	[2127]
Co/W(111)	–	–	–	–	–	5.08	TC	[531]
Co/W(110)	Co	–	1 × 10^{-10}	100 (1100)	–	5.1*	CPD	[2270]
Co	–	–	–	–	–	5.10	TC	[4024]
Co/Cu/Co(0001)	–	–	–	–	–	5.12	TC	[3490]
Co/W(112)	–	–	–	–	–	5.17	TC	[531]

Table 1 (*continued*)

Surface	Beam	Ion	P_r (Torr)	T (K)	ϕ^+ (eV)	ϕ^e (eV)	Meth.	Refs.
Co/Fe(001)	Co	–	$<5 \times 10^{-11}$	~300	–	5.20 ± 0.02	PE	[1831]
Co/Si(111)	Co	–	5×10^{-11}	~300	–	5.27	PE	[1820,2865]
Co/W(100)	–	–	–	–	–	5.28	TC	[531]
Co	–	–	–	–	–	5.32	TC	[950]
Co	–	–	–	–	–	5.44	TC	[1066]
Recommended	–	–	–	–	–	**4.71 ± 0.03**	–	–
fcc (β, $T > 695$ K for bulk)[474]								
Co/W(100)	Co	–	$<8 \times 10^{-11}$	~300	–	3.6	FE	[364]
Co/W	Co	–	$<8 \times 10^{-11}$	~300, 580	–	3.9	FE	[364]
Co/W(110)	Co	–	$<8 \times 10^{-11}$	~300	–	4.1	FE	[364]
Co[116]	–	–	$\leq 3 \times 10^{-8}$	~300 (1120)	–	4.25 ± 0.08	PE	[1632]
Co	–	–	?	?	–	4.3	TE	[3402]
Co/graphite	Co	–	$<10^{-6}$	~1400–1600	–	4.41 ± 0.02	TE	[769,2304]
Co	–	–	3×10^{-8}	>1120	–	4.41 ± 0.10	TE	[310]
Co/W(100)	–	–	$<8 \times 10^{-11}$	580	–	4.5	FE	[364]
Co[120]	–	–	?	1340–1390	–	4.6 ± 0.3	TE	[3604]
Co[120]	–	–	?	1390–1440	–	4.8 ± 0.3	TE	[3604]
Co[119]	–	–	$<4 \times 10^{-10}$	673	–	4.925	CPD	[1148]
Co	–	–	$<4 \times 10^{-10}$	720	–	4.93	CPD	[3153]
Co[119]	–	–	$<4 \times 10^{-10}$	300[E]	–	4.966	CPD	[1148]
Co/W(110)	Co	–	$<8 \times 10^{-11}$	580	–	5.1	FE	[364]
Recommended	–	–	–	–	–	**4.50 ± 0.13**	–	–
fcc (metastable, $T < 695$ K)								
Co/Cu(100)	Co	–	1×10^{-10}	<50	–	4.4	PE	[950]
Co/Cu(100)	Co	–	$\sim 1 \times 10^{-10}$	<50	–	4.5	PE	[950]
Co/Cu(100)	Co	–	$<8 \times 10^{-11}$	400	–	4.72 ± 0.03	PE	[3475]
Co/Cu(100)	Co	–	$<8 \times 10^{-11}$	400	–	4.78 ± 0.03	PE	[3475]
Co/Cu(100)	–	–	–	–	–	4.83	TC	[3377]
Co/Cu(100)	–	–	–	–	–	4.93	TC	[3377]
Co/Cu(111)	Co	–	$<8 \times 10^{-11}$	~300	–	5.02	PE	[968]
Co/Cu(001)	–	–	–	–	–	5.15	TC	[3377]
Co/Cu(001)	–	–	–	–	–	5.30	TC	[2897]
Co/Cu(001)	–	–	–	–	–	5.31	TC	[2897]
Co/Cu(001)[121]	Co	–	2×10^{-10}	30	–	5.0 ± 0.2	PE	[2879,4377]
Co/Cu(001)[122]	–	–	–	–	–	5.34	TC	[3654]
Recommended	–	–	–	–	–	**4.94 ± 0.30**	–	–

28. Nickel Ni

Surface	Beam	Ion	P_r (Torr)	T (K)	ϕ^+ (eV)	ϕ^e (eV)	Meth.	Refs.
fcc								
Ni(100)	–	–	–	–	–	4	TC	[2884]
Ni(100)	–	–	–	–	–	4.7	TC	[935,1006]
Ni(100)	–	–	$\sim 10^{-10}$	~300	–	4.75 ± 0.1	CPD	[1983]
Ni(100){95%}	–	–	–	–	(5.21 ± 0.01)	4.80 ± 0.09	TC	[283,630,1351]
Ni(100)	–	–	2×10^{-10}	460 (750)	–	4.84 ± 0.03	PE	[1032]
Ni(100)	–	–	–	–	–	4.86	TC	[3224]
Ni(100)	–	–	2×10^{-10}	343 (705)	–	4.89 ± 0.03	PE	[1032]
Ni(100)	–	–	1×10^{-9}	~1400–1600	–	4.89 ± 0.03	TE	[312,837]
Ni(100)	–	–	?	~300	–	4.9	CPD	[1379]
Ni(100)	–	–	–	–	–	4.95 ± 0.02	TC	[4331]
Ni(100)	–	–	$<5 \times 10^{-11}$	~300	–	4.95 ± 0.05	CPD	[1005,2830]
Ni(100)	–	–	–	–	–	4.96	TC	[4454]
Ni(100)	–	–	–	–	–	4.97	TC	[311]
Ni(100)	–	–	–	–	–	5.0	TC	[935,3556]
Ni(100)	–	–	–	–	–	5.02	TC	[463]
Ni(100)	–	–	–	–	–	5.05	TC	[2701]
Ni(100)	–	–	–	–	–	5.05	TC	[4258]
Ni(100)[123]	–	–	$\sim 10^{-10}$	~300	–	5.08	PE	[903]
Ni(100)	–	–	?	~300	–	5.08	PE	[2673]
Ni(100)	–	–	–	–	–	5.09	TC	[4229]
Ni(100)	–	–	?	~300	–	5.09 ± 0.03	PE	[3180]
Ni(100)	–	–	–	–	–	5.1	TC	[1006,1108,1109]
Ni(100)	–	–	$<1 \times 10^{-10}$	~300	–	5.1 ± 0.1	CPD	[1110,1517]
Ni(100)[123]	–	–	$\sim 10^{-10}$	~300 (623)	–	5.12	PE	[903]
Ni(100)/mica[124]	Ni	–	2×10^{-9}	~300{593}	–	5.12 ± 0.02	PE	[314]
Ni(100)	–	–	$\sim 10^{-10}$	~300 (?)	–	5.135	PE	[903]
Ni(100)	–	–	$\sim 10^{-10}$	~300	–	5.14	PE	[3744]
Ni(100)	–	–	4×10^{-10}	273	–	5.15 ± 0.05	PE	[484]

Table 1 (*continued*)

Surface	Beam	Ion	P_r (Torr)	T (K)	ϕ^+ (eV)	ϕ^e (eV)	Meth.	Refs.
Ni(100)/glass[125]	Ni	–	2×10^{-9}	77 (523)	–	5.17 ± 0.02	PE	[314]
Ni(100)	–	–	–	–	–	5.19	TC	[2548]
Ni(100)	–	–	1×10^{-10}	100, 300	–	5.2	PE	[1808]
Ni(100)	–	–	$\leq 3 \times 10^{-10}$	~300	–	5.2	CPD	[936]
Ni(100)	–	–	$\sim 10^{-10}$	350	–	5.2 ± 0.1	PE	[1919]
Ni(100)	–	–	6×10^{-11}	~300	–	5.2 ± 0.15	CPD	[1791]
Ni(100)	–	–	–	–	–	5.20	TC	[1159,1980,3067]
Ni(100)	–	–	2×10^{-10}	100	–	5.20	PE	[3139]
Ni(100)/glass[126]	Ni	–	2×10^{-9}	~300{573}	–	5.20 ± 0.02	PE	[314,315]
Ni(100)	–	–	4×10^{-10}	273	–	5.20 ± 0.05	PE	[484]
Ni(100)	–	–	$\sim 10^{-11}$	173	–	5.20 ± 0.11	CPD	[1417]
Ni(100){95%}	–	–	–	–	5.21 ± 0.01	(4.80 ± 0.09)	TC	[283,630,1351]
Ni(100)	–	–	–	–	–	5.22	TC	[463]
Ni(100)[123]	–	–	$\sim 10^{-10}$	~300 (1023)	–	5.22	PE	[903]
Ni(100)/glass[127]	Ni	–	5×10^{-10}	~300{523}	–	5.22	PE	[1513]
Ni(100)	–	–	5×10^{-10}	293	–	5.22 ± 0.04	PE	[314,315,2604]
Ni(100)	–	–	–	–	–	5.29	TC	[464]
Ni(100)	–	–	–	–	–	5.29	TC	[2701]
Ni(100)	–	–	$\sim 10^{-11}$	77	–	5.3	PE	[937]
Ni(100)	–	–	–	–	–	5.31	TC	[2804]
Ni(100)	–	–	–	–	–	5.31	TC	[1237]
Ni(100)	–	–	$\sim 10^{-10}$	~300	–	5.34	PE	[903]
Ni(100)	–	–	–	–	–	5.35	TC	[464]
Ni(100)	–	–	–	–	–	5.37	TC	[3614]
Ni(100)	–	–	–	–	–	5.37	TC	[466]
Ni(100)	–	–	–	–	–	5.4	TC	[2905]
Ni(100)	–	–	–	–	–	5.4	TC	[1918]
Ni(100)	–	–	–	–	–	5.5	TC	[465]
Ni(100)	–	–	$\sim 10^{-10}$	77, 300	–	5.53 ± 0.05	FE	[358]
Ni(100)	–	–	–	–	–	5.65	TC	[984]
Ni(100)	–	–	–	–	–	5.7	TC	[389]
Ni(100)	–	–	–	–	–	5.71	TC	[984]
Ni(100)	–	–	–	–	–	5.72	TC	[1234]
Ni(100)	–	–	–	–	–	5.73	TC	[464]
Ni(100)	–	–	–	–	–	5.75	TC	[229,317]
Ni(100)	–	–	–	–	–	5.84	TC	[229]
Recommended	–	–	–	–	–	**5.19 ± 0.05**	–	–
Ni(110)	–	–	$\sim 10^{-10}$	~300	–	4.20 ± 0.1	CPD	[1983]
Ni(110)	–	–	2×10^{-11}	20	–	4.45	PE	[2974,2977]
Ni(110)	–	–	–	–	–	4.46	TC	[4454]
Ni(110)	–	–	–	–	–	4.49	TC	[467]
Ni(110)	–	–	$\sim 10^{-11}$	20	–	4.55	PE	[1111,2259,3636]
Ni(110)	–	–	–	–	–	4.6	TC	[311]
Ni(110)	–	–	$\sim 1 \times 10^{-10}$	~300	–	4.62 ± 0.05	PE	[770]
Ni(110)	–	–	1×10^{-9}	~1200–1600	–	4.64 ± 0.03	TE	[312,837]
Ni(110)	–	–	$\sim 10^{-11}$	20	–	4.65 ± 0.1	PE	[2142]
Ni(110)	–	–	–	–	–	4.69	TC	[3224]
Ni(110)	–	–	$<1 \times 10^{-10}$	~300	–	4.7 ± 0.1	CPD	[1110]
Ni(110)	–	–	$\sim 1 \times 10^{-10}$	~300	–	4.7 ± 0.1	PE	[1112]
Ni(110)	–	–	$\sim 10^{-10}$	~300	–	4.82	PE	[2809]
Ni(110)	–	–	–	–	–	4.84	TC	[2548]
Ni(110)	–	–	–	–	–	4.84	TC	[1159,1980,3067]
Ni(110)	–	–	6×10^{-11}	~300	–	4.85 ± 0.15	CPD	[1791]
Ni(110)	–	–	1×10^{-10}	100, ~300	–	4.9	PE	[1808]
Ni(110)	–	–	–	–	–	4.90	TC	[1237]
Ni(110){97%}	–	–	–	–	(5.03 ± 0.01)	4.91 ± 0.04	TC	[630,1351]
Ni(110)	–	–	–	–	–	4.93	TC	[467]
Ni(110)	–	–	?	?	–	5.03	?	[2821]
Ni(110){97%}	–	–	–	–	5.03 ± 0.01	(4.91 ± 0.04)	TC	[630,1351]
Ni(110)	–	–	5×10^{-10}	293	–	5.04 ± 0.02	PE	[314,315,2604]
Ni(110)	–	–	–	–	–	5.1	TC	[2905]
Ni(110)	–	–	–	–	–	5.1	TC	[465]
Ni(110)	–	–	–	–	–	5.2	TC	[465]
Recommended	–	–	–	–	–	**4.96 ± 0.10**	–	–
Ni(111)	–	–	–	–	–	3.9	TC	[1043]
Ni(111)	Ca	Ca^+	$<10^{-6}$	~1300	4.5 ± 0.2	–	PSI	[126]
Ni(111)	Rb	Rb^+	$<10^{-6}$	1280	4.57 ± 0.05	–	PSI	[126]
Ni(111)	–	–	$\sim 10^{-10}$	~300	–	4.68 ± 0.1	CPD	[1983]

Table 1 (*continued*)

Surface	Beam	Ion	P_r (Torr)	T (K)	ϕ^+ (eV)	ϕ^e (eV)	Meth.	Refs.
Ni(111){89%}	–	–	–	–	(5.33 ± 0.01)	4.68 ± 0.10	TC	[283,630,1351]
Ni(111)	–	–	$<1 \times 10^{-10}$	~300	–	4.9	PE	[249]
Ni(111)	–	–	–	–	–	5.00	TC	[4454]
Ni(111)	–	–	?	298	–	5.07	PE	[1392]
Ni(111)	–	–	–	–	–	5.11	TC	[311]
Ni(111)/Mo(110)	Ni	–	$<6 \times 10^{-11}$	~300	–	5.14*	CPD	[3293]
Ni(111)	–	–	–	–	–	5.15	TC	[2423]
Ni(111)	–	–	$<5 \times 10^{-11}$	~300	–	5.15 ± 0.1	PE	[938]
Ni(111)	–	–	$\sim 10^{-10}$	220	–	5.17 ± 0.05	PE	[2040]
Ni(111)	–	–	?	?	–	5.2	TE	[771]
Ni(111)	–	–	?	~300	–	5.2	PE	[1113]
Ni(111)/glass	Ni	–	$<10^{-9}$	77 (~600)	–	5.2	PE	[2934]
Ni(111)/Ru(0001)	Ni	–	?	~300	–	5.2*	PE	[3591]
Ni(111)	–	–	$\sim 1 \times 10^{-10}$	~300	–	5.2 ± 0.07	PE	[1114]
Ni(111)	–	–	?	?	–	5.20	?	[1994]
Ni(111)	–	–	?	1033	–	5.20	PE	[1392]
Ni(111)	–	–	–	–	–	5.22	TC	[3224]
Ni(111)	–	–	$\sim 1 \times 10^{-9}$	~1400–1600	–	5.22 ± 0.03	TE	[312,837]
Ni(111)	–	–	–	–	–	5.23	TC	[4258]
Ni(111)	–	–	–	–	–	5.23	TC	[4317]
Ni(111)	–	–	5×10^{-11}	~300	–	5.25	PE	[939,940,1920]
Ni(111)	–	–	5×10^{-11}	~300	–	5.25 ± 0.03	PE	[922]
Ni(111)	–	–	$<2 \times 10^{-10}$	~300	–	5.27 ± 0.04	CPD	[1898]
Ni(111)	–	–	–	–	–	5.28	TC	[2068]
Ni(111)	–	–	–	–	–	5.29	TC	[4056]
Ni(111)/glass	Ni	–	$\leq 3 \times 10^{-10}$	77 (~460)	–	5.29	PE	[3058]
Ni(111)	–	–	8×10^{-11}	100	–	5.3	PE	[772]
Ni(111)	–	–	1×10^{-10}	80, ~300	–	5.3	PE	[616,2962]
Ni(111)	–	–	$\sim 10^{-10}$	~300	–	5.3	PE	[313]
Ni(111)	–	–	$<1 \times 10^{-10}$	~300	–	5.3 ± 0.1	CPD	[1110]
Ni(111)	–	–	$\sim 10^{-10}$	350	–	5.3 ± 0.1	PE	[1919]
Ni(111)/glass	Ni	–	2×10^{-9}	~300{523}	–	5.30 ± 0.04	PE	[314,315]
Ni(111)/glass	Ni	–	2×10^{-9}	77 (523)	–	5.32 ± 0.05	PE	[314]
Ni(111){89%}	–	–	–	–	5.33 ± 0.01	(4.68 ± 0.10)	TC	[283,630,1351]
Ni(111)/glass[126]	Ni	–	2×10^{-9}	~300{523}	–	5.34 ± 0.02	PE	[314]
Ni(111)	–	–	?	?	–	5.35	?	[2821]
Ni(111)/glass[128]	Ni	–	5×10^{-10}	~300{523}	–	5.35	PE	[315,1513]
Ni(111)	–	–	5×10^{-10}	293	–	5.35 ± 0.05	PE	[314,315,2604]
Ni(111)	–	–	$<2 \times 10^{-10}$	~300	–	5.36	PE	[316]
Ni(111)	–	–	$\sim 10^{-10}$	85	–	5.36	PE	[773]
Ni(111)	–	–	–	–	–	5.39	TC	[4056]
Ni(111)	–	–	6×10^{-11}	~300	–	5.40 ± 0.15	CPD	[1791]
Ni(111)	–	–	$<2 \times 10^{-10}$	27, 90	–	5.42	CPD	[4107]
Ni(111)	–	–	$\leq 3 \times 10^{-9}$	~300	–	5.42 ± 0.04	PE	[1115]
Ni(111)/Mo(110)	Ni	–	$<6 \times 10^{-11}$	~300	–	5.43	CPD	[3293]
Ni(111)	–	–	?	<85	–	5.45 ± 0.1	PE	[1033]
Ni(111)	–	–	–	–	–	5.46	TC	[2804]
Ni(111)	–	–	–	–	–	5.47	TC	[4174,4284]
Ni(111)	–	–	–	–	–	5.50	TC	[1237]
Ni(111)	–	–	–	–	–	5.56	TC	[2548]
Ni(111)	–	–	–	–	–	5.56	TC	[1159,1980,3067]
Ni(111)	–	–	–	–	–	5.6	TC	[2905]
Ni(111)	–	–	–	–	–	5.68	TC	[334,3179]
Ni(111)	–	–	–	–	–	5.70	TC	[229,317]
Ni(111)	–	–	–	–	–	5.77	TC	[229,334]
Ni(111)	–	–	3×10^{-11}	80	–	6.27	FE	[2514]
Recommended	–	–	–	–	–	**5.32 ± 0.05**	–	–
Ni(113)	–	–	–	–	–	4.52	TC	[3224]
Ni(133)	–	–	–	–	–	4.43	TC	[3224]
Ni(fp)[130]	–	–	–	–	–	2.941	TC	[2887]
Ni(fp)[130]	–	–	–	–	–	2.955	TC	[2887]
Ni(fp)[130]	–	–	–	–	–	2.972	TC	[2887]
Ni/W	Ni	–	?	~300	–	3.4 ± 0.03	FE	[1856]
Ni	–	–	$\sim 10^{-5}$	≤ 1200	–	3.60	TE	[2216]
Ni/?	Ni	–	?	~300	–	3.67	PE	[2460]
Ni	–	–	$\sim 10^{-6}$	~300	–	4.05	PE	[3388]
Ni	–	–	$\sim 10^{-6}$	~300	–	4.05 ± 0.02	PE	[3394]

Table 1 (*continued*)

Surface	Beam	Ion	P_r (Torr)	T (K)	ϕ^+ (eV)	ϕ^e (eV)	Meth.	Refs.
Ni	–	–	6×10^{-3}	~300	–	4.05 ± 0.07	PE	[2079,2080]
Ni	–	–	~10^{-6}	~300	–	4.06	PE	[3389,3394]
Ni	–	–	$<10^{-6}$	~300	–	4.12	PE	[2919]
Ni	–	–	?	~300	–	4.12 ± 0.02	CPD	[2544]
Ni$_3$(cluster)	–	–	–	–	–	4.16	TC	[2990]
Ni	–	–	?	~300	–	4.2	PE	[4278]
Ni/steel	Ni	–	3×10^{-10}	20 (~300)	–	4.2 ± 0.1	PE	[1410]
Ni	–	–	4×10^{-9}	673	–	4.23 ± 0.08	PE	[1116]
Ni	–	–	4×10^{-9}	533	–	4.24 ± 0.07	PE	[1116]
Ni/W(111)	Ni	–	$<2 \times 10^{-10}$	78 (375)	–	4.3*	FE	[1591]
Ni/W(100)	Ni	–	$<2 \times 10^{-10}$	78 (870)	–	4.3*	FE	[1591]
Ni/W(100)	Ni	–	$<2 \times 10^{-10}$	78 (375)	–	4.3*	FE	[1591]
Ni/W(112)	Ni	–	$<3 \times 10^{-10}$	~300 (580)	–	4.30	FE	[3213]
Ni	–	–	?	~300	–	4.32	CPD	[2297]
Ni/Si	–	–	–	–	–	4.33	TC	[1653]
Ni	–	–	?	~300	–	4.35	CPD	[2469]
Ni	–	–	–	–	–	4.36	TC	[1976]
Ni	–	–	?	90	–	4.37	CPD	[2294]
Ni/NaCl[131]	Ni	–	2×10^{-9}	~300{573}	–	4.39 ± 0.02	PE	[314]
Ni/W(111)	Ni	–	$<2 \times 10^{-10}$	78 (870)	–	4.4*	FE	[1591]
Ni	–	–	–	–	–	4.4*	TC	[1955]
Ni/steel	Ni	–	3×10^{-10}	20	–	4.4 ± 0.1	PE	[1410]
Ni[413]	–	–	~10^{-9}	1170–1250	–	4.41 ± 0.02	TE	[179,650,3410, 3413]
Ni	–	–	$<10^{-6}$	773	–	4.44 ± 0.05	CPD	[4142]
Ni/NaCl[131]	Ni	–	2×10^{-9}	~300{573}	–	4.47 ± 0.06	PE	[314]
Ni	–	–	–	–	–	4.49	TC	[3476]
Ni	–	–	–	–	–	4.5	TC	[3262]
Ni	–	–	–	–	–	4.5	TC	[3318]
Ni/W(111)	Ni	–	$<2 \times 10^{-10}$	78	–	4.5*	FE	[1591]
Ni/Re	Ni	–	$<4 \times 10^{-10}$	~300	–	4.5	CPD	[1586]
Ni/Al$_2$O$_3$/Si(100)	Ni	–	?	~300	–	4.5[48]	PE	[1442]
Ni[413]	–	–	?	~300	–	4.5	PE	[942]
Ni/graphite	Ni	–	$<10^{-5}$	~1400–1600	–	4.50 ± 0.02	TE	[769,2304]
Ni/W	Ni	–	$<2 \times 10^{-9}$	430	–	4.51	FE	[2239]
Ni	–	–	4×10^{-9}	294	–	4.51 ± 0.03	PE	[1116,3788,4082, 4134]
Ni/W[134]	Ni	–	2×10^{-10}	78, 300	–	4.52 ± 0.03	FE	[2249]
Ni/glass	Ni	–	$<10^{-9}$	77	–	4.54	PE	[3051]
Ni/glass	Ni	–	2×10^{-9}	77	–	4.54 ± 0.02	PE	[314]
Ni/glass	Ni	–	$<10^{-9}$	77	–	4.55	PE	[3051]
Ni/W	Ni	–	$<3 \times 10^{-10}$	~300 (580)	–	4.55	FE	[3213]
Ni/glass[369]	Ni	–	~10^{-10}	77	–	4.55 ± 0.02	PE	[2132,2133,2147]
Ni/glass	Ni	–	5×10^{-10}	~300{523}	–	4.56	PE	[1513]
Ni/glass	Ni	–	$<1 \times 10^{-10}$	78	–	4.56	PE	[414,2719]
Ni	–	–	12 (Ar)	?	–	4.56	PE	[4236]
Ni	–	–	–	–	–	4.57	TC	[3318]
Ni	–	–	–	–	–	4.57	TC	[3224]
Ni/glass	Ni	–	$<10^{-9}$	77	–	4.57	PE	[1469]
Ni/glass	Ni	–	$<10^{-9}$	77	–	4.58	PE	[2310]
Ni/glass	Ni	–	$<10^{-9}$	77	–	4.58	PE	[2929]
Ni/glass	Ni	–	$<10^{-9}$	77	–	4.59	PE	[1957]
Ni/glass	Ni	–	$<10^{-9}$	77	–	4.59	PE	[2929]
Ni	–	–	27 (Ne)	?	–	4.59	PE	[4236]
Ni/glass	Ni	–	$\leq 3 \times 10^{-10}$	77	–	4.59 ± 0.02	PE	[3058]
Ni	–	–	–	–	–	4.6	TC	[1645]
Ni	–	–	–	–	–	4.6	TC	[2583]
Ni/W(100)	Ni	–	$<2 \times 10^{-10}$	78	–	4.6*	FE	[1591]
Ni	–	–	?	~300	–	4.6	CPD	[1379]
Ni/glass	Ni	–	$<10^{-9}$	77	–	4.6	PE	[1469]
Ni/Ta(111)	Ni	–	$<1 \times 10^{-10}$	~300	–	4.60	CPD	[3302]
Ni/glass	Ni	–	$<10^{-9}$	77	–	4.60	PE	[2310]
Ni/glass	Ni	–	$<10^{-9}$	77	–	4.60	PE	[2934]
Ni/glass	Ni	–	$<10^{-9}$	77	–	4.60	PE	[1957]
Ni/glass	Ni	–	$\leq 3 \times 10^{-10}$	77	–	4.60 ± 0.02	PE	[1153]
Ni/quartz	Ni	–	$\leq 5 \times 10^{-10}$	78	–	4.60 ± 0.03	PE	[435]
Ni/glass	Ni	–	$<10^{-9}$	77	–	4.61	PE	[2763,3046]
Ni/glass	Ni	–	$<10^{-9}$	77	–	4.61	PE	[2929]
Ni/glass	Ni	–	$<10^{-9}$	77	–	4.61	PE	[2310]
Ni	–	–	3×10^{-8}	?	–	4.61 ± 0.05	TE	[310]

Table 1 (*continued*)

Surface	Beam	Ion	P_r (Torr)	T (K)	ϕ^+ (eV)	ϕ^e (eV)	Meth.	Refs.
Ni	–	–	?	~1300–1500	–	4.63	TE	[1762]
Ni/glass	Ni	–	<10⁻¹⁰	77 (196)	–	4.64 ± 0.02	PE	[2147]
Ni[132]	–	–	4 × 10⁻¹⁰	~300	–	4.645	CPD	[503]
Ni	–	–	27 (Ne)	~300	–	4.65 ± 0.02	PE	[788]
Ni[132]	–	–	4 × 10⁻¹⁰	400	–	4.653	CPD	[503]
Ni	–	–	–	–	–	4.66	TC	[3476]
Ni[132]	–	–	4 × 10⁻¹⁰	400	–	4.660	CPD	[503]
Ni	–	–	12 (Ar)	~300	–	4.67 ± 0.02	PE	[788]
Ni{89%(111)}	–	–	–	–	(5.33 ± 0.01)	4.68 ± 0.10	TC	[283,630,1351]
Ni[132]	–	–	4 × 10⁻¹⁰	660	–	4.690	CPD	[503]
Ni/?	Ni	–	~10⁻⁵	~300	–	4.7	CPD	[1376]
Ni/W(110)	Ni	–	<2 × 10⁻¹⁰	78	–	4.7*	FE	[1591]
Ni/W(110)	Ni	–	<2 × 10⁻¹⁰	78 (375)	–	4.7*	FE	[1591]
Ni/W(110)	Ni	–	<2 × 10⁻¹⁰	78 (870)	–	4.7*	FE	[1591]
Ni/W(112)	Ni	–	<2 × 10⁻¹⁰	78	–	4.7*	FE	[1591]
Ni/W(112)	Ni	–	<2 × 10⁻¹⁰	78 (375)	–	4.7*	FE	[1591]
Ni/glass	Ni	–	?	77	–	4.7	CPD	[2577]
Ni/W(112)	Ni	–	<2 × 10⁻¹⁰	78 (870)	–	4.7*	FE	[1591]
Ni	–	–	~10⁻⁹	973	–	4.7	TE	[3112]
Ni/Mo(111)	Ni	–	<1 × 10⁻¹⁰	~300	–	4.7 ± 0.1*	CPD	[3307]
Ni[132]	–	–	4 × 10⁻¹⁰	740	–	4.700	CPD	[503]
Ni/W(111)	Ni	–	<5 × 10⁻¹¹	~300	–	4.72*	CPD	[2429]
Ni	–	–	–	–	–	4.73	TC	[3264,3265,3267]
Ni	–	–	–	–	–	4.73	TC	[3352]
Ni	–	–	?	~300	–	4.74	PE	[1371]
Ni	–	–	~10⁻¹⁰	~300	–	4.74	CPD	[3131]
Ni/W(110)	–	–	–	–	–	4.74	TC	[531]
Ni/glass	Ni	–	~10⁻⁸	~300	–	4.74 ± 0.04	CPD	[133]
Ni/ZrO₂/Si(100)	Ni	–	?	~300	–	4.75[48]	PE	[1442]
Ni/glass	Ni	–	<10⁻⁹	77 (195)	–	4.76	PE	[2310]
Ni	–	–	≤10⁻⁹	1500	–	4.77	TE	[179,650]
Ni/W(100)	Ni	–	<1 × 10⁻¹¹	77	–	4.78	FE	[1549]
Ni/W	Ni	–	<3 × 10⁻¹⁰	900, 1150	–	4.78	FE	[3684]
Ni	–	–	~10⁻¹¹	~300	–	4.79	CPD	[3338]
Ni/W(110)	Ni	–	?	90	–	4.8	CPD	[3732]
Ni	–	–	–	–	–	4.8	TC	[706]
Ni[413]	–	–	~10⁻⁹	1440–1490	–	4.80 ± 0.02	TE	[179,650,3410, 3413]
Ni{95%(100)}	–	–	–	–	(5.21 ± 0.01)	4.80 ± 0.09	TC	[283,630,1351]
Ni/TiO₂(110)	Ni	–	~4 × 10⁻¹¹	~300	–	4.80 ± 0.10	PE	[2788]
Ni/glass	Ni	–	<10⁻⁹	~300	–	4.8–5.1	PE	[1469]
Ni/W	Ni	–	<3 × 10⁻¹⁰	900, 1150	–	4.82	FE	[3684]
Ni/glass[129]	Ni	–	2 × 10⁻⁹	273	–	4.82 ± 0.04	PE	[314]
Ni/mica[133]	Ni	–	2 × 10⁻⁹	~300{593}	–	4.82 ± 0.04	PE	[314]
Ni	–	–	–	–	–	4.83	TC	[1399]
Ni₆(cluster)	–	–	–	–	–	4.83	TC	[2990]
Ni/W(111)	Ni	–	<3 × 10⁻¹⁰	~300 (580)	–	4.83	FE	[3213]
Ni/glass	Ni	–	<10⁻¹⁰	77 (293)	–	4.83 ± 0.02	PE	[2147]
Ni₁₀(cluster)	–	–	–	–	–	4.84	TC	[2990]
Ni/W[134]	Ni	–	2 × 10⁻¹⁰	78, 300	–	4.85	FE	[2249]
Ni₇(cluster)	–	–	–	–	–	4.85	TC	[2990]
Ni/quartz	Ni	–	≤5 × 10⁻¹⁰	293	–	4.86 ± 0.04	PE	[435]
Ni/glass	Ni	–	<10⁻⁹	77 (293)	–	4.87	PE	[3051]
Ni	–	–	?	~300	–	4.87	PE	[2924]
Ni/glass	Ni	–	2 × 10⁻⁹	~300 (573)	–	4.87 ± 0.04	PE	[314,315]
Ni/Ni(mono)[414]	Ni	–	<5 × 10⁻¹⁰	678{~300}	–	4.87 ± 0.04	PE	[3971]
Ni/glass[369]	Ni	–	~10⁻¹⁰	77 (323)	–	4.88	PE	[2133]
Ni/glass	Ni	–	<10⁻¹⁰	77 (293)	–	4.88 ± 0.02	PE	[2147]
Ni/glass	Ni	–	<10⁻⁹	77 (293)	–	4.89	PE	[2929]
Ni	–	–	≤10⁻⁹	1380	–	4.89	TE	[179,650]
Ni/glass	Ni	–	5 × 10⁻¹⁰	~300{523}	–	4.89	PE	[1513]
Ni/glass[135]	Ni	–	2 × 10⁻⁹	273	–	4.9	PE	[315]
Ni/?	Ni	–	2 × 10⁻¹⁰	4.2 (400)	–	4.9	PE	[1506]
Ni/SiO₂	Ni	–	?	~300	–	4.9	PE	[2899]
Ni	–	–	~10⁻⁹	~300	–	4.9	PE	[2667]
Ni	–	–	–	–	–	4.9	TC	[2667]
Ni/steel	Ni	–	3 × 10⁻¹⁰	4.2	–	4.9 ± 0.1	PE	[1410]
Ni/glass	Ni	–	3 × 10⁻¹⁰	78 (~300)	–	4.90	PE	[414,2722]
Ni/glass	Ni	–	<1 × 10⁻¹⁰	78 (293)	–	4.90 ± 0.02	PE	[414,2722]
Ni{97%(110)}	–	–	–	–	(5.03 ± 0.01)	4.91 ± 0.04	TC	[630,1351]

Table 1 (*continued*)

Surface	Beam	Ion	P_r (Torr)	T (K)	ϕ^+ (eV)	ϕ^e (eV)	Meth.	Refs.
Ni	–	–	$\sim 10^{-10}$	~ 300	–	4.93	PE	[724]
Ni	–	–	1×10^{-8}	~ 300	–	4.93 ± 0.02	PE	[306]
Ni/mica[133]	Ni	–	2×10^{-9}	$\sim 300\{593\}$	–	4.93 ± 0.02	PE	[314]
Ni/glass	Ni	–	$<10^{-9}$	77 (293)	–	4.95	PE	[2310]
Ni/glass	Ni	–	$\sim 10^{-10}$	78 (293)	–	4.95	PE	[2719]
Ni/glass	Ni	–	2×10^{-10}	77	–	4.95 ± 0.01	CPD	[945]
Ni/glass	Ni	–	$<10^{-10}$	77 (373)	–	4.95 ± 0.02	PE	[2147]
Ni/mica	Ni	–	2×10^{-9}	$\sim 300\{593\}$	–	4.95 ± 0.03	PE	[314]
Ni/Si(110)	Ni	–	$\sim 10^{-10}$	220 (?)	–	4.95 ± 0.05*	CPD	[2737]
Ni/W	Ni	–	?	~ 300	–	4.96	CPD	[1460]
Ni/W(111)	–	–	–	–	–	4.97	TC	[531]
Ni/Ni(mono)[414]	Ni	–	$<5 \times 10^{-10}$	295	–	4.97 ± 0.02	PE	[3971]
Ni/glass	Ni	–	5×10^{-10}	~ 300 (523)	–	4.99	PE	[1513]
Ni	–	–	1×10^{-9}	~ 300	–	5	PE	[3511]
Ni/W	Ni	–	$\sim 10^{-9}$	~ 300	–	5–7	FE	[3619]
Ni	–	–	?	?	–	5.0	TE	[3402]
Ni[413]	–	–	?	~ 300	–	5.0	PE	[942]
Ni/W(110)	Ni	–	4×10^{-11}	~ 300 (1100)	–	5.0*	CPD	[2386]
Ni/glass[135]	Ni	–	$<2 \times 10^{-9}$	273	–	5.0	PE	[315]
Ni/glass	Ni	–	$<10^{-8}$	78	–	5.0 ± 0.02	CPD	[1646]
Ni/steel	Ni	–	3×10^{-10}	4.2	–	5.0 ± 0.1	PE	[1410]
Ni/glass[129]	Ni	–	2×10^{-9}	273	–	5.00 ± 0.02	PE	[314]
Ni/quartz	Ni	–	$\leq 5 \times 10^{-10}$	293 (~ 550)	–	5.01	PE	[435]
Ni	–	–	1×10^{-8}	~ 300	–	5.01	PE	[306]
Ni/glass	Ni	–	2×10^{-9}	$\sim 300\{523\}$	–	5.01 ± 0.04	PE	[314]
Ni	–	–	$\sim 10^{-10}$	~ 300	–	5.01 ± 0.07*	CPD	[2645]
Ni/SiO$_2$	Ni	–	?	~ 300	–	5.017	CPD	[1221]
Ni/glass	Ni	–	$<10^{-9}$	90 (380)	–	5.02	PE	[3045]
Ni/glass	Ni	–	$<10^{-9}$	90	–	5.02	PE	[3046]
Ni/W(110)	Ni	–	?	90 (800)	–	5.02	CPD	[3469]
Ni/glass	Ni	–	$<10^{-10}$	~ 300 (~ 370)	–	5.02 ± 0.02	PE	[1117]
Ni/quartz	Ni	–	$<10^{-8}$	77, 300	–	5.03	PE	[3032,3036]
Ni/quartz	Ni	–	$<5 \times 10^{-10}$	293	–	5.03	PE	[1102]
Ni/quartz	Ni	–	$<5 \times 10^{-10}$	293 (618)	–	5.03	PE	[1102]
Ni{97%(110)}	–	–	–	–	5.03 ± 0.01	(4.91 ± 0.04)	TC	[630,1351]
Ni	–	–	$\leq 3 \times 10^{-8}$	1370–1500	–	5.03 ± 0.05	TE	[3608]
Ni/glass	Ni	–	2×10^{-9}	$\sim 300\{573\}$	–	5.04 ± 0.04	PE	[314,315]
Ni/glass	Ni	–	$\leq 3 \times 10^{-10}$	77 (470)	–	5.04–5.24	PE	[1153]
Ni/glass	Ni	–	$<10^{-9}$	77 (373)	–	5.05	PE	[2763,3046]
Ni[405]	–	–	$\leq 8 \times 10^{-8}$	623	–	5.05	PE	[943]
Ni/glass	Ni	–	2×10^{-10}	77 (398)	–	5.05 ± 0.01	CPD	[945]
Ni[405]	–	–	$\leq 8 \times 10^{-8}$	623	–	5.05 ± 0.05	PE	[943]
Ni[405]	–	–	$\leq 8 \times 10^{-8}$	~ 300	–	5.06	PE	[943]
Ni/glass	Ni	–	$<10^{-9}$	77 (373)	–	5.06	PE	[2929]
Ni/glass	Ni	–	$<10^{-9}$	77 (373)	–	5.06	PE	[3051]
Ni/W	Ni	–	$<3 \times 10^{-10}$	~ 300 (580)	–	5.06	FE	[3213]
Ni/glass	Ni	–	2×10^{-9}	77{523}	–	5.06 ± 0.04	PE	[314]
Ni/SiO$_2$	Ni	–	?	~ 300	–	5.063	CPD	[1221]
Ni	–	–	$\sim 10^{-7}$	~ 300	–	5.07	CPD	[3513]
Ni/glass	Ni	–	$<10^{-9}$	90 (293)	–	5.07	PE	[3046]
Ni	–	–	–	–	–	5.09	TC	[1066]
Ni/glass	Ni	–	$\sim 10^{-10}$	90	–	5.09	PE	[3048]
Ni	–	–	–	–	–	5.1	TC	[944]
Ni(fp)[448]	–	–	$\sim 10^{-9}$	~ 300	–	5.1	PE	[2667]
Ni/W	Ni	–	3×10^{-10}	~ 300 (760)	–	5.1*	FE	[3680]
Ni/W	Ni	–	?	~ 300 (1070)	–	5.1 ± 0.03	FE	[1856]
Ni	–	–	–	–	–	5.10	TC	[3476]
Ni	–	–	–	–	–	5.10*	TC	[4185]
Ni[405]	–	–	$\leq 8 \times 10^{-8}$	770	–	5.10	PE	[943]
Ni/glass	Ni	–	$<10^{-9}$	77 (373)	–	5.10	PE	[1957]
Ni/glass	Ni	–	$\sim 10^{-10}$	78 (373)	–	5.10	PE	[2719]
Ni/Si(111)	Ni	–	$<1 \times 10^{-10}$	~ 300	–	5.10 ± 0.05	CPD	[3270]
Ni/glass	Ni	–	$<1 \times 10^{-10}$	78 (406)	–	5.11	PE	[414]
Ni/glass	Ni	–	$\sim 10^{-10}$	90	–	5.11	PE	[3048]
Ni/glass	Ni	–	$<10^{-10}$	77 (473)	–	5.11 ± 0.02	PE	[2147]
Ni/Ag(100)	–	–	–	–	–	5.12	TC	[2166]
Ni/glass	Ni	–	3×10^{-10}	78 (570)	–	5.12	PE	[2722]
Ni/mica[124]	Ni	–	2×10^{-9}	$\sim 300\{593\}$	–	5.12 ± 0.02[133]	PE	[314]
Ni/Mo(110)	Ni	–	$<6 \times 10^{-11}$	~ 300	–	5.14*	CPD	[3293]
Ni/glass	Ni	–	$<10^{-8}$	293	–	5.145	PE	[1386]

Table 1 (*continued*)

Surface	Beam	Ion	P_r (Torr)	T (K)	ϕ^+ (eV)	ϕ^e (eV)	Meth.	Refs.
Ni/W(110)	Ni	–	?	90	–	5.15	CPD	[3468,3469]
Ni/W(112)	–	–	–	–	–	5.15	TC	[531]
Ni	–	–	3×10^{-11}	~300	–	5.15	FE	[2227]
Ni	–	–	$<2 \times 10^{-10}$	27, 90	–	5.15	CPD	[4107]
Ni/W(110)	Ni	–	$<2 \times 10^{-10}$	27, 90	–	5.15	CPD	[4107]
Ni/quartz	Ni	–	$\sim10^{-10}$	~300	–	5.15 ± 0.1	PE	[304]
Ni/glass	Ni	–	$<1 \times 10^{-10}$	78 (589)	–	5.16	PE	[414]
Ni/glass[129]	Ni	–	2×10^{-9}	273	–	5.16 ± 0.03	PE	[314]
Ni/W(110)	Ni	–	4×10^{-11}	~300	–	5.16 ± 0.05*	CPD	[2386]
Ni/glass	Ni	–	$\sim10^{-10}$	78 (573)	–	5.17	PE	[2719]
Ni[405]	–	–	$\leq8 \times 10^{-8}$	975	–	5.17	PE	[943]
Ni/glass[125]	Ni	–	2×10^{-9}	77 (523)	–	5.17 ± 0.02	PE	[314]
Ni$_n$($n \to \infty$)	–	–	–	–	–	5.2	TC	[1866]
Ni/glass	Ni	–	$<10^{-9}$	77 (≤650)	–	5.2	PE	[2934]
Ni/glass[135]	Ni	–	$<2 \times 10^{-9}$	273	–	5.2	PE	[315]
Ni/ZnO(0001)Zn	Ni	–	$<5 \times 10^{-11}$	~300	–	5.2 ± 0.1	PE	[3119]
Ni/glass	Ni	–	$<10^{-9}$	77 (373)	–	5.20	PE	[2310]
Ni	–	–	–	–	–	5.20	TC	[3637]
Ni/glass	Ni	–	2×10^{-9}	~300 (523)	–	5.20 ± 0.02	PE	[314]
Ni/glass[126]	Ni	–	2×10^{-9}	~300{573}	–	5.20 ± 0.02	PE	[314,315]
Ni[405]	–	–	$\leq8 \times 10^{-8}$	1108	–	5.20 ± 0.05	PE	[943]
Ni/glass	Ni	–	$<10^{-10}$	~300 (~470)	–	>5.2	PE	[1117]
Ni/?	Ni	–	?	?	–	5.21	PE	[1403]
Ni/glass	Ni	–	$\leq3 \times 10^{-10}$	77 (373)	–	5.21	PE	[3058]
Ni	Cs	Cs$^+$	?	~300	–	5.21*	CPD	[611]
Ni{95%(100)}	–	–	–	–	5.21 ± 0.01	(4.80 ± 0.09)	TC	[283,630,1351]
Ni	–	–	3×10^{-10}	~300	–	5.21 ± 0.02	PE	[1504]
Ni/glass	Ni	–	$<10^{-9}$	77 (~600)	–	5.22	PE	[2934]
Ni/glass	Ni	–	2×10^{-9}	~300{523}	–	5.22 ± 0.02	PE	[314]
Ni/glass	Ni	–	$<10^{-9}$	77 (473)	–	5.23	PE	[2929]
Ni[405]	–	–	$\leq8 \times 10^{-8}$	≥1150	–	5.24	TE	[943]
Ni/glass	Ni	–	$<10^{-9}$	77 (423)	–	5.25	PE	[1957]
Ni/glass	Ni	–	2×10^{-10}	77	–	5.25 ± 0.03	FE	[945]
Ni	–	–	–	–	–	5.26	TC	[298]
Ni/glass	Ni	–	$<10^{-9}$	77 (423)	–	5.28	PE	[2310]
Ni/glass	Ni	–	$\leq3 \times 10^{-10}$	77 (~460)	–	5.29	PE	[3058]
Ni	–	–	?	~300	–	5.3	PE	[1371]
Ni$_{28}$(cluster)	–	–	–	–	–	5.30	TC	[4063]
Ni/glass	Ni	–	2×10^{-9}	~300{523}	–	5.30 ± 0.04	PE	[314,315]
Ni/glass	Ni	–	2×10^{-9}	77 (523)	–	5.32 ± 0.05	PE	[314]
Ni{89%(111)}	–	–	–	–	5.33 ± 0.01	(4.68 ± 0.10)	TC	[283,630,1351]
Ni/W(100)	–	–	–	–	–	5.34	TC	[531]
Ni/glass	Ni	–	$<2 \times 10^{-9}$	~300{523}	–	5.35	PE	[315]
Ni/W(110)	Ni	–	?	~300	–	5.36	CPD	[3469]
Ni/Mo(110)	Ni	–	$<6 \times 10^{-11}$	~300	–	5.43	CPD	[3293]
Ni/Cu(100)	–	–	–	–	–	5.45	TC	[1121]
Ni/W(110)	Ni	–	$<3 \times 10^{-10}$	~300 (580)	–	5.57	FE	[3213]
Ni/?	Ni	–	?	?	–	5.76	PE	[1403]
Ni/Cu(100)	–	–	–	–	–	6.10	TC	[1121]
Ni/W	Ni	–	$\sim10^{-9}$	~300	–	7.2	FE	[2225]
Recommended	–	–	–	–	**5.19 ± 0.12**	**5.06 ± 0.06**	–	–

29. Copper Cu

fcc

Surface	Beam	Ion	P_r (Torr)	T (K)	ϕ^+ (eV)	ϕ^e (eV)	Meth.	Refs.
Cu(100)	–	–	–	–	–	3.80	TC	[475]
Cu(100)	–	–	–	–	–	3.855	TC	[2914]
Cu(100)/NaCl[137]	Cu	–	?	~300 (473)	–	3.96 ± 0.02	PE	[3328]
Cu(100)[138]	–	–	$\leq8 \times 10^{-9}$	~300	–	4.07	CPD	[1183]
Cu(100)	–	–	–	–	–	4.12	TC	[947]
Cu(100)	–	–	–	–	–	4.21	TC	[949]
Cu(100)	–	–	–	–	–	4.22	TC	[2523]
Cu(100)	–	–	–	–.	–	4.26	TC	[949]
Cu(100)	–	–	$\sim10^{-10}$	~300	–	4.27	PE	[1661]
Cu(100)	–	–	–	–.	–	4.30	TC	[4034]
Cu(100)	–	–	–	–	–	4.37	TC	[949]
Cu(100)	–	–	–	–	–	4.4	TC	[2646]
Cu(100)	–	–	–	–	–	4.412	TC	[1118]
Cu(100)[138]	–	–	$\leq8 \times 10^{-9}$	~300	–	4.43	CPD	[1183]

Table 1 (*continued*)

Surface	Beam	Ion	P_r (Torr)	T (K)	ϕ^+ (eV)	ϕ^e (eV)	Meth.	Refs.
Cu(100)	–	–	–	–	–	4.44	TC	[949]
Cu(100)	–	–	$<5 \times 10^{-8}$	~300	–	4.45 ± 0.03*	CPD	[2923]
Cu(100)	–	–	?	470–670	–	4.458 ± 0.010	CPD	[948,2841]
Cu(100)	–	–	–	–	–	4.47	TC	[949]
Cu(100)	–	–	–	–	–	4.473	TC	[4135]
Cu(100)	–	–	–	–	–	4.48	TC	[949]
Cu(100)	–	–	–	–	–	4.49	TC	[949]
Cu(100)	–	–	–	–	–	4.49	TC	[705]
Cu(100)	–	–	–	–	–	4.49	TC	[1184]
Cu(100)	–	–	–	–	–	4.5	TC	[1741,1742]
Cu(100)	–	–	–	–	–	4.5	TC	[951,1108,1109]
Cu(100)/TaN/Ta	–	–	$<10^{-7}$	~300	–	4.5 ± 0.02	PE	[1238,4210]
Cu(100)	–	–	1×10^{-10}	<50	–	4.5 ± 0.05	PE	[950]
Cu(100)	–	–	–	–	–	4.506	TC	[4091]
Cu(100)	–	–	–	–	–	4.51	TC	[343]
Cu(100)	–	–	–	–	–	4.52	TC	[949]
Cu(100)	–	–	$<10^{-10}$	~300	–	4.52	PE	[1239]
Cu(100)	–	–	$<5 \times 10^{-8}$	~300	–	4.53 ± 0.03*	CPD	[2923]
Cu(100)	–	–	–	–	–	4.54	TC	[2917]
Cu(100)/Ir(100)[139]	Cu	–	?	78 (380)	–	4.55 ± 0.02	FE	[2189]
Cu(100)	–	–	$\leq 10^{-10}$	~300	–	4.56	CPD	[952]
Cu(100)	–	–	–	–	–	4.56 ± 0.01	CT	[4135]
Cu(100)	–	–	$\leq 10^{-10}$	~300	–	4.58	CPD	[952]
Cu(100)	–	–	–	–	–	4.58	TC	[3477]
Cu(100)	–	–	–	–	–	4.58	TC	[3304]
Cu(100)	–	–	$<10^{-10}$	~300	–	4.59 ± 0.03	PE	[953,2006]
Cu(100)	–	–	1×10^{-10}	~300	–	4.6	PE	[3707]
Cu(100)	–	–	$\leq 1 \times 10^{-10}$	180	–	4.6	PE	[2678]
Cu(100)	–	–	–	–	–	4.6	TC	[3205]
Cu(100)	–	–	–	–	–	4.60	TC	[479]
Cu(100)	–	–	–	–	–	4.60	TC	[949]
Cu(100)	–	–	1×10^{-10}	~300	–	4.62	PE	[2673,3005]
Cu(100)	–	–	$\sim 1 \times 10^{-11}$	~300	–	4.63	PE	[1241]
Cu(100)	–	–	?	~300	–	4.63 ± 0.01	PE	[1240]
Cu(100)	–	–	$\sim 2 \times 10^{-10}$	~300	–	4.63 ± 0.02	PE	[957,958]
Cu(100)	–	–	$<8 \times 10^{-11}$	400	–	4.63 ± 0.03	PE	[3475]
Cu(100)	–	–	?	~300	–	4.63 ± 0.03	PE	[2903]
Cu(100)	–	–	2×10^{-10}	~300	–	4.65	PE	[1151]
Cu(100)	–	–	$<5 \times 10^{-11}$	95	–	4.65	PE	[1444]
Cu(100)	–	–	?	~300	–	4.65 ± 0.05	PE	[1913,2650]
Cu(100)/Pd(100)	–	–	$\sim 10^{-9}$	~300	–	4.65 ± 0.10	PE	[1424]
Cu(100)	–	–	–	–	–	4.67	TC	[3273]
Cu(100)	–	–	–	–	–	4.67	TC	[3477]
Cu(100)[140]	–	–	?	~300	–	4.68*	CPD	[959]
Cu(100)	–	–	–	–	–	4.7	TC	[2641]
Cu(100)	–	–	–	–	–	4.71	TC	[4189]
Cu(100)	–	–	$\sim 10^{-10}$	~300	–	4.75 ± 0.1	CPD	[1507]
Cu(100)	–	–	–	–	–	4.753	TC	[1119,2989]
Cu(100)	–	–	$\leq 10^{-10}$	~300	–	4.76	CPD	[952]
Cu(100)	–	–	$\sim 1 \times 10^{-10}$	~300	–	4.76 ± 0.05	PE	[950]
Cu(100)	–	–	$\sim 10^{-10}$	~300	–	4.77 ± 0.05	PE	[955]
Cu(100)	–	–	–	–	–	4.78	TC	[2897]
Cu(100)	–	–	$<5 \times 10^{-10}$	~300	–	4.79 ± 0.05	PE	[1555]
Cu(100)	–	–	–	–	–	4.81	TC	[3477]
Cu(100)	–	–	–	–	–	4.81	TC	[4405]
Cu(100)	–	–	–	–	–	4.82	TC	[2897]
Cu(100)	–	–	–	–	–	4.83	TC	[2897]
Cu(100)	–	–	$<1 \times 10^{-10}$	~300	–	4.83 ± 0.02	PE	[1554]
Cu(100)	–	–	–	–	–	4.85	TC	[480]
Cu(100)	–	–	–	–	–	4.88	TC	[463]
Cu(100)	–	–	–	–	–	4.88	TC	[1608]
Cu(100)	–	–	–	–	–	4.88	TC	[1237]
Cu(100)	–	–	–	–	–	4.89	TC	[3477]
Cu(100)	–	–	–	–	–	4.9	TC	[2646]
Cu(100)	–	–	–	–	–	4.90	TC	[2971]
Cu(100)	–	–	–	–	–	4.91	TC	[1120]
Cu(100)	–	–	–	–	–	4.91	TC	[2897]
Cu(100)	–	–	–	–	–	4.93	TC	[950]
Cu(100)	–	–	–	–	–	4.93	TC	[1106,4386]
Cu(100)	–	–	–	–	–	4.94	TC	[1121]

Table 1 (*continued*)

Surface	Beam	Ion	P_r (Torr)	T (K)	ϕ^+ (eV)	ϕ^e (eV)	Meth.	Refs.
Cu(100)	–	–	–	–	–	4.95	TC	[956]
Cu(100)	–	–	–	–	–	4.98	TC	[962]
Cu(100)	–	–	–	–	–	4.99	TC	[1159,1980,3067]
Cu(100)	–	–	–	–	–	4.99	TC	[2548]
Cu(100)	–	–	–	–	–	5.00	TC	[4405]
Cu(100)	–	–	–	–	–	5.01	TC	[2803]
Cu(100)	–	–	–	–	–	5.02	TC	[480,4398]
Cu(100)	–	–	–	–	–	5.02	TC	[3007]
Cu(100)	–	–	–	–	–	5.03	TC	[962]
Cu(100)	–	–	–	–	–	5.05	TC	[480,4398]
Cu(100)/Ni(100)	–	–	–	–	–	5.1	TC	[2641]
Cu(100)	–	–	–	–	–	5.1	TC	[389]
Cu(100)	–	–	$\leq 1 \times 10^{-10}$	~300	–	5.1	PE	[3298]
Cu(100)	–	–	$\sim 10^{-10}$	77, ~300	–	5.10 ± 0.05	FE	[358]
Cu(100)	–	–	–	–	–	5.13	TC	[3224]
Cu(100)	–	–	–	–	–	5.14	TC	[3382]
Cu(100)	–	–	$< 1 \times 10^{-10}$	77, ~300	–	5.155 ± 0.054	CPD	[963]
Cu(100)	–	–	–	–	–	5.16	TC	[321]
Cu(100)	–	–	–	–	–	5.20	TC	[1596]
Cu(100)	–	–	–	–	–	5.20	TC	[3382]
Cu(100)	–	–	–	–	–	5.21	TC	[1703]
Cu(100)	–	–	–	–	–	5.22	TC	[1234]
Cu(100)	–	–	–	–	–	5.25	TC	[2540]
Cu(100)	–	–	–	–	–	5.26	TC	[229,334]
Cu(100)	–	–	–	–	–	5.26	TC	[962]
Cu(100)	–	–	$< 5 \times 10^{-8}$	~300	–	5.29 ± 0.04*	CPD	[2923]
Cu(100)	–	–	–	–	–	5.31	TC	[962]
Cu(100)	–	–	$< 5 \times 10^{-8}$	~300	–	5.37 ± 0.04*	CPD	[2923]
Cu(100)	–	–	–	–	–	5.6	TC	[1122]
Cu(100)	–	–	$\sim 1 \times 10^{-8}$	~300	–	5.61	PE	[3308]
Cu(100)	–	–	–	–	–	5.95	TC	[1703]
Cu(100)	–	–	–	–	–	6.11	TC	[1703]
Cu(100)	–	–	–	–	–	6.3	TC	[2646]
Cu(100)	–	–	–	–	–	6.4	TC	[2646]
Cu(100)	–	–	–	–	–	6.9	TC	[2646]
Recommended	–	–	–	–	–	**4.58 ± 0.06**	–	–
Cu(110)	–	–	–	–	–	3.55	TC	[475]
Cu(110)	–	–	–	–	–	3.56	TC	[962]
Cu(110)	–	–	–	–	–	3.648	TC	[2914]
Cu(110)	–	–	–	–	–	3.85	TC	[321]
Cu(110)	–	–	–	–	–	3.98	TC	[947]
Cu(110)	–	–	–	–	–	4.1	TC	[967]
Cu(110)	–	–	–	–	–	4.10	TC	[962]
Cu(110)	–	–	–	–	–	4.2	TC	[967]
Cu(110)	–	–	–	–	–	4.20	TC	[962]
Cu(110)	–	–	$\sim 10^{-10}$	~300	–	4.23	PE	[1661]
Cu(110)	–	–	–	–	–	4.25	TC	[3477]
Cu(110)	–	–	–	–	–	4.27	TC	[4034]
Cu(110)	–	–	–	–	–	4.272	TC	[4091]
Cu(110)	–	–	–	–	–	4.33	TC	[3477]
Cu(110)	–	–	$\leq 10^{-10}$	~300	–	4.4	CPD	[952]
Cu(110)	–	–	?	~300	–	4.4	PE	[1242]
Cu(110)/TaN/Ta	–	–	?	~300	–	4.4 ± 0.02	PE	[1238,4210]
Cu(110)	–	–	$\leq 10^{-10}$	~300	–	4.40	CPD	[952]
Cu(110)	–	–	?	470–670	–	4.400 ± 0.010	CPD	[948,2841]
Cu(110)	–	–	–	–	–	4.408	TC	[1118]
Cu(110)	–	–	–	–	–	4.421	TC	[3574]
Cu(110)	–	–	–	–	–	4.43	TC	[2917]
Cu(110)	–	–	–	–	–	4.44	TC	[3304]
Cu(110)	–	–	$< 8 \times 10^{-10}$	~300	–	4.46 ± 0.04	PE	[4195]
Cu(110)	–	–	–	–	–	4.48	TC	[334]
Cu(110)[140]	–	–	?	~300	–	4.48*	CPD	[959]
Cu(110)	–	–	3×10^{-10}	20, 42	–	4.48	PE	[2140,2642]
Cu(110)	–	–	$< 10^{-10}$	~300	–	4.48 ± 0.03	PE	[953,2006]
Cu(110)	–	–	$< 7 \times 10^{-11}$	~300	–	4.5	PE	[1123]
Cu(110)	–	–	?	~300	–	4.5	PE	[1243]
Cu(110)	–	–	$\sim 4 \times 10^{-11}$	20–200	–	4.5	PE	[2143]
Cu(110)	–	–	–	–	–	4.508	TC	[1119,2989]
Cu(110)	–	–	$< 5 \times 10^{-11}$	90	–	4.52	PE	[1444]

Table 1 (*continued*)

Surface	Beam	Ion	P_r (Torr)	T (K)	ϕ^+ (eV)	ϕ^e (eV)	Meth.	Refs.
Cu(110)	–	–	–	–	–	4.53	TC	[962]
Cu(110)	–	–	–	–	–	4.53	TC	[3477]
Cu(110)	–	–	?	~300	–	4.59	CPD	[964]
Cu(110)	–	–	–	–	–	4.61	TC	[3477]
Cu(110)	–	–	–	–	–	4.625	TC	[4189]
Cu(110)	–	–	–	–	–	4.65	TC	[1159,1980,3067]
Cu(110)	–	–	–	–	–	4.66	TC	[2548]
Cu(110)	–	–	–	–	–	4.67	TC	[480]
Cu(110)	–	–	~10^{-10}	~300	–	4.7 ± 0.1	CPD	[1507]
Cu(110)	–	–	–	–	–	4.70	TC	[4405]
Cu(110)	–	–	–	–	–	4.71	TC	[1237]
Cu(110)	–	–	–	–	–	4.78	TC	[4405]
Cu(110)	–	–	–	–	–	4.81	TC	[480,4398]
Cu(110)	–	–	–	–	–	4.83	TC	[480,4398]
Cu(110)	–	–	–	–	–	4.84	TC	[1244]
Cu(110)	–	–	<5×10^{-11}	~300	–	4.87	PE	[1124]
Cu(110)	–	–	–	–	–	4.87	TC	[3007]
Cu(110)	–	–	–	–	–	4.88	TC	[3007]
Cu(110)	–	–	–	–	–	4.9	TC	[956]
Cu(110)	–	–	<1×10^{-10}	77, ~300	–	4.92 ± 0.019	CPD	[963]
Cu(110)	–	–	–	–	–	4.94	TC	[3224]
Cu(110)	–	–	–	–	–	4.98	TC	[962]
Cu(110)	–	–	–	–	–	5.04	TC	[962]
Recommended	–	–	–	–	–	**4.43 ± 0.04**	–	–
Cu(111)	–	–	–	–	–	3.55	TC	[3491]
Cu(111)	–	–	–	–	–	3.90	TC	[475]
Cu(111)	–	–	–	–	–	4.123	TC	[2914]
Cu(111)	–	–	–	–	–	4.17	TC	[2522]
Cu(111)/NaCl[137]	Cu	–	?	~300 (423)	–	4.20 ± 0.02	PE	[3328]
Cu(111)	–	–	–	–	–	4.24	TC	[947]
Cu(111)	–	–	–	–	–	4.381	TC	[1118]
Cu(111)/ZnO(0001)[409]	Cu	–	4×10^{-10}	~300	–	4.5	TCS	[2679]
Cu(111)	–	–	~10^{-10}	~300	–	4.50	PE	[1661]
Cu(111)	–	–	–	–	–	4.54	TC	[1608]
Cu(111)	–	–	–	–	–	4.58	TC	[4034]
Cu(111)	–	–	–	–	–	4.63	TC	[2077]
Cu(111)	–	–	?	470–670	–	4.632 ± 0.010	CPD	[948,2841]
Cu(111)/Au(111)	–	–	–	–	–	4.69 ± 0.02*	TC	[3214]
Cu(111)/Si(111)	Cu	–	~10^{-10}	~300	–	4.7	PE	[1801]
Cu(111)	–	–	–	–	–	4.714	TC	[4091]
Cu(111)	–	–	–	–	–	4.76	TC	[2971]
Cu(111)	–	–	–	–	–	4.78	TC	[1028,1179]
Cu(111)	–	–	–	–	–	4.79	TC	[3477]
Cu(111)/Ru(0001)	Cu	–	≤5×10^{-10}	400–640	–	4.8*	CPD	[3705,3706,3731]
Cu(111)/W(110)[141]	Cu	–	<5×10^{-11}	~300	–	4.8	CPD	[1519]
Cu(111)/TaN/Ta	–	–	?	~300	–	4.8	PE	[1238,4210]
Cu(111)/mica[420]	Cu	–	4×10^{-10}	~300{570}	–	4.8	PE	[4001]
Cu(111)	–	–	<1×10^{-10}	~300	–	4.8 ± 0.3	CPD	[1186,1245,2284]
Cu(111)	–	–	–	–	–	4.80	TC	[3304]
Cu(111)	–	–	–	–	–	4.80	TC	[2917]
Cu(111)	–	–	–	–	–	4.80	TC	[1246]
Cu(111)	–	–	–	–	–	4.80	TC	[4317]
Cu(111)	–	–	–	–	–	4.82	TC	[1179]
Cu(111)[140]	–	–	?	~300	–	4.85*	CPD	[959]
Cu(111)	–	–	<10^{-10}	~300	–	4.85	PE	[1239]
Cu(111)	–	–	<2×10^{-10}	~300	–	4.85 ± 0.1	PE	[2415,3631,3632]
Cu(111)	–	–	–	–	–	4.86	TC	[2077]
Cu(111)	–	–	~10^{-10}	35	–	4.86	PE	[2898]
Cu(111)	–	–	1×10^{-8}	~300	–	4.86	PE	[3308]
Cu(111)	–	–	–	–	–	4.86	TC	[3486]
Cu(111)	–	–	≤1×10^{-10}	~300	–	4.87	PE	[3571]
Cu(111)	–	–	–	–	–	4.876	TC	[1119,2989]
Cu(111)	–	–	2×10^{-10}	~300	–	4.88	PE	[939,1124]
Cu(111)	–	–	2×10^{-10}	100	–	4.88	PE	[2684,2686]
Cu(111)	–	–	7×10^{-11}	~300	–	4.88 ± 0.05	PE	[1125]
Cu(111)/W(110)	Cu	–	?	~300	–	4.9	CPD	[4231]
Cu(111)	–	–	7×10^{-11}	85	–	4.9	PE	[4033]
Cu(111)	–	–	?	?	–	4.9	?	[1247]

Table 1 (*continued*)

Surface	Beam	Ion	P_r (Torr)	T (K)	ϕ^+ (eV)	ϕ^e (eV)	Meth.	Refs.
Cu(111)	–	–	?	~300	–	4.9	PE	[2509,2512]
Cu(111)/Ru(0001)	–	–	–	–	–	4.9	TC	[2641]
Cu(111)/Ru(0001)	Cu	–	~10^{-10}	539	–	4.9	CPD	[1685]
Cu(111)	–	–	–	–	–	4.90	TC	[2068]
Cu(111)	–	–	~1×10^{-11}	~300	–	4.90	CPD	[2532]
Cu(111)/Pt(111)	Cu	–	~7×10^{-11}	450	–	4.90	CPD	[2747]
Cu(111)	–	–	~2×10^{-10}	~300	–	4.90	PE	[1151]
Cu(111)	–	–	?	95	–	4.90	PE	[2687]
Cu(111)	–	–	?	~300	–	4.90	PE	[4025]
Cu(111)/W(110)[142]	Cu	–	<2×10^{-10}	~300	–	4.90*	CPD	[2598]
Cu(111)/W(110)	Cu	–	<10^{-10}	~300 (?)	–	4.90 ± 0.05	CPD	[2262]
Cu(111)/Pt(111)	Cu	–	?	450–475	–	4.91*	CPD	[2862]
Cu(111)	–	–	–	–	–	4.91	TC	[3477]
Cu(111)	–	–	?	100	–	4.92	PE	[4025]
Cu(111)/Au(111)	Cu	–	–	–	–	4.92 ± 0.02*	TC	[3214]
Cu(111)	–	–	<8×10^{-11}	~300	–	4.93	PE	[968,969]
Cu(111)	–	–	<2×10^{-10}	~300	–	4.93	PE	[1187]
Cu(111)	–	–	–	–	–	4.93	TC	[2685]
Cu(111)	–	–	?	~300	–	4.93 ± 0.03	PE	[2903]
Cu(111)	–	–	?	~300	–	4.93 ± 0.03	PE	[3180]
Cu(111)/Pt(111)	Cu	–	~7×10^{-11}	350	–	4.93 ± 0.05	CPD	[897,2747]
Cu(111)	–	–	?	400	–	4.94	CPD	[3198]
Cu(111)	–	–	<2×10^{-10}	~300	–	4.94	PE	[316]
Cu(111)	–	–	1×10^{-10}	~300	–	4.94	PE	[2907,2915]
Cu(111)	–	–	7×10^{-11}	~300	–	4.94 ± 0.02	PE	[1922]
Cu(111)	–	–	<10^{-10}	~300	–	4.94 ± 0.03	PE	[953,2006]
Cu(111)	–	–	<2×10^{-11}	85	–	4.946 ± 0.010	PE	[970]
Cu(111)	–	–	≤10^{-10}	~300	–	4.95	CPD	[952]
Cu(111)	–	–	8×10^{-11}	50, 100	–	4.95	PE	[898,3197,3603]
Cu(111)/Ru(0001)[143]	Cu	–	1×10^{-10}	290–700	–	4.95*	CPD	[1683,1685]
Cu(111)/Pd(111)	Cu	–	5×10^{-9}	~300	–	4.95	CPD	[3364]
Cu(111)	–	–	<5×10^{-8}	~300	–	4.95 ± 0.08*	CPD	[2923]
Cu(111)	–	–	–	–	–	4.958	TC	[4189]
Cu(111)	–	–	–	–	–	4.98	TC	[3273]
Cu(111)	–	–	–	–	–	4.99	TC	[3477]
Cu(111)	–	–	–	–	–	5.0	TC	[1126]
Cu(111)	–	–	–	–	–	5.0	TC	[3593]
Cu(111)	–	–	?	~300	–	5.00 ± 0.03	PE	[4213]
Cu(111)/Ru(0001)	Cu	–	?	400	–	5.01	CPD	[3198]
Cu(111)	–	–	?	~300	–	5.01	PE	[3522]
Cu(111)	–	–	–	–	–	5.03	TC	[1179]
Cu(111)	–	–	<5×10^{-8}	~300	–	5.03 ± 0.08*	CPD	[2923]
Cu(111)/Nb(110)	Cu	–	7×10^{-11}	~300	–	5.05	PE	[2986]
Cu(111)	–	–	–	–	–	5.1	TC	[1126]
Cu(111)	–	–	–	–	–	5.10	TC	[480]
Cu(111)	–	–	–	–	–	5.10	TC	[1178]
Cu(111)	–	–	–	–	–	5.17	TC	[1237]
Cu(111)	–	–	–	–	–	5.17	TC	[3491]
Cu(111)	–	–	–	–	–	5.19	TC	[956]
Cu(111)	–	–	–	–	–	5.19	TC	[2803]
Cu(111)	–	–	–	–	–	5.19	TC	[4402]
Cu(111)	–	–	–	–	–	5.22	TC	[1028,1179]
Cu(111)	–	–	–	–	–	5.22	TC	[4174,4284]
Cu(111)	–	–	–	–	–	5.24	TC	[3486,3491]
Cu(111)	–	–	–	–	–	5.25	TC	[3217]
Cu(111)	–	–	~10^{-10}	~300	–	5.25 ± 0.1	CPD	[1507]
Cu(111)	–	–	–	–	–	5.30	TC	[229,334,3179]
Cu(111)	–	–	–	–	–	5.305	TC	[2971]
Cu(111)	–	–	–	–	–	5.31	TC	[480,4398]
Cu(111)	–	–	–	–	–	5.32	TC	[480,4398]
Cu(111)	–	–	–	–	–	5.32	TC	[1159,1980,3067]
Cu(111)	–	–	–	–	–	5.32	TC	[2548]
Cu(111)	–	–	–	–	–	5.43	TC	[962]
Cu(111)	–	–	–	–	–	5.44	TC	[962]
Cu(111)	–	–	–	–	–	5.46	TC	[2540]
Cu(111)	–	–	<1×10^{-10}	77, 300	–	5.54 ± 0.012	CPD	[963]
Cu(111)	–	–	–	–	–	5.55	TC	[962]
Cu(111)	–	–	–	–	–	5.55	TC	[3224]
Cu(111)	–	–	–	–	–	5.56	TC	[962]
Recommended	–	–	–	–	–	**4.92 ± 0.05**	–	–

Table 1 (*continued*)

Surface	Beam	Ion	P_r (Torr)	T (K)	ϕ^+ (eV)	ϕ^e (eV)	Meth.	Refs.
Cu(112)	–	–	?	470–670	–	4.438 ± 0.010	CPD	[948,2841]
Cu(112)	–	–	–	–	–	4.45	TC	[3304]
Cu(112)	–	–	≲10^{-10}	~300	–	4.48	CPD	[952]
Cu(112)	–	–	–	–	–	4.48	TC	[4405]
Cu(112)	–	–	≲10^{-10}	~300	–	4.49	CPD	[952]
Cu(112)	–	–	<10^{-10}	~300	–	4.53 ± 0.03	PE	[953,2006]
Cu(112)	–	–	?	~300	–	4.54 ± 0.03	PE	[2903]
Cu(112)	–	–	?	~300	–	4.56	CPD	[964]
Recommended	–	–	–	–	–	**4.52 ± 0.03**	–	–
Cu(113)	–	–	–	–	–	4.31	TC	[479,1249]
Cu(113)	–	–	?	470–670	–	4.418 ± 0.010	CPD	[948,2841]
Cu(113)	–	–	–	–	–	4.74	TC	[3224]
Cu(114)	–	–	≲10^{-10}	~300	–	4.59	CPD	[952]
Cu(119)	–	–	~1 × 10^{-11}	~300	–	4.60	PE	[1241]
Cu(122)	–	–	≲10^{-10}	~300	–	4.54	CPD	[952]
Cu(122)	–	–	–	–	–	4.56	TC	[3304]
Cu(124)	–	–	≲10^{-10}	~300	–	4.48	CPD	[952]
Cu(210)	–	–	–	–	–	4.24	TC	[3304]
Cu(210)	–	–	?	470–670	–	4.370 ± 0.010	CPD	[948,2841]
Cu(233)	–	–	≲1 × 10^{-10}	95	–	4.35 ± 0.05	PE	[1604]
Cu(233)	–	–	≲10^{-10}	~300	–	4.57	CPD	[952]
Cu(234)	–	–	≲10^{-10}	~300	–	4.50	CPD	[952]
Cu(234)	–	–	≲10^{-10}	~300	–	4.52	CPD	[952]
Cu(236)	–	–	≲10^{-10}	~300	–	4.41	CPD	[952]
Cu(321)	–	–	?	~300	–	4.12	CPD	[964]
Cu(345)	–	–	≲10^{-10}	~300	–	4.50	CPD	[952]
Cu(356)	–	–	≲10^{-10}	~300	–	4.45	CPD	[952]
Cu(413)	–	–	?	~300	–	4.00	CPD	[964]
Cu(018)	–	–	≲10^{-10}	~300	–	4.70	CPD	[952]
Cu(???)/W	Cu	–	<1 × 10^{-9}	~300	–	4.54 ± 0.01	PE	[2313,2317]
Cu	–	–	–	–	–	3.20	TC	[2493]
Cu	–	–	–	–	–	3.21	TC	[2493]
Cu	–	–	–	–	–	3.24	TC	[1150]
Cu	–	–	–	–	–	3.32	TC	[521]
Cu	–	–	–	–	–	3.65	TC	[475]
Cu	–	–	–	–	–	3.65	TC	[2629]
Cu	–	–	–	–	–	3.66	TC	[2474]
Cu	–	–	?	~1350	–	3.85	TE	[3385]
Cu/W(100)	Cu	–	<2 × 10^{-10}	~300	–	3.9*	CPD	[1519]
Cu/Ti	Cu	–	3 × 10^{-11}	77 (400)	–	3.92	FE	[2424,3749]
Cu	–	–	?	~300	–	3.95 ± 0.02	CPD	[2544]
Cu/Ti	Cu	–	3 × 10^{-11}	77	–	3.96 ± 0.04	FE	[2424,3749]
Cu	–	–	–	–	–	4.0	TC	[2456]
Cu	–	–	~10^{-10}	~300	–	4.0	PE	[1661]
Cu	–	–	?	~300	–	4.05 ± 0.04	PE	[3394]
Cu/?	Cu	–	?	~300	–	4.07	PE	[2460]
Cu	–	–	?	?	–	4.1	TE	[3402]
Cu/Ti	Cu	–	3 × 10^{-11}	77 (800)	–	4.15	FE	[2424]
Cu/W(100)	Cu	–	<2 × 10^{-10}	78 (600)	–	4.16	FE	[2255]
Cu	–	–	~10^{-6}	~300	–	4.18	PE	[3389,3394]
Cu/glass	Cu	–	<1 × 10^{-10}	78	–	4.19	PE	[414,2728]
Cu	–	–	? (N_2)	~300	–	4.19	CPD	[2634]
Cu	–	–	–	–	–	4.2	TC	[944]

Table 1 (*continued*)

Surface	Beam	Ion	P_r (Torr)	T (K)	ϕ^+ (eV)	ϕ^e (eV)	Meth.	Refs.
Cu/W	Cu	–	4×10^{-10}	77	–	4.2	FE	[2586]
Cu	–	–	?	~300	–	4.22	CPD	[2626]
Cu	–	–	–	–	–	4.22	TC	[3352]
Cu	–	–	$\sim 10^{-7}$	~300 (753)	–	4.22 ± 0.01	CPD	[2627]
Cu/Ir	Cu	–	?	78 (~550)	–	4.23	FE	[2189]
Cu/W(310)	Cu	–	$<2 \times 10^{-10}$	78 (550)	–	4.23	FE	[2253]
Cu	–	–	4×10^{-9}	673	–	4.23 ± 0.08	PE	[1116]
Cu/W(310)	Cu	–	$<2 \times 10^{-10}$	78 (650)	–	4.24	FE	[2253]
Cu/Mo(100)	Cu	–	$<2 \times 10^{-10}$	~300 (≤965)	–	4.24*	CPD	[3121]
Cu	–	–	$\sim 4 \times 10^{-9}$	533	–	4.24 ± 0.07	PE	[1116]
Cu	–	–	$\sim 10^{-10}$	~300	–	4.25	CPD	[2426]
Cu	–	–	?	~300	–	4.25 ± 0.01	PE	[4190]
Cu/V(100)	Cu	–	$<8 \times 10^{-11}$	~300	–	4.25 ± 0.07*	PE	[3380]
Cu	–	–	?	?	–	4.26	TE	[1362]
Cu	–	–	–	–	–	4.26	TC	[1626]
Cu	–	–	–	–	–	4.26	TC	[2914]
Cu	–	–	–	–	–	4.3	TC	[706]
Cu/Ru(0001)	Cu	–	$\sim 1 \times 10^{-10}$	100	–	4.3	CPD	[2159]
Cu/Pt(111)	Cu	–	$\sim 10^{-10}$	293	–	4.3	PE	[3138]
Cu/GaP	–	–	–	–	–	4.30	TC	[1653]
Cu/Ti	Cu	–	3×10^{-11}	77 (?)	–	4.31	FE	[2424]
Cu/W(111)	Cu	–	$<2 \times 10^{-10}$	~300 (?)	–	4.32	FE	[2831]
Cu/W	Cu	–	5×10^{-10}	78 (700)	–	4.32 ± 0.01	FE	[1673,2238]
Cu/quartz	Cu	–	$\leq 5 \times 10^{-10}$	78	–	4.33 ± 0.01	PE	[435]
Cu	–	–	–	0	–	4.34	TC	[4419]
Cu	–	–	–	–	–	4.35	TC	[1885]
Cu/W(100)	Cu	–	$<2 \times 10^{-10}$	~300 (?)	–	4.35	FE	[2831]
Cu/Ni	Cu	–	4×10^{-10}	~300	–	4.35 ± 0.16*	CPD	[3367]
Cu/W	Cu	–	$<2 \times 10^{-10}$	~300 (?)	–	4.36	FE	[2831]
Cu	–	–	–	–	–	4.37	TC	[1976]
Cu	–	–	?	~1200	–	4.38	TE	[1944]
Cu/W(112)	Cu	–	$<2 \times 10^{-10}$	~300 (?)	–	4.38	FE	[2831]
Cu	–	–	–	–	–	4.39	TC	[3318]
Cu/glass	Cu	–	$<10^{-9}$	90	–	4.39	PE	[1957]
Cu/glass	Cu	–	$<10^{-8}$	78	–	4.39 ± 0.02	CPD	[1646]
Cu/glass	Cu	–	$<10^{-9}$	77–90	–	4.395	PE	[3052]
Cu[144]	–	–	$\sim 8 \times 10^{-8}$	~1350	–	4.4	TE	[1465]
Cu/W(100)	Cu	–	$<2 \times 10^{-10}$	78	–	4.4	FE	[2255]
Cu/glass[88]	Cu	–	$<10^{-9}$	~300{77}	–	4.4	CPD	[1526]
Cu/Mo(100)	Cu	–	$<2 \times 10^{-10}$	~300	–	4.4*	CPD	[3121]
Cu/W(100)	Cu	–	$<2 \times 10^{-10}$	78 (850)	–	4.40	FE	[2253]
Cu/glass[369]	Cu	–	$\sim 10^{-10}$	77	–	4.40	PE	[2133,2155]
Cu/glass	Cu	–	$\sim 10^{-10}$	90	–	4.40	PE	[2763,3046]
Cu	–	–	$\sim 10^{-9}$	~1100–1300	(4.42)	4.41 ± 0.02	TE	[179,3425]
Cu	–	–	4×10^{-9}	296	–	4.41 ± 0.03	PE	[1116]
Cu	–	–	$\leq 10^{-9}$	~1100–1250	–	4.415 ± 0.03	TE	[650]
Cu	–	–	?	~300	–	4.42*	CPD	[3621]
Cu	–	–	? (Cs)	~1100–1250	–	4.42	TE	[650,3413]
Cu	Cs	Cs$^+$	?	1073	4.42	(4.41 ± 0.02)	PSI	[179,3425]
Cu	–	–	?	~300	–	4.42 ± 0.04	PE	[1250]
Cu/W(112)	Cu	–	$<2 \times 10^{-10}$	78 (700)	–	4.43	FE	[2253]
Cu	–	–	$\sim 10^{-10}$	~300	–	4.43	PE	[724]
Cu/Si	–	–	–	–	–	4.43	TC	[1653]
Cu	–	–	–	–	–	4.45	TC	[1399]
Cu	–	–	?	~300	–	4.45	PE	[4278]
Cu	–	–	$\sim 10^{-9}$	~1100–1200	–	4.45 ± 0.05	TE	[650,3419]
Cu	–	–	2×10^{-7} (O$_2$)	~1100–1200	–	4.45 ± 0.05	TE	[3419]
Cu	–	–	–	–	–	4.46	TC	[1645]
Cu/Si	–	–	–	–	–	4.46	TC	[1653]
Cu	–	–	1×10^{-5}	~300	–	4.46	CPD	[1883]
Cu	–	–	?	~300	–	4.46	CPD	[2297]
Cu/W(110)	Cu	–	$<2 \times 10^{-10}$	78 (750)	–	4.46	FE	[2253]
Cu/glass	Cu	–	?	~300	–	4.46 ± 0.03	CPD	[243]
Cu/Ni[145]	–	–	?	~80	–	4.47	CPD	[2294]
Cu	–	–	$\leq 1 \times 10^{-10}$	~300	–	4.47	CPD	[2198]
Cu	–	–	?	~300	–	4.48	CPD	[1883]
Cu	–	–	–	–	–	4.48	TC	[4441]
Cu/W(110)	Cu	–	$<2 \times 10^{-10}$	78 (600)	–	4.48	FE	[2253]
Cu/quartz	Cu	–	$\leq 5 \times 10^{-10}$	293	–	4.48 ± 0.02	PE	[435]
Cu[146]	–	–	$\sim 10^{-6}$	~300	–	4.48 ± 0.06*	CPD	[2087]

Table 1 (*continued*)

Surface	Beam	Ion	P_r (Torr)	T (K)	ϕ^+ (eV)	ϕ^e (eV)	Meth.	Refs.
Cu	–	–	–	–	–	4.49	TC	[3515]
Cu	–	–	~10^{-7}	~300 (1173)	–	4.49 ± 0.02	CPD	[2627]
Cu/ZnO(0001)[409]	Cu	–	4×10^{-10}	~300	–	4.5	TCS	[2679]
Cu	–	–	1×10^{-9}	~300	–	4.5	PE	[3511]
Cu	–	–	–	–	–	4.5	TC	[1993]
Cu	–	–	–	–	–	4.5	TC	[2583]
Cu/Cu,Ag,Au	Cu	–	2×10^{-9}	~300	–	4.5	PE	[1155]
Cu/W(110)[141]	Cu	–	<2×10^{-10}	~300{800}	–	4.5	CPD	[1519]
Cu/Al(100)	Cu	–	1×10^{-10}	~300	–	4.5	PE	[1572]
Cu/W(100)	Cu	–	5×10^{-10}	400, 450	–	4.5	FE	[3129]
Cu/W(110)	Cu	–	≤7×10^{-11}	~300 (≤1200)	–	4.5	CPD	[2388]
Cu/W(100)	Cu	–	<2×10^{-10}	78 (700)	–	4.5	FE	[1674]
Cu	–	–	2×10^{-9}	~300	–	4.5	PE	[1155]
Cu	–	–	2×10^{-11}	~300	–	4.5 ± 0.1	PE	[1251]
Cu	–	–	–	–	–	4.50	TC	[2629]
Cu	–	–	<5×10^{-8}	~1150–1350	–	4.50	TE	[1466]
Cu	–	–	?	~300	–	4.5 ± 0.1	PE	[1461]
Cu	–	–	2×10^{-11}	~300	–	4.5 ± 0.1	PE	[1251]
Cu/Mo(110)	Cu	–	5×10^{-11}	~300–750	–	4.5 ± 0.1	CPD	[3287]
Cu/graphite	Cu	–	?	~1200–1300	–	4.50 ± 0.02	TE	[2236]
Cu	–	–	–	–	–	4.50 ± 0.05	TC	[3358]
Cu	–	–	–	–	–	4.51	TC	[3515]
Cu	–	–	–	–	–	4.51	TC	[3318]
Cu	–	–	≤1×10^{-10}	~300	–	4.51	CPD	[2198]
Cu/W(110)	Cu	–	<2×10^{-10}	78 (522)	–	4.51	FE	[2253]
Cu[463]	–	–	?	~300	–	4.52	CPD	[931,2547]
Cu/glass	Cu	–	<1×10^{-10}	78 (293)	–	4.52	PE	[414,2722,2728]
Cu/glass	Cu	–	~10^{-8}	~300	–	4.52 ± 0.04	CPD	[133]
Cu	–	–	5×10^{-10}	~300	–	4.53	AI[38]	[4027]
Cu/glass	Cu	–	5×10^{-11}	~300	–	4.53 ± 0.05	CPD	[1071]
Cu/Si(111)	Cu	–	~10^{-10}	~300	–	4.54	PE	[1801]
Cu	–	–	?	?	–	4.55	TE	[1764]
Cu	–	–	–	–	–	4.55	TC	[3264,3265]
Cu/TaN/Ta	–	–	?	~300	–	4.55 ± 0.02	PE	[1238,4210]
Cu/Ir(100)[139]	Cu	–	?	78 (380)	–	4.55 ± 0.02	FE	[2189]
Cu/Si(111)	Cu	–	~10^{-10}	~300	–	4.55 ± 0.05	CPD	[613,636,3270]
Cu/V(100)	Cu	–	<8×10^{-11}	~300	–	4.55 ± 0.05	PE	[3380]
Cu/glass	Cu	–	5×10^{-11}	~300	–	4.55 ± 0.06*	CPD	[1071]
Cu	–	–	<5×10^{-8}	~1150–1350	–	4.56	TE	[1466]
Cu/glass	Cu	–	5×10^{-11}	~300	–	4.57 ± 0.07*	CPD	[1071]
Cu/W(110)	Cu	–	<2×10^{-10}	90	–	4.58	CPD	[3983,4107]
Cu/W(110)	Cu	–	<2×10^{-10}	78 (600)	–	4.58	FE	[2253]
Cu/W(110)[147]	Cu	–	<2×10^{-10}	~300 (?)	–	4.58 ± 0.05*	FE	[2831]
Cu/Mo(110)	Cu	–	~10^{-10}	~300	–	4.6	CPD	[3679]
Cu/W[142]	Cu	–	≤2×10^{-10}	~300	–	4.6*	CPD	[2598]
Cu/Ru(0001)	Cu	–	~1×10^{-10}	100 (900)	–	4.6	CPD	[2159]
Cu	–	–	–	–	–	4.6	TC	[3556]
Cu/?	Cu	–	~10^{-5}	~300	–	4.6	CPD	[1376]
Cu/W(110)	Cu	–	?	90 (850)	–	4.6	CPD	[1701,1706]
Cu/quartz	Cu	–	≤5×10^{-10}	293 (~550)	–	4.60 ± 0.02	PE	[435]
Cu/Pt(111)	Cu	–	~10^{-10}	293	–	4.60 ± 0.08*	PE	[3138]
Cu/Ni	Cu	–	<10^{-10}	~300 (~370)	–	4.61	PE	[1152]
Cu/glass	Cu	–	<10^{-10}	~300 (~370)	–	4.61 ± 0.02	PE	[1117]
Cu/W	Cu	–	≤5×10^{-8}	~300	–	4.61 ± 0.04	CPD	[690]
Cu[144]	–	–	8×10^{-8}	1356 (m.p.)	–	4.62	TE	[1465,1466]
Cu	–	–	–	–	–	4.62	TC	[339]
Cu/W(110)	Cu	–	<1×10^{-10}	~300	–	4.62 ± 0.03	FE	[2054]
Cu/glass	Cu	–	5×10^{-11}	~300	–	4.62 ± 0.07*	CPD	[1071]
Cu/Au(111)	–	–	–	–	–	4.63	TC	[3217]
Cu	–	–	6×10^{-3}	~300	–	4.63 ± 0.05	PE	[2079,2080]
Cu/glass[369]	Cu	–	~10^{-10}	77 (323)	–	4.64	PE	[2133,2155]
Cu/glass[148]	Cu	–	?	273	–	4.64	PE	[3075]
Cu/steel	Cu	–	<6×10^{-9}	~300	–	4.64 ± 0.02	CPD	[1540]
Cu/W	Cu	–	<5×10^{-8}	~300	–	4.64 ± 0.07	CPD	[2570]
Cu	–	–	–	–	–	4.647	TC	[2649]
Cu/Au(100)	–	–	–	–	–	4.65	TC	[3217]
Cu	–	–	–	–	–	4.65	TC	[3016]
Cu	–	–	1×10^{-10}	~300	–	4.65	PE	[2907]
Cu/glass[148]	Cu	–	?	77	–	4.65	PE	[3075]
Cu	–	–	<2×10^{-10}	90	–	4.65	CPD	[4107]

Table 1 (*continued*)

Surface	Beam	Ion	P_r (Torr)	T (K)	ϕ^+ (eV)	ϕ^e (eV)	Meth.	Refs.
Cu/W(110)	Cu	–	$<2 \times 10^{-10}$	90	–	4.65	CPD	[3983]
Cu/quartz	Cu	–	$\sim10^{-10}$	~300	–	4.65 ± 0.05	PE	[304]
Cu/W(100)	Cu	–	$\leq10^{-10}$	78	–	4.66	FE	[356]
Cu/glass	Cu	–	$<10^{-10}$	~300 (~470)	–	4.66 ± 0.01	PE	[1117]
Cu/W(112)	Cu	–	?	77, 650	–	4.66 ± 0.01	FE	[4319,4320]
Cu/W(110)	Cu	–	$<1 \times 10^{-10}$	~300	–	4.66 ± 0.03	FE	[2054]
Cu/glass	Cu	–	$<10^{-9}$	90 (343)	–	4.67	PE	[2096]
Cu/Ni	Cu	–	$<10^{-10}$	~300 (~470)	–	4.68	PE	[1152]
Cu	–	–	–	–	–	4.69	TC	[3476]
Cu	–	–	–	–	–	4.69	TC	[298]
Cu/Al(111)	Cu	–	1×10^{-10}	~300	–	4.7	PE	[1572]
Cu/Ni(100)	–	–	–	–	–	4.7	TC	[3556]
Cu/Ag(110)	Cu	–	$<4 \times 10^{-9}$	~300	–	4.7	CPD	[2749]
Cu/W(110)	–	–	–	–	–	4.7*	TC	[2975]
Cu	–	–	? (H_2)	~300	–	4.70	PE	[2207]
Cu	–	–	–	–	–	4.70	TC	[3267]
$Cu_n(n \to \infty)$	–	–	?	~300	–	4.70	IP, TC	[4197]
Cu	–	–	$\sim1 \times 10^{-6}$	~300	–	4.71	CPD	[2742]
Cu/glass	–	–	$\sim10^{-10}$	90	–	4.71 ± 0.03	PE	[3048]
Cu	–	–	?	~300	–	4.71 ± 0.05	PE	[2903]
Cu	–	–	1×10^{-9}	~300	–	4.73	CPD	[1252]
Cu/Co/Cu(100)	–	–	–	–	–	4.74	TC	[2897]
Cu/W(112)	Cu	–	?	~300	–	4.74	FE	[4319]
Cu	–	–	3×10^{-11}	~300	–	4.75	FE	[2227]
Cu/Mo(110)	Cu	–	2×10^{-10}	~300	–	4.75	PE	[3288]
Cu	–	–	–	–	–	4.76	TC	[3637]
Cu	–	–	?	~300	–	4.76	PE	[3027]
Cu/Si(111)	Cu	–	$<4 \times 10^{-10}$	~300	–	4.76	PE	[3282]
Cu[463]	–	–	?	~300	–	4.76	CPD	[931,2547]
Cu/Mo(110)	Cu	–	$<6 \times 10^{-11}$	~300	–	4.79*	CPD	[3293]
Cu/W(110)[141]	Cu	–	$<2 \times 10^{-10}$	~300	–	4.8	CPD	[1519,3588]
Cu/Ru(0001)	Cu	–	$\leq5 \times 10^{-10}$	400–640	–	4.8*	CPD	[3705,3706,3731]
Cu	–	–	?	~300	–	4.8 ± 0.2	CPD	[3867]
Cu(fp)[149]	–	–	$<10^{-9}$	~300	–	4.80 ± 0.1	PE	[3190]
Cu/Co/Co(0001)	–	–	–	–	–	4.86	TC	[3490]
Cu[146]	–	–	$\sim10^{-6}$	~300	–	4.86 ± 0.01	CPD	[2087]
Cu/SiO$_2$/Si	Cu	–	?	~300 (570)	–	4.87	PE	[2355]
Cu	–	–	?	~1350	–	4.87	PE	[4139]
Cu/glass	Cu	–	$<10^{-9}$	90, 293	–	4.89	PE	[3046]
Cu	–	–	–	–	–	4.89	TC	[3476]
Cu/Co/Cu(100)	–	–	–	–	–	4.89	TC	[2897]
Cu/W(110)	Cu	–	?	90 (~300)	–	4.9	CPD	[1701,1706]
Cu/Pt(100)	–	–	–	–	–	4.90	TC	[2530]
Cu/W(110)	Cu	–	$<2 \times 10^{-10}$	90	–	4.90	CPD	[3983]
Cu/glass	Cu	–	$<10^{-9}$	90 (380)	–	4.92	PE	[3045]
Cu	–	–	–	–	–	4.93	TC	[4031]
Cu/glass	Cu	–	$\sim10^{-10}$	90 (348)	–	4.94	PE	[2763,3046]
Cu	–	–	–	–	–	4.95	TC	[1066]
Cu	–	–	–	–	–	4.95	TC	[4031]
Cu[58]	–	–	?	~300	–	4.99	CPD	[2550]
Cu/Pt(100)	–	–	–	–	–	5.02	TC	[3382]
Cu/Nb(110)	–	–	7×10^{-11}	~300	–	5.05	PE	[2986]
Cu/Mo(110)	Cu	–	$<6 \times 10^{-11}$	~300	–	5.08	CPD	[3293]
Cu$_4$(cluster)	–	–	–	–	–	5.10	TC	[3205]
Cu/glass	Cu	–	$<10^{-9}$	90 (333)	–	5.11	PE	[1957]
Cu/Co/Cu(100)	–	–	–	–	–	5.14	TC	[950]
Cu$_4$(cluster)	–	–	–	–	–	5.16	TC	[3205]
Cu/Pt(100)	–	–	–	–	–	5.16	TC	[3382]
Cu/W(110)[147]	Cu	–	$<2 \times 10^{-10}$	~300 (?)	–	5.20	FE	[2831]
Cu	–	–	–	–	–	5.24	TC	[3476]
Cu	–	–	–	–	–	5.3	TC	[1432]
Recommended	–	–	–	–	–	**4.51 ± 0.04**	–	–
Liquid ($T > 1356$ K)								
Cu[144]	–	–	8×10^{-8}	~1356	–	4.5 ± 0.1	TE	[1465,1466]
Cu	–	–	?	~1360	–	4.75	PE	[4139]
Cu	–	–	$<5 \times 10^{-8}$	1356–1520	–	5.3	TE	[1466]

Table 1 (*continued*)

Surface	Beam	Ion	P_r (Torr)	T (K)	ϕ^+ (eV)	ϕ^e (eV)	Meth.	Refs.
				30. Zinc Zn				
hcp								
Zn(0001)	–	–	–	–	–	3.0	TC	[3137]
Zn(0001)	–	–	–	–	–	3.24	TC	[3211]
Zn(0001)	–	–	–	–	–	3.500	TC	[2914]
Zn(0001)	–	–	2×10^{-7}	~300	–	3.56	PE	[1758]
Zn(0001)[150]	–	–	10^{-9}	45–290	–	3.63	PE	[2591,2601]
Zn(0001)	–	–	–	–	–	3.65	TC	[1030,1089]
Zn(0001)	–	–	?	~300	–	3.7	PE	[2264]
Zn(0001)	–	–	–	–	–	3.74	TC	[1089]
Zn(0001)	–	–	–	–	–	3.77	TC	[3467]
Zn(0001)	–	–	–	–	–	3.79	TC	[3004]
Zn(0001)	–	–	–	–	–	3.83	TC	[231,556]
Zn(0001)	–	–	–	–	–	3.92	TC	[4461][490]
Zn(0001)	–	–	–	–	–	4.00	TC	[1089]
Zn(0001)	–	–	–	–	–	4.07	TC	[1030]
Zn(0001)	–	–	–	–	–	4.075	TC	[4460][490]
Zn(0001)	–	–	–	–	–	4.15	TC	[1159,3067]
Zn(0001)	–	–	–	–	–	4.15	TC	[475,1095]
Zn(0001)	–	–	–	–	–	4.19	TC	[3004]
Zn(0001)	–	–	–	–	–	4.2	TC	[1088]
Zn(0001)	–	–	–	–	–	4.20	TC	[593]
Zn(0001)	–	–	–	–	–	4.21	TC	[4461][490]
Zn(0001)	–	–	–	–	–	4.24	TC	[553]
Zn(0001)	–	–	?	100	–	4.25	CPD	[2370,2633]
Zn(0001)	–	–	~10^{-7}	~300	–	4.26 ± 0.01	PE	[2298]
Zn(0001)	–	–	–	–	–	4.30	TC	[556]
Zn(0001)	–	–	~10^{-11}	~300	–	4.4	PE	[2137]
Zn(0001)	–	–	–	–	–	4.43	TC	[4005]
Zn(0001)	–	–	–	–	–	4.442	TC	[4460][490]
Zn(0001)	–	–	–	–	–	4.7	TC	[2375]
Zn(0001)	–	–	–	–	–	4.81	TC	[1087]
Zn(0001)	–	–	–	–	–	4.85	TC	[1095]
Zn(0001)	–	–	≤1×10^{-10}	70	–	4.9 ± 0.6	CPD	[1508]
Zn(0001)	–	–	–	–	–	6.88	TC	[321]
Recommended	–	–	–	–	–	**4.35 ± 0.28**	–	–
Zn(1010)	–	–	–	–	–	5.04	TC	[4005]
Zn(1010)	–	–	–	–	–	6.57	TC	[321]
Zn(1124)	–	–	–	–	–	5.76	TC	[321]
Zn	–	–	?	~300	–	3.08	PE	[2460]
Zn	–	–	?	~300	–	3.09 ± 0.01	PE	[2703]
Zn	–	–	?	~300	–	3.1	PE	[1454]
Zn	–	–	–	–	–	3.14	TC	[1744]
Zn	–	–	–	–	–	3.2	TC	[944]
Zn	–	–	?	648	–	3.24	PE	[1454]
Zn	–	–	?	~300	–	3.28 ± 0.01	PE	[2703]
Zn	–	–	2×10^{-7}	~300	–	3.32	PE	[1758]
Zn	–	–	–	–	–	3.4	TC	[2456]
Zn	–	–	?	~300	–	3.40	CPD	[2761]
Zn/Pt(100)	–	–	–	–	–	3.45	TC	[3168]
Zn/Au(100)	–	–	–	–	–	3.45	TC	[3168]
Zn	–	–	–	–	–	3.50	TC	[521]
Zn	–	–	–	–	–	3.51	TC	[231]
Zn	–	–	?	~300	–	3.52	PE	[4278]
Zn	–	–	2×10^{-7}	~300	–	3.57	PE	[1758]
Zn	–	–	6×10^{-3}	~300	–	3.60 ± 0.08	PE	[2079,2080]
Zn	–	–	–	–	–	3.62	TC	[1924]
Zn	–	–	?	~300	–	3.66	CPD	[2297]
Zn	–	–	–	–	–	3.68	TC	[3467]
Zn	–	–	–	0	–	3.69	TC	[4419]
Zn	–	–	?	~300	–	3.69 ± 0.09	CPD	[2544]
Zn	–	–	?	~300	–	3.72	PE	[4159]
Zn	–	–	–	–	–	3.73	TC	[231]
Zn	–	–	<10^{-6}	~300	–	3.74	PE	[2919]
Zn	–	–	–	–	–	3.77	TC	[230]

Table 1 (*continued*)

Surface	Beam	Ion	P_r (Torr)	T (K)	ϕ^+ (eV)	ϕ^e (eV)	Meth.	Refs.
Zn	–	–	–	–	–	3.77	TC	[3467]
Zn	–	–	–	–	–	3.79	TC	[3168]
Zn	–	–	–	–	–	3.8*	TC	[1955]
Zn	–	–	–	–	–	3.80	TC[3]	[475]
Zn	–	–	–	–	–	3.80	TC	[3352]
Zn	–	–	? (N_2)	~300	–	3.80 ± 0.02	CPD	[2624,4226,4232]
Zn	–	–	?	~300	–	3.84*	CPD	[3621]
Zn	–	–	?	~300	–	3.85 ± 0.01	PE	[3394]
Zn	–	–	~10^{-6}	~300	–	3.89	PE	[3389,3394]
Zn	–	–	–	–	–	3.93	TC	[2629]
Zn	–	–	–	–	–	3.95	TC	[1399]
Zn/ins/Al[47]	Zn	–	?	~300	–	3.98 ± 0.09	CPD	[2028]
Zn	–	–	1×10^{-5}	~300	–	4.01	CPD	[1883]
Zn	–	–	–	–	–	4.02	TC	[1924]
Zn	–	–	–	–	–	4.04	TC	[3318]
Zn	–	–	–	–	–	4.07	TC	[1901]
Zn	–	–	–	–	–	4.09	TC	[553]
Zn	–	–	–	–	–	4.09	TC	[3477]
Zn	–	–	–	–	–	4.1 ± 0.09	TC	[1990]
Zn	–	–	–	–	–	4.10	TC	[1626,2914]
Zn/glass[151]	Zn	–	?	~300	–	4.11 ± 0.03	CPD	[1370]
Zn	–	–	–	–	–	4.12	TC	[738]
Zn/brass	Zn	–	≤10^{-8}	~300	–	4.16 ± 0.12	PE	[2848]
Zn	–	–	–	–	–	4.18	TC	[3318]
Zn	–	–	–	–	–	4.2	TC	[1993]
Zn/steel	Zn	–	≤10^{-10}	~300	–	4.2 ± 0.05	PE	[1523]
Zn	–	–	?	~300	–	4.2 ± 0.1	CPD	[2364]
Zn/SrTiO$_3$(100)	Zn	–	?	~300	–	4.2 ± 0.1	TCS	[4220]
Zn/Mo	Zn	–	~2×10^{-8}	~300	–	4.24	PE	[1763]
Zn	–	–	–	–	–	4.24	TC	[298]
Zn[152]	–	–	~10^{-6}	~300	–	4.27 ± 0.06*	CPD	[2087]
Zn/glass[151]	Zn	–	?	~300	–	4.28 ± 0.02	CPD	[1370]
Zn	–	–	–	–	–	4.3*	TC	[706]
Zn$_n$($n \to \infty$)[472]	–	–	–	–	–	4.3*	TC	[4329]
Zn:ZnO(0001)	–	–	<5×10^{-11}	~300	–	4.3 ± 0.1	PE	[3119]
Zn	–	–	–	–	–	4.30	TC	[3264,3265,3267]
Zn/glass	Zn	–	?	90, 300	–	4.307	PE	[3031]
Zn	–	–	–	–	–	4.31	TC	[2005]
Zn	–	–	–	–	–	4.317	TC	[2649]
Zn/glass	Zn	–	<10^{-9}	90, 293	–	4.32	PE	[3046]
Zn/glass	Zn	–	~10^{-10}	77–90	–	4.33	PE	[2763,3046,3052]
Zn/glass	Zn	–	~10^{-10}	77–90 (373)	–	4.33	PE	[2763,3046]
Zn/glass	Zn	–	<10^{-9}	77–90	–	4.335	PE	[3031]
Zn/glass	Zn	–	<10^{-9}	77–90 (293)	–	4.335	PE	[3031]
Zn/glass	Zn	–	<10^{-9}	77–90	–	4.34	PE	[2307,3048]
Zn/glass	Zn	–	<10^{-9}	77–90 (383)	–	4.34	PE	[2307,3048]
Zn	–	–	–	–	–	4.34	TC	[4418,4420]
Zn	–	–	~4×10^{-9}	294	–	4.35 ± 0.03	PE	[1116]
Zn[152]	–	–	~10^{-6}	~300	–	4.65 ± 0.01	CPD	[2087]
Zn	–	–	–	–	–	4.76	TC	[3477]
Zn	–	–	–	–	–	4.85	TC	[2629]
Zn	–	–	?	~300	–	4.9*	CPD	[3867]
Zn	–	–	–	–	–	5.35	TC	[1066]
Recommended	–	–	–	–	–	**4.22 ± 0.11**	–	–

31. Gallium Ga

fcc

Ga(100)	–	–	–	–	–	3.35	TC	[3211]
Ga(110)	–	–	–	–	–	4.08	TC	[3211]
Ga(111)	–	–	–	–	–	3.79	TC	[3211]

Rhombic ($T < 303$ K for bulk)

Ga	–	–	–	–	–	3.55	TC	[3211]
Ga	–	–	–	–	–	3.56	TC	[521]
Ga	–	–	–	–	–	3.57	TC	[3211]
Ga	–	–	–	–	–	3.58	TC	[1744]
Ga	–	–	–	–	–	3.7	TC	[3318]

Table 1 (*continued*)

Surface	Beam	Ion	P_r (Torr)	T (K)	ϕ^+ (eV)	ϕ^e (eV)	Meth.	Refs.
Ga	–	–	–	–	–	3.8*	TC	[1955]
Ga	–	–	?	~300	–	3.80	CPD	[2297]
Ga	–	–	–	–	–	3.84	TC	[3211]
Ga	–	–	–	0	–	3.84	TC	[4419]
Ga	–	–	–	–	–	3.94	TC	[3318]
Ga/Au/Cu	Ga	–	5×10^{-11}	10	–	4.0	PE	[3130]
Ga	–	–	–	–	–	4.0 ± 0.05	TC	[1990]
Ga	–	–	–	–	–	4.02	TC	[1399]
Ga	–	–	–	–	–	4.02	TC	[2629]
Ga	–	–	?	293	–	4.07	PE	[4139]
Ga	–	–	–	–	–	4.1	TC	[944]
Ga	–	–	–	–	–	4.1	TC	[2583]
Ga	–	–	?	~300	–	4.12	PE	[3027]
Ga	–	–	–	–	–	4.16	TC	[298]
Ga	–	–	?	187	–	4.19	PE	[4249]
Ga	–	–	–	–	–	4.2	TC	[706]
Ga	–	–	–	–	–	4.20	TC	[1885]
Ga	–	–	$\sim10^{-7}$	~300	–	4.20 ± 0.03	CPD	[2767]
Ga	–	–	–	–	–	4.21	TC	[4418]
Ga	–	–	–	–	–	4.22	TC	[1613]
Ga	–	–	–	–	–	4.25	TC	[3267]
Ga/Cu	Ga	–	$\sim10^{-11}$	20	–	4.3	PE	[1111]
Ga	–	–	–	–	–	4.3	TC	[1645]
Ga/Au/Cu	Ga	–	5×10^{-11}	<10	–	4.3 ± 0.1	PE	[2267]
Ga	–	–	–	–	–	4.30	TC	[3264,3265]
Ga	–	–	?	~290	–	4.31	PE	[4139]
Ga/Si(111)	Ga	–	$<8 \times 10^{-11}$	~300	–	4.33	PE	[1904]
Ga	–	–	10^{-6}	~300	–	4.34 ± 0.06	CPD	[2942]
Ga	–	–	?	273	–	4.35 ± 0.03	PE	[2770,2771]
Ga/Si(111)	Ga	–	$<8 \times 10^{-11}$	~300	–	4.36	PE	[1904]
Ga	–	–	–	–	–	4.36	TC	[1901]
Ga	–	–	$<10^{-10}$	273	–	4.36 ± 0.03	PE	[2026]
Ga/Si(111)	Ga	–	5×10^{-11}	~300	–	4.37 ± 0.1	PE	[2623,2625]
Ga/glass	Ga	–	$<10^{-9}$	90	–	4.40	PE	[3046]
Ga/Al(100)	–	–	–	–	–	4.41	TC	[1932]
Ga	–	–	–	–	–	4.44	TC	[2005]
Ga/glass	Ga	–	$<10^{-9}$	90 (<273)	–	4.45	PE	[2763,3046]
Ga/glass	Ga	–	$<10^{-9}$	293	–	4.45	PE	[3052]
Ga/Si(111)	Ga	–	$<4 \times 10^{-10}$	~300	–	4.45	PE	[1566]
Ga/W(110)	Ga	–	$\sim10^{-11}$	20	–	4.5	FE	[2218]
Ga/W(112)	Ga	–	$\sim10^{-11}$	20	–	4.5	FE	[2218]
Ga/Al(100)	–	–	–	–	–	4.57	TC	[1932]
Ga/W(111)	Ga	–	$\sim10^{-11}$	20	–	4.6	FE	[2218]
Ga/Mo(111)	Ga	–	$\sim10^{-11}$	20	–	4.6	FE	[2218]
Ga/W	Ga	–	?	78 (?)	–	4.65 ± 0.1	FE	[2725]
Ga/W(114)	Ga	–	$\sim10^{-11}$	20	–	4.7	FE	[2218]
Ga/Mo(112)	Ga	–	$\sim10^{-11}$	20	–	4.7	FE	[2218]
Ga/W	Ga	–	$<2 \times 10^{-10}$	77 (≤500)	–	4.75	FE	[2727]
Ga/W	Ga	–	?	78 (?)	–	4.75 ± 0.1	FE	[2725]
Ga/Mo(110)	Ga	–	$\sim10^{-11}$	20	–	4.9	FE	[2218]
Ga	–	–	–	–	–	4.96	TC	[2629]
Recommended	–	–	–	–	–	**4.27 ± 0.06**	–	–

Liquid ($T > 303$ K)

Surface	Beam	Ion	P_r (Torr)	T (K)	ϕ^+ (eV)	ϕ^e (eV)	Meth.	Refs.
Ga	–	–	?	323	–	4.30 ± 0.01	PE	[2770,2771]
Ga	–	–	$<10^{-10}$	323	–	4.30 ± 0.02	PE	[2026]
Ga	–	–	$\leq10^{-9}$	473	–	4.31	SP	[2349]
Ga	–	–	8×10^{-10}	320–820	–	4.33 ± 0.05	PE	[2726]
Ga	–	–	$\leq10^{-9}$	473	–	4.35 ± 0.05	PE	[2345,2349,2353]
Ga	–	–	?	313	–	4.37	PE	[4139]
Ga	–	–	$\leq3 \times 10^{-9}$	>300	–	4.39 ± 0.06	CPD	[1542,3106]
Recommended	–	–	–	–	–	**4.33 ± 0.03**	–	–

32. Germanium Ge

Diamond structure

Surface	Beam	Ion	P_r (Torr)	T (K)	ϕ^+ (eV)	ϕ^e (eV)	Meth.	Refs.
Ge(100)	–	–	$<2 \times 10^{-10}$	~300	–	4.46[484]	FE	[3539]
Ge(100)	–	–	?	~300 (770)	–	4.55	CPD	[1768]
Ge(100)	–	–	?	~300 (870)	–	4.55	CPD	[1768]
Ge(100)	–	–	–	–	–	4.649	TC	[3499,3500]

Table 1 (*continued*)

Surface	Beam	Ion	P_r (Torr)	T (K)	ϕ^+ (eV)	ϕ^e (eV)	Meth.	Refs.
Ge(100)	–	–	?	?	–	4.7	?	[1857]
Ge(100)	–	–	?	~300 (620)	–	4.72	CPD	[1768]
Ge(100)	–	–	?	~300	–	4.75	CPD	[1768]
Ge(100)	–	–	$\leq 2 \times 10^{-8}$	~300	–	4.76 ± 0.3	CPD	[1382]
Ge(100)	–	–	5×10^{-10}	~300	–	4.77 ± 0.015	CPD	[1769,1770]
Ge(100)	–	–	$\sim 10^{-11}$	~300	–	4.9	FE	[3097]
Ge(100)	–	–	$\sim 10^{-11}$	~300	–	5.0	FE	[3097]
Recommended	–	–	–	–	–	**4.68 ± 0.08**	–	–
Ge(110)[436]	–	–	$\leq 2 \times 10^{-8}$	~300	–	4.72 ± 0.3	CPD	[1382]
Ge(110)[n]	–	–	5×10^{-10}	~300	–	4.73 ± 0.015	CPD	[1770]
Ge(110)	–	–	$\sim 10^{-10}$	~300	–	4.77	CPD	[3696]
Ge(110)	–	–	5×10^{-10}	~300	–	4.78 ± 0.015	CPD	[1770]
Ge(110)	–	–	$<2 \times 10^{-10}$	~300	–	4.85[484]	FE	[3539]
Ge(110)	–	–	$\sim 10^{-10}$	~300	–	4.88	PE	[3696]
Recommended	–	–	–	–	–	**4.79 ± 0.06**	–	–
Ge(111)	–	–	$\sim 10^{-6}$	~900–1050	–	4.01 ± 0.05	TE	[3272]
Ge(111)	–	–	$\sim 10^{-6}$	~900–1050	–	4.07 ± 0.05	TE	[3272]
Ge(111)	–	–	?	~1070–1170	–	4.1	TE	[1660]
Ge(111)[n153]	–	–	$\sim 10^{-9}$	~300	–	4.12	PE	[2093]
Ge(111)	–	–	–	–	–	4.5	TC	[2213]
Ge(111)[n154]	–	–	4×10^{-10}	~300 (≤470)	–	4.5	PE	[2620]
Ge(111)[n]	–	–	5×10^{-11}	~300 (623)	–	4.53 ± 0.02	PE, CPD	[2023,2029]
Ge(111)	–	–	–	–	–	4.548	TC	[4424]
Ge(111)	–	–	–	–	–	4.569	TC	[4425]
Ge(111)[p]	–	–	2×10^{-10}	~300 (450)	–	4.61	CPD	[1969]
Ge(111)[n]	–	–	5×10^{-11}	~300	–	4.65 ± 0.02	PE, CPD	[2023,2029,3109, 3819]
Ge(111)[n154]	–	–	4×10^{-10}	~300 (570)	–	4.7	PE	[2620]
Ge(111)	–	–	$\sim 10^{-10}$	~300	–	4.7	CPD	[2948]
Ge(111)	–	–	$\leq 2 \times 10^{-8}$	~300	–	4.70 ± 0.3	CPD	[1382]
Ge(111)[p]	–	–	5×10^{-11}	~300	–	4.72 ± 0.02	PE, CPD	[2029,3819]
Ge(111)[421]	–	–	$<2 \times 10^{-9}$	~300	–	4.73 ± 0.05	CPD	[1991]
Ge(111)[p]	–	–	2×10^{-10}	~300 (450)	–	4.74	CPD	[1969]
Ge(111)[n153]	–	–	$\sim 10^{-9}$	~300	–	4.75	PE	[2093]
Ge(111)[n]	–	–	5×10^{-10}	~300	–	4.79 ± 0.015	CPD	[1769,1770]
Ge(111)[p]	–	–	?	~300	–	4.8	FE	[2955]
Ge(111)[p]	–	–	$\leq 10^{-9}$	~300	–	4.8 ± 0.1	FE	[1496]
Ge(111)[p155]	–	–	2×10^{-10}	~300	–	4.80	PE	[1971]
Ge(111)[p155]	–	–	2×10^{-10}	~300	–	4.80 ± 0.05	CPD	[1969,1971]
Ge(111)/W	Ge	–	2×10^{-10}	480	–	4.85 ± 0.05	FE	[2248]
Ge(111)[n154]	–	–	4×10^{-10}	~300	–	4.9	PE	[2620]
Ge(111)	–	–	–	–	–	5.1	TC	[3151]
Ge(111)	–	–	–	–	–	5.4	TC	[3151]
Ge(111)[421]	–	–	$<2 \times 10^{-9}$	~300	–	5.45 ± 0.05	CPD	[1991]
Recommended	–	–	–	–	–	**4.60 ± 0.09**	–	–
Ge(112)	–	–	–	–	–	4.72	TC	[1627]
Ge(112)	–	–	$<2 \times 10^{-10}$	~300	–	4.94	FE	[3539]
Ge(113)	–	–	$<2 \times 10^{-10}$	~300	–	4.88	FE	[3539]
Ge(114)	–	–	$<2 \times 10^{-10}$	~300	–	4.90	FE	[3539]
Ge(122)	–	–	$<2 \times 10^{-10}$	~300	–	4.90	FE	[3539]
Ge(133)	–	–	$<2 \times 10^{-10}$	~300	–	4.85	FE	[3539]
Ge(155)	–	–	$<2 \times 10^{-10}$	~300	–	4.80	FE	[3539]
Ge(???)[p]	–	–	?	~300	–	4.87	PE	[1229]
Ge(???)	–	–	$<10^{-10}$	~300	–	5.1 ± 0.1	PE	[3333]
Ge/graphite[461]	–	–	$<5 \times 10^{-8}$	670–1230	–	2.4–3.5	TE	[1466]
Ge[n]	–	–	?	273	–	3.52	PE	[3688]
Ge/Nb	Ge	–	$<10^{-10}$	~300	–	3.55	FE	[3796]
Ge[n]	–	–	?	493	–	3.62	PE	[3688]
Ge	–	–	?	~300 (?)	–	3.82 ± 0.05	PE	[3577]

Table 1 (*continued*)

Surface	Beam	Ion	P_r (Torr)	T (K)	ϕ^+ (eV)	ϕ^e (eV)	Meth.	Refs.
Ge	–	–	?	900	–	3.97	TE	[3274]
Ge	–	–	–	–	–	4.00	TC	[298]
Ge	–	–	?	~300	–	4.00 ± 0.05	PE	[3577]
Ge/W(111)	Ge	–	1×10^{-8}	~1550–1650	–	4.1	TE	[1499]
Ge[p]	–	–	?	613–943	–	4.10 ± 0.05	PE	[3688]
Ge	–	–	?	1050	–	4.16	TE	[3274]
Ge	–	–	?	~300	–	4.16 ± 0.02	PE	[3394]
Ge	–	–	$\sim10^{-6}$	~300	–	4.29	PE	[3389,3394]
Ge[n]	–	–	?	298 (903)	–	4.32	PE	[3688]
Ge[n]	–	–	–	–	–	4.33 ± 0.05	TC	[3860]
Ge[p]	–	–	?	298	–	4.34 ± 0.05	PE	[3688]
Ge	–	–	?	~300 (?)	–	4.35	PE	[1470]
Ge[p]	–	–	?	298 (≤943)	–	4.36	PE	[3688]
Ge	–	–	–	–	–	4.4*	TC	[1955]
Ge[n]	–	–	$\sim10^{-10}$	~300	–	4.43 ± 0.05	FE	[3069]
Ge(nanowire)[71]	–	–	?	~300	–	4.43	PE	[2200]
Ge	–	–	?	~300	–	4.45	PE	[1470]
Ge/W(110)	Ge	–	1×10^{-8}	1550–1650	–	4.5	TE	[1499]
Ge[n]	–	–	$<2 \times 10^{-6}$	523	–	4.5	CPD	[1310]
Ge[n]	–	–	$<2 \times 10^{-6}$	1023	–	4.5	CPD	[1310]
Ge	–	–	?	~300	–	4.50	CPD	[2297]
Ge	–	–	–	–	–	4.59	TC	[3318]
Ge[p]	–	–	–	–	–	4.65 ± 0.03	TC	[3860]
Ge	–	–	?	~300	–	4.73	PE	[3027]
Ge/Mo	Ge	–	$<3 \times 10^{-8}$	~300	–	4.73 ± 0.07	PE	[1371]
Ge	–	–	?	~300	–	4.77	PE	[3387]
Ge	–	–	$\leq5 \times 10^{-8}$	~300	–	4.77 ± 0.04	CPD	[3658]
Ge	–	–	5×10^{-10}	~300	–	4.78 ± 0.015	CPD	[1770]
Ge	–	–	–	–	–	4.8	TC	[1993]
Ge	–	–	–	–	–	4.8	TC	[706]
Ge	–	–	$\leq10^{-10}$	~300	–	4.8	FE	[1502]
Ge/W	Ge	–	?	~300	–	4.8	FE	[3594]
Ge/W	Ge	–	?	~300	–	4.8	CPD	[2577]
Ge/W	Ge	–	$\sim10^{-9}$	~300	–	4.85 ± 0.05	CPD	[1954]
Ge/W	Ge	–	2×10^{-10}	480	–	4.85 ± 0.05	FE	[2248]
Ge[p]	–	–	$\sim10^{-10}$	~300	–	4.90 ± 0.05	FE	[3069]
Ge/W	Ge	–	$\leq10^{-10}$	~300	–	4.90 ± 0.06	FE	[3545]
Ge/Ti/W	Ge	–	$\leq10^{-10}$	~300	–	4.90 ± 0.06	FE	[3545]
Ge/W	Ge	–	$\sim10^{-10}$	~300 (~380)	–	4.95 ± 0.05	FE	[2588]
Ge/glass	Ge	–	$<10^{-9}$	77–90	–	4.98	PE	[2311]
Ge/glass	Ge	–	2×10^{-10}	77	–	4.98 ± 0.02	PE	[3052,3056,3059, 3060]
Ge/W	Ge	–	$\sim10^{-9}$	~300	–	5.0	FE	[3554]
Ge/W	Ge	–	?	~300 (400)	–	5.0	FE	[3594]
Ge/glass	Ge	–	5×10^{-10}	273 (293)	–	5.00 ± 0.02	PE	[3056]
Ge/W	Ge	–	2×10^{-10}	460	–	5.01 ± 0.02	FE	[2248]
Ge/glass	Ge	–	2×10^{-10}	273 (≤373)	–	5.02 ± 0.02	PE	[3059,3060]
Ge/glass	Ge	–	2×10^{-10}	77 (293)	–	5.03 ± 0.02	PE	[3052,3059,3060]
Ge/glass	Ge	–	$<10^{-9}$	77 (293)	–	5.04	PE	[2311]
Ge/glass	Ge	–	5×10^{-10}	293 (373)	–	5.04 ± 0.02	PE	[3056]
Ge/W(110)	Ge	–	$\leq1 \times 10^{-9}$	293	–	5.05	CPD	[1520]
Ge/glass	Ge	–	5×10^{-10}	77 (293)	–	5.05 ± 0.03	PE	[3056]
Ge	–	–	–	–	–	5.08	TC	[2554]
Ge/W	Ge	–	?	~300 (1130)	–	5.1 ± 0.05	FE	[3553,3555,3903]
Ge/W	Ge	–	$\leq10^{-9}$	~300 (380)	–	5.15 ± 0.05	FE	[3063]
Ge/W	Ge	–	$<10^{-9}$	~300 (≤400)	–	5.2	FE	[2580,2584,2596]
Ge/O/W	Ge	–	$<10^{-9}$	~300 (≤400)	–	5.2	FE	[2596]
Ge/W	Ge	–	$\leq3 \times 10^{-10}$	~300	–	5.2 ± 0.1	FE	[3544]
Ge/Mo	Ge	–	$\leq3 \times 10^{-10}$	~300	–	5.2 ± 0.1	FE	[3544]
Ge/W	Ge	–	2×10^{-10}	395	–	5.21 ± 0.01	FE	[2248]
Ge[n]	–	–	?	~300	–	5.8	FE	[1855]
Ge[p]	–	–	$\leq10^{-9}$	77	–	6.2	FE	[1395]
Ge[n]	–	–	$\leq10^{-9}$	77	–	6.2	FE	[1395]
Recommended	–	–	–	–	–	**4.76 ± 0.05**	–	–

Liquid ($T > 1232$ K)

Surface	Beam	Ion	P_r (Torr)	T (K)	ϕ^+ (eV)	ϕ^e (eV)	Meth.	Refs.
Ge/graphite[461]	–	–	$<5 \times 10^{-8}$	~1300–1500	–	3.60*	TE	[1466]

Table 1 (*continued*)

Surface	Beam	Ion	P_r (Torr)	T (K)	ϕ^+ (eV)	ϕ^e (eV)	Meth.	Refs.

33. Arsenic As

Rhombohedral (arsenic structure)

Surface	Beam	Ion	P_r (Torr)	T (K)	ϕ^+ (eV)	ϕ^e (eV)	Meth.	Refs.
As(111)	–	–	$\sim10^{-9}$	~300	–	3.75 ± 0.05	PE	[2952]
As	–	–	–	–	–	3.23	TC	[1744]
As	–	–	–	–	–	4.64	TC	[3318]
As/Cu,Ni,Ta,C	As	–	$\sim10^{-6}$	~300	–	4.66	PE	[3251,3252]
As/Ni,Mo,etc.	As	–	$<5 \times 10^{-8}$	~300	–	4.72	CPD	[1375]
As	–	–	–	–	–	4.77	TC	[298]
As/Nb,Pt,etc.	As	–	$<5 \times 10^{-8}$	~300	–	4.79	PE	[1375]
As	–	–	–	–	–	4.8 ± 0.2	TC	[1903,1905]
As	–	–	–	–	–	4.9*	TC	[1955]
As	–	–	–	–	–	5.02	TC	[1901]
As	–	–	?	~300	–	5.11	PE	[3027]
As/glass	As	–	$\sim3 \times 10^{-7}$	~300	–	5.17 ± 0.04	PE	[2950]
As	–	–	–	–	–	5.2	TC	[706]
As/Si(001)	–	–	–	–	–	5.56	TC	[2525]
Recommended	–	–	–	–	–	**4.85 ± 0.14**	–	–

34. Selenium Se

Hexagonal

Surface	Beam	Ion	P_r (Torr)	T (K)	ϕ^+ (eV)	ϕ^e (eV)	Meth.	Refs.
Se(1010)	–	–	$\sim10^{-10}$	~300	–	5.9	PE	[3429]
Se(1010)	Se	–	5×10^{-11}	~300	–	5.9 ± 0.1	PE	[4247]
Se	–	–	?	~300	–	4.42	CPD	[2297]
Se	–	–	?	~300	–	4.62	PE	[2080]
Se	–	–	–	–	–	4.8	TC	[3318]
Se/W(111)	Se	–	$<10^{-10}$	~300	–	4.80	FE	[1677]
Se/W(110)	Se	–	$<5 \times 10^{-11}$	~300	–	4.9*	CPD	[4102]
Se/W(100)	Se	–	$<10^{-10}$	~300	–	4.95	FE	[1677]
Se/W	Se	–	$<10^{-9}$	~300 (1000)	–	4.96 ± 0.03	FE	[2333]
Se/W(100)	Se	–	$<5 \times 10^{-11}$	~300	–	5.0*	CPD	[2852]
Se/W(100)	Se	–	$<5 \times 10^{-11}$	~300 (≤800)	–	5.1*	CPD	[2852]
Se/Si(111)	–	–	–	–	–	5.1*	TC	[2062,4073]
Se/GaAs(001)	Se	–	?	~300 (670)	–	5.1	PE	[3216]
Se/W	Se	–	$<10^{-10}$	~300	–	5.1 ± 0.1	FE	[1677]
Se/Ni(110)	H_2Se	–	$<1 \times 10^{-10}$	~300 (~1270)	–	5.10	CPD	[1110]
Se/?	Se	–	?	~300	–	5.11	PE	[3027]
Se/Si(100)	Se	–	?	~300	–	5.16*	CPD	[2896]
Se/Si(111)	Se	–	$<10^{-10}$	~300	–	5.17 ± 0.04*	CPD	[4160]
Se/Ni(100)	Se	–	$<5 \times 10^{-10}$	~300	–	5.26 ± 0.06*	CPD	[1790]
Se	–	–	–	–	–	5.3 ± 0.3	TC	[1905]
Se/Fe(100)	Se	–	2×10^{-11}	~300	–	5.34 ± 0.05*	CPD	[4327]
Se/Ni(100)	H_2Se	–	$<1 \times 10^{-10}$	~300 (~1270)	–	5.35	CPD	[1110]
Se/W	Se	–	$\sim10^{-9}$	~300	–	5.4	FE	[394,3342,4052]
Se/Ni(111)	H_2Se	–	$<1 \times 10^{-10}$	~300 (~1270)	–	5.43	CPD	[1110]
Se	–	–	–	–	–	5.6	TC	[706]
Se/W(112)	Se	–	$<10^{-10}$	~300	–	5.65	FE	[1677]
Se	–	–	–	–	–	5.68	TC	[1901]
Se	–	–	?	?	–	5.74 ± 0.15	PE	[3659]
Se	–	–	–	–	–	5.8*	TC	[1955]
Se/brass	Se	–	?	~300 (333)	–	5.86	PE	[2479]
Se/ss	Se	–	$\sim10^{-10}$	~300	–	5.9	PE	[3429]
Se	–	–	–	–	–	5.9	TC	[298]
Se/W(110)	Se	–	$<10^{-10}$	~300	–	6.3	FE	[1677]
Recommended	–	–	–	–	–	**5.27 ± 0.18**	–	–

37. Rubidium Rb

bcc

Surface	Beam	Ion	P_r (Torr)	T (K)	ϕ^+ (eV)	ϕ^e (eV)	Meth.	Refs.
Rb(100)	–	–	–	–	–	2.01	TC	[1254]
Rb(100)	–	–	–	–	–	2.10	TC	[475]
Rb(100)	–	–	–	–	–	2.115	TC	[4091]
Rb(100)	–	–	–	–	–	2.12	TC	[231]
Rb(100)	–	–	–	–	–	2.15	TC	[3467]
Rb(100)	–	–	–	–	–	2.16	TC	[2427]
Rb(100)	–	–	–	–	–	2.17	TC	[553]

Table 1 (*continued*)

Surface	Beam	Ion	P_r (Torr)	T (K)	ϕ^+ (eV)	ϕ^e (eV)	Meth.	Refs.
Rb(100)	–	–	–	–	–	2.177	TC	[2947]
Rb(100)	–	–	–	–	–	2.22	TC	[334]
Rb(100)	–	–	–	–	–	2.28	TC	[711]
Rb(100)	–	–	–	–	–	2.3	TC	[763]
Rb(100)	–	–	–	–	–	2.35	TC	[475]
Rb(100)	–	–	–	–	–	2.36	TC	[1030]
Rb(100)	–	–	–	–	–	2.40	TC	[472]
Rb(100)	–	–	–	–	–	2.40	TC	[321]
Rb(100)	–	–	–	–	–	2.41	TC	[3814]
Rb(100)	–	–	–	–	–	2.45	TC	[476,711]
Rb(100)	–	–	–	–	–	2.47	TC	[1095]
Rb(100)	–	–	–	–	–	2.53	TC	[476]
Rb(100)	–	–	–	–	–	2.54	TC	[1030]
Rb(100)	–	–	–	–	–	2.6	TC	[1088]
Recommended	–	–	–	–	–	**2.31 ± 0.08**	–	–
Rb(110)	–	–	–	–	–	2.2	TC	[1086]
Rb(110)	–	–	–	–	–	2.2	TC	[3137]
Rb(110)	–	–	–	–	–	2.20	TC	[475]
Rb(110)	–	–	–	–	–	2.230	TC	[2947]
Rb(110)	–	–	–	–	–	2.243	TC	[4091]
Rb(110)	–	–	–	–	–	2.25	TC	[593]
Rb(110)	–	–	–	–	–	2.28	TC	[231]
Rb(110)	–	–	–	–	–	2.32	TC	[334,3179]
Rb(110)	–	–	–	–	–	2.32	TC	[2427]
Rb(110)	–	–	–	–	–	2.33	TC	[3467]
Rb(110)	–	–	–	–	–	2.33	TC	[553]
Rb(110)	–	–	–	–	–	2.40	TC	[472]
Rb(110)	–	–	–	–	–	2.46	TC	[711]
Rb(110)	–	–	–	–	–	2.48	TC	[1086]
Rb(110)	–	–	–	–	–	2.49	TC	[1030]
Rb(110)	–	–	–	–	–	2.56	TC	[2402]
Rb(110)	–	–	–	–	–	2.56	TC	[3814]
Rb(110)	–	–	–	–	–	2.57	TC	[1095]
Rb(110)	–	–	–	–	–	2.6	TC	[763]
Rb(110)	–	–	–	–	–	2.6	TC	[1088]
Rb(110)	–	–	–	–	–	2.63	TC	[1086]
Rb(110)	–	–	–	–	–	2.63	TC	[476,711]
Rb(110)	–	–	–	–	–	2.63	TC	[2385]
Rb(110)	–	–	–	–	–	2.65	TC	[475]
Rb(110)	–	–	–	–	–	2.70	TC	[476]
Rb(110)	–	–	–	–	–	2.71	TC	[2835]
Rb(110)	–	–	–	–	–	2.72	TC	[1087]
Rb(110)	–	–	–	–	–	2.72	TC	[1030,1089]
Rb(110)	–	–	–	–	–	2.741	TC	[4069]
Rb(110)	–	–	–	–	–	2.79	TC	[321]
Rb(110)	–	–	–	–	–	2.81	TC	[3693]
Rb(110)	–	–	–	–	–	2.81	TC	[1089]
Rb(110)	–	–	–	–	–	2.83	TC	[3713]
Rb(110)	–	–	–	–	–	2.84	TC	[1086]
Rb(110)	–	–	–	–	–	2.84	TC	[1089]
Rb(110)	–	–	–	–	–	2.87	TC	[1086]
Rb(110)	–	–	–	–	–	2.88	TC	[1086]
Rb(110)	–	–	–	–	–	2.9	TC	[1088]
Rb(110)	–	–	–	–	–	2.9	TC	[1086]
Rb(110)	–	–	–	–	–	2.93	TC	[3693]
Rb(110)	–	–	–	–	–	2.94	TC	[3712]
Rb(110)	–	–	–	–	–	2.94	TC	[3713]
Rb(110)	–	–	–	–	–	2.96	TC	[3692]
Rb(110)	–	–	–	–	–	3.04	TC	[3692]
Rb(110)	–	–	–	–	–	4.96	TC	[3622]
Recommended	–	–	–	–	–	**2.65 ± 0.05**	–	–
Rb(111)	–	–	–	–	–	2.05	TC	[475]
Rb(111)	–	–	–	–	–	2.06	TC	[711]
Rb(111)	–	–	–	–	–	2.08	TC	[231]
Rb(111)	–	–	–	–	–	2.09	TC	[3467]
Rb(111)	–	–	–	–	–	2.096	TC	[4091]
Rb(111)	–	–	–	–	–	2.10	TC	[593]
Rb(111)	–	–	–	–	–	2.12	TC	[553]

Table 1 (*continued*)

Surface	Beam	Ion	P_r (Torr)	T (K)	ϕ^+ (eV)	ϕ^e (eV)	Meth.	Refs.
Rb(111)	–	–	–	–	–	2.22	TC	[472]
Rb(111)	–	–	–	–	–	2.23	TC	[476,711]
Rb(111)	–	–	–	–	–	2.25	TC	[3814]
Rb(111)	–	–	–	–	–	2.26	TC	[1030]
Rb(111)	–	–	–	–	–	2.28	TC	[1030]
Rb(111)	–	–	–	–	–	2.3	TC	[1088]
Rb(111)	–	–	–	–	–	2.30	TC	[475]
Rb(111)	–	–	–	–	–	2.30	TC	[321]
Rb(111)	–	–	–	–	–	2.32	TC	[476]
Rb(111)	–	–	–	–	–	2.42	TC	[1095]
Recommended	–	–	–	–	–	**2.21 ± 0.09**	–	–
Rb(112)	–	–	–	–	–	2.56	TC	[321]
Rb	–	–	–	~300	–	1.4	TC	[3737]
Rb/Si(100)	Rb	–	<3 × 10⁻¹⁰	~300	–	1.5*	PE	[1729,3803,3804]
Rb/Pt	Rb	–	?	~300	–	1.55	PE	[2206]
Rb/Si(100)	–	–	–	–	–	1.906*	TC	[3501]
Rb/Hf	Rb	–	?	~300	–	1.9 ± 0.1	PE	[1691]
Rb	–	–	?	302	–	1.99	PE	[4139]
Rb/Cu(110)	Rb	–	5 × 10⁻¹¹	140	–	2.0 ± 0.1	PE	[3454]
Rb	–	–	–	–	–	2.01	TC	[1254]
Rb	–	–	–	–	–	2.04	TC	[1066]
Rb/W(100)	Rb	–	<1 × 10⁻¹⁰	~150	–	2.05	PE	[2120]
Rb	–	–	–	–	–	2.06	TC	[1951]
Rb/Ni	Rb	–	<10⁻⁹	77	–	2.08	CPD	[2139,3128,3698]
Rb/Ag/glass	Rb	–	~10⁻⁸	~80	–	2.09	PE	[1452]
Rb/quartz	Rb	–	~10⁻¹⁰	90	–	2.1	PE	[2605]
Rb/Cu	Rb	–	3 × 10⁻¹¹	~300	–	2.1 ± 0.1	PE	[3091]
Rb/Ag	Rb	–	3 × 10⁻¹¹	~300	–	2.1 ± 0.1	PE	[3091]
Rb/Y	Rb	–	?	~300	–	2.1 ± 0.1	PE	[1691]
Rb	–	–	–	–	–	2.11	TC	[3728]
Rb/GaAs(110)	Rb	–	<1 × 10⁻¹⁰	~300	–	2.12	CPD	[2793]
Rb	–	–	–	–	–	2.13*	TC	[1955]
Rb	–	–	–	–	–	2.14	TC	[4150]
Rb	–	–	~10⁻⁹	310	–	2.15	PE	[4241]
Rb	–	–	–	–	–	2.16	TC	[2949]
Rb	–	–	~10⁻¹⁰	300	–	2.16	PE	[4297]
Rb/?	Rb	–	?	?	–	2.16	?	[3785]
Rb¹⁵⁶	–	–	<10⁻⁸	298	–	2.16 ± 0.03	PE	[2470,4208,4209]
Rb	–	–	~10⁻⁹	298	–	2.16 ± 0.05	PE	[2612,2613]
Rb	–	–	–	–	–	2.17	TC	[3352]
Rb	–	–	?	303	–	2.17 ± 0.02*	PE	[4141]
Rb/graphene	–	–	–	–	–	2.18	TC	[4079]
Rb	–	–	–	–	–	2.19	TC	[3467,3477]
Rb(cluster)	–	–	–	–	–	2.19	TC	[3479]
Rb	–	–	–	–	–	2.2*	TC	[1955]
Rb	–	–	–	–	–	2.20	TC	[3725]
Rb/glass	Rb	–	≤3 × 10⁻¹¹	195	–	2.20 ± 0.01	PE	[2615]
Rb/glass	Rb	–	≤10⁻¹⁰	77	–	2.21 ± 0.02	PE	[1489]
Rb/glass	Rb	–	<10⁻¹⁰	77	–	2.21 ± 0.05	PE	[2815]
Rb	–	–	–	–	–	2.22	TC	[3312]
Rb	–	–	–	–	–	2.25	TC	[298]
Rb/quartz	Rb	–	<10⁻¹⁰	140–155	–	2.261 ± 0.015	PE	[2119]
Rb	–	–	–	–	–	2.29	TC	[1744]
Rb	–	–	–	–	–	2.3	TC	[1993]
Rb	–	–	–	–	–	2.3	TC	[706]
Rb/glass	Rb	–	≤3 × 10⁻¹¹	77, 195	–	2.31 ± 0.01	PE	[2615]
Rb	–	–	–	–	–	2.33	TC	[3312]
Rb	–	–	–	–	–	2.36	TC	[231]
Rb	–	–	–	–	–	2.37	TC	[2061]
Rb	–	–	–	–	–	2.39	TC	[3477]
Rb	–	–	–	–	–	2.39	TC	[553,2427]
Rb	–	–	–	–	–	2.40	TC	[1924]
Rb/O/W	Rb	–	≤440 (Rb)	~600–700	–	2.41	TE	[2292]
Rb	–	–	–	–	–	2.41	TC	[3467]
Rb	–	–	–	–	–	2.42	TC	[767]
Rb	–	–	–	–	–	2.43	TC	[231]
Rb	–	–	–	–	–	2.45	TC	[1924]
Rb	–	–	–	–	–	2.47	TC	[2427]

Table 1 (*continued*)

Surface	Beam	Ion	P_r (Torr)	T (K)	ϕ^+ (eV)	ϕ^e (eV)	Meth.	Refs.
Rb	–	–	–	–	–	2.48	TC	[4101]
Rb	–	–	–	–	–	2.49	TC	[1613]
Rb/Al(111)	Rb	–	?	~300	–	2.52	CPD	[734]
Rb	–	–	–	–	–	2.54	TC	[738]
Rb	–	–	–	–	–	2.55	TC	[1578]
Rb	–	–	–	–	–	2.6	TC	[2845]
Rb	–	–	–	–	–	2.61	TC	[2629]
Rb	–	–	–	–	–	2.61	TC	[2382]
Rb	–	–	–	–	–	2.63	TC[3]	[475,519,2474]
Rb	–	–	–	–	–	2.64	TC	[230]
Rb	–	–	–	–	–	2.7	TC	[944]
Rb/W	Rb	–	≤440 (Rb)	~650–850	–	2.76	TE	[2292]
Recommended	–	–	–	–	–	**2.17 ± 0.05**	–	–

Liquid (*T > 312 K*)

Rb	–	–	–	–	–	1.80	TC	[4249]
Rb	–	–	?	322	–	1.93	PE	[4139]
Rb	–	–	?	350	–	2.13 ± 0.02*	PE	[4141]
Rb	–	–	~10^{-9}	313	–	2.15	PE	[4241]
Rb	–	–	~10^{-8}	313	–	2.16	PE	[4208]
Rb	–	–	~10^{-10}	313	–	2.16	PE	[4297]
Rb[156]	–	–	?	313	–	2.17 ± 0.03	PE	[2470]
Recommended	–	–	–	–	–	**2.15 ± 0.02**	–	–

38. Strontium Sr

fcc (*α, T < 488 K*)

Sr(100)	–	–	–	–	–	2.43	TC	[1254]
Sr(100)	–	–	–	–	–	2.473	TC	[4091]
Sr(100)	–	–	–	–	–	2.79	TC	[231]
Sr(100)	–	–	–	–	–	2.8	TC	[1712,1714]
Sr(100)	–	–	–	–	–	2.95	TC	[3467]
Sr(100)	–	–	–	–	–	3.42	TC	[1030]
Sr(100)	–	–	–	–	–	3.81	TC	[321]
Sr(100)	–	–	–	–	–	3.82	TC	[1030]
Recommended	–	–	–	–	–	**3.3 ± 0.4**	–	–
Sr(110)	–	–	–	–	–	2.545	TC	[4091]
Sr(110)	–	–	–	–	–	2.75	TC	[231]
Sr(110)	–	–	–	–	–	2.76	TC	[3467]
Sr(110)	–	–	–	–	–	3.05	TC	[1030]
Sr(110)	–	–	–	–	–	3.31	TC	[1030]
Sr(110)	–	–	–	–	–	3.57	TC	[321]
Recommended	–	–	–	–	–	**3.1 ± 0.3**	–	–
Sr(111)	–	–	–	–	–	2.22	TC	[3369]
Sr(111)	–	–	–	–	–	2.3	TC	[3179]
Sr(111)	–	–	–	–	–	2.38	TC	[1722]
Sr(111)	–	–	–	–	–	2.42	TC	[334]
Sr(111)	–	–	–	–	–	2.569	TC	[4091]
Sr(111)	–	–	–	–	–	2.94	TC	[231]
Sr(111)	–	–	–	–	–	3.07	TC	[2427]
Sr(111)	–	–	–	–	–	3.21	TC	[3467]
Sr(111)	–	–	–	–	–	3.57	TC	[1030,1089]
Sr(111)	–	–	–	–	–	3.61	TC	[1030]
Sr(111)	–	–	–	–	–	3.65	TC	[1089]
Sr(111)	–	–	–	–	–	3.78	TC	[1089]
Sr(111)	–	–	–	–	–	4.10	TC	[321]
Recommended	–	–	–	–	–	**3.4 ± 0.3**	–	–

hcp (*β, T = 488–878 K*)

Sr(0001)	–	–	–	–	–	4.17	TC	[321]
Sr(1010)	–	–	–	–	–	3.99	TC	[321]
Sr(1124)	–	–	–	–	–	3.49	TC	[321]

bcc (*γ, T > 878 K*)

Sr(100)	–	–	–	–	–	2.71	TC	[1159,3067]
Sr(100)	–	–	–	–	–	3.27	TC	[321]

Table 1 (*continued*)

Surface	Beam	Ion	P_r (Torr)	T (K)	ϕ^+ (eV)	ϕ^e (eV)	Meth.	Refs.
Sr(110)	–	–	–	–	–	2.39	TC	[334]
Sr(110)	–	–	–	–	–	2.63	TC	[1159,3067]
Sr(110)	–	–	–	–	–	3.81	TC	[321]
Sr(111)	–	–	–	–	–	2.80	TC	[1159,3067]
Sr(111)	–	–	–	–	–	3.13	TC	[321]
Sr(112)	–	–	–	–	–	3.61	TC	[321]
fcc (α, $T < 488$ K for bulk)								
Sr/glass	Sr	–	?	~300	–	2.06	PE	[1748]
Sr	–	–	–	–	–	2.08	TC	[1744]
Sr/?	Sr	–	?	~300	–	2.24	PE	[3027]
Sr/W	Sr	–	(~10^{-12})	~300 (819)	–	2.24	FE	[2585]
Sr/Mo(112)	Sr	–	~10^{-9}	~300	–	2.25	PE	[2398]
Sr/W	Sr	–	$\leq 1 \times 10^{-9}$	~300 (773)	–	2.35 ± 0.05	FE	[2587]
Sr/Mo(112)	–	–	–	–	–	2.43	TC	[702]
Sr	–	–	–	–	–	2.43	TC	[1254]
Sr	–	–	–	–	–	2.46	TC	[3318]
Sr	–	–	–	–	–	2.46	TC	[1066]
Sr/W	Sr	–	?	~300	–	2.5	FE	[1471]
Sr/W	Sr	–	?	~300 ($\leq$700)	–	2.5–2.6	CPD	[2578]
Sr/Mo(100)	Sr	–	$\geq 10^{-6}$(Sr)	~800–900	–	2.59	TE	[1401,1402]
Sr/?	Sr	–	5×10^{-11}	~300	–	2.6	PE	[2116]
Sr	–	–	–	–	–	2.6*	TC	[1955]
Sr	–	–	–	–	–	2.61	TC	[3318]
Sr	–	–	–	–	–	2.64	TC	[298]
Sr/W[244]	Sr	–	$\leq 2 \times 10^{-9}$	~900	–	2.64	CPD	[3530]
Sr/quartz	Sr	–	5×10^{-10}	~300	–	2.64 ± 0.05	PE	[2014,2021,2024]
Sr	–	–	–	0	–	2.68	TC	[4419]
Sr	–	–	–	–	–	2.7	TC	[1993]
Sr/?	Sr	–	?	~300	–	2.7	PE	[2115]
Sr/W[244]	Sr	–	$\leq 2 \times 10^{-9}$	~300	–	2.73	CPD	[3530]
Sr/?	Sr	–	?	~300	–	2.74	PE	[1639]
Sr/W(100)	Sr	–	$\leq 10^{-2}$(Sr)	~900–1000	–	2.74	TE	[1792]
Sr	–	–	–	–	–	2.77	TC	[3729]
Sr/Mo(112)	Sr	–	($\leq 10^{-11}$)	77	–	2.8	CPD	[2631]
Sr/glass[88]	Sr	–	<10^{-9}	~300{77}	–	2.8	CPD	[1526]
Sr	–	–	–	–	–	2.8	TC	[1711]
Sr/W(110)	Sr	–	($\leq 10^{-11}$)	5	–	2.8	CPD	[2347]
Sr/Mo(112)	Sr	–	2×10^{-11}	100 (500)	–	2.8	CPD	[2431]
Sr	–	–	–	–	–	2.81	TC	[1901]
Sr/Re(1010)	Sr	–	(<10^{-11})	77 (~300)	–	2.85	CPD	[4275]
Sr	–	–	–	–	–	2.9	TC	[706]
Sr	–	–	–	–	–	2.93	TC	[3476]
Sr	–	–	–	–	–	2.96	TC	[231]
Sr	–	–	–	–	–	2.97	TC	[3467]
Sr/W(110)[157]	Sr	–	$\leq 10^{-10}$	77	–	3.0	FE	[2344]
Sr	–	–	–	–	–	3.03	TC	[231]
Sr	–	–	–	–	–	3.04	TC	[3476]
Sr	–	–	–	–	–	3.08	TC	[1924]
Sr	–	–	–	–	–	3.09	TC	[1924]
Sr	–	–	–	–	–	3.12	TC	[1613]
Sr/W(110)	Sr	–	($\leq 10^{-11}$)	290	–	3.2	CPD	[2347]
Sr/W(110)	Sr	–	($\leq 10^{-11}$)	5 ($\leq$400)	–	3.2	CPD	[2347]
Sr/W(110)[157]	Sr	–	($\leq 10^{-10}$)	77 (300)	–	3.2	CPD	[2344]
Sr	–	–	–	–	–	3.30	TC	[3476]
Sr	–	–	–	–	–	3.33	TC	[3467]
Recommended	–	–	–	–	–	**2.71 ± 0.08**	–	–
hcp (β, $T = 488$–878 K for bulk)								
Sr/W[244]	Sr	–	$\leq 2 \times 10^{-9}$	750–850	–	2.64	CPD	[3530]
Sr	–	–	–	–	–	2.77	TC	[3729]
Sr	–	–	–	–	–	2.92	TC	[1578]
Sr/Mo(110)	Sr	–	$\leq 10^{-10}$	5 ($\leq$300)	–	3.1	CPD	[3350]
bcc (γ, $T > 878$ K for bulk)								
Sr/W	Sr	–	(<10^{-14})	~850–950	–	2.3	TE	[2572]
Sr/?	Sr	–	?	?	–	2.4	TE	[3402]

(*continued on next page*)

Table 1 (*continued*)

Surface	Beam	Ion	P_r (Torr)	T (K)	ϕ^+ (eV)	ϕ^e (eV)	Meth.	Refs.
				39. Yttrium Y[399]				
hcp (α, T < 1540 K)								
Y(0001)	–	–	<10^{-9}	? (~1700)	–	3.0 ± 0.1	TE,PE	[4230]
Y(0001){90%}	–	–	?	~300	–	3.1 ± 0.1	PE	[1691]
Y(0001)	–	–	–	–	–	3.38	TC	[334]
Y(0001)	–	–	2×10^{-9}	1400	–	3.47	TE	[3105]
Y(0001)	–	–	–	–	–	3.60	TC	[4005]
Y(0001)	–	–	2×10^{-9}	1250–1500	–	3.62	TE	[3105]
Y(0001)	–	–	–	–	–	4.67	TC	[321]
Y(1010)	–	–	–	–	–	3.08	TC	[4005]
Y(1010)	–	–	–	–	–	4.47	TC	[321]
Y(1124)	–	–	2×10^{-9}	1250–1500	–	3.27	TE	[3105]
Y(1124)	–	–	2×10^{-9}	1400	–	3.28	TE	[3105]
Y(1124)	–	–	–	–	–	3.92	TC	[321]
bcc (β, T > 1540 K)								
Y(100)	–	–	–	–	–	3.67	TC	[321]
Y(110)	–	–	–	–	–	4.28	TC	[321]
Y(111)	–	–	–	–	–	3.52	TC	[321]
Y(112)	–	–	–	–	–	3.92	TC	[321]
hcp (α, T < 1540 K for bulk)								
Y	–	–	? (N_2)	~300	–	2.54 ± 0.02	CPD	[4066]
Y	–	–	–	–	–	2.6	TC	[1744]
Y/W[158]	Y	–	≤7 × 10^{-8}	~300	–	2.6	FE	[1804]
Y/W[158]	Y	–	≤7 × 10^{-8}	~300	–	2.7	FE	[1804]
Y/W(111)	Y	–	≤10^{-9}	~300	–	2.8	FE	[1987,2011]
Y/W	Y	–	~10^{-9}	500	–	2.85	FE	[2817]
Y/W(116)	Y	–	≤10^{-9}	~300	–	2.9	FE	[1987]
Y/W(111)	Y	–	≤10^{-9}	300 (>400)	–	2.9	FE	[1975,1987]
Y/W	Y	–	~10^{-9}	~300	–	2.9	FE	[2817]
Y/W	Y	–	≤10^{-9}	~300	–	2.95 ± 0.05	FE	[2816]
Y(foil)[255]	–	–	~10^{-7}	1300	–	2.98	TE	[3071]
Y/Re–Y(4%)	–	–	~10^{-8}	1300	–	2.98	TE	[4240]
Y	–	–	–	–	–	2.99	TC	[1066]
Y[379]	–	–	–	–	–	3.0*	TC	[1955]
Y/W(116)	Y	–	≤10^{-9}	300 (>400)	–	3.0	FE	[1975,1987]
Y/W	Y	–	~10^{-9}	78	–	3.0	FE	[2817]
Y	–	–	2×10^{-10}	~300	–	3.0 ± 0.1	PE	[1813]
Y/W(111)	Y	–	(<10^{-10})	77	–	3.00	FE	[3335]
Y/W(100)	Y	–	(<10^{-10})	77	–	3.06	FE	[3335]
Y	–	–	–	–	–	3.07	TC	[1956]
Y/W	Y	–	~10^{-9}	~300	–	3.1	FE	[2819]
Y/W(100)[159]	Y	–	1×10^{-9}	~300	–	3.1	CPD	[1985]
Y/W(110)	Y	–	1×10^{-9}	~300	–	3.1	CPD	[1986]
Y/W(100)	Y	–	≤10^{-9}	~300	–	3.1	FE	[1987]
Y/W(112)	Y	–	≤10^{-9}	~300	–	3.1	FE	[1987]
Y/W(112)	Y	–	≤10^{-9}	300 (>400)	–	3.1	FE	[1987]
Y	–	–	–	–	–	3.1	TC	[1955]
Y/W	Y	–	~10^{-9}	~300	–	3.1	FE	[2819]
Y/Nb(100)	Y	–	≤10^{-8}	~1000–1150	–	3.1 ± 0.03	TE	[2359]
Y	–	–	?	~300	–	3.1 ± 0.1	PE	[1691]
Y/quartz	Y	–	~10^{-10}	~300	–	3.1 ± 0.15	PE	[304]
Y_n(n→ ∞)	–	–	–	–	–	3.11 ± 0.10	TC	[4261]
Y/W(111)	Y	–	≤10^{-8}	~1150–1250	–	3.12 ± 0.03	TE	[2330]
Y/Nb	Y	–	≤10^{-8}	~1000–1150	–	3.16 ± 0.03	TE	[2359]
Y/Ta	Y	–	≤10^{-8}	~1000–1150	–	3.16 ± 0.03	TE	[2359]
Y/W(112)	Y	–	(<10^{-10})	77	–	3.18	FE	[3335]
Y[174]	–	–	–	0^E	–	3.19	TC	[1747]
Y/W	Y	–	<10^{-9}	300 (>400)	–	3.2	FE	[1987]
Y	–	–	–	–	–	3.2	TC	[1993]
Y/W(111)	Y	–	~10^{-9}	~300	–	3.2	FE	[3082]
Y/W(012)	Y	–	~10^{-9}	~300	–	3.2	FE	[3082]

Table 1 (*continued*)

Surface	Beam	Ion	P_r (Torr)	T (K)	ϕ^+ (eV)	ϕ^e (eV)	Meth.	Refs.
Y	–	–	–	–	–	3.20	TC	[298]
Y/Zr	Y	–	≤10⁻⁸	~1000–1150	–	3.25 ± 0.03	TE	[2359]
Y/Hf	Y	–	≤10⁻⁸	~1000–1150	–	3.25 ± 0.03	TE	[2359]
Y/Ru	Y	–	≤10⁻⁸	~1000–1150	–	3.25 ± 0.03	TE	[2359]
Y/Os	Y	–	≤10⁻⁸	~1000–1150	–	3.25 ± 0.03	TE	[2359]
Y/Ir	Y	–	≤10⁻⁸	~1000–1150	–	3.25 ± 0.03	TE	[2359]
Y/Mo	Y	–	≤10⁻⁸	~1000–1150	–	3.26 ± 0.03	TE	[2359]
Y/W	Y	–	≤10⁻⁸	~1000–1150	–	3.26 ± 0.03	TE	[2359]
Y/Re	Y	–	≤10⁻⁸	~1000–1150	–	3.26 ± 0.03	TE	[2359]
Y	–	–	–	–	–	3.27	TC	[3318]
Y	–	–	~10⁻⁹	~1300–1500	–	3.27	TE	[4356]
Y[160]	–	–	–	–	–	3.3	TC	[1355]
Y/W(112)	Y	–	~10⁻⁹	~300	–	3.3	FE	[3082]
Y/Nb(110)	Y	–	≤10⁻⁸	~1000–1150	–	3.3 ± 0.03	TE	[2359]
Y/W(100)	Y	–	≤10⁻⁸	~1150–1250	–	3.38 ± 0.03	TE	[2330,2359]
Y	–	–	–	–	–	3.4	TC	[706]
Y/W(100)	Y	–	≤10⁻⁹	~300 (>400)	–	3.4	FE	[1975,1987]
Y	–	–	–	–	–	3.42	TC	[3476]
Y	–	–	–	–	–	3.51	TC	[3476]
Y/W(110)	Y	–	≤10⁻⁸	~1150–1250	–	3.53 ± 0.03	TE	[2330,2359]
Y	–	–	–	–	–	3.54	TC	[3318]
Y/W(110)	Y	–	≤10⁻⁹	~300	–	3.6	FE	[1987]
Y/W(110)	Y	–	≤10⁻⁹	~300 (>400)	–	3.7	FE	[1975,1987]
Y	–	–	–	–	–	3.8	TC	[944]
Recommended	–	–	–	–	–	**3.16 ± 0.06**	–	–
bcc (β, $T > 1540$ K for bulk)								
Y	–	–	~10⁻⁹	~1550–1650	–	3.17	TE	[4356]

40. Zirconium Zr[451]

Surface	Beam	Ion	P_r (Torr)	T (K)	ϕ^+ (eV)	ϕ^e (eV)	Meth.	Refs.
hcp (α, $T < 1135$ K)								
Zr(0001)	–	–	–	–	–	4.04	TC	[1980]
Zr(0001)	–	–	–	–	–	4.15	TC	[334]
Zr(0001)	–	–	–	–	–	4.16	TC	[4417]
Zr(0001)	–	–	–	–	–	4.24	TC	[3493]
Zr(0001)	–	–	–	–	–	4.26	TC	[1091,3516]
Zr(0001)	–	–	–	–	–	4.37	TC	[1091,3516]
Zr(0001)	–	–	–	–	–	4.42	TC	[4005]
Zr(0001)	–	–	–	–	–	4.43	TC	[892]
Zr(0001)	–	–	–	–	–	4.49	TC	[893]
Zr(0001)	–	–	–	–	–	4.51	TC	[2519]
Zr(0001)	–	–	–	–	–	5.00	TC	[321]
Recommended	–	–	–	–	–	**4.36 ± 0.09**	–	–
Zr(1010)	–	–	–	–	–	3.59	TC	[4005]
Zr(1010)	–	–	–	–	–	3.89	TC	[1980]
Zr(1010)	–	–	–	–	–	4.78	TC	[321]
Zr(1124)	–	–	–	–	–	4.18	TC	[321]
bcc (β, $T > 1135$ K)								
Zr(100)	–	–	–	–	–	3.94	TC	[321]
Zr(110)	–	–	–	–	–	4.57	TC	[321]
Zr(111)	–	–	–	–	–	3.76	TC	[321]
Zr(112)	–	–	–	–	–	4.18	TC	[321]
hcp (α, $T < 1135$ K for bulk)								
Zr/Mo–Zr(5%)[161]	–	–	1 × 10⁻¹⁰	~300 (~1000)	–	2.94 ± 0.02	FE	[790]
Zr	–	–	<10⁻³	~300	–	3.10 ± 0.07	PE	[2571]
Zr/W	Zr	–	<10⁻¹¹	?	–	3.25	FE	[3039,3042]
Zr[174]	–	–	–	0ᴱ	–	3.28	TC	[1747]
Zr	–	–	–	–	–	3.42	TC	[3476]
Zr	–	–	–	–	–	3.47	TC	[1066]
Zr	–	–	–	–	–	3.51	TC	[3476]
Zr	–	–	?	~300	–	3.60	CPD	[2297]

Table 1 (*continued*)

Surface	Beam	Ion	P_r (Torr)	T (K)	ϕ^+ (eV)	ϕ^e (eV)	Meth.	Refs.
Zr/Mo	Zr	–	$\sim 10^{-10}$	~ 300	–	3.63	CPD	[2134]
Zr/W(310)	Zr	–	$< 10^{-10}$	295	–	3.65 ± 0.03	FE	[1665]
Zr/W(100)	Zr	–	5×10^{-10}	~ 300	–	3.65 ± 0.05	CPD	[2526]
Zr	–	–	–	–	–	3.7	TC	[1993]
Zr/Ni	Zr	–	?	~ 300	–	3.73	PE	[2922]
Zr	–	–	–	–	–	3.74	TC	[3318]
Zr/W(100)	Zr	–	?	~ 300	–	3.75	CPD	[3076]
Zr	–	–	–	–	–	3.77	TC	[3318]
Zr	–	–	–	–	–	3.8*	TC	[1955]
Zr	–	–	$< 10^{-3}$	~ 300	–	3.81 ± 0.12	PE	[2571]
Zr/W	Zr	–	$< 10^{-10}$	295	–	3.84 ± 0.03	FE	[1656,1665]
Zr	–	–	–	–	–	3.85	TC	[3476]
Zr/W(100)	Zr	–	$< 10^{-10}$	295	–	3.87 ± 0.03	FE	[1665]
Zr/W	Zr	–	?	~ 300	–	3.87 ± 0.05	CPD	[3073,3076]
Zr	–	–	3×10^{-10}	~ 300	–	3.89 ± 0.05	CPD	[1812]
Zr	–	–	–	–	–	3.90	TC	[2949]
Zr/W(112)	Zr	–	$< 10^{-10}$	295	–	3.92 ± 0.03	FE	[1665]
Zr	–	–	–	–	–	3.94	TC	[1744]
Zr	–	–	–	0	–	3.94	TC	[4419]
Zr/W(111)	Zr	–	$< 10^{-10}$	295	–	3.98 ± 0.03	FE	[1665]
Zr	–	–	–	–	–	4.0	TC	[2117]
Zr/W(100)	Zr	–	$< 8 \times 10^{-11}$	~ 300	–	4.0	CPD	[1806]
Zr	–	–	?	~ 300	–	4.00	PE	[2927]
Zr	–	–	2×10^{-10}	~ 300	–	4.05	PE	[1814]
Zr/quartz	Zr	–	$\sim 10^{-10}$	~ 300	–	4.05 ± 0.1	PE	[304]
Zr/W(100)	Zr	–	$< 8 \times 10^{-11}$	<450 (1400)	–	4.1	CPD	[1806]
Zr/W(100)	Zr	–	?	~ 300	–	4.12	CPD	[3204]
Zr	–	–	–	–	–	4.19	TC	[298]
Zr	–	–	–	–	–	4.3	TC	[706]
Zr	–	–	–	–	–	4.3	TC	[944]
Zr/W(110)	Zr	–	?	~ 300	–	4.33	CPD	[3076]
Zr	–	–	–	–	–	4.33	TC	[3637]
Zr	–	–	$< 10^{-3}$	~ 300	–	4.33 ± 0.07	PE	[2571]
Zr/W(110)	Zr	–	$< 10^{-10}$	295	–	4.46 ± 0.03	FE	[1665]
Recommended	–	–	–	–	–	**3.85 ± 0.06**	–	–
bcc (β, $T > 1135$ K for bulk)								
Zr/W	Zr	–	?	?	–	3.15	TE	[1750]
Zr	–	–	$\leq 10^{-8}$	?	–	3.80	TE	[1778]
Zr	–	–	?	~ 1000–1400	–	3.95	TE	[1773]
Zr	–	–	$\sim 10^{-8}$	~ 1300–1800	–	3.95	TE	[4221]
Zr	–	–	3×10^{-9}	960–1370	–	4.0	TE	[159]
Zr	–	–	?	?	–	4.01	TE	[2117]
Zr/W	Zr	–	$< 1 \times 10^{-10}$	? (≥ 1600)	–	4.04 ± 0.03	FE	[1656]
Zr	–	–	?	?	–	4.1	TE	[3402]
Zr	–	–	?	~ 2000	–	4.12	TE	[3527]
Zr	–	–	?	?	–	4.13	TE	[3524,3525]
Recommended	–	–	–	–	–	**4.01 ± 0.05**	–	–

41. Niobium Nb

Surface	Beam	Ion	P_r (Torr)	T (K)	ϕ^+ (eV)	ϕ^e (eV)	Meth.	Refs.
bcc								
Nb(100)	–	–	–	–	–	3.552	TC	[4091]
Nb(100)	–	–	–	–	–	3.6	TC	[1154,1188]
Nb(100)	–	–	–	–	–	3.68	TC	[320]
Nb(100)	–	–	?	~ 300	–	3.76	FE	[4339]
Nb(100)	–	–	5×10^{-8}	~ 1800–2100	–	3.86 ± 0.05	TE	[774]
Nb(100)	–	–	–	–	–	3.87	TC	[4316,4412]
Nb(100)	–	–	?	77	–	3.87 ± 0.01	FE	[1303]
Nb(100)	–	–	1×10^{-9}	?	(4.04*)	3.90	TE	[739]
Nb(100)	–	–	$\sim 10^{-9}$	~ 1400–1800	–	3.95 ± 0.03	TE	[775]
Nb(100)	–	–	–	–	–	3.96	TC	[321]
Nb(100)	–	–	$\leq 5 \times 10^{-11}$	~ 300	–	3.97 ± 0.02	PE	[336]
Nb(100)	–	–	$\leq 2 \times 10^{-9}$	~ 1700–2000	–	4.0	TE	[127]
Nb(100)	–	–	$\sim 10^{-9}$	?	–	4.00	TE	[3096]
Nb(100)	–	–	$< 1 \times 10^{-10}$	~ 300	–	4.02	CPD	[1253]
Nb(100)	–	–	$\sim 10^{-10}$	~ 1600–1850	–	4.02 ± 0.06	TE	[779]
Nb(100){68%}[162]	–	–	–	–	(4.39 ± 0.08)	4.02 ± 0.07	TC	[803]
Nb(100)	Cs	Cs^+	1×10^{-9}	?	4.04*	(3.90)	PSI	[739]

Table 1 (*continued*)

Surface	Beam	Ion	P_r (Torr)	T (K)	ϕ^+ (eV)	ϕ^e (eV)	Meth.	Refs.
Nb(100)	–	–	–	–	–	4.06	TC	[2548]
Nb(100)	–	–	–	–	–	4.07	TC	[1159,1980,3067]
Nb(100)	–	–	($\leq 10^{-11}$)	~300	–	4.1	CPD	[776]
Nb(100){68%}[162]	–	–	? (Cs)	~1100–1800	–	4.1	TE	[650,3414]
Nb(100)	–	–	~10^{-10}	77, ~300	–	4.18 ± 0.02	FE	[358]
Nb(100){70%}	–	–	~10^{-9}	~1050–2100	–	4.19 ± 0.04	TE	[124]
Nb(100)	–	–	–	–	–	4.23	TC	[1254]
Nb(100){68%}[162]	–	–	–	–	4.39 ± 0.08	(4.02 ± 0.07)	TC	[803]
Recommended	–	–	–	–	–	**4.02 ± 0.05**	–	–
Nb(110)	–	–	~10^{-10}	~300	–	4.33	PE	[2764]
Nb(110)	–	–	~10^{-10}	~300	–	4.37 ± 0.01	CPD	[777]
Nb(110)	–	–	–	–	–	4.488	TC	[4091]
Nb(110)	–	–	$\leq 5 \times 10^{-11}$	~300	–	4.51 ± 0.02	PE	[336]
Nb(110)	–	–	~10^{-8}	?	–	4.57	TE	[3353]
Nb(110)	–	–	–	–	–	4.61	TC	[321]
Nb(110)	–	–	–	–	–	4.61	TC	[2913]
Nb(110)	–	–	4×10^{-10}	~300	–	4.62 ± 0.05	CPD	[2672]
Nb(110)	Cs	Cs$^+$	1×10^{-9}	?	4.64*	(4.80)	PSI	[739]
Nb(110)	–	–	~10^{-8}	~1450–1750	–	4.65 ± 0.07	TE	[960]
Nb(110)	–	–	–	–	–	4.66	TC	[320]
Nb(110)	–	–	~10^{-9}	?	–	4.67	TE	[3096]
Nb(110)	–	–	–	–	–	4.74	TC	[2548]
Nb(110)	–	–	–	–	–	4.75	TC	[1159,1980,3067]
Nb(110)	–	–	~10^{-10}	~300	–	4.75 ± 0.05	CPD	[2381]
Nb(110)	–	–	1×10^{-10}	~300	–	4.75 ± 0.05*	CPD	[2839]
Nb(110)	–	–	~10^{-9}	1290–1540	–	4.75 ± 0.08	TE	[778]
Nb(110)	–	–	1×10^{-9}	?	(4.84 ± 0.05)	4.80	TE	[726,739]
Nb(110)	–	–	~10^{-7}–10^{-9}	2200	–	4.80	TE	[3357]
Nb(110)	–	–	–	–	–	4.80	TC	[334,3179]
Nb(110)	–	–	5×10^{-9}	1673–2073	–	4.80 ± 0.02	TE	[2000,2016]
Nb(110)	–	–	?	?	–	4.80 ± 0.04	TE	[3347]
Nb(110)	–	–	~10^{-9}	~1500–1800	–	4.80 ± 0.05	TE	[775]
Nb(110)	–	–	~10^{-9}	?	–	4.82 ± 0.05	TE	[1409]
Nb(110)	–	–	–	–	–	4.82	TC	[2073]
Nb(110)	–	–	–	–	–	4.84	TC	[722]
Nb(110)	Na	Na$^+$	1×10^{-9}	925–1680	4.84 ± 0.05	(4.80)	PSI	[726]
Nb(110)	–	–	~10^{-8}	?	–	4.85	TE	[3353]
Nb(110)	–	–	?	~300	–	4.87	PE	[722]
Nb(110)	–	–	~10^{-10}	1650–1850	–	4.87 ± 0.07	TE	[779]
Nb(110)/W(110)	–	–	–	–	–	4.9	TC	[2073]
Nb(110)	–	–	5×10^{-8}	~1800–2100	–	4.90 ± 0.05	TE	[774]
Nb(110)	–	–	7×10^{-11}	~300	–	4.93	PE	[2986]
Nb(110)	–	–	7×10^{-11}	~300	–	4.98	PE	[2874]
Recommended	–	–	–	–	–	**4.77 ± 0.05**	–	–
Nb(111)	–	–	–	–	–	3.775	TC	[4091]
Nb(111)	Cs	Cs$^+$	1×10^{-9}	?	3.78*	(3.88)	PSI	[739]
Nb(111)	–	–	–	–	–	3.80	TC	[321]
Nb(111)	–	–	~10^{-9}	2200	–	3.80	TE	[3357]
Nb(111)	–	–	5×10^{-8}	~1800–2100	–	3.84 ± 0.05	TE	[774]
Nb(111)	–	–	~10^{-8}	?	–	3.85	TE	[3353]
Nb(111)	–	–	1×10^{-9}	?	(3.90 ± 0.05)	3.88	TE	[726,739]
Nb(111)	–	–	~10^{-9}	~1600–2050	–	3.88 ± 0.03	TE	[775]
Nb(111)	–	–	~10^{-8}	1450–1750	–	3.88 ± 0.07	TE	[960,3096]
Nb(111)	Na	Na$^+$	1×10^{-9}	1630–1940	3.90 ± 0.05	(3.88)	PSI	[726]
Nb(111)	–	–	–	–	–	3.93	TC	[2548]
Nb(111)	–	–	–	–	–	3.94	TC	[1159,1980,3067]
Nb(111)	–	–	?	~300	–	4.05	FE	[4339]
Nb(111)	–	–	$\leq 5 \times 10^{-11}$	~300	–	4.08 ± 0.02	PE	[336]
Nb(111)[163]	–	–	~10^{-10}	~300	–	4.09	PE	[780]
Nb(111)	–	–	~10^{-8}	?	–	4.14	TE	[3353]
Nb(111)	–	–	1×10^{-10}	~300	–	4.30 ± 0.05*	CPD	[2839]
Nb(111)	–	–	~10^{-10}	~1600–1850	–	4.36 ± 0.06	TE	[779]
Nb(111)[163]	–	–	~10^{-10}	~300	–	4.66	PE	[780,2764]
Recommended	–	–	–	–	–	**3.95 ± 0.09**	–	–
Nb(112)	–	–	–	–	–	4.20	TC	[2818]
Nb(112)	–	–	–	–	–	4.23	TC	[321]
Nb(112)	–	–	–	–	–	4.33	TC	[1980,3067]

Table 1 (*continued*)

Surface	Beam	Ion	P_r (Torr)	T (K)	ϕ^+ (eV)	ϕ^e (eV)	Meth.	Refs.
Nb(112)	Cs	Cs$^+$	1×10^{-9}	?	4.44*	(4.45)	PSI	[739]
Nb(112)	–	–	5×10^{-8}	~1800–2100	(4.44*)	4.45 ± 0.05	TE	[739,774]
Nb(112)	–	–	~10^{-10}	~1600–1850	–	4.63 ± 0.06	TE	[779]
Recommended	–	–	–	–	–	**4.33 ± 0.10**	–	–
Nb(113)	–	–	~10^{-10}	~1600–1850	–	4.29 ± 0.06	TE	[779]
Nb(116)	–	–	≤2 × 10^{-9}	~1700–2000	–	3.7	TE	[127]
Nb(116)	–	–	~10^{-9}	1450–1800	–	3.70 ± 0.03	TE	[775]
Nb(116)	–	–	–	–	–	3.94	TC	[1980,3067]
Nb(116)	–	–	~10^{-10}	~1600–1850	–	3.95 ± 0.06	TE	[779]
Nb(310)	–	–	~10^{-10}	~1600–1850	–	4.18 ± 0.05	TE	[779]
Nb(335)	–	–	~10^{-10}	~300	–	4.55	PE	[2764]
Nb/quartz[164]	Nb	–	≤10^{-8}	28	–	3.8 ± 0.2	CPD	[1686]
Nb	–	–	–	–	–	3.81	TC	[521]
Nb	–	–	–	–	–	3.83	TC	[3476]
Nb	–	–	–	–	–	3.87	TC	[3476]
Nb[165]	CsI	Cs$^+$, I$^-$	~10^{-8}	1879–1942	3.88 ± 0.04	–	PSI, NSI	[120]
Nb[165]	CsI	Cs$^+$, I$^-$	~10^{-8}	1879–1942	3.88 ± 0.04^N	–	PSI, NSI	[120]
Nb	–	–	?	295	–	3.89	CPD	[2943]
Nb/quartz[164]	Nb	–	≤10^{-8}	4.2	–	3.9 ± 0.2	CPD	[1686]
Nb/quartz[164]	Nb	–	≤10^{-8}	293	–	3.9 ± 0.2	CPD	[1686]
Nb[165]	KCl	K$^+$, Cl$^-$	~10^{-8}	1853–2025	3.90 ± 0.07	–	PSI, NSI	[120]
Nb[165]	KCl	K$^+$, Cl$^-$	~10^{-8}	1853–2025	3.90 ± 0.07^N	–	PSI, NSI	[120]
Nb[165]	RbBr	Rb$^+$, Br$^-$	~10^{-8}	1928–1940	3.91 ± 0.05	–	PSI, NSI	[120]
Nb[165]	RbBr	Rb$^+$, Br$^-$	~10^{-8}	1928–1940	3.91 ± 0.05^N	–	PSI, NSI	[120]
Nb	–	–	5×10^{-9}	1373–2073	–	3.95 ± 0.02	TE	[2000,2016]
Nb	–	–	7×10^{-8}	~1300–1600	–	3.96	TE	[121,3401]
Nb	–	–	?	295	–	3.97	CPD	[2943]
Nb	–	–	?	~300	–	3.97 ± 0.07	PE	[974]
Nb	–	–	<2 × 10^{-7}	1870	–	3.98	TE	[1970]
Nb	–	–	–	–	–	4.0	TC	[2583]
Nb	–	–	?	?	–	4.0	TE	[3402,3404]
Nb	–	–	~700 (Ar)	?	–	4.0	TE	[2007]
Nb	–	–	~10^{-9}	~1400–2100	–	4.0 ± 0.05	TE	[1775]
Nb	–	–	~10^{-5}	≤1200	–	4.00	TE	[2216]
Nb	–	–	–	–	–	4.01	TC	[4433]
Nb	–	–	?	1470–1980	–	4.01$_3$	TE	[122]
Nb	–	–	~10^{-9}	~1200–1800	–	4.02	TE	[975]
Nb	–	–	2×10^{-7}	~1800–2100	(4.76–4.88)	4.02 ± 0.05	TE	[23]
Nb{68%(100)}	–	–	–	–	(4.39 ± 0.08)	4.02 ± 0.07	TC	[803]
Nb	–	–	~10^{-8}	~1450–1750	–	4.02 ± 0.07	TE	[960]
Nb	–	–	~10^{-9}	?	–	4.03	TE	[3096]
Nb	–	–	–	–	–	4.05	TC	[2949]
Nb	–	–	≤10^{-8}	?	–	4.05	TE	[1778]
Nb/W(111)	–	–	–	–	–	4.06	TC	[531]
Nb[163]	–	–	~10^{-10}	~300	–	4.09	PE	[780,2764]
Nb	–	–	–	–	–	4.1	TC	[1993]
Nb{68%(100)}	–	–	? (Cs)	≤1100	–	4.1	TE	[650,3414]
Nb/Si(111)[166]	Nb	–	?	~300	–	4.12	PE	[1430]
Nb	–	–	?	~300	–	4.13*	PE	[3602]
Nb	–	–	~10^{-9}	~1200–1800	–	4.13 ± 0.06	TE	[975]
Nb/W(112)	–	–	–	–	–	4.15	TC	[531]
Nb	–	–	~10^{-9}	973	–	4.15	TE	[3112]
Nb	–	–	?	?	–	4.16	TE	[2117]
Nb	–	–	–	–	–	4.18	TC	[3318]
Nb{68%(100)}	–	–	~10^{-9}	~1050–2100	–	4.19 ± 0.04	TE	[124,650]
Nb	–	–	–	–	–	4.2*	TC	[1955]
Nb	–	–	–	–	–	4.20	TC	[3264,3265,3267]
Nb	–	–	–	–	–	4.22	TC	[3318]
Nb{68%(100)}	–	–	–	–	–	4.23	TC	[1254]
Nb	–	–	–	–	–	4.25	TC	[298]
Nb	–	–	–	–	–	4.28	TC	[3476]
Nb	–	–	–	–	–	4.3	TC	[706]
Nb	–	–	<10^{-7}	2200	–	4.3	TE	[2582]
Nb/quartz	Nb	–	~10^{-10}	~300	–	4.3 ± 0.15	PE	[304]
Nb	–	–	?	~300	–	4.33	PE	[2622]

Table 1 (*continued*)

Surface	Beam	Ion	P_r (Torr)	T (K)	ϕ^+ (eV)	ϕ^e (eV)	Meth.	Refs.
Nb/W(100)	–	–	–	–	–	4.37	TC	[531]
Nb	–	–	$<1 \times 10^{-9}$	~300	–	4.37 ± 0.03	CPD	[123,349]
Nb	–	–	?	~300	–	$4.39 \pm 0.02^*$	CPD	[4277]
Nb{68%(100)}	–	–	–	–	4.39 ± 0.08	(4.02 ± 0.07)	TC	[803]
Nb/W(100)	Nb	–	1×10^{-11}	77	–	4.40	FE	[2965]
Nb	–	–	$\sim10^{-11}$	~300	–	4.41	CPD	[3338]
Nb	–	–	$\sim10^{-10}$	~300	–	4.41 ± 0.1	FE	[996]
Nb	–	–	–	–	–	4.45	TC	[2629]
Nb	RbI	Rb^+	2×10^{-7}	~1800–2100	4.76 ± 0.03	(4.02 ± 0.05)	PSI	[23]
Nb/W(110)	–	–	–	–	–	4.84	TC	[531]
Nb	RbBr	Rb^+	2×10^{-7}	~1800–2100	4.87 ± 0.06	(4.02 ± 0.05)	PSI	[23]
Nb	RbCl	Rb^+	2×10^{-7}	~1800–2100	4.88 ± 0.06	(4.02 ± 0.05)	PSI	[23]
Nb[164]	–	–	$\leq10^{-8}$	5	–	5.01	FE	[1686]
Recommended	–	–	–	–	–	**4.11 ± 0.05**	–	–

42. Molybdenum Mo

bcc

Surface	Beam	Ion	P_r (Torr)	T (K)	ϕ^+ (eV)	ϕ^e (eV)	Meth.	Refs.
Mo(100)	–	–	–	–	–	3.842	TC	[4091]
Mo(100)	–	–	12 (Ar)	?	–	3.94	PE	[4236]
Mo(100)	–	–	–	–	–	3.98 ± 0.02	TC	[4428]
Mo(100)	–	–	–	–	–	4.01	TC	[4057]
Mo(100)	–	–	–	–	–	4.03	TC	[639]
Mo(100)	–	–	–	–	–	4.05	TC	[320]
Mo(100)	–	–	–	–	–	4.06	TC	[4057]
Mo(100)	–	–	5–50 (Ne)	?	–	4.1 ± 0.1	TE	[643]
Mo(100)	–	–	–	–	–	4.10	TC	[321]
Mo(100){70%}	–	–	$\sim10^{-9}$	2000	–	4.10 ± 0.07	TE	[124]
Mo(100)	–	–	–	–	–	4.11	TC	[4407]
Mo(100)	–	–	–	–	–	4.19	TC	[1034]
Mo(100){80%}	–	–	$\sim10^{-9}$	~300	–	4.2	FE	[3231]
Mo(100)	–	–	–	–	–	4.20	TC	[2181]
Mo(100)	–	–	–	–	–	4.20	TC	[639]
Mo(100)[167]	Li	Li^-, Li^+	2×10^{-8}	1964–2048	4.20 ± 0.20^N	–	NSI, PSI	[125]
Mo(100){70%}	–	–	$\sim10^{-9}$	1400	–	4.21 ± 0.09	TE	[124]
Mo(100)	–	–	$<1 \times 10^{-11}$	78	–	4.26	FE	[648]
Mo(100)	–	–	6×10^{-10}	~300	–	4.26 ± 0.03	FE	[999]
Mo(100)	Cs	Cs^+	$<10^{-6}$	1190	4.26 ± 0.05	–	PSI	[126]
Mo(100)	–	–	–	–	–	4.28	TC	[1624]
Mo(100)	–	–	–	–	–	4.28	TC	[3224]
Mo(100)	–	–	6×10^{-10}	~300	–	4.28 ± 0.01	FE	[999,1668]
Mo(100)[167]	Li	Li^+	2×10^{-8}	~1250–1450	4.28 ± 0.05	–	PSI	[129,572,573]
Mo(100)[167]	CsI	I^-	2×10^{-8}	~1750–1850	4.29 ± 0.02^N	–	NSI	[572,573]
Mo(100){80%}	–	–	$\sim10^{-9}$	~300	–	4.3	FE	[2756,2757]
Mo(100)	–	–	$<1 \times 10^{-10}$	77	–	4.3 ± 0.2	PE	[4002]
Mo(100)[168]	–	–	?	1980	–	4.33 ± 0.03	TE	[729]
Mo(100)	–	–	7×10^{-10}	77	–	4.35 ± 0.02	FE	[3691]
Mo(100)	–	–	$\leq10^{-4}$ (Br_2)	~1400–2100	(4.36 ± 0.06^N)	4.35 ± 0.05	TE	[925]
Mo(100)	–	–	$\leq10^{-5}$ (I_2)	~1500–2000	(4.36 ± 0.05^N)	4.35 ± 0.05	TE	[571]
Mo(100)	–	–	$\leq5 \times 10^{-8}$	~1600–1900	–	4.35 ± 0.07	TE	[128,3096]
Mo(100)	–	–	–	–	–	4.36	TC	[3224]
Mo(100)	I_2	I^-	$\leq10^{-5}$ (I_2)	~1500–2000	4.36 ± 0.05^N	(4.35 ± 0.05)	NSI	[571]
Mo(100)	Br_2	Br^-	$\leq10^{-4}$ (Br_2)	~1400–2100	4.36 ± 0.06^N	(4.35 ± 0.05)	NSI	[925]
Mo(100)	–	–	–	–	–	4.37	TC	[4034]
Mo(100)[168]	–	–	?	1980	–	4.37 ± 0.03	TE	[729]
Mo(100)	–	–	$\sim10^{-10}$	77	–	4.38	FE	[1304]
Mo(100)[167]	Li	Li^+	2×10^{-8}	~1400–2000	4.38 ± 0.01	–	PSI	[125]
Mo(100){72%}[172]	–	–	–	–	(4.51 ± 0.03)	4.38 ± 0.01	TC	[803]
Mo(100)[168]	–	–	?	1980	–	4.38 ± 0.03	TE	[729]
Mo(100)	–	–	$\leq10^{-5}$ (Sr)	~1400–1800	–	4.40	TE	[1401]
Mo(100)	–	–	$<2 \times 10^{-9}$	?	–	4.40	TE	[2235]
Mo(100)	–	–	$\sim10^{-10}$	?	–	4.40	?	[322]
Mo(100)	–	–	–	–	–	4.40	TC	[2701]
Mo(100)	–	–	?	77	–	4.40	FE	[1303]
Mo(100)	–	–	$\leq2 \times 10^{-9}$	~1700–2000	–	4.40 ± 0.02	TE	[127,144,323]
Mo(100)	–	–	$\sim10^{-9}$	?	(4.44 ± 0.03)	4.40 ± 0.03	TE	[727,2210,3103]
Mo(100)	–	–	3×10^{-7}	1943	–	4.40 ± 0.04	TE	[1402]
Mo(100)	–	–	$\leq10^{-9}$	~1700–2100	–	4.40 ± 0.05	TE	[323]
Mo(100)	–	–	–	–	–	4.43	TC	[2548]

Table 1 (*continued*)

Surface	Beam	Ion	P_r (Torr)	T (K)	ϕ^+ (eV)	ϕ^e (eV)	Meth.	Refs.
Mo(100)	–	–	$\leq 4 \times 10^{-9}$	~1800–2100	–	4.43 ± 0.05	TE	[739,781,1407]
Mo(100)	–	–	–	–	–	4.44	TC	[1159,1980,3067]
Mo(100)	Na	Na$^+$	~10^{-9}	~900–1700	4.44 ± 0.03	(4.40 ± 0.03)	PSI	[727,2210,3103]
Mo(100)	–	–	$\leq 1 \times 10^{-10}$	200, 300	–	4.45	FE	[783,1416]
Mo(100)	–	–	<10^{-10}	~1200–2000	–	4.45	TE	[324,527,784]
Mo(100)	–	–	$\leq 1 \times 10^{-10}$	?	(4.45)	4.45	TE	[278]
Mo(100)	Na	Na$^+$	$\leq 1 \times 10^{-10}$	?	4.45	(4.45)	PSI	[278]
Mo(100)	K	K$^+$	$\leq 1 \times 10^{-10}$	?	4.45	(4.45)	PSI	[278]
Mo(100)	–	–	~10^{-9}	~1484–1788	–	4.46 ± 0.02	CPD	[2963]
Mo(100)	–	–	~10^{-9}	~1484–1788	–	4.47 ± 0.02	TE	[2963]
Mo(100)	–	–	$\leq 10^{-6}$	~1770–2170	–	4.5	TE	[2339]
Mo(100)	–	–	~10^{-8}	~1600–1900	–	4.5 ± 0.04	TE	[3344]
Mo(100)	–	–	~10^{-10}	–1700–	–	4.5 ± 0.1	TE	[335,1650,1651, 1967]
Mo(100){72%}[172]	–	–	–	–	4.51 ± 0.03	(4.38 ± 0.01)	TC	[803]
Mo(100)[168]	–	–	?	1980	–	4.52 ± 0.03	TE	[729]
Mo(100)	–	–	~1×10^{-10}	~300	–	4.53	CPD	[2632]
Mo(100)	–	–	<1×10^{-10}	~300	–	4.53 ± 0.02	PE	[325]
Mo(100)	–	–	–	–	–	4.58	TC	[3224]
Mo(100)	–	–	2×10^{-10}	~300	–	4.60	FE	[275,440]
Mo(100)	–	–	$\leq 1 \times 10^{-8}$	1789	–	4.60 ± 0.04	TE	[2244]
Mo(100)	–	–	~10^{-11}	~300	–	4.65	PE	[326]
Mo(100)	–	–	~10^{-10}	~300	–	4.67 ± 0.03	PE	[2607]
Mo(100)	–	–	–	–	–	4.84	TC	[2701]
Recommended	–	–	–	–	**4.38 ± 0.08**	**4.38 ± 0.03**	–	–
Recommended	–	–	–	–	**4.34 ± 0.03^N**	–	–	–
Mo(110)	–	–	12 (Ar)	?	–	4.18	PE	[4236]
Mo(110)	–	–	5–50 (Ne)	?	–	4.32 ± 0.07	TE	[643]
Mo(110)	–	–	–	–	–	4.510	TC	[4091]
Mo(110)	–	–	–	–	–	4.59	TC	[4057]
Mo(110)	–	–	–	–	–	4.64	TC	[4057]
Mo(110)	–	–	~10^{-8}	~1600–1900	–	4.7 ± 0.04	TE	[3344]
Mo(110)/Si$_3$N$_4$	–	–	–	–	–	4.71	TC	[3517]
Mo(110)/Si$_3$N$_4$	Mo	–	?	~300	–	4.72	CPD	[3517]
Mo(110)	–	–	~10^{-8}	?	–	4.75	TE	[3353,3357]
Mo(110)	–	–	–	–	–	4.77	TC	[321]
Mo(110)/W(110)[169]	–	–	–	–	–	4.8	TC	[2074]
Mo(110)	–	–	7×10^{-10}	77	–	4.81 ± 0.09	FE	[3691]
Mo(110)	–	–	–	–	–	4.82	TC	[3224]
Mo(110)	–	–	–	–	–	4.820	TC	[3573,4046]
Mo(110)	–	–	<1×10^{-11}	78	–	4.83	FE	[648]
Mo(110)[169]	–	–	–	–	–	4.83	TC	[2074]
Mo(110)	–	–	–	–	–	4.84	TC	[1624]
Mo(110)	–	–	5×10^{-9}	?	–	4.85	TE	[2786]
Mo(110)	–	–	–	–	–	4.85	TC	[639]
Mo(110)	–	–	$\leq 10^{-9}$	?	–	4.85 ± 0.05	TE	[323]
Mo(110)	–	–	~10^{-9}	?	–	4.87 ± 0.03	TE	[3348]
Mo(110)	–	–	–	–	–	4.88	TC	[639]
Mo(110)	–	–	$\leq 5 \times 10^{-8}$	~1600–1900	–	4.9 ± 0.07	TE	[128,3096]
Mo(110)	–	–	?	?	–	4.9 ± 0.1	TE	[1962]
Mo(110)	–	–	~10^{-9}	?	–	4.90 ± 0.02	TE	[3331]
Mo(110)	–	–	$\leq 1 \times 10^{-8}$	1789	–	4.90 ± 0.04	TE	[2244]
Mo(110)	–	–	$\leq 4 \times 10^{-9}$	~1800–2100	–	4.90 ± 0.05	TE	[781]
Mo(110)	–	–	?	~1700–2200	–	4.90 ± 0.05	TE	[785]
Mo(110)	–	–	5×10^{-8}	?	–	4.90 ± 0.05[485]	TE	[1400]
Mo(110)	–	–	~10^{-8}	?	–	4.91	TE	[3353,3357]
Mo(110)	–	–	~10^{-10}	~300	–	4.92 ± 0.02	CPD	[777]
Mo(110)	–	–	–	–	–	4.94	TC	[320]
Mo(110)	–	–	–	–	–	4.94	TC	[3224]
Mo(110)	–	–	?	?	–	4.94 ± 0.03	TE	[3107]
Mo(110)	–	–	~10^{-8}	~1800–2100	–	4.94 ± 0.05	TE	[782]
Mo(110)	–	–	7×10^{-11}	~300	–	4.95	PE	[1035]
Mo(110)	–	–	<1×10^{-10}	~300	–	4.95 ± 0.02	PE	[325]
Mo(110)	–	–	$\leq 4 \times 10^{-9}$	~1800–2100	–	4.95 ± 0.05	TE	[739,1407]
Mo(110)	–	–	$\leq 10^{-3}$ (Cs)	>1800	–	5.0	TE	[976]
Mo(110)	–	–	$\leq 10^{-10}$	77, ~300	–	5.0	CPD	[327–329]
Mo(110)	–	–	$\leq 10^{-11}$	~300	–	5.0	CPD	[2380]
Mo(110)/W(110)	Mo	–	?	~300	–	5.0	CPD	[4231]
Mo(110)	–	–	$\leq 1 \times 10^{-10}$	200, 300	–	5.00	FE	[1416]

Table 1 (*continued*)

Surface	Beam	Ion	P_r (Torr)	T (K)	ϕ^+ (eV)	ϕ^e (eV)	Meth.	Refs.
Mo(110)	–	–	($\sim10^{-12}$)	~300	–	5.00 ± 0.02	CPD	[1795]
Mo(110)	–	–	5×10^{-9}	1673–2073	–	5.00 ± 0.02	TE	[2000,2016]
Mo(110)	–	–	$\sim10^{-9}$	?	–	5.00 ± 0.03	TE	[3331,3348]
Mo(110)	–	–	$\leq2 \times 10^{-9}$	?	–	5.00 ± 0.03	TE	[3099]
Mo(110)	–	–	3×10^{-9}	?	–	5.00 ± 0.05	TE	[2212,2214]
Mo(110)	–	–	$\sim10^{-9}$	?	–	5.00 ± 0.05	TE	[1409]
Mo(110)	–	–	$\leq2 \times 10^{-9}$	$\sim1700–2000$	–	5.00 ± 0.05	TE	[127,144]
Mo(110)	–	–	$\leq3 \times 10^{-10}$	?	–	5.00 ± 0.05	TE	[330,331,640]
Mo(110)	–	–	$\leq5 \times 10^{-9}$	?	–	5.05 ± 0.05	TE	[3084]
Mo(110)	–	–	$\leq10^{-11}$	~300	–	5.05 ± 0.07	CPD	[977]
Mo(110)	–	–	?	~300	–	5.07	FE	[2676]
Mo(110)/W(110)	Mo	–	2×10^{-10}	1023	–	5.09*	CPD	[2293]
Mo(110)	–	–	$\leq1 \times 10^{-6}$	1770–2270	–	5.1	TE	[2339]
Mo(110)	–	–	$\sim10^{-11}$	20–200	–	5.1	FE	[2218]
Mo(110)	–	–	$\sim10^{-9}$	?	(5.13 ± 0.03)	5.10 ± 0.03	TE	[727,2210,3103]
Mo(110)	–	–	$\sim10^{-9}$	?	–	5.10 ± 0.03	TE	[3331,3348]
Mo(110)	–	–	$\leq10^{-9}$	$\sim1700–2100$	–	5.10 ± 0.05	TE	[323]
Mo(110)	–	–	4×10^{-10}	~300	–	5.10 ± 0.15	FE	[999]
Mo(110)	–	–	4×10^{-10}	~300	–	5.11 ± 0.07	FE	[999,1668]
Mo(110)	–	–	7×10^{-10}	77	–	5.12 ± 0.16	FE	[3691]
Mo(110)	–	–	–	–	–	5.13	TC	[4034]
Mo(110)	Na	Na^+	$\sim10^{-9}$	$\sim900–1600$	5.13 ± 0.03	(5.10 ± 0.03)	PSI	[727,2210,3103]
Mo(110)	–	–	$\sim10^{-9}$	?	–	5.20 ± 0.02	TE	[3331]
Mo(110)	–	–	–	–	–	5.23	TC	[2548]
Mo(110)	–	–	–	–	–	5.23	TC	[1159,1980,3067]
Mo(110)	–	–	5×10^{-11}	350	–	5.25	CPD	[332,333]
Mo(110)	–	–	$\sim10^{-10}$	80	–	5.32 ± 0.02	FE	[2499]
Mo(110)	–	–	–	–	–	5.34	TC	[334,3179]
Mo(110)	–	–	$\sim10^{-10}$	–1700–	–	5.4 ± 0.2	TE	[335,1650,1651, 1967]
Mo(110)	–	–	$\sim10^{-10}$	300, 550	–	5.46 ± 0.02	FE	[2499]
Mo(110)	–	–	–	–	–	5.90	TC	[3224]
Recommended	–	–	–	–	–	**4.98 ± 0.03**	–	–
Mo(111)	–	–	–	–	–	3.86	TC	[4057]
Mo(111)	Cs	Cs^+	?	$\sim800–1050$	3.89	–	PSI	[135]
Mo(111)	–	–	–	–	–	3.93	TC	[321]
Mo(111)	–	–	6×10^{-10}	~300	–	3.94 ± 0.05	FE	[999]
Mo(111)	–	–	–	–	–	3.940	TC	[4091]
Mo(111)[170]	Cs	Cs^+	?	$\sim800–1050$	3.95*	–	PSI	[135]
Mo(111)	–	–	$\sim10^{-9}$	?	–	3.95 ± 0.02	TE	[3331]
Mo(111)	–	–	6×10^{-10}	~300	–	3.99 ± 0.02	FE	[999,1668]
Mo(111)	–	–	–	–	–	4.00	TC	[4057]
Mo(111)	–	–	7×10^{-10}	77	–	4.00 ± 0.08	FE	[1304,3691]
Mo(111)	–	–	$<1 \times 10^{-11}$	78	–	4.06	FE	[648]
Mo(111)	–	–	–	–	–	4.07	TC	[4034]
Mo(111)	–	–	$\leq2 \times 10^{-9}$	$\sim1700–2000$	–	4.10 ± 0.02	TE	[127,144]
Mo(111)	–	–	$\sim10^{-9}$	?	(4.13 ± 0.03)	4.10 ± 0.03	TE	[727,2210,3103, 3348]
Mo(111)	–	–	$\sim10^{-9}$	$\sim1100–1800$	(4.10 ± 0.03)	4.10 ± 0.03	TE	[786]
Mo(111)	Li	Li^+	$\sim10^{-9}$	$\sim1100–1800$	4.10 ± 0.03	(4.10 ± 0.03)	PSI	[786]
Mo(111)	–	–	3×10^{-9}	?	–	4.10 ± 0.05	TE	[2212,2214]
Mo(111)	–	–	$\leq4 \times 10^{-9}$	$\sim1800–2100$	–	4.10 ± 0.05	TE	[739,781,782,1407]
Mo(111)	–	–	10^{-8}	?	–	4.13	TE	[3353,3357]
Mo(111)	Na	Na^+	$\sim10^{-9}$	$\sim1600–2000$	4.13 ± 0.03	(4.10 ± 0.03)	PSI	[727,2210,3103]
Mo(111)	–	–	$\leq5 \times 10^{-9}$	?	–	4.14 ± 0.04	TE	[3084]
Mo(111)	–	–	5×10^{-8}	?	–	4.14 ± 0.05[485]	TE	[1400]
Mo(111)	–	–	2×10^{-10}	$\sim1480–1850$	–	4.15 ± 0.02	TE	[678]
Mo(111)	–	–	$\leq10^{-9}$	$\sim1700–2100$	–	4.15 ± 0.05	TE	[323]
Mo(111)	–	–	$\leq1 \times 10^{-10}$	~300	–	4.19	FE	[783]
Mo(111)	–	–	$\sim10^{-9}$	?	–	4.19 ± 0.02	TE	[3331]
Mo(111)	–	–	5×10^{-7}	$\sim1870–2270$	–	4.2	TE	[2339]
Mo(111)	–	–	$\leq1 \times 10^{-10}$	200, 300	–	4.20	FE	[1416]
Mo(111)	–	–	–	–	–	4.23	TC	[3224]
Mo(111)	–	–	–	–	–	4.25	TC	[2548]
Mo(111)	–	–	$\sim10^{-9}$	?	–	4.25 ± 0.03	TE	[3348]
Mo(111)	–	–	–	–	–	4.27	TC	[1159,1980,3067]
Mo(111)	–	–	–	–	–	4.27	TC	[639]
Mo(111)	?	?	?	?	4.3	–	PSI	[135]
Mo(111)	–	–	$\leq5 \times 10^{-10}$	~300	–	4.3	CPD	[2621]

(*continued on next page*)

Table 1 (*continued*)

Surface	Beam	Ion	P_r (Torr)	T (K)	ϕ^+ (eV)	ϕ^e (eV)	Meth.	Refs.
Mo(111)	–	–	≤10⁻⁹	1650–1850	–	4.3 ± 0.03	TE	[787]
Mo(111)	–	–	~10⁻¹⁰	–1700–	–	4.3 ± 0.1	TE	[335,1650,1651, 1967]
Mo(111)	–	–	–	–	–	4.30	TC	[1624]
Mo(111)	–	–	5 × 10⁻⁹	?	–	4.30	TE	[2786]
Mo(111)	–	–	–	–	–	4.32	TC	[639]
Mo(111)	–	–	5–50 (Ne)	?	–	4.33 ± 0.01	TE	[643]
Mo(111)	–	–	≤1 × 10⁻⁸	1789	–	4.35 ± 0.04	TE	[2244]
Mo(111)	–	–	–	–	–	4.4	TC	[1739]
Mo(111)	–	–	~10⁻⁹	?	–	4.40 ± 0.03	TE	[3348]
Mo(111)	–	–	~10⁻⁹	?	–	4.46 ± 0.03	TE	[3348]
Mo(111)[171]	–	–	<6 × 10⁻¹⁰	293	–	4.49 ± 0.06	PE	[3421]
Mo(111)	–	–	≤5 × 10⁻¹¹	~300	–	4.52 ± 0.02	PE	[336]
Mo(111)	–	–	–	–	–	4.55	TC	[3224]
Mo(111)	–	–	<1 × 10⁻¹⁰	~300	–	4.55 ± 0.02	PE	[325]
Mo(111)	–	–	~10⁻⁸	?	–	4.58	TE	[3353,3357]
Mo(111)	–	–	~10⁻¹¹	20–200	–	4.6	FE	[2218]
Mo(111)	–	–	?	~300	–	4.6*	FE	[1518]
Mo(111)[171]	–	–	<6 × 10⁻¹⁰	293	–	4.67 ± 0.02	PE	[3421]
Mo(111)	–	–	1 × 10⁻⁵	1820–2270	–	4.7	TE	[2339]
Mo(111)	–	–	~10⁻⁸	~1600–1900	–	4.8 ± 0.04	TE	[3344]
Recommended	–	–	–	–	–	**4.29 ± 0.03**	–	–
Mo(112)	–	–	–	–	–	4.11	TC	[702]
Mo(112)	–	–	–	–	–	4.12	TC	[702]
Mo(112)	–	–	–	–	–	4.25	TC	[468]
Mo(112)	–	–	–	–	–	4.28	TC	[1034]
Mo(112)	–	–	–	–	–	4.35	TC	[468]
Mo(112)	–	–	<1 × 10⁻¹⁰	~300	–	4.36 ± 0.03	PE	[325]
Mo(112)	–	–	–	–	–	4.37	TC	[3224]
Mo(112)	–	–	–	–	–	4.38	TC	[321]
Mo(112)	–	–	7 × 10⁻¹⁰	77	–	4.45 ± 0.07	FE	[3691]
Mo(112)	–	–	<1 × 10⁻¹¹	78	–	4.46	FE	[648]
Mo(112)	–	–	~10⁻⁹	~300	–	4.5	PE	[2398]
Mo(112)	–	–	~10⁻¹⁰	–1700–	–	4.5 ± 0.1	TE	[335,1643,1650, 1651,1967]
Mo(112)	–	–	≤10⁻¹¹	~300	–	4.50	CPD	[2533]
Mo(112)	–	–	≤1 × 10⁻⁸	1789	–	4.50 ± 0.04	TE	[2244]
Mo(112)	–	–	7 × 10⁻¹⁰	77	–	4.51 ± 0.07	FE	[1304,3691]
Mo(112)	–	–	≤2 × 10⁻⁹	~1700–2000	–	4.55 ± 0.05	TE	[127,144]
Mo(112)	–	–	≤4 × 10⁻⁹	~1800–2100	–	4.55 ± 0.05	TE	[726,739,781,1407]
Mo(112)	–	–	≤1 × 10⁻¹⁰	~300	–	4.58	FE	[783]
Mo(112)	–	–	~1 × 10⁻¹¹	90	–	4.6	CPD	[505]
Mo(112)	–	–	(≤10⁻¹¹)	77	–	4.6	CPD	[1255,2027,2030]
Mo(112)	–	–	~10⁻¹¹	~300	–	4.6	CPD	[2535]
Mo(112)	–	–	?	~300	–	4.6	CPD	[2404,2407]
Mo(112)	–	–	~10⁻¹⁰	200, 300	–	4.60	FE	[1416]
Mo(112)	–	–	~10⁻⁹	?	(4.63 ± 0.03)	4.60 ± 0.03	TE	[727,2210]
Mo(112)	–	–	≤5 × 10⁻⁹	?	–	4.60 ± 0.05	TE	[3084]
Mo(112)	–	–	–	–	–	4.61	TC	[3224]
Mo(112)	–	–	(<10⁻¹¹)	~300	–	4.61*	CPD	[2637]
Mo(112)	Na	Na⁺	~10⁻⁹	~800–1500	4.63 ± 0.03	(4.60 ± 0.03)	PSI	[727,2210]
Mo(112)	–	–	–	–	–	4.64	TC	[3224]
Mo(112)	–	–	2 × 10⁻¹⁰	1480–1850	–	4.67 ± 0.02	TE	[678]
Mo(112)	–	–	~10⁻¹¹	20–200	–	4.7	FE	[2218]
Mo(112)	–	–	–	–	–	4.71	TC	[1159,1980,3067]
Mo(112)	–	–	–	–	–	4.8	TC	[1739]
Recommended	–	–	–	–	–	**4.51 ± 0.03**	–	–
Mo(114)	–	–	–	–	–	4.02	TC	[3224]
Mo(114)	–	–	–	–	–	4.16	TC	[3224]
Mo(114)	–	–	≤5 × 10⁻⁸	~1600–1900	–	4.18 ± 0.07	TE	[128]
Mo(114-116)	–	–	?	?	–	4.3 ± 0.1	TE	[1962]
Mo(114)	–	–	–	–	–	4.50	TC	[3224]
Mo(114)	–	–	<1 × 10⁻¹⁰	~300	–	4.50 ± 0.04	PE	[325]
Recommended	–	–	–	–	–	**4.33 ± 0.15**	–	–
Mo(116)	–	–	–	–	–	3.90	TC	[3224]
Mo(116)	–	–	7 × 10⁻¹⁰	77	–	3.96 ± 0.01	FE	[3691]
Mo(116)	–	–	≤2 × 10⁻⁹	~1700–2000	–	4.00	TE	[127,144]

Table 1 (*continued*)

Surface	Beam	Ion	P_r (Torr)	T (K)	ϕ^+ (eV)	ϕ^e (eV)	Meth.	Refs.
Mo(116)	–	–	$\leq 5 \times 10^{-9}$	?	–	4.02 ± 0.04	TE	[3084]
Mo(116)	–	–	–	–	–	4.11	TC	[3224]
Mo(116)	–	–	$\leq 5 \times 10^{-8}$	~1600–1900	–	4.18 ± 0.07	TE	[128]
Mo(116)	–	–	~10^{-10}	–1700–	–	4.2 ± 0.1	TE	[335,1650,1651, 1967]
Mo(116)	–	–	–	–	–	4.27	TC	[1159,1980,3067]
Mo(116-114)	–	–	?	?	–	4.3 ± 0.1	TE	[1962]
Mo(116)	–	–	$<2 \times 10^{-9}$	?	–	4.33	TE	[134]
Mo(116)	–	–	$<2 \times 10^{-9}$	293, 1000	–	4.41	PE	[134]
Mo(116)	–	–	–	–	–	4.47	TC	[3224]
Recommended	–	–	–	–	–	**4.23 ± 0.08**	–	–
Mo(310)	–	–	$\leq 1 \times 10^{-10}$	~300	–	4.13	FE	[783]
Mo(310)	–	–	–	–	–	4.13	TC	[3224]
Mo(310)	–	–	–	–	–	4.20	TC	[3224]
Mo(310)	–	–	–	–	–	4.53	TC	[3224]
Mo(321)	–	–	$\leq 1 \times 10^{-10}$	~300	–	4.14	FE	[783]
Mo(321)	–	–	–	–	–	4.15	TC	[3224]
Mo(321)	–	–	–	–	–	4.20	TC	[3224]
Mo(321)	–	–	–	–	–	4.53	TC	[3224]
Mo(331)	–	–	$<2 \times 10^{-9}$	?	–	4.33	TE	[134]
Mo(331)	–	–	$<2 \times 10^{-9}$	293, 1000	–	4.41	PE	[134]
Mo(332)	–	–	–	–	–	4.04	TC	[3224]
Mo(332)	–	–	–	–	–	4.16	TC	[3224]
Mo(332)	–	–	–	–	–	4.51	TC	[3224]
Mo(332)	–	–	$<1 \times 10^{-10}$	~300	–	4.55 ± 0.02	PE	[325]
Mo(431)	–	–	7×10^{-10}	77	–	4.02 ± 0.06	FE	[3691]
Mo(431)	–	–	7×10^{-10}	77	–	4.32 ± 0.14	FE	[3691]
Mo	–	–	$\leq 2 \times 10^{-8}$	~300	–	3.22 ± 0.16	PE	[2558]
Mo	–	–	$\leq 2 \times 10^{-8}$	~1300–1600	–	3.48 ± 0.07	TE	[2558]
Mo(porous)	–	–	?	>1600	(4.15)	3.8	TE	[3762]
Mo	–	–	–	–	–	3.92	TC	[521]
Mo[170]	–	(Mo$^+$)	~10^{-7}	~2400–2550	4.0 ± 0.1	(4.19 ± 0.02)	PSI	[954]
Mo	–	–	?	?	–	4.04	TE	[1486]
Mo	–	–	$<10^{-9}$	~300	–	4.04	PE	[337]
Mo	–	–	12 (Ar)	~300	–	4.04 ± 0.02	PE	[788,1647]
Mo	–	–	27 (Ne)	~300	–	4.06 ± 0.02	PE	[788,1647]
Mo	–	–	–	–	–	4.07	TC	[3476]
Mo	–	–	12 (Ar)	?	–	4.07 ± 0.03	PE	[4236]
Mo	–	–	–	–	–	4.08	TC	[1066]
Mo	–	–	?	~300	–	4.08	CPD	[2761]
Mo/W	Mo	–	5×10^{-10}	77	–	4.1	FE	[2318]
Mo	–	–	?	~300	–	4.10	CPD	[2761]
Mo	–	–	–	–	–	4.10	TC	[3476]
Mo	–	–	27 (Ne)	?	–	4.10 ± 0.02	PE	[4236]
Mo	–	–	?	~300	–	4.11	PE	[4190]
Mo{70%(100)}[172]	–	–	~10^{-9}	1950–2070	–	4.11 ± 0.08	TE	[124]
Mo	–	–	?	~300	–	4.12 ± 0.03	PE	[1635]
Mo	–	–	?	~300	–	4.15	PE	[2237]
Mo	–	–	?	?	–	4.15	TE	[1949]
Mo(porous)	Cs	Cs$^+$	?	~1100–1400	4.15	(3.8)	PSI	[3762]
Mo[262]	–	–	$<10^{-7}$	~1400–2000	–	4.15 ± 0.01	TE	[338]
Mo[262]	–	–	$<10^{-7}$	303, 940	–	4.15 ± 0.02	PE	[338]
Mo	–	–	$\leq 2 \times 10^{-10}$	~300	–	4.15 ± 0.05	CPD	[3077]
Mo	–	–	2×10^{-7}	~300	–	4.16	CPD	[642]
Mo	–	–	$<2 \times 10^{-7}$	1870	–	4.16	TE	[1970]
Mo	–	5–50 (Ne)	?	?	–	4.16 ± 0.02	TE	[643]
Mo	–	–	$<3 \times 10^{-8}$	~1400–1700	(4.50)	4.17	TE	[131]
Mo	–	–	1×10^{-8}	~300	–	4.17	PE	[1433]
Mo	–	–	–	–	–	4.18	TC	[339]
Mo[262]	–	–	–	940$^\mathrm{E}$	–	4.18	TC	[3586]
Mo	–	–	~10^{-7}	~2400–2550	(4.0, 4.5)	4.19 ± 0.02	TE	[954]
Mo{70%(100)}[172]	–	–	~10^{-9}	1360–1460	–	4.19 ± 0.09	TE	[124]
Mo	–	–	–	–	–	4.2	TC	[1645]
Mo	–	–	–	–	–	4.2	TC	[1993]

Table 1 (*continued*)

Surface	Beam	Ion	P_r (Torr)	T (K)	ϕ^+ (eV)	ϕ^e (eV)	Meth.	Refs.
Mo	–	–	–	–	–	4.2	TC	[2583]
Mo{80%(100)}	–	–	$\sim10^{-9}$	~300	–	4.2	FE	[3231]
Mo/W	Mo	–	5×10^{-10}	800	–	4.2	FE	[2318]
Mo	–	–	4×10^{-9}	~1600–1950	–	4.2 ± 0.05	TE	[341]
Mo	–	–	?	~1000–1400	–	4.20	TE	[1773]
Mo	–	–	$\leq10^{-9}$	~1800–2200	–	4.20	TE	[66]
Mo	–	–	$\sim10^{-8}$	~1600–1800	–	4.20	TE	[4221]
Mo	–	–	?	?	(4.3, 5.1)	4.20 ± 0.02	TE	[132]
Mo	–	–	$<10^{-8}$	~300	–	4.20 ± 0.03	CPD	[1163]
Mo	–	–	$<10^{-9}$	~300	–	4.21	PE	[337]
Mo/W(100)	Mo	–	1×10^{-11}	77	–	4.21	FE	[2965]
Mo	RbC	Rb$^+$	?	?	4.21 ± 0.02	–	PSI	[2306]
Mo/glass	Mo	–	$\sim10^{-8}$	~300	–	4.21 ± 0.04	CPD	[349]
Mo	–	–	?	~300	–	4.21 ± 0.07	PE	[974]
Mo	–	–	$\sim10^{-10}$	~300	–	4.22	PE	[789]
Mo	–	–	$\sim10^{-7}$	~300	–	4.22	CPD	[3513]
Mo	–	–	$\sim10^{-9}$	~1300–2100	–	4.22 ± 0.05	TE	[1775,1777]
Mo	–	–	$\sim10^{-8}$	~300	–	4.22 ± 0.05	CPD	[133]
Mo	–	–	?	~1600–1900	–	4.23	TE	[634]
Mo	K	K$^+$	?	?	$4.23 \pm 0.10^*$	(4.41 ± 0.01)	PSI	[645]
Mo	–	–	$\sim10^{-9}$	?	–	4.24	TE	[979]
Mo{70%(100)}[172]	–	–	–	–	–	4.25	TC	[1254]
Mo	–	–	$\leq10^{-9}$	?	–	4.25 ± 0.05	TE	[650]
Mo	–	–	$\sim10^{-6}$	~1900–2100	–	4.25–4.7	TE	[1779]
Mo	–	–	$\leq4 \times 10^{-10}$	?	–	4.26	TE	[2091]
Mo	–	–	1×10^{-10}	~300	–	4.27 ± 0.02	FE	[790]
Mo	–	–	–	–	–	4.28	TC	[3224]
Mo[17]	–	–	$<10^{-9}$	1650–1950	–	4.28 ± 0.6	TE	[791]
Mo/W(100)	Mo	–	1×10^{-11}	77 (750)	–	4.3	FE	[2965]
Mo	–	–	–	–	–	4.3	TC	[2456]
Mo{80%(100)}	–	–	$\sim10^{-9}$	~300	–	4.3	PE	[2757]
Mo	–	–	?	~300	–	4.3	PE	[3640]
Mo	–	–	700 (Ar)	~2800	–	4.3	TE	[2007]
Mo	–	–	$<1 \times 10^{-6}$	?	–	4.3	TE	[3035]
Mo	–	–	?	?	–	4.3 ± 0.1	?	[3780]
Mo	–	–	–	–	–	4.30	TC	[3264,3265,3267]
Mo	–	–	?	?	–	4.30	FE	[3544]
Mo	–	–	5×10^{-9}	1373–2073	–	4.30 ± 0.02	TE	[2016]
Mo[170]	–	(Mo$^+$)	?	~2350–2500	4.3 ± 0.1	(4.20 ± 0.02)	PSI	[132]
Mo	–	–	?	?	–	4.31	TE	[2455]
Mo	–	–	$<10^{-6}$	?	–	4.31	TE	[2919]
Mo	–	–	6×10^{-7}	?	–	4.31	TE	[1521]
Mo[174]	–	–	–	0^E	–	4.31	TC	[1747]
Mo	–	–	?	~1500–2100	–	4.31 ± 0.04	TE	[792]
Mo	–	–	$\leq2 \times 10^{-8}$	~1400–1800	–	4.32	TE	[130,1363]
Mo	–	–	$<10^{-6}$	~300	–	4.33	PE	[2919]
Mo	–	–	?	~80	–	4.33	CPD	[2294]
Mo	–	–	$\leq10^{-7}$	0^E (~1800)	–	4.33	TE	[1878]
Mo[173]	–	–	$<2 \times 10^{-9}$	?	–	4.33	TE	[134]
Mo	–	–	?	~300	–	4.33	PE	[2924]
Mo	–	–	1×10^{-7}	~1900–2300	(5.02 ± 0.05)	4.33 ± 0.07	TE	[76,77]
Mo[17]	–	–	$<10^{-9}$	1650–1950	–	4.33 ± 0.16	TE	[791]
Mo	–	–	$\leq10^{-9}$	1800–2200	–	4.34	TE	[66]
Mo	–	–	?	~1600–2000	–	4.34	TE	[3526]
Mo/Re	Mo	–	$\sim10^{-9}$	~1200–1800	–	4.35	TE	[975]
Mo	–	–	$\leq4 \times 10^{-10}$	?	–	4.35	TE	[2091]
Mo{72%(100)}[172]	–	–	? (Cs)	~1200–1800	–	4.35 ± 0.05	TE	[650,3414]
Mo	–	–	4×10^{-9}	~1600–1950	–	4.35 ± 0.05	TE	[341]
Mo	–	–	$\sim10^{-11}$	~300	–	4.36	CPD	[3338]
Mo	–	–	?	?	–	4.36	TE	[2088]
Mo	–	–	$\sim10^{-10}$	–1700–	–	4.36	TE	[335,1650,1651, 1967]
Mo	–	–	?	~2350–2500	$(4.6, 5.4^*)$	4.37 ± 0.02	TE	[132]
Mo	–	–	$<3 \times 10^{-8}$	~1400–1700	(4.50)	4.38	TE	[131]
Mo	–	–	?	?	–	4.38	TE	[3524,3525]
Mo	–	–	? (Cs)	~1500–2200	–	4.38	TE	[1390,3840]
Mo	–	–	6×10^{-10}	~1400–2100	–	4.38	TE	[2091,2092]
Mo	–	–	? (Cs)	~1500–2500	–	4.38	TE	[3798,3799]
Mo{72%(100)}[172]	–	–	–	–	(4.51 ± 0.03)	4.38 ± 0.01	TC	[803]
Mo	KCl	K$^+$	?	?	4.39 ± 0.02	–	PSI	[2306]

Table 1 (*continued*)

Surface	Beam	Ion	P_r (Torr)	T (K)	ϕ^+ (eV)	ϕ^e (eV)	Meth.	Refs.
Mo	–	–	2×10^{-7}	~2000–2100	(4.90 ± 0.06)	4.39 ± 0.05	TE	[23,39]
Mo	–	–	(~10^{-12})	~300	–	4.4 ± 0.02	CPD	[1795]
Mo	–	–	?	?	–	4.40	TE	[3402]
Mo	–	–	?	~1800	–	4.40	TE	[2567]
Mo	–	–	–	–	–	4.40	TC	[2949]
Mo	–	–	≤1×10^{-6}	2055–2140	–	4.40 ± 0.01	TE	[2296]
Mo[173]	–	–	<2×10^{-9}	293	–	4.41	PE	[134]
Mo	–	–	–	–	–	4.41	TC	[3637]
Mo	–	–	?	?	(4.23 ± 0.10*)	4.41 ± 0.01	TE	[645]
Mo	–	–	1×10^{-8}	1590–2100	(4.96 ± 0.01)	4.41 ± 0.02	TE	[78]
Mo/SiO$_2$	Mo	–	?	~300	–	4.42	CPD	[3687]
Mo	–	–	–	–	–	4.42	TC	[3318]
Mo	K	K$^+$	? (K)	1000	4.42	–	PSI	[1845]
Mo	–	–	2×10^{-6}	2200	–	4.44	TE	[39]
Mo	–	–	≤1×10^{-7}	~1700–2500	–	4.45 ± 0.01	TE	[978]
Mo	–	–	–	–	–	4.46	TC	[298]
Mo	–	–	–	–	–	4.46	TC	[3318]
Mo[173]	–	–	<2×10^{-9}	1000	–	4.47 ± 0.03	PE	[134]
Mo	–	–	≤10^{-7}	~1450–2150	–	4.48	TE	[1878]
Mo	–	–	?	~300	–	4.48	CPD	[2297]
Mo	–	–	~10^{-7}	~2000	–	4.49	TE	[1398]
Mo	–	–	–	–	–	4.49	TC	[531]
Mo	Li$^+$	Li$^+$	~10^{-9}	~500–1800	4.5	–	PSI	[1440]
Mo	Na$^+$	Na$^+$	~10^{-9}	~500–1800	4.5	–	PSI	[1440]
Mo	K$^+$	K$^+$	~10^{-9}	~500–1800	4.5	–	PSI	[1440]
Mo	–	–	<1×10^{-9}	~300	–	4.5	PE	[2211]
Mo	–	–	~10^{-8}	833	–	4.5	CPD	[2050]
Mo[170]	–	(Mo$^+$)	~10^{-7}	~2400–2550	4.5 ± 0.1	(4.19 ± 0.02)	PSI	[954]
Mo	–	–	~10^{-6}	~1900–2100	–	4.5 ± 0.2	TE	[1779]
Mo[170]	–	(Mo$^+$)	<3×10^{-8}	2150–2630	4.50	(4.17, 4.38)	PSI	[131]
Mo	–	–	<8×10^{-11}	~300	–	4.500 ± 0.100	CPD	[342,3868]
Mo{72%(100)}[172]	–	–	–	–	4.51 ± 0.03	(4.38 ± 0.01)	TC	[803]
Mo	–	–	–	–	–	4.53	TC	[3476]
Mo/W(112)	–	–	–	–	–	4.55	TC	[531]
Mo	–	–	3×10^{-10}	~300	–	4.55 ± 0.03	PE	[1504]
Mo[170]	–	(Mo$^+$)	?	2350–2500	4.6 ± 0.1	(4.37 ± 0.02)	PSI	[132]
Mo	–	–	–	–	–	4.6	TC	[944]
Mo/quartz	Mo	–	~10^{-10}	~300	–	4.6 ± 0.15	PE	[304]
Mo	–	–	?	77	–	4.61 ± 0.02	PE	[793]
Mo	–	–	2×10^{-5}	2080–2200	–	4.64	TE	[3017]
Mo	–	–	? (K)	1350–1550	–	4.66	TE	[2559]
Mo	–	–	–	–	–	4.7	TC	[706]
Mo[170]	–	(Mo$^+$)	~10^{-7}	~2400–2550	4.7 ± 0.1*	(4.19 ± 0.02)	PSI	[954]
Mo/W(111)	–	–	–	–	–	4.70	TC	[531]
Mo	–	–	–	–	–	4.70	TC	[2629]
Mo	–	–	5×10^{-10}	~300	–	4.72	AI	[4027]
Mo/Si(111)[166]	Mo	–	4×10^{-11}	~300	–	4.76	PE	[1430]
Mo	–	–	–	0	–	4.78	TC	[4419]
Mo	KBr	K$^+$	2×10^{-7}	~2000–2100	4.90 ± 0.06	(4.39 ± 0.05)	PSI	[23,39,57,2422]
Mo[170]	–	(Mo$^+$)	~10^{-10}	2350–2500	4.93 ± 0.03*	–	PSI	[3886]
Mo/HfO$_2$	Mo	–	?	~300	–	4.95	CPD	[3519,3656]
Mo	Bi	Bi$^+$	1×10^{-8}	1830–2240	4.96 ± 0.01	(4.41 ± 0.02)	PSI	[78]
Mo	–	–	–	–	–	4.97	TC	[531]
Mo	In	In$^+$	1×10^{-7}	~1900–2300	5.02 ± 0.05	(4.33 ± 0.07)	PSI	[76,77]
Mo/SiO$_2$	Mo	–	?	~300 (~900)	–	5.05 ± 0.05	CPD	[3519,3687]
Mo[170]	–	(Mo$^+$)	?	2350–2500	5.1 ± 0.1*	(4.20 ± 0.02)	PSI	[132]
Mo[170]	–	(Mo$^+$)	~10^{-7}	~2100–2400	5.1 ± 0.4	(4.33 ± 0.07)	PSI	[77]
Mo	KCl	K$^+$	2×10^{-7}	~2000–2100	5.10 ± 0.07	(4.39 ± 0.05)	PSI	[23,39,2422]
Mo[170]	–	(Mo$^+$)	?	2350–2500	5.4 ± 0.1*	(4.37 ± 0.02)	PSI	[132]
Mo	–	–	–	–	–	5.80	TC	[2629]
Mo/W	Mo	–	?	~300	–	6.0	FE	[2225]
Recommended	–	–	–	–	**5.03 ± 0.06**	**4.31 ± 0.02**	–	–

43. Technetium Tc

hcp

Tc(0001)	–	–	–	–	–	4.69	TC	[4004]
Tc(0001)	–	–	–	–	–	4.95	TC	[4004]
Tc(0001)	–	–	–	–	–	5.15	TC	[4005]
Tc(0001)	–	–	–	–	–	5.30	TC	[321]

Table 1 (*continued*)

Surface	Beam	Ion	P_r (Torr)	T (K)	ϕ^+ (eV)	ϕ^e (eV)	Meth.	Refs.
Tc(0001)	–	–	–	–	–	5.36	TC	[334]
Tc(1010)	–	–	–	–	–	4.31	TC	[4005]
Tc(1010)	–	–	–	–	–	4.50	TC	[4004]
Tc(1010)	–	–	–	–	–	4.83	TC	[4004]
Tc(1010)	–	–	–	–	–	5.13	TC	[321]
Tc(1011)	–	–	–	–	–	4.70	TC	[4004]
Tc(1011)	–	–	–	–	–	5.05	TC	[4004]
Tc(1012)	–	–	–	–	–	4.31	TC	[4004]
Tc(1012)	–	–	–	–	–	4.67	TC	[4004]
Tc(1013)	–	–	–	–	–	4.25	TC	[4004]
Tc(1013)	–	–	–	–	–	4.60	TC	[4004]
Tc(1121)	–	–	–	–	–	4.09	TC	[4004]
Tc(1121)	–	–	–	–	–	4.44	TC	[4004]
Tc(1122)	–	–	–	–	–	4.28	TC	[4004]
Tc(1122)	–	–	–	–	–	4.63	TC	[4004]
Tc(1123)	–	–	–	–	–	4.23	TC	[4004]
Tc(1123)	–	–	–	–	–	4.56	TC	[4004]
Tc(1124)	–	–	–	–	–	4.43	TC	[321]
Tc(2130)	–	–	–	–	–	4.26	TC	[4004]
Tc(2130)	–	–	–	–	–	4.58	TC	[4004]
Tc(3140)	–	–	–	–	–	4.32	TC	[4004]
Tc(3140)	–	–	–	–	–	4.64	TC	[4004]
Tc	–	–	–	–	–	3.91	TC	[3476]
Tc	–	–	–	–	–	4.01	TC	[3476]
Tc[160]	–	–	–	–	–	4.4	TC	[1355]
Tc	–	–	–	–	–	4.41	TC	[3476]
Tc(wire)	–	–	5×10^{-8}	1970–2120	–	4.51 ± 0.02	TE	[3700]
Tc	–	–	–	–	–	4.66	TC	[3318]
Tc	–	–	–	–	–	4.66 ± 0.02	TC	[1045]
Tc	–	–	–	–	–	4.67	TC	[2949]
Tc	–	–	–	–	–	4.67	TC	[3318]
Tc	–	–	–	–	–	4.7	TC	[706]
Tc	–	–	–	–	–	4.8	TC	[298]
Tc	–	–	–	–	–	4.82	TC	[4270]
Tc	–	–	–	–	–	4.86 ± 0.01	TC	[895]
Tc	–	–	–	–	–	4.88 ± 0.05	TC	[895]
Tc	–	–	$\leq 1 \times 10^{-10}$	~300	–	4.9 ± 0.4	PE	[1695]
Tc	–	–	$\leq 1 \times 10^{-10}$	~300	–	5.1 ± 0.1	PE	[1695]
Tc	–	–	–	–	–	5.2	TC	[944]
Recommended	–	–	–	–	–	**4.67 ± 0.02**	–	–

44. Ruthenium Ru[435]

hcp

Surface	Beam	Ion	P_r (Torr)	T (K)	ϕ^+ (eV)	ϕ^e (eV)	Meth.	Refs.
Ru(0001)[143]	–	–	?	?	–	4.5	FE	[2348]
Ru(0001)	–	–	~10^{-10}	~300	–	4.7	PE	[4340]
Ru(0001)	–	–	–	–	–	4.97	TC	[4004]
Ru(0001)	–	–	–	–	–	5.0	TC	[3011]
Ru(0001)	–	–	–	–	–	5.03	TC	[343]
Ru(0001)	–	–	~10^{-9}	1600	–	5.04 ± 0.07	TE	[3087]
Ru(0001)	–	–	$<2 \times 10^{-10}$	~300	–	5.1	PE	[2374]
Ru(0001)	–	–	–	–	–	5.18	TC	[3734]
Ru(0001)/Mo(110)	Ru	–	1×10^{-10}	~300 (800)	–	5.26	CPD	[2876]
Ru(0001)	–	–	$\leq 1 \times 10^{-10}$	~300	–	5.26	PE	[1606]
Ru(0001)	–	–	4×10^{-11}	100	–	5.27 ± 0.08	PE	[344]
Ru(0001)	–	–	–	–	–	5.3	TC	[1707]
Ru(0001)	–	–	$\leq 1 \times 10^{-10}$	~300	–	5.3	PE	[1614]
Ru(0001)[175]	–	–	–	–	–	5.3	TC	[542]

Table 1 (*continued*)

Surface	Beam	Ion	P_r (Torr)	T (K)	ϕ^+ (eV)	ϕ^e (eV)	Meth.	Refs.
Ru(0001)	–	–	$<10^{-10}$	~300	–	5.3	PE	[3782]
Ru(0001)	–	–	?	~300	–	5.3 ± 0.1	PE	[3359]
Ru(0001)	–	–	?	~300	–	5.30	PE	[4020]
Ru(0001)	–	–	–	–	–	5.31	TC	[4004]
Ru(0001)	–	–	–	–	–	5.37	TC	[4005]
Ru(0001)	–	–	–	–	–	5.37	TC	[3473]
Ru(0001)	–	–	1×10^{-10}	100	–	5.38	PE	[759]
Ru(0001)	–	–	–	–	–	5.4	TC	[456]
Ru(0001)[175]	–	–	~10^{-11}	~300	–	5.4	PE	[542]
Ru(0001)	–	–	$<2 \times 10^{-10}$	115	–	5.4 ± 0.1	PE	[4335]
Ru(0001)	–	–	$<8 \times 10^{-11}$	130	–	5.4 ± 0.1	PE	[528]
Ru(0001)	–	–	~10^{-10}	~300	–	5.4 ± 0.1	PE	[2138]
Ru(0001)	–	–	3×10^{-10}	295	–	5.40	CPD	[1822,1827]
Ru(0001)	–	–	~10^{-9}	~1600–2000	–	5.40 ± 0.07	TE	[3085,3087,3096]
Ru(0001)	–	–	?	?	–	5.42	?	[2652]
Ru(0001)	–	–	–	–	–	5.43	TC	[1106]
Ru(0001)	–	–	~10^{-10}	~300	–	5.45	PE	[4199]
Ru(0001)	–	–	–	–	–	5.46	TC	[3224]
Ru(0001)/Mo(110)	Ru	–	1×10^{-10}	~300 (800)	–	5.48	CPD	[2876]
Ru(0001)	–	–	1×10^{-10}	100	–	5.50 ± <0.10	PE	[672]
Ru(0001)[143]	–	–	1×10^{-10}	100	–	5.52 ± 0.1	PE	[529,759,2266, 3198]
Ru(0001)	–	–	$\leq 2 \times 10^{-10}$	85	–	5.53	CPD	[2176]
Ru(0001)	–	–	?	?	–	5.58	?	[3160]
Ru(0001)	–	–	–	–	–	5.84	TC	[334]
Recommended	–	–	–	–	–	**5.35 ± 0.06**	–	–
Ru(1010)	–	–	–	–	–	4.59	TC	[4005]
Ru(1010)	–	–	3×10^{-10}	~300	–	4.6 ± 0.1	PE	[846]
Ru(1010)	–	–	–	–	–	4.79	TC	[4004]
Ru(1010)	–	–	–	–	–	4.88	TC	[703]
Ru(1010)	–	–	~10^{-9}	1600	–	5.08 ± 0.05	TE	[3087]
Ru(1010)	–	–	–	–	–	5.13	TC	[4004]
Ru(1010)	–	–	~10^{-9}	~1600–1900	–	5.14 ± 0.05	TE	[3085,3087,3096]
Recommended	–	–	–	–	–	**4.9 ± 0.2**	–	–
Ru(1011)	–	–	–	–	–	4.91	TC	[4004]
Ru(1011)	–	–	–	–	–	5.26	TC	[4004]
Ru(1012)	–	–	–	–	–	4.50	TC	[4004]
Ru(1012)	–	–	–	–	–	4.85	TC	[4004]
Ru(1013)	–	–	–	–	–	4.45	TC	[4004]
Ru(1013)	–	–	–	–	–	4.82	TC	[4004]
Ru(1121)	–	–	–	–	–	4.39	TC	[4004]
Ru(1121)	–	–	–	–	–	4.76	TC	[4004]
Ru(1122)[435]	–	–	~10^{-9}	~1510–1540	–	4.12 ± 0.05$^\beta$	TE	[3686]
Ru(1122)[435]	–	–	~10^{-9}	~1400–1500	–	4.45 ± 0.05$^\alpha$	TE	[3686]
Ru(1122)[435]	–	–	~10^{-9}	~1580–1730	–	4.45 ± 0.05$^\gamma$	TE	[3686]
Ru(1123)	–	–	–	–	–	4.43	TC	[4004]
Ru(1123)	–	–	–	–	–	4.80	TC	[4004]
Ru(1124)	–	–	~10^{-9}	~1600–1900	–	4.52 ± 0.05	TE	[3087,3096]
Ru(1124)	–	–	~10^{-9}	1600	–	4.55 ± 0.05	TE	[3085,3087]
Ru(1125)[435]	–	–	~10^{-9}	~1510–1540	–	4.10 ± 0.05$^\beta$	TE	[3686]
Ru(1125)[435]	–	–	~10^{-9}	~1400–1480	–	4.65 ± 0.05$^\alpha$	TE	[3686]
Ru(1125)[435]	–	–	~10^{-9}	~1560–1730	–	4.65 ± 0.05$^\gamma$	TE	[3686]
Ru(2130)	–	–	–	–	–	4.47	TC	[4004]
Ru(2130)	–	–	–	–	–	4.86	TC	[4004]
Ru(3140)	–	–	–	–	–	4.37	TC	[4004]
Ru(3140)	–	–	–	–	–	4.96	TC	[4004]
Ru	–	–	–	–	–	4.10	TC	[3476]
Ru	–	–	–	–	–	4.21	TC	[3476]

Table 1 (*continued*)

Surface	Beam	Ion	P_r (Torr)	T (K)	ϕ^+ (eV)	ϕ^e (eV)	Meth.	Refs.
Ru	–	–	7×10^{-10}	~300	–	4.3	PE	[2328]
Ru/glass	Ru	–	$<1 \times 10^{-10}$	78	–	4.50	PE	[414]
Ru/glass	Ru	–	5×10^{-10}	78	–	4.51	PE	[1495]
Ru/glass[363]	Ru	–	$\sim10^{-10}$	~78	–	4.52	PE	[436]
Ru	–	–	?	~300	–	4.52	CPD	[2297]
Ru	–	–	–	–	–	4.52	TC	[1399]
Ru/glass	Ru	–	$<5 \times 10^{-10}$	78	–	4.52 ± 0.03	PE	[1256]
Ru/Mo	Ru	–	$\sim10^{-8}$	~1600–2000	–	4.55 ± 0.05	TE	[794,2824]
Ru	–	–	? (Cs)	?	–	4.57	TE	[2099]
Ru	–	–	? (Cs)	?	–	4.57	TE	[2936]
Ru/Mo	Ru	–	$\sim10^{-4}$–1 (Cs)	≥2000	–	4.57 ± 0.05	TE	[794,2824]
Ru	–	–	–	–	–	4.60	TC	[1066]
Ru	–	–	–	–	–	4.61	TC	[3476]
Ru/H$_f$SiO$_x$/Si	Ru	–	2×10^{-10}	~300{620}	–	4.62	PE	[4186]
Ru	–	–	$\sim10^{-9}$	?	–	4.64	TE	[3112]
Ru	–	–	–	–	–	4.66	TC	[3318]
Ru	–	–	–	–	–	4.67	TC	[3318]
Ru	–	–	–	–	–	4.68	TC	[2949]
Ru	–	–	$\sim10^{-9}$	1600	–	4.68	TE	[3087,3096]
Ru	–	–	–	–	–	4.7	TC	[706]
Ru/glass	Ru	–	$<1 \times 10^{-10}$	78 (293)	–	4.71	PE	[414]
Ru	–	–	?	~300	–	4.730 ± 0.01	CPD	[13]
Ru/H$_f$SiO$_x$/Si	Ru	–	2×10^{-10}	~300 (700)	–	4.74 ± 0.01	CPD	[4186]
Ru	–	–	$\sim10^{-8}$	~1600–2300	–	4.75	TE	[1776,2322,2327]
Ru/82%Ru–Ta	–	–	$\sim10^{-8}$	~1700 (~2200)	–	4.75	TE	[2327]
Ru/glass	Ru	–	$<1 \times 10^{-10}$	78 (373)	–	4.76	PE	[414]
Ru	–	–	–	–	–	4.80	TC	[3264,3265,3267]
Ru	–	–	–	–	–	4.81	TC	[298]
Ru/SiO$_2$/Si	Ru	–	2×10^{-10}	~300 (700)	–	4.81	CPD	[4186]
Ru/glass	Ru	–	$<1 \times 10^{-10}$	78 (473)	–	4.82	PE	[414]
Ru	–	–	–	–	–	4.83	TC	[3224]
Ru/glass	Ru	–	$<5 \times 10^{-10}$	78 (373)	–	4.83 ± 0.03	PE	[1256]
Ru/SiO$_2$	Ru	–	?	~300	–	4.84 ± 0.1	CPD	[2906]
Ru/W	Ru	–	?	~300	–	4.865 ± 0.005	CPD	[13]
Ru	–	–	?	?	–	4.89	TE	[2105]
Ru/glass	Ru	–	$<1 \times 10^{-10}$	78 (573)	–	4.89	PE	[414]
Ru	–	–	–	–	–	4.9*	TC	[1955]
Ru	–	–	–	–	–	5.1	TC	[944]
Ru/HfO$_2$/SiO$_x$/Si	Ru	–	?	~300 (593)	–	5.1	CPD	[1835]
Ru/quartz[363]	Ru	–	$<5 \times 10^{-10}$	~78 (≥2800)	–	5.10 ± 0.05	PE	[436,1256]
Ru/glass	Ru	–	5×10^{-10}	78 (800)	–	5.11	PE	[1495]
Ru/?	Ru	–	7×10^{-10}	~300	–	5.4	PE	[2328]
Ru	–	–	–	–	–	5.46	TC	[1744]
Recommended	–	–	–	–	–	**4.71 ± 0.05**	–	–

45. Rhodium Rh

fcc

Surface	Beam	Ion	P_r (Torr)	T (K)	ϕ^+ (eV)	ϕ^e (eV)	Meth.	Refs.
Rh(100)	–	–	–	–	–	4.4	TC	[1109]
Rh(100)	–	–	?	~300	–	4.6 ± 0.1	?	[1257]
Rh(100)	–	–	–	–	–	$4.8 \pm <0.3$	TC	[1014,1108]
Rh(100)	–	–	–	–	–	4.91	TC	[980]
Rh(100)	–	–	–	–	–	4.92	TC	[981]
Rh(100)	–	–	1×10^{-10}	~300	–	4.94 ± 0.03	PE	[2396]
Rh(100)	–	–	–	–	–	4.99	TC	[321]
Rh(100)	–	–	–	–	–	5.040	TC	[4091]
Rh(100)	–	–	–	–	–	5.087	TC	[2229,2447]
Rh(100)	–	–	2×10^{-10}	100	–	5.11	PE	[1017,2859,3821]
Rh(100)	–	–	–	–	–	5.15	TC	[1008]
Rh(100)	–	–	–	–	–	5.16	TC	[705]
Rh(100)	–	–	–	–	–	5.17	TC	[2912]
Rh(100)	–	–	–	–	–	5.17	TC	[4333,4334]
Rh(100)	–	–	?	~300	–	5.2	PE	[2158]
Rh(100)	–	–	?	~300	–	5.2 ± 0.2	PE	[1127]
Rh(100)	–	–	–	–	–	5.24	TC	[1928]
Rh(100)	–	–	–	–	–	5.25	TC	[320,1012,1015]
Rh(100)	–	–	–	–	–	5.26	TC	[981]
Rh(100)	–	–	–	–	–	5.30	TC	[980]
Rh(100)[176]	–	–	–	–	–	5.36	TC	[1258]
Rh(100)	–	–	$\sim10^{-11}$	~300	–	5.38 ± 0.05	FE	[853]

Table 1 (*continued*)

Surface	Beam	Ion	P_r (Torr)	T (K)	ϕ^+ (eV)	ϕ^e (eV)	Meth.	Refs.
Rh(100)	–	–	?	40–298	–	5.40 ± 0.02	CPD	[2832]
Rh(100)	–	–	<10⁻¹⁰	80, 144, 298	–	5.41 ± 0.01	FE	[1010]
Rh(100)	–	–	–	–	–	5.43 ± 0.1	TC	[916]
Rh(100)	–	–	–	–	–	5.45	TC	[4228]
Rh(100)	–	–	–	–	–	5.46	TC	[4228]
Rh(100)	–	–	–	–	–	5.49	TC	[982]
Rh(100)	–	–	–	–	–	5.5	TC	[1009,1016]
Rh(100)[176]	–	–	–	–	–	5.57	TC	[1258]
Rh(100)	–	–	–	–	–	5.6 ± >0.2	TC	[1016,1909]
Recommended	–	–	–	–	–	**5.24 ± 0.07**	–	–
Rh(110)	–	–	–	–	–	4.53	TC	[2442]
Rh(110)	–	–	–	–	–	4.57	TC	[2442]
Rh(110)	–	–	–	–	–	4.59	TC	[980]
Rh(110)	–	–	–	–	–	4.615	TC	[2229,2447]
Rh(110)	–	–	–	–	–	4.62	TC	[2442]
Rh(110)	–	–	–	–	–	4.635	TC	[4091]
Rh(110)	–	–	–	–	–	4.67	TC	[2912]
Rh(110)	–	–	–	–	–	4.69	TC	[321]
Rh(110)[177]	–	–	~10⁻¹¹	~300	–	4.70 ± 0.05	FE	[853]
Rh(110)	–	–	–	–	–	4.72	TC	[2442]
Rh(110)	–	–	–	–	–	4.77	TC	[523]
Rh(110)	–	–	–	–	–	4.78	TC	[523]
Rh(110)	–	–	1 × 10⁻¹⁰	80	–	4.8	FE	[2146,2163]
Rh(110)[177]	–	–	~10⁻¹¹	~300	–	4.80 ± 0.05	FE	[853]
Rh(110)	–	–	<10⁻¹⁰	144, 195	–	4.86 ± 0.01	FE	[1010]
Rh(110)	–	–	–	–	–	4.94	TC	[320,980]
Rh(110)	–	–	–	–	–	4.98	TC	[523]
Rh(110)	–	–	–	–	–	4.99	TC	[523]
Rh(110)	–	–	–	–	–	5.07	TC	[4228]
Rh(110)	–	–	?	40–298	–	5.12 ± 0.02	CPD	[2832]
Recommended	–	–	–	–	–	**4.75 ± 0.06**	–	–
Rh(111)[178]	–	–	~10⁻¹¹	~300	–	4.95 ± 0.05	FE	[853]
Rh(111)	–	–	1 × 10⁻¹⁰	~300	–	5.04 ± 0.03	PE	[2396]
Rh(111)[179]	–	–	~10⁻¹⁰	~300	–	5.1	PE	[1544,1546]
Rh(111)	–	–	–	–	–	5.105	TC	[2229,2447]
Rh(111)	–	–	–	–	–	5.11	TC	[1722]
Rh(111)	–	–	–	–	–	5.12	TC	[2068]
Rh(111)	–	–	–	–	–	5.132	TC	[4008]
Rh(111)	–	–	–	–	–	5.138	TC	[4091]
Rh(111)	–	–	–	–	–	5.20	TC	[2913]
Rh(111)	–	–	–	–	–	5.21	TC	[2912]
Rh(111)	–	–	–	–	–	5.23	TC	[1013]
Rh(111)	–	–	–	–	–	5.26	TC	[3369]
Rh(111)	–	–	1 × 10⁻¹⁰	80	–	5.3	FE	[2146,2163]
Rh(111)	–	–	4 × 10⁻¹¹	40	–	5.3	PE	[1019]
Rh(111)/Mo(110)[180]	Rh	–	7 × 10⁻¹¹	~300	–	5.36	PE	[1035]
Rh(111)	–	–	–	–	–	5.39	TC	[321]
Rh(111)	–	–	<1 × 10⁻¹⁰	~300	–	5.4	PE	[568,2282]
Rh(111)	–	–	<5 × 10⁻¹¹	~300	–	5.4	PE	[1018]
Rh(111)	–	–	4 × 10⁻¹¹	~300	–	5.4 ± 0.1	PE	[2048]
Rh(111)	–	–	–	–	–	5.40	TC	[1011]
Rh(111)	–	–	–	–	–	5.44	TC	[320,1178]
Rh(111)	–	–	–	–	–	5.44	TC	[2534]
Rh(111)/W(110)	Rh	–	4 × 10⁻¹¹	350	–	5.47	CPD	[2408]
Rh(111)	–	–	–	–	–	5.56	TC	[4228]
Rh(111)	–	–	–	–	–	5.59	TC	[4228]
Rh(111)	–	–	–	–	–	5.59	TC	[1011]
Rh(111)	–	–	<10⁻¹⁰	298	–	5.59 ± 0.01	FE	[1010]
Rh(111)	–	–	–	–	–	5.6	TC	[1009,1011]
Rh(111)	–	–	~10⁻¹¹	80	–	5.6	FE	[3460]
Rh(111)	–	–	<10⁻¹⁰	195	–	5.60 ± 0.01	FE	[1010]
Rh(111)	–	–	1 × 10⁻¹⁰	45	–	5.60 ± 0.04	PE	[1128,1204,2280]
Rh(111)	–	–	<10⁻¹⁰	195	–	5.61 ± 0.01	FE	[1010]
Rh(111)	–	–	–	–	–	5.63	TC	[1011]
Rh(111)	–	–	–	–	–	5.64	TC	[1011]
Rh(111)	–	–	?	40–298	–	5.66 ± 0.02	CPD	[2832]
Rh(111)	–	–	<10⁻¹⁰	144	–	5.67 ± 0.01	FE	[1010]
Rh(111)	–	–	<10⁻¹⁰	80	–	5.69 ± 0.01	FE	[1010]

Table 1 (*continued*)

Surface	Beam	Ion	P_r (Torr)	T (K)	ϕ^+ (eV)	ϕ^e (eV)	Meth.	Refs.
Rh(111)	–	–	–	–	–	5.79	TC	[1011]
Rh(111)	–	–	–	–	–	5.91	TC	[334,3179]
Rh(111)	–	–	–	–	–	6.51	TC	[1011]
Recommended	–	–	–	–	–	**5.40 ± 0.08**	–	–
Rh(112)	–	–	$\sim 10^{-11}$	80	–	5.1	FE	[3460]
Rh(113)	–	–	1×10^{-10}	80	–	5.0	FE	[2146,2163]
Rh(210)	–	–	$\sim 10^{-11}$	~ 300	–	4.64 ± 0.05	FE	[853,2511]
Rh(310)	–	–	$\sim 10^{-11}$	~ 300	–	4.76 ± 0.05	FE	[853,2511]
Rh(320)	–	–	1×10^{-10}	80	–	4.70	FE	[2146,2163]
Rh(321)	–	–	$\sim 10^{-11}$	~ 300	–	4.75 ± 0.05	FE	[853,2511]
Rh(410)	–	–	$\sim 10^{-11}$	~ 300	–	4.90 ± 0.05	FE	[853]
Rh(430)	–	–	$\sim 10^{-11}$	~ 300	–	4.72 ± 0.05	FE	[853,2511]
Rh(520)	–	–	$\sim 10^{-11}$	~ 300	–	4.74 ± 0.05	FE	[853,2511]
Rh(531)	–	–	$\sim 10^{-11}$	~ 300	–	4.69 ± 0.05	FE	[853,2511]
Rh	–	–	–	–	–	4.19	TC	[3476]
Rh	–	–	–	–	–	4.35	TC	[3476]
Rh	–	–	?	~ 300	–	4.52	CPD	[2297]
Rh	–	–	3×10^{-11}	~ 300	–	4.53	FE	[2227]
Rh/Nb(110)	–	–	–	–	–	4.56	TC	[2913]
Rh	–	–	–	–	–	4.57	TC	[1399]
Rh	–	–	$\sim 10^{-8}$	513	–	4.57 ± 0.09	PE	[1757]
Rh	–	–	$\sim 10^{-8}$	$\sim 1300–1500$	–	4.58 ± 0.09	TE	[1757]
Rh	–	–	?	?	–	4.6	TE	[3402]
Rh	–	–	–	–	–	4.62	TC	[1066]
Rh	–	–	–	–	–	4.64	TC	[3318]
Rh	–	–	–	–	–	4.7	TC	[3318]
Rh	–	–	3×10^{-9}	$\sim 1100–1700$	–	4.72	TE	[159]
Rh	–	–	–	–	–	4.74	TC	[2949]
Rh	–	–	–	–	–	4.76	TC	[3476]
Rh	–	–	–	–	–	4.8	TC	[706]
Rh	–	–	–	–	–	4.80	TC	[298]
Rh	–	–	$\leq 2 \times 10^{-6}$	$\sim 1150–1300$	–	4.80	TE	[3396]
Rh	–	–	1×10^{-10}	~ 300	–	4.85	PE	[3125]
Rh/glass	Rh	–	$\sim 10^{-10}$	78	–	4.87	PE	[2719]
Rh/glass	Rh	–	$< 1 \times 10^{-10}$	78	–	4.88	PE	[414,2723]
Rh	–	–	?	$\sim 1550–1950$	–	4.9	TE	[668]
Rh/W(110)	Rh	–	5×10^{-11}	$\sim 300\ (1200)$	–	4.9*	CPD	[2420]
Rh/W(111)	Rh	–	$\leq 10^{-8}$	~ 300	–	4.90 ± 0.04*	CPD	[2338]
Rh/glass	Rh	–	$< 1 \times 10^{-10}$	78 (293)	–	4.98	PE	[414,2722,2723]
Rh	–	–	–	–	–	4.99	TC	[3264]
Rh/quartz	Rh	–	5×10^{-11}	~ 300	–	5.0	PE	[1022]
Rh	–	–	–	–	–	5.0	TC	[2583]
Rh	–	–	1×10^{-10}	~ 300	–	5.0	PE	[570,2368,3125]
Rh/glass	Rh	–	$\sim 10^{-10}$	78 (293)	–	5.06	PE	[2719]
Rh/W(110)	Rh	–	3×10^{-11}	200–560	–	5.1*	?	[1930]
Rh	–	–	–	–	–	5.1*	TC	[1955]
Rh/glass	Rh	–	$\sim 10^{-10}$	78 (373)	–	5.11	PE	[414,2719,2723]
Rh/W(100)	Rh	–	$\leq 10^{-8}$	~ 300	–	5.12 ± 0.03*	CPD	[2338]
Rh	–	–	–	–	–	5.15 ± 0.05	TC	[1256]
Rh/glass	Rh	–	$< 3 \times 10^{-10}$	78 (458)	–	5.18	PE	[414,2723]
Rh	–	–	$< 5 \times 10^{-9}$	?	–	5.2 ± 0.1	TE	[647]
Rh/HfO$_2$/Si[181]	Rh(ac)$_3$	–	5×10^{-6}	$\sim 300\ (423)$	–	5.25	CPD	[2908]
Rh	–	–	?	?	–	5.25	TE	[2105]
Rh	–	–	–	–	–	5.3	TC	[944]
Rh/SiO$_2$/Si[181]	Rh(ac)$_3$	–	5×10^{-6}	$\sim 300\ (423)$	–	5.43	CPD	[2908]
Rh/W(110)	Rh	–	$\leq 10^{-8}$	~ 300	–	5.51 ± 0.05*	CPD	[2338]
Recommended	–	–	–	–	–	**4.87 ± 0.07**	–	–

Table 1 (*continued*)

Surface	Beam	Ion	P_r (Torr)	T (K)	ϕ^+ (eV)	ϕ^e (eV)	Meth.	Refs.
				46. Palladium Pd				
fcc								
Pd(100)	–	–	–	–	–	4.3	TC	[2033]
Pd(100)	–	–	–	–	–	5.0	TC	[1023,1108,1109, 3126]
Pd(100)	–	–	?	~300	–	5.0 ± 0.2	PE	[1692]
Pd(100)	–	–	–	–	–	5.080	TC	[4091]
Pd(100)	–	–	–	–	–	5.11	TC	[4087]
Pd(100)	–	–	–	–	–	5.115	TC	[2229,2447]
Pd(100)	–	–	–	–	–	5.14	TC	[602,1008]
Pd(100)	–	–	–	–	–	5.16	TC	[4434]
Pd(100)/Fe(100)	–	–	–	–	–	5.2	TC	[2157]
Pd(100)	–	–	–	–	–	5.22	TC	[705]
Pd(100)	–	–	–	–	–	5.25	TC	[1024,3284]
Pd(100)	–	–	?	?	–	5.3	?	[1025]
Pd(100)	–	–	–	–	–	5.30	TC	[320,1012,1015, 1928]
Pd(100)	–	–	~10^{-11}	~300	–	5.5	PE	[2379]
Pd(100)[182]	–	–	–	–	–	5.50	TC	[704,795]
Pd(100)	–	–	–	–	–	5.50	TC	[2701]
Pd(100)	–	–	?	20	–	5.51	PE	[2642]
Pd(100)	–	–	–	–	–	5.54	TC	[2701]
Pd(100)	–	–	<10^{-9}	~300	–	5.55	PE	[1424]
Pd(100)[183]	–	–	2×10^{-11}	40–140	–	5.55 ± <0.1	PE	[1129]
Pd(100)	–	–	–	–	–	5.56	TC	[321]
Pd(100)	–	–	–	–	–	5.6	TC	[1734]
Pd(100)	–	–	?	80	–	5.60	PE	[3176]
Pd(100)	–	–	–	–	–	5.61	TC	[2405]
Pd(100)	–	–	?	?	–	5.65	?	[1809]
Pd(100)	–	–	1×10^{-10}	100	–	5.65 ± <0.1	PE	[672,914,1026, 3449]
Pd(100)	–	–	–	–	–	5.68	TC	[1259]
Pd(100)	–	–	–	–	–	5.72	TC	[704]
Pd(100)	–	–	?	110	–	5.8	PE	[2980]
Pd(100)	–	–	2×10^{-10}	~300	–	5.8 ± 0.2*	PE	[997]
Pd(100)	–	–	–	–	–	5.80	TC	[1027]
Pd(100)[182]	–	–	–	–	–	5.80	TC	[704,795]
Pd(100)	–	–	–	–	–	5.81	TC	[2405]
Pd(100)	–	–	–	–	–	5.82	TC	[704]
Pd(100)	–	–	~10^{-11}	77	–	5.9	PE	[3845]
Pd(100)	–	–	–	–	–	5.96	TC	[334]
Pd(100)	–	–	–	–	–	6.11	TC	[1259]
Recommended	–	–	–	–	–	**5.48 ± 0.04**	–	–
Pd(110)	–	–	–	–	–	4.781	TC	[2229,2447]
Pd(110)	–	–	–	–	–	4.860	TC	[4091]
Pd(110)	–	–	–	–	–	4.87	TC	[4087,4410]
Pd(110)	–	–	–	–	–	4.88	TC	[2916]
Pd(110)	–	–	–	–	–	4.90	TC	[602]
Pd(110)	–	–	–	–	–	4.98	TC	[602]
Pd(110)[184]	–	–	1×10^{-10}	100	–	~5	PE	[610]
Pd(110)	–	–	–	–	–	5.13	TC	[320]
Pd(110)	–	–	–	–	–	5.16	TC	[1931]
Pd(110)	–	–	?	110	–	5.2	PE	[2980]
Pd(110)	–	–	?	~300	–	5.2	PE	[1243]
Pd(110)[184]	–	–	1×10^{-10}	100	–	5.20 ± <0.1	PE	[672,914,1026, 3444]
Pd(110)	–	–	–	–	–	5.24	TC	[321]
Pd(110)	–	–	1×10^{-10}	100	–	5.25 ± 0.1	PE	[3449]
Pd(110)/Al(110)[185]	Pd	–	1×10^{-10}	~300	–	5.5	PE	[3495]
Pd(110)	–	–	4×10^{-10}	~300	–	5.83	PE	[1599]
Recommended	–	–	–	–	–	**5.12 ± 0.09**	–	–
Pd(111)	–	–	–	–	–	5.165	TC	[4308]
Pd(111)	–	–	–	–	–	5.18	TC	[602]
Pd(111)	–	–	–	–	–	5.198	TC	[2229,2447]
Pd(111)	–	–	–	–	–	5.20	TC	[2063]
Pd(111)	–	–	–	–	–	5.22	TC	[1028,1179]

Table 1 (*continued*)

Surface	Beam	Ion	P_r (Torr)	T (K)	ϕ^+ (eV)	ϕ^e (eV)	Meth.	Refs.
Pd(111)	–	–	–	–	–	5.23	TC	[4091]
Pd(111)	–	–	–	–	–	5.239	TC	[3657]
Pd(111)	–	–	–	–	–	5.25	TC	[1029,3991]
Pd(111)	–	–	–	–	–	5.25	TC	[4087,4410]
Pd(111)	–	–	–	–	–	5.26	TC	[1179]
Pd(111)	–	–	–	–	–	5.27	TC	[2913]
Pd(111)	–	–	–	–	–	5.30	TC	[1722]
Pd(111)	–	–	–	–	–	5.31	TC	[2068]
Pd(111)	–	–	–	–	–	5.33	TC	[3369]
Pd(111)	–	–	$<2 \times 10^{-10}$	~300	–	5.44 ± 0.03	PE	[985]
Pd(111)/Nb(110)	Pd	–	?	~300	–	5.48 ± 0.05*	PE	[3439]
Pd(111)/W(110)	Pd	–	$<1 \times 10^{-10}$	~300	–	5.5	CPD	[2857,3123]
Pd(111)/Si(111)	Pd	–	~1×10^{-10}	298 (423)	–	5.5	PE	[2972]
Pd(111)/Ta(111)	Pd	–	$<3 \times 10^{-10}$	~300	–	5.5	CPD	[3232]
Pd(111)	–	–	–	–	–	5.53	TC	[320,2534]
Pd(111)[182]	–	–	–	–	–	5.53	TC	[704]
Pd(111)	–	–	–	–	–	5.53	TC	[1720]
Pd(111)/W(100)	Pd	–	$<5 \times 10^{-11}$	~300	–	5.55	CPD	[2847]
Pd(111)/Mo(110)	Pd	–	$\leq 7 \times 10^{-11}$	~300	–	5.55	CPD	[2861]
Pd(111)	–	–	$<2 \times 10^{-10}$	27, 90	–	5.55	CPD	[4107]
Pd(111)	–	–	~1×10^{-10}	~300	–	5.55 ± 0.1	PE	[998]
Pd(111)	–	–	–	–	–	5.57	TC	[2916]
Pd(111)	–	–	–	–	–	5.58	TC	[1720]
Pd(111)	–	–	–	–	–	5.59	TC	[1720]
Pd(111)	–	–	–	–	–	5.59	TC	[4282]
Pd(111)	–	–	$<3 \times 10^{-10}$	~300	–	5.6	PE	[3645]
Pd(111)	–	–	~1×10^{-10}	80	–	5.6	PE	[616,1799]
Pd(111)	–	–	?	~300	–	5.6	PE	[1243]
Pd(111)	–	–	?	140	–	5.6*	PE	[4067]
Pd(111)/Nb(110)	Pd	–	~10^{-10}	~300	–	5.6	PE	[1864]
Pd(111)	–	–	–	–	–	5.61	TC	[4024]
Pd(111)/Cu(111)[186]	Pd	–	5×10^{-9}	~300	–	5.61	CPD	[3364]
Pd(111)/Al(111)	Pd	–	4×10^{-10}	~300	–	5.62 ± 0.02	CPD	[1826]
Pd(111)	–	–	–	–	–	5.63	TC	[1179]
Pd(111)	–	–	–	–	–	5.64	TC	[1028,1179]
Pd(111)	–	–	–	–	–	5.64	TC	[1931]
Pd(111)/Al(111)	Pd	–	4×10^{-10}	~300	–	5.66 ± 0.04*	CPD	[1826]
Pd(111)	–	–	–	–	–	5.67	TC	[1931]
Pd(111)	–	–	–	–	–	5.67	TC	[4174,4284]
Pd(111)	–	–	–	–	–	5.75	TC	[1259]
Pd(111)	–	–	–	–	–	5.76	TC	[704]
Pd(111)	–	–	–	–	–	5.8	TC	[624]
Pd(111)[182]	–	–	–	–	–	5.86	TC	[704,795]
Pd(111)	–	–	–	–	–	5.90	TC	[334,3179]
Pd(111)	–	–	1×10^{-10}	100	–	5.90 ± <0.1	PE	[672]
Pd(111)/Al(111)	Pd	–	5×10^{-11}	~300	–	5.95	PE	[1915]
Pd(111)	–	–	~1×10^{-10}	100	–	5.95 ± <0.1	PE	[914,1026,3449]
Pd(111)	–	–	–	–	–	6.02	TC	[321]
Pd(111)	–	–	–	–	–	6.18	TC	[1259]
Recommended	–	–	–	–	–	**5.58 ± 0.05**	–	–
Pd(113)	–	–	–	–	–	5.64	TC	[704,795]
Pd	–	–	–	–	–	4.01	TC	[3476]
Pd	–	–	–	–	–	4.17	TC	[3476]
Pd	–	–	1×10^{-8}	~300	–	4.2	PE	[3325]
Pd	–	–	–	–	–	4.38	TC	[2990]
Pd/Al/Ta(111)[398]	Pd	–	8×10^{-8}	~300	–	4.38	PE	[2271]
Pd/Si(111)	–	–	–	–	–	4.4	TC	[2219]
Pd/Nb(110)	–	–	–	–	–	4.44	TC	[2913]
Pd	–	–	–	–	–	4.47	TC	[2005]
Pd	–	–	?	~300	–	4.49	CPD	[2297]
Pd/Si	–	–	–	–	–	4.50	TC	[1653]
Pd	–	–	–	–	–	4.51	TC	[1976]
Pd	–	–	–	–	–	4.52	TC	[3318]
Pd/Si	–	–	–	–	–	4.53	TC	[1653]
Pd	–	–	–	–	–	4.54	TC	[3318]
Pd	–	–	~10^{-8}	~300	–	4.54 ± 0.20	PE	[3104]
Pd	–	–	–	–	–	4.57	TC	[3476]
Pd[187]	–	–	~10^{-10}	~300	–	4.6 ± 0.15	PE	[350]

Table 1 (*continued*)

Surface	Beam	Ion	P_r (Torr)	T (K)	ϕ^+ (eV)	ϕ^e (eV)	Meth.	Refs.
Pd$_6$(cluster)	–	–	–	–	–	4.61	TC	[2990]
Pd^{188}	–	–	?	~300	–	4.61*	CPD	[1953]
Pd^{188}	–	–	?	~300	–	4.69 ± 0.06*	CPD	[1953]
Pd/Nb(110)	–	–	–	–	–	4.72	TC	[722]
Pd	–	–	–	–	–	4.72	TC	[1066]
Pd	–	–	–	–	–	4.73	TC	[1399]
Pd	–	–	–	–	–	4.77	TC	[2949]
Pd/C	Pd	–	<2 × 10^{-10}	~300	–	4.8	PE	[2392]
Pd/W	Pd	–	~10^{-10}	1180	–	4.8	FE	[2779]
Pd	–	–	–	–	–	4.80	TC	[1590]
Pd	–	–	~10^{-5}	≤1200	–	4.80	TE	[2216]
Pd/W	Pd	–	<10^{-10}	800	–	4.83	FE	[2964]
Pd$_4$(cluster)	–	–	–	–	–	4.855	TC	[2990]
Pd$_4$(cluster)	–	–	–	–	–	4.858	TC	[2990]
Pd$_{10}$(cluster)	–	–	–	–	–	4.87	TC	[2990]
Pd$_7$(cluster)	–	–	–	–	–	4.875	TC	[2990]
Pd/glass	Pd	–	<3 × 10^{-10}	78	–	4.88 ± 0.02	PE	[1031]
Pd$_7$(cluster)	–	–	–	–	–	4.882	TC	[2990]
Pd/W(110)	Pd	–	?	90 (900)	–	4.9*	CPD	[3560]
Pd	–	–	–	–	–	4.9*	TC	[1955]
Pd/Re	Pd	–	<4 × 10^{-10}	~300	–	4.9*	CPD	[1586]
Pd/Nb	Pd	–	≤3 × 10^{-9}	~300	–	4.9*	CPD	[3263]
Pd/W(100)	Pd	–	?	~300 (≤500)	–	4.9*	PE	[2039]
Pd/W(110)	Pd	–	?	~300 (≤500)	–	4.9*	PE	[2039]
Pd	–	–	–	–	–	4.9	TC	[706]
Pd	–	–	–	–	–	4.9	TC	[944]
Pd	–	–	?	?	–	4.9	TE	[3402]
Pd/glass	Pd	–	<1 × 10^{-10}	78	–	4.90	PE	[414]
Pd/quartz	Pd	–	≤5 × 10^{-10}	78	–	4.93 ± 0.02	PE	[435]
Pd/glass	Pd	–	<10^{-9}	77	–	4.95	PE	[2763,3046,3052]
Pd/Ta^{187}	Pd	–	~10^{-10}	~300	–	4.95 ± 0.05	PE	[350]
Pd	–	–	?	~300	–	4.96	PE	[1760]
Pd$_7$(cluster)	–	–	–	–	–	4.96	TC	[2990]
Pd^{264}	–	–	–	400	–	4.966	TC	[3586]
Pd^{264}	–	–	<10^{-7}	400	–	4.97	PE	[1189]
Pd^{264}	–	–	<10^{-7}	925	–	4.98	PE	[1189]
Pd^{264}	–	–	–	305–1078^E	–	4.985 ± 0.016	TC	[3586]
Pd^{264}	–	–	<10^{-7}	~1200–1400	–	4.99 ± 0.04	TE	[1189]
Pd^{264}	–	–	–	925	–	4.997	TC	[3586]
Pd/Si(111)	Pd	–	1 × 10^{-10}	~300	–	5.0*	CPD	[2732]
Pd/W	Pd	–	~10^{-10}	1180	–	5.0	FE	[2779,2780]
Pd/Ru(0001)	–	–	–	–	–	5.00	TC	[2554]
Pd	–	–	–	–	–	5.00	TC	[3264,3265,3267]
Pd	–	–	–	–	–	5.01	TC	[3264]
Pd/Ta(110)	–	–	–	–	–	5.05	TC	[3473]
Pd/glass	Pd	–	<3 × 10^{-10}	77 (298)	–	5.05 ± 0.03	PE	[1031]
Pd/cnt/Si(111)^{25}	–	–	~10^{-10}	~300	–	5.05 ± 0.06	PE	[3246]
Pd/Ta(112)	Pd	–	<1 × 10^{-10}	90, 300	–	5.06	CPD	[3314]
Pd/cnt/Si(111)^{25}	–	–	~10^{-10}	~300	–	5.06 ± 0.04	CPD	[3246]
Pd^{188}	–	–	?	~300	–	5.07 ± 0.01	CPD	[1953]
Pd	–	–	–	–	–	5.08	TC	[298]
Pd/W(110)	–	–	–	–	–	5.08	TC	[3473]
Pd/Re(0001)	–	–	–	–	–	5.09	TC	[3473]
Pd/W	Pd	–	~10^{-10}	980	–	5.1	FE	[2779]
Pd	–	–	–	–	–	5.1	TC	[2583]
Pd	–	–	–	–	–	5.1	TC	[1645]
Pd/Ta(110)^{398}	Pd	–	8 × 10^{-11}	~300	–	5.1	PE	[2271]
Pd/Mo(112)	Pd	–	<1 × 10^{-10}	100	–	5.1	CPD	[3210]
Pd/glass	Pd	–	~10^{-10}	293	–	5.11	PE	[1509]
Pd/glass	Pd	–	<1 × 10^{-10}	78 (293)	–	5.12	PE	[414]
Pd/quartz	Pd	–	≤5 × 10^{-10}	293	–	5.12 ± 0.03	PE	[435]
Pd/Cu(100)	Pd	–	2 × 10^{-10}	~300	–	5.14*	PE	[2041]
Pd/W(111)	Pd	–	<5 × 10^{-11}	~300	–	5.17	CPD	[2429]
Pd/SiO$_2$/Si	Pd	–	?	~300	–	5.18	CPD	[4330]
Pd/cnt/Si(111)^{25}	–	–	~10^{-10}	~300	–	5.19 ± 0.08	CPD	[3246]
Pd/Nb(100)	Pd	–	<1 × 10^{-10}	~300	–	5.2	CPD	[1253]
Pd	–	–	–	–	–	5.20	TC	[3016]
Pd/glass	Pd	–	<1 × 10^{-10}	78 (383)	–	5.20	PE	[414]
Pd/quartz	Pd	–	≤5 × 10^{-10}	293 (550)	–	5.20 ± 0.01	PE	[435]
Pd	–	–	<8 × 10^{-11}	~300	–	5.200 ± 0.100	CPD	[342]

Table 1 (*continued*)

Surface	Beam	Ion	P_r (Torr)	T (K)	ϕ^+ (eV)	ϕ^e (eV)	Meth.	Refs.
Pd/glass	Pd	–	$<1 \times 10^{-10}$	78 (483)	–	5.22	PE	[414,1031]
Pd/glass	Pd	–	$\sim10^{-10}$	293 (573)	–	5.22	PE	[1509]
Pd/glass	Pd	–	$<1 \times 10^{-10}$	78 (583)	–	5.22	PE	[414]
Pd	–	–	$<2 \times 10^{-10}$	27, 90	–	5.22	CPD	[4107]
Pd	–	–	–	–	–	5.22	TC	[3993]
Pd/Mo(111)	Pd	–	$\leq1 \times 10^{-10}$	300	–	5.24 ± 0.07*	CPD	[1836]
Pd	–	–	–	–	–	5.25	TC	[2205]
Pd/Al/Ta(110)[398]	Pd	–	8×10^{-11}	~300	–	5.25	PE	[2271]
Pd	–	–	–	–	–	5.27	TC	[3978]
Pd/Ru(0001)	–	–	–	–	–	5.29	TC	[3473]
Pd/Ir	Pd	–	$\sim10^{-9}$	~300	–	5.3	CPD	[417]
Pd/Mo(112)	Pd	–	$<1 \times 10^{-10}$	~300	–	5.3	CPD	[3210]
Pd	–	–	1×10^{-10}	100	–	5.30 ± <0.1	PE	[672]
Pd	–	–	$\sim10^{-10}$	90	–	5.4	PE	[3048]
Pd/Au(111)	Pd	–	$<1 \times 10^{-10}$	~300	–	5.4	PE	[3140]
Pd/Mo(111)	Pd	–	$\leq1 \times 10^{-10}$	~300	–	5.4	CPD	[1836]
Pd/Au(111)	Pd	–	$<1 \times 10^{-10}$	~300	–	5.4	PE	[3140]
Pd/glass	Pd	–	$<10^{-9}$	293 (388)	–	5.40	PE	[3046,3052]
Pd(fp)[149]	–	–	$<10^{-9}$	~300	–	5.45 ± 0.1	PE	[3190]
Pd/W(110)	Pd	–	$<2 \times 10^{-10}$	27, 90	–	5.46	CPD	[4107]
Pd/Ag(111)	–	–	–	–	–	5.49	TC	[1720]
Pd	–	–	5×10^{-9}	~300	–	5.5	PE	[1020]
Pd/Ta(111)	Pd	–	$<1 \times 10^{-10}$	~300	–	5.5	CPD	[3232]
Pd/Rh(100)	–	–	–	–	–	5.5	TC	[1009]
Pd/Ag(111)	–	–	–	–	–	5.51	TC	[1720]
Pd/Ru(0001)	Pd	–	1×10^{-10}	~300	–	5.53 ± 0.06*	TC	[2880]
Pd	–	–	$<10^{-9}$	~300	–	5.55 ± 0.05	PE	[2968]
Pd/quartz	Pd	–	$\sim10^{-10}$	~300	–	5.55 ± 0.1	PE	[304]
Pd	–	–	–	–	–	5.59	TC	[1744]
Pd/W(110)	Pd	–	?	90	–	5.6	PE	[2513,3563]
Pd/Si(111)	Pd	–	$\sim1 \times 10^{-10}$	298	–	5.6	PE	[1900,1906]
Pd/Ag(111)	Pd	–	$<4 \times 10^{-11}$	~300	–	5.6	PE	[3133]
Pd/Cu(111)	Pd	–	$<1 \times 10^{-10}$	~300	–	5.6 ± 0.2	CPD	[1245,3417]
Pd/Ag(100)	–	–	–	–	–	5.67	TC	[2405]
Pd	–	–	–	–	–	5.7	TC	[944]
Pd/Cu(111)	Pd	–	$<1 \times 10^{-10}$	~300	–	5.9 ± 0.2	CPD	[1245,3417]
Recommended	–	–	–	–	–	**5.17 ± 0.06**	–	–

47. Silver Ag[404]

fcc

Surface	Beam	Ion	P_r (Torr)	T (K)	ϕ^+ (eV)	ϕ^e (eV)	Meth.	Refs.
Ag(100)	–	–	–	–	–	3.55	TC	[475]
Ag(100)	–	–	–	–	–	3.8	TC	[1260]
Ag(100)	–	–	–	–	–	3.89	TC	[2516]
Ag(100)	–	–	–	–	–	4.14	TC	[705]
Ag(100)	–	–	–	–	–	4.18	TC	[1193]
Ag(100)	–	–	–	–	–	4.19	TC	[4421]
Ag(100)	–	–	–	–	–	4.2	TC	[971,1108,1109, 2981]
Ag(100)	–	–	–	–	–	4.2	TC	[1261]
Ag(100)[189]	–	–	$<2 \times 10^{-10}$	~300	–	4.2	PE	[2128]
Ag(100)	–	–	–	–	–	4.20	TC	[4258]
Ag(100)	–	–	–	–	–	4.22	TC	[1190]
Ag(100)	–	–	$\sim10^{-10}$	~300	–	4.22 ± 0.04	PE	[625]
Ag(100)	–	–	–	–	–	4.246	TC	[4091]
Ag(100)	–	–	–	–	–	4.29	TC	[947]
Ag(100)	–	–	–	–	–	4.3	TC	[1692]
Ag(100)/V(100)	Ag	–	2×10^{-11}	250	–	4.3	PE	[3368]
Ag(100)	–	–	–	–	–	4.30	TC	[1034]
Ag(100)/NaCl[137]	Ag	–	?	~300 (473)	–	4.30 ± 0.02	PE	[3328,3330]
Ag(100)	–	–	2×10^{-10}	~300	–	4.3 ± 0.1	PE	[1263]
Ag(100)	–	–	–	–	–	4.31	TC	[4429]
Ag(100)	–	–	–	–	–	4.32 ± 0.03	TC	[3280]
Ag(100)	–	–	–	–	–	4.33	TC	[3280]
Ag(100)	–	–	–	–	–	4.33	TC	[1191,1264]
Ag(100)	–	–	$<10^{-10}$	~300	–	4.34 ± 0.03	PE	[1192]
Ag(100)	–	–	–	–	–	4.35	TC	[4117]

Table 1 (*continued*)

Surface	Beam	Ion	P_r (Torr)	T (K)	ϕ^+ (eV)	ϕ^e (eV)	Meth.	Refs.
Ag(100)	–	–	2×10^{-10}	30	–	4.35 ± 0.05	PE	[3154]
Ag(100)	–	–	–	–	–	4.38	TC	[1190]
Ag(100)	–	–	?	?	–	4.4	?	[1262]
Ag(100)	–	–	$\sim 10^{-10}$	~ 300	–	4.41 ± 0.04	PE	[2064]
Ag(100)	–	–	2×10^{-10}	~ 300	–	4.42 ± 0.02	PE	[957,958]
Ag(100)	–	–	–	–	–	4.43	TC	[320]
Ag(100)	–	–	$\sim 10^{-10}$	~ 300	–	4.43	PE	[3703]
Ag(100)	–	–	–	–	–	4.43	TC	[1928]
Ag(100)	–	–	?	~ 300	–	4.43 ± 0.01	PE	[1131]
Ag(100)	–	–	–	–	–	4.44	TC	[1190]
Ag(100)[190]	–	–	–	–	–	4.45	TC	[2405]
Ag(100)	–	–	–	–	–	4.45	TC	[1159,3067]
Ag(100)	–	–	–	–	–	4.5	TC	[1261]
Ag(100)	–	–	4×10^{-11}	~ 300	–	4.5	PE	[2164]
Ag(100)	–	–	?	50	–	4.5	PE	[2909]
Ag(100)	–	–	–	–	–	4.50	TC	[2523]
Ag(100)/Ag(100)[191]	Ag	–	?	308–313	–	4.50*	PE	[2302]
Ag(100)	–	–	–	–	–	4.53	TC	[2524]
Ag(100)/NaCl	Ag	–	?	473	–	$\leq 4.58 \pm 0.01$	CPD	[1369]
Ag(100)	–	–	–	–	–	4.60	TC	[1193]
Ag(100)/NaCl[192]	Ag	–	?	~ 300	–	4.62 ± 0.03	CPD	[1157]
Ag(100)	–	–	$< 4 \times 10^{-11}$	~ 300	–	4.64	PE	[3134]
Ag(100)[193]	–	–	$< 1 \times 10^{-9}$	290	–	4.64 ± 0.02	PE	[626]
Ag(100)/Ag(100)[193]	Ag	–	$< 2 \times 10^{-9}$	290 (525)	–	4.64 ± 0.02	PE	[626]
Ag(100)	–	–	$< 4 \times 10^{-11}$	~ 300	–	4.65	PE	[3133]
Ag(100)/Ag(100)[194]	Ag	–	$\leq 3 \times 10^{-8}$	~ 300 (red)	–	4.72 ± 0.03	PE	[1132]
Ag(100)	–	–	–	–	–	4.74	TC	[627]
Ag(100)	–	–	–	–	–	4.75	TC	[1684]
Ag(100)/Ag(100)	Ag	–	?	~ 300	–	≤ 4.76	PE	[1158]
Ag(100)[190]	–	–	–	–	–	4.78	TC	[2405]
Ag(100)/NaCl[192]	Ag	–	?	~ 300	–	4.79	CPD	[1157]
Ag(100)[194]	–	–	$\leq 3 \times 10^{-8}$	~ 300	–	4.81 ± 0.01	PE	[1132,1881]
Ag(100)/Ag(100)[194]	Ag	–	$\leq 3 \times 10^{-8}$	~ 300	–	4.81 ± 0.03	PE	[1132]
Ag(100)	–	–	–	–	–	4.82	TC	[1237]
Ag(100)	–	–	–	–	–	4.82	TC	[1264]
Ag(100)	–	–	–	–	–	4.94	TC	[1428]
Ag(100)	–	–	–	–	–	4.95	TC	[1428]
Ag(100)	–	–	–	–	–	5.02	TC	[334]
Ag(100)/V(100)[195]	–	–	–	–	–	5.02	TC	[1876]
Ag(100)	–	–	–	–	–	5.06	TC	[321]
Recommended	–	–	–	–	–	**4.46 ± 0.05**	–	–
Ag(110)	–	–	–	–	–	3.35	TC	[475]
Ag(110)	–	–	–	–	–	3.66	TC	[2516]
Ag(110)	–	–	$< 2 \times 10^{-10}$	~ 300	–	3.9	PE	[1265]
Ag(110)	–	–	–	–	–	4.059	TC	[4091]
Ag(110)	–	–	–	–	–	4.06	TC	[3480]
Ag(110)/Re(1122)	Ag	–	$(< 1 \times 10^{-11})$	78 (≤ 650)	–	4.1 ± 0.02	FE	[1421]
Ag(110)	–	–	–	–	–	4.10	TC	[947]
Ag(110)	–	–	$\sim 10^{-10}$	~ 300	–	4.14 ± 0.04	PE	[625]
Ag(110)	–	–	–	–	–	4.17	TC	[1159,3067]
Ag(110)	–	–	–	–	–	4.19	TC	[3280]
Ag(110)	–	–	?	~ 300	–	4.2	PE	[2144]
Ag(110)	–	–	1×10^{-10}	~ 300	–	4.2 ± 0.1	PE	[1678]
Ag(110)	–	–	–	–	–	4.20	TC	[4117]
Ag(110)	–	–	–	–	–	4.23	TC	[320]
Ag(110)	–	–	$< 10^{-10}$	~ 300	–	4.25 ± 0.03	PE	[1192]
Ag(110)	–	–	4×10^{-11}	~ 300	–	4.3 ± 0.1	PE	[2164]
Ag(110)	–	–	–	–	–	4.30	TC	[1264]
Ag(110)	–	–	?	570	–	4.40	PE	[3169]
Ag(110)	–	–	–	–	–	4.40	TC	[334]
Ag(110)/Ag(110)[196]	Ag	–	$< 2 \times 10^{-9}$	290 (525)	–	4.51 ± 0.01	PE	[626]
Ag(110)/mica[196]	Ag	–	$< 2 \times 10^{-9}$	290 (525)	–	4.51 ± 0.02	PE	[626]
Ag(110)[196]	–	–	$< 1 \times 10^{-9}$	290	–	4.52 ± 0.02	PE	[626]
Ag(110)	–	–	?	570	–	4.53 ± 0.05	PE	[3169]
Ag(110)	–	–	–	–	–	4.66	TC	[1264]
Ag(110)	–	–	–	–	–	4.68	TC	[1237]
Ag(110)	–	–	?	570	–	4.70 ± 0.03	PE	[3169]

Table 1 (*continued*)

Surface	Beam	Ion	P_r (Torr)	T (K)	ϕ^+ (eV)	ϕ^e (eV)	Meth.	Refs.
Ag(110)	–	–	–	–	–	4.75	TC	[1684]
Ag(110)	–	–	–	–	–	4.76	TC	[321]
Recommended	–	–	–	–	–	**4.28 ± 0.08**	–	–
Ag(111)	–	–	–	–	–	3.56	TC	[1194]
Ag(111)	–	–	–	–	–	3.70	TC	[475]
Ag(111)	–	–	–	–	–	3.96	TC	[2516]
Ag(111)/NaCl[137]	Ag	–	?	~300 (423)	–	3.98 ± 0.02	PE	[3328,3330]
Ag(111)[197]	–	–	~10^{-10}	~300	–	4.03	CPD	[1693]
Ag(111)[197]	–	–	~10^{-10}	~300	–	4.18	PE	[1693]
Ag(111)	–	–	–	–	–	4.25	TC	[4117]
Ag(111)	–	–	–	–	–	4.26	TC	[2077]
Ag(111)/quartz[198]	Ag	–	~10^{-9}	~300	–	4.35	PE	[3313]
Ag(111)	–	–	–	–	–	4.368	TC	[4091]
Ag(111)	–	–	–	–	–	4.38	TC	[2077]
Ag(111)/mica(111)	Ag	–	<5 × 10^{-11}	~300{~700}	–	4.38*	CPD	[1897]
Ag(111)	–	–	–	–	–	4.40	TC	[3280]
Ag(111)	–	–	–	–	–	4.40	TC	[947]
Ag(111)	–	–	–	–	–	4.44	TC	[2541]
Ag(111)	–	–	–	–	–	4.45	TC	[2541]
Ag(111)	–	–	–	–	–	4.45	TC	[2068]
Ag(111)	–	–	–	–	–	4.45	TC	[2983]
Ag(111)	–	–	~10^{-10}	~300	–	4.45	PE	[4143]
Ag(111)	–	–	<10^{-10}	~300	–	4.45 ± 0.03	PE	[1192]
Ag(111)	–	–	–	–	–	4.46	TC	[343]
Ag(111)[197]	–	–	~10^{-10}	~300	–	4.46 ± 0.02	PE	[625,1693]
Ag(111)	–	–	–	–	–	4.48	TC	[2523]
Ag(111)	–	–	–	–	–	4.49	TC	[2694]
Ag(111)	–	–	2 × 10^{-10}	~300	–	4.49 ± 0.02	PE	[1000]
Ag(111)	–	–	<4 × 10^{-11}	~300	–	4.5	PE	[3133]
Ag(111)	–	–	2 × 10^{-10}	~300	–	4.5	PE	[274,1196]
Ag(111)/mica[420]	Ag	–	4 × 10^{-10}	~300{570}	–	4.5	PE	[4001]
Ag(111)/Si(111)	Ag	–	1 × 10^{-10}	~300	–	4.5	PE	[1551]
Ag(111)	–	–	–	–	–	4.5 ± 0.1	TC	[3494]
Ag(111)	–	–	–	–	–	4.50	TC	[1197,4215,4413]
Ag(111)	–	–	1 × 10^{-10}	~300	–	4.50 ± 0.10	PE	[1195]
Ag(111)/W(110)	Ag	–	<10^{-10}	~300 (363)	–	4.53 ± 0.05	CPD	[2262]
Ag(111)/W(110)	Ag	–	?	~300	–	4.55	CPD	[4231]
Ag(111)/Cu(111)	Ag	–	<8 × 10^{-11}	~300	–	4.56	PE	[968]
Ag(111)	–	–	<2 × 10^{-10}	90	–	4.56	PE	[1266]
Ag(111)	–	–	<2 × 10^{-10}	~300	–	4.56	PE	[1133]
Ag(111)	–	–	–	–	–	4.56	TC	[3369]
Ag(111)	–	–	2 × 10^{-10}	~300	–	4.56	PE	[939,958]
Ag(111)	–	–	–	–	–	4.57	TC	[1722]
Ag(111)	–	–	4 × 10^{-11}	~300	–	4.6	PE	[2164]
Ag(111)/Re(1011)	Ag	–	(<1 × 10^{-11})	78 (≤650)	–	4.6 ± 0.02	FE	[1421]
Ag(111)	–	–	?	~300	–	4.60 ± 0.03	PE	[4213]
Ag(111)/W(110)	Ag	–	3 × 10^{-10}	~300	–	4.61 ± 0.05*	CPD	[2373]
Ag(111)/PTCDA[476]	Ag	–	2 × 10^{-10}	~300	–	4.61 ± 0.05	PE	[4341]
Ag(111)/quartz[198]	Ag	–	~10^{-9}	~300 (773)	–	4.64	PE	[3313]
Ag(111)	–	–	–	–	–	4.65	TC	[1264]
Ag(111)/W(110)	Ag	–	<7 × 10^{-11}	78 (450)	–	4.65 ± 0.03	FE	[2279]
Ag(111)/H:Si(111)[199]	Ag	–	~10^{-10}	~300	–	4.65 ± 0.15	PE	[1198]
Ag(111)/W(110)	Ag	–	≤2 × 10^{-10}	~300	–	4.66*	CPD	[1538]
Ag(111)	–	–	<1 × 10^{-10}	~300	–	4.66	CPD	[990]
Ag(111)/Ag(111)[194]	Ag	–	≤3 × 10^{-8}	~300 (red)	–	4.66 ± 0.03	PE	[1132]
Ag(111)	–	–	–	–	–	4.67	TC	[320,1178]
Ag(111)/W(110)	Ag	–	≤2 × 10^{-10}	500	–	4.68*	CPD	[1538]
Ag(111)	–	–	4 × 10^{-10}	100	–	4.68 ± 0.08	PE	[1579,2988]
Ag(111)/Nb(110)	Ag	–	7 × 10^{-11}	~300	–	4.69	PE	[2986]
Ag(111)	–	–	<5 × 10^{-11}	~300	–	4.69	PE	[1124]
Ag(111)/Re(0001)	Ag	–	4 × 10^{-10}	300, 740	–	4.7	CPD	[836]
Ag(111)/Si(100)	Ag	–	?	~300	–	4.7	PE	[1199]
Ag(111)/Pt(111)[200]	Ag	–	?	~300 (600)	–	4.7	PE	[2182]
Ag(111)	–	–	–	–	–	4.702 ± 0.017	TC	[2352]
Ag(111)[198]	–	–	–	–	–	4.72	TC	[3313]
Ag(111)/Ag[201]	Ag	–	?	58 (330)	–	4.72	PE	[1422]
Ag(111)/mica[202]	Ag	–	<2 × 10^{-9}	290 (525)	–	4.72 ± 0.01	PE	[626]
Ag(111)	–	–	~10^{-10}	~300	–	4.73	PE	[4340]

Table 1 (*continued*)

Surface	Beam	Ion	P_r (Torr)	T (K)	ϕ^+ (eV)	ϕ^e (eV)	Meth.	Refs.
Ag(111)/Si(100)	Ag	–	?	110 (~300)	–	4.74	PE	[3238]
Ag(111)	–	–	–	–	–	4.74	TC	[1159,3067]
Ag(111)	–	–	–	–	–	4.74	TC	[2551]
Ag(111)	–	–	<2 × 10⁻¹⁰	27, 90	–	4.74	CPD	[4107]
Ag(111)[202]	–	–	<2 × 10⁻⁹	~300	–	4.74 ± 0.02	PE	[626,1134]
Ag(111)	–	–	?	~300	–	4.75	PE	[3779]
Ag(111)	–	–	–	–	–	4.75	TC	[1720]
Ag(111)/W(112)	Ag	–	≤7 × 10⁻¹¹	~300 (800)	–	4.75	CPD	[2385]
Ag(111)[194]	–	–	≤3 × 10⁻⁸	~300	–	4.75 ± 0.01	PE	[1132,1881]
Ag(111)/Ag(111)[194]	Ag	–	≤3 × 10⁻⁸	~300	–	4.75 ± 0.03*	PE	[1132]
Ag(111)/W(110)	Ag	–	3 × 10⁻¹⁰	330–390	–	4.75 ± 0.08*	CPD	[2373]
Ag(111)[203]	–	–	2 × 10⁻¹¹	50–60	–	4.76 ± 0.1	PE	[2266]
Ag(111)	–	–	–	–	–	4.80	TC	[1720]
Ag(111)	–	–	~10⁻¹⁰	100–670	–	4.84 ± 0.03	PE	[3142]
Ag(111)	–	–	–	–	–	4.85	TC	[1684]
Ag(111)	–	–	–	–	–	4.85	TC	[233]
Ag(111)/Ru(001)[203]	Ag	–	2 × 10⁻¹¹	~60 (500)	–	4.90 ± 0.1	PE	[2266]
Ag(111)	–	–	?	~300	–	≥4.9 ± 0.1*	CPD	[1879]
Ag(111)	–	–	–	–	–	4.92	CT	[4174,4284]
Ag(111)	–	–	–	–	–	4.95	TC	[1237]
Ag(111)	–	–	–	–	–	4.98	TC	[1264]
Ag(111)	–	–	–	–	–	4.99	TC	[1720]
Ag(111)	–	–	–	–	–	5.01	TC	[334,3179]
Ag(111)	–	–	–	–	–	5.46	TC	[321]
Recommended	–	–	–	–	–	**4.64 ± 0.06**	–	–
Ag	–	–	?	~1230 (~m.p.)	–	3.09	TE	[3385]
Ag	–	–	–	–	–	3.19	TC	[521]
Ag	–	–	–	–	–	3.43	TC	[2629]
Ag	–	–	–	–	–	3.49	TC	[475]
Ag	–	–	?	~1230 (~m.p.)	–	3.56	TE	[1362]
Ag	–	–	–	–	–	3.6	TC	[3590]
Ag	–	–	6 × 10⁻³	~300	–	3.64 ± 0.07	PE	[2079,2080]
Ag	–	–	?	~300	–	3.67	PE	[2460]
Ag/W(100)	Ag	–	?	415, 550	–	3.7*	FE	[2263]
Ag	–	–	–	–	–	3.72	TC	[2523]
Ag/W(100)	Ag	–	?	370	–	3.8*	FE	[2263]
Ag/W	Ag	–	<5 × 10⁻¹⁰	~300	–	3.8	FE	[3116]
Ag	–	–	?	~300	–	3.80	PE	[3018]
Ag	–	–	–	–	–	3.82	TC	[1150]
Ag	–	–	<10⁻⁶	~300	–	3.85	PE	[2919]
Ag/W(100)	Ag	–	?	415, 550	–	3.9	FE	[2263]
Ag/W(100)	Ag	–	?	650	–	3.9*	FE	[2263]
Ag	–	–	~10⁻¹⁰	373,	–	3.94	CPD	[2118]
Ag/glass	Ag	–	~10⁻⁶	373, 473	–	3.94 ± 0.01	PE	[3507]
Ag	–	–	?	~300	–	4.0	PE	[3639]
Ag/silica	Ag	–	~10⁻⁸	~300	–	4.0	PE	[1989]
Ag/W(100)	Ag	–	?	370	–	4.0	FE	[2263]
Ag/Mo(111)	Ag	–	<1 × 10⁻¹⁰	~300	–	4.0	CPD	[1842]
Ag	–	–	–	–	–	4.0 ± 0.05	TC	[1990]
Ag/quartz	Ag	–	~10⁻¹⁰	~300	–	4.0 ± 0.15	PE	[304]
Ag	–	–	–	–	–	4.00	TC	[1885]
Ag	–	–	–	–	–	4.00 ± 0.05	TC	[3358]
Ag/glass	Ag	–	~10⁻⁶	373	–	4.01 ± 0.01	PE	[3507]
Ag	–	–	~10⁻⁶	296	–	4.01 ± 0.05	CPD	[1487,1505]
Ag	–	–	5 × 10⁻⁸	296	–	4.03 ± 0.04	CPD	[1487]
Ag	–	–	4 × 10⁻⁹	733	–	4.04 ± 0.07	PE	[1116]
Ag	–	–	5 × 10⁻⁸	296	–	4.05 ± 0.05	CPD	[1542]
Ag[209]	–	–	?	~300	–	4.06 ± 0.05	PE	[2729]
Ag	–	–	?	~1200	–	4.08	TE	[1944]
Ag₄(cluster)	–	–	–	–	–	4.08	TC	[2990]
Ag	–	–	4 × 10⁻⁹	533	–	4.08 ± 0.07	PE	[1116]
Ag/W(100)	Ag	–	?	650	–	4.1	FE	[2263]
Ag/Ta(111)	Ag	–	<1 × 10⁻¹⁰	~300	–	4.1	CPD	[2441]
Ag/W(111)	Ag	–	5 × 10⁻¹⁰	~300	–	4.1	CPD	[2363]
Ag	–	–	–	–	–	4.1	TC	[944]
Ag	–	–	–	–	–	4.1	TC	[2456]
Ag/Si(111)ⁿ	Ag	–	3 × 10⁻¹¹	60 (750)	–	4.11	PE	[2660]
Ag	–	–	–	–	–	4.13	TC	[2005]
Ag	–	–	–	–	–	4.16	TC	[3476]

Table 1 (*continued*)

Surface	Beam	Ion	P_r (Torr)	T (K)	ϕ^+ (eV)	ϕ^e (eV)	Meth.	Refs.
Ag	–	–	–	–	–	4.18	TC	[1066]
Ag/glass	Ag	–	$<1 \times 10^{-10}$	78	–	4.18	PE	[414,2723]
Ag/glass	Ag	–	$\sim 10^{-6}$	373	–	4.18 ± 0.01	PE	[3507]
Ag/W	Ag	–	8×10^{-11}	300 (450)	–	4.18 ± 0.02	FE	[3430]
Ag$_n$(n → ∞)	–	–	?	~300	–	4.19	IP, TC	[4197]
Ag	–	–	–	–	–	4.2	TC	[1993]
Ag/H:Si(111)[199]	Ag	–	$\sim 10^{-10}$	~300{210}	–	4.2	PE	[1198]
Ag/W	Ag	–	$\sim 10^{-10}$	78{920}	–	4.2	FE	[3089]
Ag/W	Ag	–	$<5 \times 10^{-10}$	800	–	4.2	FE	[3116]
Ag/Ir	Ag	–	?	78 (589)	–	4.20	FE	[2189]
Ag/glass	Ag	–	?	77–90	–	4.20	PE	[2763,3046]
Ag	–	–	?	~300	–	4.21	CPD	[3405]
Ag/W	Ag	–	8×10^{-11}	~300 (780)	–	4.22 ± 0.02	FE	[3430]
Ag/glass	Ag	–	$<10^{-9}$	77–90	–	4.23	PE	[1389]
Ag/W	Ag	–	$<5 \times 10^{-8}$	~300	–	4.23 ± 0.08*	CPD	[2570]
Ag	–	–	–	–	–	4.24	TC	[2629]
Ag/Ag[201]	Ag	–	?	60	–	4.25	PE	[1422]
Ag	–	–	?	~300	–	4.25	PE	[2992]
Ag[431]	–	–	$<5 \times 10^{-8}$	1150–1230	–	4.25*	TE	[1466]
Ag/W	Ag	–	?	~300	–	4.25	FE	[3108]
Ag(fp)[204]	–	–	? (He)	?	–	4.25 ± 0.1	PE	[1562]
Ag[205]	–	–	–	–	–	4.26	TC	[3280,3720]
Ag	–	–	–	–	–	4.26	TC	[3318]
Ag	–	–	–	–	–	4.26	TC	[339]
Ag/quartz	Ag	–	$<2 \times 10^{-9}$	290 (473)	–	4.26 ± 0.02	PE	[626]
Ag[447]	–	–	4×10^{-9}	296 (≤773)	–	4.26 ± 0.03	PE	[1116,3788,4082, 4114,4132–4134]
Ag/KBr	Ag	–	?	~300	–	4.28	PE	[1952]
Ag/W	Ag	–	($<1 \times 10^{-11}$)	78 (490)	–	4.28 ± 0.02	FE	[1421]
Ag	–	–	–	–	–	4.29	TC	[3318]
Ag	–	–	?	~300	–	4.29 ± 0.02	CPD	[2810]
Ag	–	–	$<10^{-8}$	~300	–	4.29 ± 0.02	CPD	[1163]
Ag/V(100)	Ag	–	2×10^{-11}	250	–	4.3	PE	[3368]
Ag/W(100)	Ag	–	5×10^{-10}	~300	–	4.3	CPD	[2363]
Ag/W	Ag	–	$<5 \times 10^{-10}$	680, 930	–	4.3	FE	[3116]
Ag/Fe(100)	–	–	–	–	–	4.3	TC	[2901]
Ag	–	–	–	–	–	4.3	TC	[706]
Ag	–	–	2×10^{-11}	~300	–	4.3 ± 0.1	PE	[1251]
Ag/glass	Ag	–	?	~300	–	4.30	CPD	[1157]
Ag	–	–	–	–	–	4.30	TC	[3264,3265,3267]
Ag	–	–	$<1 \times 10^{-10}$	~300	–	4.30	CPD	[2198]
Ag	–	–	–	–	–	4.30	TC	[298]
Ag/GaP	–	–	–	–	–	4.30	TC	[1653]
Ag/glass	Ag	–	$<10^{-8}$	~300	–	4.30 ± 0.02	CPD	[349]
Ag	–	–	$\sim 10^{-10}$	~300	–	4.30 ± 0.04	PE	[2064]
Ag/glass	Ag	–	5×10^{-11}	~300	–	4.30 ± 0.05	CPD	[1071]
Ag/various[404]	–	–	–	–	–	4.30 ± 0.13*	TC	[3280]
Ag	–	–	–	–	–	4.31	TC	[3637]
Ag/graphite	Ag	–	?	~1160–1200	–	4.31 ± 0.03	TE	[2236]
Ag/Ta[242]	Ag	–	?	~300	–	4.31 ± 0.03	CPD	[1050]
Ag/glass	Ag	–	$\sim 10^{-8}$	~300	–	4.31 ± 0.03	CPD	[133]
Ag	–	–	–	–	–	4.32	TC	[3476]
Ag/Ta	–	–	$<5 \times 10^{-8}$	1234(m.p.)	–	4.32	TE	[1466]
Ag/Re	Ag	–	($<1 \times 10^{-11}$)	78 (490)	–	4.32 ± 0.02	FE	[1421]
Ag/V(100)	–	–	–	–	–	4.32 ± 0.03	TC	[2437]
Ag	–	–	$<10^{-10}$	~300	–	4.32 ± 0.03	PE	[1192]
Ag/W	Ag	–	$\leq 5 \times 10^{-8}$	~300	–	4.32 ± 0.03	CPD	[690]
Ag/Mo(100)	Ag	–	$<2 \times 10^{-10}$	~300	–	4.32 ± 0.03*	CPD	[2252]
Ag/glass	Ag	–	5×10^{-11}	~300	–	4.32 ± 0.07*	CPD	[1071]
Ag/NaCl	Ag	–	?	90	–	4.33	PE	[1952]
Ag/glass	Ag	–	$<1 \times 10^{-10}$	78 (293)	–	4.33	PE	[414,1509,2723]
Ag/W	Ag	–	$<5 \times 10^{-9}$	298	–	4.33	FE	[2245]
Ag/W	Ag	–	?	~300 (550)	–	4.33	FE	[3345]
Ag	–	–	–	–	–	4.33	TC	[3931]
Ag/W	Ag	–	$\leq 8 \times 10^{-10}$	~300 (550)	–	4.33 ± 0.03	FE	[1689]
Ag/W	Ag	–	$\leq 5 \times 10^{-8}$	~300	–	4.33 ± 0.05	CPD	[690]
Ag	–	–	?	90	–	4.33 ± 0.05	CPD	[1366]
Ag/Si(111)	Ag	–	?	~300	–	4.33 ± 0.07	PE	[2776]
Ag(fp, r → ∞)[460]	–	–	?	~300	–	4.34*	IP	[4198]
Ag(fp, r → ∞)[460]	–	–	?	~300	–	4.35*	IP	[4198]

Table 1 (*continued*)

Surface	Beam	Ion	P_r (Torr)	T (K)	ϕ^+ (eV)	ϕ^e (eV)	Meth.	Refs.
Ag/glass	Ag	–	$<1 \times 10^{-10}$	78 (378)	–	4.35	PE	[414,2723]
Ag/quartz[198]	Ag	–	$\sim10^{-9}$	~300	–	4.35	PE	[3313]
Ag	–	–	?	~300	–	4.35	PE	[4159]
Ag/W	Ag	–	$\leq5 \times 10^{-8}$	~300	–	4.35 ± 0.05	CPD	[690]
Ag/Ta	Ag	–	?	~300	–	4.35 ± 0.05	CPD	[1050]
Ag	–	–	6×10^{-9}	~300	–	4.36	PE	[1139]
Ag/Ta	Ag	–	$\sim10^{-8}$	~300	–	4.36 ± 0.05	CPD	[1385]
Ag/VO$_2$(100)	–	–	–	–	–	4.365	TC	[1934]
Ag/glass	Ag	–	$<1 \times 10^{-10}$	78 (485)	–	4.37	PE	[414,2723]
Ag(fp, $r \to \infty$)[206]	–	–	–	–	–	4.37	TC	[3442]
Ag/DiMe[476]	Ag	–	2×10^{-10}	~300	–	4.37 ± 0.05	PE	[4341]
Ag/glass	Ag	–	5×10^{-11}	~300	–	$4.37 \pm 0.06^*$	CPD	[1071]
Ag/glass	Ag	–	$\sim10^{-10}$	90	–	4.38	PE	[3048]
Ag/Ir	Ag	–	?	78 (442)	–	4.38	FE	[2189]
Ag/glass	Ag	–	$<5 \times 10^{-10}$	78 (573)	–	4.38	PE	[1509]
Ag/glass	Ag	–	$<10^{-8}$	78	–	4.38 ± 0.02	CPD	[1646]
Ag/glass	Ag	–	$<10^{-9}$	90 (293)	–	4.39	PE	[2763,3046]
Ag/W	Ag	–	5×10^{-10}	78 (740)	–	4.39 ± 0.01	FE	[1673]
Ag/quartz	Ag	–	$<1 \times 10^{-9}$	323	–	4.39 ± 0.05	CPD	[1536]
Ag/glass	Ag	–	5×10^{-11}	~300	–	$4.39 \pm 0.07^*$	CPD	[1071]
Ag/Ag(100)[191]	Ag	–	?	≤300	–	4.4^*	PE	[2302]
Ag/Fe(100)	Ag	–	?	~300	–	4.4	PE	[2901]
Ag/Pd(100)	–	–	–	–	–	4.4	TC	[1692]
Ag/Mo(100)	Ag	–	$<2 \times 10^{-10}$	~300	–	4.4^*	CPD	[3121]
Ag	–	–	$<2 \times 10^{-10}$	~300	–	4.4	CPD	[4214]
Ag/glass[367]	Ag	–	$<10^{-9}$	~300 (520)	–	4.4	CPD	[1893]
Ag/Pt(111)	Ag	–	?	~300	–	4.4	CPD	[2869]
Ag/Pt(111)[200]	Ag	–	?	~300	–	4.4	PE	[2182]
Ag/Pd(100)	–	–	–	–	–	4.4	TC	[1692]
Ag	–	–	?	~300	–	4.4	PE	[1838]
Ag	–	–	$\sim10^{-9}$	~300	–	4.4 ± 0.1	PE	[1267]
Ag	–	–	$\sim10^{-6}$	623	–	4.40 ± 0.02	PE	[3098]
Ag/GaP	–	–	–	–	–	4.41	TC	[1653]
Ag/Mo[207]	Ag	–	$<5 \times 10^{-8}$	~300	–	4.41	PE	[1051]
Ag/quartz	Ag	–	$<5 \times 10^{-8}$	~300	–	4.41	PE	[1051]
Ag/Si	–	–	–	–	–	4.41	TC	[1653]
Ag/Si(111)	Ag	–	5×10^{-11}	~300	–	4.41 ± 0.05	CPD	[613,636]
Ag	–	–	–	–	–	4.42	TC	[1976]
Ag	–	–	–	–	–	4.43^*	TC	[1955]
Ag/Si	–	–	–	–	–	4.44	TC	[1653]
Ag	–	–	?	~300	–	4.44	CPD	[2297]
Ag/Ta	Ag	–	$<10^{-8}$	~300	–	4.44 ± 0.01	CPD	[349]
Ag	–	–	$\sim10^{-6}$	523	–	4.44 ± 0.03	PE	[3098]
Ag	–	–	–	–	–	4.46	TC	[1645]
Ag/Mo	Ag	–	$\sim10^{-8}$	~300	–	4.46	CPD	[299]
Ag	–	–	1×10^{-9}	~300	–	4.46	CPD	[1252]
Ag/glass	Ag	–	?	~300	–	4.46 ± 0.01	CPD	[1369]
Ag/Si	Ag	–	$<6 \times 10^{-9}$	~300	–	4.46 ± 0.02	CPD	[1540]
Ag/glass	Ag	–	?	~300	–	4.47	CPD	[1157]
Ag/W(110)	Ag	–	?	90	–	4.47	CPD	[3565]
Ag/Re(1010)[211]	Ag	–	$(<1 \times 10^{-11})$	78 (≤770)	–	$4.47 \pm 0.05^*$	FE	[1421]
Ag/Pt(111)	Ag	–	$<8 \times 10^{-11}$	$\sim300(\sim800)$	–	$4.47 \pm 0.06^*$	CPD	[4180]
Ag/W	Ag	–	$(<1 \times 10^{-12})$	800	–	4.48	FE	[1676]
Ag/glass	Ag	–	$<10^{-9}$	77 (295)	–	4.48	PE	[1389]
Ag/Si(111)	Ag	–	4×10^{-10}	~300	–	4.48	PE	[3589]
Ag	–	–	4×10^{-10}	~300	–	4.48 ± 0.02	PE	[1552]
Ag/C	Ag	–	$<10^{-9}$	~300	–	4.49	CPD	[2958]
Ag/Ta	Ag	–	$\sim10^{-8}$	~300	–	4.49 ± 0.02	CPD	[1385]
Ag/Si(111)	Ag	–	4×10^{-10}	~300	–	4.49 ± 0.02	PE	[1552]
Ag	–	–	–	–	–	4.5	TC	[2583]
Ag/W(110)	Ag	–	$\leq1 \times 10^{-10}$	90	–	4.5	CPD	[3472]
Ag	–	–	–	–	–	4.50	TC	[1399]
Ag	–	–	$<2 \times 10^{-9}$	~300	–	4.50	PE	[1575]
Ag/Ag	Ag	–	$<5 \times 10^{-8}$	~300	–	4.50 ± 0.02	PE	[1051]
Ag/Re(1010)	Ag	–	$(<1 \times 10^{-11})$	78 (≤770)	–	4.50 ± 0.05	FE	[1421]
Ag(fp)[149]	–	–	$<10^{-9}$	~300	–	4.50 ± 0.1	PE	[3190]
Ag	–	–	?	~300	–	4.51 ± 0.01	PE	[3609]
Ag/Pd(111)	–	–	–	–	–	4.54	TC	[985]
Ag/W(111)	–	–	–	–	–	4.54	TC	[531]
Ag	–	–	$\leq1 \times 10^{-9}$	~300	–	4.55	PE	[3383]

Table 1 (*continued*)

Surface	Beam	Ion	P_r (Torr)	T (K)	ϕ^+ (eV)	ϕ^e (eV)	Meth.	Refs.
Ag/W(110)	Ag	–	$<7 \times 10^{-11}$	78 (450)	–	4.55	FE	[2279]
Ag/quartz	Ag	–	?	~300	–	4.55	PE	[4202]
Ag/Pd(111)	Ag	–	$<2 \times 10^{-10}$	~300	–	4.55	PE	[985]
Ag/Mo[207]	Ag	–	$<5 \times 10^{-8}$	~300 (≤370)	–	4.55 ± 0.05	PE	[1051]
Ag/Ta(112)	Ag	–	$<1 \times 10^{-10}$	~300	–	4.56	CPD	[878]
Ag/W(110)	Ag	–	?	~300 (700)	–	4.56	CPD	[3565]
Ag[263]	–	–	$\leq 3 \times 10^{-8}$	873	–	4.56 ± 0.06	PE	[3391]
Ag/Pd(111)	–	–	–	–	–	4.57	TC	[985]
Ag/Cu(111)	Ag	–	?	~300	–	4.57 ± 0.05*	CPD	[2692]
Ag/glass	Ag	–	?	~300	–	4.58	PE	[3029]
Ag/Pt(111)	Ag	–	2×10^{-10}	350	–	4.58 ± 0.05*	CPD	[4366]
Ag	–	–	?	~300	–	4.59	PE	[4278]
Ag(fp)[208]	–	–	?	~300	–	4.59 ± 0.05	PE	[3127]
Ag	–	–	–	–	–	4.594	TC	[2649]
Ag[209]	–	–	?	~300	–	4.6	PE	[2729]
Ag/W(110)[210]	Ag	–	$<10^{-10}$	~300	–	4.6	FE	[1828]
Ag/W(110)[210]	Ag	–	5×10^{-10}	~300	–	4.6	CPD	[2363]
Ag/O/V(100)	Ag	–	4×10^{-11}	220 (≤700)	–	4.6 ± 0.1	PE	[3375]
Ag/Pd(100)[210]	Ag	–	?	~300	–	4.6 ± 0.2	PE	[1692]
Ag	–	–	~10^{-5}	<1200	–	4.60	TE	[2216]
Ag/glass	Ag	–	~10^{-10}	77 (373)	–	4.60	PE	[2155]
Ag/Pd(111)	–	–	–	–	–	4.60	TC	[985]
Ag	–	–	?	296	–	4.61	PE	[1455]
Ag/Ir(100)	Ag	–	?	78 (≤518)	–	4.63 ± 0.02	FE	[2189]
Ag/quartz[198]	Ag	–	~10^{-9}	~300 (773)	–	4.64	PE	[3313]
Ag/Ta(112)[210]	Ag	–	$<1 \times 10^{-10}$	~300	–	4.65	CPD	[878]
Ag/W(110)[210]	Ag	–	$\leq 1 \times 10^{-10}$	90 (700)	–	4.67	CPD	[3472]
Ag	–	–	?	~300	–	4.68	PE	[3025]
Ag	–	–	$<5 \times 10^{-8}$	~300	–	4.68 ± 0.01	PE	[1051]
Ag/Nb(110)[210]	Ag	–	7×10^{-11}	~300	–	4.69	PE	[2986]
Ag/W(110)[210]	Ag	–	?	~300	–	4.7	CPD	[3565]
Ag/Re(0001)	Ag	–	4×10^{-10}	~300, 740	–	4.7	CPD	[836]
Ag	–	–	?	?	–	4.7	TE	[3402]
Ag/W(110)	Ag	–	$\leq 7 \times 10^{-11}$	~300 (~950)	–	4.7	CPD	[2388]
Ag/Ru(001)	Ag	–	$<5 \times 10^{-10}$	60	–	4.7 ± 0.05	PE	[2651]
Ag	–	–	–	–	–	4.70	TC	[3476]
Ag	–	–	1×10^{-8}	~300	–	4.7 ± 0.2	PE	[3325]
Ag/Pt(100)	Ag	–	1×10^{-10}	~300	–	4.71 ± 0.15	PE	[174]
Ag	–	–	–	–	–	4.72	TC	[2990]
Ag/W(100)	–	–	–	–	–	4.72	TC	[531]
Ag	–	–	1×10^{-5}	~300	–	4.73	CPD	[1883]
Ag[263]	–	–	–	296	–	4.73 ± 0.02	TC	[1135]
Ag[263]	–	–	$\leq 3 \times 10^{-8}$	298	–	4.73 ± 0.07	PE	[3391]
Ag[263]	–	–	–	873	–	4.75 ± 0.00	TC	[1135]
Ag/cnt/Si(111)[25]	–	–	~10^{-10}	~300	–	4.75 ± 0.06	PE	[3246]
Ag/Ag(100)	Ag	–	?	~300	–	≤4.76	PE	[1158]
Ag/cnt/Si(111)[25]	–	–	~10^{-10}	~300	–	4.76 ± 0.09	CPD	[3246]
Ag/Pd(111)	–	–	–	–	–	4.77	TC	[985]
Ag/glass	Ag	–	–	~300	–	4.78	PE	[3023]
Ag/Mo[207]	Ag	–	$<5 \times 10^{-8}$	~300 (red)	–	4.78	PE	[1051]
Ag/W(112)	–	–	–	–	–	4.78	TC	[531]
Ag/Si(111)ⁿ	Ag	–	3×10^{-11}	~300	–	4.79	PE	[2660]
Ag/Si(111)	Ag	–	?	770	–	4.80 ± 0.08	PE	[2776]
Ag/Pt(997)	Ag	–	1×10^{-10}	~300	–	4.82 ± 0.15	PE	[174]
Ag/W(110)	–	–	–	–	–	4.84	TC	[531]
Ag/cnt/Si(111)[25]	–	–	~10^{-10}	~300	–	4.84 ± 0.10	CPD	[3246]
Ag/Pd(111)	–	–	–	–	–	4.86	TC	[1720]
Ag/Si(111)ᵖ	Ag	–	3×10^{-11}	~300	–	4.87	PE	[2660]
Ag	–	–	?	~300	–	4.90	PE	[3127]
Ag/Pd(111)	–	–	–	–	–	4.91	TC	[1720]
Ag/Pd(111)	–	–	–	–	–	4.92	TC	[1720]
Ag/Fe(100)	–	–	–	–	–	4.92	TC	[1105]
Ag/SiO₂/Si	Ag	–	?	~300 (570)	–	4.97	PE	[2355]
Ag/Rh(100)	–	–	–	–	–	5.0	TC	[1009]
Ag/Si(111)ᵖ	Ag	–	3×10^{-11}	60 (750)	–	5.02	PE	[2660]
Ag/Ru(0001)	–	–	–	–	–	5.03	TC	[2554]
Ag/Fe(100)	–	–	–	–	–	5.05	TC	[1105]
Ag/Rh(111)	–	–	–	–	–	5.2	TC	[1009]
Ag/Ru(0001)	Ag	–	1×10^{-10}	~300	–	5.26*	CPD	[2880]
Ag/Re(1010)[211]	Ag	–	$<1 \times 10^{-11}$	78 (≤770)	–	5.30 ± 0.02	FE	[1421]

Table 1 (*continued*)

Surface	Beam	Ion	P_r (Torr)	T (K)	ϕ^+ (eV)	ϕ^e (eV)	Meth.	Refs.
Ag	–	–	–	–	–	5.41	TC	[2551]
Recommended	–	–	–	–	–	**4.39 ± 0.02**	–	–
Liquid ($T > 1234$ **K**)								
Ag[456]	–	–	$<5 \times 10^{-8}$	1240	–	4.32*	TE	[1466]

48. Cadmium Cd

hcp

Surface	Beam	Ion	P_r (Torr)	T (K)	ϕ^+ (eV)	ϕ^e (eV)	Meth.	Refs.
Cd(0001)	–	–	–	–	–	4.17	TC	[4005]
Cd(0001)	–	–	–	–	–	4.3	TC	[1711]
Cd(0001)	–	–	–	–	–	4.6	TC	[2375]
Cd(0001)	–	–	–	–	–	6.52	TC	[321]
Cd(1010)	–	–	–	–	–	4.76	TC	[4005]
Cd(1010)	–	–	–	–	–	6.30	TC	[321]
Cd(1124)	–	–	–	–	–	5.52	TC	[321]
Cd	–	–	–	–	–	3.36	TC	[521]
Cd	–	–	–	–	–	3.36	TC	[3211]
Cd	–	–	–	–	–	3.4	TC	[944]
Cd	–	–	$\sim 10^{-8}$	~ 300	–	3.4 ± 0.6	PE	[3433]
Cd/Pt(100)	–	–	–	–	–	3.43	TC	[3168]
Cd/Au(100)	–	–	–	–	–	3.43	TC	[3168]
Cd$_n$($n \to \infty$)	–	–	–	–	–	3.54 ± 0.27	TC	[4261]
Cd	–	–	–	–	–	3.6	TC	[2583]
Cd	–	–	?	~ 300	–	3.68	PE	[3027]
Cd	–	–	–	–	–	3.68	TC	[3168]
Cd	–	–	–	–	–	3.70	TC	[2629]
Cd	–	–	?	~ 300	–	3.73	PE	[2460]
Cd	–	–	? (N$_2$)	~ 300	–	3.80 ± 0.02	CPD	[4251]
Cd	–	–	? (Ar)	~ 300	–	3.83	CPD	[4253]
Cd/ins/Al[47]	Cd	–	?	~ 300	–	3.88 ± 0.08	CPD	[2028]
Cd	–	–	–	–	–	3.89	TC	[1744]
Cd	–	–	–	–	–	3.9*	TC	[1645]
Cd	–	–	–	–	–	3.9	TC	[3318]
Cd	–	–	–	–	–	3.93	TC	[3318]
Cd	–	–	6×10^{-3}	~ 300	–	3.94 ± 0.06	PE	[2079,2080]
Cd	–	–	–	–	–	3.96	TC	[1399]
Cd	–	–	–	–	–	3.97	TC	[3264,3265]
Cd	–	–	–	–	–	4.0	TC	[1993,2005]
Cd	–	–	–	–	–	4.0 ± 0.05	TC	[1990]
Cd	–	–	?	~ 300	–	4.00	CPD	[2297]
Cd	–	–	–	–	–	4.01	TC	[3352]
Cd	–	–	? (N$_2$)	~ 300	–	4.01 ± 0.02	CPD	[2361,2626,4226]
Cd	–	–	$<1 \times 10^{-5}$	~ 300	–	4.04	CPD	[1883]
Cd[212]	–	–	$\sim 10^{-6}$	~ 300	–	4.05 ± 0.06*	CPD	[1953]
Cd/glass	Cd	–	$<10^{-6}$	~ 300	–	4.06	PE	[1451]
Cd/brass	Cd	–	$\leq 10^{-8}$	~ 300	–	4.07 ± 0.2	PE	[2848]
Cd/Ta[214]	Cd	–	?	~ 300	–	4.08 ± 0.02	CPD	[1380]
Cd/glass	Cd	–	?	90	–	4.099	PE	[3031]
Cd/glass	Cd	–	?	90 (~ 300)	–	4.099	PE	[3031]
Cd	–	–	–	–	–	4.1	TC	[706]
Cd/W	Cd	–	$\leq 3 \times 10^{-9}$	375	–	4.1 ± 0.1	FE	[3047]
Cd	–	–	–	–	–	4.10	TC	[1885]
Cd	–	–	–	–	–	4.10	TC	[738]
Cd	–	–	–	–	–	4.11	TC	[298]
Cd[213]	–	–	$\sim 10^{-6}$	~ 300	–	4.11 ± 0.06*	CPD	[2087]
Cd	–	–	–	–	–	4.12	TC	[3267]
Cd	–	–	–	–	–	4.14	TC	[1901]
Cd/Ta[214]	Cd	–	?	~ 300	–	4.22 ± 0.01	CPD	[1380]
Cd[212]	–	–	$\sim 10^{-6}$	–	–	4.43 ± 0.01	CPD	[1953]
Cd	–	–	–	–	–	4.47	TC	[1066]
Cd[213]	–	–	?	~ 300	–	4.49 ± 0.01	CPD	[2087]
Cd	–	–	–	–	–	4.57	TC	[2629]
Recommended	–	–	–	–	–	**4.06 ± 0.05**	–	–

Table 1 (*continued*)

Surface	Beam	Ion	P_r (Torr)	T (K)	ϕ^+ (eV)	ϕ^e (eV)	Meth.	Refs.
						49. Indium In		
fcc								
In(100)	–	–	–	–	–	4.2	TC	[2375]
In(100)	–	–	–	–	–	4.6	TC	[2375]
In(100)	–	–	–	–	–	4.6	TC	[1714]
In(110)/PTCDA[477]	In	–	2×10^{-10}	~300	–	4.44 ± 0.05	PE	[4341]
In(111)	–	–	5×10^{-9}	~300	–	4.14 ± 0.05	PE	[2336]
In[379]	–	–	–	–	–	3.6	TC	[1955]
In	–	–	–	–	–	3.6	TC	[3318]
In	–	–	–	–	–	3.62	TC	[1744]
In	–	–	$\sim 10^{-7}$	~300	–	3.82 ± 0.05	PE	[2814]
In	–	–	$\sim 10^{-7}$	~300	–	3.825 ± 0.01	CPD	[2814]
In	–	–	–	–	–	3.84	TC	[2629]
In/Au(111)	In	–	$<10^{-10}$	80	–	3.85	CPD	[2661]
In/quartz[215]	In	–	$\sim 10^{-6}$	~300	–	3.85 ± 0.01	PE	[1475]
In	–	–	?	293	–	3.90	PE	[4139]
In	–	–	?	~300	–	3.90	PE	[4249]
In/quartz[215]	In	–	$\sim 10^{-6}$	~300	–	3.94 ± 0.01	PE	[1475]
In	–	–	?	419	–	3.96	PE	[4139]
In	–	–	–	–	–	3.97	TC	[1613]
In	–	–	–	–	–	3.97	TC	[2005]
In[160]	–	–	–	–	–	4.0	TC	[1355]
In	–	–	–	–	–	4.0	TC	[944]
In	–	–	–	–	–	4.0	TC	[3928]
In	–	–	$<10^{-9}$	~300	–	4.0	PE	[2321]
In	–	–	–	–	–	4.0	TC	[298]
In	–	–	–	–	–	4.0	TC	[706]
In	–	–	$\sim 10^{-9}$	~430	–	4.00	PE	[4241]
In	–	–	? (N_2)	~300	–	4.00 ± 0.02	CPD	[4251]
$In_n (n \to \infty)$	–	–	–	–	–	4.04	TC	[4244]
In	–	–	–	–	–	4.05	TC	[3352]
In	–	–	? (N_2)	~300	–	4.05 ± 0.02	CPD	[2624,2626,4083]
In	–	–	?	~430	–	4.07	PE	[4328]
In	–	–	–	–	–	4.08	TC	[3264,3265,3267]
In/glass	In	–	5×10^{-11}	77–90	–	4.08 ± 0.01	PE	[3319]
In	–	–	?	403	–	4.09 ± 0.01	PE	[2770,2771]
In	–	–	–	–	–	4.1	TC	[1993]
In/DiMe[477]	In	–	2×10^{-10}	~300	–	4.10 ± 0.05	PE	[4341]
$In_n (n \to \infty)$	–	–	?	~300	–	4.12	IP, TC	[4197]
In/quartz	In	–	$<3 \times 10^{-9}$	~153	–	4.12 ± 0.02	PE	[3672]
In	–	–	–	–	–	4.13	TC	[4418,4420]
In	–	–	–	–	–	4.16	TC	[3264]
In/W(110)	In	–	1×10^{-9}	~300	–	4.25 ± 0.05	CPD	[1986]
In	–	–	–	–	–	4.30	TC	[1901]
In/Au(111)	In	–	$<10^{-10}$	80	–	4.32	CPD	[2661]
In/Si(111)	In	–	2×10^{-10}	~300	–	4.34 ± 0.1	PE	[2623]
In/Si(111)	In	–	$<4 \times 10^{-10}$	~300	–	4.35	PE	[1566]
In/W	In	–	?	78 (?)	–	4.35 ± 0.1	FE	[2725]
In/Si(111)	In	–	$<3 \times 10^{-10}$	~300	–	4.39	PE	[3285]
In/W	In	–	$<2 \times 10^{-10}$	77 (≤500)	–	4.63	FE	[2727]
In	–	–	–	–	–	4.74	TC	[2629]
In	–	–	–	–	–	4.88	TC	[738]
Recommended	–	–	–	–	–	**4.05 ± 0.06**	–	–
Liquid ($T > 430$ K)								
In[438]	–	–	?	470	–	3.88	PE	[2111]
In	–	–	?	439	–	3.93	PE	[4139]
In	–	–	10^{-9}	~430	–	3.93	PE	[4241]
In	–	–	?	~430	–	4.03	PE	[4328]
In	–	–	?	447	–	4.06 ± 0.01	PE	[2770,2771]
In	–	–	$\leq 10^{-9}$	473	–	4.08 ± 0.04	PE	[2345,2349,2353]
In	–	–	$\leq 10^{-9}$	473	–	4.10	SP	[2349]
Recommended	–	–	–	–	–	**4.00 ± 0.08**	–	–

Table 1 (*continued*)

Surface	Beam	Ion	P_r (Torr)	T (K)	ϕ^+ (eV)	ϕ^e (eV)	Meth.	Refs.
				50. Tin Sn				
bcc (α, T < 291 K)								
Sn(100)	–	–	–	–	–	3.47	TC	[3211]
Sn(100)	–	–	–	–	–	4.42	TC	[2536]
Sn(100)	–	–	–	–	–	4.43	TC	[2536]
Sn(100)	–	–	–	–	–	4.68	TC	[2536]
Sn(110)	–	–	–	–	–	4.77	TC	[3211]
Sn(111)	–	–	–	–	–	4.01	TC	[3211]
Sn(111)	–	–	$\leq 10^{-6}$	?	–	4.26	PE	[3580]
Sn(112)	–	–	–	–	–	4.46	TC	[1627]
bcc (α, T < 291 K for bulk)								
Sn	–	–	–	–	–	3.45	TC	[3211]
Sn	–	–	–	–	–	3.57	TC	[3211]
Sn/Au	Sn	–	$< 5 \times 10^{-10}$	173–203	–	4.13	CPD	[3561]
Sn	–	–	–	–	–	4.27	TC	[3211]
Sn/quartz	Sn	–	$< 10^{-6}$	20 (200)	–	4.288 ± 0.005	PE	[1467]
Sn/quartz	Sn	–	$< 10^{-6}$	14	–	4.306 ± 0.006	PE	[1467]
Sn/quartz	Sn	–	$< 10^{-6}$	20 (90)	–	4.309 ± 0.005	PE	[1467]
Sn/quartz	Sn	–	$< 10^{-6}$	90	–	4.309 ± 0.005	PE	[1467]
Sn/W	Sn	–	?	78 (?)	–	4.85 ± 0.1	FE	[2725]
Sn/W	Sn	–	$< 2 \times 10^{-10}$	77 ($\leq$500)	–	5.10	FE	[2725,2727]
Recommended	–	–	–	–	–	**4.27 $\pm$ 0.06**	–	–
Tetragonal (β, T = 291–473 K for bulk)								
Sn	–	–	?	~300	–	3.41	PE	[3683]
Sn/SiO$_2$/Si	Sn	–	?	~300 (570)	–	3.42	PE	[2355]
Sn	–	–	?	~300	–	3.62	PE	[2460]
Sn	–	–	–	–	–	3.8	TC	[2456]
Sn	–	–	–	–	–	3.8	TC	[3727]
Sn	–	–	–	–	–	3.85	TC	[2629]
Sn	–	–	6×10^{-3}	~300	–	3.87 ± 0.07	PE	[2079,2080]
Sn/Mo(110)	Sn	–	$\leq 5 \times 10^{-11}$	350	–	4.0*	CPD	[3290]
Sn	–	–	?	~300	–	4.06*	CPD	[3621]
Sn	–	–	?	~300	–	4.09	CPD	[2297]
Sn	–	–	–	–	–	4.1	TC	[298]
Sn	–	–	–	–	–	4.1	TC	[2583]
Sn	–	–	–	–	–	4.1	TC	[1993]
Sn/GaAs	–	–	–	–	–	4.10	TC	[3054]
Sn	–	–	–	–	–	4.13	TC	[2005]
Sn	–	–	?	~300	–	4.14	PE	[4159]
Sn	–	–	$\sim 10^{-9}$	293	–	4.16	PE	[2362]
Sn	–	–	?	~300	–	4.17	PE	[4249]
Sn	–	–	–	–	–	4.17	TC	[1613]
Sn	–	–	–	–	–	4.17	TC	[3352]
Sn	–	–	? (N$_2$)	~300	–	4.17 ± 0.02	CPD	[2361,2624,2628]
Sn	–	–	?	293	–	4.18	PE	[4139]
Sn	–	–	$\sim 10^{-9}$	293	–	4.18	PE	[1445]
Sn/steel	Sn	–	2×10^{-10}	~300	–	4.2 ± 0.1	PE	[1537]
Sn	–	–	?	~300	–	4.2 ± 0.2	PE	[2086]
Sn	–	–	–	–	–	4.23	TC	[1976]
Sn	–	–	$\sim 10^{-9}$	504	–	4.23	PE	[4241]
Sn	–	–	1×10^{-5}	~300	–	4.25	CPD	[1883]
Sn[216]	–	–	$\sim 10^{-6}$	~300	–	4.26 ± 0.06*	CPD	[2087]
Sn	–	–	?	~300	–	4.27 ± 0.04*	CPD	[4159]
Sn/ins/Al[47]	Sn	–	?	~300	–	4.28 ± 0.06	CPD	[2028]
Sn	–	–	–	–	–	4.29	TC	[1399]
Sn	–	–	–	–	–	4.3 ± 0.05	TC	[1990]
Sn/steel	Sn	–	($< 2 \times 10^{-10}$)	~300	–	4.3 ± 0.1	PE	[2838]
Sn/Mo	Sn	–	($< 2 \times 10^{-10}$)	~300	–	4.3 ± 0.1	PE	[2838]
Sn/Si(111)	Sn	–	$< 3 \times 10^{-10}$	~300	–	4.32	PE	[3281]
Sn	–	–	–	–	–	4.35	TC	[3264,3265,3267]
Sn	–	–	–	–	–	4.37	TC	[1885]
Sn	–	–	?	~300	–	4.38	CPD	[3256]
Sn[217]	–	–	–	358	–	4.39	TC	[1135]

Table 1 (*continued*)

Surface	Beam	Ion	P_r (Torr)	T (K)	ϕ^+ (eV)	ϕ^e (eV)	Meth.	Refs.
Sn/brass	Sn	–	≤10^{-8}	~300	–	4.39 ± 0.13	PE	[2848]
Sn/Al(111)	Sn	–	<1 × 10^{-10}	~300	–	4.4	PE	[249]
Sn/Ni(111)	Sn	–	<1 × 10^{-10}	~300	–	4.4	PE	[249]
Sn/steel	Sn	–	(<2 × 10^{-10})	~300	–	4.4 ± 0.1	PE	[2838]
Sn/Mo	Sn	–	(<2 × 10^{-10})	~300	–	4.4 ± 0.1	PE	[2838]
Sn/Al$_2$O$_3$/Al	Sn	–	?	~300	–	4.42	CPD	[3057]
Sn	–	–	4 × 10^{-9}	299	–	4.42 ± 0.03	PE	[1116]
Sn	–	–	?	~300	–	4.47	CPD	[4159]
Sn	–	–	<1 × 10^{-10}	~300	–	4.5	PE	[249]
Sn	–	–	–	–	–	4.5	TC	[706]
Sn[217]	–	–	?	358	–	4.51 ± 0.02	PE	[1945–1947]
Sn/Si(111)	Sn	–	≤3 × 10^{-10}	~300	–	4.55	PE	[3285]
Sn/Al$_2$O$_3$/Al	Sn	–	?	~300	–	4.57 ± 0.06*	CPD	[3057]
Sn	–	–	–	–	–	4.63	TC	[1901]
Sn[216]	–	–	?	~300	–	4.63 ± 0.01	CPD	[2087]
Sn/W	Sn	–	?	400	–	4.67 ± 0.07*	FE	[3741]
Sn	–	–	–	–	–	4.76	TC	[2629]
Recommended	–	–	–	–	–	**4.34 ± 0.06**	–	–

Hexagonal (γ, T = 473–505 K for bulk)

Sn	–	–	?	495	–	4.22	PE	[4139]
Sn[218]	–	–	?	483	–	4.28	PE	[1135]
Sn[218]	–	–	?	483	–	4.38 ± 0.02	PE	[1945–1947]

Liquid (T > 505 K)

Sn[218]	–	–	–	673	–	4.17	TC	[1135]
Sn	–	–	?	515	–	4.18	PE	[4139]
Sn	–	–	~10^{-9}	506	–	4.19	PE	[4241]
Sn	–	–	?	>505	–	4.21*	CPD	[3575]
Sn[218]	–	–	?	673	–	4.22 ± 0.01	PE	[1945–1947]

51. Antimony Sb

Rhombohedral (arsenic structure)

Sb(100)	–	–	?	?	–	4.69	?	[3141]
Sb(100)/W(110)[219]	Sb	–	~10^{-9}	~300 (373)	–	4.7	CPD	[1272]
Sb(111)	–	–	≤10^{-6}	~300	–	4.26	PE	[3580]
Sb	–	–	1 × 10^{-5}	~300	–	4.01	PE	[2563]
Sb/Si(001)	–	–	–	–	–	4.03	TC	[2525]
Sb	–	–	–	–	–	4.05	TC	[1885]
Sb/W	Sb	–	<10^{-8}	~300	–	4.10 ± 0.03	CPD	[1163]
Sb	–	–	?	~300	–	4.14	CPD	[2297]
Sb	–	–	? (N$_2$)	~300	–	4.18 ± 0.02	CPD	[2624,2626,4226]
Sb	–	–	–	–	–	4.19	TC	[3352]
Sb	–	–	–	–	–	4.2	TC	[298]
Sb	–	–	–	–	–	4.3	TC	[1993]
Sb/Si	–	–	–	–	–	4.35	TC	[1653]
Sb	–	–	–	–	–	4.38	TC	[1653,1976]
Sb/Si(111)	Sb	–	≤8 × 10^{-11}	~300	–	4.43	PE	[1904]
Sb	–	–	–	–	–	4.48	TC	[2005]
Sb/quartz	Sb	–	<5 × 10^{-8}	~300	–	4.52	PE	[3625]
Sb/W(100)[219]	Sb	–	~10^{-9}	~300	–	4.55	CPD	[1955]
Sb	–	–	–	–	–	4.56	TC	[3264,3265,3267]
Sb/Ni,Mo,etc.	Sb	–	<5 × 10^{-8}	~300	–	4.56	PE	[1375]
Sb/?	Sb	–	?	~300 (473)	–	4.60	PE	[3255]
Sb/Si(111)	Sb	–	<3 × 10^{-10}	~300	–	4.61	PE	[3285]
Sb/Si(111)	Sb	–	?	~300	–	4.65	PE	[2849]
Sb/W	Sb	–	?	78 (>600)	–	4.65	FE	[3642]
Sb/Au(111)	Sb	–	3 × 10^{-10}	~300	–	4.65 ± 0.04	CPD	[2690]
Sb	–	–	–	–	–	4.7	TC	[1905,1906]
Sb	–	–	–	–	–	4.79	TC	[1901]
Sb	–	–	–	–	–	4.8	TC	[706]
Sb/W(100)[219]	Sb	–	~10^{-9}	423	–	4.98	CPD	[1995]
Recommended	–	–	–	–	–	**4.45 ± 0.09**	–	–

Table 1 (*continued*)

Surface	Beam	Ion	P_r (Torr)	T (K)	ϕ^+ (eV)	ϕ^e (eV)	Meth.	Refs.
Amorphous								
Sb	–	–	–	–	–	3.92	TC	[1744]
Sb/?	Sb	–	?	~300	–	4.49	PE	[3255]
Sb/W(100)[219]	Sb	–	~10^{-9}	~300	–	4.55	CPD	[1995]
Sb/quartz	Sb	–	<5 × 10^{-8}	~300	–	4.7 ± 0.1	PE	[3625]

52. Tellurium Te

Surface	Beam	Ion	P_r (Torr)	T (K)	ϕ^+ (eV)	ϕ^e (eV)	Meth.	Refs.
Hexagonal								
Te(1010)	–	–	~10^{-11}	~300	–	4.65 ± 0.05	PE	[2482,4248]
Te(1010)	–	–	~10^{-10}	~300	–	4.95	PE	[3429]
Te/ins/Al[47]	Te	–	?	~300	–	3.95 ± 0.08	CPD	[2028]
Te	–	–	?	~300	–	4.04	PE	[3609]
Te/silica	Te	–	<2 × 10^{-10}	100 (~300)	–	4.1	PE	[4248]
Te/W(110)	Te	–	<5 × 10^{-11}	~300	–	4.5	CPD	[2855]
Te/W(100)	Te	–	<2 × 10^{-10}	~300	–	4.54	FE	[1682]
Te/W	Te	–	<2 × 10^{-10}	~300	–	4.61 ± 0.03	FE	[1680]
Te/glass[220]	Te	–	0.1 (Ar)	~300 (573)	–	4.62	CPD	[2246]
Te/Mo(100)	Te	–	<2 × 10^{-10}	~300	–	4.63	FE	[1682]
Te/W	Te	–	<2 × 10^{-10}	~300	–	4.63	FE	[1682]
Te	–	–	–	–	–	4.7	TC	[1993]
Te	–	–	?	300	–	4.70	CPD	[2297]
Te/Mo	Te	–	<2 × 10^{-10}	~300	–	4.72 ± 0.01	FE	[1680]
Te/W	Te	–	<10^{-9}	~300 (≤800)	–	4.74 ± 0.03	FE	[2333]
Te/glass[220]	Te	–	0.1 (Ar)	~300 (573)	–	4.76	CPD	[2246]
Te/glass	Te	–	<3 × 10^{-8}	~300	–	4.76	PE	[1371]
Te	–	–	–	–	–	4.78	TC	[1644]
Te/W(100)	Te	–	~10^{-11}	~300	–	4.8	CPD	[2853]
Te/Ni(100)	Te	–	<5 × 10^{-10}	~300	–	4.80 ± 0.10*	CPD	[1788,1790]
Te/Mo	Te	–	<2 × 10^{-10}	~300	–	4.81	FE	[1682]
Te/W(112)	Te	–	<2 × 10^{-10}	~300	–	4.82	FE	[1682]
Te/steel/ss	Te	–	~10^{-10}	~300	–	4.85	PE	[3429]
Te	–	–	–	–	–	4.88	TC	[1901]
Te/Cu	Te	–	5 × 10^{-6}	123, 300	–	4.89	PE	[2589]
Te/W	Te	–	<2 × 10^{-9}	1200	–	4.9	FE	[2367]
Te	–	–	–	–	–	4.9 ± 0.3	TC	[1905]
Te	–	–	–	0	–	4.92	TC	[4419]
Te/Ni(100)	Te	–	<5 × 10^{-10}	~300	–	4.94 ± 0.10*	CPD	[1790]
Te/Ni(100)	Te	–	<4 × 10^{-10}	~300	–	4.98	PE	[2693]
Te/Fe(100)	Te	–	<8 × 10^{-11}	573	–	4.98*	CPD	[2730]
Te/Ni(100)	Te	–	<5 × 10^{-10}	~300	–	4.99 ± 0.10*	CPD	[1790]
Te	–	–	–	–	–	5.0	TC	[298]
Te/glass	Te	–	?	~300	–	5.0	PE	[3254]
Te/Fe(100)	Te	–	<8 × 10^{-11}	473	–	5.07*	CPD	[2730]
Te/Ni(100)	Te	–	<5 × 10^{-10}	~300	–	5.07 ± 0.10*	CPD	[1790]
Te/quartz	Te	–	?	~300	–	5.1	PE	[3321]
Te	–	–	–	–	–	5.1*	TC	[1955]
Te/W	Te	–	<2 × 10^{-9}	900	–	5.1	FE	[2367]
Te/Fe(100)	Te	–	<8 × 10^{-11}	~300	–	5.10*	CPD	[2730]
Recommended	–	–	–	–	–	**4.86 ± 0.06**	–	–

53. Iodine I

Surface	Beam	Ion	P_r (Torr)	T (K)	ϕ^+ (eV)	ϕ^e (eV)	Meth.	Refs.
Rhombic								
I_2/Pt	I_2	–	?	~90	–	2.78 ± 0.03	PE	[3403]
Monoclinic								
I_2/Pt	I_2	–	?	~90	–	5.41 ± 0.02	PE	[3403]
Iodine Film								
I/Mo(100)	CsI	Cs^+	?	~1400–2000	4.65 ± 0.20	–	PSI	[584]
I/W(100)	I_2	–	<10^{-6} (I_2)	~300	–	4.73 ± 0.04	CPD	[581]
I/W(110)	I_2	–	?	~300	–	4.9*	CPD	[2486]
I/W(100)	I_2	–	?	~300	–	5.0*	?	[3820]
I/Fe(110)	I_2	–	5 × 10^{-11}	~300	–	5.00 ± 0.01	CPD	[4399]
I/Fe(100)	I_2	–	5 × 10^{-11}	~300	–	5.07	CPD	[4399]
I/Au[437]	I_2	–	0.20 (I_2)	~300	–	5.1	PE	[2760]
I/Fe(100)	I_2	–	<10^{-7} (I_2)	~300	–	5.1 ± 0.1*	CPD	[3760]

Table 1 (*continued*)

Surface	Beam	Ion	P_r (Torr)	T (K)	ϕ^+ (eV)	ϕ^e (eV)	Meth.	Refs.
I/Hg/Au[437]	I_2	–	0.20 (I_2)	~300	–	5.25	PE	[2760]
I/W	KI	K^+	?	<1600	5.27	–	PSI	[46]
I/W	KI	–	?	1200 (2350)	–	5.43	CPD	[3748]
Recommended	–	–	–	–	–	**5.1 ± 0.1**	–	–
Amorphous								
I_2	–	–	–	–	–	5.88	TC	[1901]
I_2/Pt	I_2	–	?	~90	–	6.75 ± 0.02	PE	[3403]

55. Cesium Cs[444]

bcc

Surface	Beam	Ion	P_r (Torr)	T (K)	ϕ^+ (eV)	ϕ^e (eV)	Meth.	Refs.
Cs(100)	–	–	–	–	–	1.881	TC	[2947]
Cs(100)	–	–	–	–	–	1.90	TC	[475]
Cs(100)	–	–	–	–	–	1.90	TC	[1254]
Cs(100)	–	–	–	–	–	1.974	TC	[4091]
Cs(100)	–	–	–	–	–	2.01	TC	[231]
Cs(100)	–	–	–	–	–	2.03	TC	[2427]
Cs(100)	–	–	–	–	–	2.03	TC	[334]
Cs(100)	–	–	–	–	–	2.03	TC	[3467]
Cs(100)	–	–	–	–	–	2.04	TC	[553]
Cs(100)	–	–	–	–	–	2.14	TC	[711]
Cs(100)	–	–	–	–	–	2.14	TC	[1159,3067]
Cs(100)	–	–	–	–	–	2.23	TC	[1030]
Cs(100)	–	–	–	–	–	2.24	TC	[1095]
Cs(100)	–	–	–	–	–	2.24	TC	[321]
Cs(100)	–	–	–	–	–	2.28	TC	[3814]
Cs(100)	–	–	–	–	–	2.3	TC	[763]
Cs(100)	–	–	–	–	–	2.3	TC	[1088]
Cs(100)	–	–	–	–	–	2.30	TC	[475]
Cs(100)	–	–	–	–	–	2.31	TC	[476,711]
Cs(100)	–	–	–	–	–	2.36	TC	[555]
Cs(100)	–	–	–	–	–	2.39	TC	[476]
Cs(100)	–	–	–	–	–	2.40	TC	[1030]
Recommended	–	–	–	–	–	**2.24 ± 0.06**	–	–
Cs(110)	–	–	–	–	–	1.929	TC	[2947]
Cs(110)	–	–	–	–	–	2.0	TC	[1723]
Cs(110)	–	–	–	–	–	2.073	TC	[4091]
Cs(110)	–	–	–	–	–	2.09	TC	[334,3179]
Cs(110)	–	–	–	–	–	2.1	TC	[3137]
Cs(110)	–	–	–	–	–	2.1	TC	[1086]
Cs(110)	–	–	–	–	–	2.17	TC	[231]
Cs(110)	–	–	–	–	–	2.19	TC	[553,2427]
Cs(110)	–	–	–	–	–	2.21	TC	[3467]
Cs(110)	–	–	–	–	–	2.23	TC	[1159,3067]
Cs(110)	–	–	–	–	–	2.25	TC	[475]
Cs(110)	–	–	–	–	–	2.30	TC	[593]
Cs(110)	–	–	–	–	–	2.34	TC	[711]
Cs(110)	–	–	–	–	–	2.35	TC	[1030]
Cs(110)	–	–	–	–	–	2.37	TC	[1086]
Cs(110)	–	–	–	–	–	2.44	TC	[2402]
Cs(110)	–	–	–	–	–	2.44	TC	[3814]
Cs(110)	–	–	–	–	–	2.49	TC	[1086]
Cs(110)	–	–	–	–	–	2.5	TC	[763]
Cs(110)	–	–	–	–	–	2.5	TC	[1088]
Cs(110)	–	–	–	–	–	2.51	TC	[476,711]
Cs(110)	–	–	–	–	–	2.56	TC	[1030,1089]
Cs(110)	–	–	–	–	–	2.57	TC	[476]
Cs(110)	–	–	–	–	–	2.58	TC	[2835]
Cs(110)	–	–	–	–	–	2.59	TC	[1095]
Cs(110)	–	–	–	–	–	2.60	TC	[321]
Cs(110)	–	–	–	–	–	2.60	TC	[475]
Cs(110)	–	–	–	–	–	2.62	TC	[555]
Cs(110)	–	–	–	–	–	2.64	TC	[2835]
Cs(110)	–	–	–	–	–	2.66	TC	[1089]
Cs(110)	–	–	–	–	–	2.666	TC	[4069]
Cs(110)	–	–	–	–	–	2.68	TC	[1089]
Cs(110)	–	–	–	–	–	2.72	TC	[1086]

Table 1 (*continued*)

Surface	Beam	Ion	P_r (Torr)	T (K)	ϕ^+ (eV)	ϕ^e (eV)	Meth.	Refs.
Cs(110)	–	–	–	–	–	2.73	TC	[1086]
Cs(110)	–	–	–	–	–	2.74	TC	[1086]
Cs(110)	–	–	–	–	–	2.74	TC	[1086]
Cs(110)	–	–	–	–	–	2.74	TC	[3693]
Cs(110)	–	–	–	–	–	2.75	TC	[3731]
Cs(110)	–	–	–	–	–	2.78	TC	[1086]
Cs(110)	–	–	–	–	–	2.8	TC	[1086,1088]
Cs(110)	–	–	–	–	–	2.81	TC	[3693]
Cs(110)	–	–	–	–	–	2.82	TC	[3712]
Cs(110)	–	–	–	–	–	2.82	TC	[3713]
Cs(110)	–	–	–	–	–	2.87	TC	[3692]
Cs(110)	–	–	–	–	–	2.90	TC	[3692]
Recommended	–	–	–	–	–	**2.54 ± 0.07**	–	–
Cs(111)	–	–	–	–	–	1.80	TC	[475]
Cs(111)	–	–	–	–	–	1.85	TC	[593]
Cs(111)	–	–	–	–	–	1.93	TC	[711]
Cs(111)	–	–	–	–	–	1.97	TC	[231]
Cs(111)	–	–	–	–	–	1.971	TC	[4091]
Cs(111)	–	–	–	–	–	1.98	TC	[3467]
Cs(111)	–	–	–	–	–	2.01	TC	[553]
Cs(111)	–	–	–	–	–	2.10	TC	[476,711]
Cs(111)	–	–	–	–	–	2.14	TC	[1159,3067]
Cs(111)	–	–	–	–	–	2.14	TC	[321]
Cs(111)	–	–	–	–	–	2.14	TC	[3814]
Cs(111)	–	–	–	–	–	2.14	TC	[1030]
Cs(111)	–	–	–	–	–	2.14	TC	[1095]
Cs(111)	–	–	–	–	–	2.19	TC	[476]
Cs(111)	–	–	–	–	–	2.2	TC	[1088]
Cs(111)	–	–	–	–	–	2.20	TC	[475]
Cs(111)	–	–	–	–	–	2.24	TC	[555]
Recommended	–	–	–	–	–	**2.09 ± 0.08**	–	–
Cs(112)	–	–	–	–	–	2.39	TC	[321]
Cs	–	–	–	–	–	1.3	TC	[3737]
Cs/GaP(111)	Cs^+	–	$\sim 10^{-10}$	80	–	1.3 ± 0.2	CPD	[1794]
Cs/GaP(111)	Cs^+	–	$\sim 10^{-10}$	~300	–	1.3 ± 0.2	CPD	[1794]
Cs/W	Cs	–	$\sim 10^{-7}$	~300	–	1.43	FE	[2335]
Cs/Os	Cs	–	? (Cs)	~500–800	–	1.44	TE	[650,3414]
Cs/Ti	Cs	–	? (Cs)	?	–	1.44	TE	[650,3413]
Cs/GaP	Cs	–	?	~300	–	1.45	PE	[3070]
Cs/Si(100)	Cs	–	$<6 \times 10^{-11}$	~300	–	1.45*	CPD	[2433]
Cs/MO$_2$C	Cs	–	? (Cs)	~500–650	–	1.48	TE	[650]
Cs/W(110)	–	–	–	–	–	1.5*	TC	[514]
Cs/Si(111)	Cs	–	$<4 \times 10^{-11}$	~300	–	1.5*	PE	[2659]
Cs/GaAs	Cs	–	?	~300	–	1.52	PE	[3070]
Cs/Si(100)	–	–	–	–	–	1.53*	TC	[2399]
Cs/Ta	Cs	–	? (Cs)	~500–650	–	1.55	TE	[650]
Cs/Fe	Cs	–	$<10^{-9}$	~300	–	1.55	PE	[307]
Cs/Ge(111)	Cs	–	$\sim 10^{-10}$	~300	–	1.55	CPD	[1396]
Cs/Cu	Cs	–	?	~300	–	1.55	PE	[1473]
Cs/W(110)	Cs	–	$(\sim 10^{-12})$	~300	–	1.55 ± 0.02	CPD	[1795]
Cs/Re	Cs	–	? (Cs)	~500–700	–	1.56	TE	[650,3414]
Cs/Ge(100)	Cs^+	–	1×10^{-10}	~300	–	1.6	CPD	[3423]
Cs/Si(111)[221]	Cs	–	$\sim 10^{-9}$	~300	–	1.6*	PE	[1823]
Cs/W(111)	–	–	–	–	–	1.6*	TC	[514]
Cs/Mo(110)	Cs	–	1×10^{-3} (Cs)	~700–850	–	1.6	TE	[976]
Cs/Si(111)	Cs	–	$\sim 10^{-10}$	~300	–	1.6	CPD	[3579]
Cs/W–Re(25%)	Cs	–	? (Cs)	690–740	–	1.60	TE	[393]
Cs/steel	Cs	–	? (Cs)	~450–700	–	1.60	TE	[650,3410,3413]
Cs/Si(111)	Cs	–	$\sim 10^{-10}$	~300	–	1.62	CPD	[1396]
Cs/Nb	Cs	–	? (Cs)	~500–700	–	1.63	TE	[650,3414]
Cs/Cu	Cs	–	? (Cs)	~450–650	–	1.64	TE	[650,3413]
Cs/W	Cs	–	? (Cs)	~500–750	–	1.64	TE	[650,3414]
Cs/Re[222]	Cs	–	?	?	–	1.64	TE	[3582]
Cs/Ag	Cs	–	?	~300	–	1.65	PE	[1473]
Cs/Pt(111)	Cs	–	$<2 \times 10^{-10}$	~300	–	1.65*	CPD	[2434]
Cs/W(100)	Cs	–	$\leq 10^{-10}$	77	–	1.65 ± 0.1	FE	[1978]
Cs/W(110)	Cs	–	6×10^{-6} (Cs)	770	–	1.654 ± 0.055	TE	[151]

Table 1 (*continued*)

Surface	Beam	Ion	P_r (Torr)	T (K)	ϕ^+ (eV)	ϕ^e (eV)	Meth.	Refs.
Cs/Pt(210)	Cs	–	? (Cs)	~500–750	–	1.66	TE	[650,3413,3414]
Cs/ZrC	Cs	–	? (Cs)	~450	–	1.68	TE	[650]
Cs/Re	Cs	–	$\geq 10^{-4}$ (Cs)	~800–850	–	1.7	TE	[1774]
Cs/Cu(100)	–	–	–	–	–	1.7	TC	[389]
Cs/Ni(100)	–	–	–	–	–	1.7	TC	[389]
Cs/Ta(100)	–	–	–	–	–	1.7	TC	[389]
Cs/W	Cs	–	? (Cs)	~800–1000	–	1.7	TE	[3808]
Cs/Pt(100)	–	–	–	–	–	1.7	TC	[389]
Cs/MoS$_2$(0001)	Cs	–	$<1 \times 10^{-10}$	140	–	1.7	CPD	[2390]
Cs/Si(100)	Cs	–	5×10^{-11}	~300 (?)	–	1.7	PE	[1869]
Cs/Se/Si(100)[226]	Cs	–	$\sim 10^{-10}$	~300	–	1.7	CPD	[3811]
Cs/W(111)	Cs	–	?	77 (≤325)	–	1.7	FE	[3079]
Cs/W(112)	Cs	–	?	77 (≤325)	–	~1.7	FE	[3079]
Cs/W	Cs$^+$	–	$<3 \times 10^{-10}$	~300	–	1.7	CPD	[3289]
Cs/W(103)	Cs	–	?	77	–	1.7	FE	[3079]
Cs/W(103)	Cs	–	?	77 (≤325)	–	1.7	FE	[3079]
Cs/W(115)	Cs	–	?	77	–	1.7	FE	[3079]
Cs/W(115)	Cs	–	?	77 (≤325)	–	1.7	FE	[3079]
Cs/Mo	Cs	–	4×10^{-8}	~300 (900)	–	1.7 ± 0.2	CPD	[3754]
Cs/Ni	Cs	–	? (Cs)	~550–800	–	1.7–2.0	TE	[650]
Cs/Ta	Cs	–	? (Cs)	~500–650	–	1.70	TE	[3414]
Cs/Mo	Cs$^+$	–	$<3 \times 10^{-10}$	~300	–	1.71 ± 0.08	CPD	[3289]
Cs/Li	Cs	–	1×10^{-8}	~300	–	1.73	PE	[1433]
Cs/W(110)	Cs	–	$\leq 1 \times 10^{-9}$	~550	–	1.73	TE	[255]
Cs/W	Cs	–	? (Cs)	500	–	1.74*	TE	[3786]
Cs/W(100)	Cs	–	?	~300	–	1.74 ± 0.06*	CPD	[3612]
Cs/W	Cs	–	? (Cs)	~600–800	–	1.74 ± 0.26	TE	[2462]
Cs/Re	Cs	–	$\sim 10^{-10}$	~300	–	1.75	FE	[2319,3864]
Cs/Mo(110)	Cs	–	$\leq 10^{-10}$	~300	–	1.76*	CPD	[3805]
Cs/W(100)	Cs	–	?	77 (?)	–	1.76 ± 0.05	FE	[340]
Cs/W(112)	Cs	–	6×10^{-6} (Cs)	780	–	1.769 ± 0.063	TE	[151]
Cs/Mo	Cs	–	? (Cs)	~500–750	–	1.77	TE	[650,3414]
Cs/W(100)	Cs	–	$<5 \times 10^{-11}$	~300	–	1.77	CPD	[1672]
Cs/Re	Cs	–	?	77 (?)	–	1.77 ± 0.05	FE	[340]
Cs/Mo	Cs	–	$\sim 10^{-10}$	~300	–	1.78	FE	[3864]
Cs/W(112)	Cs	–	$\leq 1 \times 10^{-9}$	~550	–	1.78	TE	[255]
Cs/W(100)[231]	Cs	–	$<5 \times 10^{-11}$	~300	–	1.78	CPD	[360,361,1667]
Cs/W	Cs	–	?	77	–	1.78	FE	[396]
Cs/Mo(110)	Cs	–	$(\sim 10^{-12})$	?	–	1.78 ± 0.02	CPD	[1795]
Cs/Nb(111)	Cs	–	?	?	–	1.78 ± 0.03	TE	[2329]
Cs/Ta(110)	Cs	–	$\sim 10^{-11}$	~300	–	1.79	CPD	[683,1886]
Cs/W	Cs	–	2×10^{-8}	~300	–	1.79	FE	[2335]
Cs/W(100)	Cs	–	$\leq 1 \times 10^{-9}$	~550	–	1.79	TE	[255]
Cs/W(100)	Cs	–	$<5 \times 10^{-11}$	~300	–	1.8	CPD	[3510]
Cs/Si(111)	Cs	–	3×10^{-11}	~300	–	1.8*	CPD	[3470]
Cs/Mo(111)	Cs	–	5×10^{-9}	~300	–	1.8	CPD	[2786]
Cs/TiO$_2$(110)	Cs	–	?	~300	–	1.8	PE	[1610]
Cs/TiO$_2$(110)	Cs	–	8×10^{-11}	~300	–	1.8	PE	[3188]
Cs/Pt(111)	Cs	–	$<4 \times 10^{-11}$	295	–	1.8	PE	[423]
Cs/Ir	Cs	–	?	20	–	1.8	FE	[2320]
Cs/W	–	–	–	–	–	1.8	TC	[913]
Cs/Ag(110)[224]	Cs	–	?	~300	–	1.8	PE	[2144]
Cs/Ta(110)	–	–	–	–	–	1.8	TC	[509]
Cs/Si(111)	Cs	–	?	~300	–	1.8*	CPD	[1589]
Cs	–	–	–	–	–	1.8	TC	[3030]
Cs/W(100)	Cs	–	5×10^{-11}	~300	–	1.8	CPD	[3418]
Cs/W(112)	Cs$^+$	–	$<10^{-10}$	~300	–	1.8	CPD	[2829]
Cs/W	Cs	–	8×10^{-9}	~300	–	1.8	FE	[2335]
Cs/Ni(110)	Cs	–	$\sim 10^{-11}$	20	–	1.8	PE	[2977]
Cs/NiO/Ni(100)	Cs$^+$	–	$<5 \times 10^{-11}$	~300	–	1.8	CPD	[1005]
Cs/Re(2111)	Cs	–	$\sim 10^{-9}$	~300	–	1.8	FE	[838]
Cs/W	Cs	–	$\sim 10^{-9}$	77	–	1.8	FE	[810]
Cs/W(111)	Cs	–	$\sim 10^{-9}$	77	–	1.8	FE	[810]
Cs/Si(111)	Cs	–	?	303	–	1.8*	CPD	[3230]
Cs/W(100)	Cs	–	7×10^{-10}	77 (≤500)	–	1.8	FE	[3691]
Cs/Mo	Cs	–	? (Cs)	~600–1000	–	1.8	TE	[3798,3799]
Cs/W	Cs	–	? (Cs)	~850–950	–	1.8	TE	[3798,3799]
Cs/Mo	Cs	–	? (Cs)	~600–800	–	1.8	TE	[1390]
Cs/W	Cs$^+$	–	$\leq 1 \times 10^{-10}$	~300	–	1.8*	CPD	[3812]
Cs/W	Cs	–	$<2 \times 10^{-9}$	~300	–	1.8	FE	[2367]

Table 1 (*continued*)

Surface	Beam	Ion	P_r (Torr)	T (K)	ϕ^+ (eV)	ϕ^e (eV)	Meth.	Refs.
Cs/W	Cs	–	$\sim 10^{-10}$	~ 300	–	1.8	FE	[2319,3864,3865]
Cs/W(111)	Cs	–	?	77	–	1.8	FE	[3079]
Cs/MoS$_2$(0001)	Cs	–	$< 1 \times 10^{-10}$	175	–	1.8	CPD	[2390]
Cs/W(100)	–	–	–	–	–	1.8	TC	[389]
Cs/Ir(100)	–	–	–	–	–	1.8	TC	[389]
Cs/W(100)	Cs	–	$\sim 10^{-10}$	~ 300	–	1.8	FE	[2324]
Cs/Al$_2$O$_3$/Al	Cs	–	? (Cs)	336	–	1.8 ± 0.1	CPD	[1649]
Cs/W	Cs	–	? (Cs)	620–650	–	1.80	TE	[393]
Cs(pool)	–	–	?	500	–	1.80*	TE	[3786]
Cs	–	–	–	–	–	1.80	TC	[1744]
Cs/W(100)	Cs	–	?	~ 300	–	1.80 ± 0.02	CPD	[1787,3600]
Cs/W^{228}	Cs	–	?	77 (?)	–	1.80 ± 0.05	FE	[340,3759]
Cs/Ni	Cs	–	?	77 (?)	–	1.80 ± 0.05	FE	[340]
Cs/W(100)^{225}	Cs	–	$\leq 2 \times 10^{-10}$	293	–	1.81	CPD	[1480]
Cs/Ge(111)	Cs$^+$	–	1×10^{-10}	~ 300	–	1.81	CPD	[3418,3423]
Cs/Re	Cs	–	$\sim 10^{-9}$	~ 300	–	1.81	FE	[838]
Cs/W(100)^{225}	Cs	–	$< 3 \times 10^{-11}$	~ 300	–	1.81	PE	[3435]
Cs/W	–	–	–	–	–	1.81	TC	[2465]
Cs/Mo	–	–	–	–	–	1.81	TC	[2465]
Cs	–	–	–	–	–	1.81	TC	[2949]
Cs	–	–	–	–	–	1.81	TC	[3728]
Cs/W(100)^{225}	Cs	–	?	98	–	1.81	FE	[644]
Cs/Cr	Cs	–	? (Cs)	~ 500–800	–	1.82	TE	[650,3413]
Cs/W(100)	Cs$^+$	–	$\sim 10^{-10}$	~ 300	–	1.82	CPD	[506]
Cs/W(100)	Cs	–	$< 5 \times 10^{-10}$	~ 300	–	1.82	CPD	[1887]
Cs/Ru(0001)	Cs	–	3×10^{-10}	~ 300	–	1.82	CPD	[1827]
Cs/W	Cs	–	$\leq 3 \times 10^{-10}$	~ 300	–	1.82 ± 0.01	CPD	[362]
Cs/W(100)	Cs	–	$\leq 3 \times 10^{-10}$	~ 300	–	1.82 ± 0.01	CPD	[362,1892,2481, 3830,3831]
Cs/Nb(112)	Cs	–	?	?	–	1.82 ± 0.03	TE	[2329]
Cs/W(100)	Cs$^+$	–	$\sim 10^{-10}$	~ 300	–	1.82 ± 0.04	CPD	[581]
Cs/W(100)	Cs	–	?	~ 300	–	1.82 ± 0.05	CPD	[3612]
Cs/Mo	Cs	–	?	77 (?)	–	1.82 ± 0.05	FE	[340]
Cs/Re(2112)	Cs	–	$\sim 10^{-9}$	~ 300	–	1.83	FE	[838]
Cs/W(111)	Cs	–	$\leq 1 \times 10^{-9}$	~ 550	–	1.83	TE	[255]
Cs/Fe	Cs	–	? (Cs)	~ 700–800	–	1.84	TE	[650,3413]
Cs/Al$_2$O$_3$	Cs	–	? (Cs)	?	–	1.84	TE	[650]
Cs/Mo$_2$Si$_3$	Cs	–	? (Cs)	?	–	1.84	TE	[650]
Cs/W	Cs	–	?	~ 300	–	1.84 ± 0.01	CPD	[1163]
Cs/Pt(111)	Cs	–	$< 2 \times 10^{-10}$	~ 300	–	1.85*	CPD	[2434]
Cs/W(112)	Cs	–	$\sim 10^{-9}$	77	–	1.85	FE	[810]
Cs/Fe	Cs	–	? (Cs)	?	–	1.85	TE	[650]
Cs/Ir	Cs	–	? (Cs)	~ 550–600	–	1.85	TE	[650]
Cs/Re	Cs	–	$\sim 10^{-10}$	290	–	1.85	FE	[2324]
Cs/W	Cs	–	$< 10^{-9}$	~ 300 (900)	–	1.85	FE	[2768]
Cs/Si(111)	Cs	–	$< 6 \times 10^{-11}$	~ 300	–	1.85*	CPD	[2433]
Cs/TaC	Cs	–	3×10^{-10}	~ 300	–	1.85 ± 0.05	CPD	[1504]
Cs/Ir	Cs	–	? (Cs)	~ 500–800	–	1.86	TE	[3414]
Cs/W	Cs	–	2×10^{-9}	~ 300	–	1.86	FE	[2335]
Cs/W^{232}	Cs$^+$	–	$< 3 \times 10^{-10}$	~ 300	–	1.86*	CPD	[3289,3815]
Cs/Cu	Cs	–	? (Cs)	?	–	1.86	PE	[3447]
Cs/?	Cs	–	?	?	–	1.87	?	[3785]
Cs/Ta	Cs	–	? (Cs)	~ 300	–	1.87	FE	[1972]
Cs/Si(100)^{223}	Cs	–	$< 1 \times 10^{-10}$	~ 300	–	1.87*	CPD	[2883]
Cs/W(100)	–	–	–	–	–	1.88	TC	[1539]
Cs	–	–	–	–	–	1.88	TC	[3318]
Cs/Au	Cs	–	$\sim 10^{-3}$ (Ar)	?	–	1.89	PE	[2789]
Cs/W(100)	Cs	–	$(< 10^{-11})$	~ 300	–	1.9	CPD	[776]
Cs/Mo(111)	Cs	–	?	~ 300	–	1.9	PE	[1527]
Cs/Si(100)^{226}	Cs	–	$\sim 10^{-10}$	~ 300	–	1.9*	CPD	[3811]
Cs/Si(100)	–	–	–	–	–	1.9	TC	[1223]
Cs/Au(100)	–	–	–	–	–	1.9	TC	[389]
Cs/Ta	Cs	–	$\sim 10^{-11}$	~ 300	–	1.9	CPD	[683]
Cs/Si(100)	Cs	–	7×10^{-11}	~ 300	–	1.9	CPD	[2531]
Cs/Si(100)	Cs$^+$	–	1×10^{-10}	~ 300	–	1.9	CPD	[3423]
Cs	–	–	–	–	–	1.9	TC	[1993]
Cs/W	Cs	–	$\sim 10^{-10}$	290	–	1.9	FE	[2324,3816]
Cs/Cu(111)	Cs	–	1×10^{-10}	~ 300	–	1.9*	CPD	[2491]
Cs/Ni(100)	Cs	–	$\leq 6 \times 10^{-10}$	~ 300	–	1.9	PE	[2366]
Cs/Ag(110)	Cs	–	?	80	–	1.9	PE	[2144]

Table 1 (*continued*)

Surface	Beam	Ion	P_r (Torr)	T (K)	ϕ^+ (eV)	ϕ^e (eV)	Meth.	Refs.
Cs/Ag(110)	Cs	–	?	~300	–	1.9	PE	[2144]
Cs/Mo(111)	Cs	–	?	~300	–	1.9	PE	[1527]
Cs/Be	Cs	–	$\leq 8 \times 10^{-10}$	~300	–	1.9	CPD	[3286]
Cs/W	Cs	–	? (Cs)	~700	–	1.9*	TE	[1858]
Cs/W(110)	Cs	–	?	77	–	1.9	FE	[3079,3818]
Cs/W(110)	Cs	–	?	77 (≤325)	–	1.9	FE	[3079,3818]
Cs/W(100)	Cs	–	(~10^{-11})	~300	–	1.9	CPD	[3340]
Cs/Mo	Cs, H	H$^-$	~10^{-8}	188–293	1.9^N	–	NSI	[3677]
Cs/Mo	Cs	–	7×10^{-9}	~300	–	1.9	CPD	[3756]
Cs/O/Ni(100)	Cs	–	$<5 \times 10^{-11}$	~300	–	1.9	CPD	[1005]
Cs/Cu(111)[227]	Cs	–	1×10^{-10}	~300	–	1.9*	CPD	[2496]
Cs/Ni	Cs	–	$<10^{-9}$	77	–	1.9	CPD	[2139,3128,3698]
Cs/Si(nanowire)	Cs	–	$<5 \times 10^{-9}$	~300	–	1.9	FE	[2443]
Cs/GaAs(110)	Cs	–	$<10^{-10}$	~300	–	1.9	CPD	[2793]
Cs/MoS$_2$	Cs	–	?	200	–	1.9	CPD	[2843]
Cs/Mo[232]	Cs$^+$	–	$<3 \times 10^{-10}$	~300	–	1.9*	CPD	[3289,3815]
Cs/W[232]	Cs$^+$	–	$<3 \times 10^{-10}$	~300	–	1.9*	CPD	[3289,3815]
Cs/W	Cs	–	5×10^{-10}	~77	–	1.9 ± 0.1	FE	[2590]
Cs/Mo[229]	Cs$^+$	–	$\leq 1 \times 10^{-10}$	~300	–	1.9 ± 0.1*	CPD	[3283]
Cs/Si	Cs$^+$	–	–	–	–	1.90 ± 0.09*	TC	[4367]
Cs	–	–	–	–	–	1.92	TC	[3477]
Cs	–	–	–	–	–	1.92	TC	[339]
Cs	–	–	~10^{-10}	300	–	1.92	PE	[4297]
Cs	–	–	~10^{-9}	298	–	1.93 ± 0.03	PE	[2612,2613]
Cs	–	–	–	–	–	1.94	TC	[1066]
Cs/glass	Cs	–	~10^{-9}	82	–	1.94	PE	[2576]
Cs/Re(2110)	Cs	–	~10^{-9}	~300	–	1.94	FE	[838]
Cs	–	–	~10^{-9}	~300	–	1.94	PE	[4241]
Cs/Be	Cs	–	? (Cs)	~500–800	–	1.94	TE	[650,3410,3413]
Cs/Mo(100)	Cs	–	~10^{-11}	~300	–	1.94 ± 0.05	CPD	[3855]
Cs/quartz	Cs	–	$<4 \times 10^{-10}$	100	–	1.95	PE	[1862]
Cs/Cu(111)	Cs	–	$\sim 1 \times 10^{-11}$	~300	–	1.95	CPD	[2532]
Cs/?	Cs	–	?	~300	–	1.95	PE	[3111]
Cs/surface[230]	–	–	–	–	–	≤1.95	TC	[650,3412]
Cs/O/W(100)[231]	Cs	–	?	~300	–	1.95	CPD	[1667]
Cs	–	–	~10^{-9}	298	–	1.95 ± <0.05	PE	[2612,2613]
Cs/W(111)	Cs	–	$\leq 10^{-10}$	77	–	1.95 ± 0.1	FE	[1978]
Cs/Be[232]	Cs$^+$	–	$<3 \times 10^{-10}$	~300	–	1.96	PE	[3289]
Cs/Be[232]	Cs$^+$	–	$<3 \times 10^{-10}$	~300	–	1.96	CPD	[3289]
Cs/Ag/glass	Cs	–	~10^{-8}	~80	–	1.96	PE	[1452]
Cs/W(110)	Cs	–	5×10^{-7}	~300	–	≥1.96	PE	[3765]
Cs/Al(111)	Cs	–	1×10^{-11}	~300	–	1.98*	CPD	[2867]
Cs/Ag(100)	Cs	–	$<1 \times 10^{-10}$	80	–	1.98 ± 0.06	CPD	[3186]
Cs/Ru(0001)	Cs	–	~10^{-10}	220	–	2.0	PE	[4092–4094]
Cs/W(110)	Cs	–	~10^{-9}	77	–	2.0	FE	[810]
Cs/W(110)	–	–	–	–	–	2.0	TC	[4216]
Cs/Ag(111)	–	–	–	–	–	2.0	TC	[4216]
Cs/Pt(111)	–	–	–	–	–	2.0	TC	[4216]
Cs/Mo(110)	Cs	–	5×10^{-9}	~300	–	2.0	CPD	[2786]
Cs/Ag(111)	Cs	–	$<1 \times 10^{-10}$	~300	–	2.0*	CPD	[1426]
Cs/Mo	Cs	–	1×10^{-8}	~300	–	2.0	PE	[1433]
Cs/Mo	Cs	–	7×10^{-9}	~300	–	2.0	PE	[3756]
Cs/Cu(100)	Cs	–	$<4 \times 10^{-11}$	~300	–	2.0	PE	[3809]
Cs/W(110)	–	–	–	–	–	2.0	TC	[3300]
Cs/Mo(110)	Cs	–	?	~300	–	2.0	CPD	[1420]
Cs/Au	Cs	–	1×10^{-8}	~300	–	2.0	PE	[1433]
Cs/quartz	Cs	–	~10^{-10}	90	–	2.0	PE	[2605]
Cs/Si(100)	Cs	–	~10^{-10}	200	–	2.0	CPD	[302]
Cs/W(112)	Cs	–	(≤10^{-11})	~300	–	2.0	CPD	[977]
Cs/Si(111)	Cs	–	~10^{-10}	130	–	2.0	PE	[1817]
Cs/Ru(001)	Cs	–	?	~300	–	2.0*	CPD	[2984]
Cs	–	–	–	–	–	2.0*	TC	[1955]
Cs/W	Cs	–	~10^{-10}	800	–	2.0	FE	[2324,3816]
Cs/Re	Cs	–	~10^{-10}	850	–	2.0	FE	[2324]
Cs/Ba/W(100)	Cs	–	(<10^{-11})	210	–	2.0	CPD	[776]
Cs/W(110)	Cs	–	~10^{-8}	~300	–	2.0	PE	[3218]
Cs/HfN	Cs	–	? (Cs)	~700	–	2.0*	TE	[1858]
Cs/Ag(110)	Cs	–	?	~300	–	2.0*	CPD	[1816]
Cs/Se/Si(100)[226]	Cs	–	~10^{-10}	~300	–	2.0*	CPD	[3811]
Cs/cnt	Cs	–	2×10^{-9}	~300	–	2.0	PE	[1165]

Table 1 (*continued*)

Surface	Beam	Ion	P_r (Torr)	T (K)	ϕ^+ (eV)	ϕ^e (eV)	Meth.	Refs.
Cs/TaC	Cs⁺	–	3×10^{-10}	~300	–	2.0 ± 0.02	CPD	[1504]
Cs/Cu	Cs	–	?	~300	–	2.0 ± 0.1	PE	[3091]
Cs/Ag	Cs	–	?	~300	–	2.0 ± 0.1	PE	[3091]
Cs/W(112)	Cs	–	$\leq 10^{-10}$	77	–	2.0 ± 0.1	FE	[1978]
Cs/W(110)	Cs	–	$\leq 10^{-10}$	77	–	$2.0 \pm 0.1^*$	FE	[1978]
Cs/Cu(110)	Cs	–	5×10^{-11}	140	–	2.0 ± 0.1	PE	[3453,3454]
Cs/Cu	Cs	–	3×10^{-9}	100–140	–	2.0 ± 0.1	PE	[2015]
Cs/Ni(100)	Cs⁺	–	$<5 \times 10^{-11}$	~300	–	2.00	CPD	[1005,3674]
Cs/Ta(110)	Cs⁺	–	$\sim 10^{-10}$	~300	–	2.00	CPD	[506]
Cs/Si(100)ⁿ	Cs⁺	–	4×10^{-11}	200	–	2.00 ± 0.05	CPD	[880]
Cs/GaN(0001)	–	–	–	–	–	$2.02 - 2.34$	TC	[4187]
Cs	–	–	–	–	–	2.03	TC	[4150]
Cs	–	–	$\sim 10^{-9}$	183	–	2.03 ± 0.02	PE	[2612,2613]
Cs/ss	Cs	–	(D₂-plasma)	?	–	2.03 ± 0.16	PE	[4452]
Cs/O/W(100)²³¹	Cs	–	?	~300	–	2.05	CPD	[1667]
Cs	–	–	–	–	–	2.05^*	TC	[1955]
Cs	–	–	–	–	–	2.05	TC	[1951]
Cs/graphene	–	–	–	–	–	2.05	TC	[4075]
Cs/glass	Cs	–	$\leq 3 \times 10^{-11}$	195	–	2.05 ± 0.01	PE	[2615]
Cs/W(100)	Cs	–	$\sim 10^{-9}$	77	–	2.06	FE	[810]
Cs	–	–	–	–	–	2.06	TC	[3477]
Cs(cluster)	–	–	–	–	–	2.06	TC	[3477,3479]
Cs/Mo(100)	Cs	–	7×10^{-10}	77	–	2.06	FE	[3691]
Cs/Mo(112)	Cs	–	7×10^{-10}	77	–	2.06	FE	[3691]
Cs/W(110)	Cs	–	$\leq 3 \times 10^{-10}$	~300	–	2.06 ± 0.01	CPD	[362]
Cs/W	Cs	–	$\leq 10^{-9}$	~300	–	2.07	CPD	[3857]
Cs/Cu(100)	Cs	–	$<5 \times 10^{-11}$	~300	–	2.07	CPD	[2842,2850]
Cs/W(110)	Cs	–	($\leq 10^{-11}$)	77	–	2.07^*	CPD	[3341]
Cs	–	–	–	–	–	2.07	TC	[3467]
Cs/W(110)	Cs	–	$<2 \times 10^{-10}$	~300	–	2.07 ± 0.01	CPD	[2481]
Cs/Si(100)	–	–	–	–	–	$2.08 \pm 0.10^*$	TC	[3498]
Cs/Ag(111)	–	–	–	–	–	2.09	TC	[3995]
Cs/glass	Cs	–	$\leq 3 \times 10^{-11}$	77	–	2.09 ± 0.01	PE	[2615]
Cs/Ru(001)	Cs	–	$<5 \times 10^{-10}$	80 (≫80)	–	2.1^*	CPD	[2152]
Cs/Ni(111)	Cs	–	8×10^{-11}	100	–	2.1	PE	[772]
Cs/Mo	Cs	–	2×10^{-8}	~300	–	2.1	CPD	[3770]
Cs/W(112)	Cs	–	$\sim 10^{-10}$	~300	–	2.1	FE	[2324]
Cs/Nb(110)	Cs	–	$\sim 10^{-10}$	~300	–	2.1	CPD	[2381]
Cs/HOPG	Cs	–	?	90	–	2.1	PE	[1620]
Cs/W(100)	Cs	–	($<10^{-11}$)	210	–	2.1	CPD	[776]
Cs/Cu(110)	Cs	–	?	140	–	2.1	PE	[3450]
Cs/Pt	Cs	–	4×10^{-10}	20	–	2.1^*	AI³⁸	[3496]
Cs/Ru(0001)	Cs	–	$<10^{-10}$	~300	–	2.1	PE	[3782]
Cs/W(110)	Cs	–	$<2 \times 10^{-11}$	~300	–	2.1	CPD	[2685]
Cs/Ni(100)	Cs	–	$\sim 10^{-10}$	~300	–	2.1^*	CPD	[2895]
Cs/W(111)	Cs	–	($\leq 10^{-11}$)	77	–	2.1	CPD	[2619]
Cs/Cu(110)	Cs	–	?	100, 260	–	2.1	?	[3159,3172]
Cs/W(110)	Cs	–	($<10^{-12}$)	77	–	2.1	CPD	[1085]
Cs/W(110)	Cs	–	($\leq 10^{-11}$)	~300	–	2.1	CPD	[977]
Cs/Ag(110)²²⁴	Cs	–	?	80	–	2.1	PE	[2144]
Cs/Mo(110)	Cs	–	($\leq 10^{-11}$)	~300	–	2.1	CPD	[977]
Cs	–	–	–	–	–	2.1	TC	[706]
Cs/W(110)	Cs	–	$\leq 10^{-10}$	77	–	2.1 ± 0.1	FE	[1978]
Cs/Ba/Nb(100)	Cs	–	($<10^{-11}$)	220	–	2.10 ± 0.05	CPD	[776]
Cs/Ba/Nb(110)	Cs	–	4×10^{-10}	~300	–	2.11	CPD	[2672]
Cs/W(110)	Cs	–	($<10^{-12}$)	77	–	2.11	CPD	[1085]
Cs/glass	Cs	–	$\leq 3 \times 10^{-11}$	195	–	2.11 ± 0.01	PE	[2615]
Cs	–	–	–	–	–	2.14	TC	[1711]
Cs	–	–	–	–	–	2.14	TC	[3637]
Cs/GaAs(110)	Cs	–	?	190	–	2.14	PE	[2168]
Cs/glass	Cs	–	$\leq 10^{-10}$	77	–	2.14 ± 0.02	PE	[1489]
Cs/glass	Cs	–	$<2 \times 10^{-10}$	77	–	2.14 ± 0.05	PE	[1474]
Cs/Mo(100)	Cs	–	$\sim 10^{-11}$	~300	–	$2.14 \pm 0.06^*$	CPD	[3855]
Cs/Si(100)	Cs	–	$\sim 10^{-10}$	200	–	2.15	CPD	[302]
Cs	–	–	–	–	–	2.15	TC	[1711]
Cs/W(110)	Cs	–	$<2 \times 10^{-10}$	250	–	2.15	CPD	[1807]
Cs	–	–	–	–	–	2.15	TC	[298]
Cs/W(110)	Cs	–	1×10^{-9}	~300	–	2.15	CPD	[3721–3723,3774]
Cs/Mo(110)	Cs	–	5×10^{-11}	77	–	2.15	CPD	[329]
Cs	–	–	–	–	–	2.15	TC	[3725]

Table 1 (*continued*)

Surface	Beam	Ion	P_r (Torr)	T (K)	ϕ^+ (eV)	ϕ^e (eV)	Meth.	Refs.
Cs/W(110)	Cs	–	?	~300	–	2.15	CPD	[2881]
Cs/W(110)	Cs	–	(<10⁻¹¹)	210	–	2.15	CPD	[776]
Cs/Ba/W(110)	Cs	–	(<10⁻¹¹)	210	–	2.15	CPD	[776]
Cs/W(110)	Cs	–	<10⁻⁹	~300	–	2.15	CPD	[3857]
Cs	–	–	–	–	–	2.16	TC	[1711]
Cs/Re(1011)	Cs	–	~10⁻⁹	~300	–	2.16	FE	[838]
Cs/Mo(100)	Cs	–	<5 × 10⁻¹¹	~300	–	2.16 ± 0.09*	CPD	[3736]
Cs/Ir	–	–	–	–	–	2.18	TC	[416]
Cs/W(110)	Cs	–	?	77 (?)	–	2.18 ± 0.05	FE	[340]
Cs	–	–	–	–	–	2.19	TC	[3352]
Cs/ss	Cs	–	(H₂-plasma)	?	–	2.19 ± 0.08	PE	[4452]
Cs/Cu(111)²³³	–	–	–	–	–	2.2	TC	[3697]
Cs/Ru(001)	Cs	–	<5 × 10⁻¹⁰	80 (≫80)	–	2.2	CPD	[2152]
Cs/Mo(110)	Cs	–	?	~300	–	2.2	CPD	[2676]
Cs/Ba/Mo(110)	Cs	–	?	~300	–	2.2	CPD	[2676]
Cs/cnt/Si	Cs	–	≤8 × 10⁻¹⁰	~300	–	2.2	PE	[3225]
Cs/Cu(111)²³⁴	Cs	–	~10⁻¹⁰	200	–	2.2	PE	[2512]
Cs/Ni/ss	Cs	–	~10⁻¹⁰	4.2	–	2.2 ± 0.1	PE	[1410]
Cs/W(110)	–	–	–	–	–	2.20	TC	[1539]
Cs/W(110)	Cs	–	7 × 10⁻¹⁰	77 (500)	–	2.22	FE	[3691]
Cs/Nb(100)	Cs	–	(<10⁻¹¹)	220	–	2.22	CPD	[776]
Cs/W(100)	–	–	–	–	–	2.22*	TC	[1705]
Cs	–	–	–	–	–	2.23	TC	[477]
Cs/Cu(100)	–	–	–	–	–	2.23 ± 0.01	TC	[4135]
Cs	–	–	–	–	–	2.24	TC	[231]
Cs	–	–	–	–	–	2.24	TC	[477,1924,4035]
Cs	–	–	–	150.5	–	2.241	TC	[2419]
Cs	–	–	–	–	–	2.25	TC	[3312]
Cs	–	–	–	–	–	2.25	TC	[2427]
Cs	–	–	–	–	–	2.26	TC	[3477]
Cs	–	–	–	–	–	2.26	TC	[553]
Cs/Ru(0001)	Cs	–	?	~300	–	2.26	PE	[4020]
Cs/C(0001)	Cs	–	5 × 10⁻¹⁰	80	–	2.26*	CPD	[2156]
Cs/C(0001)²³⁵	–	–	–	–	–	2.26*	TC	[2782]
Cs/C(0001)²³⁵	Cs	–	<2 × 10⁻¹⁰	~300	–	2.26*	CPD	[2782]
Cs	–	–	–	0	–	2.264	TC	[2419]
Cs/W(100)	–	–	–	–	–	2.28	TC	[385]
Cs	–	–	–	–	–	2.28	TC	[3467]
Cs/Cu(111)²³⁴	–	–	~10⁻¹⁰	200	–	2.3	PE	[2512]
Cs/Mo(112)	Cs	–	(<10⁻¹¹)	77 (300)	–	2.3	CPD	[2032]
Cs/W(100)	Cs	–	~10⁻¹⁰	~300	–	2.3	CPD	[2477,2599,2600]
Cs/Si(111)	Cs	–	<1 × 10⁻¹⁰	~300	–	2.3*	PE	[2663]
Cs/Ag(100)	Cs	–	<2 × 10⁻¹⁰	80	–	2.3 ± 0.1*	CPD	[2179]
Cs/Si(100)	Cs⁺	–	?	~300 (≤833)	–	2.3 ± 0.15	CPD	[768]
Cs	–	–	–	–	–	2.30	TC	[477]
Cs	–	–	–	–	–	2.31	TC	[767]
Cs	–	–	–	–	–	2.33	TC	[231]
Cs/graphite	–	–	–	–	–	2.33*	TC	[1843]
Cs/Al(111)	–	–	–	–	–	2.34	TC	[3158]
Cs	–	–	–	–	–	2.35	TC	[2427]
Cs	–	–	–	–	–	2.35	TC	[4101]
Cs	–	–	–	–	–	2.35	TC	[477,1924,4035, 4036]
Cs	–	–	–	–	–	2.37	TC	[1613]
Cs	–	–	–	–	–	2.37	TC	[383]
Cs/Mo(100)	–	–	–	–	–	2.39*	TC	[1705]
Cs/Cu(111)²³³	–	–	–	–	–	2.4	TC	[3697]
Cs/Nb(110)	Cs	–	4 × 10⁻¹⁰	~300	–	2.4	CPD	[2672]
Cs/cnt/GaAs²³⁶	Cs	–	2 × 10⁻⁹	~300	–	2.4	PE	[291]
Cs/MoS₂(0001)	Cs	–	<1 × 10⁻¹⁰	~300	–	2.4	CPD	[2390]
Cs/Nb(110)	Cs	–	4 × 10⁻¹⁰	~300	–	2.40	FE	[2672]
Cs/graphite	–	–	–	–	–	2.41*	TC	[1843]
Cs/Al(111)	Cs	–	8 × 10⁻¹¹	140	–	2.44	CPD	[734,2154,2162]
Cs/W(100)	–	–	–	–	–	2.44	TC	[387]
Cs/Ta	Cs	–	~10⁻¹¹	~300	–	2.47	CPD	[683]
Cs	–	–	–	–	–	2.47	TC	[1711]
Cs	–	–	–	–	–	2.49	TC³	[475,519,2474]
Cs	–	–	–	–	–	2.5	TC	[2845]
Cs/C(0001)²³⁵	–	–	–	–	–	2.5*	TC	[2782]
Cs/C(0001)²³⁵	Cs	–	<2 × 10⁻¹⁰	~300	–	2.5*	CPD	[2782]

Table 1 (*continued*)

Surface	Beam	Ion	P_r (Torr)	T (K)	ϕ^+ (eV)	ϕ^e (eV)	Meth.	Refs.
Cs	–	–	–	–	–	2.51	TC	[2629]
Cs	–	–	–	–	–	2.54	TC	[230]
Cs/W(100)	–	–	–	–	–	2.55	TC	[385]
Cs	–	–	–	–	–	2.56	TC	[2493]
Cs	–	–	–	–	–	2.60	TC	[2382]
Cs/Ru(001)	Cs	–	<5 × 10⁻¹⁰	80	–	2.62	PE	[3152]
Cs	–	–	–	–	–	2.64	TC	[521]
Cs	–	–	–	–	–	2.64	TC	[3628]
Cs	–	–	–	–	–	2.67	TC	[2493]
Cs	–	–	–	–	–	2.74	TC	[477]
Cs/W(100)	–	–	–	–	–	2.77	TC	[385]
Cs/Si(100)	–	–	–	–	–	2.8	TC	[3362]
Cs/MoS$_2$	Cs	–	<1 × 10⁻¹⁰	~300	–	2.9	CPD	[2843]
Cs/cnt	Cs	–	6 × 10⁻⁹	~300	–	3.0 ± 0.1	FE	[2436]
Cs	–	–	–	–	–	3.10	TC	[2629]
Recommended	–	–	–	–	–	**2.05 ± 0.05**	–	–

Liquid (T > 301 K)

Surface	Beam	Ion	P_r (Torr)	T (K)	ϕ^+ (eV)	ϕ^e (eV)	Meth.	Refs.
Cs	–	–	~10⁻¹⁰	302	–	1.91*	PE	[4297]
Cs	–	–	~10⁻⁹	302	–	1.94	PE	[4241]
Cs	–	–	~10⁻⁸	302	–	1.95	PE	[4208]
Cs	–	–	–	301	–	2.212	TC	[2419]

56. Barium Ba

bcc

Surface	Beam	Ion	P_r (Torr)	T (K)	ϕ^+ (eV)	ϕ^e (eV)	Meth.	Refs.
Ba(100)/BaO	–	–	–	–	–	2.22	TC	[357]
Ba(100)	–	–	–	–	–	2.31	TC	[4091]
Ba(100)	–	–	–	–	–	2.48	TC	[1254]
Ba(100)	–	–	–	–	–	2.50	TC	[1159,3067]
Ba(100)	–	–	–	–	–	2.6	TC	[1714]
Ba(100)	–	–	–	–	–	2.62	TC	[357]
Ba(100)	–	–	–	–	–	2.67	TC	[231]
Ba(100)	–	–	–	–	–	2.68	TC	[3467]
Ba(100)	–	–	–	–	–	3.00	TC	[321]
Ba(100)	–	–	–	–	–	3.06	TC	[1030]
Ba(100)	–	–	–	–	–	3.15	TC	[476]
Ba(100)	–	–	–	–	–	3.26	TC	[476]
Ba(100)	–	–	–	–	–	3.42	TC	[1030]
Recommended	–	–	–	–	–	**3.07 ± 0.06**	–	–
Ba(110)	–	–	–	–	–	2.1	TC	[1723]
Ba(110)	–	–	–	–	–	2.19	TC	[1434]
Ba(110)	–	–	–	–	–	2.28	TC	[334,3179]
Ba(110)	–	–	–	–	–	2.384	TC	[4091]
Ba(110)	–	–	–	–	–	2.71	TC	[1159,3067]
Ba(110)	–	–	–	–	–	2.83	TC	[231]
Ba(110)	–	–	–	–	–	2.88	TC	[3467]
Ba(110)	–	–	–	–	–	2.95	TC	[2427]
Ba(110)	–	–	–	–	–	3.21	TC	[476]
Ba(110)	–	–	–	–	–	3.32	TC	[476]
Ba(110)	–	–	–	–	–	3.49	TC	[321]
Ba(110)	–	–	–	–	–	3.56	TC	[1030]
Ba(110)	–	–	–	–	–	3.58	TC	[1030]
Ba(110)	–	–	–	–	–	3.59	TC	[1089]
Ba(110)	–	–	–	–	–	3.70	TC	[1089]
Ba(110)	–	–	–	–	–	3.81	TC	[1089]
Recommended	–	–	–	–	–	**3.46 ± 0.14**	–	–
Ba(111)	–	–	–	–	–	2.293	TC	[4091]
Ba(111)	–	–	–	–	–	2.48	TC	[1159,3067]
Ba(111)	–	–	–	–	–	2.72	TC	[3467]
Ba(111)	–	–	–	–	–	2.73	TC	[231]
Ba(111)	–	–	–	–	–	2.85	TC	[476]
Ba(111)	–	–	–	–	–	2.85	TC	[1030]
Ba(111)	–	–	–	–	–	2.86	TC	[1030]
Ba(111)	–	–	–	–	–	2.87	TC	[321]
Ba(111)	–	–	–	–	–	2.96	TC	[476]
Recommended	–	–	–	–	–	**2.81 ± 0.06**	–	–

Table 1 (*continued*)

Surface	Beam	Ion	P_r (Torr)	T (K)	ϕ^+ (eV)	ϕ^e (eV)	Meth.	Refs.
Ba(112)	–	–	–	–	–	3.20	TC	[321]
Ba	–	–	?	~300	–	1.73	CPD	[2297]
Ba/W	Ba	–	(<10⁻¹⁴)	770–910	–	1.96	TE	[2572]
Ba/W	Ba	–	~10⁻¹¹	1000	–	2.0	TE	[3781]
Ba/W(221)	Ba	–	(<10⁻¹¹)	78 (≤800)	–	2.0	FE	[809]
Ba	–	–	?	~300	–	2.02	PE	[3694]
Ba/Nb(100)	Ba	–	(<10⁻¹¹)	~300 (1000)	–	2.04	CPD	[776]
Ba/W(111)	Ba	–	~10⁻⁸	~1000	–	2.1	TE	[2351]
Ba/W	Ba	–	≤3 × 10⁻⁹	~300	–	2.1	FE	[218,3739]
Ba/Re	Ba	–	~10⁻⁹	~300 (800)	–	2.1	FE	[3535]
Ba/W	Ba	–	≤1 × 10⁻⁹	~300 (870)	–	2.1	FE	[2587]
Ba/W	Ba	–	(<10⁻¹¹)	78 (≤800)	–	2.1	FE	[809]
Ba/W	Ba	–	?	880–990	–	2.15 ± 0.05	TE	[2928]
Ba/W(110)	Ba	–	(<10⁻¹¹)	~300 (1000)	–	2.18	CPD	[776]
Ba/W(110)	Ba	–	~10⁻⁸	~1000	–	2.2	TE	[2351]
Ba/W(111)	Ba	–	≤1 × 10⁻¹⁰	77	–	2.2	FE	[2372]
Ba/Rh	Ba	–	≤1 × 10⁻⁹	~300 (870)	–	2.2	FE	[2587]
Ba/W(111)	Ba	–	(<10⁻¹¹)	78 (≤800)	–	2.2	FE	[809]
Ba/W	Ba	–	3 × 10⁻⁹	~300	–	2.2	CPD	[1064]
Ba/Nb(100)	Ba	–	(<10⁻¹¹)	~300 (600)	–	2.23	CPD	[776]
Ba/W	Ba	–	≤5 × 10⁻⁹	~300–800	–	2.23 ± 0.04	CPD	[3320]
Ba/W(100)	Ba	–	(<10⁻¹¹)	~300 (700)	–	2.25	CPD	[776]
Ba/W₂C	Ba	–	?	~300 (800)	–	2.25	FE	[3531]
Ba/Ni(110)	Ba	–	≤10⁻¹⁰	~300	–	2.26*	CPD	[3376]
Ba/Re	Ba	–	~10⁻⁹	~300 (600)	–	2.3	FE	[3535]
Ba/W(211)	Ba	–	(<10⁻¹¹)	78 (≤800)	–	2.3	FE	[809]
Ba/Si(001)²³⁷	Ba	–	<6 × 10⁻¹⁰	~300	–	2.3	PE	[2170]
Ba/glass	Ba	–	<3 × 10⁻⁸	~300	–	2.3	PE	[3576]
Ba/quartz	Ba	–	5 × 10⁻¹⁰	~300	–	2.3	PE	[2024]
Ba/Nb	Ba	–	≤5 × 10⁻⁹	~300	–	2.3*	CPD	[3261]
Ba/W(100)	Ba	–	(<10⁻¹¹)	210 (730)	–	2.3	CPD	[776]
Ba/Nb(100)	Ba	–	(<10⁻¹¹)	220 (850)	–	2.3	CPD	[776]
Ba/Ti/W(111)	Ba	–	≤1 × 10⁻¹⁰	77	–	2.3	FE	[2372]
Ba/W(111)	Ba	–	(<10⁻¹¹)	77	–	2.3	CPD	[2507]
Ba/Ta(112)	Ba	–	(≤10⁻¹¹)	~300 (600)	–	2.3	CPD	[347]
Ba/Nb(110)	Ba	–	≤10⁻⁸	~1000–1150	–	2.3 ± 0.03	TE	[2359]
Ba/Nb,Ta	Ba	–	≤10⁻⁸	~1000–1150	–	2.3 ± 0.03	TE	[2359]
Ba/W	Ba	–	~10⁻⁸	745–910	–	2.3 ± 0.1	TE	[3064]
Ba/W(100)	Ba	–	~10⁻⁹	~950–1100	–	2.3 ± 0.1	TE	[143]
Ba/W(110)	Ba	–	~10⁻⁹	~950–1100	–	2.3 ± 0.1	TE	[143]
Ba/W(111)	Ba	–	~10⁻⁹	~950–1100	–	2.3 ± 0.1	TE	[143]
Ba/W(112)	Ba	–	~10⁻⁹	~950–1100	–	2.3 ± 0.1	TE	[143]
Ba/Ta(112)	Ba	–	(≤10⁻¹¹)	77 (600)	–	2.30	CPD	[347]
Ba	–	–	–	–	–	2.30	TC	[1066]
Ba/Ni(110)	Ba	–	≤10⁻¹⁰	~300	–	2.30	CPD	[3376]
Ba/Mo(111)	Ba	–	≤10⁻⁹	860–980	–	2.30 ± 0.1	TE	[323]
Ba/W(100)	Ba	–	≤10⁻¹⁰	500	–	2.34	CPD	[1891]
Ba/W	Ba	–	≤1 × 10⁻⁹	~300 (?)	–	2.35	FE	[2037]
Ba/glass²³⁸	Ba	–	?	~300	–	2.35 ± 0.03	CPD	[1157]
Ba/Ru,Os,Ir	Ba	–	≤10⁻⁸	~1000–1150	–	2.36 ± 0.03	TE	[2359]
Ba/Nb(100)	Ba	–	(≤10⁻¹¹)	~300 (700)	–	2.38	CPD	[776]
Ba/W²³⁸	Ba	–	?	90	–	2.39 ± 0.05	CPD	[1365]
Ba/Ta	Ba	–	~10⁻⁸	~300	–	2.39 ± 0.06*	CPD	[1385]
Ba/Ir	Ba	–	≤1 × 10⁻⁹	300 (970)	–	2.4	FE	[2587]
Ba/W(100)	–	–	–	–	–	2.4	TC	[4258]
Ba/Pt	Ba	–	?	~1200	–	2.4	TE	[4266]
Ba/W(100)	Ba	–	(<10⁻¹¹)	78 (≤800)	–	2.4	FE	[809]
Ba/Ge	Ba	–	~10⁻⁹	~300	–	2.4	CPD	[1954]
Ba/Au	Ba	–	~10⁻⁹	~300	–	2.4	CPD	[1954]
Ba/W	Ba	–	?	77 (?)	–	2.4	FE	[3777]
Ba/W	Ba	–	?	600, 730	–	2.4	FE	[3555]
Ba/Ge/W	Ba	–	?	600, 730	–	2.4	FE	[3555]
Ba/Ir(111)	Ba	–	≤8 × 10⁻¹⁰	770–940	–	2.4	TE	[3546,3547]
Ba/C/Ir(111)	Ba	–	~10⁻¹⁰	850–980	–	2.4	TE	[3986]
Ba/?	Ba	–	?	?	–	2.4	TE	[3402]
Ba	–	–	–	–	–	2.4	TC	[1993]
Ba/Nb(100)	Ba	–	≤10⁻⁸	~1000–1150	–	2.4 ± 0.03	TE	[2359]
Ba/Zr,Hf	Ba	–	≤10⁻⁸	~1000–1150	–	2.4 ± 0.03	TE	[2359]
Ba/Mo,W	Ba	–	≤10⁻⁸	~1000–1150	–	2.4 ± 0.03	TE	[2359]

Table 1 (*continued*)

Surface	Beam	Ion	P_r (Torr)	T (K)	ϕ^+ (eV)	ϕ^e (eV)	Meth.	Refs.
Ba/W(100)	Ba	–	($<10^{-11}$)	~300 (500)	–	2.40	CPD	[776]
Ba/W(100)	Ba	–	($<10^{-11}$)	~300 (1000)	–	2.40	CPD	[776]
Ba/glass[238]	Ba	–	?	~300	–	2.41 ± 0.05*	CPD	[1157]
Ba/W(100)	Ba	–	($<10^{-11}$)	~300	–	2.42	CPD	[776]
Ba/W	Ba	–	$<10^{-10}$	77	–	2.42	FE	[2960]
Ba/W[238]	Ba	–	?	90	–	2.42 ± 0.05	CPD	[1365]
Ba/W(113)	Ba	–	$<5 \times 10^{-9}$	~300	–	2.44	CPD	[1138]
Ba/W	Ba	–	$<10^{-10}$	~300	–	2.44	FE	[1464]
Ba	–	–	–	–	–	2.45	TC	[3476]
Ba/Si(100)	Ba	–	$<10^{-10}$	~300	–	2.45*	CPD	[3370]
Ba/W(113)	Ba	–	$\leq 5 \times 10^{-9}$	~300	–	2.45	CPD	[1963]
Ba/Au	Ba	–	5×10^{-9}	300	–	2.45	PE	[2710]
Ba/W(110)	Ba	–	$\leq 10^{-8}$	~1000–1150	–	2.45 ± 0.03	TE	[2359]
Ba/quartz	Ba	–	$<5 \times 10^{-9}$	~330 (~470)	–	2.45 ± 0.05	PE	[3090]
Ba/W[244]	Ba	–	$\leq 2 \times 10^{-9}$	~900	–	2.46	CPD	[3530]
Ba	–	–	–	–	–	2.47	TC	[339]
Ba	–	–	–	–	–	2.47	TC	[3476]
Ba	–	–	–	–	–	2.48	TC	[3637]
Ba/glass	Ba	–	~2×10^{-8}	~300	–	2.48	PE	[2564]
Ba	–	–	–	–	–	2.48	TC	[1254]
Ba/W	Ba	–	$\leq 2 \times 10^{-9}$	~300	–	2.48	CPD	[3530]
Ba/Mo(110)	Ba	–	($\leq 10^{-11}$)	77	–	2.48	CPD	[1209,1895]
Ba/Ni	Ba	–	?	~300	–	2.49	PE	[1641]
Ba/Fe(110)/W(110)	Ba	–	?	77	–	2.5	CPD	[4231]
Ba/Mo(110)/W(110)	Ba	–	?	77	–	2.5	CPD	[4231]
Ba/Ag(111)/W(110)	Ba	–	?	77	–	2.5	CPD	[4231]
Ba/W(112)	Ba	–	$\leq 1 \times 10^{-10}$	77	–	2.5	FE	[2372]
Ba/Ti/W(112)	Ba	–	$\leq 1 \times 10^{-10}$	77	–	2.5	FE	[2372]
Ba/Ta(112)	Ba	–	($\leq 10^{-11}$)	77	–	2.5	CPD	[347]
Ba	–	–	–	–	–	2.5	TC	[3030]
Ba/Ta(112)	Ba	–	($\leq 10^{-11}$)	~300	–	2.5	CPD	[347]
Ba/W(111)	Ba	–	($<10^{-11}$)	~300	–	2.5	CPD	[2507]
Ba/Si(100)[239]	Ba	–	$<2 \times 10^{-11}$	~300	–	2.5*	PE	[1732]
Ba/Nb	Ba	–	$\leq 3 \times 10^{-9}$	~300	–	2.5*	CPD	[3263]
Ba/Ag(111)	Ba	–	~1×10^{-10}	~300	–	2.5	CPD	[3303]
Ba/Cu/W(110)	Ba	–	$\leq 1 \times 10^{-10}$	~300	–	2.5	FE	[2371]
Ba/Re(1010)	Ba	–	($\leq 10^{-11}$)	77	–	2.5	CPD	[2501]
Ba/Re(1010)	Ba	–	($\leq 10^{-11}$)	~300	–	2.5	CPD	[599,2501]
Ba/W(110)	Ba	–	~10^{-8}	~300	–	2.5	PE	[3218]
Ba/W	Ba	–	?	~300	–	2.5	CPD	[2577]
Ba/W	Ba	–	~10^{-10}	~300	–	2.5	CPD	[3532]
Ba/W(100)	Ba	–	$\leq 10^{-8}$	~1000–1150	–	2.5 ± 0.03	TE	[2359]
Ba/Ir(111)	Ba	–	$\leq 5 \times 10^{-9}$	<800	–	2.50	TE	[649]
Ba/Ag(111)	Ba	–	$<1 \times 10^{-10}$	~300 (≤450)	–	2.50	CPD	[990]
Ba/Ta(112)	Ba	–	($\leq 10^{-11}$)	77	–	2.50	CPD	[347]
Ba/Ta(112)	Ba	–	($\leq 10^{-11}$)	~300	–	2.50	CPD	[347]
Ba/W(100)	Ba	–	$\leq 10^{-10}$	~300	–	2.50	FE	[1891]
Ba/glass	Ba	–	?	~300–400	–	2.511 ± 0.002	PE	[1637,1638,2232]
Ba/Re[222]	Ba	–	?	?	–	2.52	TE	[3582]
Ba/Ag/Ta[242]	Ba	–	?	~300	–	2.52 ± 0.03*	CPD	[1050]
Ba/glass[373]	Ba	–	?	~300	–	2.520	PE	[2232]
Ba/W(112)	Ba	–	($\leq 10^{-11}$)	77	–	2.53	CPD	[379]
Ba/W(112)	Ba	–	($\leq 10^{-11}$)	~300	–	2.53	CPD	[379]
Ba/Nb(100)	Ba	–	($\leq 10^{-11}$)	~300	–	2.53	CPD	[776]
Ba/Ag/Ta[242]	Ba	–	?	~300	–	2.53 ± 0.03*	CPD	[1050]
Ba/W(110)	Ba	–	($\leq 10^{-11}$)	77	–	2.54	CPD	[1895]
Ba/Al(111)	Ba	–	3×10^{-11}	20 (120)	–	2.55	PE	[1427]
Ba/Ag(111)	Ba	–	$\leq 1 \times 10^{-10}$	~300	–	2.56	CPD	[990]
Ba/W(100)[241]	Ba	–	$\leq 6 \times 10^{-10}$	~300	–	2.560 ± 0.005	CPD	[2104,2108]
Ba/glass[240]	Ba	–	?	~300	–	2.57*	CPD	[1367]
Ba/W	Ba	–	$\leq 2 \times 10^{-9}$	760–775	–	2.57 ± 0.06*	CPD	[3528]
Ba/W(110)	Ba	–	($<10^{-11}$)	~300 (900)	–	2.59	CPD	[776]
Ba//W(110)	Ba	–	?	77	–	2.6	CPD	[4231]
Ba/Cu(111)/W(110)	Ba	–	?	77	–	2.6	CPD	[4231]
Ba/Ag(111)/W(110)	Ba	–	?	~300	–	2.6	CPD	[4231]
Ba/W(110)	Ba	–	?	~300	–	2.6	CPD	[2145]
Ba/W	Ba	–	?	~300	–	2.6	CPD	[3689]
Ba/Mo(110)	Ba	–	?	~300	–	2.6	FE	[2676]
Ba/W(110)	Ba	–	~10^{-10}	77 (~300)	–	2.6	CPD	[2022]
Ba/Mo(112)	Ba	–	($<10^{-11}$)	~300	–	2.6	CPD	[2637]

Table 1 (*continued*)

Surface	Beam	Ion	P_r (Torr)	T (K)	ϕ^+ (eV)	ϕ^e (eV)	Meth.	Refs.
Ba/W(110)	Ba	–	$\leq 1 \times 10^{-10}$	77	–	2.6*	FE	[2372]
Ba/Ti/W(110)	Ba	–	$\leq 1 \times 10^{-10}$	77	–	2.6*	FE	[2372]
Ba/Re(1010)	Ba	–	($<10^{-11}$)	~300	–	2.6	CPD	[2637]
Ba/W(100)	Ba	–	?	~300	–	2.6	CPD	[2145]
Ba/W	Ba	–	$<10^{-9}$	~300	–	2.6	FE	[3269]
Ba/Cu(111)	Ba	–	?	~300	–	2.6*	PE	[2515]
Ba/W[243]	Ba	–	2×10^{-9}	~300	–	2.6	CPD	[3259]
Ba	–	–	–	–	–	2.6	TC	[706]
Ba/Lu/W	Ba	–	$\leq 1 \times 10^{-9}$	~300 (?)	–	2.60	FE	[2037]
Ba/W(100)	Ba	–	$\leq 10^{-10}$	~300	–	2.60	CPD	[1891]
Ba/W(100)	–	–	–	–	–	2.62	TC	[357]
Ba/Mo(110)	Ba	–	($\leq 10^{-11}$)	~300	–	2.63	CPD	[1209,1895]
Ba/Mo(110)	Ba	–	($\leq 10^{-11}$)	77 ($\leq$500)	–	2.63	CPD	[1209,1895]
Ba/Mo(110)	Ba	–	$\leq 2 \times 10^{-10}$	77	–	2.63	CPD	[327]
Ba/W(110)	Ba	–	2×10^{-10}	77	–	2.63	CPD	[3985]
Ba/Re(0001)	Ba	–	$\leq 2 \times 10^{-9}$	77, ~300	–	2.64*	CPD	[3750]
Ba/W[244]	Ba	–	$\leq 2 \times 10^{-9}$	~300	–	2.65	CPD	[3530]
Ba	–	–	–	–	–	2.65	TC	[298]
Ba/W(110)	Ba	–	($<10^{-11}$)	~300 (1200)	–	2.65	CPD	[776]
Ba/Ir(100)	Ba	–	?	~300	–	2.65 ± 0.05	CPD	[3135,3701]
Ba/W	Ba	–	$\leq 2 \times 10^{-9}$	~300	–	2.65 ± 0.06*	CPD	[3528]
Ba	–	–	–	–	–	2.66	TC	[3729]
Ba/Ag/Ta[238]	Ba	–	?	~300	–	2.66 ± 0.01	CPD	[1050]
Ba/W(110)	Ba	–	($<10^{-11}$)	210	–	2.67	CPD	[776]
Ba/W(110)	Ba	–	2×10^{-10}	77	–	2.67	CPD	[3985]
Ba/W	Ba	–	$\leq 6 \times 10^{-10}$	~300	–	2.67 ± 0.02	CPD	[2108]
Ba/W(100)[241]	Ba	–	$\leq 3 \times 10^{-10}$	~300	–	2.69 ± 0.02	CPD	[2104]
Ba/W[243]	Ba	–	3×10^{-7}	~300	–	2.7	CPD	[3259]
Ba/Si(100)[239]	Ba	–	$<2 \times 10^{-11}$	~300	–	2.7	PE	[1732]
Ba/Nb(110)	Ba	–	4×10^{-10}	~300	–	2.7	CPD	[2672]
Ba/Cu(111)	Ba	–	$\sim 10^{-10}$	~300	–	2.7	PE	[2509]
Ba/Mo(110)	Ba	–	$\leq 3 \times 10^{-10}$	~300	–	2.7	CPD	[330]
Ba/Fe(110)/W(110)	Ba	–	?	~300	–	2.7	CPD	[4231]
Ba/Mo(110)/W(110)	Ba	–	?	~300	–	2.7	CPD	[4231]
Ba/Si(111)	–	–	–	–	–	2.7*	TC	[4075]
Ba/W(100)	Ba	–	$<10^{-10}$	~300	–	2.7*	CPD	[2055]
Ba/O/W(100)	Ba	–	$<10^{-10}$	~300	–	2.7*	CPD	[2055]
Ba/W(100)[245]	Ba	–	?	~300	–	2.7	CPD	[2149]
Ba/Ir(100)[245]	Ba	–	?	~300	–	2.7	CPD	[2149]
Ba/Pt	Ba	–	$\leq 2 \times 10^{-9}$	~300 (1400)	–	2.7 ± 0.1	FE	[3543]
Ba/W(100)	–	–	–	–	–	2.70	TC	[386]
Ba/O/W(100)	–	–	–	–	–	2.70	TC	[386]
Ba/Ni	Ba	–	?	0^E	–	2.70	PE	[3026]
Ba/W(110)	Ba	–	($\leq 10^{-11}$)	~300	–	2.70	CPD	[1895,2738]
Ba/Mo(110)	Ba	–	$\leq 2 \times 10^{-10}$	~300	–	2.73	CPD	[327]
Ba	–	–	–	–	–	2.73	TC	[550]
Ba/W(110)	Ba	–	($\leq 10^{-11}$)	~300	–	2.74	CPD	[776]
Ba	–	–	–	–	–	2.76	TC	[3467]
Ba/W(110)	Ba	–	$\leq 1 \times 10^{-10}$	77	–	2.8	FE	[2372]
Ba/W(110)	Ba	–	?	~300	–	2.8	CPD	[4231]
Ba/Cu(111)/W(110)	Ba	–	?	~300	–	2.8	CPD	[4231]
Ba/Ti/W(110)	Ba	–	$\leq 1 \times 10^{-10}$	77	–	2.8	FE	[2372]
Ba/W	Ba	–	2×10^{-11}	~300	–	2.8	CPD	[1867]
Ba/Ni	Ba	–	$<1 \times 10^{-9}$	~300	–	2.8	CPD	[3463]
Ba	–	–	–	–	–	2.80	TC	[1744]
Ba/W(100)	Ba	–	($\leq 10^{-11}$)	~300 (1200)	–	2.84	CPD	[776]
Ba/W(110)	Ba	–	1×10^{-9}	~300	–	2.9	CPD	[2017]
Ba	–	–	–	–	–	2.91	TC	[231]
Ba/W(110)[241]	Ba	–	$\leq 6 \times 10^{-10}$	~300	–	2.955 ± 0.005	CPD	[2104,2108]
Ba	–	–	–	–	–	2.96	TC	[231]
Ba/W(110)	Ba	–	($\leq 10^{-10}$)	~300	–	2.97 ± 0.02	CPD	[2595]
Ba/W(100)	Ba	–	$\sim 10^{-11}$	~300 (1100)	–	3.0	PE	[2518]
Ba/Si(111)	Ba	–	?	~300	–	3.0 ± 0.9	CPD	[2160]
Ba	–	–	–	–	–	3.01	TC	[1924]
Ba	–	–	–	–	–	3.02	TC	[1924]
Ba	–	–	–	–	–	3.02	TC	[3467]
Ba/W(110)	Ba	–	($<10^{-11}$)	~300 (600)	–	3.06	CPD	[776]
Ba	–	–	–	–	–	3.06	TC	[1613]
Ba/Pt	Ba	–	$\leq 2 \times 10^{-9}$	~300 (1720)	–	3.7 ± 0.1	FE	[3543]
Ba/W(110)[241]	Ba	–	$\leq 3 \times 10^{-10}$	~300	–	3.10 ± 0.02	CPD	[2104]

Table 1 (*continued*)

Surface	Beam	Ion	P_r (Torr)	T (K)	ϕ^+ (eV)	ϕ^e (eV)	Meth.	Refs.
Ba/W	Ba	–	2×10^{-9}	~300 (1000)	–	3.3	FE	[1966]
Ba	–	–	–	–	–	3.61	TC	[3476]
Recommended	–	–	–	–	–	**2.50 ± 0.02**	–	–

57. Lanthanum La[399]

hcp (α, $T < 583$ K)

Surface	Beam	Ion	P_r (Torr)	T (K)	ϕ^+ (eV)	ϕ^e (eV)	Meth.	Refs.
La(0001)/Mo(110)	La	–	$\leq 3 \times 10^{-10}$	~300	–	3.0	CPD	[640]
La(0001)	–	–	–	–	–	3.06	TC	[1434]
La(0001)	–	–	–	–	–	3.21	TC	[334]

fcc (β, $T = 583–1141$ K)

Surface	Beam	Ion	P_r (Torr)	T (K)	ϕ^+ (eV)	ϕ^e (eV)	Meth.	Refs.
La(100)	–	–	–	–	–	3.74	TC	[321]
La(100)	–	–	–	–	–	4.83	TC	[485,1703]
La(110)	–	–	–	–	–	3.53	TC	[321]
La(110)	–	–	–	–	–	4.84	TC	[485,1703]
La(111)	–	–	–	–	–	2.9	TC	[1723]
La(111)	–	–	–	–	–	3.30	TC	[334,3179]
La(111)	–	–	–	–	–	4.04	TC	[321]

bcc (γ, $T > 1141$ K)

Surface	Beam	Ion	P_r (Torr)	T (K)	ϕ^+ (eV)	ϕ^e (eV)	Meth.	Refs.
La(100)	–	–	–	–	–	3.23	TC	[321]
La(100)	–	–	–	–	–	4.83	TC	[1703]
La(110)	–	–	–	–	–	3.76	TC	[321]
La(110)	–	–	–	–	–	5.93	TC	[1703]
La(111)	–	–	–	–	–	3.09	TC	[321]
La(112)	–	–	–	–	–	3.44	TC	[321]

hcp (α, $T < 583$ K for bulk)

Surface	Beam	Ion	P_r (Torr)	T (K)	ϕ^+ (eV)	ϕ^e (eV)	Meth.	Refs.
La/W(111)	La	–	~10^{-9}	~300	–	2.4	FE	[2011]
La/W	La	–	4×10^{-10}	~300 (1050)	–	2.4	FE	[1583]
La	–	–	–	–	–	2.49	TC	[3476]
La/W	La	–	~10^{-10}	~300	–	2.49	FE	[378]
La/W(011)	La	–	4×10^{-10}	~300 (1050)	–	2.5	FE	[1583]
La/?	La	–	?	~300	–	2.50	CPD	[2634]
La	–	–	? (N_2)	~300	–	2.50 ± 0.02	CPD	[4066]
La	–	–	–	–	–	2.57	TC	[3476]
La/B/Mo(110)[252]	La	–	2×10^{-10}	~300	–	2.6	CPD	[3963]
La/W(111)	La	–	~10^{-10}	~300	–	2.63	FE	[378]
La/W	La	–	~10^{-10}	~300	–	2.7	FE	[2827]
La/W(111)	La	–	?	77	–	2.7	CPD	[2507]
La	–	–	–	–	–	2.71	TC	[1066]
La/W(111)	La	–	?	~300	–	2.75	CPD	[2507]
La/W(100)	La	–	~10^{-10}	~300	–	2.78	FE	[378]
La	–	–	–	–	–	2.8*	TC	[1955]
La/W	La	–	~10^{-10}	~300	–	2.8	FE	[2827]
La/B/Mo(110)[252]	La	–	2×10^{-10}	~300	–	2.8	CPD	[2700]
La	–	–	–	–	–	2.84	TC	[3476]
La/W	La	–	~10^{-10}	77	–	2.86	FE	[2827]
La/Pt(111)[246]	La	–	?	77	–	2.86	PE	[3009]
La/W(112)	La	–	~10^{-10}	~300	–	2.90	FE	[378]
La	–	–	–	–	–	3.0	TC	[1993]
La/Ta(112)	La	–	$\leq 10^{-11}$	~300 (800)	–	3.02	CPD	[801]
La/W(100)	La	–	$\leq 10^{-11}$	~300	–	3.04	CPD	[2020]
La/W(100)	La	–	$\leq 1 \times 10^{-9}$	~300	–	3.05	CPD	[1996]
La/Ta(112)	La	–	$\leq 10^{-11}$	~300 (1000)	–	3.09	CPD	[801]
La/Ta(112)	La	–	$\leq 10^{-11}$	~300 (400)	–	3.11	CPD	[801]
La/Mo(112)	La	–	($\leq 10^{-11}$)	77	–	3.12	CPD	[2502]
La/Ta(112)	La	–	$\leq 10^{-11}$	~300 (600)	–	3.13	CPD	[801]
La/W(110)	La	–	$\leq 1 \times 10^{-9}$	~300	–	3.17	CPD	[1996]
La/Mo(110)	La	–	2×10^{-10}	~300	–	3.2	CPD	[2700]
La	–	–	–	–	–	3.21	TC	[3318]
La	–	–	–	–	–	3.25	TC	[550]
La	–	–	–	0	–	3.28	TC	[4419]

Table 1 (continued)

Surface	Beam	Ion	P_r (Torr)	T (K)	ϕ^+ (eV)	ϕ^e (eV)	Meth.	Refs.
La	–	–	–	–	–	3.28	TC	[3318]
La	–	–	–	–	–	3.3	TC	[706]
La/W	La	–	?	0^E	–	3.3	TE	[3022]
La/Re(1010)	La	–	($<10^{-11}$)	77	–	3.3	CPD	[2506]
La/Mo(110)[252]	La	–	2×10^{-10}	~300	–	3.3	CPD	[3963,4276]
La/W(110)	La	–	~10^{-10}	~300	–	3.30	FE	[378]
La	–	–	–	–	–	3.30	TC	[3352]
La	–	–	–	–	–	3.30	TC	[521]
La/Cr(110)	La	–	~10^{-11}	~300	–	3.31*	CPD	[4276]
La/Nb(110)	La	–	~10^{-11}	~300	–	3.34*	CPD	[4276]
La/W(110)	La	–	($\leq10^{-10}$)	~300	–	3.4	CPD	[3350,3351,3365]
La/Mo(110)	La	–	($\leq10^{-10}$)	~300	–	3.4	CPD	[3350]
La/Mo(110)[252]	La	–	2×10^{-10}	~300	–	3.4	CPD	[2700]
La/quartz	La	–	~10^{-10}	~300	–	3.5 ± 0.2	PE	[304]
La/W(110)	La	–	~10^{-11}	~300	–	3.52	CPD	[4276]
La	–	–	–	–	–	3.58	TC	[298]
La	–	–	–	–	–	3.62	TC	[2629]
La	–	–	–	–	–	3.85	TC	[1744]
La/W	La	–	2×10^{-11}	~300	–	4.33	FE	[2397]
La	–	–	–	–	–	4.47	TC	[2629]
Recommended	–	–	–	–	–	**3.27 ± 0.04**	–	–

fcc (β, T = 583–1141 K for bulk)

Surface	Beam	Ion	P_r (Torr)	T (K)	ϕ^+ (eV)	ϕ^e (eV)	Meth.	Refs.
La/Nb(110)	La	–	$\leq10^{-8}$	~1000–1150	–	2.6 ± 0.03	TE	[2359]
La/Ta(110)	La	–	$\leq10^{-8}$	~1000–1150	–	2.6 ± 0.03	TE	[2359]
La/W	La	–	?	?	–	2.71	TE	[1750]
La	–	–	–	–	–	2.72	TC	[1066]
La/W(116)	La	–	1×10^{-9}	?	–	2.8	TE	[1975]
La/Nb(100)	La	–	$\leq10^{-8}$	~1000–1150	–	2.8 ± 0.03	TE	[2359]
La/W(111)	La	–	1×10^{-9}	?	–	2.9	TE	[1975]
La/W(100)	La	–	$\leq10^{-8}$	~1000–1150	–	2.9 ± 0.03	TE	[2359]
La/Zr,Hf	La	–	$\leq10^{-8}$	~1000–1150	–	2.9 ± 0.03	TE	[2359]
La/Nb,Ta	La	–	$\leq10^{-8}$	~1000–1150	–	2.9 ± 0.03	TE	[2359]
La/Ru,Os,Ir	La	–	$\leq10^{-8}$	~1000–1150	–	2.9 ± 0.03	TE	[2359]
La/Mo,W	La	–	$\leq10^{-8}$	~1000–1150	–	2.96 ± 0.03	TE	[2359]
La/Re	La	–	$\leq10^{-8}$	~1000–1150	–	2.96 ± 0.03	TE	[2359]
La/W(100)	La	–	$\leq10^{-11}$	650	–	2.97	TE	[2020]
La/W(100)	La	–	$\leq10^{-11}$	900	–	3.00	TE	[2020]
La/W(100)	La	–	1×10^{-9}	?	–	3.1	TE	[1975]
La/W(110)	La	–	$\leq10^{-8}$	~1000–1150	–	3.1 ± 0.03	TE	[2359]
La/W(110)	La	–	1×10^{-9}	?	–	3.2	TE	[1975]
Recommended	–	–	–	–	–	**2.98 ± 0.10**	–	–

58. Cerium Ce[399]

fcc (β, T = 263–1003 K)

Surface	Beam	Ion	P_r (Torr)	T (K)	ϕ^+ (eV)	ϕ^e (eV)	Meth.	Refs.
Ce(100)	–	–	$<5 \times 10^{-11}$	~300	–	4.05 ± 0.1	PE	[4147]
Ce(100)	–	–	–	–	–	4.62	TC	[321]
Ce(110)	–	–	–	–	–	4.35	TC	[321]
Ce(111)	–	–	–	–	–	3.26	TC	[1434]
Ce(111)	–	–	–	–	–	4.98	TC	[321]

bcc (γ, T > 1003 K)

Surface	Beam	Ion	P_r (Torr)	T (K)	ϕ^+ (eV)	ϕ^e (eV)	Meth.	Refs.
Ce(100)	–	–	–	–	–	3.98	TC	[321]
Ce(110)	–	–	–	–	–	4.63	TC	[321]
Ce(111)	–	–	–	–	–	3.81	TC	[321]
Ce(112)	–	–	–	–	–	4.24	TC	[321]

fcc (β, T = 263–1003 K for bulk)

Surface	Beam	Ion	P_r (Torr)	T (K)	ϕ^+ (eV)	ϕ^e (eV)	Meth.	Refs.
Ce/W(111)	Ce	–	~10^{-9}	~300	–	2.2	FE	[2011]
Ce	–	–	–	–	–	2.23	TC	[1744]
$Ce_n (n \rightarrow \infty)$	–	–	~10^{-6}	70	–	2.40	IP	[4263]
Ce/W[247]	Ce	–	–	~300^E	–	2.5*	TE	[3022]
Ce/W(111)	Ce	–	1×10^{-9}	?	–	2.5	TE	[1975]

Table 1 (*continued*)

Surface	Beam	Ion	P_r (Torr)	T (K)	ϕ^+ (eV)	ϕ^e (eV)	Meth.	Refs.
Ce/Pd/Ru(0001)[248]	Ce	–	~10^{-10}	~300	–	2.5 ± 0.1*	PE	[3718]
Ce/Ir–Ce(9%)	–	–	~10^{-8}	1300	–	2.57	TE	[4239]
Ce/W(116)	Ce	–	1×10^{-9}	?	–	2.6	TE	[1975]
Ce/Rh(110)	Ce	–	8×10^{-11}	~300	–	2.6*	PE	[2287]
Ce/?	Ce	–	?	~300	–	2.60	CPD	[3596]
Ce/?	Ce	–	?	~300	–	2.62	CPD	[2634]
Ce	–	–	? (N_2)	~300	–	2.62 ± 0.02	CPD	[2634,4066,4251]
Ce/quartz	–	–	~10^{-6} (Ar)	293	–	2.65 ± 0.02	CPD	[3977]
Ce	–	–	–	–	–	2.66	TC	[2750]
Ce/W	Ce	–	?	?	–	2.71	TE	[1750]
Ce/Rh(110)	Ce	–	8×10^{-11}	~300 (770)	–	2.8*	PE	[2287]
Ce/W	Ce	–	~10^{-10}	520	–	2.8	FE	[2826]
Ce	–	–	–	–	–	2.8	TC	[1955]
Ce/Pd/Ru(0001)[248]	Ce	–	~10^{-10}	~300	–	2.8 ± 0.1*	PE	[3718]
Ce/Ni	Ce	–	?	~300	–	2.84	PE	[2922]
Ce	–	–	–	–	–	2.84	TC	[3352]
Ce/W	Ce	–	~10^{-10}	~300	–	2.85	FE	[2826]
Ce/W(110)	Ce	–	1×10^{-9}	?	–	2.9	TE	[1975]
Ce/Pt(111)	Ce	–	<1×10^{-10}	~300	–	2.9*	CPD	[1601]
Ce/?	Ce	–	?	~300	–	2.9	PE	[2115]
Ce/quartz	Ce	–	~10^{-10}	~300	–	2.9 ± 0.2	PE	[304]
Ce/Ru(0001)	Ce	–	~10^{-10}	~300	–	2.90	PE	[4199]
Ce	–	–	–	–	–	2.98	TC	[1066]
Ce/Ir-0.4%Ce	–	–	?	~300 (2000)	–	3.0	FE	[3613]
Ce/Pd(110)[249]	Ce	–	~10^{-10}	~300	–	3.02*	PE	[3306]
Ce[174]	–	–	–	0^E	–	3.07	TC	[1747]
Ce/Pd(111)[249]	Ce	–	~10^{-10}	~300	–	3.10*	PE	[3306]
Ce	–	–	–	–	–	3.24	TC	[550]
Ce$_n$(n → ∞)	–	–	–	–	–	3.27 ± 0.35	TC	[4261]
Ce/W(100)	Ce	–	1×10^{-9}	?	–	3.3	TE	[1975]
Ce/Pd(110)[249]	Ce	–	~10^{-10}	~300	–	3.36	PE	[3306]
Ce/Pd(110)[249]	Ce	–	~10^{-10}	~300	–	3.55	PE	[3306]
Recommended	–	–	–	–	–	**2.89 ± 0.07**	–	–
bcc (γ, T = 1003–1068 K for bulk)								
Ce/?	Ce	–	?	1050	–	2.67	TE	[3022]
Ce/W	Ce	–	~10^{-10}	1060	–	2.96	FE	[2826]
Ce/?	Ce	–	?	~1000	–	3.18*	TE	[1747]
Ce/Re(0001)	Ce	–	≤5×10^{-8}	≥1000	–	3.20	TE	[96]

59. Praseodymium Pr[399]

hcp (α, T < 1071 K)

Surface	Beam	Ion	P_r (Torr)	T (K)	ϕ^+ (eV)	ϕ^e (eV)	Meth.	Refs.
Pr(0001)	–	–	–	–	–	3.11	TC	[1434]
bcc (β, T > 1071 K)								
Pr(100)	–	–	–	–	–	3.32	–	[321]
Pr(110)	–	–	–	–	–	3.86	–	[321]
Pr(111)	–	–	–	–	–	3.17	–	[321]
Pr(112)	–	–	–	–	–	3.54	–	[321]
hcp (α, T < 1071 K for bulk)								
Pr$_n$(n → ∞)	–	–	~10^{-6}	70	–	2.50	IP	[4263]
Pr/W(111)	Pr	–	~10^{-9}	~300	–	2.6	FE	[2011]
Pr	–	–	? (N_2)	~300	–	2.63 ± 0.02	CPD	[4251]
Pr	–	–	? (N_2)	~300	–	2.67	CPD	[2634,4066,4253]
Pr	–	–	–	–	–	2.70	TC	[3352]
Pr	–	–	–	–	–	2.8	TC	[1955]
Pr	–	–	–	–	–	2.80	TC	[2750]
Pr	–	–	–	–	–	2.81	TC	[1066]
Pr	–	–	–	–	–	3.04	TC	[550]
Pr	–	–	–	–	–	3.25	TC	[550]
Pr$_n$(n → ∞)	–	–	–	–	–	3.54 ± 0.13	TC	[4261]
Recommended	–	–	–	–	–	**2.83 ± 0.11**	–	–

Table 1 (*continued*)

Surface	Beam	Ion	P_r (Torr)	T (K)	ϕ^+ (eV)	ϕ^e (eV)	Meth.	Refs.
bcc (β, T = 1071–1208 K for bulk)								
Pr/?	Pr	–	?	1120	–	2.74	TE	[3022]

60. Neodymium Nd[399]

Surface	Beam	Ion	P_r (Torr)	T (K)	ϕ^+ (eV)	ϕ^e (eV)	Meth.	Refs.
hcp (α, T < 1141 K)								
Nd(0001)	–	–	–	–	–	3.09	TC	[1434]
Nd(0001)/W(100)	Nd	–	1×10^{-9}	~300	–	3.30	CPD	[1543,4145]
bcc (β, T > 1141 K)								
Nd(100)	–	–	–	–	–	3.63	TC	[321]
Nd(110)	–	–	–	–	–	4.23	TC	[321]
Nd(111)	–	–	–	–	–	3.48	TC	[321]
Nd(112)	–	–	–	–	–	3.87	TC	[321]
hcp (α, T < 1141 K for bulk)								
Nd/Cu(100)	Nd	–	1×10^{-10}	~300	–	2.63	CPD	[2734]
Nd	–	–	–	–	–	2.7	TC	[1744]
Nd/Cu(100)	Nd	–	?	~300	–	2.7	CPD	[2739]
Nd/W(111)	Nd	–	~10^{-9}	~300	–	2.8	FE	[2011]
Nd	–	–	? (N_2)	~300	–	2.80 ± 0.02	CPD	[4066]
Nd/Cu(100)	Nd	–	1×10^{-10}	550	–	2.88*	CPD	[2734]
Nd	–	–	–	–	–	2.92	TC	[1066]
Nd	–	–	–	–	–	2.94	TC	[2750]
Nd/W(111)	Nd	–	<10^{-10}	170	–	2.95	FE	[3793]
Nd/W	Nd	–	<10^{-10}	170	–	3.0	FE	[3793]
Nd	–	–	–	–	–	3.04	TC	[550]
Nd	–	–	–	–	–	3.1	TC	[1955]
Nd/W	Nd	–	≤1×10^{-9}	~300	–	3.1 ± 0.05	FE	[2602]
Nd/Cu(100)	Nd	–	1×10^{-10}	800	–	3.13	CPD	[2734]
Nd/W(100)	Nd	–	<10^{-10}	170	–	3.2	FE	[3793]
Nd/Cu(111)	Nd	–	<1×10^{-10}	~300	–	3.2*	CPD	[2735]
Nd/quartz	Nd	–	~10^{-10}	~300	–	3.2 ± 0.25	PE	[304]
Nd	–	–	–	–	–	3.25	TC	[550]
Nd/Mo(112)	Nd	–	~10^{-11}	~300	–	3.36	CPD	[2535]
Recommended	–	–	–	–	–	**3.14 ± 0.08**	–	–
bcc (β, T = 1141–1297 K for bulk)								
Nd/?	Nd	–	?	1150–1450	–	2.95	TE	[3022]

61. Prometium Pm

Surface	Beam	Ion	P_r (Torr)	T (K)	ϕ^+ (eV)	ϕ^e (eV)	Meth.	Refs.
hcp (α, T < ?)								
Pm(0001)	–	–	–	–	–	3.09	TC	[1434]
fcc (β, T > ?)								
Pm(100)	–	–	–	–	–	3.73	TC	[321]
Pm(110)	–	–	–	–	–	3.52	TC	[321]
Pm(111)	–	–	–	–	–	4.03	TC	[321]
hcp (α, T < ?)								
Pm[379]	–	–	–	–	–	3.0	TC	[1955]
Pm	–	–	–	–	–	3.07	TC	[1956]
Pm	–	–	–	–	–	3.08	TC	[2750]
Pm	–	–	–	–	–	3.21	TC	[550]

62. Samarium Sm[399]

Surface	Beam	Ion	P_r (Torr)	T (K)	ϕ^+ (eV)	ϕ^e (eV)	Meth.	Refs.
bcc (β, T > 1200 K)								
Sm(100)	–	–	–	–	–	3.23	TC	[321]
Sm(110)	–	–	–	–	–	3.76	TC	[321]

Table 1 (*continued*)

Surface	Beam	Ion	P_r (Torr)	T (K)	ϕ^+ (eV)	ϕ^e (eV)	Meth.	Refs.
Sm(111)	–	–	–	–	–	3.09	TC	[321]
Sm(112)	–	–	–	–	–	3.44	TC	[321]
Rhombohedral (α, $T < 1200$ K for bulk)								
Sm	–	–	–	–	–	1.8	TC	[1744]
Sm	–	–	? (N_2)	~300	–	2.52 ± 0.02	CPD	[4066]
Sm/Mo(110)	Sm	–	<8 × 10⁻¹¹	~300	–	2.56*	CPD	[3147]
Sm/?	Sm	–	~10⁻¹⁰	~300	–	2.6	PE	[1514]
Sm/Mo(110)	Sm	–	<5 × 10⁻¹¹	~300	–	2.64	CPD	[3148]
Sm/W(111)	Sm	–	~10⁻⁹	~300	–	2.7	FE	[2011]
Sm/Mo(111)	Sm	–	<1 × 10⁻¹⁰	300	–	2.7	CPD	[2449]
Sm/Au/SiO₂	Sm	–	8 × 10⁻¹¹	~300	–	2.7	PE	[4204]
Sm/quartz	Sm	–	~10⁻¹⁰	~300	–	2.7 ± 0.3	PE	[304]
Sm/Mo(112)	Sm	–	<5 × 10⁻¹¹	~300	–	2.71	CPD	[2450]
Sm/Si	Sm	–	?	~300	–	2.75	PE	[4217]
Sm/Ni(111)²⁵⁰	Sm	–	1 × 10⁻¹⁰	293	–	2.8*	PE	[3000]
Sm/Ir(111)	Sm	–	≤1 × 10⁻⁸	~1100–1200	–	2.8	TE	[3583]
Sm/Cu(111)	Sm	–	~1 × 10⁻¹⁰	~300	–	2.84	CPD	[2272]
Sm/W	Sm	–	?	?	–	2.85	?	[1360]
Sm/Si(111)	Sm	–	6 × 10⁻¹¹	~300	–	2.9	CPD	[3758]
Sm/W	Sm	–	?	750	–	2.98	TE	[2489]
Sm/Cu(111)	Sm	–	~1 × 10⁻¹⁰	680–870	–	2.99	CPD	[2272]
Sm	–	–	–	–	–	3.06	TC	[550]
Sm	–	–	–	–	–	3.1	TC	[1955]
Sm/W(112)	Sm	–	≤10⁻¹¹	~300	–	3.10	CPD	[4274]
Sm/Si(111)	Sm	–	?	~300	–	3.11*	CPD	[3755,3758]
Sm/?	Sm	–	?	~1150–1600	–	3.15	TE	[3022]
Sm/W(112)	Sm	–	(≤10⁻¹¹)	77	–	3.16	CPD	[2671]
Sm/Si(111)	–	–	–	–	–	3.2*	TC	[4076]
Sm/?	Sm	–	?	0ᴱ (≤1600)	–	3.2	TE	[3022]
Sm/Si(100)	Sm	–	<3 × 10⁻⁶	~300	–	3.20	PE	[2435]
Sm	–	–	–	–	–	3.22	TC	[2750]
Sm	–	–	–	–	–	3.27	TC	[550]
Sm/Pd(100)	Sm	–	~10⁻¹⁰	~300	–	3.3*	CPD	[1917]
Sm/W(110)	Sm	–	?	~300	–	4.38	CPD	[2542]
Recommended	–	–	–	–	–	**2.81 ± 0.10**	–	–

63. Europium Eu

Surface	Beam	Ion	P_r (Torr)	T (K)	ϕ^+ (eV)	ϕ^e (eV)	Meth.	Refs.
bcc								
Eu(100)	–	–	–	–	–	3.26	TC	[321]
Eu(110)	–	–	–	–	–	2.35	TC	[1434]
Eu(110)	–	–	–	–	–	2.42	TC	[334]
Eu(110)	–	–	–	–	–	3.80	TC	[321]
Eu(111)	–	–	–	–	–	3.12	TC	[321]
Eu(112)	–	–	–	–	–	3.48	TC	[321]
bcc								
Eu/W	Eu	–	3 × 10⁻¹⁰	78	–	2.2	FE	[2643]
Eu/W(112)	Eu	–	7 × 10⁻¹¹	300	–	2.25 ± 0.20*	CPD	[2389]
Eu/W(112)	Eu	–	7 × 10⁻¹¹	300 (<700)	–	2.25 ± 0.20*	CPD	[2389]
Eu/W(111)	Eu	–	~10⁻⁹	~300	–	2.4	FE	[2011]
Eu/W(116)	Eu	–	1 × 10⁻⁹	?	–	2.5	TE	[1975]
Eu/quartz	Eu	–	~10⁻¹⁰	~300	–	2.5 ± 0.3	PE	[304]
Eu	–	–	–	–	–	2.54	TC	[1956]
Eu	–	–	–	–	–	2.54	TC	[3352]
Eu	–	–	–	–	–	2.56	TC	[4432]
Eu/W(111)	Eu	–	1 × 10⁻⁹	?	–	2.6	TE	[1975]
Eu/W	Eu	–	?	?	–	2.7	TE	[2494]
Eu	–	–	4 × 10⁻¹⁰	~300	–	2.7 ± 0.05	CPD	[3120]
Eu	–	–	? (N_2)	~300	–	2.78 ± 0.02	CPD	[4066]
Eu/W(110)	Eu	–	1 × 10⁻⁹	?	–	2.8	TE	[1975]
Eu	–	–	–	–	–	2.8	TC	[1955]
Eu/W(110)	Eu	–	<7 × 10⁻¹¹	~300	–	2.8*	CPD	[2393]
Eu/Si(111)	–	–	–	–	–	2.8*	TC	[4076]

Table 1 (*continued*)

Surface	Beam	Ion	P_r (Torr)	T (K)	ϕ^+ (eV)	ϕ^e (eV)	Meth.	Refs.
Eu/Si(111)[445]	Eu	–	$\leq 5 \times 10^{-10}$	~300	–	2.8*	CPD	[3757,4111]
Eu	–	–	–	–	–	2.87	TC	[550]
Eu/Si(111)[445]	Eu	–	$\leq 5 \times 10^{-10}$	~300	–	2.9*	CPD	[4112]
Eu/Si(111)[445]	Eu	–	$\leq 5 \times 10^{-10}$	500	–	2.9*	CPD	[3757,4111]
Recommended	–	–	–	–	–	**2.74 ± 0.12**	–	–

64. Gadolinium Gd[399]

hcp (α, T < 1533 K)

Surface	Beam	Ion	P_r (Torr)	T (K)	ϕ^+ (eV)	ϕ^e (eV)	Meth.	Refs.
Gd(0001)	–	–	–	–	–	3.22	TC	[1434]
Gd(0001)/W(110)	Gd	–	$<2 \times 10^{-10}$	~300	–	3.25	PE	[3567]
Gd(0001)	–	–	$\sim 10^{-11}$	~300	–	3.3 ± 0.1	PE	[2148,2498,2504]
Gd(0001)/W(110)	Gd	–	$\sim 10^{-11}$	~300	–	3.3 ± 0.1	PE	[2522]
Gd(0001)[251]	–	–	–	–	–	3.67	TC	[3462]
Gd(0001)[251]	–	–	–	–	–	3.84	TC	[3462]
Gd(0001)	–	–	–	–	–	4.52	TC	[321]
Recommended	–	–	–	–	–	**3.27 ± 0.03**	–	–
Gd(1010)	–	–	–	–	–	4.31	TC	[321]
Gd(1124)	–	–	–	–	–	3.78	TC	[321]

bcc (β, T > 1533 K)

Surface	Beam	Ion	P_r (Torr)	T (K)	ϕ^+ (eV)	ϕ^e (eV)	Meth.	Refs.
Gd(100)	–	–	–	–	–	2.9	TC	[4218]
Gd(100)	–	–	–	–	–	3.55	TC	[321]
Gd(110)	–	–	–	–	–	4.13	TC	[321]
Gd(111)	–	–	–	–	–	3.40	TC	[321]
Gd(112)	–	–	–	–	–	3.78	TC	[321]

hcp (α, T < 1533 K)

Surface	Beam	Ion	P_r (Torr)	T (K)	ϕ^+ (eV)	ϕ^e (eV)	Meth.	Refs.
Gd	–	–	–	–	–	2.18 ± 0.05	TC	[2358]
Gd/W	Gd	–	?	~300	–	2.4 ± 0.3	FE	[1856]
Gd	–	–	–	–	–	2.41	TC	[1744]
Gd	–	–	–	–	–	2.45 ± 0.07	TC	[2358]
Gd	–	–	? (N_2)	~300	–	2.57 ± 0.02	CPD	[4251]
Gd/W(111)	Gd	–	1×10^{-9}	?	–	2.6	TE	[1975]
Gd/W(111)	Gd	–	1×10^{-9}	~300	–	2.6	FE	[2011]
Gd/W(111)	Gd	–	$\sim 10^{-10}$	~300	–	2.6	FE	[818]
Gd	–	–	? (N_2)	~300	–	2.65 ± 0.02	CPD	[4066]
Gd/W(111)	Gd	–	$\leq 10^{-9}$	~300	–	2.7	FE	[1987]
Gd/W(111)	Gd	–	$\leq 10^{-9}$	~300 (>400)	–	2.7	FE	[1987]
Gd/W(111)	Gd	–	1×10^{-9}	~300	–	2.7	FE	[1975]
Gd/W(116)	Gd	–	1×10^{-9}	?	–	2.7	TE	[1975]
Gd/W	Gd	–	?	~300	–	2.7 ± 0.3	FE	[1856]
Gd/W(116)	Gd	–	$\leq 10^{-9}$	~300	–	2.8	FE	[1987]
Gd/W(111)	Gd	–	($\leq 10^{-11}$)	~300 (≤ 1000)	–	2.80 ± 0.01	CPD	[2046]
Gd/W(111)	Gd	–	$\leq 10^{-9}$	77	–	2.85	FE	[3704]
Gd(slab)	–	–	5×10^{-9}	~300	–	2.9 ± 0.1	PE	[2716]
Gd/Re–Gd(4.4%)	–	–	$\sim 10^{-8}$	1300	–	2.90	TE	[4240]
Gd	–	–	?	295	–	2.90 ± 0.06	CPD	[2943]
Gd/W(111)	Gd	–	($\leq 10^{-11}$)	~300	–	2.93	CPD	[2046]
Gd/W(116)	Gd	–	$\leq 10^{-9}$	~300 (>400)	–	3.0	FE	[1975,1987]
Gd/B/Mo(110)[253]	Gd	–	2×10^{-10}	~300	–	3.0	CPD	[2700]
Gd	–	–	–	–	–	3.05	TC	[2750]
Gd	–	–	–	–	–	3.07	TC	[1956]
Gd	–	–	–	–	–	3.07	TC	[2943]
Gd(foil)	–	–	$<8 \times 10^{-11}$	~300	–	3.075 ± 0.050	PE	[342,3866,3868]
Gd/W(100)	Gd	–	$\leq 10^{-9}$	~300	–	3.1	FE	[1987]
Gd/W(112)	Gd	–	$\leq 10^{-9}$	~300	–	3.1	FE	[1987]
Gd	–	–	$\leq 10^{-9}$	~300	–	3.1	PE	[1483]
Gd/W(112)	Gd	–	$\leq 10^{-9}$	~300 (>400)	–	3.1	FE	[1987]
Gd/W	Gd	–	$\leq 10^{-9}$	~300 (>400)	–	3.1	FE	[1987]
Gd	–	–	–	–	–	3.1	TC	[1955]
Gd/Mo(111)	Gd	–	$<1 \times 10^{-10}$	~300	–	3.1	CPD	[2449]
Gd/quartz	Gd	–	$\sim 10^{-10}$	~300	–	3.1 ± 0.15	PE	[304]
Gd/W(110)	Gd	–	$\leq 10^{-9}$	77	–	3.12*	FE	[3704]

Table 1 (*continued*)

Surface	Beam	Ion	P_r (Torr)	T (K)	ϕ^+ (eV)	ϕ^e (eV)	Meth.	Refs.
Gd/W	Gd	–	?	~300 (1070)	–	3.2 ± 0.3	FE	[1856]
Gd/Mo(112)	Gd	–	1×10^{-10}	~300	–	3.23	CPD	[2452]
Gd	–	–	–	–	–	3.27	TC	[550]
Gd/W(110)	Gd	–	$\leq 10^{-9}$	~300	–	3.3	FE	[1987]
Gd/W(100)	Gd	–	$\leq 10^{-9}$	~300 (>400)	–	3.3	FE	[1975,1987]
Gd/W(110)	Gd	–	$\leq 10^{-9}$	77	–	3.31	FE	[3704]
Gd/Mo(110)	Gd	–	$\leq 3 \times 10^{-10}$	~300	–	3.4	CPD	[331]
Gd/Mo(110)	Gd	–	$\sim 10^{-10}$	~300	–	3.4	CPD	[4272]
Gd/Mo(112)	Gd	–	$\leq 10^{-11}$	~300 (1100)	–	3.40	CPD	[2533]
Gd	–	–	–	–	–	3.45	TC	[2358]
Gd/W(100)	Gd	–	$(\leq 10^{-11})$	~300 (≤800)	–	3.45 ± 0.02	CPD	[2664]
Gd/W(100)	Gd	–	$(\leq 10^{-11})$	~300 (1200)	–	3.48	CPD	[2664]
Gd/Mo(110)[253]	Gd	–	2×10^{-10}	~300	–	3.5	CPD	[2700]
Gd/W(100)	Gd	–	1×10^{-9}	?	–	3.5	TE	[1975]
Gd/W(110)	Gd	–	1×10^{-9}	?	–	3.5	TE	[1975]
Gd/W(110)	Gd	–	$<7 \times 10^{-11}$	~300 (1200)	–	3.51*	CPD	[2393]
Gd[446]	–	–	?	290.85	–	3.55 ± 0.15	PE	[3899]
Gd/W(110)	Gd	–	$\leq 10^{-9}$	~300 (>400)	–	3.6	FE	[1975,1987]
Gd/W(112)	Gd	–	$(\leq 10^{-11})$	77	–	3.6	CPD	[2043]
Gd/W(100)	Gd	–	$(\leq 10^{-11})$	~300 (1000)	–	3.60	CPD	[2664]
Gd/W(112)	Gd	–	$\leq 10^{-11}$	~300	–	3.62	CPD	[2533]
Gd/W(100)	Gd	–	$(\leq 10^{-11})$	~300	–	3.68	CPD	[2664]
Gd	–	–	–	–	–	3.70 ± 0.06	TC	[2358]
Gd/Mo(110)	Gd	–	$<5 \times 10^{-10}$	~300	–	3.75	CPD	[4238]
Gd[254]	–	–	–	–	–	3.76	TC	[2358]
Gd[254]	–	–	–	–	–	3.77	TC	[2358]
Recommended	–	–	–	–	–	**3.09 ± 0.04**	–	–

65. Terbium Tb[399]

hcp (α, $T < 1500$ K)

Surface	Beam	Ion	P_r (Torr)	T (K)	ϕ^+ (eV)	ϕ^e (eV)	Meth.	Refs.
Tb(0001)	–	–	–	–	–	3.29	TC	[1434]
Tb(0001)[450]	–	–	?	300[E]	–	4.8*	TE	[3920]
Tb(0001)	–	–	–	–	–	4.95	TC	[321]
Tb(1010)	–	–	–	–	–	4.72	TC	[321]
Tb(1124)	–	–	–	–	–	4.13	TC	[321]

bcc (β, $T > 1500$ K)

Surface	Beam	Ion	P_r (Torr)	T (K)	ϕ^+ (eV)	ϕ^e (eV)	Meth.	Refs.
Tb(100)	–	–	–	–	–	3.88	TC	[321]
Tb(110)	–	–	–	–	–	4.52	TC	[321]
Tb(111)	–	–	–	–	–	3.72	TC	[321]
Tb(112)	–	–	–	–	–	4.13	TC	[321]

hcp (α, $T < 1500$ K for bulk)

Surface	Beam	Ion	P_r (Torr)	T (K)	ϕ^+ (eV)	ϕ^e (eV)	Meth.	Refs.
Tb/W(111)	Tb	–	$(\leq 10^{-11})$	~300 (1000)	–	2.81	CPD	[2046]
Tb/W(111)	Tb	–	$(\leq 10^{-11})$	~300 (800)	–	2.83	CPD	[2046]
Tb/W(111)	Tb	–	$(\leq 10^{-11})$	~300	–	2.92	CPD	[2046]
Tb/W(023)	Tb	–	$(\leq 10^{-11})$	77	–	2.92	FE	[3157]
Tb/W(112)	Tb	–	7×10^{-11}	~300 (1000)	–	2.92*	CPD	[2389]
Tb/W(111)	Tb	–	$(\leq 10^{-11})$	77	–	2.94	FE	[3157]
Tb/W(112)	Tb	–	$(\leq 10^{-11})$	77	–	2.94	FE	[3157]
Tb/Re–Tb(5%)	–	–	$\sim 10^{-8}$	1300	–	2.95	TE	[4240]
Tb/W(113)	Tb	–	$(\leq 10^{-11})$	77	–	2.97	FE	[3157]
Tb/W(111)	Tb	–	$\leq 10^{-9}$	77	–	2.97	FE	[3704]
Tb(slab)	–	–	5×10^{-9}	~300	–	3.0 ± 0.1	PE	[2716]
Tb	–	–	–	–	–	3.06	TC	[2750]
Tb	–	–	–	–	–	3.09	TC	[1956]
Tb	–	–	–	–	–	3.1	TC	[1955]
Tb/W(110)	Tb	–	$\leq 10^{-9}$	77	–	3.11*	FE	[3704]
Tb/W(111)	Tb	–	$(<10^{-11})$	~300	–	3.14*	CPD	[4235]
Tb	–	–	$\sim 10^{-9}$	1490	–	3.19	TE	[4356]
Tb	–	–	–	–	–	3.2	TC	[1744]
Tb/W(112)	Tb	–	$(\leq 10^{-11})$	77	–	3.24	CPD	[2671]
Tb	–	–	–	–	–	3.29	TC	[550]

Table 1 (*continued*)

Surface	Beam	Ion	P_r (Torr)	T (K)	ϕ^+ (eV)	ϕ^e (eV)	Meth.	Refs.
Tb/W(110)	Tb	–	($\leq 10^{-11}$)	77	–	3.3	FE	[3157]
Tb/W(110)	Tb	–	$\leq 10^{-9}$	77	–	3.30	FE	[3704]
Tb/W(110)	Tb	–	$< 7 \times 10^{-11}$	~300	–	3.36*	CPD	[2393]
Tb/W(100)	Tb	–	($\leq 10^{-11}$)	~300 (≤ 700)	–	3.40 ± 0.01	CPD	[2664]
Tb/W(100)	Tb	–	($\leq 10^{-11}$)	~300 (1200)	–	3.44	CPD	[2664]
Tb/Mo(110)	Tb	–	1×10^{-10}	~300	–	3.46	CPD	[3181,4273]
Tb/W(100)	Tb	–	($\leq 10^{-11}$)	~300 (≤ 1000)	–	3.48 ± 0.01	CPD	[2664]
Tb/W(100)	Tb	–	($\leq 10^{-11}$)	~300	–	3.60	CPD	[2664,3201]
Tb/Mo(110)	Tb	–	1×10^{-10}	~300 (800)	–	3.63	CPD	[3181,4273]
Recommended	–	–	–	–	–	**3.14 ± 0.09**	–	–

66. Dysprosium Dy[399]

hcp (α, $T < 1657$ K)

Surface	Beam	Ion	P_r (Torr)	T (K)	ϕ^+ (eV)	ϕ^e (eV)	Meth.	Refs.
Dy(0001)	–	–	–	–	–	3.31	TC	[1434]
Dy(0001)	–	–	–	–	–	5.00	TC	[321]
Dy(1010)	–	–	–	–	–	4.77	TC	[321]
Dy(1124)	–	–	–	–	–	4.18	TC	[321]

hcp (α, $T < 1657$ K for bulk)

Surface	Beam	Ion	P_r (Torr)	T (K)	ϕ^+ (eV)	ϕ^e (eV)	Meth.	Refs.
Dy/W	Dy	–	$\leq 3 \times 10^{-9}$	300 (?)	–	2.75	FE	[2969]
Dy/W(111)	Dy	–	$\leq 10^{-9}$	77	–	2.79	FE	[3704]
Dy/W	Dy	–	?	~300 (700)	–	2.9	FE	[532,1622]
Dy/W(111)	Dy	–	?	~300	–	2.9	FE	[532]
Dy/Re–Dy(4%)	–	–	~10^{-8}	1300	–	2.90	TE	[4240]
Dy/W(100)	Dy	–	~10^{-11}	~300	–	3.0*	PE	[2900]
Dy/Ta(112)	Dy	–	$\leq 10^{-11}$	~300 (600)	–	3.06	CPD	[801]
Dy	–	–	–	–	–	3.08	TC	[2750]
Dy	–	–	–	–	–	3.09	TC	[1956]
Dy	–	–	–	–	–	3.1	TC	[1955]
Dy/Ta(112)	Dy	–	$\leq 10^{-11}$	~300 (500)	–	3.11	CPD	[801]
Dy/Mo(112)	Dy	–	$\leq 1 \times 10^{-11}$	100 (~1000)	–	3.15*	CPD	[1937]
Dy/Mo(112)	Dy	–	($\leq 10^{-11}$)	77	–	3.15	CPD	[2052]
Dy/Mo(112)	Dy	–	$\leq 1 \times 10^{-11}$	90 (≥ 600)	–	3.16 ± 0.05*	CPD	[3616]
Dy/Ta(112)	Dy	–	$\leq 10^{-11}$	~300 (400)	–	3.25	CPD	[801]
Dy/Mo(112)	Dy	–	$\leq 1 \times 10^{-11}$	100 (≤ 400)	–	3.3*	CPD	[1937]
Dy/W(112)	Dy	–	($\leq 10^{-11}$)	77	–	3.3	CPD	[2043]
Dy	–	–	–	–	–	3.30	TC	[550]
Dy/Ta(112)	Dy	–	$\leq 10^{-11}$	77	–	3.41	CPD	[801]
Dy/Ta(112)	Dy	–	$\leq 10^{-11}$	~300	–	3.41	CPD	[801]
Dy/Mo(112)	Dy	–	~10^{-11}	~300	–	3.43	CPD	[2535]
Dy/Mo(112)	Dy	–	$\leq 1 \times 10^{-11}$	90 (~550)	–	3.43 ± 0.05*	CPD	[3616]
Dy/Mo(110)	Dy	–	1×10^{-10}	~300	–	3.58	CPD	[3181]
Dy/Mo(110)	Dy	–	$\leq 2 \times 10^{-10}$	~300	–	3.60	CPD	[2655,4272]
Dy/Al$_2$O$_3$/Mo(110)	Dy	–	$\leq 2 \times 10^{-10}$	~300	–	3.60	CPD	[2655]
Recommended	–	–	–	–	–	**3.18 ± 0.08**	–	–

67. Holmium Ho[399]

hcp (α, $T < 1701$ K)

Surface	Beam	Ion	P_r (Torr)	T (K)	ϕ^+ (eV)	ϕ^e (eV)	Meth.	Refs.
Ho(0001)	–	–	–	–	–	3.37	TC	[1434]
Ho(0001)	–	–	–	–	–	4.37	TC	[321]
Ho(1010)	–	–	–	–	–	4.23	TC	[321]
Ho(1124)	–	–	–	–	–	3.71	TC	[321]

hcp (α, $T < 1701$ K for bulk)

Surface	Beam	Ion	P_r (Torr)	T (K)	ϕ^+ (eV)	ϕ^e (eV)	Meth.	Refs.
Ho/W(111)	Ho	–	$\leq 10^{-11}$	~300 (640)	–	2.73 ± 0.03	FE	[3162]
Ho/W(023)	Ho	–	$\leq 10^{-11}$	77	–	2.84	FE	[3162]
Ho/W(113)	Ho	–	$\leq 10^{-11}$	~300{77}	–	2.84	FE	[3162]
Ho/W(113)	Ho	–	$\leq 10^{-11}$	~300	–	2.93 ± 0.05	FE	[3162]
Ho/Re–Ho(3%)	–	–	~10^{-8}	1300	–	2.95	TE	[4240]
Ho/W	Ho	–	$\leq 3 \times 10^{-9}$	~300 (?)	–	3.02	FE	[2969]
Ho/W(111)	Ho	–	$\leq 10^{-9}$	77	–	3.02	FE	[3704]
Ho/W(111)	Ho	–	$\leq 10^{-11}$	~300{77}	–	3.03 ± 0.03	FE	[3162]
Ho/W(113)	Ho	–	$\leq 10^{-11}$	~300{77}	–	3.03 ± 0.05	FE	[3162]

Table 1 (*continued*)

Surface	Beam	Ion	P_r (Torr)	T (K)	ϕ^+ (eV)	ϕ^e (eV)	Meth.	Refs.
Ho/W(111)	Ho	–	≤10⁻¹¹	77	–	3.06	FE	[3162]
Ho/W(113)	Ho	–	≤10⁻¹¹	77	–	3.06	FE	[3162]
Ho/W	Ho	–	≤10⁻¹¹	~300{77}	–	3.06 ± 0.05	FE	[3162]
Ho/W(113)	Ho	–	≤10⁻¹¹	~300 (800)	–	3.07	FE	[3162]
Ho	–	–	–	–	–	3.09	TC	[1956]
Ho	–	–	–	–	–	3.09	TC	[2750]
Ho	–	–	–	–	–	3.1	TC	[1955]
Ho	–	–	–	–	–	3.30	TC	[550]
Ho/W(112)	Ho	–	≤10⁻¹¹	77	–	3.31	FE	[3162]
Ho/W(112)	Ho	–	≤10⁻¹¹	77	–	3.55	CPD	[2049]
Recommended	–	–	–	–	–	**3.05 ± 0.05**	–	–

68. Erbium Er

Surface	Beam	Ion	P_r (Torr)	T (K)	ϕ^+ (eV)	ϕ^e (eV)	Meth.	Refs.
hcp								
Er(0001)	–	–	–	–	–	3.41	TC	[1434]
Er(0001)/Mo(110)	Er	–	~10⁻¹⁰	~300	–	3.53	CPD	[3163]
Er(0001)/Mo(110)	Er	–	~10⁻¹⁰	800	–	3.68	CPD	[3163]
Er(0001)	–	–	–	–	–	4.43	TC	[321]
Er(1010)	–	–	–	–	–	4.29	TC	[321]
Er(1124)	–	–	–	–	–	3.77	TC	[321]
hcp								
Er/6H-SiC(0001)	Er	–	4 × 10⁻¹⁰	~300	–	2.9 ± 0.1	CPD	[1832,3644]
Er/W	Er	–	<3 × 10⁻⁹	300 (?)	–	2.95	FE	[2969]
Er/Si(111)	Er	–	7 × 10⁻¹¹	~300	–	3.00	PE	[3461]
Er/Re–Er(2.5%)	–	–	~10⁻⁸	1300	–	3.00	TE	[4240]
Er(foil)²⁵⁵	–	–	~10⁻⁶	1300	–	3.06	TE	[3071]
Er/W(111)	Er	–	≤10⁻⁹	77	–	3.07	FE	[3704]
Er/6H-SiC(0001)	Er	–	4 × 10⁻¹⁰	~300 (1000)	–	3.1	CPD	[1832]
Er	–	–	–	–	–	3.1	TC	[1955]
Er	–	–	–	–	–	3.11	TC	[2750]
Er	–	–	–	–	–	3.12	TC	[1956]
Er	–	–	–	–	–	3.31	TC	[550]
Er/Si(100)	Er	–	≤4 × 10⁻¹⁰	230	–	3.5	CPD	[3199]
Er/Si(100)	Er	–	≤4 × 10⁻¹⁰	370	–	3.5	CPD	[3199]
Er/Mo(110)	Er	–	1 × 10⁻¹⁰	~300	–	3.53	CPD	[3181]
Recommended	–	–	–	–	–	**3.14 ± 0.08**	–	–

69. Thulium Tm³⁹⁹

Surface	Beam	Ion	P_r (Torr)	T (K)	ϕ^+ (eV)	ϕ^e (eV)	Meth.	Refs.
hcp (α, T < 1277 K)								
Tm(0001)	–	–	–	–	–	3.46	TC	[1434]
Tm(0001)	–	–	–	–	–	4.48	TC	[321]
Tm(1010)	–	–	–	–	–	4.34	TC	[321]
Tm(1124)	–	–	–	–	–	3.81	TC	[321]
hcp (α, T < 1277 K for bulk)								
Tm/W(111)	Tm	–	≤10⁻⁹	77	–	2.94	FE	[3704]
Tm/Mo(110)	Tm	–	<4 × 10⁻¹¹	~300	–	3.0*	CPD	[2744]
Tm	–	–	–	–	–	3.1	TC	[1955]
Tm	–	–	–	–	–	3.11	TC	[550]
Tm	–	–	–	–	–	3.12	TC	[2750]
Tm	–	–	–	–	–	3.12	TC	[1956]
Tm/Re(0001)	Tm	–	≤5 × 10⁻⁸	1060–1460	–	3.15	TE	[96]
Tm/W(100)	Tm	–	<1 × 10⁻⁹	950–1300	–	3.23	TE	[1558]
Tm	–	–	–	–	–	3.32	TC	[550]
Recommended	–	–	–	–	–	**3.12 ± 0.07**	–	–

70. Ytterbium Yb³⁹⁹

Surface	Beam	Ion	P_r (Torr)	T (K)	ϕ^+ (eV)	ϕ^e (eV)	Meth.	Refs.
fcc (α, T < 1071 K)								
Yb(100)	–	–	–	–	–	4.15	TC	[321]
Yb(110)	–	–	–	–	–	3.90	TC	[321]

Table 1 (*continued*)

Surface	Beam	Ion	P_r (Torr)	T (K)	ϕ^+ (eV)	ϕ^e (eV)	Meth.	Refs.
Yb(111)	–	–	–	–	–	2.51	TC	[334,1434]
Yb(111)	–	–	–	–	–	4.47	TC	[321]
bcc (β, $T > 1071$ K)								
Yb(100)	–	–	–	–	–	3.57	TC	[321]
Yb(110)	–	–	–	–	–	2.45	TC	[334]
Yb(110)	–	–	–	–	–	4.16	TC	[321]
Yb(111)	–	–	–	–	–	3.42	TC	[321]
Yb(112)	–	–	–	–	–	3.81	TC	[321]
fcc (α, $T < 1071$ K for bulk)								
Yb	–	–	–	–	–	2.59	TC	[1956]
Yb	–	–	–	–	–	2.59	TC	[3352]
Yb/W$_2$C(111)	Yb	–	$<10^{-10}$	170	–	2.6	FE	[3792]
Yb/W(111)	Yb	–	$<10^{-10}$	170	–	2.6	FE	[3793]
Yb/W	Yb	–	$\leq 1 \times 10^{-9}$	?	–	2.6 ± 0.05	FE	[2602]
Yb	–	–	? (N_2)	~300	–	2.67	CPD	[2634,4066]
Yb/W	Yb	–	$<10^{-10}$	170	–	2.7	FE	[3793]
Yb	–	–	? (N_2)	~300	–	2.74 ± 0.02	CPD	[4251]
Yb	–	–	–	–	–	2.8	TC	[1955]
Yb/W(111)	Yb	–	$\sim 10^{-9}$	~300	–	2.8	FE	[2011]
Yb/H-Si(111)	Yb	–	1×10^{-10}	~300	–	2.80 ± 0.05	PE	[1195,2545]
Yb/Sm/Si(111)	Yb	–	$\leq 5 \times 10^{-10}$	~300	–	2.9*	CPD	[4110]
Yb/Si(111)^p	Yb	–	$<6 \times 10^{-10}$	~300	–	2.92 ± 0.02*	CPD	[4013]
Yb	–	–	–	–	–	2.95	TC	[550]
Yb/W(100)	Yb	–	$<10^{-10}$	170	–	3.0	FE	[3793]
Yb/Mo(110)	Yb	–	4×10^{-11}	~300	–	3.0*	CPD	[3146,3148]
Yb/Ta(112)	Yb	–	$\sim 10^{-11}$	~300 (600)	–	3.0*	CPD	[3316]
Yb/Si(111)	–	–	–	–	–	3.0*	TC	[4076]
Yb/Si(111)^{440}	Yb	–	$\leq 5 \times 10^{-10}$	~300	–	3.00 ± 0.03	CPD	[4109]
Yb/Si(111)^n	Yb	–	$<6 \times 10^{-10}$	~300	–	3.05*	CPD	[4012]
Yb/Ta(112)	Yb	–	$\sim 10^{-11}$	~300	–	3.1*	CPD	[3316]
Yb/Mo(112)	Yb	–	$\sim 10^{-11}$	~300 (700)	–	3.1*	CPD	[3316]
Yb/Mo(112)	Yb	–	$\sim 10^{-11}$	~300 (900)	–	3.1*	CPD	[3316]
Yb/Si(111)^n	Yb	–	$<6 \times 10^{-10}$	~300	–	3.1 ± 0.2*	CPD	[4013]
Yb/Si(111)	Yb	–	?	~300	–	3.16*	CPD	[3755]
Yb/Ir(111)	Yb	–	$\leq 5 \times 10^{-8}$	1025–1085	–	3.2	TE	[104]
Yb/Si(111)^n	Yb	–	$<6 \times 10^{-10}$	~300	–	3.27*	CPD	[4012]
Yb/Mo(112)	Yb	–	$\sim 10^{-11}$	~300	–	3.3*	CPD	[3316]
Recommended	–	–	–	–	–	**2.91 ± 0.09**	–	–

71. Lutetium Lu

Surface	Beam	Ion	P_r (Torr)	T (K)	ϕ^+ (eV)	ϕ^e (eV)	Meth.	Refs.
hcp (α, $T < $?)								
Lu(0001)	–	–	–	–	–	3.53	TC	[1434]
Lu(0001)	–	–	–	–	–	3.57	TC	[334]
Lu(0001)	–	–	–	–	–	4.45	TC	[321]
Lu(1010)	–	–	–	–	–	4.30	TC	[321]
Lu(1124)	–	–	–	–	–	3.78	TC	[321]
bcc (β, $T > $?)								
Lu(100)	–	–	–	–	–	3.54	TC	[321]
Lu(110)	–	–	–	–	–	4.13	TC	[321]
Lu(111)	–	–	–	–	–	3.39	TC	[321]
Lu(112)	–	–	–	–	–	3.77	TC	[321]
hcp (α, $T < $?)								
Lu	–	–	–	–	–	2.8	TC	[1744]
Lu/W(113)	Lu	–	($\leq 10^{-11}$)	77	–	3.05	FE	[3157]
Lu	–	–	–	–	–	3.1	TC	[1955]
Lu/W(111)	Lu	–	$\leq 10^{-9}$	77	–	3.11	FE	[3704]

Table 1 (*continued*)

Surface	Beam	Ion	P_r (Torr)	T (K)	ϕ^+ (eV)	ϕ^e (eV)	Meth.	Refs.
Lu/W(111)	Lu	–	($\leq 10^{-11}$)	77	–	3.12	FE	[3157]
Lu	–	–	–	–	–	3.14	TC	[1956]
Lu/W	Lu	–	$\leq 1 \times 10^{-9}$	~300 (?)	–	3.14	FE	[2037]
Lu/Re–Lu(4%)	–	–	~10^{-8}	1300	–	3.20	TE	[4240]
Lu/W(112)	Lu	–	($\leq 10^{-11}$)	77	–	3.28	FE	[3157]
Lu/Mo(110)	Lu	–	$\leq 5 \times 10^{-9}$	~300	–	3.3	CPD	[2603]
Lu	–	–	–	–	–	3.33	TC	[550]
Lu/Mo(110)	Lu	–	$\leq 5 \times 10^{-9}$	~300 (800)	–	3.5	CPD	[2603]
Recommended	–	–	–	–	–	**3.17 ± 0.09**	–	–

72. Hafnium Hf

hcp (α, $T < 2050$ K)

Surface	Beam	Ion	P_r (Torr)	T (K)	ϕ^+ (eV)	ϕ^e (eV)	Meth.	Refs.
Hf(0001)	–	–	5×10^{-8}	~1800–2000	–	4.10 ± 0.05	TE	[3921]
Hf(0001)	–	–	?	~1700–1900	–	4.11 ± 0.05	TE	[2967]
Hf(0001)	–	–	–	–	–	4.26	TC	[334]
Hf(0001)	–	–	–	–	–	4.51	TC	[4005]
Hf(0001)	–	–	–	–	–	5.50	TC	[321]
Hf(1010)	–	–	–	–	–	3.63	TC	[4005]
Hf(1010)	–	–	–	–	–	5.25	TC	[321]
Hf(1124)	–	–	–	–	–	4.60	TC	[321]

bcc (β, $T > 2050$ K)

Surface	Beam	Ion	P_r (Torr)	T (K)	ϕ^+ (eV)	ϕ^e (eV)	Meth.	Refs.
Hf(100)	–	–	–	–	–	4.1	TC	[3171]
Hf(100)	–	–	–	–	–	4.2	TC	[1714,3167,3171]
Hf(100)	–	–	–	–	–	4.3	TC	[321]
Hf(110)	–	–	–	–	–	5.03	TC	[321]
Hf(111)	–	–	–	–	–	4.13	TC	[321]
Hf(112)	–	–	–	–	–	4.60	TC	[321]

hcp (α, $T < 2050$ K for bulk)

Surface	Beam	Ion	P_r (Torr)	T (K)	ϕ^+ (eV)	ϕ^e (eV)	Meth.	Refs.
Hf	–	–	$<2 \times 10^{-7}$	~1700–1900	–	3.17 ± 0.02	TE	[3066]
Hf[256]	–	–	?	<1700	–	3.20	TE	[1756,3524,3527]
Hf/W[257]	Hf	–	?	1100	–	3.20	TE	[1479]
Hf/W(100)	Hf	–	~10^{-10}	965	–	3.27	FE	[501][487]
Hf/W(100)	Hf	–	~10^{-10}	852	–	3.33	FE	[501]
Hf/W(100)	Hf	–	~10^{-10}	1100	–	3.36	FE	[501]
Hf/W(100)	Hf	–	~10^{-10}	747	–	3.39	FE	[501]
Hf/W(100)	Hf	–	~10^{-10}	642	–	3.46	FE	[501]
Hf	–	–	?	?	–	3.5	TE	[3402]
Hf/W(100)	Hf	–	4×10^{-11}	600	–	3.5*	CPD	[1737]
Hf/W(100)	Hf	–	~10^{-10}	551	–	3.51	FE	[501]
Hf	–	–	–	–	–	3.52	TC	[3318]
Hf	–	–	–	–	–	3.53	TC	[2949]
Hf[256]	–	–	?	>1900	–	3.53	TE	[3524,3527]
Hf	–	–	–	–	–	3.54	TC	[3318]
Hf	–	–	–	–	–	3.56	TC	[1744]
Hf/W	Hf	–	$<10^{-10}$	~300 (1300)	–	3.56 ± 0.01	FE	[3195]
Hf	–	–	~6×10^{-10}	~1300–1900	–	3.60	TE	[2092]
Hf	–	–	~3×10^{-9}	~1000–1600	–	3.65	TE	[159]
Hf/W	Hf	–	$<8 \times 10^{-11}$	~300 (1355)	–	3.65	FE	[3222]
Hf/W(100)	Hf	–	~10^{-10}	~300	–	3.68	FE	[501]
Hf	–	–	–	–	–	3.7	TC	[1993]
Hf/1%Hf–Nb	–	–	$\leq 10^{-8}$	1550 (1800)	–	3.72	TE	[1778]
Hf	–	–	$\leq 1 \times 10^{-6}$	~1600–1800	–	3.75 ± 0.1	TE	[216]
Hf	–	–	$\leq 10^{-8}$	~1300 (1900)	–	3.82	TE	[1778]
Hf	–	–	–	–	–	3.85	TC	[3637]
Hf	–	–	–	–	–	3.89	TC	[298]
Hf/quartz	Hf	–	~10^{-10}	~300	–	3.9 ± 0.1	PE	[304]
Hf	–	–	~10^{-9}	~1500	–	3.9 ± 0.1	CPD	[1588]
Hf	–	–	2×10^{-10}	~300	–	3.90	PE	[1814]
Hf	–	–	$\leq 10^{-8}$	~1500–2100	–	3.91	TE	[1778]
Hf	–	–	~6×10^{-10}	~1400–2000	–	3.91	TE	[2092]
Hf/W[257]	Hf	–	?	2000	–	3.92	TE	[1479]
Hf	–	–	?	?	–	3.97	TE	[2105]

Table 1 (*continued*)

Surface	Beam	Ion	P_r (Torr)	T (K)	ϕ^+ (eV)	ϕ^e (eV)	Meth.	Refs.
Hf/SiO$_2$	Hf	–	?	?	–	4.0	CPD	[2689]
Hf/W	Hf	–	<8 × 10^{-11}	~300 (≥730)	–	4.0	FE	[3222]
Hf/W[257]	HfI$_4$	–	?	1900{500}	–	4.00 ± 0.01	TE	[1479]
Hf	–	–	~10^{-6}	~1600	–	4.06 ± 0.06	TE	[1780]
Hf	–	–	–	–	–	4.1	TC	[706]
Hf	–	–	–	–	–	4.20	TC	[3476]
Hf	–	–	–	–	–	4.31	TC	[3476]
Hf	–	–	–	–	–	4.66	TC	[3476]
Recommended	–	–	–	–	–	**3.64 ± 0.06**	–	–

73. Tantalum Ta

bcc

Surface	Beam	Ion	P_r (Torr)	T (K)	ϕ^+ (eV)	ϕ^e (eV)	Meth.	Refs.
Ta(100)	–	–	–	–	–	3.8 ± 0.1	TC	[470]
Ta(100)	–	–	–	–	–	3.83	TC	[1200]
Ta(100)	–	–	–	–	–	3.96	TC	[4316,4412]
Ta(100)	–	–	–	–	–	4.0 ± 0.1	TC	[470]
Ta(100)	–	–	–	–	–	4.04	TC	[1200]
Ta(100)	–	–	–	–	–	4.07	TC	[2548]
Ta(100)	–	–	–	–	–	4.08	TC	[1159,1980,3067]
Ta(100)	–	–	–	–	–	4.096	TC	[4091]
Ta(100)	–	–	<10^{-10}	?	–	4.1	TE	[694]
Ta(100)	–	–	–	–	–	4.1 ± 0.1	TC	[470]
Ta(100)	–	–	?	?	–	4.10	FE	[796]
Ta(100)	–	–	–	–	–	4.11	TC	[1200]
Ta(100)	–	–	5 × 10^{-9}	~1800–2100	–	4.12 ± 0.05	TE	[739,798,1406]
Ta(100)	–	–	–	–	–	4.14	TC	[3224]
Ta(100)	–	–	≤2 × 10^{-9}	~1700–2000	–	4.15 ± 0.02	TE	[127,144]
Ta(100)	–	–	<5 × 10^{-11}	~1500–1700	–	4.16 ± 0.05	TE	[1896]
Ta(100)	–	–	≤2 × 10^{-9}	?	(4.20 ± 0.04)	4.17 ± 0.04	TE	[797,799,2331]
Ta(100)	Na	Na$^+$	≤2 × 10^{-9}	1050–1750	4.20 ± 0.04	(4.17 ± 0.04)	PSI	[797]
Ta(100)	–	–	<5 × 10^{-11}	?	–	4.2	TE	[3776]
Ta(100)	–	–	<5 × 10^{-11}	~300	–	4.24 ± 0.05	CPD	[1896]
Ta(100)	–	–	<1 × 10^{-11}	78	–	4.25	FE	[648]
Ta(100)	–	–	–	–	–	4.3	TC	[469]
Ta(100)	–	–	–	–	–	4.3 ± 0.1	TC	[470]
Ta(100)	–	–	–	–	–	4.44	TC	[321]
Ta(100)	–	–	–	–	–	4.5	TC	[3171]
Ta(100)	F$^+$	F$^-$	2 × 10^{-10}	1965	4.51 ± 0.1^N	–	NSI	[604]
Ta(100)	Cl$^+$	Cl$^-$	2 × 10^{-10}	1985	4.55 ± 0.1^N	–	NSI	[604]
Ta(100)	Br$^+$	Br$^-$	2 × 10^{-10}	1938	4.55 ± 0.1^N	–	NSI	[604]
Ta(100)	–	–	–	–	–	4.6	TC	[389]
Ta(100)	–	–	–	–	–	4.6	TC	[3171]
Ta(100)	–	–	–	–	–	4.87	TC	[485,2791]
Recommended	–	–	–	–	–	**4.15 ± 0.05**	–	–
Ta(110)	–	–	≤2 × 10^{-9}	?	–	4.43 ± 0.05	TE	[1406]
Ta(110)	–	–	~10^{-10}	~300	–	4.47 ± 0.02	CPD	[777]
Ta(110)	–	–	–	–	–	4.6	TC	[1723]
Ta(110)	–	–	?	? (2300)	–	4.62 ± 0.04	TE	[3347]
Ta(110)	–	–	4 × 10^{-9}	?	–	4.63 ± 0.01	TE	[1477]
Ta(110)	–	–	~10^{-11}	1560–2360	–	4.73	TE	[683,1886,3846]
Ta(110)	–	–	–	–	–	4.74	TC	[2548]
Ta(110)	–	–	≤4 × 10^{-10}	~300	–	4.74 ± 0.02	PE	[680,1268]
Ta(110)	–	–	–	–	–	4.75	TC	[1159,1980,3067]
Ta(110)	–	–	?	~1200–1600	–	4.75 ± 0.06	TE	[681]
Ta(110)	–	–	?	?	–	4.76 ± 0.04	TE	[3347]
Ta(110)	–	–	–	–	–	4.77	TC	[1200]
Ta(110)	–	–	–	–	–	4.78	TC	[1200]
Ta(110)	–	–	?	? (2300)	–	4.78 ± 0.04	TE	[3347]
Ta(110)	–	–	?	80	–	4.79	FE	[1052]
Ta(110)	–	–	?	~300	–	4.8	PE	[460]
Ta(110)	–	–	≤2 × 10^{-9}	~1700–2000	–	4.80 ± 0.02	TE	[127,144]
Ta(110)	–	–	~10^{-9}	~1200–1900	(4.8)	4.80 ± 0.03	TE	[786]
Ta(110)	Li	Li$^+$	~10^{-9}	?	4.8	(4.80 ± 0.03)	PSI	[786]
Ta(110)	–	–	1 × 10^{-9}	~1000–1700	(4.85 ± 0.05)	4.81	TE	[726]
Ta(110)	–	–	≤2 × 10^{-9}	?	–	4.82 ± 0.04	TE	[797,799,2331]
Ta(110)	–	–	–	–	–	4.83	TC	[3224]
Ta(110)	–	–	5 × 10^{-9}	~1800–2100	–	4.83 ± 0.05	TE	[739,798]
Ta(110)	Na	Na$^+$	≤2 × 10^{-9}	~1000–1650	4.84 ± 0.04	(4.82 ± 0.04)	PSI	[797]

Table 1 (*continued*)

Surface	Beam	Ion	P_r (Torr)	T (K)	ϕ^+ (eV)	ϕ^e (eV)	Meth.	Refs.
Ta(110)	Na	Na$^+$	1×10^{-9}	1010–1680	4.85 ± 0.05	(4.81)	PSI	[726]
Ta(110)	–	–	$<5 \times 10^{-8}$	~1300–2000	(4.85 ± 0.06)	4.85	TE	[279]
Ta(110)	L[466]	L$^+$	$<5 \times 10^{-8}$	~1300–2000	4.85 ± 0.06	(4.85)	PSI	[279]
Ta(110)	–	–	–	–	–	4.86	TC	[1200]
Ta(110)	F$^+$	F$^-$	2×10^{-10}	2186	4.86 ± 0.1^N	–	NSI	[604]
Ta(110)	–	–	–	–	–	4.87	TC	[1200]
Ta(110)	–	–	~10^{-11}	~300	–	4.9	CPD	[1888]
Ta(110)	–	–	~10^{-9}	?	–	4.9	TE	[3909]
Ta(110)	–	–	–	–	–	4.9 ± 0.1	TC	[470]
Ta(110)	–	–	?	?	–	4.91	TE	[3407]
Ta(110)	Cl$^+$	Cl$^-$	2×10^{-10}	2183	4.92 ± 0.1^N	–	NSI	[604]
Ta(110)	–	–	~10^{-10}	~300	–	4.94 ± 0.05	PE	[506]
Ta(110)	–	–	?	?	–	4.95	FE	[796]
Ta(110)	–	–	–	–	–	4.964	TC	[4091]
Ta(110)	–	–	–	–	–	5.03	TC	[3474]
Ta(110)	–	–	–	–	–	5.08	TC	[334]
Ta(110)	–	–	–	–	–	5.08	TC	[3473]
Ta(110)	–	–	–	–	–	5.15	TC	[3179]
Ta(110)	–	–	–	–	–	5.16	TC	[321]
Ta(110)	–	–	~10^{-7} (O$_2$)	2200	–	5.2	TE	[3909]
Ta(110)	–	–	–	–	–	5.58	TC	[485,2791]
Ta(110)	–	–	–	–	–	6.06	TC	[485,2791]
Recommended	–	–	–	–	**4.84 ± 0.02**	**4.82 ± 0.06**	–	–
Ta(111)	–	–	–	–	–	3.50	TC	[1200]
Ta(111)	–	–	–	–	–	3.51	TC	[1200]
Ta(111)	–	–	$<1 \times 10^{-11}$	78	–	3.55	FE	[648]
Ta(111)	–	–	–	–	–	3.93	TC	[2548]
Ta(111)	–	–	–	–	–	3.93	TC	[1200]
Ta(111)	–	–	–	–	–	3.94	TC	[1159,1980,3067]
Ta(111)	–	–	?	?	–	3.95	FE	[796]
Ta(111)	–	–	–	–	–	3.96	TC	[1200]
Ta(111)	–	–	5×10^{-9}	~1800–2100	(4.00 ± 0.05)	3.98 ± 0.05	TE	[726,739,798,1406]
Ta(111)	–	–	?	80	–	3.99	FE	[1052]
Ta(111)	–	–	~10^{-7}	2200	–	4.00	TE	[3360]
Ta(111)	–	–	$\leq 2 \times 10^{-9}$	~1700–2000	–	4.00 ± 0.02	TE	[127,144]
Ta(111)	Na	Na$^+$	$\leq 2 \times 10^{-9}$	~1600–1800	4.00 ± 0.04	(4.02 ± 0.04)	PSI	[797]
Ta(111)	Na	Na$^+$	1×10^{-9}	~1700–2200	4.00 ± 0.05	(3.98 ± 0.05)	PSI	[726]
Ta(111)	–	–	~10^{-9}	~1500–1900	–	4.02 ± 0.02	TE	[800]
Ta(111)	–	–	$\leq 2 \times 10^{-9}$	?	(4.00 ± 0.04)	4.02 ± 0.04	TE	[797,799,2331]
Ta(111)	–	–	$<2 \times 10^{-9}$	~1700–2300	–	4.04	TE	[662]
Ta(111)	–	–	–	–	–	4.08	TC	[3224]
Ta(111)[258]	–	–	?	? (2100)	–	4.08 ± 0.03	TE	[729]
Ta(111)[258]	–	–	?	? (2100)	–	4.14 ± 0.03	TE	[729]
Ta(111)	–	–	~10^{-9}	2200	–	4.20	TE	[3360]
Ta(111)	–	–	–	–	–	4.201	TC	[4091]
Ta(111)	–	–	–	–	–	4.25	TC	[321]
Ta(111)[258]	–	–	?	? (2100)	–	4.28 ± 0.03	TE	[729]
Ta(111)	–	–	~10^{-5}	2200	–	4.40	TE	[3360]
Ta(111)[258]	–	–	?	? (2100)	–	4.46 ± 0.03	TE	[729]
Recommended	–	–	–	–	–	**4.01 ± 0.04**	–	–
Ta(112)	–	–	–	–	–	3.77	TC	[1200]
Ta(112)	–	–	–	–	–	3.80	TC	[1200]
Ta(112)	–	–	–	–	–	4.03	TC	[1200]
Ta(112)	–	–	–	–	–	4.05	TC	[1200]
Ta(112)	–	–	$<1 \times 10^{-11}$	78	–	4.05	FE	[648]
Ta(112)	–	–	–	–	–	4.25	TC	[3224]
Ta(112){70%}[267]	–	–	$\leq 10^{-9}$	~1100–2200	–	4.25 ± 0.05	TE	[124,650]
Ta(112)	–	–	?	?	–	4.30	FE	[796]
Ta(112)	–	–	–	–	–	4.31	TC	[1159,1980,3067]
Ta(112){82%}	–	–	–	–	(4.49 ± 0.04)	4.34 ± 0.03	TC	[803]
Ta(112)	–	–	$\leq 2 \times 10^{-9}$	~1700–2000	–	4.35 ± 0.05	TE	[127,144]
Ta(112)	–	–	1×10^{-10}	~1300–1900	–	4.352 ± 0.01	TE	[192]
Ta(112)	–	–	?	80	–	4.37	FE	[1052]
Ta(112)	–	–	($\leq 10^{-11}$)	77	–	4.40	CPD	[347,2662]
Ta(112)	–	–	($\leq 10^{-11}$)	~300	–	4.40	CPD	[347,801,2662]
Ta(112)	–	–	5×10^{-9}	~1800–2100	–	4.40 ± 0.05	TE	[798,1406]
Ta(112){82%}	–	–	–	–	4.49 ± 0.04	(4.34 ± 0.03)	TC	[803]
Ta(112)	–	–	1×10^{-10}	~1300–1900	–	4.58 ± 0.02	TE	[192]

Table 1 (*continued*)

Surface	Beam	Ion	P_r (Torr)	T (K)	ϕ^+ (eV)	ϕ^e (eV)	Meth.	Refs.
Ta(112)	–	–	–	–	–	4.73	TC	[321]
Ta(112)	–	–	1×10^{-10}	~1300–1900	–	4.74 ± 0.02	TE	[192]
Ta(112)	–	–	$<2 \times 10^{-9}$	1250–1650	–	4.8	TE	[802]
Ta(112)	K	K$^+$	2×10^{-9}	~1000–1500	4.8*	(4.8 ± 0.05)	PSI	[79]
Ta(112)	–	–	2×10^{-9}	~1200–2300	(4.8)	4.8 ± 0.05	TE	[79]
Recommended	–	–	–	–	–	**4.36 ± 0.04**	–	–
Ta(114)	–	–	–	–	–	3.98	TC	[3224]
Ta(116)	–	–	$\leq 2 \times 10^{-9}$	~1700–2000	–	~3.90	TE	[127,144]
Ta(116)	–	–	–	–	–	3.92	TC	[3224]
Ta(116)	–	–	–	–	–	3.94	TC	[1980,3067]
Ta(123)	–	–	–	–	–	4.04	TC	[3224]
Ta(130)[259]	–	–	$\leq 4 \times 10^{-10}$	~300	–	3.96 ± 0.04	PE	[680]
Ta(130)	–	–	–	–	–	4.03	TC	[3224]
Ta(130)	–	–	?	80	–	4.22	FE	[1052]
Ta(130)[259]	–	–	$\leq 4 \times 10^{-10}$	~300 (1670)	–	4.57 ± 0.02	PE	[680]
Ta(233)	–	–	–	–	–	3.99	TC	[3224]
Ta	^{91}Rb	^{91}Rb$^+$	~10^{-6}	~2100	>3*	–	PSI	[3861]
Ta	–	–	?	?	–	3.14	TE	[3019]
Ta/quartz[260]	Ta	–	$\leq 10^{-8}$	35	–	3.5 ± 0.2	CPD	[1686]
Ta[261]	–	(Ta$^-$)	$<2 \times 10^{-8}$	~2000–2100	3.7 ± 0.4*^{N}	–	NSI	[804]
Ta/quartz[260]	Ta	–	$\leq 10^{-8}$	4.2	–	3.8 ± 0.2	CPD	[1686]
Ta/quartz[260]	Ta	–	$\leq 10^{-8}$	293	–	3.8 ± 0.2	CPD	[1686]
Ta	–	–	–	–	–	3.80	TC	[521]
Ta	–	–	–	–	–	3.80	TC	[1901]
Ta	–	–	–	–	–	3.85	TC	[1744]
Ta[261]	–	(Ta$^-$)	$<2 \times 10^{-8}$	~2000–2100	3.9 ± 0.3^N	–	NSI	[804]
Ta	–	–	~10^{-7}	~1500–1950	–	3.90 ± 0.04	TE	[2769]
Ta	–	–	$<10^{-6}$	~300	–	3.93	PE	[2919]
Ta	–	–	?	~300	–	3.96	CPD	[2297]
Ta	–	–	2×10^{-8}	1650–2100	–	3.96	TE	[3643]
Ta	I$_2$	I$^-$	$\leq 10^{-2}$ (I$_2$)	~1900–2200	3.96 ± 0.03^N	(4.30 ± 0.02)	NSI	[81]
Ta	–	–	–	–	–	4.0	TC	[1993]
Ta	–	–	2×10^{-8}	~1200–1500	–	4.03 ± 0.04	TE	[2566]
Ta	–	–	–	–	–	4.05	TC	[2949]
Ta	–	–	?	~300	–	4.05 ± 0.03	PE	[1635]
Ta	–	–	–	–	–	4.07	TC	[2949]
Ta	–	–	?	~1400–1600	–	4.07	TE	[1949]
Ta	–	–	~10^{-9}	~1200–1800	–	4.08 ± 0.04	TE	[975]
Ta[266]	–	–	–	293^E	–	4.09	TC	[3586]
Ta	–	–	~10^{-3} (Cs)	?	–	4.09	CPD	[1642]
Ta	–	–	?	?	–	4.1	TE	[3402]
Ta(porous)	–	–	?	>1600	(4.2)	4.1	TE	[3762]
Ta/W(100)	Ta	–	1×10^{-11}	77	–	4.10	FE	[2965]
Ta/W(100)	Ta	–	1×10^{-11}	20–830	–	4.10	FE	[2965]
Ta	KCl	K$^+$	?	?	4.10 ± 0.02	–	PSI	[2306]
Ta	RbCl	Rb$^+$	?	?	4.10 ± 0.02	–	PSI	[2306]
Ta[265]	–	–	$\leq 8 \times 10^{-8}$	293	–	4.12	PE	[1633]
Ta/quartz	Ta	–	$<10^{-8}$	77, ~300	–	4.12	PE	[3036]
Ta/Ni	Ta	–	?	~300	–	4.12	PE	[2922]
Ta[265]	–	–	–	293	–	4.12 ± 0.02	TC	[1135]
Ta[266]	–	–	?	~1450–2050	–	4.12 ± 0.04	TE	[792]
Ta	–	–	?	~300	–	4.12 ± 0.07	PE	[974]
Ta[265]	–	–	$\leq 8 \times 10^{-8}$	293	–	4.13	PE	[1633,1636]
Ta[266]	–	–	–	973^E	–	4.13	TC	[3586]
Ta	–	–	–	–	–	4.13	TC	[3318]
Ta	–	–	–	–	–	4.13	TC	[3224]
Ta	–	–	$\leq 8 \times 10^{-8}$	293^E	–	4.13	TE	[1636]
Ta	–	–	$<5 \times 10^{-10}$	293	–	4.13	PE	[348]
Ta	–	–	~700 (Ar)	?	–	4.13 ± 0.013	TE	[2007]
Ta	–	–	4×10^{-11}	~300	–	4.14	PE	[1430,2733]
Ta	–	–	?	1370–1670	–	4.14	TE	[2567]
Ta	–	–	~10^{-8}	~1600–2300	–	4.14 ± 0.02	TE	[1164]
Ta/glass	Ta	–	~10^{-11}	77	–	4.14 ± 0.1	PE	[1528]
Ta/glass	Ta	–	~10^{-11}	~300	–	4.14 ± 0.1	PE	[1528]

Table 1 (*continued*)

Surface	Beam	Ion	P_r (Torr)	T (K)	ϕ^+ (eV)	ϕ^e (eV)	Meth.	Refs.
Ta	–	–	$\sim 10^{-11}$	1560–2360	–	4.15	TE	[683]
Ta	–	–	$\sim 10^{-9}$	?	–	4.15	TE	[979]
Ta	–	–	?	~ 300	–	4.15	PE	[1371]
Ta	–	–	?	?	–	4.15	TE	[2455]
Ta/Si(111)[166]	Ta	–	4×10^{-11}	~ 300	–	4.15	PE	[1430,2733]
Ta{70% (112)}[267]	–	–	–	–	–	4.15	TC	[1254]
Ta	–	–	?	~ 1500–2000	–	4.15	TE	[1306]
Ta	–	–	$\leq 5 \times 10^{-9}$	?	–	4.15 ± 0.05	TE	[806]
Ta[260]	–	–	$\leq 10^{-8}$	4.2–35	–	4.16	FE	[1686]
Ta	–	–	$<5 \times 10^{-10}$	293	–	4.16	PE	[348]
Ta	–	–	?	90	–	4.16	CPD	[2294]
Ta[265]	–	–	–	973	–	4.16 ± 0.02	TC	[1135]
Ta	–	–	4×10^{-9}	~ 300	–	4.17	PE	[1269]
Ta/Nb	Ta	–	$\sim 10^{-9}$	~ 1200–1800	–	4.17	TE	[975]
Ta	Sr	Sr⁺	$<1 \times 10^{-7}$	2450–2800	4.17	(4.21)	PSI	[80]
Ta[265]	–	–	$\leq 8 \times 10^{-8}$	973	–	4.18	PE	[1633,1636]
Ta	–	–	$\sim 10^{-6}$	?	–	4.18	TE	[3272]
Ta[265]	–	–	$\leq 8 \times 10^{-8}$	973	–	4.19	PE	[1633]
Ta	–	–	–	–	–	4.19	TC	[2005]
Ta	–	–	$<3 \times 10^{-8}$	1420–1700	(5.9 ± 0.3*)	4.19 ± 0.02	TE	[137]
Ta(porous)	Cs	Cs⁺	?	~ 1100–1400	4.2	(4.1)	PSI	[3762]
Ta	–	–	–	–	–	4.2	TC	[3318]
Ta	–	–	–	–	–	4.2	TC	[2583]
Ta	–	–	?	~ 1400–2000	–	4.2	TE	[3020]
Ta	–	–	$\leq 8 \times 10^{-8}$	973[E]	–	4.20	TE	[1636]
Ta	–	–	$<1 \times 10^{-7}$	?	(4.17, 4.23)	4.21	TE	[80]
Ta	–	–	$\leq 3 \times 10^{-9}$	~ 300	–	4.21 ± 0.06	CPD	[3106]
Ta	–	–	9×10^{-7}	2138–2440	–	4.218 ± 0.016	TE	[2296]
Ta	–	–	$\sim 1 \times 10^{-6}$	2088–2430	–	4.218 ± 0.028	TE	[2296]
Ta	–	–	–	–	–	4.22	TC	[3264,3265,3267]
Ta[269]	Br⁺	Br⁻	?	2125	4.22*[N]	(4.37 ± 0.1)	NSI	[600,641]
Ta	–	–	$<10^{-8}$	~ 300	–	4.22 ± 0.02	CPD	[349]
Ta$_n$(n → ∞)	–	–	–	–	–	4.22 ± 0.08	TC	[4261]
Ta	–	–	$\sim 1 \times 10^{-6}$	2050–2580	–	4.229 ± 0.014	TE	[2296]
Ta[269]	I⁺	I⁻	?	2125	4.23*[N]	(4.37 ± 0.1)	NSI	[600,641]
Ta	Ba	Ba⁺	$<1 \times 10^{-7}$	~ 2500–2800	4.23 ± 0.03	(4.21)	PSI	[80]
Ta	–	–	$\leq 10^{-9}$	~ 1800–2200	–	4.25	TE	[66]
Ta	–	–	?	~ 300	–	4.25	CPD	[2084]
Ta{82% (112)}[268]	–	–	? (Cs)	~ 1100–1700	–	4.25	TE	[650,3414]
Ta	–	–	$\leq 10^{-8}$	~ 1400–2100	–	4.25 ± 0.05	TE	[1775,1777,1778]
Ta{70% (112)}[267]	–	–	$\leq 10^{-9}$	~ 1100–2200	–	4.25 ± 0.05	TE	[124,650]
Ta	–	–	2×10^{-7}	~ 1800–2100	(5.10–5.19)	4.27 ± 0.04	TE	[23,67]
Ta[269]	Cl⁺	Cl⁻	?	2125	4.28*[N]	(4.37 ± 0.1)	NSI	[600,641]
Ta	–	–	?	?	–	4.3	TE	[2459]
Ta	–	–	?	1640–1890	–	4.3	TE	[2078]
Ta	–	–	$\sim 10^{-10}$	~ 300	–	4.3 ± 0.1	PE	[350]
Ta	–	–	$<10^{-9}$	~ 1900–2200	(4.64 ± 0.03)	4.30 ± 0.02	TE	[81]
Ta	–	–	$<10^{-9}$	~ 1900–2200	(3.96 ± 0.03[N])	4.30 ± 0.02	TE	[81]
Ta[174]	–	–	–	O[E]	–	4.31	TC	[1747]
Ta	–	–	1×10^{-7}	~ 1700–2200	(4.88 ± 0.05)	4.33 ± 0.03	TE	[76,77]
Ta{82% (112)}[268]	–	–	–	–	(4.49 ± 0.04)	4.34 ± 0.03	TC	[803]
Ta	–	–	$\sim 10^{-5}$	≤ 1200	–	4.35	TE	[2216]
Ta	–	–	–	–	–	4.35	TC	[3476]
Ta	–	–	?	~ 1900–2100	–	4.35 ± 0.05	TE	[1779]
Ta	–	–	–	–	–	4.37	TC	[298]
Ta	–	–	?	~ 1850–2300	(4.22–4.28)*[N]	4.37 ± 0.1	TE	[600,641]
Ta	–	–	? (K)	~ 1300–1700	–	4.38	TE	[2559]
Ta	–	–	$\sim 10^{-11}$	~ 300	–	4.38	CPD	[3338]
Ta	–	–	–	–	–	4.39	TC	[3476]
Ta	–	–	$<10^{-7}$	2200	–	4.4	TE	[2582]
Ta	–	–	–	0	–	4.41	TC	[4419]
Ta	–	–	–	–	–	4.45	TC	[2629]
Ta	–	–	~ 700 (Ar)	~ 3000	–	4.46	TE	[2007]
Ta{82% (112)}[268]	–	–	–	–	4.49 ± 0.04	(4.34 ± 0.03)	TC	[803]
Ta	–	–	~ 700 (Ar)	~ 3000	–	4.50	TE	[2007]
Ta	–	–	–	–	–	4.6	TC	[706]
Ta[270]	Na	Na⁺	$\sim 10^{-5}$ (Na)	~ 1900–2200	4.64 ± 0.03	(4.30 ± 0.02)	PSI	[81]
Ta[170,271]	–	(Ta⁺)	$<2 \times 10^{-8}$	~ 2000–2550	4.64 ± 0.14	–	PSI	[804]
Ta{mainly (110)}	–	–	0.1–6 (Cs)	~ 1700–1900	–	4.67 ± 0.07*	TE	[2609]
Ta	–	–	?	~ 300	–	4.70 ± 0.05	CPD	[3399]

Table 1 (*continued*)

Surface	Beam	Ion	P_r (Torr)	T (K)	ϕ^+ (eV)	ϕ^e (eV)	Meth.	Refs.
Ta	–	–	–	–	–	4.81	TC	[3476]
Ta	In	In$^+$	1×10^{-7}	~1700–2200	4.88 ± 0.05	(4.33 ± 0.03)	PSI	[76,77]
Ta	^{87}Br	^{87}Br$^-$	~10^{-6}	~2100	<5^{*N}	–	NSI	[3861]
Ta[170,271]	–	(Ta$^+$)	~10^{-7}	~2400–2660	5.0 ± 0.5	(4.33 ± 0.03)	PSI	[77]
Ta[271]	–	(Ta$^+$)	<7 × 10^{-7}	2550–2770	5.02 ± 0.11	–	PSI	[805,3083]
Ta	KCl	K$^+$	2×10^{-7}	~1800–2100	5.10 ± 0.01	(4.27 ± 0.04)	PSI	[23,2422]
Ta	RbBr	Rb$^+$	2×10^{-7}	~1800–2100	5.13 ± 0.03	(4.27 ± 0.04)	PSI	[23,67,2422]
Ta	RbCl	Rb$^+$	2×10^{-7}	~1800–2100	5.19 ± 0.03	(4.27 ± 0.04)	PSI	[23,67]
Ta	–	–	–	–	–	5.50	TC	[2629]
Ta[272]	–	(Ta$^+$)	<3 × 10^{-8}	~2700–2900	5.85 ± 0.3*	(4.19 ± 0.02)	PSI	[137]
Recommended	–	–	–	–	**4.95 ± 0.20**	**4.20 ± 0.03**	–	–
Recommended	–	–	–	–	**417 ± 0.13^N**	–	–	–

74. Tungsten W

bcc

Surface	Beam	Ion	P_r (Torr)	T (K)	ϕ^+ (eV)	ϕ^e (eV)	Meth.	Refs.
W(100)	–	–	–	–	–	3.7	TC	[2979]
W(100)	–	–	–	–	–	3.8	TC	[351]
W(100)	–	–	–	–	–	4.090	TC	[4091]
W(100)	–	–	–	–	–	4.10	TC	[1270]
W(100)–Re(5%)	–	–	?	~1900–2100	–	4.10 ± 0.05	TE	[438]
W(100)	–	–	–	–	–	4.13	TC	[1270]
W(100)	–	–	?	~2000–2400	–	4.15 ± 0.02	TE	[2356]
W(100)	–	–	(≤10^{-10})	77	–	4.2	FE	[1974]
W(100)	–	–	?	~300 (2200)	–	4.2	FE	[3952]
W(100)	–	–	–	–	–	4.3	TC	[2265]
W(100)	–	–	?	~2200–2450	–	4.32 ± 0.01	TE	[2340,2343]
W(100)	–	–	–	–	–	4.34	TC	[2691]
W(100)	–	–	–	–	–	4.35 ± 0.01	TC	[4188]
W(100)	–	–	–	–	–	4.37	TC	[4189]
W(100)	–	–	–	–	–	4.4	TC	[351]
W(100)	–	–	–	–	–	4.4	TC	[3615]
W(100)	–	–	2×10^{-9}	~1700–2000	–	4.40	TE	[141]
W(100)	–	–	–	–	–	4.44	TC	[1270]
W(100)	–	–	1×10^{-8}	~1900–2100	–	4.45 ± 0.05	TE	[2012]
W(100)	–	–	–	–	–	4.46	TC	[3224]
W(100)	–	–	~10^{-10}	~300	–	4.47	FE	[378]
W(100)	–	–	5×10^{-9}	~2000–2400	–	4.48	TE	[352]
W(100)	–	–	–	–	–	4.49	TC	[4405]
W(100)	–	–	(≤10^{-11})	~300	–	4.5	CPD	[259]
W(100){95%}[302]	–	–	? (Cs)	~1600–2400	–	4.5	TE	[3414]
W(100)	–	–	–	–	–	4.5 ± 0.2	TC	[381]
W(100)	–	–	~10^{-11}	~300	–	4.50	CPD	[3338]
W(100)	–	–	–	–	–	4.50	TC	[4117]
W(100)	–	–	–	–	–	4.50	TC	[4405]
W(100){almost}[277]	–	–	≤10^{-9}	~1300–2200	–	4.50 ± 0.07	TE	[650]
W(100)/W(100)[309]	WF$_6$, H$_2$	–	~10^{-7}	~1850–2450	–	4.51 ± 0.01	TE	[1053]
W(100)	Sr	Sr$^+$	~10^{-9}	~2500–2850	4.52	–	PSI	[138]
W(100)	–	–	2×10^{-9}	~1400–2000	–	4.52	TE	[150]
W(100)	–	–	2×10^{-10}	90	–	4.52	FE	[3101,3102]
W(100){95%}[302]	–	–	~10^{-9}	?	–	4.52	TE	[3414]
W(100)–Re(5%)[274]	–	–	?	~2200	–	4.52 ± 0.04	TE	[438]
W(100){probably}	–	–	2×10^{-8}	1920–2300	(4.55 ± 0.03)	4.52 ± 0.07	TE	[92]
W(100){95%}[300]	–	–	~10^{-9}	1150–2200	–	4.52 ± 0.07	TE	[124]
W(100){96%}[300]	–	–	~10^{-9}	1150–2200	–	4.52 ± 0.07	TE	[124]
W(100)	–	–	–	–	–	4.53	TC	[3356,3452]
W(100)[273]	–	–	3×10^{-8}	–1900–	–	4.53	TE	[651]
W(100)	–	–	?	~1400–2000	–	4.53	TE	[149]
W(100)	–	–	≤8 × 10^{-9}	~2200–2450	–	4.53 ± 0.05	TE	[2340,2343]
W(100)	–	–	≤10^{-5} (I$_2$)	~1500–2300	(4.55 ± 0.05)^N	4.53 ± 0.05	TE	[571]
W(100)	Br$_2$	Br$^-$	? (Br$_2$)	~1500–2300	4.53 ± 0.05^N	–	NSI	[1658]
W(100)	–	–	~10^{-10}	77	–	4.54	FE	[2714]
W(100)	–	–	~2 × 10^{-9}	~2000–2400	–	4.54	TE	[4343]
W(100)	–	–	–	–	–	4.54	TC	[2701]
W(100)	–	–	–	–	–	4.54	TC	[3224]
W(100)–Re(1%)[274]	–	–	?	1850–2270	–	4.54	TE	[3086]
W(100)–Ir(2%)[275]	–	–	?	~1800–2030	–	4.54	TE	[3086]
W(100)[310]	–	–	~10^{-7}	~1850–2450	–	4.54 ± 0.01	TE	[1053]
W(100)	–	–	?	2100–2200	–	4.54 ± 0.01	TE	[3349]

(*continued on next page*)

Table 1 (*continued*)

Surface	Beam	Ion	P_r (Torr)	T (K)	ϕ^+ (eV)	ϕ^e (eV)	Meth.	Refs.
W(100)	K	K$^+$	≤3 × 10^{-10}	1574	4.54 ± 0.02	(4.59 ± 0.03)	PSI	[82,261]
W(100)	–	–	≤2 × 10^{-8}	1670–2040	(4.60)	4.55	TE	[83]
W(100)	–	–	≤3 × 10^{-11}	1670–1820	–	4.55	TE	[353]
W(100)	–	–	–	–	–	4.55	TC	[1136]
W(100)	–	–	2 × 10^{-10}	~300	–	4.55	PE	[1859]
W(100)	–	–	<3 × 10^{-11}	~300	–	4.55	PE	[3435]
W(100){probably}	Ba	Ba$^+$	2 × 10^{-8}	2050–2550	4.55 ± 0.03	(4.52 ± 0.07)	PSI	[92]
W(100)	I$_2$	I$^-$	≤10^{-5} (I$_2$)	~1500–2300	4.55 ± 0.05^N	(4.53 ± 0.05)	NSI	[571]
W(100)	–	–	~10^{-9}	~1940–2340	–	4.55 ± 0.05	TE	[143]
W(100)	–	–	1 × 10^{-8}	~1900–2100	–	4.55 ± 0.05	TE	[1663,2012]
W(100)	–	–	~10^{-8}	1170	–	4.56	TE	[3015]
W(100)	–	–	–	–	–	4.56	TC	[1271]
W(100)	–	–	–	–	–	4.56	TC	[3224]
W(100)–Re(2%)[274]	–	–	?	1640–1840	–	4.56	TE	[353]
W(100)	–	–	?	~1400–2000	–	4.56 ± 0.02	TE	[149]
W(100)	Sr	Sr$^+$	~10^{-9}	~2500–2850	4.56 ± 0.04	–	PSI	[138]
W(100)–Os(1%)[276]	–	–	?	~1700–2030	–	4.57 ± 0.04	TE	[3086]
W(100)	–	–	~10^{-10}	77	–	4.57	FE	[340]
W(100){95%}[301]	–	–	–	–	(4.69 ± 0.05)	4.57 ± 0.00	TC	[803]
W(100)	–	–	3 × 10^{-11}	78, 295	–	4.57 ± 0.14	FE	[354]
W(100)	–	–	–	–	–	4.58	TC	[531]
W(100)–Re(6%)[274]	–	–	?	1630–1770	–	4.59	TE	[353]
W(100)	–	–	~10^{-10}	77	–	4.59 ± 0.02	FE	[502]
W(100)	–	–	≤4 × 10^{-8}	~1650–2050	–	4.59 ± 0.02	TE	[140]
W(100)	–	–	≤3 × 10^{-10}	~1150–1650	(4.54 ± 0.02)	4.59 ± 0.03	TE	[82]
W(100){96%}[300]	–	–	–	–	(4.60 ± 0.04)	4.59 ± 0.04	TC	[630,2453]
W(100)	–	–	1 × 10^{-9}	?	(4.62 ± 0.06)	4.59 ± 0.05	TE	[84]
W(100)	–	–	?	~300	–	4.6	PE	[1603]
W(100)	–	–	≤5 × 10^{-8}	~1600–2100	(4.6)	4.6	TE	[271]
W(100)	Sm	Sm$^+$	≤5 × 10^{-8}	~1650–2000	4.6	(4.6)	PSI	[271]
W(100)	–	–	<10^{-10}	170	–	4.6	FE	[3793]
W(100)	Li	Li$^+$	<10^{-9}	~1000–1300	4.6	–	PSI	[318]
W(100)	–	–	–	–	–	4.6	TC	[382,1908]
W(100)	–	–	?	?	–	4.6	FE	[1463]
W(100)	–	–	1 × 10^{-8}	~300	–	4.6	CPD	[1511]
W(100)	–	–	–	–	–	4.6	TC	[3615]
W(100)	–	–	?	~1800–2300	–	4.6	TE	[1958]
W(100)	–	–	?	?	–	4.6	FE	[1964]
W(100)	–	–	≤7 × 10^{-11}	~300	–	4.6	CPD	[2385]
W(100)	–	–	?	77	–	4.6	FE	[3079]
W(100)	–	–	?	20, 100	–	4.6	FE	[3508]
W(100)	–	–	?	?	(4.6 ± 0.1)	4.6 ± 0.1	TE	[15,649]
W(100)	Ba	Ba$^+$	?	?	4.6 ± 0.1	(4.6 ± 0.1)	PSI	[15,649]
W(100)	–	–	~10^{-10}	–1600–	–	4.6 ± 0.1	TE	[335,1650,1651, 1967]
W(100)	La	La$^+$	3 × 10^{-8}	~2000–2750	4.6 ± 0.1	–	PSI	[153]
W(100)	Nd	Nd$^+$	<10^{-8}	~1900–2550	4.6 ± 0.1	–	PSI	[153]
W(100)	K	K$^+$	≤1 × 10^{-6}	?	4.6 ± 0.1	–	PSI	[216]
W(100)	–	–	?	?	(4.6 ± 0.1)	4.6 ± 0.1	TE	[1659]
W(100)	K	K$^+$	?	?	4.6 ± 0.1	(4.6 ± 0.1)	PSI	[1659]
W(100)	–	–	?	?	–	4.6 ± 0.1	FE	[3033]
W(100)	In	In$^+$	≤2 × 10^{-8}	1630–2040	4.60	(4.55)	PSI	[83]
W(100)	–	–	≤5 × 10^{-10}	298, 613	–	4.60	CPD	[355]
W(100)	–	–	?	~1700–2200	–	4.60	TE	[2187,3664]
W(100)	–	–	~10^{-9}	?	–	4.60	TE	[3096]
W(100)	La	La$^+$	~10^{-9}	~2500–2850	4.60 ± 0.03	–	PSI	[138]
W(100)	–	–	~10^{-9}	?	(4.66 ± 0.03)	4.60 ± 0.03	TE	[3103]
W(100){96%}[300]	–	–	–	–	4.60 ± 0.04	(4.59 ± 0.04)	TC	[630,2453]
W(100)	–	–	<2 × 10^{-10}	?	–	4.60 ± 0.05	TE	[142]
W(100)	–	–	≤2 × 10^{-9}	~1700–2000	–	4.60 ± 0.05	TE	[127,144]
W(100)	–	–	–	–	–	4.60 ± 0.05	TC	[384]
W(100)	–	–	~10^{-10}	~300	–	4.60 ± 0.05	CPD	[820]
W(100)[278]	–	–	8 × 10^{-9}	?	(4.66 ± 0.11*)	4.60 ± 0.06	TE	[280]
W(100)	–	–	≤3 × 10^{-10}	~1150–1650	–	4.61 ± 0.03	TE	[652]
W(100){95%}[301]	–	–	–	–	(4.70 ± 0.04)	4.61 ± 0.04	TC	[2453]
W(100)[273]	–	–	3 × 10^{-8}	–1900–	–	4.61 ± 0.05	TE	[651]
W(100)	–	–	3 × 10^{-9}	~1500–2000	–	4.61 ± 0.05	TE	[2214,2217]
W(100)[170,278]	Cs	Cs$^+$	2 × 10^{-9}	~1000–1500	4.61 ± 0.07	(4.65 ± 0.02)	PSI	[266,2314–2316]
W(100){probably}	–	–	~10^{-10}	~300	–	4.62	CPD	[1516]
W(100)	–	–	<10^{-8}(Sr)	~2000	–	4.62	TE	[1792]

(continued on next page)

Table 1 (*continued*)

Surface	Beam	Ion	P_r (Torr)	T (K)	ϕ^+ (eV)	ϕ^e (eV)	Meth.	Refs.
W(100)	–	–	?	~300	–	4.62	CPD	[3600]
W(100)	–	–	≤10⁻⁸	~1700–2300	–	4.62 ± 0.03	TE	[1793]
W(100)	–	–	<1 × 10⁻¹⁰	~300	–	4.62 ± 0.05	PE	[2669]
W(100)	Bi	Bi⁺	1 × 10⁻⁹	?	4.62 ± 0.06	(4.59 ± 0.05)	PSI	[84]
W(100)	–	–	<5 × 10⁻¹¹	~300	–	4.63	CPD	[1672]
W(100)	–	–	≤10⁻¹⁰	78	–	4.63	FE	[356]
W(100)	–	–	–	–	–	4.63	TC	[357]
W(100)	–	–	–	–	–	4.63	TC	[383,385]
W(100)/Mo	WX₆	–	6 × 10⁻⁷	?	–	4.63	TE	[1521]
W(100)	–	–	~10⁻¹⁰	~300	–	4.63	CPD	[2110]
W(100)	–	–	–	–	–	4.63	TC	[3452]
W(100)	–	–	~10⁻¹⁰	77, 300	–	4.63 ± 0.02	FE	[358,3092]
W(100)	–	–	~10⁻⁸ (O₂)	2200	–	4.64	TE	[212]
W(100)	–	–	≤6 × 10⁻¹¹	78	–	4.64	FE	[807]
W(100)	–	–	1 × 10⁻⁹	~300	–	4.64	FE	[2220]
W(100)	–	–	2 × 10⁻¹⁰	~300	–	4.64	PE	[3436]
W(100)	–	–	<5 × 10⁻¹⁰	~300	–	4.64 ± 0.01	CPD	[2471]
W(100)	–	–	≤3 × 10⁻¹⁰	~300	–	4.64 ± 0.02	CPD	[1054]
W(100)	–	–	?	~300	–	4.645 ± 0.005	CPD	[1490]
W(100)	–	–	≤6 × 10⁻¹⁰	120, 300	–	4.65	CPD	[359,2124,2721]
W(100)	–	–	<5 × 10⁻¹¹	~300	–	4.65	CPD	[360,361]
W(100)	–	–	–	–	–	4.65	TC	[386]
W(100)	–	–	<2 × 10⁻¹⁰	~300	–	4.65	FE	[489]
W(100)	–	–	<10⁻¹⁰	295	–	4.65	FE	[1276]
W(100){99.5%}	–	–	<10⁻¹⁰	~300	–	4.65	CPD	[2058]
W(100)	–	–	–	–	–	4.65	TC	[2548]
W(100)	–	–	~10⁻¹⁰	~300	–	4.65	CPD	[3076]
W(100)	–	–	≤3 × 10⁻¹⁰	~300	–	4.65 ± 0.01	CPD	[194]
W(100)	–	–	≤3 × 10⁻¹⁰	~300	–	4.65 ± 0.01	CPD	[362,2481]
W(100)[278]	–	–	2 × 10⁻⁹	~1400–2200	(4.61 ± 0.07)	4.65 ± 0.02	TE	[266,2314–2316]
W(100)	–	–	?	~2000–2400	–	4.65 ± 0.02	TE	[2356]
W(100)	–	–	≤4 × 10⁻¹⁰	~300	–	4.65 ± 0.02	CPD	[582,2102,3088]
W(100)	–	–	≤10⁻¹⁰	~300	–	4.65 ± 0.03	PE	[3432]
W(100)	–	–	<5 × 10⁻¹⁰	~300	–	4.65 ± 0.04	CPD	[1055,1056]
W(100)	–	–	≤3 × 10⁻¹⁰	~300	–	4.655 ± 0.005	CPD	[2104]
W(100)	–	–	–	–	–	4.66	TC	[1159,1980,2129, 3067]
W(100)	Na	Na⁺	~10⁻⁹	?	4.66 ± 0.03	(4.60 ± 0.03)	PSI	[3103]
W(100)	–	–	<10⁻⁸	~1900–2400	–	4.66 ± 0.06	TE	[87]
W(100)[170,278]	Cs	Cs⁺	8 × 10⁻⁹	?	4.66 ± 0.11*	(4.60 ± 0.06)	PSI	[280]
W(100)	–	–	?	~2100–2200	–	4.66 ± 0.13	TE	[3349]
W(100)	–	–	≤4 × 10⁻¹⁰	~300	–	4.660 ± 0.005	CPD	[2108]
W(100)	–	–	–	–	–	4.67	TC	[3224]
W(100)	–	–	2 × 10⁻¹⁰	90	–	4.68	FE	[3102]
W(100)	La	La⁺	~10⁻⁹	~2500–2900	4.69	–	PSI	[138]
W(100)	–	–	?	1920	–	4.69	TE	[2187,3664]
W(100){95%}[301]	–	–	–	–	4.69 ± 0.05	(4.57 ± 0.00)	TC	[803]
W(100)	–	–	?	~300 (2200)	–	4.7	FE	[3847,3952,3953]
W(100)	–	–	<10⁻¹⁰	~300	–	4.7	CPD	[808]
W(100)	–	–	7 × 10⁻¹⁰	77	–	4.7	FE	[3691]
W(100)	–	–	≤1 × 10⁻⁹	300, 1000	–	4.7	FE	[1965]
W(100)	–	–	(<10⁻¹¹)	78	–	4.70	FE	[809]
W(100)	–	–	?	20, 100	–	4.70	FE	[812]
W(100){95%}[301]	–	–	–	–	4.70 ± 0.04	(4.61 ± 0.04)	TC	[2453]
W(100)	–	–	~10⁻¹⁰	77–600	–	4.70 ± 0.05*	FE	[502]
W(100)	–	–	?	?	–	4.71	FE	[1284]
W(100)[170,278]	Cs	Cs⁺	~10⁻¹⁰	~800–1050	4.72*	–	PSI	[265]
W(100)	–	–	≤3 × 10⁻¹⁰	1000	–	4.72 ± 0.02	CPD	[194]
W(100)	–	–	<2 × 10⁻¹⁰	78	–	4.72 ± 0.04	FE	[1674,2254–2256]
W(100)	–	–	~10⁻¹⁰	77	–	4.75	FE	[340]
W(100)	–	–	~10⁻⁸	~2050–2350	–	4.76 ± 0.05	TE	[3064]
W(100)	–	–	~10⁻⁹	77	–	4.77	FE	[363,810,811,2766]
W(100)	–	–	–	–	–	4.77	TC	[383,385]
W(100)	–	–	<1 × 10⁻¹¹	78	–	4.78	FE	[373]
W(100){95%}[277]	–	–	–	–	–	4.78	TC	[1254]
W(100)	–	–	<5 × 10⁻¹⁰	77	–	4.8	FE	[3114]
W(100)	–	–	<1 × 10⁻¹¹	77	–	4.80	FE	[1549]
W(100)	La	La⁺	~10⁻⁹	~2500–2850	4.80 ± 0.03	–	PSI	[138]
W(100)	–	–	<8 × 10⁻¹¹	~300	–	4.80 ± <0.05	FE	[364,530]
W(100)	–	–	3 × 10⁻⁹	~1500–2000	–	4.80 ± 0.05	TE	[2214,2217]

Table 1 (*continued*)

Surface	Beam	Ion	P_r (Torr)	T (K)	ϕ^+ (eV)	ϕ^e (eV)	Meth.	Refs.
W(100)	–	–	$\sim10^{-10}$	~300	–	4.82	FE	[2324]
W(100)	–	–	$<10^{-11}$	77	–	4.82	FE	[267]
W(100)	–	–	–	–	–	4.82	TC	[384]
W(100)	–	–	2×10^{-10}	~300	–	4.83 ± 0.02	FE	[999]
W(100)	–	–	$(\sim10^{-11})$	~300	–	4.86	FE	[3237]
W(100)	–	–	–	–	–	4.88	TC	[387]
W(100)	–	–	$<1\times10^{-10}$	~300	–	4.88 ± 0.02	FE	[2616]
W(100)	–	–	–	–	–	4.89	TC	[387]
W(100)	–	–	?	15	–	4.89	FE	[653]
W(100)	–	–	$<5\times10^{-10}$	77	–	4.9	FE	[3114]
W(100)	–	–	$\sim1\times10^{-10}$	~300	–	4.9	FE	[3438]
W(100)	–	–	$\sim10^{-10}$	79	–	4.90	FE	[1275]
W(100)	–	–	$<10^{-8}$	20	–	4.90 ± 0.03	FE	[813]
W(100)	–	–	$\sim10^{-10}$	78	–	4.93 ± 0.06	FE	[819]
W(100)	–	–	–	–	–	4.963	TC	[365]
W(100)	–	–	?	~300	–	4.97	FE	[1730]
W(100)	–	–	–	–	–	4.979	TC	[365]
W(100)	–	–	?	80	–	4.98	FE	[1057]
W(100)	–	–	–	–	–	5.00	TC	[2701]
W(100)	–	–	–	–	–	5.009	TC	[365]
W(100)	–	–	–	–	–	5.03	TC	[387]
W(100)	Sr	Sr^+	$\sim10^{-9}$	~1700–2200	5.07	–	PSI	[138]
W(100)	–	–	–	–	–	5.08	TC	[387]
W(100)	–	–	–	–	–	5.10	TC	[387]
W(100)–Os(1%)[276]	–	–	?	2080–2300	–	5.12 ± 0.06	TE	[3086]
W(100)	–	–	–	–	–	5.16	TC	[387]
W(100)	–	–	5×10^{-10}	~300	–	5.2	FE	[376]
W(100)–Ir(2%)[275]	–	–	?	2030–2200	–	5.28 ± 0.06	TE	[3086]
W(100)–Ir(2%)[275]	–	–	?	2030–2200	–	5.30 ± 0.06	TE	[3086]
W(100)	–	–	–	–	–	5.4	TC	[388,389,511]
W(100)	–	–	–	–	–	5.47	TC	[384]
W(100)	–	–	–	–	–	7.8	TC	[2528]
Recommended	–	–	–	–	**4.62 ± 0.05**	**4.65 ± 0.02**	–	–
W(110)[289]	–	–	1×10^{-9}	~1400–2000	–	4.58	TE	[150]
W(110)	–	–	$\sim10^{-10}$	77	–	4.6	FE	[2714]
W(110)	–	–	?	?	–	4.60 ± 0.08	FE	[1377,1378]
W(110)[279]	NaCl	Na^+, Cl^-	$<10^{-10}$	1845–2136	4.609 ± 0.014	(5.18 ± 0.08)	PSI, NSI	[89]
W(110)[279]	NaCl	Cl^-, Na^+	$<10^{-10}$	1845–2136	4.609 ± 0.014^N	(5.18 ± 0.08)	NSI, PSI	[89]
W(110)	–	–	$<10^{-8}$	~1900–2250	–	4.61	TE	[85]
W(110)	–	–	1×10^{-8}	~1900–2100	–	4.63 ± 0.05	TE	[1663,2012]
W(110)	–	–	?	~1400–2000	–	4.65 ± 0.02	TE	[149,2706]
W(110)[289]	–	–	1×10^{-9}	~1400–2000	–	4.66	TE	[150]
W(110)[279]	NaCl	Na^+, Cl^-	$<10^{-10}$	1800–2200	4.66 ± 0.09	–	PSI, NSI	[3690]
W(110)[279]	NaCl	Cl^-, Na^+	$<10^{-10}$	1800–2200	4.66 ± 0.09^N	–	NSI, PSI	[3690]
W(110)	–	–	1×10^{-8}	~1900–2100	–	4.67 ± 0.05	TE	[1663,2012]
W(110)	–	–	$\sim10^{-12}$	~300	–	4.68	FE	[3406]
W(110)	–	–	–	–	–	4.7	TC	[1723]
W(110)	–	–	?	?	–	4.7 ± 0.1	TE	[3578]
W(110)	–	–	–	–	–	4.758	TC	[4091]
W(110)	–	–	–	–	–	4.79	TC	[1270]
W(110)	–	–	–	–	–	4.8	TC	[1723]
W(110)	–	–	$<10^{-8}$	~1800–2200	(5.14)	4.8 ± 0.1	TE	[85]
W(110)	–	–	?	?	–	4.8 ± 0.1	TE	[3578]
W(110)	Gd	Gd^+	$\sim10^{-10}$	~2000–2700	$4.80\pm0.09*$	–	PSI	[416]
W(110)	–	–	$\sim10^{-10}$	79	–	4.82	FE	[1275]
W(110){80%}[311]	–	–	$<10^{-9}$	~1700–2600	–	4.82 ± 0.02	TE	[162]
W(110)[280]	Ba	Ba^+	$<10^{-8}$	~1800–2140	4.82 ± 0.06	(5.04, 5.30)	PSI	[87]
W(110)	–	–	–	–	–	4.84	TC	[1270]
W(110)	–	–	–	–	–	4.84	TC	[4309]
W(110)	–	–	$<8\times10^{-9}$	~2200–2450	–	4.87 ± 0.04	TE	[2340]
W(110){80%}[311]	–	–	–	–	(5.26 ± 0.00)	4.87 ± 0.06	TC	[2453]
W(110)/Nb(110)	–	–	–	–	–	4.9	TC	[2073]
W(110)	–	–	1×10^{-8}	~1500–1850	–	4.9	TE	[1499]
W(110)	–	–	?	?	–	>4.9	FE	[1463]
W(110)	–	–	$\leq2\times10^{-9}$	~1600–2200	(5.28 ± 0.03)	4.90 ± 0.02	TE	[88,814]
W(110){80%}[311]	–	–	–	–	(5.25 ± 0.02)	4.90 ± 0.02	TC	[630]
W(110)	–	–	5×10^{-9}	~2000–2400	–	4.92	TE	[352]
W(110)/?	WCl_6	–	?	?	–	5.0	FE	[3735]
W(110)	–	–	$\leq6\times10^{-8}$	~1800–2150	–	5.0	TE	[2247]

(continued on next page)

Table 1 (*continued*)

Surface	Beam	Ion	P_r (Torr)	T (K)	ϕ^+ (eV)	ϕ^e (eV)	Meth.	Refs.
W(110){80%}[311]	–	–	<10⁻⁹	~700–2600	–	5.0 ± 0.2	TE	[162]
W(110)	–	–	~10⁻¹⁰	–1600–	–	5.0 ± 0.2	TE	[335,1650,1651, 1967]
W(110)	–	–	~10⁻⁸	?	–	5.00	TE	[3353]
W(110)	–	–	~10⁻¹⁰	77–700	–	5.02 ± 0.03	FE	[502]
W(110)	–	–	–	–	–	5.025	TC	[4189]
W(110)	–	–	–	–	–	5.03	TC	[471]
W(110)	–	–	≤2 × 10⁻⁹	~1600–2200	(5.30 ± 0.03)	5.03 ± 0.02	TE	[3542]
W(110)[280]	–	–	<10⁻⁸	~1900–2300	(4.82, 5.14)	5.04 ± 0.06	TE	[87]
W(110)	–	–	–	–	–	5.05	TC	[367]
W(110)	–	–	–	–	–	5.05	TC	[151,2936]
W(110)[281]	–	–	<2 × 10⁻¹⁰	~300	–	5.05 ± 0.02	CPD	[815]
W(110)/W(110)[310]	W	–	~10⁻⁷	~1850–2450	–	5.06 ± 0.01	TE	[1053]
W(110)	–	–	7 × 10⁻¹¹	200	–	5.06 ± 0.05	PE	[3566]
W(110)	–	–	–	–	–	5.07	TC	[1270]
W(110)	–	–	<8 × 10⁻¹¹	~300	–	5.07 ± <0.05	FE	[364,530,3213]
W(110)	–	–	–	–	–	5.08	TC	[3115]
W(110)	–	–	≤3 × 10⁻⁹	~1200	–	5.08	FE	[2072]
W(110)	–	–	2 × 10⁻⁹	~2000	–	5.09	TE	[141]
W(110)	Li	Li⁺	<10⁻⁹	~1000–1200	5.1	–	PSI	[318,319,366]
W(110)	–	–	2 × 10⁻¹¹	~300	–	5.1	PE	[1940]
W(110)[283]	–	–	~10⁻¹⁰	~300	(5.2)	5.1	PE	[2774,3768]
W(110)	–	–	≤1 × 10⁻¹⁰	~300	–	5.1	PE	[3177,3191]
W(110)[282]	–	–	–	–	–	5.10	TC	[2073,2074]
W(110)	–	–	?	?	–	5.10	FE	[3618]
W(110)/Mo(110)[282]	–	–	–	–	–	5.10+0.01	TC	[2074]
W(110)	–	–	~10⁻¹⁰	~300	–	5.10 ± 0.01	CPD	[2106,2110]
W(110)	–	–	–	–	–	5.11	TC	[3224]
W(110)[284]	Cs	Cs⁺	2 × 10⁻⁹	~1000–1500	5.11	(5.33 ± 0.04)	PSI	[2314]
W(110)	–	–	<5 × 10⁻¹⁰	~300	–	5.11 ± 0.01	CPD	[2471]
W(110)	–	–	<5 × 10⁻¹⁰	~300	–	5.11 ± 0.02	CPD	[1055,1056,2102]
W(110)	–	–	≤3 × 10⁻¹⁰	~300	–	5.120 ± 0.005	CPD	[2104]
W(110)	–	–	≤4 × 10⁻¹⁰	~300	–	5.125 ± 0.005	CPD	[2108]
W(110)	–	–	–	–	–	5.13	TC	[4405]
W(110)[310]	–	–	~10⁻⁷	~1850–2450	–	5.13 ± 0.01	TE	[1053]
W(110)	–	–	≤4 × 10⁻¹⁰	~300	–	5.13 ± 0.02	CPD	[582]
W(110)[280]	Na[270]	Na⁺	? (Na)	~1900–2000	5.14	(5.04, 5.30)	PSI	[87]
W(110)[270]	Na	Na⁺	? (Na)	~1500–2000	5.14	(4.8 ± 0.1)	PSI	[85,3037]
W(110)	–	–	≤3 × 10⁻¹⁰	~300	–	5.14 ± 0.01	CPD	[362,2481]
W(110)	Na	Na⁺	~10⁻⁹	~1450–2000	5.14 ± 0.03	(5.30 ± 0.03)	PSI	[3103]
W(110)	–	–	?	~300	–	5.141 ± 0.007	CPD	[1490]
W(110)[281]	–	–	<2 × 10⁻¹⁰	~300 (2500)	–	5.15	CPD	[815]
W(110)	–	–	–	–	–	5.15	TC	[3224]
W(110)	KCl	K⁺	1 × 10⁻¹⁰	~1000–1500	5.15	–	PSI	[1548]
W(110)	–	–	?	80, 300	–	5.15	CPD	[2112]
W(110)	–	–	<3 × 10⁻¹⁰	~300	–	5.15 ± 0.01	CPD	[194]
W(110)[310]	–	–	~10⁻⁷	~1850–2450	–	5.15 ± 0.01	TE	[1053]
W(110)	–	–	?	~300	–	5.15 ± 0.01	CPD	[3420]
W(110)	–	–	~10⁻¹⁰	~300	–	5.15 ± 0.02	CPD	[3076,3088]
W(110)	–	–	?	77	–	5.15 ± 0.05	FE	[502]
W(110)/W(100)[309]	WF₆, H₂	–	~10⁻⁷	1850–2450	–	5.16 ± 0.01	TE	[1053]
W(110)/W(110)[309]	WCl₆, H₂	–	~10⁻⁷	1850–2450	–	5.16 ± 0.01	TE	[1053]
W(110)	–	–	?	77	–	5.16 ± 0.02	FE	[502]
W(110)[285]	Na	Na⁺	~10⁻¹⁰	1180	5.17 ± 0.01	–	PSI	[154,260]
W(110)	–	–	?	2100–2200	–	5.17 ± 0.02	TE	[3349]
W(110)	–	–	5 × 10⁻⁹ (O₂)	2050	–	5.18	TE	[212]
W(110)	–	–	–	–	–	5.18	TC	[531]
W(110)[279]	–	–	<10⁻¹⁰	~1850–2250	(4.609 ± 0.014)	5.18 ± 0.08	TE	[89]
W(110)[279]	–	–	<10⁻¹⁰	~1850–2250	(4.609 ± 0.014)ᴺ	5.18 ± 0.08	TE	[89]
W(110)[285]	Na	Na⁺	~10⁻¹⁰	1180	5.19 ± 0.01	–	PSI	[3768]
W(110)	–	–	≤3 × 10⁻¹⁰	1000	–	5.19 ± 0.01	CPD	[194]
W(110)	Tb	Tb⁺	~10⁻¹⁰	~2200–2500	5.19 ± 0.07*	–	PSI	[416]
W(110)	–	–	?	~300	–	5.2	FE	[1767]
W(110)	–	–	~10⁻⁹ (O₂)	2050	–	5.2	TE	[212]
W(110)	–	–	(≤10⁻¹⁰)	77	–	5.2	FE	[1974]
W(110)	–	–	?	~300 (2200)	–	5.2	FE	[3952]
W(110)	–	–	~10⁻¹¹	20–200	–	5.2	FE	[2218]
W(110)	–	–	7 × 10⁻¹⁰	77	–	5.2	FE	[3691]
W(110)	–	–	?	~1800–2300	–	5.2	TE	[1958]
W(110)[283]	Na	Na⁺	~10⁻¹⁰	~300	5.2	(5.1)	PSI	[2773,2774]

Table 1 (*continued*)

Surface	Beam	Ion	P_r (Torr)	T (K)	ϕ^+ (eV)	ϕ^e (eV)	Meth.	Refs.
W(110)	–	–	$<10^{-9}$	$\sim$300	–	5.20	PE	[3857]
W(110)	–	–	–	–	–	5.20	TC	[365]
W(110)	–	–	–	–	–	5.20	TC	[3224]
W(110)	Ho	Ho$^+$	$\sim$10^{-10}	$\sim$1900–2500	5.20 ± 0.05*	–	PSI	[416]
W(110)	–	–	$<10^{-10}$	$\sim$300	–	5.20 ± 0.05	FE	[2262]
W(110)	–	–	–	–	–	5.21	TC	[3473]
W(110)	–	–	3×10^{-7}	–2300–	–	5.21 ± 0.04	TE	[1402]
W(110)^{310}	–	–	$\sim$10^{-7}	$\sim$1850–2450	–	5.22 ± 0.01	TE	[1053]
W(110)	–	–	$\leq 8 \times 10^{-9}$	$\sim$1700–2160	–	5.22 ± 0.01	TE	[1183]
W(110)	–	–	$<8 \times 10^{-9}$	2300	–	5.22 ± 0.02	TE	[147,1037,2357, 3802]
W(110)	–	–	?	?	–	5.22 ± 0.05	FE	[816]
W(110)	Dy	Dy$^+$	$\sim$10^{-10}	$\sim$1850–2500	5.22 ± 0.07*	–	PSI	[416]
W(110)	–	–	$\leq 10^{-8}$	$\sim$1800–2250	–	5.24 ± 0.03	TE	[1793]
W(110){>90%}	Na^{270}	Na$^+$	1×10^{-8} (Na)	$\sim$1200–2000	5.25	(5.27)	PSI	[90]
W(110)	–	–	?	?	–	5.25	TE	[368]
W(110)	–	–	$<2 \times 10^{-10}$	$\sim$300	–	5.25	FE	[489]
W(110)	–	–	$\sim$10^{-9}	$\sim$300	–	5.25	CPD	[1272]
W(110)	–	–	2×10^{-10}	$\sim$300	–	5.25	CPD	[2592]
W(110)	–	–	?	$\sim$300	–	5.25	PE	[3443]
W(110)	–	–	$\sim$10^{-10}	77, 300	–	5.25 ± 0.02	FE	[358,3092]
W(110){80%}^{311}	–	–	–	–	5.25 ± 0.02	(4.90 ± 0.05)	TC	[630,2453]
W(110)	–	–	?	100	–	5.25 ± 0.02	PE	[1273]
W(110){>90%}	–	–	5×10^{-9}	$\sim$1500–1900	(5.25 ± 0.05)	5.25 ± 0.05	TE	[86,90,2094]
W(110){>90%}	Na	Na$^+$	5×10^{-9}	$\sim$1200–2000	5.25 ± 0.05	(5.25 ± 0.05)	PSI	[86,90,2094]
W(110)	–	–	?	$\sim$300	–	5.25 ± 0.25	FE	[1767]
W(110)	–	–	–	–	–	5.26	TC	[1271]
W(110)^{289}	–	–	–	–	–	5.26	TC	[150]
W(110)	–	–	?	1920	–	5.26	TE	[2187,3664]
W(110)	–	–	?	$\sim$300	–	5.26	PE	[3448]
W(110){80%}^{311}	–	–	–	–	5.26 ± 0.02	(4.87 ± 0.06)	TC	[2453]
W(110)	–	–	–	–	–	5.269	TC	[365]
W(110)	–	–	5×10^{-10}	$\sim$1500–1900	(5.25)	5.27	TE	[90]
W(110)^{142}	–	–	$\leq 2 \times 10^{-10}$	$\sim$300	–	5.28*	CPD	[2598]
W(110)	–	–	$\sim$10^{-8}	?	–	5.29	TE	[3353]
W(110)	Li	Li$^+$	$\leq 2 \times 10^{-9}$	$\sim$1250–1800	5.28 ± 0.03	(4.90, 5.30)	PSI	[88,814]
W(110)	–	–	?	$\sim$300 (2200)	–	5.3	FE	[3847,3952]
W(110)	–	–	($\leq 10^{-11}$)	$\sim$300	–	5.3	CPD	[259]
W(110)	Tm	Tm$^+$	?	$\sim$2000	5.3	–	PSI	[3559]
W(110)	–	–	1×10^{-11}	300, 700	–	5.3	CPD	[370]
W(110)	–	–	–	–	–	5.3	TC	[1723]
W(110)	–	–	($\leq 10^{-11}$)	$\sim$300	–	5.3	CPD	[2380]
W(110)	–	–	$<2 \times 10^{-10}$	90	–	5.3	PE	[2778]
W(110)	–	–	2×10^{-10}	$\sim$300	–	5.3	PE	[2834]
W(110)	–	–	$\sim$10^{-9}	?	–	5.3	TE	[3096]
W(110)	–	–	($\sim$10^{-12})	$\sim$300	–	5.3 ± 0.02	CPD	[1795]
W(110)	–	–	$\sim$10^{-9}	$\sim$1700–2000	–	5.3 ± 0.07	TE	[1277]
W(110)	–	–	($<1 \times 10^{-11}$)	$\sim$300	–	5.30	FE	[2251]
W(110)	–	–	$<2 \times 10^{-10}$	27, 90	–	5.30	CPD	[4107]
W(110)	–	–	?	20	–	5.30	FE	[2956,3472,3508, 3563]
W(110)	–	–	$<2 \times 10^{-10}$	78	–	5.30	FE	[1674,2251,2253, 2254]
W(110)	–	–	$<1 \times 10^{-10}$	$\sim$300	–	5.30 ± 0.02	FE	[2054]
W(110)	–	–	$\leq 2 \times 10^{-9}$	$\sim$1600–2000	(5.30 ± 0.03)	5.30 ± 0.03	TE	[88,814,3541]
W(110)	Li	Li$^+$	$\leq 2 \times 10^{-9}$	1250–1800	5.30 ± 0.03	(5.30, 5.03)	PSI	[814,3542]
W(110)	–	–	$\sim$10^{-9}	$\sim$1600–2000	(5.14 ± 0.03)	5.30 ± 0.03	TE	[3103]
W(110)	–	–	3×10^{-9}	$\sim$1500–2000	–	5.30 ± 0.05	TE	[2214,2217]
W(110)^{280}	–	–	$<10^{-8}$	$\sim$1900–2300	(4.82, 5.14)	5.30 ± 0.06	TE	[87]
W(110)	–	–	$<10^{-8}$	$\sim$1900–2400	–	5.30 ± 0.06	TE	[148]
W(110)	–	–	$<5 \times 10^{-11}$	$\sim$300	–	5.32	CPD	[1274]
W(110)	–	–	$\sim$10^{-10}	78	–	5.32 ± 0.10	FE	[819]
W(110)	–	–	2×10^{-9}	1450–2000	–	5.33 ± 0.03	TE	[817]
W(110)	–	–	$\sim$10^{-8}	$\sim$2050–2350	–	5.33 ± 0.03	TE	[372,3064]
W(110)^{284}	–	–	2×10^{-9}	$\sim$1400–2200	(5.11)	5.33 ± 0.04	TE	[266,2314–2316]
W(110)	–	–	$\sim$10^{-11}	$\sim$300	–	5.34 ± 0.03*	CPD	[2647]
W(110)	–	–	$<10^{-10}$	$\sim$300	–	5.34 ± 0.05	FE	[2044]
W(110)	–	–	–	–	–	5.345	TC	[365]
W(110)	–	–	$<2 \times 10^{-11}$	78	–	5.35	FE	[262]
W(110)	–	–	$\sim$10^{-9}	77	–	5.35	FE	[1137]

Table 1 (*continued*)

Surface	Beam	Ion	P_r (Torr)	T (K)	ϕ^+ (eV)	ϕ^e (eV)	Meth.	Refs.
W(110)	–	–	2×10^{-11}	>1200	–	5.35	TE	[1940]
W(110)	–	–	$\leq 7 \times 10^{-11}$	~300	–	5.35	CPD	[2385]
W(110)	–	–	$\leq 2 \times 10^{-9}$	~1700–2000	–	5.35 ± 0.05	TE	[127,144]
W(110)	–	–	$\leq 8 \times 10^{-10}$	~300	–	5.35 ± 0.05	FE	[1689]
W(110)	–	–	$\sim 10^{-10}$	~300	–	5.35 ± 0.05	CPD	[2381]
W(110)	–	–	$\sim 10^{-11}$	78	–	5.35 ± 0.09	FE	[654]
W(110)	–	–	6×10^{-6} (Cs)	1950–2150	–	5.37	TE	[151]
W(110)	–	–	$\leq 3 \times 10^{-9}$	~1200	–	5.37	FE	[2072]
W(110)	Sr	Sr$^+$	8×10^{-9}	~2300–2800	5.38 ± 0.03	–	PSI	[145]
W(110)	Ca	Ca$^+$	8×10^{-9}	~2300–2800	5.39 ± 0.04	–	PSI	[145]
W(110)	–	–	$\sim 10^{-10}$	80–550	–	5.40	FE	[2499]
W(110)	–	–	$\sim 10^{-9}$	~2050–2350	–	5.40 ± 0.05	TE	[143]
W(110)	–	–	$< 10^{-10}$	38, 80	–	5.42 ± 0.02	FE	[1010]
W(110)	–	–	$\leq 3 \times 10^{-9}$	~1200	–	5.43	FE	[2072]
W(110)	–	–	?	40–298	–	5.43 ± 0.03	CPD	[2832]
W(110)	–	–	–	–	–	5.44	TC	[357]
W(110)	–	–	$\leq 3 \times 10^{-9}$	~1200	–	5.44	FE	[2072]
W(110)	La	La$^+$	$\sim 10^{-9}$	~1700–2700	5.44 ± 0.05	–	PSI	[138]
W(110)	Sr	Sr$^+$	8×10^{-9}	~2300–2800	5.44 ± 0.05	–	PSI	[145]
W(110)	Ca	Ca$^+$	8×10^{-9}	~2300–2800	5.45 ± 0.05	–	PSI	[145]
W(110)[170,286]	–	(W$^+$)	$< 5 \times 10^{-8}$	~2500	5.46 ± 0.11	–	PSI	[146]
W(110)	–	–	?	80	–	5.47	FE	[1058]
W(110)	Sr	Sr$^+$	8×10^{-9}	~2300–2800	5.47 ± 0.10	–	PSI	[145]
W(110)	–	–	$< 10^{-9}$	~300	–	5.5	FE	[2354]
W(110)	–	–	?	?	–	5.5 ± 0.2	FE	[3033]
W(110)	–	–	–	–	–	5.50	TC	[2548]
W(110)	–	–	–	–	–	5.50	TC	[1159,1980,2129, 3067]
W(110)	Sr	Sr$^+$	$\sim 10^{-9}$	~1700–2700	5.52 ± 0.05	–	PSI	[138]
W(110)	–	–	?	~1700–2200	–	5.54	TE	[2187,3664]
W(110)	–	–	–	–	–	5.54	TC	[4117]
W(110)	–	–	(1×10^{-10})	~300	–	5.54 ± <0.06	FE	[1529]
W(110)	–	–	–	–	–	5.55	TC	[3179]
W(110)	–	–	?	?	–	5.6	FE	[1964]
W(110)	–	–	$\leq 5 \times 10^{-10}$	~300	–	5.6 ± 0.1	FE	[2013]
W(110)	–	–	–	–	–	5.62	TC	[334]
W(110)	–	–	2×10^{-10}	~300	–	5.66 ± 0.03	FE	[999]
W(110)	–	–	?	~300	–	5.69	FE	[3581]
W(110)	–	–	$< 10^{-7}$	2100	–	5.7	TE	[371]
W(110)	–	–	$\sim 10^{-10}$	77	–	5.70	FE	[340]
W(110)	–	–	?	20, 100	–	5.70	FE	[812]
W(110)	–	–	$(< 10^{-12})$	~300 (~2500)	(6.0)	5.70	FE	[152]
W(110)	–	–	?	~300	–	5.70 ± 0.15	FE	[1766]
W(110)	–	–	–	–	–	5.73	TC	[3224]
W(110)	–	–	$\sim 10^{-10}$	79	–	5.74	FE	[1275]
W(110)	–	–	–	–	–	5.75	TC	[4405]
W(110)	–	–	2×10^{-10}	~300	–	5.75 ± 0.03	FE	[999]
W(110)	–	–	?	77	–	5.75 ± 0.15	FE	[3079]
W(110)	–	–	?	15	–	5.76	FE	[653]
W(110)	–	–	$< 1 \times 10^{-11}$	78	–	5.79	FE	[373]
W(110)	–	–	$\sim 10^{-10}$	~300	–	5.79	FE	[378]
W(110)	–	–	$\sim 10^{-10}$	77	–	5.79 ± 0.04	FE	[502]
W(110)	–	–	$\sim 1 \times 10^{-10}$	~300	–	5.8	FE	[3438]
W(110)	–	–	$\sim 10^{-10}$	78	–	5.8 ± 0.5	FE	[819]
W(110)	–	–	$< 10^{-10}$	90	–	5.80	FE	[656,926]
W(110)	–	–	$< 10^{-8}$	20	–	5.80 ± 0.05	FE	[813]
W(110)	–	–	?	15	–	5.83	FE	[653]
W(110)	–	–	$(< 10^{-11})$	78	–	5.85	FE	[267]
W(110)	–	–	$< 10^{-10}$	~300	–	5.9	CPD	[808]
W(110)	–	–	$\sim 10^{-10}$	~300	–	5.9	FE	[2324]
W(110)	–	–	$\sim 2 \times 10^{-9}$	~300	–	5.93	FE	[2766]
W(110)	–	–	$\leq 10^{-12}$	77	–	5.96	FE	[657]
W(110)	–	–	$\sim 10^{-10}$	79	–	5.98	FE	[1275]
W(110)	–	–	$(< 10^{-12})$	~300 (~1800)	(6.0)	5.99	FE	[152]
W(110)	–	–	$< 10^{-10}$	298	–	5.99	FE	[1010]
W(110)	–	–	?	?	–	6.0	FE	[2565,2574]
W(110)	–	–	$(< 10^{-11})$	78	–	6.0	FE	[809]
W(110)	–	–	$< 10^{-10}$	79	–	6.00	FE	[1276]
W(110)	–	–	?	77	–	6.02 ± 0.06	FE	[502]
W(110)	–	–	$< 10^{-10}$	144	–	6.03 ± 0.02	FE	[1010]

Table 1 (*continued*)

Surface	Beam	Ion	P_r (Torr)	T (K)	ϕ^+ (eV)	ϕ^e (eV)	Meth.	Refs.
W(110)	–	–	(<10⁻¹²)	~300 (~1500)	–	6.10	FE	[152]
W(110)	–	–	~10⁻¹⁰	79	–	6.10	FE	[1275]
W(110)	–	–	~10⁻¹⁰	77	–	6.20 ± 0.06	FE	[502]
W(110)	–	–	~10⁻¹⁰	78	–	6.28 ± 0.08	FE	[819]
W(110)	–	–	~10⁻¹⁰	77	–	6.30	FE	[340]
W(110)	–	–	~10⁻¹⁰	79	–	6.30	FE	[1275]
W(110)	–	–	?	80	–	6.35	FE	[1057]
W(110)	–	–	?	77	–	6.40 ± 0.09	FE	[502]
W(110)	–	–	~10⁻¹⁰	77	–	6.5	FE	[2714]
W(110)	–	–	–	–	–	6.70	TC	[1059]
W(110)	–	–	~10⁻¹²	77	–	7.1	FE	[1281]
W(110)	–	–	–	–	–	7.15	TC	[1059]
W(110)	–	–	~10⁻¹²	77	–	7.2	FE	[1281]
W(110)	–	–	~10⁻¹²	77 (~1000)	–	8.78	FE	[1281]
Recommended	–	–	–	–	**5.28 ± 0.11**	**5.32 ± 0.02**	–	–
W(111)	–	–	?	~1400	–	3.25 ± 0.02	TE	[2356]
W(111)	–	–	?	?	–	3.9	FE	[1964]
W(111)	–	–	–	~2300	–	4.07 ± 0.02	TE	[2356]
W(111)	–	–	?	~1800–2300	–	4.2	TE	[1958]
W(111)	–	–	?	?	–	4.2 ± 0.1	FE	[3033]
W(111)	–	–	–	–	–	4.20	TC	[1270]
W(111)	–	–	?	~300	–	4.21	FE	[1730]
W(111)	–	–	≤3 × 10⁻⁹	~1200	–	4.24	FE	[2072]
W(111)	–	–	1 × 10⁻⁸	~1900–2100	–	4.24 ± 0.05	TE	[2012]
W(111)	–	–	–	–	–	4.240	TC	[4091]
W(111)	–	–	?	?	–	4.25	TE	[368]
W(111)	–	–	–	–	–	4.25	TC	[1270]
W(111)	–	–	1 × 10⁻⁸	~1900–2100	–	4.26 ± 0.05	TE	[1663,2012]
W(111)/W	WF₆	–	~10⁻⁸	~1800	–	4.3	TE	[2050]
W(111)	–	–	~10⁻¹⁰	~300	–	4.3	FE	[374,818]
W(111)	–	–	?	?	–	4.3 ± 0.1	FE	[1377,1378]
W(111)	–	–	<10⁻⁹	~300	–	4.32	PE	[375]
W(111)	–	–	?	~300	–	4.33	FE	[3581]
W(111)	–	–	<1 × 10⁻¹¹	78	–	4.35	FE	[373]
W(111)	–	–	?	~2000–2400	–	4.35 ± 0.02	TE	[2356]
W(111)	–	–	?	~1400–2000	–	4.35 ± 0.02	TE	[149]
W(111)	–	–	<8 × 10⁻¹¹	~300	–	4.35 ± <0.05	FE	[364,530,3213]
W(111)	–	–	2 × 10⁻⁹	~1700–2000	–	4.36	TE	[141]
W(111)	–	–	<2 × 10⁻¹⁰	78	–	4.37	FE	[1674,2253]
W(111)	KCl	K⁺	1 × 10⁻¹⁰	~1000–1300	4.37	–	PSI	[1548]
W(111)	–	–	?	~1400–2000	–	4.37 ± 0.02	TE	[149,2706]
W(111)[287]	–	–	<1 × 10⁻¹⁰	~800–1300	–	4.38	FE	[3440]
W(111)	–	–	–	–	–	4.38	TC	[4405]
W(111)	–	–	≤2 × 10⁻⁹	~1600–2200	(4.50 ± 0.03)	4.38 ± 0.02	TE	[88]
W(111)	–	–	1 × 10⁻⁹	~1400–2000	–	4.38 ± 0.02	TE	[150]
W(111)	–	–	–	–	–	4.381	TC	[4189]
W(111)	–	–	(<10⁻¹²)	~300	–	4.39	FE	[152]
W(111)	–	–	~10⁻⁸	?	–	4.39	TE	[3353]
W(111)	–	–	?	~1900	–	4.39	TE	[1581]
W(111)	–	–	<10⁻¹⁰	170	–	4.4	FE	[3793]
W(111)	–	–	?	~300 (2200)	–	4.4	FE	[3847,3952,3953]
W(111)	–	–	(≤10⁻¹¹)	~300	–	4.4	CPD	[259]
W(111)	–	–	<10⁻¹⁰	~300	–	4.4	CPD	[808]
W(111)	–	–	~10⁻⁹	77	–	4.4	FE	[363,810,811,2766]
W(111)	–	–	~10⁻⁹	?	–	4.4	TE	[3686]
W(111)	–	–	~10⁻¹⁰	–1600–	–	4.4 ± 0.1	TE	[335,1650,1651, 1967]
W(111)	–	–	5 × 10⁻¹⁰	~300	–	4.40	FE	[376]
W(111)	–	–	<10⁻¹⁰	78, 295	–	4.40	FE	[679,1276]
W(111)	–	–	?	?	–	4.40	FE	[1463]
W(111)	–	–	~10⁻¹⁰	300–1500	–	4.40	FE	[1783]
W(111)	–	–	~10⁻⁹	?	–	4.40	TE	[3096]
W(111)	–	–	≤2 × 10⁻⁹	~1600–2200	(4.50 ± 0.03)	4.40 ± 0.02	TE	[88,814,3541,3542]
W(111)	–	–	<10⁻⁸	~1900–2400	–	4.40 ± 0.02	TE	[127,144,148]
W(111)	–	–	~10⁻⁸	~2050–2350	–	4.40 ± 0.03	TE	[372,3064]
W(111)	–	–	2 × 10⁻⁹	1450–1750	(4.42, 4.44)	4.40 ± 0.03	TE	[817,3103]
W(111)	–	–	3 × 10⁻⁹	~1500–2000	–	4.40 ± 0.05	TE	[2214,2217]
W(111)	–	–	(1 × 10⁻¹⁰)	~300	–	4.40 ± <0.06	FE	[1529]
W(111)	–	–	–	695	–	4.404	TC	[377]

Table 1 (*continued*)

Surface	Beam	Ion	P_r (Torr)	T (K)	ϕ^+ (eV)	ϕ^e (eV)	Meth.	Refs.
W(111)	–	–	(<10⁻¹¹)	78	–	4.41	FE	[267]
W(111)	–	–	~10⁻¹⁰	~300	–	4.41	FE	[4237]
W(111)	–	–	–	–	–	4.41	TC	[3224]
W(111)	–	–	<10⁻¹⁰	90	–	4.41	FE	[656,926]
W(111)	–	–	?	~1500–2000	–	4.41	TE	[1581]
W(111)	–	–	~10⁻¹⁰	~300	–	4.41	FE	[2324]
W(111)	–	–	?	~300–1100	–	4.41	FE	[3426]
W(111)	–	–	–	418	–	4.415	TC	[377]
W(111)	–	–	?	?	–	4.42	FE	[1283]
W(111)	–	–	~10⁻⁹	~1900–2300	–	4.42 ± 0.03	TE	[143]
W(111)	Na	Na⁺	?	1450–1750	4.42 ± 0.03	(4.40 ± 0.03)	PSI	[3103]
W(111)	–	–	(<10⁻¹¹)	78	–	4.43	FE	[809]
W(111)	–	–	?	1920	–	4.43	TE	[2187,3664]
W(111)[287]	–	–	<1 × 10⁻¹⁰	80–500	–	4.43	FE	[3440]
W(111)	–	–	5 × 10⁻¹⁰	~1400–2150	–	4.43 ± 0.05	TE	[151]
W(111)	–	–	–	–	–	4.44	TC	[1271]
W(111)	–	–	–	–	–	4.44	TC	[4405]
W(111)	–	–	≤3 × 10⁻⁹	~1200	–	4.44	FE	[2072]
W(111)	–	–	?	2100–2200	–	4.44 ± 0.02	TE	[3349]
W(111)	Na	Na⁺	2 × 10⁻⁹	1360–1630	4.44 ± 0.03	(4.40 ± 0.03)	PSI	[817]
W(111)	Li	Li⁺	~10⁻⁹	~1400–1700	4.44 ± 0.03	(4.40 ± 0.03)	PSI	[3103]
W(111)	–	–	5 × 10⁻⁹	~2000–2400	–	4.45	TE	[352]
W(111)	–	–	≤2 × 10⁻¹⁰	~300	–	4.45	CPD	[1056]
W(111)	–	–	~10⁻¹⁰	77	–	4.45	FE	[3092]
W(111)	–	–	<8 × 10⁻¹⁰	78	–	4.45	FE	[1731]
W(111)	–	–	?	20, 100	–	4.45	FE	[3508]
W(111)	–	–	~10⁻¹⁰	~300	–	4.45 ± 0.02	CPD	[1056,3088]
W(111)	–	–	~10⁻¹⁰	77	–	4.45 ± 0.03	FE	[358,502]
W(111)	–	–	~10⁻¹⁰	78	–	4.45 ± 0.05	FE	[819]
W(111)	–	–	5 × 10⁻¹⁰	~300	–	4.46	FE	[3670]
W(111)	–	–	–	–	–	4.46	TC	[2548]
W(111)	–	–	<2 × 10⁻¹⁰	~300	–	4.47	FE	[489]
W(111)	–	–	–	–	–	4.47	TC	[1159,1980,2129, 3067]
W(111)	–	–	~10⁻¹⁰	77, 300	–	4.47 ± 0.02	FE	[358]
W(111)	–	–	2 × 10⁻¹⁰	~300	–	4.47 ± 0.03	FE	[999]
W(111)	–	–	–	–	–	4.48	TC	[1270]
W(111)	–	–	2 × 10⁻⁹	~1900–2400	–	4.48	TE	[4343]
W(111)	–	–	–	–	–	4.49	TC	[3224]
W(111)	–	–	~10⁻¹⁰	~300	–	4.49	FE	[378]
W(111)	–	–	~10⁻¹⁰	77	–	4.49 ± 0.02	FE	[502]
W(111)	–	–	~10⁻¹¹	78	–	4.49 ± 0.03	FE	[654]
W(111)	Ca	Ca⁺	8 × 10⁻⁹	~2300–2800	4.49 ± 0.04	–	PSI	[145]
W(111)	Sr	Sr⁺	8 × 10⁻⁹	~2300–2800	4.49 ± 0.04	–	PSI	[145]
W(111)	–	–	~10⁻¹⁰	79	–	4.5	FE	[1275]
W(111)	–	–	1 × 10⁻⁸	~1500–1850	–	4.5	TE	[1499]
W(111)	–	–	3 × 10⁻⁹	~300	–	4.5 ± 0.1	FE	[2215]
W(111)	–	–	?	77	–	4.50	FE	[2956,3079,3509]
W(111)	–	–	≤2 × 10⁻¹¹	78	–	4.50	FE	[262]
W(111)	–	–	–	–	–	4.50	TC	[3224]
W(111)	Li	Li⁺	≤2 × 10⁻⁹	~1400–1800	4.50 ± 0.03	(4.40 ± 0.02)	PSI	[88,3542]
W(111)	–	–	–	–	–	4.500	TC	[365]
W(111)	–	–	<5 × 10⁻¹¹	~300	–	4.51	CPD	[1274]
W(111)	–	–	?	~300–1100	–	4.51	FE	[3427]
W(111)	–	–	~10⁻¹¹	~300	–	4.53 ± 0.03*	CPD	[2647]
W(111)	–	–	?	20, 100	–	4.54	FE	[812]
W(111)	–	–	?	~1700–2200	–	4.54	TE	[2187,3664]
W(111)[310]	–	–	~10⁻⁷	~1850–2450	–	4.54 ± 0.01	TE	[1053]
W(111)	–	–	–	–	–	4.55	TC	[357]
W(111)	–	–	<10⁻¹⁰	~300	–	4.55 ± 0.01	FE	[2044]
W(111)	–	–	≤8 × 10⁻¹⁰	~300	–	4.55 ± 0.05	FE	[1689]
W(111)	–	–	~10⁻¹⁰	79	–	4.56	FE	[1275]
W(111)	–	–	≤3 × 10⁻⁹	~1200	–	4.56	FE	[2072]
W(111)	–	–	–	–	–	4.562	TC	[365]
W(111)	–	–	?	80	–	4.57	FE	[1057]
W(111)	–	–	<10⁻¹⁰	~300	–	4.57 ± 0.09	FE	[2044]
W(111)	–	–	<5 × 10⁻¹¹	~300	–	4.58	CPD	[3309]
W(111)	–	–	–	–	–	4.59	TC	[3224]
W(111)	–	–	≤10⁻⁸	~1700–2300	–	4.59 ± 0.03	TE	[1793]
W(111)	–	–	3 × 10⁻⁹ (O₂)	2050	–	4.6	TE	[212]

Table 1 (*continued*)

Surface	Beam	Ion	P_r (Torr)	T (K)	ϕ^+ (eV)	ϕ^e (eV)	Meth.	Refs.
W(111)	–	–	$\sim1 \times 10^{-10}$	~300	–	4.6	FE	[3438]
W(111)	–	–	–	–	–	4.60	TC	[531]
W(111)	–	–	$\leq4 \times 10^{-10}$	~300	–	4.60 ± 0.02	CPD	[582]
W(111)	–	–	$<10^{-8}$	20	–	4.60 ± 0.05	FE	[813]
W(111)	–	–	5×10^{-10} (O_2)	1900	–	4.61	TE	[212]
W(111)	–	–	?	~2100–2200	–	4.61 ± 0.17	TE	[3349]
W(111)	–	–	$<1 \times 10^{-10}$	~300	–	4.62 ± 0.02	FE	[2616]
W(111)	–	–	$\sim10^{-12}$	~300	–	4.64	FE	[3406]
W(111)	–	–	5×10^{-8} (O_2)	2200	–	4.67	TE	[212]
W(111)	–	–	?	15	–	4.68	FE	[653]
W(111)	–	–	$\sim10^{-8}$	?	–	4.73	TE	[3353]
W(111)	–	–	$\leq8 \times 10^{-9}$	~2000–2200	–	4.74 ± 0.15	TE	[1183]
W(111)	–	–	?	15	–	4.78	FE	[653]
W(111)	–	–	$\sim10^{-10}$	79	–	4.8	FE	[1275]
W(111)	–	–	$\sim10^{-11}$	78	–	4.8	FE	[2823]
W(111)	–	–	?	77	–	4.80 ± 0.03	FE	[502]
W(111)	–	–	3×10^{-11}	78, 295	–	4.83 ± 0.38	FE	[354]
W(111)	–	–	$\sim10^{-11}$	20–200	–	4.9	FE	[2218]
W(111)	–	–	$\leq3 \times 10^{-9}$	~1200	–	5.27	FE	[2072]
W(111)	–	–	$\sim10^{-10}$	77	–	5.3	FE	[2714]
W(111)	–	–	–	–	–	5.60	TC	[4117]
Recommended	–	–	–	–	**4.45 ± 0.04**	**4.45 ± 0.03**	–	–
W(112)	Gd	Gd$^+$	$\sim10^{-9}$	~2100–3000	$4.28 \pm 0.02*$	(4.85 ± 0.07)	PSI	[91]
W(112)	–	–	$\leq3 \times 10^{-9}$	~1200	–	4.36	FE	[2072]
W(112)	Yb	Yb$^+$	$\sim10^{-9}$	~1550–2900	$4.38 \pm 0.01*$	(4.85 ± 0.07)	PSI	[91]
W(112)	–	–	2×10^{-9}	~1700–2000	–	4.48	TE	[141]
W(112)	–	–	1×10^{-8}	~1900–2100	–	4.5 ± 0.05	TE	[1663,2012]
W(112)	–	–	2×10^{-8}	~300	–	4.50	PE	[821]
W(112)	–	–	2×10^{-9}	~1700–2000	–	4.51	TE	[141]
W(112)	–	–	$\sim10^{-8}$	~2050–2350	–	4.53 ± 0.05	TE	[3064]
W(112)	–	–	–	–	–	4.57	TC	[3224]
W(112)	–	–	$\leq10^{-10}$	77	–	4.6	FE	[1974]
W(112)	–	–	$\sim10^{-11}$	78	–	4.6 ± 0.4	FE	[2823]
W(112)	–	–	–	–	–	4.60	TC	[4405]
W(112)	–	–	$<5 \times 10^{-11}$	~300	–	4.61	CPD	[1672]
W(112)	–	–	–	–	–	4.64	TC	[3224]
W(112)	–	–	$(<10^{-12})$	~300 (~2500)	–	4.65	FE	[152]
W(112)	–	–	–	–	–	4.66	TC	[3224]
W(112)	–	–	?	~1400–2000	–	4.66 ± 0.02	TE	[149,2706]
W(112)	–	–	1×10^{-9}	~1400–2000	–	4.66 ± 0.02	TE	[150]
W(112)	–	–	$<10^{-8}$	~1800–2200	–	4.67 ± 0.02	TE	[85]
W(112)	–	–	$\sim10^{-10}$	~300	–	4.68	CPD	[2110]
W(112)	–	–	–	–	–	4.69	TC	[4405]
W(112)	–	–	$\sim10^{-11}$	~300	–	$4.69 \pm 0.03*$	CPD	[2647]
W(112)	–	–	3×10^{-8} (O_2)	2200	–	4.7	TE	[212]
W(112)	–	–	$\sim10^{-11}$	78	–	4.7	FE	[2823]
W(112)	–	–	$\sim10^{-10}$	–1600–	–	4.7 ± 0.1	TE	[335,1650,1651, 1967]
W(112)	Gd	Gd$^+$	$\sim10^{-9}$	~2100–2900	$4.70 \pm 0.02*$	(4.85 ± 0.07)	PSI	[91]
W(112)	Er	Er$^+$	$\sim10^{-9}$	~1900–2900	$4.70 \pm 0.02*$	(4.85 ± 0.07)	PSI	[91]
W(112)	–	–	?	2100	–	4.70 ± 0.02	TE	[3349]
W(112)	–	–	6×10^{-6} (Cs)	~1800–2200	–	4.71	TE	[151]
W(112)	–	–	$\sim10^{-10}$	~300	–	4.71 ± 0.05	CPD	[820]
W(112)	–	–	–	–	–	4.72	TC	[1271]
W(112)	–	–	$<5 \times 10^{-11}$	~300	–	4.72	CPD	[1274]
W(112)	Er	Er$^+$	$\sim10^{-9}$	~1800–3300	$4.72 \pm 0.06*$	(4.85 ± 0.07)	PSI	[91]
W(112)	–	–	$\leq3 \times 10^{-10}$	~300	–	4.73 ± 0.02	CPD	[1054]
W(112)	–	–	$\leq8 \times 10^{-10}$	~300	–	4.74 ± 0.05	FE	[1689]
W(112)	–	–	–	–	–	4.75	TC	[531]
W(112)	–	–	$\leq7 \times 10^{-11}$	~300	–	4.75	CPD	[2385]
W(112)	–	–	$<10^{-7}$	~1800–2300	–	4.75 ± 0.03	TE	[371]
W(112)	–	–	$\leq3 \times 10^{-10}$	~300	–	4.75 ± 0.05	FE	[530,3213]
W(112)	–	–	$<2 \times 10^{-10}$	~300	–	4.76	FE	[489]
W(112)	–	–	$\sim10^{-10}$	~300	–	4.77 ± 0.02	CPD	[2106,3088]
W(112)	–	–	$(<10^{-11})$	~300	–	$4.79 \pm 0.05*$	CPD	[2637]
W(112)	–	–	?	?	–	4.8	FE	[1463]
W(112)	–	–	$\sim10^{-11}$	20–200	–	4.8	FE	[2218]
W(112)	–	–	$(\leq10^{-11})$	77	–	4.8	CPD	[2671]
W(112)	–	–	$(\leq10^{-11})$	~300	–	4.80	CPD	[259,379,380,658]

Table 1 (*continued*)

Surface	Beam	Ion	P_r (Torr)	T (K)	ϕ^+ (eV)	ϕ^e (eV)	Meth.	Refs.
W(112)	–	–	$\leq 2 \times 10^{-11}$	78	–	4.80	FE	[262]
W(112)	–	–	$<10^{-10}$	90	–	4.80	FE	[656,926]
W(112)	–	–	$\leq 2 \times 10^{-9}$	~1700–2000	–	4.80 ± 0.05	TE	[127,143,144]
W(112)	–	–	$\sim 10^{-11}$	78	–	4.80 ± 0.05	FE	[654]
W(112)	–	–	–	–	–	4.800	TC	[365]
W(112)	–	–	–	–	–	4.811	TC	[365]
W(112)	–	–	$\leq 3 \times 10^{-9}$	~1200	–	4.82	FE	[2072]
W(112)	–	–	(1×10^{-10})	~300	–	4.82 ± <0.06	FE	[1529,4237]
W(112)	–	–	$\sim 10^{-10}$	77	–	4.84 ± 0.06	FE	[502]
W(112)	–	–	$(<10^{-11})$	78	–	4.85	FE	[267]
W(112)	–	–	–	–	–	4.85	TC	[3224]
W(112)	–	–	3×10^{-11}	78	–	4.85	FE	[822]
W(112)	–	–	$\sim 10^{-10}$	~300	–	4.85	FE	[2324]
W(112)	–	–	$\sim 10^{-9}$	~1700–2450	(4.28–4.72)	4.85 ± 0.07	TE	[91]
W(112)	–	–	$(<10^{-11})$	78	–	4.87	FE	[809]
W(112)	–	–	$(<10^{-12})$	~300 (~1700)	–	4.88	FE	[152]
W(112)	–	–	$<1 \times 10^{-11}$	78	–	4.88	FE	[373]
W(112)	–	–	3×10^{-11}	78, 295	–	4.89 ± 0.15	FE	[354]
W(112)	–	–	?	?	–	4.9 ± 0.2	FE	[3033]
W(112)	–	–	$\sim 10^{-10}$	77	–	4.90	FE	[3092]
W(112)	–	–	$(<1 \times 10^{-11})$	~300	–	4.90 ± 0.02	FE	[2254]
W(112)	–	–	$\leq 3 \times 10^{-9}$	~1200	–	4.91	FE	[2072]
W(112)	–	–	?	77	–	4.91	FE	[2956,3079]
W(112)	–	–	$\leq 3 \times 10^{-9}$	~1200	–	4.93	FE	[2072]
W(112)	–	–	$\sim 10^{-10}$	77	–	4.93 ± 0.01	FE	[502]
W(112)	–	–	–	–	–	4.94	TC	[1159,1980,2129, 3067]
W(112)	–	–	$\sim 10^{-9}$	77	–	4.95	FE	[363,810,811,2766]
W(112)	–	–	$\sim 10^{-10}$	~300	–	4.95	FE	[378]
W(112)	–	–	3×10^{-10}	~300	–	4.97 ± 0.05	FE	[999]
W(112)	–	–	?	20, 100	–	4.98	FE	[812]
W(112)	–	–	$<2 \times 10^{-10}$	78	–	5.0 ± 0.1	FE	[1674,2253]
W(112)	–	–	$\sim 10^{-10}$	77	–	5.00	FE	[502]
W(112)	–	–	?	~300–1100	–	5.01	FE	[3426]
W(112)	–	–	?	15	–	5.02	FE	[653]
W(112)	–	–	3×10^{-10}	~300	–	5.03 ± 0.02	FE	[999]
W(112)	–	–	?	15	–	5.04	FE	[653]
W(112)	–	–	$\sim 10^{-10}$	77	–	5.05 ± 0.05	FE	[502]
W(112)	–	–	$<10^{-8}$	20	–	5.05 ± 0.05	FE	[813]
W(112)	–	–	?	80	–	5.08	FE	[1057]
W(112)	–	–	$\sim 10^{-10}$	77	–	5.1	FE	[2714]
W(112)	–	–	$\sim 10^{-10}$	78	–	5.12 ± 0.07	FE	[819]
W(112)	–	–	3×10^{-10}	~300	–	5.14 ± 0.05	FE	[999]
W(112)	–	–	$\sim 10^{-10}$	79	–	5.18	FE	[1275]
W(112)	–	–	5×10^{-10}	~1500–1900	–	5.20	TE	[90]
W(112)	–	–	?	~1800–2300	–	5.3	TE	[1958]
Recommended	–	–	–	–	**4.70 ± 0.01**	**4.78 ± 0.03**	–	–
W(113)	–	–	2×10^{-9}	~1500–2000	–	4.15 ± 0.07	TE	[2468]
W(113)	–	–	$\leq 4 \times 10^{-10}$	~1450–2000	–	4.18 ± 0.04	CPD	[195]
W(113)	–	–	$\leq 4 \times 10^{-10}$	~1450–2000	–	4.235 ± 0.04	TE	[195]
W(113)	–	–	–	–	–	4.27	TC	[3224]
W(113)	–	–	–	–	–	4.35	TC	[3224]
W(113)	–	–	–	–	–	4.36	TC	[3224]
W(113)	–	–	–	–	–	4.37	TC	[3224]
W(113)	–	–	$\sim 10^{-10}$	78	–	4.46 ± 0.05	FE	[819]
W(113)	–	–	5×10^{-10}	~300	–	4.50	TE	[376]
W(113){nearly}	Sr	Sr$^+$	$\sim 10^{-9}$	~2400–2800	4.52 ± 0.03	–	PSI	[138]
W(113)	–	–	$\sim 10^{-10}$	~300	–	4.54	PE	[1060,1848,1849]
W(113)	–	–	$\sim 10^{-10}$	~300	–	4.55 ± 0.05	CPD	[820]
W(113)	–	–	$<5 \times 10^{-9}$	~300	–	4.57	CPD	[138]
W(113)	–	–	$\leq 10^{-9}$	~1600–2400	–	4.58	TE	[1225,1282]
W(113)	–	–	$<5 \times 10^{-10}$	~300	–	4.59 ± 0.01	CPD	[2471]
W(113)	–	–	$<2 \times 10^{-10}$	~300	–	4.65	CPD	[1056]
W(113)	La	La$^+$	$\sim 10^{-9}$	~2400–2800	4.79 ± 0.05	–	PSI	[138]
W(113)	–	–	1×10^{-10}	~300	–	4.82	PE	[1226]
Recommended	–	–	–	–	–	**4.43 ± 0.09**	–	–
W(114)	–	–	?	?	–	4.31	FE	[1283]
W(114)	–	–	–	–	–	4.32	TC	[3224]

Table 1 (*continued*)

Surface	Beam	Ion	P_r (Torr)	T (K)	ϕ^+ (eV)	ϕ^e (eV)	Meth.	Refs.
W(114)	–	–	$\sim 10^{-10}$	79	–	4.40	FE	[1275]
W(114)	–	–	–	–	–	4.40	TC	[3224]
W(114)	–	–	$\sim 10^{-10}$	$\sim 1800–2200$	–	4.40 ± 0.05	TE	[820,2134]
W(114)	–	–	–	–	–	4.42	TC	[3224]
W(114)	–	–	$\sim 10^{-10}$	$\sim 1100–1360$	–	4.42 ± 0.02	TE	[1394,1854]
W(114)	–	–	$\sim 10^{-10}$	78	–	4.42 ± 0.05	FE	[819]
W(114)[288]	–	–	$<5 \times 10^{-10}$	77	–	4.42 ± 0.05	CPD	[920]
W(114)	–	–	–	–	–	4.44	TC	[3224]
W(114)	–	–	$\sim 10^{-10}$	79	–	4.48	FE	[1275]
W(114)	–	–	$\sim 10^{-11}$	20–200	–	4.8	FE	[2218]
Recommended	–	–	–	–	–	**4.40 ± 0.03**	–	–
W(115)	–	–	?	77	–	4.3	FE	[3079]
W(115)	–	–	$\sim 10^{-10}$	~ 300	–	4.35 ± 0.05	CPD	[820]
W(115)	–	–	$<5 \times 10^{-11}$	~ 300	–	4.43	CPD	[1274]
W(115)	–	–	$\sim 10^{-11}$	~ 300	–	4.46 ± 0.03*	CPD	[2647]
W(116)	–	–	–	–	–	4.10	TC	[4405]
W(116)	–	–	–	–	–	4.121	TC	[365]
W(116)	–	–	–	–	–	4.152	TC	[365]
W(116)	–	–	?	?	–	4.2	FE	[1463]
W(116)	–	–	?	78	–	4.20	FE	[679]
W(116)	–	–	3×10^{-10}	~ 300	–	4.21 ± 0.05	FE	[530]
W(116)	–	–	–	–	–	4.250	TC	[365]
W(116)	–	–	2×10^{-9}	$\sim 1700–2000$	–	4.26	TE	[141]
W(116)	–	–	$\sim 10^{-10}$	79	–	4.26	FE	[1275]
W(116)	–	–	?	?	–	4.26	FE	[1284]
W(116)	–	–	–	–	–	4.27	TC	[3224]
W(116)	–	–	?	?	–	4.3	FE	[1964]
W(116)	–	–	$\sim 10^{-10}$	77	–	4.3	FE	[2714]
W(116)	–	–	1×10^{-8}	$\sim 1900–2100$	–	4.3 ± 0.05	TE	[1663,2012]
W(116)	–	–	$\sim 10^{-10}$	–1600–	–	4.3 ± 0.1	TE	[335,1650,1651, 1967]
W(116)	–	–	5×10^{-10}	~ 300	–	4.30	FE	[376]
W(116)	–	–	–	–	–	4.30	TC	[4405]
W(116)	–	–	$(<10^{-12})$	~ 300	–	4.30	FE	[152]
W(116)	–	–	$\sim 1 \times 10^{-9}$	$\sim 1350–2050$	–	4.30 ± 0.01	TE	[150]
W(116)	–	–	$\sim 10^{-8}$	$\sim 2050–2350$	–	4.30 ± 0.03	TE	[372,3064]
W(116)	–	–	$\leq 2 \times 10^{-9}$	$\sim 1700–2000$	–	4.32 ± 0.02	TE	[127,144]
W(116)	–	–	$\sim 10^{-10}$	77	–	4.32 ± 0.04	FE	[502]
W(116)	–	–	1×10^{-8}	$\sim 1900–2100$	–	4.32 ± 0.05	TE	[1663,2012]
W(116)	–	–	$\sim 10^{-10}$	78	–	4.32 ± 0.06	FE	[819]
W(116)	–	–	$\sim 10^{-10}$	~ 300	–	4.34	FE	[4237]
W(116)	–	–	–	–	–	4.35	TC	[3224]
W(116)	–	–	?	$\sim 1400–2000$	–	4.35 ± 0.02	TE	[149,2706]
W(116)	–	–	–	–	–	4.36	TC	[3224]
W(116)	–	–	$\sim 10^{-10}$	~ 300	–	4.36 ± 0.05	CPD	[820]
W(116)	–	–	2×10^{-9}	$\sim 1700–2000$	–	4.37	TE	[141]
W(116)	–	–	?	77	–	4.41 ± 0.04	FE	[502]
W(116)	–	–	–	–	–	4.47	TC	[1159,1980,2129, 3067]
Recommended	–	–	–	–	–	**4.30 ± 0.04**	–	–
W(119)	–	–	$\sim 10^{-10}$	~ 300	–	4.56 ± 0.05	CPD	[820]
W(120)	–	–	–	–	–	4.308	TC	[365]
W(120)	–	–	–	–	–	4.31	TC	[3224]
W(120)	–	–	$\leq 1 \times 10^{-10}$	78	–	4.32	FE	[1278]
W(120)	–	–	–	–	–	4.320	TC	[365]
W(120)	–	–	?	?	–	4.33	FE	[1283]
W(120)	–	–	?	~ 300	–	4.33	FE	[3581]
W(120)	–	–	$(<10^{-12})$	~ 300	–	4.34	FE	[152]
W(120)	–	–	(1×10^{-10})	~ 300	–	4.35 ± <0.06	FE	[1529]
W(120)	–	–	$\leq 1 \times 10^{-10}$	~ 300	–	4.36 ± 0.01	FE	[1278]
W(120)	–	–	$\sim 10^{-10}$	78	–	4.36 ± 0.04	FE	[819]
W(120)	–	–	?	~ 300	–	<4.39	FE	[1766]
W(120)	–	–	–	–	–	4.39	TC	[3224]
W(120)	–	–	?	20, 100	–	4.40	FE	[812]
W(120)	–	–	–	–	–	4.40	TC	[3224]
W(120)	–	–	–	–	–	4.404	TC	[365]

Table 1 (*continued*)

Surface	Beam	Ion	P_r (Torr)	T (K)	ϕ^+ (eV)	ϕ^e (eV)	Meth.	Refs.
W(120)	–	–	–	–	–	4.42	TC	[3224]
W(120)	–	–	?	20, 100	–	4.45	FE	[3508]
W(120)	–	–	?	~300–1100	–	4.46	FE	[3426]
W(120)	–	–	<10⁻⁸	20	–	4.46 ± 0.05	FE	[813]
W(120)	–	–	≤8 × 10⁻⁹	~2200–2450	–	4.47 ± 0.01	TE	[2340]
W(120)	–	–	≤8 × 10⁻⁹	~2200–2450	–	4.54 ± 0.05	TE	[2340]
W(120)	–	–	?	?	–	5.76	FE	[1964]
Recommended	–	–	–	–	–	**4.38 ± 0.05**	–	–
W(122)	–	–	–	–	–	4.133	TC	[365]
W(122)	–	–	–	–	–	4.162	TC	[365]
W(122)	–	–	–	–	–	4.259	TC	[365]
W(122)	–	–	–	–	–	4.29	TC	[3224]
W(122)	–	–	~10⁻¹⁰	78	–	4.30 ± 0.04	FE	[819]
W(122)	–	–	(<10⁻¹²)	~300	–	4.35	FE	[152]
W(122)	–	–	–	–	–	4.37	TC	[3224]
W(122)	–	–	(<10⁻¹¹)	78	–	4.37	FE	[809]
W(122)	–	–	–	–	–	4.38	TC	[3224]
W(122)	–	–	–	–	–	4.39	TC	[3224]
W(122)	–	–	?	~300–1100	–	4.40	FE	[3427]
W(122)	–	–	?	~300–1100	–	4.47	FE	[3426]
W(122)	–	–	<10⁻⁹	~300	–	4.5	FE	[2354]
Recommended	–	–	–	–	–	**4.34 ± 0.05**	–	–
W(123)	–	–	–	–	–	4.31	TC	[4405]
W(123)	–	–	–	–	–	4.37	TC	[3224]
W(123)	–	–	–	–	–	4.41	TC	[4405]
W(123)	–	–	–	–	–	4.433	TC	[365]
W(123)	–	–	–	–	–	4.442	TC	[365]
W(123)	–	–	–	–	–	4.45	TC	[3224]
W(123)	–	–	–	–	–	4.47	TC	[3224]
W(123)[290]	–	–	≤4 × 10⁻¹¹	~1200	–	4.50	FE	[2045]
W(123)	–	–	~10⁻¹⁰	78	–	4.50 ± 0.06	FE	[819]
W(123)	–	–	–	–	–	4.511	TC	[365]
W(123)	–	–	(<10⁻¹²)	~300	–	4.52	FE	[152]
W(123)	–	–	–	–	–	4.53	TC	[3224]
W(123)	–	–	~10⁻¹⁰	79	–	4.56	FE	[1275]
W(123)	–	–	?	~300–1100	–	4.58	FE	[3426]
W(123)	–	–	~10⁻¹⁰	79	–	4.61	FE	[1275]
W(123)	–	–	–	–	–	4.77	TC	[1271]
W(123)[290]	–	–	≤4 × 10⁻¹¹	80–400	–	4.90 ± 0.03	FE	[2045]
Recommended	–	–	–	–	–	**4.50 ± 0.05**	–	–
W(124)	–	–	–	–	–	4.25	TC	[3224]
W(124)	–	–	–	–	–	4.33	TC	[3224]
W(124)	–	–	?	~300–1100	–	4.33	FE	[3426]
W(124)	–	–	–	–	–	4.34	TC	[3224]
W(124)	–	–	~10⁻¹⁰	78	–	4.35 ± 0.05	FE	[819]
W(124)	–	–	–	–	–	4.35	TC	[3224]
Recommended	–	–	–	–	–	**4.33 ± 0.03**	–	–
W(130)	–	–	~10⁻¹⁰	77	–	4.16 ± 0.03	FE	[502]
W(130)	–	–	~10⁻¹⁰	77	–	4.21 ± 0.01	FE	[502]
W(130)	–	–	≤8 × 10⁻⁹	~2200–2450	–	4.24 ± 0.05	TE	[2340]
W(130)	–	–	3 × 10⁻¹¹	78, 295	–	4.25	FE	[354]
W(130)	–	–	<2 × 10⁻¹⁰	~300	–	4.25	FE	[489]
W(130)	–	–	?	?	–	4.27	FE	[1283]
W(130)	–	–	≤8 × 10⁻⁹	~2200–2450	–	4.28 ± 0.01	TE	[2340]
W(130)	–	–	~10⁻¹⁰	77	–	4.28 ± 0.01	FE	[502]
W(130)	–	–	~1 × 10⁻¹⁰	~300	–	4.3	FE	[3438]
W(130)	–	–	~10⁻¹⁰	~300–1500	–	4.30	FE	[1783]
W(130)	–	–	–	–	–	4.30	TC	[4405]
W(130)	–	–	<10⁻¹⁰	90	–	4.30	FE	[656,926]
W(130)	–	–	(<10⁻¹²)	~300	–	4.31	FE	[152]
W(130)	–	–	2 × 10⁻⁹	~300	–	4.31 ± 0.07	CPD	[2468]
W(130)	–	–	~10⁻¹⁰	77	–	4.32 ± 0.05	FE	[502]
W(130)	–	–	~10⁻¹⁰	77	–	4.34 ± 0.02	FE	[502]
W(130)	–	–	~10⁻¹⁰	78	–	4.34 ± 0.04	FE	[819]
W(130)	–	–	5 × 10⁻¹⁰	~300	–	4.35	FE	[376]
W(130)	–	–	2 × 10⁻¹⁰	~300	–	4.35	FE	[3992]

Table 1 (*continued*)

Surface	Beam	Ion	P_r (Torr)	T (K)	ϕ^+ (eV)	ϕ^e (eV)	Meth.	Refs.
W(130)	–	–	2×10^{-8}	~300	–	4.35	PE	[821]
W(130)	–	–	?	?	–	4.35	FE	[1284]
W(130)	–	–	~10^{-11}	78	–	4.35	FE	[2823]
W(130)	–	–	?	~300	–	4.35 ± 0.05	FE	[2484]
W(130)	–	–	–	–	–	4.37	TC	[3224]
W(130)	–	–	<5×10^{-10}	77	–	4.4	FE	[3114]
W(130)	–	–	~10^{-10}	77	–	4.40 ± 0.13	FE	[502]
W(130)	–	–	2×10^{-10}	~300	–	4.45	FE	[4296]
W(130)	–	–	–	–	–	4.45	TC	[3224]
W(130)	–	–	–	–	–	4.46	TC	[1271]
W(130)	–	–	–	–	–	4.46	TC	[3224]
W(130)	–	–	<2×10^{-10}	78	–	4.48	FE	[1674,2253]
W(130)	–	–	?	77	–	4.5	FE	[3079]
W(130)	–	–	–	–	–	4.52	TC	[3224]
W(130)	–	–	3×10^{-11}	78, 295	–	5.19 ± 0.16	FE	[354]
Recommended	–	–	–	–	–	**4.32 ± 0.04**	–	–
W(133)	–	–	~10^{-10}	78	–	4.68 ± 0.07	FE	[819]
W(134)	–	–	~10^{-10}	78	–	4.74 ± 0.07	FE	[819]
W(144)	–	–	<10^{-10}	295	–	5.15	FE	[1276]
W(144)	–	–	<10^{-10}	79	–	5.25	FE	[1276]
W(150)	–	–	<10^{-10}	~300	–	4.43 ± 0.01	FE	[2044]
W(160)	–	–	5×10^{-10}	~300	–	4.31	FE	[3670]
W(160)	–	–	~10^{-10}	78	–	4.43 ± 0.04	FE	[819]
W(160)	–	–	<8×10^{-10}	78	–	4.45	FE	[1731]
W(223)	–	–	~10^{-10}	78	–	4.70 ± 0.05	FE	[819]
W(227)	–	–	~10^{-10}	~300	–	4.43 ± 0.05	CPD	[820]
W(229)	–	–	~10^{-10}	~300	–	4.34 ± 0.05	CPD	[820]
W(230)	–	–	–	–	–	4.26	TC	[3224]
W(230)	–	–	(1×10^{-10})	~300	–	4.29 ± <0.06	FE	[1529]
W(230)	–	–	~10^{-10}	~300	–	4.31	FE	[4237]
W(230)	–	–	–	–	–	4.34	TC	[3224]
W(230)	–	–	–	–	–	4.35	TC	[3224]
W(230)	–	–	–	–	–	4.36	TC	[3224]
W(230)	–	–	~10^{-10}	77	–	4.4	FE	[2714]
W(230)	–	–	~10^{-10}	78	–	4.58 ± 0.06	FE	[819]
Recommended	–	–	–	–	–	**4.33 ± 0.05**	–	–
W(233)	–	–	–	–	–	4.277	TC	[365]
W(233)	–	–	–	–	–	4.291	TC	[365]
W(233)	–	–	–	–	–	4.33	TC	[3224]
W(233)	–	–	–	–	–	4.36	TC	[4405]
W(233)	–	–	–	–	–	4.378	TC	[365]
W(233)	–	–	–	–	–	4.41	TC	[3224]
W(233)	–	–	~10^{-10}	78	–	4.41 ± 0.05	FE	[819]
W(233)	–	–	–	–	–	4.42	TC	[3224]
W(233)	–	–	–	–	–	4.45	TC	[3224]
W(233)	–	–	$(<10^{-12})$	~300	–	4.46	FE	[152]
Recommended	–	–	–	–	–	**4.38 ± 0.06**	–	–
W(235)[290]	–	–	≤4×10^{-11}	~1200	–	4.30	FE	[2045]
W(235)[290]	–	–	≤4×10^{-11}	~80–400	–	4.72 ± 0.05	FE	[2045]
W(250)	–	–	~10^{-10}	~300	–	4.55 ± 0.05	CPD	[820]
W(257)[290]	–	–	≤4×10^{-11}	~1200	–	4.80	FE	[2045]
W(257)[290]	–	–	≤4×10^{-11}	~80–900	–	5.00 ± 0.01	FE	[2045]
W(334)	–	–	<10^{-10}	295	–	4.20	FE	[1276]
W(334)	–	–	~10^{-10}	78	–	4.62 ± 0.04	FE	[819]
W(650)	–	–	–	–	–	4.24	TC	[3224]

Table 1 (*continued*)

Surface	Beam	Ion	P_r (Torr)	T (K)	ϕ^+ (eV)	ϕ^e (eV)	Meth.	Refs.
W(650)	–	–	–	–	–	4.30	TC	[3224]
W(650)	–	–	–	–	–	4.32	TC	[3224]
W(650)	–	–	–	–	–	4.33	TC	[3224]
W(650)	–	–	$<8 \times 10^{-9}$	~2200–2450	–	4.67 ± 0.03	TE	[2340]
W	–	(W$^+$)	6×10^{-9}	~2900–3000	2.6 ± 0.2	–	PSI	[924]
W	–	–	–	–	–	2.80	TC	[2493]
W	–	–	–	–	–	2.85	TC	[2493]
W(fp)[291]	–	–	–	–	–	3.65	TC	[2973]
W	–	–	$<10^{-10}$	78	–	3.8*	FE	[2695]
W(fp)[291]	–	–	–	–	–	3.80	TC	[2973]
W	–	–	–	–	–	3.91	TC	[521]
W	–	–	$<4 \times 10^{-11}$	~300	–	4.0	FE	[3809]
W	–	–	$<10^{-8}$	~2200–2400	–	4.10 ± 0.20	TE	[1062]
W(porous)	Cs	Cs$^+$	?	~1150–1250	4.2	–	PSI	[3764]
W	–	–	–	–	–	4.2	TC	[1993]
W[292]	–	–	$\sim10^{-9}$	~300	–	4.2	FE	[1493]
W[292]	–	–	$\sim10^{-9}$	~300	–	4.25	FE	[1493]
W	–	–	?	?	–	4.31	TE	[2455]
W/glass[293]	W	–	$\sim10^{-10}$	77–90	–	4.33	PE	[3049]
W{46.3%(310)}[411]	–	–	–	–	(4.96 ± 0.03)	4.34 ± 0.05	TC	[630]
W[292]	–	–	$\sim10^{-9}$	~300	–	4.35	FE	[1493]
W	–	–	$\leq10^{-6}$	~1600–1800	–	4.35	TE	[2301]
W/glass	W	–	$\sim10^{-10}$	77–90	–	4.35	PE	[3052]
W	–	–	–	–	–	4.36	TC	[2005]
W/glass[293]	W	–	$<10^{-9}$	77–90	–	4.36	PE	[2095]
W	–	–	?	~300	–	4.38	CPD	[2297]
W{46.3%(310)}[411]	–	–	–	–	(4.99 ± 0.06)	4.38 ± 0.05	TC	[2453]
W	–	–	$(<10^{-13})$	21	–	4.4	CPD	[3504]
W	–	–	?	~300	–	4.4	FE	[3987]
W	–	–	–	–	–	4.40	TC	[3637]
W	–	–	–	–	–	4.40	TC	[2707]
W	–	–	–	–	–	4.40	TC	[2949]
W(fp)[291]	–	–	–	–	–	4.40	TC	[2973]
W	–	–	–	–	–	4.40	TC	[4441]
W	–	–	?	~1400–2000	–	4.40	TE	[3020]
W	–	–	$<10^{-8}$	~1900–2400	–	4.40 ± 0.05	TE	[1858]
W	–	–	$\sim10^{-8}$	~300	–	4.41	PE	[4340]
W	–	–	–	–	–	4.41	TC	[298]
W	U	U$^+$	$<1 \times 10^{-7}$	~2800–2950	4.41 ± 0.08	–	PSI	[80]
W	–	–	–	–	–	4.42	TC	[1066]
W[294]	–	–	12 (Ar)	~300	–	4.42 ± 0.02	PE	[621]
W	–	–	2×10^{-7}	~2000–2200	(5.09, 5.23)	4.42 ± 0.02	TE	[36]
W	–	–	$\leq10^{-10}$	~300	–	4.44	FE	[392]
W	–	–	$<5 \times 10^{-10}$	77, ~300	–	4.45	FE	[3822]
W	–	–	$\sim10^{-9}$	?	–	4.45 ± 0.05	TE	[1775]
W(1% oxides)	–	–	?	~1350–2200	–	4.456 ± 0.006	TE	[660]
W	–	–	–	–	–	4.46	TC	[3224]
W{25%(110)}[295]	–	–	–	2000	(5.12*)	4.46*	TC	[3844]
W	–	–	$\sim6 \times 10^{-10}$	~1400–1700	–	4.46	TE	[2089,2092]
W	CsCl	Cl$^-$	?	~2300–2600	4.46*[N]	–	NSI	[574]
W	–	–	$\sim10^{-8}$	~1600–2100	–	4.46 ± 0.09	TE	[1880,1882]
W	–	–	$\sim10^{-10}$	–1600–	–	4.47	TE	[335,1650,1651, 1967]
W	–	–	? (Cs)	~1200–2000	–	4.47	TE	[650]
W	–	–	$<6 \times 10^{-10}$	1080–1400	–	4.47 ± 0.01	TE	[161]
W/W(110)[309]	WCl$_6$, H$_2$	–	$\sim10^{-7}$	~1850–2450	–	4.47 ± 0.01	TE	[1053]
W	–	–	2×10^{-7}	~2000–2200	(5.23 ± 0.03)	4.47 ± 0.04	TE	[37]
W	–	–	?	~1400–1900	–	4.48	TE	[393]
W	–	–	5×10^{-7}	2270	–	4.48	TE	[1746]
W	–	–	2×10^{-7}	~2000–2100	(5.20 ± 0.05)	4.48 ± 0.06	TE	[23]
W/glass	W	–	?	293 (351)	–	4.49 ± 0.03	CPD	[2573]
W/glass	W	–	?	351 (428)	–	4.49 ± 0.03	CPD	[2573]
W	KCl	Cl$^-$	?	~2300–2600	4.49*[N]	–	NSI	[574]
W	KI	I$^-$	?	~2300–2550	4.49*[N]	–	NSI	[574]
W[299]	I	I$^-$	$\sim10^{-7}$	1980	4.49*[N]	(4.51)	NSI	[827]
W	–	–	2×10^{-8}	~300–1040	–	4.49 ± 0.02	PE	[826]
W[170,296]	–	(W$^+$)	$<10^{-6}$	~2800–3000	4.49 ± 0.14	(4.59 ± 0.04)	PSI	[823]
W	–	–	$\sim10^{-9}$	~1800–2600	–	4.5	TE	[394]
W[297]	–	(W$^-$)	?	~2200–2300	4.5*[N]	–	NSI	[966]

Table 1 (*continued*)

Surface	Beam	Ion	P_r (Torr)	T (K)	ϕ^+ (eV)	ϕ^e (eV)	Meth.	Refs.
W	–	–	–	–	–	4.5	TC	[1561]
W{95%(100)}[302]	–	–	? (Cs)	~1600–2400	–	4.5	TE	[3414]
W	–	–	–	–	–	4.5	TC	[1645]
W	–	–	~700 (Ar)	~3500	–	4.5	TE	[2007]
W	–	–	~10^{-10}	~2000–2800	–	4.5	TE	[2098]
W	–	–	?	~1400–2000	–	4.5	TE	[3020]
W	–	–	? (Cs)	~1200–1800	–	4.5	TE	[3414]
W[298]	–	–	≤2 × 10^{-9}	~1500–2500	–	4.5 ± 0.07	TE	[3533]
W	–	–	~10^{-6}	~1800	–	4.5 ± 0.1	TE	[1779]
W	–	–	5 × 10^{-10}	~300	–	4.50	FE	[3670]
W	–	–	<10^{-11}	78	–	4.50	FE	[267]
W/Mo	WF$_6$	–	5 × 10^{-9}	~2000–2200	–	4.50	TE	[352,4343]
W	–	–	–	–	–	4.50	TC	[3224]
W	–	–	–	–	–	4.50	TC	[2583]
W	–	–	~10^{-9}	?	–	4.50	TE	[3096]
W	–	–	?	?	–	4.50	TE	[3402]
W	–	–	~10^{-7}	?	–	4.50	TE	[3523]
W	–	–	≤5 × 10^{-10}	20	–	4.50 ± <0.02	FE	[3862]
W/glass	W	–	?	77 (293)	–	4.50 ± 0.04	CPD	[2573]
W	–	–	≤10^{-9}	1150–2200	–	4.50 ± 0.05	TE	[650]
W	–	–	5 × 10^{-8}	~1000–1500	–	4.51	TE	[395]
W{25%(110)}[295]	Cs	Cs$^+$	–	2000	4.51	–	TC	[3843]
W	RbCl	Cl$^-$	?	~2300–2600	4.51*N	–	NSI	[574]
W[299]	–	–	~10^{-7}	~1300–2000	(4.51*N)	4.51	TE	[827]
W[299]	I$_2$	I$^-$	~10^{-7}	1940	4.51*N	(4.51)	NSI	[827]
W/W(100)[309]	WF$_6$, H$_2$	–	~10^{-7}	1850–2450	–	4.51 ± 0.01	TE	[1053]
W	K	K$^+$	?	1350–2170	4.514 ± 0.002	–	PSI	[158]
W	–	–	?	~1200–2000	–	4.515	TE	[2705]
W	–	–	?	1350–2200	–	4.519	TE	[660]
W	–	–	–	–	–	4.52	TC	[3224]
W	–	–	~10^{-9}	~300	–	4.52	PE	[1609]
W	–	–	?	~1500–1900	–	4.52	TE	[1372]
W	–	–	?	?	–	4.52	TE	[1450]
W	–	–	5 × 10^{-7}	2270	–	4.52	TE	[1746]
W	–	–	3 × 10^{-9}	?	–	4.52	TE	[159]
W	–	–	5 × 10^{-10}	~300	–	4.52	FE	[1853]
W	–	–	–	–	–	4.52	TC	[2456]
W	–	–	<10^{-6}	~300	–	4.52	PE	[2919]
W	–	–	? (Cs)	~1200–1400	–	4.52	TE	[3752]
W	–	–	?	~1600–2000	–	4.52	TE	[2925,2926]
W{95%(100)}[302]	–	–	~10^{-9}	?	–	4.52	TE	[3414]
W	–	–	<10^{-6}	?	–	4.52 ± 0.01	TE	[2919]
W	–	–	<8 × 10^{-10}	77	–	4.52 ± 0.04	CPD	[920]
W	Rb	Rb$^+$	?	1150–1450	4.52 ± 0.05	–	PSI	[2107]
W{95%(100)}[300]	–	–	~10^{-9}	1150–2200	–	4.52 ± 0.07	TE	[124]
W{96%(100)}[300]	–	–	~10^{-9}	1150–2200	–	4.52 ± 0.07	TE	[124]
W	–	–	<2 × 10^{-9}	~1050–1250	–	4.52 ± 0.09	TE	[2241]
W{<35%(110)}	–	–	–	–	(5.09 ± 0.10)	4.52 ± 0.12	TC	[283,630]
W	–	–	?	~1350–2200	–	4.529	TE	[660]
W	–	–	6 × 10^{-9}	~300	–	4.53	PE	[1139]
W	–	–	?	?	–	4.53	TE	[1486]
W	–	–	≤10^{-7}	O^E (~1850)	–	4.53	TE	[1878]
W[174]	–	–	–	O^E	–	4.53	TC	[1747]
W	–	–	≤10^{-6}	~1600–1800	–	4.53	TE	[2305]
W	–	–	? (Cs)	2300	–	4.53	TE	[2341]
W/glass	–	–	~10^{-10}	90 (403)	–	4.53	PE	[3049]
W	–	–	?	~2400–2500	–	4.53 ± 0.01	TE	[2204]
W	–	–	?	~1500–2200	–	4.53 ± 0.02	TE	[792]
W	–	–	?	?	–	4.53 ± 0.05	TE	[2209]
W	–	–	~10^{-7}	O^E (~1700)	–	4.53 ± 0.07	TE	[3326]
W	–	–	?	1577	–	4.539	TE	[661]
W	–	–	–	–	–	4.54	TC	[3224]
W	–	–	~10^{-9}	?	–	4.54	TE	[979]
W	SF$_6$	SF$_6^-$	2 × 10^{-6}	~1400–1700	4.54N	–	NSI	[586]
W	–	–	~10^{-9}	>1200	–	4.54	TE	[1203]
W	–	–	?	~1100–1700	–	4.54	TE	[1949]
W	Cs	Cs$^+$	?	~1400–1800	4.54	–	PSI	[2109]
W	–	–	?	1970	–	4.54	TE	[2121]
W/glass	–	–	?	O^E (295)	–	4.54	PE	[3392]
W	–	–	?	2300–2450	–	4.54	TE	[3842]

Table 1 (*continued*)

Surface	Beam	Ion	P_r (Torr)	T (K)	ϕ^+ (eV)	ϕ^e (eV)	Meth.	Refs.
W[303]	–	–	–	~300	–	4.54$_5$	TC	[828]
W	–	–	5×10^{-9}	~2000–2400	–	4.55	TE	[352]
W	–	–	–	1800	–	4.55	TC	[471]
W	–	–	? (Cs, Ba)	~1600–2000	–	4.55	TE	[1485]
W	–	–	$\sim10^{-8}$	~1600–2300	–	4.55	TE	[1776]
W(foil)	–	–	$\leq 2 \times 10^{-10}$	~300	–	4.55	CPD	[1781]
W/glass	W	–	$\leq 2 \times 10^{-10}$	~300	–	4.55	CPD	[1781]
W	–	–	?	?	–	4.55	TE	[2233]
W	RbCl	Rb$^+$	?	?	4.55	–	PSI	[2306]
W	–	–	?	~1200–1500	–	4.55	TE	[2928]
W/glass[293]	W	–	$\sim10^{-10}$	293 (403)	–	4.55	PE	[3049]
W	–	–	–	–	–	4.55	TC	[3264,3265,3267]
W	–	–	$<6 \times 10^{-10}$	~1100–1400	–	4.55 ± 0.01	TE	[161]
W	–	–	$\leq 3 \times 10^{-10}$	~300	–	4.55 ± 0.01	CPD	[194]
W	–	–	$<5 \times 10^{-10}$	~1800–2500	–	4.55 ± 0.01	TE	[232]
W/glass	W	–	$\sim10^{-8}$	~300	–	4.55 ± 0.02	CPD	[133,349]
W	Ag	Ag$^+$	3×10^{-6}(O$_2$)	~2500–2800	4.55 ± 0.1	–	PSI	[3408,3409]
W	Ag	Ag$^+$	$<10^{-7}$(O$_2$)	~2300–2600	4.55 ± 0.1	–	PSI	[3408,3409]
W	Cu	Cu$^+$	3×10^{-6}(O$_2$)	~2500–2800	4.55 ± 0.1	–	PSI	[3408,3409]
W	Cu	Cu$^+$	$<10^{-7}$(O$_2$)	~2300–2600	4.55 ± 0.1	–	PSI	[3408,3409]
W	–	–	?	1577	–	4.556	TE	[661]
W	–	–	?	~1350–2200	–	4.557	TE	[660]
W	–	–	?	~1700–2200	–	4.56	TE	[2187,3664]
W	–	–	–	–	–	4.56	TC	[3318]
W	–	–	–	–	–	4.56	TC	[3224]
W	–	–	$<2 \times 10^{-9}$	~1700–2300	–	4.56	TE	[662]
W	–	–	$<10^{-8}$	~300	–	4.56	CPD	[829]
W	–	–	$\leq 10^{-7}$	~1500–1600	–	4.56	TE	[1777]
W	–	–	1×10^{-9}	~300 (~2100)	–	4.56	CPD	[3617]
W{46%(100)}	–	–	–	–	(4.98 ± 0.05)	4.56 ± 0.01	TC	[803]
W{46%(100)}	–	–	–	–	(5.00 ± 0.05)	4.56 ± 0.01	TC	[2453]
W	–	–	?	~2100–2200	–	4.56 ± 0.01	TE	[3349]
W	–	–	$<10^{-9}$	~1700–2300	–	4.56 ± 0.02	TE	[162]
W	–	–	$\leq 5 \times 10^{-7}$	?	–	4.56 ± 0.03	TE	[160]
W	–	–	5×10^{-10}	~300	–	4.56 ± 0.03	FE	[2492]
W	–	–	$\leq 10^{-4}$ (Na)	~1450–2450	–	4.56 ± 0.04	TE	[1063]
W	–	–	?	?	(4.65*)	4.56 ± 0.06	TE	[3834]
W	–	–	?	1577	–	4.567	TE	[661]
W	K	K$^+$	4×10^{-9}	~1000–1600	4.57	–	PSI	[188]
W	–	–	2×10^{-9}	~1900–2400	–	4.57	TE	[4343]
W{95%(100)}[301]	–	–	–	–	(4.69 ± 0.05)	4.57 ± 0.00	TC	[803]
W	–	–	$\leq 9 \times 10^{-7}$	2160–2520	–	4.57 ± 0.01	TE	[2296]
W	–	–	1×10^{-7}	~1900–2200	(5.18 ± 0.03)	4.57 ± 0.04	TE	[281]
W	–	–	1×10^{-10}	~300	(4.67 ± 0.09)	4.57 ± 0.1	PE	[3055]
W	–	–	$<10^{-8}$	~2200–2400	–	4.57 ± 0.21	TE	[1062]
W	–	–	$\leq 2 \times 10^{-6}$	~2100–2700	–	4.575 ± 0.015	TE	[2296]
W	–	–	$\leq 10^{-9}$	~1900–2200	–	4.58	TE	[66]
W	–	–	$\leq 2 \times 10^{-8}$	~1350–2050	–	4.58	TE	[130,1363]
W	KBr	Br$^-$	?	~2300–2600	4.58^N	–	NSI	[574]
W	–	–	? (Ba)	~1600–2000	–	4.58	TE	[1485]
W	–	–	?	?	–	4.58	TE	[3524,3525]
W	Ba	Ba$^+$	$<1 \times 10^{-7}$	~2400–2800	4.58 ± 0.01	–	PSI	[80]
W	–	–	1×10^{-7}	~2100–2600	(5.14 ± 0.03)	4.58 ± 0.03	TE	[76,77]
W[304]	–	–	5×10^{-7}	2300	(5.05, 5.10)	4.58 ± 0.05	TE	[94]
W	–	–	$\leq 1 \times 10^{-6}$	~2100–2700	–	4.588 ± 0.011	TE	[2296]
W	–	–	–	–	–	4.59	TC	[1744]
W/W(100)[309]	WF$_6$, H$_2$	–	$\sim10^{-7}$	~1850–2450	–	4.59 ± 0.01	TE	[1053]
W{96%(100)}[300]	–	–	–	–	(4.60 ± 0.04)	4.59 ± 0.01	TC	[630,2453]
W[296]	–	–	$<10^{-6}$	?	(4.49 ± 0.14)	4.59 ± 0.04	TE	[823]
W	–	–	$\sim10^{-7}$	~1700–2050	–	4.59 ± 0.04	TE	[2820]
W[292]	–	–	$\sim10^{-9}$	~300	–	4.6	FE	[1493]
W	–	–	$<10^{-4}$ (Cs)	~2500–3000	–	4.6	TE	[111]
W[294]	–	–	2×10^{-7}	~300 (2300)	–	4.6	PE	[621]
W	–	–	?	~300	–	4.6	PE	[1243]
W	–	–	?	?	–	4.6	TE	[1792]
W	KCl	K$^+$	?	?	4.6	–	PSI	[2306]
W/Mo(100)[305]	W	–	1×10^{-11}	77	–	4.6	FE	[2965]
W	–	–	–	–	–	4.6	TC	[3318]
W{46.3%(310)}[411]	–	–	–	–	–	4.6	TC	[489]
W	–	–	? (Cs)	~2000–2500	–	4.6	TE	[3798,3799]

Table 1 (*continued*)

Surface	Beam	Ion	P_r (Torr)	T (K)	ϕ^+ (eV)	ϕ^e (eV)	Meth.	Refs.
W	–	–	$\leq 1 \times 10^{-6}$	?	(4.75 ± 0.02)	4.6 ± 0.1	TE	[216]
W[306]	NaCl	Na⁺	$\leq 5 \times 10^{-8}$	~1550–1770	4.6 ± 0.1	–	PSI	[3113]
W{46%(100)}	Li	Li⁺	~10⁻⁹	~1800–2800	4.60	–	PSI	[534]
W/Ni	W	–	?	~300	–	4.60	PE	[2922]
W	–	–	~10⁻¹⁰	~300	–	4.60	CPD	[3532]
W	–	–	? (CsI)	~2100–2400	–	4.60 ± 0.01	TE	[1321]
W	Sr	Sr⁺	~10⁻⁹	~2400–2800	4.60 ± 0.02	–	PSI	[138]
W	La	La⁺	~10⁻⁹	~2400–2800	4.60 ± 0.02	–	PSI	[138]
W	–	–	$\leq 5 \times 10^{-8}$	?	(5.14 ± 0.05)	4.60 ± 0.04	TE	[84,93,824]
W{96%(100)}[300]	–	–	–	–	4.60 ± 0.04	(4.59 ± 0.01)	TC	[630,2453]
W	–	–	$\leq 10^{-4}$ (Na)	~1450–2450	–	4.60 ± 0.04	TE	[1063]
W	–	–	$\leq 8 \times 10^{-8}$	~1600–2500	(4.75 ± 0.05)	4.60 ± 0.05	TE	[95]
W	In	In⁺	4×10^{-10} (O₂)	~2100–2850	4.60 ± 0.05	–	PSI	[139]
W	In	In⁺	1×10^{-6} (O₂)	~2500–2850	4.60 ± 0.05	–	PSI	[139]
W	–	–	1×10^{-7}	~1900–2200	(5.19, 5.20)	4.60 ± 0.05	TE	[281]
W	–	–	<10⁻⁸	~1900–2250	(4.95 ± 0.05)	4.61	TE	[85]
W	–	–	? (NaI)	~2500–3000	–	4.61 ± 0.01	TE	[1321]
W	–	–	5×10^{-10}	~300	–	4.61 ± 0.01	PE	[2492]
W	Sr	Sr⁺	8×10^{-9}	~2300–2800	4.61 ± 0.03	–	PSI	[145]
W{35%(110)}	–	–	–	–	(5.18 ± 0.03)	4.61 ± 0.03	TC	[630,2453]
W	–	–	1×10^{-7}	~2000–2200	(5.16 ± 0.05)	4.61 ± 0.03	TE	[281]
W{95%(100)}[301]	–	–	–	–	(4.70 ± 0.04)	4.61 ± 0.04	TC	[2453]
W{46%(100)}[475]	Eu	Eu⁺	~10⁻⁹	~1800–2800	4.61 ± 0.05	–	PSI	[390,825]
W{46%(100)}	Ce	Ce⁺	~10⁻⁹	~1800–2800	4.61 ± 0.05	–	PSI	[390]
W{46%(100)}	Li	Li⁺	~10⁻⁹	~1800–2300	4.61 ± 0.05	–	PSI	[391,535,825]
W{46%(100)}	Na	Na⁺	~10⁻⁹	~1700–1950	4.61 ± 0.05	–	PSI	[535,659,825]
W{46%(100)}	K	K⁺	~10⁻⁹	~1250–1650	4.61 ± 0.05	–	PSI	[535,825]
W{46%(100)}	Rb	Rb⁺	~10⁻⁹	~1300–1650	4.61 ± 0.05	–	PSI	[535,825]
W{46%(100)}	Cs	Cs⁺	~10⁻⁹	~1150–1500	4.61 ± 0.05	–	PSI	[535,825]
W[294]	–	–	12 (Ar)	~300	–	4.62	PE	[621]
W	–	–	? (Cs)	~2000–2400	–	4.62	TE	[3808]
W	–	–	?	~1200–1500	–	4.62	TE	[3248]
W	–	–	~10⁻⁷	~1450–2250	–	4.62	TE	[1878]
W	–	–	$\leq 3 \times 10^{-10}$	1000	–	4.62 ± 0.01	CPD	[194]
W{33.6%(112)}	–	–	–	–	(5.13 ± 0.04)	4.62 ± 0.02	TC	[630,2453]
W{46%(100)}	Eu	Eu⁺	~10⁻⁹	~1800–2800	4.62 ± 0.05	–	PSI	[533,534]
W/glass[293]	W	–	~10⁻¹⁰	77 (438)	–	4.63	PE	[2095]
W{35.2%(110)}	–	–	–	–	(5.15 ± 0.03)	4.63 ± 0.01	TC	[281]
W	–	–	<10⁻⁸	~1900–2400	–	4.63 ± 0.05	TE	[1858]
W	–	–	$\leq 10^{-7}$	~1450–2250	–	4.64	TE	[1878]
W	K	K⁺	?	~1300–1400	4.64 ± 0.03*	–	PSI	[1373]
W	Ag	Ag⁺	$\leq 10^{-5}$ (O₂)	~2500–2800	4.65	–	PSI	[55]
W	Ba	Ba⁺	$\leq 10^{-4}$ (Ba)	~2600–2900	4.65*	(4.56 ± 0.06)	PSI	[3834]
W	–	–	?	1500	–	4.65	TE	[3534]
W	–	–	6×10^{-9}	1800	–	4.65	TE	[4060]
W[312]	KCl	K⁺	?	~1700–2400	4.65 ± 0.05	–	PSI	[46]
W[312]	KBr	K⁺	?	~1700–2400	4.65 ± 0.05	–	PSI	[46]
W[312]	KI	K⁺	?	~1700–2400	4.65 ± 0.05	–	PSI	[46]
W/SiO₂	W	–	?	?	–	4.65 ± 0.05	FE	[1605]
W	–	–	~10⁻⁷	~2000	–	4.65 ± 0.05	TE	[1649]
W	Ti	Ti⁺	$\leq 10^{-6}$ (O₂)	~2300–2900	4.65 ± 0.1	–	PSI	[3408]
W[307]	–	(W⁺, W⁻)	?	~2262–2353	4.65 ± 0.4*	–	PSI, NSI	[965]
W	–	–	$<8 \times 10^{-11}$	~300	–	4.650 ± 0.100	CPD	[342,3868]
W	Cu	Cu⁺	$\leq 10^{-5}$ (O₂)	~2500–2800	4.66	–	PSI	[55]
W/Mo[308]	WF₆, H₂	–	~10⁻⁷	–2000–	–	4.66	TE	[1398]
W/W(110)[309]	WCl₆, H₂	–	~10⁻⁷	~1850–2450	–	4.66 ± 0.01	TE	[1053]
W	Na	Na⁺	$\leq 5 \times 10^{-9}$	~1500–1700	4.66 ± 0.01*	–	PSI	[2594]
W/Mo[308]	WCl₆, H₂	–	~10⁻⁷	–2000–	–	4.67	TE	[1398]
W	–	–	?	1900	–	4.67	TE	[2762]
W	–	–	–	–	–	4.67	TC	[3224]
W	K	K⁺	$\leq 3 \times 10^{-9}$	1150–2000	4.67 ± 0.09	(4.57 ± 0.1)	PSI	[3055]
W	–	–	6×10^{-7} (O₂)	~2100–2500	–	4.68	CPD	[200]
W[308]	–	–	~10⁻⁷	–2000–	–	4.68	TE	[1398]
W	–	–	–	–	–	4.68	TC	[2629]
W	K	K⁺	2×10^{-7}	~1400–2200	4.68 ± 0.01*	–	PSI	[50]
W	–	–	?	~2100–2700	–	4.68 ± 0.07	TE	[228]
W	–	–	$\leq 10^{-7}$	1450–2150	–	4.69	TE	[1878]
W	–	–	?	?	–	4.69	TE	[2105]
W/W(100)[309]	WF₆, H₂	–	~10⁻⁷	~1850–2450	–	4.69 ± 0.01	TE	[1053]
W	KI	K⁺	2×10^{-7}	~1500–2200	4.69 ± 0.02*	–	PSI	[51]

Table 1 (*continued*)

Surface	Beam	Ion	P_r (Torr)	T (K)	ϕ^+ (eV)	ϕ^e (eV)	Meth.	Refs.
W	–	–	?	0^E (≤1100)	–	4.69 ± 0.03	PE	[3392]
W{95%(100)}[301]	–	–	–	–	4.69 ± 0.05	(4.57 ± 0.00)	TC	[803]
W(porous)	–	–	?	>1600	–	4.7	TE	[3762]
W(porous)	K	K$^+$	<10^{-7}	~1400–1600	4.7	–	PSI	[3763]
W	Na	Na$^+$	~10^{-4} (Na)	2000	4.7*	–	PSI	[3839]
W	–	–	<10^{-7}	2200	–	4.7	TE	[2582]
W/Mo(100)[305]	W	–	1×10^{-11}	77 (1300)	–	4.7	FE	[2965]
W/W(110)	–	–	–	–	–	4.7	TC	[2975]
W	–	–	5×10^{-8}	~300	–	4.7	PE	[3301]
W	Na	Na$^+$	?	~1600–2200	4.7 ± 0.1	–	PSI	[1061]
W	Mg	Mg$^+$	?	~1600–2200	4.7 ± 0.1	–	PSI	[1061]
W	Ca	Ca$^+$	?	~1600–2200	4.7 ± 0.1	–	PSI	[1061]
W	Sr	Sr$^+$	?	~1600–2200	4.7 ± 0.1	–	PSI	[1061]
W	Ba	Ba$^+$	?	~1600–2200	4.7 ± 0.1	–	PSI	[1061]
W	–	–	0.08 (Cs)	~2000–2350	–	4.70	TE	[2937]
W	Li	Li$^+$	2×10^{-7}	~2100–2800	4.70	–	PSI	[50]
W	Na	Na$^+$	2×10^{-7}	~2100–2800	4.70	–	PSI	[50]
W	Rb	Rb$^+$	2×10^{-7}	~1600–2600	4.70 ± 0.02*	–	PSI	[50]
W	KCl	K$^+$	2×10^{-7}	~1600–2300	4.70 ± 0.03*	–	PSI	[51]
W	KBr	K$^+$	2×10^{-7}	~1600–2300	4.70 ± 0.03*	–	PSI	[51]
W{95%(100)}[301]	–	–	–	–	4.70 ± 0.04	(4.61 ± 0.04)	TC	[2453]
W	–	–	<2×10^{-7}	~2000–2200	–	4.70 ± 0.40	TE	[3066]
W	Na	Na$^+$	≤3×10^{-7}	~1500–2900	4.71	–	PSI	[136]
W	NaI	Na$^+$	≤3×10^{-7}	~1500–2900	4.71	–	PSI	[136]
W	K	K$^+$	?	~1000	4.71*	–	PSI	[3794]
W	–	–	~10^{-9}	~300	–	4.71	CPD	[2473]
W	–	–	?	?	–	4.71	TE	[3386]
W	–	–	?	1100	–	4.71	TE	[3392]
W/W(100)[309]	WF$_6$, H$_2$	–	~10^{-7}	1850–2450	–	4.71 ± 0.01	TE	[1053]
W/Mo[308]	WF$_6$, H$_2$	–	~10^{-7}	–2000–	–	4.72	TE	[1398]
W	Li	Li$^+$	2×10^{-7}	~2100–2800	4.72 ± 0.01*	–	PSI	[50]
W	Na	Na$^+$	2×10^{-7}	~2200–2900	4.72 ± 0.01*	–	PSI	[50]
W	KF	K$^+$	2×10^{-7}	~1400–2200	4.72 ± 0.02*	–	PSI	[51]
W	KBr	K$^+$	2×10^{-7}	~1600–2400	4.72 ± 0.03*	–	PSI	[1285]
W	K	K$^+$	2×10^{-7}	~1300–2200	4.72 ± 0.04*	–	PSI	[1285]
W	–	–	6×10^{-3}	~300	–	4.72 ± 0.05	PE	[2079,2080]
W	–	–	–	–	–	4.73	TC	[3476]
W	–	–	–	1500–1900	–	4.73 ± 0.01	TC	[1372]
W	–	–	? (Cs)	~2000–2350	–	4.74	TE	[2937]
W	LiI	Li$^+$	≤3×10^{-7}	~1500–1900	4.74	–	PSI	[136]
W	KBr	K$^+$	?	~1900–2100	4.74*	–	PSI	[2208]
W	KI	K$^+$	?	~1900–2100	4.74*	–	PSI	[2208]
W	–	–	?	~2100–2200	–	4.74 ± 0.01	TE	[3349]
W(fp)[291]	–	–	–	–	–	4.75	TC	[2973]
W	–	–	~10^{-8}	?	–	4.75	TE	[196]
W[308]	–	–	~10^{-7}	–2000–	–	4.75	TE	[1398]
W	K	K$^+$	≤1×10^{-6}	~1300–1800	4.75 ± 0.02	(4.6 ± 0.1)	PSI	[216]
W	Li	Li$^+$	≤8×10^{-8}	~1800–2500	4.75 ± 0.05	(4.60 ± 0.05)	PSI	[95]
W	–	–	–	–	–	4.77	TC	[3476]
W	–	–	–	0	–	4.77	TC	[4419]
W{95%(100)}[277]	–	–	–	–	–	4.78	TC	[1254]
W	K	K$^+$	?	~1200–2100	4.78*	–	PSI	[2208]
W	–	–	?	?	–	4.79	TE	[3386]
W	–	–	7×10^{-5}	~2000–2150	–	4.79 ± 0.01	TE	[2454]
W{46.3%(310)}[411]	–	–	<2×10^{-10}	~300	–	4.8	FE	[489]
W/Si^{n}[482]	W	–	?	~300	–	4.8	CPD	[4375]
W	K	K$^+$	<10^{-9}	~1100–1200	4.8 ± 0.1*	–	PSI	[2579,3055]
W[170,297]	–	(W$^+$)	?	~2200–2600	4.8 ± 0.2*	–	PSI	[966]
W[170]	–	(W$^+$)	~10^{-7}	~2600–2900	4.8 ± 0.6	(4.58 ± 0.03)	PSI	[77]
W	Na	Na$^+$	≤10^{-4} (Na)	2300	4.80 ± 0.03*	–	PSI	[1364]
W	–	–	?	~300–1100	–	4.80 ± 0.09	PE	[3390]
W[313]	NaCl	Na$^+$	?	~1800–2600	4.82	–	PSI	[47]
W[315]	Li	Li$^+$	≤3×10^{-7}	~1800–2000	4.82 ± 0.02	–	PSI	[155]
W[315]	NaCl	Na$^+$	≤3×10^{-7}	~1550–2450	4.83 ± 0.05	–	PSI	[156]
W	NaBr	Na$^+$	?	~1700–2600	4.84	–	PSI	[47]
W/Si(111)[166]	W	–	4×10^{-11}	~300	–	4.87	PE	[1429,1430]
W{80%(110)}[311]	–	–	–	–	(5.26 ± 0.02)	4.87 ± 0.06	TC	[2453]
W/W(110)[309]	WCl$_6$, H$_2$	–	~10^{-7}	~1850–2450	–	4.88 ± 0.01	TE	[1053]
W	–	–	–	–	–	4.9	TC	[706]
W	–	–	?	~1400–2500	–	4.90	TE	[3856]

Table 1 (*continued*)

Surface	Beam	Ion	P_r (Torr)	T (K)	ϕ^+ (eV)	ϕ^e (eV)	Meth.	Refs.
W	–	–	–	–	–	4.90	TC	[339]
W	–	–	1×10^{-10}	~300	–	4.90	CPD	[2632]
W{80%(110)}[311]	–	–	–	–	(5.25 ± 0.02)	4.90 ± 0.05	TC	[630]
W	–	–	?	?	–	4.90 ± 0.05	TE	[2209]
W	–	–	? (K)	~1400–1800	–	4.95	TE	[2559]
W[312]	KCl	K⁺	?	1450	4.95	–	TC	[3747]
W[270]	Na	Na⁺	? (Na)	~1500–2000	4.95 ± 0.05	(4.61)	PSI	[85]
W[314]	KI	I⁻	$<1 \times 10^{-6}$	~1800–2300	4.95 ± 0.05[N]	–	NSI	[183]
W{46.3%(310)}	–	–	–	–	4.96 ± 0.03	(4.34 ± 0.05)	TC	[630]
W/W(100)[309]	WF₆, H₂	–	~10^{-7}	~1850–2450	–	4.98 ± 0.01	TE	[1053]
W{46%(100)}	–	–	–	–	4.98 ± 0.05	(4.56 ± 0.01)	TC	[803]
W{46.3%(310)}	–	–	–	–	4.99 ± 0.06	(4.38 ± 0.05)	TC	[2453]
W	–	–	$<10^{-9}$	~1700–2300	–	5.0	TE	[162]
W	–	–	?	~1400–1750	–	5.0	TE	[2078]
W	Nd	Nd⁺	$<1 \times 10^{-7}$	~2700–2900	5.00 ± 0.04*	–	PSI	[80]
W{46%(100)}	–	–	–	–	5.00 ± 0.05	(4.56 ± 0.01)	TC	[2453]
W/W(110)[309]	WCl₆, H₂	–	~10^{-7}	~1850–2450	–	5.03 ± 0.01	TE	[1053]
W	–	(W⁺)	$<7 \times 10^{-7}$	~2850–3000	5.04 ± 0.29	–	PSI	[805,3083]
W[313]	NaCl	Na⁺	?	1450	5.05	–	TC	[3747]
W[304]	In	In⁺	5×10^{-7}	~2300–2700	5.05 ± 0.05	(4.58 ± 0.05)	PSI	[94]
W	KCl	K⁺	2×10^{-7}	~2000–2300	5.09 ± 0.02	(4.42 ± 0.02)	PSI	[36]
W	KCl	K⁺	2×10^{-7}	~2000–2200	5.09 ± 0.06	(4.48 ± 0.06)	PSI	[23]
W{<35%(110)}	–	–	–	–	5.09 ± 0.10	(4.52 ± 0.12)	TC	[283,630]
W	Na	Na⁺	$\leq 10^{-7}$ (Na)	2400	5.1*	–	PSI	[3839]
W[304]	In	In⁺	5×10^{-7}	2350	5.10	(4.58 ± 0.05)	PSI	[94]
W[315]	LiCl	Li⁺	$\leq 3 \times 10^{-7}$	~2250–2700	5.11 ± 0.02	–	PSI	[156]
W{25%(110)}[295]	–	–	–	2000	5.12*	(4.46*)	TC	[3844]
W	KF	K⁺	2×10^{-7}	~2000–2200	5.12 ± 0.02	(4.48 ± 0.06)	PSI	[23]
W[315]	Li	Li⁺	$\leq 3 \times 10^{-7}$	~2200–2500	5.12 ± 0.02	–	PSI	[155]
W[315]	Tl	Tl⁺	$\leq 3 \times 10^{-7}$	~1900–2500	5.12 ± 0.03	–	PSI	[157]
W{33.6%(112)}	–	–	–	–	5.13 ± 0.04	(4.62 ± 0.02)	TC	[630,2453]
W	In	In⁺	1×10^{-7}	~2100–2600	5.14 ± 0.03	(4.58 ± 0.03)	PSI	[76,77]
W	Bi	Bi⁺	$\leq 5 \times 10^{-8}$	~2050–2300	5.14 ± 0.05	(4.60 ± 0.04)	PSI	[84,93,824]
W[315]	In	In⁺	$\leq 3 \times 10^{-7}$	~1900–2500	5.15 ± 0.01	–	PSI	[157,3538]
W{35.2%(110)}	–	–	–	–	5.15 ± 0.03	(4.63 ± 0.01)	TC	[281]
W/W(100)[309]	W	–	~10^{-7}	~1850–2450	–	5.16 ± 0.01	TE	[1053]
W/W(110)[309]	W	–	~10^{-7}	~1850–2450	–	5.16 ± 0.01	TE	[1053]
W	LiI	Li⁺	2×10^{-7}	~2000–2200	5.16 ± 0.05	(4.61 ± 0.03)	PSI	[281]
W[306]	Ag	Ag⁺	$\leq 5 \times 10^{-8}$	?	5.16 ± 0.1	–	PSI	[3113]
W	LiCl	Li⁺	2×10^{-7}	~2000–2200	5.18 ± 0.03	(4.57 ± 0.04)	PSI	[281]
W{35%(110)}	–	–	–	–	5.18 ± 0.03	(4.61 ± 0.03)	TC	[630,2453]
W	NaCl	Na⁺	2×10^{-7}	~1900–2200	5.19 ± 0.01	–	PSI	[208]
W	LiCl	Li⁺	2×10^{-7}	~2000–2200	5.19 ± 0.03	(4.48 ± 0.06)	PSI	[23]
W	LiF	Li⁺	2×10^{-7}	~2000–2200	5.19 ± 0.05	(4.60 ± 0.05)	PSI	[281]
W{mainly(110)}	–	–	0.1–6 (Cs)	~1700–1900	–	5.2 ± 0.1*	TE	[2609]
W	NaBr	Na⁺	2×10^{-7}	~2000–2200	5.20 ± 0.02	(4.48 ± 0.06)	PSI	[23,2422]
W	LiCl	Li⁺	2×10^{-7}	~2000–2200	5.20 ± 0.02	(4.47 ± 0.04)	PSI	[37]
W	LiBr	Li⁺	2×10^{-7}	~2000–2200	5.20 ± 0.04	(4.60 ± 0.05)	PSI	[281,2411]
W	LiBr	Li⁺	2×10^{-6}	~2100–2200	5.20 ± 0.05	–	PSI	[2411]
W	–	–	–	–	–	5.21	TC	[3476]
W	NaCl	Na⁺	2×10^{-7}	~2000–2200	5.21 ± 0.02	(4.48 ± 0.06)	PSI	[23,2411]
W	RbCl	Rb⁺	2×10^{-7}	~2000–2200	5.21 ± 0.06	(4.48 ± 0.06)	PSI	[23]
W	NaCl	Na⁺	2×10^{-7}	~2000–2200	5.22 ± 0.02	(4.47 ± 0.04)	PSI	[37,2422]
W	LiF	Li⁺	2×10^{-7}	~2000–2200	5.22 ± 0.07	(4.48 ± 0.06)	PSI	[23]
W	NaCl	Na⁺	2×10^{-7}	~2000–2300	5.23 ± 0.01	(4.42 ± 0.02)	PSI	[36]
W	NaI	Na⁺	2×10^{-7}	~2000–2200	5.23 ± 0.02	(4.48 ± 0.06)	PSI	[23,2422]
W	LiBr	Li⁺	2×10^{-7}	~2000–2200	5.23 ± 0.02	(4.48 ± 0.06)	PSI	[23,37,57,2422]
W	NaCl	Na⁺	2×10^{-7}	~2000–2200	5.24 ± 0.05	–	PSI	[57]
W{80%(110)}[311]	–	–	–	–	5.25 ± 0.02	(4.90 ± 0.05)	TC	[630]
W[314]	Cu	Cu⁺	$<1 \times 10^{-6}$	~1800–2300	5.25 ± 0.05	(4.95 ± 0.05[N])	PSI	[183]
W[314]	Ag	Ag⁺	$<1 \times 10^{-6}$	~1800–2300	5.25 ± 0.05	(4.95 ± 0.05[N])	PSI	[183]
W{80%(110)}[311]	–	–	–	–	5.26 ± 0.02	(4.87 ± 0.06)	TC	[2453]
W	LiI	Li⁺	2×10^{-7}	~2000–2200	5.26 ± 0.02	(4.48 ± 0.06)	PSI	[23]
W[170]	LiI	Li⁺	2×10^{-7}	~2000–2200	5.27 ± 0.01	(4.47 ± 0.04)	PSI	[37]
W[170]	Cs	Cs⁺	$<5 \times 10^{-8}$	770–800	5.3 ± 0.1	–	PSI	[263]
W	K	K⁺	$<5 \times 10^{-8}$	780–820	5.3 ± 0.2	–	PSI	[263,269]
W	–	–	–	–	–	5.67	TC	[3931]
W	–	–	–	–	–	5.78	TC	[2629]
W	Na	Na⁺	?	1370	5.45 ± 0.06*	–	PSI	[3766]
Recommended	–	–	–	–	**5.17 ± 0.05**	**4.56 ± 0.03**	–	–
Recommended	–	–	–	–	**4.51 ± 0.03[N]**	–	–	–

Table 1 (*continued*)

Surface	Beam	Ion	P_r (Torr)	T (K)	ϕ^+ (eV)	ϕ^e (eV)	Meth.	Refs.
				75. Rhenium Re[416]				
hcp								
Re(0001)	–	–	–	–	–	4.88	TC	[4004]
Re(0001)/Mo	Re	–	?	–1800–	–	4.9	TE	[2416]
Re(0001)/Mo	ReCl$_3$	–	~10^{-9}	~1800–2000	–	5.01 ± 0.05	TE	[398]
Re(0001)/Mo	ReCl$_3$	–	~10^{-7}	~2300–2500	–	5.02 ± 0.02	TE	[398]
Re(0001)/Mo	ReCl$_3$	–	~10^{-8}	~2100–2200	–	5.02 ± 0.04	TE	[398]
Re(0001)	–	–	–	–	–	5.09	TC	[3473]
Re(0001)	–	–	≤5 × 10^{-8}	?	(5.15 ± 0.26)	5.15 ± 0.10	TE	[96]
Re(0001)	La	La$^+$	≤5 × 10^{-8}	~2000–2100	5.15 ± 0.21	(5.15 ± 0.10)	PSI	[96]
Re(0001)	Ce	Ce$^+$	≤5 × 10^{-8}	~2300–2400	5.15 ± 0.21	(5.15 ± 0.10)	PSI	[96]
Re(0001)	Er	Er$^+$	≤5 × 10^{-8}	~1900–2000	5.15 ± 0.21	(5.15 ± 0.10)	PSI	[96]
Re(0001)	Gd	Gd$^+$	≤5 × 10^{-8}	~2100–2200	5.15 ± 0.34	(5.15 ± 0.10)	PSI	[96]
Re(0001)	Tm	Tm$^+$	≤5 × 10^{-8}	~1600–1750	5.15 ± 0.34	(5.15 ± 0.10)	PSI	[96]
Re(0001)	–	–	–	–	–	5.17	TC	[4004]
Re(0001){80%}	–	–	?	~300	–	5.20 ± 0.1	PE	[401]
Re(0001)	–	–	~10^{-10}	120	–	5.24	PE	[399]
Re(0001)	–	–	2 × 10^{-10}	100	–	5.26 ± 0.05	CPD	[3378]
Re(0001)	–	–	–	–	–	5.35	TC	[4005]
Re(0001){mainly}	–	–	~10^{-5} (air)	~2400–2600	–	5.4	TE	[56,206]
Re(0001)	–	–	~10^{-10}	~300	–	5.4	PE	[400]
Re(0001)	–	–	6 × 10^{-11}	~300	–	5.4	CPD	[836]
Re(0001)	–	–	–	–	–	5.46	TC	[3224]
Re(0001)	–	–	~10^{-10}	80	–	5.5	PE	[664]
Re(0001)	–	–	≤6 × 10^{-8}	~1800–2150	–	5.51	TE	[2247]
Re(0001)	–	–	–	–	–	5.53	TC	[1159,1980,3067]
Re(0001)	–	–	~10^{-9}	?	–	5.53 ± 0.03	TE	[1065,2593]
Re(0001)	–	–	–	–	–	5.57	TC	[3224]
Re(0001)	–	–	≤7 × 10^{-9}	~1700–2300	–	5.59 ± 0.05	TE	[402,3415,3416]
Re(0001)	–	–	–	–	–	5.71	TC	[334]
Re(0001)	–	–	–	–	–	5.77	TC	[321]
Re(0001)	–	–	≤10^{-10}	50–300	–	6.40 ± 0.02	FE	[2488,2499]
Recommended	–	–	–	–	**5.15 ± <0.34**	**5.30 ± 0.21**	–	–
Re(1010)	–	–	–	–	–	4.62	TC	[4004]
Re(1010)	–	–	–	–	–	4.93	TC	[4004]
Re(1010)	–	–	(<8 × 10^{-12})	~300	–	5.05	CPD	[599,2490]
Re(1010)	–	–	≤1 × 10^{-8}	~1900–2250	–	5.05 ± 0.04	TE	[837,2325,2326]
Re(1010)	–	–	<10^{-11}	77	–	5.1	CPD	[2506]
Re(1010)	–	–	≤7 × 10^{-9}	~1700–2300	–	5.15 ± 0.02	TE	[402,3415,3416]
Re(1010)	–	–	~10^{-9}	?	–	5.15 ± 0.03	TE	[1065,2593]
Re(1010)	–	–	≤5 × 10^{-10}	–1800–	–	5.15 ± 0.05	TE	[286,412,537,665, 839,2051,4458]
Re(1010)	–	–	–	–	–	5.20	TC	[1159,1980,3067]
Re(1010)	–	–	–	–	–	5.51	TC	[321]
Re(1010)	–	–	~10^{-10}	~300	–	5.52 ± 0.03	PE	[403]
Re(1010)	–	–	–	–	–	5.67	TC	[4005]
Re(1010)[211]	–	–	<5 × 10^{-9}	~300	–	5.95 ± 0.15	FE	[730]
Recommended	–	–	–	–	–	**5.12 ± 0.05**	–	–
Re(1011)	–	–	–	–	–	4.94	TC	[4004]
Re(1011)	–	–	≤1 × 10^{-8}	~1900–2250	–	5.04 ± 0.04	TE	[837,2325,2326]
Re(1011)	–	–	–	–	–	5.25	TC	[4004]
Re(1011)	–	–	<5 × 10^{-9}	~300 (<800)	–	5.25 ± 0.04	FE	[730]
Re(1011)	–	–	<5 × 10^{-9}	~300 (<800)	–	5.36 ± 0.04	FE	[730]
Re(1011)	–	–	≤7 × 10^{-9}	~1700–2300	–	5.37 ± 0.03	TE	[402,3415,3416]
Re(1011)	–	–	<5 × 10^{-9}	~300 (>800)	–	5.55 ± 0.03	FE	[730]
Re(1011)	–	–	~10^{-10}	~300	–	5.69 ± 0.06	PE	[403]
Re(1011)	–	–	~10^{-9}	77	–	5.75	FE	[363,811,838]
Re(1011)	–	–	~10^{-10}	~300	–	5.82 ± 0.07	PE	[403]
Re(1011)	–	–	~10^{-10}	~300	–	5.88 ± 0.10	PE	[403]
Recommended	–	–	–	–	–	**5.26 ± 0.13**	–	–
Re(1120)	–	–	–	–	–	4.55	TC	[4004]
Re(1120)	–	–	≤1 × 10^{-8}	~1900–2250	–	4.80 ± 0.04	TE	[837,2325,2326]
Re(1120)	–	–	–	–	–	4.86	TC	[4004]
Re(1120)	–	–	~10^{-10}	~300	–	4.94 ± 0.06	PE	[403]
Re(1120)	–	–	~10^{-9}	77	–	5.07	FE	[363,811,838]

(*continued on next page*)

Table 1 (*continued*)

Surface	Beam	Ion	P_r (Torr)	T (K)	ϕ^+ (eV)	ϕ^e (eV)	Meth.	Refs.
Re(1120)	–	–	$<5 \times 10^{-9}$	~300	–	5.08 ± 0.02	FE	[730]
Recommended	–	–	–	–	–	**4.95 ± 0.11**	–	–
Re(1121)	–	–	–	–	–	4.33	TC	[4004]
Re(1121)	–	–	–	–	–	4.62	TC	[4004]
Re(1121)	–	–	$\leq 1 \times 10^{-8}$	~1900–2250	–	4.70 ± 0.04	TE	[837,2325,2326]
Re(1121)	–	–	$\sim 10^{-9}$	77	–	4.82	FE	[363,811,838]
Re(1121)	–	–	$\sim 10^{-10}$	~300	–	4.93 ± 0.09	PE	[403]
Re(1121)	–	–	$\sim 10^{-10}$	~300	–	5.02 ± 0.05	PE	[403]
Recommended	–	–	–	–	–	**4.82 ± 0.14**	–	–
Re(1122)	–	–	–	–	–	4.48	TC	[4004]
Re(1122)	–	–	–	–	–	4.79	TC	[4004]
Re(1122)	–	–	$<5 \times 10^{-9}$	~300	–	4.95 ± 0.02	FE	[730]
Re(1122)	–	–	$\sim 10^{-10}$	~300	–	5.10 ± 0.02	PE	[403]
Re(1122)	–	–	$\sim 10^{-9}$	77	–	5.27	FE	[363,811,838]
Re(1122)	–	–	$\sim 10^{-10}$	~300	–	5.36 ± 0.05	PE	[403]
Recommended	–	–	–	–	–	**5.03 ± 0.18**	–	–
Re(1123)	–	–	–	–	–	4.41	TC	[4004]
Re(1123)	–	–	–	–	–	4.72	TC	[4004]
Re(1123)	–	–	$\sim 10^{-9}$	?	–	4.84 ± 0.03	TE	[1065,2593]
Re(1124)	–	–	$\leq 1 \times 10^{-8}$	~1900–2250	–	4.72 ± 0.04	TE	[837,2325,2326]
Re(1124)	–	–	–	–	–	4.83	TC	[321]
Re(1130)	–	–	–	–	–	4.44	TC	[4004]
Re(1130)	–	–	–	–	–	4.73	TC	[4004]
Re(2130)	–	–	–	–	–	4.49	TC	[4004]
Re(2130)	–	–	–	–	–	4.77	TC	[4004]
Re(3140)	–	–	–	–	–	4.55	TC	[4004]
Re(3140)	–	–	–	–	–	4.80	TC	[4004]
Re	–	–	–	–	–	3.98	TC	[521]
Re	–	–	$\sim 10^{-6}$	1620	–	4.15	TE	[1780]
Re	KI	I^-	$\leq 1 \times 10^{-6}$	1600	$>4.30^N$	(5.0 ± 0.1)	NSI	[216]
Re	–	–	$\sim 10^{-6}$	~1600	–	4.35	TE	[1780]
Re	–	–	$\sim 10^{-6}$	~1900–2100	–	4.45–5.2	TE	[1779]
Re	KI	I^-	$\leq 1 \times 10^{-6}$	1800	$>4.46^N$	(5.0 ± 0.1)	NSI	[216]
Re	–	–	–	–	–	4.53	TC	[2949]
Re	KBr	Br^-	$\leq 1 \times 10^{-6}$	1600	$>4.60^N$	(5.0 ± 0.1)	NSI	[216]
Re	–	–	–	–	–	4.62	TC	[298]
Re	–	–	–	–	–	4.67	TC	[3476]
Re	–	–	?	?	–	4.7	TE	[3402]
Re	–	–	–	–	–	4.7	TC	[706]
Re	–	–	–	–	–	4.72	TC	[3318]
Re	–	–	2×10^{-8}	~1700–2150	–	4.72	TE	[832]
Re	K	K^+	?	1660	$4.73 \pm 0.10^*$	–	PSI	[737]
Re/W[316]	–	–	5×10^{-7}	~1950–2700	–	4.74 ± 0.02^{486}	TE	[666]
Re	–	–	$\sim 10^{-9}$	~1300–2200	–	4.75	TE	[1775]
Re/W	Re	–	?	?	–	4.75	TE	[2575]
Re	Rb	Rb^+	?	1660	$4.75 \pm 0.10^*$	–	PSI	[737]
Re	KBr	Br^-	$\leq 1 \times 10^{-6}$	1800	$>4.76^N$	(5.0 ± 0.1)	NSI	[216]
Re/Cr/W	–	–	$<10^{-5}$	?	–	4.77	TE	[3041]
Re	–	–	–	–	–	4.78	TC	[3476]
Re	Sm	Sm^+	$<10^{-7}$	2100	4.78	–	PSI	[2970]
Re	–	–	$\sim 10^{-9}$	77	–	4.8	FE	[363,811,838]
Re	–	–	$\sim 10^{-6}$ (Cs)	~2000–2200	–	4.8	TE	[1774]
Re[320]	–	–	? (Cs)	~1300–2000	–	4.8	TE	[3414]
Re/SiC[323]	–	–	4×10^{-10}	~300 (700)	–	4.8 ± 0.1	CPD	[3646]
Re	–	–	–	–	–	4.81	TC	[3318]
Re/Mo[319]	$ReCl_3$, H_2	–	$\sim 10^{-7}$	~2000	–	4.82	TE	[1398]
Re	K	K^+	$\leq 1 \times 10^{-6}$	1800	4.85	(5.0 ± 0.1)	PSI	[216]
Re	–	–	$\leq 10^{-8}$	~1500	–	4.85	TE	[1778]
Re	–	–	5×10^{-8}	~1700–2500	(5.35 ± 0.05)	4.85 ± 0.05	TE	[100]
Re	–	–	$\sim 10^{-10}$	~1500–2100	–	4.85 ± 0.05	TE	[165]
Re	–	–	$\sim 10^{-9}$	~1200–1800	–	4.86	TE	[975]
Re	K	K^+	$\leq 1 \times 10^{-6}$	1600	4.87	(5.0 ± 0.1)	PSI	[216]

Table 1 (*continued*)

Surface	Beam	Ion	P_r (Torr)	T (K)	ϕ^+ (eV)	ϕ^e (eV)	Meth.	Refs.
Re	–	–	–	–	–	4.87	TC	[2629]
Re	–	–	? (Cs)	2300	–	4.87	TE	[2341]
Re	–	–	~10^{-9}	>1200	–	4.88	TE	[1203]
Re/W	Re	–	?	?	–	4.89	TE	[3257]
Re	–	–	?	1900	–	4.9	TE	[3093]
Re(porous)	–	–	?	>1600	–	4.9	TE	[3762]
Re	K	K^+	≤2×10^{-7}	~1050–1950	4.9	(4.93 ± 0.04)	PSI	[53]
Re	KCl	K^+	≤2×10^{-7}	~1150–1950	4.9	(4.93 ± 0.04)	PSI	[53]
Re[317]	Li	Li^+	<10^{-7}	?	4.9	–	PSI	[2944]
Re	–	–	~10^{-9}	?	–	4.9	TE	[979]
Re	–	–	4×10^{-9}	~1600–1950	–	4.9 ± 0.05	TE	[341]
Re[318]	–	(Re^-)	?	~2250–2500	4.9 ± 0.2*N	–	NSI	[966]
Re	–	–	–	–	–	4.90	TC	[3224]
Re	LiCl	Li^+	5×10^{-7}	2600	4.90	(5.0 ± 0.1)	PSI	[99]
Re	KBr	K^+	≤1×10^{-6}	1800	4.90	(5.0 ± 0.1)	PSI	[216]
Re	KI	K^+	≤1×10^{-6}	1800	4.90	(5.0 ± 0.1)	PSI	[216]
Re	–	–	≤7×10^{-9}	~1700–2300	–	4.93 ± 0.02	TE	[402,3415,3416]
Re	–	–	1×10^{-9}	~1750–2400	(5.43 ± 0.03)	4.93 ± 0.04	TE	[76,77,97,190]
Re	–	–	≤2×10^{-7}	~1800–2300	(5.34)	4.93 ± 0.04	TE	[53]
Re	–	–	~10^{-7}–10^{-5} (air)	2010, 2080	(5.42 ± 0.02)	4.93 ± 0.05	TE	[23]
Re	–	–	~10^{-7}–10^{-5} (air)	1830	(5.42–5.58)	4.93–5.18	TE	[23]
Re	KCl	K^+	≤1×10^{-6}	1800	4.94	(5.0 ± 0.1)	PSI	[216]
Re	–	–	3×10^{-9}	~1250–2250	–	4.94	TE	[159]
Re/Mo[319]	$ReCl_3$, H_2	–	~10^{-7}	~2000	–	4.94	TE	[1398]
Re	–	–	~10^{-7}–10^{-5} (O_2)	1715	(5.45–5.81)	4.94–5.41	TE	[23]
Re/W	$ReCl_3$, H_2	–	~10^{-7}	~2000	–	4.95	TE	[1398]
Re	–	–	–	–	–	4.95	TC	[3264,3265,3267]
Re	–	–	?	?	–	4.95	TE	[1772]
Re	–	–	~10^{-7}–10^{-5} (O_2)	2080	(5.43 ± 0.01)	4.95 ± 0.01	TE	[23]
Re	–	–	2×10^{-7}	~1800–2000	(5.48 ± 0.02)	4.95 ± 0.05	TE	[23]
Re	–	–	5×10^{-10}	~1300–2500	–	4.95 ± 0.10	TE	[404,840]
Re	–	–	~10^{-7}–10^{-5} (air)	1930	(5.43 ± 0.04)	4.96 ± 0.05	TE	[23]
Re[320]	–	–	~10^{-9}	1325–2250	–	4.96 ± 0.05	TE	[124,650,3414]
Re	–	–	≤10^{-9}	~1800–2200	–	4.97	TE	[66]
Re	KCl	K^+	≤1×10^{-6}	1600	4.97	(5.0 ± 0.1)	PSI	[216]
Re	KBr	K^+	≤1×10^{-6}	1600	4.97	(5.0 ± 0.1)	PSI	[216]
Re	KI	K^+	≤1×10^{-6}	1600	4.97	(5.0 ± 0.1)	PSI	[216]
Re	La	La^+	≤10^{-7}	~2100	4.97	–	PSI	[2970]
Re	–	–	?	~300	–	4.97	PE	[1846]
Re	–	–	≤5×10^{-7}	?	–	4.97 ± 0.03	TE	[160]
Re	–	–	~10^{-7}–10^{-5} (air)	1710	(5.42–5.70)	4.97–5.36	TE	[23]
Re	–	–	<1×10^{-8}	~1650–2400	(5.21 ± 0.01)	4.98 ± 0.03	TE	[54,3078]
Re	In	In^+	<10^{-7}	~2100	4.99	–	PSI	[2970]
Re	KCl	Cl^-	≤1×10^{-6}	2000	4.99N	(5.0 ± 0.1)	NSI	[216]
Re	–	–	5×10^{-7}	2300	(5.39 ± 0.05)	4.99 ± 0.05	TE	[94]
Re	Nd	Nd^+	<10^{-7}	~2100	5	–	PSI	[2970]
Re[317]	Li	Li^+	<10^{-7}	?	5	–	PSI	[2944]
Re/W[321]	–	–	?	?	–	5.0	FE	[1850]
Re[322]	–	–	5×10^{-7}	~1900–2500	(5.03 ± 0.07)	5.0 ± 0.1	TE	[99,216]
Re[318]	–	(Re^+)	?	~1900–2350	5.0 ± 0.1*	–	PSI	[966]
Re	–	–	2×10^{-7}	~1700–2200	(5.53 ± 0.02)	5.00 ± 0.01	TE	[101]
Re	Na	Na^+	≤10^{-3} (Na)	2300	5.00 ± 0.03*	–	PSI	[1364]
Re	NaI	Na^+	5×10^{-7}	~1900–2500	5.01	(5.0 ± 0.1)	PSI	[99]
Re	–	–	–	0	–	5.03	TC	[4419]
Re[322]	KCl	Cl^-	≤1×10^{-6}	1800	5.03 ± 0.1N	(5.0 ± 0.1)	NSI	[216]
Re	–	–	<2×10^{-7}	1870	–	5.05	TE	[1970]
Re	Li	Li^+	<10^{-7}	~2000	5.05	–	PSI	[2953,2970]
Re	Tl	Tl^+	5×10^{-9}	1700	5.05*	–	PSI	[1393]
Re	Na	Na^+	5×10^{-7}	1370	5.06	(5.0 ± 0.1)	PSI	[99]
Re	NaCl	Na^+	5×10^{-7}	1370	5.06	(5.0 ± 0.1)	PSI	[99]
Re[322]	$C_2(CN)_4$	CN^-	≤1×10^{-6}	2440	5.06 ± 0.2N	(5.0 ± 0.1)	NSI	[216]
Re	–	–	700 (Ar)	~3000	–	5.1	TE	[2007]
Re	–	–	<8×10^{-11}	~300	–	5.1 ± 0.1	CPD	[405]
Re	Ce	Ce^+	~10^{-9}	~1400–2400	5.10	–	PSI	[536]

Table 1 (*continued*)

Surface	Beam	Ion	P_r (Torr)	T (K)	ϕ^+ (eV)	ϕ^e (eV)	Meth.	Refs.
Re[170]	Na	Na$^+$	5×10^{-7}	~1300–1500	5.10 ± 0.07	–	PSI	[166]
Re	–	–	$<8 \times 10^{-11}$	~300	–	5.100 ± 0.100	CPD	[342,405,3868]
Re	Eu	Eu$^+$	~10^{-9}	~1400–2400	5.11	–	PSI	[536]
Re	NaBr	Na$^+$	5×10^{-7}	1370	5.11	(5.0 ± 0.1)	PSI	[99]
Re/W	ReCl$_3$	–	?	~1900–2700	–	5.13	TE	[841,1361]
Re	Na	Na$^+$	$\leq 2 \times 10^{-7}$	~1500–2300	5.14	(4.93 ± 0.04)	PSI	[53]
Re	NaCl	Na$^+$	$\leq 2 \times 10^{-7}$	~1700–2300	5.14	(4.93 ± 0.04)	PSI	[53]
Re/Si(111)	Re	–	$<4 \times 10^{-10}$	400 ($\leq$1100)	–	5.14	PE	[3708]
Re	Pr	Pr$^+$	$<10^{-7}$	~2100	5.16	–	PSI	[2970]
Re	Na	Na$^+$	$\leq 3 \times 10^{-7}$	~1300–2600	5.17	–	PSI	[136]
Re	Sr	Sr$^+$	$<1 \times 10^{-7}$	~2100–2700	5.17 ± 0.02	–	PSI	[80]
Re[170]	Na	Na$^+$	?	~1250–1450	5.17 ± 0.09	–	PSI	[684]
Re	–	–	$<8 \times 10^{-11}$	~300	–	5.171 ± 0.050	PE	[3866]
Re	–	–	–	–	–	5.18	TC	[3476]
Re/W	Re	–	$\leq 7 \times 10^{-8}$	~300	–	5.2	FE	[1804]
Re/6H-SiC[323]	Re	–	4×10^{-10}	~300 (500)	–	5.2 ± 0.1	CPD	[3646]
Re	–	–	$<1 \times 10^{-8}$	?	–	5.2 ± 0.1	TE	[3753]
Re	Ag	Ag$^+$	6×10^{-8} (O$_2$)	~2000–2500	5.2 ± 0.1	–	PSI	[3408,3409]
Re	Ag	Ag$^+$	~10^{-7}	~1850–2200	5.20 ± 0.1	–	PSI	[163]
Re{80%(0001)}	–	–	?	~300	–	5.20 ± 0.1	PE	[401]
Re	–	–	?	1900	–	5.21	TE	[1287]
Re	Li	Li$^+$	$<10^{-7}$	~1900	5.21	–	PSI	[2970]
Re	Li	Li$^+$	$<1 \times 10^{-8}$	~1000–2600	5.21 ± 0.01	(4.98 ± 0.03)	PSI	[54,3078]
Re	Ba	Ba$^+$	$<1 \times 10^{-7}$	~2000–2600	5.21 ± 0.02	–	PSI	[80]
Re	–	–	?	1650	–	5.22	TE	[1287]
Re	Na	Na$^+$	$\leq 2 \times 10^{-7}$	~1550–2350	5.25	–	PSI	[53]
Re	NaCl	Na$^+$	$\leq 2 \times 10^{-7}$	~1800–2350	5.25	–	PSI	[53]
Re/Mo	ReCl$_5$	–	?	1800	–	5.25 ± 0.02	TE	[1287]
Re	In	In$^+$	$\leq 1 \times 10^{-7}$	~1900–2400	5.31 ± 0.03	(4.93 ± 0.04)	PSI	[97]
Re[170]	UF$_4$	U$^+$	$<1 \times 10^{-8}$	~2400–2700	5.33 ± 0.13*	–	PSI	[276]
Re	Li	Li$^+$	$\leq 2 \times 10^{-7}$	~1700–2350	5.34	(4.93 ± 0.04)	PSI	[53]
Re	LiCl	Li$^+$	$\leq 2 \times 10^{-7}$	~1800–2350	5.34	(4.93 ± 0.04)	PSI	[53]
Re	Bi	Bi$^+$	5×10^{-8}	~1700–2500	5.35 ± 0.05	(4.85 ± 0.05)	PSI	[100]
Re[324]	–	–	1×10^{-7}	?	–	5.35 ± 0.05	TE	[166,3730]
Re	In	In$^+$	$\leq 1 \times 10^{-7}$	~1900–2400	5.38 ± 0.03	(4.93 ± 0.04)	PSI	[97]
Re	Ca	Ca$^+$	$\leq 1 \times 10^{-7}$	~1900–2400	5.38 ± 0.03	(4.93 ± 0.04)	PSI	[97]
Re	In	In$^+$	5×10^{-7}	~2300–2700	5.39 ± 0.05	(4.99 ± 0.05)	PSI	[94]
Re	Li	Li$^+$	4×10^{-9}	~1300–1600	5.4	–	PSI	[164]
Re[170]	–	(Re$^+$)	~10^{-7}	~2400–2750	5.4 ± 0.6	(4.93 ± 0.04)	PSI	[77]
Re	In	In$^+$	5×10^{-7}	2350	5.40	(4.99 ± 0.05)	PSI	[94]
Re	NaCl	Na$^+$	2×10^{-7}	~1700–2200	5.40 ± 0.05	–	PSI	[57]
Re	Mg	Mg$^+$	$\leq 1 \times 10^{-7}$	~1900–2400	5.40 ± 0.05	(4.93 ± 0.04)	PSI	[97]
Re	NaI	Na$^+$	2×10^{-7}	~1800–2000	5.41 ± 0.05	(4.95 ± 0.05)	PSI	[23]
Re	NaCl	Na$^+$	2×10^{-7}	~1800–2000	5.42 ± 0.02	(4.95 ± 0.05)	PSI	[23]
Re	NaCl	Na$^+$	~10^{-7}–10^{-5} (air)	2010	5.42 ± 0.02	(4.95 ± 0.05)	PSI	[23]
Re	NaCl	Na$^+$	~10^{-7}–10^{-5} (air)	1830	5.42–5.58	(4.93–5.18)	PSI	[23]
Re	NaCl	Na$^+$	~10^{-7}–10^{-5} (air)	1710	5.42–5.70	(4.97–5.36)	PSI	[23]
Re	NaI	Na$^+$	~10^{-7}–10^{-5} (air)	2080	5.43 ± 0.01	(4.93 ± 0.02)	PSI	[23]
Re	NaI	Na$^+$	~10^{-7}–10^{-5} (O$_2$)	2080	5.43 ± 0.01	(4.95 ± 0.01)	PSI	[23]
Re	Ag	Ag$^+$	$\leq 1 \times 10^{-7}$	~1900–2400	5.43 ± 0.02	(4.93 ± 0.04)	PSI	[97]
Re	NaCl	Na$^+$	2×10^{-7}	~1700–2000	5.43 ± 0.02	–	PSI	[208]
Re	Ca	Ca$^+$	1×10^{-7}	~1750–2400	5.43 ± 0.02	(4.93 ± 0.04)	PSI	[76,77]
Re	NaCl	Na$^+$	~10^{-7}–10^{-5} (air)	1930	5.43 ± 0.04	(4.96 ± 0.05)	PSI	[23]
Re	NaI	Na$^+$	2×10^{-6} (air)	~1900–2100	5.44 ± 0.02	–	PSI	[23]
Re	Ca	Ca$^+$	$\leq 1 \times 10^{-7}$	~1900–2400	5.44 ± 0.03	(4.93 ± 0.04)	PSI	[97]
Re	NaI	Na$^+$	2×10^{-5} (air)	~2000–2100	5.45 ± 0.02	–	PSI	[23]
Re	NaI	Na$^+$	~10^{-7}–10^{-5} (air)	1715	5.45–5.76	(4.97–5.37)	PSI	[23]
Re	NaI	Na$^+$	~10^{-7}–10^{-5} (O$_2$)	1715	5.45–5.81	(4.94–5.41)	PSI	[23]
Re	Ca	Ca$^+$	$\leq 1 \times 10^{-7}$	~1900–2400	5.46 ± 0.02	(4.93 ± 0.04)	PSI	[97]
Re	LiBr	Li$^+$	2×10^{-7}	~1800–2000	5.48 ± 0.02	(4.95 ± 0.05)	PSI	[23,2422]
Re	NaBr	Na$^+$	2×10^{-7}	~1700–2150	5.48 ± 0.03	–	PSI	[24,35]
Re	LiI	Li$^+$	2×10^{-7}	~1800–2000	5.49 ± 0.02	(4.95 ± 0.05)	PSI	[23,38]

Table 1 (*continued*)

Surface	Beam	Ion	P_r (Torr)	T (K)	ϕ^+ (eV)	ϕ^e (eV)	Meth.	Refs.
Re	$C_2(CN)_4$	CN^-	$\leq 1 \times 10^{-6}$	1800	$>5.49 \pm 0.2^N$	(5.0 ± 0.1)	NSI	[216]
Re/HfO$_2$/SiO$_x$/Si	Re	–	$<5 \times 10^{-10}$	~300	–	5.5	PE	[1296]
Re	LiI	Li^+	2×10^{-6} (air)	2000	5.53	–	PSI	[38]
Re	LiCl	Li^+	2×10^{-7}	~1800–2000	5.53 ± 0.02	(4.95 ± 0.05)	PSI	[23]
Re	LiI	Li^+	2×10^{-7}	~1750–2150	5.53 ± 0.02	(5.00 ± 0.01)	PSI	[101]
Re	–	(Re^+)	$<7 \times 10^{-7}$	2590–2780	5.62 ± 0.08	–	PSI	[805,3083]
Re	–	–	–	–	–	6.01	TC	[2629]
Recommended	–	–	–	–	**5.41 ± 0.04**	**4.96 ± 0.05**	–	–

76. Osmium Os

hcp

Surface	Beam	Ion	P_r (Torr)	T (K)	ϕ^+ (eV)	ϕ^e (eV)	Meth.	Refs.
Os(0001)	–	–	–	–	–	5.32	TC	[4004]
Os(0001)	–	–	–	–	–	5.59	TC	[1980]
Os(0001)	–	–	–	–	–	5.62	TC	[4005]
Os(0001)	–	–	–	–	–	5.64	TC	[4004]
Os(0001)	–	–	–	–	–	6.05	TC	[321]
Os(0001)	–	–	–	–	–	6.42	TC	[334]
Os(1010)	–	–	–	–	–	4.94	TC	[4005]
Os(1010)	–	–	–	–	–	5.17	TC	[4004]
Os(1010)	–	–	–	–	–	5.34	TC	[1980]
Os(1010)	–	–	–	–	–	5.45	TC	[4004]
Os(1010)	–	–	–	–	–	5.78	TC	[321]
Os(0111)	–	–	–	–	–	5.23	TC	[4004]
Os(0111)	–	–	–	–	–	5.53	TC	[4004]
Os(0112)	–	–	–	–	–	4.85	TC	[4004]
Os(0112)	–	–	–	–	–	5.15	TC	[4004]
Os(0113)	–	–	–	–	–	4.67	TC	[4004]
Os(0113)	–	–	–	–	–	4.98	TC	[4004]
Os(1121)	–	–	–	–	–	4.67	TC	[4004]
Os(1121)	–	–	–	–	–	4.98	TC	[4004]
Os(1122)	–	–	–	–	–	4.90	TC	[4004]
Os(1122)	–	–	–	–	–	5.22	TC	[4004]
Os(1123)	–	–	–	–	–	4.77	TC	[4004]
Os(1123)	–	–	–	–	–	5.09	TC	[4004]
Os(1124)	–	–	–	–	–	5.06	TC	[321]
Os(2130)	–	–	–	–	–	4.87	TC	[4004]
Os(2130)	–	–	–	–	–	5.20	TC	[4004]
Os(3140)	–	–	–	–	–	4.77	TC	[4004]
Os(3140)	–	–	–	–	–	5.09	TC	[4004]
Os	–	–	?	~300	–	4.55	CPD	[2297]
Os	–	–	? (Cs)	~1500–2000	–	4.6–5.0	TE	[3414]
Os	–	–	–	–	–	4.65	TC	[2005]
Os	–	–	–	–	–	4.66	TC	[2949]
Os	–	–	6×10^{-9}	1800	–	4.68 ± 0.04	TE	[978]
Os	–	–	$<10^{-9}$	1900	–	4.69	TE	[650]
Os	–	–	?	?	–	4.7	TE	[3402]
Os	–	–	?	2000	–	4.71 ± 0.01	TE	[1628,1629]
Os	–	–	–	–	–	4.73	TC	[298]
Os	–	–	? (Cs)	~1600–2000	–	4.8	TE	[650]
Os	–	–	–	–	–	4.83	TC	[3264,3265,3267]
Os	–	–	$\leq 3 \times 10^{-9}$	1480–1640	–	4.83 ± 0.01	TE	[171]
Os	–	–	7×10^{-9}	2200	–	4.83 ± 0.04	TE	[978]
Os	–	–	$\sim 10^{-9}$	~1400–1640	–	4.83 ± 0.05	TE	[124,3414]
Os	–	–	–	–	–	4.84	TC	[3476]
Os	–	–	$<10^{-9}$	1500	–	4.84	TE	[650]
Os	–	–	$\leq 3 \times 10^{-9}$	~600–700	–	4.84 ± 0.04	CPD	[171]
Os	–	–	–	–	–	4.9	TC	[3318]
Os	–	–	–	–	–	4.9*	TC	[1955]

Table 1 (*continued*)

Surface	Beam	Ion	P_r (Torr)	T (K)	ϕ^+ (eV)	ϕ^e (eV)	Meth.	Refs.
Os	–	–	–	–	–	4.91	TC	[1066]
Os	–	–	–	–	–	4.95	TC	[3476]
Os	–	–	–	–	–	4.95 ± 0.05	TC	[1256]
Os	–	–	<10⁻⁹	1200	–	4.96	TE	[650]
Os	–	–	–	–	–	4.99	TC	[3318]
Os	–	–	–	0	–	5.10	TC	[4419]
Os/W(100)–Os(1%)[276]	–	–	<10⁻⁸	2080–2300	–	5.12 ± 0.06	TE	[2811,3086]
Os	–	–	?	?	–	5.16	TE	[2105]
Os/W	Os	–	?	~1500	–	5.17	TE	[2101]
Os	–	–	2 × 10⁻⁷	2600	–	5.21 ± 0.04	TE	[978]
Os	–	–	–	–	–	5.3	TC	[706]
Os	–	–	–	–	–	5.37	TC	[3476]
Os/W[325]	Os	–	?	~300	–	5.93 ± 0.05	PE	[3322]
Os	–	–	–	–	–	6.06	TC	[1744]
Recommended	–	–	–	–	–	**4.97 ± 0.17**	–	–

77. Iridium Ir

fcc

Surface	Beam	Ion	P_r (Torr)	T (K)	ϕ^+ (eV)	ϕ^e (eV)	Meth.	Refs.
Ir(100)	–	–	?	4	–	4.65 ± 0.05	FE	[1391]
Ir(100)	–	–	–	–	–	4.92	TC	[1928]
Ir(100)[326]	–	–	3 × 10⁻¹¹	77	–	5.2	FE	[1810]
Ir(100)	–	–	?	~300	–	5.2	PE	[1532]
Ir(100)	–	–	–	–	–	5.20	TC	[2548]
Ir(100)	–	–	–	–	–	5.20	TC	[1980,3067]
Ir(100)	–	–	~10⁻⁹	1900	–	5.3	TE	[1288]
Ir(100)	–	–	~10⁻⁹	?	–	5.37	TE	[3096]
Ir(100)[326]	–	–	3 × 10⁻¹¹	77	–	5.4	FE	[1810]
Ir(100)[327]	–	–	2 × 10⁻¹⁰	~300 (>1200)	–	5.4	PE	[2961]
Ir(100)[327]	–	–	2 × 10⁻¹⁰	135–300	–	5.5	PE	[1533,1534,2961]
Ir(100)	–	–	–	–	–	5.52	TC	[3224]
Ir(100)	–	–	–	–	–	5.55	TC	[4091]
Ir(100)	–	–	–	–	–	5.55	TC	[4421]
Ir(100)	–	–	~10⁻¹⁰	~300	–	5.6	CPD	[669,2126]
Ir(100)	–	–	?	275	–	5.6	PE	[1534]
Ir(100)	–	–	–	–	–	5.60	TC	[3243]
Ir(100)	–	–	–	–	–	5.60	TC	[4258]
Ir(100)	–	–	–	–	–	5.61	TC	[2203]
Ir(100)	–	–	–	–	–	5.62	TC	[2696,4444]
Ir(100)	–	–	<1 × 10⁻¹⁰	78	–	5.67 ± 0.05	FE	[414,843,1140]
Ir(100)[326]	–	–	<3 × 10⁻¹¹	77	–	5.70 ± 0.05	FE	[1797,1802,1810]
Ir(100)	–	–	?	78	–	5.80 ± 0.02	FE	[2189]
Ir(100)	–	–	–	–	–	5.84	TC	[1718,1721]
Ir(100)	–	–	–	–	–	5.89	TC	[3243]
Ir(100)	–	–	–	–	–	5.92	TC	[1933]
Ir(100)	–	–	?	78	–	6.00 ± 0.02	FE	[2189]
Ir(100)	–	–	<1 × 10⁻¹⁰	100	–	6.00 ± <0.1	PE	[672,914,1289]
Ir(100)	–	–	–	–	–	6.03	TC	[321]
Ir(100)	–	–	?	~300	–	6.1 ± 0.1	CPD	[1067]
Ir(100)	–	–	1 × 10⁻¹⁰	100	–	6.15 ± <0.1	PE	[672,1289]
Recommended	–	–	–	–	–	**5.60 ± 0.06**	–	–
Ir(110)	–	–	~10⁻⁹	1900	–	4.83	TE	[1288]
Ir(110)	–	–	–	–	–	4.83	TC	[2548]
Ir(110)	–	–	–	–	–	4.84	TC	[1980,3067]
Ir(110)	–	–	~10⁻⁹	?	–	4.85	TE	[3096]
Ir(110)	–	–	–	–	–	4.958	TC	[4091]
Ir(110)	–	–	<10⁻¹⁰	80	–	5.0	FE	[414,843]
Ir(110)	–	–	<3 × 10⁻¹¹	77	–	5.0	FE	[1802]
Ir(110)	–	–	–	–	–	5.07	TC	[3243]
Ir(110)	–	–	–	–	–	5.36	TC	[3243]
Ir(110)	–	–	–	–	–	5.37	TC	[3224]
Ir(110)	–	–	~10⁻¹⁰	77, 300	–	5.42 ± 0.02	FE	[358]
Ir(110)	–	–	–	–	–	5.45	TC	[1933]
Ir(110)	–	–	–	–	–	5.67	TC	[321]
Recommended	–	–	–	–	–	**5.23 ± 0.19**	–	–
Ir(111){80%}[329]	–	–	–	–	–	4.68	TC	[1254]
Ir(111){81%}[330]	–	–	? (Cs)	~1500–2000	–	5.2	TE	[3414]
Ir(111){80%}[329]	–	–	~10⁻⁹	~1300–2100	–	5.27 ± 0.05	TE	[124]

Table 1 (*continued*)

Surface	Beam	Ion	P_r (Torr)	T (K)	ϕ^+ (eV)	ϕ^e (eV)	Meth.	Refs.
Ir(111){81%}[328]	–	–	~10^{-9}	~1300–2100	–	5.27 ± 0.05	TE	[650,3414]
Ir(111){81%}[330]	–	–	≤10^{-4}(Li)	~1400–2200	(5.4*)	5.35 ± 0.05	TE	[169]
Ir(111){81%}[328]	–	–	–	–	(5.73 ± 0.01)	5.36 ± 0.07	TC	[803]
Ir(111){81%}[330]	Li	Li$^+$	≤10^{-4}(Li)	~1100	5.4*	(5.35 ± 0.05)	PSI	[169]
Ir(111)	–	–	–	–	–	5.42	TC	[3243]
Ir(111)	–	–	–	–	–	5.497	TC	[4091]
Ir(111)	–	–	–	–	–	5.55	TC	[2548]
Ir(111)	–	–	–	–	–	5.56	TC	[1980,3067]
Ir(111)	–	–	–	–	–	5.58	TC	[2068]
Ir(111)	–	–	–	–	–	5.6	TC	[1723]
Ir(111)	–	–	–	–	–	5.60	TC	[4258]
Ir(111)	–	–	~10^{-10}	80	–	5.65 ± 0.02	FE	[2499]
Ir(111)[334]	Li	Li$^+$	2×10^{-10}	~1100–1300	5.68 ± 0.01	–	PSI	[167]
Ir(111)[334]	Li	Li$^+$	2×10^{-10}	~1150–1400	5.69 ± 0.03	–	PSI	[167]
Ir(111)[334]	Li	Li$^+$	2×10^{-10}	~1100–1400	5.70 ± 0.02	–	PSI	[167,319]
Ir(111)	–	–	–	–	–	5.72	TC	[3243]
Ir(111)[170,334]	Li	Li$^+$	2×10^{-10}	1160–1375	5.72 ± 0.03	–	PSI	[167]
Ir(111){81%}[328]	–	–	–	–	5.73 ± 0.01	(5.36 ± 0.07)	TC	[803]
Ir(111)	–	–	1×10^{-8}	1760–2150	(5.79 ± 0.03)	5.74 ± 0.06	TE	[102,410]
Ir(111)	Bi	Bi$^+$	≤8×10^{-10}	?	5.75 ± 0.05	(5.75 ± 0.05)	PSI	[105,409]
Ir(111)	–	–	≤8×10^{-10}	?	(5.75, 5.8)	5.75 ± 0.05	TE	[105,252]
Ir(111)	Yb	Yb$^+$	≤5×10^{-8}	~1800–2000	5.75 ± 0.10	(5.75 ± 0.10)	PSI	[104]
Ir(111)	–	–	≤5×10^{-8}	~1800–2000	(5.75 ± 0.10)	5.75 ± 0.10	TE	[104]
Ir(111)	–	–	~10^{-10}	77, 300	–	5.76 ± 0.04	FE	[358]
Ir(111)	–	–	3×10^{-9}	~1700–2000	–	5.78 ± 0.05	TE	[273]
Ir(111)	Bi	Bi$^+$	1×10^{-8}	1770–2150	5.79 ± 0.03	(5.74 ± 0.06)	PSI	[102,410]
Ir(111)	Tl	Tl$^+$	1×10^{-8}	1250–2200	5.79 ± 0.03	(5.74 ± 0.06)	PSI	[102,410]
Ir(111)	–	–	<10^{-10}	78	–	5.79 ± 0.05	FE	[414,843,1140]
Ir(111)	Al	Al$^+$	≤10^{-8}	~1700–2500	5.8	–	PSI	[3428]
Ir(111)	In	In$^+$	≤10^{-8}	~1400–1900	5.8	–	PSI	[3428]
Ir(111)	K	K$^+$	<1×10^{-9}	~800–2000	5.8	(5.75 ± 0.05)	PSI	[252,411]
Ir(111)	Ba	Ba$^+$	≤5×10^{-9}	?	5.8	(5.80 ± 0.05)	PSI	[649]
Ir(111)	Ba	Ba$^+$	<5×10^{-10}	?	5.8	–	PSI	[3778]
Ir(111)	Tm	Tm$^+$	?	2000	5.8	–	PSI	[3559]
Ir(111)	In	In$^+$	~10^{-8}	?	5.8 ± 0.05	–	PSI	[186]
Ir(111)	–	–	?	~300	–	5.8	CPD	[3858]
Ir(111)	–	–	~10^{-10}	~300	–	~5.8	FE	[4268]
Ir(111)	–	–	<1×10^{-10}	?	–	5.80	TE	[168,410–413,537]
Ir(111)	–	–	~10^{-9}	?	–	5.80	TE	[3096]
Ir(111)	In	In$^+$	7×10^{-9}	–1700–	5.80 ± 0.03	(5.80 ± 0.03)	PSI	[103]
Ir(111)	–	–	7×10^{-9}	–1700–	(5.80 ± 0.03)	5.80 ± 0.03	TE	[103]
Ir(111)	–	–	<3×10^{-11}	77	–	5.80 ± 0.05	FE	[1797,1802]
Ir(111)	–	–	≤5×10^{-9}	?	(5.8)	5.80 ± 0.05	TE	[649]
Ir(111)	–	–	~10^{-10}	~300	–	5.85 ± 0.04	CPD	[415,3266,3275]
Ir(111)	–	–	–	–	–	5.86	TC	[3224]
Ir(111)	–	–	–	–	–	5.87	TC	[3291]
Ir(111)	–	–	–	–	–	5.92	TC	[1933]
Ir(111)	–	–	–	–	–	6.1	TC	[1723]
Ir(111)	–	–	–	–	–	6.51	TC	[321]
Ir(111)	–	–	–	–	–	6.63	TC	[334]
Ir(111)	–	–	–	–	–	6.65	TC	[3179]
Recommended	–	–	–	–	**5.76 ± 0.04**	**5.75 ± 0.06**	–	–
Ir(210)	–	–	<1×10^{-10}	78	–	5.0 ± 0.05	FE	[414,843]
Ir(210)	–	–	–	–	–	5.10	TC	[3224]
Ir(211)	–	–	–	–	–	5.07	TC	[3224]
Ir(211)	–	–	–	–	–	5.284	TC	[4091]
Ir(311)	–	–	<3×10^{-11}	77	–	5.2	FE	[1802]
Ir(311)	–	–	–	–	–	5.20	TC	[3224]
Ir(321)	–	–	–	–	–	5.072	TC	[4091]
Ir(321)	–	–	<1×10^{-10}	78	–	5.4	FE	[414]
Ir(331)	–	–	–	–	–	5.12	TC	[3224]
Ir(331)	–	–	<1×10^{-10}	78	–	5.4	FE	[414]
Ir(731)	–	–	<10^{-10}	78	–	4.9	FE	[843]

Table 1 (*continued*)

Surface	Beam	Ion	P_r (Torr)	T (K)	ϕ^+ (eV)	ϕ^e (eV)	Meth.	Refs.
Ir	–	–	–	–	–	2.20	TC	[2493]
Ir	–	–	–	–	–	2.42	TC	[2493]
Ir	–	–	–	–	–	4.02	TC	[521]
Ir	–	–	?	~300	–	4.57	CPD	[2297]
Ir	–	–	3×10^{-9}	~1150–1900	–	4.57	TE	[159]
Ir	–	–	–	–	–	4.57	TC	[1399]
Ir	–	–	~10^{-6}	≤1700	–	~4.6	TC	[3537]
Ir	–	–	?	4	–	4.6 ± 0.6	FE	[1391]
Ir{80%(111)}[329]	–	–	–	–	–	4.68	TC	[1254]
Ir	–	–	–	–	–	4.78	TC	[2005]
Ir	–	–	–	–	–	4.86	TC	[3318]
Ir	–	–	–	–	–	4.91	TC	[3318]
Ir	–	–	–	–	–	4.97	TC	[3264]
Ir	–	–	–	–	–	5.00	TC	[3476]
Ir	–	–	–	–	–	5.02	TC	[2629]
Ir	–	–	1×10^{-9}	~300	–	5.14 ± 0.04	CPD	[845]
Ir	–	–	2×10^{-7}	~1450–1800	(5.72 ± 0.03)	5.15 ± 0.03	TE	[68]
Ir/glass	Ir	–	<1×10^{-10}	78	–	5.17	PE	[414]
Ir	–	–	–	–	–	5.17	TC	[3476]
Ir{81%(111)}[330]	–	–	? (Cs)	~1500–2000	–	5.2	TE	[3414]
Ir	–	–	1×10^{-7}	~1500–2400	–	5.2	TE	[2320]
Ir	–	–	3×10^{-7}	~1400–1700	–	5.2 ± 0.2	TE	[1290]
Ir	–	–	≤3×10^{-9}	~1600–1800	–	5.24 ± 0.03	TE	[171]
Ir/W(porous)	–	–	≤10^{-9}	~1500	–	5.25	TE	[650]
Ir	–	–	–	–	–	5.25	TC	[3224]
Ir	–	–	~10^{-7}	~1300–2100	(5.25–5.34)	5.25 ± 0.05	TE	[107]
Ir	K	K$^+$	~10^{-7}	~1200–2000	>5.25	(5.25 ± 0.05)	PSI	[107]
Ir	–	–	?	2670–2730	–	5.26 ± 0.01	TE	[495,2205]
Ir{81%(111)}[330]	–	–	~10^{-9}	?	–	5.27	TE	[3414]
Ir{80%(111)}[329]	–	–	~10^{-9}	~1300–2100	–	5.27 ± 0.05	TE	[124,650]
Ir/W(100)–Ir(2%)[275]	–	–	?	2030–2200	–	5.28 ± 0.06	TE	[3086]
Ir	–	–	?	?	–	5.29	?	[416]
Ir	Li	Li$^+$	<10^{-9}	~1000–1200	5.3	–	PSI	[318,319,366]
Ir	–	–	–	–	–	5.3	TC	[2583]
Ir	–	–	?	~1700–2200	–	5.3	TE	[668]
Ir	–	–	~10^{-9}	~300	–	5.3	CPD	[417]
Ir/Pd	Ir	–	~10^{-9}	~300	–	5.3	CPD	[417]
Ir	Na	Na$^+$	~10^{-10}	~1300	5.3	–	PSI	[844]
Ir	–	–	2×10^{-10}	?	–	5.3	TE	[669]
Ir	–	–	≤5×10^{-8}	~1900–2400	–	5.30 ± 0.01	TE	[978]
Ir	–	–	?	~2500–2600	–	5.30 ± 0.01	TE	[495,2205]
Ir	–	–	≤5×10^{-7}	?	–	5.30 ± 0.04	TE	[160]
Ir	–	–	–	–	–	5.31	TC	[298]
Ir	–	–	?	?	–	5.31	TE	[2105]
Ir	–	–	–	–	–	5.33	TC	[4441]
Ir/glass	Ir	–	<1×10^{-10}	78 (293)	–	5.33	PE	[414]
Ir	–	–	≤3×10^{-9}	~600–700	–	5.33	CPD	[171]
Ir	Na	Na$^+$	~10^{-7}	~1350–2000	5.34 ± 0.07	(5.25 ± 0.05)	PSI	[107]
Ir/glass	–	–	<5×10^{-10}	77 (373)	–	5.35	PE	[1256]
Ir{81%(111)}[330]	–	–	≤10^{-4} (Li)	~1400–2200	(5.4*)	5.35 ± 0.05	TE	[169]
Ir	–	–	3×10^{-7}	~1400–1600	–	5.36	TE	[1290]
Ir{81%(111)}[328]	–	–	–	–	(5.73 ± 0.01)	5.36 ± 0.07	TC	[803]
Ir/glass	Ir	–	<1×10^{-10}	78 (473)	–	5.38	PE	[414]
Ir{81%(111)}[330]	Li	Li$^+$	≤10^{-4} (Li)	~1100	5.4*	(5.35 ± 0.05)	PSI	[169]
Ir	Na	Na$^+$	~10^{-10}	~1300	5.4*	–	PSI	[844]
Ir	–	–	~10^{-9}	>1200	–	5.4	TE	[1203]
Ir	–	–	?	~1600–2300	–	5.40	TE	[170]
Ir	–	–	~10^{-9}	?	–	5.40	TE	[3096]
Ir	–	–	5×10^{-8}	~1550–2250	(5.80 ± 0.05)	5.40 ± 0.05	TE	[106,667]
Ir[325]	–	–	?	~300	–	5.50 ± 0.05	PE	[3322]
Ir	–	–	–	–	–	5.59	TC	[3476]
Ir/W(100)	Ir	–	~1×10^{-11}	77	–	5.60	FE	[2965]
Ir	NaBr	Na$^+$	2×10^{-7}	~1600–1900	5.72 ± 0.03	(5.15 ± 0.03)	PSI	[68]
Ir{81%(111)}[328]	–	–	–	–	5.73 ± 0.01	(5.36 ± 0.07)	TC	[803]
Ir	NaCl	Na$^+$	2×10^{-7}	~1600–1850	5.73 ± 0.02	(5.15 ± 0.03)	PSI	[68]
Ir	Bi	Bi$^+$	5×10^{-8}	~1700–2250	5.80 ± 0.05	(5.40 ± 0.05)	PSI	[106,667]
Recommended	–	–	–	–	**5.75 ± 0.04**	**5.28 ± 0.04**	–	–

Table 1 (*continued*)

Surface	Beam	Ion	P_r (Torr)	T (K)	ϕ^+ (eV)	ϕ^e (eV)	Meth.	Refs.
				78. Platinum Pt				
fcc								
Pt(100)/MgO	Pt	–	?	~300	–	4.78	PE	[2448]
Pt(100)	–	–	–	–	–	5.20	TC	[1980]
Pt(100)	–	–	–	–	–	5.20 ± 0.02	TC	[3244]
Pt(100)	–	–	–	–	–	5.32	TC	[3244]
Pt(100)	–	–	?	~300	–	5.5 ± 0.2	CPD	[1067]
Pt(100)	–	–	–	–	–	5.625	TC	[4091]
Pt(100)	–	–	–	–	–	5.63	TC	[4416]
Pt(100)	–	–	–	–	–	5.64	TC	[3244]
Pt(100)	–	–	–	–	–	5.66	TC	[4087]
Pt(100)	–	–	–	–	–	5.67	TC	[3224]
Pt(100)	–	–	–	–	–	5.7	TC	[1938]
Pt(100)	–	–	3×10^{-10}	~300	–	5.7 ± 0.1	PE	[846]
Pt(100)	–	–	–	–	–	5.71	TC	[4434]
Pt(100)	–	–	–	–	–	5.711	TC	[3245]
Pt(100)	–	–	4×10^{-11}	100	–	5.75 ± 0.05	PE	[847]
Pt(100)	–	–	–	–	–	5.78	TC	[705]
Pt(100)	–	–	1×10^{-10}	80	–	5.8	FE	[2163]
Pt(100)	–	–	$<1 \times 10^{-10}$	78	–	5.8	FE	[414,848]
Pt(100)	–	–	1×10^{-10}	~300	–	5.8	PE	[3587]
Pt(100)	–	–	$<1 \times 10^{-10}$	78	–	5.81	FE	[849]
Pt(100)	–	–	1×10^{-10}	~300	–	5.82 ± 0.15	PE	[174,3136]
Pt(100)	–	–	$<10^{-10}$	80	–	5.84	FE	[428]
Pt(100)	–	–	2×10^{-11}	~300	–	5.84	PE	[429]
Pt(100)	–	–	–	–	–	5.840	TC	[2229]
Pt(100)	–	–	–	–	–	5.85	TC	[4229]
Pt(100)	–	–	2×10^{-11}	~300	–	5.86	PE	[429,2987,2996]
Pt(100)	–	–	?	~300	–	5.9 ± 0.1	PE	[850]
Pt(100)	–	–	–	–	–	5.92 ± 0.09	TC	[851,852]
Pt(100)[331]	–	–	–	–	–	5.93	TC	[795]
Pt(100)	–	–	–	–	–	5.94	TC	[2530]
Pt(100)	–	–	–	–	–	5.96	TC	[3356]
Pt(100)	–	–	–	–	–	5.99	TC	[321]
Pt(100)	–	–	$\sim 10^{-11}$	~300	–	6.00 ± 0.06	FE	[853]
Pt(100)[331]	–	–	–	–	–	6.07	TC	[795]
Pt(100)	–	–	–	–	–	6.07	TC	[1237]
Pt(100)	–	–	–	–	–	6.08	TC	[2701]
Pt(100)	–	–	–	–	–	6.09	TC	[2701]
Pt(100)	–	–	–	–	–	6.1	TC	[1938]
Pt(100)	–	–	–	–	–	6.1	TC	[2905]
Pt(100)	–	–	–	–	–	6.11	TC	[1928]
Pt(100)	–	–	–	–	–	6.12	TC	[2846]
Pt(100)	–	–	–	–	–	6.2	TC	[854]
Pt(100)	–	–	–	–	–	6.2	TC	[3733]
Pt(100)	–	–	–	–	–	6.21	TC	[3635]
Pt(100)	–	–	–	–	–	6.23	TC	[3382]
Pt(100)	–	–	–	–	–	6.52	TC	[1201]
Pt(100)	–	–	–	–	–	6.57	TC	[3339]
Pt(100)	–	–	–	–	–	6.60	TC	[855]
Pt(100)	–	–	–	–	–	6.7	TC	[389]
Pt(100)	–	–	–	–	–	6.86	TC	[3194]
Pt(100)	–	–	–	–	–	6.93	TC	[3194]
Pt(100)	–	–	–	–	–	6.97	TC	[334]
Recommended	–	–	–	–	–	**5.75 ± 0.06**	–	–
Pt(110)	–	–	–	–	–	4.84	TC	[1980]
Pt(110)	–	–	–	–	–	4.93	TC	[3791]
Pt(110)	–	–	–	–	–	5.223	TC	[4091]
Pt(110)[332]	–	–	$\sim 10^{-11}$	~300	–	5.24 ± 0.05	FE	[853]
Pt(110)	–	–	–	–	–	5.26	TC	[4087,4410]
Pt(110)	–	–	–	–	–	5.297	TC	[3245]
Pt(110)[332]	–	–	$\sim 10^{-11}$	~300	–	5.35 ± 0.05	FE	[853]
Pt(110)	–	–	$<1 \times 10^{-10}$	78	–	5.4	FE	[849,2728]
Pt(110)	–	–	1×10^{-10}	80	–	5.4	FE	[2163]
Pt(110)	–	–	7×10^{-11}	100	–	5.4	PE	[1923]
Pt(110)	–	–	–	–	–	5.441	TC	[2229]
Pt(110)	–	–	?	77	–	5.49	FE	[1294]

Table 1 (*continued*)

Surface	Beam	Ion	P_r (Torr)	T (K)	ϕ^+ (eV)	ϕ^e (eV)	Meth.	Refs.
Pt(110)	–	–	?	?	–	5.5	?	[2042]
Pt(110)[333]	–	–	–	–	–	5.52	TC	[2543]
Pt(110)	–	–	–	–	–	5.52	TC	[3224]
Pt(110)	–	–	–	–	–	5.54	TC	[1931]
Pt(110)	–	–	–	–	–	5.63	TC	[321]
Pt(110)	–	–	$\sim10^{-11}$	~300	–	5.67	PE	[1291]
Pt(110)	–	–	–	–	–	5.69	TC	[4416]
Pt(110)	–	–	–	–	–	5.7	TC	[2905]
Pt(110)	–	–	7×10^{-11}	150	–	5.7 ± 0.1	PE	[856]
Pt(110)[333]	–	–	–	–	–	5.71	TC	[2543]
Pt(110)	–	–	2×10^{-11}	~300	–	5.72	PE	[429]
Pt(110)	–	–	–	–	–	5.74	TC	[1237]
Pt(110)	–	–	–	–	–	6.10	TC	[3194]
Pt(110)	–	–	–	–	–	6.15	TC	[3194]
Pt(110)	–	–	–	–	–	6.19	TC	[1201]
Recommended	–	–	–	–	–	**5.54 ± 0.07**	–	–
Pt(111)	–	–	–	–	–	4.54	TC	[1254]
Pt(111)	Ca	Ca$^+$	? (Ca)	?	4.7 ± 0.2	–	PSI	[126]
Pt(111)	Na	Na$^+$	$\leq6 \times 10^{-3}$ (Na)	~1450–1700	4.77 ± 0.07	–	PSI	[126,173]
Pt(111)	K	K$^+$	$\leq2 \times 10^{-2}$ (K)	1600	4.8 ± 0.2	–	PSI	[172]
Pt(111)	Ca	Ca$^+$	? (Ca)	1580	4.82 ± 0.05	–	PSI	[126]
Pt(111)/quartz	Pt	–	?	~300	–	4.93	PE	[2448]
Pt(111)/garnet	Pt	–	?	~300	–	4.93	PE	[2448]
Pt(111)/sapphire	Pt	–	?	~300	–	4.93	PE	[2448]
Pt(111)	–	–	?	?	–	4.95 ± 0.05	TE	[857]
Pt(111)	–	–	1×10^{-10}	77	–	5.40	CPD	[2993]
Pt(111)	–	–	$\sim10^{-10}$	~300	–	5.5 ± 0.1	PE	[418,3138]
Pt(111)[178]	–	–	$\sim10^{-11}$	~300	–	5.53 ± 0.06	FE	[853]
Pt(111){mainly}[344]	–	–	$<1 \times 10^{-9}$	~1300–1800	–	5.55 ± 0.1	TE	[434]
Pt(111)	–	–	–	–	–	5.56	TC	[1980]
Pt(111)	–	–	$\sim10^{-10}$	~300	–	5.6 ± 0.1	PE	[858]
Pt(111)	–	–	–	–	–	5.67 ± 0.06	TC	[3244]
Pt(111)	–	–	–	–	–	5.67 ± 0.07	TC	[3244]
Pt(111)	–	–	–	–	–	5.69	TC	[1028,1179]
Pt(111)	–	–	–	–	–	5.69	TC	[4087,4410]
Pt(111)	–	–	1×10^{-10}	80–340	–	5.7	PE	[616,1805]
Pt(111)	–	–	2×10^{-10}	~300	–	5.7	PE	[3455]
Pt(111)	–	–	$<10^{-10}$	~300	–	5.7	PE	[3715]
Pt(111)	–	–	$\sim10^{-10}$	100	–	5.7 ± 0.2	PE	[671]
Pt(111)	–	–	–	–	–	5.70	TC	[419]
Pt(111)	–	–	–	–	–	5.702	TC	[4091]
Pt(111)	–	–	–	–	–	5.72	TC	[420]
Pt(111)	–	–	–	–	–	5.73	TC	[1179]
Pt(111)	–	–	–	–	–	5.74	TC	[4258]
Pt(111)	–	–	–	–	–	5.747	TC	[3245]
Pt(111)[170,334]	Li	Li$^+$	2×10^{-10}	1320–1475	5.75 ± 0.02	–	PSI	[167]
Pt(111)	–	–	–	–	–	5.76	TC	[3244]
Pt(111)	–	–	–	–	–	5.76	TC	[343]
Pt(111)[334]	Li	Li$^+$	2×10^{-10}	1300–1340	5.76 ± 0.02	–	PSI	[167]
Pt(111)[334]	Li	Li$^+$	2×10^{-10}	1240–1475	5.77 ± 0.02	–	PSI	[167,319]
Pt(111)	–	–	?	?	–	5.79	TE	[1852]
Pt(111)	–	–	1×10^{-10}	~300	–	5.8	PE	[3989]
Pt(111){rich}	–	–	$\sim10^{-10}$	~300	–	5.8	CPD	[437]
Pt(111)/Ni(111)	Pt	–	$\sim10^{-10}$	<85 (≤500)	–	5.8	PE	[773]
Pt(111)	–	–	?	~300	–	5.8	CPD	[3518]
Pt(111)	–	–	2×10^{-10}	50	–	5.8	PE	[1437,2273,2275]
Pt(111)	–	–	–	–	–	5.8	TC	[1723]
Pt(111)[334]	Li	Li$^+$	2×10^{-10}	1240–1440	5.80 ± 0.02	–	PSI	[167]
Pt(111)	–	–	–	–	–	5.817	TC	[2229]
Pt(111)	–	–	–	–	–	5.84	TC	[1197]
Pt(111)[335]	–	–	$<10^{-10}$	85–400	–	5.84 ± 0.05	PE	[421–423,773]
Pt(111)/Pt(111)[335]	Pt	–	$<10^{-10}$	400	–	5.84 ± 0.05	PE	[421]
Pt(111)/Nb(110)	Pt	–	7×10^{-11}	~300	–	5.85	PE	[2874]
Pt(111)	–	–	2×10^{-10}	~300	–	5.85	PE	[424]
Pt(111)	–	–	4×10^{-11}	135–370	–	5.85 ± 0.05	PE	[425]
Pt(111)	–	–	?	95	–	5.85 ± 0.1	PE	[426,859]
Pt(111)	–	–	–	–	–	5.89	TC	[2068]
Pt(111)	–	–	8×10^{-11}	~300	–	5.9	PE	[427,1565]
Pt(111)	–	–	–	–	–	5.9	TC	[1723]

Table 1 (*continued*)

Surface	Beam	Ion	P_r (Torr)	T (K)	ϕ^+ (eV)	ϕ^e (eV)	Meth.	Refs.
Pt(111)	–	–	$<1 \times 10^{-10}$	78	–	5.9	FE	[848]
Pt(111)/Ni(111)	Pt	–	$\sim 10^{-10}$	≤85 (573)	–	5.9	PE	[773]
Pt(111)/Re(0001)	Pt	–	$\sim 10^{-10}$	~300	–	5.9	PE	[400]
Pt(111)	Li	Li$^+$	2×10^{-10}	400	5.91 ± 0.07	–	PSI	[167]
Pt(111)	–	–	$<10^{-10}$	80	–	5.93	FE	[428]
Pt(111)	–	–	2×10^{-11}	~300	–	5.94	PE	[429]
Pt(111)	–	–	?	77	–	5.95	FE	[1294]
Pt(111)	–	–	8×10^{-11}	50	–	5.95	PE	[898,3197]
Pt(111)	–	–	?	<85	–	5.95 ± 0.1	PE	[1033]
Pt(111)	–	–	–	–	–	5.97	TC	[430]
Pt(111)	–	–	$\sim 10^{-10}$	~300	–	5.97	PE	[2529]
Pt(111)	–	–	$<1 \times 10^{-10}$	78	–	5.99	FE	[849]
Pt(111)	–	–	1×10^{-10}	80	–	6.0	FE	[2163]
Pt(111)	–	–	–	–	–	6.01	TC	[795]
Pt(111)	–	–	–	–	–	6.01	TC	[3224]
Pt(111)	–	–	–	–	–	6.02	TC	[4024]
Pt(111)	–	–	–	–	–	6.04	TC	[3291]
Pt(111)	–	–	–	–	–	6.04	TC	[1179]
Pt(111)	–	–	–	–	–	6.06	TC	[1028,1179,1834]
Pt(111)	–	–	–	–	–	6.07	TC	[419]
Pt(111)	–	–	1×10^{-10}	~300	–	6.08 ± 0.15	PE	[174]
Pt(111)	–	–	–	–	–	6.1	TC	[1292]
Pt(111)	–	–	–	–	–	6.1	TC	[2905]
Pt(111)	–	–	–	–	–	6.10	TC	[431,1931]
Pt(111)	–	–	2×10^{-10}	~300	–	6.10 ± 0.06	PE	[175]
Pt(111)	–	–	–	–	–	6.11	TC	[1293]
Pt(111)	–	–	–	–	–	6.12	TC	[432]
Pt(111)	–	–	–	–	–	6.12	TC	[1237]
Pt(111)	–	–	–	–	–	6.13	TC	[4174,4284]
Pt(111)	–	–	–	–	–	6.14	TC	[1197]
Pt(111)	–	–	–	–	–	6.16	TC	[1593]
Pt(111)	–	–	$\leq 1 \times 10^{-10}$	~300	–	6.2	PE	[3177,3191]
Pt(111)	–	–	–	–	–	6.3	TC	[1723]
Pt(111)	–	–	1×10^{-10}	100	–	6.40 ± <0.1	PE	[672]
Pt(111)	–	–	–	–	–	6.47	TC	[321]
Pt(111)	–	–	–	–	–	6.53	TC	[1201]
Pt(111)	–	–	?	37, 95	–	6.6*	PE	[3630]
Pt(111)	–	–	–	–	–	6.60	TC	[3194]
Pt(111)	–	–	–	–	–	6.67	TC	[3194]
Pt(111)	–	–	–	–	–	6.73	TC	[3179]
Pt(111)	–	–	–	–	–	6.74	TC	[334]
Recommended	–	–	–	–	**5.80 ± 0.06**	**5.84 ± 0.05**	–	–
Pt(210){~80%}[336]	–	–	? (Cs)	~1500–1900	–	5.0	TE	[650]
Pt(210){~80%}[336]	–	–	? (Cs)	~1500–1900	–	5.1	TE	[3413,3414]
Pt(210)	–	–	$<1 \times 10^{-10}$	78	–	5.17	FE	[849]
Pt(210)	–	–	10^{-11}	~300	–	5.18	FE	[2511]
Pt(210)	–	–	?	77	–	5.18	FE	[1294]
Pt(210)	–	–	$<1 \times 10^{-10}$	78	–	5.2	FE	[414,848]
Pt(210)	–	–	–	–	–	5.25	TC	[3224]
Pt(210){~80%}[336]	–	–	$<1 \times 10^{-9}$	~1600–1950	–	5.79 ± 0.09	TE	[179,650]
Recommended	–	–	–	–	–	**5.18 ± 0.04**	–	–
Pt(211)	–	–	–	–	–	5.22	TC	[3224]
Pt(211)	–	–	–	–	–	5.555	TC	[4091]
Pt(211)	–	–	–	–	–	5.84	TC	[1293]
Pt(211)	–	–	–	–	–	5.88	TC	[1293]
Pt(221)[337]	–	–	–	–	–	5.74	TC	[1293]
Pt(221)[337]	–	–	–	–	–	5.76	TC	[1293]
Pt(221?)[337]	–	–	2×10^{-11}	~300	–	5.77	PE	[429]
Pt(310)	–	–	$\sim 10^{-11}$	~300	–	5.36 ± 0.05	FE	[853,2511]
Pt(310)	–	–	–	–	–	5.419	TC	[4091]
Pt(311)	–	–	–	–	–	5.35	TC	[3224]
Pt(311)	–	–	$<1 \times 10^{-10}$	78	–	5.5	FE	[414,848,2728]
Pt(320)	–	–	–	–	–	5.16	TC	[3224]
Pt(320)	–	–	$\sim 10^{-11}$	~300	–	5.19 ± 0.05	FE	[853,2511]

Table 1 (*continued*)

Surface	Beam	Ion	P_r (Torr)	T (K)	ϕ^+ (eV)	ϕ^e (eV)	Meth.	Refs.
Pt(320)	–	–	$<10^{-10}$	80	–	5.22	FE	[428]
Pt(321)	–	–	$\sim10^{-11}$	~300	–	5.24 ± 0.05	FE	[853,2511]
Pt(321)	–	–	$<1 \times 10^{-10}$	78	–	5.4	FE	[414,848,2728]
Pt(331)	–	–	$<10^{-10}$	80	–	5.12	FE	[428]
Pt(331)	–	–	–	–	–	5.27	TC	[3224]
Pt(331)	–	–	–	–	–	5.62	TC	[1293]
Pt(331)	–	–	–	–	–	5.69	TC	[1293]
Pt(410)	–	–	$\sim10^{-11}$	~300	–	5.50 ± 0.05	FE	[853,2511]
Pt(430)	–	–	$\sim10^{-11}$	~300	–	5.21 ± 0.05	FE	[853,2511]
Pt(520)	–	–	$\sim10^{-11}$	~300	–	5.30 ± 0.05	FE	[853,2511]
Pt(533)	–	–	–	–	–	5.90	TC	[1293]
Pt(533)	–	–	–	–	–	5.93	TC	[1293]
Pt(533)–(755)	–	–	$<1 \times 10^{-10}$	78	–	5.7	FE	[849]
Pt(741)	–	–	$\sim10^{-11}$	~300	–	5.19 ± 0.05	FE	[853,2511]
Pt(997)	–	–	1×10^{-10}	~300	–	5.78 ± 0.15	PE	[174]
Pt	–	–	?	~300	–	3.94	PE	[2460]
Pt	–	–	?	?	–	4.18	TE	[3019]
Pt	–	–	3×10^{-8}	~300	–	4.3	FE	[2082]
Pt	–	–	?	~300	–	4.34	PE	[3018]
Pt	–	–	$<10^{-6}$	~300	–	4.4	PE	[2919]
Pt[338]	Cs	Cs^+	2×10^{-7}	$\sim1400–2000$	$4.40 \pm 0.03*$	–	PSI	[50]
Pt	–	–	?	?	–	4.43	TE	[2567]
Pt	–	–	6×10^{-3}	~300	–	4.43 ± 0.06	PE	[2079,2080]
Pt	–	–	1×10^{-5}	$\sim1700–1900$	–	4.46	TE	[2458]
Pt[338]	K	K^+	2×10^{-7}	$\sim1300–2000$	$4.48 \pm 0.01*$	–	PSI	[50]
Pt[338]	Rb	Rb^+	2×10^{-7}	$\sim1200–2000$	$4.49 \pm 0.01*$	–	PSI	[50]
Pt	K	K^+	2×10^{-7}	$\sim1300–2000$	4.49 ± 0.01	–	PSI	[1285]
Pt	–	–	?	~300	–	4.52	CPD	[2297]
Pt/glass	–	–	$\sim10^{-6}$	$\sim300–720$	–	4.54	PE	[3585]
Pt/GaP	–	–	–	–	–	4.55	TC	[1653]
Pt	–	–	?	?	–	4.57	TE	[3019]
Pt/Si	–	–	–	–	–	4.57	TC	[1653]
Pt	–	–	?	$\sim1600–1700$	–	4.6	TE	[2312]
Pt/Si	–	–	–	–	–	4.60	TC	[1653]
Pt	–	–	–	–	–	4.65	TC	[3318]
Pt	–	–	$\sim10^{-7}$	~300	–	4.65 ± 0.05	CPD	[1890]
Pt/GaP	–	–	–	–	–	4.66	TC	[1653]
Pt	–	–	7×10^{-9}	?	(5.45–5.78)	4.66 ± 0.2	TE	[74]
Pt	–	–	–	–	–	4.67	TC	[2005]
Pt	–	–	?	$\sim1350–1600$	–	4.7	TE	[1753]
Pt	–	–	–	–	–	4.71	TC	[1796]
Pt[339]	–	–	?	?	–	4.72	TE	[2299,2300]
Pt	–	–	?	~300	–	4.76	PE	[1371]
Pt	–	–	?	~300	–	4.79	CPD	[2761]
Pt	–	–	$\leq1 \times 10^{-6}$	293	–	4.80	PE	[2289]
Pt	–	–	–	–	–	4.86	TC	[3476]
Pt	–	–	?	~300	–	$4.87 \pm 0.06*$	CPD	[1953]
Pt	–	–	–	–	–	4.89	TC	[1066]
Pt	–	–	–	–	–	4.9	TC	[3318]
Pt	K	K^+	$<10^{-9}$	$\sim1100–1200$	$4.9 \pm 0.1*$	–	PSI	[2579]
Pt	–	–	–	–	–	4.90	TC	[4420]
Pt	–	–	$\sim10^{-8}$	~300	–	4.93 ± 0.03	PE	[1751]
Pt[340]	K	K^+	$\leq3 \times 10^{-9}$	$\sim1200–1700$	4.94 ± 0.23	(5.27 ± 0.1)	PSI	[3055]
Pt	–	–	?	?	–	4.99	TE	[3019]
Pt/W	Pt	–	$\leq10^{-6}$	$\sim1600–1800$	–	5.0	TE	[2301]
Pt	–	–	?	~300	–	5.0	CPD	[1597,1600]
Pt	–	–	6×10^{-9}	$\sim1350–1950$	–	5.00 ± 0.05	TE	[2125]
Pt	–	–	–	–	–	5.03	TC	[3264,3267]
Pt	–	–	–	–	–	5.03	TC	[3476]
Pt	Li	Li^+	5×10^{-9}	1150	$5.03*$	–	PSI	[1393]

Table 1 (*continued*)

Surface	Beam	Ion	P_r (Torr)	T (K)	ϕ^+ (eV)	ϕ^e (eV)	Meth.	Refs.
Pt/ZrO$_2$	–	–	?	~300	–	5.05	CPD	[3681]
Pt{~80%(210)}[336]	–	–	? (Cs)	~1800–2000	–	5.1	TE	[3413,3414]
Pt/Ru(0001)	–	–	–	–	–	5.10	TC	[2554]
Pt	K	K$^+$	7×10^{-9}	~800–1800	≥5.1	(4.66 ± 0.2)	PSI	[74]
Pt	–	–	~10^{-9}	~300	–	5.12	PE	[3212]
Pt/cnt/Si(111)[25]	–	–	~10^{-10}	~300	–	5.12 ± 0.06	PE	[3246]
Pt	–	–	3×10^{-11}	~300	–	5.13	FE	[2227]
Pt	Na	Na$^+$	≤5×10^{-9}	~1250–1700	5.13 ± 0.01	–	PSI	[2594]
Pt	–	–	5×10^{-8}	1560–1920	(5.77 ± 0.05)	5.13 ± 0.05	TE	[106,667]
Pt/W[346]	Pt	–	~10^{-9}	77	–	5.2	CPD	[1137]
Pt	–	–	–	–	–	5.2	TC	[2583]
Pt/Nb	Pt	–	≤3×10^{-9}	~300	–	5.2*	CPD	[3263]
Pt	–	–	?	~300	–	5.2	PE	[3505]
Pt/W	Pt	–	?	~300	–	5.2	CPD	[2577]
Pt/W	Pt	–	?	1000	–	5.2	FE	[4115]
Pt	–	–	–	–	–	5.2	TC	[1645]
Pt	–	–	?	O^E	–	5.22	TE	[3020]
Pt/HfO$_2$	Pt	–	?	~300	–	5.23	CPD	[3651]
Pt	–	–	?	~300	–	5.25 ± 0.01	CPD	[1953]
Pt	–	–	?	~300	–	5.25 ± 0.07*	CPD	[3994]
Pt	–	–	?	>1900	–	5.27	TE	[674,1847]
Pt/W(110)	Pt	–	5×10^{-11}	~300 (880)	–	5.27*	CPD	[2420]
Pt	–	–	1×10^{-10}	~300	(4.94 ± 0.23)	5.27 ± 0.1	PE	[3055]
Pt	–	–	<3×10^{-8}	~1700–2000	–	5.28	TE	[177]
Pt	–	–	~10^{-7}	1560–1800	–	5.29*	TE	[176]
Pt/W(110)	Pt	–	5×10^{-11}	~300 (1200)	–	5.29*	CPD	[2420]
Pt	–	–	?	?	–	5.3	TE	[3402]
Pt	–	–	–	–	–	5.3	TC	[3030]
Pt	–	–	4×10^{-10}	~300	–	5.3	PE	[3124]
Pt/Ir	Pt	–	?	~300	–	5.3 ± 0.1	CPD	[1600]
Pt	–	–	4×10^{-10}	~300	–	5.3 ± 0.1	PE	[3132]
Pt	–	–	<5×10^{-11}	~300	–	5.3 ± 0.15	PE	[2724]
Pt	–	–	–	–	–	5.30	TC	[1885]
Pt/quartz	Pt	–	≤5×10^{-10}	78	–	5.30 ± 0.01	PE	[435]
Pt/Si(111)	Pt	–	<1×10^{-10}	~300 (≤320)	–	5.30 ± 0.05	CPD	[3270]
Pt	–	–	<3×10^{-8}	~1700–1900	–	5.31	TE	[177]
Pt	–	–	?	~1500–1850	–	5.31 ± 0.01	TE	[1306]
Pt	–	–	<3×10^{-8}	~1700–2000	–	5.32	TE	[177]
Pt	–	–	–	–	–	5.32	TC	[1399]
Pt	Li	Li$^+$	2×10^{-7}	~1800–1950	5.32 ± 0.05*	–	PSI	[50]
Pt	–	–	–	–	–	5.34	TC	[3931]
Pt	Tl	Tl$^+$	5×10^{-9}	~1250–1370	5.34	–	PSI	[1393]
Pt	–	–	3×10^{-9}	~1000–1600	–	5.36	TE	[159]
Pt	–	–	?	~300	–	5.36	CPD	[3256]
Pt[341]	Cs	Cs$^+$	≤6×10^{-9}	~1600–1900	5.36 ± 0.06	(5.41 ± 0.05)	PSI	[282]
Pt	–	–	?	~300	–	5.36 ± 0.06	CPD	[2762]
Pt/cnt/Si(111)[25]	–	–	~10^{-10}	~300	–	5.39 ± 0.08	CPD	[3246]
Pt	–	–	–	–	–	5.4	TC	[3161]
Pt/W	Pt	–	≤10^{-6}	~1600–1800	–	5.4	TE	[2301]
Pt	–	–	1×10^{-6}	~1600–1900	–	5.4	TE	[675]
Pt/Mo(112)	Pt	–	<1×10^{-10}	~300 (~1300)	–	5.4	CPD	[3210]
Pt/Pt(110)	Pt	–	7×10^{-11}	90, 150	–	5.4 ± 0.1	PE	[856]
Pt	–	–	?	~300	–	5.4 ± 0.1	CPD	[1600]
Pt	–	–	–	–	–	5.40	TC	[3264,3265,3267]
Pt	–	–	–	–	–	5.40	TC	[3224]
Pt	–	–	~10^{-7}	~1550–1800	–	5.40 ± 0.03	TE	[176]
Pt	–	–	?	>1900	–	5.40 ± 0.08	TE	[674,1847]
Pt/SiO$_2$/Si	Pt	–	?	~300	–	5.41	CPD	[4330]
Pt[341]	–	–	≤6×10^{-9}	~1600–1900	(5.36,5.52)	5.41 ± 0.05	TE	[282]
Pt	–	–	~10^{-6}	~1450–1550	–	5.42	TE	[3384]
Pt	–	–	<3×10^{-8}	~1700–2000	–	5.43	TE	[177]
Pt[341]	K	K$^+$	≤6×10^{-9}	~1600–1900	5.43	(5.41 ± 0.05)	PSI	[282]
Pt[341]	Cs	Cs$^+$	≤6×10^{-9}	~1600–1900	5.43	(5.41 ± 0.05)	PSI	[282]
Pt	Na	Na$^+$	4×10^{-10}	~1500–1660	5.44*	–	PSI	[3336]
Pt	–	–	–	–	–	5.45	TC	[3476]
Pt	–	–	~10^{-5}	≤1200	–	5.45	TE	[2216]
Pt/W	Pt	–	≤10^{-6}	~1600–1800	–	5.45	TE	[2305]
Pt/glass[342]	Pt	–	~10^{-10}	78	–	5.45	PE	[428,1497,2719]
Pt[457]	Li	Li$^+$	7×10^{-9}	~1300–1800	5.45 ± 0.02	(4.66 ± 0.2)	PSI	[74]
Pt	–	–	≤3×10^{-9}	1570–1720	–	5.45 ± 0.02	TE	[171]

Table 1 (*continued*)

Surface	Beam	Ion	P_r (Torr)	T (K)	ϕ^+ (eV)	ϕ^e (eV)	Meth.	Refs.
Pt[343]	–	–	$\leq 6 \times 10^{-9}$	~1000–1700	(5.5)	5.45 ± 0.05	TE	[98]
Pt	–	–	?	~90	–	5.45 ± 0.2	PE	[3403]
Pt/glass[363]	Pt	–	~10^{-10}	~78	–	5.46	PE	[436]
Pt/cnt/Si(111)[25]	–	–	~10^{-10}	~300	–	5.46 ± 0.07	CPD	[3246]
Pt/glass	Pt	–	<10^{-9}	77	–	5.48	PE	[2931]
Pt	Na	Na$^+$	2×10^{-7}	~1700–2050	5.49 ± 0.01*	–	PSI	[50]
Pt[457]	Na	Na$^+$	7×10^{-9}	~1050–1800	5.49 ± 0.05	(4.66 ± 0.2)	PSI	[74]
Pt[343]	Cs	Cs$^+$	$\leq 6 \times 10^{-9}$	~1400–1800	5.5	(5.45 ± 0.05)	PSI	[98]
Pt//Si^n[482]	Pt	–	?	~300	–	5.5	CPD	[4375]
Pt	–	–	~10^{-10}	~300	–	5.5 ± 0.1	PE	[858]
Pt/glass[369]	Pt	–	~10^{-10}	77	–	5.50	PE	[2133]
Pt	–	–	?	?	–	5.50	TE	[2105]
Pt[458]	Na	Na$^+$	7×10^{-9}	~1050–1800	5.51 ± 0.1	(4.66 ± 0.2)	PSI	[74]
Pt[170,341]	K	K$^+$	$\leq 6 \times 10^{-9}$	~1600–1900	5.52 ± 0.05	(5.41 ± 0.05)	PSI	[282]
Pt	–	–	?	~300	–	5.53 ± 0.1	PE	[3711]
Pt[458]	Li	Li$^+$	7×10^{-9}	~1300–1800	5.54 ± 0.07	(4.66 ± 0.2)	PSI	[74]
Pt[170,345]	NaNO$_3$	Na$^+$	5×10^{-7}	~1250–1350	5.54 ± 0.07	–	PSI	[178]
Pt	–	–	–	–	–	5.55	TC	[298]
Pt	–	–	4×10^{-9}	~1500–1800	–	5.55	TE	[1295]
Pt	–	–	~10^{-10}	~300	–	5.55 ± 0.02	PE	[2487]
Pt{mainly(111)}[344]	–	–	<1×10^{-9}	~1300–1800	–	5.55 ± 0.1	TE	[434]
Pt[345]	NaNO$_3$	Na$^+$	5×10^{-7}	~1250–1350	5.56	–	PSI	[178]
Pt/quartz	Pt	–	$\leq 5 \times 10^{-10}$	293	–	5.58 ± 0.04	PE	[435]
Pt/SiO$_2$	Pt	–	?	?	–	5.59	CPD	[3519,3520]
Pt	–	–	<3×10^{-8}	~1700–2000	–	5.6	TE	[177]
Pt	–	–	?	~300	–	5.6	PE	[3235]
Pt	Na	Na$^+$	2×10^{-10}	1000	5.6 ± 0.1	–	PSI	[75]
Pt	–	–	?	~300	–	5.6 ± 0.2	CPD	[3867]
Pt	–	–	?	~1500–1800	–	5.60	TE	[1753]
Pt/glass	Pt	–	<3×10^{-10}	78 (~300)	–	5.62	PE	[2722]
Pt/glass[342]	Pt	–	~10^{-10}	78 (293)	–	5.63	PE	[428,1497,2719]
Pt/glass	Pt	–	<10^{-9}	77 (293)	–	5.63	PE	[2931]
Pt/Pt(111)[335]	Pt	–	<10^{-10}	130	–	5.64	PE	[421,773]
Pt/quartz	Pt	–	$\leq 5 \times 10^{-10}$	293 (~550)	–	5.64	PE	[435]
Pt	–	–	6×10^{-9}	~300	–	5.65	PE	[1139]
Pt	–	–	?	?	–	5.65	TE	[1]
Pt/quartz	Pt	–	~10^{-10}	~300	–	5.65 ± 0.1	PE	[304]
Pt	NaBr	Na$^+$	2×10^{-7}	1450	5.66	–	PSI	[58]
Pt	–	–	$\leq 10^{-9}$	1500	–	5.66	TE	[650]
Pt	–	–	~10^{-7}	~1550–1800	–	5.66 ± 0.07	TE	[176]
Pt/glass	Pt	–	~10^{-10}	~300	–	5.68 ± 0.03	PE	[1141]
Pt/glass	Pt	–	<1×10^{-10}	78 (373)	–	5.69	PE	[414]
Pt	–	–	<5×10^{-10}	~300	–	5.7	PE	[1296]
Pt/Pt(111)[335]	Pt	–	<10^{-10}	250	–	5.7	PE	[421]
Pt/TiO$_2$(001)	Pt	–	~10^{-10}	~300	–	5.7	CPD	[1567]
Pt	–	–	2×10^{-10}	293	–	5.7 ± 0.05	PE	[1542]
Pt/glass	Pt	–	<1×10^{-10}	78 (473)	–	5.70	PE	[414]
Pt	–	–	$\leq 5 \times 10^{-10}$	~300	–	5.70 ± 0.07	PE	[3354]
Pt	–	–	<8×10^{-11}	~300	–	5.700 ± 0.100	CPD	[342,3868]
Pt/glass[369]	Pt	–	~10^{-10}	77 (323)	–	5.71	PE	[2133]
Pt[458]	Tl	Tl$^+$	7×10^{-9}	~1300–1800	5.71 ± 0.03	(4.66 ± 0.2)	PSI	[74]
Pt/glass[363]	Pt	–	<1×10^{-10}	78 ($\geq$500)	–	5.72	PE	[414,436]
Pt/glass[342]	Pt	–	<10^{-10}	78 (593)	–	5.72	PE	[428,1497]
Pt/glass	Pt	–	~10^{-10}	~300 (473)	–	5.72 ± 0.01	PE	[1141]
Pt	–	–	–	–	–	5.73	TC	[3016]
Pt	–	–	5×10^{-10}	~300	–	5.73	AI[38]	[4027]
Pt	–	–	<3×10^{-8}	~1700–2000	–	5.75	TE	[177]
Pt[337]	–	–	2×10^{-11}	~300	–	5.77	PE	[429]
Pt	Bi	Bi$^+$	5×10^{-8}	1560–1920	5.77 ± 0.05	(5.13 ± 0.05)	PSI	[106,667]
Pt[457]	Tl	Tl$^+$	7×10^{-9}	~1300–1800	5.78 ± 0.02	(4.66 ± 0.2)	PSI	[74]
Pt{80%(210)}[336]	–	–	1×10^{-9}	1620–1950	–	5.79 ± 0.09	TE	[179,650,3413]
Pt{(111)rich}	–	–	~10^{-10}	~300	–	5.8	CPD	[437]
Pt	–	–	~10^{-10}	~300	–	5.8 ± 0.1	PE	[858]
Pt	–	–	$\leq 10^{-9}$	1900	–	5.83	TE	[650]
Pt/Nb(110)	Pt	–	7×10^{-11}	~300	–	5.85	PE	[2874]
Pt/W(110)	Pt	–	4×10^{-11}	400	–	5.85	CPD	[2408]
Pt/W	Pt	–	$\leq 10^{-6}$	~1600–1800	–	6	TE	[2301]
Pt	–	–	–	–	–	6.0	TC	[706]
Pt	–	–	?	~1600–2000	–	6.0	TE	[3020]
Pt	–	–	~10^{-5} (O_2)	~300	–	6.0	PE	[2487]

Table 1 (*continued*)

Surface	Beam	Ion	P_r (Torr)	T (K)	ϕ^+ (eV)	ϕ^e (eV)	Meth.	Refs.
Pt/W(110)[346]	Pt	–	($\leq 10^{-10}$)	~300	–	6.05	CPD	[1137]
Pt/W(110)[346]	Pt	–	($\leq 10^{-10}$)	~300{800}	–	6.05	CPD	[1137]
Pt	–	–	?	~1500–1800	–	6.05	TE	[1753]
Pt	–	–	<10^{-7}	~1100–1200	–	6.1	TE	[3384]
Pt/Re	Pt	–	?	~300	–	6.1 ± 0.1	PE	[401]
Pt	–	–	?	1540–1780	–	6.16	TE	[1753]
Pt	–	–	1×10^{-9}	~600–700	–	6.17	CPD	[171]
Pt	–	–	?	~300	–	6.17	PE	[2924]
Pt	–	–	~10^{-8}	1370–1750	–	6.27 ± 0.07	TE	[860]
Pt	–	–	~10^{-8}	~300	–	6.30 ± 0.05	PE	[1751,1753]
Pt	–	–	?	?	–	6.33	TE	[1754]
Pt	–	–	–	–	–	6.35	TC	[1744]
Pt	–	–	?	1540–1780	–	6.35	TE	[1753]
Recommended	–	–	–	–	**5.58 ± 0.11**	**5.30 ± 0.07**	–	–

79. Gold Au

fcc

Surface	Beam	Ion	P_r (Torr)	T (K)	ϕ^+ (eV)	ϕ^e (eV)	Meth.	Refs.
Au(100)	–	–	–	–	–	3.318	TC	[2914]
Au(100)	–	–	–	–	–	3.65	TC	[475]
Au(100)	–	–	–	–	–	3.816	TC	[2914]
Au(100)/NaCl[137]	Au	–	?	~300 (473)	–	4.02 ± 0.02	PE	[3324,3328,3330]
Au(100)	–	–	–	–	–	4.99	TC	[1159,1980,3067]
Au(100)	–	–	–	–	–	5.02	TC	[705]
Au(100)	–	–	–	–	–	5.022	TC	[4414]
Au(100)	–	–	–	–	–	5.04	TC	[4233]
Au(100)	–	–	–	–	–	5.05	TC	[4233]
Au(100)	–	–	–	–	–	5.071	TC	[4091]
Au(100)	–	–	–	–	–	5.08	TC	[1939]
Au(100)	–	–	–	–	–	5.10	TC	[4087,4410]
Au(100)	–	–	–	–	–	5.10	TC	[4326]
Au(100)	–	–	–	–	–	5.11	TC	[1939]
Au(100)	–	–	–	–	–	5.14	TC	[2702]
Au(100)	–	–	1×10^{-10}	~300	–	5.22 ± 0.04	PE	[1068]
Au(100)	–	–	?	~300	–	5.35 ± 0.05	PE	[2995]
Au(100)	–	–	–	–	–	5.39	TC	[1873]
Au(100)	–	–	–	–	–	5.41	TC	[1011]
Au(100)/Cr(100)	–	–	–	–	–	5.42	TC	[1011]
Au(100)	–	–	–	–	–	5.43	TC	[1011]
Au(100)	–	–	–	–	–	5.44	TC	[1719]
Au(100)/Cr(100)	–	–	–	–	–	5.44	TC	[1011]
Au(100)	–	–	–	–	–	5.45	TC	[1939]
Au(100)	–	–	?	~300	–	5.47	CPD	[959]
Au(100)	–	–	–	–	–	5.48	TC	[3217]
Au(100)	–	–	–	–	–	5.53	TC	[480,4398]
Au(100)	–	–	–	–	–	5.53 ± 0.10	TC	[3217]
Au(100)	–	–	–	–	–	5.56	TC	[3317]
Au(100)	–	–	–	–	–	5.61	TC	[1928]
Au(100)	–	–	–	–	–	5.66	TC	[1011]
Au(100)	–	–	–	–	–	5.67	TC	[2803]
Au(100)	–	–	–	–	–	5.92	TC	[1011]
Au(100)	–	–	–	–	–	5.96	TC	[1011]
Au(100)	–	–	–	–	–	6.13	TC	[1011]
Au(100)	–	–	–	–	–	6.16	TC	[334]
Au(100)	–	–	–	–	–	6.16	TC	[321]
Au(100)	–	–	–	–	–	6.23	TC	[3194]
Au(100)	–	–	–	–	–	6.26	TC	[3194]
Au(100)	–	–	–	–	–	6.4	TC	[389]
Recommended	–	–	–	–	–	**5.39 ± 0.07**	–	–
Au(110)	–	–	–	–	–	3.148	TC	[2914]
Au(110)	–	–	–	–	–	3.50	TC	[475]
Au(110)	–	–	–	–	–	3.629	TC	[2914]
Au(110)	–	–	–	–	–	4.65	TC	[1159,3067]
Au(110)	–	–	–	–	–	4.91	TC	[4091]
Au(110)	–	–	–	–	–	4.93	TC	[4233]
Au(110)	–	–	–	–	–	4.98	TC	[4233]
Au(110)	–	–	–	–	–	5.04	TC	[4087,4410]
Au(110)	–	–	5×10^{-10}	298	–	5.12 ± 0.07	CPD	[1069]
Au(110)	–	–	1×10^{-10}	~300	–	5.20 ± 0.04	PE	[1068]

Table 1 (*continued*)

Surface	Beam	Ion	P_r (Torr)	T (K)	ϕ^+ (eV)	ϕ^e (eV)	Meth.	Refs.
Au(110)[347]	–	–	–	–	–	5.32	TC	[2543]
Au(110)	–	–	–	–	–	5.36	TC	[4404]
Au(110)	–	–	?	~300	–	5.37	CPD	[959]
Au(110)[347]	–	–	–	–	–	5.38	TC	[2543]
Au(110)	–	–	–	–	–	5.38	TC	[480]
Au(110)[347]	–	–	–	–	–	5.39	TC	[2543]
Au(110)	–	–	?	~300	–	5.39 ± 0.06	CPD	[4404]
Au(110)	–	–	–	–	–	5.40	TC	[334]
Au(110)	–	–	–	–	–	5.41	TC	[480,4398]
Au(110)	–	–	–	–	–	5.42	TC	[3317]
Au(110)/W(112)[348]	Au	–	<2 × 10⁻¹⁰	78{540}	–	5.45 ± 0.03	FE	[2256]
Au(110)	–	–	–	–	–	5.5	TC	[2167]
Au(110)	–	–	–	–	–	5.80	TC	[321]
Au(110)	–	–	–	–	–	5.85	TC	[3194]
Au(110)	–	–	–	–	–	5.86	TC	[3194]
Recommended	–	–	–	–	–	**5.33 ± 0.09**	–	–
Au(111)	–	–	–	–	–	3.478	TC	[2914]
Au(111)	–	–	–	–	–	3.80	TC	[475]
Au(111)/NaCl[137]	Au	–	?	~300 (423)	–	4.12 ± 0.02	PE	[3324,3328,3330]
Au(111)	–	–	–	–	–	4.165	TC	[2914]
Au(111)	–	–	<1 × 10⁻¹⁰	~300	–	4.6	PE	[3140]
Au(111)	–	–	–	–	–	4.83	TC	[2077]
Au(111)	–	–	–	–	–	4.94 ± 0.11	TC	[2902]
Au(111)	–	–	–	–	–	4.95	TC	[2077]
Au(111)	–	–	–	–	–	5.1	TC	[4233]
Au(111)	–	–	–	–	–	5.11	TC	[2702]
Au(111)	–	–	–	–	–	5.110	TC	[4091]
Au(111)	–	–	–	–	–	5.13	TC	[4233]
Au(111)	–	–	–	–	–	5.14	TC	[1939]
Au(111)	–	–	–	–	–	5.15	TC	[2068]
Au(111)	–	–	–	–	–	5.15	TC	[343]
Au(111)	–	–	–	–	–	5.15	TC	[4087,4410]
Au(111)	–	–	?	70	–	5.15 ± 0.1	PE	[1297]
Au(111)	–	–	–	–	–	5.17	TC	[4140]
Au(111)	–	–	–	–	–	5.18	TC	[1939]
Au(111)/Si(111)[419]	Au	–	~10⁻¹⁰	~300	–	5.2	PE	[3999,4000]
Au(111)/Cu(111)	Au	–	<1 × 10⁻¹⁰	~300	–	5.2 ± 0.3	CPD	[1186,3417]
Au(111)	–	–	–	–	–	5.20	CT	[4151,4408]
Au(111)	–	–	–	–	–	5.21	TC	[4155]
Au(111)	–	–	–	–	–	5.23	CT	[4181]
Au(111)	–	–	–	–	–	5.25	TC	[4152]
Au(111)	–	–	–	–	–	5.25	TC	[4154]
Au(111)	–	–	–	–	–	5.25	TC	[1197,4157,4215, 4413]
Au(111)	–	–	–	–	–	5.26	TC	[4153]
Au(111)/W(110)	Au	–	?	~300 (<934)	–	5.25 ± 0.03	CPD	[3076]
Au(111)	–	–	1 × 10⁻¹⁰	~300	–	5.26 ± 0.04	PE	[1068]
Au(111)	–	–	–	–	–	5.27	TC	[2902]
Au(111)	–	–	1 × 10⁻¹⁰	~300	–	5.3	PE	[1070]
Au(111)	–	–	5 × 10⁻¹⁰	~300	–	5.3	PE	[1142]
Au(111)/mica	Au	–	?	~300	–	5.3	CPD	[1600]
Au(111)	–	–	–	–	–	5.3 ± 0.1	TC	[3494]
Au(111)	–	–	5 × 10⁻¹⁰	298	–	5.30 ± 0.05	PE	[1069]
Au(111)	–	–	–	–	–	5.31	TC	[2551]
Au(111)	–	–	?	~300	–	5.31	CPD	[959]
Au(111)	–	–	–	–	–	5.31	TC	[3497]
Au(111)	–	–	–	–	–	5.32	TC	[1159,1980,3067]
Au(111)/W(110)[349]	Au	–	<2 × 10⁻¹⁰	78{420}	–	5.32 ± 0.03	FE	[2256]
Au(111)	–	–	5 × 10⁻¹¹	100 (730)	–	5.35	PE	[4156]
Au(111)	–	–	?	5 (900)	–	5.36	PE	[4257]
Au(111)/quartz[350]	Au	–	~10⁻⁹	~300	–	5.38	PE	[3313]
Au(111)/mica[420]	Au	–	4 × 10⁻¹⁰	~300{570}	–	5.4	PE	[4001]
Au(111)	–	–	?	~300	–	5.40 ± 0.05	PE	[2995]
Au(111)/quartz[350]	Au	–	~10⁻⁹	~300 (623)	–	5.42	PE	[3313]
Au(111)	–	–	?	30	–	5.44	PE	[2228]
Au(111)	–	–	–	–	–	5.45	TC	[4426]
Au(111)/mica	Au	–	4 × 10⁻¹¹	~300 (623)	–	5.47	PE	[1202]
Au(111)/mica(111)	Au	–	<5 × 10⁻¹¹	~300 (~700)	–	5.47 ± 0.15*	CPD	[1897]
Au(111)	–	–	–	–	–	5.5	TC	[1723]

Table 1 (*continued*)

Surface	Beam	Ion	P_r (Torr)	T (K)	ϕ^+ (eV)	ϕ^e (eV)	Meth.	Refs.
Au(111)	–	–	?	~300	–	5.5 ± 0.1	PE	[1297]
Au(111)/W(110)	Au	–	≤2 × 10⁻¹⁰	~300	–	5.50*	CPD	[1538]
Au(111)	–	–	8 × 10⁻¹¹	~300	–	5.50	PE	[4080]
Au(111)/W(112)[351]	Au	–	≤7 × 10⁻¹¹	~300	–	5.51	CPD	[2385]
Au(111)	–	–	–	–	–	5.52	TC	[1939]
Au(111)	–	–	–	–	–	5.54	TC	[233]
Au(111)	–	–	–	–	–	5.54	TC	[4174,4284]
Au(111)[351]	–	–	≤7 × 10⁻¹¹	~300	–	5.55	CPD	[2385,2871]
Au(111)	–	–	?	~300	–	5.55	PE	[2999]
Au(111)	–	–	?	~300	–	5.55 ± 0.03	PE	[4213]
Au(111)	–	–	–	–	–	5.56	TC	[3217]
Au(111)/Ir(111)	Au	–	≤5 × 10⁻¹⁰	~300 (>673)	–	5.60 ± 0.04	CPD	[415,3266]
Au(111)	–	–	–	–	–	5.60 ± 0.10	TC	[3217]
Au(111)	–	–	–	–	–	5.63	TC	[480,4398]
Au(111)	–	–	–	–	–	5.65	TC	[3317]
Au(111)	–	–	–	–	–	5.7	TC	[1723]
Au(111)	–	–	–	–	–	5.71	TC	[2803]
Au(111)	–	–	–	–	–	6.01	TC	[334]
Au(111)	–	–	–	–	–	6.05	TC	[3179]
Au(111)	–	–	–	–	–	6.08	TC	[3194]
Au(111)	–	–	–	–	–	6.65	TC	[321]
Recommended	–	–	–	–	–	**5.46 ± 0.07**	–	–
Au(112)	–	–	–	–	–	5.09	TC	[2702]
Au(113)	–	–	5 × 10⁻¹⁰	298	–	5.16 ± 0.07	CPD	[1069]
Au(210)	–	–	5 × 10⁻¹⁰	298	–	4.96 ± 0.07	CPD	[1069]
Au(532)	–	–	–	–	–	5.03	TC	[2702]
Au	–	–	–	–	–	3.07	TC	[2493]
Au	–	–	–	–	–	3.16	TC	[2493]
Au	–	–	–	–	–	3.19	TC	[521]
Au	–	–	–	–	–	3.44	TC	[2629]
Au	–	–	–	–	–	3.49	TC	[475]
Au/Si(100)ⁿ[478]	Au	–	?	~300	–	~3.5–3.8	CPD	[4368]
Au	–	–	–	–	–	3.52	TC	[2474]
Au/quartz	Au	–	~10⁻⁶	~300	–	4	PE	[2941]
Au	–	–	~10⁻⁶	~300	–	4 ± 0.5	FE	[2675]
Au/quartz[51]	Au	–	~10⁻⁵	~300	–	4.0	PE	[1973]
Au	–	–	?	?	–	4.00–4.58	TE	[1362]
Au/Ag	Au	–	~10⁻⁶	~300	–	4.03	PE	[2941]
Au/?	Au	–	~10⁻⁶	~300	–	4.1	PE	[3332]
Au(fp)[352]	–	–	–	–	–	4.1	TC	[2973]
Au/glass	Au	–	~10⁻⁶	373	–	4.17 ± 0.01	PE	[3507]
Au/glass	Au	–	~10⁻⁶–10⁻⁸	~300	–	4.2	PE	[1894]
Au[437]	–	–	?	~300	–	4.20	PE	[2760]
Au/glass	Au	–	~10⁻⁶	463	–	4.21	PE	[3507]
Au	–	–	≤4 × 10⁻¹⁰	~300	–	4.24	CPD	[2118]
Au	–	–	–	–	–	4.25	TC	[2629]
Au/glass	Au	–	~10⁻⁶	613	–	4.26	PE	[3507]
Au/glass	Au	–	~10⁻⁶	523	–	4.27	PE	[3507]
Au/graphite	Au	–	?	1170–1280	–	4.27 ± 0.03	TE	[2236]
Au	–	–	–	–	–	4.28	TC	[1626,2914]
Au	–	–	–	–	–	4.33	TC	[3318]
Au	–	–	?	~300	–	4.36 ± 0.06*	CPD	[1953]
Au/GaP	–	–	–	–	–	4.38	TC	[1653]
Au	–	–	2 × 10⁻⁵	~300	–	4.4–4.6	?	[2836]
Au(fp)[352]	–	–	–	–	–	4.4	TC	[2973]
Au	–	–	?	1323	–	4.41	TE	[1944]
Au	–	–	≤4 × 10⁻¹⁰	~300	–	4.42	CPD	[2118]
Au	–	–	–	–	–	4.45	TC	[1645]
Au	–	–	?	~300	–	4.46	CPD	[2297]
Au/?	Au	–	?	~300	–	4.48	CPD	[2708]
Au/GaP	–	–	–	–	–	4.49	TC	[1653]
Au/W(100)	Au	–	?	825	–	4.5*	FE	[2263]
Au	–	–	–	–	–	4.50	TC	[3352]
Au/Si	–	–	–	–	–	4.53	TC	[1653]
Au/Cu	Au	–	~10⁻¹⁰	~300	–	4.54 ± 0.02	PE	[2765]

Table 1 (*continued*)

Surface	Beam	Ion	P_r (Torr)	T (K)	ϕ^+ (eV)	ϕ^e (eV)	Meth.	Refs.
Au	–	–	$\sim10^{-7}$	~300	–	4.55	PE	[1890]
Au	–	–	–	–	–	4.56	TC	[1976]
Au/Si	–	–	–	–	–	4.56	TC	[1653]
Au	–	–	–	–	–	4.6	TC	[1993]
Au(fp)[352]	–	–	–	–	–	4.6	TC	[2973]
Au/W(100)	Au	–	?	900	–	4.6*	FE	[2263]
Au[353]	–	–	$<10^{-9}$	~300	–	4.64	CPD	[1072]
Au/glass[368]	Au	–	$<10^{-8}$	~300	–	4.68 ± 0.03	CPD	[133]
Au/Si(111)	–	–	–	–	–	4.69	TC	[2688]
Au/Al$_2$O$_3$/Al	Au	–	?	~300	–	4.69	CPD	[3057]
Au	–	–	–	–	–	4.69	TC	[2005]
Au/glass[367]	Au	–	$<10^{-9}$	~300	–	4.7	CPD	[1893]
Au/W(100)	Au	–	?	825	–	4.7	FE	[2263]
Au/W(110)	Au	–	?	20	–	4.7	FE	[2956]
Au	–	–	–	–	–	4.7	TC	[2583]
Au/TiO$_2$(110)	–	–	–	–	–	~4.7–5.2	TC	[4182]
Au	–	–	$<3 \times 10^{-9}$	~300	–	4.70 ± 0.01	CPD	[486,904]
Au/glass[365]	Au	–	$\sim10^{-8}$	~300	–	4.70 ± 0.03	CPD	[133]
Au/W	Au	–	$<10^{-10}$	~300	–	4.705 ± 0.010	CPD	[2940]
Au/W	Au	–	$\sim10^{-10}$	~300	–	4.709 ± 0.006	CPD	[2938]
Au	–	–	$<10^{-6}$	~300	–	4.71	PE	[2919]
Au	–	–	–	–	–	4.71	TC	[1399]
Au/glass[365]	Au	–	$<10^{-9}$	~300 (523)	–	4.71 ± 0.02	CPD	[349,1160,1163]
Au/W[365]	Au	–	$\sim10^{-10}$	~300	–	4.714 ± 0.004	CPD	[349,1161,2935]
Au	–	–	?	~300	–	4.72	PE	[3021]
Au/cnt/Si(111)[25]	–	–	$\sim10^{-10}$	~300	–	4.72 ± 0.06	PE	[3246]
Au[354]	–	–	1×10^{-8}	1013	–	4.73	PE	[2560]
Au	–	–	–	–	–	4.74	TC	[1066]
Au	–	–	?	~300	–	4.74 ± 0.01	CPD	[1953]
Au	–	–	?	~300	–	4.76	PE	[3023]
Au/Ta(112)[358]	–	–	$<1 \times 10^{-10}$	$\sim300\{1000\}$	–	4.76	CPD	[878]
Au	–	–	–	–	–	4.77	TC	[3476]
Au/glass[365]	Au (Hg)	–	5×10^{-11}	~300	–	4.77	CPD	[1071]
Au	–	–	–	–	–	4.78	TC	[3264,3265]
Au	–	–	$<10^{-7}$	~300	–	4.79–4.97	PE	[3393]
Au/steel	Au	–	?	~300	–	4.8	PE	[2466,2475]
Au	–	–	–	–	–	4.8	TC	[3268]
Au/Ta(111)	Au	–	$<1 \times 10^{-10}$	~300	–	4.8	CPD	[2440]
Au/W(100)	Au	–	?	900	–	4.8*	FE	[2263]
Au/Nb	Au	–	$\leq5 \times 10^{-9}$	~300	–	4.8*	CPD	[3261]
Au/Mo	Au	–	7×10^{-11}	~300	–	4.8	PE	[2226]
Au/glass	Au	–	$<10^{-8}$	78	–	4.8 ± 0.02	CPD	[1646]
Au[354]	–	–	–	293–1013	–	4.81 ± 0.02	TC	[1760]
Au	–	–	–	–	–	4.82	TC	[1885]
Au[354]	–	–	1×10^{-8}	293	–	4.82	PE	[2560]
Au/Ta[356]	Au	–	?	~300	–	4.83 ± 0.02	CPD	[1162]
Au	–	–	?	~300	–	4.84 ± 0.02	PE	[4155]
Au/Al$_2$O$_3$/Al	Au	–	?	~300	–	4.84 ± 0.06*	CPD	[3057]
Au/Cu	Au	–	?	~300	–	4.85 ± 0.05	PE	[3178]
Au/cnt/Si(111)[25]	–	–	$\sim10^{-10}$	~300	–	4.85 ± 0.11	CPD	[3246]
Au	–	–	–	–	–	4.88	TC	[298]
Au	–	–	–	–	–	4.88 ± 0.05	TC	[3358]
Au[355]	–	–	–	733	–	4.89	TC	[3586]
Au/W(110)[366]	–	–	5×10^{-10}	78 (300)	–	4.89 ± 0.01	FE	[1673]
Au[353]	–	–	$<10^{-9}$	~300	–	4.89 ± 0.06	CPD	[1072]
Au	–	–	?	~300	–	4.9	PE	[3639]
Au/quartz	Au	–	5×10^{-9}	~300	–	4.9	CPD	[2606]
Au	–	–	?	?	–	4.9	?	[1838]
Au$_2$/TiO$_2$(110)	–	–	–	–	–	~4.9–5.2	TC	[4182]
Au	–	–	?	~300	–	4.9 ± 0.1	PE	[3014]
Au[354]	–	–	–	296–1013	–	4.90 ± 0.03	TC	[1135]
Au	–	–	1×10^{-9}	~300	–	4.91	CPD	[1252]
Au	–	–	–	–	–	4.91	TC	[339]
Au[355]	–	–	–	1013	–	4.92	TC	[3586]
Au[355]	–	–	–	733, 1013	–	4.92	TC	[1135]
Au/W	Au	–	$<5 \times 10^{-9}$	78	–	4.92	FE	[2240]
Au/cnt/Si(111)[25]	–	–	$\sim10^{-10}$	~300	–	4.92 ± 0.10	CPD	[3246]
Au	–	–	–	–	–	4.93	TC	[3476]
Au[354]	–	–	–	296–1013	–	4.93 ± 0.03	TC	[1135]
Au	–	–	?	~300	–	4.95	PE	[2752]

Table 1 (*continued*)

Surface	Beam	Ion	P_r (Torr)	T (K)	ϕ^+ (eV)	ϕ^e (eV)	Meth.	Refs.
Au/W(111)[361]	Au	–	$\sim 10^{-11}$	~ 300 (~ 1000)	–	4.96*	CPD	[2647]
Au/glass[369]	Au	–	$\sim 10^{-10}$	77	–	4.96	PE	[2133]
Au/Ta[356]	Au	–	?	~ 300	–	4.97 ± 0.02	CPD	[1162]
Au	–	–	1×10^{-10}	~ 300	–	5.0	PE	[1678]
Au/glass	–	–	$< 10^{-9}$	~ 300	–	5.0	PE	[2717]
Au/?	Au	–	$\sim 10^{-5}$	~ 300	–	5.0	CPD	[1376]
Au(fp)[352]	–	–	–	–	–	5.0	TC	[2973]
Au/W(100)	Au	–	?	750	–	5.0*	FE	[2263]
Au/W	Au	–	?	~ 300	–	5.0	FE	[2225]
Au/Si	Au	–	1×10^{-9}	~ 300	–	5.0	PE	[3221]
Au	–	–	4×10^{-10}	~ 300	–	5.0 ± 0.1	PE	[3132]
Au	–	–	?	~ 300	–	5.00	PE	[4159]
Au[357]	–	–	$\sim 10^{-9}$	~ 300	–	5.01	CPD	[2473]
Au	–	–	?	~ 300	–	5.03 ± 0.05	PE	[4003]
Au/Ta(112)[358]	Au	–	$< 1 \times 10^{-10}$	~ 300	–	5.04	CPD	[878]
Au/W(100)	Au	–	$\leq 2 \times 10^{-10}$	$\sim 300\{900\}$	–	5.05*	CPD	[1538]
Au/ZrO_2/Si(100)	Au	–	?	~ 300	–	5.05[48]	PE	[1442]
Au/SiO_2/Si	Au	–	?	~ 300 (570)	–	5.06	PE	[2355]
Au/glass	Au	–	$< 1 \times 10^{-10}$	78	–	5.06	PE	[414]
Au/W(111)	–	–	–	–	–	5.07	TC	[531]
Au/W(100)	Au	–	?	20 (330)	–	5.07*	FE	[2959]
Au[357]	–	–	$\sim 10^{-9}$	~ 300	–	5.08	CPD	[2473]
Au/Mo(111)[364]	Au	–	$< 1 \times 10^{-10}$	~ 300	–	5.08	CPD	[1842]
Au/Ta(112)[358]	Au	–	$< 1 \times 10^{-10}$	~ 300	–	5.08	CPD	[878]
Au/W(112)[361]	Au	–	$\sim 10^{-11}$	~ 300 (~ 1000)	–	5.08*	CPD	[2647]
Au/CdTe(110)	Au	–	$\leq 2 \times 10^{-11}$	~ 300	–	5.08 ± 0.02	CPD	[3068]
Au/quartz	Au	–	$\leq 5 \times 10^{-10}$	78	–	5.08 ± 0.04	PE	[435]
Au/Al_2O_3/Si(100)	Au	–	?	~ 300	–	5.1[48]	PE	[1442]
Au	–	–	4×10^{-10}	~ 300	–	5.1	PE	[3120]
Au/quartz	Au	–	$\leq 5 \times 10^{-9}$	~ 300	–	5.1	PE	[2309]
Au/W(111)	Au	–	?	20	–	5.1	FE	[2956]
Au	–	–	?	~ 300	–	5.1	PE	[1449]
Au/ITO	Au	–	5×10^{-10}	~ 300	–	5.1*	PE	[4183]
Au	–	–	$\sim 10^{-9}$	~ 300	–	5.1 ± 0.1	PE	[1267]
Au/quartz	Au	–	$\sim 10^{-10}$	~ 300	–	5.1 ± 0.1	PE	[304]
Au–Cu(2.4%)/Si	Au, Cu	–	?	293	–	5.1 ± 0.1	PE	[3998]
Au	–	–	?	~ 300	–	5.1 ± 0.15	CPD	[1600]
Au	–	–	–	–	–	5.10	TC	[3637]
Au/Ir[359]	Au	–	?	78 (520)	–	5.10	FE	[2189]
Au/Si(111)	Au	–	5×10^{-11}	~ 300	–	5.10 ± 0.05	CPD	[613,636]
Au/Si(111)	Au	–	$< 4 \times 10^{-10}$	~ 300	–	5.11 ± 0.04	PE	[3279]
Au/W	Au	–	$< 5 \times 10^{-9}$	78	–	5.12	FE	[2240]
Au/Au[360]	Au	–	$< 5 \times 10^{-8}$	~ 300	–	5.12*	PE	[3502]
Au[357]	–	–	$\sim 10^{-9}$	~ 300 (~ 1200)	–	5.13	CPD	[2473]
Au/W(100)[361]	Au	–	$\sim 10^{-11}$	~ 300 (~ 1000)	–	5.14*	CPD	[2647]
Au/W(100)	Au	–	?	20	–	5.14*	FE	[2959]
Au/W(110)	Au	–	($< 1 \times 10^{-11}$)	~ 300	–	5.15 ± 0.02	FE	[2251]
Au	–	–	–	–	–	5.16	TC	[3016]
Au	–	–	$\sim 10^{-5}$	≤ 1200	–	5.16	TE	[2216]
Au/W(111)[361]	Au	–	$\sim 10^{-11}$	~ 300	–	5.17*	CPD	[2647]
Au[357]	–	–	$\sim 10^{-9}$	~ 300 (~ 1200)	–	5.18	CPD	[2473]
Au/W(112)	–	–	–	–	–	5.18	TC	[531]
Au/Si(111)[419]	Au	–	$\sim 10^{-10}$	~ 300	–	5.2	PE	[3999,4000]
Au/W(100)	Au	–	?	750	–	5.2	FE	[2263]
Au	–	–	$\sim 10^{-10}$	100	–	5.2	PE	[2720]
Au	–	–	–	–	–	5.2	TC	[1561]
Au/Re	Au	–	$< 4 \times 10^{-10}$	~ 300	–	5.2*	CPD	[515]
Au	–	–	$\sim 4 \times 10^{-10}$	~ 300	–	5.2 ± 0.05	PE	[1298]
Au	–	–	2×10^{-11}	~ 300	–	5.2 ± 0.1	PE	[1251]
Au/W(111)	Au	–	?	20	–	5.2 ± 0.1	FE	[3509]
Au	–	–	$\leq 1 \times 10^{-10}$	~ 300	–	5.2 ± 0.3	PE	[1695]
Au/W[362]	Au_n	–	$\sim 10^{-5}$ (He, Ar)	77	–	5.2 ± 0.4	FE	[1713]
Au/W(112)[361]	Au	–	$\sim 10^{-11}$	~ 300	–	5.20*	CPD	[2647]
Au/W(115)	Au	–	$\sim 10^{-11}$	~ 300	–	5.20*	CPD	[2647]
Au/W(100)	Au	–	$< 2 \times 10^{-10}$	78	–	5.20	FE	[2256]
Au	–	–	?	~ 300	–	5.20	PE	[4242]
Au/W	Au	–	($< 1 \times 10^{-11}$)	~ 300	–	5.20 ± 0.02	FE	[2251]
Au[353]	–	–	$< 10^{-9}$	~ 300 (1170)	–	5.20 ± 0.05	CPD	[1072]
Au	–	–	4×10^{-10}	~ 300	–	5.20 ± 0.05	PE	[1181]
Au/glass	Au	–	5×10^{-11}	~ 300	–	5.20 ± 0.07*	CPD	[1071]

Table 1 (*continued*)

Surface	Beam	Ion	P_r (Torr)	T (K)	ϕ^+ (eV)	ϕ^e (eV)	Meth.	Refs.
Au(f.p.)[149]	–	–	<10⁻⁹	~300	–	5.20 ± 0.1	PE	[1562,3190]
Au/Mo(111)[364]	Au	–	<1 × 10⁻¹⁰	~300{1000}	–	5.22	CPD	[1842]
Au/glass[363]	Au	–	~10⁻¹⁰	~78	–	5.22	PE	[436]
Au/glass[365]	Au	–	5 × 10⁻¹¹	~300	–	5.22 ± 0.05	CPD	[1071,2100]
Au	–	–	<1 × 10⁻⁹	~300	–	5.22 ± 0.05	CPD	[1072]
Au	–	–	<5 × 10⁻⁹	78	–	5.23	FE	[2240]
Au	–	–	~10⁻⁹	~300 (~1100)	–	5.24	CPD	[2473]
Au/W(110)[366]	Au	–	2 × 10⁻¹⁰	~300 (750)	–	5.25 ± 0.01	FE	[1670,1673]
Au/glass	Au	–	5 × 10⁻¹¹	~300	–	5.25 ± 0.08*	CPD	[1071]
Au/Cu	Au	–	?	~300	–	5.26	CPD	[3716]
Au/glass	Au	–	2 × 10⁻¹⁰	~300	–	5.26	PE	[1621]
Au/W	Au	–	(<1 × 10⁻¹¹)	~300 (600)	–	5.26	FE	[730]
Au[357]	–	–	~10⁻⁹	~300	–	5.27	CPD	[2473]
Au[357]	–	–	~10⁻⁹	~300 (~1100)	–	5.27	CPD	[2473]
Au/glass	Au	–	<1 × 10⁻¹⁰	78 (293)	–	5.28	PE	[414,2722]
Au/quartz	Au	–	≤5 × 10⁻¹⁰	293	–	5.28 ± 0.01	PE	[435]
Au/Ru[368]	Au	–	~10⁻¹⁰	~300	–	5.28 ± 0.02	CPD	[1073]
Au/glass	Au	–	5 × 10⁻¹¹	~300	–	5.28 ± 0.06*	CPD	[1071]
Au/Ir[359]	Au	–	?	78 (501)	–	5.29	FE	[2189]
Au	–	–	≤1 × 10⁻¹⁰	~300	–	5.29	CPD	[2198]
Au/Si(111)	Au	–	<5 × 10⁻¹¹	60 (770)	–	5.3	PE	[2893]
Au/Ta	Au	–	~10⁻¹⁰	~300	–	5.3	PE	[2985]
Au/Nb(110)	Au	–	7 × 10⁻¹¹	~300	–	5.3	PE	[2986]
Au/W	Au	–	?	~300	–	5.3	FE	[3095]
Au/W	Au	–	?	?	–	5.3	FE	[1501]
Au/W(100)	Au	–	?	~300	–	5.3*	FE	[2263]
Au/W(110)[349]	Au	–	<2 × 10⁻¹⁰	78	–	5.3	FE	[2256]
Au/W(112)[348]	Au	–	<2 × 10⁻¹⁰	78	–	5.3	FE	[2256]
Au/W(112)	Au	–	?	20	–	5.3	FE	[2956]
Au/glass[367]	Au	–	<10⁻⁹	~300 (520)	–	5.3	CPD	[1893]
Au	–	–	<5 × 10⁻¹⁰	~300	–	5.3	PE	[1296]
Au	–	–	<2 × 10⁻¹⁰	~300	–	5.3	CPD	[4214]
Au/glass	Au	–	~10⁻¹⁰	323	–	5.30	PE	[1074]
Au/W(100)	Au	–	1 × 10⁻¹¹	330	–	5.30	FE	[2965]
Au/Co/Pt	Au	–	?	~300	–	5.30 ± 0.06	PE	[4423]
Au[357]	–	–	~10⁻⁹	~300	–	5.31	CPD	[2473]
Au/Au[360]	Au	–	<5 × 10⁻⁸	~300 (≤723)	–	5.31*	PE	[3502]
Au/Ru(0001)	Au	–	1 × 10⁻¹⁰	~300	–	5.31*	CPD	[2880]
Au[357]	–	–	~10⁻⁹	~300	–	5.32	CPD	[2473]
Au/W(100)	Au	–	<2 × 10⁻¹⁰	78{200}	–	5.32	FE	[2256]
Au/glass	Au	–	<1 × 10⁻¹⁰	78 (≤573)	–	5.32 ± 0.01	PE	[414]
Au/W	Au	–	(<1 × 10⁻¹¹)	~300	–	5.32 ± 0.02	FE	[2251]
Au	–	–	–	–	–	5.33	TC	[3476]
Au/W(100)	Au	–	~10⁻¹⁰	~300{≤900}	–	5.33	CPD	[2858]
Au[357]	–	–	~10⁻⁹	~300	–	5.33	CPD	[2473]
Au/W(100)	Au	–	≤10⁻¹⁰	78	–	5.33 ± 0.02	FE	[356]
Au/O–Si(100)	Au	–	~10⁻¹⁰	~300	–	5.33 ± 0.05	PE	[2281]
Au/W(110)	–	–	–	–	–	5.34	TC	[531]
Au/W(110)	Au	–	~10⁻¹¹	~300	–	5.34*	CPD	[2647]
Au/W(100)	–	–	–	–	–	5.35	TC	[531]
Au/W(100)[361]	Au	–	~10⁻¹¹	~300	–	5.36*	CPD	[2647]
Au/quartz	Au	–	≤5 × 10⁻¹⁰	293 (~550)	–	5.36 ± 0.01	PE	[435]
Au/Re	Au	–	(<1 × 10⁻¹¹)	~300 (600)	–	5.37	FE	[730]
Au/W(100)	Au	–	~1 × 10⁻¹¹	20	–	5.37	FE	[2965]
Au/steel	Au	–	<6 × 10⁻⁹	~300	–	5.37 ± 0.02	FE	[1540]
Au/glass[363]	Au	–	~10⁻¹⁰	~300 (≥400)	–	5.38	PE	[436,1074]
Au	–	–	–	–	–	5.38	TC	[3016]
Au/glass	Au	–	~10⁻¹⁰	~300	–	5.38 ± 0.02	PE	[1141]
Au/quartz[350]	Au	–	~10⁻⁹	~300	–	5.38 ± 0.02	PE	[3313]
Au/glass	Au	–	~10⁻¹⁰	~300 (473)	–	5.39 ± 0.01	PE	[1141]
Au/W(100)	Au	–	?	78	–	5.4*	FE	[2263]
Au	–	–	2 × 10⁻¹⁰	130	–	5.4	PE	[4212]
Au/W(112)	Au	–	~10⁻¹⁰	~300{≤1000}	–	5.4	CPD	[2858]
Au/W(110)[349]	Au	–	<2 × 10⁻¹⁰	78{160}	–	5.4	FE	[2256]
Au/Pt(100)	Au	–	1 × 10⁻¹⁰	~300	–	5.4 ± 0.15	PE	[174]
Au/glass[369]	Au	–	~10⁻¹⁰	77 (373)	–	5.40	PE	[2133]
Au	–	–	?	?	–	5.40	?	[2610]
Au/Mo(110)	Au	–	<1 × 10⁻¹⁰	~300{900}	–	5.40*	CPD	[2864]
Au	–	–	–	–	–	5.400	TC	[2649]
Au/steel	Au	–	≤2 × 10⁻¹¹	~300	–	5.40 ± 0.05	CPD	[3068]

Table 1 (*continued*)

Surface	Beam	Ion	P_r (Torr)	T (K)	ϕ^+ (eV)	ϕ^e (eV)	Meth.	Refs.
Au/glass	Au	–	$\sim10^{-10}$	~300	–	5.41	PE	[1141]
Au/quartz	Au	–	$\sim10^{-9}$	~300 (673)	–	5.41	PE	[3313]
Au/quartz[350]	Au	–	$\sim10^{-9}$	~300 (623)	–	5.42	PE	[3313]
Au/W(110)	Au	–	$\leq7\times10^{-11}$	~300 (≤1200)	–	5.42	CPD	[2388]
Au/Pt(100)	Au	–	$\sim10^{-10}$	~300	–	5.42 ± 0.02	PE	[3136]
Au/Mo(110)	Au	–	$<1\times10^{-10}$	~300	–	5.43*	CPD	[2864]
Au/glass[368]	Au	–	2×10^{-10}	77	–	5.43 ± 0.01	CPD	[945]
Au/glass	Au	–	10^{-9}	~300 (>573)	–	5.45	CPD	[1074]
Au/W(110)	Au	–	$<7\times10^{-11}$	78 (750)	–	5.45	FE	[2279]
Au/glass[368]	Au	–	2×10^{-10}	77	–	5.45 ± 0.01	CPD	[945]
Au/W(100)	Au	–	?	~300	–	5.5	FE	[2263]
Au/W(110)	Au	–	$\sim10^{-10}$	~400	–	5.5 ± 0.05*	CPD	[3676]
Au/W (110)	Au	–	5×10^{-11}	~300	–	5.51	CPD	[2384]
Au/Pt (997)	Au	–	1×10^{-10}	~300	–	5.52 ± 0.15	PE	[174]
Au/W(110)	Au	–	$\sim10^{-10}$	$\sim300\{\leq900\}$	–	5.55	CPD	[2858]
Au/W(100)	Au	–	$<2\times10^{-10}$	78{500}	–	5.55	FE	[2256]
Au/Cr/Au(100)	–	–	–	–	–	5.57	TC	[1911]
Au/ZnO(1120)	Au	–	$\leq2\times10^{-11}$	~300	–	5.59 ± 0.03	CPD	[3068]
Au/CdS(1120)	Au	–	$\leq2\times10^{-11}$	~300	–	5.59 ± 0.03	CPD	[3068]
Au	–	–	–	–	–	5.6	TC	[706]
Au/W(100)	Au	–	?	78	–	5.6	FE	[2263]
Au/W(100)	Au	–	?	78 (330)	–	5.6*	FE	[2263]
Au/Cr	Au	–	4×10^{-11}	~300	–	5.6	CPD	[2123]
Au/V(100)	Au	–	$<8\times10^{-11}$	120	–	5.6 ± 0.1	PE	[3372]
Au/Ru(001)	Au	–	$<5\times10^{-10}$	60	–	5.60 ± 0.05	PE	[2651]
Au/Cr/Au(100)	–	–	–	–	–	5.65	TC	[1911]
Au/W(110)	Au	–	$\sim10^{-10}$	900	–	5.65 ± 0.05*	CPD	[3676]
Au/Si(111)	Cs, Li	Cs$^+$	?	~300	5.7*	–	CPD	[1342]
Au/W[362]	Au$_n$	–	$\sim10^{-5}$ (He, Ar)	77	–	5.7 ± 0.5	FE	[1713]
Au/W(110)	Au	–	$\sim10^{-10}$	600	–	5.70 ± 0.05*	CPD	[3676]
Au/W(100)	Au	–	?	78 (330)	–	5.8	FE	[2263]
Au/Pt(111)	Au	–	1×10^{-10}	~300	–	5.8 ± 0.15	PE	[174]
Au/Ir(100)[359]	Au	–	?	78 (520)	–	5.80	FE	[2189]
Au/Ir(100)[359]	Au	–	?	78 (482)	–	5.86 ± 0.02	FE	[2189]
Au/W[362]	Au$_n$	–	$\sim10^{-5}$ (He, Ar)	77	–	5.9 ± 0.6	FE	[1713]
Au/Pt(100)	–	–	–	–	–	6.17	TC	[855]
Au	–	–	–	–	–	6.79	TC	[2551]
Recommended	–	–	–	–	–	**5.30 ± 0.04**	–	–

80. Mercury Hg

Liquid (T > 234 K)

Surface	Beam	Ion	P_r (Torr)	T (K)	ϕ^+ (eV)	ϕ^e (eV)	Meth.	Refs.
Hg	–	–	–	–	–	3.33	TC	[3211]
Hg	–	–	?	~300	–	3.9–4.9	PE	[1745]
Hg	–	–	–	–	–	3.9–5.0	TC	[2261]
Hg	–	–	?	~300	–	4.054 ± 0.027	PE	[3247]
Hg/Ag	Hg	–	$\sim10^{-9}$	~300	–	4.16 ± 0.07*	CPD	[1530]
Hg/Ag/Al	Hg	–	$\sim10^{-6}$	~300	–	4.3 ± 0.1	CPD	[2250]
Hg	–	–	?	~300	–	4.33	PE	[2081]
Hg/Mo	Hg	–	?	~240	–	~4.4	FE	[3074]
Hg$_n$(n → ∞)	–	–	–	–	–	4.42 ± 0.58	TC	[4261]
Hg	–	–	–	–	–	4.43*	TC	[1955]
Hg/W(110)	Hg	–	7×10^{-11}	~240	–	4.46	PE	[3566]
Hg	–	–	?	243	–	4.475 ± 0.01	PE	[2770,2771]
Hg	–	–	?	~300	–	4.48 ± 0.02	CPD	[2334,2597]
Hg	–	–	–	–	–	4.49	TC	[2005]
Hg[370]	–	–	$<2\times10^{-10}$	273	–	4.49 ± 0.01	PE	[1669]
Hg[156]	–	–	$<10^{-8}$	298	–	4.49 ± 0.05	PE	[2470,4207,4209, 4223–4225]
Hg	–	–	–	–	–	4.5	TC	[1645]
Hg	–	–	–	–	–	4.5	TC	[2583]
Hg/Cu/Al	Hg	–	$\sim10^{-6}$	~300	–	4.5 ± 0.1	CPD	[2250]
Hg	–	–	–	–	–	4.50	TC	[3264,3265,3267]
Hg	–	–	?	~300	–	4.50	PE	[1634]
Hg	–	–	–	–	–	4.50	TC	[3352]
Hg	–	–	$\sim10^{-6}$	~300	–	4.50	CPD	[2942]
Hg	–	–	$\sim10^{-6}$	~300	–	4.50 ± 0.01	PE	[1752]
Hg	–	–	$\sim10^{-7}$	~300	–	4.50 ± 0.03	CPD	[1542,2767]
Hg	–	–	? (N$_2$)	~300	–	4.51	CPD	[2186]

Table 1 (*continued*)

Surface	Beam	Ion	P_r (Torr)	T (K)	ϕ^+ (eV)	ϕ^e (eV)	Meth.	Refs.
Hg	–	–	?	~300	–	4.51	PE	[2290]
Hg	–	–	–	–	–	4.51	TC	[1399]
Hg	–	–	?	~300	–	4.51 ± 0.02	PE	[2920]
Hg	–	–	–	–	–	4.510	TC	[2649]
Hg	–	–	–	–	–	4.52	TC	[1990]
Hg	–	–	<10⁻⁵	~300	–	4.52	PE	[2291]
Hg	–	–	?	~300	–	4.52 ± 0.02	PE	[2081]
Hg/O=Fe	Hg	–	?	>234	–	4.52 ± 0.02	PE	[2921]
Hg	–	–	–	–	–	4.53	TC	[1885]
Hg/W(100)	Hg	–	2 × 10⁻¹⁰	~300	–	4.55	PE	[1859]
Hg	–	–	~10⁻⁹	298	–	4.55 ± 0.05*	PE	[2613]
Hg	–	–	–	–	–	4.59	TC	[298]
Hg/W	Hg	–	?	293	–	4.59 ± 0.04*	CPD	[2573]
Hg/W[371]	Hg	–	?	~240	–	~4.6	FE	[3074]
Hg	–	–	?	~300	–	4.60	PE	[2614]
Hg	–	–	?	~300	–	4.60	PE	[2081]
Hg/W	Hg	–	~10⁻⁹ (Hg)	295	–	4.616 ± 0.046*	FE	[3143]
Hg/Mo	Hg	–	~10⁻⁹	~300	–	4.62 ± 0.07*	CPD	[1530]
Hg/Au	Hg	–	<10⁻⁹ (Hg)	~300	–	4.64	CPD	[1072]
Hg/W	Hg	–	~10⁻⁹ (Hg)	900–980	–	4.647 ± 0.007*	FE	[3143]
Hg/W	Hg	–	~10⁻⁹ (Hg)	750,780	–	4.680 ± 0.004*	FE	[3143]
Hg	–	–	–	–	–	4.7	TC	[706]
Hg/Au/Al	Hg	–	~10⁻⁶	~300	–	4.7 ± 0.1	CPD	[2250]
Hg/W	Hg	–	~10⁻⁹ (Hg)	295	–	4.73 ± 0.04*	FE	[3143]
Hg	–	–	?	~300	–	4.744	PE	[2806]
Hg/Au/glass	Hg	–	5 × 10⁻¹¹	~300	–	4.77	CPD	[1071]
Hg	–	–	–	–	–	4.79	TC	[1744]
Hg	–	–	? (O₂, air)	~300	–	4.83	PE	[2081]
Hg/Au	Hg	–	2 × 10⁻⁹ (Hg)	~300	–	4.89 ± 0.06	CPD	[1072]
Hg/W[371]	Hg	–	1 × 10⁻¹⁰	~300	–	4.9	FE	[3726]
Hg/Ni(111)[372]	Hg	–	<10⁻¹⁰	240–310	–	4.90 ± 0.08	PE	[3165,3166]
Hg/Re	Hg	–	~10⁻⁹	~300	–	5.08 ± 0.03*	CPD	[1530]
Hg/Au	Hg	–	~10⁻⁹	~300	–	5.15 ± 0.08*	CPD	[1530]
Recommended	–	–	–	–	–	**4.50 ± 0.02**	–	–
Rhombohedral (α, $T < 234$ K for bulk)								
Hg/W(110)	Hg	–	7 × 10⁻¹¹	200	–	4.46	PE	[3566]
Hg	–	–	?	173	–	4.47 ± 0.03	PE	[2770]
Hg[370]	–	–	<2 × 10⁻¹⁰	<234	–	4.49 ± 0.01	PE	[1669]
Hg[156]	–	–	<10⁻⁸	<234	–	4.49 ± 0.05	PE	[2470]
Hg	–	–	?	83–230	–	4.49 ± 0.04	PE	[2920]
Hg/O=Fe	–	–	?	83	–	4.52 ± 0.02	PE	[2921]
Hg/W(110)	Hg	–	?	90	–	4.59	CPD	[3562]
Hg/W	Hg	–	?	~200	–	~4.6	FE	[3074]
Recommended	–	–	–	–	–	**4.52 ± 0.05**	–	–

81. Thallium Tl

hcp (α, $T < 503$ K)

Surface	Beam	Ion	P_r (Torr)	T (K)	ϕ^+ (eV)	ϕ^e (eV)	Meth.	Refs.
Tl(0001)	–	–	–	–	–	3.90	TC	[4005]
Tl(0001)	–	–	–	–	–	4.48	TC	[321]
Tl(1010)	–	–	–	–	–	3.93	TC	[4005]
Tl(1010)	–	–	–	–	–	4.27	TC	[321]
Tl(1124)	–	–	–	–	–	3.75	TC	[321]
bcc (β, $T > 503$ K)								
Tl(100)	–	–	–	–	–	3.52	TC	[321]
Tl(110)	–	–	–	–	–	4.10	TC	[321]
Tl(111)	–	–	–	–	–	3.36	TC	[321]
Tl(112)	–	–	–	–	–	3.75	TC	[321]
hcp (α, $T < 503$ for bulk)								
Tl	–	–	–	–	–	3.03	TC	[1066]
Tl	–	–	–	–	–	3.23	TC	[1744]
Tl$_n$(n → ∞)	–	–	–	–	–	3.23 ± 0.11	TC	[4261]

Table 1 (*continued*)

Surface	Beam	Ion	P_r (Torr)	T (K)	ϕ^+ (eV)	ϕ^e (eV)	Meth.	Refs.
Tl	–	–	–	–	–	3.40	TC	[521]
Tl/?	Tl	–	?	?	–	3.68	PE	[3029]
Tl	–	–	?	293	–	3.69	PE	[4139]
Tl	–	–	–	–	–	3.7	TC	[1993]
Tl	–	–	–	–	–	3.7	TC	[2583]
Tl	–	–	–	–	–	3.70	TC	[1885]
Tl	–	–	?	~300	–	3.70	PE	[2614]
Tl/Au(100)	–	–	–	–	–	3.71	TC	[3168]
Tl	–	–	?	567	–	3.72	PE	[4139]
Tl	–	–	–	–	–	3.73	TC	[3168]
Tl	–	–	–	–	–	3.75*	TC	[1955]
Tl	–	–	–	–	–	3.76	TC	[1399]
Tl	–	–	–	–	–	3.78	TC	[2629]
Tl	–	–	–	–	–	3.83	TC	[4418,4420]
Tl	–	–	?	~300	–	3.84	CPD	[2297]
Tl	–	–	–	–	–	3.84	TC	[3264,3265]
Tl	–	–	9×10^{-10}	~300	–	3.84 ± 0.05	PE	[3437]
Tl	–	–	–	–	–	3.88	TC	[298]
Tl$_n$(n → ∞)	–	–	?	~300	–	3.89	IP, TC	[4197]
Tl	–	–	–	–	–	3.90	TC	[1613]
Tl	–	–	–	–	–	4.0 ± 0.05	TC	[1990]
Tl	–	–	–	–	–	4.02	TC	[3264,3265,3267]
Tl/Cu(100)	Tl	–	$<5 \times 10^{-10}$	~300	–	4.04	PE	[1555]
Tl	–	–	–	–	–	4.07	TC	[2005]
Tl	–	–	–	–	–	4.08	TC	[3264]
Tl/Si(111)	Tl	–	2×10^{-10}	~300	–	4.1*	PE	[3634]
Tl	–	–	–	–	–	4.2	TC	[706]
Recommended	–	–	–	–	–	**3.82 ± 0.05**	–	–

Liquid ($T > 577$ K)

Tl	–	–	?	587	–	3.64	PE	[4139]
Tl	–	–	9×10^{-10}	~680	–	3.84 ± 0.05	PE	[3437]

82. Lead Pb

fcc

Surface	Beam	Ion	P_r (Torr)	T (K)	ϕ^+ (eV)	ϕ^e (eV)	Meth.	Refs.
Pb(100)	–	–	–	–	–	3.04	TC	[1159,3067]
Pb(100)	–	–	–	–	–	3.45	TC	[476]
Pb(100)	–	–	–	–	–	3.48	TC	[3211]
Pb(100)	–	–	–	–	–	3.50	TC	[231]
Pb(100)	–	–	–	–	–	3.57	TC	[553]
Pb(100)	–	–	–	–	–	3.67	TC	[476]
Pb(100)	–	–	–	–	–	3.76	TC	[3467]
Pb(100)	–	–	–	–	–	3.79	TC	[3004]
Pb(100)	–	–	–	–	–	3.79 ± 0.02*	TC	[3521]
Pb(100)	–	–	–	–	–	3.8	TC	[1088]
Pb(100)	–	–	–	–	–	3.81	TC	[1030]
Pb(100)	–	–	–	–	–	3.84	TC	[3492]
Pb(100)	–	–	–	–	–	3.88	TC	[1030]
Pb(100)	–	–	–	–	–	3.95	TC	[475]
Pb(100)	–	–	–	–	–	4.0	TC	[1088]
Pb(100)	–	–	–	–	–	4.07	TC	[3004]
Pb(100)	–	–	–	–	–	4.07 ± 0.01*	TC	[3521]
Pb(100)	–	–	–	–	–	4.10	TC	[556,1030]
Pb(100)	–	–	–	–	–	4.12	TC	[2516]
Pb(100)	–	–	–	–	–	4.31	TC	[555]
Pb(100)	–	–	–	–	–	4.4	TC	[1712,1714]
Pb(100)	–	–	–	–	–	4.5	TC	[1711]
Pb(100)	–	–	–	–	–	4.50	TC	[475]
Pb(100)	–	–	–	–	–	4.65	TC	[1095]
Pb(100)	–	–	–	–	–	4.95	TC	[321]
Recommended	–	–	–	–	–	**3.96 ± 0.11**	–	–
Pb(110)	–	–	–	–	–	2.99	TC	[1159,3067]
Pb(110)	–	–	–	–	–	3.26	TC	[1684]
Pb(110)	–	–	–	–	–	3.46	TC	[553]
Pb(110)	–	–	–	–	–	3.51	TC	[3467]
Pb(110)	–	–	–	–	–	3.64 ± 0.01*	TC	[3521]
Pb(110)	–	–	–	–	–	3.73	TC	[2516]
Pb(110)	–	–	–	–	–	3.77	TC	[231]

Table 1 (*continued*)

Surface	Beam	Ion	P_r (Torr)	T (K)	ϕ^+ (eV)	ϕ^e (eV)	Meth.	Refs.
Pb(110)	–	–	–	–	–	3.8	TC	[1088]
Pb(110)	–	–	–	–	–	3.80	TC	[3004]
Pb(110)	–	–	–	–	–	3.80	TC	[475]
Pb(110)	–	–	–	–	–	3.82	TC	[476]
Pb(110)	–	–	–	–	–	3.84	TC	[3004]
Pb(110)	–	–	–	–	–	3.84	TC	[1030]
Pb(110)	–	–	–	–	–	3.89	TC	[3211]
Pb(110)	–	–	–	–	–	3.90	TC	[556,1030]
Pb(110)	–	–	–	–	–	3.92 ± 0.01*	TC	[3521]
Pb(110)	–	–	–	–	–	3.98	TC	[555]
Pb(110)	–	–	–	–	–	4.01	TC	[476]
Pb(110)	–	–	–	–	–	4.08	TC	[1030]
Pb(110)	–	–	–	–	–	4.4	TC	[1088]
Pb(110)	–	–	–	–	–	4.50	TC	[1095]
Pb(110)	–	–	–	–	–	4.66	TC	[321]
Recommended	–	–	–	–	–	**3.84 ± 0.09**	–	–
Pb(111)	–	–	–	–	–	3.16	TC	[1159,3067]
Pb(111)	–	–	–	–	–	3.31	TC	[476]
Pb(111)	–	–	–	–	–	3.39	TC	[1684]
Pb(111)	–	–	–	–	–	3.51	TC	[476]
Pb(111)	–	–	–	–	–	3.59	TC	[231]
Pb(111)	–	–	–	–	–	3.65	TC	[1030]
Pb(111)	–	–	–	–	–	3.7	TC	[1086,1088]
Pb(111)	–	–	–	–	–	3.71	TC	[1086]
Pb(111)	–	–	–	–	–	3.78 ± 0.01	TC	[3521]
Pb(111)	–	–	–	–	–	3.79	TC	[3004]
Pb(111)	–	–	–	–	–	3.80	TC	[1086]
Pb(111)	–	–	–	–	–	3.82 ± 0.02	TC	[3483]
Pb(111)	–	–	–	–	–	3.85	TC	[475]
Pb(111)	–	–	–	–	–	3.9	TC	[1088]
Pb(111)	–	–	–	–	–	3.90	TC	[553]
Pb(111)	–	–	–	–	–	4.05	TC	[1086]
Pb(111)	–	–	2×10^{-11}	20 ± 5	–	4.05	PE	[2268]
Pb(111)	–	–	?	30	–	4.05	PE	[2228]
Pb(111)	–	–	–	–	–	4.06	TC	[1086]
Pb(111)	–	–	–	–	–	4.08 ± 0.01	TC	[3521]
Pb(111)	–	–	–	–	–	4.11	TC	[3004]
Pb(111)	–	–	–	–	–	4.12	TC	[1086]
Pb(111)	–	–	–	–	–	4.14	TC	[1086]
Pb(111)	–	–	–	–	–	4.14	TC	[2516]
Pb(111)	–	–	–	–	–	4.15	TC	[475]
Pb(111)/W(100)	Pb	–	$\sim 10^{-9}$	~300	–	4.28	CPD	[2002]
Pb(111)	–	–	–	–	–	4.30	TC	[555]
Pb(111)	–	–	–	–	–	4.34	TC	[3467]
Pb(111)	–	–	–	–	–	4.55	TC	[1095]
Pb(111)/W(110)	Pb	–	5×10^{-11}	548	–	4.70	CPD	[1525]
Pb(111)	–	–	–	–	–	4.79	TC	[3211]
Pb(111)	–	–	–	–	–	5.21	TC	[1089]
Pb(111)	–	–	–	–	–	5.23	TC	[1030]
Pb(111)	–	–	–	–	–	5.24	TC	[1089]
Pb(111)	–	–	–	–	–	5.35	TC	[321]
Pb(111)	–	–	–	–	–	5.47	TC	[1089]
Pb(111)	–	–	–	–	–	5.9	TC	[1086]
Pb(111)	–	–	–	–	–	5.9	TC	[3137]
Recommended	–	–	–	–	–	**4.14 ± 0.09**	–	–
Pb	–	–	–	–	–	3.0–4.6	TC	[2704]
Pb	–	–	–	–	–	3.31	TC	[1066]
Pb	–	–	–	–	–	3.50	TC	[521]
Pb	–	–	–	–	–	3.50	TC	[3211]
Pb	–	–	–	–	–	3.51	TC	[231]
Pb	–	–	–	–	–	3.55	TC	[3211]
Pb	–	–	$\sim 10^{-8}$	298	–	3.58	PE	[4206]
Pb/Si(111)	Pb	–	8×10^{-11}	77{~300}	–	3.6 ± 0.1	CPD	[4400]
Pb	–	–	–	–	–	3.73	TC	[231]
Pb	–	–	–	–	–	3.79	TC	[2005]
Pb	–	–	–	–	–	3.80	TC[3]	[475]
Pb/Ge(111)	–	–	–	–	–	3.81 ± 0.01	TC	[2286]
Pb	–	–	–	–	–	3.82	TC	[2286]

Table 1 (*continued*)

Surface	Beam	Ion	P_r (Torr)	T (K)	ϕ^+ (eV)	ϕ^e (eV)	Meth.	Refs.
Pb/glass[373]	–	–	?	~300	–	3.83 ± 0.02	CPD	[1381]
Pb	–	–	–	–	–	3.84	TC	[230]
Pb	–	–	–	–	–	3.87	TC	[3467]
Pb/ins/Al[47]	Pb	–	?	~300	–	3.89 ± 0.06	CPD	[2028]
Pb/Cu(111)	–	–	–	–	–	3.91	TC	[2286]
Pb	–	–	1×10^{-5}	~300	–	3.92	CPD	[1883]
Pb/Si(111)	Pb	–	1×10^{-10}	78	–	3.92	CPD	[4311]
Pb	–	–	–	–	–	3.92	TC	[2629]
Pb	–	–	?	~300	–	3.92 ± 0.02	TC	[4265]
Pb	–	–	?	~300	–	3.94	CPD	[2297]
Pb/quartz	Pb	–	$\sim10^{-10}$	~300	–	3.95	PE	[2718]
Pb/Cu	Pb	–	$\sim10^{-10}$	~300	–	3.95	PE	[2718]
Pb[374]	–	–	5×10^{-10}	~300	–	3.95 ± 0.05	PE	[3437]
Pb/steel	Pb	–	2×10^{-10}	~300	–	3.95 ± 0.05	PE	[1537]
Pb	–	–	?	~300	–	3.97	PE	[2460]
Pb	–	–	–	–	–	3.98	TC	[1399]
Pb	–	–	$\sim10^{-9}$	293	–	3.98	PE	[2362]
Pb/quartz	Pb	–	$<10^{-6}$	20	–	3.983 ± 0.004	PE	[1467]
Pb/quartz	Pb	–	$<10^{-6}$	20 (90)	–	3.995 ± 0.004	PE	[1467]
Pb	–	–	–	–	–	4.0	TC	[298]
Pb	–	–	–	–	–	4.00	TC	[3352]
Pb/glass[373]	Pb	–	?	~300	–	4.00 ± 0.02	CPD	[1381]
Pb	–	–	? (N_2)	~300	–	4.00 ± 0.02	CPD	[2361,4083]
Pb	–	–	–	–	–	4.01	TC	[3264,3265]
Pb/quartz	Pb	–	$<10^{-6}$	20 (250)	–	4.013 ± 0.004	PE	[1467]
Pb	–	–	?	~300	–	4.05 ± 0.05	CPD	[1542,2334]
Pb	–	–	?	293	–	4.06	PE	[4139]
Pb	–	–	?	~300	–	4.06	PE	[4249]
Pb	–	–	–	–	–	4.09	TC	[553]
Pb	–	–	–	–	–	4.09	TC	[3477]
Pb	–	–	–	–	–	4.1	TC	[1993]
Pb/Ag(111)/mica	Pb	–	2×10^{-10}	~300	–	4.1*	CPD	[3276]
Pb	–	–	–	–	–	4.10	TC	[3211]
Pb	–	–	–	–	–	4.10	TC	[1613]
Pb	–	–	?	597	–	4.11	PE	[4139]
Pb/Cu(100)	Pb	–	?	~300	–	4.11 ± 0.01*	CPD	[1423]
Pb	–	–	–	–	–	4.12	TC	[1885]
Pb	–	–	?	298	–	4.13	PE	[4305]
Pb	–	–	6×10^{-3}	~300	–	4.14 ± 0.07	PE	[2079,2080]
Pb/brass	Pb	–	$\leq10^{-8}$	~300	–	4.14 ± 0.1	PE	[2848]
Pb	–	–	–	–	–	4.18	TC	[3264,3265,3267]
Pb/Al(111)	Pb	–	$<1 \times 10^{-10}$	~300	–	4.2	PE	[249]
Pb/Ni(111)	Pb	–	$<1 \times 10^{-10}$	~300	–	4.2	PE	[249]
Pb	–	–	–	–	–	4.2 ± 0.05	TC	[1990]
Pb/Si(111)	Pb	–	5×10^{-11}	~300	–	4.25 ± 0.05	CPD	[613,636]
Pb/Ni(111)	Pb	–	2×10^{-11}	~300	–	4.3	PE	[2269]
Pb/Cu(111)	Pb	–	?	~300	–	4.34*	CPD	[1423]
Pb	–	–	$\sim6 \times 10^{-9}$	~300	–	4.36	PE	[1139]
Pb/Pt(111)	Pb	–	$<3 \times 10^{-10}$	~300	–	4.39 ± 0.07*	CPD	[2670]
Pb/W(110)	Pb	–	?	~300	–	4.4	CPD	[1984]
Pb/Pt(111)	Pb	–	$<3 \times 10^{-10}$	~300	–	4.4 ± 0.1	CPD	[2670]
Pb/Ni(100)	Pb	–	3×10^{-10}	~300	–	4.4 ± 0.1	CPD	[1439]
Pb/W	Pb	–	$(<1 \times 10^{-11})$	~300 (526)	–	4.40 ± 0.02	FE	[2254]
Pb/Mo(110)	Pb	–	$\leq5 \times 10^{-11}$	550	–	4.45*	CPD	[3290]
Pb/W(110)	Pb	–	5×10^{-11}	~300	–	4.45	CPD	[1525,3588]
Pb/Mo(110)	Pb	–	$\leq5 \times 10^{-11}$	680	–	4.48*	CPD	[3290]
Pb	–	–	–	–	–	4.5	TC	[706]
Pb/W	Pb	–	$(<1 \times 10^{-11})$	~300 (730)	–	4.50 ± 0.02	FE	[2254]
Pb/Mo(110)	Pb	–	$\leq5 \times 10^{-11}$	350 (550)	–	4.50*	CPD	[3290]
Pb/Mo(110)	Pb	–	$\leq5 \times 10^{-11}$	350 (680)	–	4.56*	CPD	[3290]
Pb/W(100)	Pb	–	?	300–800	–	4.56	FE	[2257]
Pb/W(100)	Pb	–	?	77 (415)	–	4.58 ± 0.03*	FE	[2260]
Pb/W(112)	Pb	–	$(<1 \times 10^{-11})$	~300 (526)	–	4.59 ± 0.02	FE	[2254]
Pb/W(100)	Pb	–	$(<1 \times 10^{-11})$	~300 (843)	–	4.59 ± 0.02	FE	[2254]
Pb	–	–	–	–	–	4.64	TC	[3467]
Pb/Si(111)	Pb	–	$<8 \times 10^{-11}$	100 (600)	–	4.68*	PE	[2445]
Pb/W(100)	Pb	–	$(<1 \times 10^{-11})$	~300 (463)	–	4.68 ± 0.02	FE	[2254]
Pb/W	Pb	–	$\leq5 \times 10^{-10}$	300 (520)	–	4.70 ± 0.05	FE	[3548]
Pb/W(100)	Pb	–	?	77 (415)	–	4.71 ± 0.01	FE	[2260]
Pb/W(112)	Pb	–	$<8 \times 10^{-11}$	80	–	4.72 ± 0.01	FE	[3959]

Table 1 (*continued*)

Surface	Beam	Ion	P_r (Torr)	T (K)	ϕ^+ (eV)	ϕ^e (eV)	Meth.	Refs.
Pb/W(112)	Pb	–	($<1 \times 10^{-11}$)	~300 (730)	–	4.74 ± 0.02	FE	[2254]
Pb	–	–	–	–	–	4.76	TC	[3477]
Pb	–	–	–	–	–	4.84	TC	[2629]
Pb/W(110)	Pb	–	($<1 \times 10^{-11}$)	~300 (≤658)	–	4.94 ± 0.02	FE	[2254]
Recommended	–	–	–	–	–	**4.07 ± 0.05**	–	–

Liquid ($T > 601$ K)

Pb[374]	–	–	8×10^{-10}	~700	–	3.95 ± 0.05	PE	[3437]
Pb	–	–	?	617	–	4.04	PE	[4139]

83. Bismuth Bi

Rhombohedral (arsenic structure)

Bi(0001)	–	–	~10^{-7}	~300	–	4.35 ± 0.02	PE	[2807]
Bi(0001)	–	–	5×10^{-10}	100, ~300	–	4.5*	PE	[2480]
Bi(0001)	–	–	~10^{-6}	~300	–	4.81 ± 0.02	PE	[2807]
Bi(1011)	–	–	5×10^{-10}	100, ~300	–	4.3*	PE	[2480]
Bi	–	–	–	–	–	3.77	TC	[1744]
Bi/Pt(111)	Bi	–	?	110–625	–	3.8 ± 0.1*	CPD	[2868]
Bi/ins/Al[47]	Bi	–	?	~300	–	3.85 ± 0.07	CPD	[2028]
Bi	–	–	–	–	–	3.92	TC	[2005]
Bi/Au(111)[375]	Bi	–	$<5 \times 10^{-10}$	298	–	3.94*	CPD	[3678]
Bi	–	–	–	–	–	4.1	TC	[298]
Bi	–	–	–	–	–	4.1	TC	[706]
Bi	–	–	–	–	–	4.12	TC	[1885]
Bi	–	–	?	~300	–	4.14	PE	[2080]
Bi	–	–	?	~300	–	4.17	CPD	[2297]
Bi	–	–	?	~300	–	4.17	PE	[4249]
Bi/quartz	Bi	–	$<10^{-6}$	6.5–12.5	–	4.1746	PE	[1467]
Bi/quartz	Bi	–	$<10^{-6}$	20	–	4.2160	PE	[1467]
Bi/glass	Bi	–	$<10^{-9}$	90	–	4.22	PE	[1383,1389,3038, 3052]
Bi/Au(111)	Bi	–	2×10^{-10}	~300	–	4.22	PE	[4448]
Bi	–	–	–	–	–	4.22	TC	[4418,4420]
Bi/glass	Bi	–	$<10^{-9}$	90	–	4.223	PE	[3038]
Bi/glass	Bi	–	2×10^{-8}	297–299	–	4.23 ± 0.01	PE	[2234]
Bi/quartz	Bi	–	$<10^{-6}$	20 (270)	–	4.2348	PE	[1467]
Bi/glass	Bi	–	≤10^{-7}	90	–	4.243	PE	[3040]
Bi/glass[376]	Bi	–	$<10^{-9}$	90 (293)	–	4.245	PE	[3038]
Bi/glass[376]	–	–	–	–	–	4.25	TC	[1403]
Bi/glass	Bi	–	$<10^{-9}$	90 (363)	–	4.25	PE	[1383]
Bi[377]	–	–	5×10^{-10}	~300	–	4.25 ± 0.05	PE	[3437]
Bi/glass	Bi	–	≤10^{-7}	90	–	4.251	PE	[3040]
Bi/glass	Bi	–	$<10^{-9}$	90 363)	–	4.26	PE	[1389]
Bi/Ni, etc.	Bi	–	$<5 \times 10^{-8}$	~300	–	4.26	PE	[1375]
Bi/InAs(111)[n]	Bi	–	?	~300 (503)	–	4.28	PE	[4090]
Bi/glass	Bi	–	$<10^{-9}$	293{90}	–	4.288	PE	[3038]
Bi	–	–	–	–	–	4.29	TC	[3264,3265]
Bi	–	–	–	–	–	4.29	TC	[1399]
Bi	–	–	–	–	–	4.3	TC	[1993]
Bi	–	–	–	–	–	4.3	TC	[1955]
Bi	–	–	–	–	–	4.3 ± 0.05	TC	[1990]
Bi/glass	Bi	–	≤10^{-7}	293	–	4.307	PE	[3040]
Bi	–	–	–	–	–	4.32	TC	[3352]
Bi	–	–	? (N_2)	~300	–	4.32 ± 0.02	CPD	[2361,4083]
Bi/Mo, etc.	Bi	–	$<5 \times 10^{-8}$	~300	–	4.34	PE	[1375]
Bi	–	–	?	293	–	4.35	PE	[4139]
Bi	–	–	–	–	–	4.36	TC	[3264,3267]
Bi/glass[376]	Bi	–	$<10^{-9}$	90 (293)	–	4.370	PE	[3038]
Bi	–	–	?	534	–	4.39	PE	[4139]
Bi/W	Bi	–	5×10^{-10}	~300	–	4.40	FE	[2018]
Bi/glass	Bi	–	?	~300	–	4.43	PE	[3397]
Bi/glass	Bi	–	?	20, 77	–	4.44	PE	[3028]
Bi/W(100)	Bi	–	?	77 (415)	–	4.45 ± 0.04*	FE	[2260]
Bi/W	Bi	–	≤10^{-10}	~300{700}	–	4.5	FE	[2966]
Bi/glass	Bi	–	$<10^{-9}$	90 (363)	–	4.54	PE	[1389]
Bi/W(100)	Bi	–	?	77 (415)	–	4.58 ± 0.03	FE	[2260]
Bi/glass[376]	–	–	–	–	–	4.6	TC	[1403]

Table 1 (*continued*)

Surface	Beam	Ion	P_r (Torr)	T (K)	ϕ^+ (eV)	ϕ^e (eV)	Meth.	Refs.
Bi/glass	Bi	–	?	220–298	–	4.76–5.06	PE	[3395]
Bi/glass	Bi	–	?	220–298	–	4.82–5.03	PE	[3395]
Bi[378]	–	–	?	<544	–	4.86*	CPD	[1755]
Bi/glass	Bi	–	?	195–295	–	4.969 ± 0.011	PE	[3398]
Recommended	–	–	–	–	–	**4.28 ± 0.05**	–	–

Liquid (T > 544 K)

Bi[377]	–	–	8×10^{-10}	~640	–	4.25 ± 0.05	PE	[3437]
Bi	–	–	≤10^{-9}	573	–	4.34 ± 0.05	PE	[2349,2353]
Bi	–	–	?	554	–	4.42	PE	[4139]
Bi[378]	–	–	?	>544	–	4.88*	CPD	[1755]

84. Polonium Po

Cubic (α, T < 348 K for bulk)

Po[160]	–	–	–	–	–	4.6	TC	[1355]
Po[379]	–	–	–	–	–	4.8	TC	[1955]
Po	–	–	–	–	–	5.0	TC	[298]

85. Astatine At

At	–	–	–	–	–	5.3		[1955]

87. Francium Fr

bcc

Fr(111)	–	–	–	–	–	2.13	TC	[2410]
Fr[160]	–	–	–	–	–	1.5	TC	[1355]
Fr[379]	–	–	–	–	–	1.8	TC	[1955]
Fr	–	–	–	–	–	2.0	TC	[298]
Fr	–	–	–	–	–	2.01	TC	[550]
Fr	–	–	–	–	–	2.02	TC	[550]
Fr	–	–	–	–	–	2.14	TC	[550]

88. Radium Ra

bcc

Ra(110)	–	–	–	–	–	2.25	TC	[334]
Ra(111)	–	–	–	–	–	2.03	TC	[2410]
Ra	–	–	–	–	–	2.0	TC	[3928]
Ra[379]	–	–	–	–	–	2.2*	TC	[1955]
Ra[379]	–	–	–	–	–	2.4	TC	[1955]
Ra	–	–	–	–	–	2.78	TC	[550]
Ra	–	–	–	–	–	2.8	TC	[298]
Ra	–	–	–	–	–	3.23	TC	[550]

89. Actinium Ac

fcc

Ac(111)	–	–	–	–	–	3.44	TC	[2410]
Ac[379]	–	–	–	–	–	2.7	TC	[1955]
Ac	–	–	–	–	–	3.0	TC	[3928]
Ac	–	–	–	–	–	3.20	TC	[550]
Ac	–	–	–	–	–	3.38	TC	[550]
Ac	–	–	–	–	–	3.58	TC	[298]

90. Thorium Th

fcc (α, T < 1623 K)

Th(100)	–	–	–	–	–	3.52	TC	[1254]
Th(100)	–	–	–	–	–	3.57	TC	[1980]
Th(110)	–	–	–	–	–	3.38	TC	[1980]
Th(111)	–	–	–	–	–	3.44	TC	[2410]
Th(111)	–	–	–	–	–	3.75	TC	[1980]

Table 1 (*continued*)

Surface	Beam	Ion	P_r (Torr)	T (K)	ϕ^+ (eV)	ϕ^e (eV)	Meth.	Refs.
Th/Pt	Th	–	?	~1500	–	2.40	TE	[1306]
Th/Ta	Th	–	?	~1500	–	2.54	TE	[1306]
Th/ThO₂-W[380]	–	–	?	~1300 (2200)	–	2.63	TE	[1749,1750]
Th/ThO₂-W[380]	–	–	?	1230 (1920)	–	2.64	TE	[3667,3668]
Th/ThO₂-W	–	–	?	~1300–2500	–	2.7	TE	[3652]
Th/Ta	Th	–	2×10^{-8}	1468	–	2.73	TE	[2566]
Th/ThO₂-W	–	–	1×10^{-9}	~1800 (~2800)	–	2.75 ± 0.15	FE	[3050]
Th/ThO₂-W	–	–	~10^{-8}	~900–1200	–	2.77	TE	[196]
Th/ThO₂-W	–	–	?	1160–1600	–	2.77	TE	[2925]
Th/ThO₂-W	–	–	~10^{-7}	?	(3.3*)	2.8 ± 0.1	TE	[216]
Th/ThO₂-W	–	–	~10^{-8}	~900–1200	–	2.82	TE	[196]
Th/ThO₂-W	–	–	<10^{-7}	~1300 (2040)	–	2.91	TE	[3800]
Th	–	–	<10^{-6}	?	–	2.94	TE	[2919]
Th[174]	–	–	–	0[E]	–	2.94	TC	[1747]
Th(foil)[381]	–	–	<10^{-10}	~300	–	2.988 ± 0.008	CPD	[2932]
Th/W	–	–	?	?	–	3.0	TE	[2459]
Th/ThO₂-W	–	–	<10^{-7}	~1300 (2040)	–	3.0	TE	[3800]
Th/W(111)	Th	–	?	~300	–	3.0	FE	[2574]
Th/W	Th	–	≤3×10^{-9}	~300	–	3.0	FE	[218]
Th/Re–Th(2%)	–	–	10^{-8}	1600	–	3.09	TE	[4252]
Th/ThO₂-W	–	–	?	~1250–1600	–	3.1	TE	[3801]
Th	–	–	–	–	–	3.1	TC	[1744]
Th/W	–	–	–	1400	–	3.1	TC	[3271]
Th/W	Th	–	≤7×10^{-8}	~300	–	3.1	FE	[1804]
Th/ThO₂-W	–	–	?	0[E]	–	3.18–3.60	CPD	[3972]
Th/ThO₂-W	–	–	<10^{-9}	~1300 (2040)	–	3.26	TE	[3800]
Th	–	–	–	–	–	3.28	TC	[550]
Th/W(foil)	Cl	Cl⁻	2×10^{-7}	1721–1831	3.29 ± 0.16[N]	–	NSI	[597]
Th/ThO₂-W	KCl	K⁺	≤1×10^{-6}	1800	3.3*	(2.8 ± 0.1)	PSI	[216]
Th	–	–	4×10^{-10}	~300	–	3.3 ± 0.2	PE	[3132]
Th/ThO₂-W	–	–	?	1230 (1920)	–	3.3 ± 0.2	TE	[3668]
Th/Re	Th	–	~10^{-10}	1354	–	3.31	TE	[165]
Th/W	Th	–	≤3×10^{-9}	~1500–1800	–	3.31 ± 0.02	TE	[218]
Th/Re(0001)	–	–	–	–	–	3.33	TC	[3848]
Th/W	Th	–	5×10^{-9}	1150–1540	–	3.34	TE	[1453]
Th[382]	–	–	–	–	–	3.35	TC	[1759]
Th/ThO₂-Mo,Pt	–	–	<1×10^{-6}	~1100–1700	–	3.35	TE	[3035]
Th	–	–	?	?	–	3.36	?	[1761]
Th/W(114)	Th	–	~10^{-10}	1360	–	3.36 ± 0.02	TE	[1394,1854]
Th/Ni	Th	–	?	~300	–	3.38	PE	[2922]
Th	–	–	?	?	–	3.39	TE	[1844]
Th/W	ThI₄	–	?	~300 (?)	–	3.39	PE	[2927]
Th/W(114)	Th	–	~10^{-10}	1118	–	3.39 ± 0.02	TE	[1394,1854]
Th	–	–	–	–	–	3.4	TC	[2456]
Th/ThO₂-W	K	K⁺	≤1×10^{-6}	1800	3.4*	(2.8 ± 0.1)	PSI	[216]
Th	–	–	?	?	–	3.4	TE	[3402]
Th/W	–	–	–	–	–	3.4	TC	[509]
Th/W(110)	Th	–	<10^{-8}	~1300–1500	–	3.4	TE	[148]
Th/W(111)	Th	–	<10^{-8}	~1350–1500	–	3.4	TE	[148]
Th/ThO₂-W	–	–	<10^{-7}	~1300 (2040)	–	3.40	TE	[3800]
Th[382]	–	–	–	–	–	3.41	TC	[2932]
Th/W	Th	–	<10^{-9}	~300	–	3.42	FE	[3529]
Th[382]	–	–	–	–	–	3.44	TC	[2932]
Th/Mo, Pt[383]	–	–	–	–	–	3.44	TC	[2932]
Th	–	–	?	~300	–	3.44	PE	[2924]
Th/W	Th	–	<10^{-10}	~300	–	3.44 ± 0.01	CPD	[13,349]
Th/W(100)	Th	–	≤3×10^{-9}	~1200	–	3.45	TE	[1854]
Th[382]	–	–	?	1250–1800	–	3.45 ± 0.01	TE	[3524,3525]
Th/ThO₂W[381]	Th	–	<10^{-10}	~300	–	3.455 ± 0.012	CPD	[2932]
Th	–	–	?	~300	–	3.46	CPD	[2297]
Th/ThO₂-W	–	–	~10^{-7}	~1300–2000	(3.60*[N])	3.46	TE	[827]
Th/W	Th	–	<10^{-10}	~300	–	3.460 ± 0.010	CPD	[2938]
Th/Ni	Th	–	?	~300	–	3.47	PE	[2927]
Th/W(100)	–	–	–	–	–	3.5	TC	[913,4344]
Th/ThO₂-W	–	–	?	~1000 (?)	–	3.5 ± 0.5	TE	[3973]
Th	–	–	–	–	–	3.52	TC	[1254]
Th/ThO₂-W[383]	–	–	?	1260 (≥1300)	–	3.55	TE	[872]
Th/ThO₂-Pt[383]	–	–	?	1260 (≤1650)	–	3.55	TE	[872]
Th	–	–	?	~300	–	3.57	PE	[2080]

Table 1 (*continued*)

Surface	Beam	Ion	P_r (Torr)	T (K)	ϕ^+ (eV)	ϕ^e (eV)	Meth.	Refs.
Th/ThO$_2$-W	I	I$^-$	~10^{-7}	1422	3.58*[N]	(3.46)	NSI	[827]
Th/W(100)	Th	–	6×10^{-11}	~300	–	3.6*	CPD	[2825]
Th/ThO$_2$-W	–	–	≤3×10^{-9}	2000 (2700)	–	3.6	TE	[3960]
Th/ThO$_2$-W	I$_2$	I$^-$	~10^{-7}	1405	3.60*[N]	(3.46)	NSI	[827]
Th/W[383]	–	–	–	–	–	3.61	TC	[2932]
Th	–	–	?	~300	–	3.66	PE	[3027]
Th	–	–	<10^{-10}	~300	–	3.71 ± 0.01	CPD	[13,349]
Th(foil)[381]	–	–	<10^{-10}	~300 (1900)	–	3.728 ± 0.010	CPD	[2932]
Th/Ta	Th	–	2×10^{-8}	1214	–	3.83	TE	[2566]
Recommended	–	–	–	–	–	**3.37 ± 0.04**	–	–

91. Protactinium Pa

Surface	Beam	Ion	P_r (Torr)	T (K)	ϕ^+ (eV)	ϕ^e (eV)	Meth.	Refs.
Pa(111)	–	–	–	–	–	3.76	TC	[2410]
Pa[160]	–	–	–	–	–	3.3	TC	[1355]
Pa	–	–	–	–	–	3.3	TC	[1955]
Pa	–	–	–	–	–	3.5	TC	[1955]
Pa	–	–	–	–	–	3.73	TC	[550]

92. Uranium U[400]

Surface	Beam	Ion	P_r (Torr)	T (K)	ϕ^+ (eV)	ϕ^e (eV)	Meth.	Refs.
bcc (γ, $T > 1050$ K)								
U(100)	–	–	–	–	–	3.49	TC	[321]
U(100)	–	–	–	–	–	3.60	TC	[2180]
U(100)	–	–	–	–	–	3.82	TC	[2180]
U(110)	–	–	–	–	–	4.07	TC	[321]
U(111)	–	–	–	–	–	3.33	TC	[321]
U(112)	–	–	–	–	–	3.72	TC	[321]
Rhombic (α, $T < 940$ K for bulk)								
U	–	–	–	–	–	2.94	TC	[1744]
U (foil)	–	–	<5×10^{-11}	~300	–	3.080 ± 0.005	CPD	[2933]
U/W	U	–	<8×10^{-12}	~300	–	3.181 ± 0.013	CPD	[1161]
U/W	U	–	<5×10^{-11}	~300	–	3.19 ± 0.01	CPD	[13,349,2939]
U/W	U	–	<5×10^{-11}	~300	–	3.203 ± 0.013	CPD	[2933]
U (foil)	–	–	≤10^{-10}	~300–938	–	3.47 ± 0.01	PE	[1884]
U	–	–	4×10^{-10}	~300	–	3.5	PE	[3124]
U	–	–	5×10^{-9}	~300	–	3.5 ± 0.03	FE	[3110]
U	–	–	4×10^{-10}	~300	–	3.5 ± 0.1	PE	[3132]
U/W	U	–	<2×10^{-10}	295	–	3.56 ± 0.05	FE	[1657]
U/W(116)	U	–	<1×10^{-10}	295	–	3.57 ± 0.03	FE	[1664]
U/W(113)	U	–	<1×10^{-10}	295	–	3.60 ± 0.03	FE	[1664]
U/W	U	–	<2×10^{-10}	295	–	3.60 ± 0.03	FE	[1654,1655,1657]
U/Ni	U	–	?	~300	–	3.63	PE	[2922]
U/W	U	–	<2×10^{-10}	~300–940	–	3.63 ± 0.01	CPD	[1476,1484,2103]
U/W(111)	U	–	<1×10^{-10}	295	–	3.64 ± 0.03	FE	[1664]
U/W	U	–	<2×10^{-10}	295–900	–	3.65 ± 0.01	PE	[2467]
U/W(113)[408]	U	–	<5×10^{-10}	~300	–	3.66 ± 0.03	PE	[2471]
U/W(113)[408]	U	–	<5×10^{-10}	~300	–	3.67 ± 0.03	CPD	[2471]
U/W	–	–	–	–	–	3.68	TC	[2478]
U/W(112)	U	–	<1×10^{-10}	295	–	3.70 ± 0.03	FE	[1664]
U/W(100)[408]	U	–	<5×10^{-10}	~300	–	3.73 ± 0.02	CPD	[2471]
U/W(100)[408]	U	–	<5×10^{-10}	~300	–	3.73 ± 0.02	PE	[2471]
U/W(113)[408]	U	–	<5×10^{-10}	~300	–	3.73 ± 0.04	CPD	[2471]
U/W(100)[408]	U	–	<5×10^{-10}	~300	–	3.78 ± 0.03	CPD	[2471]
U/W(100)	U	–	?	~300	–	3.80 ± 0.03	CPD	[3076]
U/W(100)	U	–	<1×10^{-10}	295	–	3.88 ± 0.03	FE	[1664]
U/W(110)	U	–	?	~300	–	3.90 ± 0.03	CPD	[3076]
U/W(110)[408]	U	–	<5×10^{-10}	~300	–	3.90 ± 0.03	CPD	[2471]
U/W(110)[408]	U	–	<5×10^{-10}	~300	–	3.90 ± 0.03	PE	[2471]
U	–	–	–	–	–	3.97	TC	[550]
U/W(110)[408]	U	–	<5×10^{-10}	~300	–	4.00 ± 0.04	CPD	[2471]
U/W(110)	U	–	<1×10^{-10}	295	–	4.04 ± 0.03	FE	[1664]
U	–	–	?	~300	–	4.32 ± 0.05	CPD	[2297]
Recommended	–	–	–	–	–	**3.64 ± 0.04**	–	–

Table 1 (*continued*)

Surface	Beam	Ion	P_r (Torr)	T (K)	ϕ^+ (eV)	ϕ^e (eV)	Meth.	Refs.
Tetragonal (β, $T \simeq$ 940–1050 K for bulk)								
U/W	U	–	$<2 \times 10^{-10}$	1040	–	3.05 ± 0.03	FE	[1657]
U/W(111)	U	–	$<1 \times 10^{-10}$	950	–	3.36 ± 0.03	FE	[1664]
U(foil)	–	–	$\leq 10^{-10}$	940–1040	–	3.52 ± 0.01	PE	[1884]
U/W	U	–	$<1 \times 10^{-10}$	~1000	–	3.53 ± 0.03	FE	[1654,1655,1657]
U/W	U	–	$<2 \times 10^{-10}$	950–1050	–	3.58 ± 0.01	CPD	[1484]
U/W	U	–	$<2 \times 10^{-10}$	940–1030	–	3.59 ± 0.01	PE	[2467]
U/W(100)	U	–	$<1 \times 10^{-10}$	950	–	3.61 ± 0.03	FE	[1664]
U/W(112)	U	–	$<1 \times 10^{-10}$	960	–	3.64 ± 0.03	FE	[1664]
U/W(110)	U	–	$<1 \times 10^{-10}$	950	–	3.99 ± 0.03	FE	[1664]
Recommended	–	–	–	–	–	**3.58 ± 0.04**	–	–
bcc (γ, $T >$ 1050 K for bulk)								
U/W	U	–	?	?	–	2.84	TE	[1750]
U/W[384]	U	–	$<6 \times 10^{-10}$	1250–1400	–	3.0	TE	[232]
U/W[386]	U	–	$<2 \times 10^{-10}$	~1000–1300	–	3.14 ± 0.02	TE	[1484]
U/W[385]	U	–	$\sim 10^{-10}$	1250	–	3.2*	TE	[2098]
U(wire)[388]	–	–	$\sim 10^{-8}$	~950–1300	–	3.27 ± 0.05	TE	[2085,3961]
U[174,387]	–	–	–	0^E	–	3.28	TC	[1747]
U/W(112)	U	–	$<1 \times 10^{-10}$	1120	–	3.29 ± 0.03	FE	[1664]
U/W(111)	U	–	$<1 \times 10^{-10}$	1120	–	3.31 ± 0.03	FE	[1664]
U/W[386]	–	–	–	1400	–	3.36 ± 0.04	TC	[1484]
U/W[384]	–	–	–	1400	–	3.38	TC	[1484]
U(foil)	–	–	$\leq 10^{-10}$	1040–1060	–	3.39 ± 0.01	PE	[1884]
U/W	U	–	$<2 \times 10^{-10}$	~1200–1400	–	3.4 ± 0.2	FE	[1657]
U[387]	–	–	–	1100	–	3.42*	TC	[1747]
U/W[386]	U	–	$<2 \times 10^{-10}$	~1000–1400	–	3.42 ± 0.04	TE	[1484]
U/W	U	–	$<1 \times 10^{-10}$	1200	–	3.43 ± 0.03	FE	[1654]
U/W(116)	U	–	$<1 \times 10^{-10}$	1120	–	3.43 ± 0.03	FE	[1664]
U/W[386]	–	–	–	1400	–	3.44 ± 0.03	TC	[Here]
U/W[388]	–	–	–	–	–	3.45	TC	[2467]
U/W	U	–	$<2 \times 10^{-10}$	1060–1200	–	3.45 ± 0.01	PE	[2467]
U/W[386]	–	–	–	1400	–	3.45 ± 0.1	TC	[1484]
U/W[386]	U	–	$\leq 10^{-5}$ (H$_2$)	~1000–1400	–	3.46 ± 0.02	TE	[1484]
U/W[384]	U	–	$<5 \times 10^{-10}$	~1250–1400	–	3.47 ± 0.03	TE	[232,2930]
U/W[384]	–	–	–	1400	–	3.48 ± 0.03	TC	[1484]
U/W[385]	–	–	–	1250	–	3.5*	TC	[Here]
U/W	U	–	$<2 \times 10^{-10}$	~1050–1500	–	3.53 ± 0.01	CPD	[1484]
U/Mo	U	–	5×10^{-11}	1275	–	3.53 ± 0.01	TE	[2644]
U/W(113)	U	–	$<1 \times 10^{-10}$	1120	–	3.53 ± 0.03	FE	[1664]
U/Mo	U	–	5×10^{-11}	~1100–1300	–	3.54	TE	[2644]
U(wire)[388]	–	–	–	–	–	3.56 ± 0.05	TC	[2467]
U/W(100)	U	–	$<1 \times 10^{-10}$	1120	–	3.82 ± 0.03	FE	[1664]
U/W(110)	U	–	$<1 \times 10^{-10}$	1120	–	4.00 ± 0.03	FE	[1664]
U(wire)	F$_2$	UF$_6^-$	5×10^{-5}(F$_2$)	1140–1290	4.20 ± 0.14^N	–	NSI	[2630]
Recommended	–	–	–	–	–	**3.42 ± 0.05**	–	–

93. Neptunium Np

Np(111)	–	–	–	–	–	4.00	TC	[2410]
Np	–	–	–	–	–	2.8	TC	[1955]
Np	–	–	–	–	–	3.90	TC	[550]

94. Plutonium Pu

Monoclinic (α, $T <$ 398 K)								
Pu(020)	–	–	–	–	–	3.51	TC	[1448]
Pu(020)	–	–	–	–	–	3.62	TC	[1448]
fcc (δ, $T =$ 593–736 K)								
Pu(100)	–	–	–	–	–	2.97 ± 0.05	TC	[3488]
Pu(100)	–	–	–	–	–	3.01 ± 0.06j	TC	[3488]
Pu(100)	–	–	–	–	–	3.05 ± 0.03	TC	[3488]
Pu(100)	–	–	–	–	–	3.11	TC	[2069]
Pu(100)	–	–	–	–	–	3.14 ± 0.01	TC	[2549]
Pu(100)	–	–	–	–	–	3.43 ± 0.06	TC	[3488]
Pu(100)	–	–	–	–	–	3.44 ± 0.06	TC	[3488]

Table 1 (*continued*)

Surface	Beam	Ion	P_r (Torr)	T (K)	ϕ^+ (eV)	ϕ^e (eV)	Meth.	Refs.
Pu(100)	–	–	–	–	–	3.5	TC	[2172]
Pu(100)	–	–	–	–	–	3.68	TC	[2172]
Pu(100)	–	–	–	–	–	3.7	TC	[1870]
Recommended	–	–	–	–	–	**3.3 ± 0.2**	–	–
Pu(110)	–	–	–	–	–	2.99	TC	[2069]
Pu(111)	–	–	–	–	–	2.85 ± 0.20	TC	[3012,3013]
Pu(111)	–	–	–	–	–	3.260	TC	[1446–1448]
Pu(111)	–	–	–	–	–	3.32	TC	[1447]
Pu(111)	–	–	–	–	–	3.41	TC	[2069,2070]
Pu(111)	–	–	–	–	–	3.488	TC	[1446]
Pu(111)	–	–	–	–	–	3.49	TC	[1448]
Pu(111)	–	–	–	–	–	3.98	TC	[2410]
Pu(111)	–	–	–	–	–	4.14	TC	[2172]
Pu(111)	–	–	–	–	–	4.3	TC	[2165]
Pu(111)	–	–	–	–	–	8.4	TC	[2165]
Recommended	–	–	–	–	–	**3.8 ± 0.3**	–	–
Monoclinic (α, $T < 398$ K for bulk)								
Pu	–	–	–	–	–	3.3	TC	[1955]
fcc (δ, $T = 593$–736 K for bulk)								
Pu	–	–	–	–	–	3.1–3.3	TC	[1833,1841]
Pu	–	–	–	–	–	3.72	TC	[550]
Pu	–	–	–	–	–	3.89	TC	[550]

95. Americium Am

Surface	Beam	Ion	P_r (Torr)	T (K)	ϕ^+ (eV)	ϕ^e (eV)	Meth.	Refs.
dhcp (α, $T < ?$ K)								
Am(0001)	–	–	–	–	–	2.90	TC	[2075]
Am(0001)	–	–	–	–	–	4.35	TC	[321]
Am(1010)	–	–	–	–	–	4.21	TC	[321]
Am(1124)	–	–	–	–	–	3.70	TC	[321]
fcc (β, $T = ?$–$?$ K)								
Am(100)	–	–	–	–	–	2.93	TC	[2071,2076]
Am(110)	–	–	–	–	–	2.86	TC	[2071,2076]
Am(111)	–	–	–	–	–	3.06	TC	[2071,2076]
hcp (α, $T < ?$ K for bulk)								
Am	–	–	–	–	–	3.3	TC	[1955]
Am	–	–	–	–	–	3.33	TC	[550]
Am	–	–	–	–	–	3.7	TC	[550]

96. Curium Cm

Surface	Beam	Ion	P_r (Torr)	T (K)	ϕ^+ (eV)	ϕ^e (eV)	Meth.	Refs.
hcp								
Cm	–	–	–	–	–	3.3	TC	[1955]
Cm	–	–	–	–	–	3.32	TC	[550]
Cm	–	–	–	–	–	3.9	TC	[550]

97. Berkelium Bk

Surface	Beam	Ion	P_r (Torr)	T (K)	ϕ^+ (eV)	ϕ^e (eV)	Meth.	Refs.
hcp								
Bk	–	–	–	–	–	3.3	TC	[1955]
Bk	–	–	–	–	–	3.37	TC	[550]
Bk	–	–	–	–	–	3.8	TC	[550]

98. Californium Cf

Surface	Beam	Ion	P_r (Torr)	T (K)	ϕ^+ (eV)	ϕ^e (eV)	Meth.	Refs.
hcp								
Cf	–	–	–	–	–	3.3	TC	[1955]
Cf	–	–	–	–	–	3.38	TC	[550]
Cf	–	–	–	–	–	4.0	TC	[550]

Table 1 (*continued*)

Surface	Beam	Ion	P_r (Torr)	T (K)	ϕ^+ (eV)	ϕ^e (eV)	Meth.	Refs.
				99. Einsteinium Es				
fcc								
Es	–	–	–	–	–	2.88	TC	[550]
Es	–	–	–	–	–	3.3	TC	[550]

[1] The Li films at 3–5 or 4–6 monolayers on W(110) and Mo(110) are suggested to have the (110) bcc orientation at 300 K, in contrast to the (0001) rhombohedral one at 77 K [3361].

[2] The value of 2.32 ± 003 eV for Li/glass [349] is based on the correction [349] of 2.49 ± 0.02 eV [1374] by taking $\phi^e = 2.35 \pm 0.03$ eV [349] instead of 2.52 eV [1374] as the reference work function of Ba.

[3] For further information about the theoretical calculation [475] and comparison between the calculated values [475] and the recommended ones for Li, Na, Mg, Al, K, Zn, Rb, Cs and Pb in Table 2 [Here], see Section 6.

[4] The Be-films on mica ($\phi^e = 4.98$ eV) [2009] and on glass (5.08 eV) [1782] presumably consist, to a considerable extent, of the (0001) surface [2025], which is generally expected to have 5.27 ± 011 eV (see Table 2).

[5] The values of $\phi^e = 2.9$ and 3.6 eV for C(100)^B correspond to the diamond cone-height to -radius ratios of $\beta = h/r = 700$ and 1000, respectively [2751].

[6] The work function of C(100)^B [1830] changes from 5.3 to 5.7 eV as the boron content increases from 10^{16} to 10^{20} atoms/cm^3.

[7] As the mean grain size (S_d) of diamond prepared by electrophoresis onto a Mo-sheet [544,4059] increases from 0.32 to 3.9 and to 108.0 μm, the surface area (A_d) of the (111) plane on the film increases from 76 to 92 and to 99%, thereby changing in ϕ^e from 5.1 to 3.2 and to 4.8 eV, respectively, determined by PE [544,4059]. Similarly, other films with (S_d, A_d) = (0.25, ~76), (3, ~88) and (6, ~96) on another Mo-sheet are found to have $\phi^e = 3.8$, 3.3 and 3.2 eV, respectively, done by PE [1205].

[8] By the same way as above (Footnote 7), the diamond films on Mo-tips [1205] having (S_d μm, A_d%) = (0.25, 76), (3, ~88) and (6, ~96) are observed to have $\phi^e = 3.8$, 3.5 and 3.4 eV, respectively, determined by FE [1205]. The first value of 3.8 eV on the tip is equal to that for the film of (0.25, ~76) on a Mo-sheet [1205] (see Footnote 7).

[9] For both systems of C/Si and C/Mo prepared by dielectrophoresis [3568], ϕ^e is found to have 3.7 and 7.1 eV for thin and thick diamond films, respectively.

[10] This diamond-like-carbon having 4.1 eV [2230] is formed on a tungsten tip by electro-deposition in methanol. For further information, see Ref. [3938].

[11] This is the mean value calculated for C(0001), whose ϕ^e ranges from 4.44 to 5.23 eV depending complicatedly upon the slab thickness of 1–14 [1174].

[12] The value of 3.93 eV for a freshly prepared monocrystalline graphite decreases to 3.25 eV after exposing to air [2581].

[13] The specimens of C(HOPG) cleaved in air and vacuum [3215] have different values of $\phi^e = 4.7$ and 5.0 eV, respectively.

[14] The sample of C/Si having $\phi^e = 4.2$ or 4.3 eV [1611] is used as received from other workers, but ϕ^e is decreased from 4.2 to 4.0 eV by annealing in vacuum at ~770 K [1611].

[15] By incidence of C_6H_6 upon a heated Re foil, graphitic layers ($\phi^e = 4.4 \pm 0.3$ eV) are formed at $T < 1900$ K, above which carbidic ones (5.25 eV) are done [407,408].

[16] The surface of C/Pt–W(8%) ($\phi^+ = 4.42$ eV) at 1290 K has the ionization efficiency (β^+) of 50% for the incident K atoms, but only $\beta^+ = 1$% for KI molecules [1299], thereby suggesting that the degree of dissociation (γ) of KI is greatly decreased on the graphitic carbon surfaces, in contrast to carbidic or carbon-free metal surfaces (see Section 4.2.4 [1351]).

[17] The surface of C/Mo [791] having $\phi^e = 4.71$ or 4.73 eV is due to carbon contamination, and its ϕ^e is reduced to 4.28 or 4.33 corresponding to an essentially clean Mo surface after it is heated in O_2 [791].

[18] The surface consisting of carbon layers sputtered onto an Al–Mg alloy disk [2743] changes in ϕ^e from 4.79 eV (unlubricated) to 5.32 eV (lubricated) as proceeding to saturation.

[19] The values of 4.81 and 5.23 eV are calculated for mono- and dilayers of graphite, respectively [296].

[20] The values of 5.8 and 5.85 eV for graphite are estimated from Fig. 2 [1735] by other workers [291,3223].

[21] The value of 4.73 eV corresponding to graphene [767] is determined from the linear relationship between the work function of semiconducting single-walled carbon nanotubes and their inverse diameter ($1/d$) after extrapolation of $d \to \infty$, whilst 4.84 eV [767] is done similarly from metallic tubes.

[22] On the basis of the calculated data on $\phi^e = 4.85$ and 5.54 eV for Ag(111) and Au(111) [233], the systems of C_{60}-monolayer adsorbed on Ag(111) and Au(111) are determined, respectively, to have 4.96 and 4.94 eV evaluated from the work function changes ($\Delta\phi_\mu = +0.11$ and -0.60 eV) calculated from the changes in the surface dipole moment ($\Delta\mu = +0.24$ and -1.37 debye) induced by adsorption of C_{60} [233]. Direct calculation made for the respective systems yields $\phi^e = 4.99$ and 4.96 eV [233]. The four values agree excellently with each other irrespective of the differences in both calculation method and substrate species, and also do well with 4.87 ± 0.06 eV recommended for C_{60} in Table 2 [Here]. In addition by taking $\Delta\phi_\mu = -0.09$ eV due to $\Delta\mu = -0.21$ debye [233] and $\phi^e = 4.94$ eV determined for Cu(111) [316], C_{60}/Cu(111) is calculated to have $\phi^e = 4.85$ eV, which agrees exactly with 4.86 determined by PE [316].

[23] The monolayer of C_{60} on Ru(111) is stable ($\phi^e = 5.05$ eV) until ~750 K, above which C_{60} is decomposed to graphitic carbon remaining on Rh(111) at ~1000–1300 K [1007].

[24] By doping N and B (1–2% in concentration), the pristine tube is calculated to change in ϕ^e from ~4.5 to ~3.9 and ~5.2 eV, respectively, each value of which fluctuates dependently upon the tube diameter (~0.5–1 nm), in a narrow range of about ±0.1 eV [1168].

[25] The value of $\phi^e_{PE} = 4.62 \pm 0.06$ eV determined for the single-walled cnt/Si(111) system by PE is smaller than $\phi^e_{CPD} = 4.97 \pm 0.07$ and 4.86 ± 0.10 eV done by CPD-measurements before and after the PE-measurement, respectively [3246]. The same tendency that ϕ^e_{PE} is always smaller than ϕ^e_{CPD} even after PE-measurement is found also for several metal/cnt/Si(111) systems having Pd, Ag, Pt and Au [3246]. Typically for Pt/sw-cnt/Si(111), the successive measurements by CPD, PE and CPD yield $\phi^e_{CPD} = 5.46$ eV, $\phi^e_{PE} = 5.12$ eV and $\phi^e_{CPD} = 5.39$ eV, showing that ϕ^e_{CPD} decreases after PE-measurement and also ϕ^e_{PE} is smaller than both of ϕ^e_{CPD}. For further information, see Section 2.8.2.

[26] For the system of cnt/Si(111) treated with HNO_3 acid, ϕ^e_{CPD} by CPD-measurement is decreased from 5.01 to 4.94 eV by exposure of UV during PE-measurement [3246], quite similarly to the normal system free from the acid treatment (see Footnote 25 just above).

[27] The open-ended tubes at mouth before and after relaxation are calculated to have slightly different values of 4.86 and 4.95 eV, respectively, whilst those at the first neighbor to the mouth are done similarly to have different ones (5.25 and 5.20 eV) according to the relaxation [3570].

[28] The value of 5.08 eV calculated for a perfect tip of chirality (5, 5) is considered [3570] to be close to experimental data of ~5 eV [291,1171]. About the structure and property of single-walled carbon nanotubes with several types of chirality, see excellent review papers [3969,4030].

[29]The polycrystalline diamond films prepared by chemical vapor deposition onto p-type Si(100) are decreased in ϕ^e from 5.6 to 5.2 eV by arc discharge activation [698].

[30]Oxygen contamination of C(pentagon)/Ta decreases ϕ^e from ~4.8 to 4.2–4.3 eV [3942].

[31]The vertically aligned type of C/Si having $\phi^e = 4.4$ eV is smaller by 0.2 eV compared with the random one [3223].

[32]The conductive (metallic) and semiconductive types of multi-walled carbon nanotube are found to have $\phi^e = 4.7$ and 5.6 eV, respectively, depending upon their helical angles [545].

[33]The values of 5.7 and 5.75 eV for the random multi-walled carbon nanotubes are estimated from the spectral data [1735] by other workers [291,3223], together with such a comment that both values seem too large.

[34]Individual tubes are stacked onto a W-tip by the van der Waals-forces alone or by a conductive carbon glue, and they are heated in vacuum at ~1000 K for 30 s to remove contaminants [1170].

[35]The clean Na(110) layers [1417] are prepared on the clean Ni(100) surface ($\phi^e = 5.20 \pm 0.11$ eV, essentially equal to 5.19 ± 0.05 eV in Table 2) at 173 K and ~10^{-11} Torr, and the layers (2.90 eV) are checked to have the bcc structure exposing the (110) surface parallel to the Ni(100) surface. For further information, see Refs. [3944,3945].

[36]Work function measurements of the Na/Mo systems prepared at either 293 K or 80 K (preannealing at 293 K) by both Fowler and photoemission threshold methods yield nearly the same result of either 2.36 ± 0.02 or 2.45 ± 0.04 eV [3336].

[37]Similarly to the above cases (Footnote 36), the values of ϕ^e at 80 K (no annealing) are virtually the same (2.45 ± 0.05 eV and 2.40 ± 0.03 eV) between the two methods of Fowler and threshold, respectively [3336].

[38]Work function is determined from AI (autoionization) electron spectra observed by 700 eV–Ne^+ impact of both a clean reference surface of Al (ϕ^e taken as 4.26 eV) and a sample surface of Na/Cr, which show the peak positions of Ne-II at the kinetic energies of 23.55 and 22.08 eV, respectively (see Fig. 1 and Table 1 [1103]). Consequently, we have $\phi^e = 4.26 - (23.55 - 22.08) = 2.79$ eV for Na [1103,4027]. The reference value for Al is the same with ours (4.26 ± 0.03 eV), but the value for Na itself is slightly larger than ours (2.54 ± 0.03 eV) (see Table 2 herein). Similarly to another case [3789], $\phi^e = 2.80$ and 3.80 eV are estimable for Na and Mg, respectively, when 4.25 eV [3789] is taken for Al, while 2.70 eV for Na is so by taking 3.70 eV [3789] for Mg. Additionally, 1 keV–Ne^+ is impinged on Cs/Pt and Na/Cs/Pt systems [3496], thereby determining $\phi^e = 2.1$ and 2.62 eV for Cs and Na, respectively [3496].

[39]By taking $\phi^e = 5.2$, 4.6 and 4.4 eV for the substrates of W(110), W(112) and W(111), respectively, Li is estimated to be 2.75 eV by FE [1974], which may be improved to be 2.87, 2.93 and 2.80 eV if we take 5.32, 4.78 and 4.45 eV recommended for the respective substrates in Table 2. All of the latter values become closer to our most probable value of 2.90 ± 0.03 eV for Li (Table 2). Later by the same group of workers, Li/W(112) is found to have 2.88 or 2.93 eV by CPD [380].

[40]By extension of n→∞ (cluster → bulk) for closed-shell Na clusters (n = 2–137), ϕ^e is experimentally determined to be 2.68 eV from a plot of $n^{-1/3}$ vs. the ionization energy of each cluster, whilst $\phi^e = 2.56$ eV is theoretically evaluated from the classical law [2171] (see Section 11.3).

[41]Bulk sodium work function is determined to be 2.75 eV [2860] by such a graphic method that a plot of $1/r$ (inverse cluster radius) vs. $\phi_c - W_{im}$ (difference between cluster's work function and image force equal to $3e^2/8r$) is extrapolated as $r \to \infty$, where ϕ_c is taken from the experimental data on ionization potential [2383].

[42]Analysis of the photo-ionization yield observed for fine particles (3–5 nm radius, 2×10^3–3×10^4 atoms) of Li, Na and K reveals that the ionization threshold energies for Fowler plots (2.93, 2.75 and 2.28 eV, respectively) [3482] are substantially equal or close to our respective values of $\phi^e = 2.90$, 2.54 and 2.30 eV (Table 2).

[43]The value of 2.8 eV calculated for the Na/Al(111) system at one monolayer is near to 2.9 eV done for Na(100) by five-layer slab model following the same calculational scheme [2222].

[44]Sodium clusters having the atom number (n) up to 22 000 are employed to determine the bulk work function of Na (2.81 eV) by extrapolation of n→∞ (cluster → bulk) in a plot of $n^{-1/3}$ vs. the ionization energy of each cluster [2053].

[45]The sample cut from a pure Mg boule and mechanically polished is cleaned in vacuum by sputtering with 1 keV–Ne^+ and then annealed to 500 K for 10 min, thereby yielding 3.65 eV for Mg(0001) [3174].

[46]The work function of Mg(0001) free-standing thin films with the thickness of up to 30 ML is calculated by first-principles, thus yielding 3.75 ± 0.05* eV for relaxed atomic geometry at 10–30 ML [2552].

[47]Each surface system consists of such a sandwich structure as sample metal/barium stearate-Al_2O_3/Al/glass, where the metal is Mg, Cr, Mn, Zn, Cd, Sn, Te, Pb or Bi [2028]. Both preparation and properties of the systems are summarized in Ref. [3948].

[48]Each work function for an M/oxide/Si(100) system (M = Mg, Al, Ni or Au) is evaluated by other workers [3519] using the data on conduction band barrier height at metal–dielectric interface [1442].

[49]The work function (3.78 eV) for the Mg/glass system [1368] is corrected to be 3.61 eV by other workers [13,349] taking the reference (ϕ^e for Ba) as 2.35 ± 0.03 eV instead of 2.52 eV.

[50]A mirror-like surface of Mg/glass ($\phi^e = 3.65$ eV) [1368] is smaller in ϕ^e by 0.13 eV than a macrocrystalline (matte) one (3.78 eV) [1368].

[51]The sample systems of Mg, Al, Fe and Au layers on quartz prepared in a poor vacuum (~10^{-5} Torr) are as thick as ~100–110, ~80–100, ~40–50 and ~30–40 nm, respectively [1973]. The work function determined for Al (3.47 eV, lower than the generally accepted value of ~4.3 eV, for example, seems unlikely to correspond to its clean surface. Such a low value is probably due to the adsorption of water vapor [725]. For further information about the adsorption, see Footnote 59.

[52]The system of Al(100)/Ge(100) is theoretically constructed by a lattice-matched interface model using an ideal Ge(100) substrate and a 45°-rotated Al(100) film, thus resulting in $\phi^e = 3.94$ eV [3949].

[53]Each monocrystalline surface is prepared by deposition of Al-vapor on each monocrystalline bulk substrate of aluminium at ~300 K and annealed often at 473–573 K during the course of the deposition [612]. A linear relationship is found between surface atom density (D_s) and work function (ϕ^e) among Al(111), Al(100) and Al(110), as illustrated in Fig. 4 [612]. The values of both D_s and ϕ^e for the surfaces [612] are listed in Table 8 [Here]. By intermittent repetition of Ar^+-impact and annealing (473–573 K), ϕ^e of Al(110) is decreased from 4.26 to 4.06 ± 0.03 eV [612].

[54]The work function of Al(111) ought to lie in 3.83–4.59 eV [1101], whose middle value may be calculated to be 4.21 eV, virtually equal to the most provable value of 4.24 ± 0.04 eV estimated in the present article and also to other recommended ones (4.24–4.28 eV) listed in Table 2.

[55]By annealing at 623 K for 1 h, the Al-layer (0.15 nm thick) prepared on quartz at ~300 K is decreased in ϕ^e from 4.31 to 4.29 eV as the degree (δ_m) of monocrystallization forming the (111) face is increased from 57 to 88% [3313].

[56]Deposition of Al-vapor up to 4 monolayers on an Ag(111) surface at 150 or 300 K causes a work function decrease by up to 0.38 eV [2888], which accords with the work function difference (0.40 ± 0.07 eV) between the most provable values of 4.64 ± 0.06 eV for Ag(111) and 4.24 ± 0.04 eV for Al(111), as shown in Table 2 [Here]. This accordance may give an additional evidence to support the conclusion [2888] that the Al-layers have the same orientation as the Ag(111) substrate.

[57]By consideration of the work function decrease by 1.17 eV after Al-deposition of 5 monolayers on Ru(0001) [301] and also by employment of the work function values for Ru(0001) as 5.35 ± 0.06 eV [Here], 5.42 eV [2652] and 5.58 eV [3160], we find those values for Al(111)/Ru(0001) [301] to be 4.18 ± 0.06, 4.25 and 4.41 eV, respectively, the middle (or average = 4.28 ± 0.10 eV) of which is nearest to the most probable value of 4.24 ± 0.04 eV for Al(111) in Table 2 [Here].

[58]Both experiment and theory indicate that Al-plates are decreased in ϕ^e from 4.3 to ~4.1 eV by deformation due to tension or compression [2550]. Similarly, a decrease (from 4.99 to ~4.7 eV) is observed also for Cu-ones [2550].

[59]Fresh Al-film ($\phi^e = 4.17 \pm 0.07$ eV) and oxygen pre-exposed one (4.08 ± 0.05 eV) on glass are reduced by up to ~1 eV by admission of water vapor from ~10^{-7} to 10^{-4} Torr min [2100] (see also Footnote 51).

[60]The ionization potential (IP) measurement of clusters (Al_{2000} and Al_{32000} at different charge states, $Z = -1$ up to +5) makes it possible to determine the bulk work function ($\phi^e(\infty)$) from Eq. (20). The value of 4.28 ± 0.03 eV thus determined [2199] is essentially the same with ours (4.26 ± 0.03 eV) recommended for polycrystalline Al in Table 2 [Here] (see Section 11.3).

[61]The Al-surface (~300–600 K) is scratched by irradiation with an increased light power, thereby decreasing in ϕ^e from 4.90 to 4.75 eV [1222].

[62]The work function of 4.41 eV for Si(100) at 300 K is evaluated from $\phi^e(T) = 4.30 + 3.75 \times 10^{-4}\ T$ found at ~1300–1650 K [1225].

[63]A free energy model is employed to derive the work function (ϕ^+) effective for positive ion emission from alkali (Li, Na or K) or Tl atom incident upon Si(100)^n and Si(111)^n, thereby yielding nearly the same values (averages derived from free energies) of $\phi^+ = 4.80 \pm 0.05$ eV for Si(100)^n and 4.82 ± 0.05 eV for Si(111)^n, irrespective of the difference in four incident atom species [74]. On the other hand, the value of $\phi^+ \approx 4.8$ eV for Si(100)^n and Si(111)^n are different from $\phi^e \approx 4.5$ eV for the two monocrystalline surfaces [74], affording $\Delta\phi^* \equiv \phi^+ - \phi^e \simeq 0.3$ eV $\neq 0$. The authors [74] suggest that the discrepancy ($\Delta\phi^* \neq 0$) would be accounted by partial covering with graphitic carbon or SiC having lower work function (4.4–4.6 eV).

[64]Similarly as above in Footnote 63, another enthalpy model is adopted to determine ϕ^+ by PSI of four different samples on Si(100)^n and Si(111)^n, yielding the averages of $\phi^+ = 4.67 \pm 0.08$ and 4.77 ± 0.05 eV for Si(100)^n and Si(111)^n, respectively [74]. Each of the values is nearly equal to that determined by the free energy model (see Footnote 63).

[65]On the basis of $\phi^e = 4.30 + 5.6 \times 10^{-4}\ T$ [2097], each ϕ^e of both Si(100) and Si(110) is evaluated to be 4.47, 4.86 or 5.14 eV for 300, 1000 or 1500 K. The theoretical value of the temperature coefficient (5.6×10^{-4} eV/K) [2097] is close to the experimental one (3.75×10^{-4} eV/K) determined for the both surfaces by another worker [1225].

[66]The value of ϕ^e for Si(111)^p by TE is determined to be 4.84 ± 0.14 or 4.86 ± 0.10 eV at ~1500 K by electron retarding method [73]. Each value is in excellent agreement with $\phi^+ = 4.85 \pm 0.08$ and 4.88 ± 0.10 eV by PSI of Cs incident upon the same Si(111)^p specimen at ~1100–1600 K [73] and, hence, $\Delta\phi^* \equiv \phi^+ - \phi^e$ is essentially zero, quite similarly as found generally for monocrystalline metals (see Table 5). On the contrary, ϕ^e of the same specimen is found to be as small as 4.07 ± 0.05 eV from Richardson plots at virtually the same temperature range (~1300–1600 K) as above [73], where the apparent Richardson constant is very small ($A_r = 0.2$–0.4 A/cm² K²) [73]. Quite similarly, $\phi^e = 4.05 \pm 0.04$ eV and $A_r \approx 0.2$–2 A/cm² K² for another Si(111)^p specimen are determined by another group of workers [635]. The above results suggest that the internal reflection coefficient (r^e) of electron is very large, as may be understandable from the inequality of $A_r \equiv A_R(1 - r^e) < A_R = 120$ A/cm²/K² [2]. Therefore, it may be concluded for silicon surfaces that the true value of the thermionic contrast ($\Delta\phi^*$) can hardly be obtainable by direct comparison between ϕ^+ (by PSI) and ϕ^e (by TE using Richardson plots) without correcting ϕ^e by a suitable method. It should be noted that $\phi^e = 4.07$ eV [73] may be corrected to be 4.83 ± 0.04 eV by substitution of $A_r = 0.3 \pm 0.1$ A/cm² K² into Eq. (8) (see Section 2.8.6), and hence that $\Delta\phi^* = 4.85 - 4.83 \approx 0$ eV instead of $4.85 - 4.07 \approx 0.8$ eV. In the same way, $\phi^e = 4.04 \pm 0.05$ eV for Si(111)^n [72] is corrected to be 4.80 ± 0.04 eV, which yields $\Delta\phi^* = 0.06 \pm 0.08$ eV, 0.07 ± 0.05 eV and 0.10 ± 0.11 eV since $\phi^+ = 4.86 \pm 0.07$, 4.87 ± 0.03 and 4.90 ± 0.10 eV by PSI of Li, Na and In, respectively [72]. See the data with the superscript of d in Table 4.

[67]The samples of Si(111)^n and Si(111)^p are found to have the same value of 5.05 eV at ~300 K, but to show a large difference of either 4.65 and 5.56 eV or 4.5 and 5.4 eV at 60 K for n- and p-types, respectively [2660,2893].

[68]The sample of Si(111)^n freshly cleaved at ~300 K has the 2×1 super structure with $\phi^e = 4.83$ eV, stable for a few hours at $P_r < 3 \times 10^{-11}$ Torr. But, it is changed to 4.56 and 4.74 eV by annealing at 550 and 800 K according to changes to the 1×1 and 7×7 structures, respectively [1228].

[69]The surfaces of Si(111)^p heated to 1000 K after cleaving and done so after sputtering are little different in ϕ^e between the two [118].

[70]The Richardson constants (A_R) determined for Si(110)^n having $\phi^e = 3.76$ and 4.14 eV are 0.1 ± 0.03 and 3 ± 0.1 A/cm² K² at 1250–1400 and 1400–1625 K, respectively, while those for Si(110)^p having 3.17 and 4.12 eV are 0.03 ± 0.01 and 1 ± 0.3 A/cm² K² in the above respective temperature ranges [1500]. Regarding both n- and p-types of Si(112) and Si(541), nearly the same values are found to range from 0.04 ± 0.01 to 2 ± 0.8 A/cm² K² [1500], all of which are very small similarly as in the cases [73,635] mentioned in Footnote 66. For further information, see Section 2.8.6.

[71]The nanowires of Si (20 nm in diameter) and Ge (17 nm) are found to have $\phi^e = 4.13$ and 4.43 eV, respectively [2200], which are smaller than the respective values of 4.65 ± 0.09 and 4.76 ± 0.06 eV (see Table 2) recommended for much larger sizes of usual specimens.

[72]The work function of the Si/Ba/W(110) system changes from 4.2 to 4.6 eV depending upon the Ba-thickness of ~(1–9) × 10^{14} atoms/cm² [2013]. The upper value (4.6 eV) is close to our recommended one (4.65 ± 0.09 eV) as shown in Table 2.

[73]The surface of Si/Si(111) consists of vapor-quenched amorphous silicon films [2822].

[74]As the Si-coverage increases from 0 to 1 monolayer on W, the work function calculated theoretically for the Si/W system changes from about 4.5 to 4.7 eV [913], the latter of which is in good agreement with the experimental value of 4.72 ± 0.02 eV [1231].

[75]The coverage of Si on Co/CoSi$_2$(111) is 3 monolayers [2169], where 4.70 ± 0.05 eV is very close to ours recommended for Si (Table 2).

[76]At the Si-coverage of $\theta = 3$–4 ML, the Si/W system prepared at 77 K is found to have $\phi^e = 4.78$ and 4.6 eV after annealing at 460 (or 525) and 580 (or 640) K, respectively. Such a decrease by 0.2 eV as found around 600 K is due to the diffusion of Si into W. When annealing is done at 990 K, $\phi^e = 4.6$ eV is kept at $\theta = 2$–3 ML, above which ϕ^e is sharply decreased down to 3.7 eV by alloying between Si and W [2248].

[77]The calculated values of $\phi^e = 4.98$, 4.999 and 5.08 eV for the monolayer adsorption of S on Fe(110) correspond to the hollow, bridge and atop sites, respectively [4313].

[78]The layer of S ($\theta = 0.53$ ML) on Fe(100) is formed by effusion of S included in Fe(100) after annealing at 970 K. Its work function increases from 5.21 to 5.26 eV as θ increases from 0.53 to 0.66 ML [565,3311].

[79]Incidence of S$_2$ upon Pd(111) forms a bulk sulfide layer, three-dimensional sulfide crystallites and elemental bulk sulfur layer at ~300, 550 and 100 (or 150) K, thereby decreasing the work function by ~0.3, 0.35 and 0.24 (or 0.20) eV, respectively, at ~6× 10^{15} S$_2$ molecules/cm² [2877]. By taking $\phi^e = 5.55$ eV [1351] for Pd(111), we have 5.25, 5.20 and 5.31 (or 5.35) eV at the respective temperatures.

[80]At 273 K, K is deposited on KF(100) and NaCl(100) to form K(100) and K(110), respectively, and their work functions are measured, the respective values of which are determined to be 2.33 and 2.41 eV after extrapolation to 0° K [2946].

[81]On the basis of $\phi^e = 5.85$ eV for W(110), K/W(110) is determined to have 2.0 eV at $\theta = 1.1$ ML by both theory and experiment [267,3818].

[82]The value of $\phi^e = 2.55$ eV determined for K/W(110) according to $\phi^e = 5.80$ eV for W(110) [373] may be revised to be 2.05 eV by taking the latter as 5.30 eV (see Table 2).

[83]The work function of K/Ag/glass [1456] depends upon the K-coverage of $\theta = 2$, 3 and 30 ML and holds $\phi^e = 2.16$, 2.12 and 2.24 eV, respectively, thereby affording 2.17 ± 0.05 eV as their average. However, it should be noted that the last (2.24 eV) is nearest to the values of 2.22–2.30 eV recommended by several authors (see Table 2). This fact suggests that such layers as thick as $\theta = 30$ ML have essentially the same property of a usual polycrystalline surface. In other words, the bulk work function can hardly be determined correctly unless θ is much greater than several ML.

[84]The plot of ϕ^e vs. θ observed for a K/Ru(001) system at 130 K shows $\phi^e \approx 2.2$ eV at $\theta = 0.8$ ML and 2.4 eV at much higher values of θ, corresponding to the bulk potassium [528].

[85]The substrate consists of microcrystallites having the same (0001) direction [2193] with $\phi^e = 4.7$ eV [1725], resulting in about 2.5 eV for K/C(0001) [1725,2193].

[86]The value of 3.3 eV observed for a system of K-encapsulated into single-walled carbon nanotubes [3229] is rather close to 3.6 eV calculated for a K-doped (10, 10) tube bundle of $K_{0.1}C$ [767].

[87]The system of Ca/silica is found to have $\phi^e = 2.2$, 2.55 and 2.98 eV for the layers of 5.5, 3 and 10 nm, respectively [1418].

[88]Each sample of Mg, Ca, Cu and Sr is deposited onto glass at 77 K to form a layer of $\theta = 2$–3 ML, and their work functions at ~300 K are measured to be 3.7, 3.0, 4.4 and 2.8 eV, respectively [1526].

[89]The systems of Ca/Mo consist of the Mo-foils implanted with 50- and 60-keV Ca^+ ions in doses of $2 \times$ and 1×10^{17} ions/cm^2, showing the minimum work functions of 3.13 and 3.26 eV, respectively, much lower than ~4.5 for pure Mo [2211].

[90]The system of Sc(0001)/W(110) with $\phi^e = 3.8$ eV is found at the surface concentration of 1.5×10^{15} Sc-atoms/cm^2 at 300 K. Even at the same concentration, however, ϕ^e shows different constant values of 4.0, 3.6 and 4.6 eV at 1050, 1200 and 1500 K, respectively [1982], suggesting that the Sc-layers have different structures.

[91]The Sc/W systems have $\phi^e = 2.8$ and 2.9 eV at $\theta = 1.0$ and 2.0 ML, respectively [1811].

[92]The Sc-layers with $\phi^e = 3.3$–3.4 eV are prepared from the alloys of Re–Sc (4–9%) after heating at 1700–1800 K for a long time [1979].

[93]The value of 4.10 eV is estimated for the (0001)-oriented titanium microcrystal grown on W(110) at 600–700 K [2196].

[94]The value of 5.0 eV corresponds to Ti(0001) formed as a main component of the titanium layers on glass, while the layers over the entire surface area are found to have 4.76 eV as the mean value of Ti(poly) [2378].

[95]The work function values of 4.15 and 4.75 eV correspond to Ti(1010) and Ti(1011), respectively, formed as the major and minor components of titanium layers on oxidized titanium (O=Ti), where they have 4.60 eV as the average over the entire surface area [2378].

[96]The surface layer structures of Ti grown on W(011) and both W(111) and W(001) are epitaxially oriented toward Ti{0001} and Ti<11$\bar{2}$0>, respectively having 3.52, 3.50 and 3.75 eV, in contrast to 3.03 eV for Ti/W(016) and 3.95 eV for Ti/W(112) [3222].

[97]The systems ($\theta \gtrsim 3$ ML) of Ti/W(001) and Ti/Re(10$\bar{1}$0) with $\phi^e = 3.88$ and 4.00 eV, respectively, have the same structure of α-hcp at 293 K [1404], but the former undergoes allotropic transformation to β-bcc after annealing at 1300 K for 1 min, thereby changing in ϕ^e from 3.88 to 3.65 eV [1404,1405].

[98]Similarly as mentioned above in Footnote 97, Ti/W(111) shows the allotropic transformation from α- to β-Ti after heating at 1100 K, together with a decrease in ϕ^e from 3.95 to 3.6 eV [2194].

[99]The same phenomenon as just above Footnotes (97 and 98) is found for Ti/W, changing ϕ^e from 3.95 to 3.65 eV according to transforming from α- to β-Ti, respectively, after annealing at 1100 for 15 s [1522].

[100]The theoretical values of 4.61 and 4.19 ± 0.02 eV are obtained for the non-magnetic V(100) films consisting of 1 and 3–7 layers, respectively [3671].

[101]At $T = 4.2$ and 15 K, the thin film system of V/quartz is measured to have $\phi^e = 3.1 \pm 0.2$ and 2.9 ± 0.2 eV by CPD, respectively, and ϕ^e seems to change by 0.2 ± 0.3 eV at the superconducting transition temperature ($T_S = 5.4$ K), although $\phi^e = 3.1$ and 2.9 eV are considerably smaller than 3.77 eV found for bulk-V by FE at the same range of 4.2–15 K [1686]. About the quantitative relation between ϕ^e and T around T_S, fine measurements at a meV level may be necessary in general to determine accurately the minute change in ϕ^e according to the transition (see Section 9 and Table 14).

[102]At 4.2 and 5 K slightly above the superconducting transition temperature (1.2 K), Al/quartz and Al-bulk systems are observed to have 4.1 ± 0.2 and 4.20 eV by CPD and FE, respectively [1686], where the disagreement between the two is smaller compared with the case of V mentioned just above (Footnote 101).

[103]Although the system of Cr(100)/Au(100) as well as Cr(011)/Au(010) satisfies the exceptionally close lattice match (0.02%), Cr forms fcc alloy with Au even at room temperature, and Au diffuses to the Cr-surface. Consequently, ϕ^e of the surface even at $\theta \simeq 60$ ML shows a value (4.05 ± 0.1 eV) higher by ~0.15 eV compared with that (3.90 ± 0.1 eV) of pure bulk Cr(100) [2870,3951].

[104] The system of Cr/Au/glass [3207] is prepared at room temperature by deposition of Cr (10 nm thick) on Au (250 nm thick) and determined to have $\phi^e = 4.6$ eV for Cr by taking $\phi^e = 5.1$ eV for Au [304], while the former is evaluated to be 4.8 eV if the latter is taken as 5.3 eV from Table 2 [Here]. However, both of 4.6 and 4.8 eV are considerably higher than 4.38 ± 0.04 eV recommended in Table 2, thereby suggesting that the system is alloyed to some extent by diffusion of Au (see Footnote 103).

[105]The work function of Cr/Au(100) [3557] is evaluated to be 4.87 eV for Cr by taking 5.47 eV for Au(100) [959,1045,1358], but the former is larger than both 4.10 eV [2638] and 4.46 eV [3445,3446] for Cr(100) and also than both 4.5 eV [304,1045,1358] and 4.38 eV [Here, see Table 2] for Cr (poly). Such discrepancies may suggest again the alloy formation between Cr and Au due to diffusion of Au, quite similarly as already mentioned above (see Footnotes 103 and 104).

[106]Mn atoms deposited onto Cu(111) at ~300 K are incorporated into the first Cu layer, and they form compact alloy islands according to further deposition, thereby decreasing ϕ^e by ~1.0 eV for the Mn/Cu(111) system (3.9 eV) [3710]. Here, ϕ^e for Cu(111) is taken as 4.94 eV [953].

[107]The Mn/Cu(100) system at $\theta \simeq 2.5$ ML at 293 K is found to have $\phi^e = 4.2 \pm 0.1$ eV, which corresponds to bulk Mn [1554], in contrast to the above case [3710] (see Footnote 106). It is generally 4.1 eV that is recommended for Mn (see Table 2).

[108]The system of Mn/ins/Al (see Footnote 47 for the sandwich structure) [2028] is determined to have $\phi^e = 3.60$ eV by taking the reference work function as 3.43 eV for Al [2028], in contrast to 4.40 eV by doing as 4.23 eV recommended for Al (Table 2 [1351]).

[109]The values of $\phi^e = 3.7$ and 3.9 eV calculated for the strained and unstrained Fe(100) crystals, respectively, are much smaller than 4.24 eV by experiment [2901].

[110]The value of $\phi^e = 4.17$ eV for Fe(100) [920,3044] is corrected to be 4.24 eV by another worker [13] taking not 4.49 eV [826] but 4.54_5 eV [828] for W (see Footnote 303) as the reference for CPD measurements.

[111] The ions of Na$^+$ and K$^+$ are due to the impurities (Na and K) occluded in the Fe filament employed [277], thereby making it possible to measure $\phi^+ = 3.6$ and 3.8 (or 4.3) eV by PSI.

[112] Regarding the γ- and β-phases of Fe [303], the differences of both ϕ^+ and ϕ^e between the two phases are estimated to be $\Delta\phi^+_{\gamma\beta} \equiv \phi^+_\gamma - \phi^+_\beta = 4.55-4.49 = 0.06$ eV and $\Delta\phi^e_{\gamma\beta} \equiv \phi^e_\gamma - \phi^e_\beta = 0.09$ eV, respectively [303] (see Table 11).

[113] The Richardson plot for Fe has a break at ~1170 K, below and above which both slopes are identical, thus yielding 4.77 eV for β- and γ-Fe [3024].

[114] The films of Fe(100) and Fe grown epitaxially on Cu(100) are found to have *metastable* and ferromagnetic fcc-structure, whose Curie temperature (T_C) changes depending upon the film thickness in contrast to the stable and ferromagnetic α-bcc-bulk iron with T_C constant at 1042 K. For details, see Section 8.2.

[115] By temperature increase from 703 to 763 K, α-hcp-Co(0001) with $\phi^e = 5.264$ eV is allotropically transformed to β-fcc-Co(111) with 5.266 eV [3192,3193].

[116] The Co sample cooled slowly from above 1120 K to ~300 K is found to have the α-hcp structure with $\phi^e = 4.12 \pm 0.04$ eV, whilst that done so suddenly retains the β-fcc one with 4.25 ± 0.08 eV [1631,1632].

[117] The systems of Co/substrate prepared by deposition of Co at 4.2 and 400 K consist of noncrystal and polycrystal Co-layers having $\phi^e = 4.4 \pm 0.1$ and 4.9 ± 0.1 eV, respectively [1506].

[118] The Co/Si(111) system at $\theta \simeq 3$–10 ML is found to have $\phi^e = 4.86 \pm 0.05$ eV at ~300 K, but it forms Co- and Si-rich CoSi$_2$ films with 4.94 ± 0.01 and 4.81 ± 0.01 eV depending upon the annealing temperatures at 610–690 and 760–870 K, respectively [2451].

[119] The values of $\phi^e = 4.960$ and 4.923 eV are determined at 300 and 663 K, respectively, for α-hcp-Co, whereas 4.925 and 4.966 eV are found at 673 and 300 K (extrapolated from ~770 K passing through the allotropic transition temperature of 663–673 K) for β-fcc-Co, respectively [1148]. For further information, see Section 7.1.

[120] The specimen of β-Co is found to have $\phi^e = 4.6 \pm 0.3$ eV (ferromagnetic state) and 4.8 ± 0.3 eV (paramagnetic one) below (1340–1390 K) and above (1390–1440 K) the Curie point (1390 K), respectively [3604].

[121] The Co films (1–9 ML) grown epitaxially on Cu(100) at 300–400 K are ferromagnetic and have the β-like fcc structure with $\phi^e = 5.0 \pm 0.2$ eV [2879,4377].

[122] The β-like fcc-Co films on Cu(100) is theoretically evaluated to have 5.34 eV, being ferromagnetic at temperatures up to the Curie point (~1400 K) [3654].

[123] The work function of Ni(100) after Ar$^+$ impact is found to have 5.08 eV, which is increased to 5.12 and 5.22 eV by annealing at 623 and 1023 K for 4 and 30 min, respectively [903].

[124] The Ni films (>1000 Å thick) prepared on vacuum- and air-cleaved mica at 593 K consist mainly (85 and 92%) of Ni(100), respectively, both having $\phi^e = 5.12 \pm 0.02$ eV [314], which is very close to 5.19 ± 0.05 eV for bulk Ni(100) (Table 2).

[125] About 67% of the Ni film surface (prepared on glass at 77 K and annealed at 523 K) have $\phi^e = 5.17 \pm 0.02$ eV [314], yielding nearly the same ϕ^e as above (see Footnote 124).

[126] Similarly as above (Footnotes 124 and 125), about 95 and 94% of the Ni film surfaces on glass at 573 and 523 K have 5.20 ± 0.02 eV [314,315] and 5.34 ± 0.02 eV [314], respectively, which are close to 5.19 ± 0.05 eV for Ni(100) and 5.32 ± 0.05 eV for Ni(111), respectively (Table 2).

[127] About 85–90% of the nickel layer surface on glass after annealing at 523 K have $\phi^e = 5.22$ eV, corresponding virtually to Ni(100) [1513].

[128] Identically as above (Footnote 126), 90% of the nickel surface have $\phi^e = 5.35$ eV [315,1513], essentially the same as 5.32 ± 0.05 eV for Ni(111) (Table 2).

[129] Only 3% of the whole surface area of Ni deposited on glass at 273 K (without annealing) correspond to $\phi^e = 4.82$ eV, with the remainders of 45 and 52% correspondent to 5.00 and 5.16 eV, respectively [314].

[130] Regarding fine particles of Ni, the calculated values (~2.9 eV) [2887] are found to be very discrepant from the experimental ones (~4.2 eV) [2887]. Such a discrepancy is found for Al, too; theory (~3.2 eV) and experiment (~3.7 eV) [2887].

[131] About 25 and 75% of the layer surface of Ni deposited on NaCl at 573 K correspond to 4.39 and 4.47 eV, respectively [314].

[132] The polycrystalline Ni is observed to have $\phi^e = 4.645$ eV (extrapolated from ~550 to 300 K), 4.660 eV (at 400 K), 4.690 eV (at 660 K, slightly above the Curie point of $T_C = 631$ K), or 4.700 eV (at 740 K) [503]. The ferromagnetic state at 400 K below T_C has the difference of $\Delta\phi^e_{PF} \equiv \phi^e_P - \phi^e_F = 4.653 - 4.660 = -0.007$ eV in comparison to the paramagnetic value extrapolated from 700 to 400 K [503]. The theoretical value of the difference is reported to be –135 meV [3673], –50 meV [3954] or 9 meV [2358] in contrast to –7 meV mentioned above (see Table 13).

[133] About 2, 13 and 85% of the overall surface area of Ni deposited on vacuum-cleaved mica at 593 K are found to have 4.82, 4.93 and 5.12 eV, respectively [314], the last of which is nearly the same with ϕ^e of Ni(100) (see Footnote 124).

[134] The Ni/W system is found to have 4.52 and 4.85 eV for the layers at 1 and 4–5 ML, respectively [2249].

[135] About 12, 35 and 53% of the layer surface area of Ni deposited on glass at 273 K have 4.9, 5.2 and 5.0 eV, respectively [315], the last of which is substantially the same with our recommended value (4.96 eV) for Ni(110) (see Table 2).

[136] The surface of Ni having 5.21 eV [1403] is partially oxidized.

[137] The Cu/NaCl systems annealed at 473 and 423 K are found to have the Cu(100) and Cu(111) orientations with $\phi^e = 3.96$ and 4.20 eV, respectively [3328]. After annealing at the same temperatures, Ag and Au on NaCl systems show the same orientations with $\phi(100) = 4.30$ eV and $\phi(111) = 3.98$ eV for Ag and with $\phi^e(100) = 4.02$ eV and $\phi^e(111) = 4.12$ eV for Au [3328]. Any of the above values, however, has a large difference ($\Delta\phi$) from ours recommended for each surface in Table 2. Typically for Ag, $\phi(100)$ and $\phi(111)$ are smaller by $\Delta\phi = 0.16$ and 0.66 eV than our respective values (Table 2), and $\phi(100) > \phi(111)$ does not follow the Smoluchowski rule of $\phi(111) > \phi(100) > \phi(110)$ found generally for Ag and also for many fcc metals except Al (see Table 10 and Section 5.3).

[138] The Cu(100) surface is determined to have 4.07 and 4.43 eV, neither of which is representative of a truly clean surface [1183].

[139] The layers (5–6 ML) of Cu deposited on Ir(100) at 78 K and annealed at 380 K are observed to have 4.55 ± 0.02 eV [2189], very close to both 4.59 ± 0.03 eV [953] and 4.58 ± 0.06 eV (Table 2) found for Cu(100).

[140] The work functions of Cu(100), Cu(110) and Cu(111) are estimated to be 4.68, 4.48 and 4.85 eV, respectively, by the present author using $\phi^e = 4.34$ eV estimated for SnO (the reference for CPD measurements) from the data in Table II [959], the reference value of which is constant in the presence of O$_2$ below ~10^{-6} Torr [831].

[141] The growth of Cu layers ($\theta > 3$ ML) on W(110) at ~300 K leads to recrystallization, thereby forming {111}-oriented patches with $\phi^e = 4.8$ eV (near to 4.92 ± 0.05 eV recommended for Cu(111) in Table 2) in a predominantly lateral direction on further condensation [1519]. On the other hand, $\phi^e = 4.5$ eV (equal to 4.51 ± 0.04 eV for Cu(poly) in Table 2) is found by deposition at 800 K [1519].

[142] When ϕ^e of the reference (W) is taken as 4.55 eV [828,1056,2103], the Cu layers prepared on W(110) at ~300 K [2598] are estimated to have 4.90 eV, essentially equal to our recommended value of 4.92 ± 0.05 eV (Table 2) for bulk Cu(111), whereas those on W(poly) [2598] are done to have 4.6 eV, nearly to $\phi^e = 4.51 \pm 0.04$ eV recommended for Cu(poly) (see Table 2). In a similar way, ϕ^e for W(110) [2598] is evaluated to be $4.55 + 0.73 = 5.28$ eV, well agreeing with our value (5.32 $\pm$ 0.02 eV in Table 2).

[143]In contrast to the work function decrease ($\Delta\phi = -0.32$ eV) upon Cu-condensation on Ru(0001) [2876], the large increase ($\Delta\phi = +0.40$ eV) reported for Cu/Ru(0001) [1683,1685] is due to an inadvertent error in the sign of $\Delta\phi$ measured with a Kelvin prove [3955], as stated in Ref. [2876]. In addition, $\phi^e = 4.5$ eV for Ru(0001) cited in Ref. [1683] from Ref. [2348] is too low [2266] compared with 5.52 ± 0.1 eV [2266] and also with our recommended value (5.35 ± 0.06 eV, see Table 2). Consequently, Cu/Ru(0001) [1683,1685] is estimated to have $\phi^e = 5.35 - 0.40 = 4.95$ eV, which is substantially equal to our value of 4.92 ± 0.05 eV for Cu(111). This result supports the conclusion [1683,1685] that Cu(111) is formed on Ru(0001).

[144]Around the melting point ($T_m = 1356$ K) of Cu, ϕ^e is found to be 4.4, 4.62 and 5.5 eV just below T_m, at T_m and above T_m, respectively [1465].

[145]Cu is deposited onto Ni by electroplating and found to have 4.47 eV [2294], which is very close to 4.51 ± 0.04 eV recommended for Cu (Table 2).

[146]When the reference work function of Ag used for CPD is taken as 4.36 eV [1351] by the present author instead of 4.74 eV adopted by the corresponding author [2087], the work function of Cu [2087] is corrected to be 4.48 eV instead of 4.86 eV [2087], the former of which is much closer to our recommended one (4.51 ± 0.04 eV, see Table 2).

[147]Regarding Cu/W(110) [2831], ϕ^e may be evaluated to be 4.58 eV [Here] and 5.20 eV [2831] for Cu by taking 5.31 eV [Here] and 5.93 eV [2831] for W(110) by the present and corresponding authors [2831], respectively, thereby yielding a more reasonable result ($4.58 \approx 4.51 \pm 0.04$ eV) from the former similarly as above (Footnote 146).

[148]Preparation of Cu layers on glass with 103 and 114 Å thick at 273 and 77 K affords $\phi^e = 4.64$ and 4.65 eV, respectively [3075].

[149]Fine particles ($r \approx 30$ Å in radius) of four metals are produced from each metal vapor by passing through He steam evaporating from liquid He [3190]. They are found to have $\phi^e(r) = 4.80$ eV (Cu), 5.45 eV (Pd), 4.50 eV (Ag) and 5.20 eV (Au) [3190], respective values of which are nearly equal to ours calculated from Eq. (17′) by citing $\phi^e(\infty)$ from Table 2 (see Section 11.1).

[150]The orientation of this single zinc crystal with 3.63 eV [2591,2601] is taken as (0001) in Ref. [475], although it is not clearly done so in Ref. [1312]. The crystal is treated as a polycrystal in CRC handbooks [11,1358,1859,4191] (see Section 3.2).

[151]Concerning the Zn/glass system [1370], $\phi^e = 4.28$ eV [1370] is corrected to be 4.11 eV [13,349] for Zn by other workers [13,349] taking $\phi^e = 2.35$ eV [13,349] instead of 2.52 eV [1370] as the reference work function for Ba used in CPD measurements.

[152]Employment of $\phi^e = 4.36$ eV [1351] instead of 4.74 eV [2087] for Ag (reference for CPD) yields 4.27 eV [Here] instead of 4.65 eV [2087] for Zn under study, the former of which is much closer to our recommended value (4.22 ± 0.11 eV for Zn in Table 2).

[153]Work function of the Ge(111) sample [2093] is measured to be 4.12 and 4.75 eV after cleavage in air and vacuum, respectively.

[154]The surface of Ge(111) cleaved in vacuum [2620] is found to have 4.9 eV, which changes to 4.5 and 4.7 eV after annealing at 370–470 and 570 K, respectively [2620].

[155]By both PE and CPD, exactly the same value of 4.80 eV is measured for Ge(111) cleaved in vacuum [1971]. See Section 2.8.2 for comparison of work function data obtained by different methods.

[156]Regarding K, Rb and Hg [2470], each of their work functions (2.29, 2.16 and 4.49 eV, respectively) does not undergo any substantial changes (less than 0.01 eV) during the transition through each melting point. See Table 12 for further information about the work function change due to liquefying.

[157]The layer ($\theta = 1.3$ or 1.5 ML) of Sr deposited onto W(110) at 77 K [2344] is measured to have 3.0 eV (by FE) or 3.2 eV (by CPD), the latter of which does not change even after annealing at 300 K.

[158]The systems of Y/W with $\theta = 1$ and 1.5–2.0 ML [1804] have $\phi^e = 2.6$ and 2.7 eV, respectively.

[159]The layer of Y deposited onto W(100) at ~300 K ($\phi^e = 3.1$ eV) is changed to that of Y(0001) ($\phi^e = ?$) after annealing up to ~1070 K [1985].

[160]The work functions of Sc, Y, Tc, In, Po, Fr and Pa are estimated to be 3.3, 3.3, 4.4, 4.0, 4.6, 1.5 and 3.3 eV, respectively, from the periodic trend of published data on ϕ^e for several elements neighbor to each metal [1355]. These values for Po, Fr and Pa have a trend to be smaller than other theoretical ones of 4.8–5.0, 1.8–2.14 and 3.3–3.73 eV, respectively. Of course, the three elements have no experimental data on ϕ^e available yet today.

[161]The smooth layers of Zr are formed by thermal processing of a Mo–Zr (5%) alloy heated to ~1000 K [790]. The value of 2.94 eV [790] is smaller than any other data on ϕ^e for α-Zr in this table.

[162]The specimen of Nb(100) with 68%-(100) orientation over the surface area [650,3414] is determined to have a "clean" cesiated work function of 4.1 eV [3414], whilst its really clean one is theoretically calculated to be 4.02 ± 0.07 eV [803], nearly the same between the two. It should be noted that the specimen is theoretically evaluated to have the thermionic contrast of $\Delta\phi^* = \phi^+ - \phi^e = 4.39 - 4.02 = 0.37$ eV [803].

[163]By Ar$^+$ impact on Nb(111), ϕ^e is decreased from 4.66 to 4.09 eV [780].

[164]At 4.2 K below the superconducting point ($T_s = 9.2$ K), the Nb/quartz system [1686] is found by CPD to have $\phi^e = 3.9 \pm 0.2$ eV, which is not clearly different from both 3.8 ± 0.2 and 3.9 ± 0.2 eV measured by CPD at 28 and 293 K above T_s. However, the above Nb film (3.9 eV at 4.2 K) is much smaller in ϕ^e than the bulk Nb (5.01 eV by FE) at 5 K below T_s [1686] (see Table 14).

[165]With respect to the niobium work function, it is criticized in Section 3.1.4 [13] that 3.88–3.91 eV determined by combination of both PSI and NSI of several alkali halides [120] is too low compared with 4.37 ± 0.03 eV by CPD [123]. The former [120] is also less than by ~0.2 eV compared with our recommended value (see Table 2). Such a discrepancy may be caused mainly by the implicit assumption [120] that the work functions (ϕ^+ and ϕ^-) effective for positive and negative ionic emissions are the same with each other without considering the thermionic contrast ($\Delta\phi^* = \phi^+ - \phi^- = \phi^+ - \phi^e = 4.81 \pm 0.05 - 4.11 \pm 0.05 = 0.70 \pm 0.07$ eV (see Table 5 and Section 4.1). It should be noted that the relation of $\phi^+ = \phi^- = \phi^e$ holds exactly with a clean and smooth monocrystalline surface alone, as already stated in Section 1.

[166]The layers of Nb, Mo, Ta and W on Si(111) ($\phi^e = 4.53$ eV) are as thick as ~30 ML, showing 4.12, 4.76, 4.15 and 4.87 eV, respectively [1430].

[167]Each molybdenum surface [125,129,572,573] is assigned to the (100) plane arranged naturally by recrystallization of Mo through annealing for many hours above 2200 K [573]. This assignment is supported by the result that $\phi^+ = \phi^e = 4.28 \pm 0.05$ eV [573] and hence $\Delta\phi^* = 0.0$ eV in contrast to ~0.7 eV for Mo (see Table 5). Such a work function change due to thermal monocrystallization is reported also for many other metals (see Section 4.5 in Ref. [1351]).

[168]The work function of Mo(100) is found to be 4.52 and 4.38 eV after heating at 1980 K by a.c. for initially 40 h and successively 50 h until giving constancy in ϕ^e, respectively, while it is 4.37 and 4.33 eV after doing so by d.c. for firstly 25 h and additionally 235 h until so, respectively [729]. In both cases, ϕ^e decreases gradually by the heating and finally becomes constant at 4.38 ± 0.03 and 4.33 ± 0.03 eV, both of which are essentially equal to our recommended values of $\phi^e = 4.38 \pm 0.03$ eV, $\phi^+ = 4.38 \pm 0.08$ eV and $\phi^- = 4.34 \pm 0.03$ eV (see Table 2 and also Footnote 258).

[169]The theoretical values of ϕ^e for Mo(110) layers (1–4 ML) on W(110) and for Mo(110) bulk are 4.8 and 4.83 eV, respectively, well agreeing with each other [2074].

[170]The work function (ϕ^+) for each specimen is calculated by either the corresponding workers or the present author substituting each of workers' data on ionic and neutral desorption energies (E^+ and E^0) [77,131,132,135,146,166,167,178,263,265,266,269,276,280,282,397,684,804,823,954,966,1049,3886] and also literature value (ionization energy, I) into the Schottky equation (9) of $\phi^+ + E^+ = E^0 + I$, where E^0 is cited in some cases (for details, see Section 4.1).

[171]The "clean" and "gassy" surfaces of Mo(111) are measured to have $\phi^e = 4.49$ and 4.67 eV, respectively [3421].

[172]About the Mo surface consisting of 70–72% (100), 20–22% (112), 5% (111) and less than 2% (110) [124,3414], ϕ^e is estimated to be 4.25 eV by another worker [1254], while our theoretical evaluation yields $\phi^e = 4.38 \pm$ eV and $\phi^+ = 4.51 \pm 0.03$ eV [803], and hence $\Delta\phi^* = 0.13 \pm 0.03$ eV in contrast to $\Delta\phi^* = 0.0$ eV for ∼100% Mo(100) (see Table 5). Experimentally on the other hand, ϕ^e is found to be temperature-dependent like as 4.32–4.17 and 4.18–4.01 eV at ∼1400 and 2000 K, respectively [124], or roughly 4.0–4.3 eV [124,3414].

[173]The Mo surface consists of the planes of mainly (116) and (331), and its ϕ^e is measured to be 4.33 eV by TE and 4.41 or 4.47 eV by PE [134].

[174]The work function at 0 K for each of the nine polycrystalline surfaces is evaluated from $\phi_0 = kb_0 = \phi_T - (3/2)kT$ after determination of b_0 using published data on thermionic emission from Ca, Y, Zr, Mo, Ce, Ta, W, Th or U at various temperatures [1747].

[175]By theory and experiment, ϕ^e for Ru(0001) is evaluated to be 5.3 and 5.4 eV, respectively [542], both of which are close to our recommended value of 5.35 ± 0.06 eV (see Table 2).

[176]The theoretical values of 5.36 and 5.57 eV correspond to the ferromagnetic and paramagnetic states of Rh(100), respectively [1258].

[177] The work function (4.70 eV) for a roughened surface of Rh(110) is lower than that (4.80 eV) for a smooth one [853], just as expected generally (see Section 4.2.5 in Ref. [1351]).

[178]The work function values of roughened surfaces of Rh(111) and Pt(111) are 4.95 and 5.53 eV, respectively [853], both of which are much smaller than the respective ones of 5.40 and 5.84 eV recommended mainly for smooth surfaces (see Table 2), quite similarly as above (see Footnote 177).

[179]The value (5.1 eV) for Rh(111) is deduced by Feibelman [456,1011] from the photoemission data obtained by other workers [1544,1546].

[180]The Rh layers (2–3 ML) on Mo(110) are found to have $\phi^e = 5.36$ eV [1035], very close to our value of 5.40 eV for Rh(111) (see Table 2).

[181]On the two species of insulator/semiconductor substrates, the Rh layers (>10 Å thick) are prepared from rhodium acetylacetonate at 423 K, resulting in $\phi^e = 5.25$ or 5.43 eV [2908].

[182]The work function of a 6 × (100) stepped face of Pd is calculated to be 5.50 eV, which is smaller than 5.80 eV for a normal Pd(100) face [704,795]. Similarly to Pd(111), 5.53 eV for a 6 × (111) stepped face is lower than 5.86 eV for the normal one [704,795].

[183]This is a stepped surface of Pd(S)–[8(100) × 1(110)] having 5.55 eV [1129]. For this nomenclature, see Ref. [1130].

[184]The value of ∼5 eV for Pd(110) [610] is roughly equal to 5.20 ± <0.1 eV determined later by the same group [914].

[185]The work function of 5.5 eV for Pd(110) is determined for thick layers (10 ML) of Pd deposited onto Al(110) ($\phi^e = 4.2$ eV) at ∼300 K [3495].

[186]The substrate of Cu(111) is prepared on mica at 398 K, after which Pd(111) layers are formed on Cu(111), thereby yielding $\phi^e = 5.61$ eV at ∼300 K [3364]. This is virtually the same with our recommended value (5.58 ± 0.05 eV, see Table 2).

[187]With respect to Pd(foil) and Pd layers (400–700 Å) on Ta, ϕ^e is determined to be 4.6 and 4.95 eV respectively [350], the latter being close to our value (5.17 eV).

[188]The values of 4.61, 4.69 and 5.07 eV for Pd [1953] are based on the Ag reference ones of 4.28 eV [1355], 4.36 eV [1351] and 4.74 eV [2087] for Ag, respectively, the last of which is too large compared with our recommended one of 4.39 eV for Ag (see Table 2).

[189]The work function of 4.2 eV is estimated by another worker [971] using the PE data for Ag(100) [2128], the topic of which is introduced in Ref. [1261].

[190]The value of 4.45 eV for 20%-vacant Ag(100) is much lower than 4.78 eV for normal one [2405].

[191]Preparation of an Ag-film on Ag(100) at ∼300 K or less makes ϕ^e lower by 0.1 eV than that of the clean substrate [2302], where the latter may be estimated to have 4.50 eV according to the value recommended for Ag(100) in Ref. [1351]. By heating the system to 308–313 K, however, the difference of 0.1 eV is decreased to ∼0 eV [2302], thereby indicating that the film becomes equivalent to the substrate. In other words, a polycrystalline metal film on a monocrystalline surface of the same metal species may be monocrystallized to have the same orientation by annealing at suitable temperatures.

[192]About the Ag(100)/NaCl system [1157], ϕ^e for Ag(100) is corrected to be 4.62 eV from 4.79 eV by other workers [349] taking 2.35 eV [13,349] instead of 2.52 eV [2232] for Ba employed as the reference [1157], the topic of which is mentioned in Ref. [626].

[193]The system of Ag/Ag(100) annealed at 525 K is found to have the same work function (4.64 eV) with bulk Ag(100) [626], quite similarly as mentioned already in Footnote 191.

[194]In the case of a low vacuum ($\leq 3 \times 10^{-8}$ Torr), both bulk Ag(100) and Ag film formed on the bulk at ∼300 K are found to have the same work function of 4.81 eV, which is decreased by 0.09 ± 0.03 eV after heating the film to red [1132]. The same decrease (from 4.75 to 4.66 eV) is observed also for the Ag film on bulk Ag(111) [1132].

[195]The work function of Ag film on V(100) (4.56 eV) is calculated to be 5.72, 5.44 and 5.02 eV at 1, 2 and ≫2 ML, respectively. For larger coverage, ϕ^e oscillates around the value (5.02 eV) for semi-infinite Ag(100) [1876].

[196]After annealing at 525 K, the Ag films formed on Ag(110) and on mica are found to have $\phi^e = 4.51$ eV, which is essentially the same (4.52 eV) with Ag(110) [626].

[197]A clean and smooth surface of Ag(111) is found to have $\phi^e = 4.46 \pm 0.02$ eV measured by PE [625,1693]. On the other hand, ϕ^e for a surface of Ag(111) damaged by Ar$^+$ impact is 4.18 eV done by PE, larger than 4.03 eV by CPD [1693]. This result does not follow the general trend of a normal surface that ϕ^e by PE is smaller than ϕ^e by CPD, thereby indicating that application of PE to such a damaged surface is not suitable because any surface defect gives some effect to the surface potential barrier and hence to photothreshold [1693]. For further information, see Section 2.8.2.

[198]By annealing at 773 K for 1 h, the Ag layer (1.7 nm thick) prepared on quartz at ∼300 K is increased in ϕ^e from 4.35 to 4.64 eV as the degree of monocrystallization (δ_m) forming the (111) face is increased from 54 to 86% by annealing at ∼773 K [3313]. Theoretically, 4.72 eV is evaluated for Ag(111) [3313], close to 4.64 eV (Table 2).

[199]The thick Ag-film (above ∼20 ML) formed at ∼300 K on the H-terminated Si(111) 1 × 1 ($\phi^e = 4.50 \pm 0.04$ eV) is found to have $\phi^e = 4.65 \pm 0.15$ eV [1198], which is essentially the same with our recommended value of 4.64 ± 0.06 eV for Ag(111) (see Table 2). On the other hand, the thin film (below ∼5 ML) prepared by annealing at ∼300 K after deposition at ∼210 K shows roughly 4.2 eV [1198], near to the selected value of 4.26 eV [1045] for polycrystalline Ag (see Table 2).

[200]The Ag-film (10 ML) formed on Pt(111) at ∼300 K has $\phi^e = 4.4$ eV, which is increased to 4.7 eV by annealing at 600 K, thereby changing the film structure from polycrystalline Ag to Ag(111) [2182].

[201]The Ag-film prepared on bulk Ag at 58 K is highly porous with $\phi^e = 4.25$ eV, which is increased to 4.72 eV after annealing at 330 K, corresponding to Ag(111) [1422].

[202]The Ag-film annealed at 525 K after deposition on mica at 425 K shows $\phi^e = 4.72 \pm 0.01$ eV, well agreeing with 4.74 ± 0.02 eV measured for bulk Ag(111) [626,1134].

[203]For the Ag-film (19 ML)/Ru(001) system annealed at 500 K after deposition at ∼60 K, ϕ^e is determined to be 4.90 ± 0.1 eV [2266], which does not well agree with 4.76 ± 0.1 eV measured for bulk Ag(111) at 50–60 K [2266] and also with our value of 4.64 ± 0.06 eV for Ag(111) (Table 2).

[204]The fine particles (50 ± 20 Å in radius) are produced by passing Ag-vapor through the He-gas boiling off from liquid He and found to have $\phi^e = 4.25 \pm 0.1$ eV [1562]. This is smaller than 4.39 ± 0.02 eV recommended for bulk Ag in Table 2. See Section 11.1.

[205]According to a patchy surface model of Ag [3720], work function is calculated to be 4.26 eV for a hypothetical polycrystalline surface of Ag [3280]. This value, however, corresponds to neither ϕ^e nor ϕ^+ but to a simple average (ϕ^a). It should be noted that $\phi^e < \phi^a < \phi^+$ holds with any polycrystalline surfaces (see Section 1). By substitution of the data included in the above model into Eqs. (2) and (1), ϕ^e and ϕ^+ are calculated to be 4.21 and 4.32 eV, respectively [3956]. Here, the polycrystalline surface of Ag is considered to consist of the three main faces of Ag(100), Ag(110) and Ag(111), and their compositions of (F_i, ϕ_i) are taken as (23%, 4.22 eV), (46%, 4.14 eV) and (31%, 4.46 eV), respectively [3720].

[206]The work function of fine particles of Ag is studied according to Eq. (17′), where the polycrystalline work function of ϕ^e ($r = \infty$) is estimated to be 4.37 eV for Ag [3442]. It well agrees with 4.39 ± 0.02 eV for the planar Ag (Table 2). No value of ϕ^e (r), however, is determined there [3442]. Further information about nanometer metal particles may be obtained from Section 11 and also from excellent reviews [3669,4138,4194,4261,4269,4301–4304].

[207]The heavy layer of Ag deposited onto Mo at ~300 K is observed to have $\phi^e = 4.41$ eV [1051], equivalent to our value (4.39 ± 0.02 eV). The former is increased to 4.78 eV by annealing at a high temperature (red), but returns to 4.41 eV by subsequent deposition of Ag [1051]. On the other hand, the annealing of the Ag layer (4.41 eV) at $T \leq 370$ K increases ϕ^e by 0.1–0.2 eV [1051], thereby affording the estimated value of 4.55 ± 0.05 eV.

[208]The work functions of fine particles of Ag (20, 27 and 30 Å in radius) are determined to be 4.65, 4.57 and 4.55 eV, respectively, yielding the average of 4.59 ± 0.05 eV [3127]. This is larger than 4.25 ± 0.1 eV for a larger particle of Ag (50 ± 20 Å in radius) [1562] (see Footnote 204), and also than $\phi^e(\infty) = 4.39 \pm 0.02$ eV recommended for Ag(poly), just as expected from Eq. (17′).

[209]Compared with 4.6 eV for Ag [2729], much lower value of 4.06 ± 0.05 eV is found for air-oxidized Ag [2729], strongly suggesting that these Ag-surfaces ($\phi^e \simeq 4.1$ eV or less) studied in low vacua may be oxygenated partly or considerably.

[210]For Ag/W(110), ϕ^e is determined to be 4.5 and 4.6 eV at $\theta \simeq 2$ and 3 ML, corresponding to a minimum and nearly a flat saturation, respectively [1828]. The latter is very near to our value of 4.64 ± 0.05 eV for Ag(111) (Table 2), the nearness to which is found also in many other cases of Ag/W(110) [2363,3472,3565], Ag/Pd(100) [1692], Ag/Ta(112) [878] and Ag/Nb(110) [2986], as may be seen in Table 1.

[211]The work function of Ag-layers (9 ML) on Re(1010) after annealing at 350–770 K is determined to be 5.30 ± 0.02 eV by FE [1421], which is too large compared with any other experimental data on Ag listed in Table 1. This may be mainly because ϕ^e of the substrate is taken as 5.95 ± 0.15 eV by FE [730], which is also extremely larger than any other data on Re(1010) in Table 1. If the latter is taken from our value of 5.12 ± 0.05 eV (see Table 2), then, ϕ^e of the above system is evaluated to be 4.47 eV, becoming very near to our value of 4.46 eV recommended for Ag(100) (see Table 2).

[212]By taking 4.74 ± 0.03 eV [1135] and 4.36 ± 0.06 eV [1351] as the reference work function of Ag, ϕ^e of Cd is evaluated to be 4.43 ± 0.01 eV [1953] and 4.05 ± 0.06 eV by the present author [Here], respectively, the latter of which is essentially the same with our value of 4.06 ± 0.05 eV recommended in Table 2. All of the above experimental data, however, are obtained in low vacua (above ~10^{-9} Torr), strongly suggesting that further work in ultrahigh vacua is needed to obtain more reliable data for Cd.

[213]Quite similarly as above (Footnote 212), ϕ^e of Cd [2087] is corrected from 4.49 eV [2087] to 4.11 eV by the present author, the difference (0.38 eV) of which corresponds to that (4.74–4.36 eV) for the reference work functions selected for Ag.

[214]About the Cd/Ta system [1380], ϕ^e is adjusted from 4.08 eV [1380] to 4.22 eV by others [13,349] taking the reference of $\phi^e = 2.66$ eV [13,349] instead of 2.52 eV [3582] for Ba, thereby yielding such a negative result that deviation from our value (4.06 eV) recommended for Cd increases from 0.02 to 0.16 eV. It should be noted that 2.52 eV [3582] is substantially the same with our value (2.50 ± 0.02 eV) recommended for Ba.

[215]Under the conditions without and with the magnetic field of 0.05 tesla, ϕ^e is measured to be 3.85 and 3.94 eV, respectively, for the In/quartz system [1475].

[216]About the specimen of Sn [2087], 4.63 ± 0.01 eV [2087] is corrected to be 4.26 ± 0.06 eV (close to our value, see Footnote 217) by the present author taking our value of 4.36 ± 0.06 eV [1351] instead of 4.73 ± 0.07 eV [3391] as the reference work function of Ag.

[217]The work function of 4.51 ± 0.02 eV measured for Sn [1945–1947] is improved to be 4.39 eV by another worker [1135] after theoretical analysis of the experimental data [1945–1947], thereby yielding the result that the latter [1135] approaches closely to our value (4.34 ± 0.06 eV) for β-Sn.

[218]Quite similarly as just above (Footnote 217), the work function values for γ- and liquid-Sn are adjusted from 4.38 eV [1945–1947] to 4.28 eV [1135] and from 4.22 eV [1945–1947] to 4.17 eV [1135], respectively.

[219]The Sb-films prepared on W(100) at ~300 and 423 K are found to have 4.55 and 4.98 eV, respectively, the former being apparently amorphous [1995]. On the other hand, the Sb-film on W(110) at ~300 K is concluded to form pseudocubic Sb(100) having 4.7 eV [1272].

[220]The systems of Te-layers (200 and 1000 Å thick) deposited onto glass at less than 5×10^{-6} Torr and 573 K are studied at ~300 K in the flowing Ar-gas (0.1 Torr), yielding $\phi^e = 4.62$ and 4.76 eV, respectively [2246].

[221]About the systems of K and Cs on Si(111) [1823], the plots of work function change vs. alkali deposition time do not show a clear minimum, and a small oxygen contamination is observed at 10^{-9} Torr, thereby yielding such a result that ϕ^e for the both systems is estimated to be 1.6 eV, smaller than ϕ^e usually expected.

[222]The work function of a Cs/Re system is measured to be 1.64 eV [3582], smaller than usual, whilst that of Ba/Re is 2.52 eV [3582], in excellent agreement with our value of 2.50 ± 0.02 eV for Ba (see Table 2).

[223]On the flat surface of Si(100) at ~300 K, Cs is deposited until the work function decrease ($\Delta\phi$) becomes independent of the Cs-deposition time (t), thereby yielding $\Delta\phi = -2.95$ eV = constant [2883]. This constancy, however, does not correspond to a saturation ($\theta \geq 1$ ML) but does to $\theta \leq 0.58$ [2883]. If ϕ^e of the substrate is taken as 4.82 eV from Table 2 [Here], ϕ^e of the Cs-film is estimated to be 1.87 eV. Such a constancy as above is observed also for the Cs-film prepared on stepped and Ar$^+$-sputtered surfaces of Si(100), showing $\Delta\phi$ = constant = −2.89 and −3.44 eV even at $\theta = 0.69$ and 0.78 eV, respectively [2883]. These results suggest that the film thickness of $\theta \geq 1$ ML is not always guaranteed simply because $\Delta\phi$ is found to be constant independently of t.

[224]The work function of Cs on Ag(110) is estimated to be 1.8 eV at ~300 K, where Cs as well as other alkali metals do not form multilayers [2144]. At lower temperatures (e.g., 80 K), ϕ^e of Cs-multilayers tends to rise up to 2.1 eV correspondent to metallic Cs [2144].

[225]About the Cs/W(100) system at $\theta \simeq 0.4$–0.7 ML, ϕ^e is found to be 1.81 eV [3435], which is the same with that at $\theta = 1$ [644,1480].

[226]By taking $\phi^e = 4.8$ eV for Si(100) from Table 2 [Here], Cs/Si(100) at $\theta \approx 1.5$ ML is estimated to have 1.9 eV [3811], while the Cs/Se/Si(100) systems at $\theta = 0.5$ and 1.0 ML of Se are done to have the sandwiching values of 2.0 and 1.7 eV, respectively, owing to formation of such compounds as CsSe and $Si_xCs_ySe_z$ [3811].

[227]In the plot of $\Delta\phi$ vs. θ, Na- and Cs-films on Cu(111) are found to have $\phi \approx$ constant at 2.7 and 1.9 eV at $\theta \geq 0.25$ and 0.35 ML, respectively [2496], even at less than 1 ML. It should be emphasized that the former and the latter are slightly larger and smaller than our recommended values of 2.54 and 2.05 eV for Na and Cs, respectively (see Table 2).

[228]About the relation between ϕ^e and θ, some interesting information is added by other workers [2122] to the Cs/W system (1.80 ± 0.05 eV) [340] after theoretical analysis of the data [340] from the viewpoints of Cs-flux and surface temperature [2122]. About a Cs/W system at 400 K, surface coverages are evaluated to be ~1.1 and 0.9 ML at the incident Cs-fluxes of ~10^{17} and 10^{15} atoms/cm^2 s [2122].

[229]Through the Cs$^+$-impact with the energy (E_i) of 45 or 90 eV, ϕ^e of the Cs/Mo system at $\theta \approx 1$ ML is estimated to be 1.9 ± 0.1 eV, which increases to about 2.0 and 2.6 eV at E_i = 150 and 450 eV according as θ decreases from ~1 to ~0.45 and 0.25 ML, respectively, at the same dosage of ~10^{16} ions/cm^2 [3283]. Here, ϕ^e of Mo is taken as 4.3 eV from our Table 2. For further information, see Footnote 232 below.

[230]From the experiments and data-analyses performed for 25 substrates (mainly pure metals) in Cs-vapor by TE and PSI, the minimum- and heavily-cesiated work functions are estimated to have a range of 1.45 to 1.95 eV, which show no correlation with both the effective vacuum work function (ϕ^e) and chemical property of each substrate species [650,3412].

[231]About the Cs/O/W(100) systems with saturation Cs coverage prepared after oxygen exposure of 1 and 1.5 Langmuirs onto W(100), ϕ^e is measured to be 1.95 and 2.05 eV, respectively, in contrast to 1.78 eV for Cs/W(100) [361,1667].

[232]For the Cs/Be system prepared by Cs$^+$-incidence up to the dosage of 1×10^{16} ions/cm^2 ($\theta = 1.0$ ML), ϕ^e is measured by both PE and CPD, showing the same value of 1.96 eV [3289] (see Section 2.8.2), in contrast to the case of Ar$^+$-bombarded Ag(111) with difference in ϕ^e between PE and CPD [1693] mentioned in Footnote 197. This value is independent of the Cs$^+$-impact energy (E_i) of 8–900 eV because θ is kept at 1.0 ML independently of E_i [3289]. For these substrate systems of Mo (96 amu) and W(183 amu) much heavier than Be (9.0 amu), on the other hand, ϕ^e remains higher by up to ~0.6 and ~1.6 eV above ϕ^e at 45 eV, respectively, as E_i increases from 45–50 up to 300 eV, where θ decreases from 1.0 down to 0.35 and to 0.15 ML, respectively [3289,3815]. At $E_i \leq 50$ eV alone, therefore, ϕ^e at $\theta = 1$ is found to have 1.9 eV for Cs/Mo and Cs/W [3289,3815].

[233]About the systems of Cs/Cu(111) at $\theta = 1$ and 2–4 ML, ϕ^e is theoretically evaluated to be 2.2 and 2.4 eV respectively [3697], both of which are in fair agreement with the experimental results [2512] (see the next Footnote).

[234]About Cs/Cu(111) at $\theta = 1$–2 and 3–4 ML at 200 K, ϕ^e is experimentally determined to be 2.2 and 2.3 eV, respectively [2512].

[235]By both theoretical and experimental studies made for a Cs/C(0001) system, the work function decrease is determined to be 2.19 eV [2782], from which ϕ^e of the system is evaluated to be 2.26 and 2.5 eV by taking ϕ^e = 4.45 eV [286,1174] and 4.7 eV [235,236,525] for C(0001), respectively.

[236]The work function is found to be 2.4 eV for the Cs-intercalated single-walled carbon nanotube bundles deposited on GaAs [291].

[237]The work function of Ba/Si(100) at $\theta = 4.0$ ML is found to be 2.3 eV, which tends to increase gradually with increasing θ, thereby getting close to 2.5 eV for bulk Ba [2170].

[238]For the systems of Ba/glass [1157], Ba/W [1365] and Ba/Ag/Ta [1050], Anderson has assumed or measured the Ba-work function as 2.520 eV [2232], 2.39 ± 0.05 eV [1365] and 2.520 eV [2232], which are corrected to be 2.35 ± 0.03, 2.42 ± 0.05 and 2.66 ± 0.01 eV, respectively, by Rivière [13,349].

[239]About Ba/Si(100), ϕ^e is determined to be 2.7 eV [1732], which may be corrected to be 2.5 eV by taking 4.7 eV [1351] instead of 4.9 eV [1732] for Si(100), thereby yielding a good agreement with our value (2.50 ± 0.02 eV) recommended for Ba in Table 2.

[240]Between Mg and Ba, the difference in ϕ^e is measured to be 1.08 eV [1367], which affords ϕ^e = 3.58 eV for Mg and 2.57 eV for Ba according to our citation of 2.50 eV for Ba and 3.65 eV for Mg, respectively, from Table 2.

[241]By employment of Kelvin and retarding potential methods [2104], ϕ^e = 2.560 and 2.69 eV are determined for Ba/W(100), respectively, and also 2.955 and 3.10 eV are done for Ba/W(110), respectively, clearly showing a difference (~0.14 eV) between the two methods [2104]. The difference can be explained either in terms of two-patch model [2104].

[242]In contrast to the cases of Ba/W(100) and Ba/W(110) [2104] mentioned just above in Footnote 241, ϕ^e of Ba/Ag/Ta is found to be essentially the same values of 2.52 and 2.53 eV by retarding and Kelvin methods, respectively [1050], while ϕ^e = 4.31 eV is determined for Ag/Ta [1050].

[243]At the residual gas pressure of 2×10^{-9} Torr, Ba/W is found to have ϕ^e = 2.6 eV, which increases to 2.7 eV at 3×10^{-7} Torr [3259].

[244]For the systems of Ca/W, Sr/W and Ba/W at ~300 K, ϕ^e is determined to be 2.90, 2.73 and 2.65 eV, respectively, all of which decrease to 2.84, 2.64 and 2.46 eV, respectively, at ~900 K, while Mg/W remains at 3.76 eV [3530].

[245]At $\theta = 10$ ML, ϕ^e is determined to be 2.7 eV for both Ba/W(100) and Ba/Ir(100), in contrast to 1.8 and 1.5 eV for BaO/W(100) and BaO/Ir(100), respectively [2149].

[246]Regarding La/Pt(111) at $\theta = 1.0$–1.2 ML, work function at 77 K is found to be 2.86 eV, which is increased to 5.0 eV by alloy formation after annealing at 900 K [3009]. Here, ϕ^e for Pt(111) is taken as 5.86 eV from Ref. [1351].

[247]About Ce/W [3022], ϕ^e is evaluated to be 2.5 eV at ~300 K according to the temperature dependence of $2.48 + 1.8 \times 10^{-4} T$ determined at 1060–1450 K [3022].

[248]For the systems of Ce/Pd/Ru(0001) at ~300 K with the thickness of 2.8 Å Pd and 5.5 Å Ce and at 6.2 Å Pd and 5.1 Å Ce [3718], ϕ^e is evaluated to be 2.5 ± 0.1 and 2.8 ± 0.1 eV, respectively, by the present author taking 5.4 eV for Ru(0001) from Table 2.

[249]By citing ϕ^e = 5.19 and 5.55 eV for Pd(110) and Pd(111) from Ref. [1351] (see Table 2), the systems of Ce/Pd(110) with 4.8 and 2.1 Å thick [3306] are estimated to have ϕ^e = 3.02 and 3.36 eV, respectively, while those of Ce/Pd(111) with 5.8 and 2.2 Å thick are done to have 3.10 and 3.55 eV, respectively. Due to alloy formation at 970 K, ϕ^e = 4.54 eV is found for the former, while 5.05 or 5.25 eV for the latter [3306].

[250]By citation of ϕ^e = 5.3 eV for Ni(111) from Table 2, ϕ^e of Sm/Ni(111) at 293 K [3000] is estimated to be 2.8 eV, which is increased to 3.3 eV at 800 K by formation of such a surface alloy as $Ni_{17}Sm_2$ [3000].

[251]The values of 3.67 and 3.84 eV correspond to the antiferromagnetic and ferromagnetic surfaces of Gd(0001), respectively [3462].

[252]About La/B/Mo(110) and La/Mo(110), ϕ^e is determined to be 2.8 and 3.4 eV, respectively [2700], while B/La/Mo(110) as well as B/Gd/Mo(110) and B/Mo(110) are done to have the same value of 5.8 eV [2700].

[253]The work function for Gd/B/Mo(110) is 3.0 eV, which is different from 3.5 eV for Gd/Mo(110) [2700], similarly as the above cases mentioned for La/B/Mo(110) and La/Mo(110) in Footnote 252.

[254]The ferromagnetic and paramagnetic surfaces of Gd are theoretically calculated to have ϕ^e = 3.76 and 3.77 eV, respectively [2358] (see Table 13), which are larger than 3.1 eV [304,1045] and also our value of 3.09 eV recommended for Ga in Table 2.

[255]At 1150–1500 K, the temperature dependence is expressed by $\phi^e = A + B \times 10^{-5} T$, where (A, B) is (3.126, 8.0) for Sc, (2.954, 2.0) for Y and (2.975, 6.5) for Er [3071]. Therefore, 3.23, 2.98 and 3.06 eV are evaluated for the respective polycrystals at 1300 K.

[256]The work function of Hf is reported to be 3.53 eV [3524,3527], which is claimed to hold only above 1900 K and also to be 3.20 eV below 1700 K [1756].

[257]For the layers of Hf on W, ϕ^e is measured to be 3.20 eV at 1100 K and 3.92 eV at 2000 K, the latter of which is gradually decreased to 3.70 ± 0.03 eV by formation of Hf–W alloy [1479]. When HfI_4 is deposited onto W at 500 K and decomposed at 1100 K, on the other hand, ϕ^e of the Hf/W system at 1900 K shows 4.00 ± 0.01 eV without forming the alloy [1479].

[258]The work function of Ta(111) is observed to be 4.28 and 4.08 eV after heating at 2100 K by a.c. for firstly 40 h and additionally 50 h until reaching to constancy in ϕ^e, respectively, while it is 4.14 and 4.46 eV after doing so by d.c. for initially 25 h and successively 235 h until so, respectively [729]. Similarly to Mo(100) (see Footnote 168), very long aging of Ta(111) at a high temperature around ~2000 K makes finally ϕ^e constant at 4.08 ± 0.03 or 4.46 ± 0.03 eV [729]. The former is close to 4.01 ± 0.04 eV recommended for Ta(111) (Table 2).

[259]With respect to Ta(130), ϕ^e is determined to be 3.96 eV without annealing, while it is 4.57 eV with annealing up to 1670 K after argon ion impact at 200–2000 eV [680].

[260]At 4.2 K below the superconducting transition temperature (T_S = 4.4 K), ϕ^e for Ta-film on quartz is found to be 3.8 ± 0.2 eV, while it is 3.5 ± 0.2 and 3.8 ± 0.2 eV at 35 and 293 K, respectively [1686]. This result does not show clearly how ϕ^e alters at T_S. In addition, any of the three values for the film by CPD is smaller than ϕ^e = 4.16 eV at 4.2–35 K for bulk Ta by FE [1686]. In considering the temperature dependence of ϕ^e (~10^{-5} eV/K for Ta, see Table 6 in Ref. [1351]), it may be necessary to measure ϕ^e continuously at a meV level in order to determine precisely a probably very minute change (<0.1 eV) around T_S (see Section 9 and Table 14).

[261]According to the Schottky equation (22) (see Section 8.1 in Ref. [1351]) of $\phi^- = E^- - E^0 + E = 11 - 7.94 + E$ [804], ϕ^- for Ta is determined to be 3.7 ± 0.4 and 3.9 ± 0.3 eV by taking the electron affinity (E) of 0.6 ± 0.4 eV [578] and 0.8 ± 0.3 eV [946], respectively. Here, E^- and E^0 are the desorption energies of Ta$^-$ and Ta^0, respectively. In the case of self-NSI, E^- can hardly be determined correctly owing to the space-charge effect due to much stronger thermal electron emission. For production of Ta$^+$ by self-PSI [77,804,805,3083], see Footnote 271.

[262]By critical analysis of the experimental data about Mo by both TE (4.15 eV at ~1400–2000 K) and PE (4.14 eV at 303 K and 4.16 eV at 940 K) [338], Becker deduces ϕ^e = 4.18 eV from TE [3586], well agreeing with 4.16 eV based on PE (4.14 eV at 303 K and 4.16 eV at 940 K) [338] at the same temperature of 940 K in spite of the difference in the two methods.

[263]By theoretical analysis of the experimental data on 4.73 and 4.56 eV obtained for Ag at 298 and 873 K, respectively [3391], Fowler finds 4.73 and 4.75 eV at 296 and 873 K, respectively [1135], the former agreeing excellently between experiment and theory, in contrast to the latter at the higher temperature.

[264]With respect to Pd at ~1200–1400 K, the work function value (4.99 ± 0.04 eV) obtained by TE [1189] is theoretically analyzed by Becker to estimate ϕ^e = 4.997 and 4.966 eV at much lower temperatures (typically, 925 and 400 K) [3586], the respective values of which well agree with 4.98 and 4.97 eV measured by PE [1189]. In other words, ϕ^e for Pd by TE may be extrapolated to be 4.985 ± 0.016 eV at 305–1078 K [3586].

[265]Similarly as above (Footnotes 217 and 218 for Sn and 263 for Ag), Fowler analyzes theoretically the experimental data on 4.12–4.13 eV at 293 K and 4.18–4.19 eV at 973 K observed for Ta by PE [1633,1636], and yields 4.10–4.13 eV and 4.14–4.18 eV at the respective temperatures [1135], fairly agreeing with each other between the two methods.

[266]By theoretical analysis of the data (4.12 ± 0.04 eV) obtained for Ta at ~1450–2050 K by TE [792], Becker yields ϕ^e = $4.07 + 6.0 \times 10^{-5}\,T$ [3586], which affords 4.09 and 4.13 eV at 293 and 973 K, respectively [3586]. The respective values thus extrapolated are in good agreement with the above values (4.10 and 4.14 eV, see Footnote 265) evaluated theoretically by Fowler [1135] from the experimental data achieved by PE [1633].

[267]About the Ta specimen consisting of 70%–(112) face [124], ϕ^e is calculated to be 4.15 eV [1254], which is smaller than the experimental value of 4.25 ± 0.05 eV determined by TE [124,650].

[268]With regard to the 82%–(112)-oriented Ta surface [3414], ϕ^e is determined experimentally to be 4.25 eV by TE [3414], whereas theoretical calculation yields ϕ^e = 4.34 ± 0.03 eV and ϕ^+ = 4.49 ± 0.04 eV [803].

[269]The values of ϕ^- = 4.22, 4.23 and 4.28 eV are determined at 2125 K by simultaneous two–electron capture of the ions of Br$^+$, I$^+$ and Cl$^+$ on Ta, respectively [600,641], where the incident beam flux is correctly countable and, hence, the negative surface ionization efficiency (β^-) by NSI (see Eq. (6)) is more readily determinable compared with the case of neutral halogen beam incidence. In fact, each of the above three values is very close to our recommended ones of ϕ^- = 4.17 ± 0.13 eV and also ϕ^e = 4.20 ± 0.03 eV (see Table 2).

[270]Instead of probing beam incidence upon Ta, W or W(110), the vacuum tube is filled with sodium vapor after evacuation below ~10^{-9} Torr [81,85,87]. Typically, the vapor pressure is ~2×10^{-5} Torr [81]. Thus, ϕ^+ = 4.64, 4.95 and 5.14 eV are determined for Ta [81], W [85] and W(110) [85,87], respectively. About a Na/W(110) system, see Footnote 280.

[271]By production of Ta$^+$ by self-PSI of Ta at very high temperatures (≥2000 K), the effective work function is estimated from Eq. (9). Namely, $\phi^+ = E^0 + I - E^+ = 7.94 + 7.88 - 11.18 \pm 0.1 = 4.64 \pm 0.14$ eV [804], where I is the ionization energy of tantalum atom. In the same way, ϕ^+ is determined to be 5.0 ± 0.5 eV for Ta [77], while ϕ^+ = 5.02 ± 0.11 eV is evaluated from the data on Ta$^+$ produced by self-PSI of Ta independently of Eq. (9) [805,3083]. For production of Ta$^-$ by self-NSI [804], see Footnote 261.

[272]Similarly as above [804] in Footnote 271, ϕ^+ for Ta is evaluated from $E^0 + I - E^+ = 7.97 \pm 0.03 + 7.88 - 10.0 \pm 0.3 = 5.85 \pm 0.3$ eV, where E^0 and I are cited from literatures. However, E^+ = 10.0 eV [137] is unreliable because positive ionic species is not assigned to be Ta$^+$ alone by mass spectrometry.

[273]The work function of W(100) at 1900 K is found to decrease from 4.61 to 4.53 eV as the dislocation density increases from $(4–5) \times 10^6$ to 1×10^8/cm^2 [651].

[274]For the (100) surface of Re (y-atomic %)–W alloys at ~1600–2300 K, two groups of workers [438,3086] and [353] find ϕ^e = 4.54 eV at y = 1% [3086], 4.56 eV at 2% [353], 4.52 eV at 5% after 40–50 h annealing at 2200 K [438] and 4.59 eV at 6% [353], all of which are nearly the same with 4.55 eV for pure W(100) [353], with little dependence upon y = 1–6%.

[275]About the (100) face of 2% Ir–W alloy [3086], ϕ^e is observed to be 4.54 eV at ~1800–2000 K, apparently correspondent to pure W(100). At ~2000–2200 K, on the other hand, ϕ^e increases to 5.28–5.30 eV, showing the same property of Ir (5.28 ± 0.04 eV, see Table 2) and hence suggesting the entire surface covering by Ir-spillover.

[276]Regarding the (100) surface of 1% Os–W alloy [3086], ϕ^e is measured to be 4.57 eV at ~1700–2000 K, corresponding to pure W(100). On the other hand, ϕ^e becomes 5.12 eV at ~2100–2300 K [3086], closing to 4.97 ± 0.17 eV for pure Os (see Table 2).

[277]With respect to the almost (100)-oriented W specimens [124,650,3414], ϕ^e is experimentally determined by TE to be 4.50 ± 0.07 eV [650] and 4.52 ± 0.07 eV (see Footnote 300) [124,3414]. On the other hand, ϕ^e is calculated to be 4.78 eV [1254]. The specimens are theoretically studied in detail by the present author (see Footnotes 300–302, and also both W(F) and W(G) in Table 6).

[278]Similarly as in Footnote 271, Schottky equation (9) is employed to evaluate ϕ^+ of W(100) by PSI of Cs. Namely, $\phi^+ = E^0 + I - E^+ = 2.77 \pm 0.05 + 3.89 - 2.05 \pm 0.05 = 4.61 \pm 0.07$ eV, which well agrees with ϕ^e = 4.65 ± 0.02 eV [266,2314–2316]. By the same way, ϕ^+ is evaluated to be 4.72 eV from $2.83 + 3.89 - 2.00$ eV by PSI of Cs on W(100) [265]. Similarly, ϕ^+ is estimated to be $2.61 \pm 0.07 + 3.89 - 1.84 \pm 0.09 = 4.66 \pm 0.11$ eV by PSI of Cs on W(100), well agreeing with ϕ^e = 4.60 ± 0.06 eV for W(100) by TE [280].

[279]Both PSI and NSI of Na$^+$ and Cl$^-$ from NaCl on W(110) yield $\phi^+ = \phi^- = 4.609 \pm 0.014$ eV [89] and 4.66 ± 0.09 eV [3690], which are much smaller than ϕ^e = 5.18 ± 0.08 eV by TE [89]. The discrepancy (~0.5 eV) between ϕ^+ and ϕ^e is mainly attributable to the fact that the ionization energy (I = 5.14 eV) of Na is smaller than $\phi^+ = \phi^e$ = 5.3 eV (generally expected) for clean W(110). It should be emphasized that the temperature dependence of ionization efficiency (β^+) for Na is generally insensitive to the actual value of work function unless $I > \phi^+$ (see pp. 76 and 77 in Ref. [1351]). In order to avoid such a systematic error due to the insensitivity, not NaCl but TlCl, for example, should have been adopted, where I = 6.11 eV for Tl is much larger than ϕ^+.

[280]By PSI of Ba on W(110), ϕ^+ is found to be 4.82 eV [87], which is much smaller than $\phi^e = 5.04$ or 5.30 eV [87]. The discrepancy (=0.2–0.5 eV) may be principally because the ionization energy ($I = 5.21$ eV) for Ba is not larger than ϕ^+ (~5.3 eV) and hence PSI is affected by the insensitivity mentioned just above in Footnote 279. Quite similarly, ϕ^+ is underestimated to be 5.14 eV (=I for Na) by PSI of Na on W(110) [87].

[281]With respect to W(110) at ~300 K by CPD, ϕ^e is measured to be 5.05 eV, which is increased to 5.15 eV by annealing at 2500 K for 20 h in O_2 at ~10^{-6} Torr [815].

[282]For the (2–4) overlayers of W(110) on Mo(110), ϕ^e is theoretically evaluated to be 5.10 ± 0.01 eV [2074], which is in good agreement with the theoretical value of 5.10 eV for bulk W(110) [2073,2074]. But, they are lightly smaller by 0.10–0.22 eV than any values (5.20–5.32 eV) recommended for W(110) in Table 2.

[283]The actual work function of W(110) is estimated to be $\phi^e = 5.2$ eV instead of 5.1 eV [2774] by the authors [2773,3768] considering a slight underestimation (by 0.1 eV) by a photoemission method [2774]. Consequently, $\phi^e = 5.2$ eV agrees with $\phi^+ = 5.2$ eV by PSI of fast Na atom (100 eV) incident on W(110) [2773,2774], thereby yielding $\Delta\phi^* = \phi^+ - \phi^e = 0.0$ eV just as expected by theory and experiment for clean monocrystalline surfaces (see Table 5). However, the above estimation seems to admit a question (for the detail, see Section 2.8.2).

[284]By applying Schottky equation (9) to PSI of Cs on W(110), the author [2314] mentioned in Footnote 278 determines $\phi^+ = 3.28 + 3.89 - 2.06 = 5.11$ eV, which is smaller than our recommended value of 5.28 ± 0.11 eV (see Table 2). On the other hand, ϕ^e is observed to be 5.33 ± 0.04 eV [2314], equal to our value of 5.32 ± 0.02 eV. The difference ($\Delta\phi^* \equiv \phi^+ - \phi^e = -0.22$ eV $\neq 0$ eV) suggests that some systematic errors are accompanied for E^+ and E^0 included in the equation. This result shows a large contrast to the case reported for PSI of Cs on W(100) by the same author who finds little difference between $\phi^+ = 4.61 \pm 0.07$ eV and $\phi^e = 4.65 \pm 0.02$ eV [266,2314–2316], as already mentioned in Footnote 278.

[285]By incidence of hyperthermal Na atom (0.5–9 eV) on W(110), ϕ^+ is determined to be 5.17 ± 0.01 eV [154,260] or 5.19 ± 0.01 eV [3768] at 1180 K. Similarly, $\phi^+ = 5.2$ eV is measured by 100 eV–Na incidence at ~300 K [2773,2774] (see Footnote 283).

[286]By production of W^+ by self-PSI of W(110), ϕ^+ is evaluated from Schottky equation (9). Namely, $\phi^+ = E^0 + I - E^+ = 8.79 + 7.98 - 11.31 \pm 0.11 = 5.46 \pm 0.11$ eV [146]. Here, the desorption energy of tungsten atom is evaluated from the data compiled in JANAF Thermochemical Tables [26].

[287]By thermal-field emission from W(111), ϕ^e is determined to be 4.43 eV at 80–500 K, while ϕ^e is 4.38 eV at 800–1300 K, according to dϕ/d$T < 10^{-5}$ eV/K [3440].

[288]The work function data on W having various orientations are compared between Refs. [920] and [150], thereby concluding $\phi^e = 4.42 \pm 0.05$ eV for W(114) [920]. Here, 4.17 eV is estimated as the reference work function of Fe(100) [920] (see also Footnote 110).

[289]Among the various single crystals grown in W-wire adopted for experimental study of thermionic emission from different planes, W(110) is estimated to have $\phi^e = 5.26$ eV by subtraction of spurious current to give 120 A/cm^2 K^2 just as the theoretical value of the Richardson constant (A_R) [150]. Both values are quite different really from own experimental data of (ϕ^e, A_r) = (4.58, 8.0) and (4.66, 12) [150]. Tentative substitution of the data into Eq. (8) in Section 2.8.6, on the other hand, yields 5.0 eV, smaller than the value estimated above.

[290]For W(123) and W(235), ϕ^e is found to decrease from 4.90 to 4.50 eV and from 4.72 to 4.30 eV, respectively, by the increase from 80–400 K up to 1200 K [2045]. Similarly for W(257), ϕ^e decreases from 5.00 to 4.80 eV according to the increase from 80–900 K to 1200 K [2045]. Each of the values at 1200 K seems to be nearer to the most probable one for each surface. Typically for W(123), 4.50 eV [2045] is the same with our value of 4.50 ± 0.05 eV (see Table 2).

[291]About the fine tungsten particles with the radius of ~8 and ~40–90 Å, ϕ^e is calculated to be 3.65 and 4.75 eV for real sphere, respectively, in contrast to the respective values of 3.80 and 4.40 eV for cube [2973]. As shown typically as above, ϕ^e changes according to the size, structure and shape of the particles [2973] (for detail, see Section 11.1).

[292]In the magnetic field of 10 kOe, the Fowler–Nordheim plots for W yield $\phi^e = 4.2$ and 4.6 eV above and below the applied voltage of 6 kV, respectively [1493]. In that of 15 kOe, the respective values are 4.25 and 4.35 eV, again different from 4.5 eV taken in absence of the field [1493].

[293]For the W/glass systems (50 Å thick) prepared at 77–90 K, ϕ^e is increased from 4.33 to 4.55 eV by annealing at 403 K [3049], and similarly from 4.36 to 4.63 eV at 438 K [2095], thus approaching to the bulk work function of 4.56 ± 0.03 eV (see Table 2).

[294]The work function of W is found to be 4.6 and 4.62 eV at $P_r = 2 \times 10^{-7}$ Torr and $P(Ar) = 12$ Torr, respectively, while ϕ^e is decreased to 4.42 ± 0.02 eV by ion impact in a high-current glow discharge in Ar [621].

[295]On the basis of such a patchy surface model that W consists of four faces of W(111), W(100), W(112) and W(110) having the local work function (ϕ_i) = 4.35, 4.56, 4.69 and 5.35 eV, respectively, with the fractional area (F_i) = 25% for each face [3843], ϕ^+ is calculated to be 4.51 eV from the ionization efficiency (β^+) = 0.954 for Cs at 2000 K, as shown in Fig. 1 [3843]. Under the same condition, on the other hand, ϕ^e and ϕ^+ are calculated to be 4.46 and 5.12 eV from Eqs. (2) and (1) by the present author, respectively, while $\phi^a = 4.74$ eV calculated from Eq. (4) is intermediate between ϕ^e and ϕ^+, just as predicted by theory [3844].

[296]Similarly as in Footnote 286, ϕ^+ is determined from the data on self-PSI of W according to Schottky equation (9). Namely, $\phi^+ = E^0 + I - E^+ = 8.44 + 7.98 - 11.93 \pm 0.14 = 4.49 \pm 0.14$ eV [823], which is much smaller than our value of $\phi^+ = 5.17 \pm 0.05$ eV for W (see Table 2) but rather near to ours of 4.62 ± 0.06 eV for W(100) (see Table 2). On the other hand, $\phi^e = 4.59 \pm 0.04$ eV [823] is essentially the same with our value of $\phi^e = 4.56 \pm 0.03$ eV for W and near to ours of 4.65 ± 0.02 eV for W(100) (see Table 2). Suppose that the W-specimen [823] is already changed mainly to W(100) by re-crystallization due to aging at high temperatures up to ~3000 K for a long time before the work function measurements, then, both of ϕ^+ and ϕ^e are generally expected to be near to ~4.6 eV (see Table 2). If so, both of the above values [823] may be accepted to be reasonable. If not so, on the other hand, the above result ($\phi^+ = 4.49$ eV $< \phi^e = 4.59$ eV) suggests that the measurements of E^+ as well as E^0 are accompanied with the systematic error of up to ~0.7 eV ($\approx \phi^+ - \phi^e$) mainly for E^+. About such re-crystallization as mentioned above, further information may be obtainable from Section 4.5 in Ref. [1351].

[297]The work function effective for negative ion emission by self-NSI of W is evaluated from the Schottky equation [966], thereby yielding $\phi^- = E^- - E^0 + E = 12.6 - 8.9 + 0.8 = 4.5$ eV. Here, the electron affinity (E) is cited by the present author from Refs. [972], [3957] and [3958], where $E = 0.815$–0.816 eV for W-atom is determined experimentally from negative ion photodetachment threshold. In addition, the data on self-PSI of W afford that $\phi^+ = E^0 + I - E^+ = 8.9 + 7.98 - 12.1 \pm 0.15 = 4.8 \pm 0.2$ eV [966], thereby yielding $\Delta\phi^* \equiv \phi^+ - \phi^e = \phi^+ - \phi^- = 4.8 - 4.5 = 0.3$ eV. This is smaller than our value of 0.6 eV for W (see Table 5). The decrease from 0.6 to 0.3 eV suggests that a considerable part (δ_m) of the tungsten surface is recrystallized to W(100) by high-temperature heating up to ~3000 K during measurements (see Fig. 1 for the relation between $\Delta\phi^*$ and δ_m).

[298]Both W and W_2C are found to have almost the same work functions of 4.5 ± 0.07 and 4.58 ± 0.08 eV, respectively [3533].

[299]The same value of $\phi^e = \phi^- = 4.51$ eV (or $\phi^- = 4.49$ eV for I-incidence) is determined for W [827], yielding $\Delta\phi^{**} \equiv \phi^- - \phi^e = 0$ eV, just as predicted by theory. Further information about the thermionic contrast ($\Delta\phi^{**}$) is obtainable from Table 7.

[300]Each W-surface consisting of 95 or 96%-W(100) and of the remainder with almost W(111) is determined experimentally to have $\phi^e = 4.52 \pm 0.07$ eV [124]. The latter taken as 96%-(100) and 4%-(111) is theoretically calculated to have $\phi^e = 4.59 \pm 0.04$ eV [630,2453], which is very close to the above experimental value [124]. However, both are smaller by $\Delta\phi = 0.13$ or 0.06 eV than $\phi^e = 4.65 \pm 0.02$ eV recommended for 100%-W(100) (see Table 2). This smallness is quite reasonable because $\phi^e = 4.45 \pm 0.03$ eV for W(111) (Table 2) is smaller by 0.20 eV than the above for W(100). In other words, only 4%-W(111) has a considerable contribution to lowering the work function of the 96%-W(100) specimen by $\Delta\phi \approx 0.1$ eV. On the contrary, our theoretical value of $\phi^+ = 4.60 \pm 0.04$ eV for the specimen [630,2453] is virtually the same with 4.62 $\pm$ 0.06 eV for 100%-(100) (Table 2). This result shows that 4%-W(111) with the work function smaller by 0.20 eV compared with W(100) has little contribution to lowering ϕ^+. This is mainly because positive ion is emitted predominantly from the higher work function face (100), in contrast to electron done so from the lower one (111) (see Section 1).

[301]For the W-surface consisting of 95%-(100), 1%-(110), <1%-(111) and 2%-(112) faces [3414], ϕ^e is theoretically evaluated to be 4.57 $\pm$ 0.00 eV [803] and 4.61 $\pm$ 0.04 eV [2453], the former of which is closer to $\phi^e = 4.52$ eV determined experimentally for the surface [3414]. Both are smaller by 0.04–0.08 eV than $\phi^e = 4.65 \pm 0.02$ eV for 100%-W(100) recommended in Table 2. This result, however, is quite natural because the (110) and (112) faces have the respective values of $\phi^e = 5.32 \pm 0.02$ eV and 4.78 $\pm$ 0.03 eV (Table 2), higher than 4.65 $\pm$ 0.02 eV for the (100) face. Consequently, both of the former have the smaller contribution to electron emission compared with the latter. On the other hand, the work function (ϕ^+) effective for positive ion emission from the 95%-W(100) specimen is calculated to be 4.69 $\pm$ 0.05 eV [803] and 4.70 $\pm$ 0.04 eV [2453], both of which are slightly larger by 0.07–0.08 eV than $\phi^+ = 4.62 \pm 0.06$ eV for 100%-W(100) (Table 2), on the contrary to the above case where ϕ^e is smaller by 0.04–0.08 eV. Again, this is reasonable because the (110) and (112) faces with larger work functions ($\phi^+ = 5.28 \pm 0.11$ and 4.70 $\pm$ 0.01 eV, see Table 2), compared with the (100) face ($\phi^+ = 4.62 \pm 0.06$ eV), have the larger contribution to positive ion emission in comparison with the latter.

[302]About the W-specimen having the surface composition of 95%-(100), 2%-(112), 1%-(110) and <1%-(111) [3414], ϕ^e is experimentally determined to be 4.52 eV in vacuum ($\sim 10^{-9}$ Torr) and 4.5 eV as the "clean" cesiated work function in Cs-vapor [3414]. Theoretical evaluation of both ϕ^e and ϕ^+ for the specimen is summarized in Footnote 301. It should be noted that this 95%-(100) specimen [3414] is different from another 95%-(100) one with the remainder consisting of almost (111) face [124], although the experimental value of $\phi^e = 4.52$ eV is the same between the two. With respect to the theoretical values of ϕ^e and ϕ^+, see Footnotes 300 and 301 and also W(F) in Table 6.

[303]By critical analysis of work function data obtained for W by several methods by many groups of workers, $\phi^e = 4.54_5$ eV for well-aged polycrystalline tungsten is recommended as the reference for CPD at $\sim$300 K by Hopkins and Rivière [828].

[304]By PSI of In on W at $\sim$2300–2700 and 2350 K, ϕ^+ of W is determined to be 5.05 $\pm$ 0.05 and 5.10 eV from the slope of a semi-Saha–Langmuir plot (see Section 4.2.1 in Ref. [1351]) and from the ionization efficiency (β^+) (see Eq. (6) in Ref. [1351]), respectively [94]. It should be emphasized that In has the ionization energy of $I = 5.79$ eV, larger than $\phi^+ = 5.10$ eV mentioned above and also than our value of 5.17 $\pm$ 0.05 eV (Table 2), thereby making it reasonable to employ the above plot. In addition, ϕ^e is measured to be 4.58 $\pm$ 0.05 eV by TE at 2300 K [94], consequently affording $\Delta\phi^* = \phi^+ - \phi^e = 0.47 \pm 0.07$ eV or 0.52 $\pm$ >0.05 eV (see Table 4).

[305]Regarding the W/Mo(100) system with $\theta = 0.6$–1.0 ML, ϕ^e at 77 K is determined to be 4.6 eV, which is increased to 4.7 eV by annealing up to 1300 K [2965].

[306]From the temperature dependence of Na$^+$ and Ag$^+$ currents originating from PSI of NaCl and Ag, ϕ^+ of W is determined to be 4.6 $\pm$ 0.1 and 5.16 $\pm$ 0.1 eV, respectively [3113], which are much smaller than and substantially equal to, respectively, our recommended value of $\phi^+ = 5.17 \pm 0.05$ eV (Table 2). In contrast to Ag (ionization energy, $I = 7.54$ eV), Na (5.14 eV) does not satisfy the prerequisite condition ($I \geq \phi^+ + 0.3 \simeq 5.5$ eV) for semi-Saha–Langmuir plot (Section 4.2.1 in Ref. [1351]). This may be the main reason for the above result. It should be noted that the by-production of Na$_2$Cl$^+$ is as small as $\sim 1 \times 10^{-4}$ in comparison with Na$^+$, consequently giving no effect to the above result.

[307]From the experimental data on W$^+$ and W$^-$ produced by self-PSI and self-NSI, respectively [965], the present author estimates $\phi^+ = 4.65 \pm 0.4$ eV, where he takes $E = 0.6 \pm 0.4$ eV for electron affinity of W [578] and also does $\phi^- = \phi^e = 4.55$ eV instead of $\phi^- = \phi^+ = 4.55$ eV [965] because of $\phi^- \neq \phi^+$ and of $\phi^e \neq \phi^+$ for any polycrystalline specimen (see Tables 4, 5 and 7).

[308]About the W-layers prepared by chemical vapor deposition (CVD) of WF$_6$ and WCl$_6$ together with H$_2$ onto Mo (or Nb, Ta or W), ϕ^e is measured to be 4.66 and 4.67 eV, respectively [1398], the former of which is increased slightly to 4.72 eV by electro-etching [1398]. This is close to 4.75 eV for bulk-W after the etching, instead of 4.68 eV for the bulk before the etching [1398].

[309]The system of W/W(100) prepared by CVD of WF$_6$ and H$_2$ at $\sim$1850–2450 K is determined to have $\phi^e = 4.69$ eV, which is changed to 4.71, 4.51, 4.59 and 4.98 eV by lightly electropolishing, both grinding and electropolishing, both grinding and 3h-heating at 2300 K, and chemically etching in NaOH-solution, respectively. The surface with 4.51 eV consists mainly of sections of grains oriented close to (100) [1053]. Similarly, W/W(110) done by WCl$_6$ and H$_2$ is found to have 4.66 eV, which changes to 4.47, 4.88 and 5.03 eV after electropolishing, both grinding and 3h-heating at 2600 K, and both grinding and electropolishing, respectively [1053]. In addition, W is deposited onto ground W(100) and W(110), both of which are observed to have 5.16 eV [1053]. This is very close to 5.13 and 5.15 observed for W(110) after both abrading and heating at 2800 K [1053], as outlined in Footnote 310 below.

[310]Under the same condition as above (Footnote 309), ϕ^e is measured to be 5.22 eV for W(110) after electropolishing or next heating at 2400 K for 16 h, and also to be 5.13 or 5.15 eV after both abrading and heating at 2800 K for 3 h [1053]. In addition, ϕ^e is determined to be 5.06 eV for W/W(110) prepared by W-deposition [1053]. This value is slightly lower than those for the above bulk surfaces subjected to several processing, but much larger than 4.54 eV found for the electropolished W(100) and W(111) faces [1053].

[311]With respect to the W-surface consisting fractionally of 80%-(110), 14%-(100), 5%-(112) and 1%-(111) [162], ϕ^e is theoretically evaluated to be 4.90 $\pm$ 0.05 eV [630] and 4.87 $\pm$ 0.06 eV [2453], both of which are near to 5.0 $\pm$ 0.2 eV determined after outgassing at temperatures up to 2600 K over 8 h [162] and also to 4.82 $\pm$ 0.02 eV done after heating at 2400 K for 17 h [162]. Theoretical evaluation of ϕ^+ yields 5.25 $\pm$ 0.02 eV [630] and 5.26 $\pm$ 0.02 eV [2453], thereby leading to $\Delta\phi^* = \phi^+ - \phi^e = 0.35 \pm 0.07$ eV [630] and 0.39 $\pm$ 0.07 eV [2453], respectively (see Table 4). For further information about the surface, see W(E) in Table 6.

[312]By PSI of KCl, KBr or KI on W, ϕ^+ is determined to be 4.65 $\pm$ 0.05 eV [46], which is corrected to 4.95 eV [3747] by theoretical analysis of the data on PSI of KCl [46].

[313]From the experimental data on PSI of NaCl on W, ϕ^+ is evaluated to be 4.82 eV [47], which is corrected to 5.05 eV [3747] by theoretical analysis of the data [47]. The latter is closer to our recommended value of $\phi^+ = 5.17 \pm 0.05$ eV (see Table 2).

[314]By NSI of KI on W, ϕ^- is determined to be 4.95 $\pm$ 0.05 eV [183], which is much larger than $\phi^- = 4.46$–4.58 eV [574,586,827,966] (see Table 7), and than our value of $\phi^- = 4.51 \pm 0.03$ eV (Table 2), and also than ϕ^e (=ϕ^- in general, see Table 7) = 4.56 $\pm$ 0.03 eV (Table 2). On the other hand, PSI of Cu and Ag on W yields $\phi^+ = 5.25 \pm 0.05$ eV [183], fairly agreeing with our value of $\phi^+ = 5.17 \pm 0.05$ eV (Table 2).

[315]In the strong electric fields of $F \approx 6 \times 10^4 - 1 \times 10^6$ V/cm [155,156] and $3 \times 10^3 - 2 \times 10^6$ V/cm [157], PSI of Li [155], NaCl and LiCl [156] and In and Tl [157] is performed on W at $\sim$1600–2700 K, thereby yielding $\phi^+ = 4.82$ and 5.12 eV [155], 4.83 and 5.11 eV [156], and 5.15 and 5.12 eV [157]. In these cases, the slope of semi-Saha–Langmuir plot is given by $\phi^+ + e(eF)^{1/2} - I$ [2], where I is the ionization energy of incident atom such as Li, In or Tl. In usual PSI, the Schottky term can be neglected since $e(eF)^{1/2}$ is less than 0.012 eV for $F < 1$ kV/cm [2]. In self-NSI of metals (typically, W and Re [966]) at very high temperatures, the term must be considered in general because F is usually applied so strongly as to overcome the space charge effect due to much stronger electron emission current accompanied with the negative metal ion current under study.

[316]Re is electroplated onto W in solution of KReO$_4$ [666], thereby resulting in 4.74 eV.

[317]This is a capillary type ion source consisting of six Re-wires ($\phi^+ = 4.9$ or 5 eV) in a Ta-tube [2944].

[318]From the experimental data on Re$^-$ produced by self-NSI of Re at high temperatures [966], the present author evaluates $\phi^- = E^- - E^0 + E = 12.55 \pm 0.15 - 7.8 \pm 0.15 \pm 0.10 \approx 4.9 \pm 0.2$ eV, where the electron affinity (E) of Re is cited from Ref. [578]. Similarly for Re$^+$ [966], ϕ^+ is estimated from $E^0 + I - E^+ = 7.8 + 7.87 - 10.72 \pm 0.12 \approx 5.0 \pm 0.1$ eV.

[319]With regard to Re/Mo prepared by CVD of ReCl$_3$ and H$_2$ on Mo, ϕ^e is determined to be 4.82 eV, which increases to 4.94 eV after electroetching [1398].

[320] The Re-surface composed of various patchy faces [3414] is found to have 4.8 eV as the "clean" cesiated work function in Cs-vapor [3414], but 4.96 ± 0.05 eV in vacuum [124,650,3414], exactly the same with our recommended value (Table 2).

[321] This Re-surface is prepared by electrolytic coating on W with ~1500 atomic layers [1850]. Its work function (5.0 eV) is virtually the same with ours (Table 2).

[322] To evaluate ϕ^- for Re [216], the electron affinity of CN is taken as 3.7 ± 0.2 eV from Ref. [930]. The result of $\phi^- = 5.06 \pm 0.1$ eV is essentially equal to 5.03 ± 0.1 eV by NSI of Cl and also to $\phi^e = 5.0 \pm 0.1$ eV for Re [99,216].

[323]The Re-film (2 nm thick) prepared on 6H-SiC(0001) ($\phi^e = 4.5 \pm 0.1$ eV) at ~300 K or annealed at ~500 K is found to have $\phi^e = 5.2 \pm 0.1$ eV, and decreases by ~0.4 eV after further annealing at 700 K [3646].

[324]The Re-surface ($\phi^e = 5.35 \pm 0.05$ eV) appears to be covered with oxygen at ~0.5 ML [166,3730], thereby being larger than the generally accepted value of about 5.0 eV (see Table 2).

[325]The work functions of 5.93 and 5.50 eV for Os and Ir, respectively [3322], are determined by another worker in the same laboratory [3536].

[326]For stepped faces of Ir(100), ϕ^e is determined by FE to be 5.2 and 5.4 eV [1810], which are lower than 5.70 ± 0.05 eV for a perfect face of Ir(100) [1797,1802]. The latter is near to our value of 5.60 ± 0.06 eV (Table 2). According to increase in step density, ϕ^e decreases in general, as already outlined in Section 4.2.5 [1351].

[327]The normal (1 × 1)Ir(100) with $\phi^e = 5.5$ eV [1534,1553,2961] is changed to the reconstructed (1 × 5)Ir(100) with 5.4 eV by heating above 1200 K [2961].

[328]Regarding the Ir surface consisting of 81%-(111), 15%-(100) and <3%-(110) faces [650,3414], ϕ^e is theoretically evaluated to be 5.36 ± 0.07 eV [803], which is slightly larger than the experimental value of 5.27 ± 0.05 eV [650,3414], but considerably smaller than ours (5.75 ± 0.06 eV for 100%-(111) face, see Table 2). This may be mainly due to the co-existent (110) face having the smallest value of 5.23 ± 0.19 eV (Table 2) among the three faces. On the other hand, the theoretical value of $\phi^+ = 5.73 \pm 0.01$ eV [803] for the above patchy surface [650,3414] is essentially the same with our value of 5.76 ± 0.04 eV for 100%-(111) surface (Table 2). Namely, the lower work function faces oriented with (110) and (100) have little contribution to ϕ^+ effective for positive ion emission, on the contrary to the above ϕ^e effective for electron emission occurring predominantly from lower work function faces.

[329] About the Ir-surface with 80%-(111) and 15%-(100) oriented [124], ϕ^e is calculated to be 4.68 eV [1254], which is smaller than 5.27 ± 0.05 eV determined experimentally [124]. Regarding almost the same surface of Ir [650,3414], see Footnote 328 just above.

[330]The "clean" work function of Ir-surface with 81%-(111), 15%-(100) and <3%-(110) oriented at ~1400–2200 K in Li-vapor ($\leq 2.5 \times 10^{-4}$ Torr) is measured to be $\phi^e = 5.35 \pm 0.05$ eV [169], which is larger than 5.2 eV for the "clean" cesiated one [3414] and also than 5.27 eV found in vacuum [650,3414], but which is essentially the same with our calculated value of 5.36 ± 0.07 eV [803]. For additional information, see Footnote 328. About PSI of Li, $\phi^+ = 5.4$ eV is evaluated from the data in Fig. 5 [169], from which $\beta^+ = 0.34$ at ~1100 K is selected by the present author.

[331]The work function of a 6 × (100) stepped surface of Pt is calculated to be 5.93 eV, which is smaller than 6.07 eV for a flat one [795]. Such a difference is found for Pd(100), too (see Footnote 182). For further information about stepped surfaces, see Section 4.2.5 [1351].

[332]A rough surface of Pt(110) is determined to have $\phi^e = 5.24$ eV, which is smaller than 5.35 eV for a smooth one [853]. Such a difference as ~0.1 eV depending upon surface roughness is observed for Rh(110), too [853] (see Footnote 177).

[333]With respect to the unreconstructed (1 × 1) and reconstructed (1 × 2) Pt(110) surfaces, ϕ^e is theoretically evaluated to be 5.52 and 5.71 eV, respectively [2543], the former of which is the same with our value of 5.54 ± 0.07 eV (Table 2).

[334]By three different experimental methods of ionic emission, atomic desorption and mean residence time of Li-atom incident upon Ir(111) at ~1100–1400 K, ϕ^+ is determined to be 5.68 ± 0.01, 5.69 ± 0.03 and 5.72 ± 0.03 eV, respectively, which yield the average of 5.70 ± 0.02 eV [167], well agreeing with our recommended value of $\phi^+ = 5.76 \pm 0.04$ eV for Ir(111) (see Table 2). Similarly, the respective methods applied to Pt(111) at ~1200–1500 K afford 5.80 ± 0.02, 5.76 ± 0.02 and 5.75 ± 0.02 eV and, hence, yield the mean of 5.77 ± 0.02 eV [167,319]. Again, this is in good agreement with our value of $\phi^+ = 5.80 \pm 0.06$ eV (Table 2).

[335]Onto the Pt(111) surface determined to have 5.84 ± 0.05 eV [421–423,773], Pt is deposited at 130 K, forming a highly disordered and complex surface ($\phi^e = 5.64$ eV) dominated probably by clusters. At 250 K, ϕ^e continues to decrease according to $\theta^{1/2}$-dependence down to about 5.7 eV at $\theta = 1$ ML because Pt-adatoms are organized in islands [421]. At 400 K, on the other hand, ϕ^e is kept virtually constant at 5.84 eV = ϕ^e (111) in the covered range of $\theta = 0$–1.25 ML, indicating that Pt-adatoms are incorporated rapidly at existing steps and hence ϕ^e remains unchanged [421].

[336]Regarding the Pt-surface estimated roughly to consist of 80%-(210), ~10%-(100) and 10%-(111) faces [179], ϕ^e is determined to be 5.79 ± 0.09 eV [179,650], while the "clean" cesiated work function is done to be 5.0 eV [650] or 5.1 eV [3413,3414].

[337]The Pt-surface [429] is experimentally determined to have $\phi^e = 5.77$ eV, which is very close to the theoretical values of 5.74 and 5.76 eV for Pt(221) [1293].

[338] The Pt-surface [50] seems to be not clean but considerably contaminated with carbon because its $\phi^+ = 4.40$–4.49 eV is much smaller than $\phi^+ = 5.58 \pm 0.11$ eV of our value recommended for a clean Pt surface (Table 2), but rather very close to $\phi^+ = 4.50 \pm 0.04$ eV of ours done for a C-film on metals (see Table 2). About the physico-chemical properties of the film, see Section 4.2.4 [1351]. Consideration of the above results and of the film properties outlined in the above section may suggest that many of the Pt-surfaces having $\phi^e \approx 4.3$–4.7 eV found in Table 1 may probably be heavily or considerably covered with graphitic films.

[339]The experimental data on Pt yields the empirical equation of $\log_{10} A = -6.85 + 1.87\phi^e$, affording $\phi^e = 4.72$ eV for $A = 92.8$ A/cm^2 K^2 [2299,2300].

[340]The work function of Pt measured by PE is found to be $\phi^e = 5.27 \pm 0.1$ eV [3055], well agreeing with our recommended value of 5.30 ± 0.07 eV (Table 2). However, $\phi^+ = 4.94 \pm 0.23$ eV by PSI of K [3055] is not larger than the above ϕ^e and it is smaller than ours of $\phi^+ = 5.58 \pm 0.11$ eV. This is probably because the ionization energy (I) of K (4.34 eV) does not satisfy the prerequisite condition of $I \geq \phi^+ + 0.3$ eV (see Section 4.2.3 in Ref. [1351]). In other words, not K but Ca or Tl, for instance, should have been adopted because the latter satisfies $I = 6.1 > 5.3 + 0.3$ eV.

[341]By PSI of Cs and K on Pt, $\phi^+ = 5.43$ eV [282] is determined from Saha–Langmuir equation (5) of $k^+/k^0 = \alpha^+ = 0.5 \exp[(\phi^+ - I)/kT]$. In addition, ϕ^+ is determined from Schottky equation (9) of $\phi^+ = E^0 + I - E^+ = 3.27 \pm 0.04 + 3.89 - 1.80 \pm 0.05 = 5.36 \pm 0.06$ eV according to the data on Cs and also from that of $\phi^+ = 3.65 \pm 0.03 + 4.34 - 2.47 \pm 0.04 = 5.52 \pm 0.05$ eV according to those on K [282], only the latter of which is larger than $\phi^e = 5.41 \pm 0.05$ eV determined from a Richardson plot [282]. In the above equations, k^+/k^0 is the ionic to atomic desorption rate constant ratio [98,282,397], whilst E^+, E^0 and I are the ionic and atomic desorption energies and ionization energy, respectively (see Section 4.1). The above values [282] do not well accord to ours of $\phi^+ = 5.58 \pm 0.11 > \phi^e = 5.30 \pm 0.07$ eV and $\Delta\phi^* = 0.28 \pm 0.13$ eV for Pt (Tables 2 and 4).

[342]The Pt-films prepared on glass at 78–80 K are found to have $\phi^e = 5.45$ eV, which increases to 5.63 and 5.72 eV after annealing at about 300 and 600 K, respectively [428,1497,2719], more deviating from our value of Pt (5.30 $\pm$ 0.07 eV, see Table 2) and much closing to ours of Pt(110) (5.54 $\pm$ 0.07 eV) or Pt(100) (5.75 $\pm$ 0.06 eV) by the annealing at higher temperatures.

[343]By PSI of Cs on Pt [98], $\phi^+ = 5.5$ eV is determined from the data on $\alpha^+ = k^+/k^0$, the method of which is outlined in Footnote 341.

[344]The Pt-specimen [434] is a considerably (111)-oriented wire prepared by aging at 1600 K for 150 h, thereby showing $\phi^e = 5.55 \pm 0.1$ eV [434]. This is intermediate between 5.84 eV for Pt(111) and 5.30 eV for Pt in Table 2.

[345]By PSI of NaNO$_3$ on Pt [178], ϕ^+ is determined to be 5.54 $\pm$ 0.07 and 5.56 eV from Schottky equation (9) and $\alpha^+ = 20$ in Saha–Langmuir equation (5), respectively [178], both values of which are virtually the same with ours of $\phi^+ = 5.58 \pm 0.11$ eV for Pt (Table 2).

[346]By deposition of Pt (1–2 ML thick) onto W(110) at $\sim$300 or 800 K, ϕ^e increases from 5.35 to 6.05 eV [1137], the latter of which is near to 5.7–5.9 eV recommended for Pt(111) in Table 2.

[347]Regarding the unreconstructed (1 $\times$ 1) and also reconstructed (1 $\times$ 2) and (1 $\times$ 3) Au(110) surfaces, ϕ^e is calculated to be 5.39, 5.38 and 5.32 eV, respectively [2543], all of which are virtually the same with 5.33 $\pm$ 0.09 eV recommended for Au(110) in Table 2.

[348]After Au-films ($\theta \geq 3.5$ ML) are prepared on W(112) at 78 and 540 K, ϕ^e is measured at 78 K to be 5.3 and 5.45 $\pm$ 0.03 eV, which correspond to Au and Au(110), respectively [2256]. The former agrees well with our recommended value of 5.30 $\pm$ 0.04 eV for bulk Au, but the latter is slightly larger than ours of 5.33 $\pm$ 0.09 eV (Table 2).

[349]The Au-films ($\theta = 5$ and 4 ML) formed on W(110) at 78 and 160 K are observed at 78 K to have $\phi^e = 5.3$ and 5.4 eV, respectively [2256]. On the other hand, Au-film ($\theta \geq 3.5$ ML) done at 420 K is found at 78 K to have 5.32 $\pm$ 0.03 eV with an Au(111) structure [2256], slightly smaller than our value of 5.46 $\pm$ 0.07 eV for Au(111) (Table 2).

[350]By annealing at 623 K for 1 h, the Au-film (0.12 nm thick) prepared on quartz at $\sim$300 K is increased in ϕ^e from 5.38 to 5.42 eV as the degree (δ_m) of monocrystallization forming the (111) face is increased from $F_i = 61$ to 91% [3313]. The latter is essentially the same with 5.46 $\pm$ 0.07 eV for Au(111) (Table 2). For further information about δ_m and F_i (fractional surface area), see Sections 4.2 and 4.3.

[351]The Au-film ($\theta = 7$ ML) formed on W(112) at $\sim$300 K is observed to have $\phi^e = 5.51$ eV [2385], which is virtually the same with 5.55 eV for the bulk Au(111) surface studied in a similar way [2385,2871].

[352]Regarding the fine Au-particles of $\sim$8 and 90 Å in radius, ϕ^e is calculated to be about 4.1 and 4.6 eV for real sphere, respectively, and also to be about 4.4 and 5.0 eV for octahedron, respectively [2973]. For further information, see Section 11.1.

[353]For an Au-ribbon at $\sim$300 K in an Hg-pumping system at the residual gas pressure less than $\sim$10^{-9} Torr (2 $\times$ 10^{-9} Torr as the partial pressure of Hg), ϕ^e is found to be 4.64 or 4.89 $\pm$ 0.06 eV [1072]. However, it increases to 5.20 $\pm$ 0.05 eV when the measurement by CPD is done soon after flashing to remove Hg-adatoms, all of which desorb at 1170 K [1072]. About the work function change due to amalgamation, see Point (6) in Section 3.2.

[354]With respect to a gold filament at 293 and 1013 K, ϕ^e is determined by PE to be 4.82 and 4.73 eV, respectively [2560], the theoretical analysis of which yields 4.81 $\pm$ 0.02 eV [1760] and also 4.90 $\pm$ 0.03 or 4.93 $\pm$ 0.03 eV [1135] in the above temperature range.

[355]By theoretical analysis of the data on temperature dependence of work function for ordinary metals [3586], the thermionic work function of Au is estimated to be 4.89 and 4.92 eV at 733 and 1013 K, respectively [3586]. They are in good agreement with 4.92 eV theoretically evaluated [1135] from the photoelectric data (nearly the same values in Footnote 354) [2560] at the respective temperatures, but they are smaller than ours (see Table 2).

[356]In regard to an Au/Ta system, ϕ^e is determined to be 4.83 $\pm$ 0.02 eV [1162], which is corrected to be 4.97 $\pm$ 0.02 eV [349] by taking the reference work function of Ba as 2.66 $\pm$ 0.01 eV [1050] (see Footnote 238) instead of 2.51 eV [2232] adopted by the author [1162]. However, both values are still much smaller than ours (5.30 $\pm$ 0.04 eV, Table 2), probably because the above system is contaminated with Hg (see p. 77 in Ref. [1351]).

[357]For an Au-ribbon at $\sim$10^{-9} Torr evacuated by an Hg-pump [2473], ϕ^e is found to be 5.01 and 5.08 eV at $\sim$300 K after Ar$^+$-impact (335 V), the values of which increase to 5.13 and 5.18 eV, respectively, after annealing up to $\sim$1200 K. Similarly, $\phi^e = 5.27$ and 5.31–5.33 eV at $\sim$300 K after the impact (85 and 635 eV by Ar$^+$) become common at 5.27 eV after the annealing at $\sim$1100 K [2473], thus yielding the data affected little by Hg-contamination.

[358]About the Au-layers (10 and 5 ML thick) deposited onto Ta(112) at $\sim$300 K, ϕ^e is measured to be 5.04 and 5.08 eV at $\sim$300 K [878], while the layers deposited at 1000 K have 4.76 eV, corresponding likely to a surface alloy with Ta [878].

[359]With regard to Au-layers ($\theta \approx$ 4–5 ML) prepared on Ir(100) at 78 K, ϕ^e is found to be 5.86 $\pm$ 0.02 and 5.80 eV after annealing at 482 and 520 K, respectively [2189]. On the other hand, the Au-layers ($\theta \approx$ 2–3 ML) on Ir is observed to have the different values of 5.29 and 5.10 eV after annealing at 501 and 520 K, respectively, indicating a change in overlayer structure in the above temperature range [2189].

[360]By deposition of Au onto bulk Au at $\sim$300 K, ϕ^e is decreased by 0.19 eV, which becomes zero by heating up to 723 K [3502]. Provided that the latter corresponds to 5.31 eV [1351], the former may be estimated to 5.12 eV.

[361]About the Au-films ($\sim$30 ML thick) on W of (111), (112) and (100) faces at $\sim$300 K, ϕ^e is measured to be 5.17, 5.20 and 5.36 eV, the respective values of which are decreased to 4.96, 5.08 and 5.14 eV by annealing at $\sim$1000 K [2647].

[362]Regarding the Au-clusters (Au$_n$) on W systems at 77 K, ϕ^e is determined to be 5.2 $\pm$ 0.4 and 5.7 $\pm$ 0.5 (or 5.9 $\pm$ 0.6) eV for the incident cluster diameters of 30 and 15 Å, respectively [1713]. Supposing that $r = 15$ and 7.5 Å are kept unchanged on W, $\phi^e \approx 5.7$ and 6.0 eV for Au$_n$/W, respectively, may be estimated from Eq. (17′), where $\phi^e(\infty)$ is taken as 5.3 eV. The latter seems to be consistent with the experimental data.

[363]The layers (250–500 Å thick) of Ru, Pt and Au deposited on glass at $\sim$78 K are found to have $\phi^e = 4.52$, 5.46 and 5.22 eV, respectively, which are increased to the stable values of 5.10, 5.72 and 5.38 eV by annealing at the temperatures (T_a) above $\sim$800, $\sim$500 and $\sim$400 K, respectively [436]. These results indicate that T_a should be selected to satisfy the condition of roughly $T_a \geq T_m/3$ in order to make the layers equilibrated fully on glass [436]. Here, T_m is the melting points of 2723, 2047 and 1336 K for the respective metals (see Section 2.5).

[364]The Au-layers formed on Mo(111) at $\sim$300 and 1000 K are found to have $\phi^e = 5.08$ and 5.22 eV at $\sim$300 K, respectively [1842]. The latter is nearer to the recommended value of 5.30 $\pm$ 0.04 eV (Table 2), just as expected from the annealing condition mentioned in Footnote 363.

[365]The work function of Au/glass at $\sim$300 K is measured to be 5.22 $\pm$ 0.05 eV, which is decreased to 4.77 eV by intentional admission of Hg [1071]. The latter corresponds to $\sim$4.7–4.8 eV found for Au in Hg-pumping systems [typically, 133,1160–1162,1893], where the surface reaction (amalgamation) is ready to occur between Au and Hg (see Point (6) in Section 3.2). For related subject, see Footnote 368.

[366]The Au-layers ($\theta > 2$ ML) formed on W(110) at 78 K in an Hg-pumping system is found to have $\phi^e = 4.89$ eV at $\sim$300 K, but ϕ^e increases to 5.25 eV after heating at 750 K [1670,1673]. The heating is effective for removing Hg from the Au-layers.

[367]Similarly as above (Footnote 366), ϕ^e of an Au/glass system is found to increase from 4.7 to 5.3 eV after heating at 520 K [1893], which is also effective for making an Ag/glass surface substantially free from Hg.

[368]By using an ion-pumping system in order to escape from Hg-contamination, ϕ^e for Au/Ru is measured to be 5.28 eV [1073], which is much higher than 4.68 and 4.71 eV determined previously for Au/glass and Au/W, respectively, by the same author [133,1161] using an Hg-pumping system. In brief discussion, the Hg-contamination data on 4.68–4.97 eV for Au on glass, W and Ta [133,1160–1162] are compared with the Hg-free ones on 5.22–5.45 eV for Au/glass [945,1071,1073]. For related subject, see Footnote 365.

[369]For metal films (7–12 nm thick) made on glass at 77 K, ϕ^e is found to increase from m to n eV by annealing (smoothing) at 323 K (or 373 K for Au alone). Namely, metal ($m \to n$ in eV) results in α-Fe (4.10 → 4.40); Co (4.44 → 4.91); Ni (4.55 → 4.88); Cu (4.40 → 4.64); Pt (5.50 → 5.71); and Au (4.96 → 5.40) [2133]. Typically, α-Fe and Ni are made to approach their work function values to ours (4.55 and 5.06 eV, respectively, in Table 2) by the annealing.

[370]The work function of Hg is found to be 4.49 ± 0.01 eV at 273 K, and no measurable change around the melting point of 234 K can be observed [1669].

[371]The W covered "fully" with Hg at 300 K is found to have ϕ^e = 4.9 eV [3726]. This value, however, corresponds not to $\theta \geq 1$ ML but to ~0.4 ML [3074] according to the data on Hg/W at the equilibration temperature of 370 K [3074]. At about 240 K, the Hg/W system is found to have ~4.6 eV at $\theta \approx 1$ ML [3074].

[372]About Hg/Ni(111) at $\theta = 0.75$ ML and $T = 240$–310 K, ϕ^e is determined to be 4.90 eV [3166]. This value is much larger than ours (4.50 eV in Table 2), similarly as in the case [3726] in Footnote 371.

[373]With respect to Pb/glass at ~300 K, ϕ^e is determined to be 4.00 eV [1381], which is corrected to be 3.83 eV [349] by taking the reference work function of Ba as 2.35 eV [13,349] instead of 2.52 eV [1380,1381]. As shown in Table 2, our values for Pb and Ba are 4.07 ± 0.05 and 2.50 ± 0.02 eV, respectively, to which the former (4.00 and 2.52 eV) [1381] is nearer than the latter (3.83 and 2.35 eV) [349]. It should be noted that $\phi^e = 2.52$ eV employed as the reference work function of Ba is cited from the original value (2.520 eV at ~300 K) in Ref. [2232]. See also Ref. [1157] in Footnote 238.

[374]The work function of Pb at ~300 K is found to be 3.95 ± 0.05 eV, which does not change at the melting point (601 K) [3437] (see Table 12).

[375]The work function of a Bi/Au(111) system is found to decrease by 1.52 eV as θ increases to 1 ML, and ϕ^e remains constant up to at least 4 ML. Here, Bi forms a monolayer followed by the growth of a Bi–Au compound beneath the former consisting of Bi alone [3678]. The system is estimated to have $\phi^e = 3.94$ eV provided that ϕ^e is 5.46 eV for Au(111) (Table 2).

[376]Regarding the Bi-layers deposited on glass at 90 K and also annealed at 293 K, ϕ^e is determined to be 4.245 and 4.370 eV, corresponding to an emission from the conduction and valence bands, respectively [3038]. Theoretical analysis of the respective data yields 4.25 and 4.6 eV [1403].

[377]The work function of Bi at ~300 K is measured to be 4.25 ± 0.05 eV, which does not change even at ~640 K much above the melting point (544 K) [3437] (see Table 12).

[378]From the experimental data on the work function difference (−0.020 eV) between Bi(sol) and Bi(liq) and also that (0.350 eV) between Bi(sol) and Cu(sol) [1755], $\phi^e = 4.86$ and 4.88 eV are estimated for Bi(sol) and Bi(liq), respectively, by taking $\phi^e = 4.51$ eV for Cu(sol) from Table 2 (see Table 12).

[379]From the empirical equation (7) of $\phi^e = 2.27X + 0.34$ [1955], ϕ^e for Ra is evaluated to be 2.2 and 2.4 eV by taking the electronegativity (in Pauling unit) of $X = 0.8$ [Here] and 0.9 [1955], respectively. Similarly for Pm, Po, Fr and Ac, any of which has no experimental data available still today, ϕ^e is evaluated to be 3.0, 4.8, 1.8 and 2.7 eV, respectively, from the above equation. Also for Sc, Y and In, ϕ^e is calculated to be 3.2, 3.0 (corrected from 2.0) and 3.6, respectively [1955], but they are not in good agreement with our values (almost by experiment) of 3.33 ± 0.04, 3.16 ± 0.06 and 4.05 ± 0.06 eV (Table 2), respectively.

[380]With respect to the Th-monatomic layer prepared by activation of thoriated W (1.8%-ThO$_2$ contained) at temperatures up to 2200 K, ϕ^e is determined to be 2.63 eV [1749,1750]. Similarly, ϕ^e is measured to be 2.64 eV for W–ThO$_2$ (1%) activated at 1920 K [3667,3668].

[381]The work function of Th-foil is measured initially to be 2.988 ± 0.008 eV, which increases to 3.728 ± 0.010 eV after electron impact at 1900 K [2932]. On the other hand, Th/W is found to have 3.455 ± 0.012 eV [2932], nearer to our value (3.37 ± 0.04 eV, see Table 2).

[382]Experimentally, the work function of Th is determined to be 3.45 ± 0.01 eV [3524,3525], by critical analysis of whose data ϕ^e is theoretically evaluated to be 3.41 or 3.44 eV [2932] and 3.35 eV [1759]. The last is essentially the same with our value (3.37 ± 0.04) recommended in Table 2.

[383]For the Th-films which are prepared by coating ThO$_2$ on W or Pt by a molecular gun and then activated at 1300–1650 K in vacuum, ϕ^e at 1260 K is determined to be 3.55 eV for Th/W (3 ML of the coating) and Th/Pt (4–8 ML) [872]. When W and Mo are employed as the substrate, reduction of ThO$_2$ to Th becomes insufficient at the coating thickness above 3 ML, thereby yielding $\phi^e \approx 2.4$ and 2.6 eV, respectively [872]. By critical analysis of the data on Richardson constant, the above value (3.55 eV) is corrected to 3.61 eV [2932]. Similarly, 3.44 eV is theoretically evaluated [2932] from the experimental data (3.3–3.4 eV) on Th/Mo and Th/Pt systems [3035].

[384]About the γ-U/W systems ($\theta = 1$ and 10–200 ML), ϕ^e is determined to be 3.0 and 3.47 ± 0.03 eV, respectively [232], which are corrected to be 3.38 and 3.48 ± 0.03 eV [1484] by substituting $A_r = 5$ and 114 ± 12 A/cm^2 K^2 and $T = 1400$ K into Hensley's equation (8); $\phi^e = \phi^e_r + kT \ln(120/A_r)$ [3623]. Here, ϕ^e_r is the work function corresponding to $A_r \neq 120$ A/cm^2 K^2. Especially the former, as well as the latter, is well corrected to be essentially the same with our value of 3.42 ± 0.05 eV for γ-U (Table 2).

[385]A γ-U/W system is found to have the relation of $\phi^e = 2.9 + 2.3 \times 10^{-4}\,T$ [2098], from which ϕ^e is evaluated to be 3.2 eV at 1250 K. This is corrected to be 3.5 eV [Here] by substituting $A_r = 8$ A/cm^2 K^2 and $T = 1250$ K into Hensley's equation (8) (see Footnote 384 and Section 2.8.6), thereby becoming very close to our recommended value (3.42 ± 0.05 eV) for γ-U (see Table 2).

[386]For the γ-U/W systems ($\theta = 1$–2 and 10–20 ML) at ~1000–1300 and ~1000–1400 K, ϕ^e is found to be 3.14 ± 0.02 and 3.42 ± 0.04 eV, respectively [1484]. Again, the respective values are appropriately corrected to be 3.36 ± 0.04 and 3.45 ± 0.1 eV [1484] by substituting $A_r = 20 \pm 7$ and 80 ± 30 A/cm^2 K^2 and also $T = 1400$ K into Hensley's equation (8). Similarly for the γ-U/W system ($\theta = 50$ ML) in H$_2$ ($\leq 10^{-5}$ Torr) at 1250–1400 K, $\phi^e = 3.46 \pm 0.02$ eV under $A_r = 140 \pm 20$ A/cm^2 K^2 [1484] is corrected to be 3.44 ± 0.03 eV [Here], becoming closer to our value for γ-U (3.42 ± 0.05 eV). The more A_r deviates from 120 A/cm^2 K^2, the more ϕ^e is effectively corrected as we may expect in general if A_r itself is free from systematic errors.

[387]Theoretical analysis of thermionic emission data on U yields $\phi^e = 3.28 + (3/2)kT$ [1747], which yields 3.28 and 3.42 eV for γ-U at 0 and 1100 K. The latter accords exactly with our value (see Table 2).

[388]By correction of the thermionic emission data on $\phi^e = 2.9 + 2.3 \times 10^{-4}\,T$ found for U/W [2098], ϕ^e is evaluated to be 3.45 eV for γ-U [2467]. Similarly, 3.27 ± 0.05 eV for U (wire) [2085] is corrected to be 3.56 ± 0.05 eV for γ-U [2467].

[389]By the theories of LDA and LECP models about Li-clusters (n = 2–68, Z = 1, $r_s = 3.25$ bohr and $d_G = 1.31$ bohr), $\phi^e(\infty)$ is evaluated to be 2.25 and 3.21 eV together with $C_p = 0.51$ and $0.48 \approx 1/2$, respectively [4262] (see Section 11).

[390]About a Be/Al$_2$O$_3$/Al system, ϕ^e is determined to be 3.89 eV [3057], which is corrected to be 3.905 eV [13] and 4.04 [Here] by taking the reference work function of Al as 4.095 eV [13] and 4.23 eV [1351], respectively, instead of 4.08 eV [3057], thereby approaching to our recommended value of 4.28 eV for α-Be (Table 2).

[391]Each specimen consists of monocrystal of β-rhombohedral boron [1415,3100].

[392]The work function dependence upon θ of B on W is found to agree well between theory [913,4344] and experiment [3503] over the entire range of θ = 0–1 ML, showing 4.5 eV at monolayer [913,3503].

[393]By incidence of C_2H_4 upon TaC(111) at 1570 and 1270 K, single- and double-layer graphite films are formed to have $\phi^e = 3.7 \pm 0.1$ and 4.2 ± 0.1 eV, respectively [290], both of which are considerably lower than 4.6 ± 0.1 eV for graphitic crystal [290] and also than 4.47 ± 0.05 eV found for a graphitic carbon film (see Table 2).

[394]For C_{60}-layers of $\theta = 1$ and 2–8 ML on freshly cleaved GeS(001), the films of C_{60}(111) are found to have $\phi^e \approx 4.7$ and 4.8 eV, respectively [457,543].

[395]About the C_{60} films on clean metals (Cu, Ag and Au) at 5 and 500 nm in thickness, ϕ^e is found to range from 4.60 to 4.72 and from 4.39 to 4.47 eV, yielding the average (μ) of 4.65 and 4.44 eV, respectively [2198]. Similarly, $\mu = 4.62$ and 4.42 eV are observed, respectively, for the thin and thick C_{60} ones formed on the metals exposed preliminarily to air [2198]. By deposition onto Cu at ~300–600 nm thick, sublimation-purified C_{60} yields $\phi^e = 4.59$ eV, larger than 4.39 eV found for as-received C_{60} [2198].

[396]The work function is measured to be 5.4 eV for a C_{60}/Ta(110) system at ~300 K, where some fraction of the C_{60} film decomposes on the clean substrate, leading to a thin film of carbon between the assembled film and the substrate [460]. Such a system [460] is discussed in comparison with other various ones of monolayer-C_{60} (4.82–5.25 eV) [316,1007,2681,3002] on monocrystalline metals (Al, Ni, Cu, Rh and Au) by other workers [316].

[397]The C_{60}-film formed on Pt(111) at 100 K and annealed at 900 K is estimated to have $\phi^e = 5.7$ eV and found to be stable up to ~1050 K, above which C_{60} decomposes to leave disordered graphitic multidomains [697]. On the other hand, an ordered C_{60} layer grown on Ni(110) at 700 K decomposes at 760 K and forms a carbidic carbon layer, which transforms into graphitic carbon at higher temperatures [697]. In another case of a C_{60}/Si(111) system prepared at ~300 K, C_{60} decomposes on the substrate at ~1100 K and reacts with the Si atoms to form SiC islands [3941]. See p. 80 [1351] for further information about the work function and thermal stability of C_{60} on various substrates.

[398]For the Al/Ta(110) and Pd/Ta(110) systems at ~300 K, ϕ^e is found to be 4.27 and 5.1 eV [2271], the respective values of which are substantially equal to 4.26 ± 0.03 and 5.17 ± 0.06 eV (Table 2). In addition, deposition of Al on Pd/Ta(110) decreases from initially 5.1 eV finally to a constant at 4.1 eV [2271], roughly corresponding to bulk Al. By deposition of Pd on Al/Ta(110), on the contrary, ϕ^e increases slowly from 4.27 eV ($\theta = 0$ ML) to 4.38 eV (1 ML) and up to 5.25 eV (5.0 ML), at which Pd forms surface alloys of both $PdAl_3$ and PdAl intermetallic compounds at ~300 K [2271].

[399]Allotropic transformation temperatures are listed for 13 rare earth metals other than Pm, Eu, Er and Lu [3966].

[400]According to the literature values summarized for U [3967], the allotropic transition temperature of β to α has a range of 918–948 K, while that of γ to β has 1037–1053 K.

[401]Both synthesis and structure of graphene overlays on monocrystalline metals are reviewed together with their electronic structure and promising potential [3968,4173]. Ir(111) films grown on Si(111) wafers with buffer layers are successfully applied to scalable synthesis of graphene, which has the quality comparable to that grown on bulk Ir(111) [4007]. A review about graphene is focused on production, structure, reactivity, etc. from the viewpoint of chemistry [4104]. Another review is focused on the experimental methods and conditions for preparing mono-, di- and multilayer graphene on various substrates by chemical vapor deposition [4106].

[402]Field emission studies reported for carbon nanotubes during the first five years after 1995 are reviewed comprehensively about their structural and electronic properties, fabrication of their field emitters, their emission characteristics, etc., containing some data on their work function [3969].

[403]About the C/Si(100)^p system, $\phi^e \approx 5$ eV for cnt [3649] is reported to be 5.3 ± 0.2 eV in related studies [698,2425,3943].

[404]Regarding Ag-films on various substrates, much data on ϕ^e are listed together with each experimental method and condition [3280]. There, ϕ^e ranges from 4.0 to 4.46 eV and has the mean of 4.30 ± 0.13 eV, which is nearly equal to our value of 4.39 ± 0.02 eV recommended for polycrystalline Ag (Table 2).

[405]With respect to Ni at the ferromagnetic state, ϕ^e is determined to be 5.06 and 5.05 ± 0.05 eV at ~300 and 623 K below the Curie point (631 K), respectively [943]. At the paramagnetic state, ϕ^e is found to be 5.10, 5.17, 5.20 and 5.24 eV at 770, 975, 1108 K and above 1150 K, respectively [943]. See Table 13 for the work function change due to magnetic transformation.

[406]With respect to the α-phase ($T < 1042$ K) of Fe, ϕ^e is measured to be 4.70 and 4.65 eV at ~300 and 870 K, respectively [305]. For β (1042–1179 K) and γ (1179–1674 K), ϕ^e is found to be 4.62 and 4.68 eV at 1125 and 1243 K, respectively [305]. About the work function change due to the allotropic transformation of several metals, see Table 11.

[407]As an interesting phenomenon, the metastable Fe-layers grown epitaxially on Cu(100) at ~300 K are found to show a structural transition from m-fcc Fe(100) to α-bcc Fe(110) when θ increases beyond ~10 ML [3913]. Unfortunately to us, no data on work function are given there. About the features of such metastable iron layers, see Sections 7.1 and 8.2.

[408]By application of Kelvin, photoelectric and electron beam retarding methods to the U-layers ($\theta \approx 2$ ML) on W(100) at ~300 K, ϕ^e is determined to be 3.73 ± 0.02, 3.73 ± 0.02 and 3.78 ± 0.03 eV, respectively, for α-U [2471] (see Section 2.8.2).

[409]From the position of a primary peak appearing in TCS (total current spectrum; $dJ(E)/dE$ vs. $E - E_F$, the difference between the incident energy and the Fermi level), ϕ^e of 6 layers of Cu on ZnO(0001) is determined to be 4.5 eV [2679]. This is equal to our value of 4.51 ± 0.04 eV recommended for bulk Cu (Table 2), but much smaller than 4.94 eV [953,2006] and 4.92 ± 0.05 eV (Table 2) done for bulk Cu(111). This is because the substrate is covered by Cu(111) islands without its surface covered completely [2679].

[410]Regarding Si(111) [73], $\phi^e = 4.07 \pm 0.05$ eV may be corrected to be 4.83 ± 0.04 eV from Eq. (8), as described in Section 2.8.6. For further information about related subject, see Footnote 66.

[411]With respect to a tungsten specimen consisting of these faces of (310), (111), (100), (112) and (110) having $(\phi_i, F_i) = $ (4.25 eV, 46.3%), (4.47, 5.4), (4.65, 14.0), (4.76, 15.5) and (5.25, 18.9), respectively [489], $\phi^a = 4.6$ eV calculated from Eq. (4) is taken as ϕ^e and considered to agree well with $\phi^e = 4.8$ eV measured by FE [489]. However, both values are much larger than those estimated from the fact that the main face of (310) is lowest in ϕ_i and largest in F_i among the five faces. Namely, ϕ^e is naturally expected to be ~4.3 eV or so corresponding to face (310). In fact, our calculation from Eq. (2) yields $\phi^e = 4.34 \pm 0.05$ eV [630] or 4.38 ± 0.05 eV [2453] (see Footnote (22) for W(D) in Table 6).

[412]The metastable β-like fcc-Co(100) film is grown by sublimation of Co onto Cu(100) at ~300 K, thereby resulting in $\phi^e = 4.72$ eV [2673]. Similarly, fcc-Fe(100) is done so, yielding 4.62 or 4.67 eV [2673] (see Footnote 114). The former and latter values are much smaller than ours (Table 2) of 5.25 eV for normal β-fcc-Co(100) and 5.28 eV for γ-fcc-Fe(100), rather near to 4.50 eV for β-fcc-Co(poly) and 4.54 eV for γ-fcc-Fe(poly), respectively (see Section 8.2).

[413]Ni is found to have bivalued work functions of 4.5 and 5.0 eV by PE at ~300 K [942], and 4.41 ± 0.02 eV (1170–1250 K) and 4.80 ± 0.02 eV (1440–1490 K) by TE [179,650,3410,3413]. It is worthwhile to solve perfectly the interesting problem why this phenomenon occurs, especially at quite different temperature ranges between the two cases.

[414]In regard to the system of the Ni-film (~1500 Å thick) prepared on a monocrystalline Ni ($T_C = 6.31$ K), $\phi^e = 4.97$ and 4.87 eV are measured by PE at 295 and 678 K, respectively [3971]. This difference by 0.10 ± 0.04 eV, however, does not originate from ferro- to paramagnetic transition alone but does considerably from the thermal effect due to α (~-10^{-4} eV/K for Ni, see Table 6 in Ref. [1351]). For further information, see Section 8.1.

[415]From the data on $\phi^+(Re) - \phi^+(C/Re) = 0.466$ eV [3753], $\phi^+(C/Re)$ is estimated to be 4.94 eV by taking $\phi^+(Re) = 5.41$ eV from Table 2.

[416]A comprehensive review on Re affords us general information about thermionic properties and chemico-physical characteristics of Re in comparison with Mo, Ta and W [190].

[417]High strength metallurgical graphene (ϕ^e = 4.63–4.79, ±0.01 eV) is formed by chemical vapor deposition (CVD) of a mixture (C_2H_2, CH_2CH_2, H_2) on a 72%Cu–28%Ni composite at ~1500 K in Ar-atmosphere (750 Torr) [3996], while a commercially available CVD graphene grown on a Cu-foil is found to have 4.67–4.78, ±0.01 eV [3996].

[418]Graphene ($\phi^e = 4.81 \pm 0.06$ eV) is formed on Si(100) covered with silicon oxide (300 nm thick) [3997], whilst another (4.92 ± 0.06 eV) is grown from CH_4 (83 Torr) on a Cu-foil at 1308 K [3997].

[419]The Au-layers (200 nm thick) prepared on Si(111) have a dominant (111) orientation with 5.2 eV [3999,4000]. The Au-layers in these systems of K/Au/Si(111) and K/C_{12}/Au/Si(111) are similarly predominant in the (111) plane, resulting in 2.0 and 2.66 eV, respectively, for K. Here, C_{12} is $C_{12}H_{25}SH$(1-dodecanethiol) [3999].

[420]The film (200–300 nm thick) of Cu, Ag or Au is grown on mica (~570 K), and it is sputtered by Ar^+ (800–1500 eV) and also annealed at ~520–620 K for several hours, thereby forming a nearly defect-free (111) terrace with 4.8, 4.5 and 5.4 eV, respectively [4001]. Each of them is very near to ours (see Section 2.5 and Table 2).

[421]The work function of Ge(111) is found to have 4.73 ± 0.05 eV immediately after vacuum cleavage, but to change to 5.45 ± 0.05 eV at the moment of the $2 \times 1 \rightarrow 1 \times 1$ structural transition [1991].

[422]The work function values of Li/Si(100)^p and K/Si(100)^p are determined to be 2.53 and 2.2 eV [4016] by citing two different values of 4.85 eV for vacuum-cleaved Si^n [613,1045] and 4.7 eV for Si(111)^n [1228], respectively [4016]. By citing our best estimate of 4.82 eV for Si(100) (Table 2), for instance, the latter becomes 2.3 eV, nearer to 2.29 eV recommended for K(poly) in Table 2.

[423]On the basis of the calculated values of $\Delta\phi^e$ = 1.1, 1.9 and 2.6 eV due to adsorption of S on the hollow, bridge and atop sites on Fe(100) [4019], ϕ^e for S/Fe(100) is estimated to be 5.0, 5.8 and 6.5 eV, respectively, by the present author citing the theoretical value of $\phi^e = 3.94$ eV for α-Fe(100) from Table 1 [4019].

[424]Regarding the B-doped Si(111)-specimens of p-type (0.002 and 260 Ω cm), ϕ^e is measured by PE to be 4.9 and 5.2 eV, respectively, while As-doped one of n-type (0.002 Ω cm) is done to be 5.0 eV [1226].

[425]Similarly by the same authors above [1226], ϕ^e of Si(111) is found to vary from about 4.7 to 4.9 eV in going from extremely n- to p-types, being close to 4.83 eV throughout most of the doping range [117].

[426]The work function of Si(111) is observed to have a difference of 0.18 ± 0.02 eV between p- and n-types, which are estimated to have 4.97 and 4.79 eV, respectively [1889].

[427]Regarding the adsorption of C, S and P on paramagnetic β-bcc-Fe(100), the work function changes are calculated to be 2.1, 1.3 and 0.9 eV, which yield ϕ^e = 6.3, 5.5 and 5.1 eV for the respective surface systems [4026] since ϕ^e for the substrate is calculated to be 4.2 eV [1104].

[428]A "missing" metastable phase of single-crystalline bcc-Co film is successfully synthesized on GaAs(110) by molecular beam epitaxial growth [4028]. A later study, however, indicates that the bcc-Co film does not correspond to a true metastable state and suggests that the existing bcc-Co film is stabilized by the presence of impurities or other defects [4205]. Interestingly, on the other hand, monocrystals of GaAs are usable as the substrates for preparing single-crystalline films of Fe [4028,4095–4097] and of Al [4098]. A distorted bcc–Co phase can be stabilized on Au(001)–hex [4325].

[429]The values of 5.10 and 5.55 eV correspond to the paramagnetic five- and monolayer of metastable bcc-Co(100) slabs, respectively [4023].

[430]The data on 4.66, 4.75 and 5.20 eV are obtained theoretically for the spin-polarized five-, nine- and monolayer bcc-Co(100) films, respectively [4023].

[431]Compared with literature values such as 4.31 eV [1050] and 4.33 eV [690], ϕ^e = 2.04 eV determined for Ag by TE at ~1150–1230 K [1466] is extremely small, but it is corrected by the present author to be 4.25 eV by substitution of ϕ_r^e = 2.04 eV, T = 1200 K and $A_r = 6.4 \times 10^{-8}$ A/cm^2 K^2 into Eq. (8), thereby coming close to our value of 4.39 ± 0.02 eV (Table 2).

[432]For Si(111) of p-type, ϕ_r^e and A_r are measured to be 3.2 eV and 4×10^{-3} A/cm^2 K^2 at ~1100–1150 K [3540], by substitution of which ϕ^e is calculated to be 4.2 eV from Eq. (8). This value agrees exactly with 4.2 eV determined directly from a Richardson plot for the same specimen at ~1150–1450 K, where A_r is found to be 130 A/cm^2/K^2 [3540]. This result suggests that the reflection coefficient of $r^e = 1 - 4 \times 10^{-3}$ has a very high value of above 0.99 in the former temperature range in contrast to ~0.0% in the latter. However, 4.2 eV is much smaller than 4.6–4.8 eV recommended for Si(111) (Table 2).

[433]Formation of C_{60}(111) is observed on various substrates as follows: GeS(001) at ~400–500 K [457,543,4037], CaF$_2$(111) at ~500 K [4038], MoS$_2$(0001) at ~300 K [4039], Au(111)/Ag(111)/mica at ~500 K [4040], Cu(111)/mica and Cu(111)/Ag(111)/mica at ~400–500 K [4041]. Unlike graphite and diamond, solid C_{60} is a molecular crystal, the structure of which is illustrated in Fig. 1 [3940].

[434]By PSI of Na (or K) on Si(110)^p, ϕ^+ as well as ϕ^e is found to increase linearly from ~3.3 to 4.3 eV as T increases from ~1000 to 1300 K [1472]. At ~1500–1600 K, on the other hand, ϕ^+ remains virtually constant at ~4.4 eV and decreases gradually from ~4.4 to 4.1 eV by incidence of weak and strong sample beams, respectively, while ϕ^e gradually increases from ~4.3 eV up to a constant of ~4.7 eV at ~1500–1600 K without the beam incidence [1472]. Consequently, the discrepancy between ϕ^+ and ϕ^e increases from ~0 up to ~0.6 eV, which suggests the chemical reaction of the beam with the substrate [1472].

[435]Recently, anomalies in the temperature dependence of ϕ^e have been found for Ru(11$\bar{2}$2) and Ru(11$\bar{2}$5) having the three phases of α, β and γ, and the respective values of ϕ^e at β (1510–1540 K) are lower by 0.38 and 0.55 eV than those at both α (<1510 K) and γ (>1560 K) [3686]. See Section 7.1 for further information about the phase transitions in Ru.

[436]For the n- and p-types of Ge-samples (B and D) doped with As and In having 0.005 and 0.10 Ω cm, the work function difference of $\phi(100) - \phi(111)$ is found to be 0.064 ± 0.005 and 0.045 ± 0.009 eV, respectively, while $\phi(110) - \phi(111)$ is 0.013 ± 0.05 and 0.022 ± 0.009 eV, respectively, by CPD. Here, Ge(110) is determined to have $\phi(110) = 4.72 \pm 0.3$ eV equally for both types [1382]. Similarly for n- and p-types of Ge(110) doped with Sb and In having 0.058 and 0.39 Ω cm, the work function difference between the two is found to be as small as 0.002 ± 0.004 eV by CPD [3611].

[437]The surfaces of Au (4.20 eV) and both substrates (Au and Hg/Au to be adsorbed with iodine) are not clean, but heavily contaminated with air [2760] and also with Hg.

[438]According to the temperature coefficient of 1.2×10^{-2} eV/K, work function of liquid indium increases from 3.88 to 4.13 eV with increasing temperature from 470 to 670 K [2111].

[439]First-principles calculations of ϕ^e for graphene yield 4.5 eV, which increases up to 4.8 or 5.2 eV according to isotropic strains [4105].

[440]An Yb/Si(111) system at θ = 6.0 ML is determined to have $\phi^e = 3.00 \pm 0.03$ and 3.95 eV at ~300 and 800 K, respectively. The latter corresponds to ytterbium silicide [4109].

[441]About doped silicon samples, ϕ^e is theoretically evaluated to be 5.03–5.10 eV for Si^p (7.5–20 Ω cm) and 4.42–4.63 eV for Si^n (0.071–14.5 Ω cm) [4119].

[442]The single- and double-layer graphene samples prepared by mechanical exfoliation on Si-wafers are found to have $\phi^e = 4.57$ and 4.69 eV, respectively [4128].

[443]Regarding the two-dimensional graphite films on various metals, a compact review outlines their structure and physico-chemical properties [450].

[444]A comprehensive review entitled "Unravelling the secrets of Cs controlled secondary ion formation: Evidence of the dominance of site-specific surface chemistry, alloying and ionic bonding" [4118] contains both experimental data on work function changes and their analytical results achieved for various substrates (Be, Al, Si, etc.) covered mainly with Cs.

[445]With respect to an Eu-film ($\theta = 1.1$ ML)/Si(111) system, ϕ^e is determined by CPD to be 2.8, 2.9 and 3.8 eV at $\sim$300, 500 and 900–1000 K, respectively, the last case of which corresponds to europium silicide [4111].

[446]The work function of Gd is 3.55 ± 0.15 eV at the Curie temperature of 290.85 K [3899].

[447]At room temperature, Ag is found to have 4.26 ± 0.03 eV, which decreases to 4.15 ± 0.07 and 4.04 ± 0.08 eV at 530 and 780 K, respectively, thereby affording $\alpha = -4.58 \times 10^{-4}$ eV/K [4114,4132].

[448]For the nickel particles (usually, $r = 60$–100 Å in radius) produced by a spark discharge in He, $\phi(r) = 5.1$ eV is determined by PE [2667]. This is in good agreement with our value of $\phi(r) = 5.13 \pm 0.06$ eV calculated from Eq. (17') by using both $\phi(\infty) \equiv \phi(\text{poly}) = 5.06 \pm 0.06$ eV (Table 2) and $r = 80$ Å, although it is 4.9 eV that is estimated as $\phi(\infty)$ for a flat nickel surface [2667] from these values of 4.90 eV [414] and of 4.5 and 5.0 eV [942] measured by PE at $\sim$300 K (see Section 11.1).

[449]The values of 4.36 ± 0.03 and 4.51 ± 0.03 eV are calculated from Eq. (17') by the present author using the data on $e^2/R_{\text{eff}} = 0.272$ and 0.66 eV [2199], which afford 52.9 and 22 Å as the effective values of radius ($R_{\text{eff}} \equiv r_c + \delta$) in Eq. (20) for Al$_{32000\pm150}$ and Al$_{2000}$, respectively. Here, each value of $\phi^e(r) = 4.36$ or 4.51 eV is calculated from both $\phi^e(\infty) = 4.26 \pm 0.03$ eV (Table 2) and $3e^2/8(r_c + \delta) = 0.10$ or 0.251 eV, while $\phi^e(\infty) = 4.28 \pm 0.03$ eV is determined by experiment [2199] (see Footnote 60 in Table 1 and also Results (1)–(2) in Section 11.1).

[450]According to the data in Fig. 1 [4146], where ϕ^e for Tb(0001) increases from 3.09 to 3.18 eV with decreasing temperature from $\sim$1440 to 1380 K [3920], α is estimated to be -1.5×10^{-3} eV/K, which affords 4.8 eV at $\sim$300 K. Above $\sim$1450 K, on the other hand, ϕ^e retains a constant at 2.94 ± 0.05 eV, thereby yielding $\Delta\phi^e_{\beta\alpha} = -0.15 \pm 0.07$ eV (see Table 11).

[451]According to the Burgers orientation relationship [4163], α-hcp-Zr(0001) transforms to β-bcc-Zr(110) at the allotropic transition temperature (1135 K) (see Section 7.1).

[452]With respect to the ultra-thin films of graphite, their formation, structure and physical properties are outlined together with the work function data (3.7–4.8 eV) for the films prepared on several metals and carbides [695].

[453]The nanowires ($\sim$10–15 bohr in width) of Na and Al are found by a theoretical study to have $\phi^e = 2.55 \pm 0.05$ and 4.15 ± 0.05 eV, which are slightly lower than 2.75 and 4.28 eV for respective semi-infinite metals [4178].

[454]Regarding the films prepared by simultaneous incidence of both a C$_{60}$/C$_{70}$ mixture (85:15 in weight) and Ni-acetate upon a Mo-tape, photoelectric measurements reveal $\phi^e = 2.93 \pm 0.1$ eV (3% in weight of Ni-content), 2.65 ± 0.1 eV ($\sim$5%) and 2.76 ± 0.1 eV (11.7%), the last of which decreases to 2.4 eV after cleaning by pulsed laser beam [4176]. It is very interesting that all of the above values are much lower than any of 4.47 ± 0.05 eV for graphite film, 4.87 ± 0.06 eV for C$_{60}$(poly) and 5.06 ± 0.06 eV for Ni(poly) (see Table 2).

[455]The work function for cnt with the armchair conformation is calculated to be $\sim$4.5 eV being close to 4.48 eV for graphene, while that for the zigzag and chiral conformations increases drastically from $\sim$4.5 eV up to $\sim$5.9 eV as the diameter decreases from $\sim$7 to 3 Å [3240].

[456]The value of 4.32 eV for liquid Ag is obtained by substitution of $T = 1240$ K, $\phi^e_r = 3.86$ eV and $A_r = 1.6$ A/cm^2 K^2 [1466] into Eq. (8). The value corrected by the present author is equal to 4.32 eV determined experimentally for solid Ag at $T_m = 1234$ K [1466], thereby indicating that work function change due to liquefying is less than ± 0.01 eV.

[457]All the values of $\phi^+ = 5.1$–5.78 eV for Pt [74] are derived by the free energy model using the data on PSI of Li, Na, K or Tl.

[458]Each of ϕ^+ for Pt ($\geq$5.1, 5.51, 5.54 or 5.71 eV) [74] is determined by the enthalpy model according to the PSI data on alkali or Tl.

[459]Theoretical evaluation of both ionization energy (I) and electron affinity (E) of Al$_n$ ($n = 3$–70 and 3–150) yields $\phi^e(\infty) = 4.25$ eV for Al(poly) [4194,4197], which is strongly supported by the experimental data on I [4196] and E [4197] and also by $\phi^e = 4.26 \pm 0.03$ eV recommended in Table 2.

[460]See Section 11.1 about the details of $\phi^e(\infty)$ determined from the data on IP for these fine particles ($r \approx 3$–30 Å) of Na, K and Ag [4198].

[461]According to the experimental data ($\phi^e_r = 2.57$ eV, $A_r = 0.023$ A/cm^2 K^2 and $T \approx 1300$–1500 K) for liquid Ge contained in a crucible (graphite or quartz made) [1466], Eq. (8) yields 3.60 eV, which is near to the upper value of 3.5 eV for solid Ge around $T_m = 1232$ K [1466]. The latter, however, is much smaller than 4.76 eV [Here, [1354]] and 5.0 eV [1045,1358] recommended for Ge (see Table 2).

[462]A simple method by chemical vapor deposition of CH$_4$ and H$_2$ on melted Cu (1360 K) is reported for synthesizing large 200 μm single crystals of monolayer graphene within a continuous film [4201].

[463]As the root-mean-square roughness of a Cu surface increases from $\sim$30 to 65 nm, ϕ^e is found experimentally to decrease from 4.76 to 4.52 eV, the result of which accords well with the theoretical prediction [931,2547]. For further information about such a dependence, see Section 4.2.5 of the "Effect of local surface irregularities" [1351].

[464]Theoretical study of the work function decrease due to adsorption of K on graphite yields 2.34 eV at 1.0 ML [4211], which affords $\phi^e = 2.36$ and 2.29 eV for K when 4.7 and 4.63 eV are taken for graphite from a book [4211] and Table 2 [Here], respectively. The latter value for K well agrees with ours of 2.29 ± 0.02 eV (Table 2).

[465]The work function of 4.85 eV measured for the fresh surface of Si cleaved at $\sim$5 $\times$ 10^{-11} Torr is very close to that for Si(100) (see Table 2) in contrast to 4.45 eV found after exposing it to the residual gases for $\sim$100 h [613].

[466]Regarding PSI on Ta(110) [279], L represents lanthanides (12 elements).

[467]Experimental and theoretical studies about conical carbon nanotubes seem to be scanty compared with single- and multi-walled ones, but further information about the former may be obtained from several articles [4287–4295], which well outline its synthesis, structure, property, applicability, etc.

[468]In contrast to free-standing graphene ($\phi^e = 4.48$ eV), adsorbed graphene is calculated to have 3.66, 4.03 and 4.87 eV on the substrates of Ni(111), Pd(111) and Pt(111) [4174,4284], the dependence of which may be supported by the experimental data of 3.9, 4.3 and 4.8 eV [695], respectively. Such a dependence is caused by the formation of an interface dipole and the electron transfer between the metal and graphene levels driven by the work function difference, as well as the chemical interaction between graphene and the substrate metal [4174,4284].

[469]A comprehensive review is focused on the work function data published for Li in 1916–2009, thereby concluding that ϕ^e for Li is recommended to be not less than 2.64 eV [4298].

[470]Regarding multi-walled nanotubes heated directly at $\sim$1800–2200 K, Richardson plots are found to exhibit an upward bend deviating from linearity and also a current density much higher than that usually expected from Richardson's law, thereby concluding it necessary to devise new theoretical descriptions of thermal electron emission from individual low-dimensional nanostructures [4307].

[471]A theoretical study of graphene yields that ϕ^e changes from $\sim$4.3 to 4.6 eV depending upon the size (length and width) and upon the shape (armchair or zigzag) [4332].

[472]The value (4.3 eV) for Zn [4329] is estimated by the present author by extrapolating the plot (I vs. $n^{-1/3}$) for Zn-clusters (n = 2–20) in Fig. 5 [4329] based on classical CSD model [4101]. For general information about clusters, see Section 11.

[473]The original value of 4.21 eV for γ-Fe [310] may be corrected to be 4.66 eV according to Eq. (8) (see Section 2.8.6).

[474]With respect to Co, the allotropic transition temperature (T_A) for hcp $\leftrightarrow$ fcc is estimated to be 695 K [4336] in contrast to 720 K [364]. It should be noted that supported cobalt crystallites with a small size ($\sim$10–500 Å) have the fcc structure even below T_A [4338].

[475]The specimen of W{46%(100)} [390,391,533–535,659,825] corresponds to W(C) [825] in Table 6, where our theoretical value of $\phi^+ = 5.00 \pm 0.05$ eV [2453] is much larger than $\phi^a = 4.72$ eV [825,2453], in contrast to $\phi^+ = 4.61 \pm 0.05$ eV $< \phi^a = 4.72$ eV [825]. For further information, see Table 6 and Section 4.

[476]For the Ag-films ($\sim$1–50 nm thick) on two perylene derivatives (DiMe–PTCDI and PTCDA (10 nm thick)) prepared on S–GaAs(100), their work functions are found to be constant at 4.37 $\pm$ 0.05 eV and to increase up to 4.61 $\pm$ 0.05 eV at 50 nm thick [4341], the respective values of which are substantially equal to ours of 4.39 $\pm$ 0.02 and 4.64 $\pm$ 0.06 eV recommended for Ag(poly) and Ag(111) in Table 2. In fact, a stronger peak of Ag(111) is observed for the latter system by X-ray analysis [4341].

[477]The films ($\sim$5–50 nm thick) of In on DiMe–PTCDI and PTCDA (see Footnote 476 just above) are found to have $\phi^c = 4.10 \pm 0.05$ and 4.44 $\pm$ 0.05 eV, respectively [4341], the former of which is nearly equal to 4.05 $\pm$ 0.06 eV recommended for In(poly) in Table 2. According to X-ray analysis, the latter consists mainly of In(101) [4341], but its work function has not yet been reported probably by any other worker (see Tables 1 and 2).

[478]For Au-nanoparticles formed on a Si-wafer covered with a monolayer of alkyl chains providing a tunnel junction, ϕ^c is found to change from $\sim$3.5 to 3.8 eV as the particle radius increases from $\sim$20 to 80 Å together with doing from -2 to -8 in charge state inside the particle [4368].

[479]Regarding the boron sheets of alpha, distorted hexagonal and buckled triangular types, ϕ^c is theoretically evaluated to be 4.09, 4.89 and 5.39 eV, respectively [4359].

[480]With respect to heavily phosphorus-doped nano-crystalline diamond prepared by CVD of PH_3, CH_4 and H_2 on Mo at $\sim$1200 K, ϕ^c is measured by TE ($\sim$600–800 K) to be 2.3 eV [4371], which is corrected to be $\sim$2.4 eV by substituting $A_r = 15$ A/cm^2 K^2 into Eq. (8).

[481]A comprehensive review is focused on the theoretical problems connecting with both development and operation of carbon nanotube field emitters [4372].

[482]For the film ($\sim$15 nm thick) of Pt deposited on n-type silicon, ϕ^c is found to be decreased from 5.5 to 5.3 eV by illumination (18 mW/cm^2) [4375]. Similarly for W and Au films, ϕ^c is done so from 4.8 and 5.2 eV to 4.7 and 5.1 eV, respectively [4375].

[483]Together with typical work function data, a concise review summarizes the first-principles density-functional study about graphene which is expected as a potential device material for gas sensor applications [4403].

[484]The data on $\phi(100) = 4.46$ eV and $\phi(110) = 4.85$ eV measured according to the reference of $\phi(111) = 4.80$ eV by FE for Ge [3539] are taken erroneously for Si [Ref. 2040 in [1354]].

[485]Both $\phi(110) = 4.90 \pm 0.05$ eV and $\phi(111) = 4.14 \pm 0.05$ eV determined by TE for Mo [1400] are taken erroneously for W [Ref. 39 in [1354]].

[486]The datum on $\phi(poly) = 4.74 \pm 0.02$ eV measured by TE for Re [666] is taken not only for Re but also for Rh erroneously [Ref. 1522 in [1354]].

[487]Each of the work function values (3.27–3.46 eV) corresponds to these two-dimensional islands which are formed from Hf (0.05–0.2 ML) near (100) faces of W heated up to 1100 K [501].

[488]A comprehensive review is focused on the alkali metal adsorption on various types of carbon by outlining the theoretical and experimental studies on the surface structure, charge transfer, work function change, etc. [1860].

[489]Graphene films with a very high uniformity in work function are epitaxially grown by heating silicon carbides at $\sim$1300–1900 K in vacuum or argon [4455–4457].

[490]Only a part of the very plentiful work function data included in the articles [4460,4461] is added to Table 1 because the present author found the articles just before sending the final version of this article to the Editor.

2.1. Column 1; Surface species

For each chemical element, the surface species of various monocrystals under study are listed according to the face of lower crystallographic index, ahead of any polycrystalline surface of bulk and layers. The system of A/B means that A is the sample layer(s) or film(s), and that B is the substrate (metal, insulator, etc.) for supporting A. The superscript of n (or p) in such a form typically as Si(100)^n means the n-type silicon including typically antimony as a dopant [2059]. Similarly, Si(100)^p is the p-type silicon doped typically with boron [1872]. With respect to C(100)^B, the diamond specimen is doped with boron, for instance [224,1830,2751, etc.]. The annex of (fp) to Ag, for example, indicates that the Ag sample (4.25 $\pm$ 0.1 eV) consists of fine particles having a radius of 5 $\pm$ 2 nm [1562] (see Footnote 204 in Table 1 and also Section 11.1). The expression of W{46.3%(310)} [489] indicates that the sample surface consists *mainly* (46.3% = δ_m) of the (310) plane. This sample corresponds to W(D) [489] in Table 6 to be shown later.

Other symbols included in this column are as follows; HOPG = highly oriented pyrolytic graphite [e.g., 284], cnt = carbon nanotube exemplified as Cs/cnt/GsAs [291] and Cs/cnt/Si [3225], ins = insulator such as Al_2O_3-barium-stearate layers in Mg/ins/Al [2028], ITO = indium tin oxide, like as cnt of C/ITO [284,1441,3795], nw = nanowire, shown typically as diamond of C/Si(nw)/Si [3305], O=Ti = oxygenated titanium such as Ti/O=Ti [2378] (see Footnote 95 in Table 1), ss = stainless steel substrate such as Se/ss and Te/ss [3429], and d = diameter, like as cnt of C (d $\geq$ 1 nm) [1169].

The crystal structures (bcc, fcc, hcp, etc.) of various chemical elements are compactly summarized in tables and figures [4021], and the theoretically predicted structures of 3d–5d transition metals are found to accord with the experimental ones with only one exception ($_{79}$Au) [4022].

2.2. Column 2; Incident beam (or vapor) for either probing work function or forming sample layers on a substrate

In an A/B system, the surface material (A) to be studied is directed onto the substrate (B, generally foreign material) in the form of beam or vapor in order to prepare the sample film(s) or layer(s) of A. In stead of such a beam direction, the "spillover" is utilized for preparing a Th-film by activation of thoriated tungsten (1–2% ThO_2 contained) at $\sim$2000 K [1749,1750,3667,3668] (see

Footnote 380 in Table 1 and also the typical data (1)–(4) in Section 2.8.6). In a similar way, the layers of Sc and Y are successfully formed from the alloys of Re–Sc (4–9%) [1979] (see Footnote 92) and Re–Y (4%) [4240], respectively. Occasionally, A is formed on B not in vacuum but in solution by electroplating, typically preparing the systems of Cu/Ni [2294] and Re/W [1850]. Usually, A on B is annealed (equilibrated) at a temperature higher than that of sample deposition. Then, work function of the sample (A) is measured by a usual method (e.g., CPD = contact potential difference method). For the film or layer (A) having the coverage (θ) above 1 ML, ϕ^e is listed in Table 1 in order to estimate the bulk work function of the sample (A) under study.

In some cases, A is prepared by chemical vapor deposition (CVD), where a sample gas (e.g., C_6H_6) is impinged to form a layer (e.g., graphitic carbon) on B (e.g., Pt(111), initially $\phi^e = 4.95$ eV) heated tentatively to a moderate temperature (e.g., 1200 K), and the work function of the graphitic film (C/Pt(111)) thus prepared on Pt(111) is measured to be 4.45 eV at a lower temperature (e.g., ~300 K) [527,857,889].

In the case of thermal ion emission (usually called the "surface ionization"), on the other hand, a foreign beam (or vapor) of alkali halide (MX), for example, is impinged as a probing gas to be changed into positive or negative ions (M^+ or X^- in Column 3) on a heated sample surface (Column 1) in order to determine ϕ^+ or ϕ^- (Column 6) by PSI or NSI (see Column 8). Typically for Mo(100) (see Footnote 167 in Table 1), $\phi^+ = 4.28 \pm 0.05$ eV by PSI of Li to Li^+ [129,572,573] and $\phi^- = 4.29 \pm 0.02^N$ eV by NSI of CsI to I^- [572,573] are entered in the same column (6) but on the separate lines adjacent with each other. Here, "N" means that the work function value originates from NSI, corresponding to ϕ^- instead of ϕ^+.

As known very well, ϕ^e of any A/B system changes largely depending upon the surface coverage (θ), reaching to a nearly constant value (saturation) usually at $\theta \geq 1$ ML after passing a minimum (ϕ_μ^e). In Table 1, such a saturated value is adopted as ϕ^e of the sample A (bulk) under study. For a variety of A/B systems, the quantitative relation between ϕ^e and θ or ϕ^e and ϕ_μ^e has long been investigated both experimentally and theoretically by great many workers. The Cs/metal systems, for instance, are deduced empirically to have the relation of $\phi_\mu^e = 1.94 - 0.09\phi^e$ or $\phi_\mu^e - \phi^e = 1.09(1.78 - \phi^e)$ [4362]. For estimating the relation, ϕ^e is cited from the data reported for Ru, Rh, Hf, W, Os, Ir and Pt [2105]. Much further information about the work function dependence upon θ is obtainable from excellent reviews [1209,1312,3818,3901,4118, etc.].

2.3. Column 3; Ionic species employed to measure the work function effective for positive or negative ion emission

This column shows the species of thermal positive or negative ion (e.g., K^+ or Cl^-) produced from a probing beam or vapor (e.g., KCl, see Column 2) incident upon a hot sample surface (e.g., Nb at $1853-2025$ K) [120] listed in Column 1 (for further information, see Footnote 165 in Table 1). From the data on thermal positive or negative ion current, the effective work function (ϕ^+ or ϕ^-) is determined according to Saha–Langmuir's equation applicable to PSI or NSI (see Eq. (5) or (6) herein and also Sections 2.1 or 8.1 in Ref. [1351]).

In some special cases, the probing ion (M^+ or M^-) to be used for work function measurement by PSI or NSI is produced by self-surface ionization (SSI), where the ion is produced directly from the sample surface itself by heating to very high temperatures (usually, above 2000 K). The species of ion thus produced is given in the parentheses like as (M^+) or (M^-) in the 3rd column. Such production is reported to be applicable to graphite ($C_1^- - C_8^-$) [3872], nickel (Ni^+) [3874–3876], niobium (Nb^+) [120,121,946,3401, 3874,3877,3878] and (Nb^-) [946], molybdenum (Mo^+) [77,131,132,946–954,961,3869–3871,3877,3879,3880,3884,3886,3891] and (Mo^-) [946,961], rhodium (Rh^+) [3874,3877,3879], tantalum (Ta^+) [77,137,804,805,946,3083,3877–3881,3887,3888,3891] and (Ta^-) [804,946], tungsten (W^+) [3,77,146,805,924,946,965,966,3083,3869,3870,3877,3879,3880,3882,3885,3887–3891] and (W^-) [946,965,966], and also rhenium (Re^+) [77,805,946,966,3083,3882,3883] and (Re^-) [946,966]. It should be noted that the above metals have both high melting point (~2700–3800 K except Ni and Rh) and moderate values of effective work functions ($\phi^+ \approx 4.8$–5.4 and $\phi^e \approx 4.1$–5.0 eV, see Table 2) and, hence, that production of both M^+ and M^- from the same metal by SSI is strongly governed by $\Delta\phi^* \equiv \phi^+ - \phi^e \approx 0.4$–0.7 eV for Nb, Mo, Ta, W and Re (see Table 5). Further information about the determination of ϕ^+ by positive SSI or usual PSI may be obtained from Footnote 170 in Table 1.

Especially, negative SSI is employed as a useful technique to produce negative ions directly from both refractory metals and graphite, and also it is applied successfully to the determination of electron affinity (E) of C_1–C_3 [3872,3873], Nb [946], Mo [946,961], Ta [946], W [946,965,966] and Re [946,966], although it is not easy to measure accurately the temperature dependence of the negative ion current according to Eq. (18) [1351] because the current is subject to the space charge effect due to much stronger electron current arising from TE simultaneously [946,965,966].

2.4. Column 4; Pressure of residual gases around a sample surface

Since all of the work functions (ϕ^+, ϕ^e and ϕ^-) are generally very sensitive to the pressure (P_r) of residual gases surrounding the sample surface under study, it is very important to consider whether or not the sample surface in the vacuum system employed is essentially free from any gas adsorption effect. Usually, P_r in Column (4) is the background pressure during each measurement of work function. Here and there, unfortunately, P_r is marked with a question mark in the column although the present author has tried to do best for finding its value.

In an A/B system, on the other hand, P_r is somewhat higher than the value indicated therein during the periods while A is deposited on B and also while A is annealed on B to prepare equilibrated (smoothed) layers. The value in parentheses, such as ($<10^{-10}$) for a Li/W system [2711], is not the total gas pressure but the partial one of active (chemisorptive) gases such as oxygen and its compounds.

Here, the pressure units have the relation of 1 Torr = 133.3 Pa (or N/m^2) = 1333 dyne/cm^2 = 1.333 mbar = 1.316 matm.

2.5. Column 5; Surface temperature or its range for measuring work function

This column indicates the surface temperature (or its range) at which each work function is measured. In ultrahigh vacuum such as below $\sim 10^{-10}$ Torr, a contact potential difference (CPD) method, for example, is generally applicable safely to the surface even much below ~ 1000 K. Even in usual high vacuum around $\sim 10^{-8}$ Torr, thermal ionic and electronic emissions from refractory metals (e.g., Ta and Re), on the other hand, may be applied normally to those surfaces kept at $T > 1800$ K [65,67,104]. Under such conditions, the surfaces are usually expected to be substantially clean.

With respect to A/B systems, work function (usually, ϕ^e to be measured) of the sample layers (A) is very sensitive to the thermal processing after deposition upon the substrate (B). Each figure in parentheses in Column 5 is the annealing temperature (T_a) for equilibrating (smoothing) the layers under study. For instance, the expression of ~ 300 (~ 900) for B/Mo(110) [2698] in Table 1 indicates that ϕ^e is measured at ~ 300 K after the boron layers are annealed at ~ 900 K or in the range of 600–1200 K.

In typical cases of the layers (250–590 Å) of Ru, Pt and Au deposited on quartz or glass at 85 or 78 K [436], T_a should be selected to be higher than roughly one-third ($T_a \geq T_m/3 \approx 900$, 680 and 450 K, respectively) of melting point ($T_m = 2723, 2047$ and 1336 K, respectively) in order that each of the layers may be expected to have the work function corresponding to each bulk [436]. The respective values ($\phi^e = 5.10, 5.72$ and 5.38 eV measured after annealing above $T_m/3$) are much higher than those (4.52, 5.46 and 5.22 eV) observed before the annealing [436] (see Footnote 363 in Table 1). In other words, any layers deposited much below room temperature are generally low in ϕ^e, and the *bulk* work function is hardly determinable for the sample (A) without moderate annealing.

According to Fig. 1 [3280] based on much data on Ag-films prepared on glass, mica, etc. [349,414,1893,1897, etc.], the annealing above ~ 460 K $> T_m/3 \approx 410$ K yields a constant value of 4.4 eV, which is considerably higher than both of 4.2 and 4.25 eV found at 78 and 300 K without annealing, respectively [3280], and also which is essentially the same with ours of 4.39 ± 0.02 eV recommended for *bulk* Ag, as will be shown in Table 2.

Such data as exemplified above suggest that the lattice defects in deposited layers at start may largely be removed on annealing [3610]. As may be known well, ϕ^e decreases generally as the surface defects (e.g., step, kink, dislocation, vacancy) increase in density. Typically for a W/W(110) system at ~ 290–370 K, ϕ^e is found to decrease by up to 0.6 eV linearly as a function of the square root of coverage (θ) with increasing step atom density [1039,1093]. A similar phenomenon is observed for bulk-W(110), too, reducing from ~ 5.2 to 4.9 eV as the step density increases from ~ 0 to 7×10^6/cm [1037], as shown clearly in Fig. 19 [1037] in Ref. [1351]. The local work function reductions at Au–Au and Cu–Cu monatomic steps are theoretically evaluated to be ~ 0.8 and ~ 1.3 eV, the respective values of which are in good agreement with those determined experimentally, as shown in Figs. 2 and 3 [1186]. For much further information about the effect of local surface irregularities upon work function, see Sections 3.3 [1313], 4.2 [1312] and 4.2.5 [1351].

In addition, a moderate annealing is very effective for promoting the monocrystallization of sample layers. Typically for an Ag(111)/quartz system prepared at ~ 300 K, its work function is increased by annealing at 773 K from 4.35 eV (54%) to 4.64 eV (86%) [3313], the latter of which is equal to 4.64 ± 0.06 eV ($\sim 100\%$) recommended for Ag(111) (see Table 2). Here, each value in parentheses is the fractional surface area ($F_{111} = \delta_m$) largest among various ones (F_i's), and it *mainly* governs ϕ^e for the "polycrystal" ($\delta_m < 50\%$ in general) and also for the "submonocrystal" ($50 < \delta_m < 100\%$), as will be demonstrated typically for W(A)–W(D) ($\delta_m = 33.6$–46.3%) and also for W(E)–W(G) ($\delta_m = 80$–96%) in Section 4 and Table 6. For further information about such an annealing effect for forming the "monocrystals" of Al(111), Ni(100), Ag(111) and Au(111), see Footnotes 55, 125, 198 and 350 in Table 1, respectively. Of course, Table 1 includes a variety of monocrystal/substrate systems such as Li(110)/Mo(111) [3361], Be(1010)/W(110) [3122], C$_{60}$(111)/GeS(001) [457,543], Na(110)/Ni(110) [1417], Al(100)/Ge(100) [3949], Si(100)/W(110) [3448], K(100)/KF(100) [2946], Sc(0001)/W(110) [1982], Ti(0001)/W(110) [4234], Sb(100)/W(110) [1272], La(0001)/Mo(100) [640], Pt(111)/Ni(111) [773] and Au(110)/W(112) [2256]. Similarly, the plates of mica, quartz, glass and so on are very useful as the substrate under a selected condition for preparing monocrystalline samples such as (1) Be(0001) [2009], Ni(100) [314], Cu(111) [4001,4041,4379], Pd(111) [4379], Ag(110) [626,4001], Ag(111) [626,1897,3276,4001,4040,4041,4378,4380–4382] and Au(111) [1202,1600,1897,4001,4380,4381] on mica, (2) Al(111) [612, 3313], Ag(111) [3313,4001], Pt(111) [2448] and Au(111) [3313] on quartz, and (3) Be(0001) [1782], K(110) [2476], Ti(0001) [2378] and Ni(100) [314,315,1523], Ni(111) [314,315,1513,2934,3058] on glass, and also (4) Pt(111) on garnet or sapphire [2448].

Typically for growing Au(111) at ~ 300–700 K, the substrates of mica and quartz make it possible to yield the results of $\phi^e = 5.3$–5.47 eV [1202,1600,1897,4001] and 5.38–5.42 eV [3313] (Table 1), all of which are in fair or good agreement with our values of 5.46 ± 0.07 eV and also with 5.31 eV [959] recommended for Au(111) in Refs. [1045,1358] (see Table 2). In addition, various species of foreign metal substrates as well as those exemplified above are employed to grow a variety of metal monocrystals and also to find their work function data to be acceptable today, as may be seen here and there in the first and 7th columns, respectively, in Table 1.

When the sample deposition temperature (T_d) is higher than the work function measurement one (T), both of them are shown as $T\{T_d\}$ in Table 1. For example, 78{540} [2256] means that Au is deposited onto W(112) at 540 K and, then, ϕ^e is measured at 78 K, thereby yielding that Au(110)/W(112) has $\phi^e = 5.45 \pm 0.03$ eV without additional annealing. The value thus determined is close to ours of 5.33 ± 0.09 eV recommended for bulk Au(110) in Table 2. On the other hand, $T = T_d = 78$ K yields $\phi^e = 5.3$ eV [2256], which corresponds not to Au(110) but to Au(poly) (see Table 1). Such an effect due to the difference between T and T_d for gold/W(mono) systems [2256] may be typically summarized below. Here, the first item is the sample layer/surface system whose layer structure is assigned by the authors [2256] and also {A/B}, $< C >$ and (D/E) show that $A = T$ (K), $B = T_d$ (K), $C = \theta$ (ML) and $D = \phi^e$ (eV) measured experimentally [2256] and $E = \phi^e$ (eV) cited from Column 3 in Table 2.

(1) Au/W(100) // {78/78} < ≥3 > (5.20/5.30 ± 0.04).
(2) Au/W(100) // {78/200} < ≥3 > (5.32/5.30 ± 0.04).
(3) Au/W(100) // {78/500} < ≥3 > (5.55/5.30 ± 0.04).
(4) Au/W(110) // {78/78} < 5 > (5.3/5.30 ± 0.04).
(5) Au/W(110) // {78/160} < 4 > (5.4/5.30 ± 0.04).
(6) Au(111)/W(110) // {78/420} < ≥3.5 > (5.32 ± 0.03/5.46 ± 0.07).
(7) Au/W(112) // {78/78} < ≥3.5 > (5.3/5.30 ± 0.04).
(8) Au(110)/W(112) // {78/540} < ≥3.5 > (5.45 ± 0.03/5.33 ± 0.09.

As may be seen above, the increase in T_d has a tendency to increase ϕ^e for Au(poly), and that to form Au(mono) according to its suitable selection. Further information about (4)–(6) and (7)–(8) is obtainable from Footnotes 349 and 348 in Table 1, respectively.

For depositing a sample onto a substrate successfully, it is very important to select T_d properly. For instance, C_{60} forms the layers (~1500 Å thick) on Si(111) at $T_d \approx 300$ K, but it does not appear to stick to the substrate at such a slightly high temperature as 393 K [3990]. It should be underlined that C_{60} on Mo(100) at ~300 K remains intact in the adsorbed state up to 760 K [322]. Similarly, C_{60}/Rh(111) at ~300 K is stable up to 750 K, above which it is decomposed into graphite like carbon [1007]. Interestingly, C_{60} decomposes on Ta(110) even at room temperature [316]. Formation of C_{60}(111) is observed on various substrates at ~300–500 K, and its typical examples [457,543,4037–4041] are outlined in Footnote 433 in Table 1.

Instead of such a type of ribbon, wire or tip for supporting a sample to be investigated, another type of boat or box (typically, quartz or ceramic made) is employed to prepare a binary system of metals with low melting point, and both temperature and composition dependences of ϕ^e have long been investigated [2613,4144]. Typically for these systems of Na–Rb, Na–Cs, K–Rb and K–Cs, each plot of work function vs. alloy component ($\gamma_c = 0$–100% in mole fraction) is found to overlap well between theory [4150] and experiment [2613, etc.]. Experimental results thus obtained at $\gamma_c = 0$ or 100% afford us work function data for a variety of pure metals, too; such as Na [2612,2613], K [2470,2612–2614], Cu [2626,2634], Zn [2624], Rb [2470,2613,4150,4297], Cd [2626], In [2624,2626], Sn [2624], Sb [2624,2626], Cs [2612,2613,4150,4297], Hg [2470,2613,2614] and Tl [2614] (for each data on ϕ^e, see Table 1). In contrast to the other substrate systems (wire, ribbon and tip types) mentioned above, the boat or box system is generally free from the physico-chemical effect of the supporting system upon the sample under study and, hence, it provides us bulk work function data even after preheating the sample up to melting point or over.

The expression of 0^E in Column 5 (e.g., Ca, Y, Zr, etc. [1747], see Footnote 174 in Table 1) means that the work function given in Column 7 corresponds to ϕ_0^e at 0 K after extrapolation of ϕ_T^e measured at higher temperature(s) according to $\phi_0^e = \phi_T^e - \alpha T$, where α is taken as $3\,k/2 = 1.29 \times 10^{-4}$ eV/K [1747]. Strictly speaking, however, the temperature coefficient (α) is not universal at $3\,k/2$, but dependent upon the surface species. It is reported to have a wide range between $\sim \pm 10^{-4}$ and $\pm 10^{-5}$ eV/K (see Table 6 in Ref. [1351]). Such a dependence makes it very difficult to determine exactly a minute work function change (usually, $\sim 10^{-2}$–10^{-3} eV to be estimated as the *net* change due to each transition alone) initiated either by allotropic, magnetic or superconductive transformation or by solid to liquid phase transition occurring at each critical temperature (e.g., Curie point), as will be outlined later (see Tables 11–14 and Sections 7–10).

2.6. Column 6; Work function (ϕ^+ or ϕ^-) effective for positive or negative ion emission

This column shows mainly the work function value (ϕ^+) generally determined by positive surface ionization (PSI) from the data on thermal positive ion current (i^+) of M$^+$ entered in Column 3, and ϕ^+ is listed according to an increase in value as exactly following the increasing value of ϕ^e for each surface species. The figure in parentheses such as (4.44 ± 0.03) for Mo(100) [727,2210,3103] is the value of ϕ^+ determined for the same specimen done for ϕ^e such as 4.40 ± 0.03 [727, etc.] entered on the identical line. Here, all of the items in Columns 2–5 and 8 (TE) correspond to ϕ^e instead of ϕ^+. On the other hand, the items corresponding to ϕ^+ are given on another line below by six lines (PSI), where $\phi^+ = 4.44 \pm 0.03$ eV and $\phi^e = (4.40 \pm 0.03)$ eV are determined for the *same* specimen in a separate experiment [727, etc.].

Experimentally, ϕ^+ is usually determined from the slope ($\phi^+ - I$) of a semi-Saha–Langmuir plot (ln i^+ vs. $1/kT$) based on Eq. (5) [2,1351].

$$\alpha^+ = \beta^+/(1 - \beta^+) = (w^+/w^0)\exp[(\phi^+ - I)/kT]. \tag{5}$$

Here, α^+ is the ionization coefficient, β^+ is the ionization efficiency of incident atom or molecule (e.g., M or MX), w^+/w^0 is the statistical weight ratio of ion to atom (e.g., 1/2 for alkali metal), and I is the ionization energy of M. The ratio is equivalent to exp $[\Delta S^+/k]$, where ΔS^+ is the entropy change due to the ionization of M. Typically for alkali metals, the ratio is calculated to be 0.503–$0.496 \approx 1/2$ at ~1000–2000 K by using entropy data compiled in thermochemical tables [26–28].

The value of ϕ^- is measured usually by negative surface ionization (NSI) and evaluated from another Saha–Langmuir equation [2,1351].

$$\alpha^- = \beta^-/(1 - \beta^-) = (w^-/w^0)\exp[(E - \phi^-)/kT]. \tag{6}$$

Here, E is the electron affinity of the sample atom (X), and w^-/w^0 equivalent to exp $[\Delta S^-/k]$ is the statistical weight ratio of X$^-$ to X (e.g., 1/4 for halogen). The latter is calculable from the entropy change (ΔS^-) by using thermochemical data [26–28]. Column 3 shows the species of X$^-$ produced by NSI of the beam (e.g., MX or X$_2$ specified in Column 2) under the condition in Columns 4 and 5. The data on ϕ^- are given in Column 6, as in the form of either 5.4^N for diamond of C(111) [3771] or (4.4^N) for a graphite

film of C/Pt [675] in order to avoid the confusion with the data on ϕ^+. The latter example [675] shows that the surface of C/Pt has the same value of $\phi^- = (4.4)$ eV and $\phi^e = 4.4$ eV determined for the *same* specimen (see the same line in Column 7 for ϕ^e). The condition and method employed for determining $\phi^e = (4.4)$ eV in Column 7 [675] are entered on the adjacent line just above, where ϕ^- is shown as (4.4^N) in Column 6 [675]. Quite similarly, $\phi^- = 4.36 \pm 0.05^N$ eV determined for Mo(100) by NSI of I_2 [571] is essentially equal to $\phi^e = (4.35 \pm 0.05)$ eV listed on the same line. The latter is determined by thermal electron emission (TE) from the *same* specimen in a separate experiment under substantially the same condition, as shown above by three lines including (4.36 $\pm$ 0.05^N) [571] (for further information, see Fig. 28 [571] in Ref. [1351]).

Each of the values with an asterisk, such as $\phi^+ = 4.66 \pm 0.11^*$ eV determined by PSI of Cs on W(100) [280] (see Footnote 278 in Table 1) and as $\phi^- = 4.49^{*N}$ eV done by NSI of KCl on W [574], is evaluated by the present author using the respective data on PSI and NSI reported therein [280,574] and also citing other factor(s) from other literatures. Typically, the latter [574] is evaluated from the experimental data on the slope of a semi-Saha–Langmuir plot of $\phi^- - E = 0.87$ eV found by NSI of KCl upon W [574] and also from the literature value of $E = 3.62$ eV as the electron affinity of Cl [577]. The feature of such a plot is outlined in Section 4.2.1 in Ref. [1351].

Interestingly, the thermal positive ion emission from the thick layers of a binary mixture (1:1 in mole ratio) of alkali halides (e.g., LiI and NaI) deposited on a metal surface shows such a "suppression effect" that the integrated ion current of Li ($I = 5.39$ eV) at 1080 K is reduced to 60% by the presence of NaI, although the ion emission of Na (5.14 eV) is little affected by the coexistent LiI [1950]. This result is consistent with Eq. (5) predicting that the metal having a higher value of I is less ionizable by PSI. Similarly, the thermal negative ion emission of I ($E = 3.06$ eV) from CsI is reduced by the coexistence (50% in mole fraction) of CsBr, in contrast to little change in that of Br (3.36 eV) from CsBr [3626]. This result consists with Eq. (6) indicating the less efficiency in negative ion emission by NSI in accordance with the smaller electron affinity.

Generally, there holds the relation of 1 eV = 0.07350 Ryd = 0.03675 hartree = 1.602 picoerg = 96.49 kJ/mol = 23.06 kcal/mol. In a Fowler plot, ϕ^e (in eV) is determinable from $12336/\lambda_0$, where λ_0 is the threshold wave length in Å (10^{-8} cm).

2.7. Column 7; Work function (ϕ^e) effective for electron emission

In this column, the work function (ϕ^e) effective for electron emission is listed according to the order of increasing value for each surface species. The value of ϕ^e in parentheses in Column 7 and that of ϕ^+ (or ϕ^-) in Column 6 on the same line are determined separately for the *same* specimen in Column 1 under essentially the same condition specified in Columns 4 and 5. Typically, the condition (5×10^{-9} Torr and ~1200−2000 K) for $\phi^+ = 5.25 \pm 0.05$ eV determined for W(110){>90% = δ_m} by PSI of Na is listed on the same line [86,90,2094] together with $\phi^e = (5.25 \pm 0.05)$ eV, whilst that (5×10^{-9} Torr and ~1500−1900 K) for $\phi^e = (5.25 \pm 0.05)$ eV by TE is given on the adjacent line just above [86,90,2094] together with $\phi^+ = (5.25 \pm 0.05)$ eV. Such arrangement of either both ϕ^+ and (ϕ^e) or both (ϕ^+) and ϕ^e listed on the same line makes it ready to recognize the thermionic contrast ($\Delta\phi^* \equiv \phi^+ - \phi^e = 5.25 - 5.25 = 0.00$ eV), the data of which will be summarized in Tables 4 and 5. Similarly on the adjacent lines, either both $\phi^- = (4.51^{*N})$ eV and $\phi^e = 4.51$ eV by TE [827] or both $\phi^- = 4.51^{*N}$ eV by NSI of I_2 and $\phi^e = (4.51)$ eV for W [827] are listed each on the same line (see Footnote 299 in Table 1). Therefore, this specific arrangement affords us directly the contrast ($\Delta\phi^{**} \equiv \phi^- - \phi^e = 0.00$ eV). Such a result is compiled later together with many other data on $\Delta\phi^{**}$ for both mono- and polycrystals in Table 7.

When either ϕ^e and ϕ^+ or ϕ^e and ϕ^- are determined by either TE and PSI or TE and NSI during incidence of a sample such as either Yb on Ir(111) [104] or I_2 on Mo(100) [571], of course, it is very important to select the working temperature to be high (either > 1800 K or > 1500 K) enough to avoid any sample adsorption effect on the measurements of either ϕ^e and ϕ^+ or ϕ^e and ϕ^- (see either Fig. 17 [104] or Fig. 28 [571] in Refs. [1351]).

2.8. Column 8; Method employed for evaluating each work function

The symbols contained in this column are explained briefly below, and some of the typical methods are outlined together with their results and accuracy compared with those by other methods.

2.8.1. General aspect

Each symbol listed as the method for evaluating the work function (ϕ^+, ϕ^e or ϕ^-) is fully expressed below. An outline about the principle, technique, feature, etc. for each method may be obtained from the references given at each end. A full detail for each method is omitted in this article because it is outside the present scope, which is intended mainly to establish an up-to-date and enriched database on work functions (ϕ^e, ϕ^+ and ϕ^-) for almost all the chemical elements and also which is aimed to estimate the most probable values for various surface species as much as possible.

AI = autoionization [1103,3496,3789,4027] (see Footnote 38 in Table 1).
CPD = contact potential difference [12,13,1312,1354,3256,3894,3898,3902,3970].
CS = conductance spectroscopy [2993].
FE = field emission [12,13,1312,1354,3894,3906].
IP = ionization potential [2199,3208] (see Footnote 60 in Table 1).
NSI = negative surface ionization (thermal negative ion emission) [2,13,15,18,1351,3896].
PE = photoelectric effect [12,13,1312,1354,3894].
PSI = positive surface ionization (thermal positive ion emission) [12,13,15,18,1351,3896].
SP = stopping potential [2349,3922].

TC = theoretical calculation [12,475,723,1312,1354,2427,3895,3901,3904,3905].

TCS = total current spectroscopy [2679,4050,4184] (see Footnote 409 in Table 1).

TE = thermal electron emission [1,12,13,1312,1351,1354,2129,3623,3724,3892–3894].

A brief discussion is made on the features of the absolute methods (FE, PE, PSI, TE) and the relative one (CPD), together with comparison of the work function values obtained by different methods [13,358,654,890,1058,1693,2471,3586,3897]. Typically, application of PE and CPD to Si(111)^p yields 5.10 and 4.83 eV, respectively [1971], while that to Ge(111)^p does the same value of 4.80 eV [1971] (see Footnote 155 in Table 1). For another example about several metals (Mo, Pd, Ag, Ta and Au), work function values estimated at various temperatures (293–1078 K) are found to have little difference (0.00–0.09 eV) at each temperature between the methods of PE and TE [3586]. Such a comparison among different methods will be discussed briefly in Section 2.8.2.

Regarding TC, many workers have tried to estimate ϕ^e using a variety of methods based on empirical or semi-empirical equations, which correlate ϕ^e quantitatively with various chemico-physical properties such as (1) atomic sublimation energy (in 1928) [3926], (2) atomic volume (1932–1936) [3927–3930] (see Section 2.8.4), (3) compressibility factor (1934) [3931] (see Section 2.8.4), (4) specific surface energy (1947, 1969) [837,4049], (5) zero charge potential and atomic radius (1953–1956) [3932,3933], (6) first ionization energy and either surface atomic density (1955) [1066] or covalent radius (1970) [4053], (7) electronegativity (1956–1978) [706,1645,1955,3267,3512,3975] (see Section 2.8.3), (8) atomic radius (1958) [3318], (9) atomic weight, density and the number of free electrons (1958) [3318], (10) both surface atom size and the sum of fractional bond numbers (1967–1979) [1159,1980,2129,3067], (11) electronegativity and covalent radius of metal atom (1970) [1993], (12) surface energy of monocrystal, lattice constant and number of valence electrons (1970) [4078] (see Section 5.5.2), (13) atomic sublimation entropy (1979) [3925,4051], (14) melting point of monocrystal and atomic volume (1979) [1684] (see Section 5.5.4), (15) first ionization energy and electron affinity (1982) [4136], and (16) atomic chemical potential (1999) [4270].

In contrast to the above classical theory, a modern theory about work function has been developed by many workers and, nowadays, quantum theory is widely employed to calculate ϕ^e of various surface species, as will be outlined roughly for some of the typical models in Section 2.8.5 and also discussed briefly in Section 6.

2.8.2. Comparison of work function data among different methods

A theoretical study of ϕ^e yields that $\phi^e_{PE} \geq \phi^e_{TE} \geq \phi^e_{true}$ and also $\phi^e_{PE} \geq \phi^e_{FE} \geq \phi^e_{true}$ for a given species [3897]. Here, ϕ^e_{PE}, ϕ^e_{TE} and ϕ^e_{FE} are the work functions to be measured by PE, TE and FE, respectively, and ϕ^e_{true} is the true work function. For monocrystals, however, the above inequalities are not fully examined by experiment mainly because of the poverty in available experimental data [3897]. For polycrystals, on the other hand, the data on ϕ^e_{CPD} measured for various metal films and bulk by CPD [349] are taken as those on ϕ^e_{true} [3897], and the experimental data obtained by the three different methods for 14 metals reported by other authors [488,1763, etc.] are compared among the above four species of ϕ^e's [3897], thereby yielding several exceptions against the above inequalities. In addition, the above relation of $\phi^e_{PE} \geq \phi^e_{true} \equiv \phi^e_{CPD}$ is opposite to that of $\phi^e_{PE} < \phi^e_{CPD}$, as will be discussed later in this section.

It should be noted that the above comparison of the data on ϕ^e_{CPD}, ϕ^e_{PE}, etc. reported for each metal species is made neither for the same specimen nor under the identical conditions. We should always take it into consideration that ϕ^e for any surface species is apt to change considerably from worker to worker or specimen to specimen, as may be seen in Table 1. Typically, ϕ^e for even Ag-bulk (neither film nor layer) is found to have the wide ranges of 3.09–4.7 eV by TE, 3.64–4.90 eV by PE and 3.94–4.73 eV by CPD, although these ranges are partly or considerably responsible for possible errors in measuring and/or processing.

In contrast to the above, let's consider the application of both PE and CPD to the *same* specimen under *common* conditions (P_r and T). About the Cs/Be system prepared by Cs$^+$ incidence up to $\theta = 1.0$ ML, for instance, ϕ^e is measured by both PE and CPD, thereby yielding the same value of 1.96 eV [3289]. By application of Kelvin, photoelectric and electron beam retarding methods to the U-layers ($\theta \approx 2$ ML) on W(100) at ~300 K, ϕ^e is determined to be 3.73 ± 0.02, 3.73 ± 0.02 and 3.78 ± 0.03 eV, respectively, for α-U [2471], thus showing essentially the same among the three.

In principle, the photoelectrically measured work function (ϕ^e_{PE}) of a patchy surface is known to be weighted towards *low* values (smaller local work functions), whereas the work function (ϕ^e_{CPD}) measured by CPD yields the *mean* value (local work function average) of the inhomogeneous surface under study [1693]. In practice, however, it is not so easy to confirm experimentally the inequality of $\phi^e_{PE} < \phi^e_{CPD}$ and also very difficult to evaluate accurately the difference between the two, because ϕ^e_{CPD} depends largely upon the accuracy of the reference work function value to be employed. Typically for a Ba/W system [1365], $\phi^e_{CPD} = 2.39 \pm 0.05$ eV [1365] is corrected to be 2.42 ± 0.05 eV [349] by taking 4.55 ± 0.02 eV [349] instead of 4.52 eV [1365] as the reference work function of W (see Footnote 238 in Table 1). Similarly to Ba/glass [1157], 2.52 eV [1157] may be corrected to be 2.35 ± 0.03 eV [349] by taking not 4.79 [1147] but 4.62 ± 0.03 eV [349] as the reference for Ag(100). Regarding Ba/Ag/Ta [1050], $\phi^e = 2.53$ eV [1050] is corrected to be 2.66 ± 0.01 eV [349] by taking 4.44 ± 0.01 eV [349] instead of 4.31 ± 0.03 eV [1050] as the reference work function of Ag. In another case where the reference work function of Au cited as 5.1 ± 0.1 eV [304] by the authors [4159] is replaced with 5.30 ± 0.04 eV (Table 2, to be shown later), $\phi^e_{CPD} = 4.47$ eV for Sn [4159] is corrected to be 4.27 ± 0.04 eV. These four examples indicate that ϕ^e_{CPD} is subject to change by up to ~0.2 eV depending upon the choice of the reference work function and hence upon its accuracy. The above change (0.03–0.20 eV) due to the selected reference work function seems generally to be not negligibly small compared with the probably minute difference between ϕ^e_{CPD} and ϕ^e_{PE}.

Comparison of the data obtained for the *same* specimen in each measurement is summarized below as in the form of (ϕ^e_{PE}/ϕ^e_{CPD}) in eV. Namely,

  (1) $(3.82 \pm 0.05/3.825 \pm 0.01)$ for In [2814].
  (2) $(1.96/1.96)$ for Cs/Be [3289].
  (3) $(4.73 \pm 0.07/4.73 \pm 0.07)$ for Si(111)^n [117,118].
  (4) $(3.73 \pm 0.02/3.73 \pm 0.02$ or $3.78 \pm 0.03)$ for α-U/W(100) [2471].
  (5) $(3.90 \pm 0.03/3.90 \pm 0.03$ or $4.00 \pm 0.04)$ for α-U/W(110) [2471].
  (6) $(3.66 \pm 0.03/3.67 \pm 0.03$ or $3.73 \pm 0.04)$ for α-U/W(113) [2471].
  (7) $(4.62 \pm 0.06/4.97 \pm 0.07$ or $4.86 \pm 0.10)$ for cnt/Si(111) [3246].
  (8) $(5.05 \pm 0.06/5.19 \pm 0.08$ or $5.06 \pm 0.04)$ for Pd/cnt/Si(111) [3246].
  (9) $(4.75 \pm 0.06/4.84 \pm 0.10$ or $4.76 \pm 0.09)$ for Ag/cnt/Si(111) [3246].
 (10) $(5.12 \pm 0.06/5.46 \pm 0.07$ or $5.39 \pm 0.08)$ for Pt/cnt/Si(111) [3246].
 (11) $(4.72 \pm 0.06/4.92 \pm 0.10$ or $4.85 \pm 0.11)$ for Au/cnt/Si(111) [3246].
 (12) $(5.38/5.45)$ for Au/glass [1074].
 (13) $(4.56/4.60)$ for Sb [1375].
 (14) $(4.26/4.34)$ for Bi [1375].
 (15) $(4.79/4.72)$ for As [1375].
 (16) $(4.14/4.27 \pm 0.04)$ for Sn [4159].
 (17) $(3.91/3.97 \pm 0.04)$ for Sn_{91}–Zn_9 [4159].
 (18) $(4.12/4.27 \pm 0.04)$ for $Sn_{96.5}$–$Ag_{3.5}$ [4159].
 (19) $(4.28/4.38 \pm 0.04)$ for Sn_{90}–Au_{10} [4159].
 (20) $(4.59/4.64 \pm 0.04)$ for Sn_{20}–Au_{80} [4159].

Results (1), (2) (see Footnote 232 in Table 1) and (3) indicate that $\Delta\phi^e_{C-P} \equiv \phi^e_{CPD} - \phi^e_{PE} \approx 0.0$ eV. Those (4) (see Footnote 408 in Table 1), (5) and (6) yield $\Delta\phi^e_{C-P} = 0.00$–$0.01$ and 0.05–0.10 eV by Kelvin and electron current retarding methods, respectively. Results (7)–(11) (see Footnote 25 in Table 1) show $\Delta\phi^e_{C-P} = 0.09$–$0.35$ and 0.01–0.27 eV before and after PE-measurements, respectively. Those (13)–(15) afford that $\Delta\phi^e_{C-P} = 0.04$ and 0.08 eV for Sb and Bi, respectively, in contrast to -0.07 eV for As. Those (16)–(20) indicate that $\Delta\phi^e_{C-P}$ is as small as 0.05–0.15 eV for both Sn and its binary alloys. This is because the work function of Au used as the reference for CPD [4159] is corrected from 5.1 ± 0.1 eV [304] to 5.30 ± 0.04 eV for Au (Table 2), as already indicating above that $\phi^e = 4.27$ eV corrected from 4.47 eV [4159] becomes nearer to our value of 4.34 eV recommended for β-Sn in Table 2. Here, the former $(5.1$ eV) [304] is included in Michaelson's review [1045] (see Table 2) and in a CRC Handbook (77th Ed., 1996–1997) [4137], but not done in any of the CRC handbooks (82nd–97th Eds., 2001–2017). It should be noted that $\Delta\phi^e_{C-P} = 0.05$–$0.15$ eV for Results (16)–(20) becomes larger by 0.20 eV unless the reference work function is corrected. Provided that each reference work function employed is free from a systematic error, then, many of the above results (1)–(20) except (15) may be concluded to have a tendency of $\phi^e_{CPD} > \phi^e_{PE}$ as an average of $\Delta\phi^e_{C-P} = 0.07 \pm 0.08$ eV for various *polycrystalline* surfaces with inhomogeneity in work function over the entire surface area, just as expected by consideration of each principle in work function measurement. This conclusion is opposite to that of $\phi^e_{PE} \geq \phi^e_{true} \equiv \phi^e_{CPD}$ [3897], as already mentioned above in this section.

For a *monocrystalline* sample of W(110) having the most probable values of $\phi^+ = 5.28$ or 5.29 eV and $\phi^e = 5.32$ or 5.31 eV recommended in Table 2 [Here or 1351], the actual work function is estimated to be 5.2 eV rather than 5.1 eV [2774] measured by the authors [2773,3768] in considering a slight underestimation (by 0.1 eV) by a photoemission method [2774]. In consequence, $\phi^e = 5.2$ eV thus estimated reaches an agreement with $\phi^+ = 5.2$ eV determined by PSI of fast Na atom (100 eV) incident on W(110) [2773,2774], thereby affording $\Delta\phi^* \equiv \phi^+ - \phi^e = 0.0$ eV instead of 0.1 eV. However, it does not seem adequately acceptable to consider such a large correction of 0.1 eV due to the underestimation by PE if the surface of W(110) is really homogeneous $(\delta_m = 100\%$ and hence $\Delta\phi^* = 0.00$ eV) in work function over the entire surface area and also if the measurement itself is essentially free from any systematic errors. Suppose that the surface under study has $\delta_m \approx 95\%$ instead of 100% in the degree of monocrystallization, for example, such a large correction as 0.1 eV may be acceptable when we consider such an actual example that 95%-W(100) has $\Delta\phi^* \approx 0.1$ eV, as exemplified for W(F) having $\Delta\phi^* = 0.09 \pm 0.05$ eV (see Table 6). It should be noted that the difference $(\Delta\phi^*)$ between ϕ^+ and ϕ^e becomes larger from 0.0 up to ~0.5 eV for W according as δ_m decrease from 100% to ~50% or less (see Section 4.3).

A clean and smooth surface of Ag(111) is found to have $\phi^e = 4.46 \pm 0.02$ eV measured by PE [625,1693]. On the other hand, ϕ^e for a surface of Ag(111) damaged by Ar^+ impact (400 eV, 15 $\mu A/cm^2$, 30 min) is 4.18 eV done by PE, slightly larger than 4.08 eV by CPD [1693]. This result indicates that application of PE to such a damaged surface is not suitable because any surface defect gives some effect to the surface potential barrier and hence to photothreshold [1693].

In the case of β-Be ($T \approx 900$–1200 K), a marked discrepancy (1.0 eV) of ϕ^e is found between 3.67 ± 0.01 eV measured by TE for bulk (ribbon) by Wilson [179,650,3410,3413,3413] and 4.67 ± 0.10 eV done by CPD (electron beam retarding) for Be-films on W(100) or W(110) by Zuber et al. [3550] (see Table 1). Further studies are desired to settle the question whether the above discrepancy originates from the difference between the methods (TE and CPD) or/and that between the surface structures (bulk and film).

2.8.3. Evaluation of work function from electronegativity

Regarding the quantitative relation between electronegativity and work function, the following equation [1955] is proposed first by Gordy and Thomas (in 1956).

$$\phi^e = 2.27X + 0.34 \text{ (in eV)} \tag{7}$$

Here, X is the electronegativity of each element in Pauling unit, and all of the work function values are cited from the review (first edition) published by Michaelson in 1950 [1355] in order to establish this equation. The constant of 0.34 eV is the energy required for electron to overcome the image force, identical for all metals [4047]. Much later (in 1973) by Miedema et al. [4048], Eq. (7) is modified as $\phi^e = 2.6X + 0.3$ (in eV), which is based on the work function data in Ref. [10] (Fomenko in 1966) and Ref. [304] (Eastman in 1970), in addition to Ref. [1355] (Michaelson in 1950). Recently (2008), Zhou et al. have proposed other relations such as $\phi^e = 1.92X + 0.99$ and $1.06X + 2.51$ (eV) for $X = 0.5$–2.5 and 1.2–2.4 in Pauling unit, respectively [4203], where ϕ^e is based on the review (second edition) published by Michaelson in 1977 [1045]. Consequently, we can not deny the possibility that the above coefficient and the constant may change considerably according to the reference data on both ϕ^e and X to be taken from various literatures for establishing the quantitative relation between the two. Nevertheless, such a relation as Eq. (7) is very useful for estimating ϕ^e of some elements (e.g., Pm, Po and Ra), which have no experimental data still today (see Footnote 379 in Table 1). This equation is successfully applied to many metals such as Sc (3.30/3.33 ± 0.04), Rb (2.13/2.17 ± 0.05), Ag (4.43/4.39 ± 0.02), Cs (2.05/2.05 ± 0.05) and Hg (4.43/4.50 ± 0.02), where the numerator and denominator in each parentheses correspond to the work function values (in eV) calculated from Eq. (7) and to ours recommended in this article (see Table 2), respectively, clearly showing a good agreement between the two in each parentheses.

About many other metals, however, the work function values based on Eq. (7) are found to be considerably different from ours (Table 2); typically, graphite (6.02/4.63 ± 0.06), Mg (3.07/3.65 ± 0.05), Ni (4.43/5.06 ± 0.06), and Ga (3.75/4.27 ± 0.06), where the numerator and denominator originate from Eq. (7) and Table 2, respectively. Such a large difference or discrepancy found between the two values in each of the parentheses (Eq. (7)/Table 2) may originate probably from the uncertainty of X depending upon the methods for estimating X and also from the incorrectness in ϕ^e [1355] taken as the reference to establish Eq. (7). It should be noted that the mean of work function estimated for each element by Michaelson [1355] is based on those literatures published before 1950 and, hence, that many of the mean values therein are much different from ours (Table 2); typically, such as Se (4.72/5.27 ± 0.18), Ir (4.57/5.28 ± 0.04) and Au (4.58/5.30 ± 0.04). Here, (a/b) corresponds to (mean [1355]/ours (Table 2)). By taking other data (published before 1970) compiled by Fomenko [10,12], the quantitative relation between ϕ^e and X are examined, thereby reaching the conclusion that Eq. (7) is valid especially for some of the elements of low work functions [3975], in contrast to those of high work functions. The concept of both electronegativity and Pauling unit may be thoroughly understandable from the original paper [4006] and a comprehensive review [3974].

Gyftopoulos and Hatsopoulos show that the work function of a uniform surface equals the neutral orbital electronegativity of a spin-orbital localized around a surface atom [2153].

2.8.4. Evaluations of work function from atomic volume and from compressibility factor

As already mentioned in Section 2.8.1, work function studies have produced various ideas for expressing the quantitative relations between ϕ^e and physico-chemical properties. Among the sixteen ideas mentioned there, let's examine here the two typical examples of (2) atomic volume and (3) compressibility factor, which were published in an early stage (1930's) of the historical progress in work function calculations. In this section, some of the calculated results alone will be summarized compactly below.

The atomic volume model (2) proposed by Rother and Bomke (in 1933) [3928] yields the typical results of B (4.8/4.50 ± 0.09), Ti (3.5/3.87 ± 0.06), V (4.0/4.10 ± 0.05), Nb (3.9/4.11 ± 0.05), In (4.0/4.05 ± 0.06), La (3.2/3.27 ± 0.04), Hf (3.6/3.64 ± 0.06), Ra (2.0/2.4 ± 0.3) and Ac (3.0/3.2 ± 0.3). Here, the numerator and denominator in parentheses correspond to the calculated value [3928] and ours (Table 2) in eV, respectively. Between the two, a good or fair agreement is found for each element. Especially, the data on both Ra and Ac may be useful for supplementing several scanty data achieved to date by other theoretical models (see Table 1). It is worthy to underline that any experimental data are unavailable as yet today for the two as well as other radioactive elements such as Po, At, Fr, etc. (see Table 1). On the other hand, the values calculated for Be, Mn, Ga, Zr and U [3928] have a large difference (~0.6–1.5 eV) from ours in Table 2.

The model of compressibility factor (3) proposed by Chittum (in 1934) [3931] yields the data on nineteen elements, among which (numerator) a good agreement to our most probable value (denominator) is found for Ca (3.00/2.91 ± 0.03), Ag (4.33/4.39 ± 0.03) and Pt (5.34/5.30 ± 0.07) alone. The values calculated for the other sixteen elements (K, Co, Zn, Pd, W, etc.) result in a considerable difference (by ~0.2–1.0 eV) from ours in Table 2.

Unluckily, almost all the empirical or semiempirical equations based on the models (1)–(16) mentioned in Section 2.8.1 are limited to evaluating ϕ^e for polycrystals alone. It is only three equations based on the model (10) proposed by Steiner and Gyftopoulos (in 1967, 1980) [1159,1980,3067], on (12) by Zadumkin et al. (in 1970) [4078] and on (14) by Chatterjee (in 1979) [1684] alone, that are applicable to evaluation of ϕ^e for monocrystals. At present, however, such classical models are made less important by an amazing progress in quantum theory applicable not only to polycrystals but also to monocrystals with various orientations, as will be exemplified briefly below.

2.8.5. Evaluation of work function by quantum theory

Modern theory about work function is initiated by Wigner and Barden (in 1935), who apply the quantum calculation of ϕ^e to alkali metals [3725], thus evaluating $\phi^e = 2.19, 2.15, 2.20, 2.20$ and 2.15 eV for Li, Na, K, Rb and Cs, respectively, in addition to 2.0 or 2.35 eV for Na by Bardeen (in 1936) [1458]. Such values either much deviate from or well agree with ours of 2.90, 2.54, 2.29, 2.17 and 2.05 eV for respective alkali metals (see Table 2). In the next stage, Kohn has made a great contribution to developing the better calculation of ϕ^e, the effectual framework for which originates from the density functional theory reported in 1964–1966 by Kohn et al. [3638,4043,4044]. Further information about his brilliant achievements is obtainable from his Nobel lecture entitled the "Electronic structure of matter — wave functions and density functionals" [1698] and also from several

topics [4395–4397]. Hereafter, many workers have developed various models, the principle and feature of which are outlined in excellent reviews [723,1312,2004,2427,3895,3982,4035]. Some of the models are exemplified together with the results calculated for aluminum monocrystalline surfaces [1943]. For instance, the generalized gradient approximation with Perdew–Burke–Ernzerhof (GGA/PBE) functional model applied to Al(111) yields 4.06 eV [482,1175] and 4.09 eV [1177], both slightly smaller than our value of 4.24 ± 0.04 eV (see Table 2). On the other hand, the local density approximation with Coperly–Alder (LDA/CA) functional model done so affords 4.19 eV [557], 4.21 eV [1179], 4.22 eV [1943] and 4.25 eV [721], entirely well agreeing with ours cited just above. An outline about GGA etc. is given in each reference attached with the corresponding model. As brief supplements to the comprehensive data book published in 1981 [1354], Fomenko compiles the theoretical work function data published for mono- and polycrystals during the period of mainly ~1980–1990 [485,4116], and also he summarizes theoretical and experimental data reported for both Y and lanthanide monocrystals during 1976–1992 [4146].

In contrast to the above quite short and rough tracing about the development of quantum treatments of work function, much further information is obtainable from the excellent reviews mentioned above [723, etc.]. In addition, a long and interesting history of work function studies is compactly summarized as the "100 years of work function" by Halas in 2006 [4058] and as the "Electron work function — past, present and future" in 2005 [4099] together with the "Fundamental physics of vacuum electron sources" in 2006 [2243] by Yamamoto. Interesting information may be obtained from the "Hundred years of anniversary of the oxide cathode — A historical review" by Gaertner and den Engelsen in 2005 [1648] and also from the "Centennial Symposium on Electron" held in 1997 [1419].

The work function dependence upon both surface and bulk properties is theoretically investigated by Lang and Kohn using the uniform-positive-background model [475], a typical result of which will be outlined in Section 6.1, together with a brief comparison with our most probable values listed in Table 2.

2.8.6. Correction of work function values measured from Richardson plots

The Richardson constant of A_R in Richardson equation [1,2,1351] has seldom been measured exactly to be the theoretical value of 120 A/cm² K² for any surface species (e.g., Be, Si, Ta and Pt) by many experimental attempts, as may be seen in handbooks compiled by Fomenko [10,12,1354]. Typically, A_R for Si is reported to be 0.2–38 A/cm² K² [10,12,1354], similarly for Si(110), Si(111), Si(112) and Si (541) as to be 0.004–3 A/cm² K² with one exception of ~130 A/cm² K² [1354]. Particularly for molten Ag above 1234 K, A_R is found to be extremely as small as 6.4×10^{-8} A/cm² K² [1466] (see Footnote 431 in Table 1). Such a reduction in A_R is mainly because a great part of the electrons has no energy enough to escape from the surface into vacuum and also because such "internal reflection" is subject to dependence upon surface temperature and, hence, ϕ^e is generally measured to be considerably smaller than the normal value, as will be demonstrated just below.

Typically, Si(111) is found to have $\phi^e \approx$ ~4.0–4.8 eV by TE [72–75, etc.], in contrast to ~4.4–4.8 eV by PE [1181,3969, etc.] and also to ~4.6–4.9 eV by CPD [117,1959, etc.], as may be seen in Table 1. In addition, the former by TE is again smaller than $\phi^+ \approx 4.6$–5.2 eV [72–75] by PSI even in nearly the same temperature range. Consequently, Si(111) is often found to yield the results of $\Delta\phi^* \equiv \phi^+ - \phi^e \neq 0$ eV, although many other monocrystalline surfaces of Ta, W, etc. are usually determined to have $\Delta\phi^* = 0.0$ eV just as predicted by theory, as will be shown in Tables 4 and 5.

In order to avoid such a typical error due to the reduction in A_R, Hensley proposes the simple method (in 1961) that the work function to be measured directly by TE may be adequately corrected according [3623] to

$$\phi_H^e = \phi_r^e + kT \ln(120/A_r). \tag{8}$$

Here, ϕ_r^e is the work function (ϕ^e) measured directly together with $A_r \neq A_R = 120$ A/cm² K² from a Richardson plot, where A_r is the apparent Richardson constant corresponding to $(1 - r^e) A_R$ and r^e is the internal reflection coefficient [2,12,13,1354]. Firstly (in 1967) by Hopkins et al. [1484], Eq. (8) is applied to U/W systems ($\theta = 1$–50 ML), thereby yielding such a typical result that $\phi_r^e = 3.14 \pm 0.02$ is corrected to be $\phi_H^e = 3.36 \pm 0.04$ eV according to the data on $A_r = 20 \pm 7$ A/cm² K². The latter is nearer to 3.42 ± 0.05 eV for γ-U(poly) recommended by us in Table 2.

Regarding a specimen of p-type Si(111)^p measured to have $\phi_r^e = 3.2$ eV and $A_r = 4 \times 10^{-3}$ A/cm² K² at ~1100–1150 K [3540], for example, ϕ_H^e is calculated by the present author to be 4.2 eV from Eq. (8). This value agrees exactly with $\phi^e = 4.2$ eV determined directly with the same specimen at ~1150–1450 K [3540], where A_r is measured to be 130 A/cm² K² [3540]. Comparison of the results between the two temperature ranges indicates that the probability of these electrons escaping to vacuum after overcoming the surface barrier on Si(111) is extremely small in the lower temperature range and also suggests that the silicon specimen has $r^e > 0.99$ (larger than 99%) in the lower temperature range in contrast to the higher one of $r^e \approx 0$, if the above experimental data are free from any systematic errors.

In another case of Si(111)^p [73], $\phi_r^e = 4.07 \pm 0.05$ eV with $A_r = 0.2$–0.4 A/cm² K² at ~1300–1600 K by TE [73] may be corrected to be $\phi_H^e = 4.83 \pm 0.04$ eV $= \phi^e$, similarly above by the present author. This is essentially equal to 4.84 ± 0.14 and 4.86 ± 0.11 eV determined not from a Richardson plot but from an electron retarding field one (Anderson method [1365]) at ~1500 K [73]. In addition, ϕ_H^e ($=\phi^e$) is in good agreement with $\phi^+ = 4.88 \pm 0.10$ and 4.85 ± 0.08 eV determined for the same specimen by a cesium ion retarding method based on PSI at ~1500 K [73], thereby yielding $\Delta\phi^* \equiv \phi^+ - \phi^e = 0.02 \pm 0.02$ eV $= 0.0$ eV, just as predicted by theory for a monocrystalline surface under the normal condition accepted in general (see Footnote 66 in Table 1).

In the same way as Si(111)^p with $A_r = 0.2$–0.4 A/cm² K² [73] exemplified just above, $\phi_r^e = 4.04 \pm 0.05$ eV measured for n-type Si(111)^n ($A_r = 0.3$ A/cm² K², estimated) by TE (1340–1600 K) [72] may be similarly corrected to be 4.80 ± 0.04 eV $= \phi_H^e$, which yields $\Delta\phi^* = 0.06 \pm 0.08$, 0.07 ± 0.05 and 0.10 ± 0.11 eV since $\phi^+ = 4.86 \pm 0.07$, 4.87 ± 0.03 and 4.90 ± 0.10 eV by PSI of Li, Na and In on the same way, respectively [72]. Again, $\Delta\phi^* \approx 0.0$ eV is obtained in contrast to $\Delta\phi^* = 0.82$–0.86 $\neq 0$ eV in the former

($\phi^e = 4.04$ eV) measured directly from a Richardson plot. These results may suggest that many couples of the data on $\phi^+ > \phi^e$, such as $\phi^+ = 4.78 \pm 0.05$ eV $> \phi^e = 4.59 \pm 0.05$ eV determined for a specimen (A) of Si(111), as well as others (B–E) [75], are mainly caused by underestimation of ϕ^e due to $r^e > 0$ mentioned above. Additional information on the above problem is obtainable from Footnote 66 in Table 1.

In respect of γ-U (flat strip) [3961], $\phi_r^e = 3.27 \pm 0.05$ eV is corrected to be $\phi_H^e = 3.56 \pm 0.05$ eV, slightly larger than ours (3.42 $\pm$ 0.05 eV) in Table 2. This may be mainly because $A_r = 6$ A/cm^2 K^2 is only roughly estimated [3961].

Another study of β- and γ-Fe yields $\phi_r^e = 4.48 \pm 0.06$ eV with $A_r = 26$ A/cm^2 K^2 for β and $\phi_r^e = 4.21 \pm 0.05$ eV and 1.5 A/cm^2 K^2 for γ [310], the respective work function values of which may be corrected to be 4.64 ± 0.06 and 4.66 ± 0.05 eV by Eq. (8) (see Table 1). Consequently, the allotropic work function change ($\Delta\phi_{\gamma\beta}^e \equiv \phi_\gamma^e - \phi_\beta^e$) is corrected from -0.27 ± 0.08 to 0.02 ± 0.08 eV, only the latter of which is in fair agreement with any other five values of $\Delta\phi_{\gamma\beta}^e = 0.00$–0.09 eV and also well agrees with their mean value of 0.04 ± 0.03 eV, as will be shown in Table 11.

Regarding the two surface species of Th/ThO$_2$-W and γ-U/W, some of the typical data are summarized below as in the form of (T) in K, $\{A_r\}$ in A/cm^2 K^2 and (ϕ_r^e/ϕ_H^e) in eV, where ϕ_H^e with # is calculated by Hopkins et al. [1484] while the others are done by the present author. In addition, our most probable value of ϕ^e (Table 2) is given together with Means of ϕ_r^e and ϕ_H^e. For Data (1)–(4) below, the Th-films on W are prepared from a sintered cathode (67% thoria and 33% tungsten) by activation at 2040 K [3800], which corresponds to the "spillover" method mentioned in Section 2.2.

(1) Th/ThO$_2$-W ($\sim$1100–1500) // {69.1} (3.40/3.46) [3800].
(2) Th/ThO$_2$-W ($\sim$1100–1500) // {61.6} (3.26/3.33) [3800].
(3) Th/ThO$_2$-W ($\sim$1100–1500) // {10.6} (2.91/3.18) [3800].
(4) Th/ThO$_2$-W ($\sim$1100–1500) // {9.6} (3.0/3.28) [3800].
  (1)–(4) Means of $\phi_r^e = 3.14 \pm 0.40$ eV and $\phi_H^e = 3.31 \pm 0.10$ eV, while $\phi^e = 3.37 \pm 0.04$ eV (Table 2).
(5) γ-U/W (1250–1400) // {114 $\pm$ 12} (3.47 $\pm$ 0.03/3.48 $\pm$ 0.03#) [232].
(6) γ-U/W ($\sim$1000–1400) // {80 $\pm$ 30} (3.42 $\pm$ 0.04/3.45 $\pm$ 0.1#) [1484].
(7) γ-U/W ($\sim$1000–1300) // {20 $\pm$ 7} (3.14 $\pm$ 0.02/3.36 $\pm$ 0.04#) [1484].
(8) γ-U/W (1250) // {8} (3.2/3.5) [2098].
(9) γ-U/W (1250–1400) // {5} (3.0/3.38#) [232].
  (5)–(9) Means of $\phi_r^e = 3.25 \pm 0.18$ eV and $\phi_H^e = 3.43 \pm 0.06$ eV, while $\phi^e = 3.42 \pm 0.05$ eV (Table 2).

As may be seen in Data (1)–(4) as well as those (5)–(9) above, with exceptions of (3) and (8), ϕ_r^e tends to decrease generally with decreasing A_r, but each mean value of ϕ_H^e becomes nearer to ours of ϕ^e, just as expected in general. Additional information about such a correction according to Eq. (8) may be obtained from Footnotes 384–386, 431 and 456 in Table 1.

As a quantitative relationship between ϕ_r^e and A_r, the equation of $\log_{10} A_r = -6.85 + 1.87\phi_r^e$ is determined experimentally for Pt [2299,2300]. This is consistent with the above result that the more A_r becomes smaller, the more ϕ_r^e does so.

2.9. Column 9; References for each work function study

Plural references on the same line in the 9th column correspond to the same author(s) or group(s). References of [1]–[1350] are contained also in the previous review [1351], and many of them afford us further information and data on the work functions (ϕ^+, ϕ^e and ϕ^-) for both chemical elements and compounds. But, work function data on the latter (e.g., SiC, LaB$_6$ and ZrC) are not included in Table 1 herein. Of course, all of the data on the three kinds of work functions for about 400 surface species of 18 kinds of chemical elements ($_6$C–$_{79}$Au) covered previously [1351] are also included here together with newly cited ones (about 200 surface species of 70 elements) for both mono- and polycrystals covering the total of about 600 surface species of 88 elements ($_1$H–$_{99}$Es) on the bases of 4461 references published to date.

2.10. Footnotes for further information

Table 1 is attached with 490 footnotes, which afford additional information about the correlations of work function (ϕ^e or ϕ^+) with (1) its variation according to T, P_r, θ, etc. employed for the specimen under study, (2) its dependence on the size of either fine particles, nanowires or clusters, (3) its revision or correction by the present or other authors, (4) its dependence upon the degree of monocrystallization (δ_m) estimated for film or bulk samples, (5) its coincidence between theory and experiment done for the same specimen, (6) its changes at critical temperatures causing various physical transitions, (7) its increase by annealing (smoothing) the layer surface under study, (8) its coincidence among different measuring methods, and so on.

3. Most probable values of effective work functions (ϕ^+, ϕ^- and ϕ^e)

This section outlines the method to estimate the most probable values of the three kinds of work functions for essentially clean surfaces of both mono- and polycrystals after examining the reliability or acceptability for each of the great many data listed in Table 1 and also summarizes the results in Table 2 together with literature values recommended previously for each surface species independently by other several authors in order to examine the objective reliability or acceptability of our most probable value for each species.

Table 2

Effective work functions (ϕ^e, ϕ^+ and ϕ^-) recommended as the most probable values [Here] by the present author using the data in Table 1, and the effective one (ϕ^e) selected as either typical or preferable value by other authors [1045,1358], and also that (ϕ^e) recommended formerly by another author [12,1354] and previously by the present author [1351] for essentially clean surfaces.

No.	Surface	ϕ^e (eV) [Here]	ϕ^+ (eV) [Here]	ϕ^- (eV) [Here]	ϕ^e (eV) [1358]	ϕ^e (eV) [1045]	ϕ^e (eV) [12,1354]	ϕ^e (eV) [1351]
1	H(100)[f(1)]	3.7[z(4)]	–	–	–	–	–	–
1	H(110)[f]	3.8[z]	–	–	–	–	–	–
1	H(111)[f]	3.8[z]	–	–	–	–	–	–
1	H(poly)[f]	3.89 ± 0.09[(3)]	–	–	–	–	–	–
3	Li(100)[b]	3.12 ± 0.03[(3)]	–	–	–	–	–	–
3	Li(110)[b]	3.37 ± 0.05	–	–	–	–	–	–
3	Li(111)[b]	3.04 ± 0.08	–	–	–	–	–	–
3	Li(112)[b]	3.3[z(4)]	–	–	–	–	–	–
3	Li(poly)[b]	2.90 ± 0.03	–	–	2.93 [363]	2.9 [363]	2.38	–
4	α-Be(0001)[hc]	5.27 ± 0.11	–	–	–	–	–	–
4	α-Be(1010)[hc]	4.6 ± 0.1[y(4)]	–	–	–	–	–	–
4	α-Be(0111)[hc]	5.1 ± 0.1[x]	–	–	–	–	–	–
4	α-Be(0112)[hc]	4.9 ± 0.1[x]	–	–	–	–	–	–
4	α-Be(0113)[hc]	4.6 ± 0.1[x]	–	–	–	–	–	–
4	α-Be(1121)[hc]	4.7 ± 0.1[x]	–	–	–	–	–	–
4	α-Be(1122)[hc]	4.9 ± 0.1[x]	–	–	–	–	–	–
4	α-Be(1123)[hc]	4.3 ± 0.1[x]	–	–	–	–	–	–
4	α-Be(1124)[hc]	5.7[z]	–	–	–	–	–	–
4	α-Be(2130)[hc]	4.3 ± 0.1[x]	–	–	–	–	–	–
4	α-Be(3140)[hc]	4.4 ± 0.2[x]	–	–	–	–	–	–
4	α-Be(poly)[hc]	4.28 ± 0.13	–	–	4.98 [2009][(8)]	4.98 [2009][(8)]	3.92	–
4	β-Be(poly)[h]	4.2 ± 0.5	–	–	–	–	–	–
5	B(poly)	4.50 ± 0.09	–	–	–	–	4.5	–
6	C(100)[d]	5.0 ± 0.6	–	–	–	–	–	–
6	C(111)[d]	5.4 ± 0.5	–	–	–	–	–	–
6	C(112)[d]	5.2[z]	–	–	–	–	–	–
6	C(poly)[d]	4.6 ± 0.6	–	–	–	–	–	–
6	C(0001)[h]	4.6 ± 0.3	–	–	–	–	–	–
6	C(HOPG)[h]	4.66 ± 0.05	4.65 ± 0.12	–	–	–	–	–
6	C(film)	4.47 ± 0.05	4.50 ± 0.04	4.4 ± 0.1[x]	–	–	–	–
6	C(poly)	4.63 ± 0.06	4.45 ± 0.05[x]	4.6 ± 0.2[z]	5.0 [299]	5.0 [299]	4.7	4.6 ± 0.1
6	C(graphene)	4.67 ± 0.11	–	–	–	–	–	–
6	C_{60}(111)	4.76 ± 0.05[y]	–	–	–	–	–	–
6	C_{60}(poly)	4.87 ± 0.06	–	–	–	–	–	–
6	C(swnt)	4.78 ± 0.06	–	–	–	–	–	–
6	C(mwnt)	4.63 ± 0.04	–	–	–	–	–	–
6	C(conical)	4.3 ± 0.2[y]	–	–	–	–	–	–
11	Na(100)[b]	2.80 ± 0.04	–	–	–	–	–	–
11	Na(110)[b]	3.05 ± 0.04	–	–	–	–	–	–
11	Na(111)[b]	2.68 ± 0.06	–	–	–	–	–	–
11	Na(112)[b]	3.1[z]	–	–	–	–	–	–
11	Na(poly)[b]	2.54 ± 0.03	–	–	2.36 [3337][(11)]	2.75 [3424][(11)]	2.35[(11)]	–
11	Na(liquid)	2.6 ± 0.2[y]	–	–	–	–	–	–
12	Mg(0001)[hc]	3.79 ± 0.07	–	–	–	–	–	–
12	Mg(1010)[hc]	3.7 ± 0.1[y]	–	–	–	–	–	–
12	Mg(0111)[hc]	3.8 ± 0.1[x]	–	–	–	–	–	–
12	Mg(0112)[hc]	3.7 ± 0.1[x]	–	–	–	–	–	–
12	Mg(0113)[hc]	3.6 ± 0.1[x]	–	–	–	–	–	–

(continued on next page)

Table 2 (*continued*)

No.	Surface	ϕ^e (eV) [Here]	ϕ^+ (eV) [Here]	ϕ^- (eV) [Here]	ϕ^e (eV) [1358]	ϕ^e (eV) [1045]	ϕ^e (eV) [12,1354]	ϕ^e (eV) [1351]
12	Mg(1121)[hc]	3.6 ± 0.1^x	–	–	–	–	–	–
12	Mg(1122)[hc]	3.7 ± 0.1^x	–	–	–	–	–	–
12	Mg(1123)[hc]	3.6 ± 0.1^x	–	–	–	–	–	–
12	Mg(2130)[hc]	3.6 ± 0.1^x	–	–	–	–	–	–
12	Mg(3140)[hc]	3.6 ± 0.1^x	–	–	–	–	–	–
12	Mg(poly)[hc]	$\underline{3.65 \pm 0.05}$	–	–	3.66 [1968]	3.66 [1968]	3.64	–
13	Al(100)[f]	$\underline{4.28 \pm 0.05}$	–	–	4.20 [612]	4.41 [241]	–	4.36 ± 0.10
13	Al(110)[f]	$\underline{4.05 \pm 0.05}$	–	–	4.06 [612]	4.06 [612]	–	4.21 ± 0.09
13	Al(111)[f]	$\underline{4.24 \pm 0.04}$	–	–	4.26 [612]	4.24 [241]	–	4.28 ± 0.04
13	Al(poly)[f]	$\underline{4.26 \pm 0.03}$	4.9 ± 0.1^x	–	–	4.28 [612]	4.25	4.23 ± 0.06
14	Si(100)[d]	$\underline{4.82 \pm 0.05}$	4.72 ± 0.10	–	4.91^p [1225]	4.91^p [1225]	–	4.71 ± 0.16
14	Si(110)[d]	4.44 ± 0.24	$\underline{4.36 \pm 0.03}$	–	–	–	–	–
14	Si(111)[d]	$\underline{4.86 \pm 0.09}$	$\underline{4.83 \pm 0.07}$	–	4.60^p [118]	4.60^p [118]	–	4.79 ± 0.07
14	Si(112)[d]	4.1 ± 0.2	–	–	–	–	–	–
14	Si(541)[d]	4.0 ± 0.3^y	–	–	–	–	–	–
14	Si(poly)[d]	$\underline{4.65 \pm 0.09}$	–	–	4.85^n [613]	4.85^n [613]	4.8	4.6 ± 0.1
15	P(111)	1.4^z	–	–	–	–	–	–
15	P(poly)	5.0 ± 0.1^y	–	–	–	–	–	–
16	α-S(poly)[r]	$\underline{5.31 \pm 0.08}$	–	–	–	–	–	–
19	K(100)[b]	$\underline{2.47 \pm 0.04}$	–	–	–	–	–	–
19	K(110)[b]	$\underline{2.74 \pm 0.04}$	–	–	–	–	–	–
19	K(111)[b]	$\underline{2.39 \pm 0.02}$	–	–	–	–	–	–
19	K(112)[b]	2.7^z	–	–	–	–	–	–
19	K(poly)[b]	$\underline{2.29 \pm 0.02}$	–	–	2.29 [?]	2.30 [3337]	2.22	–
19	K(liquid)	2.28 ± 0.02^y	–	–	–	–	–	–
20	α-Ca(100)[f]	3.4 ± 0.4	–	–	–	–	–	–
20	α-Ca(110)[f]	3.3 ± 0.3	–	–	–	–	–	–
20	α-Ca(111)[f]	3.5 ± 0.2	–	–	–	–	–	–
20	γ-Ca(100)[b]	3.5^z	–	–	–	–	–	–
20	γ-Ca(110)[b]	3.5 ± 0.6^x	–	–	–	–	–	–
20	γ-Ca(111)[b]	3.4^z	–	–	–	–	–	–
20	γ-Ca(112)[b]	3.8^z	–	–	–	–	–	–
20	α-Ca(poly)[f]	$\underline{2.91 \pm 0.03}$	–	–	2.87 [1997]	2.87 [1997]	2.80	–
21	α-Sc(0001)[hc]	3.7 ± 0.1	–	–	–	–	–	–
21	α-Sc(1010)[hc]	3.5 ± 0.2^y	–	–	–	–	–	–
21	α-Sc(1124)[hc]	4.0^z	–	–	–	–	–	–
21	β-Sc(100)[f]	4.4^z	–	–	–	–	–	–
21	β-Sc(110)[f]	4.1^z	–	–	–	–	–	–
21	β-Sc(111)[f]	4.3 ± 0.4^x	–	–	–	–	–	–
21	α-Sc(poly)[hc]	$\underline{3.33 \pm 0.04}$	–	–	3.5 [304]	3.5 [304]	3.3	–
21	β-Sc(poly)[f]	3.4^x	–	–	–	–	–	–
22	α-Ti(0001)[hc]	$\underline{4.53 \pm 0.10}$	–	–	–	–	–	–
22	α-Ti(1010)[hc]	4.2 ± 0.4^y	–	–	–	–	–	–
22	α-Ti(1011)[hc]	4.8^z	–	–	–	–	–	–
22	α-Ti(1124)[hc]	4.2^z	–	–	–	–	–	–
22	β-Ti(100)[b]	3.9^z	–	–	–	–	–	–
22	β-Ti(110)[b]	4.6^z	–	–	–	–	–	–
22	β-Ti(111)[b]	3.8^z	–	–	–	–	–	–

Table 2 (*continued*)

No.	Surface	ϕ^e (eV) [Here]	ϕ^+ (eV) [Here]	ϕ^- (eV) [Here]	ϕ^e (eV) [1358]	ϕ^e (eV) [1045]	ϕ^e (eV) [12,1354]	ϕ^e (eV) [1351]
22	β-Ti(112)[b]	4.2[z]	–	–	–	–	–	–
22	α-Ti(poly)[hc]	3.87 ± 0.05	–	–	4.33 [304]	4.33 [304]	3.95	–
22	β-Ti(poly)[b]	3.93 ± 0.16	–	–	–	–	–	–
23	V(100)[b]	4.27 ± 0.05	–	–	–	–	–	–
23	V(110)[b]	5.04 ± 0.07	–	–	–	–	–	–
23	V(111)[b]	4.13 ± 0.04[y]	–	–	–	–	–	–
23	V(112)[b]	4.3 ± 0.3[x]	–	–	–	–	–	–
23	V(116)[b]	4.0 ± 0.1[x]	–	–	–	–	–	–
23	V(poly)[b]	4.10 ± 0.05	–	–	4.3 [304]	4.3 [304]	4.12	–
24	Cr(100)[b]	4.43 ± 0.14	–	–	–	–	–	–
24	Cr(110)[b]	4.99 ± 0.19	–	–	–	–	–	–
24	Cr(111)[b]	3.8 ± 0.1[y]	–	–	–	–	–	–
24	Cr(112)[b]	4.1 ± 0.1[x]	–	–	–	–	–	–
24	Cr(116)[b]	3.8[z]	–	–	–	–	–	–
24	Cr(210)[b]	4.2[z]	–	–	–	–	–	–
24	Cr(poly)[b]	4.38 ± 0.04	–	–	4.5 [304]	4.5 [304]	4.58	–
25	γ-Mn(100)[f]	5.2 ± 0.3[y]	–	–	–	–	–	–
25	γ-Mn(110)[f]	4.7[z]	–	–	–	–	–	–
25	γ-Mn(111)[f]	5.3 ± 0.1[y]	–	–	–	–	–	–
25	δ-Mn(100)[b]	4.8 ± 0.4[y]	–	–	–	–	–	–
25	δ-Mn(110)[b]	5.3 ± 0.3[y]	–	–	–	–	–	–
25	δ-Mn(111)[b]	4.1[z]	–	–	–	–	–	–
25	δ-Mn(112)[b]	4.6[z]	–	–	–	–	–	–
25	$\alpha-\beta$-Mn(poly)[c]	4.08 ± 0.11	–	–	4.1 [304]	4.1 [304]	3.83	–
25	γ-Mn(poly)[f]	4.3 ± 0.1[x]	–	–	–	–	–	–
25	δ-Mn(poly)[b]	3.8[z]	–	–	–	–	–	–
26	α-Fe(100)[b]	4.64 ± 0.05	–	–	4.67 [921]	4.67 [921]	–	4.59 ± 0.13
26	α-Fe(110)[b]	4.99 ± 0.04	–	–	–	–	–	5.19 ± 0.08
26	α-Fe(111)[b]	4.4 ± 0.3	–	–	4.81 [487]	4.81 [487]	–	–
26	α-Fe(210)[b]	4.2 ± 0.1[x]	–	–	–	–	–	–
26	α-Fe(211)[b]	4.4 ± 0.4[y]	–	–	–	–	–	–
26	α-Fe(310)[b]	4.0 ± 0.1[x]	–	–	–	–	–	–
26	α-Fe(321)[b]	4.3 ± 0.1[x]	–	–	–	–	–	–
26	β-Fe(100)[b]	4.6 ± 0.4[y]	–	–	–	–	–	–
26	β-Fe(110)[b]	5.8[z]	–	–	–	–	–	–
26	β-Fe(111)[b]	4.8[z]	–	–	–	–	–	–
26	γ-Fe(100)[f]	5.28 ± 0.19	–.	–	–	–	–	–
26	γ-Fe(110)[f]	5.0[z]	–	–	–	–	–	–
26	γ-Fe(111)[f]	5.6 ± 0.1[x]	–	–	–	–	–	–
26	m-Fe(100)[f]/Cu(100)[(16)]	5.38 ± 0.22	–	–	–	–	–	–
26	α-Fe(poly)[b]	4.55 ± 0.05	–	–	–	4.5 [304]	4.31	4.66 ± 0.08
26	β-Fe(poly)[b]	4.52 ± 0.17	–	–	–	4.62 [305]	–	–
26	γ-Fe(poly)[f]	4.54 ± 0.05	–	–	–	4.68 [305]	–	–
26	δ-Fe(poly)[b]	4.76 ± 0.1[x]	–	–	–	–	–	–
26	m-Fe[f]/Cu(100)	4.58 ± 0.10[y]	–	–	–	–	–	–
27	α-Co(0001)[hc]	5.30 ± 0.18	–	–	–	–	–	–
27	α-Co(1010)[hc]	5.5[z]	–	–	–	–	–	–
27	α-Co(1011)[hc]	5.3[z]	–	–	–	–	–	–
27	α-Co(1120)[hc]	4.1[z]	–	–	–	–	–	–
27	α-Co(1124)[hc]	4.8[z]	–	–	–	–	–	–
27	β-Co(100)[f]	5.25 ± 0.17	–	–	–	–	–	–
27	β-Co(110)[f]	5.0[z]	–	–	–	–	–	–

Table 2 (*continued*)

No.	Surface	ϕ^e (eV) [Here]	ϕ^+ (eV) [Here]	ϕ^- (eV) [Here]	ϕ^e (eV) [1358]	ϕ^e (eV) [1045]	ϕ^e (eV) [12,1354]	ϕ^e (eV) [1351]
27	β-Co(111)[f]	5.39 ± 0.23	–	–	–	–	–	–
27	m-Co(100)[b] /GaAs(110)[(7)]	5.0 ± 0.3[y]	–	–	–	–	–	–
27	m-Co(100)[f] /Cu(100)[(17)]	4.7[z]	–	–	–	–	–	
27	α-Co(poly)[hc]	4.71 ± 0.03	–	–	5.0 [304]	5.0 [304]	4.41	–
27	β-Co(poly)[f]	4.50 ± 0.13	–	–	–	–	–	–
27	m-Co[f] /Cu(100)[(17)]	4.94 ± 0.30	–	–	–	–	–	–
28	Ni(100)[f]	5.19 ± 0.05	5.2[z]	–	5.22 [314]	5.22 [314]	–	5.23 ± 0.10
28	Ni(110)[f]	4.96 ± 0.10	5.0[z]	–	5.04 [314]	5.04 [314]	–	4.64 ± 0.05
28	Ni(111)[f]	5.32 ± 0.05	5.3[z]	–	5.35 [314]	5.35 [314]	–	5.28 ± 0.05
28	Ni(113)[f]	4.5[z]	–	–	–	–	–	–
28	Ni(133)[f]	4.4[z]	–	–	–	–	–	–
28	Ni(poly)[f]	5.06 ± 0.06	5.19 ± 0.12[y]	–	–	5.15 [304]	4.50	4.87 ± 0.16
29	Cu(100)[f]	4.58 ± 0.06	–	–	5.10 [358][(15)]	4.59 [953]	–	4.57 ± 0.08
29	Cu(110)[f]	4.43 ± 0.04	–	–	4.48 [953]	4.48 [953]	–	4.48 ± 0.06
29	Cu(111)[f]	4.92 ± 0.05	–	–	4.94 [953]	4.94 [953]	–	4.91 ± 0.03
29	Cu(112)[f]	4.52 ± 0.03	–	–	4.53 [953]	4.53 [953]	–	4.50 ± 0.04
29	Cu(113)[f]	4.5 ± 0.2[y]	–	–	–	–	–	–
29	Cu(114)[f]	4.6[z]	–	–	–	–	–	–
29	Cu(119)[f]	4.6[z]	–	–	–	–	–	–
29	Cu(122)[f]	4.5 ± 0.1[x]	–	–	–	–	–	–
29	Cu(124)[f]	4.5[z]	–	–	–	–	–	–
29	Cu(210)[f]	4.3 ± 0.1[x]	–	–	–	–	–	–
29	Cu(233)[f]	4.5 ± 0.1[x]	–	–	–	–	–	–
29	Cu(234)[f]	4.5 ± 0.1[x]	–	–	–	–	–	–
29	Cu(236)[f]	4.4[z]	–	–	–	–	–	–
29	Cu(321)[f]	4.1[z]	–	–	–	–	–	–
29	Cu(345)[f]	4.5[z]	–	–	–	–	–	–
29	Cu(356)[f]	4.5[z]	–	–	–	–	–	–
29	Cu(413)[f]	4.0[z]	–	–	–	–	–	–
29	Cu(018)[f]	4.7[z]	–	–	–	–	–	–
29	Cu(poly)[f]	4.51 ± 0.04	–	–	–	4.65 [3319][(10)]	4.40	4.51 ± 0.07
29	Cu(liquid)	4.6 ± 0.1[y]	–	–	–	–	–	–
30	Zn(0001)[hc]	4.35 ± 0.28	–	–	–	4.9 [1508][(14)]	–	–
30	Zn(1010)[hc]	5.8 ± 0.7[x]	–	–	–	–	–	–
30	Zn(1124)[hc]	5.8[z]	–	–	–	–	–	–
30	Zn(poly)[hc]	4.22 ± 0.11	–	–	3.63 [2601][(14)]	4.33 [3052]	4.24	–
31	Ga(100)[f]	3.4[z]	–	–	–	–	–	–
31	Ga(110)[f]	4.1[z]	–	–	–	–	–	–
31	Ga(111)[f]	3.8[z]	–	–	–	–	–	–
31	Ga(poly)[r]	4.27 ± 0.06	–	–	4.32 [2770]	4.2 [2767]	3.96	–
31	Ga(liquid)	4.33 ± 0.03	–	–	–	–	–	–
32	Ge(100)[d]	4.68 ± 0.08	–	–	–	–	–	–
32	Ge(110)[d]	4.79 ± 0.06	–	–	–	–	–	–
32	Ge(111)[d]	4.60 ± 0.09	–	–	–	4.80[p] [1971]	–	–
32	Ge(112)[d]	4.8 ± 0.1[x]	–	–	–	–	–	–
32	Ge(113)[d]	4.9[z]	–	–	–	–	–	–

Table 2 (*continued*)

No.	Surface	ϕ^e (eV) [Here]	ϕ^+ (eV) [Here]	ϕ^- (eV) [Here]	ϕ^e (eV) [1358]	ϕ^e (eV) [1045]	ϕ^e (eV) [12,1354]	ϕ^e (eV) [1351]
32	Ge(114)[d]	4.9^z	–	–	–	–	–	–
32	Ge(122)[d]	4.9^z	–	–	–	–	–	–
32	Ge(133)[d]	4.9^z	–	–	–	–	–	–
32	Ge(155)[d]	4.8^z	–	–	–	–	–	–
32	Ge(poly)[d]	4.76 ± 0.05	–	–	5.0 [1520]	5.0 [1520]	4.76	–
33	As(111)[rh]	3.8^z	–	–	–	3.75 [2952]	–	–
33	As(poly)[rh]	4.85 ± 014	–	–	–	–	5.11	–
34	Se(1010)[h]	5.9^x	–	–	–	–	–	–
34	Se(poly)[h]	5.27 ± 0.18	–	–	5.9 [3429]	5.9 [3429]	4.72	–
37	Rb(100)[b]	2.31 ± 0.08	–	–	–	–	–	–
37	Rb(110)[b]	2.65 ± 0.05	–	–	–	–	–	–
37	Rb(111)[b]	2.21 ± 0.09	–	–	–	–	–	–
37	Rb(112)[b]	2.6^z	–	–	–	–	–	–
37	Rb(poly)[b]	2.17 ± 0.05	–	–	2.261 [2119]	2.16 [2470]	2.16	–
37	Rb(liquid)	2.15 ± 0.02	–	–	–	–	–	–
38	α-Sr(100)[f]	3.3 ± 0.4	–	–	–	–	–	–
38	α-Sr(110)[f]	3.1 ± 0.3	–	–	–	–	–	–
38	α-Sr(111)[f]	3.4 ± 0.3	–	–	–	–	–	–
38	β-Sr(0001)[hc]	4.2^z	–	–	–	–	–	–
38	β-Sr(1010)[hc]	4.0^z	–	–	–	–	–	–
38	β-Sr(1124)[hc]	3.5^z	–	–	–	–	–	–
38	γ-Sr(100)[b]	3.0 ± 0.3^x	–	–	–	–	–	–
38	γ-Sr(110)[b]	3.2 ± 0.6^y	–	–	–	–	–	–
38	γ-Sr(111)[b]	3.0 ± 0.2^x	–	–	–	–	–	–
38	γ-Sr(112)[b]	3.6^z	–	–	–	–	–	–
38	α-Sr(poly)[f]	2.71 ± 0.08	–	–	2.59 [1401]	2.59 [1401]	2.35	–
38	β-Sr(poly)[hc]	2.9 ± 0.2^y	–	–	–	–	–	–
38	γ-Sr(poly)[b]	2.35 ± 0.05^x	–	–	–	–	–	–
39	α-Y(0001)[hc]	3.4 ± 0.2	–	–	–	–	–	–
39	α-Y(1010)[hc]	3.1^x	–	–	–	–	–	–
39	α-Y(1124)[hc]	3.3 ± 0.1^y	–	–	–	–	–	–
39	β-Y(100)[b]	3.7^z	–	–	–	–	–	–
39	β-Y(110)[b]	4.3^z	–	–	–	–	–	–
39	β-Y(111)[b]	3.5^z	–	–	–	–	–	–
39	β-Y(112)[b]	3.9^z	–	–	–	–	–	–
39	α-Y(poly)[hc]	3.16 ± 0.06	–	–	3.1 [304]	3.1 [304]	3.3	–
39	β-Y(poly)[b]	3.2^z	–	–	–	–	–	–
40	α-Zr(0001)[hc]	4.36 ± 0.09	–	–	–	–	–	–
40	α-Zr(1010)[hc]	4.1 ± 0.5^y	–	–	–	–	–	–
40	α-Zr(1124)[hc]	4.2^z	–	–	–	–	–	–
40	β-Zr(100)[b]	3.9^z	–	–	–	–	–	–
40	β-Zr(110)[b]	4.6^z	–	–	–	–	–	–
40	β-Zr(111)[b]	3.8^z	–	–	–	–	–	–
40	β-Zr(112)[b]	4.2^z	–	–	–	–	–	–
40	α-Zr(poly)[hc]	3.85 ± 0.06	–	–	4.05 [304]	4.05 [304]	3.9	–
40	β-Zr(poly)[b]	4.01 ± 0.05	–	–	–	–	–	–
41	Nb(100)[b]	4.02 ± 0.05	4.0^z	–	4.02 [779]	4.02 [779]	–	3.95 ± 0.05
41	Nb(110)[b]	4.77 ± 0.05	4.74 ± 0.10^x	–	4.87 [779]	4.87 [779]	–	4.83 ± 0.05
41	Nb(111)[b]	3.95 ± 0.09	3.84 ± 0.06^x	–	4.36 [779]	4.36 [779]	–	3.86 ± 0.03
41	Nb(112)[b]	4.33 ± 0.10	4.4^z	–	4.63 [779]	4.63 [779]	–	–
41	Nb(113)[b]	4.3^z	–	–	4.29 [779]	4.29 [779]	–	–

Table 2 (*continued*)

No.	Surface	ϕ^e (eV) [Here]	ϕ^+ (eV) [Here]	ϕ^- (eV) [Here]	ϕ^e (eV) [1358]	ϕ^e (eV) [1045]	ϕ^e (eV) [12,1354]	ϕ^e (eV) [1351]
41	Nb(116)[b]	3.82 ± 0.12[y]	–	–	3.95 [779]	3.95 [779]	–	–
41	Nb(310)[b]	4.2[z]	–	–	4.18 [779]	4.18 [779]	–	–
41	Nb(335)[b]	4.6[z]	–	–	–	–	–	–
41	Nb(poly)[b]	<u>4.11 ± 0.05</u>	4.81 ± 0.05[y]	–	–	4.3 [304]	3.99	4.02 ± 0.05
42	Mo(100)[b]	<u>4.38 ± 0.03</u>	<u>4.38 ± 0.08</u>	<u>4.34 ± 0.03[y]</u>	4.53 [325]	4.53 [325]	–	4.40 ± 0.03
42	Mo(110)[b]	<u>4.98 ± 0.03</u>	5.1[z]	–	4.95 [325]	4.95 [325]	–	4.96 ± 0.06
42	Mo(111)[b]	<u>4.29 ± 0.03</u>	4.17 ± 0.09[y]	–	4.55 [325]	4.55 [325]	–	4.09 ± 0.07
42	Mo(112)[b]	<u>4.51 ± 0.03</u>	4.6[z]	–	4.36 [325]	4.36 [325]	–	4.58 ± 0.05
42	Mo(114)[b]	4.33 ± 0.15	–	–	4.50 [325]	4.50 [325]	–	–
42	Mo(116)[b]	<u>4.23 ± 0.08</u>	–	–	–	–	–	–
42	Mo(310)[b]	4.15 ± 0.03[y]	–	–	–	–	–	–
42	Mo(321)[b]	4.16 ± 0.03[y]	–	–	–	–	–	–
42	Mo(331)[b]	4.37 ± 0.04[x]	–	–	–	–	–	–
42	Mo(332)[b]	4.3 ± 0.2[y]	–	–	4.55 [325]	4.55 [325]	–	–
42	Mo(431)[b]	4.2 ± 0.1[x]	–	–	–	–	–	–
42	Mo(poly)[b]	<u>4.31 ± 0.02</u>	5.03 ± 0.06	–	–	4.6 [304]	4.3	4.34 ± 0.06
43	Tc(0001)[hc]	5.1 ± 0.2[y]	–	–	–	–	–	–
43	Tc(1010)[hc]	4.7 ± 0.2[y]	–	–	–	–	–	–
43	Tc(1011)[hc]	4.9 ± 0.2[x]	–	–	–	–	–	–
43	Tc(1012)[hc]	4.5 ± 0.2[x]	–	–	–	–	–	–
43	Tc(1013)[hc]	4.4 ± 0.2[x]	–	–	–	–	–	–
43	Tc(1121)[hc]	4.3 ± 0.2[x]	–	–	–	–	–	–
43	Tc(1122)[hc]	4.5 ± 0.2[x]	–	–	–	–	–	–
43	Tc(1123)[hc]	4.4 ± 0.2[x]	–	–	–	–	–	–
43	Tc(1124)[hc]	4.4[z]	–	–	–	–	–	–
43	Tc(2130)[hc]	4.4 ± 0.2[x]	–	–	–	–	–	–
43	Tc(2140)[hc]	4.5 ± 0.2[x]	–	–	–	–	–	–
43	Tc(poly)[hc]	<u>4.67 ± 0.02</u>	–	–	–	–	–	–
44	Ru(0001)[hc]	<u>5.35 ± 0.06</u>	–	–	–	–	–	–
44	Ru(1010)[hc]	4.9 ± 0.2	–	–	–	–	–	–
44	Ru(1011)[hc]	5.1 ± 0.2[x]	–	–	–	–	–	–
44	Ru(1012)[hc]	4.7 ± 0.2[x]	–	–	–	–	–	–
44	Ru(1013)[hc]	4.6 ± 0.2[x]	–	–	–	–	–	–
44	Ru(1121)[hc]	4.6 ± 0.2[x]	–	–	–	–	–	–
44	Ru(1122)[hc]	4.3 ± 0.2[y]	–	–	–	–	–	–
44	Ru(1123)[hc]	4.6 ± 0.2[x]	–	–	–	–	–	–
44	Ru(1124)[hc]	4.5 ± 0.1[x]	–	–	–	–	–	–
44	Ru(1125)[hc]	4.5 ± 0.2[y]	–	–	–	–	–	–
44	Ru(2130)[hc]	4.7 ± 0.2[x]	–	–	–	–	–	–
44	Ru(3140)[hc]	4.7 ± 0.2[x]	–	–	–	–	–	–
44	Ru(poly)[hc]	<u>4.71 ± 0.05</u>	–	–	4.71 [414]	4.71 [414]	4.60	4.75 ± 0.11
45	Rh(100)[f]	<u>5.24 ± 0.07</u>	–	–	–	–	–	5.29 ± 0.07
45	Rh(110)[f]	<u>4.75 ± 0.06</u>	–	–	–	–	–	4.77 ± 0.06
45	Rh(111)[f]	<u>5.40 ± 0.08</u>	–	–	–	–	–	5.50 ± 0.10
45	Rh(112)[f]	5.1[z]	–	–	–	–	–	–
45	Rh(113)[f]	5.0[z]	–	–	–	–	–	–
45	Rh(210)[f]	4.6[z]	–	–	–	–	–	–
45	Rh(310)[f]	4.8[z]	–	–	–	–	–	–
45	Rh(320)[f]	4.7[z]	–	–	–	–	–	–
45	Rh(321)[f]	4.8[z]	–	–	–	–	–	–
45	Rh(410)[f]	4.9[z]	–	–	–	–	–	–
45	Rh(430)[f]	4.7[z]	–	–	–	–	–	–
45	Rh(520)[f]	4.7[z]	–	–	–	–	–	–

Table 2 (*continued*)

No.	Surface	ϕ^e (eV) [Here]	ϕ^+ (eV) [Here]	ϕ^- (eV) [Here]	ϕ^e (eV) [1358]	ϕ^e (eV) [1045]	ϕ^e (eV) [12,1354]	ϕ^e (eV) [1351]
45	Rh(531)[f]	4.7[z]	–	–	–	–	–	–
45	Rh(poly)[f]	4.87 ± 0.07	–	–	4.98 [414]	4.98 [414]	4.75	4.90 ± 0.08
46	Pd(100)[f]	5.48 ± 0.04	–	–	–	–	–	5.59 ± 0.05
46	Pd(110)[f]	5.12 ± 0.09	–	–	–	–	–	5.19 ± 0.04
46	Pd(111)[f]	5.58 ± 0.05	–	–	5.6 [616,1799]	5.6 [616,1799]	–	5.55 ± 0.07
46	Pd(113)[f]	5.6[z]	–	–	–	–	–	–
46	Pd(poly)[f]	5.17 ± 0.06	–	–	5.22 [1031]	5.12 [414]	4.8	5.24 ± 0.05
47	Ag(100)[f]	4.46 ± 0.05	–	–	4.64 [626]	4.64 [626]	–	4.50 ± 0.10
47	Ag(110)[f]	4.28 ± 0.08	–	–	4.52 [626]	4.52 [626]	–	4.16 ± 0.05
47	Ag(111)[f]	4.64 ± 0.06	–	–	4.74 [1134]	4.74 [1134]	–	4.56 ± 0.15
47	Ag(poly)[f]	4.39 ± 0.02	–	–	–	4.26 [626]	4.3	4.36 ± 0.06
47	Ag(liquid)	4.3[z]	–	–	–	–	–	–
48	Cd(0001)[hc]	4.9 ± 0.9[y]	–	–	–	–	–	–
48	Cd(1010)[hc]	5.5 ± 0.8[x]	–	–	–	–	–	–
48	Cd(1124)[hc]	5.5[z]	–	–	–	–	–	–
48	Cd(poly)[hc]	4.06 ± 0.05	–	–	4.08 [1380]	4.22 [1380][(9)]	4.1	–
49	In(100)[f]	4.5 ± 0.2[y]	–	–	–	–	–	–
49	In(110)[f]	4.4[z]	–	–	–	–	–	–
49	In(111)[f]	4.1[z]	–	–	–	–	–	–
49	In(poly)[f]	4.05 ± 0.06	–	–	4.09 [2770]	4.12 [3672]	3.8	–
49	In(liquid)	4.00 ± 0.08	–	–	–	–	–	–
50	α-Sn(100)[b]	4.5 ± 0.1[y]	–	–	–	–	–	–
50	α-Sn(110)[b]	4.8[z]	–	–	–	–	–	–
50	α-Sn(111)[b]	4.2 ± 02[y]	–	–	–	–	–	–
50	α-Sn(112)[b]	4.5[z]	–	–	–	–	–	–
50	α-Sn(poly)[b]	4.27 ± 0.06	–	–	–	–	–	–
50	β-Sn(poly)[t]	4.34 ± 0.06	–	–	4.42 [3057]	4.42 [3057]	4.38	–
50	γ-Sn(poly)[h]	4.29 ± 0.06[y]	–	–	–	–	–	–
50	Sn(liquid)	4.20 ± 0.02[y]	–	–	–	–	–	–
51	Sb(100)[p]	4.7 ± 0.1[x]	–	–	4.7 [1272]	4.7 [1272]	–	–
51	Sb(111)	4.3[z]	–	–	–	–	–	–
51	Sb(poly)[rh]	4.45 ± 0.09	–	–	–	–	4.08	–
51	Sb(amorphous)	4.5 ± 0.1[y]	–	–	4.55 [1995]	4.55 [1995]	–	–
52	Te(1010)[h]	4.80 ± 0.15[x]	–	–	4.95 [3429]	4.95 [3429]	–	–
52	Te(poly)[h]	4.86 ± 0.06	–	–	–	–	4.73	–
53	I[r]	2.8[z]	–	–	–	–	–	–
53	I[m]	5.4[z]	–	–	–	–	–	–
53	I(film)	5.1 ± 0.1	5.3[x]	–	–	–	–	–
53	I(amorphous)	6.3 ± 0.4[x]	–	–	–	–	–	–
55	Cs(100)[b]	2.24 ± 0.06	–	–	–	–	–	–
55	Cs(110)[b]	2.54 ± 0.07	–	–	–	–	–	–
55	Cs(111)[b]	2.09 ± 0.08	–	–	–	–	–	–
55	Cs(112)[b]	2.4[z]	–	–	–	–	–	–
55	Cs(poly)[b]	2.05 ± 0.05	–	–	1.95 [2613]	2.14 [1489]	1.81	–
55	Cs(liquid)	2.00 ± 0.12[y]	–	–	–	–	–	–
56	Ba(100)[b]	3.07 ± 0.06	–	–	–	–	–	–

Table 2 (*continued*)

No.	Surface	ϕ^e (eV) [Here]	ϕ^+ (eV) [Here]	ϕ^- (eV) [Here]	ϕ^e (eV) [1358]	ϕ^e (eV) [1045]	ϕ^e (eV) [12,1354]	ϕ^e (eV) [1351]
56	Ba(110)[b]	3.46 ± 0.14	–	–	–	–	–	–
56	Ba(111)[b]	<u>2.81 ± 0.06</u>	–	–	–	–	–	–
56	Ba(112)[b]	3.2[z]	–	–	–	–	–	–
56	Ba(poly)[b]	<u>2.50 ± 0.02</u>	–	–	2.52 [379]	2.7 [330]	2.49	–
57	α-La(0001)[hc]	3.09 ± 0.05[y]	–	–	–	–	–	–
57	β-La(100)[f]	4.3 ± 0.5[x]	–	–	–	–	–	–
57	β-La(110)[f]	4.2 ± 0.6[x]	–	–	–	–	–	–
57	β-La(111)[f]	3.4 ± 0.5[x]	–	–	–	–	–	–
57	γ-La(100)[b]	4.0 ± 0.8[x]	–	–	–	–	–	–
57	γ-La(110)[b]	4.8 ± 1.1[x]	–	–	–	–	–	–
57	γ-La(111)[b]	3.1[z]	–	–	–	–	–	–
57	γ-La(112)[b]	3.4[z]	–	–	–	–	–	–
57	α-La(poly)[hc]	<u>3.27 ± 0.04</u>	–	–	3.5 [304]	3.5 [304]	3.3	–
57	β-La(poly)[f]	<u>2.98 ± 0.10</u>	–	–	–	–	–	–
58	β-Ce(100)[f]	4.3 ± 0.3[x]	–	–	–	–	–	–
58	β-Ce(110)[f]	4.4[z]	–	–	–	–	–	–
58	β-Ce(111)[f]	4.1 ± 0.9[x]	–	–	–	–	–	–
58	γ-Ce(100)[b]	4.0[z]	–	–	–	–	–	–
58	γ-Ce(110)[b]	4.6[z]	–	–	–	–	–	–
58	γ-Ce(111)[b]	3.8[z]	–	–	–	–	–	–
58	γ-Ce(112)[b]	4.2[z]	–	–	–	–	–	–
58	β-Ce(poly)[f]	<u>2.89 ± 0.07</u>	–	–	2.9 [304]	2.9 [304]	2.7	–
58	γ-Ce(poly)[b]	3.1 ± 0.1[y]	–	–	–	–	–	–
59	α-Pr(0001)[hc]	3.1[z]	–	–	–	–	–	–
59	β-Pr(100)[b]	3.3[z]	–	–	–	–	–	–
59	β-Pr(110)[b]	3.9[z]	–	–	–	–	–	–
59	β-Pr(111)[b]	3.2[z]	–	–	–	–	–	–
59	β-Pr(112)[b]	3.5[z]	–	–	–	–	–	–
59	α-Pr(poly)[f]	2.83 ± 0.11	–	–	–	–	2.7	–
60	α-Nd(0001)[hc]	3.2 ± 0.1[x]	–	–	–	–	–	–
60	β-Nd(100)[b]	3.6[z]	–	–	–	–	–	–
60	β-Nd(110)[b]	4.2[z]	–	–	–	–	–	–
60	β-Nd(111)[b]	3.5[z]	–	–	–	–	–	–
60	β-Nd(112)[b]	3.9[z]	–	–	–	–	–	–
60	α-Nd(poly)[hc]	<u>3.14 ± 0.08</u>	–	–	3.2 [304]	3.2 [304]	3.2	–
61	α-Pm(0001)[hc]	3.1[z]	–	–	–	–	–	–
61	β-Pm(100)[f]	3.7[z]	–	–	–	–	–	–
61	β-Pm(110)[f]	3.5[z]	–	–	–	–	–	–
61	β-Pm(111)[f]	4.0[z]	–	–	–	–	–	–
61	α-Pm(poly)[hc]	3.09 ± 0.08[y]	–	–	–	–	–	–
62	β-Sm(100)[b]	3.2[z]	–	–	–	–	–	–
62	β-Sm(110)[b]	3.8[z]	–	–	–	–	–	–
62	β-Sm(111)[b]	3.1[z]	–	–	–	–	–	–
62	β-Sm(112)[b]	3.4[z]	–	–	–	–	–	–
62	α-Sm(poly)[rh]	<u>2.81 ± 0.10</u>	–	–	2.7 [304]	2.7 [304]	2.7	–
63	Eu(100)[b]	3.3[z]	–	–	–	–	–	–
63	Eu(110)[b]	2.9 ± 0.6[y]	–	–	–	–	–	–
63	Eu(111)[b]	3.1[z]	–	–	–	–	–	–
63	Eu(112)[b]	3.5[z]	–	–	–	–	–	–
63	Eu(poly)[b]	2.74 ± 0.12	–	–	2.5 [304]	2.5 [304]	–	–
64	α-Gd(0001)[hc]	<u>3.27 ± 0.03</u>	–	–	–	–	–	–

Table 2 (*continued*)

No.	Surface	ϕ^e (eV) [Here]	ϕ^+ (eV) [Here]	ϕ^- (eV) [Here]	ϕ^e (eV) [1358]	ϕ^e (eV) [1045]	ϕ^e (eV) [12,1354]	ϕ^e (eV) [1351]
64	α-Gd(1010)[hc]	4.3[z]	–	–	–	–	–	–
64	α-Gd(1124)[hc]	3.8[z]	–	–	–	–	–	–
64	β-Gd(100)[b]	3.2 ± 0.3[x]	–	–	–	–	–	–
64	β-Gd(110)[b]	4.1[z]	–	–	–	–	–	–
64	β-Gd(111)[b]	3.4[z]	–	–	–	–	–	–
64	β-Gd(112)[b]	3.8[z]	–	–	–	–	–	–
64	α-Gd(poly)[hc]	<u>3.09 ± 0.04</u>	–	–	2.90 [2943]	3.1 [304]	3.1	–
65	α-Tb(0001)[hc]	4.4 ± 0.5[y]	–	–	–	–	–	–
65	α-Tb(1010)[hc]	4.7[z]	–	–	–	–	–	–
65	α-Tb(1124)[hc]	4.1[z]	–	–	–	–	–	–
65	β-Tb(100)[b]	3.9[z]	–	–	–	–	–	–
65	β-Tb(110)[b]	4.5[z]	–	–	–	–	–	–
65	β-Tb(111)[b]	3.7[z]	–	–	–	–	–	–
65	β-Tb(112)[b]	4.1[z]	–	–	–	–	–	–
65	α-Tb(poly)[hc]	<u>3.14 ± 0.09</u>	–	–	3.0 [2716]	3.0 [2716]	3.15	–
66	α-Dy(0001)[hc]	4.2 ± 0.8[x]	–	–	–	–	–	–
66	α-Dy(1010)[hc]	4.8[z]	–	–	–	–	–	–
66	α-Dy(1124)[hc]	4.2[z]	–	–	–	–	–	–
66	α-Dy(poly)[hc]	<u>3.18 ± 0.08</u>	–	–	–	–	3.25	–
67	α-Ho(0001)[hc]	3.9 ± 0.5[x]	–	–	–	–	–	–
67	α-Ho(1010)[hc]	4.2[z]	–	–	–	–	–	–
67	α-Ho(1124)[hc]	3.7[z]	–	–	–	–	–	–
67	Ho(poly)[hc]	<u>3.05 ± 0.05</u>	–	–	–	–	3.22	–
68	Er(0001)[hc]	3.8 ± 04[y]	–	–	–	–	–	–
68	Er(1010)[hc]	4.3[z]	–	–	–	–	–	–
68	Er(1124)[hc]	3.8[z]	–	–	–	–	–	–
68	Er(poly)[hc]	<u>3.14 ± 0.08</u>	–	–	–	–	3.25	–
69	α-Tm(0001)[hc]	4.0 ± 0.5[x]	–	–	–	–	–	–
69	α-Tm(1010)[hc]	4.3[z]	–	–	–	–	–	–
69	α-Tm(1124)[hc]	3.8[z]	–	–	–	–	–	–
69	α-Tm(poly)[hc]	<u>3.12 ± 0.07</u>	–	–	–	–	3.10	–
70	α-Yb(100)[f]	4.2[z]	–	–	–	–	–	–
70	α-Yb(110)[f]	3.9[z]	–	–	–	–	–	–
70	α-Yb(111)[f]	3.5 ± 1.0[x]	–	–	–	–	–	–
70	β-Yb(100)[b]	3.6[z]	–	–	–	–	–	–
70	β-Yb(110)[b]	3.3 ± 0.8[x]	–	–	–	–	–	–
70	β-Yb(111)[b]	3.4[z]	–	–	–	–	–	–
70	β-Yb(112)[b]	3.8[z]	–	–	–	–	–	–
70	α-Yb(poly)[f]	<u>2.91 ± 0.09</u>	–	–	–	–	–	–
71	α-Lu(0001)[hc]	3.9 ± 0.4[y]	–	–	–	–	–	–
71	α-Lu(1010)[hc]	4.3[z]	–	–	–	–	–	–
71	α-Lu(1124)[hc]	3.8[z]	–	–	–	–	–	–
71	β-Lu(100)[b]	3.5[z]	–	–	–	–	–	–
71	β-Lu(110)[b]	4.1[z]	–	–	–	–	–	–
71	β-Lu(111)[b]	3.4[z]	–	–	–	–	–	–
71	β-Lu(112)[b]	3.8[z]	–	–	–	–	–	–
71	α-Lu(poly)[hc]	<u>3.17 ± 0.09</u>	–	–	3.3 [2603]	3.3 [2603]	–	–
72	α-Hf(0001)[hc]	4.2 ± 0.1[y]	–	–	–	–	–	–
72	α-Hf(1010)[hc]	4.4 ± 0.8[x]	–	–	–	–	–	–
72	α-Hf(1124)[hc]	4.6[z]	–	–	–	–	–	–
72	β-Hf(100)[b]	4.2 ± 0.1[y]	–	–	–	–	–	–

Table 2 (*continued*)

No.	Surface	ϕ^e (eV) [Here]	ϕ^+ (eV) [Here]	ϕ^- (eV) [Here]	ϕ^e (eV) [1358]	ϕ^e (eV) [1045]	ϕ^e (eV) [12,1354]	ϕ^e (eV) [1351]
72	β-Hf(110)[b]	5.0[z]	–	–	–	–	–	–
72	β-Hf(111)[b]	4.1[z]	–	–	–	–	–	–
72	β-Hf(112)[b]	4.6[z]	–	–	–	–	–	–
72	α-Hf(poly)[hc]	3.64 ± 0.06	–	–	3.9 [304]	3.9 [304]	3.53	–
73	Ta(100)[b]	4.15 ± 0.05	4.2[z]	–	4.15 [127]	4.15 [127]	–	4.17 ± 0.09
73	Ta(110)[b]	4.82 ± 0.06	4.84 ± 0.02[y]	4.89 ± 0.03[x]	4.80 [127]	4.80 [127]	–	4.81 ± 0.05
73	Ta(111)[b]	4.01 ± 0.04	4.00 ± 0.05[x]	–	4.00 [127]	4.00 [127]	–	4.00 ± 0.04
73	Ta(112)[b]	4.36 ± 0.04	–	–	–	–	–	4.37 ± 0.03
73	Ta(114)[b]	4.0[z]	–	–	–	–	–	–
73	Ta(116)[b]	3.92 ± 0.02[y]	–	–	–	–	–	–
73	Ta(123)[b]	4.0[z]	–	–	–	–	–	–
73	Ta(130)[b]	4.2 ± 0.2[y]	–	–	–	–	–	–
73	Ta(233)[b]	4.0[z]	–	–	–	–	–	–
74	Ta(poly)[b]	4.20 ± 0.03	4.95 ± 0.20	4.17 ± 0.13[y]	4.25 [124]	4.25 [124]	4.12	4.25 ± 0.05
74	W(100)[b]	4.65 ± 0.02	4.62 ± 0.05	4.54 ± 0.01[x]	4.63 [358]	4.63 [358]	4.65 ± 0.10[#(2)]	4.57 ± 0.03
74	W(110)[b]	5.32 ± 0.02	5.28 ± 0.11	–	5.22 [3802]	5.25 [358]	5.20 ± 0.10[#]	5.31 ± 0.05
74	W(111)[b]	4.45 ± 0.03	4.45 ± 0.04	–	4.45 [819]	4.47 [358]	4.40 ± 0.05[#]	4.38 ± 0.04
74	W(112)[b]	4.78 ± 0.03	4.70 ± 0.01[y]	–	–	–	4.85 ± 0.10[#]	4.83 ± 0.20
74	W(113)[b]	4.43 ± 0.09	–	–	4.46 [819]	4.18 [195]	4.50 ± 0.10[#]	4.55 ± 0.06
74	W(114)[b]	4.40 ± 0.03	–	–	–	–	–	4.40 ± 0.05
74	W(115)[b]	4.39 ± 0.06[y]	–	–	–	–	–	–
74	W(116)[b]	4.30 ± 0.04	–	–	4.32 [819]	4.30 [372]	4.26 ± 0.10[#]	4.32 ± 0.20
74	W(119)[b]	4.6[z]	–	–	–	–	–	–
74	W(120)[b]	4.38 ± 0.05	–	–	–	–	–	4.38 ± 0.06
74	W(122)[b]	4.34 ± 0.05	–	–	–	–	–	–
74	W(123)[b]	4.50 ± 0.05	–	–	–	–	–	4.49 ± 0.04
74	W(124)[b]	4.33 ± 0.03	–	–	–	–	–	–
74	W(130)[b]	4.32 ± 0.04	–	–	–	–	4.31 ± 0.10[#]	4.32 ± 0.04
74	W(133)[b]	4.7[z]	–	–	–	–	–	–
74	W(134)[b]	4.7[z]	–	–	–	–	–	–
74	W(144)[b]	5.2 ± 0.1[x]	–	–	–	–	–	–
74	W(150)[b]	4.4[z]	–	–	–	–	–	–
74	W(160)[b]	4.40 ± 0.06[y]	–	–	–	–	–	–
74	W(223)[b]	4.7[z]	–	–	–	–	–	–
74	W(227)[b]	4.4[z]	–	–	–	–	–	–
74	W(229)[b]	4.3[z]	–	–	–	–	–	–
74	W(230)[b]	4.33 ± 0.05	–	–	–	–	–	–
74	W(233)[b]	4.38 ± 0.06	–	–	–	–	–	–
74	W(235)[b]	4.5 ± 0.2[x]	–	–	–	–	–	–
74	W(250)[b]	4.6[z]	–	–	–	–	–	–
74	W(257)[b]	4.9 ± 0.1[x]	–	–	–	–	–	–
74	W(334)[b]	4.4 ± 0.2[x]	–	–	–	–	–	–
74	W(650)[b]	4.4 ± 0.1[y]	–	–	–	–	–	–
74	W(poly)[b]	4.56 ± 0.03	5.17 ± 0.05	4.51 ± 0.03	4.55 [828]	4.55 [828]	4.54 4.50[#]	4.55 ± 0.04
75	Re(0001)[hc]	5.30 ± 0.21	5.15 ± <0.34	–	–	–	–	5.13 ± 0.16
75	Re(1010)[hc]	5.12 ± 0.05	–	–	–	–	–	–
75	Re(1011)[hc]	5.26 ± 0.13	–	–	–	5.75 [363]	–	–
75	Re(1120)[hc]	4.95 ± 0.11	–	–	–	–	–	–
75	Re(1121)[hc]	4.82 ± 0.14	–	–	–	–	–	–
75	Re(1122)[hc]	5.03 ± 0.18	–	–	–	–	–	–
75	Re(1123)[hc]	4.7 ± 0.2[y]	–	–	–	–	–	–
75	Re(1124)[hc]	4.8 ± 0.1[x]	–	–	–	–	–	–

Table 2 (*continued*)

No.	Surface	ϕ^e (eV) [Here]	ϕ^+ (eV) [Here]	ϕ^- (eV) [Here]	ϕ^e (eV) [1358]	ϕ^e (eV) [1045]	ϕ^e (eV) [12,1354]	ϕ^e (eV) [1351]
75	Re(1130)[hc]	4.6 ± 0.1[x]	–	–	–	–	–	–
75	Re(2130)[hc]	4.6 ± 0.1[x]	–	–	–	–	–	–
75	Re(3140)[hc]	4.7 ± 0.1[x]	–	–	–	–	–	–
75	Re(poly)[hc]	4.96 ± 0.05	5.41 ± 0.04	5.00 ± 0.06[y]	4.72 [832]	4.96 [124]	5.0	4.95 ± 0.03
76	Os(0001)[hc]	5.6 ± 0.2	–	–	–	–	–	–
76	Os(1010)[hc]	5.3 ± 0.3[y]	–	–	–	–	–	–
76	Os(0111)[hc]	5.4 ± 0.1[x]	–	–	–	–	–	–
76	Os(0112)[hc]	5.0 ± 0.1[x]	–	–	–	–	–	–
76	Os(0113)[hc]	4.8 ± 0.1[x]	–	–	–	–	–	–
76	Os(1121)[hc]	4.8 ± 0.1[x]	–	–	–	–	–	–
76	Os(1122)[hc]	5.1 ± 0.1[x]	–	–	–	–	–	–
76	Os(1123)[hc]	4.9 ± 0.1[x]	–	–	–	–	–	–
76	Os(1124)[hc]	5.1[z]	–	–	–	–	–	–
76	Os(2130)[hc]	5.0 ± 0.1[x]	–	–	–	–	–	–
76	Os(3140)[hc]	4.9 ± 0.1[x]	–	–	–	–	–	–
76	Os(poly)[hc]	4.97 ± 0.17	–	–	5.93 [3322]	4.83 [124]	4.7	4.84 ± 0.07
77	Ir(100)[f]	5.60 ± 0.06	–	–	5.67 [414][(12)]	5.67 [414]	–	5.72 ± 0.27
77	Ir(110)[f]	5.23 ± 0.19	–	–	5.42 [358][(12)]	5.42 [358]	–	–
77	Ir(111)[f]	5.75 ± 0.06	5.76 ± 0.04	–	5.76 [358][(12)]	5.76 [358]	–	5.77 ± 0.03
77	Ir(210)[f]	5.05 ± 0.05[x]	–	–	5.00 [414][(12)]	5.00 [414]	–	–
77	Ir(211)[f]	5.2 ± 0.1[x]	–	–	–	–	–	–
77	Ir(311)[f]	5.2[x]	–	–	–	–	–	–
77	Ir(321)[f]	5.2 ± 0.1[x]	–	–	–	–	–	–
77	Ir(331)[f]	5.3 ± 0.1[x]	–	–	–	–	–	–
77	Ir(731)[f]	4.9[z]	–	–	–	–	–	–
77	Ir(poly)[f]	5.28 ± 0.04	5.75 ± 0.04	–	–	5.27 [124]	4.7	5.27 ± 0.02
78	Pt(100)[f]	5.75 ± 0.06	–	–	5.84* [428][(5)]	–	–	5.82 ± 0.07
78	Pt(110)[f]	5.54 ± 0.07	–	–	–	–	–	5.61 ± 0.13
78	Pt(111)[f]	5.84 ± 0.05	5.80 ± 0.06	–	5.93 [428]	5.7** [616][(6)]	–	5.86 ± 0.06
78	Pt(210)[f]	5.18 ± 0.04	–	–	–	–	–	–
78	Pt(211)[f]	5.7 ± 0.1[y]	–	–	–	–	–	–
78	Pt(221)[f]	5.76 ± 0.01[y]	–	–	–	–	–	–
78	Pt(310)[f]	5.4 ± 0.1[x]	–	–	–	–	–	–
78	Pt(311)[f]	5.4 ± 0.1[x]	–	–	–	–	–	–
78	Pt(320)[f]	5.19 ± 0.03[y]	–	–	5.22 [428]	–	–	–
78	Pt(321)[f]	5.3 ± 0.1[x]	–	–	–	–	–	–
78	Pt(331)[f]	5.4 ± 0.2[y]	–	–	5.12 [428]	–	–	–
78	Pt(410)[f]	5.5[z]	–	–	–	–	–	–
78	Pt(430)[f]	5.2[z]	–	–	–	–	–	–
78	Pt(520)[f]	5.3[z]	–	–	–	–	–	–
78	Pt(533)[f]	5.9[x]	–	–	–	–	–	–
78	Pt(741)[f]	5.2[z]	–	–	–	–	–	–
78	Pt(997)[f]	5.8[z]	–	–	–	–	–	–
78	Pt(poly)[f]	5.30 ± 0.07	5.58 ± 0.11	–	5.64 [435]	5.65 [304]	5.32	5.27 ± 0.08
79	Au(100)[f]	5.39 ± 0.07	–	–	5.47 [959]	5.47 [959]	–	5.41 ± 0.12
79	Au(110)[f]	5.33 ± 0.09	–	–	5.37 [959]	5.37 [959]	–	5.31 ± 0.11
79	Au(111)[f]	5.46 ± 0.07	–	–	5.31 [959]	5.31 [959]	–	5.29 ± 0.02
79	Au(112)[f]	5.1[z]	–	–	–	–	–	–
79	Au(113)[f]	5.2[z]	–	–	–	–	–	–

Table 2 (*continued*)

No.	Surface	ϕ^e (eV) [Here]	ϕ^+ (eV) [Here]	ϕ^- (eV) [Here]	ϕ^e (eV) [1358]	ϕ^e (eV) [1045]	ϕ^e (eV) [12,1354]	ϕ^e (eV) [1351]
79	Au(210)[f]	5.0[z]	–	–	–	–	–	–
79	Au(532)[f]	5.0[z]	–	–	–	–	–	–
79	Au(poly)[f]	5.30 ± 0.04	5.7[z]	–	–	5.1 [304]	4.30	5.31 ± 0.07
80	Hg(liquid)	4.50 ± 0.02	–	–	4.475 [2770]	4.49 [2470]	4.52	–
80	α-Hg(poly)[rh]	4.52 ± 0.05	–	–	–	–	–	–
81	α-Tl(0001)[hc]	4.2 ± 0.3[x]	–	–	–	–	–	–
81	α-Tl(1010)[hc]	4.1 ± 0.2[x]	–	–	–	–	–	–
81	α-Tl(1124)[hc]	3.8[z]	–	–	–	–	–	–
81	β-Tl(100)[b]	3.5[z]	–	–	–	–	–	–
81	β-Tl(110)[b]	4.1[z]	–	–	–	–	–	–
81	β-Tl(111)[b]	3.4[z]	–	–	–	–	–	–
81	β-Tl(112)[b]	3.8[z]	–	–	–	–	–	–
81	α-Tl(poly)[hc]	3.82 ± 0.05	–	–	3.84 [2297]	3.84 [2297]	3.7	–
81	Tl(liquid)	3.7 ± 0.1[x]	–	–	–	–	–	–
82	Pb(100)[f]	3.96 ± 0.11	–	–	–	–	–	–
82	Pb(110)[f]	3.84 ± 0.09	–	–	–	–	–	–
82	Pb(111)[f]	4.14 ± 0.09	–	–	–	–	–	–
82	Pb(poly)[f]	4.07 ± 0.05	–	–	4.25 [613]	4.25 [613]	4.0	–
82	Pb(liquid)	4.00 ± 0.05[x]	–	–	–	–	–	–
83	Bi(0001)[tr]	4.5 ± 0.2[y]	–	–	–	–	–	–
83	Bi(1011)[tr]	4.3[z]	–	–	–	–	–	–
83	Bi(poly)[tr]	4.28 ± 0.05	–	–	4.34 [2349][(13)]	4.22 [3052]	4.4	–
83	Bi(liquid)	4.34 ± 0.07[y]	–	–	–	–	–	–
84	α-Po(poly)[c]	4.8 ± 0.2[y]	–	–	–	–	–	–
85	At	5.3[z]	–	–	–	–	–	–
87	Fr(111)[b]	2.1[z]	–	–	–	–	–	–
87	Fr(poly)[b]	2.0 ± 0.1	–	–	–	–	–	–
88	Ra(110)[b]	2.3[z]	–	–	–	–	–	–
88	Ra(111)[b]	2.0[z]	–	–	–	–	–	–
88	Ra(poly)[b]	2.4 ± 0.3	–	–	–	–	–	–
89	Ac(111)[f]	3.4[z]	–	–	–	–	–	–
89	Ac(poly)[f]	3.2 ± 0.3[y]	–	–	–	–	–	–
90	α-Th(100)[f]	3.5 ± 0.1[x]	–	–	–	–	–	–
90	α-Th(110)[f]	3.4[z]	–	–	–	–	–	–
90	α-Th(111)[f]	3.6 ± 0.2[x]	–	–	–	–	–	–
90	α-Th(poly)[f]	3.37 ± 0.04	3.4 ± 0.1[x]	3.5 ± 0.1[y]	3.4 [1854]	3.4 [1854]	3.30	–
91	Pa(111)[c]	3.8[z]	–	–	–	–	–	–
91	Pa(poly)[c]	3.4 ± 0.1[y]	–	–	–	–	–	–
92	γ-U(100)[b]	3.7 ± 0.1[y]	–	–	–	–	–	–
92	γ-U(110)[b]	4.1[z]	–	–	–	–	–	–
92	γ-U(111)[b]	3.3[z]	–	–	–	–	–	–
92	γ-U(112)[b]	3.7[z]	–	–	–	–	–	–
92	α-U(poly)[r]	3.64 ± 0.04	–	–	3.63 [2103]	3.63 [2103]	3.3	–
92	β-U(poly)[t]	3.58 ± 0.04	–	–	–	–	–	–
92	γ-U(poly)[b]	3.42 ± 0.05	–	–	–	–	–	–

Table 2 (*continued*)

No.	Surface	ϕ^e (eV) [Here]	ϕ^+ (eV) [Here]	ϕ^- (eV) [Here]	ϕ^e (eV) [1358]	ϕ^e (eV) [1045]	ϕ^e (eV) [12,1354]	ϕ^e (eV) [1351]
93	Np(111)^c	4.0^z	–	–	–	–	–	–
93	Np(poly)^c	3.4 ± 0.5^x	–	–	–	–	–	–
94	α-Pu(020)^m	3.6 ± 0.1^x	–	–	–	–	–	–
94	δ-Pu(100)^f	3.3 ± 0.2	–	–	–	–	–	–
94	δ-Pu(110)^f	3.0^z	–	–	–	–	–	–
94	δ-Pu(111)^f	3.8 ± 0.3	–	–	–	–	–	–
94	α-Pu(poly)^m	3.3^z	–	–	–	–	–	–
94	δ-Pu(poly)^f	3.6 ± 0.3^y	–	–	–	–	–	–
95	α-Am(0001)^{dhc}	3.6 ± 0.7^x	–	–	–	–	–	–
95	α-Am(1010)^{dhc}	4.2^z	–	–	–	–	–	–
95	α-Am(1124)^{dhc}	3.7^z	–	–	–	–	–	–
95	β-Am(100)^f	2.9^z	–	–	–	–	–	–
95	β-Am(110)^f	2.9^z	–	–	–	–	–	–
95	β-Am(111)^f	3.1^z	–	–	–	–	–	–
95	α-Am(poly)^{hc}	3.4 ± 0.1^y	–	–	–	–	–	–
96	Cm(poly)^{hc}	3.5 ± 0.2^y	–	–	–	–	–	–
97	Bk(poly)^{hc}	3.5 ± 0.2^y	–	–	–	–	–	–
98	Cf(poly)^{hc}	3.5 ± 0.2^y	–	–	–	–	–	–
99	Es(poly)^{hc}	3.1 ± 0.2^x	–	–	–	–	–	–
	Total element species (N_e)	88	14	6	60	63	66	18
	Total surface species (N_s)	609	39	9	103	114	66	72

(1) The superscripts (b–tr) in the 2nd column are the abbreviations indicating the crystal structures as follows.
b body-centered cubic
c cubic
d diamond
dhc double hexagonal closed packing
f face-centered cubic
h hexagonal
hc hexagonal closed packing
m monoclinic
p pseudocubic
r rhombic
rh rhombohedral
t tetragonal
tr trigonal
(2) The values with the superscript (#) for tungsten in the last 2nd column are estimated as the probable ones from many published data on tungsten by Collins and Blott [1664,1665,3964] instead of Fomenko [12,1354].
(3) The values with double and single underlines in the 3rd–5th columns may be reliable to within the errors of ±0.05 and ±0.1 eV, respectively, whilst the others in the columns may have a possible error of up to ∼0.1 eV or more.
(4) The superscripts (x and y) in the 3rd–5th columns indicate that the numbers of the work function data available for estimating these values with x and y are 2 and 3–5, respectively, whilst the value with the superscript (z) originates from a single datum alone. Consequently, many of the values (x, y or z attached) may probably be less reliable compared with those based on much abundant data (up to about 400 in total number, typically, for each of Cs and W).
(5) Regarding the plane of Pt in the CRC handbooks [11,1358,1359], "(110)" should be read "(100)" partly because any of these references (1)–(3) [13,1045,1312] cited in the handbooks does not include Pt(110) and mainly because 5.84 eV by FE corresponds exactly to Pt(100) [428] alone among the four planes of Pt tabulated in Ref. (1) [1312] and also in the original data source [428]. This is the reason why 5.84* for Pt(100) in Column 6 here is accompanied with an asterisk.
(6) The value of ϕ^e = 5.7** eV for Pt(111) [1045] in 7th column originates from Demuth's paper [616] instead of his another [1799], because the latter cited as reference 45 by Michaelson [1045] includes the datum of 5.6 eV for Pd(111) alone and does not 5.7 eV for Pt(111).
(7) The m-Co(100)^b indicates the metastable bcc–phase–Co(100) on GaAs(110) [4023,4028]. For further information, see Footnotes 428–430 in Table 1.
(8) Among the many surface species listed herein, Columns (6) [1358] and (7) [1045] for each species are found to have the same value originating from a common article selected by Michaelson [1045], while each value [1358] different from that [1045] comes from that done by Rivière [13] or Hölzl [1312]. In any cases, all of the values in the columns, in addition to those recommended by Fomenko in Column (8), are based on those data published before ∼1980.
(9) The value of 4.22 eV for Cd(poly) [349] is reported by Hopkins and Rivière after correcting the original one of 4.08 eV [1380] (see Footnote 214 in Table 1).
(10) Regarding 4.65 eV for Cu(poly), [3319] corresponding to Ref. 9 [1045] should be read [304] doing to Ref. 8 [1045] because the former [3319] includes 4.08 eV for In(poly) alone in contrast to the latter [304] including 4.65 eV for Cu(poly).

(11) In respect of Na(poly), 2.75 eV (PE, 77 K, film on quartz) [3424] and both 2.36 eV (PE, 293 K, film on Mo) [3337] and 2.35 eV [1354] are considerably larger and smaller than 2.54 eV [Here], respectively, thereby suggesting that the valid reason for such a large gap (~0.2 eV) should be found by further investigations.

(12) CRC Handbooks (78–98th Eds., 1997–2017) [1358, etc.] indicate that all of the data on Ir(100)–Ir(210) [[358] or [414]] are obtained by PE. But, PE should be read FE, just as indicated in a CRC Handbook (77th Ed., 1996) [4137] and a review [1045].

(13) On the basis of Ref. 1 [1312], CRC Handbooks (78–98 Eds., 1997–2017) [1358, etc.] recommend 4.34 eV at 300 °C by PE [2349] for Bi(poly). But, it should be read Bi(liq) measured at 573 K above T_m [2349] (see Table 1), although the value may be acceptable because the work function difference ($\Delta\phi_{LS}^e$) between the two phases is as small as 0.03 eV (see Table 12).

(14) The work function of 3.63 eV for Zn(mono) [2601] is recommended as that for Zn(poly) in CRC Handbooks (78–98 Eds., 1997–2017) [1358, etc.], while it is taken as that for Zn(0001) [475] although not clearly done so [1312,2601]. On the other hand, 4.9 eV [1508] is recommended for Zn(0001) in a CRC Handbook (77th Ed., 1996) [4137] and in a review [1045]. However, 3.63 and 4.9 eV are respectively much smaller and larger than our most probable values of 4.22 and 4.35 eV recommended for Zn(poly) and Zn(0001) in Table 2 and also than many others listed in Table 1 for the respective surfaces, thereby suggesting that any of the former values may be acceptable today as a reliable work function value for neither Zn(poly) nor Zn(0001).

(15) The value of 5.10 eV [358] recommended for Cu(100) in CRC Handbooks (78–98th Eds., 1997–2017) [1358, etc.] is extremely larger than any others (4.57–4.59 eV) [Here, 1045,1351] recommended for Cu(100) herein and also considerably larger than those (4.91–4.94 eV) done for Cu(111) having the largest among all of the copper monocrystals (see Tables 2 and 10). On the other hand, a CRC Handbook (77th Ed., 1996) [4137] as well as a review [1045] adopts 4.59 ± 0.03 eV [953,2006], which is the same with ours (4.58 ± 0.06 eV) for Cu(100).

(16) The m-Fe(100)^f grown epitaxially on Cu(100) represents the metastable fcc-Fe(100) (see Footnote 114 in Table 1 and also Sections 7.1 and 8.2).

(17) Metastable fcc-films of Co and Co(100) grown epitaxially on Cu(100) are much different in physical property from the two allotropes of bulk cobalt (see Section 8.2).

3.1. Estimation of the most probable values

On the basis of the theoretical and experimental data compiled in Table 1, the most probable values of the effective work functions (ϕ^+, ϕ^e and ϕ^-) for each of the essentially clean surface species will be estimated according to the fundamental aspects and policies as follows.

(1) In the case of thermal electron emission (TE) studied usually in relatively low vacuum conditions ($P_r \approx 10^{-7}$–10^{-9} Torr) as may be found frequently in the 4th column in Table 1, we should not overlook the important point whether or not the temperature or its range (Column 5) selected for work function measurements is high enough to keep the surface essentially clean. Typically, $T \geq 1800$ K for Re [65] and Ir [104] and also above 1900 K for W [69] may be acceptable as the normal condition even in such a low vacuum as mentioned above.

(2) Similarly in thermal positive (or negative) ion emission (PSI or NSI), T should be selected to be so high that the surface may be kept substantially clean even during the probing beam (or vapor) incidence. How to select T is readily understandable from such typical examples as Figs. 3 [58], 17 [104] and 28 [571] shown in Ref. [1351].

(3) Since other methods such as field emission (FE), photoelectric effect (PE) and contact potential difference (CPD) are usually adopted at $T \leq 300$ K, a very high vacuum below ~10^{-10} Torr should be maintained in general to insure the surface cleanness. It should be noted that adsorption lifetime of impinging residual gasses generally becomes longer with a decrease in T and hence that the surface coverage of foreign atoms and molecules (degree of surface contamination) becomes larger with decreasing temperature.

(4) With respect to a sample layers/substrate system (A/B) usually investigated around room temperature, it should be examined whether the layer(s) is adequately equilibrated (smoothed) by annealing at T_a (or $T_d) \geq T_m/3$) so as to correspond to its *bulk* sample (see Section 2.5 and Footnote 363 in Table 1) and also whether ultrahigh vacuum during work function measurements is maintained so as to keep the layer(s) substantially free from any effect owing to residual gas adsorption.

(5) Strictly speaking, all of ϕ^+, ϕ^e and ϕ^- are dependent upon surface temperature with the coefficient (α) of ~$\pm 10^{-4}$–10^{-5} eV/K (see both Section 5 and Table 6 in Ref. [1351]), which yields the work function differences of about ± 0.05–0.005 eV and of ± 0.2–0.02 eV according to the temperature differences by ~500 K (e.g., ~100–600 K, usually adopted in FE, PE or CPD) and by ~2000 K (~2300–300 K, extrapolated to room temperature in TE, PSI or NSI), respectively. However, such differences are tentatively disregarded here because of the reasons to be outlined as follows. (i) As may be seen in Table 1, the work function of any surface species changes by up to ~0.5 eV or much more from specimen to specimen or worker to worker, even in a common temperature range. Typically, ϕ^+ and ϕ^e for W(100) by PSI and TE are scattered widely in the ranges of mainly ~4.5–5.1 and ~4.4–5.0 eV, respectively, in a usual range (~1800–2300 K) among different experimental workers. Much wider scattering ($\phi^e \approx 3.7$–7.8 eV) is found for W(100) among different theoretical ones (see Table 1). All of the scattering widths (0.6–4.1 eV) are much larger than these differences (0.005–0.2 eV) due to the temperature difference mentioned just above. (ii) Such a fact as mentioned just above (i) indicates that the work function data based on both theoretical and experimental methods available today are usually not so convergent (or concentrated) enough to determine accurately the absolute value at a specified temperature (e.g., ~300 K) for any surface species to within the uncertainty of about ± 0.1 eV or so and, hence, that the estimated range of work function change (~0.005–0.2 eV) due to the actual difference in temperature may be considered to be much more narrower than the range (~0.6–4.1 eV) owing to the difference among various specimens or workers. (iii) This is the main reason why the present author has tried to estimate the most probable values of work function here without considering its temperature dependence, quite similarly as many other authors do so in handbooks and reviews [10–13,1045,1352–1355,1358]. Of course, it is needless to say that work function dependence upon surface temperature inherent in any crystal must be taken into consideration whenever the *net* work function change due to physical transition alone at a critical temperature (e.g., Curie point) is to be determined accurately (see Sections 7–10).

(6) In addition, all the data obtained for each surface species listed in Table 1 are critically analyzed from the viewpoints of (i) the reproducibility of the data reported, (ii) the surface cleanness (subject to dependence upon P_r and T), (iii) the correctness

of the reference work function adopted for CPD, etc., (iv) both method and condition selected for sample preparation, and (v) the measurement procedure employed.

(7) As will be shown typically for W in Sections 4.2–4.4, (i) ϕ^e of the "polycrystals" having the largest fractional area (δ_m) of less than 0.5 (=50% in fraction) (e.g. W(A)–W(D)) is nearly constant at 4.52 ± 0.10 eV [2453] (see Footnote (25) in Table 6) with little dependence upon the difference in both $\delta_m = 0.336$–0.463 and $\phi_m = 5.35$–4.25 eV belonging each to δ_m correspondent to the planes of (110)–(310), but (ii) ϕ^e of the "submonocrystals" with $0.5 < \delta_m < 1$ (namely, $50 < \delta_m < 100\%$), on the other hand, changes considerably depending upon both δ_m and ϕ_m (see Sections 4.4 and 4.5) and, hence, (iii) the work function data for the latter (ii) (typically, $\phi^e = 4.87$ eV for $\delta_m = 0.80$ and $\phi_m = 5.3$ eV of W(E) [2453], see Footnote (33) in Table 6) should be eliminated whenever the most probable work function value for the usually called "polycrystal" alone is taken into consideration. In other words, any "submonocrystal" should be treated as another type (category) different from both poly- and monocrystals. This is entirely because the former has generally such an anomaly that its work function depends principally upon δ_m without having a constant and unique value characteristic of the surface species (material) itself even under the normal condition accepted generally (see Section 4.5), in contrast to the "polycrystal" ($\delta_m < 0.5$) having a unique work function value with little dependence upon δ_m (see Conclusions (4)–(7) in Section 4.4). Of course, each surface of monocrystal ($\delta_m = 1$) is generally expected to have a unique value of work function characteristic of the surface species itself when the surface is essentially clean and smooth.

According to the above aspects and policies (1)–(7), the present author has tried to examine critically the work function data for each surface species listed in Table 1. As a result, about 50% or more of the very abundant data listed for such popular surface species as Cu, Mo, W, etc. are naturally eliminated in general because of (i) the poverty in surface condition, (ii) some errors in determination and/or (iii) the anomaly of $0.5 < \delta_m < 1$ corresponding to "submonocrystals" (see Sections 4.4 and 4.5). In consequence, such elimination leads to the result that both average and standard deviation for ϕ^e or ϕ^+ are calculated mainly from these data in the middle group (usually ~30–40%) alone, without including those in lower and higher groups (usually 70–60%) for each surface species. In this way, the statistical processing is applied to almost all the surface species included in Table 1, thereby yielding the most probable values of ϕ^e and ϕ^+ listed respectively in the 3rd and 4th columns in Table 2, together with ϕ^- in the 5th one. In the last column are recorded the most probable values of ϕ^e recommended by the present author previously [1351] in the same manner as above, although they are not so abundant (only 72 surface species) as the present ones (about 600 species) in the 9th and 3rd columns, respectively.

When the available data are extremely scanty in such a typical case as less-popular surface species and/or when they are much scattered in value over a very wide range, on the other hand, it is generally very difficult to find the most probable value for each species. This is the main reason why many of the surface species are not accompanied with the recommended values in the last line for the corresponding species in Table 1. Regarding those surface species having relatively scanty and/or divergent data, however, the present author dares to estimate tentatively the probable values and also to enter all of them in Column 3 of Table 2. Here, the superscripts of x and y indicate that the total numbers of work function data listed in Table 1 are 2 and 3–5, respectively. Especially, even the value of ϕ^e based on a single datum alone is purposely added with a superscript of z in order to summarize compactly all of the surface species investigated here and also to compare ϕ^e readily among different surface species for each element. Therefore, these values with x, y or z superscripted may possibly be less reliable or accurate compared with the others that are generally based on much abundant data (by up to ~400 data on each of Cs and W as typical cases) and hence that may be convincing in general. In other words, it may be safe to say that some of them (especially those with z attached) should be taken as the values estimated roughly by the present author. For quite many surface species (x–z) other than the ten species of Nb(113)^z, Nb(116)^y, Nb(310)^z, Mo(332)^y, Sb(100)^x, Sb(amorphous)^y, Te(1010)^x, Ir(210)^x, Pt(320)^y and Pt(331)^y, however, neither selected nor recommended values are found in Columns 6–8 in Table 2. Such an unfavorable situation at present suggests that much data on these species (x–z) should be accumulated hereafter by both theoretical and experimental studies.

3.2. Comparison with previously recommended values

In order to examine the important problem whether our most probable values estimated for ϕ^e as well as the previous ones [1351] are rational from the standpoint of scientific objectivity, the typical values of ϕ^e selected formerly by other authors [1045,1358] and also those recommended by another [12,1354] are listed in the 6–8th columns in Table 2. As known very well, these publications [12,1045,1354,1358] together with others [13,1312,1352,1355] have long been consulted as reliable and convenient data sources by many workers still to date. Especially, many of the values selected by Michaelson [1045] are adopted in CRC handbooks [11,1358,1359,4137, etc.], as may readily be understood from the fact that Columns 6 and 7 are often found to have the same value originating from the same reference selected for each surface species by the author [1045]. Typically, $\phi^e = 5.22, 5.04$, and 5.35 eV for Ni(100), Ni(110) and Ni(111) originating from Ref. [314], respectively, are found in both Columns 6 and 7, and all the values of which come from the selection by Michaelson [1045]. In addition, Ref. [1045] has long been widely cited to date by about 2000 groups of workers, as already mentioned in Section 1. Similarly, a handbook compiled by Fomenko [1354] has constantly been consulted especially in Russian and previous USSR countries. However, the total numbers (N_e and N_s) of the species (element and surface) covered by them [1045,1354,1358] in Table 2 are much smaller ($N_e = 60, 63$ and 66 species and $N_s = 103, 114$ and 66 species, respectively) compared with the present ones ($N_e = 88$ and $N_s = 609$ species, see the last two lines in Table 2). In addition, even CRC handbook (97th Ed.) [1358] published in 2016 is based entirely on the references [13,1045,1312], all of which were published more than ~40 years ago (1969–1979). Therefore, it may be necessary to examine the question whether all of the data listed in the above publications are fully accurate or reliable enough to be still acceptable even today.

From the above point of view, let's try to compare the recommended data [1045,1354,1358] with ours [Here] according to the typical forty examples listed below, where the figures are given as in the form of (A), {B}, [C] and (D/E). Namely, A is our

most probable value of ϕ^e (in eV) recommended in the 3rd column in Table 2, *B* is the experimental data on ϕ^e (in eV) which is achieved originally by the corresponding author [C] and also which is recommended in the 6–8th columns by one or two of the authors [1045,1354,1358], *D* is the difference (in eV) equal to $\Delta \equiv B - A$, and *E* is the percent of Δ/A. For the examinations (1)–(40) below, our value (*A*) is tentatively employed as the reference to examine the degree of difference or discrepancy (*E*) between our and other values (*A* and *B*) recommended in Table 2.

(1) α-Be(poly); (4.28 ± 0.13) // {4.98 ± 0.10} [2009] // (0.70 ± 0.16/16 ± 4)#.
(2) C(poly); (4.63 ± 0.06) // {5.0 ± 0.1} [299] // (0.37 ± 0.12/8 ± 3).
(3) Na(poly); (2.54 ± 0.03) // {2.35 ± ?} [1354] // (−0.19 ± 0.03/−7 ± 1).
(4) Na(poly); (2.54 ± 0.03) // {2.36 ± 0.02} [3337] // (−0.18 ± 0.04/−7 ± 2).
(5) Si(111); (4.86 ± 0.09) // {4.60 ± 0.13} [118] // (−0.26 ± 0.16/−5 ± 3).
(6) α-Ti(poly); (3.87 ± 0.05) // {4.33 ± 0.1} [304] // (0.46 ± 0.11/12 ± 3)#.
(7) α-Fe(poly); (4.55 ± 0.05) // {4.31 ± ?} [1354] // (−0.24 ± 0.05/−5 ± 1).
(8) α-Co(poly); (4.71 ± 0.03) // {4.41 ± ?} [1354] // (−0.30 ± 0.03/−6 ± 1).
(9) α-Co(poly); (4.71 ± 0.03) // {5.0 ± 0.1} [304] // (0.29 ± 0.1/6 ± 2).
(10) Cu(100); (4.58 ± 0.06) // {5.10 ± 0.05} [358] // (0.52 ± 0.08/11 ± 2)#.
(11) Zn(poly); (4.22 ± 0.11) // {3.63 ± ?} [2601] // (−0.59 ± 0.11/−14 ± 3)#.
(12) Ga(poly); (4.27 ± 0.06) // {3.96 ± ?} [1354] // (−0.31 ± 0.06/−7 ± 2).
(13) Ge(poly); (4.76 ± 0.05) // {5.0 ± ?} [1520] // (0.24 ± 0.05/5 ± 1).
(14) Se(poly); (5.27 ± 0.18) // {4.72 ± ?} [1354] // (−0.55 ± 0.18/−10 ± 4)#.
(15) Se(poly); (5.27 ± 0.18) // {5.9 ± ?} [3429] // (0.63 ± 0.18/12 ± 4)#.
(16) α-Sr(poly); (2.71 ± 0.08) // {2.35 ± ?} [1354] // (−0.36 ± 0.08/−13 ± 3)#.
(17) Nb(111); (3.95 ± 0.09) // {4.36 ± 0.06} [779] // (0.41 ± 0.11/10 ± 3)#.
(18) Nb(112); (4.33 ± 0.10) // {4.63 ± 0.06} [779] // (0.30 ± 0.12/7 ± 3).
(19) Mo(100); (4.38 ± 0.03) // {4.53 ± 0.02} [325] // (0.15 ± 0.04/3 ± 1).
(20) Mo(111); (4.29 ± 0.03) // {4.55 ± 0.02} [325] // (0.26 ± 0.04/6 ± 1).
(21) Mo(poly); (4.31 ± 0.02) // {4.6 ± 0.15} [304] // (0.29 ± 0.15/7 ± 3).
(22) Pd(poly); (5.17 ± 0.06) // {4.8 ± ?} [1354] // (−0.37 ± 0.06/−7 ± 1).
(23) In(poly); (4.05 ± 0.06) // {3.8 ± ?} [1354] // (−0.25 ± 0.06/−6 ± 2).
(24) Sb(poly); (4.45 ± 0.09) // {4.08 ± ?} [1354] // (−0.37 ± 0.09/−8 ± 3).
(25) Cs(poly); (2.05 ± 0.05) // {1.81 ± ?} [1354] // (−0.24 ± 0.05/−12 ± 2)#.
(26) α-La(poly); (3.27 ± 0.04) // {3.5 ± 0.2} [304] // (0.23 ± 0.20/7 ± 6).
(27) β-Ce(poly); (2.89 ± 0.07) // {2.7 ± ?} [1354] // (−0.19 ± 0.07/−7 ± 3).
(28) Eu(poly); (2.74 ± 0.12) // {2.5 ± 0.3} [304] // (−0.24 ± 0.32/−9 ± 11).
(29) α-Hf(poly); (3.64 ± 0.06) // {3.9 ± 0.1} [304] // (0.26 ± 0.12/7 ± 3).
(30) Re(1011); (5.26 ± 0.13) // {5.75 ± ?} [363] // (0.49 ± 0.13/9 ± 3).
(31) Re(poly); (4.96 ± 0.05) // {4.72 ± ?} [832] // (−0.24 ± 0.05/−5 ± 1).
(32) Os(poly); (4.97 ± 0.17) // {4.7 ± ?} [1354] // (−0.27 ± 0.17/−5 ± 4).
(33) Os(poly); (4.97 ± 0.17) // {5.93 ± 0.05} [3322] // (0.96 ± 0.18/19 ± 4)#.
(34) Ir(poly); (5.28 ± 0.04) // {4.7 ± ?} [1354] // (−0.58 ± 0.04/−11 ± 1)#.
(35) Pt(poly); (5.30 ± 0.07) // {5.64 ± ?} [435] // (0.34 ± 0.07/6 ± 2).
(36) Pt(poly); (5.30 ± 0.07) // {5.65 ± ?} [304] // (0.35 ± 0.07/7 ± 2).
(37) Au(poly); (5.30 ± 0.04) // {4.30 ± ?} [1354] // (−1.00 ± 0.04/−19 ± 1)#.
(38) Au(poly); (5.30 ± 0.04) // {5.1 ± 0.1} [304] // (−0.20 ± 0.11/−4 ± 2).
(39) Pb(poly); (4.07 ± 0.05) // {4.25 ± 0.05} [613] // (0.18 ± 0.07/4 ± 2).
(40) α-U(poly); (3.64 ± 0.04) // {3.3 ± ?} [1354] // (−0.34 ± 0.04/−9 ± 1).

As shown above, the difference of $|D| \equiv |B - A| \equiv |\Delta|$ has a wide range of 0.15–1.00 eV corresponding to $|E| \equiv |\Delta/A| = 3$–19%. In a typical case (11), we have $\Delta = -0.59$ eV and $\Delta/A = -14\%$ for Zn [2601]. The value of 3.63 eV [2601] is recommended for Zn(poly) in the CRC Handbook [1358], but it is treated as Zn(0001) [475]. Even in the latter, however, $B = 3.63$ eV for Zn(0001) yields $\Delta = -0.72 \pm 0.28$ eV and $\Delta/A = -17 \pm 6\%$ because our most probable value for Zn(0001) is 4.35 ± 0.28 eV (see Table 2). In another case (17), $B = 4.36 \pm 0.06$ eV for Nb(111) [779] is much larger than $A = 3.95 \pm 0.09$ eV for Nb(111) [Here] and not smaller than 4.02 ± 0.06 eV for Nb(100) [779], thereby leading to such a result that the triple set [779] of 4.87, 4.02 and 4.36 eV (see Table 2) does not perfectly follow the Smoluchowski rule of $\phi^e(110) > \phi^e(100) > \phi^e(111)$ to be expected generally for bcc-surfaces (for full detail, see Section 5.2 and 41–Nb–[779] in Table 9 and also Conclusion (8) in Section 5.4). In other words, it may be concluded that 4.36 eV for Nb(111) should be replaced with another to be less than 4.02 eV for Nb(100), such a typical value as 3.84 eV [774], 3.88 eV [726,775,960] or 3.95 eV [Here] (see Table 1).

Among the typical examinations (1)–(40) listed above, particularly those with # attached show that each of the value (*B*) recommended by one or two of the authors [1045,1354,1358] has a very large deviation ($|\Delta| \equiv |B - A| > 0.2$ eV and also $|\Delta/A| > 10\%$) from ours (*A*). Namely, they correspond to the examples of (1), (6), (10), (11), (15), (17) and (33) in CRC [1358], those of (1), (6), (15) and (17) in Michaelson [1045] and those of (14), (16), (25), (34) and (37) in Fomenko [1354]. The recommended values (*B*) with # attached, together with many others (*B*) included in the above forty examples, have long been consulted widely by a

great many workers. However, it does not seem to the present author that those with # may be very accurate or reliable enough to be straight or undoubtedly acceptable today, although any of our most probable values (*A*) employed as the reference for estimating the deviation or discrepancy (*Δ*) is not yet insured generally to be fully acceptable at present.

In the next step, let's examine the distribution of the work function difference ($D \equiv B - A$) for all of the recommended data (*B*) including the above forty examples.

Among our 609 surface species having the data on ϕ^e listed in the 3rd column in Table 2, it is only 134 species that can be compared with the other values of $\phi^e \equiv B$ (at least one or up to four values for each species) recommended previously in the 6–9th columns [1045,1351,1354,1358]. The difference ($|\Delta|$) between ϕ^e [Here] and each ϕ^e [1045,1354,1358] or [1351] has a wide distribution from 0.00 to 1.00 eV, which may be divided into the eleven categories as shown in Table 3; (1) good agreement of $|\Delta| \leq 0.05$ eV, (2) fair agreement of $|\Delta| = 0.06$–0.10 eV, (3) less-fair agreement of $|\Delta| = 0.11$–0.20 eV, and so on up to (11) wide gap of $|\Delta| = 0.91$–1.00 eV. The number (N_c) of those species contained in each category is different among the four references. The percentage (N_c/N_t) of the data corresponding to each category is also shown in Table 3, where N_t is the total number of the surface species contained in each of the four references (see the last line in Table 3).

Table 3
Distribution of the work function difference ($|\Delta|$) of ϕ^e between the most probable value [Here] and each one recommended by others [12,1045,1351,1354,1358] in Table 2. Here, N_t is the total number of ϕ^e–data listed in the last line and N_c is that corresponding to each category.

Category	Difference $|\Delta|$ (eV)	Ref. [1358]		Ref. [1045]		Refs. [12,1354]		Ref. [1351]	
		N_c	N_c/N_t (%)	N_c	N_c/N_t (%)	N_c	N_c/N_t (%)	N_c	N_c/N_t (%)
1	≤0.05	45	44	44	39	22	33	44	61
2	0.06–0.10	16	16	16	14	8	12	13	18
3	0.11–0.20	23	22	33	29	18	27	14	19
4	0.21–0.30	10	10	12	11	7	11	0	0
5	0.31–0.40	2	2	2	2	6	11	1	1
6	0.41–0.50	2	3	3	3	0	0	0	0
7	0.51–0.60	4	4	3	3	4	6	0	0
8	0.61–0.70	1	1	1	1	0	0	0	0
9	0.71–0.80	0	0	0	0	0	0	0	0
10	0.81–0.90	0	0	0	0	0	0	0	0
11	0.91–1.00	0	0	0	0	1	2	0	0
N_t	–	103	–	114	–	66	–	72	–

The essential points of Table 3 in addition to Table 2 may be summarized as follows.

(1) In the first category, many of our most probable values of ϕ^e [Here] in the 3rd column in Table 2 show a good agreement ($|\Delta| \leq 0.05$ eV) with about 44% ($N_c = 45$ species) of the values [1358], 39% ($N_c = 44$) of those [1045], 33% ($N_c = 22$) [12,1354] and 61% ($N_c = 44$) [1351] of the selected or recommended ones in the four references in the 6–9th columns in Table 2 (except those# for tungsten inserted with sharp in Column 8), respectively. Regarding the above "good agreement", each of the four references has the highest percentage ($N_c/N_t = 44, 39, 33$ or 61%) among the eleven categories. Especially, the following species satisfy the best agreement ($|\Delta| \leq 0.05$ eV) between each of our present values (Column 3 in Table 2) and more than two values referred for the same species in Columns 6–9 in Table 2. Namely, Li(poly); Mg(poly); Al(110), Al(111) and Al(poly); K(poly); α-Ca(poly); $\alpha-\beta$-Mn(poly); α-Fe(100); Ni(100) and Ni(111); Cu(100), Cu(110), Cu(111) and Cu(112); Rb(poly); Nb(100); Mo(110) and Mo(poly); Ru(poly); Pd(111) and Pd(poly); Cd(poly); Ba(poly); β-Ce(poly); Gd(poly); Ta(100), Ta(110), Ta(111) and Ta(poly); W(100), W(111), W(116) and W(poly); Re(poly); Ir(111) and Ir(poly); Au(110); Hg(liquid); α-Tl(poly); α-Th(poly) and α-U(poly). The recommended value of ϕ^e [Here] for each surface species mentioned just above may be fitly concluded to have a higher reliability or accuracy in comparison with that for any other species having $|\Delta| > 0.05$ eV.

(2) In the 2nd category, rather small percentages ($N_c/N_t = 12$–18% of $N_c = 8$–16 species) of the values recommended in the four references [1358, etc.] correspond to a fair agreement ($|\Delta| = 0.06 - 0.10$ eV) with our most probable value estimated for a common surface species [Here]. Among the four references, usually more than two are found to satisfy a fair agreement with the following species: Al(100); Si(100); Ni(110); Ga(poly); α-Y(poly); Nb(110); Ag(111); In(poly); β-Sn(poly); Cs(poly); α-Nd(poly); W(110) and W(113); Ir(100); Pt(100); Au(100) and Bi(poly). Our most probable values for the above species in Column 3 in Table 2 may probably be accepted to be considerably reliable in contrast to the others with $|\Delta| > 0.10$ eV.

(3) In the 3rd category, a less-fair agreement ($|\Delta| = 0.11 - 0.20$ eV) between the present and other four values is not small in percentage ($N_c/N_t = 22, 29, 27$ and 19% for $N_c = 23, 33, 18$ and 14 species, respectively). The following species belong to this category: Na(poly); Si(poly); α-Sc(poly); V(poly); Cr(poly); α-Fe(poly); Ni(poly); Cu(poly); Zn(poly); α-Sr(poly); α-Zr(poly); Nb(116) and Nb(poly); Mo(100), Mo(112) and Mo(114); Rh(poly); Ag(100) and Ag(poly); Sb(100) and Sb(amorphous); Te(1010); Sm(poly); α-Tb(poly); Lu(poly); Os(poly); Ir(110); Pt(111); Au(111) and Pb(poly). For each species, more than two values in Columns 6−9 in Table 2 correspond to $|\Delta| = 0.11 - 0.20$ eV. The present values [Here] as well as the others [1045,1351,1354,1358] for the above species may possibly be needed to be examined after accumulating much more data of ϕ^e achieved by both experiment and theory. Among the forty examinations listed above, these (3) and (4) Na(poly) [1354,3337], (19) Mo(100) [325], (27) β-Ce(poly) [1354] and (39) Pb(poly) [613] belong to the 3rd category, whilst the other thirty five ones ($|\Delta| = 0.21 - 1.00$ eV) do to those 4th–11th ones.

(4) In the 4th category, a considerable percentage of $N_c/N_t \approx 10\%$ ($N_c = 10, 12$ and 7 corresponding to Refs. [1045,1358] and [1354], respectively), in contrast to $N_c/N_t = 0\%$ [1351], is still found to have $|\Delta| = 0.21 - 0.30$ eV, being little agreeable to ϕ^e in the present and previous studies [Here, 1351]. The following surface species belong to this category; Si(111); α-Co(poly); Ge(poly); Nb(112); Mo(111) and Mo(332); Ag(110); α-La(poly); and α-Hf(poly). Much further study about these nine species may probably be needed to find the accurate or reliable value of ϕ^e so as to be convincing in general.

(5) In the 5–8th categories, a considerable discrepancy ($|\Delta| = 0.31 - 0.70$ eV) is found for the seven species of α-Be(poly); C(poly); α-Ti(poly); α-Fe(111); Se(poly); Nb(111); and Pt(poly). Typically, a marked discrepancy of $|\Delta| = |5.27 - 5.9| \approx 0.6$ eV is observed for Se(poly) between Column 3 [Here] and Columns 6 and 7 [1045,1358] in Table 2. The value of $\phi^e = 5.9$ eV by PE originating from Ref. [3429] is extraordinarily larger than any others except both 5.9 eV by TC [298] and 6.3 eV by FE [1677] listed in Table 1. In addition, 4.72 eV for Se(poly) [12,1354] corresponding to $|\Delta| = 0.55$ eV (Category 7) is exceedingly smaller than 4.8–5.8 eV (except 4.42 and 4.62 eV and also 5.9 and 6.3 eV above) among about 30 data obtained by various methods in Table 1. Therefore, none of the above values (5.9 and 4.72 eV) recommended for Se(poly) seems to be reliable enough to be acceptable today. With respect to the above seven species, it may be necessary to accumulate much data reliable enough to settle the question which value of ϕ^e for each species is nearer to the true or most probable one among those recommended by present or other authors.

(6) In the 11th category for $|\Delta| = 0.91 - 1.00$ eV, a wide gap of $|\Delta| = |5.30 - 4.30| = 1.00$ eV for Au(poly) exists between the present [Here] and the other [10,12,1354]. The latter (4.30 eV) seems to be affected strongly by the data obtained by using mercury diffusion pump systems which were very popular until ~1970. Table 1 includes many data determined for Au to be $\phi^e < 4.8$ eV, most of which were reported before ~1980. It should be noted that Au is subject to surface reaction (amalgamation) with Hg [1071–1073] having $\phi^e = 4.475$–4.52 eV (see Table 2). Typically, $\phi^e = 5.22$ eV for Au is reduced by ~0.45 eV by intentional admission of Hg-vapor [1071]. Several topics on Au may be added as follows: (i) Remove of Hg adsorbed on Au and Ag can be done readily by baking above 520 K [1893]. Typically, 5.25 ± 0.01 eV is observed for Au/W(110) after annealing at 750 K at $P_r = 5 \times 10^{-10}$ Torr attained by using a mercury pumping system [1670,1673], and similarly 5.24–5.27 eV is found for an Au ribbon after baking around 1070 K [2473]. Similarly at $P_r < 10^{-9}$ Torr (2×10^{-10} Torr as the partial pressure of Hg), ϕ^e of an Au-ribbon is increased from 4.89 ± 0.06 eV to 5.20 ± 0.05 eV by flashing at 1170 K [1072]. (ii) Further information about the mercury contamination of Au may be obtained from Section 4.2.3 in Ref. [1351]. (iii) Instead of 4.30 eV [10,12,1354], either 5.30 ± 0.04 eV [Here] or 5.31 ± 0.07 eV [1351] for Au may be recommended to be the most probable value of ϕ^e according to those data achieved in Hg-free systems. Employment of the latter makes it possible to establish much better the linear relationship between ϕ^e and X (see Fig. 1 [1955] and Fig 4.1 [1312]) expressed by Eq. (7). (iv) Regarding amorphous gold film on glass, on the other hand, ϕ^e is considered to be 4.7 eV [4113], which is currently interpreted on the basis of plasmon-assisted multiphoton emission [4369,4370]. (v) According to another study about Au-nanoparticles grown on a Si-wafer covered with a monolayer of alkyl chain, ϕ^e is found to change from ~3.5 to 3.8 eV as the particle radius increases from ~20 to 80 Å [4368] (see Footnote 478 in Table 1). The above typical examples suggest that some of the Au-layers having $\phi^e < 4.7$ eV (see Table 1) measured in an Hg-free atmosphere may possibly consist of fine crystallites.

(7) In order to list up compactly all of the surface species studied for their work functions in this article and also to demonstrate the present state how scanty the work function data are for a variety of less-common or unfamiliar surface species, the probable values of ϕ^e, ϕ^+ and ϕ^- with superscript (x, y or z) are also included in Table 2. Here, each of the values is estimated from the scanty data whose total numbers available in Table 1 are 2 and 3–5 for x and y, respectively, and only one for z. Consequently, any of them may possibly be less accurate or reliable than the others estimated from much abundant data (e.g., ~400 in number for each of Cs and W) listed in Table 1. With the eleven exceptions of As(111), Nb(113), Nb(116), Nb(310), Mo(332), Sb(100), Sb(amorphous), Te(1010), Ir(210), Pt(320) and Pt(331), many (97%) of our data on ϕ^e with x, y or z (387 surface species in total) in Column 3 (Table 2) can not be compared with any others in Columns 6–8 in Table 2.

(8) Accumulation of many new data on ϕ^e is generally expected particularly for the species attached with a superscript (x, y or z) as follows: α-Sc(1010); α-Ti(1010) and β-Ti(100)–(112); α-Co(1010)–(1124); Zn(1010); Ga(100)–(111); α-Y(1010) and β-Y(100)–(112); α-Zr(1010) and β-Zr(100)–(112); Cd(1010); In(100)–(111); Sb(111); β-La(100)–(112); β- and γ-Ce(100)–(112); α-Pr(0001) and β-Pr(100)–(112); β-Nd(100)–(112); Sm(100)–(112); Eu(100)–(112); α-Gd(1010) and (1124) and also β-Gd(100)–(112); α-Tb(1010) and (1124) and also β-Tb(100)–(112); α-Dy(1010) and (1124); α-Ho(1010) and (1124); α-Er(1010) and (1024); α-Tm(0001), (1010) and (1124); α- and β-Yb(100)–(112); α-Lu(0001), (1010) and (1124) and also β-Lu(100)–(112); α-Hf(0001), (1010) and (1124) and also β-Hf(100)–(112); Os(1010)–(1124); Au(112); α-Tl(0001)–(1124); Bi(0001) and (1011); Th(100)–(111); γ-U(100)–(112); and so on. Many of the above species may be interested in some workers active in the fields of pure and applied physics. Addition of new reliable data on the above species is strongly expected to fill out such great blanks as found in Columns 6–8th in Table 2.

(9) The most probable values of ϕ^e without any of x–z attached are estimated for 213 surface species in the 3rd column in Table 2, whilst their large part (36%, 77 species) is not covered in the 6–8th columns by any of the other authors [1045,1354,1358]. Namely, any of the 77 species has long been left without ϕ^e recommended in spite of the fact that a considerable number (≥ 6) of data on ϕ^e have already been published for each species. Of our all data (about 600 surface species including those with x–z attached), such a high percentage as ~80% (about 480 surface species) is not covered in any data list compiled by other authors, as may readily be understandable from the great blank in the three columns in Table 2. In other words, not only the best estimates but also even preferable ones of ϕ^e have not yet been reported for the latter 480 species by any other authors. Consequently, much further work is needed to accumulate many reliable data on ϕ^e particularly for those less-common species with x–z attached.

(10) To the best of the present author's knowledge, any other authors have not yet published the most probable values (or recommended data) of both ϕ^+ and ϕ^-, and hence of the thermionic contrasts ($\Delta\phi^*$ and $\Delta\phi^{**}$) for any surface species (see Section 4).

(11) Our values of ϕ^e with double underlines in the 3rd column (93 kinds of surface species, only 15% of the total 609 ones including those with x–z attached) in Table 2 may probably be acceptable at present as the most reliable values of ϕ^e with a possible

uncertainty of less than ± 0.05 eV for each of the surface species. In addition, our data with a single underline (73 species, 12% of the total ones) may be usable as considerably reliable values of ϕ^e with a possible uncertainty of less than ± 0.1 eV.

(12) Citation of these data on ϕ^e having no underline (443 species, 73% of the total ones) may be accompanied with a possible uncertainty of up to ~0.1 eV or much more. Namely, more than half of the total 606 surface species surveyed comprehensively from 4461 literatures cannot yield us any convincing estimates of ϕ^e within possible uncertainty of less than ± 0.1 eV, in contrast to the above 166 species of underlined data mentioned in Point (11). This is mainly because the work function data available for the species without any underline attached are very small in number less than 6 or partly because the data themselves are scattered in value in a wide range of up to 1 eV or more. Typically, the five data on α-Sc(0001) largely range from 2.1 to 4.81 eV (see Table 1).

(13) Disappointingly, no data are found for quite many surface species such as $C_{60}(100)$, Al(112), P(100), α-Ca(112), Zn(1011), As(100), Sc(0001), α-Y(1011), α-Zr(1011), Pd(112), Ag(112), Cd(1011), In(112), Sb(110), Te(0001), α-La(1010), α-Pr(1010), α-Nd(1010), α-Gd(1011), α-Tb(1011), α-Dy(1011), α-Ho(1011), α-Tm(1011), α-Lu(1011), α-Hf(1011), α-Tl(1011), Pb(112) and Bi(1010), although they may be interested in some of the workers active in various fields of physics and chemistry. As may be seen in Column 3 of Table 2, the work function data on high-Miller index surfaces are reported for several species alone (e.g., Cu, W and Pt). Such data are generally expected for many other metals and metalloids, too.

(14) The actual situation exemplified in Points (7)–(9) and (13) indubitably indicates that accumulation of work function data for great many surface species is quite poor still to date and hence that much further survey or study is needed to establish more reliable estimates of ϕ^e (within the uncertainty of ± 0.1 eV) for quite many surface species mentioned partly in Points (3)–(5) in addition to those listed typically in Points (7), (8) and (13).

With respect to the "Electron Work Function of the Elements" in CRC handbooks (78th−98th Editions published in 1997−2017), it seems to the present author that Pt(110) should be read Pt(100) because any of the references (1)–(3) [13,1045,1312] has no datum on Pt(110), whilst 5.84 eV cited from Ref. [1312] in the handbooks originates from Ref. [428], accurately corresponding not to Pt(110) but to Pt(100) studied by FE (see also Footnote # in Table 2 in Ref. [1351]). Consequently, it may be reasonable to suggest that "5.84 eV" cited by Logovoi et al. [2543] as ϕ^e for "Pt(110)" from the CRC Handbook (78th Ed.) [4318], for example, should be replaced with "5.54 $\pm$ 0.07 eV" recommended for Pt(110) by us (see Table 2). If so replaced, then, the theoretical value of 5.52 eV [2543] as well as 5.54 eV [1931] calculated for Pt(110) (see Table II in Ref. [2543]) agrees exactly with ours cited just above without having the "unreasonable discrepancy of 0.32 eV" against the "literature value of 5.84 eV for Pt(110)".

4. Peculiarity of polycrystalline work function

In contrast to monocrystals, polycrystals have generally the different work functions of ϕ^+ and ϕ^e, as already shown in Tables 1 and 2. This peculiarity brings about the "thermionic contrast" of $\Delta\phi^* \equiv \phi^+ - \phi^e > 0$ and, hence, it poses very interesting problems and new information about work function. After analyzing the data on $\Delta\phi^*$, an exhaustive discussion is devoted to the peculiarity of polycrystals ($\delta_m < 0.5$) and also to the anomaly of submonocrystals ($0.5 < \delta_m < 1$) in this section, where δ_m is focused as the *key* factor governing both ϕ^+ and ϕ^e as well as $\Delta\phi^*$.

4.1. Polycrystalline thermionic contrast ($\Delta\phi^*$) between ϕ^+ and ϕ^e

Positive surface ionization (PSI), often called thermal positive ion emission, has long been utilized by great many workers in a variety of fields of both science and technology in order to (1) generate positive ion beams of various species of atoms (M) having relatively low ionization energy ($I < 6$ eV), (2) detect neutral beams (or vapor) of atoms (M) or molecules (MX), (3) analyze a microsize of materials including M or MX, (4) investigate both surface reactions and phenomena related with work function, its change and so on [2,5,15–22]. For these purposes, almost all the workers have employed polycrystals and, hence, they are inevitably required to employ reliable values of ϕ^+ instead of ϕ^e for either analyzing or predicting correctly the positive ion emission data to be obtained in a given experiment under a specified experimental condition. In other words, the accuracy of the analyzed result to be achieved is generally affected by that of the value of ϕ^+ or $\phi^e + \Delta\phi^*$, strongly dependent upon the size of $\Delta\phi^*$.

Nevertheless, the thermionic contrast ($\Delta\phi^* \equiv \phi^+ - \phi^e$) has long been overlooked or disregarded often by many groups of workers in spite of the fact that $\Delta\phi^* = 0$ holds for a clean and smooth monocrystalline surface alone, as already mentioned in Section 1 and also explained in Section 4.4 in Ref. [1351]. In addition, these data on ϕ^+ and $\Delta\phi^*$ are hardly found in many handbooks available today. The latter may be largely responsible for such a present status that the emission predominance peculiar to polycrystalline surfaces ($\phi^+ > \phi^a > \phi^e = \phi^- = \phi$) has not yet fully been recognized to date. Without considering or examining the surface homogeneity in work function of the various specimens (usually polycrystals) under study, ϕ^e instead of ϕ^+ is employed to analyze these data on the positive ion emission from the specimens under study by many groups of workers [3–9,14,16,17,20,98,99,120,132,137,160,228,232,323,416,490–494,522,611,804,823,924,932–934,946, 954,961,965,966,979,1003,1004,1252,1320–1350,3823–3829,3832,3834–3839,3849–3854,3869–3871,3884,3907]. Without being recognized or perceived by each of the corresponding workers themselves, of course, some of the above specimens may have possibly been changed already from polycrystals into nearly monocrystals owing to previous or preliminary aging for a very long time at high temperatures. When the specimen under study is almost monocrystallized ($\delta_m \approx 1$) by high temperature aging prior to work function measurements, of course, ϕ^e may generally be employable as the equivalence to ϕ^+ with safety.

Needless to say, even refractory metals are subject to recrystallization according to heating at high temperatures (usually above ~2000 K) for very long hours, thereby generally leading to such a change as follows:

Polycrystal ($\delta_m < 0.5$) → "Submonocrystal" ($0.5 < \delta_m < 1$) → Monocrystal ($\delta_m = 1$).

According to the above change in surface structure, work function also changes considerably in general. The peculiarity of polycrystal and the anomaly of submonocrystal will be outlined later in Sections 4.3–4.5.

In a typical case of W [3834], ϕ^+ and ϕ^e are determined to be 4.65 and 4.56 eV by PSI of Ba and by TE, respectively (see Table 1), thereby yielding that $\Delta\phi^* = 4.65 - 4.56 = 0.09$ eV is much smaller than the most probable value of $\Delta\phi^* = 0.61 \pm 0.06$ eV usually expected for polycrystalline tungsten specimens with $\delta_m < 0.5$ (see Tables 4 and 5 to be shown later). This discrepancy (0.09 vs. 0.61 eV) may be reasonably explained by considering that the specimen [3834] having subjected up to ~2900 K prior to measurements consists probably almost ($\delta_m > 0.9$) of the W(100) face developed after thermal recrystallization without being sufficiently recognized by the worker [3834], like as the specimen of W(F) with $\delta_m = 0.95$–(100) oriented [3414] having (43) $\Delta\phi^* = 4.70 \pm 0.04 - 4.61 \pm 0.04 = 0.09 \pm 0.05$ eV [2453] (to be shown later in Table 6). Both of the tungsten specimens [3414,3834] are the typical examples of submonocrystal ($0.5 < \delta_m < 1$ and $\Delta\phi^* > 0$ eV).

Table 4
Thermionic contrast ($\Delta\phi^* \equiv \phi^+ - \phi^e$) determined for the *same* specimen under substantially the same condition in each study.

Surface	δ_m (%)	Beam	Ion	ϕ^+ (eV)	ϕ^e (eV)	$\Delta\phi^*$ (eV)	Meths.	Refs.
				6. Highly Oriented Pyrolytic Graphite				
C(HOPG)	?	Cs	Cs$^+$	4.51 ± 0.15	4.58 ± 0.02	-0.07 ± 0.15	PSI, TE	[1049]
C(HOPG)	?	Cs	Cs$^+$	4.60 ± 0.11	4.58 ± 0.02	0.02 ± 0.11	PSI, TE	[112,524,1049]
C(HOPG)	?	Cs	Cs$^+$	4.62 ± 0.17	4.58 ± 0.02	0.04 ± 0.17	PSI, TE	[1049]
C(HOPG)	?	Cs	Cs$^+$	4.69 ± 0.19	4.58 ± 0.02	0.11 ± 0.19	PSI, TE	[1049]
C(HOPG)	?	Cs	Cs$^+$	4.82 ± 0.14	4.58 ± 0.02	0.24 ± 0.14	PSI, TE	[1049]
Mean	–	–	–	–	–	**0.07 ± 0.10**	PSI, TE	–
M.P.V.	–	–	–	4.65 ± 0.12	4.66 ± 0.05	**−0.01 ± 0.13**	various	Table 2
				6. Graphitic Carbon Film				
C/Ir	?	Cs	Cs$^+$	4.2 ± 0.1	4.5 ± 0.1	-0.3 ± 0.14	PSI, TE	[1290]
C/Re(1010)	?	Na	Na$^+$	4.30 ± 0.05	4.30 ± 0.05	0.00 ± 0.07	PSI, TE	[4458]
C/Ir(111)	?	Ba	Ba$^+$	4.5	4.5	0.0	PSI, TE	[168]
C/Ir(111)	?	In	In$^+$	4.5	4.5	0.0	PSI, TE	[168]
C/Pt–W(8%)	?	K	K$^+$	4.50 ± 0.05	4.50 ± 0.02	0.00 ± 0.05	PSI, TE	[108]
C/Pt–W(8%)	?	K	K$^+$	4.55 ± 0.07	4.63 ± 0.06	-0.08 ± 0.09	PSI, TE	[108]
C/Pt–W(8%)	?	Na	Na$^+$	4.58 ± 0.03	4.54 ± 0.06	0.04 ± 0.07	PSI, TE	[676]
C/Ir	?	K	K$^+$	4.6 ± 0.1	4.4	0.2 ± 0.1	PSI, TE	[107]
C/Ir(111)	?	Cs	Cs$^+$	4.8	4.8	0.0	PSI, TE	[103]
C/Ir(111)	?	In	In$^+$	4.8	4.8	0.0	PSI, TE	[103]
Mean	–	–	–	–	–	**−0.02 ± 0.12**	PSI, TE	–
M.P.V.	–	–	–	4.50 ± 0.04	4.47 ± 0.05	**0.03 ± 0.06**	various	Table 2
				13. Polycrystalline Aluminium				
Al/Si(111)	?	Cs, Li	Cs$^+$	4.8[a]	4.23 ± 0.06[b]	$0.6 \pm >0.06$	CPD, various	[1342]
Al	?	Cs	Cs$^+$	4.96[a]	4.23 ± 0.06[b]	$0.73 \pm >0.06$	CPD, various	[611]
Mean	–	–	–	–	–	**0.66 ± >0.06**	CPD, various	–
M.P.V.	–	–	–	4.9 ± 0.1	4.26 ± 0.03	**0.6 ± 0.1**	various	Table 2
				14. Monocrystalline Silicon				
Si(100)[n]	~100	K	K$^+$	4.54 ± 0.2	4.53 ± 0.1	0.01 ± 0.2	PSI, TE	[74]
Si(100)[n]	~100	Li	Li$^+$	4.60 ± 0.03	4.53 ± 0.1	0.07 ± 0.1	PSI, TE	[74]
Si(100)[n]	~100	Na	Na$^+$	4.70 ± 0.02	4.53 ± 0.1	0.17 ± 0.1	PSI, TE	[74]
Si(100)[n]	~100	Li	Li$^+$	4.74 ± 0.05	4.53 ± 0.1	0.21 ± 0.1	PSI, TE	[74]
Si(100)[n]	~100	Tl	Tl$^+$	4.81 ± 0.03	4.53 ± 0.1	0.28 ± 0.1	PSI, TE	[74]
Si(100)[n]	~100	Tl	Tl$^+$	4.81 ± 0.07	4.53 ± 0.1	0.28 ± 0.1	PSI, TE	[74]
Si(100)[n]	~100	Na	Na$^+$	4.84 ± 0.03	4.53 ± 0.1	0.31 ± 0.1	PSI, TE	[74]
Si(100)[n]	~100	K	K$^+$	≥ 4.84	4.53 ± 0.1	$\geq 0.31 \pm 0.1$	PSI, TE	[74]
Mean	–	–	–	–	–	**0.20 ± 0.10**[g]	PSI, TE	–
M.P.V.	–	–	–	4.72 ± 0.10	4.82 ± 0.10	**−0.10 ± 0.14**	various	Table 2
Si(110)[p]	~100	Na	Na$^+$	3.32	3.40	-0.08	PSI, TE	[1472]
Si(110)[p]	~100	K	K$^+$	3.32	3.40	-0.08	PSI, TE	[1472]
Si(110)[p]	~100	Na	Na$^+$	4.31	4.31	0.00	PSI, TE	[1472]
Si(110)[p]	~100	K	K$^+$	4.31	4.31	0.00	PSI, TE	[1472]
Si(110)[p]	~100	Na	Na$^+$	4.38 ± 0.01	4.69 ± 0.01	-0.31 ± 0.01	PSI, TE	[1472]

Table 4 (*continued*)

Surface	δ_m (%)	Beam	Ion	ϕ^+ (eV)	ϕ^e (eV)	$\Delta\phi^*$ (eV)	Meths.	Refs.
Si(110)[p]	~100	K	K$^+$	4.38 ± 0.01	4.69 ± 0.01	−0.31 ± 0.01	PSI, TE	[1472]
Mean	–	–	–	–	–	**−0.13 ± 0.13**	PSI, TE	–
Mean (revised)[c]	–	–	–	–	–	**−0.04 ± 0.04**	PSI, TE	–
M.P.V.	–	–	–	4.36 ± 0.03	4.44 ± 0.24	**−0.08 ± 0.24**	various	Table 2
Si(111)[n]	~100	K	K$^+$	4.44 ± 0.1	4.55 ± 0.1	−0.11 ± 0.14	PSI, TE	[74]
Si(111)[n]	~100	Na	Na$^+$	4.63 ± 0.05	4.59 ± 0.05	0.04 ± 0.07	PSI, TE	[75]
Si(111)[n]	~100	K	K$^+$	4.69 ± 0.1	4.55 ± 0.1	0.14 ± 0.14	PSI, TE	[74]
Si(111)[n]	~100	Li	Li$^+$	4.75 ± 0.03	4.55 ± 0.1	0.20 ± 0.10	PSI, TE	[74]
Si(111)[p]	~100	Na	Na$^+$	4.76 ± 0.05	4.58 ± 0.05	0.18 ± 0.07	PSI, TE	[75]
Si(111)[n]	~100	Na	Na$^+$	4.78 ± 0.05	4.59 ± 0.05	0.19 ± 0.07	PSI, TE	[75]
Si(111)[n]	~100	Tl	Tl$^+$	4.79 ± 0.03	4.55 ± 0.1	0.24 ± 0.10	PSI, TE	[74]
Si(111)[p]	~100	K	K$^+$	4.80	4.1 ± 0.1	0.7 ± >0.1	PSI, TE	[272]
Si(111)[n]	~100	Na	Na$^+$	4.80 ± 0.04	4.55 ± 0.1	0.25 ± 0.11	PSI, TE	[74]
Si(111)[n]	~100	Na	Na$^+$	4.81 ± 0.02	4.55 ± 0.1	0.26 ± 0.10	PSI, TE	[74]
Si(111)	~100	Na	Na$^+$	4.81 ± 0.05	4.55 ± 0.05	0.26 ± 0.07	PSI, TE	[75]
Si(111)[n]	~100	Li	Li$^+$	4.84 ± 0.03	4.55 ± 0.1	0.29 ± 0.10	PSI, TE	[74]
Si(111)[p]	~100	Cs	Cs$^+$	4.85 ± 0.08	4.07 ± 0.05	0.78 ± 0.09	PSI, TE	[73]
Si(111)[p]	~100	Cs	Cs$^+$	4.85 ± 0.08	4.83 ± 0.04[d]	0.02 ± 0.09	PSI, TE	[73]
Si(111)[p]	~100	Cs	Cs$^+$	4.85 ± 0.08	4.86 ± 0.11	−0.01 ± 0.14	PSI, CPD	[73]
Si(111)[n]	~100	Li	Li$^+$	4.86 ± 0.07	4.04 ± 0.05	0.82 ± 0.09	PSI, TE	[72]
Si(111)[n]	~100	Li	Li$^+$	4.86 ± 0.07	4.80 ± 0.04[d]	0.06 ± 0.08	PSI, TE	[72]
Si(111)[n]	~100	Na	Na$^+$	4.87 ± 0.03	4.04 ± 0.05	0.83 ± 0.06	PSI, TE	[72]
Si(111)[n]	~100	Na	Na$^+$	4.87 ± 0.03	4.80 ± 0.04[d]	0.07 ± 0.05	PSI, TE	[72]
Si(111)[p]	~100	Cs	Cs$^+$	4.88 ± 0.10	4.07 ± 0.05	0.81 ± 0.11	PSI, TE	[73]
Si(111)[p]	~100	Cs	Cs$^+$	4.88 ± 0.10	4.83 ± 0.04[d]	0.05 ± 0.11	PSI, TE	[73]
Si(111)[p]	~100	Cs	Cs$^+$	4.88 ± 0.10	4.84 ± 0.14	0.04 ± 0.17	PSI, CPD	[73]
Si(111)[n]	~100	In	In$^+$	4.90 ± 0.10	4.04 ± 0.05	0.86 ± 0.11	PSI, TE	[72]
Si(111)[n]	~100	In	In$^+$	4.90 ± 0.10	4.80 ± 0.04[d]	0.10 ± 0.11	PSI, TE	[72]
Si(111)[n]	~100	Tl	Tl$^+$	4.99 ± 0.05	4.55 ± 0.1	0.44 ± 0.11	PSI, TE	[74]
Si(111)	~100	Na	Na$^+$	5.00 ± 0.05	4.51	0.49 ± >0.05	PSI, TE	[75]
Si(111)[p]	~100	Na	Na$^+$	5.05	4.1 ± 0.1	0.95 ± >0.1	PSI, TE	[272]
Si(111)[p]	~100	Na	Na$^+$	5.06	4.1 ± 0.1	0.96 ± >0.1	PSI, TE	[272]
Si(111)	~100	Li	Li$^+$	5.23 ± 0.05	4.51 ± 0.05	0.72 ± 0.07	PSI, TE	[75]
Mean	–	–	–	–	–	**0.35 ± 0.33**	PSI, SIE, TE	–
Mean (revised)[e]	–	–	–	–	–	**0.05 ± 0.03**	PSI, CPD, Eq. (8)	–
M.P.V.	–	–	–	4.83 ± 0.07	4.86 ± 0.09	**−0.03 ± 0.11**	various	Table 2

14. Polycrystalline Silicon

Surface	δ_m (%)	Beam	Ion	ϕ^+ (eV)	ϕ^e (eV)	$\Delta\phi^*$ (eV)	Meths.	Refs.
Si	?	Cs	Cs$^+$	5.14[a]	4.6 ± 0.1[b]	0.5 ± >0.1	CPD, various	[611]

41. Monocrystalline Niobium

Surface	δ_m (%)	Beam	Ion	ϕ^+ (eV)	ϕ^e (eV)	$\Delta\phi^*$ (eV)	Meths.	Refs.
Nb(100)	~100	Cs	Cs$^+$	4.04	3.90	0.14	PSI, TE	[739]
M.P.V.	–	–	–	4.04	4.02 ± 0.05	**0.02 ± >0.05**	various	Table 2
Nb(110)	~100	Cs	Cs$^+$	4.64	4.80	−0.16	PSI, TE	[739]
Nb(110)	~100	Na	Na$^+$	4.84 ± 0.05	4.80	0.04 ± >0.05	PSI, TE	[726]
Mean	–	–	–	–	–	**−0.06 ± 0.10**	PSI, TE	–
M.P.V.	–	–	–	4.74 ± 0.10	4.77 ± 0.05	**−0.03 ± 0.11**	various	Table 2
Nb(111)	~100	Cs	Cs$^+$	3.78	3.88	−0.10	PSI, TE	[739]
Nb(111)	~100	Na	Na$^+$	3.90	3.88	0.02	PSI, TE	[726]
Mean	–	–	–	–	–	**−0.04 ± 0.06**	PSI, TE	–
M.P.V.	–	–	–	3.84 ± 0.06	3.95 ± 0.09	**−0.11 ± 0.11**	various	Table 2
Nb(112)	~100	Cs	Cs$^+$	4.44	4.45 ± 0.05	−0.01 ± >0.05	PSI, TE	[739]
M.P.V.	–	–	–	4.44	4.33 ± 0.10	**0.11 ± >0.1**	various	Table 2

41. Polycrystalline Niobium

Surface	δ_m (%)	Beam	Ion	ϕ^+ (eV)	ϕ^e (eV)	$\Delta\phi^*$ (eV)	Meths.	Refs.
Nb–(100)[f]	68	–	–	4.39 ± 0.08	4.02 ± 0.07	0.37 ± 0.11	TC	[803]
Nb	?	RbI	Rb$^+$	4.76 ± 0.03	4.02 ± 0.05	0.74 ± 0.06	PSI, TE	[23]
Nb	?	RbBr	Rb$^+$	4.87 ± 0.06	4.02 ± 0.05	0.85 ± 0.08	PSI, TE	[23]
Nb	?	RbCl	Rb$^+$	4.88 ± 0.06	4.02 ± 0.05	0.86 ± 0.08	PSI, TE	[23]
Mean	–	–	–	–	–	**0.70 ± 0.12**	TC, PSI, TE	–
M.P.V.	–	–	–	4.81 ± 0.05	4.11 ± 0.05	**0.70 ± 0.07**	various	Table 2

Table 4 (*continued*)

Surface	δ_m (%)	Beam	Ion	ϕ^+ (eV)	ϕ^e (eV)	$\Delta\phi^*$ (eV)	Meths.	Refs.
				42. Monocrystalline Molybdenum				
Mo(100)	~100	Na	Na$^+$	4.44 ± 0.03	4.40 ± 0.03	0.04 ± 0.04	PSI, TE	[727,3103]
Mo(100)	~100	Na	Na$^+$	4.45	4.45	0.00	PSI, TE	[278]
Mo(100)	~100	K	K$^+$	4.45	4.45	0.00	PSI, TE	[278]
Mean	–	–	–	–	–	**0.01 ± 0.01**	PSI, TE	–
M.P.V.	–	–	–	4.38 ± 0.08	4.38 ± 0.03	**0.00 ± 0.09**	various	Table 2
Mo(110)	~100	Na	Na$^+$	5.13 ± 0.03	5.10 ± 0.03	0.03 ± 0.04	PSI, TE	[727]
M.P.V.	–	–	–	5.1	4.98 ± 0.03	**0.1 ± >0.03**	various	Table 2
Mo(111)	~100	Li	Li$^+$	4.10 ± 0.03	4.10 ± 0.03	0.00 ± 0.04	PSI, TE	[786]
Mo(111)	~100	Na	Na$^+$	4.13 ± 0.03	4.10 ± 0.03	0.03 ± 0.04	PSI, TE	[727,3103]
Mean	–	–	–	–	–	**0.02 ± 0.04**	PSI, TE	–
M.P.V.	–	–	–	4.17 ± 0.09	4.29 ± 0.03	**−0.12 ± 0.09**	various	Table 2
Mo(112)	~100	Na	Na$^+$	4.63 ± 0.03	4.60 ± 0.03	0.03 ± 0.04	PSI, TE	[727,2210]
M.P.V.	–	–	–	4.6	4.51 ± 0.03	**0.1 ± >0.03**	various	Table 2
				42. Polycrystalline Molybdenum				
Mo(porous)	?	Cs	Cs$^+$	4.15	3.8	0.35	PSI, TE	[3762]
Mo	?	K	K$^+$	4.23 ± 0.10	4.41 ± 0.01	−0.18 ± 0.10	PSI, TE	[645]
Mo	?	–	Mo$^+$	4.3 ± 0.1	4.20 ± 0.02	0.1 ± 0.1	PSI, TE	[132]
Mo	?	–	Mo$^+$	4.5 ± 0.1	4.19 ± 0.02	0.3 ± 0.1	PSI, TE	[954]
Mo	?	–	Mo$^+$	4.50	4.17	0.33	PSI, TE	[131]
Mo	?	–	Mo$^+$	4.6 ± 0.1	4.37 ± 0.02	0.2 ± 0.1	PSI, TE	[132]
Mo	?	–	Mo$^+$	4.7 ± 0.1	4.19 ± 0.02	0.5 ± 0.1	PSI, TE	[954]
Mo	?	KBr	K$^+$	4.90 ± 0.06	4.39 ± 0.05	0.51 ± 0.08	PSI, TE	[23,39]
Mo	?	Bi	Bi$^+$	4.96 ± 0.01	4.41 ± 0.02	0.55 ± 0.02	PSI, TE	[78]
Mo	?	In	In$^+$	5.02 ± 0.05	4.33 ± 0.07	0.69 ± 0.09	PSI, TE	[76,77]
Mo	?	–	Mo$^+$	5.1 ± 0.1	4.20 ± 0.02	0.9 ± 0.1	PSI, TE	[132]
Mo	?	–	Mo$^+$	5.1 ± 0.4	4.33 ± 0.07	0.8 ± 0.41	PSI, TE	[77]
Mo	?	KCl	K$^+$	5.10 ± 0.07	4.39 ± 0.05	0.71 ± 0.09	PSI, TE	[23,39]
Mo	?	–	Mo$^+$	5.4 ± 0.1	4.37 ± 0.02	1.0 ± 0.1	PSI, TE	[132]
Mean	–	–	–	–	–	**0.48 ± 0.31**	PSI, TE	–
M.P.V.	–	–	–	5.03 ± 0.06	4.31 ± 0.02	**0.72 ± 0.06**	various	Table 2
				73. Monocrystalline Tantalum				
Ta(100)	~100	Na	Na$^+$	4.20 ± 0.04	4.17 ± 0.04	0.03 ± 0.06	PSI, TE	[797]
M.P.V.	–	–	–	4.2	4.15 ± 0.05	**0.05 ± >0.05**	various	Table 2
Ta(110)	~100	Li	Li$^+$	4.8	4.80 ± 0.03	0.0 ± >0.03	PSI, TE	[786]
Ta(110)	~100	Na	Na$^+$	4.84 ± 0.04	4.82 ± 0.04	0.02 ± 0.06	PSI, TE	[797]
Ta(110)	~100	Na	Na$^+$	4.85 ± 0.05	4.81	0.04 ± >0.05	PSI, TE	[726]
Ta(110)	~100	L^h	L$^+$	4.85 ± 0.06	4.85	0.00 ± >0.05	PSI, TE	[279]
Mean	–	–	–	–	–	**0.02 ± 0.01**	PSI, TE	–
M.P.V.	–	–	–	4.84 ± 0.02	4.82 ± 0.06	**0.02 ± 0.06**	various	Table 2
Ta(111)	~100	Na	Na$^+$	4.00 ± 0.04	4.02 ± 0.04	−0.02 ± 0.06	PSI, TE	[797]
Ta(111)	~100	Na	Na$^+$	4.00 ± 0.05	3.98 ± 0.05	0.02 ± 0.07	PSI, TE	[726]
Mean	–	–	–	–	–	**0.00 ± 0.02**	PSI, TE	–
M.P.V.	–	–	–	4.00 ± 0.05	4.01 ± 0.04	**−0.01 ± 0.06**	various	Table 2
Ta(112)	~100	K	K$^+$	4.8	4.8 ± 0.05	0.0 ± >0.05	PSI, TE	[79]
				73. Polycrystalline Tantalum				
Ta(porous)	?	Cs	Cs$^+$	4.2	4.1	0.1	PSI, TE	[3762]
Ta–(112)^i	82	–	–	4.49 ± 0.04	4.34 ± 0.03	0.15 ± 0.05	TC	[803]
Ta	?	Na	Na$^+$	4.64 ± 0.03	4.30 ± 0.02	0.34 ± 0.04	PSI, TE	[81]
Ta	?	In	In$^+$	4.88 ± 0.05	4.33 ± 0.03	0.55 ± 0.06	PSI, TE	[76,77]
Ta	?	–	Ta$^+$	5.0 ± 0.5	4.33 ± 0.03	0.7 ± 0.5	PSI, TE	[77]
Ta	?	KCl	K$^+$	5.10 ± 0.01	4.27 ± 0.04	0.83 ± 0.04	PSI, TE	[23,2422]

Table 4 (*continued*)

Surface	δ_m (%)	Beam	Ion	ϕ^+ (eV)	ϕ^e (eV)	$\Delta\phi^*$ (eV)	Meths.	Refs.
Ta	?	RbBr	Rb$^+$	5.13 ± 0.03	4.27 ± 0.04	0.86 ± 0.05	PSI, TE	[23,67]
Ta	?	RbCl	Rb$^+$	5.19 ± 0.03	4.27 ± 0.04	0.92 ± 0.05	PSI, TE	[23,67]
Mean	–	–	–	–	–	**0.56 ± 0.30**	TC, PSI, TE	–
M.P.V.	–	–	–	4.95 ± 0.20	4.20 ± 0.03	**0.75 ± 0.20**	various	Table 2

74. Monocrystalline Tungsten

Surface	δ_m (%)	Beam	Ion	ϕ^+ (eV)	ϕ^e (eV)	$\Delta\phi^*$ (eV)	Meths.	Refs.
W(100)	~100	K	K$^+$	4.54 ± 0.02	4.59 ± 0.03	−0.05 ± 0.04	PSI, TE	[82,261]
W(100)	~100	Ba	Ba$^+$	4.55 ± 0.03	4.52 ± 0.07	0.03 ± 0.08	PSI, TE	[92]
W(100)	~100	Sm	Sm$^+$	4.6	4.6	0.0	PSI, TE	[271]
W(100)	~100	Ba	Ba$^+$	4.6 ± 0.1	4.6 ± 0.1	0.0 ± 0.1	PSI, TE	[15,649]
W(100)	~100	K	K$^+$	4.6 ± 0.1	4.6 ± 0.1	0.0 ± 0.1	PSI, TE	[1659]
W(100)	~100	In	In$^+$	4.60	4.55	0.05	PSI, TE	[83]
W(100)	96	–	–	4.60 ± 0.04	4.59 ± 0.04	0.01 ± 0.06	TC	[630]
W(100)	~100	Cs	Cs$^+$	4.61 ± 0.07	4.65 ± 0.02	−0.04 ± 0.07	PSI, TE	[266]
W(100)	~100	Bi	Bi$^+$	4.62 ± 0.06	4.59 ± 0.05	0.03 ± 0.08	PSI, TE	[84]
W(100)	~100	Na	Na$^+$	4.66 ± 0.03	4.60 ± 0.03	0.06 ± 0.04	PSI, TE	[3103]
W(100)	~100	Cs	Cs$^+$	4.66 ± 0.11	4.60 ± 0.06	0.06 ± 0.13	PSI, TE	[280]
W(100)	95	–	–	4.69 ± 0.05	4.57 ± 0.00	0.12 ± 0.05	TC	[803]
W(100)	95	–	–	4.70 ± 0.04	4.61 ± 0.04	0.09 ± 0.06	TC	[2453]
Mean	–	–	–	–	–	**0.03 ± 0.05**	TC, PSI, TE	–
M.P.V.	–	–	–	4.62 ± 0.05	4.65 ± 0.02	**−0.03 ± 0.05**	various	Table 2
W(110)	~100	Ba	Ba$^+$	4.82 ± 0.06	5.04	−0.22 ± >0.06	PSI, TE	[87]
W(110)	~100	Cs	Cs$^+$	5.11	5.33 ± 0.04	−0.22 ± >0.04	PSI, TE	[2314]
W(110)	~100	Na	Na$^+$	5.14	5.04 ± 0.06	0.10 ± >0.06	PSI, TE	[87]
W(110)	~100	Na	Na$^+$	5.14	4.8 ± 0.1	0.34 ± >0.1	PSI, TE	[85]
W(110)	~100	Na	Na$^+$	5.14 ± 0.03	5.30 ± 0.03	−0.16 ± 0.04	PSI, TE	[3103]
W(110)	~100	Na	Na$^+$	5.2	5.2	0.0	PSI, TE	[2773]
W(110)	~100	Na	Na$^+$	5.25	5.27	−0.02	PSI, TE	[86,90]
W(110)	80	–	–	5.25 ± 0.02	4.90 ± 0.05	0.35 ± 0.05	TC	[630]
W(110)	>90	Na	Na$^+$	5.25 ± 0.05	5.25 ± 0.05	0.00 ± 0.07	PSI, TE	[86,90]
W(110)	~100	Li	Li$^+$	5.28 ± 0.03	5.30 ± 0.03	−0.02 ± 0.04	PSI, TE	[88]
W(110)	~100	Li	Li$^+$	5.30 ± 0.03	5.30 ± 0.03	0.00 ± 0.04	PSI, TE	[814]
Mean	–	–	–	–	–	**0.01 ± 0.11**	TC, PSI, TE	–
M.P.V.	–	–	–	5.28 ± 0.11	5.32 ± 0.02	**−0.04 ± 0.11**	various	Table 2
W(111)	~100	Na	Na$^+$	4.42 ± 0.03	4.40 ± 0.03	0.02 ± 0.04	PSI, TE	[3103]
W(111)	~100	Na	Na$^+$	4.44 ± 0.03	4.40 ± 0.03	0.04 ± 0.04	PSI, TE	[817]
W(111)	~100	Li	Li$^+$	4.44 ± 0.03	4.40 ± 0.03	0.04 ± 0.04	PSI, TE	[3103]
W(111)	~100	Li	Li$^+$	4.50 ± 0.03	4.40 ± 0.02	0.10 ± 0.04	PSI, TE	[88]
Mean	–	–	–	–	–	**0.05 ± 0.03**	PSI, TE	–
M.P.V.	–	–	–	4.45 ± 0.04	4.45 ± 0.03	**0.00 ± 0.05**	various	Table 2
W(112)	~100	Gd	Gd$^+$	4.70 ± 0.02	4.85 ± 0.07	−0.15 ± 0.07	PSI, TE	[91]
W(112)	~100	Er	Er$^+$	4.70 ± 0.02	4.85 ± 0.07	−0.15 ± 0.07	PSI, TE	[91]
W(112)	~100	Er	Er$^+$	4.72 ± 0.06	4.85 ± 0.07	−0.13 ± 0.09	PSI, TE	[91]
Mean	–	–	–	–	–	**−0.15 ± 0.07**	PSI, TE	–
M.P.V.	–	–	–	4.70 ± 0.01	4.78 ± 0.03	**−0.08 ± 0.03**	various	Table 2

74. Polycrystalline Tungsten

Surface	δ_m (%)	Beam	Ion	ϕ^+ (eV)	ϕ^e (eV)	$\Delta\phi^*$ (eV)	Meths.	Refs.
W	?	–	W$^+$	4.8 ± 0.6	4.58 ± 0.03	0.2 ± 0.6	PSI, TE	[77]
W	?	Na	Na$^+$	4.95 ± 0.05	4.61	0.34 ± >0.05	PSI, TE	[85]
W–(310)^f	46.3	–	–	4.96 ± 0.03	4.34 ± 0.05	0.62 ± 0.06	TC	[630]
W–(100)	46	–	–	4.99 ± 0.05	4.56 ± 0.01	0.43 ± 0.05	TC	[803]
W–(310)	46.3	–	–	4.99 ± 0.06	4.38 ± 0.05	0.61 ± 0.08	TC	[2453]
W–(100)	46	–	–	5.00 ± 0.05	4.56 ± 0.01	0.44 ± 0.05	TC	[2453]
W	?	In	In$^+$	5.05 ± 0.05	4.58 ± 0.05	0.47 ± 0.07	PSI, TE	[94]
W	?	KCl	K$^+$	5.09 ± 0.02	4.42 ± 0.02	0.67 ± 0.03	PSI, TE	[36]
W	?	KCl	K$^+$	5.09 ± 0.06	4.48 ± 0.06	0.61 ± 0.08	PSI, TE	[23]
W–(110)	<35	–	–	5.09 ± 0.10	4.52 ± 0.12	0.57 ± 0.16	TC	[283]
W	?	In	In$^+$	5.10	4.58 ± 0.05	0.52 ± >0.05	PSI, TE	[94]
W–(110)	25	–	–	5.12	4.46	0.66	TC	[3844]
W	?	KF	K$^+$	5.12 ± 0.02	4.48 ± 0.06	0.64 ± 0.06	PSI, TE	[23]
W–(112)	33.6	–	–	5.13 ± 0.04	4.62 ± 0.02	0.51 ± 0.04	TC	[630]
W	?	In	In$^+$	5.14 ± 0.03	4.58 ± 0.03	0.56 ± 0.04	PSI, TE	[76,77]
W	?	Bi	Bi$^+$	5.14 ± 0.05	4.60 ± 0.04	0.54 ± 0.06	PSI, TE	[84,93]

(*continued on next page*)

Table 4 (*continued*)

Surface	δ_m (%)	Beam	Ion	ϕ^+ (eV)	ϕ^e (eV)	$\Delta\phi^*$ (eV)	Meths.	Refs.
W–(110)	35.2	–	–	5.15 ± 0.03	4.63 ± 0.01	0.52 ± 0.03	TC	[281]
W	?	LiI	Li$^+$	5.16 ± 0.05	4.61 ± 0.03	0.55 ± 0.06	PSI, TE	[281]
W	?	LiCl	Li$^+$	5.18 ± 0.03	4.57 ± 0.04	0.61 ± 0.05	PSI, TE	[281]
W–(110)	35	–	–	5.18 ± 0.03	4.61 ± 0.03	0.57 ± 0.04	PSI, TE	[630]
W	?	LiCl	Li$^+$	5.19 ± 0.03	4.48 ± 0.06	0.71 ± 0.07	PSI, TE	[23]
W	?	LiF	Li$^+$	5.19 ± 0.05	4.60 ± 0.05	0.59 ± 0.07	PSI, TE	[281]
W	?	NaBr	Na$^+$	5.20 ± 0.02	4.48 ± 0.06	0.72 ± 0.06	PSI, TE	[23]
W	?	LiCl	Li$^+$	5.20 ± 0.02	4.47 ± 0.04	0.73 ± 0.04	PSI, TE	[37]
W	?	LiBr	Li$^+$	5.20 ± 0.04	4.60 ± 0.05	0.60 ± 0.06	PSI, TE	[281]
W	?	NaCl	Na$^+$	5.21 ± 0.02	4.48 ± 0.06	0.73 ± 0.06	PSI, TE	[23]
W	?	RbCl	Rb$^+$	5.21 ± 0.06	4.48 ± 0.06	0.73 ± 0.08	PSI, TE	[23]
W	?	NaCl	Na$^+$	5.22 ± 0.02	4.47 ± 0.04	0.75 ± 0.04	PSI, TE	[37]
W	?	LiF	Li$^+$	5.22 ± 0.07	4.48 ± 0.06	0.74 ± 0.09	PSI, TE	[23]
W	?	NaCl	Na$^+$	5.23 ± 0.01	4.42 ± 0.02	0.81 ± 0.02	PSI, TE	[36]
W	?	NaI	Na$^+$	5.23 ± 0.02	4.48 ± 0.06	0.75 ± 0.06	PSI, TE	[23]
W	?	LiBr	Li$^+$	5.23 ± 0.02	4.48 ± 0.06	0.75 ± 0.06	PSI, TE	[23,37]
W–(110)	80	–	–	5.25 ± 0.02	4.90 ± 0.05	0.35 ± 0.05	TC	[630]
W–(110)	80	–	–	5.26 ± 0.02	4.87 ± 0.05	0.39 ± 0.06	TC	[2453]
W	?	LiI	Li$^+$	5.26 ± 0.02	4.48 ± 0.06	0.78 ± 0.06	PSI, TE	[23]
W	?	LiI	Li$^+$	5.27 ± 0.01	4.47 ± 0.04	0.80 ± 0.04	PSI, TE	[37]
Mean	–	–	–	–	–	**0.60 ± 0.13**	TC, PSI, TE	–
M.P.V.	–	–	–	5.17 ± 0.05	4.56 ± 0.03	**0.61 ± 0.06**	various	Table 2

75. Monocrystalline Rhenium

Surface	δ_m (%)	Beam	Ion	ϕ^+ (eV)	ϕ^e (eV)	$\Delta\phi^*$ (eV)	Meths.	Refs.
Re(0001)	~100	La	La$^+$	5.15 ± 0.21	5.15 ± 0.10	0.00 ± 0.23	PSI, TE	[96]
Re(0001)	~100	Ce	Ce$^+$	5.15 ± 0.21	5.15 ± 0.10	0.00 ± 0.23	PSI, TE	[96]
Re(0001)	~100	Er	Er$^+$	5.15 ± 0.21	5.15 ± 0.10	0.00 ± 0.23	PSI, TE	[96]
Re(0001)	~100	Gd	Gd$^+$	5.15 ± 0.34	5.15 ± 0.10	0.00 ± 0.35	PSI, TE	[96]
Re(0001)	~100	Tm	Tm$^+$	5.15 ± 0.34	5.15 ± 0.10	0.00 ± 0.35	PSI, TE	[96]
Mean	–	–	–	–	–	**0.00 ± 0.28**	PSI, TE	–
M.P.V.	–	–	–	5.15 ± <0.34	5.30 ± 0.21	**−0.15 ± <0.40**	various	Table 2

75. Polycrystalline Rhenium

Surface	δ_m (%)	Beam	Ion	ϕ^+ (eV)	ϕ^e (eV)	$\Delta\phi^*$ (eV)	Meths.	Refs.
Re	?	NaI	Na$^+$	5.01	5.0 ± 0.1	0.0 ± >0.1	PSI, TE	[99]
Re	?	Na	Na$^+$	5.06	5.0 ± 0.1	0.1 ± >0.1	PSI, TE	[99]
Re	?	NaCl	Na$^+$	5.06	5.0 ± 0.1	0.1 ± >0.1	PSI, TE	[99]
Re	?	NaBr	Na$^+$	5.11	5.0 ± 0.1	0.1 ± >0.1	PSI, TE	[99]
Re	?	Na	Na$^+$	5.14	4.93 ± 0.04	0.21 ± >0.04	PSI, TE	[53]
Re	?	NaCl	Na$^+$	5.14	4.93 ± 0.04	0.21 ± >0.04	PSI, TE	[53]
Re	?	Li	Li$^+$	5.21 ± 0.01	4.98 ± 0.03	0.23 ± 0.03	PSI, TE	[54]
Re	?	In	In$^+$	5.31 ± 0.03	4.93 ± 0.04	0.38 ± 0.05	PSI, TE	[97]
Re	?	Li	Li$^+$	5.34	4.93 ± 0.04	0.41 ± >0.04	PSI, TE	[53]
Re	?	LiCl	Li$^+$	5.34	4.93 ± 0.04	0.41 ± >0.04	PSI, TE	[53]
Re	?	Bi	Bi$^+$	5.35 ± 0.05	4.85 ± 0.05	0.50 ± 0.07	PSI, TE	[100]
Re	?	In	In$^+$	5.38 ± 0.03	4.93 ± 0.04	0.45 ± 0.05	PSI, TE	[97]
Re	?	Ca	Ca$^+$	5.38 ± 0.03	4.93 ± 0.04	0.45 ± 0.05	PSI, TE	[97]
Re	?	In	In$^+$	5.39 ± 0.05	4.99 ± 0.05	0.40 ± 0.07	PSI, TE	[94]
Re	?	–	Re$^+$	5.4 ± 0.6	4.93 ± 0.04	0.5 ± 0.6	PSI, TE	[77]
Re	?	In	In$^+$	5.40	4.99 ± 0.05	0.41 ± >0.05	PSI, TE	[94]
Re	?	Mg	Mg$^+$	5.40 ± 0.05	4.93 ± 0.04	0.47 ± 0.06	PSI, TE	[97]
Re	?	NaI	Na$^+$	5.41 ± 0.05	4.95 ± 0.05	0.46 ± 0.07	PSI, TE	[23]
Re	?	NaCl	Na$^+$	5.42	4.93	0.49	PSI, TE	[23]
Re	?	NaCl	Na$^+$	5.42	4.97	0.45	PSI, TE	[23]
Re	?	NaCl	Na$^+$	5.42 ± 0.02	4.95 ± 0.05	0.47 ± 0.05	PSI, TE	[23]
Re	?	NaI	Na$^+$	5.43 ± 0.01	4.93 ± 0.02	0.50 ± 0.02	PSI, TE	[23]
Re	?	NaI	Na$^+$	5.43 ± 0.01	4.95 ± 0.01	0.48 ± 0.01	PSI, TE	[23]
Re	?	Ag	Ag$^+$	5.43 ± 0.02	4.93 ± 0.04	0.50 ± 0.04	PSI, TE	[97]
Re	?	Ca	Ca$^+$	5.43 ± 0.02	4.93 ± 0.04	0.50 ± 0.04	PSI, TE	[76,77]
Re	?	NaCl	Na$^+$	5.43 ± 0.04	4.96 ± 0.05	0.47 ± 0.06	PSI, TE	[23]
Re	?	Ca	Ca$^+$	5.44 ± 0.03	4.93 ± 0.04	0.51 ± 0.05	PSI, TE	[97]
Re	?	NaI	Na$^+$	5.45	4.97	0.48	PSI, TE	[23]
Re	?	NaI	Na$^+$	5.45	4.94	0.51	PSI, TE	[23]
Re	?	Ca	Ca$^+$	5.46 ± 0.02	4.93 ± 0.04	0.53 ± 0.04	PSI, TE	[97]
Re	?	LiBr	Li$^+$	5.48 ± 0.02	4.95 ± 0.05	0.53 ± 0.05	PSI, TE	[23]
Re	?	LiI	Li$^+$	5.49 ± 0.02	4.95 ± 0.05	0.54 ± 0.05	PSI, TE	[23,38]
Re	?	LiCl	Li$^+$	5.53 ± 0.02	4.95 ± 0.05	0.58 ± 0.05	PSI, TE	[23]
Re	?	LiI	Li$^+$	5.53 ± 0.02	5.00 ± 0.01	0.53 ± 0.02	PSI, TE	[101]

Table 4 (*continued*)

Surface	δ_m (%)	Beam	Ion	ϕ^+ (eV)	ϕ^e (eV)	$\Delta\phi^*$ (eV)	Meths.	Refs.
Re	?	NaCl	Na$^+$	5.58	5.18	0.40	PSI, TE	[23]
Re	?	NaCl	Na$^+$	5.70	5.36	0.34	PSI, TE	[23]
Re	?	NaI	Na$^+$	5.76	5.37	0.39	PSI, TE	[23]
Re	?	NaI	Na$^+$	5.81	5.41	0.40	PSI, TE	[23]
Mean	–	–	–	–	–	**0.41 ± 0.14**	PSI, TE	–
M.P.V.	–	–	–	5.41 ± 0.04	4.96 ± 0.05	**0.45 ± 0.06**	various	Table 2

77. Monocrystalline Iridium

Surface	δ_m (%)	Beam	Ion	ϕ^+ (eV)	ϕ^e (eV)	$\Delta\phi^*$ (eV)	Meths.	Refs.
Ir(111)	~100	Bi	Bi$^+$	5.75 ± 0.05	5.75 ± 0.05	0.00 ± 0.07	PSI, TE	[105,409]
Ir(111)	~100	Yb	Yb$^+$	5.75 ± 0.10	5.75 ± 0.10	0.00 ± 0.14	PSI, TE	[104]
Ir(111)	~100	Bi	Bi$^+$	5.79 ± 0.03	5.74 ± 0.06	0.05 ± 0.07	PSI, TE	[102,410]
Ir(111)	~100	Tl	Tl$^+$	5.79 ± 0.03	5.74 ± 0.06	0.05 ± 0.07	PSI, TE	[102,410]
Ir(111)	~100	K	K$^+$	5.8	5.75 ± 0.05	0.05 ± >0.05	PSI, TE	[252,411]
Ir(111)	~100	Ba	Ba$^+$	5.8	5.80 ± 0.05	0.0 ± >0.05	PSI, TE	[649]
Ir(111)	~100	In	In$^+$	5.80 ± 0.03	5.80 ± 0.03	0.00 ± 0.04	PSI, TE	[103]
Mean	–	–	–	–	–	**0.02 ± 0.02**	PSI, TE	–
M.P.V.	–	–	–	5.76 ± 0.04	5.75 ± 0.06	**0.01 ± 0.07**	various	Table 2

77. Polycrystalline Iridium

Surface	δ_m (%)	Beam	Ion	ϕ^+ (eV)	ϕ^e (eV)	$\Delta\phi^*$ (eV)	Meths.	Refs.
Ir	?	NaBr	Na$^+$	5.72 ± 0.03	5.15 ± 0.03	0.57 ± 0.04	PSI, TE	[68]
Ir–(111)	81	–	–	5.73 ± 0.01	5.36 ± 0.07	0.37 ± 0.07	TC	[803]
Ir	?	NaCl	Na$^+$	5.73 ± 0.02	5.15 ± 0.03	0.58 ± 0.04	PSI, TE	[68]
Ir	?	Bi	Bi$^+$	5.80 ± 0.05	5.40 ± 0.05	0.40 ± 0.07	PSI, TE	[106,667]
Mean	–	–	–	–	–	**0.48 ± 0.10**	TC, PSI, TE	–
M.P.V.	–	–	–	5.75 ± 0.04	5.28 ± 0.04	**0.47 ± 0.06**	various	Table 2

78. Monocrystalline Platinum

Surface	δ_m (%)	Beam	Ion	ϕ^+ (eV)	ϕ^e (eV)	$\Delta\phi^*$ (eV)	Meths.	Refs.
Pt(111)	~100	Li	Li$^+$	5.75 ± 0.02	5.86 ± 0.06[b]	−0.11 ± 0.06	PSI, various	[167]
Pt(111)	~100	Li	Li$^+$	5.76 ± 0.02	5.86 ± 0.06[b]	−0.10 ± 0.06	PSI, various	[167]
Pt(111)	~100	Li	Li$^+$	5.77 ± 0.02	5.86 ± 0.06[b]	−0.09 ± 0.06	PSI, various	[167]
Pt(111)	~100	Li	Li$^+$	5.80 ± 0.02	5.86 ± 0.06[b]	−0.06 ± 0.06	PSI, various	[167]
Pt(111)	~100	Li	Li$^+$	5.91 ± 0.02	5.86 ± 0.06[b]	0.05 ± 0.06	PSI, various	[167]
Mean	–	–	–	–	–	**−0.06 ± 0.06**	PSI, various	–
M.P.V.	–	–	–	5.80 ± 0.06	5.84 ± 0.05	**−0.04 ± 0.08**	various	Table 2

78. Polycrystalline Platinum

Surface	δ_m (%)	Beam	Ion	ϕ^+ (eV)	ϕ^e (eV)	$\Delta\phi^*$ (eV)	Meths.	Refs.
Pt	?	Na	Na$^+$	5.44	5.27 ± 0.08[b]	0.17 ± >0.08	PSI, various	[3336]
Pt	?	Na	Na$^+$	5.49 ± 0.01	5.27 ± 0.08[b]	0.22 ± 0.08	PSI, various	[50]
Pt	?	Cs	Cs$^+$	5.5	5.45 ± 0.05	0.05 ± >0.05	PSI, TE	[98]
Pt	?	K	K$^+$	5.52 ± 0.05	5.41 ± 0.05	0.11 ± >0.07	PSI, TE	[282]
Pt	?	NaNO$_3$	Na$^+$	5.54 ± 0.07	5.27 ± 0.08[b]	0.27 ± 0.11	PSI, various	[178]
Pt	?	NaNO$_3$	Na$^+$	5.56	5.27 ± 0.08[b]	0.29 ± >0.08	PSI, various	[178]
Pt	?	Na	Na$^+$	5.6 ± 0.1	5.27 ± 0.08[b]	0.3 ± 0.13	PSI, various	[75]
Pt	?	NaBr	Na$^+$	5.66	5.27 ± 0.08[b]	0.39 ± >0.08	PSI, various	[58]
Pt	?	Bi	Bi$^+$	5.77 ± 0.05	5.13 ± 0.05	0.64 ± 0.07	PSI, TE	[106,667]
Mean	–	–	–	–	–	**0.27 ± 0.16**	PSI, various	–
M.P.V.	–	–	–	5.58 ± 0.11	5.30 ± 0.07	**0.28 ± 0.13**	various	Table 2

79. Polycrystalline Gold

Surface	δ_m (%)	Beam	Ion	ϕ^+ (eV)	ϕ^e (eV)	$\Delta\phi^*$ (eV)	Meths.	Refs.
Au/Si(111)	?	Cs, Li	Cs$^+$	5.7[a]	5.31 ± 0.07[b]	0.4 ± >0.07	CPD, various	[1342]
M.P.V.	–	–	–	5.7	5.30 ± 0.04	**0.4 ± >0.04**	various	Table 2

[a]Each of the values of ϕ^+ (e.g., 4.8 eV for Al and 5.7 eV for Au) is calculated by the present author using each of the data included in the corresponding reference.

[b]Each value (ϕ^e) is taken tentatively from the most probable value listed in Table 2 [1351] because each of the corresponding references [611,1342,1342,3336, etc.] has no data on ϕ^e for the specimen itself (Al, Si, Pt or Au) under study.

[c]The mean (revised) for Si(110)^p is obtained after disregarding the last two data [1472], which correspond to the composite surface covered partially with the reaction products between Na (or K) and Si (see Footnote 434 in Table 1).

[d]The values of ϕ^e = 4.83 and 4.80 eV for Si(111)^p [73] and Si(111)^n [72] are corrected from those of 4.07 and 4.04 eV, respectively, by using Eq. (8) (see Footnote 66 in Table 1). It should be noted that the former (4.83 ± 0.04 eV) is essentially equal to 4.86 ± 0.11 eV determined directly for the same specimen by CPD [73]. For further information about the data on Si(100)–Si(111) [72–75, etc.], see Footnotes 63–70 in Table 1.

[e]The mean (revised) for Si(111) is based on these data alone whose ϕ^e is determined by CPD or calculated from Eq. (8).

[f]The expression such as W–(310) denotes that the surface consists mainly (δ_m = 46.3%) of the (310) face of W [630]. For further information about the surface, see W(D) [489] in Table 6. On the other hand, Nb–(100) consists mainly (68%) of the (100) plane (see Table 2 in Ref. [803]).

[g]The authors [74] suggest that the discrepancy of $\phi^+ - \phi^e \neq 0$ eV would be accounted by surface contamination of Si(100)[n] (see Footnotes 63 and also 64 in Table 1).

[h]L represents lanthanides for measuring ϕ^+ of Ta(110) by PSI [279] (see Footnote 466 in Table 1).

[i]Ta–(112) designates that its surface consists mainly of the (112) face with $\delta_m = 82\%$ [803], similarly as in other cases of Nb and W (see Footnote f).

Table 5
Summary of the thermionic contrast ($\Delta\phi^*$) determined by the two methods of the "mean" originating from each common pair of ϕ^+ and ϕ^e measured for the same specimen under virtually the same condition and of the "most probable value" due to heterogeneous pairs measured separately for various specimens under different conditions by a variety of workers (see Table 4 and also the values in Table 1).

No.	Surface	$\Delta\phi^*$ (eV) (mono)			$\Delta\phi^*$ (eV) (poly)		
		Mean	M.P.V.	[1351]	Mean	M.P.V.	[1351]
6	C(HOPG)	0.07 ± 0.10	−0.01 ± 0.13	–	–	–	–
6	C(film)[a]	−0.02 ± 0.12	0.03 ± 0.06	–	–	–	–
13	Al(poly)	–	–	–	0.66 ± >0.06	0.6 ± 0.1	0.6
14	Si(100)	–[b]	−0.10 ± 0.14	0.02 ± 0.19	–	–	–
14	Si(110)	−0.04 ± 0.04	−0.08 ± 0.24	–	–	–	–
14	Si(111)	0.05 ± 0.03	−0.03 ± 0.11	0.03 ± 0.12	–	–	–
14	Si(poly)	–	–	–	0.5 ± >0.1	–	–
41	Nb(100)	0.14[c]	0.02 ± >0.05	–	–	–	–
41	Nb(110)	−0.06 ± 0.10	−0.03 ± 0.11	0.04 ± 0.05	–	–	–
41	Nb(111)	−0.04 ± 0.06	−0.11 ± 0.11	0.02 ± 0.05	–	–	–
41	Nb(112)	−0.01 ± >0.05	0.11 ± >0.1	–	–	–	–
41	Nb(poly)	–	–	–	0.70 ± 0.12	0.70 ± 0.07	0.78 ± 0.11
42	Mo(100)	0.01 ± 0.01	0.00 ± 0.09	−0.03 ± 0.08	–	–	–
42	Mo(110)	0.03 ± 0.04	0.1 ± >0.03	0.03 ± 0.30	–	–	–
42	Mo(111)	0.02 ± 0.04	−0.12 ± 0.09	−0.02 ± 0.15	–	–	–
42	Mo(112)	0.03 ± 0.04	0.1 ± >0.03	0.03 ± 0.30	–	–	–
42	Mo(poly)	–	–	–	0.48 ± 0.31	0.72 ± 0.06	0.66 ± 0.07
73	Ta(100)	0.03 ± 0.06	0.05 ± >0.05	0.03 ± 0.06	–	–	–
73	Ta(110)	0.02 ± 0.01	0.02 ± 0.06	0.04 ± 0.07	–	–	–
73	Ta(111)	0.00 ± 0.02	−0.01 ± 0.06	0.00 ± 0.06	–	–	–
73	Ta(poly)	–	–	–	0.56 ± 0.30	0.75 ± 0.20	0.71 ± 0.23
74	W(100)	0.03 ± 0.05	−0.03 ± 0.05	0.03 ± 0.06	–	–	–
74	W(110)	0.01 ± 0.11	−0.04 ± 0.11	−0.02 ± 0.09	–	–	–
74	W(111)	0.05 ± 0.03	0.00 ± 0.05	0.07 ± 0.06	–	–	–
74	W(112)	−0.15 ± 0.07	−0.08 ± 0.03	0.07 ± 0.32	–	–	–
74	W(poly)	–	–	–	0.60 ± 0.13	0.61 ± 0.06	0.59 ± 0.06
75	Re(0001)	0.00 ± 0.28	−0.15 ± <0.40	0.02 ± 0.19	–	–	–
75	Re(poly)	–	–	–	0.41 ± 0.14	0.45 ± 0.06	0.45 ± 0.05
77	Ir(111)	0.02 ± 0.02	0.01 ± 0.07	−0.01 ± 0.05	–	–	–
77	Ir(poly)	–	–	–	0.48 ± 0.10	0.47 ± 0.06	0.48 ± 0.04
78	Pt(111)	−0.06 ± 0.06	−0.04 ± 0.08	−0.06 ± 0.08	–	–	–
78	Pt(poly)	–	–	–	0.27 ± 0.16	0.28 ± 0.13	0.34 ± 0.14
79	Au(poly)	–	–	–	0.4 ± >0.07	0.4 ± >0.04	0.4
	Average[d]	**0.00 ± 0.06**	**−0.02 ± 0.07**	**0.02 ± 0.03**	–	–	–
	Range[e]	–	–	–	**~0.3–0.7**	**~0.3–0.7**	**~0.3–0.8**

[a]The value of $\Delta\phi^* = -0.02$ or $0.03 \approx 0.0$ eV for C(film) is substantially equal to that (0.07 or $-0.01 \approx 0.0$ eV) for C(HOPG), thereby showing that the graphitic film formed on a foreign substrate (typically, Mo, Re or Pt) has usually the same thermionic property with monocrystalline graphite. In other words, carbon is subject to forming a two-dimensional film with the graphitic monocrystalline structure under some conditions such as ~1700 K on Ir(111) ($\phi^+ = \phi^e = 4.5$ eV) [168] and ~1500 K on Pt–W(8%) ($\phi^+ = \phi^e = 4.50$ eV) [108]. For further information about the chemico-physical peculiarity of the graphitic film in contrast to a carbidic one, see Section 4.2.4 in Ref. [1351].

[b]The mean of $\Delta\phi^* = 0.20 \pm 0.10$ eV evaluated for Si(100) from the data in Ref. [74] alone is disregarded because of the reason outlined in Footnote g in Table 4.

[c]This value of 0.14 eV for Nb(100) may be disregarded in statistical examination of $\Delta\phi^*$ because it is based on a single datum alone.

[d]As may be seen in the last 2 line, the overall average for monocrystalline surfaces has $\Delta\phi^* = 0.00, -0.02$ or $0.02 \approx 0.0$ eV as a whole covering the 21, 23 or 18 surface species, just as predicted by theory.

[e]As shown in the last line, on the other hand, $\Delta\phi^*$ for any polycrystalline surfaces studied here is much larger than 0.0 eV for any species, ranging from ~0.3 to ~0.8 eV, just as expected from Eqs. (1) and (2).

In addition, we may cite such an example that a Mo-specimen [125,129,572] is assigned later to have the (100) plane arranged naturally by recrystallization of the Mo ribbon through thermal annealing for very long hours above ~2200 K [573], where $\phi^+ = 4.28 \pm 0.05$ [129,572,573] or 4.38 ± 0.01 eV [125] (see Footnote 167 in Table 1) is in good agreement with our best estimates of $\phi^+ = 4.38 \pm 0.08$ eV and also $\phi^e = 4.38 \pm 0.03$ eV for Mo(100) (see Table 2). Consequently, the annealed specimen may be assigned to be Mo(100) ($\delta_m = 1$ and $\Delta\phi^* = 0$ eV). A persuasive example may be added for a nanocrystalline Ni [4142]. Namely, ϕ^e is found to increase from 3.92 ± 0.05 eV to 4.40 ± 0.05 eV as the specific grain boundary length (per grain size of 1 μm^2) decreases from ~12 to 0.3 μm according to the recrystallization due to annealing from ~300 up to 773 K [4142]. About such a thermal instability in surface crystal structure mentioned just above, further information may be obtained from Section 4.5 in Ref. [1351].

As may be seen in the 6th column on many lines much below W(650) in Table 1, the data on $\phi^+ \approx 4.5$–4.7 eV $\approx \phi^e$ (=4.5–4.6 eV accepted today for W) are reported for many "polycrystalline" tungsten specimens, which have typically $\phi^+ = 4.49$ and $\phi^e = 4.59$ eV [823] (see Footnotes 170 and 296 in Table 1), 4.65 and 4.56 eV [3834] and 4.67 and 4.57 eV [3055]. They may possibly consist predominantly ($\delta_m > 0.9$) of W(100) without each worker's recognition if the data on both ϕ^+ and ϕ^e are free from systematic errors. In consequence, such data may possibly afford to many workers the incorrect apprehension or conclusion that $\Delta\phi^*$ of W is always negligibly small to be less than ~0.1 eV instead of ~0.6 ± 0.1 eV (see Table 5) to be expected usually.

If the various specimens mentioned above [[3–9], etc., ranging to [3907]] consist of mainly ($\delta_m > 0.9$) monocrystalline surfaces owing to thermal recrystallization, then, such analysis as taking ϕ^e instead of ϕ^+ may hardly yield unreasonable results from the data on positive ion emission from apparent polycrystals. If not or little so, on the other hand, any analytical results obtained by employment of ϕ^e may be affected by systematic errors according to the degree of inhomogeneity in work function and hence to the size of $\Delta\phi^*$ up to ~0.6 eV.

In a typical case [3863], the ionization efficiency (β^+) of Na emitted as Na^+ from a Pt surface heated to 1200 or 1500 K is theoretically calculated from Eq. (5) to be respectively 0.94 or 0.89 by taking $\phi^+ = 5.5$ eV [98], which is nearly the same with the most probable value of 5.6 ± 0.1 eV [1351, Here]. Employment of $\phi^e = 5.3$ eV [12,1351,1354, Here], on the other hand, would yield $\beta^+ = 0.70$ or 0.63, thereby decreasing by 26 or 29% in comparison with the former, according to $\Delta\phi^* = 0.2$ eV. In another case of Na^+ from W ($\Delta\phi^* = 0.61$ eV, see Table 5) at the same temperatures just above, on the other hand, employment of $\phi^e = 4.56$ eV (see the 3rd column for W(poly) in Table 2) would afford a very small value of $\beta^+ = 0.002$ or 0.006, whilst that of $\phi^+ = 5.17$ eV (see 4th column for W(poly) in Table 2) would yield such a much larger value as $\beta^+ = 0.40$ or 0.39, thus demonstrating that the neglect of $\Delta\phi^*$ is subject to committing a large systematic error to the analytical results of positive ion emission from polycrystals.

The importance of $\Delta\phi^*$ is concerned also with the Schottky equation [251]:

$$\phi + E^+ = E^0 + I, \tag{9}$$

where E^+ is the desorption energy of positive ion (M^+), E^0 is that of neutral atom (M), and I is the ionization energy of M (see Fig. 25 [256] in Ref. [1351]). Here, E^+ and E^0 are determinable from the data either on adsorption lifetimes (τ^+ and τ^0) according to Frenckel's equation [14,15,86,178,260], on desorption rate constants (k^+ and k^0) [98,282,397] or on the slope of an Arrhenius plot of $\ln i^+ T^n$ vs. $1/T$ [77]. Here, i^+ is the ion current of M^+, and n = 1/2 [77]. Generally, E^0 can be determined from a similar plot (n = 1) mentioned just above after converting M into M^+ by electron impact of M [77]. In the case of self-surface ionization (SSI, see Section 2.3), E^0 can be calculated from the data on the standard heat of formation in thermochemical tables [26–28]. Unless the surface under study is substantially both clean and monocrystalline, ϕ^+ instead of ϕ^e should be employed as ϕ in Eq. (9). Otherwise, the energy cycle of $\Delta E^* \equiv (\phi^e + E^+) - (E_0 + I)$ yields $-\Delta\phi^* \neq 0$ even if the other three terms are free from errors. Such failure in closing the cycle ($\Delta E^* \neq 0$) is reported by several authors [132,137,804,924,3869–3871], where SSI on polycrystalline metals (Mo, Ta, W) is studied together with the emissions of neutral atom and electron, but where ϕ^+ itself (or $\Delta\phi^*$) is neither considered nor measured. Typically, the data on Ta [137] yields $\Delta E^* \equiv (\phi^e + E^+) - (E^0 + I) = (4.19 \pm 0.02 + 10.0 \pm 0.3) - (7.97 \pm 0.03 + 7.3 \pm 0.3) = -1.1 \pm 0.4$ eV, falling to close the cycle by 1.1 eV. There is still lacking -0.4 eV even for the limit values [137]. This is mainly because ϕ^e is taken as ϕ in Eq. (9) and partly because the other values are not so accurate as ϕ^e. Here, $\phi^e = 4.19 \pm 0.02$ eV [137] is equal to 4.20 ± 0.03 eV (see Table 2) but much smaller than $\phi^+ = 4.95 \pm 0.20$ eV recommended for Ta (Table 2). Citation of the latter (ϕ^+) could reduce ΔE^* from -1.1 to about -0.3 eV, which covers amply the above limit (-0.4 eV). Similarly, the data on E^+, E^0 and ϕ^e for Re [76,77] yield such an unreasonable result that $\Delta E^* = (4.93 + 10.2) - (7.7 + 7.87) = -0.44$ eV $\neq 0$ when $\phi^e = 4.93 \pm 0.04$ eV [77] (see Table 1) is employed as ϕ in Eq. (9).

On the other hand, adoption of $\phi^+ = 5.43$ eV (larger than $\phi^e = 4.93$ eV by $\Delta\phi^* = 0.50$ eV for Re) [76,77] (see Table 1) affords a reasonable result of $\Delta E^* = 0.06$ eV ≈ 0.0 eV. Similarly to Mo [76,77], employment of $\phi^+ = 5.02 \pm 0.05$ eV as ϕ yields $\Delta E^* = -0.08$ eV ≈ 0.0 eV, in contrast to $\Delta E^* = -0.77$ eV $\neq 0$ owing to $\phi^e = 4.33 \pm 0.07$ eV. In the latter case, $\Delta E^* = -0.77$ eV is nearly equal to $-\Delta\phi^* \equiv \phi^e - \phi^+ = -0.69 \pm 0.09$ eV, where the difference of -0.08 eV between -0.77 and -0.69 eV is mainly due to the errors in E^+ and/or E^0 because $\Delta\phi^* = 0.69 \pm 0.09$ eV well accords with our most probable value (M.P.V.) of 0.72 ± 0.06 eV for Mo (see Table 5). These examples indicate that employment of ϕ^e instead of ϕ^+ falls to close the Schottky cycle by $\Delta\phi^*$ even if the other data (E^+, E^0 and I) themselves are essentially free from any error.

Let's consider another case of PSI on a monocrystalline surface instead of the polycrystalline ones exemplified above. When Cs^+ and Cs are desorbed from a substantially clean surface of W(100) with $\phi^e = 4.65 \pm 0.02$ eV [266], we find $\Delta E^* = (4.65 \pm 0.02 + 2.05 \pm 0.05) - (2.77 \pm 0.05 + 3.89) = 0.04 \pm 0.07 \approx 0.0$ eV, showing clearly that even adoption of ϕ^e affords the reasonable result in a monocrystalline surface system. Of course, adoption of $\phi^+ = 4.61 \pm 0.07$ eV [266] yields $\Delta E^* = 0.00 \pm 0.10$ eV, just closed exactly. This is because W(100) has the most probable values of $\phi^e = 4.65 \pm 0.02$ and $\phi^+ = 4.62 \pm 0.06$ eV (see Table 2), essentially equivalent between the two within the error of 0.03 ± 0.06 eV. An interesting information about the dependence of E^+ upon ϕ^+ may be acquired from Table 9 and Section 7.1 in Ref. [1351].

As described above by citing some of the typical examples, consideration of $\Delta\phi^* \neq 0$ inherent in polycrystalline surfaces is always necessary to avoid systematic errors in quantitative analysis of experimental data on PSI on any polycrystals, which have long been employed widely as useful and convenient ionizing materials in many fields of both physics and chemistry.

In addition, both theoretical and experimental studies of $\Delta\phi^*$ afford us a clue to the very important problem how the effective work functions of ϕ^e and ϕ^+ for polycrystals depend upon the surface components (F_i and ϕ_i) and particularly upon both $\delta_m (\equiv F_m)$ and ϕ_m, as will be discussed next together with those of the "submonocrystals" in Sections 4.2–4.5.

From the viewpoint mentioned above, all of the data on $\Delta\phi^*$ surveyed by the present author are listed in Table 4, where each of the data on ϕ^+ is achieved at the temperatures high enough to keep the ionizing surface essentially clean even during sample

beam incidence (see Section 2.2 in Ref. [1351]). In the first column in Table 4, a typical example of W–(310) [630] means that the polycrystalline surface of W consists mainly ($\delta_m = 46.3\% = 0.463$ in fractional surface area) of the (310) plane.

Similarly as in Table 1, the "Beam" and "Ion" in the 3rd and 4th columns in Table 4, respectively, show the species of probing atom (or molecule) impinging upon the surface under investigation and that of ion produced from the atom (or molecule) usually by PSI. Thus, the value of ϕ^+ in the 5th column is either determined by experiment usually according to a semi-Saha–Langmuir plot (see Section 4.2.1 in Ref. [1351]) or calculated by theory using Eq. (1).

Each value of ϕ^e in the 6th column is determined usually by TE according to the Richardson equation in a separate experiment, where nearly the same surface condition during TE and PSI on the same specimen is maintained by selection of suitable experimental conditions (namely, P_r, T and incident beam intensity), irrespective of the beam incidence (see Section 4.1 in Ref. [1351]). Needless to say, ϕ^e as well as ϕ^+ is determined in the temperature range high enough to avoid sample adsorption effect upon the surface under study (see Fig. 17 [104] in Ref. [1351]). Theoretical calculation (TC) of both ϕ^+ and ϕ^e is made, of course, for the same specimen by using the published data on F_i's and ϕ_i's (see Section 4.2).

The values of $\Delta\phi^*$ ($\equiv \phi^+ - \phi^e$) thus determined experimentally or theoretically for various surfaces by many workers are given in the 7th column in Table 4. The 2nd line above the last for each surface species shows the mean value (Mean) of $\Delta\phi^*$ based on the data (ϕ^+ and ϕ^e) obtained for the *same* specimen listed therein. On the other hand, the last line for each species shows the most probable value (M.P.V.) of $\Delta\phi^*$ evaluated from those data on both ϕ^e and ϕ^+ listed in the 3rd and 4th columns in Table 2. In contrast to the former, the latter is based on those much more data which are based on a variety of *distinct* specimens by different workers using various methods under a variety of conditions (see Table 1). Consequently, comparison between the two values of $\Delta\phi^*$ (Mean and M.P.V.) is helpful for examining the objective accuracy or reliability of each $\Delta\phi^*$. In Table 5, the two types of the best estimates (Mean and M.P.V.) originating from the data in Table 4 are summarized compactly together with another estimate achieved previously [1351] so that the values of $\Delta\phi^*$ may readily be compared between mono- and polycrystals and also among different surface species investigated by the present author.

Speaking in general about the monocrystals in Table 5, almost all the means of $\Delta\phi^*$ are found to be Mean ≈ 0.0 eV, exactly following to Eqs. (1) and (2). Regarding such an unreasonable result as M.P.V. $= -0.15$ eV against Mean $= 0.00$ eV for Re(0001), further studies are needed to find a valid reason for the discrepancy between the two. On the contrary to the monocrystals, all of the polycrystals have $\Delta\phi^* > 0$, just as predicted by our theoretical model. Namely, $\Delta\phi^*$ has a range from ~0.3 eV (Pt) to ~0.7 eV (Nb), which satisfies the fundamental condition of $\Delta\phi^* < \phi_{max} - \phi_{min} \approx 0.8$–1 eV (see Section 4.3 and Fig. 1). It is worthwhile to note that C(film) has $\Delta\phi^* = -0.02$ or $0.03 \approx 0.0$ eV, quite similarly to C(HOPG) with 0.07 or $-0.01 \approx 0.0$ eV, as shown in Table 5.

Carbonaceous overlayers grown on transition metal surfaces generally consist of the two types of carbidic and graphitic carbon [3939]. Compared with the latter, the former is usually stable at lower temperatures alone ($T < 600$ K), higher in work function ($\phi^e > 5$ eV) and more active as a catalyst. On the contrary, the latter has a very *anomalous* insensitivity to PSI of incident alkali halide molecules (MX), for example, because the degree of dissociation (MX $\to$ M + X) reduces to ~$10^{-3} \approx 0$ (and hence $\beta^+ \approx 0$ for producing M$^+$ from MX) compared with a normal detection sensitivity ($\beta^+ > 0$) to alkali atoms (M) incident upon a graphitized metal surface. Such a notable difference in detection sensitivity between the two surfaces affords us a very convenient technique of the "differential surface ionization" [222,223,226,737], by which the currents of M$^+$ originating from M alone and of M$^+$ from a mixture of M and MX are distinctively measurable without using mass spectrometry (for further information, see Sections 4.2.4 and 6.4 in Ref. [1351]).

Regarding graphitic film formation, a typical example is shown in Fig. 18 [103] in Ref. [1351], thus indicating that both ϕ^+ and ϕ^e of Ir(111) change from 5.8 to 4.8 eV according to graphitic film formation ($\theta = 1$ ML) at 1685 K [103] (see Table 1). About carbonaceous overlayers, both preparation methods and conditions and also chemico-physical properties are comprehensively reviewed by Gall' et al. [450] and Oshima et al. [695] and also outlined in Section 4.2.4 in Ref. [1351].

The work function of C$_{60}$/metal system ($\theta = 1$) is found experimentally to depend upon the metal species, showing that $\phi^e = 4.53, 5.06, 5.07$ and 5.19 eV on the substrates of Au(111), Cu(100), Cu(111) and Ag(111), respectively [4449]. Such a substrate dependence is reported also for other systems (Cu, Ag and Au) having a range of 4.39–4.72 eV [2198] (see Table 1).

In contrast to free-standing graphene ($\phi^e = 4.48$ eV) [4174,4284], adsorbed graphene is calculated to have 3.66, 4.03 and 4.87 eV on the substrates of Ni(111), Pd(111) and Pt(111) [4174,4284], the dependence of which may be supported by the experimental data of 3.9, 4.3 and 4.8 eV [695], respectively. Such a substrate dependence is caused by the formation of an interface dipole and the electron transfer between the metal and graphene levels driven by the work function difference, as well as the chemical interaction between graphene and the substrate metal [4174,4282,4284]. Since many of the carbon film systems are not clearly described for their surface structure, tentatively, Table 1 lists their work function data separately in the two groups of the "graphitic carbon films" and "graphene". But, some of the former of graphite/metal systems ($\phi^e = 3.32$–6.3 eV) seem to belong probably to the graphene/metal ones (4.03–4.96 eV). Such a large divergence in ϕ^e seems to support the above conclusion [4174,4284] that the work function of adsorbed graphene depends upon the substrate species. Similar dependence by up to 0.15 eV is observed [4435,4436].

Interestingly, highly ordered graphene films are epitaxially grown by thermal desorption of silicon from silicon carbide by high-temperature annealing (~1300–1900 K) in vacuum or under an argon atmosphere [4455–4457]. Typically, the variation in work function is as small as 12 meV over the single layer surface [4455], and the difference is only 139 ± 9 meV between single and bilayers thus prepared [4456].

The chief points of Tables 4 and 5 may be summarized as follows.

(1) As shown in Columns 3–5 in Table 5, the experimental determination for an essentially clean surface of W(100), for example, indicates that $\Delta\phi^* = 0.03$ or -0.03 eV ≈ 0.0 eV [Here, 1351], just as predicted by theory. On the other hand, a non-clean

monocrystalline surface such as an oxygenated W(100) face is observed to have $\phi^+ = 6.50 \pm 0.05$ eV and $\phi^e \approx 5.8$ eV [84,833], thereby giving $\Delta\phi^* \approx 0.7$ eV (see Table 1 in Ref. [1351]). This is near to $0.59-0.61$ eV determined for many polycrystalline W specimens (see Table 5), but considerably smaller than $\Delta\phi^* = 6.75 \pm 0.01 - 5.75 \pm 0.05 = 1.00 \pm 0.05$ eV found for an oxygenated polycrystalline W face [84,93,824,833] (Table 1 in Ref. [1351]).

(2) With the two exceptions of 0.14 and -0.15 eV for Nb(100) and W(112), respectively, almost all the species show that Mean is inside the range of -0.06 to 0.07 eV. Consideration of all the species affords Average $= 0.00 \pm 0.06$ eV, as shown on the 2nd line above the bottom in Table 5. In addition, quite many species have M.P.V. $= -0.10-0.10$ eV, but the average of all the species yields M.P.V. $= -0.02 \pm 0.07$ eV. In our previous study [1351], it is found to be 0.02 ± 0.03 eV. Consequently, essentially clean monocrystalline surfaces may be concluded to have $\Delta\phi^* = 0.0$ eV, just as expected by theory.

(3) Even when we try to analyze quantitatively these data on positive ionization and related phenomena on an essentially clean monocrystalline surface, therefore, our employment of ϕ^e instead of ϕ^+ of the surface may be generally expected to be substantially free from a systematic error.

(4) For any of the clean polycrystalline surfaces, on the other hand, $\Delta\phi^*$ is found to be considerably higher than 0.0 eV. Typically, Ir has Mean $= 0.48 \pm 0.10$ eV and M.P.V. $= 0.47 \pm 0.06$ eV [Here], both of which are equal to 0.48 ± 0.04 eV estimated in the previous review [1351] (see Table 5). Similarly, Nb has 0.70 ± 0.12 or 0.70 ± 0.07 eV [Here], nearly equal to 0.78 ± 0.11 eV [1351]. The last line in Table 5 indicates that $\Delta\phi^*$ has Range of $\sim 0.3-0.7 > 0.0$ eV, largely depending upon the surface species.

(5) Consequently, employment of ϕ^e instead of ϕ^+ always results in a systematic error depending upon the size of $\Delta\phi^*$ (up to ~ 0.7 eV) whenever we try to analyze these data on positive ionization phenomena on any polycrystalline surface. From this point of view, such data on $\Delta\phi^*$ as listed in Tables 4 and 5 may be very useful for better understanding the thermionic peculiarity of polycrystal ($\Delta\phi^* \geq 0.3$ eV), in contrast to monocrystal ($\Delta\phi^* = 0.0$ eV).

(6) Regarding a typical case of W, the dependence of $\Delta\phi^*$ upon the surface compositions of both F_i and ϕ_i is thoroughly studied for not imaginary but actual specimens [2453]. For instance, it is clearly shown for W that the theoretical values of $\Delta\phi^* = 0.62$ eV [630] and 0.57 eV [283] for $\delta_m = 0.46$ and 0.34, respectively, are in good agreement with these experimental data on 0.61 eV [23] and 0.56 eV [76,77]. The quantitative relation between δ_m and $\Delta\phi^*$ will be discussed for W in Section 4.3.

(7) It should be emphasized here that theoretical analysis of such data on $\Delta\phi^*$ as exemplified in Tables 4–6 affords us a promising clue to the long-pending problem how the polycrystalline work function is decided by the surface components of F_i and ϕ_i [4406], as will be discussed in Sections 4.4 and 4.5.

Disappointedly, the present author can find neither the best estimates nor the most probable values recommended statistically from abundant data on $\Delta\phi^*$ for any surface species by other authors in any literatures published to date. Consequently, any of our values on $\Delta\phi^*$ in Table 5 cannot be examined objectively by comparison with those to be recommended possibly by others.

4.2. Theoretical evaluation of the contrast ($\Delta\phi^*$)

Eqs. (1) and (2) indicate that $\Delta\phi^* \equiv \phi^+ - \phi^e$ can be evaluated theoretically when the data on both ϕ_i and F_i for a given specimen are available from literatures. The present author has already published the values of $\Delta\phi^*$ calculated for actual specimens of Ni [283,630], of Nb, Mo, Ta and Ir [803], and also of W [281,283,630,803,2453]. Typically for the seven specimens (A)–(G) of W having different values of $\delta_m = 0.336-0.96$, the data on $\Delta\phi^*$ evaluated from Eqs. (1) and (2) are summarized in Table 6, together with experimental data available on ϕ^e to be compared with the theoretical ones for the *same* specimen under study. Typically, the specimen of W(G) is found to have Footnote (59) $\phi^e = 4.59 \pm 0.04$ eV as Mean by theory [2453] and Footnote (60) 4.52 ± 0.07 eV as the actual data on the same specimen by experiment [124,3414], both of which well agree with each other, thereby strongly supporting the validity of the above equations symbolic of our theoretical model.

Table 6
Typical data on the fractional surface area (F_i), the local work function (ϕ_i) reported for tungsten specimens (A–G, Q, R and U) having different values of the degree of monocrystallization (δ_m), and also the thermionic contrast ($\Delta\phi^*$) calculated from the data on both F_i and ϕ_i listed herein, thereby yielding Fig. 1.

Specimen	δ_m	Footnote	Fractional surface area, Local work function, and Thermionic contrast						Refs.
W(A)	0.336	(1)	Plane	(111)	(100)	(112)	(110)		[488]
		(2)	F_i	0.062	0.331	0.336	0.271		[488]
		(3)	ϕ_i (eV)	4.35	4.56	4.69	5.35		[488]
		(4)	$\Delta\phi^*$ (eV) $\equiv \phi^+ - \phi^e = \underline{5.13 \pm 0.04 - 4.62 \pm 0.02 = \mathbf{0.52 \pm 0.04}}$				ϕ^a (eV) = 4.80		[2453]
W(B)	0.352	(5)	Plane	(111)	(100)	(112)	(110)		[488]
		(6)	F_i	0.089	0.254	0.343	0.352		[488]
		(7)	ϕ_i (eV)	4.35	4.56	4.69	5.35		[488]
		(8)	$\Delta\phi^*$ (eV) $\equiv \phi^+ - \phi^e = \underline{5.18 \pm 0.03 - 4.61 \pm 0.03 = \mathbf{0.57 \pm 0.04}}$				ϕ^a (eV) = 5.04		[2453]
W(C)	0.46	(9)	Plane	(011)	(001)	(112)	(013)	(222)	(123)	[825]
		(10)	F_i	0.16	0.46	0.09	0.06	0.22	0.01	[825]
		(11)	ϕ_i (eV)	5.25	4.63	5.12	4.34	4.45	4.50	[825]

(continued on next page)

Table 6 (*continued*)

Specimen	δ_m	Footnote	Fractional surface area, Local work function, and Thermionic contrast						Refs.
		(12)	ϕ_i (eV)	5.31	4.63	4.83	4.32	4.45	4.49	[825,1351]
		(13)	$\Delta\phi^*$ (eV) $\equiv \phi^+ - \phi^e = 4.98 \pm 0.05 - 4.56 \pm 0.01 = 0.42 \pm 0.05$				ϕ^a (eV) = 4.72		[2453]
		(14)	$\Delta\phi^*$ (eV) $\equiv \phi^+ - \phi^e = 5.01 \pm 0.05 - 4.56 \pm 0.01 = 0.45 \pm 0.05$				ϕ^a (eV) = 4.70		[2453]
		(15)	$\Delta\phi^*$ (eV) $\equiv \phi^+ - \phi^e = \underline{5.00 \pm 0.05 - 4.56 \pm 0.01} = \mathbf{0.44 \pm 0.05}$ (Mean of 13 and 14)						[2453]
W(D)	0.463	(16)	Plane	(310)	(111)	(100)	(112)	(110)	[489]
		(17)	F_i	0.463	0.054	0.140	0.155	0.189	[489]
		(18)	ϕ_i (eV)	4.25	4.47	4.65	4.76	5.25	[489]
		(19)	ϕ_i (eV)	4.32	4.38	4.57	4.83	5.31	[1351]
		(20)	$\Delta\phi^*$ (eV) $\equiv \phi^+ - \phi^e = 4.96 \pm 0.03 - 4.37 \pm 0.02 = 0.59 \pm 0.04$				ϕ^a (eV) = 4.59 [489]		[2453]
		(21)	$\Delta\phi^*$ (eV) $\equiv \phi^+ - \phi^e = 5.02 \pm 0.07 - 4.42 \pm 0.01 = 0.60 \pm 0.07$				ϕ^a (eV) = 4.63		[2453]
		(22)	$\Delta\phi^*$ (eV) $\equiv \phi^+ - \phi^e = \underline{4.99 \pm 0.06 - 4.38 \pm 0.05} = \mathbf{0.61 \pm 0.08}$ (Mean of 20 and 21)						[2453]
		(23)	ϕ^e (eV) = 4.38 ± 0.05 (Mean by calculation)						[2453]
		(24)	ϕ^e (eV) = 4.8 ± 0.05 (by experiment)						[489]
W(A)–(D)	<0.5	(25)	$\Delta\phi^*$ (eV) $\equiv \phi^+ - \phi^e = \underline{5.05 \pm 0.09 - 4.52 \pm 0.10} = \mathbf{0.53 \pm 0.09}$ (Mean of 4, 8, 15 and 22)						[2453]
W(P)	<0.5	(26)	$\Delta\phi^*$ (eV) $\equiv \phi^+ - \phi^e = \underline{5.14 \pm 0.05 - 4.55 \pm 0.04} = \mathbf{0.59 \pm 0.06}$ (M.P.V. by experiment)						[1351]
W(E)	0.80	(27)	Plane	(110)	(112)	(100)	(111)		[162]
		(28)	F_i	0.80	0.05	0.14	0.01		[162]
		(29)	ϕ_i (eV)	5.3	4.8	4.66	4.35		[162]
		(30)	ϕ_i (eV)	5.31	4.83	4.57	4.38		[1351]
		(31)	$\Delta\phi^*$ (eV) $\equiv \phi^+ - \phi^e = 5.25 \pm 0.02 - 4.90 \pm 0.05 = 0.35 \pm 0.05$				ϕ^a (eV) = 5.18		[2453]
		(32)	$\Delta\phi^*$ (eV) $\equiv \phi^+ - \phi^e = 5.27 \pm 0.01 - 4.85 \pm 0.05 = 0.42 \pm 0.05$				ϕ^a (eV) = 5.17		[2453]
		(33)	$\Delta\phi^*$ (eV) $\equiv \phi^+ - \phi^e = \underline{5.26 \pm 0.02 - 4.87 \pm 0.06} = \mathbf{0.39 \pm 0.06}$ (Mean of 31 and 32)						[2453]
W(F)	0.95	(34)	Plane	(100)	(110)	(111)	(112)	(116)	[3414]
		(35)	F_i	0.95	0.01	<0.01	0.02	–	[3414]
		(36)	F_i	0.95	0.01	<0.01	0.02	0.01	[2453]
		(37)	ϕ_i (eV)	4.65	5.25	4.47	4.67	4.32	[489,1351]
		(38)	ϕ_i (eV)	4.57	5.31	4.38	4.83	4.32	[1351]
		(39)	$\Delta\phi^*$ (eV) $\equiv \phi^+ - \phi^e = 4.70 \pm 0.03 - 4.65 \pm 0.00 = 0.05 \pm 0.03$				ϕ^a (eV) = 4.61		[2453]
		(40)	$\Delta\phi^*$ (eV) $\equiv \phi^+ - \phi^e = 4.70 \pm 0.03 - 4.64 \pm 0.00 = 0.06 \pm 0.03$				ϕ^a (eV) = 4.65		[2453]
		(41)	$\Delta\phi^*$ (eV) $\equiv \phi^+ - \phi^e = 4.69 \pm 0.05 - 4.57 \pm 0.00 = 0.12 \pm 0.05$				ϕ^a (eV) = 4.54		[2453]
		(42)	$\Delta\phi^*$ (eV) $\equiv \phi^+ - \phi^e = 4.69 \pm 0.05 - 4.56 \pm 0.01 = 0.12 \pm 0.05$				ϕ^a (eV) = 4.58		[2453]
		(43)	$\Delta\phi^*$ (eV) $\equiv \phi^+ - \phi^e = \underline{4.70 \pm 0.04 - 4.61 \pm 0.04} = \mathbf{0.09 \pm 0.05}$ (Mean of 39–42)						[2453]
		(44)	ϕ^e (eV) = 4.61 ± 0.04 (Mean by calculation)						[2453]
		(45)	ϕ^e (eV) = 4.52 ± 0.07 (by experiment)						[124,3414]
W(G)	0.96	(46)	Plane	(100)	(111)				[124]
		(47)	F_i	0.96	0.04				[124]
		(48)	ϕ_i (eV)	4.65	4.47				[489]
		(49)	ϕ_i (eV)	4.66	4.35				[162]
		(50)	ϕ_i (eV)	4.60	4.40				[144]
		(51)	ϕ_i (eV)	4.55	4.42				[143]
		(52)	ϕ_i (eV)	4.57	4.38				[1351]
		(53)	$\Delta\phi^*$ (eV) $\equiv \phi^+ - \phi^e = 4.64 \pm 0.01 - 4.64 \pm 0.00 = 0.00 \pm 0.01$				ϕ^a (eV) = 4.64		[2453]
		(54)	$\Delta\phi^*$ (eV) $\equiv \phi^+ - \phi^e = 4.65 \pm 0.01 - 4.63 \pm 0.01 = 0.02 \pm 0.01$				ϕ^a (eV) = 4.65		[2453]
		(55)	$\Delta\phi^*$ (eV) $\equiv \phi^+ - \phi^e = 4.59 \pm 0.00 - 4.58 \pm 0.00 = 0.01 \pm 0.00$				ϕ^a (eV) = 4.59		[2453]
		(56)	$\Delta\phi^*$ (eV) $\equiv \phi^+ - \phi^e = 4.54 \pm 0.00 - 4.53 \pm 0.00 = 0.01 \pm 0.00$				ϕ^a (eV) = 4.54		[2453]
		(57)	$\Delta\phi^*$ (eV) $\equiv \phi^+ - \phi^e = 4.56 \pm 0.01 - 4.55 \pm 0.01 = 0.01 \pm 0.01$				ϕ^a (eV) = 4.56		[2453]
		(58)	$\Delta\phi^*$ (eV) $\equiv \phi^+ - \phi^e = \underline{4.60 \pm 0.04 - 4.59 \pm 0.04} = \mathbf{0.01 \pm 0.01}$ (Mean of 53–57)						[2453]
		(59)	ϕ^e (eV) = 4.59 ± 0.04 (Mean by calculation)						[2453]
		(60)	ϕ^e (eV) = 4.52 ± 0.07 (by experiment)						[124,3414]
W(Q)	1.00	(61)	Plane	(100)					[1351]
		(62)	$\Delta\phi^*$ (eV) $\equiv \phi^+ - \phi^e = \underline{4.60 \pm 0.05 - 4.57 \pm 0.03} = \mathbf{0.03 \pm 0.06}$ (M.P.V.)						[1351]
W(R)	1.00	(63)	Plane	(110)					[1351]
		(64)	$\Delta\phi^*$ (eV) $\equiv \phi^+ - \phi^e = \underline{5.29 \pm 0.08 - 5.31 \pm 0.05} = \mathbf{-0.02 \pm 0.09}$ (M.P.V.)						[1351]
W(U)	–	(65)	$\phi_{max} - \phi_{min} \simeq 1.0{-}0.8$ eV $> \phi^+ - \phi^e \equiv \Delta\phi^* \simeq 0.6{-}0.0$ eV						[2453]

(1)–(4) From the experimental data (1)–(3) [488], the values (4) are theoretically obtained from Eqs. (1), (2) and (4) [2453].

(5)–(8) Similarly as above, the data (5)–(7) [488] yield the theoretical values (8) [2453].

(9)–(15) By using the data of (11) ϕ_i and (12) ϕ_i together with (10) F_i for the specimen of W(C) (9), we obtain the results of (13) $\Delta\phi^*$ and (14) $\Delta\phi^*$, respectively, thereby yielding the mean value of (15) $\Delta\phi^*$.

(16)–(22) Similarly, the local work function sets (18) and (19) together with the set (17) afford the results (20) and (21), respectively, which give the mean value (22).

(23)–(24) The theoretical value (23) based on the mean (22) is found to be poor in agreement with the experimental one (24) determined with the specimen of W(D) by the corresponding workers [489]. For this reason, see Chief point (4) in Section 4.2.

(25) The contrast (25) is the mean value for the four specimens of (A)–(D) having the values of $\delta_m < 0.5$.

(26) The contrast (26) is the most probable value determined from quite many specimens of polycrystalline tungsten (see Table 2 in Ref. [1351]).

(27)–(33) The sets (29) and (30) together with the set (28) afford the contrasts (31) and (32), respectively, which give the mean of (33) $\Delta\phi^*$.

(34)–(45) Combinations of (35)–(37), (35)–(38), (36)–(37) and (36)–(38) give the four values of (39)–(42), respectively, which yield Mean (43). The mean of (44) $\phi^e = 4.61 \pm 0.04$ eV thus calculated is in fair agreement with (45) $\phi^e = 4.52 \pm 0.07$ eV determined experimentally for the specimen of W(F) by the corresponding worker [124,3414].

(46)–(60) Employment of ϕ_i (48)–ϕ_i (52) yields $\Delta\phi^*$ (53)–$\Delta\phi^*$ (57), respectively, which afford the mean (58). Our calculated value of ϕ^e (59) = 4.59 $\pm$ 0.04 eV well agrees with the experimental data of ϕ^e (60) = 4.52 $\pm$ 0.07 eV determined with W(G) by the worker [124,3414].

(61)–(62) The contrast (62) is the most probable value determined from quite many specimens of W(100) (see Table 2 in Ref. [1351]).

(63)–(64) Similarly, the value (64) for W(110) is cited from Ref. [1351].

(65) The range (1.0–0.8 eV) is generally estimated for bcc metals such as W, Ta and Mo [2453]. Polycrystalline tungsten exemplified as W(U) consists generally of various faces, among which W(110) and W(116) seem to have the largest and smallest values of $\phi_{max} \approx 5.3$ eV and $\phi_{min} \approx 4.3$ eV, respectively (see Table 2). The range (0.6–0.0 eV) is determinable also from the data on (22) and (62) of $\Delta\phi^* = 0.61$ and 0.0 eV, respectively, contained above [Here].

The main points of Table 6 may be summarized below, where the numbers of (1)–(65) regarding various items (e.g., plane, F_i and ϕ_i) correspond to those of Footnote in Column 3.

(1) Regarding the specimen of W(A) consisting of the four planes (1) of (111)–(110) with $\delta_m = F(112) = 0.336$ [488], substitution of both Footnote (2) $F_i = 0.062$–0.271 and that (3) $\phi_i = 4.35$–5.35 eV into Eqs. (1) and (2) yields the result (4) of $\phi^+ = 5.13 \pm 0.04$ and $\phi^e = 4.62 \pm 0.02$ eV and, hence, $\Delta\phi^* = 0.52 \pm 0.04$ eV. Each of the three values is very close to that listed as the most probable value (M.P.V.) for the generally called "polycrystalline" tungsten ($\delta_m < 0.5$, usually considered) in Table 4, which shows $\phi^+ = 5.17 \pm 0.05$ eV, $\phi^e = 4.56 \pm 0.03$ eV and $\Delta\phi^* = 0.61 \pm 0.06$ eV as M.P.V. for polycrystalline W. In addition, the result (4) [2453] shows that the sequence of $\phi^+ = 5.13$ eV $> \phi^a = 4.80$ eV $> \phi^e = 4.62$ eV holds just as predicted by theory in Section 1 (see Eqs. (1), (2) and (4)).

(2) With regard to W(B) having $\delta_m = F(110) = 0.352$ [488], the data on (6) F_i and (7) ϕ_i afford theoretically the result (8) of $\phi^+ = 5.18 \pm 0.03$ and $\phi^e = 4.61 \pm 0.03$ eV and, hence, $\Delta\phi^* = 0.57 \pm 0.04$ eV. With respect to W(A) and W(B), both (3) ϕ_i and (7) ϕ_i are common for each of the planes (1) and (5), but (2) F_i and (6) F_i are different (by up to 0.081) with each other between the two. Each of ϕ^+, ϕ^e and $\Delta\phi^*$, however, is essentially the same (within 0.05 eV gapped) between the results of (4) and (8) [2453], in spite of the fact that $\phi^a = 4.80$ eV for W(A) is very different (by 0.24 eV) from $\phi^a = 5.04$ eV for W(B). In addition, $\phi^a = 5.04$ eV is quite different from both $\phi^+ = 5.18 \pm 0.03$ and $\phi^e = 4.61 \pm 0.03$ eV for W(B). Such difference among the three is observed also for W(C)–W(E) to be mentioned below. These results indicate that employment of ϕ^a as ϕ^e or ϕ^+ is not very reasonable for any polycrystals, as already mentioned in Section 1.

(3) About W(C) with $\delta_m = F(001) = 0.46$ [825], adoption of the two sets (11) and (12) of ϕ_i's gives the results (13) and (14), respectively. Each of the three values of ϕ^+, ϕ^e and $\Delta\phi^*$ is essentially the same between the results of (13) and (14), irrespective of the difference in ϕ_i by up to 0.29 eV between the two sets of (11) and (12) for ϕ_i. They lead to the mean (15). Again, $\phi^a = 4.71 \pm 0.01$ eV is different from both $\phi^+ = 5.00 \pm 0.05$ and $\phi^e = 4.56 \pm 0.01$ eV by 0.29 $\pm$ 0.05 and 0.15 $\pm$ 0.01 eV, respectively, showing again $\phi^+ > \phi^a > \phi^e$. On the other hand, the authors [825] report that $\phi^a = 4.72$ eV differs from $\phi^+ = 4.61 \pm 0.05$ eV determined by PSI of Li and Eu on W(C). The difference itself is quite natural, but the result of $\phi^+ = 4.61$ eV $< \phi^a = 4.72$ eV does not accord with ours of $\phi^+ = 5.00$ eV $> \phi^a = 4.71 \pm 0.01$ eV.

(4) With respect to W(D) having $\delta_m \equiv F_m = F(310) = 0.463$ [489], the two sets (18) and (19) of ϕ_i's together with (17) F_i afford the two results of (20) and (21), respectively. Again, each of ϕ^+, ϕ^e and $\Delta\phi^*$ is almost the same (gap ≤ 0.06 eV) between the results of (20) and (21), nearly independent of the considerable difference (by up to 0.09 eV) between the two ϕ_i sets of (18) and (19). Of course, each of $\phi^a = 4.59$ and 4.63 eV is intermediate between $\phi^+ = 4.99$ eV and $\phi^e = 4.38$ eV, as shown in the mean (22)). On the other hand, the corresponding workers [489] conclude that the data (24) of $\phi^e = 4.8$ eV measured for W(D) by FE is in good agreement with the calculated value (20) of $\phi^a = 4.59 \approx 4.6$ eV. This conclusion, however, does not seem very reasonable, mainly because $\phi^e = \phi^a$ or $\phi^e > \phi^a$ does not hold in principle for any polycrystalline surface and also because $\phi^e = 4.8$ eV is much larger than the most probable value (26) of $\phi^e = 4.55 \pm 0.04$ eV [1351] and also than such values of 4.56 $\pm$ 0.03 eV [Here], 4.55 eV [1045,1358] and 4.54 eV [1354] as generally accepted today for the usually called "polycrystalline" tungsten (see Table 2).

(5) About the four specimens of W(A)–W(D) having $\delta_m < 0.5$ [488,489,825], we obtain Mean (25) from the results (4), (8), (15) and (22). Namely, $\phi^+ = 5.05 \pm 0.09$, $\phi^e = 4.52 \pm 0.10$ eV and $\Delta\phi^* = 0.53 \pm 0.09$ eV, each of which is comparable with each of the means for W(A)–W(D) in spite of the fact that both δ_m and ϕ^a are considerably different by up to 0.127 and to 0.45 eV, respectively, among the four specimens.

(6) The result (26) for W(P) is achieved by various experimental methods (FE, PE, CPD, TE, PSI, etc.) for a variety of specimens of the generally called "polycrystalline" tungsten (usually $\delta_m < 0.5$). Namely, the data (26) $\phi^+ = 5.14 \pm 0.05$ (or 5.17 $\pm$ 0.05) eV, $\phi^e = 4.55 \pm 0.04$ (or 4.56 $\pm$ 0.03) eV and $\Delta\phi^* = 0.59 \pm 0.06$ (or 0.61 $\pm$ 0.06) eV are cited as the most probable values from Table 2 in Ref. [1351] or as those (given in each parentheses) from M.P.V. in Table 4. Comparison between the theoretical results (25) and the experimental ones (26) shows that each of the three values is in fair agreement between the two to within 0.09 eV gapped. Especially, ϕ^e is substantially the same (only 0.03 eV gapped) between theory and experiment, irrespective of the fact that ϕ^a has a wide gap (0.45 eV in the range of 4.59–5.04 eV) among the four specimens of W(A)–W(D). Again, this result indicates that ϕ^a is quite different in both nature and value from both ϕ^e and ϕ^+ for polycrystalline surfaces, in contrast to the treatment ($\phi^a \approx \phi^e$) [489] mentioned in Point (4) above.

(7) Regarding W(E) with $\delta_m = F(110) = 0.80$ [162], calculation using the two different sets (29) and (30) of ϕ_i's [162,1351] together with F_i (28) [162] yields results (31) and (32), respectively, and also does their Mean (33). Compared with W(A)–W(D)

having $\delta_m < 0.5$, W(E) has a larger value of $\delta_m = 0.80$ (submonocrystal), considerably near to ~1 for the monocrystal ($\Delta\phi^* = 0$) of W(110). In consequence, it is quite natural that $\Delta\phi^*$ decreases from 0.53 eV (25) to 0.39 eV (33), becoming nearer to zero.

(8) In the case of W(F) having $\delta_m = F(100) = 0.95$ [3414], the two combinations of F_i (35) and ϕ_i (37) and of F_i (35) and ϕ_i (38) afford the results (39) and (41), respectively, while those of F_i (36) and ϕ_i (37) and of F_i (36) and ϕ_i (38) yield the respective results (40) and (42). These results indicate that each of ϕ^+, ϕ^e, $\Delta\phi^*$ and ϕ^a is nearly identical (within 0.09 eV gapped) in spite of the difference in the sets of F_i's and ϕ_i's among those (39)–(42). In addition, Mean (43) shows that $\Delta\phi^* = 0.09 \pm 0.05$ eV is much smaller than Mean (33) of $\Delta\phi^* = 0.39 \pm 0.06$ eV for W(E) according as δ_m becomes larger from 0.80 to 0.95 and, hence, as it does nearer to unity for the monocrystalline tungsten ($\delta_m = 1$) of W(100). Mean (44) of $\phi^e = 4.61 \pm 0.04$ eV by calculation [2453] is in fair agreement with the experimental data (45) on $\phi^e = 4.52 \pm 0.07$ eV determined directly for W(F) itself by TE (Richardson plots) [124,3414].

(9) With respect to W(G) having $\delta_m = F(100) = 0.96$ [124], the five sets (48)–(52) of ϕ_i's combined with the set (47) of F_i yield the results of (53)–(57), respectively, from which Mean (58) is obtained. Again, Mean (59) of $\phi^e = 4.59 \pm 0.04$ eV yielded by theory [2453] well agrees with the data (60) of $\phi^e = 4.52 \pm 0.07$ eV done for W(G) by TE [124,3414]. The mean of the five values (53)–(57) for $\phi^a = 4.59 \pm 0.04$ eV coincides exactly with Mean (59) of $\phi^e = 4.59 \pm 0.04$ eV. This is quite natural because W(G) is essentially equivalent in electrophysical property to W(100) listed as (61) W(Q). Namely, each of the three averages (58) of $\phi^+ = 4.60 \pm 0.04$ eV, $\phi^e = 4.59 \pm 0.04$ eV and $\Delta\phi^* = 0.01 \pm 0.01 \approx 0.00$ eV is essentially the same (within 0.02 eV gapped) with each of the most probable values (62) of $\phi^+ = 4.60 \pm 0.05$ eV and $\phi^e = 4.57 \pm 0.03$ eV and $\Delta\phi^* = 0.03 \pm 0.06$ eV based on those data achieved for W(100) by a great many workers (see Table 2 in Ref. [1351]). These results of $\phi^+ = \phi^e = \phi^a = 4.59 \pm 0.04$ eV and also $\Delta\phi^* = 0.0$ eV indicate that W(G) with $\delta_m = F(100) = 0.96$ is substantially equivalent in work function to W(100) with $\delta_m = 1$. This is one of the important outcomes that can be deduced theoretically by our simple model leading to Eqs. (1), (2) and (4).

(10) As partly mentioned above, each of the three values (58) calculated for W(G) are essentially equal to each of those (62) determined by using various experimental methods, thus giving an additional evidence to support the validity of our theoretical model.

(11) With respect to W(110) listed as (63) W(R), the most probable values (64) of ϕ^+ and ϕ^e are determined from a good many data listed in Table 1 [1351], giving $\Delta\phi^* = -0.02 \pm 0.09 \approx 0.0$ eV (see Table 2 [1351] and Table 5 [Here]), just as predicted by theory.

(12) Regarding the "polycrystalline" tungsten expressed as (65) W(U), its maximum and minimum local work function values (ϕ_{max} and ϕ_{min}) seem to correspond to $\phi^e(110) \approx 5.3$ eV and $\phi^e(116) \approx 4.3$ eV (see Table 2), respectively. Compared with the difference of $\phi_{max} - \phi_{min} \approx 1.0$ eV, our value of $\Delta\phi^* \approx 0.6 - 0.0$ eV for W(A)–W(G) [2453] is reasonably smaller, just as expected on principle.

(13) Quite similarly for W as exemplified in Points (6) and (10) above, a fair agreement of ϕ^e between theory and experiment is observed also for Ni [283,630] and for Nb, Mo, Ta and Ir [803]. Typically, we have the results of (i) Nb($\delta_m = 0.68$) as ($4.02 \pm 0.07/4.1$–4.19), (ii) Mo(0.72) as ($4.38 \pm 0.03/4.0$–4.4), (iii) Ta(0.82) as ($4.34 \pm 0.03/4.25 \pm 0.05$) and (iv) Ir(0.81) as ($5.36 \pm 0.07/5.27 \pm 0.05$ or 5.35 ± 0.05). Here, the figures of numerator and denominator in the second parentheses correspond to the values of ϕ^e (in eV) calculated by the present author [803] and measured directly for each specimen by Wilson [124,169,3414], respectively. These specimens ($\delta_m = 0.68$–0.82) correspond to the "submonocrystals", the anomaly of which is outlined in Sections 4.4 and 4.5.

(14) Such an agreement between theory and experiment is generally expected to hold for ϕ^-, too, because both ϕ^e and ϕ^- are given theoretically by the same equations of Eqs. (2) and (3) (see Section 1), and also $\Delta\phi^{**} \equiv \phi^- - \phi^e = 0.0$ eV is found experimentally for W together with other species of polycrystals such as C, Mo and Ta, too (see Table 7).

The results summarized in the above points (1)–(14) give an additional evidence to support that our theoretical model is very reasonable and useful, although it is very simple and plain and also may seem crude and coarse apparently.

4.3. Quantitative relation between the contrast ($\Delta\phi^*$) and the degree of monocrystallization (δ_m)

As may be seen in Table 6, δ_m corresponds simply to the largest (F_m) among the fractional surface areas (F_i's) for each specimen. Apparently, therefore, δ_m itself may seem to be neither chief nor basic (key) factor decisive actually of the work functions (ϕ^+ and ϕ^e) of the specimen under study. The points (1)–(9) in Section 4.2, however, suggests it by δ_m that $\Delta\phi^*$ is governed substantially. Such a suggestion leads to the idea that δ_m may be taken as an indicator representative of the two types of $\Delta\phi^*$. Namely, $\Delta\phi^*$ is nearly constant with little dependence upon δ_m so long as δ_m is below 0.5. At $\delta_m > 0.5$, on the contrary, $\Delta\phi^*$ decreases gradually with increasing δ_m, generally converging to zero as $\delta_m \to 1$. To find the quantitative relation between the two, the data on $\Delta\phi^*$ in Table 6 are plotted against δ_m, as shown in Fig. 1 [2453]. Here, the solid circles of (A)–(G) correspond to the theoretical values of $\Delta\phi^*$ for the seven specimens of W(A)–W(G) in Table 6, respectively, while the horizontal line crossed with a vertical arrow (A–D) shows Mean (25) of $\Delta\phi^* = 0.53 \pm 0.09$ eV at $\delta_m < 0.5$ for the four specimens of W(A)–W(D). Here, the number of (25) corresponds to that of Footnote in Table 6, quite similarly as above in Section 4.2. The horizontal line with arrow (P) at $\delta_m < 0.5$ corresponds to W(P) of M.P.V. (26) having $\Delta\phi^* = 0.59 \pm 0.06$ eV [1351] based on the data achieved experimentally by a great many workers applying different methods and processes to a variety of polycrystalline tungsten specimens under various conditions. The open circles of (Q) and (R) at $\delta_m = 1.00$ correspond to W(Q) and W(R), originating from the experimental data ($\Delta\phi^* = 0.03 \pm 0.06$ and -0.02 ± 0.09 eV) [1351] on the monocrystals of W(100) and W(110), respectively (see M.P.V.'s (62) and (64) in Table 6). Consideration of both Fig. 1 and the above points (1)–(9) in Section 4.2 leads to the conclusion that the quantitative relation between the two is given by the empirical formulae [2453] as follows:

$$\Delta\phi^* = c \quad \text{for } 0 < \delta_m < 0.5 \text{ (polycrystal)}. \tag{10}$$

Fig. 1. Dependence of the thermionic contrast ($\Delta\phi^*$) upon the degree of monocrystallization (δ_m) of tungsten [2453]. Each of the data (A)–(G) as well as those (P)–(R) is cited from Table 6 [Here].

$$\Delta\phi^* = 4c\delta_m(1 - \delta_m) \quad \text{for } 0.5 < \delta_m < 1 \text{ ("submonocrystal").} \tag{11}$$

$$\Delta\phi^* = 0 \quad \text{for } \delta_m = 1 \text{ (monocrystal).} \tag{12}$$

From the data on $\Delta\phi^*$ at $\delta_m < 0.5$ for W, the constant of c is evaluated theoretically to be 0.53 ± 0.09 eV (Mean (25) [2453] in Table 6), as shown by the horizontal line crossed with vertical arrow (A–D). This value is substantially equal to 0.59 ± 0.06 eV (M.P.V. (26) [1351] in Table 6), which is shown by the horizontal line with the arrow (P) originating from the experimental data obtained by many workers (see Tables 1 and 2 in Ref. [1351]). At $\delta_m > 0.5$, on the other hand, the theoretical values of $\Delta\phi^* = 0.39 \pm 0.06$, 0.09 ± 0.05 and 0.01 ± 0.01 eV (Means (33), (43) and (58) evaluated respectively for (E)–(G) in Table 6) are well expressed by a parabolic curve according to Eq. (11), as may be seen in Fig. 1. These results indicate that the so-called "polycrystal" should be divided into the two different categories of the usually called "polycrystal" ($\delta_m < 0.5$, corresponding to Eq. (10)) and the tentatively named "submonocrystal" ($0.5 < \delta_m < 1$, doing to Eq. (11)) because the dependence of ϕ^+, ϕ^e and $\Delta\phi^*$ upon δ_m is quite different between the two, as will be discussed in Sections 4.4 and 4.5.

In the present case of W, ϕ_{max} and ϕ_{min} may be estimated to be $\phi(110) \approx 5.3$ eV and $\phi(116) \approx \phi(013) \approx 4.3$ eV (see Table 2), respectively, which are partly included as ϕ_i in the present calculation of $\Delta\phi^*$ for almost all the seven specimens of W(A)–W(G) in Table 6. At $\delta_m < 1$, the sequence of $\phi_{max} > \phi^+ > \phi^a > \phi^e > \phi_{min}$ holds for tungsten polycrystals [1351] and, hence, we have the relation of $\Delta\phi^* \equiv \phi^+ - \phi^e < \phi_{max} - \phi_{min} \approx 5.3 - 4.3 = 1.0$ or ≈ 0.9 eV [3965]. In other words, the actual value of $\Delta\phi^*$ is strongly governed by both ϕ_{max} and ϕ_{min} included in ϕ_i's that are considered for either calculation or measurement of $\Delta\phi^*$. In respect of W(G), ϕ_{max} and ϕ_{min} correspond to $\phi(100) \approx 4.6$ eV for $F(100) = 0.96$ and to $\phi(111) \approx 4.4$ eV for $F(111) = 0.04$, respectively. Even in this case for $\delta_m \approx 1$, of course, $\Delta\phi^* = 0.01 \pm 0.01$ eV (see Mean (58) in Table 6) fully satisfies the above condition of $\Delta\phi^* < \phi_{max} - \phi_{min} \approx 1.0$ eV. In a typical case of bcc-metals (e.g., Nb, Mo, Ta and W), the difference of $\phi_{max} - \phi_{min}$ is generally estimated to have a range of ~ 0.9–1.0 [127] or ~ 0.8–1.0 eV [1351], the latter of which is inserted as dotted horizontal lines (U) in Fig. 1. Even at $\delta_m < 0.5$ having the largest values of $\Delta\phi^*$, the present value of $\Delta\phi^* = c$ is limited to 0.44–0.65 eV (see the probable ranges indicated with two arrows of (A–D) and (P) in Fig. 1) and, hence, our values of $\Delta\phi^*$ are always (at any value of δ_m) much smaller than the upper limit of 0.8–1.0 eV mentioned just above. Consequently, the theoretical result about W satisfies perfectly the essential condition of $\Delta\phi^* \leq c < \phi_{max} - \phi_{min}$ for any value of δ_m. For additional examples of fcc-polycrystals, Ir and Pt are estimated from Table 2 to have $\phi_{max} - \phi_{min} \approx 0.9$ and 0.7 eV, respectively, which are much larger than $\Delta\phi^* \approx 0.5$ and 0.3 eV (see Table 5), respectively. For hcp-Re, the former (~ 0.7 eV) is also larger than the latter (~ 0.4 eV), quite similarly for the bcc-metals mentioned just above (~ 0.8–1.0 eV $> \sim 0.6$–0.7 eV, see Tables 2 and 5).

In the range of $\delta_m \approx 0.5$–1.0 for "submonocrystals", $\Delta\phi^*$ is given by Eq. (11), where c for W is theoretically evaluated to be 0.53 ± 0.09 eV by the present author [2453] (Mean (25) in Table 6). This is in good agreement with $\Delta\phi^* = 0.59 \pm 0.06$ eV [1351] (M.P.V. (26) in Table 6) and also with both 0.60 ± 0.13 and 0.61 ± 0.06 eV (Mean and M.P.V., respectively, in Tables 4 and 5) determined by the present author according to the abundant data on both ϕ^+ and ϕ^e achieved for W mainly by experiment by a great many workers (see Table 1). Eq. (11) may be expected to be available to other metals, too. According to a preliminary study about Ir, for instance, the constant (c) may be estimated to be 0.60 ± 0.13 eV [2453], which is consistent with $\Delta\phi^* = 0.48 \pm 0.10$ eV (Mean) and 0.47 ± 0.06 eV (M.P.V.) based on much data by experiment (see Table 5). However, it needs much further work to confirm the general applicability of Eq. (11) to any other metals.

4.4. Effect of the degree of monocrystallization (δ_{m}) upon both ϕ^{e} and ϕ^+ for polycrystal ($\delta_{\mathrm{m}} < 50\%$) and also submonocrystal ($50 < \delta_{\mathrm{m}} < 100\%$)

Considerations of the analytical results in Section 4.3 and of the data in Table 6 may lead to the conclusions as follows:

(1) Substitution of a probable combination of F_i and ϕ_i into Eqs. (1) and (2) affords the theoretical values of ϕ^+ and ϕ^{e} and also of $\Delta\phi^*$, each of which is usually expected to agree well or fairly with each value to be determined by experiment within the error of ± 0.1 eV. Namely, our model is useful for estimating theoretically the effective work functions (ϕ^+ and ϕ^{e}) of any polycrystalline surfaces probably within the uncertainty of less than ± 0.1 eV if the reliable data on F_i and ϕ_i are available for the surface under study.

(2) Typically for the four specimens (W(A)–W(D)) of polycrystalline tungsten ($\delta_{\mathrm{m}} = 0.336$–$0.463 < 0.5$) having a large difference in surface components (F_i's and ϕ_i's), all of the theoretical values of ϕ^+, ϕ^{e} and $\Delta\phi^*$ are in good agreement with the respective ones determined by experiment to within the discrepancy of ± 0.09 eV, as may readily be understandable from the comparison between the two data in Table 6. Typically, our theoretical value of (25) $\phi^{\mathrm{e}} = 4.52$ eV for the four actual specimens ($\delta_{\mathrm{m}} < 0.5$) well agrees with the experimental data on (26) $\phi^{\mathrm{e}} = 4.55$ eV [1351] and also with those on 4.50[#] eV [1665], 4.54 eV [1354] and 4.55 eV [1045,1358] recommended for polycrystalline W by other authors in Table 2. This agreement suggests such new information that the work function data on polycrystals listed in Table 2 may usually correspond to the surfaces of $\delta_{\mathrm{m}} < 0.5$.

(3) The above agreement between theory and experiment indicates that each of the three values (ϕ^+, ϕ^{e} and $\Delta\phi^*$) is generally common and nearly constant with little dependence upon the difference in specimen and hence in surface components (F_i's and ϕ_i's, changing considerably from specimen to specimen even of the same species) so long as $\delta_{\mathrm{m}} < 0.5$ corresponding to Eq. (10).

(4) The agreement and constancy found for W just above suggest that any species of the so called "polycrystals" may have a nearly constant value of ϕ^{e} among a variety of distinct specimens. This suggestion is strongly supported by the fact that every polycrystal ($\delta_{\mathrm{m}} < 0.5$ estimated in general) is found to have an essentially constant value characteristic of its surface species (see Column (3) in Table 2). In other wards, each polycrystal has the universal constancy in ϕ^{e} unique of the surface material (element) itself so long as $\delta_{\mathrm{m}} < 0.5$, thus giving a definite answer to the long pending problem why every "polycrystal" as well as every monocrystal is generally recognized to have a constant value of work function (ϕ^{e}) characteristic of its species. Quite similarly to ϕ^{e}, such a universal constancy for any polycrystal may be concluded also for both ϕ^+ and $\Delta\phi^*$ from the theoretical result (25) in Table 6. In addition, the constancy may be done also from the experimental data on ϕ^+ in Column (4) in Table 2 and from those on $\Delta\phi^*$ in Columns (6)–(8) in Table 5.

(5) Thus, our model leading to Eqs. (1), (2) and (10) furnishes a new and sound basis for supporting theoretically the experimental fact that every polycrystal ($\delta_{\mathrm{m}} < 0.5$ in general) has a nearly constant value (with the uncertainty of less than about ± 0.1 eV) of work function under the normal condition accepted in general, irrespective of a considerable difference in surface components (F_i's and ϕ_i's) among various specimens so long as $\delta_{\mathrm{m}} \equiv F_{\mathrm{m}} < 0.5$. In other words, it may be reasonable to interpret that the so-called "polycrystal" appearing in many publications is implicitly recognized to correspond to $\delta_{\mathrm{m}} < 0.5$ alone, instead of $\delta_{\mathrm{m}} < 1$ including the "submonocrystal". The above theoretical support may be considered a new contribution of our model to the work function studies developed to date.

(6) As described in (1)–(5) above, δ_{m} has such a strong governance as to keep each of ϕ^+, ϕ^{e} and $\Delta\phi^*$ to be nearly constant representatively of the surface species itself so long as $\delta_{\mathrm{m}} < 0.5$. On the contrary, ϕ_{m} belonging to δ_{m} does not possess such an impartial effect upon all of the work functions. Typically for W(A) of mainly W(112) and W(B) of mainly W(110) with $\delta_{\mathrm{m}} < 0.5$, their values of $\phi_{\mathrm{m}} = 4.69$ and 5.35 eV have a considerable effect upon the determination of $\phi^{\mathrm{e}} = 4.62$ eV and $\phi^+ = 5.18$ eV, respectively, but have little to do with $\phi^+ = 5.13$ eV and $\phi^{\mathrm{e}} = 4.61$ eV, respectively (see Footnotes (1)–(8) in Table 6). This differential effect originates in the emission predominance emphasized in Section 1. Namely, ϕ_{m} has less effect upon ϕ^{e} and ϕ^+ when ϕ_{m} is relatively higher and lower among ϕ_i's, respectively. In conclusion, it is not ϕ_{m} but δ_{m} that substantially governs all of ϕ^+, ϕ^{e} and $\Delta\phi^*$ under the condition of $\delta_{\mathrm{m}} < 0.5$, as shown in Footnote (25) in Table 6. Here, each of the three values is found to be nearly constant to within ± 0.1 eV, irrespective of the large difference in ϕ_{m} ranging from 4.25 to 5.35 eV among the four different specimens of W(A)–W(D). It should be emphasized here again that our theoretical results thus achieved (Footnote (25)) are strongly supported by the experimental data shown in Footnote (26) in Table 6.

(7) In the case of the "submonocrystal" ($0.5 < \delta_{\mathrm{m}} < 1$) corresponding to Eq. (11), on the contrary to any polycrystal ($\delta_{\mathrm{m}} < 0.5$) mentioned just above, ϕ^{e} as well as $\Delta\phi^*$ depends upon δ_{m}. Typically, W(E) of mainly W(110) ($\delta_{\mathrm{m}} = 0.80$) has $\phi^{\mathrm{e}} = 4.87 \pm 0.06$ eV, which is very different from $\phi^{\mathrm{e}} = 4.61 \pm 0.04$ eV for W(F) of mainly W(100) ($\delta_{\mathrm{m}} = 0.95$) (see Table 6). In addition, each of them is considerably or somewhat different from 4.56 ± 0.03 eV for W(poly) ($\delta_{\mathrm{m}} < 0.5$) and also largely or slightly different from 5.32 ± 0.02 eV for W(110) ($\delta_{\mathrm{m}} = 1.0$) or 4.65 ± 0.02 eV for W(100) ($\delta_{\mathrm{m}} = 1.0$) (see Column (3) in Table 2). Namely, any "submonocrystal" ($0.5 < \delta_{\mathrm{m}} < 1$) has such an anomaly that ϕ^{e} is not independent of δ_{m}, changing considerably according to the surface compositions (F_i's and ϕ_i's) without having a universal constancy unique of the surface material itself. With regard to such a work function dependence upon δ_{m} as certified theoretically for W-submonocrystals above, we can find many other examples here and there in Table 1. Typically, $\phi^{\mathrm{e}} = 4.80$ eV for Ni(100) ($\delta_{\mathrm{m}} = 0.95$) [283] and 4.68 eV for Ni(111) (0.89) [283] are radically different from any of 5.06 eV for Ni(poly) ($\delta_{\mathrm{m}} < 0.5$), 5.19 eV for Ni(100) ($\delta_{\mathrm{m}} = 1$) and 5.32 eV for Ni(111) ($\delta_{\mathrm{m}} = 1$) (see Table 2). About the work function for any element, therefore, submonocrystal ($0.5 < \delta_{\mathrm{m}} < 1$) should be treated *separately* as another type (category) different from both polycrystal ($\delta_{\mathrm{m}} < 0.5$) and monocrystal ($\delta_{\mathrm{m}} = 1$), as already pointed out in Aspect and Policy (7) in Section 3.1. For a given specimen, of course, the work function value of any submonocrystal becomes nearer to the unique value characteristic of the poly- or monocrystalline surface itself as δ_{m} approaches to 0.5 or 1. It should be emphasized here again that δ_{m} is the key factor governing mainly the work function at a different mode between poly- and submonocrystal according to the conditions of $\delta_{\mathrm{m}} < 0.5$

and $0.5 < \delta_m < 1$, respectively. Our new findings of both the "key factor" (δ_m) and the anomaly of "submonocrystal" ($0.5 < \delta_m < 1$) outlined above originate entirely from our simple model leading to Eqs. (1)–(3) and (10)–(12), and they may be considered as an additional contribution to the work function studies developed to date [4406].

(8) Regarding submonocrystals, theoretical studies are made for other metals, too. Typically for Ir(111) ($\delta_m = 0.81$) [169], ϕ^e is theoretically evaluated to be 5.36 eV [803], which is in good agreement with 5.35 eV [169] determined experimentally for the same specimen. However, they are different from both 5.75 eV for Ir(111) ($\delta_m = 1$) and 5.28 eV for Ir(poly) ($\delta_m < 0.5$) (Table 2), thus showing again the anomaly of submonocrystal. In addition, our theoretical value of $\Delta\phi^* \equiv \phi^+ - \phi^e = 5.73 \pm 0.01 - 5.36 \pm 0.07$ eV $= 0.37 \pm 0.07$ eV [803] is smaller than $\Delta\phi^* = 0.48$ and 0.47 eV for Ir(poly) (see Columns 6–8 in Table 5). This difference is quite natural because $\delta_m = 0.81$ for Ir (submonocrystal) [3414] is larger than that ($\delta_m < 0.5$) of the generally called "polycrystal". Namely, the former is near to the "monocrystal" ($\delta_m = 1$) having $\Delta\phi^* = 0.0$ eV (see Average at the bottom of Table 5). The tendency of $\Delta\phi^* \rightarrow 0$ as $\delta_m \rightarrow 1$ is typically shown for W in Fig. 1.

(9) So long as $\delta_m < 1$, therefore, distinction between ϕ^+ and ϕ^e is very important to avoid the systematic errors due to $\Delta\phi^*$, although $\Delta\phi^*$ itself has long been overlooked or ignored by many workers without considering or examining the homogeneity of work function over the surface under study. Such errors due to $\Delta\phi^*$ inherent in any polycrystals and submonocrystals are accompanied typically with the evaluation of β^+ from Eq. (5) and of E^+ or E^0 from Eq. (9), as already exemplified in Section 4.1.

(10) In a typical case of $\delta_m \approx 1.0$ such as W(G) with $\delta_m = 0.96$ for the (100) plane, of course, all of ϕ^+, ϕ^a and ϕ^e have a substantially common value ($\phi_m \approx 4.6$ eV) characteristic of the main surface components ($F(100) = 0.96$ and $\phi(100) = 4.60$ eV), as may be seen in Footnote (58) in Table 6. Namely, our theoretical values of $\phi^+ = 4.60$ eV and $\phi^e = 4.59$ eV are essentially equal to $\phi^+ = 4.60$ eV and $\phi^e = 4.57$ eV [1351] (see Footnote (62)) and also to $\phi^+ = 4.62$ eV and $\phi^e = 4.65$ eV (Table 2) recommended for W(100) according mainly to the experimental data.

(11) Our model leads to the conclusion that the sequence of $\phi^+ > \phi^a > \phi^e$ holds always for $\delta_m < 1$ independent of the species of both poly- and submonocrystal. For W(F) alone among W(A)–W(G), for example, it may seem to be the "exceptions" that Footnote (39) $\phi^a = 4.61$ eV $< \phi^e = 4.65$ eV and also that (41) $\phi^a = 4.54$ eV $< \phi^e = 4.57$ eV. Both of them, however, are concluded to be not real but only apparent, being entirely due to the disregard of $F(116) = 0.01$ in Footnote (35). This conclusion may readily be understandable from the comparison with the results that (40) $\phi^a = 4.65$ eV $> \phi^e = 4.64$ eV and that (42) $\phi^a = 4.58$ eV $> \phi^e = 4.56$ eV. For the calculated values of these (40) and (42), $F(116) = 0.01$ in Footnote (36) is tentatively taken into consideration by the present author so that the total of $\Sigma F(hkl)$ may be exactly equal to 1.00 in contrast to 0.99 due to the above disregard (35). Such a treatment is entirely because it is for the four planes of (100)–(112) alone that the data on (35) $F_i = 0.95$–0.02 are specified by the corresponding author [3414].

(12) As δ_m increases from ~ 0.5 up to ~ 1, $\Delta\phi^*$ converges gradually to zero, closely approaching to the usually called "monocrystalline" surface ($\phi^+ = \phi^a = \phi^e = \phi$ and $\Delta\phi^* = 0$), just as concluded by both theory and experiment (see Table 5). Here, ϕ is the "work function" generally used without distinction among ϕ^+, ϕ^a and ϕ^e. Of course, any monocrystal with $\delta_m = 1$ is generally expected to have the unique work function value characteristic of the surface species itself within the uncertainty of about ± 0.1 eV under the normal condition (see Table 2).

4.5. Anomaly of submonocrystal work functions (ϕ^+ and ϕ^e)

The conclusions (7) and (8) described in Section 4.4 open a novel aspect as follows. In terms of work function, elemental crystals should be classified into the three different types as follows.

(1) Polycrystal ($\delta_m < 0.5$) having a nearly constant value (within ± 0.1 eV in fluctuation) of each ϕ^e and ϕ^+ ($\Delta\phi^* > 0$) characteristic of its elemental species in spite of a considerable difference in the surface components (ϕ_i and F_i) among different specimens.

(2) Submonocrystal ($0.5 < \delta_m < 1$) having such an anomaly that both ϕ^e and ϕ^+($\Delta\phi^* > 0$) are strongly dependent upon δ_m and hence any of them doesn't possess the constant value unique of its elemental species.

(3) Monocrystal ($\delta_m = 1$) with $\phi^e = \phi^+ = $ constant and $\Delta\phi^* = 0$ characteristic of its surface species.

For better understanding the anomaly of the submonocrystal work functions together with the key factor of δ_m, let's consider the work function change in two different solid systems. As may be known very well, every binary alloy changes in ϕ^e depending upon its alloy component (γ_c) [2626,2634,4251,4253]. Typically, the alloy of Ag–Yb shows that its ϕ^e decreases nonlinearly from 4.5 eV (Ag) to 2.7 eV (Yb) as γ_c of Yb increases from 0 to 1 in mole fraction [4251]. Typically, ϕ^e is found to be about 3.5 and 2.9 eV at γ_c (Yb) $= 0.3$ and 0.8, respectively. Namely, ϕ^e of the alloy is not constant but variable with a strong dependence upon γ_c in the range of between 0 and 1, while $\gamma_c = 0$ and 1 alone yield the constant values of ϕ^e unique of the surface species of polycrystalline Ag and Yb, respectively. Comparison of the effect on the work function between the surface component (δ_m) and the alloy one (γ_c) indicates that the dependence of ϕ^e on δ_m (>0.5, but $\neq 1$) resembles strongly that on γ_c ($\neq 0$ and $\neq 1$). The anomaly of submonocrystal (cf. Conclusion (7) in Section 4.4) may readily be understood by consideration of the resemblance that δ_m (surface component) corresponds closely to γ_c (alloy component) in terms of the governance of work function in the two different solid systems [4406].

It should be emphasized here again that the work functions (ϕ^e and ϕ^+) of polycrystal ($\delta_m < 0.5$) remain nearly constant (within ± 0.1 eV in fluctuation) independently of the difference in both ϕ_i and F_i among various specimens of the same species, but that both ϕ^e and ϕ^+ of submonocrystal ($0.5 < \delta_m < 1$) are governed differentially by the ϕ_i's values lower and higher than the others according to the principle of emission predominance (see Section 1). Namely, δ_m functions as the key factor having the critical point of 0.5, above which any of ϕ^e, ϕ^+ and $\Delta\phi^*$ of submonocrystal has no longer the independency of δ_m ($0.5 < \delta_m < 1$) and also the constancy characteristic of its elemental species, quite similarly to the case of a binary alloy ($0 < \gamma_c < 1$) exemplified just above.

4.6. Contrast ($\Delta\phi^{**}$) between ϕ^- and ϕ^e

Comparison between Eqs. (2) and (3) predicts that $\Delta\phi^{**} \equiv \phi^- - \phi^e$ should be zero without depending upon the heterogeneity in work function over the entire surface because both negative ions and electrons are emitted predominantly from lower work function sites, on the contrary to positive ions to be done so from higher ones. To confirm the prediction of $\Delta\phi^{**} = 0$ eV, the present author has tried to find the experimental data on both ϕ^- and ϕ^e measured usually by NSI and TE, respectively, for the *same* specimen under substantially the same condition. In NSI as well as PSI, the working temperatures are selected to be high enough to avoid the surface contamination due to the incident sample beam or vapor, as already mentioned in Section 2.7.

Table 7
Thermionic contrast ($\Delta\phi^{**} \equiv \phi^- - \phi^e$) determined for the same surface specimen under substantially the same condition in each study.

No.	Surface	Beam	Ion	ϕ^- (eV)	ϕ^e (eV)	$\Delta\phi^{**}$ (eV)	Meths.	Refs.
				A. Monocrystalline Surface				
6	C(111)	I_2	I_2^-	5.4	5.4 ± 0.5^d	$0.0 \pm >0.5$	NSI, various	[3771, Here]
42	Mo(100)	CsI	I^-	4.29 ± 0.02	4.38 ± 0.04^d	-0.09 ± 0.04	NSI, various	[572, Here]
42	Mo(100)	I_2	I^-	4.36 ± 0.05	4.35 ± 0.05	0.01 ± 0.07	NSI, TE	[571]
42	Mo(100)	Br_2	Br^-	4.36 ± 0.06	4.35 ± 0.05	0.01 ± 0.08	NSI, TE	[925]
73	Ta(110)	F^+	F^-	4.86 ± 0.1	4.82 ± 0.06^d	0.04 ± 0.12	NSI, various	[604, Here]
73	Ta(110)	Cl^+	Cl^-	4.92 ± 0.1	4.82 ± 0.06^d	0.10 ± 0.12	NSI, various	[604, Here]
74	W(100)	Br_2	Br^-	4.53 ± 0.05	4.65 ± 0.02^d	-0.12 ± 0.05	NSI, various	[1658, Here]
74	W(100)	I_2	I_2^-	4.55 ± 0.05	4.53 ± 0.05	0.02 ± 0.07	NSI, TE	[571]
Mean	–	–	–	–	–	**-0.04 ± 0.02^e**	–	–
				B. Polycrystalline Surface				
6	C/Pt	UF_6	UF_6^-	4.4	4.4	0.0	NSI, TE	[675]
6	C/Pt–W(8%)	UF_6	UF_6^-	4.4	4.4	0.0	NSI, TF	[675]
6	C(ribbon)	N_2^+	CN^-	4.6 ± 0.2	4.63 ± 0.06^d	0.0 ± 0.2	NSI, various	[617, Here]
42	Mo	Ag	Ag^-	$(1.38 \pm 0.10)^a$	$(1.30)^b$	$0.08 \pm >0.10^c$	NSI, TE	[569,1351]
42	Mo	Au	Au^-	$(2.34 \pm 0.10)^a$	$(2.31)^b$	$0.03 \pm >0.10^c$	NSI, TE	[569,1351]
42	Mo	KI	I^-	$(3.08 \pm 0.07)^a$	$(3.06)^b$	$0.02 \pm >0.07^c$	NSI, TE	[569,1351]
73	Ta	Br^+	Br^-	4.22	4.37 ± 0.1	$-0.15 \pm >0.1$	NSI, TE	[600,641]
73	Ta	I^+	I^-	4.23	4.37 ± 0.1	$-0.14 \pm >0.1$	NSI, TE	[600,641]
73	Ta	Cl^+	Cl^-	4.28	4.37 ± 0.1	$-0.09 \pm >0.1$	NSI, TE	[600,641]
74	W	CsCl	Cl^-	4.46	4.56 ± 0.03^d	$-0.10 \pm >0.03$	NSI, various	[574, Here]
74	W	KCl	Cl^-	4.49	4.56 ± 0.03^d	$-0.07 \pm >0.03$	NSI, various	[574, Here]
74	W	KI	I^-	4.49	4.56 ± 0.03^d	$-0.07 \pm >0.03$	NSI, various	[574, Here]
74	W	I	I^-	4.49	4.51	-0.02	NSI, TE	[827]
74	W	–	W^-	4.5	4.56 ± 0.03^d	$-0.06 \pm >0.03$	NSI, various	[966, Here]
74	W	RbCl	Cl^-	4.51	4.56 ± 0.03^d	$-0.05 \pm >0.03$	NSI, various	[574, Here]
74	W	I_2	I^-	4.51	4.51	0.00	NSI, TE	[827]
74	W	SF_6	SF_6^-	4.54	4.56 ± 0.03^d	$-0.02 \pm >0.03$	NSI, various	[586, Here]
74	W	KBr	Br^-	4.58	4.56 ± 0.03^d	$0.02 \pm >0.03$	NSI, various	[574, Here]
74	W	H_2	H^-	$(0.8 \pm 0.1)^a$	$(0.75)^b$	$0.05 \pm >0.1^c$	NSI, TE	[587,1351]
74	W	Cl_2	Cl^-	$(3.72 \pm 0.04)^a$	$(3.62)^b$	$0.10 \pm >0.04^c$	NSI, TE	[588,1351]
74	W	$SnCl_4$	Cl^-	$(3.72 \pm 0.04)^a$	$(3.62)^b$	$0.10 \pm >0.04^c$	NSI, TE	[588,1351]
74	W	Br_2	Br^-	$(3.49 \pm 0.02)^a$	$(3.36)^b$	$0.13 \pm >0.02^c$	NSI, TE	[589,1351]
74	W	KI	I^-	$(3.08 \pm 0.07)^a$	$(3.06)^b$	$0.02 \pm >0.07^c$	NSI, TE	[569,1351]
74	W	I_2	I^-	$(3.1)^a$	$(3.06)^b$	0.04^c	NSI, TE	[591,1351]
74	W	I_2	I^-	$(3.14 \pm 0.07)^a$	$(3.06)^b$	$0.08 \pm >0.07^c$	NSI, TE	[590,1351]
74	W	Ag	Ag^-	$(1.38 \pm 0.10)^a$	$(1.30)^b$	$0.08 \pm >0.10^c$	NSI, TE	[569,1351]
74	W	Au	Au^-	$(2.34 \pm 0.10)^a$	$(2.31)^b$	$0.03 \pm >0.10^c$	NSI, TE	[569,1351]
90	Th	I_2	I^-	3.58	3.46	0.12	NSI, TE	[827]
90	Th	I	I^-	3.60	3.46	0.14	NSI, TE	[827]
Mean	–	–	–	–	–	**0.01 ± 0.07^e**	–	–

[a] Each value in parentheses is not ϕ^- but electron affinity (E) determined for a probing atom (Ag, Au, I, etc.) by the corresponding author(s).

[b] Each value in parentheses is not ϕ^e but the electron affinity (E^*) accepted today as the most probable value [577,578,972,973].

[c] Each of the contrasts is estimated from the difference ($\Delta\phi^{**} = E - E^*$) as the possible error due to the assumption that ϕ^- is equal to ϕ^e (see Table 12 in Ref. [1351]).

[d] Each value (e.g., $\phi^e = 4.38 \pm 0.03$ eV for Mo(100)) is cited tentatively from the most probable value in Table 2 [Here] because each of the corresponding references (e.g. [572]) has no data on ϕ^e characteristic of the surface specimen itself (e.g., Mo(100)) under study.

[e] Just as predicted theoretically by Eqs. (2) and (3), polycrystals as well as monocrystals are verified experimentally to have $\Delta\phi^{**} \approx 0.0$ eV in contrast to $\Delta\phi^* \approx 0.0$ eV for clean and smooth monocrystals alone and also to $\Delta\phi^* > 0.0$ eV for any polycrystals (see Table 5).

The results thus achieved for $\Delta\phi^{**}$ is summarized in Table 7. Here, the total data are much scanty, disappointingly, compared with those on $\Delta\phi^* \equiv \phi^+ - \phi^e$ summarized in Table 4. From the data in Table 7, however, we may draw the conclusions as follows.

Table 8 (*continued*)

Surface	D_s (atoms/10^{14} cm^2)	ϕ^e (eV)	ϕ^e (eV)	ϕ^e (eV)	ϕ^e (eV)	ϕ^e (eV)	ϕ^e (eV)
				Re. hcp[d]			
Re(0001)	15.1	5.26 ± 0.05	5.30 ± 0.21	5.53	5.59 ± 0.05	–	–
Re(1011)	14.3	–	5.26 ± 0.13	–	5.37 ± 0.03	5.55 ± 0.03	5.69 ± 0.06
Re(1010)	8.1	–	5.12 ± 0.05	5.20	5.15 ± 0.02	5.95 ± 0.15	5.52 ± 0.03
Meth.	–	CPD	various	TC	TE	FE	PE
Refs.	[340]	[3378]	[Here][a]	[1159,1980]	[402,3416]	[730]	[403]

[a] The data on ϕ^e [Here] are cited from the most probable values in Table 2.

[b] Its unit for Al is atoms/10^{18} cm^2.

[c] Regarding the triple set investigated for Al by the same worker(s) under the common condition, the present author has not yet found any data by CPD, FE, etc. other than PE and TC.

[d] To the best of the present author's knowledge, it is by TE alone that the complete set for Re is studied under the same condition and method.

As exemplified in Table 8, the data on W of the bcc-type show the normal trend that ϕ^e(hkl) decreases monotonically with decreasing D_s(hkl), irrespective of the difference in determination method, except PE having single datum alone [1273]. About the fcc-type of Ni, all the methods except FE [1898] affords the general trend well accordant to D_s(hkl). With respect to the hcp-type of Re(hkil), a similar tendency may be expectable, although the available data are much scanty than those of W and Ni and also they include one exception by FE [730] against the above trend.

Regarding the listed data on Al of fcc-type, in contrast to Ni, only two examples [556,612] follow the sequence of ϕ^e(111) > ϕ^e(100) > ϕ^e(110) with a decrease in D_s(hkl), in contrast to the four other examples [239,241], Here, [718] determined mainly by PE or TC. To the best of the present author's knowledge, the triple set of ϕ^e(hkl) determined by the same worker(s) using CPD, FE or TE has not yet been reported for Al. According to the examples shown in Table 8, the data on Al alone seem to be anomalous frequently to the corresponding sequence, in contrast to the others to be so rather seldom.

The above result strongly suggests it very interesting to examine carefully the problem whether the sequences of ϕ^e(110) > ϕ^e(100) > ϕ^e(111) for bcc-metals and also of ϕ^e(111) > ϕ^e(100) > ϕ^e(110) for fcc-ones in accordance with the decrease in D_s(hkl) may hold surely for many metals listed in Table 1. Many results to be thus examined will be discussed below in Sections 5.2–5.4. In addition, let's examine other anisotropic sequences of surface energy (ε) and melting point (T_m) in Section 5.5, where the quantitative relations between ε and ϕ^e and also between T_m and ϕ^e will be summarized briefly.

5.2. Examination of the anisotropic work function sequence for bcc-metals

From the above viewpoint, the present author has tried to examine the sequence of ϕ^e(110) > ϕ^e(100) > ϕ^e(111) for various bcc-metals by citing many triple sets of work function data from Table 1, where each set is investigated by the same worker(s) employing either the identical method under the same condition or the same theoretical model. The results thus obtained are summarized in Table 9, which shows the examination of the sequence found for 32 species of bcc-metals ranging from Li to U. Here, "Yes" and "No" mean that the sequence of ϕ^e(110) > ϕ^e(100) > ϕ^e(111) holds exactly and never, respectively. Especially, each triple sequence with double underlines for each metal species originates from the most probable values estimated by the present author using much data achieved by many groups of workers adopting various methods (see Table 2), and the sequence with a single underline comes from the data recommended previously in Table 2 in Ref. [1351]. Therefore, both of the two may be expected probably to be more accurate or reliable than any of the others based on a single method (or model) employed by an individual group of workers, although the data available for each metal in the latter [1351] are generally not so abundant as those in the former [Here].

Table 9

Examination of the work function sequence of ϕ^e(110) > ϕ^e(100) > ϕ^e(111) for the three principal planes of bcc metals.

No.	Metal.	ϕ^e(110) (eV)		ϕ^e(100) (eV)		ϕ^e(111) (eV)	Seq.	Meth.	Refs.
3	Li	2.40	=	2.40	>	2.30	No	TC	[475]
3	Li	2.78	>	2.61	>	2.58	Yes	TC	[1980]
3	Li	3.00	=	3.00	>	2.90	No	TC	[1095]
3	Li	3.09	>	2.92	>	2.90	Yes	TC	[231]
3	Li	3.18	>	3.11	>	2.96	Yes	TC	[711]
3	Li	3.221	>	2.986	>	2.746	Yes	TC	[4091]
3	Li	3.27	>	3.03	>	2.93	Yes	TC	[553]
3	Li	3.31	>	3.25	>	3.12	Yes	TC	[476,711]
3	Li	3.31	>	3.26	>	3.12	Yes	TC	[711]
3	Li	3.32	>	3.04	>	2.94	Yes	TC	[3467]
3	Li	3.37 ± 0.05	>	3.12 ± 0.03	>	3.04 ± 0.08	Yes	TC	[Here][a]
3	Li	3.40	>	3.36	<	3.44	No	TC	[637]
3	Li	3.43	>	3.03	<	3.12	No	TC	[637,2418]

Table 9 (*continued*)

No.	Metal.	$\phi^e(110)$ (eV)		$\phi^e(100)$ (eV)		$\phi^e(111)$ (eV)	Seq.	Meth.	Refs.
3	Li	3.43	>	3.28	>	3.15	Yes	TC	[3814]
3	Li	3.44	>	3.39	>	3.26	Yes	TC	[476]
3	Li	3.46	>	3.06	<	3.09	No	TC	[637,2418]
3	Li	3.5	>	3.4	>	3.2	Yes	TC	[1088]
3	Li	3.54	>	3.27	>	3.13	Yes	TC	[1237]
3	Li	3.55	>	3.30	>	3.25	Yes	TC	[475]
3	Li	3.55	>	3.32	>	3.13	Yes	TC	[556]
3	Li	3.58	>	3.30	>	3.16	Yes	TC	[1030]
3	Li	3.61	>	3.10	>	2.97	Yes	TC	[321]
3	Li	3.63	>	3.32	>	3.19	Yes	TC	[555]
3	Li	3.77	>	3.56	>	3.42	Yes	TC	[472]
3	Li	3.87	>	3.47	>	3.20	Yes	TC	[1030]
Conformity $(N_{yes}/N_{total})^d$				–		–	**80%**	–	–
11	Na	2.52	>	2.40	>	2.39	Yes	TC	[1159]
11	Na	2.75	>	2.58	>	2.54	Yes	TC	[231]
11	Na	2.76	>	2.60	>	2.57	Yes	TC	[3467]
11	Na	2.839	>	2.638	>	2.585	Yes	TC	[4091]
11	Na	2.86	>	2.69	>	2.63	Yes	TC	[4222]
11	Na	2.87	>	2.66	>	2.26	Yes	TC	[3477]
11	Na	2.88	>	2.66	>	2.59	Yes	TC	[553]
11	Na	2.9	>	2.7	>	2.6	Yes	TC	[2851]
11	Na	2.91	>	2.77	>	2.56	Yes	TC	[711]
11	Na	2.98	>	2.80	>	2.79	Yes	TC	[4398]
11	Na	2.99	>	2.80	>	2.77	Yes	TC	[4398]
11	Na	3.00	>	2.86	>	2.71	Yes	TC	[473]
11	Na	3.00	>	2.83	>	2.48	Yes	TC	[3477]
11	Na	3.00	>	2.80	>	2.79	Yes	TC	[721]
11	Na	3.04	>	2.89	>	2.72	Yes	TC	[3814]
11	Na	3.05 ± 0.04	>	2.80 ± 0.04	>	2.68 ± 0.06	Yes	TC	[Here]^a
11	Na	3.06	>	2.93	>	2.73	Yes	TC	[476,711]
11	Na	3.08	>	2.88	>	2.75	Yes	TC	[1030]
11	Na	3.1	>	2.9	>	2.8	Yes	TC	[1088]
11	Na	3.10	>	2.75	>	2.65	Yes	TC	[475]
11	Na	3.11	>	2.88	>	2.76	Yes	TC	[555]
11	Na	3.13	>	2.84	>	2.76	Yes	TC	[556]
11	Na	3.16	>	3.04	>	2.85	Yes	TC	[476]
11	Na	3.22	>	3.03	>	2.82	Yes	TC	[472,554]
11	Na	3.3	>	3.0	>	2.7	Yes	TC	[1088]
11	Na	3.33	>	3.07	>	2.79	Yes	TC	[1030]
11	Na	3.44	>	2.95	>	2.83	Yes	TC	[321]
11	Na	3.62	>	3.27	>	3.17	Yes	TC	[1095]
Conformity $(N_{yes}/N_{total})^d$				–		–	**100%**	–	–
19	K	2.35	>	2.25	>	2.24	Yes	TC	[1159,3067]
19	K	2.37	>	2.21	>	2.17	Yes	TC	[231]
19	K	2.372	>	2.24	>	2.18	Yes	TC	[4091]
19	K	2.43	>	2.26	>	2.21	Yes	TC	[3467]
19	K	2.44	>	2.27	>	2.19	Yes	TC	[553]
19	K	2.58	>	2.43	>	2.21	Yes	TC	[711]
19	K	2.72	>	2.51	>	2.39	Yes	TC	[1030]
19	K	2.74 ± 0.04	>	2.47 ± 0.04	>	2.39 ± 0.02	Yes	TC	[Here]^a
19	K	2.75	>	2.60	>	2.38	Yes	TC	[476,711]
19	K	2.75	>	2.40	>	2.35	Yes	TC	[475]
19	K	2.76	>	2.59	>	2.42	Yes	TC	[472]
19	K	2.82	>	2.68	>	2.48	Yes	TC	[476]
19	K	2.9	>	2.7	>	2.5	Yes	TC	[55,1088]
19	K	2.90	>	2.49	>	2.39	Yes	TC	[321]
19	K	2.96	>	2.55	>	2.40	Yes	TC	[3814]
19	K	3.01	>	2.71	>	2.45	Yes	TC	[1030]
19	K	3.15	>	2.80	>	2.75	Yes	TC	[1095]
Conformity $(N_{yes}/N_{total})^d$				–		–	**100%**	–	–
20	γ-Ca	4.09	>	3.52	>	3.37	Yes	TC	[321]
22	β-Ti	4.57	>	3.94	>	3.76	Yes	TC	[321]
22	β-Ti	$a_0 + 0.3673$	>	a_0	>	$a_0 - 0.3982$	Yes	TC	[4259]^f
23	V	4.52	>	3.88	>	3.72	Yes	TC	[321]

Table 9 (*continued*)

No.	Metal.	$\phi^e(110)$ (eV)		$\phi^e(100)$ (eV)		$\phi^e(111)$ (eV)	Seq.	Meth.	Refs.
23	V	4.96	>	4.29	>	4.10	Yes	TC	[2548]
23	V	4.97	>	4.28	>	4.11	Yes	TC	[1980,3067]
23	V	5.00	>	4.46	>	4.19	Yes	TE	[3695]
23	V	5.04 ± 0.07	>	4.27 ± 0.05	>	4.13 ± 0.04	Yes	various	[Here][a]
23	V	$b_0 + 0.3735$	>	b_0	>	$b_0 - 0.4237$	Yes	TC	[4259][f]
Conformity $(N_{yes}/N_{total})^d$				–		–	**100%**	–	–
24	Cr	4.44	>	4.27	>	3.78	Yes	TC	[4034]
24	Cr	4.53	>	3.90	>	3.72	Yes	TC	[321]
24	Cr	4.70	>	3.88	=	3.88	No	TC	[2818]
24	Cr	4.99 ± 0.19	>	4.43 ± 0.14	>	3.8 ± 0.1	Yes	various	[Here][a]
24	Cr	$c_0 + 0.4143$	>	c_0	>	$c_0 - 0.4319$	Yes	TC	[4259][f]
Conformity $(N_{yes}/N_{total})^d$				–		–	**80%**	–	–
25	δ-Mn	4.97	>	4.27	>	4.09	Yes	TC	[321]
25	δ-Mn	5.3 ± 0.3	>	4.8 ± 0.4	>	4.1	Yes	TC	[Here][a]
26	α-Fe	4.75	>	3.87	<	3.89	No	TC	[1625]
26	α-Fe	4.76	>	3.91	<	3.95	No	TC	[1625]
26	α-Fe	4.81	>	3.86	<	3.90	No	TC	[1619]
26	α-Fe	4.82	>	3.91	=	3.91	No	TC	[1619]
26	α-Fe	4.99 ± 0.04	>	4.64 ± 0.05	>	4.4 ± 0.3	Yes	various	[Here][a]
26	α-Fe	5.07 ± 0.04	>	4.60 ± 0.33	<	4.81 ± 0.29	No	various	[4088]
26	α-Fe	5.12	>	3.85	>	3.81	Yes	TC	[4222]
26	α-Fe	5.30	>	4.55	>	4.35	Yes	TC	[321]
Conformity $(N_{yes}/N_{total})^d$				–		–	**38%**	–	–
37	Rb	2.20	>	2.10	>	2.05	Yes	TC	[475]
37	Rb	2.243	>	2.115	>	2.096	Yes	TC	[4091]
37	Rb	2.28	>	2.12	>	2.08	Yes	TC	[231]
37	Rb	2.33	>	2.15	>	2.09	Yes	TC	[3467]
37	Rb	2.33	>	2.17	>	2.12	Yes	TC	[553]
37	Rb	2.40	=	2.40	>	2.22	No	TC	[472]
37	Rb	2.46	>	2.28	>	2.06	Yes	TC	[711]
37	Rb	2.49	>	2.36	>	2.26	Yes	TC	[1030]
37	Rb	2.56	>	2.41	>	2.25	Yes	TC	[3814]
37	Rb	2.57	>	2.47	>	2.42	Yes	TC	[1095]
37	Rb	2.63	>	2.45	>	2.23	Yes	TC	[476,711]
37	Rb	2.65	>	2.35	>	2.30	Yes	TC	[475]
37	Rb	2.65 ± 0.05	>	2.31 ± 0.08	>	2.21 ± 0.09	Yes	TC	[Here][a]
37	Rb	2.70	>	2.53	>	2.32	Yes	TC	[476]
37	Rb	2.72	>	2.54	>	2.28	Yes	TC	[1030,1089]
37	Rb	2.79	>	2.40	>	2.30	Yes	TC	[321]
37	Rb	2.9	>	2.6	>	2.3	Yes	TC	[1088]
Conformity $(N_{yes}/N_{total})^d$				–		–	**94%**	–	–
38	γ-Sr	2.63	<	2.71	<	2.80	No	TC	[1159]
38	γ-Sr	3.2 ± 0.6	>	3.0 ± 0.3	=	3.0 ± 0.2	No	TC	[Here][a]
38	γ-Sr	3.81	>	3.27	>	3.13	Yes	TC	[321]
39	β-Y	4.28	>	3.67	>	3.52	Yes	TC	[321]
39	β-Y	$d_0 + 0.303$	>	d_0	>	$d_0 - 0.355$	Yes	TC	[4246][f]
40	β-Zr	4.57	>	3.94	>	3.76	Yes	TC	[321]
40	β-Zr	$e_0 + 0.367$	>	e_0	>	$e_0 - 0.407$	Yes	TC	[4246][f]
41	Nb	4.488	>	3.552	<	3.775	No	TC	[4091]
41	Nb	4.51 ± 0.02	>	3.97 ± 0.02	<	4.08 ± 0.02	No	PE	[336]
41	Nb	4.61	>	3.96	>	3.80	Yes	TC	[321]
41	Nb	4.63 ± 0.17	>	4.08 ± 0.17	<	4.37 ± 0.19	No	various	[4088]
41	Nb	4.64^{+e}	>	4.04^+	>	3.78^+	Yes	PSI	[739]
41	Nb	4.74	>	4.06	>	3.93	Yes	TC	[2548]
41	Nb	$4.74 \pm 0.10^+$	>	4.04^+	>	$3.84 \pm 0.06^+$	Yes	PSI	[Here][a]
41	Nb	4.75	>	4.07	>	3.94	Yes	TC	[1159]
41	Nb	4.77 ± 0.05	>	4.02 ± 0.05	>	3.95 ± 0.09	Yes	various	[Here][a]
41	Nb	4.80	>	3.90	>	3.88	Yes	TE	[739]
41	Nb	4.80 ± 0.05	>	3.95 ± 0.03	>	3.88 ± 0.03	Yes	TE	[775,2811]

(*continued on next page*)

Table 9 (*continued*)

No.	Metal.	ϕ^e(110) (eV)		ϕ^e(100) (eV)		ϕ^e(111) (eV)	Seq.	Meth.	Refs.
41	Nb	4.83 ± 0.05	>	3.95 ± 0.05	>	3.86 ± 0.03	Yes	various	[1351][b]
41	Nb	4.87 ± 0.07	>	4.02 ± 0.06	<	4.36 ± 0.06	No	TE	[779]
41	Nb	4.90 ± 0.05	>	3.86 ± 0.05	>	3.84 ± 0.05	Yes	TE	[774]
41	Nb	$f_0 + 0.443$	>	f_0	>	$f_0 - 0.435$	Yes	TC	[4246][f]
41	Nb	$p_0 + 0.56$	>	p_0	>	$p_0 - 0.07$	Yes	TC	[4078][g]
Conformity (N_{yes}/N_{total})[d]				–		–	**75%**	–	–
42	Mo	4.32 ± 0.07	>	4.1 ± 0.1	<	4.33 ± 0.01	No	TE	[643]
42	Mo	4.510	>	3.842	<	3.940	No	TC	[4091]
42	Mo	4.59	>	4.01	>	4.00	Yes	TC	[4057]
42	Mo	4.64	>	4.06	>	3.86	Yes	TC	[4057]
42	Mo	4.7 ± 0.04	>	4.5 ± 0.04	<	4.8 ± 0.04	No	TE	[3344]
42	Mo	4.77	>	4.10	>	3.93	Yes	TC	[321]
42	Mo	4.81 ± 0.09	>	4.35 ± 0.02	>	4.00 ± 0.08	Yes	FE	[3691]
42	Mo	4.82	>	4.28	>	4.23	Yes	TC	[3224]
42	Mo	4.83	>	4.26	>	4.06	Yes	FE	[648]
42	Mo	4.84	>	4.28	<	4.30	No	TC	[1624]
42	Mo	4.85	>	4.20	<	4.27	No	TC	[639]
42	Mo	4.85 ± 0.05	>	4.40 ± 0.05	>	4.15 ± 0.05	Yes	TE	[323]
42	Mo	4.88	>	4.03	<	4.32	No	TC	[639]
42	Mo	4.90 ± 0.04	>	4.60 ± 0.04	>	4.35 ± 0.04	Yes	TE	[2244]
42	Mo	4.90 ± 0.05	>	4.43 ± 0.05	>	4.10 ± 0.05	Yes	TE	[781]
42	Mo	4.92 ± 0.05	>	4.46 ± 0.11	>	4.37 ± 0.24	Yes	various	[4088]
42	Mo	4.94	>	4.58	>	4.55	Yes	TC	[3224]
42	Mo	4.95 ± 0.02	>	4.53 ± 0.02	<	4.55 ± 0.02	No	PE	[325]
42	Mo	4.95 ± 0.05	>	4.43 ± 0.05	>	4.10 ± 0.05	Yes	TE	[739,1407]
42	Mo	4.96 ± 0.06	>	4.40 ± 0.03	>	4.09 ± 0.07	Yes	various	[1351][b]
42	Mo	4.98 ± 0.03	>	4.38 ± 0.03	>	4.29 ± 0.03	Yes	various	[Here][a]
42	Mo	5.00	>	4.45	>	4.20	Yes	FE	[1416]
42	Mo	5.00 ± 0.05	>	4.40 ± 0.02	>	4.10 ± 0.02	Yes	TE	[127,144]
42	Mo	5.1^+	>	$4.38 \pm 0.08^+$	>	$4.17 \pm 0.09^+$	Yes	PSI	[Here][a]
42	Mo	5.1	>	4.5	>	4.2	Yes	TE	[2339]
42	Mo	5.10 ± 0.03	>	4.40 ± 0.03	>	4.10 ± 0.03	Yes	TE	[727,3103]
42	Mo	5.10 ± 0.05	>	4.40 ± 0.05	>	4.15 ± 0.05	Yes	TE	[323]
42	Mo	5.10 ± 0.15	>	4.26 ± 0.03	>	3.94 ± 0.05	Yes	FE	[999]
42	Mo	5.11 ± 0.07	>	4.28 ± 0.01	>	3.99 ± 0.02	Yes	FE	[999,1668]
42	Mo	5.13	>	4.37	>	4.07	Yes	TC	[4034]
42	Mo	$5.13 \pm 0.03^+$	>	$4.37 \pm 0.07^+$	>	$4.07 \pm 0.13^+$	Yes	PSI	[1351][b]
42	Mo	$5.13 \pm 0.03^{+e}$	>	$4.44 \pm 0.03^+$	>	$4.13 \pm 0.03^+$	Yes	PSI	[727,3103]
42	Mo	5.23	>	4.43	>	4.25	Yes	TC	[2548]
42	Mo	5.23	>	4.44	>	4.27	Yes	TC	[1980]
42	Mo	5.4 ± 0.2	>	4.5 ± 0.1	>	4.3 ± 0.1	Yes	TE	[335,1650]
42	Mo	5.90	>	4.36	>	4.23	Yes	TC	[3224]
42	Mo	$q_0 + 0.43$	>	q_0	>	$q_0 - 0.22$	Yes	TC	[4078][g]
42	Mo	$g_0 + 0.470$	>	g_0	>	$g_0 - 0.453$	Yes	TC	[4246][f]
Conformity (N_{yes}/N_{total})[d]				–		–	**82%**	–	–
50	α-Sn	4.77	>	3.47	<	4.01	No	TC	[3211]
55	Cs	2.073	>	1.974	>	1.971	Yes	TC	[4091]
55	Cs	2.17	>	2.01	>	1.97	Yes	TC	[231]
55	Cs	2.19	>	2.04	>	2.01	Yes	TC	[553,2427]
55	Cs	2.21	>	2.03	>	1.98	Yes	TC	[3467]
55	Cs	2.23	>	2.14	=	2.14	No	TC	[1159]
55	Cs	2.25	>	1.90	>	1.80	Yes	TC	[475]
55	Cs	2.34	>	2.14	>	1.93	Yes	TC	[711]
55	Cs	2.35	>	2.23	>	2.14	Yes	TC	[1030]
55	Cs	2.44	>	2.28	>	2.14	Yes	TC	[3814]
55	Cs	2.51	>	2.31	>	2.10	Yes	TC	[476,711]
55	Cs	2.54 ± 0.07	>	2.24 ± 0.06	>	2.09 ± 0.08	Yes	TC	[Here][a]
55	Cs	2.56	>	2.40	>	2.14	Yes	TC	[1030,1089]
55	Cs	2.57	>	2.39	>	2.19	Yes	TC	[476]
55	Cs	2.59	>	2.24	>	2.14	Yes	TC	[1095]
55	Cs	2.60	>	2.24	>	2.14	Yes	TC	[321]
55	Cs	2.60	>	2.30	>	2.20	Yes	TC	[475]
55	Cs	2.62	>	2.36	>	2.24	Yes	TC	[555]
55	Cs	2.8	>	2.3	>	2.2	Yes	TC	[1086,1088]
Conformity (N_{yes}/N_{total})[d]				–		–	**94%**	–	–

Table 9 (*continued*)

No.	Metal.	ϕ^e(110) (eV)		ϕ^e(100) (eV)		ϕ^e(111) (eV)	Seq.	Meth.	Refs.
56	Ba	2.384	>	2.31	>	2.293	Yes	TC	[4091]
56	Ba	2.71	>	2.50	>	2.48	Yes	TC	[1159]
56	Ba	2.83	>	2.67	<	2.73	No	TC	[231]
56	Ba	2.88	>	2.68	<	2.72	No	TC	[3467]
56	Ba	3.21	>	3.15	>	2.85	Yes	TC	[476]
56	Ba	3.32	>	3.26	>	2.96	Yes	TC	[476]
56	Ba	3.46 ± 0.14	>	3.07 ± 0.06	>	2.81 ± 0.06	Yes	TC	[Here][a]
56	Ba	3.49	>	3.00	>	2.87	Yes	TC	[321]
56	Ba	3.56	>	3.06	>	2.86	Yes	TC	[1030]
56	Ba	3.58	>	3.42	>	2.85	Yes	TC	[1030]
Conformity $(N_{yes}/N_{total})^d$				–		–	**80%**	–	–
57	γ-La	3.76	>	3.23	>	3.09	Yes	TC	[321]
57	γ-La	$h_0 + 0.281$	>	h_0	>	$h_0 - 0.334$	Yes	TC	[4246][f]
58	γ-Ce	4.63	>	3.98	>	3.81	Yes	TC	[321]
59	β-Pr	3.86	>	3.32	>	3.17	Yes	TC	[321]
60	β-Nd	4.23	>	3.63	>	3.48	Yes	TC	[321]
62	Sm	3.76	>	3.23	>	3.09	Yes	TC	[321]
63	Eu	3.80	>	3.26	>	3.12	Yes	TC	[321]
64	β-Gd	4.13	>	3.55	>	3.40	Yes	TC	[321]
65	β-Tb	4.52	>	3.88	>	3.72	Yes	TC	[321]
71	β-Lu	4.13	>	3.54	>	3.39	Yes	TC	[321]
72	β-Hf	5.03	>	4.32	>	4.13	Yes	TC	[321]
72	β-Hf	4.31	>	3.30	<	3.35	No	TC	[4057]
72	β-Hf	4.31	>	3.30	<	3.39	No	TC	[4057]
72	β-Hf	$i_0 + 0.358$	>	i_0	>	$i_0 - 0.4177$	Yes	TC	[4246][f]
73	Ta	4.74	>	4.07	>	3.93	Yes	TC	[2548]
73	Ta	4.74 ± 0.09	>	4.10 ± 0.25	>	3.50 ± 0.21	Yes	various	[4088]
73	Ta	4.75	>	4.08	>	3.94	Yes	TC	[1980]
73	Ta	4.77	>	3.83	<	3.93	No	TC	[1200]
73	Ta	4.78	>	3.83	<	3.96	No	TC	[1200]
73	Ta	4.80 ± 0.02	>	4.15 ± 0.02	>	4.00 ± 0.02	Yes	TE	[127,144]
73	Ta	4.81 ± 0.05	>	4.17 ± 0.09	>	4.00 ± 0.04	Yes	various	[1351][b]
73	Ta	4.82 ± 0.06	>	4.15 ± 0.05	>	4.01 ± 0.04	Yes	various	[Here][a]
73	Ta	4.83 ± 0.05	>	4.12 ± 0.05	>	3.98 ± 0.05	Yes	TE	[739,798]
73	Ta	$4.84 \pm 0.02^+$	>	4.20^+	>	$4.00 \pm 0.05^+$	Yes	PSI	[Here][a]
73	Ta	$4.84 \pm 0.04^+$	>	$4.20 \pm 0.04^+$	>	$4.00 \pm 0.04^+$	Yes	PSI	[797]
73	Ta	$4.85 \pm 0.05^+$	>	$4.20 \pm 0.04^+$	>	$4.00 \pm 0.05^+$	Yes	PSI	[1351][b]
73	Ta	4.86	>	4.04	>	3.51	Yes	TC	[1200]
73	Ta	4.87	>	4.11	>	3.50	Yes	CT	[1200]
73	Ta	4.95	>	4.10	>	3.95	Yes	FE	[796]
73	Ta	4.964	>	4.096	<	4.201	No	TC	[4091]
73	Ta	5.16	>	4.44	>	4.25	Yes	TC	[321]
73	Ta	$r_0 + 0.29$	>	r_0	>	$r_0 - 0.36$	Yes	TC	[4078][g]
73	Ta	$j_0 + 0.499$	>	j_0	>	$j_0 - 0.491$	Yes	TC	[4246][f]
Conformity $(N_{yes}/N_{total})^d$				–		–	**84%**	–	–
74	W	4.58	>	4.52	>	4.38	Yes	TE	[150]
74	W	4.6	>	4.54	<	5.3	No	FE	[2714]
74	W	4.65	>	4.53	>	4.38	Yes	TE	[2706]
74	W	4.65 ± 0.02	>	4.56 ± 0.02	>	4.35 ± 0.02	Yes	TE	[149]
74	W	4.66 (4.58)	>	4.52	>	4.38 ± 0.02	Yes	TE	[150]
74	W	4.67 ± 0.05	>	4.55 ± 0.05	>	4.26 ± 0.05	Yes	TE	[1663,2012]
74	W	4.758	>	4.090	<	4.240	No	TC	[4091]
74	W	4.9	>	4.6	>	4.4	Yes	FE	[1463]
74	W	4.92	>	4.48	>	4.45	Yes	TE	[352]
74	W	5.0 ± 0.2	>	4.6 ± 0.1	>	4.4 ± 0.1	Yes	TE	[335,1650]
74	W	5.02 ± 0.03	>	4.59 ± 0.02	>	4.49 ± 0.02	Yes	FE	[502]
74	W	5.025	>	4.37	<	4.381	No	TC	[4189]

Table 9 (*continued*)

No.	Metal.	ϕ^e(110) (eV)		ϕ^e(100) (eV)		ϕ^e(111) (eV)	Seq.	Meth.	Refs.
74	W	5.09	>	4.40	>	4.35	Yes	TE	[141]
74	W	5.11	>	4.46	>	4.41	Yes	TC	[3224]
74	W	5.11 ± 0.02	>	4.65 ± 0.04	>	4.45	Yes	CPD	[1056]
74	W	5.13	>	4.50	>	4.44	Yes	TC	[4405]
74	W	5.13 ± 0.02	>	4.65 ± 0.02	>	4.60 ± 0.02	Yes	CPD	[582]
74	W	5.14 ± 0.03[+e]	>	4.66 ± 0.03[+]	>	4.42 ± 0.03[+]	Yes	PSI	[3103]
74	W	5.15	>	4.54	>	4.49	Yes	TC	[3224]
74	W	5.15 ± 0.02	>	4.65 ± 0.02	>	4.45 ± 0.02	Yes	CPD	[3088]
74	W	5.17 ± 0.01	>	4.54 ± 0.01	>	4.44 ± 0.02	Yes	TE	[3349]
74	W	5.18	>	4.64	>	4.61[c]	Yes	TE	[212]
74	W	5.18	>	4.64	<	4.67[c]	No	TE	[212]
74	W	5.18	>	4.58	<	4.60	No	TC	[531]
74	W	5.2	>	4.64	>	4.6	Yes	TE	[212]
74	W	5.2	>	4.6	>	4.2	Yes	TE	[1958]
74	W	5.20	>	4.963	>	4.562	Yes	TC	[365]
74	W	5.20	>	4.56	>	4.50	Yes	TC	[3224]
74	W	5.22 ± 0.01	>	4.54 ± 0.01	=	4.54 ± 0.01	No	TE	[1053]
74	W	5.24 ± 0.03	>	4.62 ± 0.03	>	4.59 ± 0.03	Yes	TE	[1793]
74	W	5.25	>	4.65	>	4.47	Yes	FE	[489]
74	W	5.25 ± 0.02	>	4.63 ± 0.02	>	4.47 ± 0.02	Yes	FE	[358,3092]
74	W	5.26	>	4.52	>	4.38	Yes	TE	[150]
74	W	5.26	>	4.56	>	4.44	Yes	TC	[1271]
74	W	5.26	>	4.69	>	4.43	Yes	TE	[2187,3664]
74	W	5.269	>	4.979	>	4.500	Yes	TC	[365]
74	W	5.28 ± 0.11[+]	>	4.62 ± 0.06[+]	>	4.45 ± 0.04[+]	Yes	PSI	[Here][a]
74	W	5.29 ± 0.08[+]	>	4.60 ± 0.05[+]	>	4.45 ± 0.05[+]	Yes	PSI	[1351][b]
74	W	5.3	>	4.5	>	4.4	Yes	CPD	[259]
74	W	5.3	>	4.60	>	4.40	Yes	TE	[3096]
74	W	5.30	>	4.60	>	4.45	Yes	FE	[3508]
74	W	5.30 ± 0.03	>	4.60 ± 0.03	>	4.40 ± 0.03	Yes	TE	[3103]
74	W	5.30 ± 0.05	>	4.61 ± 0.05	>	4.40 ± 0.05	Yes	TE	[2214,2217]
74	W	5.31 ± 0.05	>	4.57 ± 0.03	>	4.38 ± 0.04	Yes	various	[1351][b]
74	W	5.32	>	4.59	>	4.51	Yes	CPD	[1274]
74	W	5.32 ± 0.02	>	4.65 ± 0.02	>	4.45 ± 0.03	Yes	various	[Here][a]
74	W	5.32 ± 0.10	>	4.93 ± 0.06	>	4.45 ± 0.05	Yes	FE	[819]
74	W	5.33 ± 0.03	>	4.76 ± 0.05	>	4.40 ± 0.03	Yes	TE	[372,3064]
74	W	5.345	>	5.009	>	4.500	Yes	TC	[365]
74	W	5.35 ± 0.05	>	4.60 ± 0.05	>	4.40 ± 0.02	Yes	TE	[127]
74	W	5.40 ± 0.05	>	4.55 ± 0.05	>	4.42 ± 0.03	Yes	TE	[143]
74	W	5.44	>	4.63	>	4.55	Yes	TC	[357]
74	W	5.44 ± 0.14	>	4.70 ± 0.06	>	4.44 ± 0.03	Yes	various	[4088]
74	W	5.5 ± 0.2	>	4.6 ± 0.1	>	4.2 ± 0.1	Yes	FE	[3033]
74	W	5.50	>	4.65	>	4.46	Yes	TC	[2548]
74	W	5.50	>	4.66	>	4.47	Yes	TC	[1980]
74	W	5.54	>	4.60	>	4.54	Yes	TE	[2187,3664]
74	W	5.54	>	4.50	<	5.60	No	TC	[4117]
74	W	5.6	>	4.6	>	3.9	Yes	FE	[1964]
74	W	5.66 ± 0.03	>	4.83 ± 0.02	>	4.47 ± 0.03	Yes	FE	[999]
74	W	5.70	>	4.70	>	4.54	Yes	FE	[812]
74	W	5.73	>	4.67	>	4.59	Yes	TC	[3224]
74	W	5.75	>	4.49	>	4.38	Yes	TC	[4405]
74	W	5.75 ± 0.03	>	4.83 ± 0.02	>	4.47 ± 0.03	Yes	FE	[999]
74	W	5.75 ± 0.15	>	4.6	=	4.6	No	FE	[3079]
74	W	5.79	>	4.78	>	4.35	Yes	FE	[373]
74	W	5.79	>	4.47	<	4.49	No	FE	[378]
74	W	5.8	>	4.9	>	4.6	Yes	FE	[3438]
74	W	5.8 ± 0.3	>	4.93 ± 0.06	>	4.45 ± 0.05	Yes	FE	[819]
74	W	5.80 ± 0.05	>	4.90 ± 0.03	>	4.60 ± 0.05	Yes	FE	[813]
74	W	5.83	>	4.89	>	4.68	Yes	FE	[653]
74	W	5.85	>	4.82	>	4.41	Yes	FE	[267]
74	W	5.9	>	4.82	>	4.41	Yes	FE	[2324]
74	W	5.93	>	4.77	>	4.4	Yes	FE	[2766]
74	W	6.0	>	4.70	>	4.43	Yes	FE	[809]
74	W	6.00	>	4.65	>	4.40	Yes	FE	[1276]
74	W	6.28 ± 0.08	>	4.93 ± 0.06	>	4.45 ± 0.05	Yes	FE	[819]
74	W	6.35	>	4.98	>	4.57	Yes	FE	[1057]
74	W	6.5	>	4.54	<	5.3	No	FE	[2714]
74	W	$s_0 + 0.52$	>	s_0	>	$s_0 - 0.31$	Yes	TC	[4078][g]
74	W	$k_0 + 0.538$	>	k_0	>	$k_0 - 0.520$	Yes	TC	[4246][f]

(continued on next page)

Table 9 (*continued*)

No.	Metal.	ϕ^e(110) (eV)		ϕ^e(100) (eV)		ϕ^e(111) (eV)	Seq.	Meth.	Refs.
Conformity (N_{yes}/N_{total})[d]				–		–	**89%**	–	–
81	β-Tl	4.10	>	3.52	>	3.36	Yes	TC	[321]
92	γ-U	4.07	>	3.49	>	3.33	Yes	TC	[321]

[a] Each of the work function data with double underlines is cited from the most probable value listed in Table 2 [Here].

[b] Similarly, each of the data with a single underline is cited from the value recommended in Table 2 in the previous review [1351].

[c] The values of ϕ^e(111) = 4.61 and 4.67 eV for W(111) [212] are determined at $P(O_2) = 5 \times 10^{-10}$ Torr and $T = 1900$ K and done at 5×10^{-8} Torr and 2200 K, respectively, thereby yielding the result that the sequence changes from Yes to No in accordance with the work function increase by 0.06 eV due to the oxygen gas pressure increase. Both of the above values, however, are considerably larger than 4.45 eV recommended in Table 2, although 4.64 eV for W(100) [212] well agrees with 4.65 eV [Here].

[d] In the last line for each metal with $N_{total} \geq 5$, the conformity ($C_Y \equiv N_{yes}/N_{total}$) of the listed triple sets to the Smoluchowski rule is entered, where N_{yes} and N_{total} are the number of the sequence corresponding to Yes and that including both Yes and No, respectively. As may be seen above, many of the metals have very high values of $C_Y \approx$ 80–100%.

[e] These work function values such as ϕ(110) = 4.64$^+$ eV for Nb(110) [739], 5.13 ± 0.03$^+$ eV for Mo(110) [727,3103] and 5.14 ± 0.03$^+$ eV for W(110) [3103] are not ϕ^e but ϕ^+ determined by positive surface ionization of Cs [739] or Na [727,3103].

[f] The absolute values of a_0–c_0 [4259] and d_0–k_0 [4246] are not listed anywhere in the tables [4246,4259].

[g] None of the absolute valves (p_0–s_0) is given in the table [4078].

On the last line for each metal, the conformity ($C_Y \equiv N_{yes}/N_{total}$) of the listed triple sets following the Smoluchowski rule [1040] is entered, where N_{yes} and N_{total} are the numbers of the sequence corresponding to Yes and of that including both Yes and No, respectively. However, C_Y is omitted for any of the metals with N_{total} less than three.

In Table 9, "Yes" is found for all of the sequences (C_Y = 100%) listed for Na, K and V ($N_{total} \geq 6$) and also for γ-Ca, β-Ti, δ-Mn, β-Y, β-Zr, γ-La, γ-Ce, β-Pr, β-Nd, Sm, Eu, β-Gd, β-Tb, β-Lu, β-Tl and γ-U ($N_{total} \leq 2$). In addition, very high percentages of "Yes" (C_Y = 75–94%) are found for Li, Rb, Nb, Mo, Cs, Ba, Ta and W (N_{total} = 10–81) as well as Cr (C_Y = 80%, N_t = 5). Quite similarly in the former cases (Na–V), all of our present sequences [Here] originating from the most probable values in Table 2 have "Yes", of course, together with the latter cases (Li–W and Cr), too. On the other hand, α-Fe, γ-Sr and β-Hf are found to have a very small value of C_Y = 38, 33 and 50%, respectively, while α-Sn (N_{total} = 1) has C_Y = 0% [3211]. These results are probably due to the poverty in set size (N_{total} = 8, 3, 4 or 1 alone) and, hence, they may be less reliable than the others (C_Y = 75–100%) based on N_{total} = 10–78. Therefore, much further study is needed to answer definitely the question whether the above four species (α-Fe, γ-Sr, α-Sn and β-Hf) do not obey inherently the Smoluchowski rule. Except the four species to be pendent, almost all the bcc-metals listed in Table 9 may be concluded to follow faithfully the sequence of ϕ^e(110) > ϕ^e(100) > ϕ^e(111). Consequently, all of the examples (except the four above) having "No" may be considered to indicate that at least one of the three values for each triple set is inaccurate or incorrect. Typically, all of ϕ^e(100) = 3.86, 3.87 and 3.91 eV by TC for α-Fe(100) [1619,1625] mentioned above to be pendent are extremely smaller than our most probable value of 4.64 ± 0.05 eV [Here] and also than the others of both 4.67 eV [1045,1358] and 4.59 eV [1351] recommended in Table 2. This is probably the main reason why the conformity is reduced to 38% from 50% or more that might be expected from the other sequences alone [Here, 321,4088,4222] except the above four [1619,1625]. In other words, the real value of C_Y for α-Fe will be improved to be much larger than ∼50% by further investigations.

As additional examples for several bcc-metals, a theoretical study yields the anomalous sequence of ϕ^e(110) > ϕ^e(100) < ϕ^e(111) for Nb, Mo, Ta and W [4091], whilst it gains the normal one of ϕ^e(110) > ϕ^e(100) > ϕ^e(111) for the five species of such alkali metals and Ba [4091]. Similarly to fcc-metals to be discussed mainly in the next section, the study [4091] yields ϕ^e(111) > ϕ^e(100) < ϕ^e(110) for fcc-metals (Ca and Sr), on the contrary to ϕ^e(111) > ϕ^e(100) > ϕ^e(110) for fcc-transition metals (typically, Ni, Cu, Rh, Pd and Ag having C_Y = 90–100%) to be shown in Table 10. These results against the above rule [1040] suggest that the theoretical calculation should be examined by further investigation.

It should be pointedly emphasized that ϕ^+(110) > ϕ^+(100) > ϕ^+(111) based on PSI also holds for the bcc-metals of Nb [739, Here], Mo [727,1351,3103, Here], Ta [797,1351, Here] and W [1351,3103, Here], quite similarly to each of their sequences of ϕ^e(hkl). The former is our new finding reported here first, and also it does support strongly our theoretical model that ϕ^+(hkl) is equivalent to ϕ^e(hkl) for clean monocrystalline samples, just as concluded directly from Eqs. (1) and (2).

5.3. Examination of the anisotropic work function sequence for fcc-metals

Quite similarly as above, many triple sets for fcc-metals are cited from Table 1 in order to examine the sequence of ϕ^e(111) > ϕ^e(100) > ϕ^e(110) corresponding to D_s(111) > D_s(100) > D_s(110). As shown in Table 10, "Yes" is found entirely ($C_Y \equiv N_{yes}/N_{total}$ = 100%) for β-Sc, γ-Mn, γ-Fe, β-Co, Ni and Rh (N_{total} = 1–17), while "No" is done seldom ($I_N \equiv N_{no}/N_{total} \leq 10$%) for Cu, Pd, and Ag ($N_{total}$ = 12–44). Here, I_N is the inconformity, while N_{no} and N_{total} are the numbers of the sequence having "No" and of the total one including both "No" and "Yes", respectively. Regarding the above eight species (γ-Mn to Rh and Cu to Ag, $C_Y \geq 90$%), "Yes" is observed also for all of our sequences [Here] based on the most probable values in Table 2. Quite similarly as in the cases of bcc-metals mentioned in Section 5.2, the sequence of ϕ^+(111) > ϕ^+(100) > ϕ^+(110) determined by PSI is found to hold for the

fcc-metal of Ni, too [Here, 283,630]. Again, this is the interesting and important finding reported here first, as already mentioned in Section 5.2 just above.

Table 10
Examination of the work function sequence of $\phi^e(111) > \phi^e(100) > \phi^e(110)$ for the three principal planes of <u>fcc</u> metals.

No.	Metal	$\phi^e(111)$ (eV)		$\phi^e(100)$ (eV)		$\phi^e(110)$ (eV)	Seq.	Meth.	Refs.
13	Al	3.11 ± 0.10	<	3.38 ± 0.07	<	3.80	No	PE	[239]
13	Al	3.13	<	3.22	>	2.83	No	TC	[2697]
13	Al	3.47	<	4.16	>	3.95	No	TC	[1030,1089]
13	Al	3.48	<	3.83	<	4.10	No	TC	[476]
13	Al	3.72	>	3.62	<	3.81	No	TC	[231]
13	Al	3.73	<	4.06	<	4.28	No	TC	[476]
13	Al	3.73	>	3.63	<	3.82	No	TC	[3467]
13	Al	3.77	>	3.71	>	3.60	Yes	TC	[473][20]
13	Al	3.86	<	3.87	<	3.88	No	TC	[3004]
13	Al	3.9	>	3.8	>	3.7	Yes	TC	[2982]
13	Al	3.92	<	4.30	>	3.89	No	TC	[1030]
13	Al	4.0	<	4.7	>	4.5	No	TC	[1088]
13	Al	4.02	<	4.30	>	4.09	No	TC	[4087,4410]
13	Al	4.05	<	4.20	>	3.65	No	TC	[475]
13	Al	4.05	<	4.27	>	4.06	No	TC	[4233]
13	Al	4.059	>	3.782	>	3.642	Yes	TC	[1626]
13	Al	4.06	<	4.24	>	4.07	No	TC	[1175]
13	Al	4.08	<	4.29	>	4.11	No	TC	[4233]
13	Al	4.09	>	3.77	>	3.59	Yes	TC	[553][20]
13	Al	4.1	=	4.1	>	3.7	No	TC	[2851]
13	Al	4.1	>	3.9	>	3.8	Yes	TC	[1088]
13	Al	4.117	>	3.805	>	3.643	Yes	TC	[1626,2914]
13	Al	4.12	>	3.92	>	3.73	Yes	TC	[1159]
13	Al	4.17	<	4.36	>	4.19	No	TC	[1943]
13	Al	4.17	<	4.27	>	3.87	No	TC	[3004]
13	Al	4.18	<	4.27	>	3.88	No	TC	[555,715]
13	Al	4.18	<	4.38	>	4.20	No	TC	[1943]
13	Al	4.181	>	3.831	>	3.643	Yes	TC	[1626]
13	Al	4.19	<	4.41	>	4.20	No	TC	[557]
13	Al	4.19	<	4.30	>	3.85	No	TC	[1435]
13	Al	4.2	>	4.1	>	3.7	Yes	TC	[2851]
13	Al	4.21	=	4.21	=	4.21	No	TC	[2548]
13	Al	4.22	<	4.46	>	4.26	No	TC	[1943]
13	Al	4.23	<	4.42	>	4.29	No	TC	[482,721,4398]
13	Al	4.24 ± 0.02	<	4.41 ± 0.03	>	4.28 ± 0.02	No	PE	[241,242]
13	Al	4.24 ± 0.04	<	4.28 ± 0.05	>	4.05 ± 0.06	No	various	[Here][a]
13	Al	4.25	<	4.38	>	4.30	No	TC	[561,721,4398]
13	Al	4.25	<	4.50	>	4.25	No	TC	[3203]
13	Al	4.25	<	4.30	>	4.17	No	TC	[723][19]
13	Al	4.26 ± 0.03	>	4.20 ± 0.03	>	4.06 ± 0.03	Yes	PE	[612]
13	Al	4.27	>	4.25	>	4.02	Yes	TC	[556]
13	Al	4.28 ± 0.04	<	4.36 ± 0.10	>	4.21 ± 0.09	No	various	[1351][b]
13	Al	4.3	<	4.4	>	4.2	No	TC	[2905]
13	Al	4.31	>	4.27	>	3.92	Yes	TC	[4401]
13	Al	4.31 ± 0.03	<	4.51 ± 0.03	>	4.32 ± 0.03	No	TC	[718]
13	Al	4.32 ± 0.06	>	4.31 ± 0.18	>	4.23 ± 0.13	Yes	various	[4088]
13	Al	4.32	>	4.00	>	3.76	Yes	TC	[321]
13	Al	4.32	<	4.56	>	4.36	No	TC	[1943]
13	Al	4.33	<	4.43	>	4.28	No	TC	[4117]
13	Al	4.60	<	4.69	>	4.30	No	TC	[2697]
13	Al	4.75	<	4.90	>	4.35	No	TC	[1095]
13	Al	4.77	<	4.86	>	4.47	No	TC	[2697]
13	Al	4.81	>	4.69	>	3.97	Yes	TC	[1563]
13	Al	4.99	>	4.85	>	4.44	Yes	TC	[3477][20]
13	Al	5.35	>	5.24	>	4.91	Yes	TC	[3477][20]
13	Al	$\phi(111)$	>	$\phi(100)$	>	$\phi(110)$	Yes	TC	[227][20]
Conformity $(N_{yes}/N_{total})^e$				–		–	**32%**	–	–
20	Ca	2.916	>	2.758	<	2.813	No	TC	[4091]
20	Ca	2.98	>	2.87	>	2.83	Yes	TC	[4222]
20	Ca	3.10	>	2.94	>	2.92	Yes	TC	[231]
20	Ca	3.14	>	2.97	>	2.92	Yes	TC	[3467]
20	Ca	3.35	<	3.38	>	3.29	No	TC	[476]
20	Ca	3.49	<	3.52	>	3.41	No	TC	[476]

Table 10 (*continued*)

No.	Metal	ϕ^e(111) (eV)		ϕ^e(100) (eV)		ϕ^e(110) (eV)	Seq.	Meth.	Refs.
20	Ca	3.5 ± 0.2	>	3.4 ± 0.4	>	3.3 ± 0.3	Yes	TC	[Here][a]
20	Ca	3.68	<	3.96	>	3.43	No	TC	[1030]
20	Ca	3.70	>	3.57	>	3.20	Yes	TC	[1030]
20	Ca	4.40	>	4.09	>	3.84	Yes	TC	[321]
Conformity (N_{yes}/N_{total})[e]				–		–	60%	–	–
21	β-Sc	4.73	>	4.39	>	4.13	Yes	TC	[321]
25	γ-Mn	5.36	>	4.97	>	4.67	Yes	TC	[321]
25	γ-Mn	5.3 ± 0.1	>	5.2 ± 0.3	>	4.7	Yes	TC	[Here][a]
26	γ-Fe	5.70	>	5.28	>	4.97	Yes	TC	[321]
26	γ-Fe	5.6 ± 0.1	>	5.3 ± 0.2	>	5.0	Yes	various	[Here][a]
27	β-Co	5.68	>	5.25	>	4.95	Yes	TC	[321]
27	β-Co	5.39 ± 0.23	>	5.25 ± 0.17	>	5.0	Yes	various	[Here][a]
27	β-Co	$a_0 + 0.1574$	>	a_0	>	$a_0 - 0.3448$	Yes	TC	[4259][h]
28	Ni	5.11	>	4.97	>	4.6	Yes	TC	[311]
28	Ni	5.22	>	4.86	>	4.69	Yes	TC	[3224]
28	Ni	5.22 ± 0.03	>	4.89 ± 0.03	>	4.64 ± 0.03	Yes	TE	[312,837]
28	Ni	5.24 ± 0.07	>	5.17 ± 0.11	>	4.72 ± 0.13	Yes	various	[4088]
28	Ni	5.28 ± 0.05	>	5.23 ± 0.10	>	4.64 ± 0.05	Yes	various	[1351][b]
28	Ni	5.3[+f]	>	5.2[+]	>	5.0[+]	Yes	PSI	[Here][a]
28	Ni	5.3 ± 0.1	>	5.1 ± 0.1	>	4.7 ± 0.1	Yes	CPD	[1110]
28	Ni	5.32 ± 0.05	>	5.19 ± 0.05	>	4.96 ± 0.10	Yes	various	[Here][a]
28	Ni	5.33 ± 0.01[+f]	>	5.21 ± 0.01[+]	>	5.03 ± 0.01[+g]	Yes	TC	[283,630]
28	Ni	5.35 ± 0.05	>	5.22 ± 0.04	>	5.04 ± 0.02	Yes	PE	[314,315]
28	Ni	5.40 ± 0.15	>	5.2 ± 0.15	>	4.85 ± 0.15	Yes	CPD	[1791]
28	Ni	5.50	>	5.31	>	4.90	Yes	TC	[1237]
28	Ni	5.56	>	5.19	>	4.84	Yes	TC	[2548]
28	Ni	5.56	>	5.20	>	4.84	Yes	TC	[1980]
28	Ni	5.6	>	5.4	>	5.1	Yes	TC	[2905]
28	Ni	$b_0 + 0.1651$	>	b_0	>	$b_0 - 0.3438$	Yes	TC	[4259][h]
28	Ni	$x_0 + 0.21$	>	x_0	>	$x_0 - 0.38$	Yes	TC	[4078][i]
Conformity (N_{yes}/N_{total})[e]				–		–	100%	–	–
29	Cu	3.90	>	3.80	>	3.55	Yes	TC	[475]
29	Cu	4.123	>	3.855	>	3.648	Yes	TC	[2914]
29	Cu	4.24	>	4.12	>	3.98	Yes	TC	[947]
29	Cu	4.381	<	4.412	>	4.408	No	TC	[1118]
29	Cu	4.50	>	4.27	>	4.23	Yes	PE	[1661]
29	Cu	4.58	>	4.30	>	4.27	Yes	TC	[4034]
29	Cu	4.632 ± 0.010	>	4.458 ± 0.010	>	4.400 ± 0.010	Yes	CPD	[948,2841]
29	Cu	4.714	>	4.506	>	4.272	Yes	TC	[4091]
29	Cu	4.79	>	4.67	>	4.33	Yes	TC	[3477]
29	Cu	4.8	>	4.5	>	4.4	Yes	PE	[1238,4210]
29	Cu	4.80	>	4.58	>	4.44	Yes	TC	[3304]
29	Cu	4.80	>	4.54	>	4.43	Yes	TC	[2917]
29	Cu	4.80	>	4.53	<	4.56	No	TC	[723][19]
29	Cu	4.85	>	4.68	>	4.48	Yes	CPD	[959]
29	Cu	4.876	>	4.753	>	4.508	Yes	TC	[1119,2989]
29	Cu	4.90 ± 0.02	>	4.73 ± 0.10	>	4.56 ± 0.10	Yes	various	[4088]
29	Cu	4.91	>	4.58	>	4.25	Yes	TC	[3477]
29	Cu	4.91	>	4.81	>	4.53	Yes	TC	[3477]
29	Cu	4.91 ± 0.03	>	4.57 ± 0.08	>	4.48 ± 0.06	Yes	various	[1351][b]
29	Cu	4.92 ± 0.05	>	4.58 ± 0.06	>	4.43 ± 0.04	Yes	various	[Here][a]
29	Cu	4.93 ± 0.03	>	4.63 ± 0.03	>	4.48 ± 0.03	Yes	PE	[2903]
29	Cu	4.94 ± 0.03	>	4.59 ± 0.03	>	4.48 ± 0.03	Yes	PE	[953,2006]
29	Cu	4.95	>	4.56	>	4.40	Yes	CPD	[952]
29	Cu	4.95	>	4.76	>	4.40	Yes	CPD	[952]
29	Cu	4.958	>	4.71	>	4.625	Yes	TC	[4189]
29	Cu	4.99	>	4.89	>	4.61	Yes	TC	[3477]
29	Cu	5.10	>	4.85	>	4.67	Yes	TC	[480]
29	Cu	5.17	>	4.88	>	4.71	Yes	TC	[1237]
29	Cu	5.19	>	4.95	>	4.9	Yes	TC	[956]
29	Cu	5.25 ± 0.1	>	4.75 ± 0.1	>	4.7 ± 0.1	Yes	CPD	[1507]
29	Cu	5.30	>	5.26	>	4.48	Yes	TC	[229,334]

Table 10 (*continued*)

No.	Metal	ϕ^e(111) (eV)		ϕ^e(100) (eV)		ϕ^e(110) (eV)	Seq.	Meth.	Refs.
29	Cu	5.31	>	5.02	>	4.81	Yes	TC	[480,4398]
29	Cu	5.32	>	5.05	>	4.83	Yes	TC	[480,4398]
29	Cu	5.32	>	4.99	>	4.65	Yes	TC	[1980]
29	Cu	5.32	>	4.99	>	4.66	Yes	TC	[2548]
29	Cu	5.43	>	5.26	>	4.53	Yes	TC	[962]
29	Cu	5.44	>	5.31	>	4.98	Yes	TC	[962]
29	Cu	5.44	>	5.31	>	5.04	Yes	TC	[962]
29	Cu	5.54 ± 0.012	>	5.155 ± 0.054	>	4.92 ± 0.019	Yes	CPD	[963]
29	Cu	5.55	>	4.98	>	3.56	Yes	TC	[962]
29	Cu	5.55	>	5.13	>	4.94	Yes	TC	[3224]
29	Cu	5.56	>	5.03	>	4.10	Yes	TC	[962]
29	Cu	5.56	>	5.03	>	4.20	Yes	TC	[962]
29	Cu	5.57	>	5.16	>	3.85	Yes	TC	[321]
Conformity (N$_{yes}$/N$_{total}$)[e]				–		–	**95%**	–	–
31	Ga	3.79	>	3.35	<	4.08	No	TC	[3211]
38	α-Sr	2.569	>	2.473	<	2.545	No	TC	[4091]
38	α-Sr	2.94	>	2.79	>	2.75	Yes	TC	[231]
38	α-Sr	3.21	>	2.95	>	2.76	Yes	TC	[3467]
38	α-Sr	3.4 ± 0.3	>	3.3 ± 0.4	>	3.1 ± 0.3	Yes	TC	[Here][a]
38	α-Sr	3.57	<	3.82	>	3.31	No	TC	[1030]
38	α-Sr	3.61	>	3.42	>	3.05	Yes	TC	[1030]
38	α-Sr	4.10	>	3.81	>	3.57	Yes	TC	[321]
Conformity (N$_{yes}$/N$_{total}$)[e]				–		–	**71%**	–	–
45	Rh	5.105	>	5.087	>	4.615	Yes	TC	[2229,2447]
45	Rh	5.138	>	5.040	>	4.635	Yes	TC	[4091]
45	Rh	5.21	>	5.17	>	4.67	Yes	TC	[2912]
45	Rh	5.39	>	4.99	>	4.69	Yes	TC	[321]
45	Rh	5.40 ± 0.08	>	5.24 ± 0.07	>	4.75 ± 0.06	Yes	various	[Here][a]
45	Rh	5.44	>	5.25	>	4.94	Yes	TC	[320,1178]
45	Rh	5.46 ± 0.09	>	5.30 ± 0.15	>	4.86 ± 0.21	Yes	various	[4088]
45	Rh	5.50 ± 0.10	>	5.29 ± 0.07	>	4.77 ± 0.06	Yes	various	[1351][b]
45	Rh	5.56	>	5.46	>	5.07	Yes	TC	[4228]
45	Rh	5.59	>	5.45	>	5.07	Yes	TC	[4228]
45	Rh	5.66 ± 0.02	>	5.40 ± 0.02	>	5.12 ± 0.02	Yes	?	[2832]
45	Rh	5.67 ± 0.01	>	5.41 ± 0.01	>	4.86 ± 0.01	Yes	FE	[1010]
645	Rh	c_0 + 0.196	>	c_0	>	c_0 − 0.371	Yes	TC	[4246][h]
Conformity (N$_{yes}$/N$_{total}$)[e]				–		–	**100%**	–	–
46	Pd	5.18	>	5.14	>	4.90	Yes	TC	[602]
46	Pd	5.198	>	5.115	>	4.781	Yes	TC	[2229,2447]
46	Pd	5.23	>	5.080	>	4.860	Yes	TC	[4091]
46	Pd	5.25	>	5.11	>	4.87	Yes	TC	[4087,4410]
46	Pd	5.53	>	5.30	>	5.13	Yes	TC	[320,2534]
46	Pd	5.55 ± 0.07	<	5.59 ± 0.05	>	5.19 ± 0.04[c]	No	various	[1351][b]
46	Pd	5.58 ± 0.05	>	5.48 ± 0.04	>	5.12 ± 0.09	Yes	various	[Here][a]
46	Pd	5.67 ± 0.12	>	5.48 ± 0.23	>	5.07 ± 0.20	Yes	various	[4088]
46	Pd	5.90 ± <0.1	>	5.65 ± <0.1	>	5.20 ± <0.1	Yes	PE	[672]
46	Pd	5.95 ± <0.1	>	5.65 ± <0.1	>	5.20 ± <0.1	Yes	PE	[914,1026,3449]
46	Pd	6.02	>	5.56	>	5.24	Yes	TC	[321]
46	Pd	d_0 + 0.179	>	d_0	>	d_0 − 0.340	Yes	TC	[4246][h]
Conformity (N$_{yes}$/N$_{total}$)[e]				–		–	**92%**	–	–
47	Ag	3.70	>	3.55	>	3.35	Yes	TC	[475]
47	Ag	3.96	>	3.89	>	3.66	Yes	TC	[2516]
47	Ag	4.25	<	4.35	>	4.20	No	TC	[4117]
47	Ag	4.368	>	4.246	>	4.059	Yes	TC	[4091]
47	Ag	4.40	>	4.33	>	4.19	Yes	TC	[3280]
47	Ag	4.40	>	4.29	>	4.10	Yes	TC	[947]
47	Ag	4.45 ± 0.03	>	4.34 ± 0.03	>	4.25 ± 0.03	Yes	PE	[1192]
47	Ag	4.46 ± 0.02	>	4.22 ± 0.04	>	4.14 ± 0.05	Yes	PE	[625,1693]
47	Ag	4.53 ± 0.07	>	4.36 ± 0.05	>	4.10 ± 0.15	Yes	various	[4088]
47	Ag	4.56 ± 0.15	>	4.50 ± 0.10	>	4.16 ± 0.05	Yes	various	[1351][b]
47	Ag	4.64 ± 0.06	>	4.46 ± 0.05	>	4.28 ± 0.08	Yes	various	[Here][a]

Table 10 (*continued*)

No.	Metal	ϕ^e(111) (eV)		ϕ^e(100) (eV)		ϕ^e(110) (eV)	Seq.	Meth.	Refs.
47	Ag	4.65	>	4.33	>	4.30	Yes	TC	[1264]
47	Ag	4.67	>	4.43	>	4.23	Yes	TC	[320,1178]
47	Ag	4.74	>	4.45	>	4.17	Yes	TC	[1159]
47	Ag	4.74 ± 0.02	>	4.64 ± 0.02	>	4.52 ± 0.02	Yes	PE	[626,1134]
47	Ag	4.95	>	4.82	>	4.68	Yes	TC	[1237]
47	Ag	4.98	>	4.82	>	4.66	Yes	TC	[1264]
47	Ag	5.01	<	5.02	>	4.40	No	TC	[334,3179]
47	Ag	5.46	>	5.06	>	4.76	Yes	TC	[321]
47	Ag	$e_0 + 0.151$	>	e_0	>	$e_0 - 0.293$	Yes	TC	[4246][h]
Conformity (N_{yes}/N_{total})[e]				–		–	**90%**	–	–
57	β-La	4.04	>	3.74	>	3.53	Yes	TC	[321]
57	β-La	$f_0 + 0.126$	>	f_0	>	$f_0 - 0.268$	Yes	TC	[4246][h]
58	β-Ce	4.98	>	4.62	>	4.35	Yes	TC	[321]
61	Pm	4.03	>	3.73	>	3.52	Yes	TC	[321]
70	α-Yb	4.47	>	4.15	>	3.90	Yes	TC	[321]
77	Ir	5.42	<	5.60	>	5.07	No	TC	[3243]
77	Ir	5.497	<	5.55	>	4.958	No	TC	[4091]
77	Ir	5.55	>	5.20	>	4.83	Yes	TC	[2548]
77	Ir	5.56	>	5.20	>	4.84	Yes	TC	[1980]
77	Ir	5.72	<	5.89	>	5.36	No	TC	[3243]
77	Ir	5.75 ± 0.06	>	5.60 ± 0.06	>	5.23 ± 0.19	Yes	various	[Here][a]
77	Ir	5.77 ± 0.03	>	5.72 ± 0.27	>	5.31 ± 0.35[d]	Yes	various	[1351][b]
77	Ir	5.78 ± 0.04	<	5.95 (5.97)	>	5.42 ± 0.32	No	various	[4088]
77	Ir	5.80 ± 0.05	>	5.70 ± 0.05	>	5.0	Yes	FE	[1797,1802]
77	Ir	5.86	>	5.52	>	5.37	Yes	TC	[3224]
77	Ir	5.92	=	5.92	>	5.45	No	TC	[1933]
77	Ir	6.51	>	6.03	>	5.67	Yes	TC	[321]
77	Ir	$g_0 + 0.237$	>	g_0	>	$g_0 - 0.499$	Yes	TC	[4246][h]
Conformity (N_{yes}/N_{total})[e]				–		–	**62%**	–	–
78	Pt	5.56	>	5.20	>	4.84	Yes	TC	[1980]
78	Pt	5.69	>	5.66	>	5.26	Yes	TC	[4087,4410]
78	Pt	5.702	>	5.625	>	5.223	Yes	TC	[4091]
78	Pt	5.747	>	5.711	>	5.297	Yes	TC	[3245]
78	Pt	5.817	<	5.840	>	5.441	No	TC	[2229]
78	Pt	5.84 ± 0.05	>	5.75 ± 0.06	>	5.54 ± 0.07	Yes	various	[Here][a]
78	Pt	5.86 ± 0.06	>	5.82 ± 0.27	>	5.61 ± 0.13	Yes	various	[1351][b]
78	Pt	5.91 ± 0.08	>	5.67 (5.75)	>	5.53 ± 0.13	Yes	various	[4088]
78	Pt	5.94	>	5.86	>	5.72	Yes	PE	[429]
78	Pt	6.01	>	5.67	>	5.52	Yes	TC	[3224]
78	Pt	6.1	=	6.1	>	5.7	No	TC	[2905]
78	Pt	6.12	>	6.07	>	5.74	Yes	TC	[1237]
78	Pt	6.47	>	5.99	>	5.63	Yes	TC	[321]
78	Pt	6.53	>	6.52	>	6.19	Yes	TC	[1201]
78	Pt	6.60	<	6.86	>	6.10	No	TC	[3194]
78	Pt	6.67	<	6.93	>	6.15	No	TC	[3194]
78	Pt	$h_0 + 0.218$	>	h_0	>	$h_0 - 0.414$	Yes	TC	[4246][h]
Conformity (N_{yes}/N_{total})[e]				–		–	**76%**	–	–
79	Au	3.478	>	3.318	>	3.148	Yes	TC	[2914]
79	Au	3.80	>	3.65	>	3.50	Yes	TC	[475]
79	Au	4.165	>	3.816	>	3.629	Yes	TC	[2914]
79	Au	5.1	>	5.05	>	4.93	Yes	TC	[4233]
79	Au	5.110	>	5.071	>	4.91	Yes	TC	[4091]
79	Au	5.13	>	5.04	>	4.98	Yes	TC	[4233]
79	Au	5.15	>	5.10	>	5.04	Yes	TC	[4087,4410]
79	Au	5.26 ± 0.04	>	5.22 ± 0.04	>	5.20 ± 0.04	Yes	PE	[1068]
79	Au	5.29 ± 0.02	<	5.41 ± 0.12	>	5.31 ± 0.11	No	various	[1351][b]
79	Au	5.31	<	5.47	>	5.37	No	CPD	[959]
79	Au	5.32	>	4.99	>	4.65	Yes	TC	[1980]
79	Au	5.33 ± 0.06	>	5.22 ± 0.31	>	5.16 ± 0.22	Yes	various	[4088]
79	Au	5.46 ± 0.07	>	5.39 ± 0.07	>	5.33 ± 0.09	Yes	various	[Here][a]

Table 10 (*continued*)

No.	Metal	$\phi^e(111)$ (eV)		$\phi^e(100)$ (eV)		$\phi^e(110)$ (eV)	Seq.	Meth.	Refs.
79	Au	5.63	>	5.53	>	5.41	Yes	TC	[480,4398]
79	Au	5.65	>	5.56	>	5.42	Yes	TC	[3317]
79	Au	6.01	<	6.16	>	5.40	No	TC	[334]
79	Au	6.08	<	6.23	>	5.85	No	TC	[3194]
79	Au	6.13	<	6.26	>	5.86	No	TC	[3194]
79	Au	6.65	>	6.16	>	5.80	Yes	TC	[321]
79	Au	$i_0 + 0.190$	>	i_0	>	$i_0 - 0.363$	Yes	TC	[4246][h]
Conformity $(N_{yes}/N_{total})^e$				–		–	<u>**75%**</u>	–	–
82	Pb	3.16	>	3.04	>	2.99	Yes	TC	[1159]
82	Pb	3.31	<	3.45	<	3.82	No	TC	[476]
82	Pb	3.51	<	3.67	<	4.01	No	TC	[476]
82	Pb	3.59	>	3.50	<	3.77	No	TC	[231]
82	Pb	3.65	<	3.81	<	3.84	No	TC	[1030]
82	Pb	3.7	<	3.8	<	4.4	No	TC	[1088]
82	Pb	3.76	<	3.78	>	3.65	No	TC[1]	[3521]
82	Pb	3.77	>	3.75	>	3.65	Yes	TC[2]	[3521]
82	Pb	3.78	>	3.77	>	3.64	Yes	TC[3]	[3521]
82	Pb	3.78	>	3.77	>	3.64	Yes	TC[4]	[3521]
82	Pb	3.78	<	3.79	>	3.63	No	TC[5]	[3521]
82	Pb	3.78	<	3.80	>	3.63	No	TC[6]	[3521]
82	Pb	3.78	<	3.80	>	3.66	No	TC[7]	[3521]
82	Pb	3.78	<	3.83	>	3.63	No	TC[8]	[3521]
82	Pb	3.78 ± 0.01	<	3.79 ± 0.02	>	3.64 ± 0.01	No	TC[9]	[3521]
82	Pb	3.79	=	3.79	<	3.80	No	TC	[3004]
82	Pb	3.85	<	3.95	>	3.80	No	TC	[475]
82	Pb	3.9	<	4.0	>	3.8	No	TC	[1088]
82	Pb	3.90	>	3.57	>	3.46	Yes	TC	[553]
82	Pb	4.07	>	4.06	>	3.92	Yes	TC[10]	[3521]
82	Pb	4.07	>	4.06	>	3.93	Yes	TC[11]	[3521]
82	Pb	4.07	=	4.07	>	3.92	No	TC[12]	[3521]
82	Pb	4.07	=	4.07	>	3.92	No	TC[13]	[3521]
82	Pb	4.08	>	4.07	>	3.92	Yes	TC[14]	[3521]
82	Pb	4.08	>	4.07	>	3.93	Yes	TC[15]	[3521]
82	Pb	4.09	>	4.07	>	3.92	Yes	TC[16]	[3521]
82	Pb	4.09	>	4.07	>	3.93	Yes	TC[17]	[3521]
82	Pb	4.08 ± 0.01	>	4.07 ± 0.01	>	3.92 ± 0.01	Yes	TC[18]	[3521]
82	Pb	4.11	>	4.07	>	3.84	Yes	TC	[3004]
82	Pb	4.14	>	4.12	>	3.73	Yes	TC	[2516]
82	Pb	<u>4.14 ± 0.09</u>	>	<u>3.96 ± 0.11</u>	>	<u>3.84 ± 0.09</u>	Yes	various	[Here][a]
82	Pb	4.15	<	4.50	>	3.80	No	TC	[475]
82	Pb	4.30	<	4.31	>	3.98	No	TC	[555]
82	Pb	4.34	>	3.76	>	3.51	Yes	TC	[3467]
82	Pb	4.55	<	4.65	>	4.50	No	TC	[1095]
82	Pb	4.79	>	3.48	<	3.89	No	TC	[3211]
82	Pb	5.23	>	3.88	<	4.08	No	TC	[1030]
82	Pb	5.35	>	4.95	>	4.66	Yes	TC	[321]
Conformity $(N_{yes}/N_{total})^e$				–		–	<u>**45%**</u>	–	–
90	Th	3.75	>	3.57	>	3.38	Yes	TC	[1980]
94	δ-Pu	3.4	>	3.11	>	2.99	Yes	TC	[2069]
95	β-Am	3.06	>	2.93	>	2.86	Yes	TC	[2071,2076]

[a]<u>Each of the work function data</u> with double underlines is cited from the most probable value recommended in Table 2 [Here].

[b]Similarly, <u>each of the data</u> with a single underline is cited from the value recommended in Table 2 in the previous review [1351].

[c]This is obtained by correction of 5.08 ± 0.13 eV for Pd (110) in Table 2 [1351].

[d]This is tentatively evaluated from the three data on Ir(110) listed in Table 1 [1351].

[e]The conformity shows the percentage for each metal whose triple sets have "Yes" among the whole listed here (see Footnote d in Table 9).

[f]These work function values such as $\phi(111) = 5.3^+$ eV for Ni(111) [Here][a] and $5.33 \pm 0.01^+$ eV for Ni(111) [283,630] are not ϕ^e but ϕ^+ determined by PSI.

[g]This triple set is tentatively listed to examine the conformity of $\phi^+(hkl)$ for Ni although δ_m for each surface is slightly less than unity [283,630].

[h]No table includes the absolute values of $a_0 - b_0$ [4259] and $c_0 - i_0$ [4246].

[i]The absolute value of x_0 for Ni(100) is not given in the table [4078].

[1–9]By using different values for several parameters in a model of local density approximation for lead, the work function values calculated theoretically afford the averages.[9] Depending upon the parameters, the sequences[1–8] change from Yes to No, and vice versa. For a full detail, see Ref. [3521].

[10–18] The theoretical values for lead[10–17] based on a generalized gradient approximation model yield the averages.[18] Similarly as above[1–8], the sequences[10–17] vary also between Yes and No according to the parametric values employed for calculating ϕ^e (see Ref. [3521] for further information).

[19] Each of the three values for Al or Cu is the average calculated by the authors [723] from published experimental data.

[20] Theoretical study of the face-dependent work function yields the conclusion that Smoluchowski rule holds with Al(111)–Al(110) without showing numerical data [227]. Some typical data supporting the conclusion are found in their later publications [473,553,3477] as listed in this table.

On the contrary, the sequences of Al show "No" frequently ($I_N = 68\%$) among the 56 examples reported by many authors, and "No" is found also for our present and previous ones [Here, 1351] listed with double and single underline, respectively, in Table 10. In addition, Al is experimentally found to have the differences of $\Delta \equiv \phi^e(100) - \phi^e(111) = 0.220 \pm 0.050$ eV [4267] and 0.17 ± 0.04 eV [241,1045]. Both correspond to "No", in contrast to $\Delta = -0.06$ eV [1358]. Interestingly, a theoretical investigation for Al yields that atomically flat surfaces follow exactly the Smoluchowski rule ($4.31 > 4.27 > 3.92$ eV) but that rough surfaces have the direct opposite sequence (typically, $4.03 < 4.19 < 4.23$ eV) [4401]. Here, both $\phi^e(111)$ and $\phi^e(100)$ decrease from 4.31 and 4.27 eV to 4.03 and 4.19 eV, respectively, the result of which is consistent with the general tendency that ϕ^e reduces with an increase in surface roughness (see Footnotes 177, 331 and 332 in Table 1 and also Section 4.2.5 in Ref. [1351]). On the contrary, $\phi^e(110)$ alone increases irregularly from 3.92 to 4.23 eV with increasing roughness, the basic reason for which is naturally expected to be ascertained clearly.

Similarly to Al exemplified just above, Pb also indicates frequently "No" ($I_N = 55\%$ of $N_{total} = 38$), although our sequence [Here] has "Yes". These inconformity percentages ($I_N = 68$ and 55%) for the two metals are much larger than those (e.g., $I_N = 38, 24$ and 25% of $N_{total} = 13, 17$ and 20) for other fcc-metals (e.g., Ir, Pt and Au, respectively) and also extremely higher than those (typically, $I_N = 0, 0$ and 5% of $N_{total} = 17, 13$ and 44) found for others (namely, Ni, Rh and Cu, respectively).

5.4. Concluding remarks on the work function sequences

The data on work function sequences exemplified for many metals in Tables 9 and 10 and also the above consideration may lead to the conclusions as follows.

(1) Following well the sequence of $D_s(110) > D_s(100) > D_s(111)$, both of $\phi^e(110) > \phi^e(100) > \phi^e(111)$ and $\phi^+(110) > \phi^+(100) > \phi^+(111)$ hold generally for bcc-metals. Typically, the percentage of "Yes" for the sequence of ϕ^e is actually found to be $C_Y = 100\%$ for both Na and K and also 94% for both Rb and Cs according to the data obtained wholly by TC, while 89% for W, 82% for Mo and 75% for Nb by various methods. The sequences with double underlines [Here] coming from our most probable values in Table 2 show "Yes" for all the bcc-metals, with only one exception of γ-Sr by TC. This exception, however, can hardly be frankly acceptable, because each of the three values for γ-Sr(hkl) with double underlines [Here] is estimated from only two or three data sources [321,334,1159] (see Table 1) and also because any surface species with the same orientation has a very wide gap of 0.33–1.42 eV among the two or three different groups of workers [321,334,1159]. For making the accurate determination of either "Yes" or "No", much further work is needed to accumulate abundant data on γ-Sr(hkl).

(2) The sequence of $\phi^e(111) > \phi^e(100) > \phi^e(110)$ holds for many fcc-metals, and also $\phi^+(111) > \phi^+(100) > \phi^+(110)$ does so for Ni [Here], as shown in Table 10. The percentages of "Yes" for the former (ϕ^e) are found to be very high such as $C_Y = 100\%$ for both Ni and Rh, 95% for Cu, 92% for Pd, 90% for Ag and 71% for α-Sr, where N_t ranges from 7 up to 44. The sequences with double underlines [Here] originating from Table 2 have "Yes" for almost all the fcc-metals including Pb ($I_N = 55\%$), too, while our sequence [Here] for Al has "No" similarly together with many other sequences for Al ($I_N = 68\%$).

(3) With the two exceptions of Al ($C_Y = 32\%$) and Pb (45%), many of the bcc- and fcc-metals examined here have such sequences as follow strictly the Smoluchowski rule [1040]. Namely, $\phi^e(hkl)$ decreases as $D_s(hkl)$ reduces and hence as the surface becomes more open. In addition, both $\phi^e(hkl)$ and $\phi^+(hkl)$ have the same sequence in each case, thereby giving an additional evidence to support strongly our theoretical model that $\phi^+(hkl)$ is identically equivalent to $\phi^e(hkl)$ for essentially clean monocrystalline surfaces ($\delta_m = 1.0$ and $\Delta\phi^* = 0.0$ eV).

(4) In both cases of bcc- and fcc-metals with the two exceptions (Al and Pb), each triple set with "Yes" indicates that the *relative* values among the three are generally reasonable, but does not insure that the *absolute* value of each in the set is always accurate or correct enough to be acceptable today. Typically, the sequence of $5.12 > 3.85 > 3.81$ eV for α-Fe [4222] has "Yes", but both $\phi^e(100)$ and $\phi^e(111)$ alone are much smaller than ours ($4.99 > 4.64 > 4.4$ eV), as may be seen in Table 9. The above indications are quite natural because "Yes" exactly fulfills the *necessary* condition but does not always satisfy the *sufficient* one for insuring the accuracy or acceptability of each $\phi^e(hkl)$ among the three in the set under study.

(5) Except the cases of Al and Pb, each triple set with "No" generally indicates that at least one of the three values among $\phi^e(100)$–$\phi^e(111)$ is inaccurate either due to some errors in the experimental measurements and/or analyses performed, or due to those in the model itself and/or parameters selected for theoretical calculations for each set (see Footnotes 1–9 and 10–18 for Pb in Table 10).

(6) Consequently, such an examination as "Yes" or "No" exemplified in Tables 9 and 10 is very useful for answering quickly the question whether the three values in the set under study are partly inaccurate or unreliable. If "No", then, either the experimental and analytical procedures or the theoretical model and parameters employed should be improved until yielding "Yes", although "Yes" itself does not always insure that all of the improved values in the new set to be thus achieved are absolutely correct (see Conclusion (4) above).

(7) The triple set of Cu(100)–Cu(111) in 6th column [1358] (see Footnote (15) in Table 2) does not completely follow the Smoluchowski rule [1040], in contrast to that in the 7th column [1045] where $\phi^e(111) = 4.94$ eV $> \phi^e(100) = 4.59$ eV $> \phi^e(110) = 4.48$ eV [953] holds similarly to the most (95%) of the 44 sequences [475–321] in Table 10. On the basis of Conclusion (6) above, therefore, it may be advised that $\phi^e(100) = 5.10$ eV [358] adopted in CRC Handbooks (78–98th Eds., 1997–2017)

[1358, etc.] should be returned to 4.59 eV [953] which was once selected in the 77th Ed. (1996) [4137]. If done so, the revised triple set becomes reasonable similarly to those three sets in the 3rd, 7th and 9th columns for Cu(100)–Cu(111) in Table 2.

(8) Quite similarly to Conclusion (7) just above, the triple set of Nb(hkl) [779] recommended by both CRC and Michaelson in Table 2 also does not follow the above rule. If 4.36 eV for Nb(111) [779] is replaced typically with 3.95 eV [Here], then, the normal sequence of 4.87 eV [779] (or 4.77 eV [Here]) > 4.02 eV [779, Here] > 3.95 eV [Here] holds clearly, as already mentioned in Section 3.2 (see Examination (17)).

(9) In addition, the set of 4.95 > 4.53 < 4.55 eV [325] recommended in Table 2 for bcc-Mo(hkl) by both CRC [1358] and Michaelson [1045] also seems to be partly incorrect, although $\phi(110) = 4.95$ eV alone agrees well with ours (4.98 eV). Namely, both of $\phi(111) = 4.55$ eV and $\phi(100) = 4.53$ eV [325] are considerably larger than ours of 4.29 and 4.38 eV, respectively, and also than many others (see Table 1). Therefore, both seem to need a suitable correction (see Examinations (19) and (20) in Section 3.2).

(10) Interestingly, Al (fcc) is found to have an extremely high percentage ($I_N = 68\%$ among $N_{total} = 56$ sequences) of "No" including also the two sequences of our most probable values [Here, 1351], in contrast to many other fcc-metals having very low percentages of the inconformity; such as Ni and Rh ($I_N = 0\%$, both $N_{total} \geq 13$), Cu ($I_n = 5\%$, $N_{total} = 44$), and Ag ($I_N = 10\%$, $N_{total} = 20$).

(11) Several workers [227,241,721] have tried to examine the applicability of the Smoluchowski rule [1040] to the work function sequence of the three low-index planes of Al. Typically, it is stated to be difficult [227] to understand such *anomalous* behavior as $\phi^e(111) = 4.24 < \phi^e(100) = 4.41 > \phi^e(110) = 4.28$ eV observed for Al by PE [241,242] since other fcc-metals (e.g., Cu by PE [953,2006] and Ni by TE [312,837], see Table 10) behave correctly, regarding the above rule [1040]. On the other hand, Fall et al. [721] arrive at the conclusion that the *anomaly* in the anisotropy of Al against the rule (such as 4.23 < 4.42 > 4.29 eV [482,721] and 4.25 < 4.38 > 4.30 eV [561,721] by TC) originates from the increased *p*-atomic-like character of the density of the states at the Fermi energy, in comparison with most other fcc-metals.

(12) According to theoretical studies published recently (2017) by Perdew et al. [4312], all of the five different models (LDA, PBE, etc.) applied to Pd and Ag (both fcc) yields $\phi^e(111) > \phi^e(100) > \phi^e(110)$. Typically, 5.66 > 5.54 > 5.32 eV for Pd and 4.97 > 4.64 > 4.61 eV for Ag (both calculated by LDA) are listed together with those data by other models in Table 3 [4312]. These results with $C_Y = 100\%$ found by the five models are well accordant to many ($C_Y \geq 90\%$) of other examples of Pd and Ag in Table 10 [Here], which does not include any of the "latest" data listed in Table 3 [4312]. On the contrary, all of the five models afford $\phi^e(111) < \phi^e(100) > \phi^e(110)$ for Al alone among the eight fcc-metals (Cu, Rh, Pt, Au, etc.) under study [4312]. Typically, 4.36 < 4.41 > 4.08 eV by LDA and 4.2 < 4.27 > 3.96 eV by PBE are listed for Al in Table 3 [4312]. These anomalous results against the rule support our result with very high inconformity ($I_N = 68\%$ of $N_{total} = 56$ sequences for Al, see Table 10).

(13) Quite similarly to Al mentioned above, Pb also has a high percentage ($I_N = 55\%$ of $N_{total} = 38$ sequences) of "No", whilst the sequence of our most probable values based on various methods (see Table 2) is consistent with the Smoluchowski rule. Unfortunately, the "latest" data on Pb are not included in Table 3 [4312]. The anomaly (21 examples) found for Pb by many workers is probably first reported here comprehensively. However, it should be noted that no experimental data on Pb(100) and Pb(110) are available today and also that even the four data on Pb(111) determined by PE [2228,2268] or CPD [1525,2002] are scattered in a wide range of 4.05–4.70 eV (see Table 1). Not only by theory but also by experiment, much further investigation is expected to be done in order to examine the above anomaly found almost by theoretical studies.

(14) Any of the sequences with "No" in Tables 9 and 10, tentatively with the exceptions of Al and Pb at present, may not be employed without partial or entire corrections after consulting with the most probable values in Table 2. It should be emphasized here again that many of our most probable values are generally established from much abundant database (Table 1) published to date, and also that most of ours except those with x–z attached are generally expected to be more reliable or accurate at present, compared with others recommended according to those articles published before ~1980.

5.5. Other anisotropic dependence sequences

Concerning the three main planes of bcc- and fcc-monocrystals, similar anisotropic sequences are found to hold for other chemico-physical properties such as surface energy (ε) and melting point (T_m). Some of their data available today will be outlined below, together with the quantitative relations between $\phi^e(hkl)$ and $\varepsilon(hkl)$ and also between $\phi^e(hkl)$ and $T_m(hkl)$.

5.5.1. Anisotropy of surface energy

A theoretical study of ε [320] on fcc-Pd, for example, yields the sequence of $\varepsilon(111) = 0.68 < \varepsilon(100) = 0.89 < \varepsilon(110) = 1.33$ eV, thus increasing as the surface-atom density (D_s, see Table 8) decreases and, hence, as the surface becomes more open. This sequence is in diametric opposition to $\phi^e(111) = 5.53 > \phi^e(100) = 5.30 > \phi^e(110) = 5.13$ eV for Pd by TC [320]. Such opposition is found theoretically also for fcc-Rh and Ag [320,4061]. Another theoretical investigation yields the sequence of $\varepsilon(111) < \varepsilon(100) < \varepsilon(110)$ for all of the six fcc-metals (Ni, Cu, Pd, Ag, Pt and Au) [4064]. Such a normal sequence of ε is theoretically found also for fcc-Al [1175,4077] and Ir [3243], in contrast to an anomalous one of $\phi^e(111) < \phi^e(100) > \phi^e(110)$ for both Al [1175] and Ir [3243] (see Table 10).

Regarding bcc-crystals, α-Fe [4124] and both Mo and β-Hf [4057] are theoretically found to have the sequence of $\varepsilon(111) > \varepsilon(100) > \varepsilon$ (110)]. Again, this is directly opposite to that of $\phi^e(111) < \phi^e(100) < \phi^e(110)$ observed for the most (82%) of Mo crystals in Table 9, although only 38 and 50% of α-Fe and β-Hf, respectively, satisfy the latter sequence of $\phi^e(hkl)$.

Another theoretical study on 14 kinds of metals reports that fcc-metals (Ca, α-Sr, Cu, Ag and Au) and bcc-ones (Li, Na, K, Rb and Cs) have the sequences of $\varepsilon(111) < \varepsilon(100) < \varepsilon(110)$ and $\varepsilon(110) < \varepsilon(100) < \varepsilon(111)$, respectively [4085]. Both sequences are opposite

to the respective ones of ϕ^e(hkl) (see Tables 10 and 9). Such opposite sequences of ε(hkl) against ϕ^e(hkl) are derived theoretically for the fcc-metals of Pd, Pt and Au, although Al alone is found to have the anomalous sequence of ϕ^e(111) = 4.02 eV $< \phi^e$ (100) = 4.30 eV $> \phi^e$(110) = 4.09 eV [4087] (Table 10), contrary to the normal one of ε(111) = 0.30 eV $< \varepsilon$ (100) = 0.45 (or 0.44) eV $< \varepsilon$(110) = 0.70 (or 0.68) eV for Al [4087].

On the other hand, other theoretical studies on fcc-metals (e.g., Ni, Cu, Ag) yield the anomalous result of ε(111) $> \varepsilon$(100) $< \varepsilon$(110) [4070,4072], in contrast to ε(111) $< \varepsilon$(100) $< \varepsilon$(110) for fcc-Al [4070]. Similarly, bcc-metals (e.g., Nb, Mo, W) are observed theoretically to have ε(111) $< \varepsilon$(100) $> \varepsilon$(110) [4071,4072], on the contrary to ε(111) $> \varepsilon$(100) $> \varepsilon$(110) for bcc-Cr alone [4071].

As exemplified above, the sequence of ε(hkl) evaluated theoretically for a given species (e.g., Mo or Ag) is often found to be different with each other depending upon theoretical models employed by different workers, quite similarly to those of ϕ^e(hkl) done so especially for Al and Pb (see Table 10). Such a status suggests it desirable to promote much further studies on ε(hkl) as well as ϕ^e(hkl).

According to the theoretical data on surface energy calculated for 60 kinds of chemical elements, on the other hand, all of the fcc-metals (both Al and Pb included) and of bcc-ones under study are found to satisfy the normal sequences of ε(111) $< \varepsilon$(100) $< \varepsilon$(110) and ε(110) $< \varepsilon$(100) $< \varepsilon$(111), respectively [4077], both of which are directly opposite to the respective sequences of ϕ^e(hkl). Unfortunately, no experimental datum on ε(hkl) except fcc-In and Pb seems to be available today [4077], in contrast with much data on ε(poly) [4077]. Therefore, theoretical determination of ε(hkl) is vitally important [4077]. For thirteen hcp-metals (e.g., Be, Co, Zr, Re), a theoretical study is focused on the surface energy and its anisotropy [4342].

Recently (2014), another theoretical study has been made on both ε(hkl) and ϕ^e(hkl) for many elements such as five alkali metals, three alkali earth metals, four bcc-transition metals and also seven fcc-transition metals (see Tables 1–4 in Ref. [4091]), thereby yielding that many of the metals have the inverse-proportional relation between the sequences of ε(hkl) and ϕ^e(hkl) [4091].

5.5.2. Quantitative relation between surface energy and work function

After consideration of both theoretical values of ε(hkl) and experimental data on ϕ^e(hkl) for fcc-Ni and for bcc-Nb, Mo, Ta and W, Zadumkin et al. (in 1970) [4078] derive a quantitative relationship between the two on the basis of statistical–electronic theory. Namely,

$$\phi^e(\text{hkl}) + (Ba^2/z)\varepsilon(\text{hkl}) = \text{const.} \tag{13}$$

Here, a is the lattice constant, z is the number of valence electrons per atom, B is the constant depending only upon the type of crystal structure. Typically for fcc-Ni, they [4078] yield the theoretical values of the differences such as ϕ^e(100) $- \phi^e$(110) = 0.38 eV, as ϕ^e(100) $- \phi^e$(111) = -0.21 eV (see Table 10) and as ϕ^e(110) $- \phi^e$(111) = -0.55 eV. These differences calculated from Eq. (13) are in good or fair agreement with the experimental ones of 0.25, -0.33 and -0.58 eV determined by TE [312,837] (see Table 10), respectively. Namely, the gap ($|\Delta\phi|$) between the theory [4078] and the experiment [312,837] is as small as $0.03-0.13$ eV. Similarly for bcc-Nb, Mo, Ta and W, such an agreement as $|\Delta\phi| = 0.00 - 0.29$ eV is found between the theory [4078] and the experiment [144,775]. On the basis of these results, it is concluded that the facets with lower surface energy have higher work function, and vice versa [4078]. In other words, any theoretical value of ε(hkl) under study may readily be examined from Eq. (13) by substituting some experimental data on ϕ^e(hkl) for the same surface species (hkl) according to such data as listed in Table 2 [Here].

From another equation (12) derived theoretically by Zadumkin et al. [4084], ε(poly) is theoretically evaluated by using experimental data on ϕ^e(poly) for both alkali and alkali-earth metals, thereby indicating that substitution of an accurate work function value into the above equation (12) may yield a good agreement (within the gap of ~5%) between theoretical and experimental values of ε(poly) for alkalis (Na–Cs). In other words, an accurate value of ε by experiment may be applied to examining the accuracy of ϕ^e from a quite different viewpoint.

Using a modified Frenkel'–Gombas–Zadumkin theory correlating ε with ϕ^e, Shebzukhova and Aref'eva have recently calculated the allotropic work function differences for several metals [4259]. Typically for fcc-Ni, ϕ^e(111) $- \phi^e$(100) = 0.1651 eV and ϕ^e(100) $- \phi^e$(110) = 0.3438 eV by theory [4259] are in fair agreement with 0.33 and 0.25 eV by experiment [312] and also with 0.21 and 0.38 eV by the previous theoretical model [4078], respectively. Both of the theoretical results for Ni follow the normal sequence of ϕ^e(111) $> \phi^e$(100) $> \phi^e$(110), as shown in Table 10 (see Footnotes (h) and (i)). Others on bcc-metals (Nb, Mo, Ta and W) [4078] are listed in Table 9 (see Footnote (g)), normally following ϕ^e(110) $> \phi^e$ (100) $> \phi^e$(111).

A recent study by Shebzukhova et al. using Eq. (13) reports that the work function difference between theory and experiment is estimated to range from ~8 to 1% for Cd(0001), Zn(0001) and Hg(001) [4459].

By the theoretical studies on both ϕ(hkl) and ε(hkl) for six close-packed surfaces of 19 common fcc and bcc metals, Wang et al. find a roughly inverse proportional relationship between the two [4091].

5.5.3. Anisotropy of melting point

The melting point (T_m) of fcc-Cu, for example, is theoretically calculated by Chatterjee, who uses a variety of known parameters for both surface and bulk such as Debye temperature, atomic weight, mean-square amplitude of atomic vibration. Consequently, he yields the sequence of T_m(111) = 866 K $> T_m$(100) = 836 K $> T_m$(110) = 809 K for Cu [1684,4062]. This sequence is identical with that of ϕ^e(111) = 4.94 eV $> \phi^e$(100) = 4.59 eV $> \phi^e$(110) = 4.48 eV for Cu by PE [953] (see Table 10). Such an identity in anisotropic sequence is found also for fcc-metals of Ni, Ag, Pt and Pb [4062]. Typically, Pt has T_m(111) = 2023 K $> T_m$(100) = 1851 K $> T_m$(110) = 1837 K, in harmony with ϕ^e(111) = 5.84 $\pm$ 0.05 eV $> \phi^e$(100) = 5.75 $\pm$ 0.06 eV $> \phi^e$(110) = 5.54 $\pm$ 0.07 eV (see our most probable values in Table 2). Unfortunately, it seems to the present author that any data on T_m(hkl) have not yet been reported for bcc-metals by any worker.

5.5.4. Correlation between melting point and work function

By consideration of the above fact that the anisotropic sequence is identical between $T_m(hkl)$ and $\phi^e(hkl)$, Chatterjee (in 1979) yields the empirical equation as follows [1684].

$$\log[\phi^e(hkl)] = \log[T_m(hkl)^{1/4}/V^{1/6}] - 2.87 \pm 0.04. \tag{14}$$

Here, V is the atomic volume.

Application of Eq. (14) to fcc-Ag yields $\phi^e(111) = 4.85$ eV and $\phi^e(110) = 4.75$ eV [1684]. The respective values, however, are not well accordant to ours of 4.64 ± 0.06 and 4.28 ± 0.08 eV (Table 2), although the former [1684] also follows exactly the normal sequence of $\phi^e(111) > \phi^e(110)$, just as expected from the high conformity ($C_Y = 90\%$ among $N_t = 20$ examples) for Ag-sequence in Table 10. Similarly for fcc-Pb, the calculated values of 3.39 and 3.26 eV [1684] are in poor agreement with ours of 4.14 ± 0.09 and 3.84 ± 0.09 eV (Table 2) for $\phi^e(111)$ and $\phi^e(110)$, respectively, although the sequence of $\phi^e(111) > \phi^e(110)$ itself is identical again between theory and experiment, following the Smoluchowski rule [1040].

It may be worthwhile to inspect the reason why the values of $\phi^e(hkl)$ calculated from Eq. (14) are not well accordant with ours. In addition, it is fully expected to solve the problem whether the work function values to be calculated for bcc-metals from such an empirical equation as Eq. (14) are well accordant to ours in Table 2 [Here].

6. Work function dependence upon the Wigner–Seitz radius

In this section, theoretical evaluation of work function by two typical quantum models will be outlined below together with comparison between calculated values and experimental data.

6.1. Theoretical evaluation of work function by the Lang–Kohn model

The work function may be expressed fundamentally as a function of the external and internal components governed solely by the surface and bulk properties of the solid, respectively. Namely,

$$\phi = D_b - E_F. \tag{15}$$

Here, D_b is the dipole barrier against electrons' escape from the surface into vacuum, and E_F is the Fermi energy or chemical potential of electrons in the bulk.

Lang and Kohn calculate the work function (ϕ) of nine simple metals by using the uniform-positive-background model published in 1971 [475], the result of which may be summarized below in comparison with our most probable values.

As the Wigner–Seitz radius (r_s) increases from 2.0 to 6.0 bohr (1 bohr = 0.0529 nm), D_b and E_F decrease monotonically from 6.80 to 0.04 and 2.91 to -2.37 eV, respectively, thereby affording that ϕ decreases gradually from 3.89 to 2.41 eV (see Table I in Ref. [475]). Such a dependence of D_b, $-E_F$ and ϕ is shown as Curves (1)–(3), respectively, in Fig. 2. Consequently, the contribution of D_b to ϕ becomes smaller with increasing r_s. Typically, the ratio (D_b/ϕ) is (i) about 30% for Na ($r_s = 3.99$ bohr) having $\phi = D_b - E_F = 0.91 + 2.15 = 3.06$ eV, (ii) about 13% for K ($r_s = 4.96$ bohr) with $\phi = 0.36 + 2.38 = 2.74$ eV, and (iii) only about 5% for Cs ($r_s = 5.63$ bohr) with $\phi = 0.12 + 2.37 = 2.49$ eV. In other words, ϕ is governed more strongly (from ~70% for Na, to 87% for K, and further to 95% for Cs) by the bulk component (E_F) as r_s increases from 3.99 to 4.96 and moreover to 5.63 bohr, respectively.

The plot of Curve (3) for ϕ based on the theoretical values in Table II (e.g., 3.06, 2.74 and 2.49 eV for Na, K and Cs, respectively) [475] does not well overlap with that of Curve (4) for our ϕ^e in Table 2 [Here] (e.g., 2.54, 2.29 and 2.05 eV for Na, K and Cs, respectively), thus showing the mean discrepancy of $|\phi - \phi^e| = 0.38 \pm 0.15$ eV for the nine metals (Al–Cs) entered in Fig. 2. But, both plots have the same tendency, gradually lowering their positions with increasing r_s. Regarding another curve to be obtainable from the experimental values of work function (e.g., $\phi_{exp} = 2.7$ eV for Na by CPD [1992], 2.39 ± 0.01 eV for K by PE [1481] and 2.14 ± 0.02 eV for Cs by PE [1489], entirely published before 1970) cited in Table II [475], we shall find that the supposed curve of ϕ_{exp} might attain the position nearer to Curve (3) within the mean difference ($|\phi - \phi_{exp}|$) of 0.31 ± 0.14 eV. This is slightly smaller than $|\phi - \phi^e| = 0.38 \pm 0.15$ eV mentioned just above, but still showing a considerable difference between ϕ and ϕ_{exp}.

Another theoretical study [4089] evaluates E_F for 19 species of metals, and it yields typically -2.0, -2.2 and -2.2 eV for Na, K and Cs [4089], which are different (by $0.15-0.18$ eV) from -2.15, -2.38 and -2.37 eV in Table I [475], respectively. By substitution of both the former values of E_F [4089] and the literature ones of ϕ_{exp} cited in Table II [475] into Eq. (15), D_b is calculated to be 0.7, 0.2 and -0.06 eV [4089], which are similarly different (by $0.16-0.21$ eV) from 0.91, 0.36 and 0.12 eV [475] for Na, K and Cs, respectively. Such a difference may be quite natural because both of E_F and work function (ϕ or ϕ_{exp}) are different between the two studies [475,4089]. In other words, any theoretical evaluation of D_b is usually subject to the uncertainty of ± 0.1 eV or so.

For eleven polyvalent metals ($r_s < 3$ bohr) of higher electron density, the theoretical study [4089] leads to the conclusion that ϕ is stabilized very efficiently around 4.1 ± 0.4 eV by D_b, in spite of a considerable variation in E_F. In fact, our most probable values of ϕ^e for typical metals (e.g., Be, Al, Zn, Cd, In, α-Sn and Pb with r_s ranging from 1.87–2.59 bohr) are found to have 4.17 ± 0.10 eV (see Table 2). Regarding monovalent metals such as alkalis ($r_s > 3$ bohr), on the other hand, D_b becomes less contributable to ϕ because E_F becomes less variable with increasing r_s, as may be readily understandable from Fig. 2.

Quantitative relation between D_b and E_F is investigated theoretically and summarized in Fig. 1 [4054], showing that D_b tends to decrease monotonically (non-linearly) with increasing $-E_F$ [4054], quite similarly as above.
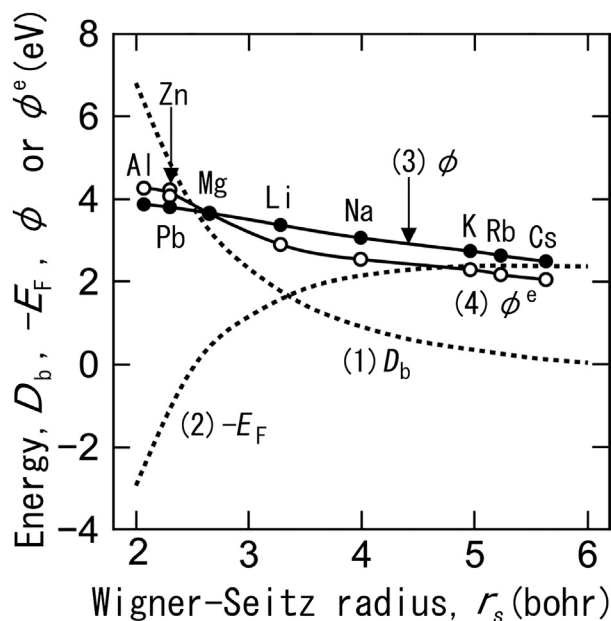
Fig. 2. Wigner–Seitz radius dependence of (1) dipole barrier (D_b), (2) Fermi energy (E_F), (3) work function (ϕ) evaluated from Eq. (15) [475], and (4) the most probable value of work function (ϕ^e) cited from Table 2 [Here].

In the above study [475] summarized in Fig. 2, it is $\phi = 3.66$ eV for Mg alone that agrees well (within 0.01 ± 0.02 eV) with our most probable value of $\phi^e = 3.65 \pm 0.05$ eV and also with other recommended values of 3.66, 3.66 and 3.64 eV in Refs. [1358], [1045] and [1354], respectively (see Table 2). Typically, another example of Na ($\phi = 3.06$ eV [475]) has the largest deviation (0.52 ± 0.03 eV) from our value ($\phi^e = 2.54 \pm 0.03$ eV in Table 2), and the former has a large discrepancy (0.31–0.71 eV) also from others (2.75–2.35 eV) recommended in Refs. [1045,1354,1358]. In other words, many of the theoretical values of ϕ calculated by the original model [475] are not yet so well accordant even to the literature values of ϕ_{exp} [1992, etc.] available at that time (~1970).

However, it should be noted that the original theory initiated in 1964 by Kohn and co-workers [475,3638,4044,4045] has made thereafter a definite contribution to better calculations of work function. As briefly mentioned in Section 2.8.5, they have constructed an epoch-making framework [1698,4395–4397], which has contributed greatly as the motive power to promote the amazing progress in precise evaluation of work function for various surface species. Namely, a variety of theoretical models have been published thereafter to evaluate ϕ^e for various mono- and polycrystalline surfaces, and many of them have achieved very accurate values of ϕ^e. Typically for W(100) reported in 1982–2004, $\phi^e = 4.6$ eV [382,1908], 4.63 eV [383,385], 4.63 eV [3452], 4.63 eV [357] and 4.65 eV [386] by quantum theory (see Table 1) agree exactly with our most probable value of 4.65 ± 0.02 eV based mainly on experiment and also do well with other recommended values of 4.63 eV [1045,1358] and 4.65 ± 0.10 eV# [1664,1665,3964] (see Table 2) and again fairly with 4.70 ± 0.06 eV recommended recently (in 2015) [4088]. Such a good agreement between a theoretical value and ours is found for many other surface species such as Al(hkl) [482,561], Cu(hkl) [3477] and Ag(hkl) [1264] (see Table 1). Regarding the comparison between theory and experiment about ϕ^e, further information is obtained from a compact review by Kiejna [2427,3901]. Recently, De Waele et al. have published the error estimates for density function theory of work function [4108], whose data are summarized in Appendices A and B added to Master's dissertation [4460].

6.2. Theoretical evaluation of work function by the Halas–Durakiewicz model

Recently (in 2010), Halas and Durakiewicz have discussed the problem whether work function is a surface or bulk property, and indicated that ϕ is derived solely from the bulk properties of both the Wigner–Seitz radius (r_s) and the Fermi energy (E_F). Namely [298,495,510,2205,3978],

$$\phi = 43.46/r_s^{3/2} E_F^{1/2}, \qquad (16)$$

which is applicable to work function changes from a clean surface to a gas-covered one and finally to gas-reacted compound one. Typically, Pd is calculated to have 5.25 eV [510,2205], which decreases gradually by hydrogen gas adsorption and finally to 3.2 eV for PdH [510,2205]. Such a gradual decrease estimated by theory is well accordant to that found by experiment [3979]. The former value (5.25 eV) for Pd agrees fairly with 5.17 ± 0.06 eV [Here], 5.22 eV [1358], 5.12 eV [1045] and 5.24 ± 0.05 eV [1351] (see Table 2). With respect to many other polycrystalline surfaces (59 species), Eq. (16) is successfully applied to the calculation of ϕ^e-values [298], many of which are found to agree well or fairly with ϕ^e recommended in a CRC-handbook (77th Ed. in 1996–1997) [4137]. There, all of the work function values are cited from those selected in 1977 by Michaelson [1045].

7. Work function change due to phase transition

This section will summarize briefly the work function changes due to allotropic transition from α to β or β to γ phase and also due to the phase change from solid to liquid, together with their experimental data available today.

7.1. Work function change due to allotropic transition

As known well, many solid elements (typically, C, Ca, Ti, Mn, Fe, Co, Sr, Y, Zr, Sn, La, Ce, Pr, Nd, Tb, Dy, Tm, Hf, U, Pu and Am) have several allotropes, each crystal structure of which changes usually at the allotropic transition temperature (T_A) characteristic of the solid species, thereby showing one of the different phases of α, β, γ, etc. with somewhat different work function values of ϕ_α^e, ϕ_β^e, ϕ_γ^e, etc. among them. The work function change due to allotropic transition may be generally expected to afford us some interesting information about chemico-physical properties characteristic of the surface and bulk under study. The experimental data reported for such a change are summarized in Table 11, where $\Delta\phi_{\beta\alpha}^e \equiv \phi_\beta^e - \phi_\alpha^e$ and $\Delta\phi_{\gamma\beta}^e \equiv \phi_\gamma^e - \phi_\beta^e$ are the work function changes corresponding to the differences between the final and initial stages of $\beta \leftarrow \alpha$ and $\gamma \leftarrow \beta$, respectively. Of course, each of the data on allotropic transition temperatures (T_A) for any metal species entered therein is scattered in a wide range dependent upon specimens or workers. Typically for Hf, nine groups of workers have reported that T_A for $\alpha \leftrightarrow \beta$ is 1583, 1970, 1990–2003, 2007–2100, 2013 $\pm$ 20, 2028, 2033, 2050 $\pm$ 5 or 2236–2266 K [2967]. Similarly, Co also has a large scatter of $T_A \approx 650$–720 K. According to Ref. [1148], $T_A = 670$ K is tentatively adopted for Co in Table 11, although 695 K [4336] is employed in Table 1.

Table 11
Work function changes due to allotropic transformation.

α-phase	β-phase	γ-phase	ϕ_α^e (eV)	$\Delta\phi_{\beta\alpha}^e$ (eV)[a]	ϕ_β^e (eV)	$\Delta\phi_{\gamma\beta}^e$ (eV)[a]	ϕ_γ^e (eV)	Meth.	Refs.
				21. Sc (α = hcp, $T < 1660$ K; β = fcc, $T > 1660$ K for bulk)					
Sc	Sc	–	3.62	−0.16	3.46	–	–	TE	[4356]
				22. Ti (α = hcp, $T < 1155$ K; β = bcc, $T > 1155$ K for bulk)					
Ti/W(100)	Ti/W(100)	–	3.88 $\pm$ 0.09	−0.23 $\pm$ 0.10	3.65 $\pm$ 0.05	–	–	FE	[1404]
Ti/W	Ti/W	–	3.95	−0.30	3.65	–	–	FE	[1522]
Ti/W(111)	Ti/W(111)	–	3.95	−0.35	3.6	–	–	FE	[2194]
Mean	–	–	–	**−0.29 $\pm$ 0.05[m]**	–	–	–	–	–
Ti	Ti	–	3.76	0.00	3.76	–	–	TE	[179]
Ti	Ti	–	4.26	−0.03	4.23	–	–	TE	[179]
Ti	Ti	–	4.36	−0.04	4.32	–	–	TE	[179]
Ti	Ti	–	3.87 $\pm$ 0.05	0.06 $\pm$ 0.17	3.93 $\pm$ 0.16	–	–	various	[Here][b]
Mean	–	–	–	**0.00 $\pm$ 0.03**	–	–	–	–	–
				26. Fe (α = bcc, $T < 1042$ K; β = bcc; γ = fcc, $T = 1179$–1674 K for bulk)[g]					
–	Fe	Fe	–	–	4.48 $\pm$ 0.06	−0.27 $\pm$ 0.08[k]	4.21 $\pm$ 0.05	TE	[310]
–	Fe	Fe	–	–	4.64 $\pm$ 0.06	0.02 $\pm$ 0.08	4.66 $\pm$ 0.05	TE	[310]
Fe	Fe	–	4.53	−0.08	4.45	–	–	TC	[3318]
Fe	Fe	–	4.65 $\pm$ 0.01	−0.03 $\pm$ 0.01	4.62 $\pm$ 0.01	–	–	PE	[305]
Fe	Fe	Fe	4.63 $\pm$ 0.01	−0.01 $\pm$ 0.01[l]	4.62 $\pm$ 0.01	0.06 $\pm$ 0.01	4.68 $\pm$ 0.01	PE	[305]
–	Fe	Fe	–	–	?	0.09	?	TE	[303]
–	Fe	Fe	–	–	4.49+	0.06	4.55+	PSI	[303][c]
–	Fe	Fe	–	–	4.77	0.00	4.77	TE	[3024]
Fe	Fe	Fe	4.55 $\pm$ 0.05	−0.03 $\pm$ 0.18	4.52 $\pm$ 0.17	0.02 $\pm$ 0.18	4.54 $\pm$ 0.05	various	[Here][b]
Mean	–	–	–	**−0.04 $\pm$ 0.03**	–	**0.04 $\pm$ 0.03**	–	–	–
				27. Co (α = hcp, $T < 670$ K; β = fcc, $T > 670$ K for bulk)					
Co(0001)	Co(111)	–	5.264	0.002	5.266	–	–	CPD	[3192]
Co	Co	–	4.923[n]	0.002	4.925[n]	–	–	CPD	[1148]
Co	Co	–	4.923	0.043	4.966	–	–	CPD	[1148]
Co	Co	–	4.960	−0.035	4.925	–	–	CPD	[1148]
Co	Co	–	4.960[n]	0.006	4.966[n]	–	–	CPD	[1148]
Co	Co	–	4.97	−0.04	4.93	–	–	CPD	[3153]
Co	Co	–	4.12 $\pm$ 0.04	0.13 $\pm$ 0.09	4.25 $\pm$ 0.08	–	–	PE	[1632]

Table 11 (*continued*)

α-phase	β-phase	γ-phase	ϕ_α^e (eV)	$\Delta\phi_{\beta\alpha}^e$ (eV)[a]	ϕ_β^e (eV)	$\Delta\phi_{\gamma\beta}^e$ (eV)[a]	ϕ_γ^e (eV)	Meth.	Refs.
Co	Co	–	4.71 ± 0.03	−0.21 ± 0.13	4.50 ± 0.13	–	–	various	[Here][b]
Mean	–	–	–	**−0.02 ± 0.10**	–	–	–	–	–
				39. Y (α = hcp, $T < 1540$ K; β = bcc, $T > 1540$ K for bulk)					
Y	Y	–	3.62	−0.18	3.44	–	–	TE	[4356]
Y	Y	–	3.27	−0.10	3.17	–	–	TE	[4356]
Y	Y	–	3.16 ± 0.06	0.01 ± 0.06	3.17	–	–	various	[Here][b]
				50. Sn (α = bcc, $T < 291$ K; β = tetragonal; γ = hexagonal, $T > 473$ K for bulk)					
–	Sn	Sn	–	–	4.39	−0.11	4.28	PE	[1135]
–	Sn	Sn	–	–	4.51	−0.13	4.38	PE	[1945–1947]
Sn	Sn	Sn	4.27 ± 0.06	0.07 ± 0.08	4.34 ± 0.06	−0.05 ± 0.08	4.29 ± 0.06	various	[Here][b]
Mean	–	–	–	**0.07 ± 0.08**	–	**−0.10 ± 0.03**	–	–	–
				65. Tb (α = hcp, $T < 1500$ K; β = bcc, $T > 1500$ K for bulk)					
Tb(0001)	Tb(???)[h]	–	3.09 ± 0.05	−0.15 ± 0.07	2.94 ± 0.05	–	–	TE	[3920]
Tb	Tb	–	3.19	−0.18	3.01	–	–	TE	[4356]
				72. Hf (α = hcp, $T < 2050$ K; β = bcc, $T > 2050$ K for bulk)[i]					
Hf(0001)	Hf(???)[h]	–	4.10 ± 0.05	−0.20 ± 0.07	3.90 ± 0.05	–	–	TE	[3921]
Hf(0001)	Hf(???)[h]	–	4.11 ± 0.05	−0.21 ± 0.07	3.90 ± 0.05	–	–	TE	[2967]
Mean	–	–	–	**−0.21 ± 0.07**	–	–	–	–	–
				92. U (α = rhombic, $T < 940$ K; β = tetragonal; γ = bcc, $T > 1050$ K for bulk)[f]					
U(foil)	U	U	3.47 ± 0.01	0.05 ± 0.01	3.52 ± 0.01	−0.13 ± 0.01	3.39 ± 0.01	PE	[1884]
U/W	U/W	U/W	3.56 ± 0.05	−0.51 ± 0.06*	3.05 ± 0.03	0.35 ± 0.20**	3.4 ± 0.2	FE	[1657]
U/W(116)	–	U/W(116)	3.57 ± 0.03	–	–	–	3.43 ± 0.03	FE	[1664]
U/W(113)	–	U/W(113)	3.60 ± 0.03	–	–	–	3.53 ± 0.03	FE	[1664]
U/W	U/W	U/W	3.60 ± 0.03	−0.07 ± 0.04	3.53 ± 0.03	−0.10 ± 0.04	3.43 ± 0.03	FE	[1654]
U/W	U/W	U/W	3.63 ± 0.01	−0.05 ± 0.01	3.58 ± 0.01	−0.05 ± 0.01	3.53 ± 0.01	CPD	[1484]
U/W(111)	U/W(111)	U/W(111)	3.64 ± 0.03	−0.28 ± 0.04*	3.36 ± 0.03	−0.05 ± 0.04	3.31 ± 0.03	FE	[1664]
U/W	U/W	U/W	3.65 ± 0.01	−0.06 ± 0.01	3.59 ± 0.01	−0.14 ± 0.01	3.45 ± 0.01	PE	[2467]
U/W(112)	U/W(112)	U/W(112)	3.70 ± 0.03	−0.06 ± 0.04	3.64 ± 0.03	−0.35 ± 0.04**	3.29 ± 0.03	FE	[1664]
U/W(100)	U/W(100)	U/W(100)	3.88 ± 0.03	−0.27 ± 0.04*	3.61 ± 0.03	0.21 ± 0.04**	3.82 ± 0.03	FE	[1664]
U/W(110)	U/W(110)	U/W(110)	4.04 ± 0.03	−0.05 ± 0.04	3.99 ± 0.03	0.01 ± 0.04	4.00 ± 0.03	FE	[1664]
U	U	U	3.64 ± 0.04	−0.06 ± 0.06	3.58 ± 0.04	−0.16 ± 0.06	3.42 ± 0.05	various	[Here][b]
Mean	–	–	–	**−0.04 ± 0.04[d]**	–	**−0.09 ± 0.06[e]**	–	–	–
Partial mean	–	–	–	**−0.03 ± 0.06[j]**	–	**−0.04 ± 0.08**	–	–	–

[a]The work function changes due to the $\alpha \to \beta$ and $\beta \to \gamma$ transformations are shown as $\Delta\phi_{\beta\alpha}^e \equiv \phi_\beta^e - \phi_\alpha^e$ and $\Delta\phi_{\gamma\beta}^e \equiv \phi_\gamma^e - \phi_\beta^e$, respectively.

[b]The work function data [Here] are cited from Table 2.

[c]The value with the superscript (+) for Fe indicates ϕ^+ instead of ϕ^e (see Footnote 112 in Table 1).

[d]This mean for U is evaluated after disregarding the three values* with an asterisk in the fifth column.

[e]Similarly, this is estimated without including these data** in the seventh column for U.

[f]The allotropic transition temperatures of U from β to α and γ to β are found to range from 918 to 948 K and from 1037 to 1053 K, respectively [3967] (see Footnote 400 in Table 1).

[g]Even at a constant temperature of ~300 K, allotropic transformation from γ-like fcc-Fe(100) to α-bcc-Fe(110) is found to occur when the Fe-layers on Cu(100) increase beyond ~10 ML [3913] (see Sections 7.1 and 8.2).

[h]Regarding β-Tb(???) and Hf(???), further investigation by both theory and experiment may be necessary to assign correctly their orientation, although both Zr and Ti are already established to have the allotropic orientation relationship of α-hcp-{0001}∥ β-bcc-{110} (see Section 7.1).

[i]The allotropic transition temperature of Hf is measured to be 2050 ± 5 K [2967], while 1997 ± 7, 2013 ± 20, 2028 and 2033 K are reported by other workers [2967]. This spread may be caused by the difference in impurity concentration of Zr.

[j]This is not overall but partial mean for $\Delta\phi_{\beta\alpha}^e$, which is evaluated from the above data on Ti, Fe, Co, Sn and U alone because the five metals seem to be somewhat different in $\Delta\phi_{\beta\alpha}^e$ from Y, Tb and Hf (see Section 7.1).

[k]This may be corrected to be $\Delta\phi_{\gamma\beta}^e = 0.02 \pm 0.08$ eV for Fe [310] by substitution of ϕ_β^e and ϕ_γ^e into Eq. (8), as listed on the next line (for details, see Section 2.8.6).

[l]This is estimated as the *net* change due to the transition alone, where both $\phi_\alpha^e = 4.70 \pm 0.01$ eV (at 300 K) and 4.65 ± 0.01 eV (870 K) for α-Fe are corrected to be 4.63 ± 0.01 eV (1125 K) by extrapolation of the linear relationship (its coefficient $\alpha = -9 \times 10^{-5}$ eV/K) between ϕ^e and T [305] (see Section 7.1). It should be noted that the other values (−0.08 eV [3318] and −0.03 eV [305]) are not corrected by the effect due to α.

[m]This value may be corrected to be 0.00 ± 0.16 eV by adoption of our most probable value ($\phi_\beta^e = 3.93 \pm 0.16$ eV for β-Ti in Table 2) instead of the experimental data (3.65–3.6 eV [1404,1522,2194] in Table 11) (see Section 7.1).

[n]The values of ϕ_α^e = 4.923 and 4.960 eV for α-Co are measured at 663 and 300 K, respectively, while ϕ_β^e = 4.966 eV at 300 K is estimated from 4.925 eV at 673 K by extrapolation of the linear relation between ϕ^e and T [1148] (see Section 7.1 for further information).

As a typical example, bulk iron possesses the four allotropic phases of α–δ having T_A = 1042, 1179 and 1674 K corresponding to the boundary temperatures between the respective adjacent phases (see Table 11). The work function change ($\Delta\phi_{\beta\alpha}^e$) for bulk Fe is evaluated to be −0.08 eV by TC [3318]. An experimental study by the Fowler method [305] yields ϕ_β^e = 4.62 eV (1125 K) and also ϕ_α^e = 4.70 eV (300 K) or 4.65 eV (870 K). By extrapolation of ϕ_α^e from both 300 and 870 K to 1125 K according to α = −0.05 eV/570 K = −9 × 10^{-5} eV/K, however, ϕ_α^e is corrected by −0.07 and −0.02 eV at 1125 K (extrapolated temperature). Consequently, the present author estimates $\Delta\phi_{\beta\alpha}^e$ = ϕ_β^e (1125 K) − ϕ_α^e (1125 K) = 4.62 − 4.63 = −0.01 eV (see Footnote (l) in Table 11), which is different from ϕ_β^e (1125 K) − ϕ_α^e (870 K) = 4.62 − 4.65 = −0.03 eV [305] (see Table 11). The former is the *net* change due to the transition alone without including the effect of the temperature coefficient of α. It should be noted that any of the other data on $\Delta\phi_{\beta\alpha}^e$ is not corrected by the temperature effect due to α. On the other hand, $\Delta\phi_{\gamma\beta}^e \equiv \phi_\gamma^e - \phi_\beta^e$ for Fe is found to have the positive values such as 0.06 eV by PE [305] and 0.02 eV by various methods [Here], in contrast to −0.27 eV by TE [310]. The latter, however, may be corrected from −0.27 to 0.02 eV because substitution of ϕ_β^e = 4.48 eV and ϕ_γ^e = 4.21 eV into Eq. (8) yields 4.64 and 4.66 eV, respectively, as already explained in Section 2.8.6 and also in Footnote (k) in Table 11. By another study on Fe [303], the transition ($\beta \to \gamma$) is observed to *increase* by $\Delta\phi_{\gamma\beta}^e$ = 0.09 eV, which is nearly equal to $\Delta\phi_{\gamma\beta}^+ \equiv \phi_\gamma^+ - \phi_\beta^+$ = 4.55 − 4.49 = 0.06 eV determined by PSI of K on Fe at 1183 K [303] (see Footnote 112 in Table 1). The result of $\Delta\phi_{\gamma\beta}^e \approx \Delta\phi_{\gamma\beta}^+$ is very interesting and also important as the first report in this research field.

According to the fine measurements by CPD [1148], α-hcp-Co has ϕ_α^e = 4.923 and 4.960 eV at 663 and 300 K, respectively, in contrast to ϕ_β^e = 4.925 eV for β-fcc-Co at 673 K. In consequence, $\Delta\phi_{\beta\alpha}^e$ may be calculated to be 0.002 or −0.035 eV if the thermal effect due to the temperature coefficient (α) is disregarded in the latter case having a larger difference in temperature (ΔT = 373 K). On the other hand, the extrapolation from 673 to 300 K yields ϕ_β^e = 4.966 eV [1148], which affords $\Delta\phi_{\beta\alpha}^e$ = 0.006 eV as the *net* change due to the phase transition alone because ϕ_α^e = 4.960 eV is measured at 300 K (ΔT = 0 K).

In the case of the Ti-film on W (mono or poly), $\Delta\phi_{\beta\alpha}^e$ determined by FE [1404,1522,2194] has Mean = −0.29 ± 0.05 eV (see Table 11), which is very different from Mean = 0.00 ± 0.03 eV for bulk Ti [179, Here]. The latter is near to Means of $\Delta\phi_{\beta\alpha}^e$ (−0.04, −0.02, 0.07 and −0.04 eV) found for bulk Fe, Co, Sn and U, respectively. According to the data on Ti/W(mono or poly) by FE [1404,1522,2194], ϕ_α^e = 3.88–3.95 eV (mean = 3.93 ± 0.03 eV) is substantially the same with our most probable value of ϕ_α^e = 3.87 ± 0.05 eV (Table 2), but ϕ_β^e = 3.6–3.65 eV [1404,1522,2194] is *smaller* by 0.30 eV than ours of 3.93 eV (Table 2). This difference is exactly corresponding to Mean = −0.29 eV mentioned just above. This fact suggests that $\Delta\phi_{\beta\alpha}^e$ may be corrected to be (3.93 ± 0.16) − (3.93 ± 0.03) = 0.00 ± 0.16 eV. This is just equal to 0.00 ± 0.03 eV found for bulk Ti (see Table 11), although the former has a very large uncertainty of ±0.16 eV. Much further work on $\Delta\phi_{\beta\alpha}^e$ for Ti, however, is needed to clarify the reasons for the large difference (∼0.3 eV) between the film [1404,1522,2194] and the bulk [179]. For example, it may be worth while to resolve the question whether the Ti-film on W is kept substantially unchanged in both surface thickness and smoothness over the temperature range covering α–β phases without depending upon either the annealing at 1300 (or 1100) K or the heating to 1100 K (see Footnotes 97–99 in Table 1).

Regarding both of the uranium bulk and film on tungsten, $\Delta\phi_{\beta\alpha}^e \equiv \phi_\beta^e - \phi_\alpha^e$ is found to have Mean = −0.04 ± 0.04 eV, while $\Delta\phi_{\gamma\beta}^e \equiv \phi_\gamma^e - \phi_\beta^e$ has Mean = −0.09 ± 0.06 eV. The former value for U (−0.04 ± 0.04 eV) is close to $\Delta\phi_{\beta\alpha}^e$ = 0.00 ± 0.03, −0.04 ± 0.03 and −0.02 ± 0.10 eV for the bulks of Ti, Fe and Co, respectively. The latter value for U ($\Delta\phi_{\gamma\beta}^e$ = −0.09 ± 0.06 eV) is essentially equal to $\Delta\phi_{\gamma\beta}^e$ = −0.10 ± 0.03 eV for bulk Sn. The above values for U are estimated tentatively by disregarding the three values of −0.51*, −0.28* and −0.27* eV for $\Delta\phi_{\beta\alpha}^e$ (see Footnote (d) in Table 11) and also by doing those of 0.35**, −0.35** and 0.21** eV for $\Delta\phi_{\gamma\beta}^e$ (see Footnote (e) in id.). The latter example of a wide divergence (−0.35 to 0.35 eV) suggests that both accurate and abundant data around each transition temperature should be accumulated by further investigations. Typically, ϕ_α^e = 3.56 ± 0.05 eV and ϕ_γ^e = 3.4 ± 0.2 eV for the U/W system [1657] are nearly equal to our most probable values of 3.64 ± 0.04 and 3.42 ± 0.05 eV (Table 2), respectively. On the contrary, ϕ_β^e = 3.05 ± 0.03 eV alone [1657] is much smaller by ∼0.5 eV than ours of 3.58 ± 0.04 eV (Table 2). This gap may be ascribed to the anomalous result that both of $\Delta\phi_{\beta\alpha}^e$ = −0.51 ± 0.06* eV and $\Delta\phi_{\gamma\beta}^e$ = 0.35 ± 0.20** eV [1657] (see Table 11) are largely different from many other respective values such as −0.05 ± 0.04 and 0.01 ± 0.04 eV [1664] and as −0.07 ± 0.04 and −0.10 ± 0.04 eV [1654]. Such a gap is the main reason why the asterisked values mentioned above are tentatively disregarded from calculating any Mean about uranium. Of course, much further work is necessary to confirm the acceptability of the above disregarding.

In general, it is very interesting to solve the problem how the monocrystal under study changes in surface orientation according to the allotropic transition, typically from α to β. An X-ray analysis indicates that α-hcp-Zr(0001) changes to β-bcc-Zr(110), which was discovered in 1934 by Burgers [4163]. Such a "Burgers orientation relationship" between $\alpha \leftrightarrow \beta$ transition has long been investigated to date for Zr [3908,3918,4170–4172], Ti [3745,3910,4164–4169], Sn [4363] and so on. Typically, the relationship of α-{0001}∥ β-{110} and α-⟨1120⟩∥β-⟨111⟩ is found to hold by experiment and theory for Ti, too [3910,4164–4169], as well as Zr [4170–4172]. In another case of Hf, α-hcp-Hf(0001) [2967] is stated to transfer to β-bcc-Hf(210) according to the description [3908]. On the other hand, α-hcp-Co(0001) is reported to transfer to β-bcc-Co(111) at T_A = 720 ± 10 K [3192]. For α-hcp-{0001} metals such as Sc, Co, Y, Gd, Tb, Hf, etc., it seems to the present author that the orientation relationship for the $\alpha \leftrightarrow \beta$ transition should be examined in more detail and also that the work function change due to the transition should be investigated precisely by both experiment and theory.

With respect to Y, $\Delta\phi^e_{\beta\alpha}$ is extremely different between the data [4356] and [Here] and, hence, we can hardly estimate correctly its probable value without addition of much data. According to Figs. 1 and 3 for Tb(0001) [4146], ϕ^e decreases from 3.09 ± 0.05 eV (at 1440 K) to 2.94 ± 0.05 eV (1450–1500 K) [3920], while Fig. 3 for Hf(0001) [2967] shows the decrease from 4.11 ± 0.05 eV ($\sim$1800−2040 K) to 3.90 ± 0.05 eV ($\sim$2050−2100 K) [2967]. Consequently, we have $\Delta\phi^e_{\beta\alpha} = -0.15 \pm 0.07$ and -0.21 ± 0.07 eV for Tb and Hf, respectively, as shown in Table 11. Both of the net values are considerably different from the partial mean of -0.03 ± 0.06 estimated for Ti, Fe, Co, Sn and U (see Footnote (j) in Table 11). Strongly, it is desirable to ascertain the reason why $\Delta\phi^e_{\beta\alpha}$ (about -0.15 and -0.21 eV) for Tb(0001) and Hf(0001) is much different from that (-0.03 eV) for the other five metals and to promote the study about the general rule how the various species of monocrystals change in crystallographic orientation according the allotropic transitions of α to β and β to γ, and also to determine the precise *net* values of $\Delta\phi^e_{\beta\alpha}$ and $\Delta\phi^e_{\gamma\beta}$ for many species of metals at the level of 10 meV or less.

With respect to Ru($11\bar{2}2$) and Ru($11\bar{2}5$), anomalous work function change is observed to drop by 0.38 and 0.55 eV, respectively, at 1510 ± 10 K, but to jump up at 1530 ± 10 K to the initial levels of 4.45 and 4.65 eV, respectively [3686]. These changes are assumed to be caused by allotropic transformations, where $\phi^e_\alpha = \phi^e_\gamma$ and $\Delta\phi^e_{\beta\alpha} = -\Delta\phi^e_{\gamma\beta}$ [3686]. Specific heat study about Ru suggests that its crystal has four different types of α ($T < 1308 \pm 5$ K), β (1308–1500 K), γ (1500–1800 K) and δ ($T > 1800$ K) [3980]. The transition temperature corresponding to $\gamma \to \beta$ phase for Ru is changed from 1530 to 1230 ± 10 K by repetition of 500 heating–cooling cycles [3919]. The latent heat of transition at 1230 K is calculated to range from 3.9 to 5.2 kJ/mol [3919], corresponding to as small as 0.040 and 0.054 eV, respectively. According to available literature data, however, the question on possible allotropic modification in Ru is still open [3919].

We may obtain general information about the temperature-dependent allotropic structures of the elements [4382], the number of allotropes of the elements [4383], both allotropic crystal transformation and transition temperatures of rare earth metals [4364, 4384] and those of many metals and several non-metals [4385].

Finally in this section, let's enjoy such interesting topics on allotropy as follows.

(1) In the case of a bulk sample, the paramagnetic γ-fcc-Fe ($\phi^e = 4.54 \pm 0.05$ eV, Table 2) is generally retained at 1179–1674 K alone, and it turns to ferromagnetic α-bcc-Fe (4.55 ± 0.05 eV) at room temperature [3980]. On the other hand, a thin layer system (usually $\theta \leq 10$ ML) of ferromagnetic fcc-Fe/Cu(100) is found to exist at room temperature [2056,3911,3912] (see Footnote 114 in Table 1). Such a *metastable* film system is found by PE to have $\phi^e = 4.59$ eV by deposition at $\sim$300 K and 4.46 eV after annealing at 400 K [2175]. The former value alone is close to 4.62 and 4.67 eV observed by PE for metastable fcc-Fe(100)/Cu(100) prepared at $\sim$300 K [2673].

(2) Such an iron film formed on Cu(100) at $\sim$300 K is found to have the phase corresponding apparently to γ-fcc-Fe(100) at the iron thickness below the critical coverage of $\theta_c \approx 10$ ML [3913]. Above θ_c, on the other hand, the metastable γ-like fcc-Fe(100) ($\phi^e = 4.59$–4.67 eV) undergoes transition to α-bcc-Fe(110) ($\phi^e = ?$ eV) [3913]. This discovery is quite interesting from the viewpoint of solid state physics because the transition of $\gamma \to \alpha$ is undergone by crossing over θ_c alone at a constant temperature ($\sim$300 K), having nothing to do with the transition temperature ($T_A = 1179$ K for γ-phase usually found for bulk Fe). In addition, the transition of γ-like fcc-Fe(100)/Cu(100) to α-bcc-Fe(110)/Cu(100) is also very interesting from the stand point of allotropic orientation relationship, as partly mentioned above. For the metastable films of such as Fe, Co and Ni grown epitaxially on Cu(100), Cu(111) and so on, their peculiarity will be summarized briefly in Section 8.2 together with the data on work function and Curie point having dependence upon film thickness.

(3) At $T_A = 670$ K, α-hcp-Co(0001) with 5.264 eV by CPD [3192] transforms to β-fcc-Co(111) [3192,3914,3916,3917] with 5.266 eV [3192] (see Table 11), but repetition of the transformation changes it into polycrystalline Co ($\phi^e = ?$) [3915].

(4) When a β-fcc-cobalt strip with $\phi^e = 4.25 \pm 0.08$ eV at 1120 K is cooled slowly to room temperature, its phase and ϕ^e are changed to α-hcp-Co and 4.12 ± 0.04 eV, respectively [1631,1632]. By sudden cooling, on the contrary, the former is retained without change in both phase and ϕ^e. This finding is also very interesting as well as the above discoveries [3913,3915] together with both of the θ_c-dependence of Fe [3913] and the polycrystallization of Co owing to repeated transformations [3915]. In addition, it may be worth while to settle the question why the above value of $\phi^e_\alpha = 4.12$ eV for α-Co(poly) [1632] is much smaller than any of the recommended values of 5.0 eV [1045,1358], 4.71 eV [Here] and 4.41 eV [1354], quite similarly to $\phi^e_\beta = 4.25$ eV [1632] being less than 4.50 eV [Here] (see Table 2).

(5) In contrast to Co-crystals existing generally in an α-hcp-phase below T_A ($\approx$ 650–720 K, already mentioned above), Co-fine particles (crystallites, $\sim$10–500 Å) supported on a foreign substrate (e.g., SiO_2, Al_2O_3 or C) have the phase of not hcp- but fcc-structure corresponding to β-phase even below T_A [4338]. Such a phenomenon is observed also for Co/W(mono) systems [364] (see Footnote 474 in Table 1).

(6) Regarding the thickness dependence of both surface structure and work function, it is reported for an Ag/H:Si(111) system at room temperature that $\theta < 5$ and > 20 ML afford $\sim$4.2 and 4.65 ± 0.15 eV, corresponding to Ag(poly) and Ag(111), respectively [1198].

7.2. Work function change due to liquefying

Among many solid elements, these of alkali metals, P, S, Ga, Se, Sn, I, In, Tl, Pb and Bi are well known to have relatively low melting points ($T_m \approx$ 300–600 K). However, it is eight elements alone except Hg (234 K) that the work function data at the liquid state are surveyed by the present author.

The work functions evaluated from Fowler plots are 3.84 ± 0.05 eV for Tl, 3.95 ± 0.05 eV for Pb and 4.25 ± 0.05 eV for Bi [3437]. No significant difference is detected for the three between the solid phase ($\sim$300 K) and liquid one ($T_m + 100$ K) [3437].

The values of ϕ^e for Na, K, Rb and Cs measured by PE are 2.38, 2.28, 2.16 and 1.95 eV, respectively [4208]. Each is the same between the states of solid (298 K) and liquid ($\sim T_m$) within the limit of experimental error [4208], which may be estimated to be ± 0.03 eV from another article [2470].

With respect to Hg, ϕ^e is determined by PE to be 4.510 ± 0.016 and 4.486 ± 0.041 eV at ~ 300 and $83{-}234$ K, respectively [2920], thus yielding $\Delta\phi^e_{LS} \equiv \phi^e_L - \phi^e_{So} = 0.024 \pm 0.044$ eV. Here, ϕ^e_{So} and ϕ^e_L are the work function values at the solid and liquid states, respectively. A thick layer of Hg on FeO at 90 K is found by PE to have $\phi^e = 4.52 \pm 0.02$ eV, which does not change even when the mercury is allowed to melt [2921].

Some experimental data on the work function change ($\Delta\phi^e_{LS}$) due to the phase transition from solid to liquid are summarized for the thirteen elements in Table 12. All of the solid species except γ-Sn show that each mean of $\Delta\phi^e_{LS}$ stays in the range of -0.05 to 0.03 eV, although the work function data available for each element are very scanty. On the other hand, the six data on γ-Sn [1135,1945–1947,3575,4139,4241, Here] are observed to range from -0.04 to -0.17 eV, resulting in the mean value of -0.10 ± 0.05 eV in contrast to any mean mentioned above. A considerable gap between γ-Sn and the other metals should be examined by further study of both theory and experiment.

Table 12
Work function change due to liquefying.

No.	Solid	Liquid	T_m (K)	ϕ^e_{So} (eV)	$\Delta\phi^e_{LS}$ (eV)[a]	ϕ^e_L (eV)	Meth.	Refs.
11	Na	Na	371	2.38	0.00	2.38	PE	[4208]
11	Na	Na	371	2.39	0.00	2.39	PE	[4241]
11	Na	Na	371	2.949	−0.025	2.924	TC	[2419]
11	Na	Na	371	2.54 ± 0.03	0.03 ± 0.26	2.57 ± 0.26	various	[Here][b]
Mean	–	–	–	–	**0.00 ± 0.01**	–	–	–
13	Al	Al	933	4.259	−0.018	4.241	TC	[2419]
19	K	K	337	2.27	0.00	2.27	PE	[4241]
19	K	K	337	2.28	0.00	2.28	PE	[4208]
19	K	K	337	2.29 ± 0.015	0.01 ± 0.02	2.30 ± 0.015	PE	[2476]
19	K	K	337	2.29 ± 0.03	0.01 ± 0.04	2.30 ± 0.03	PE	[2470]
19	K	K	337	2.29 ± 0.02	−0.01 ± 0.03	2.28 ± 0.02	various	[Here][b]
Mean	–	–	–	–	**0.00 ± 0.02**	–	–	–
31	Ga	Ga	303	4.31	0.06	4.37	PE	[4139]
31	Ga	Ga	303	4.35 ± 0.03	−0.05 ± 0.03	4.30 ± 0.01	PE	[2770]
31	Ga	Ga	303	4.36 ± 0.03	−0.06 ± 0.04	4.30 ± 0.02	PE	[2026]
31	Ga	Ga	303	4.27 ± 0.06	0.06 ± 0.07	4.33 ± 0.03	various	[Here][b]
Mean	–	–	–	–	**0.00 ± 0.06**	–	–	–
37	Rb	Rb	312	1.85	−0.05	1.80	TC	[4249]
37	Rb	Rb	312	1.99	−0.06	1.93	PE	[4139]
37	Rb	Rb	312	2.15	0.00	2.15	PE	[4241]
37	Rb	Rb	312	2.16	0.00	2.16	PE	[4208]
37	Rb	Rb	312	2.16	0.00	2.16	PE	[4297]
37	Rb	Rb	312	2.16 ± 0.03	0.01 ± 0.04	2.17 ± 0.03	PE	[2470]
37	Rb	Rb	312	2.17 ± 0.02	−0.04 ± 0.03	2.13 ± 0.02	PE	[4141]
37	Rb	Rb	312	2.17 ± 0.05	−0.02 ± 0.05	2.15 ± 0.02	various	[Here][b]
Mean	–	–	–	–	**−0.02 ± 0.03**	–	–	–
47	Ag	Ag	1234	4.32	0.00	4.32[d]	TE	[1466]
49	In	In	430	3.96	−0.03	3.93	PE	[4139]
49	In	In	430	4.00	−0.07	3.93	PE	[4241]
49	In	In	430	4.07	−0.04	4.03	PE	[4328]
49	In	In	430	4.09 ± 0.01	−0.03 ± 0.01	4.06 ± 0.01	PE	[2770]
49	In	In	430	4.05 ± 0.06	−0.05 ± 0.10	4.00 ± 0.08	various	[Here][b]
Mean	–	–	–	–	**−0.04 ± 0.02**	–	–	–
50	γ-Sn	Sn	505	4.22	−0.04	4.18	PE	[4139]
50	γ-Sn	Sn	505	4.23	−0.04	4.19	PE	[4241]
50	γ-Sn	Sn	505	4.28	−0.11	4.17	PE	[1135]
50	γ-Sn	Sn	505	4.38 ± 0.02	−0.16 ± 0.03	4.22 ± 0.02	PE	[1945–1947]
50	γ-Sn	Sn	505	?	−0.17	?	CPD	[3575]
50	γ-Sn	Sn	505	4.29 ± 0.06	−0.09 ± 0.06	4.20 ± 0.02	various	[Here][b]
Mean[c]	–	–	–	–	**−0.10 ± 0.05**	–	–	–
55	Cs	Cs	301	1.92	−0.01	1.91	PE	[4297]
55	Cs	Cs	301	1.94	0.00	1.94	PE	[4241]
55	Cs	Cs	301	1.95	0.00	1.95	PE	[4208]

Table 12 (*continued*)

No.	Solid	Liquid	T_m (K)	ϕ^e_{So} (eV)	$\Delta\phi^e_{LS}$ (eV)[a]	ϕ^e_L (eV)	Meth.	Refs.
55	Cs	Cs	301	2.241	−0.029	2.212	TC	[2419]
55	Cs	Cs	301	2.05 ± 0.05	−0.05 ± 0.13	2.00 ± 0.12	various	[Here][b]
Mean	–	–	–	–	**−0.02 ± 0.03**	–	–	–
80	α-Hg	Hg	234	4.47 ± 0.03	0.00 ± 0.03	4.475 ± 0.01	PE	[2770]
80	α-Hg	Hg	234	4.486 ± 0.041	0.024 ± 0.044	4.510 ± 0.016	PE	[2920]
80	α-Hg	Hg	234	4.49 ± 0.01	0.00 ± 0.01	4.49 ± 0.01	PE	[1669]
80	α-Hg	Hg	234	4.49 ± 0.01	0.00 ± 0.07	4.49 ± 0.05	PE	[2470]
80	α-Hg	Hg	234	4.52 ± 0.05	−0.02 ± 0.05	4.50 ± 0.02	various	[Here][b]
Mean	–	–	–	–	**0.00 ± 0.01**	–	–	–
81	α-Tl	Tl	577	3.72	−0.08	3.64	PE	[4139]
81	α-Tl	Tl	577	3.84 ± 0.05	0.00 ± 0.07	3.84 ± 0.05	PE	[3437]
81	α-Tl	Tl	577	3.82 ± 0.05	−0.08 ± 0.11	3.74 ± 0.10	various	[Here][b]
Mean	–	–	–	–	**−0.05 ± 0.04**	–	–	–
82	Pb	Pb	601	3.95 ± 0.05	0.00 ± 0.07	3.95 ± 0.05	PE	[3437]
82	Pb	Pb	601	4.11	−0.07	4.04	PE	[4139]
82	Pb	Pb	601	4.07 ± 0.05	−0.07 ± 0.07	4.00 ± 0.05	various	[Here][b]
Mean	–	–	–	–	**−0.05 ± 0.03**	–	–	–
83	Bi	Bi	544	4.25 ± 0.05	0.00 ± 0.07	4.25 ± 0.05	PE	[3437]
83	Bi	Bi	544	4.39	0.03	4.42	PE	[4139]
83	Bi	Bi	544	4.86	0.02	4.88	CPD	[1755]
83	Bi	Bi	544	4.28 ± 0.05	0.06 ± 0.09	4.34 ± 0.07	various	[Here][b]
Mean	–	–	–	–	**0.03 ± 0.02**	–	–	–
Overall mean	–	–	–	–	**−0.02 ± 0.03**	–	–	–

[a] The work function change due to liquefying is shown as $\Delta\phi^e_{LS} \equiv \phi^e_L - \phi^e_{So}$, where ϕ^e_L and ϕ^e_{So} are the work functions at liquid and solid states, respectively.

[b] The work function data [Here] are cited from Table 2.

[c] All of the six data on $\Delta\phi^e_{LS}$ for γ-Sn are found to have the mean value of −0.10 ± 0.05 eV. This is slightly different from any one (−0.05 up to 0.03 eV) for the other twelve species listed herein. As a whole for the thirteen species, we have the overall mean of $\Delta\phi^e_{LS} = -0.02 \pm 0.03$ eV. If the data for γ-Sn are disregarded, we have −0.01 ± 0.02 eV. At any rate, the work function *decrease* due to the phase change from solid to liquid may be generally concluded to be in the order of ∼10 meV or less. Much further work by both experiment and theory may be necessary to settle definitely the problem whether $\Delta\phi^e_{LS} \approx$ 0.00 eV in general.

[d] This is the value corrected from 3.86 eV measured for molten Ag by TE [1466] by the present author (see Footnote 456 in Table 1).

At any rate, the overall means of $\Delta\phi^e_{LS}$ are estimated to be −0.02 ± 0.03 and −0.01 ± 0.02 with and without including the data on γ-Sn, respectively, thus suggesting that $\Delta\phi^e_{LS}$ may generally be in the order of ±10 meV or less. In order to determine a more precise value of $\Delta\phi^e_{LS}$ for each element, however, work function measurements of both ϕ^e_S and ϕ^e_L should be done at the level of 10 meV or less in such a narrow temperature range ($\Delta T \approx 10$ K) of about −5 and +5 K sandwiching T_m so as to minimize the thermal effect due to α·ΔT.

Alchagirov et al. have developed a two-frequency photoelectric method for continuously measuring the fast changes in ϕ^e owing to adsorption, phase transition, modification of surface structure and so on, thereby showing such a typical result for In that $\Delta\phi^e_{LS}$ can be measured more precisely compared with the Fowler method [4328].

8. Work function change due to magnetic transformation

This section summarizes the work function change due to magnetic transformation at the Curie temperature (T_C) from ferro- to paramagnetic state of both bulk metals and metastable metal films together with the dependence of T_C upon film thickness.

8.1. Work function change of bulk metal at the Curie point

These metals of Fe, Co, Ni and Gd are well known to change from ferro- to paramagnetic state at the Curie points (T_C) of typically 1042, 1390, 631 and 290 K [3980, etc.], respectively. Speaking in general, however, the experimental data on T_C as well as T_A (see Section 7.1) fluctuate widely from literature to literature. For instance, the values reported for Co by the five groups of workers have a range of $T_C = 1367–1404$ K [4336]. In this section, let's treat the problem how the work function changes at T_C.

Typically, the α-bcc-Fe below $T_C = 1042$ K is ferromagnetic, but the β-bcc-Fe at 1042–1179 is paramagnetic. The γ-fcc-Fe (1179–1674 K) and δ-bcc-Fe (1674–1811 K) are paramagnetic, too [1916,2056,3980]. Work function change of $\Delta\phi^e_{PF} \equiv \phi^e_P - \phi^e_F$ due to the magnetic transition from ferro- to paramagnetic state is equivalent to that of $\Delta\phi^e_{\beta\alpha} \equiv \phi^e_\beta - \phi^e_\alpha$ since T_C is equal to T_A for the α → β transition of Fe. As already shown in Section 7.1 and Table 11, the values of $\phi^e_\alpha = 4.70$ eV (300 K) and 4.65 eV (870 K) [305] are corrected to be 4.63 eV (1125 K) by extrapolation according to $\alpha = -9 \times 10^{-5}$ eV/K and, hence, $\Delta\phi^e_{\beta\alpha}$ is concluded

to be $\phi_\beta^e - \phi_\alpha^e = 4.62 - 4.63 = -0.01$ eV instead of $4.62 - 4.70 = -0.08$ and of $4.62 - 4.65 = -0.03$ eV [305] (see Footnote (l) in Table 11).

In Table 13, all of the data available at present are summarized for Co, Ni and Gd in addition to Fe. Theoretical investigation concludes that $\Delta\phi_{PF}^e = -0.135$ eV in general [3673]. As shown in Table 13, the values of $\Delta\phi_{PF}^e$ for Ni have a range from -0.050 to 0.045 eV, thus yielding Mean = 0.01 ± 0.03 eV (see the last line for Ni). This value is very close to Mean = 0.00 ± 0.01 eV for Gd.

Table 13
Work function change due to magnetic transformation[a].

No.	Ferromag.	Paramag.	T_C (K)	ϕ_F^e (eV)[c]	$\Delta\phi_{PF}^e$ (eV)[b]	ϕ_P^e (eV)[c]	Meth.	Refs.
26	α-bcc-Fe	β-bcc-Fe	1042	4.63 (1125)[1]	-0.01	4.62 (1125)	PE	[305]
26	α-bcc-Fe	β-bcc-Fe	1042	4.65 (870)	-0.03	4.62 (1125)	PE	[305]
26	α-bcc-Fe	β-bcc-Fe	1042	4.53	-0.08	4.45	TC	[3318]
26	α-bcc-Fe	β-bcc-Fe	1042	4.55 ± 0.05 (~300)	-0.03 ± 0.18	4.52 ± 0.17 (~1100)	various	[Here][d]
Mean	–	–	–	–	$\mathbf{-0.04 \pm 0.03}$	–	–	–
27	β-fcc-Co	β-fcc-Co	1390	4.65 ± 0.22 (~1050)	-0.05 ± 0.30	4.60 ± 0.19 (~1500)	various	[Here][e]
28	fcc-Ni	fcc-Ni	631	4.645 (300)	0.045[k]	4.690 (660)	CPD[i]	[503]
28	fcc-Ni	fcc-Ni	631	4.660 (400)	0.040[k]	4.700 (740)	CPD[i]	[503]
28	fcc-Ni	fcc-Ni	631	4.660 (400)	-0.007[f]	4.653 (400)	CPD[i]	[503]
28	fcc-Ni	fcc-Ni	631	5.05 (623)	0.05	5.10 (770)	PE	[943]
28	fcc-Ni	fcc-Ni	631	? (?)	-0.050[g]	? (?)	TC	[3954]
28	fcc-Ni	fcc-Ni	631	? (?)	0.009[g]	? (?)	TC	[2358]
28	fcc-Ni(100)	fcc-Ni(100)	631	? (~600—631)	0.00	? (631–700)	CPD[i]	[3924]
28	fcc-Ni(100)	fcc-Ni(100)	631	? (413)	-0.004	? (631)	CPD[i]	[496]
Mean	–	–	–	–	$\mathbf{0.01 \pm 0.03}$[h]	–	–	–
64	hcp-Gd(0001)	hcp-Gd(0001)	290	? (220)	-0.016	? (220)[j]	CPD[i]	[3924]
64	hcp-Gd	hcp-Gd	290	3.76	0.01	3.77	TC	[2358]
Mean	–	–	–	–	$\mathbf{0.00 \pm 0.01}$	–	–	–
Overall mean[m]	–	–	–	–	$\mathbf{-0.01 \pm 0.04}$	–	–	–

[a]Theoretical study on the work function change due to para- to ferromagnetic transition yields 0.135 eV = $-\Delta\phi_{PF}^e$ in general [3673].

[b]The work function change due to ferromagnetic to paramagnetic transformation beyond the Curie point (T_C) is shown as $\Delta\phi_{PF}^e \equiv \phi_P^e - \phi_F^e$.

[c]In parentheses in the 5th or 7th column is given the temperature (in K) adopted for determining each work function value (ϕ_F^e or ϕ_P^e) corresponding to the ferro- or paramagnetic state (see Footnote 1 below).

[d]The work function data [Here][d] are cited from Table 2.

[e]The values of ϕ_F^e and ϕ_P^e for β-Co [Here][e] are estimated from these data obtained in the ranges of 720–1390 K [310,3153,3604] and of 1390–1600 K [769,2304,3604], respectively (see Table 1).

[f]The change ($\Delta\phi_{PF}^e \equiv \phi_P^e - \phi_F^e = -0.007$[f] eV) for Ni is determined at the same temperature (400 K) for both ϕ_P^e and ϕ_F^e after extrapolating the former in the range from 750–600 K to 400 K [503] (see also Footnote 132 in Table 1). This is the *net* change due to the magnetic transition alone. On the contrary, the others ($\Delta\phi_{PF}^e = 0.045$[k] and 0.040[k] eV) are tentatively estimated by the present author taking the data on ϕ_F^e and ϕ_P^e determined at respectively different temperatures (by ~350 K gapped) indicated in the parentheses beside each ϕ_F^e and ϕ_P^e. In other words, the work function change ($\Delta\phi_T^e \approx -0.05$ eV) due to the temperature decrease by ~350 K in the range covering T_C is disregarded in the latter estimation. Such a fine measurement as excluding the effect due to $\Delta\phi_T^e$ is needed for any samples, too, in order to determine precisely the *net* value of $\Delta\phi_{PF}^e$ itself in the order of 1 meV.

[g]Both of the values for Ni are cited from Ref. [503].

[h]This mean for Ni is obtained without including the data[k] (see Footnote k below).

[i]The piezoelectric driven Kelvin probe improved by Saito et al. has an accuracy of ±1 meV in work function measurements at ~100–1000 K [4065].

[j]The linear relation between T and ϕ^e at the paramagnetic state above T_C (~460–300 K) for Gd is extrapolated down to 220 K, where ϕ^e is found to be lower by 14 meV than ϕ^e at T_C, while ϕ^e at the ferromagnetic state at 220 K is higher by 2 meV than ϕ^e at T_C. Therefore, $\Delta\phi_{PF}^e \equiv \phi_P^e - \phi_F^e$ is estimated to be -16 meV at 220 K [3924].

[k]Both of the values of $\Delta\phi_{PF}^e = 0.045$ and 0.040 eV for Ni are estimated from ϕ_P^e and ϕ_F^e measured at different temperatures and, hence, any of them is not the *net* value originating from the transition alone. Consideration of the temperature coefficient (α) of ϕ^e (see Table 6 in Ref. [1351]) yields $\Delta\phi_{PF}^e = -0.007$ eV (see Footnote f above).

[1] The value of $\phi_F^e = 4.63$ eV (1125 K) for Fe is corrected from 4.70 eV (300 K) by consideration of the thermal change due to the temperature coefficient of $\alpha = -9 \times 10^{-5}$ eV/K (for detail, see Section 7.1 and Footnote 1 in Table 11).

[m]The overall mean including all of the data on the above four metals affords $\Delta\phi_{PF}^e = -0.01 \pm 0.04$ eV. Consideration of the above fine measurement for Ni [503], however, may lead to the conclusion that the work function change due to the magnetic transition is generally in the order of ~10 meV or less.

Regarding the most probable value of $\Delta\phi_{PF}^e$ for Co, it is very difficult to estimate such a minute change probably as in order of 10 meV or less because both ϕ_F^e and ϕ_P^e [Here] originating from various specimens and methods are very large in standard deviation (±0.22 and ±0.19 eV, respectively) and also in temperature difference (~450 K). For the same specimen at nearly the same temperatures sandwiching T_C, therefore, both ϕ_F^e and ϕ_P^e should be measured not intermittently and indirectly by TE (Richardson plot) but continuously and directly by another method.

The work function of Ni(100) is found to change considerably with the temperature coefficient of $\alpha = -1.83 \times 10^{-4}$ eV/K in the range from ~760 to 631 K (T_C) at paramagnetic state [496]. But, an upper deviation from the linearity starts at T_C, gradually

increasing $\Delta\phi_{PF}^{e}$ from 0 up to 4 meV in the range of 631 K down to 140 K at ferromagnetic state [496]. Namely, $\Delta\phi_{PF}^{e}$ for Ni(100) is −0.004 eV [496]. According to a previous study by the same group of workers [503], $\Delta\phi_{PF}^{e}$ for Ni(poly) is evaluated to be $\Delta\phi_{PF}^{e} \equiv \phi_{P}^{e} - \phi_{F}^{e} = 4.653 - 4.660 = -0.007$ eV at the same temperature (400 K) after extrapolation of ϕ_{P}^{e} from ~700 to 400 K. This is the *net* change due to the transition alone without including the thermal effect ($\alpha \cdot \Delta T$) upon the work function. On the other hand, $\Delta\phi_{PF}^{e} = 0.045$ eV is estimated from both $\phi_{P}^{e} = 4.690$ eV at 660 K (above $T_{C} = 631$ K) and $\phi_{F}^{e} = 4.645$ eV at 300 K, thus yielding a difference by 0.045 eV in comparison with the above (−0.007 eV). This difference estimated tentatively by the present author is caused by disregarding the temperature dependence of ϕ^{e} inherent in any metal (see Table 6 in Ref. [1351]). Namely, the comparison of ϕ_{P}^{e} and ϕ_{F}^{e} at different temperatures does never yield accurately the *net* value of $\Delta\phi_{PF}^{e}$ itself.

According to the fine measurement (at ~1 meV level) made about 10 years later for Ni(100) by the same group using a CPD method again, however, noticeable change (>1 meV at level) is not observed at T_{C} [3924].

In respect of Gd(0001) [3924], ϕ^{e} at the paramagnetic state decreases almost linearly by ~20 meV with decreasing temperature from ~400 K down to T_{C} (~290 K). Below T_{C} at the ferromagnetic state, however, ϕ^{e} shows a minimum (shallow valley) at ~280 K and does a maximum (small hump) at ~250–230 K. Then, ϕ^{e} at ~230–220 K remains nearly at a constant, which is higher by 2 meV than ϕ^{e} at T_{C} [3924]. Regarding the paramagnetic state, on the other hand, ϕ^{e} at 220 K is found to have a value lower by 14 meV than that at T_{C} after extrapolating the above linearity from T_{C} down to 220 K according to the temperature dependence of D_{b} (dipole barrier) [3924]. Consequently, the above transformation affords the work function change of $\Delta\phi_{PF}^{e} \equiv \phi_{P}^{e} - \phi_{F}^{e} = -16$ meV at 220 K (about 70 K below T_{C}).

The overall mean of the four bulk metals is estimated to be −0.01 ± 0.04 eV, as shown in Table 13. On the other hand, the results based on the *fine* measurements for the bulks of Ni(poly) [503], Ni(100) [496] and Gd(0001) [3924] studied by the same group of Saito et al. indicate that $\Delta\phi_{PF}^{e}$ is as small as −0.009 ± 0.005 eV. Therefore, such a minute value may be disregarded in a usual treatment of ϕ^{e} accompanied with an error of ±0.05 eV or more in general (see Table 2). In other words, it is very difficult to determine $\Delta\phi_{PF}^{e}$ precisely at the level of 1 meV by means of usual methods employed by many workers.

At present, $\Delta\phi_{PF}^{e}$ may be roughly estimated to be at the level of −0.01 eV or so in general, although the data themselves are very scanty and also they are scattered in a rather wide range from −0.08 to +0.05 eV even among the four metal species (see Table 13).

8.2. Both work function and Curie point of metastable metal films

In addition to the four allotropes of bulk Fe mentioned in Section 7.1, the metastable film of Fe grown epitaxially on Cu(100) has the peculiarity different from bulk Fe. Namely,

(1) α-bcc-Fe ($T_{A} = 1042$ K, ferromag., $T_{C} = 1042$ K, $\phi^{e} = 4.55 \pm 0.05$ eV).
(2) β-bcc-Fe (1042–1179 K, paramag., $\phi^{e} = 4.52 \pm 0.17$ eV).
(3) γ-fcc-Fe (1179–1674 K, paramag., $\phi^{e} = 4.54 \pm 0.05$ eV).
(4) δ-bcc-Fe (1674–1808 K, paramag., $\phi^{e} = 4.76 \pm 0.1$ eV).
(5) m-fcc-Fe (<1042 K, ferromag., $T_{C} = variable$, $\phi^{e} = 4.58 \pm 0.10$ eV).
(6) m-fcc-Fe(100) (<1042 K, ferromag., $T_{C} = variable$, $\phi^{e} = 5.38 \pm 0.22$ eV).

Here, "m" means the "metastable" and, T_{A} and T_{C} are cited from Ref. [3980], while each value of ϕ^{e} is done from the 3rd column in Table 2.

Typically for the metastable γ-like fcc-Fe(100)/Cu(100) system (6) above, already mentioned in Topics (1) and (2) in Section 7.1, ϕ^{e} is theoretically evaluated to be 4.95 or 5.00 eV [1914], 5.48 or 5.58 eV [1913,4386] and 5.6 eV [1916], some of which are well accordant to some of the experimental data on 4.62 or 4.67 eV [2673], 4.95 eV [2650], and 5.4 or 5.5 eV [1916] determined by PE at ~300 K, although the wide divergence by up to ~0.65 or 0.9 eV makes it very difficult to compare decisively the data among different authors. The value of $\phi_{F}^{e} = 4.62$ eV found for the ferromagnetic m-Fe(100) film grown at room temperature [2673] is slightly different from $\phi_{P}^{e} = 4.67$ eV for the paramagnetic one established after annealing above 500 K [2673], thereby resulting in $\Delta\phi_{PF}^{e} = 0.05$ eV. This value is somewhat different from −0.04 ± 0.03 eV for bulk Fe (see Table 13). The most provable value of 5.38 ± 0.22 eV (Table 2) for m-fcc-ferromagnetic film-Fe(100) (~300 K) seems to be near to 5.28 ± 0.19 eV for γ-fcc-paramagnetic bulk of Fe (100) (1179–1674 K), although the gap of 0.1 eV between the two is accompanied with a large standard deviation of ±0.29 eV. On the contrary, the former is certainly different from 4.64 ± 0.05 eV recommended for α-bcc-ferromagnetic bulk-Fe(100) (Table 2).

On the other hand, m-fcc-ferromagnetic film-Fe on Cu(100) listed above (5) is found to have 4.58 ± 0.10 eV (Table 2), which is very near to 4.55 ± 0.05 eV for α-bcc-ferromagnetic bulk-Fe (Table 2). In contrast to the latter with T_{C} kept constant at 1042 K, the former changes in T_{C} from 230 to 390 K as θ increases from 1 to 3–5 ML having $\phi_{F}^{e} = 4.7 \pm 0.1$ eV [2878]. In another case, the m-fcc-Fe-film is reported to have $T_{C} = 150$ and 300 K at $\theta = 5$ and 7 ML, respectively [4345]. Similarly, such an fcc-film is observed to have $T_{C} \approx 380$ and 290 K at $\theta \approx 3$ and 6–10 ML, respectively, above which the film structure is changed to bcc [3912]. In contrast, the film formed at 463 K is found to have the ferromagnetism, which disappears after keeping for 1 h or cooling to ~300 K [4386]. The film grown at ~300 K is not ferromagnetic [4386]. Regarding the m-fcc-Fe film ($\theta_{Fe} = 3$ or 7 ML) prepared on Cu-capped films ($\theta_{Cu} = 0$–5 ML) [4361], T_{C} is found to depend on θ_{Fe} and also to have an oscillatory dependence upon θ_{Cu}, showing nearly the same pattern between theory and experiment. As θ_{Cu} increases from 0 to 5 ML at $\theta_{Fe} = 3$ ML, for example, T_{C} oscillates between ~370 and 265 K (experiment) and ~530 to 480 K (theory), all of which are much below 1042 K characteristic of α-bcc-bulk Fe. For such an interesting and complicated magnetic behavior, much further work is fully expected to be done by both theory and experiment together with precise measurements of ϕ^{e} around each T_{C} changing dependently upon θ.

The metastable film of Co grown epitaxially on Cu(100) has the property different from the two allotropes of bulk cobalt. Namely,

(1) α-hcp-Co (T_A = 695 K, ϕ^e(0001) = 5.30 eV, ϕ^e = 4.71 eV).
(2) β-fcc-Co (695–1675 K, ϕ^e(100) = 5.25 eV, ϕ^e = 4.50 eV, T_C = 1390 K).
(3) m-fcc-Co (<695 K, ϕ^e(100) = 4.72 eV, $\phi^e \approx$ 4.8 eV, T_C = *variable*).

The metastable fcc-phase of ferromagnetic Co(100) film grown epitaxially on Cu(100) is found by PE to have ϕ^e = 4.72 eV [2673], which is intermediate between our values of 5.25 ± 0.17 eV for β-fcc-Co(100) and 4.50 ± 0.13 eV for β-fcc-Co (Table 2). Similarly, the metastable Co-films (1–9 ML) grown on Cu(100) at ~300–400 K exhibits the β-like fcc-structure, and they are determined by PE to have ϕ^e = 5.0 ± 0.2 eV [2879] (see Footnote 121 in Table 1) and evaluated by TC to have 5.34 eV [3654] (see id. 122).

As shown for m-fcc-Co on Cu(100) or Cu(111) in Table 1, the average of ϕ^e = 4.94 ± 0.30 eV is calculated from the twelve data achieved for the Co-films by PE or TC, while that of ϕ^e = 4.74 ± 0.23 eV done from six ones by PE alone. The average of 4.74 eV is quite near to 4.72 eV for m-Co(100) [2673] mentioned above, thereby suggesting that the Co-films [950,968,2879,3475] listed in Table 1 consist mainly of the (100) face, although the former is accompanied with a very large standard deviation (±0.23 eV) and the latter is due to a single datum alone [2673]. It may be strongly expected to accumulate much abundant data for the both films by theory and experiment.

Regarding the metastable fcc-Co-film on Cu(100), its Curie point (T_C) is reported to have a linear dependence upon Co-coverage (θ). Namely, T_C increases from ~100 to 500 K as θ increases from 1.5 to 2.5 ML, showing a bulk-like behavior (T_C = 1390 K) at $\theta \approx$ 5–6 ML [3923]. This result suggests strongly that the thick film (θ > 5 ML) is equivalent to bulk cobalt with respect to the magnetic property. Such a dependence is observed also for a Co/Cu(111) system, where T_C increases from 207 to 500 K with increasing θ from 1.0 to 1.7 ML [4355]. Interestingly, T_C is found to have the dependence upon the deposition temperature (T_{dep}), too [4394]. Typically for 2 ML, T_C increases from 170 to 325 K when T_{dep} is changed from 340 to 275 K [4394].

Similarly for Ni/Cu(100) and Ni/Cu(111) with increasing in θ from ~3 to 16 and ~2 to 17 ML, T_C increases from 210 to 540 K and 197 to 603 K, respectively [4355], both of which are lower than $T_C \approx$ 630 K accepted generally for bulk nickel.

Experimental and theoretical studies [e.g., 3743,4345–4355,4387–4394] are made on the magnetism of metastable metal films (Fe, Co, Ni, Gd, etc.) grown epitaxially on monocrystalline metal substrates (Cu, Ag, W, Au, etc.). For these systems, additional studies are strongly expected to measure finely the work function values around T_C as a function of θ.

9. Work function change due to superconductive transition

All the data available at present for the work function change due to superconductive transition are summarized in Table 14, where T_S and T_M are the temperatures correspondent to the superconductive transition and the work function measurement, respectively, while ϕ^e_C and ϕ^e_{FE} are the work functions determined for each metal film/quartz system by CPD and for each bulk metal by FE, respectively. The 7th column shows Footnote numbers of 102, etc. (see Table 1), which may be helpful for obtaining further information about each experiment.

Table 14
Work function change due to superconductive transition.

Surface	T_S (K)[a]	T_M (K)[b]	ϕ^e_C (eV)[c]	ϕ^e_{FE} (eV)[d]	$\Delta\phi^e_{SN}$ (eV)[e]	Note[f]	Ref.
Al	1.2	293	4.2 ± 0.2	–	–	102	[1686]
		135	4.2 ± 0.2	–			
		77	–	4.20			
		5	–	4.20			
		4.2	4.1 ± 0.2	–			
V	5.4	293	3.0 ± 0.2	–	0.2 ± 0.3	101	[1686]
		15	2.9 ± 0.2	–			
		4.2–15	–	3.77			
		4.2	3.1 ± 0.2	–			
Nb	9.2	293	3.9 ± 0.2	–	0.1 ± 0.3	164	[1686]
		28	3.8 ± 0.2	–			
		5	–	5.01			
		4.2	3.9 ± 0.2	–			
Ta	4.4	293	3.8 ± 0.2	–	0.3 ± 0.3	260	[1686]
		35	3.5 ± 0.2	–			
		4.2–35	–	4.16			
		4.2	3.8 ± 0.2	–			
BSCCO	85	85	4.849	–	0.004	#	[912]
		50	4.851	–			
		50 (extrap.)	4.847[g]				

[a]T_S is the superconductive transition temperature.

[b]T_M is the temperature selected for measuring each work function.

[c]ϕ_C^e is the work function determined by CPD for each metal film prepared on quartz (Al–Ta).

[d]ϕ_{FE}^e is the work function measured by FE for each bulk metal (Al–Ta).

[e]$\Delta\phi_{SN}^e \equiv \phi_S^e - \phi_N^e$ is the work function change due to the transition from the normal to superconductive state, where the change for each metal (V–Ta) is estimated by the present author. Frankly speaking, it is impossible to determine $\Delta\phi_{SN}^e$ precisely at the level of ~ 0.01 eV or less because a fine measurement of ϕ^e for any of V–Ta is not made continuously around T_C, in contrast to the below case [912] (see Footnote g below).

[f]Each of the four numbers shows the Footnote number in Table 1, whilst the mark (#) corresponds to a monocrystalline compound of $Bi_2Sr_2CaCu_2O_8$.

[g]Fig. 3 [912] shows that ϕ^e has the temperature coefficient of $d\phi^e/dT = 5.5\times$ and -5.1×10^{-5} eV/K above and below $T_C = 85$ K, respectively. Extrapolation of the former from 85 K (4.849 eV) to 50 K yields 4.847 eV, which affords $\Delta\phi_{SN}^e = 0.004$ eV because the latter is directly determined to have 4.851 eV at 50 K. Even at 0 K more below T_C, the change is still small as 0.009 eV [912].

As may be seen in Column 4 in Table 14, each of the data (ϕ_C^e) by CPD for the V–Ta films [1686] is accompanied with a large standard deviation of ± 0.2 eV. Therefore, it is very difficult to estimate finely the work function change ($\Delta\phi_{SN}^e \equiv \phi_S^e - \phi_N^e$) due to the transition between the two states, although Column 6 includes the values of $\Delta\phi_{SN}^e = 0.2 \pm 0.3$, 0.1 ± 0.3 and 0.3 ± 0.3 eV estimated tentatively by the present author for the three metals of V, Nb and Ta, respectively. Here, ϕ_S^e and ϕ_N^e correspond to the superconductive and normal states, respectively. On the other hand, the data on ϕ_{FE}^e measured for each bulk by FE (see Column 5) seem to be considerably different from those on ϕ_C^e by CPD for each film (except Al), thereby suggesting that the absolute values of both ϕ_S^e and ϕ_N^e around T_S are also different between the film and bulk for each species. According to the description in text [1686], the transition has no effect on the pattern of Fowler–Nordheim graphs. In other words, it may be considered that an appreciable change in ϕ^e is not detected around T_S, thereby leading to the tentative estimation as follows. Namely, $\Delta\phi_{SN}^e$ is as small as ± 0.01 eV or less by consideration of the data that $\phi_F^e = 3.77 \pm ?$ eV $=$ constant in the range of 4.2–15 K sandwiching $T_S = 5.4$ K for V and also that $\phi_F^e = 4.16 \pm ?$ eV $=$ constant at 4.2–35 K covering $T_S = 4.4$ K for Ta. At any rate, such a fine measurement as the level of ~ 10 meV or less may be necessary in general in order to measure a very minute change around T_S. From this point of view, let's examine the below data obtained for a chemical compound since no datum achieved by fine measurements of $\Delta\phi_{SN}^e$ for any metal is yet found by the present author.

Regarding a monocrystalline specimen of $Bi_2Sr_2CaCu_2O_8$ [912], a plot of work function vs. temperature is found to have a minimum ($\phi^e = 4.849$ eV) at the transition temperature ($T_S = 85$ K), where the temperature coefficient ($d\phi^e/dT$) changes from 5.5×10^{-5} eV/K for the normal state to -5.1×10^{-5} eV/K for the superconductive one [912]. Therefore, the latter work function (ϕ_S^e) increases up to 4.851 eV at 50 K, while the former one (ϕ_N^e) extrapolated from T_S to 50 K is estimated to be 4.847 eV. In consequence, the *net* change in work function ($\Delta\phi_{SN}^e \equiv \phi_S^e - \phi_N^e$) is determined to be 0.004 eV at 50 K or 0.009 eV at 0 K [912]. Namely, ϕ^e *increases* only by less than 0.01 eV according to the transition from the normal to superconductive state.

For another sample of $YBa_2Cu_3O_{7-x}$ ($T_S \approx 80-90$ K) [4365], the work function is found to increase by 19 or 31 meV as T decreases from ~ 80 or 89 to 30 K. Such an increase, however, is not equal to the *net* value of $\Delta\phi_{SN}^e$ itself because the former includes the change of the thermal effect ($\Delta\phi^e \equiv \alpha \cdot \Delta T$) coming from the temperature difference of $\Delta T \approx 50$ or 59 K (see Section 10).

10. Remark on work function measurements around critical temperatures

As already mentioned for the transition from ferro- to paramagnetic state in Section 8.1, the *net* change of $\Delta\phi_{PF}^e = 0.00$ or -0.004 eV is found for Ni(100) (see Table 13) by the same group of workers [496,3924] on the basis of very precise measurements at the level of ~ 1 meV. Such a minute change as below 0.01 eV can hardly be observed accurately by usual work function measurements accompanied with uncertainty of about ± 0.05 eV or more in general. In other words, the low level of ~ 0.01 eV or less is usually disregarded in the treatment of work function data in many fields of physics and chemistry. However, such fine measurements of both $\Delta\phi_{PF}^e \equiv \phi_P^e - \phi_F^e$ and $\Delta\phi_{SN}^e \equiv \phi_S^e - \phi_N^e$ owing to the magnetic and superconductive transformations [496,3924], respectively, are very interesting and important from the viewpoint of fundamental physics. In consequence, it is fully expected to investigate the changes much further by both theory and experiment, although they seem generally to be very minute (at the level of ~ 0.01 eV or less) comparably to such a thermal work function change ($\Delta\phi^e \approx 3\ kT/2 \approx 1.3 \times 10^{-4} \times 50 \approx 0.006$ eV) even in a narrow range of less than ~ 50 K at the intermediate temperatures sandwiching the magnetic or superconductive transition temperature (T_C or T_S). In other words, the temperature dependence of ϕ^e inherent in any metals (see just below for typical examples) should be taken into consideration whenever the *net* work function change due to the transition itself alone is to be measured precisely in some temperature range covering the critical point (T_C or T_S) under study. Such a precise measurement is needed around T_A and T_m, too.

With respect to the temperature dependence of work function, theoretical and experimental studies are made by many workers [495–502,3741,4122,4123, etc.], and much data on the temperature coefficient (α) are summarized in Table 6 [1351]. Usually, α is found to range largely from about $\pm 10^{-4}$ to $\pm 10^{-5}$ eV/K depending upon metal species and also to scatter widely from specimen to specimen even for the same species. Typically for W(100) and W(110), α changes in a wide range from $<+1 \times 10^{-4}$ eV/K [84] to -1.09×10^{-4} eV/K [502] and from $+(6.3 \pm 0.6) \times 10^{-5}$ eV/K [194] to -3.7×10^{-4} eV/K [1084], respectively. Similarly for Ni and Mo, it varies greatly from $-(9.9 \pm 1.7) \times 10^{-6}$ eV/K [499] to -1.0×10^{-3} eV/K [179,650] and from $+(7.86 \pm 0.04) \times 10^{-5}$ eV/K [909] to -2.21×10^{-4} eV/K [124], respectively, from worker to worker. Such situation generally makes it very difficult to measure precisely a very minute change (probably much less than ± 0.1 eV) in work function at the critical temperature of allotropic, magnetic, superconductive or solid to liquid state transition, as already summarized in Sections 7–9 and Tables 11–14.

It should be emphasized here again that the work function change due to the above transitions should be measured precisely at the level of ± 1 meV (see Footnote (i) in Table 13). In other words, we should try to determine precisely (1) the temperature coefficient

(α) in a suitable range covering the critical temperature (T_A, T_C, T_S or T_m), (2) the work function values after extrapolating the relationship (ϕ^e vs. T) to the temperatures lower or higher than the critical point under study, and (3) the *net* value of work function change due to the transition alone without including the considerable effect due to α. Regarding the work function change due to $\alpha = \pm 10^{-4}$ eV/K in a narrow range of 100 K, for instance, it is estimated to be ± 0.01 eV, which is comparable to many of the values found as the probable change (*net* value) owing to the transition alone under study (for further information, see Footnote (l) in Table 11 and also Footnotes (k) and (l) in Table 13).

In conclusion, much further work is needed for any sample to determine accurately the minute value of work function change due to transition alone at T_A, T_C, T_S or T_m.

11. Work function dependence upon the size of fine particles

In this section, a classical theory of work function about fine particles will be summarized briefly together with the comparison between the theoretical values and the experimental data on work function available for various metal particles. After outlining a quantum theory about the energetics correlating either ionization energy or electron affinity of atom with work function of bulk solid, photoelectron spectroscopic studies will be focused on a variety of metal clusters and also on the determination of bulk work function from spectroscopic data.

11.1. Classical theory for fine particles

With respect to the fine particle having a small radius (r), a classical theory about its work function based on the image-potential model affords the following equation [3442].

$$\phi^e(r) = \phi^e(\infty) + C_p e^2/r, \tag{17}$$

$$= \phi^e(\infty) + 5.40/r \text{ (Å)} \quad \text{(for } C_p = 3/8\text{)}. \tag{17'}$$

Here, $\phi^e(\infty)$ is equivalent to $\phi^e(\text{poly})$ for bulk corresponding to $r \to \infty$, and e is the elementary electric charge. By taking the coefficient of $C_p = 3/8$, $\phi^e(\infty)$ for bulk Ag is estimated from Eq. (17') to be 4.37 eV [3442] as the best fit to the experimental data on $\phi^e(r) = 4.65$, 4.57 and 4.55 eV for $r = 20$, 27 and 30 Å, respectively [3127]. The value of $\phi^e(\text{poly}) = \phi^e(r \to \infty) = 4.37$ eV thus calculated [3442] is considerably different from the experimental value of $\phi^e(\text{poly}) = 4.90$ eV determined directly by PE for the macroscopic surface [3127] (see Footnote 208 in Table 1), but the former agrees exactly with ours of 4.39 ± 0.02 eV recommended for polycrystalline Ag in Table 2.

Tentatively, the available data on both $\phi^e(\infty)$ and $r(\text{Å})$ are substituted into Eq. (17'). Then, the values of $\phi^e(r)$ thus calculated by the present author are compared with those determined experimentally by the corresponding author(s), thereby yielding the results of (1)–(13) below. Here, the values in {A}, <B> and (C/D) indicate that A is the polycrystalline work function of $\phi^e(\text{poly})$ (in eV) cited as $\phi^e(\infty)$ from Column 3 in Table 2, B is the radius of r (in Å) either reported by the corresponding author(s) or estimated by the present author (see Section 11.3), C is the work function of $\phi^e(r)$ (in eV) calculated from Eq. (17') by the present author employing $A \equiv \phi^e(\text{poly})$ and $B \equiv r(\text{Å})$, and D is $\phi^e(r)$ measured by the corresponding author(s) by means of photoelectric quantum yield of each metal particle. In the last parentheses is given the footnote number in Table 1 so as to provide further information about each data.

(1) Al {4.26 ± 0.03} // < 22 > ($4.51 \pm 0.03/?$) [2199] (449).
(2) Al {4.26 ± 0.03} // < 52.9 > ($4.36 \pm 0.03/?$) [2199] (449).
(3) Ni {5.06 ± 0.06} // < 60–100 > ($5.13 \pm 0.02/5.1$) [2667] (448).
(4) Cu {4.51 ± 0.04} // < 30 > ($4.69 \pm 0.04/4.80 \pm 0.1$) [3190] (149).
(5) Pd {5.17 ± 0.06} // < 30 > ($5.35 \pm 0.06/5.45 \pm 0.1$) [3190] (149).
(6) Ag {4.39 ± 0.02} // < 20 > ($4.66 \pm 0.02/4.65$) [3127] (208).
(7) Ag {4.39 ± 0.02} // < 27 > ($4.59 \pm 0.02/4.57$) [3127] (208).
(8) Ag {4.39 ± 0.02} // < 30 > ($4.57 \pm 0.02/4.55$) [3127] (208).
(9) Ag {4.39 ± 0.02} // < 30 > ($4.57 \pm 0.02/4.50$) [3190] (149).
(10) Ag {4.39 ± 0.02} // < 50 ± 20 > ($4.52 \pm 0.05/4.25 \pm 0.1$) [1562] (204, 208).
(11) Ag {4.39 ± 0.02} // < 50 ± 20 > ($4.52 \pm 0.05/4.65$) [1562].
(12) Au {5.30 ± 0.04} // < 30 > ($5.49 \pm 0.04/5.20 \pm 0.1$) [3190] (149).
(13) Au {5.30 ± 0.04} // < 60 ± 30 > ($5.42 \pm 0.07/5.2 \pm 0.1$) [1562].

As may be seen for the results (3)–(13) with (10)–(13) excluded, each theoretical value of $C \equiv \phi^e(r)$ is found to agree well or fairly with each experimental data on $D \equiv \phi^e(r)$. However, it should be emphasized that any value of $C \equiv \phi^e(r)$ to be calculated is strongly dependent upon $A \equiv \phi^e(\infty)$ to be cited from literatures. As typically shown in (6)–(8) for Ag [3127], the experimental value of $\phi^e(r)$ increases from $D = 4.55$ to 4.65 eV as r decreases from 30 to 20 Å, just as predicted by theory ($C = 4.57 \to 4.66$ eV). The results of (1) and (2) above are outlined in Section 11.3, but the experimental data on $\phi^e(r)$ are not described in Ref. [2199].

Fine particles of Ag (50 ± 20 Å) are formed by passing Ag-vapor through the He-gas boiling off from liquid-He, and $\phi^e(r)$ is measured to be 4.25 ± 0.1 eV [1562]. This is smaller than our calculated value of 4.52 ± 0.05 eV (see Result (10) above). In a separate experiment after purification of the particles by passing through a trap at ~77 K, however, $\phi^e(r)$ is measured to be

D = 4.65 eV [1562] (see Result (11)). This value for $r = 50 \pm 20$ Å is not smaller but larger (by 0.08−0.15 eV) than the others (D = 4.57−4.50 eV) measured for these smaller particles of Ag for 27−30 Å [3127,3190] (see Results (7)−(9)). The former for a larger particle (50 ± 20 Å) [1562] is as large as D = 4.65 eV found for a smaller particle of Ag (20 Å) (see Result (6)) [3127], thereby suggesting it necessary to examine the question whether the actual size of Ag-particle decreases from 50 ± 20 to mostly ~20 Å after the above purification.

For another result of (3) Ni [2667], fine particles (r = 60−100 Å) are produced by a spark discharge between a nickel plane and a nickel tip in He as a carrier gas, and ϕ^e(poly) = 4.9 eV is estimated from literature values (see Footnote 448 in Table 1) and also determined directly for a flat Ni surface by photothreshold [2667]. Substitution of both $\phi^e(\infty)$ = 4.9 eV and r = 80 ± 20 Å into Eq. (17′) yields the result of $C \equiv \phi^e(r)$ = 4.97 ± 0.02 eV < $A \equiv \phi^e$(poly) = 5.06 ± 0.06 eV (Table 2). On the other hand, substitution of the latter (our value of 5.06 eV) yields $C \equiv \phi^e(r)$ = 5.13 ± 0.07 eV, which is essentially equal to the experimental value of $D \equiv \phi^e(r)$ = 5.1 eV [2667], as shown in the result (3) above. On the contrary, substitution of $\phi^e(\infty)$ = 4.9 eV and $\phi^e(r)$ = 5.1 eV into Eq. (17′) yields r = 27 Å [2667]. This is smaller than r = 60−100 Å mentioned just above, thereby suggesting it necessary to examine the effective values of r and/or $\phi^e(\infty)$ under study.

As demonstrated above for six metal species (1)−(13), substitution of our most probable value of $\phi^e(\infty)$ into Eq. (17′) yields that $\phi^e(r)$ is in good or fair agreement between theory (C) and experiment (D). This result affords an additional evidence to support that many of our most probable values of ϕ^e(poly) recommend in Table 2 are reasonably accurate and reliable.

In the next step, let's examine the theoretical values of $\phi^e(r)$ calculated by Rudnitskiĭ et al. [2973,4100] exemplified below. Here, {A} and (B/C) indicate that A is the ϕ^e(poly) cited as $\phi^e(\infty)$ from Table 2, B is $\phi^e(r)$ calculated from Eq. (17′) by the present author, and C is $\phi^e(r)$ evaluated by the original theory considering both structure and shape of the small particles (typically, r = 90 Å) under study [2973].

(1) W {4.56 ± 0.03} ∥ (4.62 ± 0.03/4.25), octahedron.
(2) W {4.56 ± 0.03} ∥ (4.62 ± 0.03/4.36), truncated octahedron.
(3) W {4.56 ± 0.03} ∥ (4.62 ± 0.03/4.40), cube.
(4) W {4.56 ± 0.03} ∥ (4.62 ± 0.03/4.42), cubic octahedron.
(5) W {4.56 ± 0.03} ∥ (4.62 ± 0.03/4.75), real sphere.
(6) W {4.56 ± 0.03} ∥ (4.62 ± 0.03/5.30), rhombododecahedron.
(7) Au {5.30 ± 0.04} ∥ (5.36 ± 0.04/4.44), rhombododecahedron.
(8) Au {5.30 ± 0.04} ∥ (5.36 ± 0.04/4.58), real sphere.
(9) Au {5.30 ± 0.04} ∥ (5.36 ± 0.04/4.72), cube.
(10) Au {5.30 ± 0.04} ∥ (5.36 ± 0.04/4.84), cubic octahedron.
(11) Au {5.30 ± 0.04} ∥ (5.36 ± 0.04/4.93), truncated octahedron.
(12) Au {5.30 ± 0.04} ∥ (5.36 ± 0.04/5.01), octahedron.

In the case of r = 90 Å for both W and Au, both of the results (1)−(6) and (7)−(12) indicate that the respective six values of $C \equiv \phi^e(r)$ owing to the original theory [2973] are different notably with each other among the six shapes and also that the values (C) differ considerably from those ($B = \phi^e(r)$ = 4.62 and 5.36 eV) calculated for W and Au, respectively, by the present author using Eq. (17′) based on the *real sphere* model. Among the respective six models, the smallest difference (0.13 eV) between B and C is found for the real sphere model (5) for W, whilst that (0.35 eV) is done for the octahedron model (12) instead of the real sphere one (8) for Au.

Interestingly, Makov et al. [4198] as well as Peterson et al. [4322] point out that Schumacher and co-workers employ the coefficient of C_p = 1/2 in their earlier paper (in 1978) [4200] but they replace it later (in 1984) by 3/8 [2383]. With a special attention added to this replacement, the present author adopts the compiled data [4198] in order to examine the relative correctness of 1/2 and 3/8, thus yielding the following results.

(1) Na {2.54 ± 0.03} ∥ ⟨3.4−7.5⟩ (2.49/2.48) [4198].
(2) K {2.29 ± 0.02} ∥ ⟨4.1−7.4⟩ (2.40/2.50) [4198].
(3) Ag {4.39 ± 0.02} ∥ ⟨20−32⟩ (4.35/4.34) [4198].

Here, the values in {A} and ⟨B⟩ indicate that A (in eV) is the work function of ϕ^e(poly) cited from Table 2 and B (in Å) is the radius (r) of the particle under study. The dual values of $\phi^e(\infty)$ (in eV) given as in the form of (C/D) are tentatively estimated by the present author using the experimental data [4148,4200] compiled as Figs. 3−5 (plots of I vs. $1/r$) [4198], where C and D correspond to C_p = 3/8 and 1/2 in Eq. (17), respectively, and I is the ionization energy of the particle under study. As shown by Results (1) and (3), the differences between C and D and between A and C are as small as 0.01 and 0.05 (or 0.04) eV, respectively, whilst Result (2) indicates that each of the differences among A, C and D is too large as 0.10 eV or more to be taken into consideration for the present purpose. These typical results suggest it not easy to solve experimentally the problem which coefficient of 3/8 or 1/2 is more correct or reasonable.

With respect to Li-clusters (n = 2−68), the local exchange–correlation potential model yields $\phi^e(\infty)$ = 2.25 eV and C_p = 0.51, whilst the local density approximation model does 3.21 eV and 0.48, respectively [4262]. Namely, C_p is found to be very close to 1/2, but both of $\phi^e(\infty)$ themselves are considerably different from ϕ^e(poly) = 2.90±0.03 eV [Here] and 2.93 eV [363] recommended in Table 2.

According to Fig. 2 [4321], where the plot of $1/r$ vs. $I - \phi^e(\infty)$ has the two straight lines corresponding to 3/8 r and 1/2 (r + 1.54), all of the values calculated theoretically for I are found to exist inside alone between the two lines, slightly nearer to the former (3/8 r) [4321].

By analysis of the experimental data on K_n (n = 30–101) [3552,4227], the coefficient (C_p) is determined to be 0.34 or 0.38, the respective values of which afford $\phi^e(\infty)$ = 2.30 and 2.29 eV for K(poly) [4244], identically equal to our most probable value of ϕ^e(poly) = 2.29 ± 0.02 eV and also to 2.29 eV [?] and 2.30 eV [3337] recommended in Table 2. Interestingly, both of C_p's are considerably smaller than 1/2 and much nearer to 3/8, similarly exemplified just above [4321]. According to the conclusion [4198], C_p = 1/2 and 3/8 account better for the experimental observations for relatively large and small clusters, respectively. Further information about the coefficient may be obtainable from Refs. [4197,4302,4323].

11.2. Quantum theory about the energetics correlating either ionization energy or electron affinity with work function

On the basis of the quantum theory about the energetics correlating ionization energy (or electron affinity) of atom with work function of bulk solid, Perdew [4101] yields,

$$I(r_s) = \phi^e(\infty) + e^2/2(r_s + d_G). \tag{18}$$

$$E(r_s) = \phi^e(\infty) - e^2/2(r_s + d_G). \tag{19}$$

Here, r_s is the Wigner–Seitz radius, and d_G is the microscopic distance from the infinite planer Gibbs surface to its image plane. Typically for Na (r_s = 3.93 bohr, $d_G(r_s)$ = 1.24 bohr and $\phi^e(\infty) = \phi^e$ = 2.75 eV cited from Ref. [1045]), Eqs. (18) and (19) afford $I(r_s)$ = 5.38 eV and $E(r_s)$ = 0.12 eV [4101]. On the contrary, our citation of ϕ^e = 2.54 eV (Table 2) yields 5.17 eV and $E(r_s)$ = −0.09 eV, which are in better and worse agreements with I = 5.14 eV and E = 0.55 eV for Na–atom, respectively. Generally, the agreement between $E(r_s)$ and E is not better than that between $I(r_s)$ and I for many of the eight elements listed in Table II [4101].

11.3. Photoelectron spectroscopy of clusters

The ionization energies of the different charge states of a spherical metal cluster are given [2199] by

$$I(Z) = \phi^e(\infty) + (Z + \rho)e^2/(r_c + \delta). \tag{20}$$

Here, r_c is the effective radius of the spherical cluster as calculated from its density and weight, Z is its charge state, ρ is the quantum correction of bulk work function for spherical cluster, and δ is the correction of the cluster radius owing to the electron spillover into vacuum. In the case of Al, ρ = 0.49 ± 0.04 is determined by experiment [2199] and δ = 0.54–1.1 Å is estimated by theory [553], in contrast to 0.42 < ρ < 0.45 calculated by quantum theory [3208] and to ρ = 0.50 and δ = 0 in the classical theory [3208].

On the basis of the experimental data on the linear relationship between $I(Z)$ and Z for Al_{2000} or $Al_{32000\pm150}$ with Z = −1 up to +5 and ρ = 0.49, Fig. 2 [2199] affords $\phi^e(\infty)$ = 4.28 ± 0.03 eV (see Footnote 60 in Table 1), where the clusters are produced by sputtering through a magnetron discharge into a stream of liquid-nitrogen-cooled rare gas. The above value of $\phi^e(\infty)$ is just equal to ϕ^e(poly) = 4.28 ± 0.01 eV determined by PE for the Al/quartz system [612,1045] and also essentially equal to ours of 4.26 ± 0.03 eV recommended for polycrystalline Al (see Table 2). By substitution of $\phi^e(\infty)$ = 4.26 ± 0.03 eV and of r_c = 22 and 52.9 Å into Eq. (17'), $\phi^e(r_c)$ = 4.51 ± 0.03 and 4.36 ± 0.03 eV are evaluated for the clusters of Al_{2000} and $Al_{32000\pm150}$, respectively (see Footnote 449 in Table 1 and also Results (1) and (2) Al [2199] compiled together with many other examples (3)–(13) in Section 11.1).

In regard to neutral clusters (M_n, typically n = 4–34 for K_n) formed in adiabatic expansions of neutral vapor from a high temperature oven [4148], photoionization mass spectrometry of M_n^+ makes it possible to measure the first ionization energy of I(n) and, hence, to determine $\phi^e(\infty)$ from the intercept (n → ∞) of a plot (I(n) vs. $n^{-1/3}$) according to Eq. (21) [2171].

$$I(n) = \phi^e(\infty) + (3e^2/8r_s)n^{-1/3}. \tag{21}$$

Some of the typical results are summarized below together with the sample size (n) under study. Regarding {A}, (B) and ⟨C⟩ below, A is our most probable value of ϕ^e(poly) (in eV) listed in Table 2, B is the experimental value of $\phi^e(\infty)$ (in eV) determined from the above plot for each cluster (M_n) by the corresponding worker(s), and C is the number (n) of the atom constituent of M_n under study.

(1) Na; {2.54 ± 0.03} // (2.52 ± 0.04) ⟨15–65⟩ [2383,4148].
(2) Na; {2.54 ± 0.03} // (2.68) ⟨2–137⟩ [2171].
(3) Na; {2.54 ± 0.03} // (2.71) ⟨3–150⟩ [4197].
(4) Al; {4.26 ± 0.03} // (4.25) ⟨3–70⟩ [4197].
(5) Al; {4.26 ± 0.03} // (4.338) ⟨32–95⟩ [4192].
(6) Al; {4.26 ± 0.03} // (4.349) ⟨32–95⟩ [4192].
(7) K; {2.29 ± 0.02} // (2.23 ± 0.04) ⟨4–34⟩ [4148].
(8) K; {2.29 ± 0.02} // (2.28) ⟨19–200⟩ [4161].
(9) K; {2.29 ± 0.02} // (2.28) ⟨70–300⟩ [4161].
(10) K; {2.29 ± 0.02} // (2.29) ⟨30–101⟩ [4227].
(11) K; {2.29 ± 0.02} // (2.30) ⟨3–110⟩ [4197].
(12) K; {2.29 ± 0.02} // (2.52) ⟨30–101⟩ [4227].
(13) Fe; {4.55 ± 0.05} // (3.81 ± 0.04) ⟨?⟩ [4148].
(14) Cu; {4.51 ± 0.04} // (4.70 ± 0.04) ⟨3–500⟩ [4197].

(15) Ag; {4.39 ± 0.02} // (4.19) ⟨3–20⟩ [4197].
(16) In; {4.05 ± 0.06} // (4.12) ⟨3–18⟩ [4197].
(17) Ce; {2.89 ± 0.07} // (2.40) ⟨2–17⟩ [4263].
(18) Pr; {2.83 ± 0.11} // (2.50) ⟨2–21⟩ [4263].
(19) Hg; {4.50 ± 0.02} // (6.88 ± 0.05) ⟨≤12⟩ [4148].
(20) Hg; {4.50 ± 0.02} // (?) ⟨1–70⟩ [4149].
(21) Hg; {4.50 ± 0.02} // (?) ⟨2–35⟩ [4162].
(22) Tl; {3.82 ± 0.05} // (3.89) ⟨3–20⟩ [4197].
(23) Pb; {4.07 ± 0.05} // (4.00 ± 0.10) ⟨?⟩ [4148].

Regarding Result (2) for Na [2171] and that (4) for Al [4197] above, further information is obtainable from Footnotes 40 and 459 in Table 1, respectively. The experimental data on $B \equiv \phi^e(\infty) = 4.338$ and 4.349 eV for Results (5) and (6) for Al [4192] are obtained at 230 and 65 K, respectively, whilst $B = 2.29$ and 2.52 eV in Results (10) and (12) for K [4227] are determined from the data on both Fowler and linear plots according to Figs. 1 and 2 [4227], respectively. The value of $B = 2.28$ eV for K in Results (8) and (9) is calculated from the experimental data on K_n^{2+} and K_n^{3+}, respectively, by using another equation [4161], in contrast to the others (1)–(7) and (10)–(23) where B comes from the data on M_n^+.

As may be seen above, some of the metals are very poor in agreement between $B \equiv \phi^e(\infty)$ and $A \equiv \phi^e(\text{poly})$. Regarding Hg, for example, it is for n > 70 alone that the extrapolation (n → ∞) of a plot (I_n vs. $n^{-1/3}$) converges linearly to $\phi^e(\infty) = 4.49$ eV [1669,4149] or equal to 4.475–4.52 eV for Hg recommended by several authors in Table 2.

Further information about clusters is obtainable from excellent reviews [3669,4138,4194,4261,4269,4301–4304], which summarize concisely or comprehensively both experimental methods and theoretical analyses and also typical data on ionization energy (I), electron affinity (E), bulk work function ($\phi^e(\infty)$) and so on for various species of clusters.

12. Overall summary and conclusions

From the greatly abundant data summarized in Tables 1–14 and Figs. 1–2 and also from the above critical analysis and discussion given in Sections 1–11, we may yield the essential points of the various contents as follows.

(1) The experimental and theoretical data mainly on ϕ^e, in addition to ϕ^+ and ϕ^-, for mono-, submono- and polycrystalline surfaces are compiled in Table 1, which includes more than ten thousands of work function data for about 600 surface species covering 88 kinds of the chemical elements. The data are based upon as much as 4461 references selected from about ten thousands of articles surveyed during the last 20 years. However, even the former seems to be merely less than a half of the literatures published for the elemental work function to date in the world. The probable lack of more than the half is mainly because it is practically difficult to thoroughly cover almost all the related literatures by the single author himself alone. About the work function data on the latter half to be properly included herein, both survey and compilation are confidently expected to be made by other authors in the near future (cf. Section 1).

(2) Owing to the above difficulty, it is only about 200 surface species alone that are found to have more than five data on ϕ^e for each surface species to be practicable for estimating its most probable value. At present, however, Table 1 may be usable as the most abundant and latest database for ϕ^e, ϕ^+ and ϕ^-, each of which is accompanied with a note about the experimental condition and measuring method and some of which are attached with 490 footnotes in total. In addition, Table 1 may also be very useful for readily grasping the outline of work function studies accumulated to date for a variety of surface species under various conditions (cf. Section 2).

(3) Many of the experimental data on ϕ^e, ϕ^+ and ϕ^- listed in Table 1 may be useful for examining the theoretical predictions according to Eqs. (1)–(3). Namely, they make it possible to solve the problems whether (i) $\phi^+ = \phi^e$ holds for a clean and smooth monocrystalline surface alone, (ii) $\phi^+ > \phi^e$ does for all of poly- and submonocrystalline surfaces and (iii) $\phi^- = \phi^e$ applies to any ones, although the data on ϕ^+ and ϕ^- tabulated therein are very scanty in surface species (less than 39) compared with those (about 600) on ϕ^e (cf. Section 4).

(4) Among the sample layer/substrate systems listed in Column 1 of Table 1, some of them are inhomogeneous (patchy, bumpy and/or lattice-defective) in surface structure over the entire area and, hence, the work function for each layer is generally *lower* than that for bulk. To prepare a smooth layer equivalent substantially to bulk, it is necessary in general to select either annealing or deposition at a temperature (T_a or T_d) higher than the working temperature (T) so as to satisfy the condition of T_a (or T_d) ≥ $T_m/3$, as expressed in (T_a) or {T_d} at the back of T (e.g., ~300) in Column 5 of Table 1 (cf. Section 2.5 and Footnote 363 in Table 1).

(5) Typically for Si, both work function and Richardson constant to be measured directly from Richardson plots are generally subject to underestimation mainly because the internal reflection coefficient (r^e) of electron is not negligibly small compared with unity. In such a case, we can estimate the correct value (ϕ_H^e) from the measured one (ϕ_r^e) by using Eq. (8) proposed by Hensley, where the measured value (A_r) corresponds to $(1 - r^e) A_R$. Many attempts made by the present author using Eq. (8) yield very reasonable results, thereby suggesting that it should be employed by many workers in various cases of thermionic emission studies (cf. Section 2.8.6).

$$\phi_H^e = \phi_r^e + kT \ln(120/A_r). \tag{8}$$

Table 1 includes many values of both ϕ_H^e and ϕ_r^e (cf. Footnotes 384–386, 431 and 456).

(6) The most probable values of ϕ^e estimated from the data in Table 1 are summarized in Column 3 in Table 2, and many of them may probably be consultable as a more useful and reliable source on ϕ^e, compared with the others in Columns 6–8 [1045,1354,1358].

This is mainly because the former is much abundant in surface species and also because it covers these newer data published after ~1980, compared with the latter based entirely on those data published more than about forty years ago (cf. Section 3.2).

(7) Regarding about 200 surface species in Table 2, the most probable values of ϕ^e are estimated from relatively abundant data (larger than 5 in number). Among the work function values, especially those with double and single underline have much smaller standard deviations of $\leq \pm 0.05$ and $\leq \pm 0.10$ eV, respectively and, hence, both of them may probably be more reliable than the others with no underline. On the other hand, the values with the superscript (x, y or z) originate from a small number (2, 3–5 or 1) of work function data in Table 1 and, hence, they may possibly be less reliable or accurate than the others based on much abundant data (up to the larger number of ~400 for Cs and W). Consequently, the former is needed to be further investigated in order to accumulate much data worth while to be consultable with confidence (cf. Section 3).

(8) In spite of the fact that work function is one of the important chemico-physical properties of solid surfaces, its data are still very scanty in total number and rather doubtful in accuracy for some of the lanthanides and actinides, in contrast to many of the alkali-, alkali earth- and transition-metals. The former species, as well as those having no data in the 6–8th columns in Table 2, are expected to be added with accurate data on ϕ^e by further investigation (cf. Section 3).

(9) In addition to ϕ^e, the most probable values of ϕ^+ and ϕ^- are listed in Columns 4 and 5 in Table 2, both of which cannot be examined objectively by comparison with any others because none of the literatures [typically, 12,1045,1354,1358] has any recommended values of ϕ^+ and ϕ^-. However, the values of ϕ^+ in Table 2 may also be usable as a convenient source when we try to analyze these data on positive ion emission from polycrystalline surfaces, although the total number of surface species investigated for ϕ^+ to date is very small (only 39 surface species) (cf. Section 3).

(10) Of the work function values (B) recommended for 66–114 surface species (see the last line in Table 2) by other authors [1045,1354,1358], those for typical 40 species have a large discrepancy ($|B - A| = 0.15$–1.00 eV and $(|B - A|)/A = 3$–19%) compared with each of our most probable values (A). This is probably because some of B are entirely based on these less-abundant and less-reliable data published more than ~40 years ago (cf. Examinations (1)–(40) in Section 3.2).

(11) Particularly, each of the values (B) recommended by the other authors for 12 surface species among the above 40 ones has a very large discrepancy ($|B - A| > 0.2$ eV and also $(|B - A|)/A > 10\%$) from ours (A) (cf. Section 3.2); namely, (1) 4.98 eV for α-Be, (6) 4.33 eV for α-Ti, (10) 5.10 eV for Cu(100), (37) 4.30 eV for Au and so on with # attached (cf. Section 3.2).

(12) Both Michaelson and Fomenko have made a valuable contribution to compiling critically the work function data published up to ~1980, and all of the values recommended have long been widely consulted still to date by a great many workers in the world (cf. Section 3.2). About 20–30% of the values, however, have a large discrepancy ranging from ~0.2 to 1.0 eV against ours, as shown in Categories (4)–(11) in Table 3 and also in the list of Examinations (1)–(40) in Section 3.2. Namely, such discrepant values don't seem to be accurate or reliable enough to be straight or undoubtedly acceptable today, as mentioned in Points (10) and (11) above. Therefore, it may be advised that at least those values with # attached in the above list should be revised tentatively after our most probable values estimated from much more abundant and reliable data published to date, although any of ours is not yet insured to be correct enough to be straight acceptable today (cf. Section 3.2).

(13) Among our 609 surface species listed for 88 elements in Table 2, about 480 surfaces of 21 elements don't find any values of work function recommended by other authors. Especially, many of the monocrystalline work function values are newly recommended here for about 70 surface species of 42 elements (e.g., alkalis, alkali earths, V, Cr, Rh, Pb), many of which are based generally on the abundant source including more than five work function data published to date. This is one of the unique merits of the present article exceeding the other publications (cf. Section 3.2).

(14) The work function values with x, y or z superscripted according to scanty data (only 2, 3–5 or 1 in total number) are tentatively added as a rough estimate for each of about 390 surface species (e.g. monocrystals of γ-Ca, γ- and δ-Mn, Tc, Cd, In, α-Sn, Eu, α- and β-Tb, α- and β-Hf, etc., and also polycrystals of P, γ- and δ-Mn, δ-Fe, β- and γ-Sr, γ-Sn, I, β-Tb, At, Ac, Cm, etc.) in Table 2. Much data should be accumulated by further investigations so that each of the values may be insured or increased in accuracy (cf. Section 3.2).

(15) Disappointedly, Table 2 does not include many important surface species such as C(110), C_{60}(100), C_{60}(110), Al(112), β- and γ-Fe(112), Ni(112), Zn(1011), Ga(112), As(100), As(110), Se(0001), α-Sr(112), α-Y(1011), α-Zr(1011), Pd(112), Ag(112), Cd(1011), In(112), Sb(110), Sb(112), Te(0001), β-Ce(112), Hf(1011), Tl(1011), Pb(112), Bi(1010) and so on, although they seem to be interested by many workers as the fundamental species in surface science. Such a present situation indicates that further investigations by both theory and experiment are needed to accumulate the reliable work function data for many surface species covering not only the above but also many others such as exemplified in Point (14) just above (cf. Section 3.2).

(16) The effective work functions (ϕ^+, ϕ^e and ϕ^-) for the emissions of positive ion, electron and negative ion by the mechanism of thermal stimulation are generally given by Eqs. (1)–(3), respectively, and their values for any patchy surface are different from ϕ^a given by Eq. (4) (cf. Sections 1 and 4).

$$\phi^+ = kT \ln[\Sigma F_i \exp(\phi_i/kT)], \tag{1}$$

$$\phi^e = -kT \ln[\Sigma F_i \exp(-\phi_i/kT)], \tag{2}$$

$$\phi^- = -kT \ln[\Sigma F_i \exp(-\phi_i/kT)], \tag{3}$$

$$\phi^a = \Sigma F_i \phi_i. \tag{4}$$

(17) By using the literature values of ϕ_i and F_i, the theoretical values of ϕ^+ and ϕ^e calculated for seven W-specimens from Eqs. (1) and (2) are generally in fair agreement with the experimental data in a wide range of the degree of monocrystallization

($\delta_m \approx 0.34 - 0.96$), which corresponds to the largest among the fractional surface areas (F_i's) for each specimen under study. Such agreement is found for other metals (Ni, Nb, Mo, Ta and Ir), too, thus supporting again our equations (cf. Section 4.2 and Table 6).

(18) Consequently, it may be safe to conclude that each of the work function values to be thus calculated theoretically is generally expected to agree well with the data to be obtained experimentally for the specimen under study. Here, the local work function (ϕ_i) may ready be citable from Table 1 or 2 according to the local face species corresponding to the area (F_i) to be cited from literatures. Of course, each of the work function values to be calculated from Eqs. (1)–(3) based on PSI, TE and NSI, respectively, is generally expected to be equivalent to that to be determined for the same species by any other methods such as FE and PE without depending upon the emission mechanisms or processes (cf. Sections 1 and 4).

(19) For any polycrystalline surface consisting of patchy faces (1–i) with the fractional area (F_i) over the entire surface and also with the local work function (ϕ_i) ranging from the maximum (ϕ_{max}) to the minimum (ϕ_{min}), there holds the inequality of $\phi_{max} > \phi^+ > \phi^a > \phi^e = \phi^- > \phi_{min}$. This is because positive ions and electrons (negative ions, too) are emitted predominantly from these faces having high and low work functions (ϕ_i's) near to ϕ_{max} and ϕ_{min}, respectively (cf. Sections 1 and 4).

(20) Therefore, each polycrystalline surface has the thermionic contrast of $\Delta\phi^* \equiv \phi^+ - \phi^e > 0$, which depends upon the surface species ranging from $\sim$0.3 eV (Pt) to 0.7 eV (Nb) (cf. Tables 4 and 5). Whenever we try to analyze quantitatively the data (β^+ or E^+) on positive ion emission from polycrystals by using Eq. (5) or (9) to be shown below or in Point (22) later, we should employ ϕ^+ instead of ϕ^e. Otherwise, the analyzed results may be accompanied with the systematic error corresponding to $\Delta\phi^*$ (cf. Section 2.6 or 4.1).

$$\alpha^+ = \beta^+/(1 - \beta^+) = \{w^+/w^0\} \exp[(\phi^+ - I)/kT]. \tag{5}$$

(21) On the other hand, each monocrystalline surface has the relation of $\phi_{max} = \phi^+ = \phi^a = \phi^e = \phi^- = \phi_{min}$ and, hence, $\Delta\phi^* \approx 0.0$ eV holds generally so long as the surface is essentially clean and smooth (cf. Table 5). If not so, $\Delta\phi^* \approx 0.0$ eV does not hold. Typically, oxygenated W(100) surface has $\Delta\phi^* = 0.7$ eV in contrast to $\sim$0.0 eV for clean and smooth W(100) (cf. Section 4.1 and also the lines for O=W(100) in Table 1 in Ref. [1351]).

(22) Similarly as mentioned in Points (20) and (21) just above, the employment of ϕ^e as ϕ in Eq. (9) is limited to PSI on substantially clean and smooth monocrystalline surfaces alone. In the case of polycrystalline surfaces, ϕ^+ should be generally adopted as ϕ instead of ϕ^e. Otherwise, the Schottky cycle does never close exactly. Namely, $\Delta E^* \equiv (\phi + E^+) - (E^0 + I) = -\Delta\phi^* \neq 0$ (cf. Section 4.1).

$$\phi + E^+ = E^0 + I. \tag{9}$$

(23) Regarding the relationship between $\Delta\phi^*$ and δ_m, there hold the following equations derived empirically by the present author.

$$\Delta\phi^* = c \quad \text{for } 0 < \delta_m < 0.5 \text{ (polycrystal).} \tag{10}$$

$$\Delta\phi^* = 4c\delta_m(1 - \delta_m) \quad \text{for } 0.5 < \delta_m < 1 \text{ ("submonocrystal").} \tag{11}$$

$$\Delta\phi^* = 0 \quad \text{for } \delta_m = 1 \text{ (monocrystal).} \tag{12}$$

Each of the values calculated from Eqs. (10)–(12) is in fair agreement with each of the experimental data on the several specimens under study, as illustrated typically for tungsten in Fig. 1 (cf. Section 4.3).

(24) At $\delta_m < 0.5$, $\Delta\phi^*$ is kept nearly constant at c, as shown for polycrystal by Eq. (10). Quite similarly, both ϕ^+ and ϕ^e are also found by theory and experiment to be little dependent upon the difference in the surface components (ϕ_i and F_i) among various specimens of the same species (cf. Table 6). This result may afford us the conclusion that each of the polycrystalline surface species, like as each monocrystalline one, is usually expected to have a nearly constant (within $\pm$0.1 eV in variation) and unique value characteristic of the species itself under the normal condition (cf. Section 4.2). Although ϕ_m itself has the "differential effect" on both ϕ^+ and ϕ^e of any patchy surface according to the "emission predominance" (cf. Section 1), each of ϕ^+, ϕ^e and $\Delta\phi^*$ remains nearly constant independently of δ_m so long as $\delta_m < 0.5$ (see Points (25) and (31) below).

(25) The above conclusion in Point (24) is strongly supported by the fact that the most probable value of ϕ^e for any polycrystalline surface species (usually $\delta_m < 0.5$) is substantially common or nearly identical among various specimens in spite of a considerable difference in the surface components (ϕ_i and F_i). Typically for polycrystalline tungsten, our theoretical value ($\phi^e = 4.52$ eV, see Footnote (25) in Table 6) is in good agreement with 4.54–4.56 eV [Here, 12,1045,1351,1354,1358] (cf. Section 3.2 and Table 2). The latter is estimated from various values scattered in a wide range (e.g., $\phi^e \approx$ 3.8–5.2 eV by experiment and 2.8–5.8 eV by theory for W, see Table 1). In addition, both ϕ^+ and $\Delta\phi^*$ as well as ϕ^e show a good agreement (within $\pm$0.1 eV in gap) between Footnotes (25) and (26), thus affording an additional evidence to support our theoretical model (cf. Table 6).

(26) The wide scattering mentioned for polycrystals just above is mainly due to the reasons of (i) the error in experimental measurement or the incompletion in theoretical calculation, (ii) the difference in various surface conditions (e.g., contamination, irregularity and heteroatom density) and/or, probably, (iii) the inclusion of these specimens of "submonocrystals" with $0.5 < \delta_m < 1$ (cf. Section 3.1).

(27) By natural elimination of these data corresponding to some of the above reasons of (i)–(iii) mentioned just above, ϕ^e may naturally be converged to a very narrow range, which brings about the result mentioned in Point (24) above, thus yielding the most probable value with the uncertainty of less than $\pm$0.1 eV for many polycrystalline species ($\delta_m < 0.5$ in general) (cf. Section 4.4).

(28) In contrast to the "polycrystal" ($\delta_{\mathrm{m}} < 0.5$) mentioned just above, the "submonocrystal" ($0.5 < \delta_{\mathrm{m}} < 1$) has such an anomaly as changes in ϕ^{e} as well as ϕ^{+} and $\varDelta\phi^{*}$ depending upon δ_{m} and, hence, the latter is neither constant nor unique in ϕ^{e} without having the work function characteristic of the surface species itself. The above anomaly may readily be understood by consideration of the analogy between the surface area component (δ_{m}) and the binary alloy component (γ_{c}), both of which are identical with each other in terms of the governance of work function according to each fractional value (cf. Section 4.5). Such a work function dependence on δ_{m} is observed for not only W but also done for other metals, too (cf. Section 4.2). Therefore, the "submonocrystal ($0.5 < \delta_{\mathrm{m}} < 1$)" should be treated as another species (category) different from the "generally called polycrystal ($\delta_{\mathrm{m}} < 0.5$)" (cf. Section 4.4).

(29) As summarized in Points (24)–(27), Eqs. (1), (2) and (10) afford a sound basis for supporting *theoretically* the *experimental* results (cf. Column 3 in Table 2) that every polycrystal ($\delta_{\mathrm{m}} < 0.5$) is usually expected to be nearly constant within the variation of ± 0.1 eV in ϕ^{e} with little dependence upon the difference in both F_{i} and ϕ_{i} among various specimens and also that it has the unique value of ϕ^{e} characteristic of its surface species so long as $\delta_{\mathrm{m}} < 0.5$ (cf. Sections 4.2 and 4.4).

(30) Consequently, the above theoretical support gives a definite answer to the long-pending problem why every "polycrystal" as well as every monocrystal is generally recognized to have a constant value of work function, irrespective of a large difference in the surface components (F_{i} and ϕ_{i}) among polycrystal specimens. In other words, it may be reasonable to interpret that the so-called "polycrystal" appearing in many publications is implicitly recognized to correspond to $\delta_{\mathrm{m}} < 0.5$ alone instead of $\delta_{\mathrm{m}} < 1$ including the "submonocrystal" (cf. Section 4.4).

(31) When ϕ_{m} belonging to δ_{m} has relatively higher and lower values among ϕ_{i}'s, ϕ_{m} gives the differential effect to ϕ^{+} and ϕ^{e}, respectively, mainly due to the emission predominance inherent in every patchy surface (cf. Section 1). For polycrystal ($\delta_{\mathrm{m}} < 0.5$), however, both ϕ^{+} and ϕ^{e} remain nearly constant independently of both δ_{m} and ϕ_{m}, whilst submonocrystal ($0.5 < \delta_{\mathrm{m}} < 1$) changes in both ϕ^{+} and ϕ^{e} depending strongly upon δ_{m} and differentially upon ϕ_{m}, thus showing that both δ_{m} and ϕ_{m} have a complicate governance of the both work functions of any patchy surface (cf. Section 4.3).

(32) As mentioned in Points (23) and (28), Eqs. (1), (2) and (11) lead to the conclusion that the "submonocrystal" ($0.5 < \delta_{\mathrm{m}} < 1$) changes in work function depending upon the surface components (F_{i} and ϕ_{i}) without having a constant value, in contrast to both poly- and monocrystalline surfaces having each a constant and unique value characteristic of the surface species itself. Interestingly, δ_{m} thus acts as the *key factor* governing strongly both ϕ^{e} and ϕ^{+} at a *different* mode between poly- and submonocrystals according to the conditions of $\delta_{\mathrm{m}} < 0.5$ and $0.5 < \delta_{\mathrm{m}} < 1$, respectively. Namely, $\delta_{\mathrm{m}} = 0.5$ functions as the critical point governing differentially the work functions between the two crystal species (cf. Sections 4.4 and 4.5).

(33) Our findings of (i) the *sound basis* marked for polycrystal ($\delta_{\mathrm{m}} < 0.5$) in Point (29), (ii) the *anomaly* outlined for submonocrystal ($0.5 < \delta_{\mathrm{m}} < 1$) in Point (28) and (iii) the *key factor* of δ_{m} governing both ϕ^{e} and ϕ^{+} (Point (32)) may be considered to add a new contribution to the work function studies developed to date, although our theoretical model is very simple and plain and also may seem crude and coarse apparently (cf. Section 4.4). Without our deep analysis made for ϕ^{+}, ϕ^{e} and $\varDelta\phi^{*}$ on the basis of Eqs. (1)–(3) and (10)–(12), any of the above new findings could not have been made successfully (cf. Table 6, Fig. 1 and Sections 4.2–4.5).

(34) Another thermionic contrast ($\varDelta\phi^{**} \equiv \phi^{-} - \phi^{\mathrm{e}}$) for negative ion emission is experimentally confirmed to be substantially zero for a given specimen of any surface species (poly-, submono- and monocrystals) under any condition, irrespective of their surface contamination and/or surface irregularity (cf. Section 4.6 and Table 7). In other words, ϕ^{e} as well as ϕ^{-} is usable in safety for analyzing the data on negative ion emission from any surfaces, as may readily be understandable from the theoretical prediction that Eq. (2) is identically equivalent to Eq. (3) (cf. Section 1).

(35) Consequently, ϕ^{e} to be measured by TE is reasonably considered to be effective for NSI, too, on the same specimen under virtually the same condition whenever we try to use Eq. (6) (cf. Section 2.6).

$$\alpha^{-} = \beta^{-}/(1 - \beta^{-}) = \{w^{-}/w^{0}\}\exp[(E - \phi^{-})/kT]. \tag{6}$$

(36) As a special case, the graphitic carbon film formed on a metal substrate has $\varDelta\phi^{*} \approx 0.0$ eV, thermionically equivalent to monocrystalline graphite like as C(HOPG) (cf. Table 5). Both of them have the same chemico-physical properties in contrast to carbidic carbon films (cf. Section 4.1).

(37) In contrast to free-standing graphene ($\phi^{\mathrm{e}} \approx 4.5$ eV), adsorbed graphene is found by both theory and experiment to have a strong dependence of its work function (by up to ~1 eV) upon the substrate species (Ni(111), Pd(111), etc.) (cf. Section 4.1).

(38) Work function values of the three low-Miller-index surfaces have a tendency to decreasing as the surface atom density (D_{s}) reduces. Typically for hcp-Re, our most probable values of ϕ^{e} in Table 2 show the sequence of $\phi^{\mathrm{e}}(0001) > \phi^{\mathrm{e}}(10\bar{1}1) > \phi^{\mathrm{e}}(10\bar{1}0)$ in good accordance with $D_{\mathrm{s}}(0001) > D_{\mathrm{s}}(10\bar{1}1) > D_{\mathrm{s}}(10\bar{1}0)$, strictly following the Smoluchowski rule (cf. Table 8). Namely, ϕ^{e} reduces as the surface becomes more open (cf. Section 5.1).

(39) Regarding bcc-metals such as Na, Rb, Nb, Mo, Cs, Ba, Ta and W, most (~75–100%) of the experimental and theoretical data on $\phi^{\mathrm{e}}(hkl)$ for each metal are found to have the sequence of $\phi^{\mathrm{e}}(110) > \phi^{\mathrm{e}}(100) > \phi^{\mathrm{e}}(111)$, just as expected from the above rule. Quite similarly, all of the data obtained by PSI of Nb, Mo, Ta and W yield $\phi^{+}(110) > \phi^{+}(100) > \phi^{+}(111)$. The latter gives an additional evidence to support strongly our theoretical model that $\phi^{+}(hkl)$ is fundamentally equivalent to $\phi^{\mathrm{e}}(hkl)$ for essentially clean and smooth monocrystalline surfaces ($\delta_{\mathrm{m}} = 1.00$ and $\varDelta\phi^{*} = 0.00$ eV) (cf. Table 9 and Section 5.2).

(40) In the case of fcc-metals (e.g., Ni, Cu, Rh, Pd, Ag, Pt and Au), most (~60–100%) of the work function data on $\phi^{\mathrm{e}}(hkl)$ are observed to have $\phi^{\mathrm{e}}(111) > \phi^{\mathrm{e}}(100) > \phi^{\mathrm{e}}(110)$, exactly following the above rule. In addition, $\phi^{+}(111) > \phi^{+}(100) > \phi^{+}(110)$ is found to hold for Ni, thereby supporting again the equivalence between $\phi^{+}(hkl)$ and $\phi^{\mathrm{e}}(hkl)$ (cf. Table 10 and Section 5.3).

(41) In another case of fcc-Al, on the contrary, 68% of the 56 sets don't obey the Smoluchowski rule, quite similarly to the result that our two sets of Al [Here] and [1351] also don't so (see those with double and single underlines, respectively, in Table 10).

Such an anomalous result against the rule is concluded by Fall et al. to originate from the increased *p*-atomic-like character of the density of states at the Fermi energy, in comparison with most other fcc-metals (cf. Section 5.4).

(42) Of the 38 triple sets of fcc-Pb, 55% don't follow the above rule, whilst our set [Here] (see that with double underlines in Table 10) has the normal sequence proving the rule. Therefore, much further investigations by both theory and experiment are necessary to find a valid reason for the above discrepancy between the former and the latter, in contrast the above case of Al (cf. Section 5.4).

(43) Irrespective of the species of bcc- and fcc-metals (except Al and Pb), each triple set with "Yes" in Tables 9 and 10 indicates that the *relative* values among the three are generally reasonable, but any set does not insure that all of the *absolute* values in the set are always accurate or correct enough to be straight acceptable today. This is naturally because "Yes" does satisfy the *necessary* condition but does not the *sufficient* one for insuring the above acceptability of each ϕ^e(hkl) among the three in the set under study (cf. Section 5.4).

(44) Except the cases of Al and Pb, each triple set with "No" generally indicates that at least one of the three values among ϕ^e(100)–ϕ^e(111) is inaccurate due to some errors either in the experimental determinations or in the theoretical calculations for each set under study (cf. Section 5.4).

(45) Therefore, such an examination as exemplified in Tables 9 and 10 is very useful for answering quickly the question whether the three values in the set under study are partly inaccurate or incorrect. If "No", then, either the experimental methods and conditions employed or the theoretical model and parameters adopted should be improved until yielding "Yes", although the new set yielded to be so does not always insure its accuracy as already mentioned in Point (43) above (cf. Section 5.4).

(46) In regard to the anomalous set of ϕ^e(110) = 4.87 eV > ϕ^e(100) = 4.02 eV < ϕ^e(111) = 4.36 eV recommended for bcc-Nb (hkl) by both CRC [1358] and Michaelson [1045] (cf. Table 2), our examination according to Point (44) suggests that ϕ^e(111) = 4.36 eV [1045,1358] should be replaced with 3.95 eV [Here], for instance, so as to follow the Smoluchowski rule. Similarly, appropriate corrections should be made for the irregular sets of Cu and Mo recommended by Michaelson and/or CRC (cf. Examinations (10), (17), (19) and (20) in Section 3.2 and also Conclusions (7)–(9) in Section 5.4).

(47) Among many empirical formulae derived to evaluate ϕ^e for various polycrystals by using the data on a variety of chemico-physical properties, especially, Eq. (7) proposed first by Gordy and Thomas has a historically important contribution to the evaluation of ϕ^e for various polycrystalline surface species including particularly these of Pm, Po and Ra, the latter of which has no experimental data still to date (cf. Section 2.8.3).

$$\phi^e = 2.27X + 0.34 \text{ (in eV).} \tag{7}$$

(48) Substitution of theoretical data on surface energy (ε) into Eq. (13) derived by Zadumkin et al. makes it possible to evaluate ϕ^e, the calculated value of which is found to be in fair or good agreement to the experimental data on ϕ^e for several metals such as fcc-Ni and bcc-Nb (cf. Section 5.5.2).

$$\phi^e(\text{hkl}) + (Ba^2/z)\varepsilon(\text{hkl}) = \text{const.} \tag{13}$$

(49) By the theoretical investigation of the quantitative relation between the melting point (T_m) and ϕ^e, Chatterjee yields Eq. (14).

$$\log[\phi^e(\text{hkl})] = \log[T_m(\text{hkl})^{1/4}/V^{1/6}] - 2.87 \pm 0.04. \tag{14}$$

Disappointingly, any of the work function values thus calculated for fcc-monocrystalline surfaces of Ag and Pb does not well agree with ours listed in Table 2. The reason for the disagreement should be clarified by further investigation (cf. Section 5.5.4).

(50) As the Wigner–Seitz radius (r_s) increases from ~2 bohr (Al) to ~6 bohr (Cs), the work function (ϕ) becomes less dependent upon its surface property (D_b) on the contrary to its bulk one (E_F), exactly according to Eq. (15).

$$\phi = D_b - E_F. \tag{15}$$

In consequence, ϕ becomes smaller from ~4 to 2 eV with increasing r_s. This tendency is identical to that of the experimental data on ϕ^e (cf. Section 6.1 and Fig. 2). After Kohn and co-workers initiated the density functional theory in 1960's, the theoretical studies on work function have greatly progressed and, hence, a better agreement between theoretical values and experimental data on work function has been achieved today for a variety of monocrystalline surface species (cf. Sections 2.8.5 and 6.1).

(51) After inquiring the problem whether work function is a surface or bulk property, Eq. (16) is theoretically derived by Halas and Durakiewicz as a function of the Wigner–Seitz radius and the Fermi energy alone.

$$\phi = 43.46/r_s^{3/2} E_F^{1/2}. \tag{16}$$

This is successfully applied to calculating also the work function change due to surface reaction of hydrogen with Pd, thus yielding such a reasonable result as $\phi = \phi^e = 5.25$ eV (Pd) and 3.2 eV (PdH) (cf. Section 6.2).

(52) The work function changes due to allotropic transitions ($\Delta\phi^e_{\beta\alpha} \equiv \phi^e_\beta - \phi^e_\alpha$ and $\Delta\phi^e_{\gamma\beta} \equiv \phi^e_\gamma - \phi^e_\beta$) are estimated to be -0.03 ± 0.06 eV for Ti, Fe, Co, Sn and U and -0.04 ± 0.08 eV for Fe, Sn and U, respectively, while $\Delta\phi^e_{\beta\alpha}$ is found to range from -0.16 to -0.21 eV for Sc, Tb and Hf. Accumulation of much data on these metals and also on other metals, however, is desired to determine more finely the above changes at the level of 1 meV in a very narrow temperature range sandwiching each transition temperature and also to settle the problem how each change depends upon metal species (cf. Table 11 and Section 7.1).

(53) As an interesting topic of allotropic transformation, β-fcc-Co with $\phi^e = 4.25$ eV is changed to α-hcp-Co with 4.12 eV by cooling slowly from ~1100 K to 300 K, but the former is kept unchanged by sudden cooling to room temperature even after passing the allotropic transition temperature (670 K) (cf. Section 7.1).

(54) Normally, α-hcp-Co(0001) with $\phi^e = 5.264$ eV transfers at 670 K to β-fcc-Co(111) with 5.266 eV (cf. Table 11). However, repetition of the transformation alters it to polycrystalline Co (cf. Section 7.1), whose work function is generally expected to have 4.71 and 4.50 eV for α- and β-Co, respectively (cf. Table 2).

(55) According to the Burgers orientation relationship between the two phases before and after allotropic transition, α-hcp-Zr(0001) changes to β-bcc-Zr(110), the relationship of which is also the case for Ti. For many monocrystalline surfaces of such as Sc, Y, Gd, Tb and Hf in addition to Ti, Co and Zr, much further studies by both theory and experiment are strongly expected to accumulate the accurate data on both the work function change and the orientation relationship due to the allotropic transition (cf. Table 11 and Section 7.1).

(56) The work function change ($\Delta\phi^e_{LS} \equiv \phi^e_L - \phi^e_{So}$) due to the phase transition between solid and liquid is found for thirteen metals to range from −0.10 to 0.03 eV, which affords the average of −0.02 ± 0.03 eV. In order to determine more precisely such a *minute* change, however, work function measurements are generally desired to be done at the level of 1 meV in such a narrow temperature range ($\Delta T \approx 10$ K) sandwiching T_m so as to minimize the thermal effect due to $\alpha \cdot \Delta T$ (cf. Table 12 and Section 7.2).

(57) The work function change ($\Delta\phi^e_{PF} \equiv \phi^e_P - \phi^e_F$) due to the transition between ferro- and paramagnetic phases is found for Fe, Co, Ni and Gd to range from −0.05 to 0.01 eV, which yields the mean of −0.01 ± 0.04 eV. Such a fine measurement (e.g., −0.007 eV for Ni at 400 K after extrapolation) as excluding the thermal effect ($\alpha \cdot \Delta T$), however, is generally expected to be done for many other metals, too, by further investigations (cf. Table 13 and Section 8.1).

(58) A metastable γ-like fcc-ferromagnetic Fe-film grown epitaxially on a Cu(100) substrate has generally $\phi^e = 4.58 \pm 0.10$ eV, which is very near to 4.55 ± 0.05 eV for α-bcc-ferromagnetic bulk-Fe (cf. Table 2). The former, however, changes in the Curie point (T_C) typically from 230 to 390 K as θ increases from 1 to 3–5 ML with $\phi^e = 4.7 \pm 0.1$ eV, in contrast to the latter having $T_C =$ constant at 1040 K (cf. Section 8.2).

(59) A metastable fcc-Co-film on a Cu(100)-substrate is ferromagnetic below T_C, which is found to increase linearly from ~100 to 500 K as θ increases from ~1.5 to 2.5 ML. At $\theta \approx$ 5–6 ML, T_C reaches to 1390 K, just corresponding to bulk cobalt. Much further work is expected to be done for various metastable systems in order to elucidate the dependence of both ϕ^e and T_C upon the film thickness (cf. Section 8.2).

(60) On the basis of the experimental data for a chemical compound ($Bi_2Sr_2CaCu_2O_8$) in Table 14, the work function change due to the transition between the normal and superconductive states may be concluded to be as small as $\Delta\phi^e_{SN} \equiv \phi^e_S - \phi^e_N = 4$ meV or so. On the other hand, the possible change due to the transition studied for the film of metals (V, Nb and Ta) is accompanied with so large a standard deviation (±0.3 eV) by CPD that the possible change can hardly be estimated accurately, while any appreciable change at the level of 0.01 eV is not observed for any of the above three metals studied by FE. Further studies by both theory and experiment are strongly expected to determine $\Delta\phi^e_{SN}$ for various metals on the level of 10 meV or less (cf. Table 14 and Section 9).

(61) For any species of metals, ϕ^e is well-known to change widely with the temperature coefficient of $\alpha \approx \pm 10^{-5} - \pm 10^{-4}$ eV/K (cf. Table 6 in Ref. [1351]). Therefore, it is emphasized here again that the work function values at the two different states (phases) should be compared at the *common* temperature (around the critical point such as T_A, T_m, T_C or T_S) after extrapolation so as to eliminate the thermal effect of $\alpha \cdot \Delta T$. Otherwise, the *net* change due to the transition alone can not be determined accurately at the level of less than 10 meV (cf. Section 10).

(62) According to a classical theory, the work function of a fine particle is given by

$$\phi^e(r) = \phi^e(\infty) + C_p e^2/r. \tag{17}$$

The value of $\phi^e(r)$ calculated therefrom is generally found to agree either well or fairly with that determined by experiment when the reliable data on $\phi^e(\infty) \equiv \phi^e(\text{poly})$ cited typically from Table 2 and on r (particle radius reported in each article) are substituted to the above equation. Here, $C_p = 3/8$ instead of 1/2 is usually adopted like as shown by Eq. (17′) (cf. Section 11.1 and also Point (65) below).

(63) Quantum theory about the energetics correlating atom with bulk solid yields:

$$I(r_s) = \phi^e(\infty) + e^2/2(r_s + d_G), \tag{18}$$

$$E(r_s) = \phi^e(\infty) - e^2/2(r_s + d_G). \tag{19}$$

Typically by adopting $\phi^e(\infty) = 2.75$ eV, $I(r_s)$ and $E(r_s)$ are evaluated to be 5.38 and 0.12 eV for Na–atom, respectively. But, our adoption of 2.54 eV yields 5.17 and −0.09 eV, which are in better and worse agreements with $I = 5.14$ and $E = 0.55$ eV. Agreement between $E(r_s)$ and E is not better than that between $I(r_s)$ and I for many of the elements studied (cf. Section 11.2).

(64) By measuring the ionization energies of such clusters (r_c in radius) as Al_{2000} and $Al_{32000\pm150}$ with several charges ($Z = -1$ up to +5), the work function of $\phi^e(\infty)$ for bulk Al is determined from

$$I(Z) = \phi^e(\infty) + (Z + \rho)e^2/(r_c + \delta). \tag{20}$$

The value of $\phi^e(\infty) = 4.28 \pm 0.03$ eV determined from the plot of $I(Z)$ vs. Z with $\rho = 0.49$ is essentially equal to our most probable value of 4.26 ± 0.03 eV for polycrystalline Al (cf. Section 11.3).

(65) In regard to neutral clusters (M_n) to be investigated generally by mass spectrometry, we have

$$I(n) = \phi^e(\infty) + (3e^2/8r_s)n^{-1/3}. \tag{21}$$

Here, $C_p = 3/8$ is replaced with $1/2$ in some cases. From the plot of $I(n)$ vs. $n^{-1/3}$ according to experimental data on the first ionization energy (I) and the number (n) of atoms constituting the cluster under study, we can determine $\phi^e(poly) = \phi^e(\infty)$ at the intercept ($n \to \infty$). Between the two, we can find a good agreement among many examples (cf. Section 11.3).

(66) Some of the experimental and theoretical studies indicate that C_p tends to be nearer to $3/8$ rather than to $1/2$, and another study concludes that $1/2$ and $3/8$ account better for the experimental observations for relatively large and small clusters, respectively. Since the linearity of the relationship between I and r^{-1} (or $n^{-1/3}$) is not so good generally as we may expect, it is not easy to verify experimentally which coefficient of $1/2$ or $3/8$ is more accurate or reasonable in general for all of the sizes and species of clusters (cf. Section 11.1).

(67) Finally as to be emphasized particularly, both experimental and theoretical studies on work function and related subjects ought to be developed much more, typically for accumulating the accurate or reliable data on the work function characteristic of each of the various surface species including minor or less-common ones in order to enrich the fundamental data important in solid state physics, although such studies themselves may possibly be no longer greatly attractive and deeply interesting at present compared with many other current topics prevailing today in surface science.

Afterword

The main purposes of this article are (1) to establish comprehensively an abundant and up-to-date database on ϕ^e as well as ϕ^+ and ϕ^- determined by theory and experiment for both mono- and polycrystalline surfaces of almost all the chemical elements under specified conditions, (2) to estimate accurately the most probable values of the three kinds of work functions of essentially clean surfaces for a variety of the both crystals, (3) to compare critically the recommended work function values between the present and other authors for examining their objective reliability, (4) to summarize compactly the steady progress in theoretical and experimental studies on work function, (5) to outline briefly the methods and techniques developed for work function measurements, (6) to introduce concisely the interesting topics about work function and related subjects, (7) to indicate concretely the important problems to be solved for work function by further investigations by theory and experiment, (8) to determine fully the validity of $\phi_{max} > \phi^+ > \phi^a > \phi^e = \phi^- > \phi_{min}$ for various polycrystals studied by theory and experiment, (9) to establish firmly the universal recognition of $\Delta\phi^* \equiv \phi^+ - \phi^e > 0$ as the peculiarity characteristic of polycrystals, (10) to demonstrate amply the strong governance of ϕ^+, ϕ^e and $\Delta\phi^*$ by δ_m working as the *key* factor with the critical point of 0.5 (50% in surface fraction), (11) to clarify theoretically the *differential* effect of ϕ_m upon ϕ^+ and ϕ^e according to the emission predominance, (12) to afford well the theoretical ground to the experimental fact that every polycrystal ($\delta_m < 0.5$) usually has a nearly constant value of ϕ^e under the normal condition in spite of a large difference in both ϕ_i and F_i among various specimens, (13) to explain exactly the fundamental difference in work function between submono- and polycrystals and, finally, (14) to examine objectively a new contribution of our simple model to the work function studies developed to date.

For the above purposes, the present author has tried to do best during the last $\sim$20 years after his retirement from Ehime University in order to search thoroughly more than ten thousands of literatures published for work function and related subjects to date in the fields of both pure and applied physics and chemistry. This trial for preparing the present article as well as the previous one [1351] has long been very laborious to him, but the results thus achieved especially as Tables 1 and 2 may be useful and convenient to many workers whenever they try to grasp easily the outline of both method and condition adopted for evaluating each work function and also to refer quickly to the most probable value of elemental work function for the mono- or polycrystalline surface under study.

This article is based on 4461 references which the present author has selected from the amazing number of literatures mentioned just above. In consideration of the fact that more than 500 articles about work function and related subjects have long been published every year [SciFinder, CAS Solution], however, the above references seem to be much less than a half of the literatures published to date for reporting originally the theoretical or experimental data on work function (ϕ^e, ϕ^+ and/or ϕ^-) of the chemical elements and also for including both criticism and discussions about work function and related subjects. But, it is practically impossible to cover the remnant half or more by a single author alone.

Unfortunately, the present author has little time and health enough (1) to enrich sufficiently both contents and explanation in text, (2) to analyze fully the large amount of experimental and theoretical data listed in Table 1, (3) to integrate comprehensively the progress and results achieved by theoretical studies about work function and related subjects, (4) to examine carefully the possibility of overlooking very important articles on work function, (5) to survey adequately these literatures published especially after $\sim$2013, (6) to check thoroughly his inadvertent errors and inattentive mistakes made probably in this article, and also (7) to improve acceptably the readability of this article writing until convincing himself. This is mainly because he has long been much suffered by disease and disorder due to advancing in age. In consequence, for example, he has little analyzed critically these work function data achieved by quantum theory for various surface species by a good many workers and also hardly discussed quite many other important subjects and problems. At least, however, Table 1 including more than ten thousands of work function data and also 490 footnotes may be helpful to many readers for inspecting a variety of work function studies made to date under various conditions and methods in many fields of both pure and applied physics and chemistry. In addition, Table 2 may be useful as an up-to-date and reliable source for quickly finding the most probable values of ϕ^e, ϕ^+ and ϕ^- with regard to both mono- and polycrystalline surfaces of most or several of the chemical elements.

In this article, a theoretical analysis is made deeply for the experimental data on thermionic contrasts ($\Delta\phi^*$) for various mono-, submono- and polycrystalline surfaces, thereby yielding the new findings that δ_m is the key factor mainly governing the effective work functions of patchy surfaces ($\delta_m < 1$) and also that submonocrystal ($0.5 < \delta_m < 1$) should be taken into consideration as

another type (category) much different in work function characteristic from both polycrystal ($\delta_\mathrm{m} < 0.5$) and monocrystal ($\delta_\mathrm{m} = 1$). Such a deep analysis, however, is little attempted here for the work function data achieved by quantum theory and also for the work function changes around various critical temperatures, mainly because of his poverty in health.

As already exemplified in Footnotes 484–486 in Table 1 and also in those 5, 6, 10, 12 and 13 in Table 2, it is generally very difficult for any authors to be perfectly free from inattentive errors in any publications. On account of the poverty in both time and health mentioned above, particularly, the present author has the strong fear that both inadvertent errors and unconscious mistakes have been made probably here and there in this article. He hopes that such probable failures and defects may be adequately corrected and improved in the future by other authors.

Finally, he strongly desires and expects that the insufficient database and inadequate analysis as tentatively compiled in this article should be much enriched and improved in both quantity and quality by next generation so as to respond adequately to a continuous progress in the fields of work function and related subjects.

Acknowledgments

Appendix. List of main symbols

a	lattice constant (cf. Section 5.5.2 and Eq. (13))
A_R	Richardson constant = 120 A/cm^2 K^2 (cf. Section 2.8.6)

A_r	apparent Richardson constant $= (1 - r^e) A_R$ (cf. Section 2.8.6 and Eq. (8))
AI	autoionization (cf. Section 2.8.1 and Table 1)
cnt	carbon nanotube (cf. Section 2.1 and Table 1)
C_p	coefficient of 1/2 or 3/8 (cf. Eq. (17) and Section 11.1)
CPD	contact potential difference (cf. Sections 2.8.1 and 2.8.2 and also Table 1)
CS	conductive spectroscopy (cf. Section 2.8.1 and Table 1)
CVD	chemical vapor deposition (cf. Table 1 and Section 2.2)
D_b	dipole barrier on a surface (cf. Eq. (15), Section 6.1 and Fig. 2)
D_s	surface-atom density (cf. Table 8 and Section 5)
d	diameter (cf. Section 2.1 and Table 1)
d_G	distance from Gibbs surface to the image surface (cf. Section 11.2 and Eqs. (18) and (19))
dhcp	double hexagonal close-packed structure
e	elementary electric charge (cf. Eqs. (17)–(21) and Section 11)
E	electron affinity (cf. Eqs. (6) and (19) and also Sections 2.3, 2.6 and 11.2)
E^+	desorption energy of positive ion (e.g., M^+) (cf. Section 4.1 and Eq. (9))
E^0	desorption energy of neutral atom (e.g., M) (cf. Section 4.1 and Eq. (9))
E_F	Fermi energy of bulk (cf. Eqs. (15) and (16), Sections 6.1 and 6.2 and also Fig. 2)
0^E	extrapolation of temperature down to 0 K in order to estimate ϕ_0^e (cf. Section 2.5 and Table 1)
F_i	fractional surface area of the patchy face (i) (cf. Sections 1 and 4 and also Eqs. (1)–(4))
FE	field emission (cf. Sections 2.8.1 and 9 and also Tables 1, 8–11 and 14)
F_m	fractional surface area largest among F_i's, corresponding to the degree of monocrystallization (δ_m) and having ϕ_m (cf. Section 4)
fp	fine particle (cf. Section 2.1 and Table 1)
HOPG	highly oriented pyrolytic graphite (cf. Section 2.1 and Tables 1, 2, 4 and 5)
I	ionization energy (cf. Eqs. (5), (9), (18), (20) and (21) and also Sections 2.6, 4.1, 11.2 and 11.3)
i^+	positive ion current (cf. Sections 2.6 and 4.1)
ins	insulator (cf. Section 2.1 and Table 1)
IP	ionization potential (cf. Sections 2.8.1 and 11.3 and also Table 1)
ITO	indium tin oxide (cf. Section 2.1 and Table 1)
k	Boltzmann constant (8.617×10^{-5} eV K^{-1}) (cf. Eqs. (1)–(3), (5), (6) and (8))
k^0	neutral desorption rate constant having the relation of $k^0 = $ (const) $\times$ exp $[-E^0/kT]$ (cf. Section 4.1)
k^+	ionic desorption rate constant correlated as $k^+ = $ (const) $\times$ exp $[-E^+/kT]$ and also done with the positive ionization coefficient (α^+) by $\alpha^+ = k^+/k^0$ (cf. Sections 2.6 and 4.1)
M	neutral atom (e.g., alkali) (cf. Section 2.6)
M^+	positive ion of M (cf. Sections 2.3 and 2.6)
M^-	negative ion of M (cf. Sections 2.3 and 2.6)
ML	monolayer (cf. Sections 2.2, 7.1 and 8.2)
MX	diatomic molecule (e.g., alkali halide) (cf. Section 2.6)
nw	nanowire (cf. Section 2.1 and Table 1)
NSI	negative surface ionization (thermal negative ion emission) (cf. Sections 2.6 and 2.8.1 and also Table 1)
O=Ti	oxygenated titanium (cf. Section 2.1 and Table 1)
P_r	residual gas pressure inside the vacuum vessel including a sample surface (cf. Section 2.4 and Table 1)
PE	photoelectric effect (cf. Section 2.8.1 and Table 1)
PSI	positive surface ionization (thermal positive ion emission) (cf. Sections 2.6, 2.8.1 and 4.1 and also Table 1)
r	radius of a fine particle (cf. Eqs. (17) and (17′) and also Section 11.1)
r_c	effective radius of a spherical cluster as calculated from its density and weight (cf. Section 11.3 and Eq. (20))
r^e	internal reflection coefficient of electron, usually treated as in the form of $(1 - r^e) A_R$ (cf. Section 2.8.6)
r_s	Wigner–Seitz radius (cf. Fig. 2, Eqs. (16), (18), (19) and (21) and also Sections 6.1, 6.2, 11.2 and 11.3)
ΔS^+	entropy change due to positive ion production of M^+ from M (cf. Section 2.6)
ΔS^-	entropy change due to negative ion production of X^- from X (cf. Section 2.6)
SP	stopping potential (cf. Section 2.8.1 and Table 1)
SSI	self surface ionization (cf. Section 2.3)
T	temperature of a sample surface adopted for work function measurement (cf. Section 2.5 and Tables 1 and 14)
T_a	annealing temperature, usually recommended to be above $T_m/3$ (cf. Section 2.5) and given in parentheses at the back of T like as ~300 (~900) in the 5th column in Table 1
T_A	allotropic transition temperature (cf. Section 7.1)
T_C	Curie temperature (cf. Section 8)
T_d	sample deposition temperature listed as in the form of $\{T_d\}$, which is usually different from that (T) selected for work function measurements (cf. Table 1 and Section 2.5)
T_m	melting point (cf. Sections 2.5, 5.5.3, 5.5.4 and 7.2 and also Eq. (14))
T_S	superconductive transition temperature (cf. Section 9)
TC	theoretical calculation (cf. Sections 2.8.1, 2.8.3–2.8.5, 4.2, 5.5.2, 5.5.4, 6.1, 6.2 and 11 and also Tables 1, 6 and 9–13, in addition to Eqs. (1)–(3), (7) and (13)–(21))
TCS	total current spectroscopy (cf. Section 2.8.1 and Table 1)
TE	thermal electron emission (cf. Section 2.8.1 and Table 1)
V	atomic volume (cf. Section 5.5.4 and Eq. (14))
w^+/w^0	statistical weight ratio of ion (M^+) to atom (M), generally equivalent to exp $[\Delta S^+/k]$ (cf. Eq. (5) and Section 2.6)
w^-/w^0	statistical weight ratio of ion (X^-) to atom (X), generally equivalent to exp $[\Delta S^-/k]$ (cf. Eq. (6) and Section 2.6)
X	neutral atom (e.g., halogen) (cf. Section 2.6)
X^-	negative ion of X (e.g., halogen) (cf. Section 2.6)
X	electronegativity (cf. Eq. (7) and Section 2.8.3)
z	number of valence electrons per atom (cf. Section 5.5.2 and Eq. (13))
Z	charge state (cf. Section 11.3 and Eq. (20))
α	temperature coefficient of the work function of a clean surface, usually treated as in the form of $\phi_T^e = \phi_0^e + \alpha T$ (cf. Sections 2.5 and 7–10)
α^+	positive ionization coefficient of sample atom (e.g., M) (cf. Eq. (5) and Section 2.6)

α^-	negative ionization coefficient of sample atom (e.g., X) (cf. Eq. (6) and Section 2.6)
β^+	positive ionization efficiency of sample atom or molecule (e.g. M or MX) (cf. Eq. (5) and Section 2.6)
β^-	negative ionization efficiency of sample molecule (e.g., X_2 or MX) (cf. Eq. (6) and Section 2.6)
γ_c	binary alloy component having the range of 0–1 = 0–100% in mole fraction (cf. Sections 2.5 and 4.5)
δ	correction of the spherical cluster radius according to the electron spillover into vacuum (cf. Section 11.3 and Eq. (20))
δ_m	degree of monocrystallization corresponding to the largest (F_m) among the fractional surface areas (F_i's) with the range of 0–1 = 0–100%, governing strongly ϕ^+, ϕ^e and $\Delta\phi^*$ in a different mode between polycrystal ($\delta_m < 0.5$) and submonocrystals ($0.5 < \delta_m < 1$) (cf. Section 4, Eqs. (10)–(12), Table 6 and Fig. 1)
ε	surface energy (cf. Sections 5.5.1 and 5.5.2 and also Eq. (13))
ρ	quantum correction of bulk work function for spherical cluster (cf. Section 11.3 and Eq. (20))
Δ	difference of ϕ^e between our most probable value and another recommended for each surface species by Ref. [1045,1358] or [1354] in Table 2 (cf. Section 3.2 and Table 3)
$\Delta\phi^*$	thermionic contrast between the effective work functions for positive-ionic and electronic emissions, equal to the difference ($\phi^+ - \phi^e > 0$ for both poly- and submonocrystal surfaces) (cf. Tables 4–6, Sections 4.1–4.4 and Fig. 1)
$\Delta\phi^{**}$	thermionic contrast between the effective work functions for negative-ionic and electronic emissions, equal to the difference ($\phi^- - \phi^e = 0$ for any surface species) (cf. Section 4.6 and Table 7)
θ	surface coverage of adsorbate (cf. Sections 2.2, 7.1 and 8.2)
θ_c	critical coverage at which the metastable film changes in both phase and Curie point (cf. Sections 7.1 and 8.2)
ϕ	so-called "work function" generally used without distinction among ϕ^e, ϕ^+ and ϕ^- (cf. Eqs. (9), (15) and (16) and also Sections 1, 4.1, 6.1 and 6.2)
ϕ_i	local work function corresponding to the patch face (i) of a poly- or submonocrystalline surface (cf. Eqs. (1)–(4), Table 6, and also Sections 1 and 4)
ϕ^a	simply averaged work function of a poly- or submonocrystalline surface, generally intermediate between ϕ^+ and ϕ^e (cf. Eq. (4), Table 6, and Sections 1 and 4)
ϕ^e	effective work function for electron emission, generally equal to ϕ^- for any surface, but different from both ϕ^+ and ϕ^a for any poly- and submonocrystals (cf. Sections 1, 2 and 4, Eq. (2) and Tables 1–4 and 6–14)
ϕ^e_0	work function at 0 K (cf. Section 2.5 and Table 1)
ϕ^e_H	work function to be evaluated from Eq. (8) (cf. Section 2.8.6)
ϕ^-	effective work function for negative ion emission, generally equal to ϕ^e for any surface species (cf. Eqs. (3) and (6), Tables 1 and 7 and also Sections 1, 2.6, 3 and 4.5)
ϕ^+	effective work function for positive ion emission, generally larger than ϕ^e for any poly- and submonocrystalline surfaces (cf. Eqs. (1) and (5), Tables 1, 2, 4, 6, 9 and 10 and Sections 1, 2.6, 3, 4 and 5.2–5.4)
ϕ_m	local work function belonging to the largest surface area (F_m) and hence to the degree of monocrystallization (δ_m) (cf. Section 4)
ϕ_{max}	maximum value among the local work functions (ϕ_i's) of various patchy faces (1–i) of poly- or submonocrystalline surface, generally having the sequence of $\phi_{max} > \phi^+ > \phi^a > \phi^e > \phi_{min}$ (cf. Fig. 1 and Section 4.3)
ϕ_{min}	minimum value among the local work functions (ϕ_i's) of various patchy faces (1–i) of poly- or submonocrystalline surface (cf. Fig. 1 and Section 4.3)
ϕ_μ	minimum value to be usually found for an A/B sample system at $\theta < 1$ ML in a plot of ϕ^e vs. θ (cf. Section 2.2)
ϕ^e_0	work function effective for electron emission at the temperature extrapolated to 0 K, corresponding to 0^E (cf. Section 2.5 and Table 1)
ϕ^e_r	work function to be found experimentally together with $A_r \neq 120$ A/cm^2 K^2 (cf. Section 2.8.6 and Eq. (8))
$\phi^e(r)$	work function of a fine particle with a radius of r (cf. Section 11.1 and Eqs. (17) and (17′))
ϕ^e_T	work function effective for electron emission at T, usually having the relation of $\phi^e_T = \phi^e_0 + \alpha T$ (cf. Section 2.5)
$\phi^e(\infty)$	work function equivalent to ϕ^e(poly) of bulk (cf. Eqs. (17)–(21) and Section 11)
τ^0	neutral atom adsorption lifetime correlated with E^o by Frenkel's equation of $\tau^0 = $ (const) $\times$ exp $[E^o/kT]$ (cf. Section 4.1)
τ^+	positive ion adsorption lifetime correlated with E^+ by Frenkel's equation of $\tau^+ = $ (const) $\times$ exp $[E^+/kT]$ (cf. Section 4.1)

References

[1] O.W. Richardson, The Emission of Electricity from Hot Bodies, 2nd ed., Longmans, New York, 1921, pp. 27–59 and 69–92.

[2] H. Kawano, F.M. Page, Experimental methods and techniques for negative ion production by surface ionization, I–III, Int. J. Mass Spectrom. Ion Phys. 50 (1983) 1–128.

[3] P.B. Moon, The emission of positive ions from tungsten, Proc. Camb. Phil. Soc. 28 (1932) 490–496.

[4] B.H. Wolf, Characterization of ion sources, in: B.H. Wolf (Ed.), Handbook of Ion Sources, CRC Press, Boca Raton, 1995, pp. 313–318.

[5] I.T. Platzner, Ion formation processes, in: I.T. Platzner (Ed.), Modern Isotope Ratio Mass Spectrometry, John Wiley, Chichester, 1997, pp. 153–157.

[6] H. Zhang, Ion Sources, Science Press/Springer, Beijing/Berlin, 1999, pp. 13–16 and 165–168.

[7] D. Colodner, V. Salters, D.C. Duckworth, Ion sources for analysis of inorganic solids and liquids by MS, Anal. Chem. 66 (1994) 1079A–1089A.

[8] H. Iwabuchi, M. Nomura, K. Iio, Y. Fujii, T. Suzuki, Surface ionization mechanism of alkali halides, Vacuum 47 (1996) 501–504.

[9] G.D. Alton, R.F. Welton, B. Cui, S.N. Murray, G.D. Mills, A new concept positive (negative) surface ionization source equipped with a high porosity ionizer, Nucl. Instrum. Methods B 142 (1998) 578–591.

[10] V.S. Fomenko, in: G.S. Samsonov (Ed.), Handbook of Thermionic Properties: Electronic Work Functions and Richardson Constants of Elements and Compounds, Plenum, New York, 1966, 151 pp.

[11] D.R. Lide (Ed.), Electron work function of the elements, in: CRC Handbook of Chemistry and Physics, 88th ed., CRC Press, Boca Raton, 2007–2008, p. 12–118.

[12] V.S. Fomenko, Emission Properties of Materials, JPRS–56579 (English translation), 3rd ed., Joint Publications Research Service, Arlington, Virginia, 1972, 172 pp.

[13] J.C. Rivière, Work function: Measurements and results, in: M. Green (Ed.), Solid State Surface Science, Vol. 1, Marcel Dekker, New York, 1969, pp. 179–289.

[14] M. Kaminsky, Atomic and Ionic Impact Phenomena on Metal Surfaces, Springer–Verlag, Berlin, 1965, pp. 98–135.

[15] É.Ya. Zandberg, N.I. Ionov, Surface Ionization, Israel Program for Scientific Translations, Jerusalem, 1971, 355 pp.

[16] R.G. Wilson, G.R. Brewer, Ion Beams with Applications to Ion Implantation, John Wiley, New York, 1973, pp. 26–32 and 72–77.

[17] L. Vályi, Atom and Ion Sources, John Wiley, London, 1977, pp. 46–52 and 134–140.

[18] É.Ya. Zandberg, N.I. Ionov, Surface ionization, Sov. Phys. Uspehki 2 (1959) 255–281.

[19] A.H. Turnbull, Surface Ionization Techniques in Mass Spectrometry, United Kingdom Atomic Energy Authority Research Group Report AERE–R 4295, 1963, 23 pp. (Chem. Abstr. 59 (1963) 10874f).

[20] J.B. Moreau, Contact ionization, Rev. Phys. Appl. 3 (1968) 286–304.

[21] N.I. Ionov, Surface ionization and its applications, Prog. Surf. Sci. 1 (1972) 237–354.

[22] É.Ya. Zandberg, U.Kh. Rasulev, Surface ionization of organic compounds, Russ. Chem. Rev. 51 (1982) 819–832.

[23] H. Kawano, K. Funato, S. Matsui, K. Ogasawara, H. Kobayashi, Y. Zhu, Effective work functions of polycrystalline refractory metals heated for thermal positive–ionic and electronic emissions, Thermochim. Acta 299 (1997) 67–80.

[24] H. Kawano, T. Kenpō, Temperature dependence of thermal positive ion production from sodium bromide molecules incident upon a glowing rhenium surface, J. Chem. Phys. 81 (1984) 1248–1250.

[25] H. Kawano, K. Funato, T. Maeda, Y. Zhu, Sticking probability of metal halide molecules incident upon refractory metal surfaces heated in high vacua, Appl. Surf. Sci. 119 (1997) 341–345.

[26] D.R. Stull, H. Prophet, JANAF Thermochemical Tables, 2nd ed., National Bureau of Standards, Washington, 1971.

[27] I. Barin, Thermochemical Data of Pure Substances, VCH, Weinheim, 1989, 1829 pp.

[28] V.P. Glushko (Ed.), Thermodynamic Properties of Individual Substances, Vols. 1–4, Nauka, Moscow, USSR, 1978–1982.

[29] H. Kawano, T. Kenpō, Temperature dependence and time variation of thermal positive ion production through dissociation of lithium chloride molecules impinging on a heated rhenium surface, Int. J. Mass Spectrom. Ion Processes 62 (1984) 137–153.

[30] H. Kawano, K. Ohgami, S. Matsui, Y. Zhu, Optimum temperature range for positive ion production from metal halide molecules incident upon heated metal catalysts, Appl. Surf. Sci. 144/145 (1999) 404–408.

[31] H. Kawano, T. Kenpō, Y. Hidaka, Determination of the vapor pressures of cesium fluoride and cesium chloride by means of surface ionization, Bull. Chem. Soc. Jpn. 57 (1984) 581–582.

[32] H. Kawano, Ion emission from various solids heated or electron–stimulated in vacua, in: S.G. Pandalai (Ed.), Recent Research Developments in Vacuum Science and Technology, Vol. 3, Transworld Research Network, Trivandrum, 2001, pp. 1–39 (Chem. Abstr. 138 (2003) 278784h).

[33] H. Kawano, T. Kenpō, Determination of the vapor pressures of lithium iodide and potassium chloride by molecular beam surface ionization, Bull. Chem. Soc. Jpn. 57 (1984) 3399–3402.

[34] H. Kawano, K. Ohgami, N. Serizawa, Thermal positive ion production from thallium chloride molecules impinging upon tungsten surface heated in high vacua, Appl. Surf. Sci. 100/101 (1996) 199–202.

[35] H. Kawano, T. Kenpō, Thermal positive ion production from KCl impinging upon Re: Comparison between theory and experiment, J. Chem. Phys. 81 (1984) 6310–6312.

[36] H. Kawano, K. Ohgami, K. Inada, Thermal dissociation and positive ionization of potassium chloride on tungsten, Int. J. Mass Spectrom. Ion Processes 107 (1991) 393–407.

[37] H. Kawano, K. Ohgami, S. Takahashi, N. Nakajima, K. Funato, Influence of sample species upon the positive lithium ion production from lithium halides incident on a glowing tungsten surface, Ann. Univ. Mariae Curie–Skłodowska, Sect. AAA 46/47 (1991/1992) 183–198 (Chem. Abstr. 122 (1995) 228515v).

[38] H. Kawano, S. Itasaka, S. Ohnishi, Additional evidence for the work function increase due to adsorption of residual gases and for its decrease due to co–adsorption of the gases and alkali metal halide molecules during positive surface ionization in high vacua, Int. J. Mass Spectrom. Ion Processes 73 (1986) 145–151.

[39] H. Kawano, K. Ohgami, K. Funato, J. Nakamura, Helpful effect of residual gases upon the thermal positive ion emission from metal surfaces heated in high vacua, Vacuum 46 (1995) 1139–1143.

[40] H. Kawano, K. Ohgami, K. Funato, J. Nakamura, Determination of the rates of both work function change and residual gas adsorption on a tungsten surface heated in a high vacuum, Vacuum 46 (1995) 1145–1148.

[41] H. Kawano, T. Kenpō, A simple method for analyzing the causes of a change in effective work function for thermal positive ionization, Int. J. Mass Spectrom. Ion Processes 66 (1985) 93–100.

[42] H. Kawano, T. Kenpō, A new method to determine the mean adsorption lifetime of alkali halide molecules on a hot metal surface, Int. J. Mass Spectrom. Ion Processes 65 (1985) 299–305.

[43] H. Kawano, Y. Kutsuna, K. Ohgami, K. Funato, A new method to determine the accumulation rate and mean adsorption lifetime of alkali–halide molecules impinging on a metal surface heated for thermal positive ionization, Appl. Surf. Sci. 70/71 (1993) 158–162.

[44] H. Kawano, Y. Zhu, K. Funato, K. Ogasawara, Proc. of the 4th Int. Conf. on Spillover and Migration of Surface Species on Catalysts, Dailian, China, 1997, Stud. Surf. Sci. Catal. 112 (1997) 151–161.

[45] H. Kawano, S. Matsui, N. Serizawa, Thermal positive–ion source developed for molecular beam detection, Rev. Sci. Instrum. 67 (1996) 1193–1195.

[46] J.O. Hendricks, T.E. Phipps, M.J. Copley, Evidence for halogen films on tungsten in the surface ionization of potassium halides, J. Chem. Phys. 5 (1937) 868–872.

[47] A.A. Johnson, T.E. Phipps, A differential method applied to the surface ionization of sodium halides on tungsten, J. Chem. Phys. 7 (1939) 1039–1046.

[48] B.H. Zimm, J.E. Mayer, Vapor pressures, heats of vaporization and entropies of some alkali halides, J. Chem. Phys. 12 (1944) 362–369.

[49] G.E. Cogin, G.E. Kimball, The vapor pressures of some alkali halides, J. Chem. Phys. 16 (1948) 1035–1048.

[50] S. Datz, E.H. Taylor, Ionization on platinum and tungsten surfaces. I. The alkali metals, J. Chem. Phys. 25 (1956) 389–394.

[51] S. Datz, E.H. Taylor, Ionization on platinum and tungsten surfaces. II. The potassium halides, J. Chem. Phys. 25 (1956) 395–397.

[52] J.J. Stoffels, C.R. Lagergren, On the real time measurements of particles in air by direct–inlet surface–ionization mass spectrometry, Int. J. Mass Spectrom. Ion Phys. 40 (1981) 243–254.

[53] É.Ya. Zandberg, A.Ya. Tontegode, Surface ionization of Li, Na, K and Cs atoms and, LiCl, KCl and CsCl molecules, Sov. Phys. Tech. Phys. 10 (1965) 858–866.

[54] E.N. Sloth, M.H. Studier, P.G. Wahlbeck, Effect of anionic constituents on the surface ionization of lithium salts, J. Phys. Chem. 78 (1974) 820–827 (see Ref. [3078]).

[55] W. Weiershausen, Ionization of silver and copper in a triple–filament ion source, in: J.D. Waldron (Ed.), Advances in Mass Spectrometry, Pergamon, Oxford, 1959, pp. 120–124 (Chem. Abstr. 54 (1960) 13847c).

[56] W.D. Davis, Continuous mass spectrometric analysis of particulates by use of surface ionization, Environment. Sci. Technol. 11 (1977) 587–592.

[57] H. Kawano, K. Ohgami, K. Funato, J. Nakamura, How to select the best condition for operating a positive ion source of molecular beam surface ionization type, Rev. Sci. Intrum. 65 (1994) 1766–1769.

[58] H. Kawano, H. Mine, M. Moriyama, M. Tanigawa, Y. Zhu, Selection of the substrate metal best for thermal positive ionization, Rev. Sci. Instrum. 71 (2000) 856–858.

[59] H. Kawano, S. Kaneda, H. Karigō, Y. Kutsuna, Y. Hidaka, Main factors decisive of the threshold temperature range causing a sharp change in thermal positive ionization efficiency of alkali halide molecules incident upon a rhenium surface, Int. J. Mass Spectrom. Ion Processes 94 (1989) 179–187.

[60] H. Kawano, K. Ohgami, S. Matsui, Y. Kitayama, Empirical formulae of the threshold temperature range for dissociative positive ionization of alkali halides on heated metal surfaces, Appl. Surf. Sci. 100/101 (1996) 193–198.

[61] H. Kawano, S. Matsui, Y. Zhu, General applicability of our empirical formulae expressing the threshold temperature range for dissociative positive ionization of halide molecules on heated metal surfaces, Appl. Surf. Sci. 108 (1997) 113–119.

[62] H. Kawano, K. Ohgami, K. Funato, S. Matsui, Relationship between the residual gas pressure and the lowest temperature keeping metal surfaces essentially clean in high vacua, Vacuum 46 (1995) 1149–1150.
[63] B. Weber, B. Bigeard, J.P. Mihe, A. Cassuto, Auger–electron spectroscopy of high–temperature oxygen–rhenium interactions by AES, J. Vac. Sci. Technol. 12 (1975) 338–340.
[64] H. Kawano, K. Ogasawara, H. Kobayashi, A. Tanaka, T. Takahashi, Y. Tagashira, Selection of the residual gas pressure suitable for operating a positive ion source of thermal ionization, Rev. Sci. Instrum. 69 (1998) 1182–1185.
[65] H. Kawano, T. Takahashi, Y. Tagashira, H. Mine, M. Moriyama, Work function of refractory metals and its dependence upon working conditions, Appl. Surf. Sci. 146 (1999) 105–108.
[66] W. Greaves, R.E. Stickney, Adsorption studies based on thermionic emission measurements, Surf. Sci. 11 (1968) 395–410.
[67] H. Kawano, S. Matsui, H. Kobayashi, Y. Zhu, Effective work functions for thermal positive–ionic and electronic emissions from tantalum heated in a high vacuum, Vacuum 48 (1997) 629–631.
[68] H. Kawano, Y. Zhu, Thermal positive–ionic and electronic emissions from iridium heated in vacua, IEEE Trans. Plasma Sci. 29 (2001) 781–784.
[69] H. Kawano, K. Ohgami, K. Funato, J. Nakamura, Thermionic contrast of polycrystalline refractory metals and its dependence upon the experimental conditions employed during thermal positive–ionic and electronic emissions, Appl. Surf. Sci. 70/71 (1993) 142–146.
[70] H. Kawano, K. Ohgami, S. Matsui, Effect of constituent halogens upon the thermal alkali ion production from alkali halides on tungsten, Appl. Surf. Sci. 169/170 (2001) 671–674.
[71] É.Ya. Zandberg, V.I. Paleev, Surface ionization on electrographite with formation of positive ions of atoms of In, K, Rb, and Cs and of molecules of CsCl, RbCl, and KCl, Sov. Phys. Tech. Phys. 9 (1965) 1575–1580.
[72] É.Ya. Zandberg, V.I. Paleev, Surface ionization on silicon, Sov. Phys. Tech. Phys. 10 (1966) 1602–1606.
[73] V.I. Paleev, V.I. Karataev, É.Ya. Zandberg, Applicability of the Saha–Langmuir equation to the temperature dependence of the positive–ion current in surface ionization of atoms on silicon, Sov. Phys. Tech. Phys. 11 (1967) 1089–1095.
[74] E.F. Greene, J.T. Keeley, M.A. Pickering, Interaction of K, Na, Li and Tl with silicon (111) and (100) surfaces; Surface ionization and kinetics of desorption, Surf. Sci. 120 (1982) 103–126.
[75] Y. Bu, E.F. Greene, D.K. Stewart, The ionization of thermal and hyperthermal beams of Na, K, and Cs on Si(111) surfaces, J. Chem. Phys. 92 (1990) 3899–3908.
[76] É.Ya. Zandberg, A.Ya. Tontegode, Thermionic emission constants of molybdenum, tantalum, and tungsten wires, Sov. Phys. Tech. Phys. 10 (1966) 1162–1163.
[77] É.Ya. Zandberg, N.I. Ionov, A.Ya. Tontegode, Mass–spectrometer determination of the heat of vaporization of atoms and positive ions in sublimation of polycrystalline rhenium, tungsten, tantalum, and molybdenum, Sov. Phys. Tech. Phys. 10 (1966) 1164–1172.
[78] É.Ya. Zandberg, M.V. Knat'ko, V.I. Paleev, U.Kh. Rasulev, Work function of oxidized molybdenum wires, Sov. Phys. Tech. Phys. 29 (1984) 1367–1371.
[79] É.F. Chaikovskii, E.D. Kovtun, V.T. Sotnikov, Effect of oxygen on the surface ionization of potassium on tantalum (112) face, Sov. Phys. Tech. Phys. 25 (1980) 116–117.
[80] J.R. Werning, Thermal Ionization At Hot Metal Surfaces, U. S. Atomic Energy Comm., Report UCRL–8455, 1958, 63 pp. (Chem. Abstr. 53 (1959) 13784 i).
[81] E.P. Sytaya, N.G. Shuppe, Surface ionization of I and Na on an incandescent polycrystalline Ta filament, Nauchn. Tr., Tashkentsk. Gos. Univ. (221) (1963) 103–112 (Chem. Abstr. 60 (1964) 15248e).
[82] W. Körner, Electron work function of Tungsten (100)–vicinals, Phys. Status Solidi (a) 22 (1974) 523–534.
[83] M.V. Loginov, M.A. Mittsev, Surface ionization of KCl on tungsten, Sov. Phys. Tech. Phys. 20 (1976) 1497–1499.
[84] É.Ya. Zandberg, É.G. Nazarov, U.Kh. Rasulev, Oxidized tungsten strips as ion emitters for surface ionization of organic compounds, Sov. Phys. Tech. Phys. 25 (1980) 473–477.
[85] G.N. Shuppe, E.P. Sytaya, R.M. Kadyrov, Work function of the (110) face of a tungsten single crystal and positive surface ionization of sodium on this face, Bull. Acad. Sci. USSR, Phys. Ser. 20 (1956) 1035–1043 (Chem. Abstr. 51 (1957) 6324d).
[86] F.L. Hughes, H. Levinstein, Mean adsorption lifetime of Rb on etched tungsten single crystals: Ions, Phys. Rev. 113 (1959) 1029–1035.
[87] E.P. Sytaya, M.I. Smorodinova, N.I. Imangulova, Electron and ion emission from the (110) and (100) faces of a large tungsten monocrystal, Sov. Phys.—Solid State 4 (1962) 750–753.
[88] K.Zh. Zhanabergenov, E.P. Sytaya, Electron and ion emission of faces of a tungsten crystal, Sov. Phys. J. 13 (1970) 697–700 (Chem. Abstr. 73 (1970) 114328a).
[89] J. Fine, T.E. Madey, M.D. Scheer, The determination of work function from the ratio of positive to negative surface ionization of an alkali halide, Surf. Sci. 3 (1965) 227–233.
[90] F.L. Hughes, H. Levinstein, R. Kaplan, Surface properties of etched tungsten single crystals, Phys. Rev. 113 (1959) 1023–1028.
[91] M.J. Dresser, D.E. Hudson, Surface ionization of some rare earths on tungsten, Phys. Rev. 137 (1965) A673–A682.
[92] M.A. Mittsev, N.I. Ionov, Surface ionization of barium on a tungsten surface, Sov. Phys. Tech. Phys. 12 (1968) 1643–1646.
[93] É.Ya. Zandberg, U.Kh. Rasulev, Thermionic emission properties of tungsten oxide, Sov. Phys. Tech. Phys. 13 (1969) 1446–1449.
[94] N.D. Konovalov, V.A. Kuznetsov, B.M. Tsarev, The emission properties of tungsten–rhenium alloys, Sov. Phys. Tech. Phys. 14 (1969) 834–836.
[95] A.M. Romanov, Ionization of lithium on tungsten, Sov. Phys. Tech. Phys. 2 (1957) 1125–1130.
[96] N.I. Ionov, B.K. Medvedev, Thermal desorption and thermionic emission of lanthanide films on a rhenium surface, Sov. Phys.—Solid State 16 (1975) 1719–1721.
[97] É.Ya. Zandberg, A.Ya. Tontegode, Some thermal emission properties of polycrystalline rhenium wires, Sov. Phys. Tech. Phys. 10 (1965) 260–265.
[98] L. Holmlid, K. Möller, Cesium ion desorption from oxygen and carbon adlayers on platinum surfaces with nanosecond time resolution: Variation of desorption parameters with time available for surface diffusion and degree of surface heterogeneity, Surf. Sci. 149 (1985) 609–620.
[99] A. Persky, Positive surface ionization of Na, NaCl, NaBr, NaI, and LiCl on rhenium and on oxygenated rhenium surfaces, J. Chem. Phys. 50 (1969) 3835–3839.
[100] É.Ya. Zandberg, É.G. Nazarov, Yu.Kh. Rasulev, Oxidized–rhenium thermionic emitters of positive ions, Sov. Phys. Tech. Phys. 26 (1981) 706–709.
[101] H. Kawano, S. Itasaka, S. Ohnishi, Y. Hidaka, Temperature dependence of the effective work functions for thermal positive–ionic and electronic emissions from a polycrystalline rhenium surface in a high vacuum, Int. J. Mass Spectrom. Ion Processes 70 (1986) 195–201.
[102] É.Ya. Zandberg, A.Ya. Tontegode, Work function of the iridium (111) face, Sov. Phys.—Solid State 12 (1970) 878–880.
[103] É.Ya. Zandberg, A.Ya. Tontegode, F.K. Yusifov, Thermionic emission of an Ir(111)–C film, Sov. Phys. Tech. Phys. 16 (1972) 1920–1925.
[104] N.I. Ionov, B.K. Medvedev, Study of the adsorption of lanthanides on the surface of iridium and the effect of oxygen on the concentration dependence of the work function of the film systems Ir–Yb, Sov. Phys.—Solid State 17 (1975) 509–512.
[105] É.Ya. Zandberg, E.V. Rut'kov, A.Ya. Tontegode, Effect of valence bond saturation in the adsorbent surface layer on the desorption kinetics, Sov. Phys. Tech. Phys. 20 (1976) 1191–1195.
[106] É.Ya. Zandberg, A.Ya. Tontegode, Thermionic properties of polycrystalline wires of platinum and iridium, Sov. Phys. Tech. Phys. 13 (1968) 550–553.
[107] M.A.C. Assunção, A.M.C. Moutinho, Na and K ionization on polycrystalline Ir, Portugal. Phys. 10 (1979) 43–51 (Chem. Abstr. 93 (1980) 101598b).
[108] L. Holmlid, J.O. Olsson, Molecular beam surface ionization detection, Surf. Sci. 55 (1976) 523–544.

[109] B.I. Mikhailovs'kii, Electronic and ionic emission of some materials in connection with their utilization in a thermoelectron energy converter, Ukr. Fiz. Zh. 7 (1962) 75–77 (Chem. Abstr. 57 (1962) 10629h).

[110] É.Ya. Zandberg, V.I. Paleev, Intrinsic thermionic emission of lanthanum hexaboride and surface ionization of cesium atoms on lanthanum hexaboride, Sov. Phys. Tech. Phys. 10 (1966) 1014–1016.

[111] B.I. Mikhailovskii, Electron and ion emission of zirconium carbide, lanthanum hexaboride, and thorium oxide in cesium vapor at low pressure, Bull. Acad. Sci. USSR, Phys. Ser. 28 (1964) 1404–1407.

[112] K. Möller, L. Holmlid, Desorption of cesium from polycrystalline graphite basal surfaces with strongly non–equilibrium behavior, Surf. Sci. 163 (1985) L635–L640.

[113] A. Braun, G. Busch, Thermal electron emission from graphite, silicon and silicon carbide, Helv. Phys. Acta 20 (1947) 33–66.

[114] G. Glockler, J.W. Sausville, Thermionic emission from carbon, J. Electrochem. Soc. 95 (1949) 292–294.

[115] A.L. Reimann, Thermionic emission from carbon, Proc. Phys. Soc. London 50 (1938) 496–500.

[116] J.A. Dillon Jr., H.E. Farnsworth, Work function and sorption properties of silicon crystals, J. Appl. Phys. 29 (1958) 1195–1202.

[117] F.G. Allen, G.W. Gobeli, Work function, photoelectric threshold, and surface state of atomically clean silicon, Phys. Rev. 127 (1962) 150–158.

[118] F.G. Allen, G.W. Gobeli, Comparison of the photoelectric properties of cleaved, heated, and sputtered silicon surfaces, J. Appl. Phys. 35 (1964) 597–605.

[119] L.C. Burton, Temperature dependence of the silicon work function by means of a retarding potential technique, J. Appl. Phys. 47 (1976) 1189–1191.

[120] M.D. Scheer, J. Fine, Surface ionization of niobium, J. Chem. Phys. 42 (1965) 3645–3648.

[121] H.B. Wahlin, L.O. Sordahl, Positive and negative thermionic emission from columbium (niobium), Phys. Rev. 45 (1934) 886–889.

[122] A.L. Reimann, C.K. Grant, Some high–temperature properties of niobium, Phil. Mag. 22 (1936) 34–48.

[123] B.J. Hopkins, K.J. Ross, The contact potential difference between tungsten and niobium, Br. J. Appl. Phys. 15 (1964) 89–92.

[124] R.G. Wilson, Vacuum thermionic work functions of polycrystalline Nb, Mo, Ta, W, Re, and Ir, J. Appl. Phys. 37 (1966) 3170–3172.

[125] M.D. Scheer, J. Fine, Electron affinity of lithium, J. Chem. Phys. 50 (1969) 4343–4347.

[126] É.F. Chaikovskii, G.M. Pyatigorskii, G.V. Ptitsyn, Temperature hysteresis in positive surface ionization and the work function of a homogeneous emitter, Sov. Phys. Tech. Phys. 10 (1965) 871–876.

[127] O.D. Protopopov, E.V. Mikheeva, B.N. Sheinberg, G.N. Schuppe, Emission parameters of tantalum and molybdenum single crystals, Sov. Phys.—Solid State 8 (1966) 909–914.

[128] E.M. Savitskii, I.V. Burov, L.N. Litvak, G.S. Burkhanov, N.N. Bokareva, Anisotropic work functions of molybdenum single crystals, Sov. Phys. Tech. Phys. 11 (1967) 974–976.

[129] M.D. Scheer, R. Klein, J.D. McKinley, Surface lifetimes of alkali metals on molybdenum, J. Chem. Phys. 55 (1971) 3577–3584.

[130] A.J. Ahearn, The effect of temperature on the emission of electron field current from tungsten and molybdenum, Phys. Rev. 44 (1933) 277–286.

[131] H.B. Wahlin, J.A. Reynolds, Positive and negative thermionic emission from molybdenum, Phys. Rev. 48 (1935) 751–754.

[132] R.W. Wright, Positive and negative thermionic emission from molybdenum, Phys. Rev. 60 (1941) 465–467.

[133] J.C. Rivière, Contact potential difference measurements by the Kelvin method, Proc. Phys. Soc. B 70 (1957) 676–686 (see Ref. [349]).

[134] R.C. Jaklevic, D.W. Juenker, Field dependence of photoelectric emission from molybdenum, J. Appl. Phys. 33 (1962) 562–568.

[135] R. Klein, J. Fine, Desorption of cesium from molybdenum (111): Positive ion and neutral lifetime measurements, in: Proc. 4th Int. Conf. Solid Sur., Vide 201 (1980) 361–364 (Chem. Abstr. 93 (1980) 226128e).

[136] K.R. Wilson, R.J. Ivanetich, Surface Ionization of Na, Rb, LiI, and NaI on Tungsten, Rhenium, and Platinum–Tungsten, Report UCRL–11606, 1964, 24 pp. (Chem. Abstr. 63 (1965) 2402g).

[137] M.D. Fiske, The temperature scale, thermionics, and thermatomics of tantalum, Phys. Rev. 61 (1942) 513–519.

[138] F.L. Reynolds, Surface ionization: An experimental study of strontium and lanthanum on tungsten, Surf. Sci. 14 (1969) 327–339.

[139] H.-W. Wassmuth, R. Müller, Surface ionization and desorption kinetics of indium on pure and oxidized tungsten surfaces, Surf. Sci. 46 (1974) 441–456.

[140] A.A. Brown, L.J. Neelands, H.E. Farnsworth, Thermionic work function of the (100) face of a tungsten single crystal, J. Appl. Phys. 21 (1950) 1–4.

[141] A.R. Hutson, Velocity analysis of thermionic emission from single–crystal tungsten, Phys. Rev. 98 (1955) 889–901.

[142] É.F. Chaikovskii, G.M. Pyatigorskii, Yu.F. Derkach, Determination of emission and adsorption parameters from transient surface ionization, Sov. Phys. Tech. Phys. 21 (1976) 472–475.

[143] U.V. Azizov, G.N. Shuppe, Emission and adsorption characteristics of faces of a tungsten single crystal, Sov. Phys.—Solid State 7 (1966) 1591–1594.

[144] G.N. Shuppe, Emission parameters of different faces of tungsten, molybdenum and tantalum single crystals (clean and contaminated), Bull. Acad. Sci. USSR, Phys. Ser. 30 (1966) 2016–2023.

[145] F.L. Reynolds, Ionization on tungsten single–crystal surfaces, J. Chem. Phys. 39 (1963) 1107–1114.

[146] R.L. Floyd, M.J. Dresser, The surface ionization of gadolinium, terbium and dysprosium on tungsten, Surf. Sci. 84 (1979) 387–407.

[147] B. Krahl-Urban, E.A. Niekisch, H. Wagner, Work function of stepped tungsten single crystal surfaces, Surf. Sci. 64 (1977) 52–68.

[148] L.K. Dikova, E.P. Sytaya, G.N. Shuppe, Thermoelectronic properties of the (110) and (111) faces of a tungsten single crystal coated with a layer of thorium, Sov. Phys.—Solid State 8 (1966) 746–748.

[149] M.H. Nichols, The thermionic constants of tungsten as a function of crystallographic direction, Phys. Rev. 57 (1940) 297–306.

[150] G.F. Smith, Thermionic and surface properties of tungsten crystals, Phys. Rev. 94 (1954) 295–308.

[151] J.L. Coggins, R.E. Stickney, Adsorption studies based on thermionic emission measurements. I. Cesium on single–crystal tungsten, Surf. Sci. 11 (1968) 355–369.

[152] E.W. Müller, Work function of tungsten single crystal planes measured by the field emission microscope, J. Appl. Phys. 26 (1955) 732–737.

[153] N.I. Ionov, Ts.S. Marinova, B.V. Yakshinskii, Determination of the kinetic characteristics of the desorption of lanthanum and neodymium atoms and ions from the (001) face of tungsten by the temperature modulation method, Sov. Phys.—Solid State 14 (1973) 2717–2720.

[154] A. Hurkmans, E.G. Overbosch, J. Los, Surface resonance ionization: Total ionization cross–sections of alkali atoms impinging on a tungsten (110) surface, Nucl. Instrum. Methods 132 (1976) 453–458.

[155] É.Ya. Zandberg, N.I. Ionov, The surface ionization of lithium atoms on polycrystalline tungsten in electrical fields up to 1.3× 106 V/cm, Sov. Phys. Tech. Phys. 3 (1958) 2243–2251.

[156] É.Ya. Zandberg, The surface ionization of NaCl and LiCl molecules on tungsten in electrical fields up to 1.3×106 V/cm, Sov. Phys. Tech. Phys. 3 (1958) 2233–2241.

[157] É.Ya. Zandberg, The surface ionization of indium and thallium atoms on polycrystalline tungsten in electrical fields up to 2 · 10 6 V/cm, Sov. Phys. Tech. Phys. 5 (1961) 1152–1157.

[158] M.J. Copley, T.E. Phipps, The surface ionization of potassium on tungsten, Phys. Rev. 48 (1935) 960–968.

[159] B.Ch. Dyubua, B.N. Popov, Metals with high oxygen stability of thermionic emission against the action of oxygen, Radio Tech. Electron. Phys. 7 (1962) 1454–1462.

[160] N.I. Alekseev, D.L. Kaminskii, Ionization of some rare earth elements on the surfaces of tungsten, rhenium, and iridium, Sov. Phys. Tech. Phys. 9 (1965) 1177–1180.

[161] M. Camp, S.M.A. Lecchini, The work function of polycrystalline tungsten foil, Proc. Phys. Soc. 85 (1965) 815–817.

[162] E.P. Sytaya, N.G. Shuppe, Variation of the emission of tungsten wires as a function of the time of heating by direct and alternating current, Bull. Acad. Sci. USSR, Phys. Ser. 26 (1962) 1372–1375 (Chem. Abstr. 58 (1963) 7467b).

[163] K.F. Zmbov, A. Neubert, H.R. Ihle, Ionization of lanthanum sulfide molecules on heated metal surfaces, Adv. Mass Spectrom. 8 A (1981) 428–432 (Chem. Abstr. 94 (1981) 36483q).

[164] F. Stienkemeier, M. Wewer, F. Meier, H.O. Lutz, Langmuir–Taylor surface ionization of alkali (Li, Na, K) and alkaline earth (Ca, Sr, Ba) atoms attached to helium droplets, Rev. Sci. Instrum. 71 (2000) 3480–3484.

[165] J. Anderson, W.E. Danforth, A.J. Williams III, Work function and thermal desorption in the system thorium–on–rhenium, J. Appl. Phys. 34 (1963) 2260–2265.

[166] L. Holmlid, J.O. Olsson, Molecular beam surface ionization detection. II. Field reversal and surface ionization study of Na on Re with adsorbed oxygen, Surf. Sci. 67 (1977) 61–76.

[167] M. Kaack, D. Fick, Determination of the work functions of Pt(111) and Ir(111) beyond 1100 K surface temperature, Surf. Sci. 342 (1995) 111–118.

[168] R.M. Abdullaev, A.Ya. Tontegode, F.K. Yusifov, Adsorption and initial stages of condensation of samarium on iridium covered with a monolayer of graphite, Sov. Phys.—Solid State 20 (1978) 1856–1860.

[169] R.G. Wilson, E.D. Wolf, Electron and ion emission from iridium in lithium vapor, J. Appl. Phys. 37 (1966) 4458–4462.

[170] D.L. Goldwater, W.E. Danforth, Thermionic emission constants of iridium, Phys. Rev. 103 (1956) 871–872.

[171] V.V. Nikulov, G.A. Kudintseva, Emissive–adsorptive properties of barium oxide films and barium activated barium oxide films, on metals of the platinum group, Radio Eng. Electron. Phys. 14 (1969) 443–446.

[172] É.F. Chaikovskii, G.V. Ptitsyn, Positive surface ionization of potassium on textured platinum ribbons, Sov. Phys. Tech. Phys. 10 (1965) 410–415.

[173] É.F. Chaikovskii, G.V. Ptitsyn, Positive surface ionization of Na on textured platinum ribbons, Sov. Phys. Tech. Phys. 10 (1965) 893–894.

[174] M. Salmerón, S. Ferrer, M. Jazzar, G.A. Somorjai, Photoelectron–spectroscopy study of the electronic structure of Au and Ag overlayers on Pt(100), Pt(111), and Pt(997) surfaces, Phys. Rev. B 28 (1983) 6758–6765.

[175] G.N. Derry, J.-Z. Zhong, Work function of Pt(111), Phys. Rev. B 39 (1989) 1940–1941.

[176] H.L. Van Velzer, The thermionic constants for platinum, Phys. Rev. 44 (1933) 831–836.

[177] L.V. Whitney, The thermionic emission of platinum, Phys. Rev. 50 (1936) 1154–1157.

[178] P. Zazula, Surface ionization and desorption energies, Ark. Fys. 38 (1968) 97–111.

[179] R.G. Wilson, Vacuum thermionic work functions of polycrystalline Be, Ti, Cr, Fe, Ni, Cu, Pt, and type 304 stainless steel, J. Appl. Phys. 37 (1966) 2261–2267.

[180] J.M. Lafferty, Boride cathodes, J. Appl. Phys. 22 (1951) 299–309.

[181] J.D. Buckingham, Thermionic emission properties of a lanthanum hexaboride/rhenium cathode, Br. J. Appl. Phys. 16 (1965) 1821–1832.

[182] H.E. Gallagher, Poisoning of LaB_6 cathodes, J. Appl. Phys. 40 (1969) 44–51.

[183] I.N. Bakulina, N.I. Ionov, A determination of the electron affinity of atoms of copper, silver, and gold by the surface ionization method, Sov. Phys. Dokl. 9 (1964) 217–218.

[184] E.K. Storms, B.A. Mueller, A study of surface stoichiometry and thermionic emission using LaB_6, J. Appl. Phys. 50 (1979) 3691–3698.

[185] D.L. Goldwater, R.E. Haddad, Certain refractory compounds as thermionic emitters, J. Appl. Phys. 22 (1951) 70–73.

[186] A.Ya. Tontegode, F.K. Yusifov, Measurement of isothermal heats of evaporation and mean lifetimes for positive and negative ions on solid surfaces, Sov. Phys. Tech. Phys. 16 (1972) 1353–1357.

[187] R.G. Wilson, W.E. McKee, Vacuum thermionic work functions and thermal stability of TaB_2, ZrC, Mo_2C, $MoSi_2$, $TaSi_2$, and WSi_2, J. Appl. Phys. 38 (1967) 1716–1718.

[188] Y. Hirai, S. Hyodo, Mean residence time of potassium ions on tungsten as measured with reference to ionization efficiency, Surf. Sci. 65 (1977) 93–108.

[189] J. Zegenhagen, J. Ulbricht, R. Beckmann, U. Holm, Lithium adsorption on hot oxygen covered tungsten surfaces, Surf. Sci. 109 (1981) 621–640.

[190] É.Ya. Zandberg, A.Ya. Tontegode, Thermionic emission from rhenium (Review), Sov. Phys. Tech. Phys. 11 (1966) 713–725.

[191] H. Kawano, T. Kenpō, Y. Hidaka, A new and simple method to determine the temperature coefficient of effective work function for thermal positive ion production on a clean polycrystalline metal surface, Int. J. Mass Spectrom. Ion Processes 67 (1985) 137–145.

[192] H. Shelton, Thermionic emission from a planar tantalum crystal, Phys. Rev. 107 (1957) 1553–1557.

[193] G.F. Smith, Velocity analysis of thermionic emission from single–crystal tungsten, Phys. Rev. 100 (1955) 1115–1116.

[194] B.J. Hopkins, T.J. Lee, C.B. Williams, Temperature coefficients of the work functions of the (110) and (100) surfaces of tungsten single crystals and of polycrystalline tungsten foil, J. Appl. Phys. 40 (1969) 1728–1732.

[195] H.M. Love, G.L. Dyer, Work function of the (311) plane of tungsten, Canad. J. Phys. 40 (1962) 1837–1840.

[196] W.B. Nottingham, Thermionic emission from tungsten and thoriated tungsten filaments, Phys. Rev. 49 (1936) 78–97.

[197] A.T. Waterman, J.G. Potter, Contact potential between filaments in vacuum by Kelvin method, Phys. Rev. 51 (1937) 63.

[198] J.G. Potter, Temperature dependence of the work function of tungsten from measurement of contact potentials by the Kelvin method, Phys. Rev. 58 (1940) 623–632.

[199] D.B. Langmuir, Contact potential measurements on tungsten filaments, Phys. Rev. 49 (1936) 428–435.

[200] C.A. Haque, E.E. Donaldson, Continuously oxygenated tungsten as a surface ionization source, Rev. Sci. Instrum. 34 (1963) 409–412.

[201] T.L. Matskevich, Thermionic emission properties of metal alloys (Survey), Sov. Phys. Tech. Phys. 13 (1968) 295–307.

[202] J.A. Becker, E.J. Becker, R.G. Brandes, Reactions of oxygen with pure tungsten and tungsten containing carbon, J. Appl. Phys. 32 (1961) 411–423.

[203] K.-H. Möbius, K. Blatt, The source for negative sodium ions at the Heidelberg MP–tandem accelerator, Nucl. Instrum. Methods 225 (1984) 293–297.

[204] K.H. Kingdon, Electron emission from adsorbed films on tungsten, Phys. Rev. 24 (1924) 510–522.

[205] B.K. Annis, S. Datz, Ion pair formation and atom abstraction in collisions of Cs and UF_6, J. Chem. Phys. 69 (1978) 2553–2561.

[206] W.D. Davis, Continuous mass spectrometric analysis of environmental pollutants using surface ionization, in: T.Y. Toribara, J.R. Coleman, B.E. Dahneke, I. Feldman (Eds.), Environmental Pollutants, Plenum, New York, 1978, pp. 395–411.

[207] T. Fujii, H. Suzuki, M. Obuchi, Surface ionization of some basic organics on an oxidized rhenium emitter: Thermionic emission in a protonated form, J. Phys. Chem. 89 (1985) 4687–4690.

[208] H. Kawano, K. Ohgami, T. Saiki, K. Higaki, C. Murakami, Temperature dependence of the positive ionization efficiency of sodium chloride molecules incident upon a polycrystalline tungsten surface heated in a high vacuum, Int. J. Mass Spectrom. Ion Processes 97 (1990) 131–141.

[209] T.F. Gallagher Jr., R.C. Hilborn, N.F. Ramsey, Hyperfine spectra of $^7Li^{35}Cl$ and $^7Li^{37}Cl$, J. Chem. Phys. 56 (1972) 5972–5979.

[210] O.K. Fomin, M.V. Tikhomirov, Surface ionization of organic molecules on platinum, Russ. J. Phys. Chem. 38 (1964) 383–385.

[211] V.E. Aushev, N.I. Zaika, A.V. Mokhnach, Properties of a lithium atomic beam, Sov. Phys. Tech. Phys. 27 (1982) 878–880.

[212] W. Engelmaier, R.E. Stickney, Adsorption studies based on thermionic emission measurements. II. Oxygen on single–crystal tungsten, Surf. Sci. 11 (1968) 370–394.

[213] O.K. Fomin, M.V. Tikhomirov, N.N. Tunitskii, Mass spectrum of organic ions formed in an atmosphere of mass–spectrometer residual gases on heated oxidized molybdenum, Sov. Phys. Tech. Phys. 9 (1965) 1114–1116.

[214] É.Ya. Zandberg, U.Kh. Rasulev, Sh.M. Khalikov, Emitters for surface–ionization detectors of organic compounds, Sov. Phys. Tech. Phys. 21 (1976) 483–486.

[215] R.V. Golovnya, I.L. Zhuravleva, M.B. Terenina, U.Kh. Rasulev, A.G. Kamenev, É.Ya. Zandberg, Gas–chromatographic functional analysis of amines using parallel detection with surface–ionization and flame–ionization detectors, J. Anal. Chem. USSR 36 (1981) 364–368 (Chem. Abstr. 95 (1981) 17674g).

[216] A. Persky, E.F. Greene, A. Kuppermann, Formation of positive and negative ions on rhenium, oxygenated tungsten, hafnium, lanthanum hexaboride, and thoriated tungsten surfaces, J. Chem. Phys. 49 (1968) 2347–2357.

[217] É.Ya. Zandberg, N.I. Ionov, U.Kh. Rasulev, Sh.M. Khalikov, Method for determination of the lifetime and kinetic characteristics of the thermal desorption of polyatomic ions, Sov. Phys. Tech. Phys. 23 (1978) 79–84.

[218] Yu.V. Zubenko, I.L. Sokol'skaya, Field emission and thermionic emission of thorium and barium layers on tungsten, Sov. Phys.—Solid State 3 (1961) 1133–1136.

[219] L. Bañares, A.G. Ureña, Collision energy effects in the Cs + ICH$_3$ → CsI + CH$_3$ reaction, J. Chem. Phys. 93 (1990) 6473–6483.

[220] A.P.M. Baede, J. Los, Total cross sections for charge transfer and production of free electrons by collisions between alkali atoms and some molecules, Physica 52 (1971) 422–440.

[221] A.M.C. Moutinho, J.A. Aten, J. Los, Temperature dependence of the total cross section for chemi–ionization in alkali–halogen collisions, Physica 53 (1971) 471–492.

[222] T.R. Touw, J.W. Trischka, Large differences in surface ionization efficiencies between K and its halides on the contaminated surface of a Pt alloy (8% W) wire, J. Appl. Phys. 34 (1963) 3635–3636.

[223] A.E. Grosser, A.R. Blythe, R.B. Bernstein, Internal energy of reaction products by velocity analysis. I. Scattered KBr from the crossed molecular beam reaction K + HBr, J. Chem. Phys. 42 (1965) 1268–1273.

[224] G.R. Brandes, A.P. Mills Jr., Work function and affinity changes associated with the structure of hydrogen–terminated diamond (100) surfaces, Phys. Rev. B 58 (1998) 4952–4962.

[225] É.Ya. Zandberg, Surface–ionization detection of particles (Review), Tech. Phys. 40 (1995) 865–884.

[226] H. Pauly, J.P. Toennies, The study of intermolecular potentials with molecular beams at thermal energies, in: D.R. Bates (Ed.), Advances in Atomic and Molecular Physics, Vol. 1, Academic Press, London, 1965, pp. 195–344.

[227] A. Kiejna, K.F. Wojciechowski, Work function changes on single crystal planes, Solid State Commun. 31 (1979) 857–859.

[228] S.D. Dey, S.B. Karmohapatro, First atomic ionization potential of dysprosium and praseodymium, J. Phys. Soc. Japan 22 (1967) 682–683.

[229] M. Aldén, H.L. Skriver, S. Mirbt, B. Johansson, Surface energy and magnetism of the 3d metals, Surf. Sci. 315 (1994) 157–172.

[230] J.C. Inkson, Non–local–density based self–consistent surface calculations: I. Thomas–Fermi lives, J. Phys. C 10 (1977) 567–572.

[231] J.P. Perdew, H.Q. Tran, E.D. Smith, Stabilized jellium: Structureless pseudopotential model for the cohesive and surface properties of metals, Phys. Rev. B 42 (1990) 11627–11636.

[232] E.G. Rauh, R.J. Thorn, Thermionic properties of uranium, J. Chem. Phys. 31 (1959) 1481–1485.

[233] L.-L. Wang, H.-P. Cheng, Density functional study of the adsorption of a C$_{60}$ monolayer on Ag(111) and Au(111) surfaces, Phys. Rev. B 69 (2004) 165417/1–12.

[234] R.F. Willis, B. Fitton, G.S. Painter, Secondary–electron emission spectroscopy and the observation of high–energy excited states in graphite: Theory and experiment, Phys. Rev. B 9 (1974) 1926–1937.

[235] R. Claessen, H. Carstensen, M. Skibowski, Conduction–band structure of graphite crystals studied by angle–resolved inverse photoemission and target–current spectroscopy, Phys. Rev. B 38 (1988) 12582–12588.

[236] D. Neumann, G. Meister, U. Kürpick, A. Goldmann, J. Roth, V. Dose, Interaction of atomic hydrogen with the graphite single–crystal surface, Appl. Phys. A 55 (1992) 489–492.

[237] K. Balik, V. Malat, P. Schneider, Electron emission properties of pyrolytic carbon, Czech. J. Phys. B 31 (1981) 693–694 (Chem. Abstr. 95 (1981) 107084u).

[238] B.V. Bondarenko, V.I. Makukha, E.A. Tishin, E.P. Sheshin, Electron work function of carbon materials, in: B.V. Bondarenko (Ed.), Fiz. Yavleniya Prib. Elektron. Lazernoi Tekh., Mosk. Fiz.-Tekh. Inst., Moscow, USSR, 1983, pp. 13–18 (Chem. Abstr. 102 (1985) 177519b).

[239] B. Sieroczynska-Wojas, External photoelectric effect in Al single crystals, Sov. Phys.—Solid State 10 (1968) 544–552.

[240] J.E. Inglesfield, G.A. Benesh, Bulk and surface states on Al(001), Surf. Sci. 200 (1988) 135–143.

[241] J.K. Grepstad, P.O. Gartland, B.J. Slagsvold, Anisotropic work function of clean and smooth low–index faces of aluminum, Surf. Sci. 57 (1976) 348–362.

[242] P.O. Gartland, Adsorption of oxygen on clean single crystal faces of aluminium, Surf. Sci. 62 (1977) 183–196.

[243] P.A. Anderson, The work function of copper, Phys. Rev. 76 (1949) 388–390.

[244] E. Caruthers, L. Kleinman, G.P. Alldredge, Energy bands for the (001) surface of aluminum, Phys. Rev. B 8 (1973) 4570–4577.

[245] E.V. Chulkov, V.M. Silkin, Electronic structure of the Al(001) surface with adsorbed Na halfmonolayer, Surf. Sci. 215 (1989) 385–393.

[246] S.F. Huang, T.C. Leung, B. Li, C.T. Chan, First–principles study of field–emission properties of nanoscale graphite ribbon arrays, Phys. Rev. B 72 (2005) 035449/1–8.

[247] K.M. Ho, K.P. Bohnen, Investigation of multilayer relaxation on Al(110) with the use of self–consistent total–energy calculations, Phys. Rev. B 32 (1985) 3446–3450.

[248] C. Tejedor, F. Flores, The ionic structure and the electronic potential of metal surfaces, J. Phys. F 6 (1976) 1647–1659.

[249] K. Gürtler, K. Jacobi, Coverage and adsorption–site dependence of core–level binding energies for tin and lead on Al(111) and Ni(111), Surf. Sci. 134 (1983) 309–328.

[250] S.A. Sardar, J.A. Syed, K. Tanaka, F.P. Netzer, M.G. Ramsey, The aluminium–alcohol interface: Methanol on clean Al(111) surface, Surf. Sci. 519 (2002) 218–228.

[251] W. Schottky, Thermodynamics of the uncommon states in vapor spaces (Thermal ionization and thermal luminosity) I, Ann. Phys. 62 (1920) 113–155.

[252] E.V. Rut'kov, A.Ya. Tontegode, The nature of the adsorption bond between graphite islands and iridium, Sov. Phys. Tech. Phys. 27 (1982) 589–594.

[253] A. Khakimov, N.A. Gorbatyi, Evaporation isotherm for Cs ions at a crystal face, Sov. Phys. Tech. Phys. 23 (1978) 366–368.

[254] A. Khakimov, Desorption of Cs ions from W(112), Bull. Acad. Sci. USSR, Phys. Ser. 43 (1979) 15–17.

[255] N.A. Gorbatyi, L.V. Reshetnikova, V.M. Sultanov, Behavior of cesium on the faces of a large tungsten single crystal, Sov. Phys.—Solid State 10 (1968) 940–946.

[256] T.J. Lee, R.E. Stickney, Molecular beam study of the desorption of cesium ions from tungsten crystals, Surf. Sci. 32 (1972) 100–118.

[257] N.I. Ionov, E.N. Lebedeva, M.A. Mittsev, Surface–ionization kinetics of cesium on tungsten by the flash method, Sov. Phys. Tech. Phys. 14 (1970) 1432–1436.

[258] K. Sendecka, R. Męclewski, Field desorption of potassium from (001), (011) and (112) tungsten planes, Surf. Sci. 70 (1978) 255–264.

[259] V.K. Medvedev, T.P. Smereka, Lithium adsorption onto the fundamental faces of tungsten single crystal, Sov. Phys.—Solid State 16 (1974) 1046–1049.

[260] A. Hurkmans, E.G. Overbosch, J. Los, Trapping probabilities and desorption energies of alkali atoms on a clean and an oxygen covered tungsten (110) surface, Surf. Sci. 59 (1976) 488–508.

[261] W. Körner, Investigation of work function and of desorption kinetics on tungsten in dependence on surface structure, Dissertation, Marburg, 1973, 108 pp.

[262] C.J.T.N. Rhodin, Adsorption of single alkali atoms on tungsten using field emission and field desorption, Surf. Sci. 42 (1974) 109–138.

[263] L.D. Schmidt, R. Gomer, Neutral and ionic desorption of cesium from tungsten, J. Chem. Phys. 43 (1965) 2055–2063.

[264] V.M. Gavrilyuk, Yu.S. Vedula, A.G. Naumovets, A.G. Fedorus, Binding energy of Cs atoms adsorbed on (110) and (100) faces of a tungsten crystal, Sov. Phys.—Solid State 9 (1967) 881–883.

[265] V.N. Ageev, N.I. Ionov, B.K. Medvedev, B.V. Yakshinskiï, Kinetics of thermal desorption of cesium atoms and ions from the (001) face of tungsten, Sov. Phys.—Solid State 20 (1978) 767–770.

[266] D.R. Koenig, T.H. Pigford, Work Function and Cesium Desorption Energies for Planar Tungsten Single Crystals, AEC Accession No. 27788, Report No. UCRL–16804, 1966, 22 pp. (Chem. Abstr. 65 (1966) 19423h).

[267] L.D. Schmidt, R. Gomer, Adsorption of potassium on tungsten: Measurements on single–crystal planes, J. Chem. Phys. 45 (1966) 1605–1623.

[268] E.V. Klimenko, A.G. Naumovets, Electron state of sodium atoms adsorbed on tungsten and effect of electronic field on adsorption energy, Surf. Sci. 14 (1969) 141–155.

[269] L. Schmidt, R. Gomer, Adsorption of potassium on tungsten, J. Chem. Phys. 42 (1965) 3573–3598.

[270] K.F. Wojciechowski, Quantum theory of adsorption on metals. II, Acta Phys. Pol. 33 (1968) 363–379 (Chem. Abstr. 69 (1968) 90005g).

[271] B.K. Medvedev, N.I. Ionov, Yu.I. Belyakov, Thermal desorption of lanthanide atoms and ions from the surface of tungsten, Sov. Phys.—Solid State 15 (1974) 1743–1746.

[272] É.F. Chaikovskii, L.I. Kaisheva, Heats of evaporation of atoms and ions of alkali metals and their ionization coefficients on the surface of a silicon single crystal, Sov. Phys. Tech. Phys. 17 (1972) 1043–1044.

[273] É.Ya. Zandberg, E.V. Rut'kov, A.Ya. Tontegode, Time dependence of ion currents produced through surface ionization. Ionization of Ba on the (111) face of iridium, Sov. Phys. Tech. Phys. 19 (1974) 261–263.

[274] E.M. Staicu-Casagrande, L. Guillemot, S. Lacombe, V.A. Esaulov, M. Canepa, L. Mattera, L. Pasquali, S. Nannarone, Adsorbate phase transformations and the coverage–dependent oscillation of electron transfer probabilities, J. Chem. Phys. 113 (2000) 2064–2067.

[275] W.A. Mackie, T. Xie, P.R. Davis, Field emission from carbide film cathodes, J. Vac. Sci. Technol. B 13 (1995) 2459–2463.

[276] D.H. Smith, Mass spectrometric investigation of surface ionization. X. Desorption of uranium ions and neutrals from carburized rhenium, J. Chem. Phys. 55 (1971) 4152–4154.

[277] E.K. Stefanakos, M.J. Dresser, R.F. Tinder, Mechanisms controlling the positive ion emission from heated Fe filaments, J. Appl. Phys. 41 (1970) 3236–3244.

[278] N.R. Gall', E.V. Dut'kov, A.Ya. Tontegode, Carbon diffusion between the volume and surface of (100) molybdenum, Tech. Phys. 47 (2002) 484–490.

[279] B.K. Medvedev, Thermal desorption of lanthanide atoms from the surface of tantalum, Sov. Phys.—Solid State 16 (1975) 1242–1244.

[280] É.G. Nazarov, Observation of atomic desorption dynamics with a voltage–modulation method, Sov. Phys. Tech. Phys. 24 (1979) 707–710.

[281] H. Kawano, Thermionic contrast between the mean work functions effective for positive–ionic and electronic emissions from polycrystalline tungsten surfaces heated in vacuum: Comparison between theory and experiment, Appl. Surf. Sci. 249 (2005) 238–245.

[282] K. Möller, L. Holmlid, Simultaneous determination of desorption parameters and barrier heights for release of previously absorbed tracer amounts of cesium and potassium from a platinum sample, Surf. Sci. 179 (1987) 267–282.

[283] H. Kawano, The mean work function effective for positive ion emission from poly– and monocrystalline surfaces, Surf. Rev. Lett. 12 (2005) 107–113.

[284] H. Ago, T. Kugler, F. Cacialli, W.R. Salaneck, M.S.P. Shaffer, A.H. Windle, R.H. Friend, Work functions and surface functional groups of multiwall carbon nanotubes, J. Phys. Chem. B 103 (1999) 8116–8121.

[285] H.F. Ivey, Thermionic electron emission from carbon, Phys. Rev. 76 (1949) 567.

[286] N.R. Gall, S.N. Mikhailov, E.V. Rut'kov, A.Ya. Tontegode, Carbon interaction with the rhenium surface, Surf. Sci. 191 (1987) 185–202.

[287] W.N. Hansen, G.J. Hansen, Standard reference surfaces for work function measurements in air, Surf. Sci. 481 (2001) 172–184.

[288] C. Edgcombe, U. Valdrè, Determination of F–N parameters for carbon contamination grown nano–tip field emitters: A combined experimental and computational approach, electron, in: A. Kirkland, P.D. Brown (Eds.), Proc. Int. Centen. Symp. Electron, 1997, Institute of Materials, London, 1998, pp. 318–325 (Chem. Abstr. 131 (1999) 178236t).

[289] T. Takahashi, H. Tokailin, T. Sagawa, Angle–resolved ultraviolet photoelectron spectroscopy of the unoccupied band structure of graphite, Phys. Rev. B 32 (1985) 8317–8324.

[290] A. Nagashima, H. Itoh, T. Ichinokawa, C. Oshima, S. Otani, Change in the electronic states of graphite overlayers depending on thickness, Phys. Rev. B 50 (1994) 4756–4763.

[291] S. Suzuki, C. Bower, Y. Watanabe, O. Zhou, Work functions and valence band states of pristine and Cs–intercalated single–walled carbon nanotube bundles, Appl. Phys. Lett. 76 (2000) 4007–4009.

[292] P.G. Schroeder, M.W. Nelson, B.A. Parkinson, R. Schlaf, Investigation of band bending and charging phenomena in frontier orbital alignment measurements of para–quaterphenyl thin films grown on highly oriented pyrolytic graphite and SnS$_2$, Surf. Sci. 459 (2000) 349–364.

[293] I. Schäfer, M. Schlüter, M. Skibowski, Conduction–band structure of graphite studied by combined angle–resolved inverse photoemission and target current spectroscopy, Phys. Rev. B 35 (1987) 7663–7670.

[294] R.F. Willis, B. Feuerbacher, B. Fitton, Experimental investigation of the band structure of graphite, Phys. Rev. B 4 (1971) 2441–2452.

[295] K. Balik, V. Malat, P. Schneider, Electron emission properties of pyrolytic carbon, Czech. J. Phys. B 31 (1981) 693–694 (Chem. Abstr. 95 (1981) 107084u).

[296] S.B. Trickey, F. Müller-Plathe, G.H.F. Diercksen, J.C. Boettger, Interplanar binding and lattice relaxation in a graphite dilayer, Phys. Rev. B 45 (1992) 4460–4468.

[297] A. Ilie, A. Hart, A.J. Flewitt, J. Robertson, W.I. Milne, Effect of work function and surface microstructure on field emission of tetrahedral amorphous carbon, J. Appl. Phys. 88 (2000) 6002–6010.

[298] S. Halas, T. Durakiewicz, Work functions of elements expressed in terms of the Fermi energy and the density of free electrons, J. Phys. Condens. Matter 10 (1998) 10815–10826.

[299] B. Robrieux, R. Faure, J.-P. Dussauley, Resistivity and electric work function of very thin carbon films, C. R. Acad. Sci. Paris B 278 (1974) 659–662.

[300] S. Ciraci, I.P. Batra, Metallization of silicon upon potassium adsorption, Phys. Rev. Lett. 58 (1987) 1982–1985.

[301] I.D. Baikie, U. Petermann, B. Lägel, *In situ* work function study of oxidation and thin film growth on clean surfaces, Surf. Sci. 433–435 (1999) 770–774.

[302] J.E. Ortega, E.M. Oellig, J. Ferrón, R. Miranda, Cs and O adsorption on Si(100) 2×1: A model system for promoted oxidation of semiconductors, Phys. Rev. B 36 (1987) 6213–6216.

[303] R.V. Hill, E.K. Stefanakos, R.F. Tinder, Changes in the work function of iron in the $\alpha \leftrightarrow \gamma$ transformation region, J. Appl. Phys. 42 (1971) 4296–4298.

[304] D.E. Eastman, Photoelectric work functions of transition, rare–earth, and noble metals, Phys. Rev. B 2 (1970) 1–2.

[305] A.B. Cardwell, Photoelectric studies of iron, Phys. Rev. 92 (1953) 554–556.

[306] G.N. Glasoe, Contact potential difference between iron and nickel and their photoelectric work functions, Phys. Rev. 38 (1931) 1490–1496.

[307] A.J. Blodgett Jr., W.E. Spicer, Experimental determination of the optical density of states in iron, Phys. Rev. 158 (1967) 514–523.

[308] G.A. Antypas, R.F. Tinder, E.E. Donaldson, Positive–ion and electron emission from Fe in the region of $\alpha \leftrightarrow \gamma$ transformation, J. Appl. Phys. 39 (1968) 1967–1975.

[309] R.F. Tinder, G.A. Antypas, E.E. Donaldson, Effects of metal defects on positive ion emission from heated iron filaments, J. Appl. Phys. 35 (1964) 3452–3455.

[310] H.B. Wahlin, Thermionic properties of the iron group, Phys. Rev. 61 (1942) 509–512.

[311] F. Mittendorfer, A. Eichler, J. Hafner, Structural, electronic and magnetic properties of nickel surfaces, Surf. Sci. 423 (1999) 1–11.

[312] A. Kashetov, N.A. Gorbatyi, Thermoelectronic parameters of the faces of a nickel single crystal, Sov. Phys.—Solid State 10 (1969) 1673–1677.

[313] R. Rosei, S. Modesti, F. Sette, C. Quaresima, A. Savoia, P. Perfetti, Electronic structure of carbidic and graphitic carbon on Ni(111), Phys. Rev. B 29 (1984) 3416–3422.

[314] B.G. Baker, B.B. Johnson, G.L.C. Maire, Photoelectric work function measurements on nickel crystals and films, Surf. Sci. 24 (1971) 572–586.

[315] B.G. Baker, B.B. Johnson, The surface properties of nickel films evaporated in ultrahigh vacuum, Vacuum 21 (1971) 91–94.

[316] K.-D. Tsuei, J.-Y. Yuh, C.-T. Tzeng, R.-Y. Chu, S.-C. Chung, K.-L. Tsang, Photoemission and photoabsorption study of C_{60} adsorption on Cu(111) surfaces, Phys. Rev. B 56 (1997) 15412–15420.

[317] M. Aldén, S. Mirbt, H.L. Skriver, N.M. Rosengaard, B. Johansson, Surface magnetism in iron, cobalt, and nickel, Phys. Rev. B 46 (1992) 6303–6312.

[318] M. Riehl-Chudoba, D. Fick, Sorption of single lithium atoms on metal surfaces, Surf. Sci. 251–252 (1991) 97–100.

[319] M. Kaack, D. Fick, Binding of Li atoms adsorbed on metal surfaces, Phys. Rev. B 51 (1995) 17902–17909.

[320] M. Methfessel, D. Hennig, M. Scheffler, Trends of the surface relaxation, surface energies, and work functions of the 4d transition metals, Phys. Rev. B 46 (1992) 4816–4829.

[321] Yu.I. Kostikov, V.F. Dvoryankin, Work function of an electron from the low–index faces of b.c.c., f.c.c., and h.c.p. metals, Russ. J. Phys. Chem. 66 (1992) 277–281.

[322] N.R. Gall', E.V. Rut'kov, A.Ya. Tontegode, M.M. Usufov, Interaction of C_{60} molecules with a (100) Mo surface, Tech. Phys. 44 (1999) 1371–1376.

[323] U.V. Azizov, U.V. Vakhidov, V.M. Sulmanov, B.N. Sheinberg, G.N. Shuppe, Emission properties of a molybdenum single crystal, Sov. Phys.—Solid State 7 (1966) 2232–2234.

[324] E.V. Rut'kov, A.Ya. Tontegode, M.M. Usufov, N.R. Gall', Interaction of carbon with hot molybdenum, Sov. Phys. Tech. Phys. 37 (1992) 1038–1041.

[325] S. Berge, P.O. Gartland, B.J. Slagsvold, Photoelectric work function of a molybdenum single crystal for the (100), (110), (111), (112), (114) and (332) faces, Surf. Sci. 43 (1974) 275–292.

[326] P. Soukiassian, R. Riwan, Y. Borensztein, J. Lecante, Electronic properties of the Cs and O co–adsorption on Mo(100) at room temperature, J. Phys. C, Solid State Phys. 17 (1984) 1761–1773.

[327] D.A. Gorodetsky, Yu.P. Melnik, D.P. Proskurin, V.K. Sklyar, V.A. Usenko, A.A. Yas'ko, Barium films on molybdenum (110): LEED and EELS study, Surf. Sci. 416 (1998) 255–263.

[328] D.A. Gorodetskiĭ, Yu.P. Mel'nik, V.A. Usenko, A.A. Yas'ko, Structure and electronic properties of vanadium films on molybdenum (110), Phys. Solid State 37 (1995) 859–864.

[329] D.A. Gorodetsky, Yu.P. Melnik, V.A. Usenko, A.A. Yas'ko, V.I. Yarigin, Cesium on molybdenum (110), Surf. Sci. 315 (1994) 51–61.

[330] B.V. Bondarenko, V.I. Makhov, Adsorption of barium on a (110) face of a molybdenum single crystal, Sov. Phys.—Solid State 12 (1971) 1522–1524.

[331] B.V. Bondarenko, V.I. Makhov, Structure and work function of films of gadolinium on molybdenum, Sov. Phys.—Solid State 12 (1971) 1525–1526.

[332] M.-L. Ernst-Vidalis, C. Papageorgopoulos, U. Stawinski, E. Bauer, Electron– and ion–stimulated desorption of H and Cs ions from Mo(110), Phys. Rev. B 45 (1992) 1793–1799.

[333] M.-L. Ernst-Vidalis, E. Bauer, Hydrogen on Mo(110): Adsorption and electron stimulated H^+ desorption, Surf. Sci. 215 (1989) 378–384.

[334] H.L. Skriver, N.M. Rosengaard, Surface energy and work function of elemental metals, Phys. Rev. B 46 (1992) 7157–7168.

[335] F.M. Gardner, F.E. Girouard, W.L. Boeck, E.A. Coomes, Thermionic emission from single–crystal filaments, Surf. Sci. 26 (1971) 605–623.

[336] I. Buribayev, N.A. Nurmatov, UV photoelectron spectra of Nb and Mo single–crystal surfaces, J. Electron Spectrosc. Relat. Phenom. 68 (1994) 547–554.

[337] P.N. Chistyakov, R.A. Milovanova, Effect of processing on the work function of molybdenum, Sov. Phys. Tech. Phys. 17 (1973) 1707–1708.

[338] L.E. DuBridge, W.W. Roehr, The thermionic and photoelectric work functions of molybdenum, Phys. Rev. 42 (1932) 52–57.

[339] I. Brodie, Uncertainty, topography, and work function, Phys. Rev. B 51 (1995) 13660–13668.

[340] L.W. Swanson, R.W. Strayer, Field–electron–microscopy studies of cesium layers on various refractory metals, J. Chem. Phys. 48 (1968) 2421–2442.

[341] E.M. Savitskii, I.V. Burov, L.N. Litvak, Work function of molybdenum–rhenium alloys, Sov. Phys. Tech. Phys. 14 (1969) 535–537.

[342] I.D. Baikie, U. Peterman, B. Lägel, K. Dirscherl, Study of high– and low–work function surfaces for hyperthermal surface ionization using an absolute Kelvin probe, J. Vac. Sci. Technol. A 19 (2001) 1460–1466.

[343] Y. Morikawa, H. Ishii, K. Seki, Theoretical study of n–alkane adsorption on metal surfaces, Phys. Rev. B 69 (2004) 041403/1–4.

[344] C. Bromberger, H.J. Jänsch, D. Fick, Determination of the coverage dependent work function for Li adsorbed on Ru(001), Surf. Sci. 506 (2002) 129–136.

[345] W. Mannstadt, A.J. Freeman, LDA theory of the coverage dependence of the local density of states: Li adsorbed on Ru(001), Phys. Rev. B 57 (1998) 13289–13294.

[346] W. Mannstadt, Coverage dependence of the work function of Li adsorbed on Ru(001): *ab initio* studies within DFT, Surf. Sci. 525 (2003) 119–125.

[347] V.K. Medvedev, T.P. Smereka, I.M. Ubogiĭ, Ya.B. Lozovyĭ, G.V. Babkin, Interaction of adsorbed barium atoms of the (112) face of a tantalum single crystal, Sov. Phys.—Solid State 33 (1991) 403–405.

[348] J.L. Gumnick, D.W. Juenker, Field dependence of photoelectric emission from tantalum, J. Appl. Phys. 31 (1960) 102–108.

[349] B.J. Hopkins, J.C. Rivière, Work function values from contact potential difference measurements, Br. J. Appl. Phys. 15 (1964) 941–946.

[350] R. Jaeckel, B. Wagner, Photo–electric measurement of the work function of metals and its alteration after gas adsorption, Vacuum 13 (1963) 509–511.

[351] D.R. Jennison, P.A. Schultz, D.B. King, K.R. Zavadil, BaO/W(100) thermionic emitters and the effects of Sc, Y, La, and the density functional used in computation, Surf. Sci. 549 (2004) 115–120.

[352] P. Batzies, Influence of oxygen on the work function of tungsten, in: 2nd Int. Conf. Electr. Power Generation, 1968, pp. 1357–1365 (Chem. Abstr. 72 (1970) 71956p).

[353] A.E. Abey, Work function of the (100) surface of tungsten–rhenium alloys, J. Appl. Phys. 39 (1968) 120–127.

[354] T.V. Vorburger, D. Penn, E.W. Plummer, Field emission work functions, Surf. Sci. 48 (1975) 417–431.

[355] B.A. Boĭko, D.A. Gorodetskiĭ, Structure and work function of silicon films on (100) faces of tungsten, Sov. Phys.—Solid State 18 (1976) 1861–1864.

[356] R.L. Billington, T.N. Rhodin, Surface resonance on W(100): Effect of Au and Cu adsorption, Phys. Rev. Lett. 41 (1978) 1602–1605.

[357] K.C. Mishra, R. Garner, P.C. Schmidt, Model of work function of tungsten cathodes with barium oxide coating, J. Appl. Phys. 95 (2004) 3069–3074.

[358] R.W. Strayer, W. Mackie, L.W. Swanson, Work function measurements by the field emission retarding potential method, Surf. Sci. 34 (1973) 225–248.

[359] B.J. Hopkins, G.R. Shah, Adsorption of methane, ethane and propane on the (100) face of tungsten single crystal, Vacuum 22 (1972) 267–271.

[360] C.A. Papageorgopoulos, J.M. Chen, Coadsorption of electropositive and electronegative elements. I. Cs and H_2 on W(100), Surf. Sci. 39 (1973) 283–312.

[361] C.A. Papageorgopoulos, J.M. Chen, Coadsorption of electropositive and electronegative elements. II. Cs and O_2 on W(100), Surf. Sci. 39 (1973) 313–332.

[362] T.J. Lee, B.H. Blott, B.J. Hopkins, The work functions of cesium on the (100) and (110) oriented faces of tungsten single crystals, Appl. Phys. Lett. 11 (1967) 361–363.

[363] A.P. Ovchinnikov, B.M. Tsarev, Field emission of lithium films on faces of tungsten and rhenium single crystals, Sov. Phys.—Solid State 9 (1968) 2766–2768.

[364] R.B. Sharma, A.D. Adsool, N. Pradeep, D.S. Joag, Adsorption studies of cobalt on tungsten (110), (100) and (111) planes by probe–hole field emission microscopy, Appl. Surf. Sci. 94/95 (1996) 177–185.

[365] A. Modinos, The electronic work function of the different faces of tungsten, Surf. Sci. 75 (1978) 327–341.

[366] K. Wassmuth, D. Fick, Local density of states in Fermi energy for Li atoms adsorbed on metal surfaces, Phys. Rev. Lett. 59 (1987) 3007–3010.

[367] O. Jepsen, R.O. Jones, Surface barrier in W(110). I. Self–consistent film calculations, Phys. Rev. B 34 (1986) 6695–6698.

[368] D.Kh. Azizova, N.A. Gorbatyi, Temperature dependence of the work function of tungsten (110) and (111) crystal faces, Dokl. Akad. Nauk Uzb.SSR 10 (1983) 25–26 (Chem. Abstr. 100 (1984) 166398u).

[369] H. Schall, W. Huber, H. Hoermann, W. Maus-Friedrichs, V. Kempter, Excitation of Li(2p) in slow collisions of Li$^+$ ions with cesiated W(110) surfaces, Surf. Sci. 210 (1989) 163–174.

[370] B.Ya. Melamed, V.I. Silant'ev, N.A. Shevchenko, Work function of the (110) face of tungsten on adsorption of oxygen, Sov. Phys.—Solid State 23 (1981) 1416–1418.

[371] V.P. Kobyakov, V.A. Koryukin, V.P. Obrezumov, Thermoemissive properties of the surfaces of tubular epitaxial tungsten crystals, Tech. Phys. 41 (1996) 834–837.

[372] V.M. Sultanov, Emission properties in different crystallographic directions of a monocrystalline tungsten sphere, Radio Engin. Electron. Phys. 9 (1964) 252–254.

[373] R. Błaszczyszyn, M. Błaszczyszyn, R. Męclewski, Work function of the adsorption system of potassium on tungsten, Surf. Sci. 51 (1975) 396–408.

[374] S.A. Shakirova, E.V. Serova, Gd silicides formation: Heat treatment of coadsorbed Si and Gd ultrathin films on a W(111) surface, Appl. Surf. Sci. 219 (2003) 363–369.

[375] D.F. Stafford, A.H. Weber, Photoelectric and thermionic Schottky deviations for tungsten single crystals, J. Appl. Phys. 34 (1963) 2667–2670.

[376] A.A. Holscher, Surface potentials of nitrogen on individual crystal faces of tungsten, J. Chem. Phys. 41 (1964) 579–580.

[377] J.K. Wysocki, Utilization of the Boltzmann tail of the total energy distribution for the calculation of the "absolute" work function and local field strength in a field electron microscope, Surf. Sci. 137 (1984) 506–514.

[378] B.M. Palyukh, A.I. Yakivchuk, Adsorption of lanthanum on individual faces of tungsten single crystals, Sov. Phys.—Solid State 12 (1971) 2189–2190.

[379] V.K. Medvedev, T.P. Smereka, Adsorption of barium on the (112) faces of tungsten, Sov. Phys.—Solid State 15 (1973) 507–512.

[380] V.K. Medvedev, A.G. Naumovets, T.P. Smereka, Lithium adsorption on the (112) face of tungsten, Surf. Sci. 34 (1973) 368–384.

[381] M. Posternak, H. Krakauer, A.J. Freeman, D.D. Koelling, Self–consistent electronic structure of surfaces: Surface states and surface resonances on W(001), Phys. Rev. B 21 (1980) 5601–5612.

[382] S. Ohnishi, E. Wimmer, A.J. Freeman, Electronic structure of relaxed and reconstructed W(001) surfaces, Bull. Am. Phys. Soc. 27 (1982) 210.

[383] E. Wimmer, A.J. Freeman, J.R. Hiskes, A.M. Karo, All–electron local–density theory of alkali–metal bonding on transition–metal surfaces: Cs on W(001), Phys. Rev. B 28 (1983) 3074–3091.

[384] S. Ohnishi, A.J. Freeman, E. Wimmer, Bonding of surface states on W(001): All–electron local–density–functional studies, Phys. Rev. B 29 (1984) 5267–5278.

[385] E. Wimmer, A.J. Freeman, M. Weinert, H. Krakauer, J.R. Hiskes, A.M. Karo, Cesiation of W(001): Work function lowering by multiple dipole formation, Phys. Rev. Lett. 48 (1982) 1128–1131.

[386] L. Hemstreet, S.R. Chubb, W.E. Pickett, Electronic properties of stoichiometric Ba and O overlayers adsorbed on W(001), Phys. Rev. B 40 (1989) 3592–3599.

[387] L.-J. Chen, N. Wang, D.-S. Wang, E. Luo, Basis functions of the linear augmented–plane–wave method and the work function of an overlayer–substrate system: Cs on W(001), Phys. Rev. B 44 (1991) 8942–8949.

[388] R. Wu, K.-l. Chen, D. Wang, Interaction, electron transfer, and work function of a chemisorbed alkali–metal submonolayer on a W(001) surface, Phys. Rev. B 38 (1988) 3180–3188.

[389] R.-q. Wu, D.-s. Wang, Effect of the surface states of different transition–metal substrates on a Cs overlayer, Phys. Rev. B 41 (1990) 12541–12552.

[390] L. Gładyszewski, Thermoemission of Ce$^+$ ions and its fluctuations, Int. J. Mass Spectrom. Ion Processes 140 (1994) 123–126.

[391] L. Gładyszewski, Surface diffusion of the alkali isotopes on tungsten, Vacuum 48 (1997) 185–186.

[392] D.P. Bernatskiĭ, A.M. Mechetin, V.G. Pavlov, A.Ya. Tontegode, Cesium vapor pressure and residual gas pressure in photoelectron devices, Sov. Phys. Tech. Phys. 33 (1988) 370–371.

[393] G.F. Dionne, Thermionic emission from polycrystalline W–25Re in vacuum and low–pressure Cs vapor, J. Chem. Phys. 46 (1967) 1212–1213.

[394] N.V. Volkov, Yu.K. Gus'kov, Z.N. Kononova, Yu.I. Kostikov, Effect of selenium and sulfur on the work function of tungsten, Sov. Phys. Tech. Phys. 19 (1974) 144–145.

[395] S.J. Mroczkowski, Electron emission characteristics of sputtered lanthanum hexaboride, J. Vac. Sci. Technol. A 9 (1991) 586–590.

[396] L.W. Swanson, L.C. Crouser, F.M. Charbonnier, Energy exchanges attending field electron emission, Phys. Rev. 151 (1966) 327–340.

[397] J.O. Olsson, L. Holmlid, Desorption of potassium from carbon film surfaces, Mater. Sci. Eng. 42 (1980) 121–126.

[398] D.R. Bosch, D.L. Jacobson, The high–temperature effective work function of chemically vapor deposited rhenium on a polycrystalline molybdenum substrate, J. Mater. Eng. Perform. 2 (1993) 97–100.

[399] S. Tatarenko, M. Alnot, R. Ducros, Nitric oxide chemisorption on Re(0001) at 100 and 300 K: Evolution of the adsorbed layer during annealing from 100 to 700 K: XPS, UPS, TDS and work function measurements, Surf. Sci. 163 (1985) 249–265.

[400] M. Alnot, V. Gorodetskiĭ, A. Cassuto, J.J. Ehrhardt, Auger electron spectroscopy, X–ray photoelectron spectroscopy, work function measurements and photoemission of adsorbed xenon on thin films of Pt–Re(111) alloys, Thin Solid Films 151 (1987) 251–262.

[401] M. Alnot, A. Cassuto, J.J. Ehrhardt, B. Slavin, B. Weber, Growth of platinum on rhenium and evolution of the interface under thermal treatment, Appl. Surf. Sci. 10 (1982) 85–99.

[402] R. Wichner, Work Functions of Single Crystalline and Polycrystalline Rhenium, U. S. At. Energy Comm. UCRL–16662, 1966, 108 pp. (Chem. Abstr. 67 (1967) 26720t).

[403] J. Robichaud, F.E. Girouard, Thermionic work function of low index planes of rhenium, Canad. J. Phys. 58 (1980) 43–47.

[404] A. Cassuto, A. Pentenero, P. le Goff, Thermal electron emission of rhenium in ultrahigh vacuum and in the presence of oxygen, Compt. Rend. 260 (1965) 1974–1976.

[405] I.D. Baikie, U. Petermann, A. Speakman, B. Lägel, K.M. Dirscherl, P.J. Estrup, Work function study of rhenium oxidation using an ultra high vacuum scanning Kelvin probe, J. Appl. Phys. 88 (2000) 4371–4375.

[406] Z. Rosenzweig, M. Asscher, Optical second–harmonic generation from surfaces as a monitor for adsorbate introduced work function changes, Surf. Sci. 204 (1988) L732–L738.

[407] P.G. Pallmer Jr., R.L. Gordon, M.J. Dresser, The work function of carburized rhenium, J. Appl. Phys. 51 (1980) 3776–3779.

[408] P.G. Pallmer Jr., R.L. Gordon, M.J. Dresser, The emissivity of carburized rhenium, J. Appl. Phys. 51 (1980) 1798–1801.

[409] A.Ya. Tontegode, Intercalation by atoms of a two–dimensional graphite film on a metal, Phys.-Uspekhi 36 (1993) 1053–1067.

[410] E.V. Rut'kov, A.Ya. Tontegode, A study of the carbon adlayer on iridium, Surf. Sci. 161 (1985) 373–389.

[411] N.M. Nasrullaev, E.V. Rut'kov, A.Ya. Tontegode, Adsorption, desorption, and migration of CsCl molecules on a graphite monolayer on iridium, Sov. Phys. Tech. Phys. 32 (1987) 211–213.

[412] A.Ya. Tontegode, F.K. Yusifov, Superefficient diffusion of cesium atoms into rhenium covered by a two–dimensional graphite film, Appl. Surf. Sci. 90 (1995) 185–190.

[413] N.A. Kholin, E.V. Rut'kov, A.Y. Tontegode, The nature of the adsorption bond between graphite islands and iridium surface, Surf. Sci. 139 (1984) 155–172.

[414] B.E. Nieuwenhuys, R. Bouwman, W.M.H. Sachtler, The changes in work function of group Ib and III metals on xenon adsorption, determined by field electron and photoelectron emission, Thin Solid Films 21 (1974) 51–58.

[415] R.E. Thomas, Interference effects in the reflection of low–energy electrons from thin films of Au on Ir, J. Appl. Phys. 41 (1970) 5330–5334.

[416] G.D. Alton, R.F. Welton, B. Cui, S.N. Murray, G.D. Mills, A new concept positive (negative) surface ionization source equipped with a high porosity ionizer, Nucl. Instrum. Methods B 142 (1998) 578–591.

[417] U. Harms, R.B. Schwarz, Anomalous modulus and work function at the interfaces of thin films, Phys. Rev. B 65 (2002) 085409/1–8.

[418] D.M. Collins, J.B. Lee, W.E. Spicer, A photoemission and thermal desorption study of carbon monoxide and oxygen adsorbed on platinum, Surf. Sci. 55 (1976) 389–402.

[419] G. Boisvert, L.J. Lewis, M. Scheffler, Island morphology and adatom self–diffusion on Pt(111), Phys. Rev. B 57 (1998) 1881–1889.

[420] G.S. Karlberg, F.E. Olsson, M. Persson, G. Wahnström, Energetics, vibrational spectrum and scanning tunneling microscopy images for the intermediate in water production reaction on Pt(111) from density functional calculations, J. Chem. Phys. 119 (2003) 4865–4872.

[421] M. Alnot, J.J. Ehrhardt, J.A. Barnard, A characterization of heterogeneous Pt surfaces by work function measurements and photoemission of adsorbed xenon, Surf. Sci. 208 (1989) 285–305.

[422] A. Cassuto, J.J. Ehrhardt, J. Cousty, R. Riwan, Angle–resolved photoemission of xenon adsorbed on Pt(111): The $(\sqrt{3} \times \sqrt{3})$R30° commensurate layer, Surf. Sci. 194 (1988) 579–596.

[423] J. Cousty, C.A. Papageorgopoulos, R. Riwan, Electronic properties of Cs layers adsorbed on Pt(111), Surf. Sci. 223 (1989) 479–492.

[424] S.K. Jo, J.M. White, Characterization of adsorption states of atomic iodine on Pt(111), Surf. Sci. 261 (1992) 111–117.

[425] W. Ranke, W. Weiss, Photoemission of ethylbenzene adsorbed on Pt(111) and on epitaxial films of FeO(111) and Fe3O4(111): Electronic structure and isosteric heats of adsorption, Surf. Sci. 414 (1998) 236–253.

[426] A. Cassuto, M. Mane, M. Hugenschmidt, P. Dolle, J. Jupille, The effect of K, Cs and O atoms on ethylene adsorption on the Pt(111) surface, Surf. Sci. 237 (1990) 63–71.

[427] M. Kiskinova, G. Pirug, H.P. Bonzel, Coadsorption of potassium and CO on Pt(111), Surf. Sci. 133 (1983) 321–343.

[428] B.E. Nieuwenhuys, W.M.H. Sachtler, Crystal face specificity of nitrogen adsorption on a platinum field emission tip, Surf. Sci. 34 (1973) 317–336.

[429] H.H. Rotermund, S. Jakubith, S. Kubala, A. Von Oertzen, G. Ertl, Invesigation of surfaces by scanning photoemission microscopy, J. Electron Spectrosc. Relat. Phenom. 52 (1990) 811–819.

[430] P.J. Feibelman, D.R. Hamann, Theory of H bonding and vibration on Pt(111), Surf. Sci. 182 (1987) 411–422.

[431] P.J. Feibelman, J.S. Nelson, G.L. Kellogg, Energetics of Pt adsorption on Pt(111), Phys. Rev. B 49 (1994) 10548–10556.

[432] P.J. Feibelman, First–principles calculations of stress induced by gas adsorption on Pt(111), Phys. Rev. B 56 (1997) 2175–2182.

[433] R. Lewis, R. Gomer, Adsorption of oxygen on platinum, Surf. Sci. 12 (1968) 157–176.

[434] A. Cassuto, J. Fusy, A. Pentenero, Thermionic emission of platinum under an ultra–vacuum and in the presence of oxygen, C. R. Acad. Sci. Paris C 265 (1967) 896–898.

[435] P.E.C. Franken, V. Ponec, Ethylene adsorption on thin films of Ni, Pd, Pt, Cu, Au and Al: Work function measurements, Surf. Sci. 53 (1975) 341–350.

[436] R. Bouwman, W.M.H. Sachtler, Photoelectric determination of the equilibration of metal and alloy films, Surf. Sci. 24 (1971) 350–352.

[437] I.N. Yakovkin, V.I. Chernyi, A.G. Naumovets, Effect of Li on the adsorption of CO and O on Pt, J. Phys. D 32 (1999) 841–844.

[438] N.B. Smirnova, B.G. Smirnov, S.M. Mikhailov, E.P. Sytaya, Thermionic emission from (100) faces of single crystals of tungsten, rhenium, tantalum, and molybdenum alloys, Sov. Phys.—Solid State 11 (1969) 784–786.

[439] H. Yamauchi, K. Takagi, I. Yuito, U. Kawabe, Work function of LaB$_6$, Appl. Phys. Lett. 29 (1976) 638–640.

[440] T. Xie, W.A. Mackie, P.R. Davis, Field emission from ZrC films on Si and Mo single emitters and emitter arrays, J. Vac. Sci. Technol. B 14 (1996) 2090–2092.

[441] B.J. Hopkins, K.J. Ross, The work function of Zirconium carbide, Proc. Phys. Soc. 79 (1962) 447–448.

[442] T.L. Matskevich, Work function of zirconium carbide–oxygen, Sov. Phys. Tech. Phys. 23 (1978) 972–975.

[443] T.L. Matskevich, T.V. Krachino, Thermionic emission of zirconium carbide in hydrogen, Sov. Phys. Tech. Phys. 22 (1977) 710–716.

[444] R.G. Wilson, Electron and ion emission from surfaces originally of TaB$_2$, ZrC, Mo$_2$C, MoSi$_2$, TaSi$_2$, and WSi$_2$ in cesium vapor, J. Appl. Phys. 39 (1968) 2306–2310.

[445] R.W. Pidd, G.M. Grover, D.J. Roehling, E.W. Salmi, J.D. Farr, N.H. Krikorian, W.G. Witteman, Characteristics of UC, ZrC, and (ZrC) (UC) as thermionic emitters, J. Appl. Phys. 30 (1959) 1575–1578.

[446] G.V. Samsonov, N.I. Siman, I.A. Podchernyaeva, V.S. Fomenko, Adsorption energy of Cs and K on refractory carbides, Sov. Phys. Tech. Phys. 21 (1976) 223–226.

[447] W.E. Danforth, A.J. Williams III, On the thermionic properties of ZrC, UC, and a ZrC·UC mixture, J. Appl. Phys. 32 (1961) 1181.

[448] T.C. Tessner, P.R. Davis, Preparation and characterization of crystalline ZrC films, J. Vac. Sci. Technol. A 11 (1993) 1–5.

[449] H.W. Hugosson, O. Eriksson, U. Jansson, A.V. Ruban, P. Souvatzis, I.A. Abrikosov, Surface energies and work functions of the transition metal surfaces, Surf. Sci. 557 (2004) 243–254.

[450] N.R. Gall', E.V. Rut'kov, A.Ya. Tontegode, Two–dimensional graphite films on metals and their interaction, Internat. J. Modern Phys. B 11 (1997) 1865–1911.

[451] N.R. Gall', E.V. Rut'kov, A.Ya. Tontegode, M.M. Usufov, Interaction of two–dimensional graphite films on metals by atoms and molecules, Tech. Phys. 44 (1999) 1066–1068.

[452] N.R. Gall', N.P. Lavrovskaya, E.V. Rut'kov, A.Ya. Tontegode, Thermal destruction of two–dimensional graphite islands on refractory metals (Ir, Re, Ni, and Pt), Tech. Phys. 49 (2004) 245–249.

[453] X.Q.D. Li, T. Radojicic, R. Vanselow, Carbon on platinum: Work function changes caused by atomic carbon and by two–dimensional graphite islands, Surf. Sci. 225 (1990) L29–L32.

[454] É.Ya. Zandberg, A.Ya. Tontegode, F.K. Yusifov, Surface ionization of CsCl on an Ir(111)–C film, Sov. Phys. Tech. Phys. 17 (1972) 134–138.

[455] T. Livneh, M. Asscher, The adsorption and decomposition of C$_2$H$_4$ on Ru(001): A combined TPR and work function change study, J. Phys. Chem. B 104 (2000) 3355–3363.

[456] P.J. Feibelman, Electronic structure of clean and carbon–covered closed–packed rhodium and ruthenium surfaces, Phys. Rev. B 26 (1982) 5347–5356.

[457] G. Gensterblum, J.-J. Pireaux, P.A. Thiry, R. Caudano, T. Buslaps, R.L. Johnson, G. Le Lay, V. Aristov, R. Günther, A. Taleb-Ibrahimi, G. Indlekofer, Y. Petroff, Experimental evidence for 400–meV valence–band dispersion in solid C$_{60}$, Phys. Rev. B 48 (1993) 14756–14759.

[458] A.J. Maxwell, P.A. Brühwiler, D. Arvanitis, J. Hasselström, M.K.-J. Johansson, N. Mårtensson, Electronic and geometric structure of C$_{60}$ on Al(111) and Al(110), Phys. Rev. B 57 (1998) 7312–7326.

[459] V. Saltas, C.A. Papageorgopoulos, Adsorption and decomposition of C$_{60}$ on Ni(110) surfaces, Surf. Sci. 488 (2001) 23–31.

[460] M.W. Ruckman, B. Xia, S.L. Qiu, Adsorption of C$_{60}$ on Ta(110): Photoemission and C K–edge studies, Phys. Rev. B 48 (1993) 15457–15460.

[461] J.C. Boettger, Theoretical strain–dependent properties of square and hexagonal Fe monolayers, Phys. Rev. B 48 (1993) 10247–10253.

[462] R. Wu, A.J. Freeman, Structural, electronic, and magnetic properties of an open surface: Fe(111), Phys. Rev. B 47 (1993) 3904–3910.

[463] O. Eriksson, A.M. Boring, R.C. Albers, G.W. Fernando, B.R. Cooper, Spin and orbital contributions to surface magnetism in 3d elements, Phys. Rev. B 45 (1992) 2868–2875.

[464] O. Jepsen, J. Madsen, O.K. Andersen, Spin–polarized electronic structure of the Ni(001) surface and thin films, Phys. Rev. B 26 (1982) 2790–2809.

[465] H. Krakauer, A.J. Freeman, E. Wimmer, Magnetism of the Ni(110) and Ni(100) surfaces: Local–spin–density–functional calculations using the thin–slab linearized augmented–plane–wave method, Phys. Rev. B 28 (1983) 610–623.

[466] E. Wimmer, A.J. Freeman, H. Krakauer, Magnetism at the Ni(001) surface: A high–precision, all–electron local–spin–density–functional study, Phys. Rev. B 30 (1984) 3113–3123.

[467] F. Favot, A. Dal Corso, A. Baldereschi, *Ab initio* study of CO adsorption on Ni(110): Effects on surface magnetism at low coverage, Phys. Rev. B 63 (2001) 115416/1–5.

[468] A. Kiejna, R.M. Nieminen, First–principles calculation of Li adatom structure on the Mo(112) surface, Phys. Rev. B 66 (2002) 085407/1–8.

[469] H. Krakauer, Self–consistent electronic structure of tantalum (001): Evidence for the primary role of surface states in driving reconstructions on tungsten (001), Phys. Rev. B 30 (1984) 6834–6840.

[470] C.J. Wu, L.H. Yang, J.E. Klepeis, C. Mailhiot, *Ab initio* pseudopotential calculations of the atomic and electronic structure of the Ta(100) and (110) surfaces, Phys. Rev. B 52 (1995) 11784–11792.

[471] G.H.M. Gubbels, R. Metselaar, On the effective bare work function of bcc thermionic electrode materials, Surf. Sci. 226 (1990) 407–411.

[472] A.N. Andriotis, Work–function changes due to surface anisotropy and imperfections, Phys. Rev. B 32 (1985) 5062–5067.

[473] J. Peisert, K.F. Wojciechowski, Surface–inhomogeneous jellium model: Face–dependent work function, Surf. Sci. 336 (1995) 205–208.

[474] K.F. Wojciechowski, Quantum size effect in the work function of jellium slabs confined by a finite well of thickness–dependent depth, Phys. Rev. B 60 (1999) 9202–9203.

[475] N.D. Lang, W. Kohn, Theory of metal surfaces: Work function, Phys. Rev. B 3 (1971) 1215–1223.

[476] A. Kiejna, A note on face–dependent surface properties of simple metals, J. Phys. C 15 (1982) 4717–4725.

[477] J.P. Perdew, J.A. Chevary, S.H. Vosko, K.A. Jackson, M.R. Pederson, D.J. Singh, C. Fiolhais, Atoms, molecules, solids, and surfaces: Applications of the generalized gradient approximation for exchange and correlation, Phys. Rev. B 46 (1992) 6671–6689.

[478] H. Bogdanów, K.F. Wojciechowski, Size–dependent work function of ultrathin jellium films, Vacuum 54 (1999) 269–271.

[479] F.E. Olsson, M. Persson, A density functional study of adsorption of sodium–chloride overlayers on a stepped and a flat copper surface, Surf. Sci. 540 (2003) 172–184.

[480] C.J. Fall, N. Binggeli, A. Baldereschi, Work–function anisotropy in noble metals: Contributions from *d* states and effects of the surface atomic structure, Phys. Rev. B 61 (2000) 8489–8495.

[481] W. Hummel, H. Bross, Determining the electronic properties of semi–infinite crystals, Phys. Rev. B 58 (1998) 1620–1632.

[482] C.J. Fall, N. Binggeli, A. Baldereschi, Work functions at facet edges, Phys. Rev. Lett. 88 (2002) 156802/1–4.

[483] R.D. Young, H.E. Clark, Effect of surface patch fields on field–emission work–function determinations, Phys. Rev. Lett. 17 (1966) 351–353.

[484] W. Eib, S.F. Alvarado, Spin–polarized photoelectrons from nickel single crystals, Phys. Rev. Lett. 37 (1976) 444–446.

[485] V.S. Fomenko, Electron work function for single crystals modeled by a film of various atomic thickness, Metallofiz. 14 (2) (1992) 71–85 (Chem. Abstr. 117 (1992) 157806z).

[486] P.A.W. van der Heide, F.V. Azzarello, Work function, valence band and secondary ion intensity variations noted during the initial stages of SIMS depth profiling of Si and SiO_2 by Cs^+, Surf. Sci. 531 (2003) L369–L377.

[487] H. Kobayashi, S. Kato, Observations on the photoelectric work function and LEED pattern from the (111) surface of an iron single crystal, Surf. Sci. 18 (1969) 341–349.

[488] C. Herring, M.H. Nichols, Thermionic emission, Rev. Modern Phys. 21 (1949) 185–270.

[489] Y. Yamamoto, T. Miyokawa, Emission characteristics of a conical field emission gun, J. Vac. Sci. Technol. B 16 (1998) 2871–2875.

[490] R. Kirchner, On the thermoionization in hot cavities, Nucl. Instrum. Methods A 292 (1990) 203–208.

[491] V.P. Afanas'ev, V.A. Obukhov, V.I. Raiko, Thermoionization efficiency in the ion source cavity, Nucl. Instrum. Methods 145 (1977) 533–536.

[492] D.M. Wayne, W. Hang, D.K. McDaniel, R.E. Fields, E. Rios, V. Majidi, The thermal ionization cavity (TIC) source: Elucidation of possible mechanisms for enhanced ionization efficiency, Int. J. Mass Spectrom. 216 (2002) 41–57.

[493] G.D. Alton, Characterization of a cesium surface ionization source with a porous tungsten ionizer. I, Rev. Sci. Instrum. 59 (1988) 1039–1044.

[494] G.D. Alton, M.T. Johnson, G.D. Mills, A simple positive/negative surface ionization source, Nucl. Instrum. Methods A 328 (1993) 154–159.

[495] T. Durakiewicz, A.J. Arko, J.J. Joyce, D.P. Moore, S. Halas, Thermal work function shifts for polycrystalline metal surfaces, Surf. Sci. 478 (2001) 72–82.

[496] S. Saito, Temperature and magnetic effects on the work function, Japan. J. Appl. Phys. 26 (1987) 1838–1843.

[497] A. Kiejna, K.F. Wojciechowski, J. Żebrowski, The temperature dependence of metal work functions, J. Phys. F 9 (1979) 1361–1366.

[498] Y. Gao, R. Reifenberger, Field emission energy distribution study of laser–induced thermal effects, J. Vac. Sci. Technol. A 4 (1986) 1289–1293.

[499] G. Comsa, A. Gelberg, B. Iosifescu, Temperature dependence of the work function of metals (Mo, Ni), Phys. Rev. 122 (1961) 1091–1100.

[500] G.A. Gaudin, M.J.G. Lee, Temperature dependence of the work function of low–index surfaces of tungsten, Surf. Sci. 201 (1988) 540–558.

[501] O.L. Golubev, T.I. Sudakova, V.N. Shrednik, Temperature dependence of the work function of hafnium islands on tungsten, Tech. Phys. 45 (2000) 1575–1580.

[502] L.W. Swanson, L.C. Crouser, Total–energy distribution of field–emitted electrons and single–plane work functions for tungsten, Phys. Rev. 163 (1967) 622–641.

[503] S. Saito, T. Maeda, T. Soumura, Temperature variation of the work function of sputter–cleaned nickel surface, Surf. Sci. 143 (1984) L421– L426.

[504] K. Wandelt, Work function changes due to alkali–metal adsorption, in: H.P. Bonzel, A.M. Bradshaw, G. Ertl (Eds.), Physics and Chemistry of Alkali Metal Adsorption, Elsevier, Amsterdam, 1989, pp. 25–44.

[505] D. Kolthoff, H. Pfnür, Geometrical implications of lateral interactions in chain systems: Li (1×2) and Li (1× 4) on molybdenum (211), Surf. Sci. 457 (2000) 134–146.

[506] D.L. Fehrs, R.E. Stickney, Contact potential measurements of the adsorption of alkali metals on Ta(110) and W(100) crystals, Surf. Sci. 24 (1971) 309–331.

[507] G.N. Derry, P.N. Ross, A work function change study of oxygen adsorption on Pt(111) and Pt(100), J. Chem. Phys. 82 (1985) 2772–2778.

[508] R.O. Unãc, J.L. Sales, M.V. Gargiulo, G. Zgrablich, Desorption kinetics of alkali atoms from transition metals, J. Phys.: Condens. Matter 9 (1997) 9469–9482.

[509] G.D. Alton, Semi–empirical mathematical relationships for electropositive adsorbate induced work function changes, Surf. Sci. 175 (1986) 226–240.

[510] S. Halas, T. Durakiewicz, P. Mackiewicz, Temperature–dependent work function shifts of hydrogenated/deuterated palladium: A new theoretical explanation, Surf. Sci. 555 (2004) 43–50.

[511] N. Wang, K. Chen, D. Wang, Work function of transition–metal surface with submonolayer alkali–metal coverage, Phys. Rev. Lett. 56 (1986) 2759–2762.

[512] R.W. Verhoef, W. Zhao, M. Asscher, Repulsive interactions of potassium on Re(001), J. Chem. Phys. 106 (1997) 9353–9361.

[513] R.W. Verhoef, M. Asscher, The work function of adsorbed alkalis on metals revisited: A coverage–dependent polarizability approach, Surf. Sci. 391 (1997) 11–18.

[514] O.M. Braun, L.G. Il'chenko, É.A. Pashitskiĭ, Adsorption of alkali metal atoms on transition metal surfaces with allowance for the image potential, Sov. Phys.—Solid State 22 (1980) 963–966.

[515] D.R. Baer, R.L. Gordon, C.W. Hubbard, Work function and UPS study of Au and O on Re, Appl. Surf. Sci. 45 (1990) 71–83.

[516] Y. Xu, M. Mavrikakis, Adsorption and dissociation of O_2 on Ir(111), J. Chem. Phys. 116 (2002) 10846–10853.

[517] Y. Lilach, L. Romm, T. Livneh, M. Asscher, The first layers of water on Ru(001), J. Phys. Chem. B 105 (2001) 2736–2742.

[518] T. Livneh, Y. Lilach, M. Asscher, Dipole–dipole interactions among CH_3Cl molecules on Ru(001): Correlation between work function change and thermal desorption studies, J. Chem. Phys. 111 (1999) 11138–11146.

[519] N.D. Lang, Theory of work–function changes induced by alkali adsorption, Phys. Rev. B 4 (1971) 4234–4245.

[520] R. Gomer, J.K. Hulm, Adsorption and diffusion of oxygen on tungsten, J. Chem. Phys. 27 (1957) 1363–1376.

[521] J.R. Smith, Self–consistent many electron–theory of electron work functions and surface potential characteristics for selected metals, Phys. Rev. 181 (1969) 522–529.

[522] G.J. Beyer, E. Herrmann, A. Piotrowski, V.J. Raiko, H. Tyrroff, A new method for rare–earth isotope separation, Nucl. Instrum. Methods 96 (1971) 437–439.

[523] K. Stokbro, Mixed ultrasoft/norm–conserved pseudopotential scheme, Phys. Rev. B 53 (1996) 6869–6872.

[524] K. Möller, L. Holmlid, Cesium ion desorption from graphite surfaces: Kinetics and dynamics of diffusion and desorption steps, Sur. Sci. 173 (1986) 264–282.

[525] M.A. Gleeson, K. Mårtensson, B. Kasemo, D.V. Chakarov, Co–adsorption and reactions of Na and H_2O on graphite, Appl. Surf. Sci. 235 (2004) 91–96.

[526] B. Reihl, J.K. Gimzewski, J.M. Nicholls, E. Tosatti, Unoccupied electronic states of graphite as probed by inverse–photoemission and tunneling spectroscopy, Phys. Rev. B 33 (1986) 5770–5779.

[527] E.V. Rut'kov, A.Ya. Tontegode, M.M. Usufov, N.R. Gall, Carbon interaction with heated molybdenum surface, Appl. Surf. Sci. 78 (1994) 179–184.

[528] J.J. Weimer, E. Umbach, D. Menzel, The properties of K and coadsorbed CO + K on Ru(001), Surf. Sci. 159 (1985) 83–107.

[529] K. Markert, K. Wandelt, The short range of the electronic promoter effect of potassium, Surf. Sci. 159 (1985) 24–34.

[530] A.D. Adsool, R. Pande, R.B. Sharma, M.A. More, D.S. Joag, Adsorption studies of iron on tungsten by probe–hole field emission microscopy, Appl. Surf. Sci. 87–88 (1995) 37–44.

[531] T.C. Leung, C.L. Kao, W.S. Su, Y.J. Feng, C.T. Chan, Relationship between surface dipole, work function and charge transfer: Some exceptions to an established rule, Phys. Rev. B 68 (2003) 195408/1–6.

[532] T. Biernat, R. Błaszczyszyn, Surface diffusion of dysprosium on the W(111) facet, Appl. Surf. Sci. 230 (2004) 81–87.

[533] L. Gładyszewski, Thermoemission of Eu^+ ions and its fluctuations, Surf. Sci. 200 (1988) 386–393.

[534] L. Gładyszewski, Power spectra and autocorrelation functions for surface diffusion of lithium on tungsten, Surf. Sci. 213 (1989) 481–487.

[535] L. Gładyszewski, Alkali migration and desorption energies on polycrystalline tungsten at low coverages, Surf. Sci. 231 (1990) 120–124.

[536] L. Gładyszewski, Ionization degree for alkali atoms on a rhenium surface, Vacuum 45 (1994) 289–291.

[537] N.R. Gall', S.N. Mikhailov, E.V. Rut'kov, A.Ya. Tontegode, Effect of Cs and Ba adsorption on the electronic properties of carbon films adsorbed on metals (Ir, Re), Surf. Sci. 226 (1990) 381–388.

[538] I. Baikie, U. Petermann, B. Lägel, UHV–compatible spectroscopic scanning Kelvin probe for surface analysis, Surf. Sci. 433–435 (1999) 249–253.

[539] I.D. Hughes, H.M. Montagu-Pollock, Field emission microscopy of carbon, J. Phys. D 3 (1970) 228–230.

[540] D.W. Goodman, J.M. White, Measurement of active carbon on ruthenium (110): Relevance to catalytic methanation, Surf. Sci. 90 (1979) 201–203.

[541] D.W. Goodman, R.D. Kelley, T.E. Madey, J.M. White, Summary abstract: Kinetics of carbon deposition from CO on Ru(110) and Ni(100), J. Vac. Sci. Technol. 17 (1980) 143.

[542] F.J. Himpsel, K. Christmann, P. Heimann, D.E. Eastman, P.J. Feibelman, Adsorbate band dispersions for C on Ru(0001), Surf. Sci. 115 (1982) L159–L164.

[543] G. Gensterblum, K. Hevesi, B.-Y. Han, L.-M. Yu, J.-J. Pireaux, P.A. Thiry, R. Caudano, A.-A. Lucas, D. Bernaerts, S. Amelinckx, G. Van Tendeloo, G. Bendele, T. Buslaps, R.L. Johnson, M. Foss, R. Feidenhans'l, G. Le Lay, Growth mode and electronic structure of the epitaxial C_{60}(111)/GeS(001) interface, Phys. Rev. B 50 (1994) 11981–11995.

[544] P. Abbott, E.D. Sosa, D.E. Golden, Effect of average grain size on the work function of diamond films, Appl. Phys. Lett. 79 (2001) 2835–2837.

[545] R. Gao, Z. Pan, Z.L. Wang, Work function at the tips of multiwalled carbon nanotubes, Appl. Phys. Lett. 78 (2001) 1757–1759.

[546] J.P. Sun, Z.X. Zhang, S.M. Hou, G.M. Zhang, Z.N. Gu, X.Y. Zhao, W.M. Liu, Z.Q. Xue, Work function of single–walled carbon nanotubes determined by field emission microscopy, Appl. Phys. A 75 (2002) 479–483.

[547] D. Lovall, M. Buss, E. Graugnard, R.P. Andres, R. Reifenberger, Electron emission and structural characterization of a rope of single–walled carbon nanotubes, Phys. Rev. B 61 (2000) 5683–5691.

[548] G. Zhou, Y. Kawazoe, First–principles study on work function of carbon nanotubes, Physica B 323 (2002) 196–198.

[549] S. Ohnishi, A.J. Freeman, M. Weinert, Surface magnetism of Fe(001), Phys. Rev. B 28 (1983) 6741–6748.

[550] T. Durakiewicz, S. Halas, A. Arko, J.J. Joyce, D.P. Moore, Electronic work function calculations of polycrystalline metal surfaces revisited, Phys. Rev. B 64 (2001) 045101/1–8.

[551] P.J. Feibelman, Structure of "carbidic" and "graphitic" phases on Ru(0001), Surf. Sci. 103 (1981) L149–L154.

[552] E. Wimmer, All–electron local density functional study of metallic monolayers: I. Alkali metals, J. Phys. F 13 (1983) 2313–2321.

[553] A. Kiejna, Surface properties of simple metals in a structureless pseudopotential model, Phys. Rev. B 47 (1993) 7361–7364.

[554] A.N. Andriotis, Theory of semi–infinite metals, Surf. Sci. 116 (1982) 501–512.

[555] P.A. Serena, J.M. Soler, N. García, Work function and image–plane position of metal surfaces, Phys. Rev. B 37 (1988) 8701–8706.

[556] R. Monnier, J.P. Perdew, D.C. Langreth, J.W. Wilkins, Change–in–self–consistent–field theory of the work function, Phys. Rev. B 18 (1978) 656–666.

[557] M. Heinrichsmeier, A. Fleszar, A.G. Eguiluz, LDA calculation of the surface states on the (001), (110), and (111) surfaces of aluminum, Surf. Sci. 285 (1993) 129–141.

[558] J.C. Boettger, Persistent quantum–size effect in aluminum films up to twelve atoms thick, Phys. Rev. B 53 (1996) 13133–13137.

[559] A. Kiejna, J. Peisert, P. Scharoch, Quantum–size effect in thin Al(110) slabs, Surf. Sci. 432 (1999) 54–60.

[560] V.V. Pogosov, V.P. Kurbatsky, Density–functional theory of elastically deformed finite metallic system: Work function and surface stress, J. Exp. Theor. Phys. 92 (2001) 304–311.

[561] C.J. Fall, N. Binggeli, A. Baldereschi, Work functions and surface charges at metallic facet edges, Phys. Rev. B 66 (2002) 075405/1–10.

[562] J.A. Chaney, P.E. Pehrsson, Work function changes and surface chemistry of oxygen, hydrogen, and carbon on indium tin oxide, Appl. Surf. Sci. 180 (2001) 214–226.

[563] P.A.W. van der Heide, Secondary ion emission and work function measurements over the transit region from n and p type Si under Cs^+ irradiation, Appl. Surf. Sci. 231–232 (2004) 97–100.

[564] H. Kobayashi, S. Kato, Observations on the photoelectric work function and LEED pattern from the (100) surface of an iron single crystal, Surf. Sci. 12 (1968) 398–402.

[565] K. Ueda, R. Shimizu, Photoelectric work function study on iron (100) surface combined with Auger electron spectroscopy, Japan. J. Appl. Phys. 12 (1973) 1869–1873.

[566] S.A. Sardar, R. Duschek, R.I.R. Blyth, F.P. Netzer, M.G. Ramsey, The bonding of aldehydes on aluminium: Benzaldehyde on Al(111), Surf. Sci. 468 (2000) 10–16.

[567] J. Neugebauer, M. Scheffler, Mechanisms of island formation of alkali–metal adsorbates on Al(111), Phys. Rev. Lett. 71 (1993) 577–580.

[568] L.Q. Jiang, B.E. Koel, Charge transfer from potassium into the t_{1g} band of C_{60}, Phys. Rev. Lett. 72 (1994) 140–143.

[569] É.Ya. Zandberg, A.G. Kamenev, V.I. Paleev, Surface–ionization determination of the electron affinities of silver and gold, Sov. Phys. Tech. Phys. 19 (1974) 385–389.

[570] M.E. Belyaeva, L.A. Larin, T.V. Kalish, Relation of the work function of rhodium on the heat treatment temperature under ultravacuum conditions, Elektrokhim. 12 (1976) 567–570 (Chem. Abstr. 85 (1976) 115361r).

[571] É.F. Chaikovskii, L.G. Mel'nik, G.M. Pyatigorskii, Negative surface ionization of iodine on single–crystal ribbons of molybdenum and tungsten, Sov. Phys. Tech. Phys. 15 (1970) 163–165.

[572] M.D. Scheer, R. Klein, J.D. McKinley, Surface lifetimes of the alkalis and halogens on molybdenum, in: F. Ricca (Ed.), Adsorption–Desorption Phenomena, Academic Press, London, 1972, pp. 169–188.

[573] M.D. Scheer, R. Klein, J.D. McKinley, Halogens adsorbed on molybdenum: Their surface lifetimes and desorption kinetics, Surf. Sci. 30 (1972) 251–262.

[574] N.I. Ionov, Mass–spectrometric study of the formation of negative halogen ions in the interaction between halides and the surface of incandescent tungsten, Zh. Eksper. Teor. Fiz. 18 (1948) 174–186 (Chem. Abstr. 42 (1948) 6229d).

[575] B.M. Mårtenson, S.O. Wilhelmsson, Thermal desorption and surface lifetimes of bromine and iodine adsorbed on an ionizer of LaB_6, Surf. Sci. 161 (1985) 181–201.

[576] A. Berrada, J.P. Mercurio, J. Etourneau, F. Alexandre, J.B. Theeten, T.M. Duc, Thermionic emission properties of LaB_6 and CeB_6 in connection with their surface states, examination by XPS, Auger spectroscopy and the Kelvin method, Surf. Sci. 72 (1978) 177–188.

[577] E.C.M. Chen, W.E. Wentworth, The experimental values of atomic electron affinities, J. Chem. Educ. 52 (1975) 486–489.

[578] H. Hotop, W.C. Lineberger, Binding energies in atomic negative ions, J. Phys. Chem. Ref. Data 4 (1975) 539–576.

[579] P. Goodman, H. Homonoff, Considerations in the selection of materials for thermionic converter components, in: J.B. Schroeder (Ed.), Metallurgy of Semiconductor Materials, Interscience Publishers, New York, 1962, pp. 309–331.

[580] D.E. Zuccaro, C.R. Dulgeroff, A contact ionization negative ion source, in: Proc. 2nd Symp. on Ion Sources and Formation of Ion Beams, Berkeley, 1974, pp. VIII–8–1/8–6 (Chem. Abstr. 86 (1977) 11172j).

[581] D.L. Fehrs, R.E. Stickney, Contact–potential measurements of the adsorption of I_2, Br_2, and Cl_2 on bare and cesiated W(100), Surf. Sci. 17 (1969) 298–315.

[582] C.W. Jowett, B.J. Hopkins, Work function changes due to the adsorption of chlorine, bromine and iodine on tungsten single crystal surfaces, Surf. Sci. 22 (1970) 392–410.

[583] E.F. Chaikovskii, G.M. Pyatigorskii, Yu.F. Derkach, Positive surface ionization of KCl molecules on the molybdenum (100), Bull. Acad. Sci. USSR, Phys. Ser. 38 (1974) 178–181.

[584] E.F. Chaikovskii, G.M. Pyatigorskii, Yu.F. Derkach, Work function of a (100) molybdenum surface during adsorption of monatomic films of chlorine, bromine and iodine, Sov. Phys.—Solid State 17 (1976) 1585.

[585] M. Hohenegger, E. Bechtold, R. Schennach, Coadsorption of oxygen and chlorine on Pt(111), Surf. Sci. 412/413 (1998) 184–191.

[586] I.M. Beterov, N.V. Fateyev, Laser–assisted negative surface ionization, in: Proc. Int. Conf. Lasers, 1980, pp. 875–881 (Chem. Abstr. 96 (1982) 149481x).

[587] V.I. Khvostenko, V.M. Dukel'skii, Formation of negative hydrogen ions on an incandescent tungsten surface, Sov. Phys.—JETP 10 (1960) 465–466.

[588] K.J. McCallum, J.E. Mayer, A direct experimental determination of the electron affinity of chlorine, J. Chem. Phys. 11 (1943) 56–63.

[589] P.M. Doty, J.E. Mayer, Electron affinity of bromine and a study of its decomposition on hot tungsten, J. Chem. Phys. 12 (1944) 323–328.

[590] P.P. Sutton, J.E. Mayer, A direct experimental determination of electron affinities: The electron affinity of iodine, J. Chem. Phys. 3 (1935) 20–28.

[591] N.I. Ionov, Temperature dependence of the formation of negative iodine ions on the surface of incandescent tungsten, Zh. Eksper. Teor. Fiz. 17 (1947) 272–277 (Chem. Abstr. 42 (1948) 815d).

[592] I.N. Bakulina, N.I. Ionov, Absolute electron affinities of halogen and sulphur atoms, Russ. J. Phys. Chem. 39 (1965) 78.

[593] J.H. Rose Jr., D.J.W. Shore, M. Geldart, H.B. Rasolt, Calculation of ground state surface properties of simple metals including non–local effects of the exchange and correlation energy, Solid State Commun. 19 (1976) 619–622.

[594] C.-y. Park, T. Sagawa, Charge transfer in the Al–Mg alloy, J. Appl. Phys. 60 (1986) 1310–1312.

[595] J.C. Blais, G. Bolbach, A. Brunot, M. Cottin, A new technique for negative surface ionization studies and electron affinity determinations, Adv. Mass Spectrom. 7 A (1978) 380–383 (Chem. Abstr. 89 (1978) 83570x).

[596] J.C. Blais, A. Brunot, M. Cottin, A tandem mass spectrometer and energy analyzer for negative surface ionization studies: Determination of electron affinity, Int. J. Mass Spectrom. Ion Phys. 22 (1976) 71–83.

[597] H.H. Stroke, Surface ionization of the halogens (Master's thesis), MIT, 1952, 54 pp.

[598] P.R. Davis, M.A. Gesley, G.A. Schwind, L.W. Swanson, J.J. Hutta, Comparison of thermionic cathode parameters of low index single crystal faces of LaB_6, CeB_6 and PrB_6, Appl. Surf. Sci. 37 (1989) 381–394.

[599] Kh.I. Lakh, Z.V. Stasyuk, Adsorption of barium and oxygen on the (10$\bar{1}$0) surface of rhenium, Sov. Phys. Tech. Phys. 27 (1982) 848–850.

[600] J.C. Blais, G. Bolbach, Study of negative surface ionization on complex emitters, Int. J. Mass Spectrom. Ion Phys. 24 (1977) 413–427.

[601] F.M. Page, G.C. Goode, Negative Ions and the Magnetron, Wiley-Interscience, London, 1962, 156 pp.

[602] W. Dong, V. Ledentu, Ph. Sautet, A. Eichler, J. Hafner, Hydrogen adsorption on palladium: A comparative theoretical study of different surfaces, Surf. Sci. 411 (1998) 123–136.

[603] J. Pelletier, C. Pomot, Negative surface ionization hysteresis phenomena, J. Appl. Phys. 50 (1979) 1512–1518.

[604] G. Bolbach, J.C. Blais, Desorption of halogens from some Nb, Mo, Ta and W single crystal surfaces, Surf. Sci. 137 (1984) 327–338.

[605] K.G. Heumann, Isotope dilution mass spectrometry, Int. J. Mass Spectrom. Ion Process. 118/119 (1992) 575–592.

[606] A.J. Đerić, L.S. Vasić, M.V. Veljković, O.M. Sešković, M.B. Miletić, K.F. Zmbov, Surface ionization study of the electron affinity of fullerene, Hem. Ind. 52 (1998) 524–526 (Chem. Abstr. 130 (1999) 345844c).

[607] L.-S. Wang, J. Conceicao, C. Jin, R.E. Smalley, Threshold photodetachment of cold C_{60}^-, Chem. Phys. Lett. 182 (1991) 5–11.

[608] J.K. Nørskov, B.I. Lundqvist, Secondary–ion emission probability in sputtering, Phys. Rev. B 19 (1979) 5661–5665.

[609] M.L. Yu, Anomalous coverage dependence of secondary–ion emission from overlayers, Phys. Rev. B 29 (1984) 2311–2313.

[610] J. Küppers, F. Nitschké, K. Wandelt, G. Ertl, The adsorption of Xe on Pd(110), Surf. Sci. 87 (1979) 295–314.

[611] T. Wirtz, H.-N. Migeon, Work function shifts and variations of ionization probabilities occurring during SIMS analyses using an *in situ* deposition of Cs^0, Surf. Sci. 561 (2004) 200–207.

[612] R.M. Eastment, C.H.B. Mee, Work function measurements on (100), (110) and (111) surfaces of aluminium, J. Phys. F 3 (1973) 1738–1745.

[613] A. Thanailakis, Metal contacts on ultra–high vacuum cleaved silicon, Inst. Phys. Conf. Ser. 22 (1974) 59–66 (Chem. Abstr. 82 (1975) 163912f).

[614] R.C. Weast (Ed.), Electron work function of the elements, in: CRC Handbook of Chemistry and Physics, 66th ed., 1985–1986, pp. E–86/E–87.

[615] M.L. Yu, Velocity dependence of the ionization probability of sputtered atoms, Phys. Rev. Lett. 47 (1981) 1325–1328.

[616] J.E. Demuth, Ultraviolet photoemission studies of hydrogen chemisorption bonding to Ni, Pd and Pt surfaces, Surf. Sci. 65 (1977) 369–375.

[617] Z.W. Deng, R. Souda, Dissociative thermal–electron attachment at a surface: CN–emission from nitrogen ion irradiated graphite, Surf. Sci. 488 (2001) 393–398.

[618] H. Gnaser, Exponential scaling of sputtered negative–ion yields with transient work–function changes on Cs^+–bombarded surfaces, Phys. Rev. B 54 (1996) 16456–16459.

[619] P.G. Musket, W. McLean, C.A. Colmenares, D.M. Makowiecki, W.J. Siekhaus, Preparation of atomically clean surfaces of selected elements: A review, Appl. Surf. Sci. 10 (1982) 143–207.

[620] H. Ueta, M. Saida, C. Nakai, Y. Yamada, M. Sakaki, S. Yamamoto, Highly oriented monolayer graphite formation on Pt(111) by a supersonic methane beam, Surf. Sci. 560 (2004) 183–190.

[621] P.N. Chistyakov, R.A. Milovanova, V.V. Lytkin, Investigation of the work function of a tungsten cathode after bombardment, Sov. Phys. Tech. Phys. 19 (1974) 148–149.

[622] Y. Koguchi, T. Meguro, A. Hida, H. Takai, K. Maeda, Y. Yamamoto, Y. Aoyagi, Modification of highly oriented pyrolytic graphite (HOPG) surfaces with highly charged ion (HCI) irradiation, Nucl. Instrum. Methods B 206 (2003) 202–205.

[623] H.M. Kennett, A.E. Lee, The initial oxidation of molybdenum. I. LEED and RHEED observations on (110) molybdenum, Surf. Sci. 48 (1975) 591–605.

[624] S.G. Louie, Electronic states and adsorbate–induced photoemission structure on the Pd(111) surface, Phys. Rev. Lett. 40 (1978) 1525–1528.

[625] M. Chelvayohan, C.H.B. Mee, Work function measurements on (110), (100) and (111) surfaces of silver, J. Phys. C 15 (1982) 2305–2312.

[626] A.W. Dweydari, C.H.B. Mee, Work function measurements on (100) and (110) surfaces of silver, Phys. Status Solidi (a) 27 (1975) 223–230.

[627] H. Erschbaumer, A.J. Freeman, C.L. Fu, R. Podloucky, Surface states, electronic structure and surface energy of the Ag(001) surface, Surf. Sci. 243 (1991) 317–322.

[628] V.N. Ageev, N.I. Ionov, Oxidation kinetics of tungsten, Sov. Phys.—Solid State 11 (1970) 2593–2595.

[629] V.N. Ageev, Yu.A. Kuznetsov, The effect of the degree of oxidation of a tungsten surface on the energy distribution of lithium atoms in electron–stimulated desorption, Sov. Tech. Phys. Lett. 16 (1990) 179–180.

[630] H. Kawano, Mean work functions effective for negative–ionic, electronic and positive–ionic emissions from polycrystalline surfaces, Appl. Surf. Sci. 252 (2006) 5233–5242.

[631] V.S. Neshpor, I.A. Podchernyaeva, N.I. Siman, N.A. Skaletskaya, V.S. Fomenko, Thermal emission of pyrolytic graphite, in: Konfiguratsionnye Predstavleniya Elektron. Str. Fiz. Materialoved, 2nd, 1976 (pub. 1977), pp. 88–94 (Chem. Abstr. 89 (1978) 189641m).

[632] J. Krieg, P. Oelhafen, H.-J. Güntherodt, Observation of unfilled electron states in alkali graphite intercalation compounds by secondary electron spectroscopy, Solid State Commun. 42 (1982) 831–833.

[633] S.C. Jain, K.S. Krishnan, The thermionic constants of metals and semiconductors. I. Graphite, Proc. R. Soc. A 213 (1952) 143–157.

[634] S.B.L. Mathur, A new method for obtaining thermionic constants. I. The thermionic constants of molybdenum, Proc. Natl. Inst. Sci. India 19 (1953) 153–163 (Chem. Abstr. 47 (1953) 11958h).

[635] R. Bachmann, G. Busch, A.H. Madjid, The emission of electrons from hot silicon surfaces, Surf. Sci. 2 (1964) 396–401.

[636] A. Thanailakis, Contacts between simple metals and atomically clean silicon, J. Phys. C 8 (1975) 655–668.

[637] K. Kokko, P.T. Salo, R. Laihia, K. Mansikka, Work function and surface energy of optimized lithium slabs, Phys. Rev. B 52 (1995) 1536–1539.

[638] J. Lee, C.P. Hanrahan, J. Arias, R.M. Martin, H. Metiu, Local modifications of the surface work function by potassium adsorption, Surf. Sci. 161 (1985) L543–L548.

[639] A.A. Knizhnik, I.M. Iskandarova, A.A. Bagatur'yants, B.V. Potapkin, Impact of oxygen on the work functions of Mo in vacuum and on ZrO_2, J. Appl. Phys. 97 (2005) 064911/1–6.

[640] B.V. Bondarenko, V.I. Makhov, Structure and work function of lanthanum films on a (100) molybdenum single crystal surface, Sov. Phys.—Solid State 12 (1971) 1646–1648.

[641] J.C. Blais, G. Bolbach, A. Brunot, M. Cottin, A. Marilier, A comparison of low electronic work function surfaces for negative ion production, in: Proc. 7th Int. Vac. Congr. and 3rd Int. Conf. Solid Surfaces, Vienna, 1, 1977, pp. 667–670 (Chem. Abstr. 88 (1978) 79339r).

[642] A.R. Shul'man, E.I. Myakinin, Threshold of the secondary electron emission of nickel and molybdenum, Dokl. Akad. Nauk SSSR 91 (1953) 1075–1078, (Chem. Abstr. 48 (1954) 10423i).

[643] P. Pech, Normal cathodic potential drop of glow discharge in neon and the electronic work function of pure and gas–covered molybdenum surfaces, Beitr. Plasma Phys. 7 (1967) 419–448 (Chem. Abstr. 69 (1968) 71705u).

[644] L.W. Swanson, R.W. Strayer, F.M. Charbonnier, The effect of electronic field on adsorbed layers of cesium on various refractory metals, Surf. Sci. 2 (1964) 177–187.

[645] H.V. Thapliyal, E.K. Stefanakos, R.F. Tinder, Desorption of K^+ from molybdenum, Surf. Sci. 38 (1973) 231–233.

[646] A. Kotarba, J. Dmytrzyk, W. Raróg-Pilecka, Z. Kowalczyk, Surface heterogeneity and ionization of Cs promoter in carbon–based ruthenium catalyst for ammonia synthesis, Appl. Surf. Sci. 207 (2003) 327–333.

[647] A.Ya. Tontegode, F.K. Yusifov, Surface ionization of CsCl molecules on a Rh–C film emitter with carbon diffusion across the crystal interface, Sov. Phys. Tech. Phys. 18 (1973) 661–666.

[648] M. Błaszczyszyn, Work function of adsorption systems potassium on tantalum and on molybdenum, Surf. Sci. 59 (1976) 533–540.

[649] É.Ya. Zandberg, E.V. Rut'kov, A.Ya. Tontegode, Concentration dependence of the kinetic characteristics of thermal desorption of barium atoms and ions from the Ir(111) face, Sov. Phys.—Solid State 19 (1977) 214–217.

[650] R.G. Wilson, Ion Thruster Electrode Surface Physics Studies, NASA CR–54680, HRL–6278–SR, 1966, 209 pp.

[651] É.F. Chaikovskii, A.A. Taran, Effect of dislocations on the thermionic emission of a tungsten single crystal, Sov. Tech. Phys. Lett. 5 (1979) 381–382.

[652] W. Körner, A method for the determination of the electron work function of vicinal–faces and its applications on the tungsten–(100)–vicinals, Vide (167) (1973) 174–175.

[653] C. Lea, R. Gomer, Energy distribution in field emission from krypton covered tungsten, J. Chem. Phys. 54 (1971) 3349–3359.

[654] C.J. Todd, T.N. Rhodin, Work function in field emission: The (110) plane of tungsten, Surf. Sci. 36 (1973) 353–369.

[655] C.T. Kirk Jr., E.E. Huber Jr., The oxidation of aluminum films in low–pressure oxygen atmospheres, Surf. Sci. 9 (1968) 217–245.

[656] C. Workowski, J. Czyżewski, Dependence of the work function of tungsten single crystal planes on oxygen adsorption, Acta Phys. Pol. A 36 (1969) 1095–1097 (Chem. Abstr. 73 (1970) 70737b).

[657] R.D. Young, E.W. Müller, Progress in field–emission work–function–measurements of atomically perfect crystal planes, J. Appl. Phys. 33 (1962) 91–95.

[658] V.K. Medvedev, A.I. Yakivchuk, Potassium adsorption on the tungsten (112) face, Sov. Phys.—Solid State 16 (1974) 634–638.

[659] L. Gładyszewski, G. Gładyszewski, T. Pieńkos, Surface ionization of the lanthanides, Vacuum 74 (2004) 301–304.

[660] M.H. Nichols, Average thermionic constants of polycrystalline tungsten wires, Phys. Rev. 78 (1950) 158–161.

[661] R.L.E. Seifert, T.E. Phipps, Evidence of a periodic deviation from the Schottky line. I, Phys. Rev. 56 (1939) 652–663.

[662] Y. Higashiguchi, P. Son, M. Miyake, T. Sano, Work Function Measurements using a Planar Triode in Conjunction with a Magnetic Field, Technol. Rep. Osaka Univ. 20, 1970, pp. 607–615 (Chem. Abstr. 75 (1971) 121575y).

[663] T. Radoń, A field emission study of carbon on tungsten, Acta Phys. Pol. A 58 (1980) 377–382 (Chem. Abstr. 93 (1980) 246126f).

[664] J. Fusy, M. Alnot, J. Jupille, P. Pareja, J.J. Ehrhardt, Interaction of H_2O with rhenium basal surface; An UPS–XPS study, Appl. Surf. Sci. 17 (1984) 415–428.

[665] N.R. Gall', S.N. Mikhailov, E.V. Rut'kov, A.Ya. Tontegode, Structure and properties of a graphite monolayer on rhenium, Sov. Phys. Tech. Phys. 31 (1986) 441–444.

[666] R. Levi, G.A. Espersen, Preparation of rhenium emitters and measurements of their thermionic properties, Phys. Rev. 78 (1950) 231–234.

[667] A.Ya. Tontegode, É.Ya. Zandberg, Thermionic properties of polycrystalline platinum and iridium emitters, in: 8th Int. Conf. Phenom. Ionized Gases, Vienna, 1967, p. 69 (Chem. Abstr. 69 (1968) 111217v).

[668] O.A. Weinreich, Thermionic properties of uncoated and thoria–coated rhodium and iridium cathodes, Phys. Rev. 82 (1951) 573.

[669] T. Pankey Jr., R.E. Thomas, Orientation dependence of work function: BaO on Ir, Appl. Surf. Sci. 8 (1981) 50–65.

[670] É.Ya. Zandberg, E.V. Rut'kov, A.Ya. Tontegode, Submonolayer films of thorium on bare iridium and on iridium with a graphite monolayer on the surface, Sov. Phys. Tech. Phys. 25 (1980) 843–845.

[671] G.B. Fisher, The electronic structure of two forms of molecular ammonia adsorbed on Pt(111), Chem. Phys. Lett. 79 (1981) 452–458.

[672] J. Hulse, J. Küppers, K. Wandelt, G. Ertl, UV–photoelectron spectroscopy from xenon adsorbed on heterogeneous metal surfaces, Appl. Surf. Sci. 6 (1980) 453–463.

[673] I.D. Hughes, H.M. Montague-Pollock, Field–emission microscopy of carbon, in: 3rd Conf. Industrial Carbons and Graphite, 1970, pp. 10–12 (Chem. Abstr. 76 (1972) 51513w).

[674] A. Ertel, Effect of impurities on thermionic emission from platinum, J. Appl. Phys. 22 (1951) 353.

[675] P.F. Dittner, S. Datz, Molecular negative surface ionization of UF_6, J. Chem. Phys. 68 (1978) 2451–2456.

[676] L. Holmlid, J.O. Olsson, A molecular–beam study of the reactions of Na and CsCl on a carbon–covered surface, J. Catalysis 71 (1981) 9–20.

[677] B.S. Kul'varskaya, A.I. Rekov, V.Ye. Serebrennikova, V.A. Nikolayeva, Kh.S. Kan, Thermionic emission of certain refractory materials and their possible application in devices filled with complex gaseous medium, Radio Eng. Electron. Phys. 13 (1968) 1131–1134 (Chem. Abstr. 69 (1968) 71722x).

[678] D.Kh. Azizova, N.A. Gorbatyi, Temperature dependence of the work function of the molybdenum (112) face, Izv. Akad. Nauk Uzb.SSR, Ser. Fiz.-Math. Nauk (1) (1988) 61–62 (Chem. Abstr. 109 (1988) 30889h).

[679] A. van Oostrom, Temperature dependence of the work function of single crystal planes of tungsten in the range 78–293 K, Phys. Lett. 4 (1963) 34–36.

[680] J.E. Boggio, H.E. Farnsworth, Low–energy electron diffraction and photoelectric study of (110) tantalum as a function of ion bombardment and heat treatment, Surf. Sci. 1 (1964) 399–406.

[681] W.T. Norris, Work function of the (110) face of tungsten in cesium vapor, J. Appl. Phys. 35 (1964) 467–469.

[682] A. Yutani, A. Kobayashi, A. Kinbara, Work functions of thin LaB_6 films, Appl. Surf. Sci. 70/71 (1993) 737–741.

[683] D.L. Fehrs, R.E. Stickney, Contact–potential measurements of the adsorption of Cs, O_2 and H_2 on (110) Ta, Surf. Sci. 8 (1967) 267–287.

[684] L. Holmlid, J.O. Olsson, Simple surface ionization detector with field reversal for absolute ionization coefficient and ionic and neutral desorption measurements, Rev. Sci. Instrum. 47 (1976) 1167–1171.

[685] B. Lang, A LEED study of the deposition of carbon on platinum crystal surfaces, Surf. Sci. 53 (1975) 317–329.

[686] Z.-p. Hu, D.F. Ogletree, M.A. van Hove, G.A. Somorjai, LEED theory for incommensurate overlayers: Application to graphite on Pt(111), Surf. Sci. 180 (1987) 433–459.

[687] R.K. Roy, S. Gupta, B. Deb, A.K. Pal, Electron field emission properties of electro–deposited diamond–like carbon coatings, Vacuum 70 (2003) 543–549.

[688] J.A. Scheer, M. Wieser, P. Wurz, P. Bochsler, E. Hertzberg, S.A. Fuselier, F.A. Koeck, R.J. Nemanich, M. Schleberger, High negative ion yield from light molecule scattering, Nucl. Instrum. Methods B 230 (2005) 330–339.

[689] L. Papagno, L.S. Caputi, Determination of graphitic carbon structure adsorbed on Ni(110) by surface extended energy–loss fine–structure analysis, Phys. Rev. B 29 (1984) 1483–1486.

[690] E.W. Mitchell, J.W. Mitchell, The work functions of copper, silver and alminium, Proc. R. Soc. A 210 (1951) 70–84.

[691] J.P. Coad, J.C. Rivière, Auger spectroscopy of carbon on nickel, Surf. Sci. 25 (1971) 609–624.

[692] J.G. McCarty, R.J. Madix, The adsorption of CO, H_2, CO_2 and H_2O on carburized and graphitized Ni(110), Surf. Sci. 54 (1976) 121–138.

[693] J.G. McCarty, R.J. Madix, Formic acid desorption from graphitized Ni(110), Surf. Sci. 54 (1976) 210–228.

[694] N.R. Gall', E.V. Rut'kov, A.Ya. Tontegode, Sequential Ta(100) carbonization: From adsorption of single carbon atoms to bulk carbide production, Surf. Sci. 472 (2001) 187–194.

[695] C. Oshima, A. Nagashima, Ultra–thin epitaxial films of graphite and hexagonal boron nitride on solid surfaces, J. Phys.: Condens. Matter 9 (1997) 1–20.

[696] V. Saltas, C.A. Papageorgopoulos, Adsorption of Li on C_{60}–covered Ni(110) surfaces, Surf. Sci. 497 (2002) 70–80.

[697] C. Cepek, A. Goldoni, S. Modesti, Chemisorption and fragmentation of C_{60} on Pt(111) and Ni(110), Phys. Rev. B 53 (1996) 7466–7472.

[698] O. Gröning, O.M. Küttel, P. Gröning, L. Schlapbach, Field emission spectroscopy from discharge activated chemical vapor deposition diamond, J. Vac. Sci. Technol. B 17 (1999) 1064–1071.

[699] D. Vouagner, Cs. Beleznai, J.P. Girardeau-Montaut, C. Templier, H. Gonnord, Characterization of diamond–like carbon films before and after pulsed laser irradiation, Appl. Surf. Sci. 154–155 (2000) 201–205.

[700] G. Zhou, W. Duan, B. Gu, Dimensional effects on field emission properties of the body for single–walled carbon nanotube, Appl. Phys. Lett. 79 (2001) 836–838.

[701] A.A. Avdienko, M.D. Malev, Poisoning of LaB_6 cathodes, Vacuum 27 (1977) 583–588.

[702] A. Kiejna, R.M. Nieminen, Energies of Sr adatom interactions on the Mo(112) surface, Phys. Rev. B 69 (2004) 235424/1–7.

[703] S. Schwegmann, A.P. Seitsonen, V. De Renzi, H. Dietrich, H. Bludau, M. Gierer, H. Over, K. Jacobi, M. Scheffler, G. Ertl, Oxygen adsorption on the Ru(10$\bar{1}$0) surface: Anomalous coverage dependence, Phys. Rev. B 57 (1998) 15487–15495.

[704] I. Merrick, J.E. Inglesfield, G.A. Attard, Local work function and induced screening effects at stepped Pd surfaces, Phys. Rev. B 71 (2005) 085407 /1–11.

[705] A. Migani, C. Sousa, F. Illas, Chemisorption of atomic chlorine on metal surfaces and the interpretation of the induced work function changes, Surf. Sci. 574 (2005) 297–305.

[706] H.B. Michaelson, Relation between an atomic electronegativity scale and the wok function, IBM J. Res. Dev. 22 (1978) 72–80.

[707] E. Wimmer, A. Neckel, A.J. Freeman, TiC(001) surface: All–electron local–density–functional study, Phys. Rev. B 31 (1985) 2370–2378.

[708] D.L. Price, J.M. Wills, B.R. Cooper, Linear–muffin–tin–orbital calculation of TaC(001) surface relaxation, Phys. Rev. B 48 (1993) 15301–15310.

[709] F. Viñes, C. Sousa, P. Liu, J.A. Rodriguez, F. Illas, A systematic density functional theory study of the electronic structure of bulk and (001) surface of transition–metals carbides, J. Chem. Phys. 122 (2005) 174709 /1–11.

[710] D.L. Price, B.R. Cooper, J.M. Wills, Effect of carbon vacancies on carbide work functions, Phys. Rev. B 48 (1993) 15311–15315.

[711] A. Kiejna, K.F. Wojciechowski, Surface properties of alkali–metal alloys, J. Phys. C 16 (1983) 6883–6896.

[712] H.L. Skriver, N.M. Rosengaard, Self–consistent Green's–function technique for surfaces and interfaces, Phys. Rev. B 43 (1991) 9538–9549.

[713] H. Krakauer, M. Posternak, A.J. Freeman, D.D. Koelling, Initial oxidation of the Al(001) surface: Self–consistent electronic structure of clean Al(001) and Al(001)–$p(1\times1)$O, Phys. Rev. B 23 (1981) 3859–3876.

[714] G.A. Benesh, J.E. Inglesfield, Electronic structure and surface states of Al(001), J. Phys. C 19 (1986) L539–L543.

[715] P.A. Serena, N. García, Self–consistent calculations of work functions and relaxations of metals upon alkali adsorption, Surf. Sci. 189–190 (1987) 232–237.

[716] P.J. Feibelman, Local–orbital basis for defect electronic structure calculations of an Al(100) film, Phys. Rev. B 38 (1988) 1849–1855.

[717] K.-P. Bohnen, K.-M. Ho, First principles calculation of lattice relaxation and surface phonons on Al(100), Surf. Sci. 207 (1988) 105–117.

[718] J. Schöchlin, K.P. Bohnen, K.M. Ho, Structure and dynamics at the Al(111)–surface, Surf. Sci. 324 (1995) 113–121.

[719] G.A. Benesh, D. Gebreselasie, Relaxation of Al(001) and Al(110): Surface embedded Green function total–energy and force calculation, Phys. Rev. B 54 (1996) 5940–5945.

[720] D. Gebreselasie, G.A. Benesh, Approximating infinite–k representations: Surface relaxations and work functions of Al(001) and Be(0001), J. Phys.: Condens. Matter 9 (1997) 8359–8368.

[721] C.J. Fall, N. Binggeli, A. Baldereschi, Anomaly in the anisotropy of the aluminum work function, Phys. Rev. B 58 (1998) R7544–R7547.

[722] M. El-Batanouny, D.R. Hamann, S.R. Chubb, J.W. Davenport, Electronic structure of a Pd monolayer on Nb(110), Phys. Rev. B 27 (1983) 2575–2578.

[723] A. Kiejna, K.F. Wojciechowski, Work function of metals: Relation between theory and experiment, Prog. Surf. Sci. 11 (1981) 293–338.

[724] Y. Takasu, H. Konno, T. Yamashina, Work function of well–defined surface of copper–nickel alloy plates, Surf. Sci. 45 (1974) 321–324.

[725] R.J. Batt, C.H.B. Mee, Effect of film structure on photoelectric emission from thin films of aluminium, J. Vac. Sci. Technol. 6 (1969) 737–740.

[726] U.V. Azizov, T. Islamova, D. Azizova, S.T. Sabirov, Determination of thermoemission parameters of hemispherical niobium and tantalum single crystals by surface ionization (difficultly ionizable elements) and thermoemission, Nauchn. Tr. Tashk. Gos. Univ. 447 (1973) 92–97 (Chem. Abstr. 83 (1975) 89490u).

[727] N.G. Imangulova, E.P. Sytaya, Determination of the work function of molybdenum single crystal faces by thermionic emission and surface ionization, Nauchn. Tr. Tashk. Gos. Univ. 463 (1974) 21–24 (Chem. Abstr. 83 (1975) 200849j).

[728] D.N. Vasil'kvosky, E.M. Tadzhieva, Concerning the formation of a special surface structure on wires heated to incandescence by DC current, Sov. Phys.—Solid State 4 (1962) 63–66.

[729] M.A. Vakhabova, E.P. Sytaya, Electron emission of the (100) face of molybdenum and the (111) face of tantalum single crystals during various thermal treatments, Nauchn. Tr. Tashk. Gos. Univ. 463 (1974) 16–20 (Chem. Abstr. 83 (1975) 200848h).

[730] S.J.T. Coles, J.P. Jones, Adsorption of gold on low planes of rhenium, Surf. Sci. 68 (1977) 312–327.

[731] V.I. Veksler, Crystallographic anisotropy of the temperature coefficient of the work function, Sov. Phys.—Solid State 23 (1981) 1054–1055.

[732] S.Yu. Davydov, A.V. Pavlyk, Adsorption of alkali metals on the (100) silicon surface: Calculation of the adatom charge and work function, Tech. Phys. 49 (2004) 1050–1054.

[733] T. Kato, K. Ohtomi, M. Nakayama, Theory on spectroscopy and work function of alkali chains adsorbed on Si(001)2×1, Surf. Sci. 158 (1985) 505–514.

[734] A. Hohlfeld, K. Horn, Leed, $\Delta\phi$ and electron energy loss studies of adsorbed alkali layers on Al(111), Surf. Sci. 211–212 (1989) 844–856.

[735] A. Kiejna, B.I. Lundqvist, First–principle study of surface and subsurface o structures at Al(111), Phys. Rev. B 63 (2001) 085405/1–10.

[736] J.A. Becker, R.G. Brandes, On the adsorption of oxygen on tungsten as revealed in the field emission electron microscope, J. Chem. Phys. 23 (1955) 1323–1330.

[737] G. Aniansson, R.P. Creaser, W.D. Held, L. Holmlid, J.P. Toennies, Molecular beam scattering experiments on the reaction K + RbCl: Absolute angular distributions and integral cross sections, J. Chem. Phys. 61 (1974) 5381–5388.

[738] G. Paasch, H. Eschrig, W. John, Work function and surface structure of simple metals, Phys. Status Solidi (b) 51 (1972) 283–293.

[739] U.V. Azizov, D. Azizova, T.A. Karabaev, Crystallographic anisotropy of emission and adsorption properties of cesium films on the basal faces of single crystals of high–melting metals (molybdenum, niobium and tantalum) with a bcc lattice, Nauchn. Tr., Tashk. Gos. Univ. 459 (1974) 34–37 (Chem. Abstr. 83 (1975) 200850c).

[740] Y.-L. Wang, Velocity and work–function dependence of secondary–ion emission, Phys. Rev. B 38 (1988) 8633–8639.

[741] M.A. Gleeson, W.R. Koppers, K. Tsumori, A.W. Kleyn, Negative ion yields in hydrogen scattering from graphite surfaces, AIP Conf. Proc. 439 (1998) 37–40 (Chem. Abstr. 130 (1998) 59714s).

[742] H. Kawano, S. Kamidoi, H. Shimizu, Development of a surface ionization type dual–ion source applicable to ionic crystalline samples, Rev. Sci. Instrum. 67 (1996) 1387–1389.

[743] H. Kawano, Y. Zhu, J. Nakamura, S. Sugimoto, Thermochemical and thermionic properties of ionic crystalline films, Thin Solid Films 375 (2000) 114–122.

[744] H. Kawano, Y. Zhu, S. Sugimoto, Thermodynamic properties of alkali–chloride films, Appl. Surf. Sci. 175–176 (2001) 105–110.

[745] H. Kawano, General quantitative expression of the positive ionization efficiency in dissociative self–surface ionization of ionic crystals, J. Chem. Phys. 78 (1983) 7012–7013.

[746] H. Kawano, T. Kenpō, H. Koga, Y. Hidaka, Evaluation of the effective work functions of a binary salt using thermochemical data on its two constituent elements, Int. J. Mass Spectrom. Ion Phys. 52 (1983) 241–246.

[747] H. Kawano, T. Kenpō, General expressions of positive– and negative–ionic emission currents in dissociative self–surface ionization of binary salt, Int. J. Mass Spectrom. Ion Processes 54 (1983) 127–134.

[748] H. Kawano, T. Kenpō, Y. Hidaka, Additional evidence for the existence of active sites forming the dissociative self–surface ionization of heated polycrystalline ionic crystals, Int. J. Mass Spectrom. Ion Processes 67 (1985) 331–341.

[749] C.B. Magee, Saline hydrides, in: W.M. Mueller, J.P. Blackledge, G.G. Libowitz (Eds.), Metal Hydrides, Academic Press, New York, 1968, pp. 165–240.

[750] H. Kawano, H. Nagayasu, N. Serizawa, H. Ohta, M. Takeda, M. Wada, M. Sasao, Negative hydrogen ion emission from heated metal hydride powder, Rev. Sci. Instrum. 67 (1996) 1190–1192.

[751] H. Kawano, N. Serizawa, A. Tanaka, M. Wada, M. Sasao, K. Miyake, Simultaneous production of H⁻ by both thermal and electron–stimulated desorption from saline hydrides, Rev. Sci. Instrum. 69 (1998) 953–955.

[752] H. Kawano, A. Tanaka, S. Sugimoto, T. Iseki, Y. Zhu, M. Wada, M. Sasao, Selection of the powdery metal hydride best for producing H⁻ by thermal desorption, Rev. Sci. Instrum. 71 (2000) 853–855.

[753] H. Kawano, M. Wada, M. Sasao, Production of H⁻ from H₂ impinging upon heated saline hydride powder, Rev. Sci. Instrum. 73 (2002) 946–948.

[754] H. Kawano, T. Iseki, Production of H⁻ from heated SrH₂ powder and from H₂ introduced onto the powder, Appl. Surf. Sci. 193 (2002) 60–69.

[755] H. Kawano, N. Serizawa, M. Takeda, Work function and desorption energy of H⁻ from heated CaH₂, Appl. Phys. Lett. 67 (1995) 3904–3905.

[756] H. Kawano, N. Serizawa, M. Takeda, T. Maeda, A. Tanaka, Y. Zhu, Desorption energy of H⁻ from heated saline hydrides and their work function effective for thermal electron emission, Thermochim. Acta 299 (1997) 81–85.

[757] H. Kawano, Y. Zhu, A. Tanaka, S. Sugimoto, A new method to determine the work function of powdery samples, Appl. Surf. Sci. 169–170 (2001) 675–678.

[758] H. Kawano, Y. Zhu, A. Tanaka, S. Sugimoto, Activation energies for the desorption of H₂, H⁻ and electron from saline hydrides heated in vacuum, Thermochim. Acta 371 (2001) 155–161.

[759] K. Wandelt, J. Hulse, J. Küppers, Site–selective adsorption of xenon on a stepped Ru(0001) surface, Surf. Sci. 104 (1981) 212–239.

[760] E.V. Protsykov, Energy distribution of electrons in polycrystalline graphite, in: Materialy 4–oi Nauchn. Konf. Aspirantov Sb., 1962, pp. 70–72 (Chem. Abstr. 60 (1964) 10029e).

[761] S.V. Shulepov, E.M. Baitinger, Thermal emission properties of carbon materials, in: 17th Radiofiz. Issled. Svoistv Veshchestva, Mater. Zon. Konf., 1976, pp. 95–97 (Chem. Abstr. 90 (1979) 213907w).

[762] E. Taft, L. Apker, Photoelectric emission from polycrystalline graphite, Phys. Rev. 99 (1955) 1831–1832.

[763] K.-P. Bohnen, S.C. Ying, Self–consistent study of surfaces of simple metals by the density–matrix method: (100) and (110) surfaces of Na, K, Rb, and Cs, Phys. Rev. B 22 (1980) 1806–1817.

[764] V.S. Robinson, T.S. Fisher, J.A. Michel, C.M. Lukehart, Work function reduction of graphitic nanofibers by potassium intercalation, Appl. Phys. Lett. 87 (2005) 061501/1–3.

[765] F.A. Matsen, methyl. affinities, Electron affinities, and ionization energies of condensed ring aromatic hydrocarbons, J. Chem. Phys. 24 (1956) 602–606.

[766] J. Burns, E. Yelke, Work function of conductive coatings on glass, Rev. Sci. Instrum. 40 (1969) 1236–1237.

[767] J. Zhao, J. Han, J.P. Lu, Work functions of pristine and alkali–metal intercalated carbon nanotubes and bundles, Phys. Rev. B 65 (2002) 193401/1–4.

[768] R.G. Musket, M. Balooch, Creation of stable, low work function surfaces on Si by implantation of 3 keV Cs⁺, J. Vac. Sci. Technol. A 20 (2002) 2049–2051.

[769] S.C. Jain, K.S. Krishnan, Thermionic constants of metals and semiconductors. II. Metals of the first transition group, Proc. R. Soc. A 215 (1952) 431–437.

[770] R. Clauberg, W. Gudat, E. Kisker, E. Kuhlmann, Spin polarized threshold–photoemission from Ni(110) with transverse sample magnetization, Z. Phys. B 43 (1981) 47–54.

[771] E.V. Rut'kov, A.Ya. Tontegode, M.M. Usufov, Carbon interacting with nickel surface, Bull. Russ. Acad. Sci. Phys. 58 (1994) 1669–1672.

[772] P. Dolle, M. Tommasini, J. Jupille, The adsorption of oxygen on a cesiated Ni(111) surface: Evidence for the formation of molecularly chemisorbed oxygen species, Surf. Sci. 211/212 (1989) 904–911.

[773] J.A. Barnard, J.J. Ehrhardt, H. Azzouzi, M. Alnot, Thermal evolution of very thin platinum films deposited on Ni(111): A PAX/work function study, Surf. Sci. 211/212 (1989) 740–748.

[774] T.A. Karabaev, D. Azizova, U.V. Azizov, Thermionic emission parameters of the faces of a niobium single crystal and behavior of barium on niobium, Izv. Akad. Nauk Uzb.SSR, Ser. Fiz.-Mat. Nauk 13 (1969) 48–50 (Chem. Abstr. 73 (1970) 19527f).

[775] O.D. Protopopov, I.V. Strigushchenko, Emission parameters of faces of a niobium single crystal, Sov. Phys.—Solid State 10 (1968) 747–748.

[776] Yu.M. Konoplev, A.G. Naumovets, A.G. Fedorus, Simultaneous adsorption of cesium and barium onto tungsten and niobium crystal surfaces, Sov. Phys.—Solid State 14 (1972) 273–278.

[777] B.J. Hopkins, M. Ibrahim, Oxygen adsorption on the (110) face of tantalum, niobium, molybdenum and tungsten single crystals, Vacuum 23 (1973) 135–137.

[778] J. Jupille, B. Bigeard, J. Fusy, A. Cassuto, Study on the variation of work function of the interaction of oxygen with niobium (110), Surf. Sci. 84 (1979) 190–200.

[779] R.P. Leblanc, B.C. Vanbrugghe, F.E. Girouard, Thermionic emission from a niobium single crystal, Can. J. Phys. 52 (1974) 1589–1593.

[780] R.M. Oman, J.A. Dillon Jr., Some electrical and chemical properties of the (111) niobium surface, Surf. Sci. 2 (1964) 227–235.

[781] U.V. Azizov, D. Azizova, T.A. Karabaev, Behavior of barium on the main faces of a spherical molybdenum single crystal, Nauchn. Tr. Tashk. Gos. Univ. 447 (1973) 159–163 (Chem. Abstr. 83 (1975) 48795d).

[782] U.V. Azizov, T.A. Karabaev, T.I. Mikhailova, Kh.M. Sattarov, Coadsorption of cesium and oxygen on a molybdenum single crystal, Bull. Acad. Sci. USSR, Ser. Phys. 40 (1976) 151–153 (Chem. Abstr. 85 (1976) 198694a).

[783] G. Bergeret, M. Abon, B. Tardy, S.J. Teichner, Relative work function of clean molybdenum single–crystal planes determined by field emission microscopy, J. Vac. Sci. Technol. 11 (1974) 1193–1194.

[784] N.R. Gall', E.V. Rut'kov, A.Ya. Tontegode, M.M. Usofov, Chemisorption of sulfur on (100) Mo: The growth of surface and bulk sulfides, absolute calibration, thermal desorption of sulfur, Tech. Phys. 41 (1996) 483–487.

[785] H. Steele, K. Shimada, Evaluation of single–crystal molybdenum as an emitter material, in: Rept. Thermionic Convers. Specialist Conf. Schenectady, 1963, pp. 240–246 (Chem. Abstr. 62 (1965) 2338b).

[786] K.Zh. Zhanabergenov, The behavior of lithium atoms on the faces of refractory metal single crystals of bcc refractory metals, Sov. Phys. J. 14 (1971) 1734–1736 (Chem. Abstr. 76 (1973) 91275b).

[787] E.S. Bekmukhambetov, A.A. Dzhaimurzin, Zh.Zh. Imanbekov, Method for determining the work function of refractory metals subjected to ionizing radiation, Sov. Phys. Tech. Phys. 24 (1979) 71–73.

[788] R.A. Milovanova, P.N. Chistyakov, Work function and normal cathode fall of molybdenum and nickel in inert gases, Sov. Phys. Tech. Phys. 8 (1963) 262–264.

[789] J.D. Clewley, A.D. Crowell, D.W. Juenker, Changes in photoelectron emission from molybdenum due to gases, J. Vac. Sci. Technol. 9 (1972) 877–881.

[790] R.C. Bradley, L.A. D'Asaro, Investigation of an alloy surface with the field emission microscope, J. Appl. Phys. 30 (1959) 226–233.

[791] D.W. Vance, Auger electron emission from clean and carbon–contaminated Mo, Phys. Rev. 164 (1967) 372–380.

[792] S. Dushman, H.N. Rowe, J. Ewald, C.A. Kidner, Electron emission from tungsten, molybdenum and tantalum, Phys. Rev. 25 (1925) 338–360.

[793] L.D. López-Carreño, J.M. Heras, L. Viscido, Adsorption and dissociation of CO_2 on polycrystalline Mo, Surf. Sci. 377–379 (1997) 615–618.

[794] J. Psarouthakis, R.D. Huntington, Thermionic work function of polycrystalline ruthenium, Surf. Sci. 7 (1967) 279–292.

[795] I. Merrick, J.E. Inglesfield, G.A. Attard, Electron field emission from surfaces with steps, Phys. Rev. B 72 (2005) 033403/1–4.

[796] N. Drundarov, Determination of the work function and the intensity of the electric field for separate faces of a tantalum micro single crystal by a field emission microscope, Izv. Inst. Elektron. Bulg. Akad. Nauk 6 (1972) 5–11 (Chem. Abstr. 78 (1973) 35258c).

[797] R.Ya. Kamilova, Surface ionization of sodium atoms on large single–crystal faces of tantalum, Izv. Akad. Nauk Uzb.SSR, Ser. Fiz.-Mat. Nauk 20 (1976) 80–82 (Chem. Abstr. 86 (1977) 24918g).

[798] U.V. Azizov, T.A. Karabaev, S.M. Mikhailov, Thermoemission properties of the main faces of a spherical tantalum single crystal, Izv. Akad. Nauk Uzb.SSR, Ser. Fiz.-Mat. Nauk 15 (2) (1971) 66–67 (Chem. Abstr. 75 (1971) 41931w).

[799] R.Ya. Kamilova, E.P. Sytaya, Thermionic emission properties of the main facets of a tantalum single crystal, Dokl. Akad. Nauk Uzb.SSR 27 (5) (1970) 20–22 (Chem. Abstr. 75 (1971) 123793s).

[800] R.Ya. Kamilova, M. Shamsiev, Thermionic properties of clean and cesium–covered (111) faces of a tantalum crystal, Sov. Phys. J. 13 (1970) 820–822.

[801] T.P. Smereka, I.M. Ubogyi, Ya.B. Losovyi, The role of electron structure of substrates in interaction of adsorbed atoms on furrow faces of transition metals, Vacuum 46 (1995) 429–432.

[802] É.F. Chaikovskii, V.T. Sotnikov, E.D. Kovtun, Influence of sulfur impurities on the work function of tantalum, Sov. Tech. Phys. Lett. 2 (1976) 336–337.

[803] H. Kawano, Theoretical evaluation of the effective work functions for positive–ionic and electronic emissions from polycrystalline metal surfaces, Appl. Surf. Sci. 254 (2008) 7187–7192.

[804] M.D. Scheer, J. Fine, The positive and negative self–surface ionization of tantalum, in: Proc. 4th Int. Material Symp. Berkeley, 1968, pp. 39/1–15.

[805] N. Sasaki, K. Kubo, M. Asano, Mass–spectrometric studies of the work function and the heats of sublimation of atoms and positive ions, Mass Spectrosc. 18 (1970) 1189–1194 (Chem. Abstr. 74 (1971) 17135y).

[806] J.G. Ociepa, S. Mróz, The adsorption of lanthanum hexaboride on tantalum, Vacuum 29 (1979) 241–244.

[807] Y.-M. Gong, H.-S. Zeng, Adsorption and desorption of oxygen on the W(100) plane, Surf. Sci. 246 (1991) 169–172.

[808] T.A. Delchar, G. Ehrlich, Chemisorption on single–crystal planes: Nitrogen on tungsten, J. Chem. Phys. 42 (1965) 2686–2702.

[809] L.D. Schmidt, Adsorption of barium on tungsten: Measurements on individual crystal planes, J. Chem. Phys. 46 (1967) 3830–3841.

[810] A.P. Ovchinnikov, B.M. Tsarev, Cesium adsorption on the faces of a tungsten single crystal, Sov. Phys.—Solid State 8 (1966) 1187–1190.

[811] A.P. Ovchinnikov, B.M. Tsarev, Field–emission study of the adsorption of sodium on faces of tungsten and rhenium single crystals, Sov. Phys.—Solid State 9 (1968) 1519–1524.

[812] T. Engel, R. Gomer, Adsorption of oxygen on tungsten: Field emission from single planes, J. Chem. Phys. 52 (1970) 1832–1841.

[813] T. Engel, R. Gomer, Adsorption of CO on tungsten: Field emission from single crystal planes, J. Chem. Phys. 50 (1969) 2428–2437.

[814] K.Zh. Zhanabergenov, E.P. Sytaya, Determination of the thermal ionic emission parameters of the faces of a tungsten single crystal, Izv. Akad. Nauk Kaz. SSR, Ser. Fiz.-Mat. 8 (4) (1970) 62–67 (Chem. Abstr. 74 (1971) 58430j).

[815] B.J. Hopkins, K.R. Pender, The work function of a (110) oriented tungsten single–crystal face, Br. J. Appl. Phys. 17 (1966) 281–282.

[816] J. Marien, Use of the analog simulation on Teledeltos paper to determine the local field strength and local work function distribution relative to field emitters, Bull. Soc. R. Sci. Liége 45 (1976) 240–253 (Chem. Abstr. 86 (1977) 11117v).

[817] N.G. Imangulova, E.P. Sytaya, Thermoemission properties of some faces of a tungsten single crystal in a beam of sodium atoms, Izv. Akad. Nauk Uzb.SSR, Ser. Fiz.-Mat. Nauk 17 (2) (1973) 45–49 (Chem. Abstr. 86 (1977) 84598t).

[818] S.A. Shakirova, E.V. Serova, Work function measurements of Gd/W(111) with and without silicon interface layers: Field emission study, Sur. Sci. 422 (1999) 24–32.

[819] S. Hellwig, J.H. Block, Measurement of work function of tungsten by field emission, Z. Phys. Chem. 83 (1973) 269–286.

[820] G.A. Haas, R.E. Thomas, Distribution of crystal orientation and work function in tungsten ribbons, J. Appl. Phys. 40 (1969) 3919–3924.

[821] C.E. Mendenhall, C.F. DeVoe, The photoelectric work functions of the 211 and 310 planes of tungsten, Phys. Rev. 51 (1937) 346–349.

[822] J. Żebrowski, Ch. Kleint, Photo–field emission from the (211) tungsten plane, Phys. Lett. A 121 (1987) 463–465.

[823] H.B. Wahlin, L.V. Whitney, Positive and negative thermionic emission from tungsten, Phys. Rev. 50 (1936) 735–738.

[824] É.Ya. Zandberg, U.Kh. Rasulev, M.R. Sharapudinov, Thermal ionization of some nitrogen–containing organic compounds on tungsten and its oxides to form positive ions, Theor. Exp. Chem. 6 (1970) 267–275 (Chem. Abstr. 74 (1971) 7689t).

[825] L. Gładyszewski, G.Gł adyszewski, Atom–ion transition energies for alkali atoms on a tungsten surface, Surf. Sci. 247 (1991) 274–278.

[826] L. Apker, E. Taft, J. Dickey, Energy distribution of photoelectrons from polycrystalline tungsten, Phys. Rev. 73 (1948) 46–50.

[827] F. Rozenkranz, H.G. Wagner, Measurement of the ionization yield of molecular and atomic iodine on tungsten, tungsten (1.6 % thorium dioxide), and platinum (8 % tungsten) surfaces, Z. Phys. Chem. 68 (1969) 317–320.

[828] B.J. Hopkins, J.C. Rivière, Work function of polycrystalline tungsten foil, Proc. Phys. Soc. 81 (1963) 590–592.

[829] I. Beck, V.K. Josepovits, J. Sneider, Z. Toth, Investigation of electron emission properties of Ba–activated tungsten cathodes, J. Phys. D 38 (2005) 3865–3869.

[830] A.E. Bell, L.W. Swanson, L.C. Crouser, A field emission study of oxygen adsorption on the (110), (211), (111) and (100) planes of tungsten, Surf. Sci. 10 (1968) 254–274.

[831] J.C. Tracy, J.M. Blakely, A study of faceting of tungsten single crystal surfaces, Surf. Sci. 13 (1969) 313–336.

[832] B.Y. Chao, F.A. White, Work functions of rhenium and tungsten determined by thermionic and mass spectrometric measurements, Int. J. Mass Spectrom. Ion Phys. 12 (1973) 423–432 (see p. 92 in Ref. [1312]).

[833] É.Ya. Zandberg, É.G. Nazarev, U.Kh. Rasulev, Transient processes during surface ionization of particles on nonuniformly emitting surfaces. I. Method of voltage modulation, Sov. Phys. Tech. Phys. 25 (1980) 1024–1030.

[834] L. Gładyszewski, Influence of oxygen on the surface ionization of europium on tungsten, Ann. Univ. Mariae Curie–Skłodowska, Sect. AA, Phys. Chem. 34/35 (1981) 23–29.

[835] R. Klein, Investigation of the surface reaction of oxygen with carbon on tungsten with the field ion microscope, J. Chem. Phys. 21 (1953) 1177–1180.

[836] D. Schlatterbeck, M. Parschau, K. Christmann, Silver films grown on a rhenium (0001) surface: A combined TDS, XPS, and Δφ study, Surf. Sci. 418 (1998) 240–255.

[837] A. Kashetov, N.A. Gorbatyi, Correlation of the work function of faces of cubic and hexagonal single crystals with the surface energy of the faces, Sov. Phys.—Solid State 11 (1969) 389–390.

[838] A.P. Ovchinnikov, Work function of faces of a rhenium single crystal in vacuum and in a stream of cesium atoms, Sov. Phys.—Solid State 9 (1968) 1508–1511.

[839] N.R. Gall', S.N. Mikhaïlov, E.V. Rut'kov, A.Ya. Tontegode, Nature of the adsorption binding between a graphite monolayer and rhenium surface, Sov. Phys.—Solid State 27 (1985) 1410–1414.

[840] A. Cassutto, A. Pentenero, P. Le Goff, Work function of rhenium in ultravacuum: Effect of oxygen adsorption, J. Chim. Phys. 62 (1965) 1113–1118.

[841] C. Agte, H. Althertum, K. Becker, G. Heyne, K. Moers, The physical properties of rhenium, Naturwissenschaften 19 (1931) 108–109.

[842] W.D. Davis, Surface ionization mass spectroscopy of airborne particulates, J. Vac. Sci. Technol. 10 (1973) 278.

[843] B.E. Nieuwenhuys, D.Th. Meijer, W.M.H. Sachtler, Adsorption of nitrogen on single crystal faces of iridium, studied by field emission microscopy, Surf. Sci. 40 (1973) 125–140.

[844] R.L. Gerlach, T.N. Rhodin, Structure analysis of alkali metal adsorption on single crystal nickel surfaces, Surf. Sci. 17 (1969) 32–68.

[845] G.M. Kornacheva, N.A. Shurmovskaya, Effect of adsorption of oxygen and hydrogen on the work function of iridium, Elektrokhim. 12 (1976) 992–994.

[846] H.P. Bonzel, T.E. Fischer, An UV photoemission study of NO and CO adsorption on Pt(100) and Ru(10$\bar{1}$0) surfaces, Surf. Sci. 51 (1975) 213–227.

[847] B. Pennemann, K. Oster, K. Wandelt, Hydrogen adsorption on Pt(100) at low temperatures: Work function and thermal desorption data, Surf. Sci. 249 (1991) 35–43.

[848] B.E. Nieuwenhuys, D.Th. Meijer, W.M.H. Sachtler, Adsorption of xenon on platinum studied by field emission microscopy, Phys. Status Solidi (a) 24 (1974) 115–122.

[849] B.E. Nieuwenhuys, Influence of the surface structure on the adsorption of hydrogen on platinum, as studied by field emission probe–hole microscopy, Surf. Sci. 59 (1976) 430–446.

[850] R. Drube, V. Dose, A. Goldmann, Empty electronic states at the (1×1) and (5×20) surfaces of Pt(100): An inverse photoemission study, Surf. Sci. 197 (1988) 317–326.

[851] G.A. Benesh, L.S.G. Liyanage, J.C. Pingel, The surface electronic structure of (1×1)Pt(001), J. Phys.: Condens. Matter 2 (1990) 9065–9076.

[852] G.A. Benesh, L.S.G. Liyanage, The surface electronic structure of oxygen on Pt (001)(1×1), Surf. Sci. 261 (1992) 207–216.

[853] R. Vanselow, X.Q.D. Li, The work function of kinked areas on clean, thermally rounded Pt and Rh crystallites: Its dependence on the structure of terraces and edges, Surf. Sci. Lett. 264 (1992) L200–L206.

[854] M. Weinert, A.J. Freeman, Relativistic spin polarization and magnetization: Knight shift of Pt(001), Phys. Rev. B 28 (1983) 6262–6269.

[855] D.-s. Wang, A.J. Freeman, H. Krakauer, Electronic structure of Pt(001) surface with and without an adsorbed gold monolayer, Phys. Rev. B 29 (1984) 1665–1673.

[856] M. Alnot, J.J. Ehrhardt, Pt(110)(1×1) surfaces prepared by low temperature platinum deposition: Surface characterization and stability, Surf. Sci. 287/288 (1993) 325–329.

[857] E.V. Rut'kov, Interaction of carbon atoms with platinum, Tech. Phys. 38 (1993) 220–224.

[858] D.M. Collins, W.E. Spicer, The adsorption of CO, O$_2$, H$_2$, on Pt. II. Ultraviolet photoelectron spectroscopy studies, Surf. Sci. 69 (1977) 114–132.

[859] A. Cassuto, M. Mane, V. Kronneberg, J. Jupille, Molecular orbital shifts of π –bonded ethylene adsorbed on Pt(111) in the presence of potassium atoms, Surf. Sci. 251/252 (1991) 1133–1137.

[860] L.A. DuBridge, The thermionic emission from clean platinum, Phys. Rev. 32 (1928) 961–966.

[861] L.I. Kaisheva, Surface ionization of alkali–metal atoms on a silicon carbide single crystal, Sov. Phys.—Solid State 14 (1973) 2108–2109.

[862] B.S. Kul'varskaya, A.I. Rekov, V.E. Serebrennikova, V.A. Nikolaeva, Kh.S. Kan, Thermionic emission of certain refractory metals and possible use as cathodes in gaseous devices, Sov. Phys. Tech. Phys. 14 (1969) 122–128.

[863] M. Asano, K. Kubo, S. Magari, Vaporization of strontium atom and ion from strontium oxide on tungsten and rhenium, Mass Spectrosc. 16 (1968) 315–322 (Chem. Abstr. 70 (1969) 51299g).

[864] M. Asano, T. Harada, K. Kubo, Energy distribution of Sr$^+$ thermal ion emitted from strontium (II) oxide–tungsten surface, Mass Spectrosc. 29 (1981) 167–172 (Chem. Abstr. 95 (1981) 160621t).

[865] M.I. Elinson, G.A. Kudintseva, Field emission cathodes of high–melting metal compounds, Radio Engin. Electron. Phys. 7 (1962) 1417–1423.

[866] L.W. Swanson, T. Dickinson, Single–crystal work–function and evaporation measurements of LaB$_6$, Appl. Phys. Lett. 28 (1976) 578–580.

[867] M. Futamoto, M. Nakazawa, K. Usami, S. Hosoki, U. Kawabe, Thermionic emission properties of a single–crystal LaB$_6$ cathode, J. Appl. Phys. 51 (1980) 3869–3876.

[868] L.W. Swanson, M.A. Gesley, P.R. Davis, Crystallographic dependence of the work function and volatility of LaB$_6$, Surf. Sci. 107 (1981) 263–289.

[869] L.W. Swanson, D.R. McNeely, Work functions of the (001) face of the hexaborides of Ba, La, Ce and Sm, Surf. Sci. 83 (1979) 11–28.

[870] C. Oshima, E. Bannai, T. Tanaka, S. Kawai, Thermionic work function of LaB$_6$ single crystals and their surfaces, J. Appl. Phys. 48 (1977) 3925–3927.

[871] R.S. Khairnar, P.W. Mahajan, D.S. Joag, A.S. Nigavekar, P.L. Kanitkar, Processing and characterization of LaB_6–coated hairpin cathodes, J. Vac. Sci. Technol. A 3 (1985) 398–402.

[872] A.R. Shul'man, The work function of thin films of thorium oxide and thorium on tungsten, Sov. Phys. Tech. Phys. 3 (1958) 1579–1581.

[873] D.A. Wright, Thermionic properties of thoria, Nature 160 (1947) 129–130.

[874] Yu.M. Goryachev, I.A. Podchernyaeva, N.I. Siman, V.S. Sinel'nikova, I.I. Timofeeva, G.S. Burkhanov, Work function of ZrC_x and NbC_x single crystals, Sov. Phys. Tech. Phys. 23 (1978) 321–324.

[875] R.E. Haddad, D.L. Goldwater, F.H. Morgan, Zirconium carbide as a thermionic emitter, J. Appl. Phys. 20 (1949) 886.

[876] V.Kh. Burkhanova, N.A. Gorbatyi, V.A. Chekina, F.A. Fekhretdinov, Thermoemission properties of zirconium carbide and hafnium carbide pressed cathodes, Nauch. Tr., Tashkent. Gos Univ. 332 (1969) 64–71 (Chem. Abstr. 73 (1970) 71062q).

[877] J. Myatt, Thermionic emission from zirconium carbide with caesium vapour present, Adv. Energy Convers. 3 (1963) 279–285.

[878] S. Stepanovskyy, I. Ubogyi, J. Kołaczkiewicz, Ag and Au thin layers on Ta(211) face, Surf. Sci. 572 (2004) 206–216.

[879] P. Kisliuk, Reflection of slow electrons from tungsten single crystals, clean and with adsorbed monolayers, Phys. Rev. 122 (1961) 405–411.

[880] A.E. Souzis, M. Seidl, W.E. Carr, H. Huang, Electronic surface changes induced in silicon by hydrogen, oxygen, and cesium coverages, J. Vac. Sci. Technol. A 7 (1989) 720–723.

[881] W. Arabczyk, U. Narkiewicz, On the cleaning of monocrystalline metallic samples from impurities, Appl. Surf. Sci. 252 (2005) 98–103.

[882] S. Gupta, M.P. Chowdhury, A.K. Pal, Field emission characteristics of diamond–like carbon films synthesized by electrodeposition technique, Appl. Surf. Sci. 236 (2004) 426–434.

[883] A.Ya. Tontegode, Reduction in hydrogen permeability of palladium foils with carbon films, Sov. Tech. Phys. Lett. 3 (1977) 260–261.

[884] A.J.B. Robertson, E.M.A. Willhoft, Kinetics of the decomposition of ammonia on platinum at low pressures, Trans. Faraday Soc. 63 (1967) 476–486.

[885] E.M.A. Willhoft, Kinetics of decomposition of ammonia at low pressures on metal surfaces, Trans. Faraday Soc. 64 (1968) 1925–1933.

[886] D.W. Goodman, Single crystals as model catalysts, J. Vac. Sci. Technol. 20 (1982) 522–526.

[887] J. McCarty, R.J. Madix, A study of the kinetics and mechanism of the decomposition of formic acid on carburized and graphitized Ni(110) using AES, LEED and flash desorption, J. Catalysis 38 (1975) 402–417.

[888] D.W. Goodman, R.D. Kelley, T.E. Madey, J.T. Yates Jr., Kinetics of the hydrogenation of CO over a single crystal nickel catalyst, J. Catalysis 63 (1980) 226–234.

[889] A.Ya. Tontegode, Carbon on transition metal surfaces, Prog. Surf. Sci. 38 (1991) 201–429.

[890] S. Yamamoto, I. Watanabe, S. Sasaki, T. Yaguchi, Absolute work function measurements with the retarding potential method utilizing a field emission electron source, Surf. Sci. 266 (1992) 100–106.

[891] B. Shan, K. Cho, First–principles study of work functions of single wall carbon nanotubes, Phys. Rev. Lett. 94 (2005) 236602/1–4.

[892] P.J. Feibelman, Relaxation of hcp(0001) surfaces: A chemical view, Phys. Rev. B 53 (1996) 13740–13746.

[893] J.-H. Cho, K. Terakura, Plane–wave–basis pseudopotential calculations of the surface relaxations of Ti(0001) and Zr(0001), Phys. Rev. B 56 (1997) 9282–9285.

[894] M.N. Huda, L. Kleinman, Density functional calculations of the influence of hydrogen adsorption on the surface relaxation of Ti(0001), Phys. Rev. B 71 (2005) 241406/1–3.

[895] S. Trasatti, Accurate estimation of the work function and surface energy of polycrystalline technetium, Surf. Sci. 32 (1972) 735–738.

[896] A. Rose, The absence of surface dipole contributions to metal work functions, Solid State Commun. 45 (1983) 859–864.

[897] K. Wandelt, The local work function: Concept and implications, Appl. Surf. Sci. 111 (1997) 1–10.

[898] U. Schneider, G.R. Castro, H. Busse, T. Janssens, J. Wesemann, K. Wandelt, Xe adsorption on the $Cu_3Pt(111)$, Surf. Sci. 269/270 (1992) 316–320.

[899] K. Hermann, B. Gumhalter, K. Wandelt, Perturbation of the adsorbate electronic structure by local fields at surface defects, Surf. Sci. 251/252 (1991) 1128–1132.

[900] A. Sinsarp, Y. Yamada, M. Sasaki, S. Yamamoto, Local tunneling barrier height imaging of a reconstructed Pt(100) surface, Appl. Surf. Sci. 237 (2004) 587–592.

[901] L.A. Rudnitskii, Work function of a nonideal metal surface. I. Terraced surface, Sov. Phys. Tech. Phys. 23 (1978) 1483–1484.

[902] J. Eisinger, Electrical properties of hydrogen adsorbed on silicon, J. Chem. Phys. 30 (1959) 927–930.

[903] H.H. Farnsworth, H.E. Madden Jr., Mechanism of chemisorption, place exchange, and oxidation on a (100) nickel surface, J. Appl. Phys. 32 (1961) 1933–1937.

[904] P.A.W. van der Heide, Secondary ion formation/survival during the initial stages of sputtering Si and SiO_2 with Cs^+, Surf. Sci. 555 (2004) 193–208.

[905] K. Christmann, G. Ertl, O. Schober, Temperature dependence of the work function of nickel, Z. Naturforsch. 29 a (1974) 1516–1517.

[906] G. Comsa, The temperature dependence of the work function of nickel surfaces, Acad. Rep. Populare Romîne, Inst. Fiz. Atomică şi Inst. Fiz. Studii Cercetări Fiz. 10 (1959) 163–167 (Chem. Abstr. 53 (1959) 21179i).

[907] L.K. Dikova, I.V. Strigushchenko, A determination of the temperature coefficients of the work function of the faces of a niobium single crystal, Radio Eng. Electron. Phys. 20 (1975) 143–144 (Chem. Abstr. 84 (1976) 37705u).

[908] D.Kh. Azizova, N.A. Gorbatyi, A.F. Chumachenko, Temperature dependence of work function of principal faces of molybdenum, Bull. Acad. Sci. USSR, Phys. Ser. 46 (7) (1982) 71–73 (Chem. Abstr. 97 (1982) 102687z).

[909] B. Iosifescu, The temperature dependence of the work function of molybdenum surfaces, Acad. Rep. Populare Romîne, Inst. Fiz. Atomică şi Inst. Fiz. Studii Cercetări Fiz. 10 (1959) 177–186 (Chem. Abstr. 53 (1959) 21180b).

[910] G.Ya. Pikus, V.P. Teterya, Mechanism of the oxide cathode emission capacity changes with emission current take–off, Ukr. Fiz. Zh. 17 (1972) 472–476 (Chem. Abstr. 76 (1972) 159785a).

[911] G.G. Gnesin, G.S. Oleinik, L.N. Okhremchuk, I.A. Podchernayaeva, G.V. Samsonov, V.S. Fomenko, Emissive properties of polycrystalline silicon carbide, Poroshk. Metall. 10 (5) (1970) 67–72 (Chem. Abstr. 73 (1970) 71049r).

[912] S. Saito, T. Sutou, Y. Norimitsu, N. Yajima, Y. Uhara, T. Uenosono, T. Soumura, T. Tani, Temperature dependence of the work function of $Bi_2Sr_2CaCu_2O_8$ single crystal cleaved at low temperature, Appl. Surf. Sci. 252 (2005) 379–384.

[913] T.A. Flaim, P.D. Ownby, Adsorbate–induced work function changes, Surf. Sci. 32 (1972) 519–526.

[914] K. Wandelt, Surface characterization by photoemission of adsorbed xenon (PAX), J. Vac. Sci. Technol. A 2 (1984) 802–807.

[915] J. Hölzl, L. Fritsche, Alkal– and transition–metal adsorption on metal surfaces studied by work function measurements, Surf. Sci. 247 (1991) 226–238.

[916] D.R. Hamann, P.J. Feibelman, Anharmonic vibrational modes of chemisorbed H on the Rh(001) surface, Phys. Rev. B 37 (1988) 3847–3855.

[917] N.D. Lang, Theory of alkali adsorption on metal surfaces, in: H.P. Bonzel, A.M. Bradshaw, G. Ertl (Eds.), Physics and Chemistry of Alkali Metal Adsorption, Elsevier, Amsterdam, 1989, pp. 11–24.

[918] H.A.C.M. Hendrickx, B.E. Nieuwenhuys, Surface structure effects in the adsorption and desorption of nitric oxide on rhodium, Surf. Sci. 175 (1986) 185–196.

[919] A.M. Turner, Y.J. Chang, J.L. Erskine, Surface states and the photoelectron spin polarization of Fe(100), Phys. Rev. Lett. 48 (1982) 348–351.

[920] R.E. Simon, Work function of iron surfaces produced by cleavage in vacuum, Phys. Rev. 116 (1959) 613–617 (see Ref. [13]).

[921] K. Ueda, R. Shimizu, LEED–work function studies on Fe(100), Japan. J. Appl. Phys. 11 (1972) 916–917.

[922] R. Fischer, N. Fischer, S. Schuppler, Th. Fauster, F.J. Himpsel, Image states on Co(0001) and Fe(110) probed by two–photon photoemission, Phys. Rev. B 46 (1992) 9691–9693.

[923] G.K. Hall, C.H.B. Mee, The surface potential of oxygen on iron, cobalt and manganese, Surf. Sci. 28 (1971) 598–606.

[924] H. Gienapp, Thermal ion emission of tungsten, Acta Phys. Austriaca 25 (1967) 239–242 (Chem. Abstr. 68 (1968) 63602x).

[925] E.F. Chaikovskii, L.G. Mel'nik, Negative surface ionization of bromine at the (100) face of molybdenum, Ukr. Fiz. Zh. 14 (1969) 1398–1400 (Chem. Abstr. 71 (1969) 106474p).

[926] C.J. Workowski, Adsorption of oxygen on single–crystal planes of tungsten, Acta Phys. Pol. A 42 (1972) 9–18 (Chem. Abstr. 77 (1972) 119586a).

[927] H. Kawano, Determination of electron affinities by surface ionization mass spectrometry, Adv. Mass Spectrom. 8 (1980) 255–261 (Chem. Abstr. 94 (1981) 7900t).

[928] I.N. Bakulina, N.I. Ionov, Energy of the electron affinity of the halogen atoms, Dokl. Akad. Nauk SSSR 105 (1955) 680–682, (Chem. Abstr. 50 (1956) 11805b).

[929] I.N. Bakulina, N.I. Ionov, Determination of the electron affinity of sulfur by surface ionization, Sov. Phys. Dokl. 2 (1957) 423–425.

[930] I.N. Bakulina, N.I. Ionov, Determination of the electron affinities of halogen and sulphur atoms and the cyano radical by the surface ionization method, Russ. J. Phys. Chem. 33 (1959) 286–291.

[931] W. Li, D.Y. Li, On the correlation between surface roughness and work function in copper, J. Chem. Phys. 122 (2005) 064708/1–6.

[932] V.M. Dukel'skiĭ, N.I. Ionov, Formation of negative halogen ions in the interaction of alkali halides with the surface of incandescent tungsten, Zh. Eksper. Teort. Fiz. 10 (1940) 1248–1256 (Chem. Abstr. 35 (1941) 5387₅).

[933] N.I. Ionov, Formation of negative ions in the process of surface ionization of alkali halides on heated tungsten, Compt. Rend. Acad. Sci. USSR 28 (1940) 512–513 (Chem. Abstr. 35 (1941) 2411₈).

[934] I.N. Bakulina, N.I. Ionov, The determination of the energy of electron affinity of cyanogen from the surface ionization of KCN and KCNS molecules, Dokl. Akad. Nauk SSSR 99 (1954) 1023–1024 (Chem. Abstr. 49 (1955) 12951c).

[935] X.-y. Zhu, J. Hermanson, F.J. Arlinghaus, J.G. Gay, R. Richter, J.R. Smith, Electronic structure and magnetism of Ni(100) films: Self–consistent local–orbital calculations, Phys. Rev. B 29 (1984) 4426–4438.

[936] A.C. Papageorgopoulos, M. Kamaratos, C.A. Papageorgopoulos, Li on S covered Ni(100) surfaces, Surf. Sci. 481 (2001) 143–149.

[937] K. Christmann, J.E. Demuth, Interaction of inert gases with a nickel (100) surface, Surf. Sci. 120 (1982) 291–318.

[938] F.J. Himpsel, J.A. Knapp, D.E. Eastman, Angle–resolved photoemission study of the electronic structure of chemisorbed hydrogen on Ni(111), Phys. Rev. B 19 (1979) 2872–2875.

[939] K. Giesen, F. Hage, F.J. Himpsel, H.J. Riess, W. Steinmann, Hydrogenic image–potential states: A critical examination, Phys. Rev. B 33 (1986) 5241–5244.

[940] S. Schuppler, N. Fischer, W. Steinmann, R. Schneider, E. Bertel, Image–potential states on Ni(111): A two–photon photoemission study, Phys. Rev. B 42 (1990) 9403–9408.

[941] R. Wu, A.J. Freeman, Structural and magnetic properties of Fe/Ni(111), Phys. Rev. B 45 (1992) 7205–7210.

[942] A.J. Blodgett Jr., W.E. Spicer, Experimental determination of the density of states in nickel, Phys. Rev. 146 (1966) 390–402.

[943] A.B. Cardwell, Photoelectric and thermionic properties of nickel, Phys. Rev. 76 (1949) 125–127.

[944] M. Weinert, R.E. Watson, Contributions to the work function of crystals, Phys. Rev. B 29 (1984) 3001–3008.

[945] A.A. Holscher, A field emission retarding potential method for measuring work function, Surf. Sci. 4 (1966) 89–102.

[946] M.D. Scheer, Positive and negative ion sublimation from transition metal surfaces: A review of some recent results, J. Res. NBS 74 A (1970) 37–43.

[947] V. Russier, J.P. Badiali, Calculation of the electronic work function of Cu and Ag from an extended jellium model, Phys. Rev. B 39 (1989) 13193–13200.

[948] L. Peralta, E. Margot, Y. Berthier, J. Oudar, Effect of crystal orientation on the work function of copper with and without adsorbed sulfur, J. Microsc. Spectrosc. Electron. 3 (1978) 151–156.

[949] J.R. Smith, J.G. Gay, F.J. Arlinghaus, Self–consistent local–orbital method for calculating surface electronic structure: Application to Cu(100), Phys. Rev. B 21 (1980) 2201–2221.

[950] S.-K. Kim, J.-S. Kim, J.Y. Han, J.M. Seo, C.K. Lee, S.C. Hong, Surface alloying of a Co film on the Cu(001) surface, Surf. Sci. 453 (2000) 47–58.

[951] J.G. Gay, J.R. Smith, F.J. Arlinghaus, Large surface–state/surface–resonance density on copper (100), Phys. Rev. Lett. 42 (1979) 332–335.

[952] G.A. Haas, R.E. Thomas, Work function and secondary emission studies of various Cu crystal faces, J. Appl. Phys. 48 (1977) 86–93.

[953] P.O. Gartland, S. Berge, B.J. Slagsvold, Photoelectric work function of a copper single crystal for the (100), (110), (111), and (112) faces, Phys. Rev. Lett. 28 (1972) 738–739.

[954] H. Grover, Thermionic emission of positive ions from molybdenum, Phys. Rev. 52 (1937) 982–986.

[955] G.G. Tibbetts, J.M. Burkstrand, J.C. Tracy, Electronic properties of adsorbed layers of nitrogen, oxygen, and sulfur on copper (100), Phys. Rev. B 15 (1977) 3652–3660.

[956] Th. Rodach, K-P. Bohnen, K.M. Ho, First principles calculations of lattice relaxation at low index surfaces of Cu, Surf. Sci. 286 (1993) 66–72.

[957] K. Giesen, F. Hage, F.J. Himpsel, H.J. Riess, W. Steinmann, Binding energy of image–potential states: Dependence on crystal structure and material, Phys. Rev. B 35 (1987) 971–974.

[958] K. Giesen, F. Hage, F.J. Himpsel, H.J. Riess, W. Steinmann, N.V. Smith, Effective mass of image–potential states, Phys. Rev. B 35 (1987) 975–978.

[959] H.C. Potter, J.M. Blakely, LEED, Auger Spectroscopy, and contact potential studies of copper–gold alloy single crystal surfaces, J. Vac. Sci. Technol. 12 (1975) 635–642.

[960] E.M. Savitskii, I.V. Burov, L.N. Litvak, G.S. Burkhanov, I.V. Mal'tseva, Anisotropy of the work function of niobium single crystals, in: 1st–2nd Monokrist. Tugoplavkikh Redk. Metal., Tr. Soveshch. Poluch., Strukt., Fiz. Svoistvam Primen. Monokrist. Tugoplavkikh Redk. Metal., 1966–1967, pp. 110–112 (Chem. Abstr. 73 (1970) 113847g).

[961] J. Fine, M.D. Sheer, Positive and negative self–surface ionization of molybdenum, J. Chem. Phys. 47 (1967) 4267–4268.

[962] L. Szunyogh, B. Újfalussy, P. Weinberger, J. Kollár, Self–consistent localized KKR scheme for surfaces and interfaces, Phys. Rev. B 49 (1994) 2721–2729.

[963] T.A. Delchar, Oxygen chemisorption on copper single crystals, Surf. Sci. 27 (1971) 11–20.

[964] D.Y. Li, W. Li, Electron work function: A parameter sensitive to the adhesion behavior of crystallographic surfaces, Appl. Phys. Lett. 79 (2001) 4337–4338.

[965] M.D. Scheer, J. Fine, Electron affinity of tungsten determined by its positive and negative self–surface ionization, Phys. Rev. Lett. 17 (1966) 283–284.

[966] M.D. Scheer, J. Fine, Positive and negative self–surface ionization of tungsten and rhenium, J. Chem. Phys. 46 (1967) 3998–4003.

[967] C.-K. Yang, Y.-C. Cheng, K.S. Dy, S.-Y. Wu, Self–consistent method for the calculation of surface electronic structure and its application to Cu(110), Phys. Rev. B 52 (1995) 10803–10806.

[968] W. Wallauer, Th. Fauster, Growth of Ag, Au, and Co on Cu(111) studied by high–resolution spectroscopy of image states, Surf. Sci. 331–333 (1995) 731–735.

[969] N. Fischer, S. Schppler, Th. Fauster, W. Steinmann, Coverage–dependent electronic structure of Na on Cu(111), Surf. Sci. 314 (1994) 89–96.

[970] K. Takeuchi, A. Suda, S. Ushioda, Local variation of the work function of Cu(111) surface deduced from the low energy photoemission spectra, Surf. Sci. 489 (2001) 100–106.

[971] J.R. Smith, F.J. Arlinghaus, J.G. Gay, Electronic structure of silver (100), Phys. Rev. B 22 (1980) 4757–4763.

[972] H. Hotop, W.C. Lineberger, Binding energies in atomic negative ions: II, J. Phys. Chem. Ref. Data 14 (1985) 731–750.

[973] T.M. Miller, Electron affinities, in: D.R. Lide (Ed.), CRC Handbook of Chemistry and Physics, 83rd ed., CRC Press, Boca Raton, 2002–2003, p. **10**–147.

[974] H. Merz, Isochromat spectroscopic determination of work functions, Phys. Status Solidi (a) 1 (1970) 707–713.

[975] W.C. Niehaus, E.A. Coomes, Surface–barrier analysis for niobium and tantalum and tantalum–on–niobium from periodic deviations in the thermionic Scottky effect, Surf. Sci. 27 (1971) 256–266.

[976] J.-L. Desplat, Work function of Mo(110) in mixed cesium and cesium monoxide vapors, J. Appl. Phys. 54 (1983) 5494–5497.

[977] E.V. Klimenko, A.G. Naumovets, Common adsorption of cesium and oxygen on the (110) and (112) faces of tungsten and the (110) face of molybdenum, Sov. Phys. Tech. Phys. 24 (1979) 710–714.

[978] R.N. Wall, D.L. Jacobson, The high–temperature work function behavior of polycrystalline osmium, Metall. Trans. 22 A (1991) 1609–1613.

[979] O.K. Husmann, Alkali–ion desorption energies on polycrystalline refractory metals at low surface coverage, Phys. Rev. 140 (1965) A546–A551.

[980] J. Xie, M. Scheffler, Structure and dynamics of Rh surfaces, Phys. Rev. B 57 (1998) 4768–4775.

[981] J.-H. Cho, M. Scheffler, Surface relaxation and ferromagnetism of Rh(001), Phys. Rev. Lett. 78 (1997) 1299–1302.

[982] P.J. Feibelman, D.R. Hamann, LAPW calculations of Rh(001) surface relaxation, Surf. Sci. 234 (1990) 377–383.

[983] M.A. Vakhabova, E.P. Sytaya, Emission and structure changes in tungsten, molybdenum, and niobium crystal faces during direct current heat treatment in vauum, Izv. Akad. Nauk Uzb.SSR, Ser. Fiz.-Mat. Nauk 28 (5) (1984) 91–92 (Chem. Abstr. 102 (1985) 37990y).

[984] J.E. Ingesfield, G.A. Benesh, Surface electronic structure: Embedded self–consistent calculations, Phys. Rev. B 37 (1988) 6682–6700.

[985] R. Fischer, S. Shuppler, N. Fisher, Th. Fauster, W. Steinmann, Image states and local work function for Ag/Pd(111), Phys. Rev. Lett. 70 (1993) 654–657.

[986] J.-C. Blais, A. Blunot, M. Cottin, M.H. Ducroquet, B. Gitton, C. Martiens, Use of surface negative ionization for isotopic analysis and detection of elements with high electron affinity, C. R. Acad. Sci. Ser. C 271 (1970) 1347–1350.

[987] J.N.M. van Wunnik, J.J.C. Geerlings, J. Los, The velocity dependence of the negatively charged fraction of hydrogen scattered from cesiated tungsten surfaces, Surf. Sci. 131 (1983) 1–16.

[988] J.N.M. van Wunnik, J.J.C. Geerlings, E.H.A. Granneman, J. Los, The scattering of hydrogen from a cesiated tungsten surface, Surf. Sci. 131 (1983) 17–33.

[989] U. van Slooten, O.M.N.D. Teodoro, A.W. Kleyn, J. Los, D. Teillet-Billy, J.P. Gauyacq, Negative ion formation in proton scattering from Ba/Ag(111), Chem. Phys. 179 (1994) 227–240.

[990] U. van Slooten, W.R. Koppers, A. Bot, H.M. van Pinxteren, A.M.C. Moutinho, J.W.M. Frenken, A.W. Kleyn, The adsorption of Ba on Ag(111), J. Phys.: Condens. Matter 5 (1993) 5411–5428.

[991] H. Kawano, Negative hydrogen ion production by low energy electron impact of alkali metal hydride powder, Int. J. Mass Spectrom. Ion Processes 104 (1991) 23–34.

[992] H. Kawano, Y. Ashida, H. Nagayasu, M. Wada, M. Sasao, K. Miyake, Development of an electron–stimulated desorption type negative ion source using a powdery sample, Rev. Sci. Instrum. 65 (1994) 1227–1229.

[993] M. Wada, H. Kawano, M. Sasao, Development of a compact negative ion source using powdery samples, Rev. Sci. Instrum. 67 (1996) 1233–1235.

[994] M. Wada, T. Kasuya, M. Sasao, H. Kawano, Characteristics of ion beams extracted from a compact powdery sample ion source, Rev. Sci. Instrum. 71 (2000) 719–721.

[995] J. Los, J.J.C. Geerlings, Charge exchange in atom–surface collisions, Phys. Rep. 190 (1990) 133–190.

[996] W.R. Savage, Field electron microscope study of niobium surfaces, Phys. Status Solidi 25 (1968) 131–138.

[997] S.C. Wu, D.M. Poirier, M.B. Jost, J.H. Weaver, Inverse–photoemission study of the Pd(001) surface, Phys. Rev. B 45 (1992) 8709–8713.

[998] G.D. Kubiak, Two–photon photoelectron spectroscopy of Pd(111), J. Vac. Sci. Technol. A 5 (1987) 731–734.

[999] E. Chrzanowski, Field emission study of adsorption of hydrogen on tungsten and molybdenum, Acta Phys. Pol. A 44 (1973) 711–729 (Chem. Abstr. 80 (1974) 64128g).

[1000] K. Giesen, F. Hage, F.J. Himpsel, H.J. Riess, W. Steinmann, Two–photon photoemission via image–potential states, Phys. Rev. Lett. 55 (1985) 300–303.

[1001] D.-s. Wang, A.J. Freeman, H. Krakauer, M. Posternak, Self–consistent linearized–augmented–wave–method determination of electronic structure and surface states on Al(111), Phys. Rev. B 23 (1981) 1685–1691.

[1002] E. Wimmer, M. Weinert, A.J. Freeman, H. Krakauer, Theoretical 2p–core–level shift and crystal–field splitting at the Al(001) surface, Phys. Rev. B 24 (1981) 2292–2294.

[1003] H.-D. Schmick, H.-W. Wassmuth, Rapid separation of isobar nuclides of alkali and alkaline earth elements by use of a surface ion source, Nucl. Instrum. Methods 169 (1980) 139–148.

[1004] R.J. Zollweg, Electron and ion emission from cesium–coated refractory metals in electric fields, Appl. Phys. Lett. 2 (1963) 27–29.

[1005] C.A. Papageorgopoulos, J.M. Chen, Coadsorption of cesium and oxygen on Ni(100). I. Cesium probing of Ni–O bonding, Surf. Sci. 52 (1975) 40–52.

[1006] F.J. Arlinghaus, J.G. Gay, J.R. Smith, Self–consistent local–orbital calculation of the surface electronic structure of Ni(100), Phys. Rev. B 21 (1980) 2055–2059.

[1007] A. Sellidj, B.E. Koel, Vibrational and electronic properties of monolayer and multilayer C_{60} films on Rh(111), J. Phys. Chem. 97 (1993) 10076–10082.

[1008] A. Eichler, J. Hafner, G. Kresse, Hydrogen adsorption on the (100) surfaces of rhodium and palladium: The influence of non–local exchange–correlation interactions, J. Phys.: Condens. Matter 8 (1996) 7659–7675.

[1009] P.J. Feibelman, D.R. Hamann, Electronic structure of metal overlayers on rhodium, Phys. Rev. B 28 (1983) 3092–3099.

[1010] R.S. Polizzotti, G. Ehrlich, Chemisorption on perfect surfaces: Hydrogen and nitrogen on tungsten and rhodium, J. Chem. Phys. 71 (1979) 259–270.

[1011] P.J. Feibelman, D.R. Hamann, Quantum–size effects in work functions of free–standing and adsorbed thin metal films, Phys. Rev. B 29 (1984) 6463–6467.

[1012] S. Wilke, D. Hennig, R. Löber, *Ab initio* calculations of hydrogen adsorption on (100) surfaces of palladium and rhodium, Phys. Rev. B 50 (1994) 2548–2560.

[1013] M.V. Ganduglia-Pirovano, M. Scheffler, Structural and electronic properties of chemisorbed oxygen on Rh(111), Phys. Rev. B 59 (1999) 15533–15543.

[1014] J.G. Gay, J.R. Smith, F.J. Arlinghaus, Surface electronic structure of rhodium (100), Phys. Rev. B 25 (1982) 643–649.

[1015] D. Hennig, S. Wilke, R. Löber, M. Methfessel, The adsorption of hydrogen on Pd(100) and Rh(100) surfaces: A comparative theoretical study, Surf. Sci. 287/288 (1993) 89–93.

[1016] P.J. Feibelman, D.R. Hamann, Modification of transition metal electronic structure by P, S, Cl, and Li adatoms, Surf. Sci. 149 (1985) 48–66.

[1017] D.E. Peebles, H.C. Peebles, J.M. White, Electron spectroscopic study of the interaction of coadsorbed CO and D_2 on Rh(100) at low temperature, Surf. Sci. 136 (1984) 463–487.

[1018] E. Bertel, G. Rosina, F.P. Netzer, The structure of benzene on Rh(111): Coadsorption with CO, Surf. Sci. 172 (1986) L515–L522.

[1019] P. Brault, H. Range, J.P. Toennies, Ch. Wöll, The low temperature adsorption of oxygen on Rh(111), Z. Phys. Chem. 198 (1997) 1–17.

[1020] A.Y.-C. Yu, W.E. Spicer, Photoemission and optical studies of the electronic structure of palladium, Phys. Rev. 169 (1968) 497–507.

[1021] K. Christmann, Interaction of hydrogen with solid surfaces, Surf. Sci. Rep. 9 (1988) 1–163.

[1022] D.T. Pierce, W.E. Spicer, Photoemission studies of rhodium, Phys. Rev. B 5 (1972) 2125–2130.

[1023] J.G. Gay, J.R. Smith, F.J. Arlinghaus, T.W. Capehart, Electronic structure of palladium (100), Phys. Rev. B 23 (1981) 1559–1566.

[1024] D. Tománek, Z. Sun, S.G. Louie, *Ab initio* calculation of chemisorption systems: H on Pd(001) and Pd(110), Phys. Rev. B 43 (1991) 4699–4713.

[1025] A.M. Bradshaw, Private communication (see Refs. [1009,1023,1108]).

[1026] K. Wandelt, J.E. Hulse, Xenon adsorption on palladium. I. The homogeneous (110), (100), and (111) surfaces, J. Chem. Phys. 80 (1984) 1340–1352.

[1027] A. Wachter, K.P. Bohnen, K.M. Ho, Structure and dynamics at the Pd(100) surface, Surf. Sci. 346 (1996) 127–135.

[1028] J.L.F. Da Silva, C. Stampfl, M. Scheffler, Xe adsorption on metal surfaces: First–principles investigations, Phys. Rev. B 72 (2005) 075424/1–19.

[1029] M. Todorova, K. Reuter, M. Scheffler, Density–functional theory study of the initial oxygen incorporation in Pd(111), Phys. Rev. B 71 (2005) 195403/1–8.

[1030] V. Sahni, J.P. Perdew, J. Gruenebaum, Variational calculations of low–index crystal face–dependent surface energies and work functions of simple metals, Phys. Rev. B 23 (1981) 6512–6523.

[1031] P.E.C. Franken, R. Bouwman, B.E. Nieuwenhuys, W.M.H. Sachtler, Photoelectric determination of the equilibrium of thin Pd films (80–120 Å), Thin Solid Films 20 (1974) 243–249.

[1032] C. Weiser, Photoelectric response of a contaminated nickel (100) surface, Surf. Sci. 20 (1970) 143–156.

[1033] D. Fargues, J.J. Ehrhardt, M. Abon, J.C. Bertolini, Photoemission of adsorbed xenon on Pt_xNi_{1-x}(111) single crystal alloy surfaces, Surf. Sci. 194 (1988) 149–158.

[1034] L. Giordano, F. Cinquini, G. Pacchioni, Tuning the surface metal work function by deposition of ultrathin oxide films: Density functional calculations, Phys. Rev. B 73 (2005) 045414/1–6.

[1035] L.Q. Jiang, M. Strongin, Structural and electronic properties of Rh overlayers on Mo(110), Phys. Rev. B 42 (1990) 3282–3289.

[1036] G.A. Benesh, H. Krakauer, D.E. Ellis, M. Posternak, Na chemisorption on the Al(001) surface, Surf. Sci. 104 (1981) 599–608.

[1037] K. Besocke, B. Krahl-Urban, H. Wagner, Dipole moments associated with edge atoms: A comparative study on stepped Pt, Au and W surfaces, Surf. Sci. 68 (1977) 39–46.

[1038] J. Hölzl, G. Porsch, P. Schrammen, New experiments of the adsorption of Ni on Ni(111), Surf. Sci. 97 (1980) 529–536.

[1039] K. Besocke, H. Wagner, Adsorption of W on W(110): Work–function reduction and island formation, Phys. Rev. B 8 (1973) 4597–4600.

[1040] R. Smoluchowski, Anisotropy of the electronic work function of metals, Phys. Rev. 60 (1941) 661–674.

[1041] J.-W. He, U. Memmert, P.R. Norton, Interaction of oxygen with a Pd(110) surface. II. Kinetics and energetics, J. Chem. Phys. 90 (1989) 5088–5093.

[1042] B.N.J. Persson, H. Ishida, Depolarization and metallization in alkali–metal overlayers, Phys. Rev. B 42 (1990) 3171–3174.

[1043] N.D. Lang, Theory of work–function changes induced by submonolayer alkali adsorption, Solid State Commun. 9 (1971) 1015–1019.

[1044] M.V. Ganduglia-Pirovano, K. Reuter, M. Scheffler, Stability of subsurface oxygen at Rh(111), Phys. Rev. B 65 (2002) 245426/1–9.

[1045] H.B. Michaelson, The work function of the elements and its periodicity, J. Appl. Phys. 48 (1977) 4729–4733.

[1046] L.J. Richter, T.A. Germer, J.P. Sethna, W. Ho, Electron–energy–loss spectroscopy of H adsorbed on Rh(100): Interpretation of overtone spectra as two–photon bound states, Phys. Rev. B 38 (1988) 10403–10420.

[1047] R.J. Behm, K. Christmann, G. Ertl, Adsorption of hydrogen on Pd(100), Surf. Sci. 99 (1980) 320–340.

[1048] H. Conrad, G. Ertl, E.E. Latta, Adsorption of hydrogen on palladium single crystal surfaces, Surf. Sci. 41 (1974) 435–446.

[1049] K. Möller, L. Holmlid, Rate constants for cesium bulk diffusion and neutral desorption on pyrolytic graphite basal surfaces: A field reversal kinetic study, Surf. Sci. 204 (1988) 98–112.

[1050] P.A. Anderson, A direct comparison of the Kelvin and electron beam methods of contact potential measurement, Phys. Rev. 88 (1952) 655–658.

[1051] L.L. Blackmer, H.E. Farnsworth, Effect of the type of support on the photoelectric work function of silver films, Phys. Rev. 77 (1950) 826–829.

[1052] J. Heffner, Study of xenon adsorption on tantalum, Acta Univ. Wratislav. Mat. Fiz. Astron. 15 (1975) 95–100 (Chem. Abstr. 87 (1977) 32641x).

[1053] L. van Someren, Work function measurements on macroscopic tungsten specimens, Surf. Sci. 20 (1970) 221–234.

[1054] B.J. Hopkins, S. Usami, The surface potentials of carbon monoxide on (112) and (100) oriented tungsten single–crystal surfaces, Nuovo Cimento, Suppl. 5 (1967) 535–542.

[1055] B.J. Hopkins, K.R. Pender, The adsorption of oxygen on the surfaces of (110) and (100) oriented tungsten single crystals, Surf. Sci. 5 (1966) 155–159.

[1056] B.J. Hopkins, K.R. Pender, The adsorption of hydrogen on (110), (100), (111), and (113) oriented tungsten single crystal surfaces, Surf. Sci. 5 (1966) 316–324.

[1057] Z. Dworecki, Study of xenon adsorption on tungsten, Acta Univ. Wratislav., Mat., Fiz., Astron. 15 (1975) 87–94 (Chem. Abstr. 87 (1977) 94143v).

[1058] R.S. Polizzotti, G. Erhlich, The work function of perfect W(110) planes: Fowler–Nordheim studies, Surf. Sci. 91 (1980) 24–36.

[1059] J.R. Smith, Beyond the local–density approximation: Surface properties of (110)W, Phys. Rev. Lett. 25 (1970) 1023–1026.

[1060] J. Eisinger, Properties of hydrogen chemisorbed on tungsten, J. Chem. Phys. 29 (1958) 1154–1160.

[1061] Yu.K. Szhenov, On the mechanism of surface ionization of atoms of the alkali earth metals, Sov. Phys.—JETP 10 (1960) 239–241.

[1062] T. Durakiewicz, S. Halas, Cooling of an incandescent filament by thermionic emission, Int. J. Mass Spectrom. 177 (1998) 155–161.

[1063] A.M. Romanov, S.V. Starodubtsev, Adsorption and ionization of sodium by hot tungsten, Sov. Phys. Tech. Phys. 2 (1957) 652–662.

[1064] Yu.S. Vedula, V.M. Gavrilyuk, N.D. Morgulis, Electronic and adsorption properties of a film of barium atoms on a tungsten surface covered by oxygen, Sov. Phys.—Solid State 1 (1959) 1569–1571.

[1065] O.D. Protopopov, E.V. Mikheeva, B.N. Sheinberg, G.N. Shuppe, Thermal emission parameters of the faces of a Re single crystal, Dokl. Akad. Nauk Uzb.SSR 23 (6) (1966) 21–22 (Chem. Abstr. 66 (1967) 50190v).

[1066] W.M.H. Sachtler, Semiempirical method for the calculation of the thermionic work function of metals, Z. Elektrochem. 59 (1955) 119–122.

[1067] R. Drube, J. Noffke, R. Schneider, J. Rogozik, V. Dose, Target–current spectroscopy of reconstructing $5d$–transition–metal surfaces as a tool for testing bulk–band–structure calculations, Phys. Rev. B 45 (1992) 4390–4397.

[1068] G.V. Hansson, S.A. Flodström, Photoemission study of the bulk and surface electronic structure of single crystals of gold, Phys. Rev. B 18 (1978) 1572–1585.

[1069] J. Lecoeur, J.P. Bellier, C. Koehler, Comparison of crystallographic anisotropy effects on potential of zero charge and electronic work function for gold {111}, {311}, {110} and {210} orientations, Electrochim. Acta 35 (1990) 1383–1392.

[1070] C.-T. Tzeng, W.-S. Lo, J.-Y. Yuh, R.-Y. Chu, K.-D. Tsuei, Photoemission, near–edge X–ray absorption spectroscopy, and low–energy electron–diffraction study of C_{60} on Au(111) surfaces, Phys. Rev. B 61 (2000) 2263–2272.

[1071] E.E. Huber Jr., The effect of mercury contamination on the work function of gold, Appl. Phys. Lett. 8 (1966) 169–171.

[1072] R.P.W. Lawson, G. Carter, The desorption of mercury and the work function of polycrystalline gold, Appl. Phys. Lett. 9 (1966) 85–87.

[1073] J.C. Rivière, The work function of gold, Appl. Phys. Lett. 8 (1966) 172.

[1074] W.M.H. Sachtler, G.J.H. Dorgelo, A.A. Holscher, The work function of gold, Surf. Sci. 5 (1966) 221–229.

[1075] P.H. Schmidt, L.D. Longinotti, D.C. Joy, S.D. Ferris, H.J. Leamy, Z. Fisk, Design and optimization of directly heated LaB_6 cathode assemblies for electron–beam instruments, J. Vac. Sci. Technol. 15 (1978) 1554–1560.

[1076] P.H. Schmidt, D.C. Joy, Low work function electron emitter hexaborides, J. Vac. Sci. Technol. 15 (1978) 1809–1810.

[1077] R. Nishitani, M. Aono, T. Tanaka, C. Oshima, S. Kawai, H. Iwasaki, S. Nakamura, Surface structures and work functions of the LaB_6(100), (110) and (111) clean surfaces, Surf. Sci. 93 (1980) 535–549.

[1078] P. Hafner, E.B. Bas, Investigation on bolt cathodes with floating zone melted polycrystalline and monocrystalline LaB_6 emitters, in: 7th Int. Conf. on Electron and Ion Beam Sci. and Technol., 1976, pp. 3–17 (Chem. Abstr. 89 (1978) 172388m).

[1079] M. Gesley, L.W. Swanson, A determination of the low work function planes of LaB_6, Surf. Sci. 146 (1984) 583–599.

[1080] R. Monnier, B. Delley, Properties of LaB_6 elucidated by density functional theory, Phys. Rev. B 70 (2004) 193403/1–4.

[1081] H. Kishi, H. Kawano, Negative surface ionization mass spectrometry of atmospheric iodine, Int. J. Mass Spectrom. Ion Proc. 85 (1988) 301–318.

[1082] E.H. Blevis, C.R. Crowell, Temperature dependence of the work function of single–crystal faces of copper, Phys. Rev. 133 (1964) A580–A584.

[1083] G. Porsch, J. Hölzl, Temperature dependence of the work function of polycrystalline Ni in the region $230° \leq T \leq 450$ °C, Thin Solid Films 34 (1976) 235–238.

[1084] V.K. Medvedev, A.G. Naumovets, A.G. Fedorus, Structure and adsorption behavior of sodium films on (011) faces of tungsten, Sov. Phys.—Solid State 12 (1970) 301–306.

[1085] A.G. Fedorus, A.G. Naumovets, Cesium on tungsten (011) face: Structure and work function, Surf. Sci. 21 (1970) 426–439.

[1086] Z.Y. Zhang, D.C. Langreth, J.P. Perdew, Planar–surface charge densities and energies beyond the local–density approximation, Phys. Rev. B 41 (1990) 5674–5684.

[1087] E. Krotscheck, W. Kohn, G.-X. Qian, Theory of inhomogeneous quantum systems. IV. Variational calculations of metal surfaces, Phys. Rev. B 32 (1985) 5693–5712.

[1088] R. Monnier, J.P. Perdew, Surfaces of real metals by the variational self–consistent method, Phys. Rev. B 17 (1978) 2595–2611.

[1089] V. Sahni, J. Gruenebaum, Rayleigh–Ritz variational calculations of real–metal–surface properties, Phys. Rev. B 19 (1979) 1840–1854.

[1090] P.J. Feibelman, D.R. Hamann, Surface states of Sc(0001) and Ti(0001), Solid State Commun. 31 (1979) 413–417.

[1091] M. Yamamoto, C.T. Chan, K.M. Ho, First–principles calculations of the surface relaxation and electronic structure of Zr(0001), Phys. Rev. B 50 (1994) 7932–7939.

[1092] P. Liu, Y. Wei, K. Jiang, Q. Sun, X. Zhang, S. Fan, S. Zhang, C. Ning, J. Deng, Thermionic emission and work function of multiwalled carbon nanotube yarns, Phys. Rev. B 73 (2006) 235412/1–5.

[1093] K. Besocke, H. Wagner, Adsorption of tungsten on stepped tungsten surfaces studied by work function measurement, Surf. Sci. 53 (1975) 351–358.

[1094] A.R. Law, J.J. Barry, H.P. Hughes, Angle–resolved photoemission and secondary electron emission from single–crystal graphite, Phys. Rev. B 28 (1983) 5332–5335.

[1095] K.H. Lau, W. Kohn, Non–local corrections to the electronic structure of metal surfaces, J. Phys. Chem. Solids 37 (1976) 99–104.

[1096] K. Mednick, L. Kleinman, Self–consistent Al(111) film calculations, Phys. Rev. B 22 (1980) 5768–5773.

[1097] D.-S. Wang, A.J. Freeman, H. Krakauer, Comment on "Comparison of two self–consistent Al(111) film calculations", Phys. Rev. B 24 (1981) 3614–3615.

[1098] E. Caruthers, L. Kleinman, G.P. Alldredge, Electronic surface states on (111) aluminum, Phys. Rev. B 9 (1974) 3330–3336.

[1099] D.M. Bylander, L. Kleinman, K. Mednick, Comparison of two self–consistent Al(111) film calculations, Phys. Rev. B 24 (1981) 3612–3613.

[1100] J.R. Chelikowsky, M. Schlüter, S.G. Louie, M.L. Cohen, Self–consistent pseudopotential calculation for the (111) surface of aluminum, Solid State Commun. 17 (1975) 1103–1106.

[1101] D.M. Bylander, L. Kleinman, K. Mednick, Position of the oxygen overlayer on Al(111), Phys. Rev. Lett. 48 (1982) 1544–1547.

[1102] P.E.C. Franken, V. Ponec, Photoelectric work functions of Ni–Al alloys: Clean surfaces and adsorption of CO, J. Catalysis 35 (1974) 417–426.

[1103] A. Bonanno, P. Zoccali, F. Xu, Ne autoionization electron emission in collisions with clean and Cs and Na covered Mg, Al, and Si surfaces, Phys. Rev. B 50 (1994) 18525–18534 (see Ref. [3789]).

[1104] G.W. Fernando, J.W. Wilkins, Linearized augmented–plane–wave study of chemisorption of sulfur on Fe(001), Phys. Rev. B 33 (1986) 3709–3716.

[1105] S. Ohnishi, M. Weinert, A.J. Freeman, Interface magnetism in metals: Ag/Fe(001), Phys. Rev. B 30 (1984) 36–43.

[1106] G.W. Fernando, B.R. Cooper, M.V. Ramana, H. Krakauer, C.Q. Ma, Practical method for highly accurate large–scale surface calculations, Phys. Rev. Lett. 56 (1986) 2299–2302.

[1107] S. Kato, H. Kobayashi, LEED study of iron single crystal surfaces, Surf. Sci. 27 (1971) 625–634.

[1108] F.J. Arlinghaus, J.G. Gay, J.R. Smith, Surface states on *d*–band metals, Phys. Rev. B 23 (1981) 5152–5155.

[1109] J.R. Smith, F.J. Arlinghaus, J.G. Gay, Theory of chemisorption on *d*–band metals, J. Vac. Sci. Technol. 18 (1981) 411–415.

[1110] G.E. Becker, H.D. Hagstrum, Orbital energy spectra of electrons in chemisorption bonds: O, S, Se on Ni(110) and Ni(111), Surf. Sci. 30 (1972) 505–524.

[1111] K. Jacobi, Y.-p. Hsu, H.H. Rotermund, Photoemission from Ne, Ar, Kr and Xe layers on Ni(110) and Ga films, Surf. Sci. 114 (1982) 683–691.

[1112] W. Gudat, E. Kisker, E. Kuhlmann, M. Campagna, Strong itinerant ferromagnetism in Ni: Spin polarization of photoelectrons from the (110) surface, Phys. Rev. B 22 (1980) 3282–3287.

[1113] F.J. Himpsel, D.E. Eastman, Observation of a Λ_1–symmetry surface state on Ni(111), Phys. Rev. Lett. 41 (1978) 507–511.

[1114] E. Kisker, W. Gudat, M. Campagna, E. Kuhlmann, H. Hopster, Crossover from negative to positive spin polarization in the photoyield from Ni(111) near threshold, Phys. Rev. Lett. 43 (1979) 966–969.

[1115] T.A. Callcott, A.U. Mac Rae, Photoemission from clean and cesium–covered nickel surfaces, Phys. Rev. 178 (1969) 966–978.

[1116] M. Akbi, A. Lefort, Work function measurements of contact materials for industrial use, J. Phys. D 31 (1998) 1301–1308.

[1117] W.M.H. Sachtler, G.J.H. Dorgelo, The surface of copper–nickel alloy films. I. Work function and phase composition, J. Catalysis 4 (1965) 654–664.

[1118] D.G. Dempsey, L. Kleinman, Extended–Hückel study of the (111), (100), and (110) surfaces of copper, Phys. Rev. B 16 (1977) 5356–5366.

[1119] S. Romanowski, An application of the extended CPA method to electron work function and surface charge calculation for Cu single crystals, Phys. Status Solidi (b) 145 (1988) 467–482.

[1120] A. Euceda, D.M. Bylander, L. Kleinman, K. Mednick, Self–consistent electronic structure of 7– and 19–layer Cu(001) films, Phys. Rev. B 27 (1983) 606–659.

[1121] D.-s. Wang, A.J. Freeman, H. Krakauer, Electronic structure and magnetism of Ni overlayers on a Cu(001) substrate, Phys. Rev. B 26 (1982) 1340–1351.

[1122] J.G. Gay, J.R. Smith, F.J. Arlinghaus, Self–consistent calculation of work function, charge densities, and local densities of states for Cu(100), Phys. Rev. Lett. 38 (1977) 561–564.

[1123] C. Mariani, K. Horn, A.M. Bradshaw, Photoemission studies of the commensurate–incommensurate transition in the system Xe–Cu(110), Phys. Rev. B 25 (1982) 7798–7806.

[1124] D. Straub, F.J. Himpsel, Spectroscopy of image–potential states with inverse photoemission, Phys. Rev. B 33 (1986) 2256–2262.

[1125] G.D. Kubiak, Study of image potential surface states on Cu(111): Characterization of the $n = 1$ and $n = 2$ members via two–photon photoemission, Surf. Sci. 201 (1988) L475–L484.

[1126] J.A. Appelbaum, D.R. Hamann, Electronic structure of the Cu(111) surface, Solid State Commun. 27 (1978) 881–883.

[1127] H. Hochst, M.K. Kelly, G.B. Fisher, Unpublished (see Ref. [982]).

[1128] G.R. Castro, H. Busse, U. Schneider, T. Janssens, K. Wandelt, Geometric and electronic structure of potassium on Rh(111), Phys. Scrip. T 41 (1992) 208–212.

[1129] R. Miranda, S. Daiser, K. Wandelt, G. Ertl, Thermodynamics of xenon adsorption on Pd(s)[8(100)×(110)]: From steps to multilayers, Surf. Sci. 131 (1983) 61–91.

[1130] B. Lang, R.W. Joyner, G.A. Somorjai, Low energy electron diffraction studies of high index crystal surfaces of platinum, Surf. Sci. 30 (1972) 440–453.

[1131] S. Schuppler, N. Fischer, Th. Fauster, W. Steinmann, Bichromatic two–photon photoemission spectroscopy of image potential states on Ag(100), Appl. Phys. A 51 (1990) 322–326.

[1132] H.E. Farnsworth, R.P. Winch, Photoelectric work function of (100) and (111) faces of silver single crystals and their contact potential difference, Phys. Rev. 58 (1940) 812–819.

[1133] W. Steinmann, Spectroscopy of image–potential states by two–photon photoemission, Appl. Phys. A 49 (1989) 365–377.

[1134] A.W. Dweydari, C.H.B. Mee, Oxygen adsorption on the (111) face of silver, Phys. Status Solidi (a) 17 (1973) 247–250.

[1135] R.H. Fowler, The analysis of photoelectric sensitivity curves for clean metals at various temperatures, Phys. Rev. 38 (1931) 45–56.

[1136] L.F. Mattheiss, D.R. Hamann, Electronic structure of the tungsten (001) surface, Phys. Rev. B 29 (1984) 5372–5381.

[1137] A.G. Naumovets, A.G. Fedorus, Investigation of the structure and work function of platinum films on tungsten and of adsorption of cesium on such films, Sov. Phys.—Solid State 10 (1968) 627–633.

[1138] V.M. Gavrilyuk, V.K. Medvedev, The adsorption of barium atoms and carbon monoxide molecules on the (113) face of a tungsten single crystal, Sov. Phys.—Solid State 4 (1963) 1737–1744.

[1139] S. Evans, Work function measurements by X–PE spectroscopy, and their relevance to the calibration of X–PE spectra, Chem. Phys. Lett. 23 (1973) 134–138.

[1140] B.E. Nieuwenhuys, W.M.H. Sachtler, Crystal face specificity of xenon adsorption on iridium field emitters, Surf. Sci. 45 (1974) 513–529.

[1141] R. Bouwman, W.M.H. Sachtler, Photoelectric determination of the work function of gold–platinum alloys, J. Catalysis 19 (1970) 127–140.

[1142] F. Meier, D. Pescia, Band–structure investigation of gold by spin–polarized photoemission, Phys. Rev. Lett. 47 (1981) 374–377.

[1143] M. Aono, T. Tanaka, E. Bannai, S. Kawai, Structure and initial oxidation of the LaB_6(001) surface, Appl. Phys. Lett. 31 (1977) 323–325.

[1144] D. Purdie, H. Bernhoff, B. Reihl, The electronic structure of Ag(110)c(4×4)C_{60} and Au(110)(6×5)C_{60}, Surf. Sci. 364 (1996) 279–286.

[1145] P.A.W. van der Heide, Secondary ion emission and work function measurements over the transient region from n and p type Si under Cs^+ irradiation, Appl. Surf. Sci. 231–232 (2004) 97–100.

[1146] C. Oshima, M. Aono, T. Tanaka, R. Nishitani, S. Kawai, Low work function and surface structure of the LaB_6(210) surface studied by angle–resolved X–ray spectroscopy, ultraviolet spectroscopy, and low–energy electron diffraction, J. Appl. Phys. 51 (1980) 997–1000.

[1147] P.R. Davis, G.A. Schwind, Low work function emitter electrodes for advanced thermionic converters, Appl. Surf. Sci. 25 (1986) 355–363.

[1148] S. Saito, T. Maeda, Temperature variation of the work function of polycrystalline cobalt in the temperature range 100 °C $\leq T \leq$ 485 °C, Phys. Status Solidi (a) 100 (1987) K21–K24.

[1149] J. Hölzl, G. Porsch, Contact potential difference measurements on polycrystalline Ni during and after deposition with evaporated Ni in the temperature range 230 °C $\leq T \leq$ 450 °C, Thin Solid Films 28 (1975) 93–106.

[1150] C.R. Crowell, R.A. Armstrong, Temperature dependence of the work function of silver, sodium, and potassium, Phys. Rev. 114 (1959) 1500–1506.

[1151] J.E. Rowe, N.V. Smith, Photoemission spectra and band structures of d–band metals. V. The (100) and (111) faces of single–crystal copper, Phys. Rev. B 10 (1974) 3207–3212.

[1152] W.M.H. Sachtler, R. Jongepier, The surface of copper–nickel alloy films. II. Phase equilibrium and distribution and their implications for work function, chemisorption, and catalysis, J. Catalysis 4 (1965) 665–671.

[1153] G. Wedler, C. Wölfing, P. Wissmann, The photoelectric properties of vapor–deposited nickel films: Effect of layer thickness and annealing, Surf. Sci. 24 (1971) 302–308.

[1154] S.G. Louie, K.-M. Ho, J.R. Chelikowsky, M.L. Cohen, Self–consistent pseudopotential calculations for the ideal (001) surface of Nb, Phys. Rev. B 15 (1977) 5627–5635.

[1155] W.F. Krolikowski, W.E. Spicer, Photoemission studies of the noble metals. I. Copper, Phys. Rev. 185 (1969) 882–900.

[1156] P.H. Schmidt, D.C. Joy, L.D. Longinotti, H.J. Leamy, S.D. Ferris, Z. Fisk, Anisotropy of thermionic electron emission values for LaB_6 single–crystal emitter cathodes, Appl. Phys. Lett. 29 (1976) 400–401.

[1157] P.A. Anderson, A new technique for preparing monocrystalline metal surfaces for work function study: The work function of Ag(100), Phys. Rev. 59 (1941) 1034–1041.

[1158] E.N. Clarke, H.E. Farnsworth, Observations on the photoelectric work functions and low speed electron diffraction from thin films of silver on the (100) face of a silver single crystal, Phys. Rev. 85 (1952) 484–485.

[1159] D. Steiner, E.P. Gyftopoulos, An equation for the prediction of bare work functions, in: Proc. 27th Conf. Phys. Electron. Boston, 1967, pp. 160–168 (see Refs. [321,625,777,783,1115,1312]).

[1160] B.J. Hopkins, C.H.B. Mee, D. Parker, The surface potential of oxygen on vapour deposited gold on glass, Br. J. Appl. Phys. 15 (1964) 865–866.

[1161] J.C. Rivière, The surface potential of oxygen on uranium, Br. J. Appl. Phys. 15 (1964) 1341–1348.

[1162] P.A. Anderson, Work function of gold, Phys. Rev. 115 (1959) 553–554.

[1163] B.J. Hopkins, Marden, D. Parker, Unpublished (see Ref. [349]).

[1164] E.P. Sytaya, N.G. Shuppe, Ionization of iodine atoms at the surface of incandescent tantalum, Izv. Vysshikh Uchebn. Zavedeniĭ, Fiz. (6) (1961) 52–56 (Chem. Abstr. 57 (1962) 1696c).

[1165] S. Suzuki, C. Bower, T. Kiyokura, K.G. Nath, Y. Watanabe, O. Zhou, Photoemission spectroscopy of single–walled carbon nanotubes bundles, J. Electron Spectrosc. Relat. Phenom. 114–116 (2001) 225–228.

[1166] M. Shiraishi, M. Ata, Work function of carbon nanotubes, Carbon 39 (2001) 1913–1917.

[1167] J.C. Boettger, S.B. Trickey, Quantum size effects in equilibrium lithium ultrathin layers, Phys. Rev. B 45 (1992) 1363–1372.

[1168] V. Barone, J.E. Peralta, J. Uddin, G.E. Scuseria, Screened exchange hybrid density–functional study of the work function of pristine and doped single–walled carbon nanotubes, J. Chem. Phys. 124 (2006) 024709/1–5.

[1169] B. Shan, K. Cho, First–principles study of work functions of double–wall carbon nanotubes, Phys. Rev. B 73 (2006) 081401/1–4.

[1170] M.J. Fransen, Th.L. van Rooy, P. Kruit, Field emission energy distributions from individual multiwalled carbon nanotubes, Appl. Surf. Sci. 146 (1999) 312–327.

[1171] O. Gröning, O.M. Küttel, Ch. Emmenegger, P. Gröning, L. Schlapbach, Field emission properties of carbon nanotubes, J. Vac. Sci. Technol. B 18 (2000) 665–678.

[1172] S. Suzuki, Y. Watanabe, Y. Homma, S. Fukuba, S. Heun, A. Locatelli, Work function of individual single–walled carbon nanotubes, Appl. Phys. Lett. 85 (2004) 127–129.

[1173] H.B. Shore, J.H. Rose, Theory of ideal metals, Phys. Rev. Lett. 66 (1991) 2519–2522.

[1174] N. Ooi, A. Rairkar, J.B. Adams, Density functional study of graphite bulk and surface properties, Carbon 44 (2006) 231–242.

[1175] J.L.F. Da Silva, All–electron first–principles calculations of clean surface properties of low–miller–index Al surfaces, Phys. Rev. B 71 (2005) 195416/1–12.

[1176] I.P. Batra, S. Ciraci, G.P. Srivastava, J.S. Nelson, C.Y. Fong, Dimensionality and size effects in simple metals, Phys. Rev. B 34 (1986) 8246–8257.

[1177] A. Kiejna, B.I. Lundqvist, First–principles study of surface and subsurface O structures at Al(111), Phys. Rev. B 63 (2001) 085405/1–10.

[1178] H.M. Polatoglou, M. Methfessel, M. Scheffler, Vacancy–formation energies at the (111) surface and in bulk Al, Cu, Ag, and Rh, Phys. Rev. B 48 (1993) 1877–1883.

[1179] J.L.F. Da Silva, C. Stampfl, M. Scheffler, Converged properties of clean metal surfaces by all–electron first–principles calculations, Surf. Sci. 600 (2006) 703–715.

[1180] P.A.W. van der Heide, Secondary ion emission from polycrystalline Al under Cs^+ irradiation, Appl. Surf. Sci. 231–232 (2004) 86–89.

[1181] V. Papaefthimiou, A. Siokou, S. Kennou, The electronic structure of the interface between thin conjugated oligomer films and inorganic substrates with different work function, Surf. Sci. 600 (2006) 3987–3991.

[1182] G. Pirug, G. Brodén, H.P. Bonzel, Coadsorption of potassium and oxygen on Fe(110), Surf. Sci. 94 (1980) 323–338.

[1183] S.I. Schreiner, Thermionic Emission from Planar Single–Crystalline Tungsten, AEC Acc. No. 39635, Rept. No. UCRL–16699, 1966, 54 pp (Chem. Abstr. 66 (1967) 69963w).

[1184] X.-M. Tao, M.-Q. Tan, X.-X. Zhao, W.-B. Chen, X. Chen, X.-F. Shang, A density–functional study on the atomic geometry and adsorption of the Cu(100)c(2×2)/N surface, Surf. Sci. 600 (2006) 3419–3426.

[1185] T. Aruga, H. Tochihara, Y. Murata, Valence–electronic structure of potassium adsorbed on Cu(001) deduced from work–function change and electron–energy–loss spectroscopy, Phys. Rev. B 34 (1986) 8237–8245.

[1186] J.F. Jia, K. Inoue, Y. Hasegawa, W.S. Yang, T. Sakurai, Variation of the local work function at steps on metal surfaces studied with STM, Phys. Rev. B 58 (1998) 1193–1196.

[1187] S. Pagliara, G. Ferrini, G. Galimberti, E. Pedersoli, C. Giannetti, F. Parmigiani, Angle resolved photoemission study of image potential states and surface states on Cu(111), Surf. Sci. 600 (2006) 4290–4293.
[1188] S.G. Louie, K.-M. Ho, J.R. Chelikowsky, M.L. Cohen, Surface states on the (001) surface of Nb, Phys. Rev. Lett. 37 (1976) 1289–1292.
[1189] L.A. DuBridge, W.W. Roehr, Photoelectric and thermionic properties of palladium, Phys. Rev. 39 (1932) 99–107.
[1190] M. Gajdoš, A. Eichler, J. Hafner, *Ab initio* density functional study of O on the Ag(001) surface, Surf. Sci. 531 (2003) 272–286.
[1191] Y. Wang, L.-L. Jia, W. Wang, K. Fan, O/Ag(100) surface: A density functional study with slab model, J. Phys. Chem. B 106 (2002) 3662–3667.
[1192] W.Y. Li, K. Goto, R. Shimizu, PEEM is a stable tool for absolute work function measurements, Surf. Interf. Anal. 37 (2005) 244–247.
[1193] G. Cipriani, D. Loffreda, A. Dal Corso, S. de Gironcoli, S. Baroni, Adsorption of atomic oxygen on Ag(001): A study based on density–functional theory, Surf. Sci. 501 (2002) 182–190.
[1194] K. Doll, Density–functional study of the adsorption of K on the Ag(111) surface, Phys. Rev. B 66 (2002) 155421/1–9.
[1195] H.-N. Li, X.-X. Wang, S.-L. He, K. Ibrahim, H.-J. Qian, R. Su, J. Zhong, M.I. Abbas, C.-H. Hong, Electronic state of C₆₀ monolayer on Ag(111) before and after Yb intercalation, Surf. Sci. 586 (2005) 65–73.
[1196] R.C. Monreal, L. Guillemot, V.A. Esaulov, On Auger neutralization of He⁺ ions on a Ag(111) surface, J. Phys.: Condens. Matter 15 (2003) 1165–1171.
[1197] P.C. Rusu, G. Brocks, Work functions of self–assembled monolayers on metal surfaces by first–principles calculations, Phys. Rev. B 74 (2006) 073414/1–4.
[1198] T. Müller, H. Nienhaus, Ultrathin Ag films on H:Si(111)–1×1 surfaces deposited at low temperatures, J. Appl. Phys. 93 (2003) 924–929.
[1199] C. Kennerknecht, S. Dantscher, W. Pfeiffer, O. Autzen, C. Wesenberg, E. Hasselbrink, Electron dynamics in a heterogeneous system: Thin Ag films on Si(100), Surf. Sci. 600 (2006) 4269–4274.
[1200] A. Kiejna, Surface atomic structure and energetics of tantalum, Surf. Sci. 598 (2005) 276–284.
[1201] S. Baud, C. Ramseyer, G. Bihlmayer, S. Blügel, C. Barreteau, M.C. Desjonquères, D. Spanjaard, N. Bernstein, Comparative study of *ab initio* and tight–binding electronic structure calculations applied to platinum surfaces, Phys. Rev. B 70 (2004) 235423/1–11.
[1202] P.G. Schroeder, C.B. France, J.B. Park, B.A. Parkinson, Orbital alignment and morphology of pentacene deposited on Au(111) and SnS₂ studied using photoemission spectroscopy, J. Phys. Chem. B 107 (2003) 2253–2261.
[1203] O.K. Hunsmann, Improved surface ionization efficiency by high work function refractory metals and alloys, J. Appl. Phys. 37 (1966) 4662–4670.
[1204] T. Janssens, G.R. Castro, H. Busse, U. Schneider, K. Wandelt, Local effects in the interaction of potassium with Rh(111), Surf. Sci. 269/270 (1992) 664–668.
[1205] A.A. Rouse, J.B. Bernhard, E.D. Sosa, D.E. Golden, Variation of field emission and photoelectric thresholds of diamond films with average grain size, Appl. Phys. Lett. 75 (1999) 3417–3419.
[1206] S. Suzuki, Y. Watanabe, Y. Homma, S. Fukuba, S. Locatelli, S. Heun, Photoemission electron microscopy of individual single–walled carbon nanotubes, J. Electron Spectrosc. Relat. Phenom. 144–147 (2005) 357–360.
[1207] C.M. Tan, J. Jia, W. Yu, Temperature dependence of the field emission of multiwalled carbon nanotubes, Appl. Phys. Lett. 86 (2005) 263104/1–3.
[1208] Z. Xu, X.D. Bai, E.G. Wang, Z.L. Wang, Field emission of individual carbon nanotubes with *in situ* tip image and real work function, Appl. Phys. Lett. 87 (2005) 163106/1–3.
[1209] L.A. Bol'shov, A.P. Napartovich, A.G.N. Naumovets, A.G. Fedorus, Submonolayer films on the surface of metals, Sov. Phys. Usp. 20 (1977) 432–451.
[1210] R.D. Diehl, R. McGrath, Current progress in understanding alkali metal adsorption on metal surfaces, J. Phys.: Condens. Matter 9 (1997) 951–968.
[1211] J. Wang, M. Zhu, X. Zhao, R.A. Outlaw, D.M. Manos, B.C. Holloway, C. Park, T. Anderson, V.P. Mammana, Synthesis and field–emission testing of carbon nanoflake edge emitters, J. Vac. Sci Technol. B 22 (2004) 1269–1272.
[1212] A.P. Seitsonen, B. Hammer, M. Scheffler, to be published (see Ref. [559]).
[1213] A.P. Seitsonen, Private comm. (see Ref. [559]).
[1214] E. Caruthers, L. Kleinman, G.P. Alldredge, Electronic surface states on (110) aluminum, Phys. Rev. B 9 (1974) 3325–3329.
[1215] P.J. Feibelman, Static quantum–size effects in thin crystalline, simple–metal films, Phys. Rev. B 27 (1983) 1991–1996.
[1216] S. Ciraci, I.P. Batra, Theory of the quantum size effect in simple metals, Phys. Rev. B 33 (1986) 4294–4297.
[1217] A.G. Borisov, H. Winter, G. Dierkes, R. Zimny, Detailed study on the neutralization of fast Na⁺–ions in grazing collisions with an Al(111) surface, Europhys. Lett. 33 (1996) 229–234.
[1218] T. Mandel, Private communication (see Ref. [422]).
[1219] T.-C. Chiang, G. Kaindl, D.E. Eastman, Photoemission from physisorbed CO on clean and Xe–covered Al(111), Solid State Commun. 36 (1980) 25–28.
[1220] S.K.M. Jönsson, W.R. Salaneck, M. Fahlman, Photoemission of Alq₃ and C₆₀ films on Al and LiF/Al substrates, J. Appl. Phys. 98 (2005) 014901/1–7.
[1221] T. Matsukawa, C. Yasumuro, H. Yamauchi, M. Masahara, E. Suzuki, S. Kanemaru, Work function uniformity of Al–Ni alloys obtained by scanning Maxwell–stress microscopy as an effective tool for evaluating metal transistor gates, Appl. Phys. Lett. 86 (2005) 094104/1–3.
[1222] T. Sakurai, Y. Momose, K. Nakayama, New method to determine the work function using photoelectron emission, e–J, Surf. Sci. Nanotech. 3 (2005) 179–183 (Chem. Abstr. 143 (2005) 218618a) (http://www.jstage.jst.go.jp/article/ejssnt/3/0/179/-pdf).
[1223] R. Shaltaf, E. Mete, Ş. Ellialtıoğlu, Cs adsorption on Si(001) surface: An *ab initio* study, Phys. Rev. B 72 (2005) 205415/1–8.
[1224] T. Abukawa, Y. Enta, T. Kashiwakura, S. Suzuki, S. Kono, T. Sakamoto, Photoemission study of the negative electron affinity surfaces of O/Cs/Si(001) 2×1 and O/K/Si(001)2×1, J. Vac. Sci. Technol. A 8 (1990) 3205–3209.
[1225] F.G. Allen, Work function and emission studies on clean silicon surfaces, J. Phys. Chem. Solids 8 (1959) 119–121.
[1226] G.W. Gobeli, F.G. Allen, Direct and indirect excitation processes in photoelectric emission from silicon, Phys. Rev. 127 (1962) 141–149.
[1227] V. Papaefthimiou, A. Siokou, S. Kennou, Growth and interfacial studies of conjugated oligomer films on Si and SiO₂ substrates, J. Appl. Phys. 91 (2002) 4213–4219.
[1228] M. Erbudak, T.E. Fischer, Relationship between atomic structure and electronic properties of (111) surfaces of silicon, Phys. Rev. Lett. 29 (1972) 732–735.
[1229] J.J. Scheer, J. van Laar, Photo–emission from semiconductor surfaces, Phys. Lett. 3 (1963) 246–247.
[1230] C. Sebenne, D. Bolmont, G. Guichar, M. Balkanski, Surface states from photoemission threshold measurements on a clean, cleaved, Si(111) surface, Phys. Rev. B 12 (1975) 3280–3285.
[1231] R.A. Collins, Silicon adsorption on tungsten field emitters, Surf. Sci. 26 (1971) 624–636.
[1232] G. Brodén, H.P. Bonzel, Potassium adsorption on Fe(110), Surf. Sci. 84 (1979) 106–120.
[1233] D.G. Dempsey, W.R. Grise, L. Kleinman, Energy bands of (100) and (110) ferromagnetic Ni films, Phys. Rev. B 18 (1978) 1270–1280.
[1234] J. Kudrnovský, I. Turek, V. Drchal, P. Weinberger, S.K. Bose, A. Pasturel, Self–consistent Green's–function method for surfaces of random alloys, Phys. Rev. B 47 (1993) 16525–16531.
[1235] B. Lescop, A. Galtayries, G. Fanjoux, Thermal chemistry of NH₃ on oxygen–pretreated Ni(111) studied by metastable induced electron spectroscopy and ultraviolet photoelectron spectroscopy, J. Phys. Chem. B 108 (2004) 13711–13718.
[1236] D.G. Dempsey, W.R. Grise, L. Kleinman, Energy bands of (111) ferromagnetic Ni films, Phys. Rev. B 18 (1978) 1550–1553.
[1237] K. Doll, Calculation of the work function with a local basis set, Surf. Sci. 600 (2006) L321–L325.
[1238] O. Renault, R. Brochier, P.-H. Haumesser, N. Barrett, B. Krömker, D. Funnemann, Energy–filtered PEEM imaging of polycrystalline Cu surfaces with work function contrast and high lateral resolution, e–J, Surf. Sci. Nanotech. 4 (2006) 431–434 (Chem. Abstr. 145 (2006) 496012r) (http://www.jstage.jst.go.jp/article/ejssnt/4/0/431/-pdf).

[1239] P.O. Gartland, B.J. Slagsvold, Transitions conserving parallel momentum in photoemission from the (111) face of copper, Phys. Rev. B 12 (1975) 4047–4058.

[1240] T. Wegehaupt, D. Rieger, W. Steinmann, Observation of empty bulk states on Cu(100) by two–photon photoemission, Phys. Rev. B 37 (1988) 10086–10089.

[1241] M. Roth, M. Pickel, W. Jinxiong, M. Weinelt, T. Fauster, Electron scattering at steps: Image–potential states on Cu(119), Phys. Rev. Lett. 88 (2002) 096802/1–4.

[1242] B. Woratschek, W. Sesselmann, J. Küppers, G. Ertl, H. Haberland, $4s$ valence level of adsorbed K atoms probed by metastable–He deexcitation spectroscopy, Phys. Rev. Lett. 55 (1985) 1231–1234.

[1243] W. Sesselmann, B. Woratschek, J. Küppers, G. Ertl, H. Haberland, Interaction of metastable noble–gas atoms with transition–metal surfaces: Resonance ionization and Auger neutralization, Phys. Rev. B 35 (1987) 1547–1559.

[1244] J. Redinger, P. Weinberger, H. Erschbaumer, R. Podloucky, C.L. Fu, A.J. Freeman, Inverse–photoemission spectra and electronic structure of the Cu(110) surface, Phys. Rev. B 44 (1991) 8288–8293.

[1245] Y. Hasegawa, J.F. Jia, K. Inoue, A. Sakai, T. Sakurai, Elemental contrast of local work function studied by scanning tunneling microscopy, Surf. Sci. 386 (1997) 328–334.

[1246] J.M. Carlsson, B. Hellsing, First–principles investigation of the quantum–well system Na on Cu(111), Phys. Rev. B 61 (2000) 13973–13982.

[1247] N. Fischer, S. Schuppler, R. Fischer, Th. Fauster, W. Steinmann, Unpublished (see Ref. [1178]).

[1248] J.F. Jia, K. Inoue, Y. Hasegawa, W.S. Yang, T. Sakurai, Local work function for Cu(111)–Au surface studied by scanning tunneling microscopy, J. Vac. Sci. Technol. B 15 (1997) 1861–1864.

[1249] F.E. Olsson, M. Persson, J. Repp, G. Meyer, Scanning tunneling microscopy and spectroscopy of NaCl overlayers on the stepped Cu(311) surface: Experimental and theoretical study, Phys. Rev. B 71 (2005) 075419/1–8.

[1250] Y. Terunuma, K. Takahashi, T. Yoshizawa, Y. Momose, Temperature dependence of the photoelectron emission from intentionally oxidized copper, Appl. Surf. Sci. 115 (1997) 317–325.

[1251] B.W. Hoogenboom, R. Hesper, L.H. Tjeng, G.A. Sawatzky, Charge transfer and doping–dependent hybridization of C_{60} on noble metals, Phys. Rev. B 57 (1998) 11939–11942.

[1252] P.A.W. van der Heide, Secondary ion emission from Ti, V, Cu, Ag and Au surfaces under keV Cs^+ irradiation, Nucl. Instrum. Methods B 229 (2005) 35–45.

[1253] J. Brona, A. Ciszewski, Structural and compositional changes of the ultrathin Pd layers on Nb(001) caused by annealing, Appl. Surf. Sci. 222 (2004) 432–440.

[1254] H.E. Albrecht, Model for the calculation of the work function of pure metal surfaces, Phys. Status Solidi (a) 6 (1971) 135–142.

[1255] V.K. Medvedev, T.P. Smereka, L.P. Zadorozhnyi, F.M. Gonchar, Influence of oxygen on electronic–adsorption properties of dysprosium films on the (112) face of a molybdenum crystal, Sov. Phys.—Solid State 35 (1993) 636–639.

[1256] R. Bouwman, W.M.H. Sachtler, Photoelectric determination of the work function of Ru–films as a function of sintering temperature (78 °K–925 °K), Surf. Sci. 24 (1971) 140–148.

[1257] G.B. Fisher, Private comm. (see Refs. [1014,1017]).

[1258] I. Morrison, D.M. Bylander, L. Klienman, Ferromagnetism of the Rh(001) surface, Phys. Rev. Lett. 71 (1993) 1083–1086.

[1259] M. Heinrichsmeier, A. Fleszar, W. Hanke, A.G. Eguiluz, Nonlocal density–functional calculations of the surface electronic structure of metals: Application to aluminum and palladium, Phys. Rev. B 57 (1998) 14974–14982.

[1260] H.S. Greenside, D.R. Hamann, Cl chemisorption on the Ag(001) surface: Geometry and electronic structure, Phys. Rev. B 23 (1981) 4879–4887.

[1261] D.R. Hamann, L.F. Mattheiss, H.S. Greenside, Comparative LCAO–LAPW study of Cl chemisorption on the Ag(001) surface, Phys. Rev. B 24 (1981) 6151–6155.

[1262] J.E. Rowe, Private communication (see Refs. [1260,1261]).

[1263] G. Ferrini, C. Giannetti, G. Galimberti, S. Pagliara, D. Fausti, F. Banfi, F. Parmigiani, Violation of the electric–dipole selection rules in indirect multiphoton excitation of image–potential states on Ag(100), Phys. Rev. Lett. 92 (2004) 256802/1–4.

[1264] Y. Wang, W. Wang, K.-N. Fan, J. Deng, Structural and electronic properties of silver surfaces: *ab initio* pseudopotential density functional study, Surf. Sci. 490 (2001) 125–132.

[1265] H.Q. Qian, H.Y. Mao, Q. Chen, F. Song, Y.W. Hu, H. Huang, H.J. Zhang, H.Y. Li, P.M. He, S.N. Bao, The growth of thin fluorescein films on Ag (110), Appl. Surf. Sci. 253 (2006) 2336–2339.

[1266] S. Ryu, J. Chang, S.K. Kim, Interfacial electron dynamics and hot–electron–driven surface photochemistry of carbon tetrachloride on Ag(111), J. Chem. Phys. 123 (2005) 114710/1–9.

[1267] S.C. Veenstra, U. Stalmach, V.V. Krasnikov, G. Hadziioannou, H.T. Jonkman, A. Heeres, G.A. Sawatzky, Energy level alignment at the conjugated phenylenevinylene oligomer/metal interface, Appl. Phys. Lett. 76 (2000) 2253–2255.

[1268] J.E. Boggio, H.E. Farnsworth, Low energy electron diffraction study of the formation of TaO (111) on Ta(110), Surf. Sci. 3 (1964) 62–70.

[1269] D. Vouagner, Cs. Beleznaï, J.P. Girardeau-Montaut, Characterization of surface processes on metals under pulsed picosecond laser irradiation by photoelectric work function measurements, Appl. Surf. Sci. 171 (2001) 288–305.

[1270] S.F. Huang, R.S. Chang, T.C. Leung, C.T. Chan, Cohesive and magnetic properties of Ni, Co, and Fe on W(100), (110), and (111) surfaces: A first–principles study, Phys. Rev. B 72 (2005) 075433/1–8.

[1271] C.J. Fall, N. Binggeli, A. Baldereschi, Theoretical maps of work–function anisotropies, Phys. Rev. B 65 (2001) 045401/1–6.

[1272] D.A. Gorodetskii, A.A. Yas'ko, Structure of antimony films on tungsten (110) surfaces, Sov. Phys.—Solid State 13 (1971) 1085–1088.

[1273] U. Thomann, Ch. Reuß, Th. Fauster, F. Passek, M. Donath, Image–potential states on bcc (110) surfaces of iron and tungsten, Phys. Rev. B 61 (2000) 16163–16167.

[1274] T.M. Gardiner, H.M. Kramer, E. Bauer, The surface structure of the ⟨110⟩ zone of tungsten: A LEED and work function study, Surf. Sci. 112 (1981) 181–196.

[1275] A. van Oostrom, Validity of the Fowler–Nordheim model for field electron emission, Philips Res. Rep. 21 (Suppl. 1) (1966) 102 pp. (Thesis, Univ. of Amsterdam, June 1965) (Chem. Abstr. 64 (1966) 18595e).

[1276] A. van Oostrom, Adsorption of nitrogen on single–crystal faces of tungsten, J. Chem. Phys. 47 (1967) 761–769.

[1277] E.M. Savitskii, G.S. Burkhanov, L.G. Baranov, N.N. Raskatov, E.V. Ottenberg, Structure and properties of large tungsten single crystals, in: 1st–2nd Monokrist. Tugoplavkikh Redk. Metal. Tr. Soveshch. Poluch. Strukt. Fiz. Svoistvam Primen. Monokrist. Tugoplavkikh Redk. Metal., 1966–1967, pp. 50–58 (Chem. Abstr. 73 (1970) 113834a).

[1278] J.K. Wysocki, Anomaly of the thermal–field emission and total–energy distribution of the (012), (013) and (023) tungsten faces, Phys. Rev. B 28 (1983) 834–841.

[1279] T.E. Madey, Adsorption of oxygen on W(100): Adsorption kinetics and electron stimulated desorption, Surf. Sci. 33 (1972) 355–376.

[1280] Ya.P. Zingerman, V.A. Ishchuk, T.A. Krutilina, Some characteristics of the interaction of oxygen with the surface of a tungsten single crystal, Sov. Phys.—Solid State 7 (1966) 2078–2079.

[1281] R.D. Young, H.F. Clark, Anomalous work function of the tungsten (110) plane, Appl. Phys. Lett. 9 (1966) 265–268.

[1282] F.G. Allen, Private communication (see Ref. [145]).

[1283] J.A. Becker, Study of surfaces by using new tools, Solid State Phys. 7 (1958) 379–424 (Chem. Abstr. 53 (1959) 19585g).

[1284] J.M. Houston, Field emission from a tungsten single crystal as a function of electric field and temperature (Ph.D. thesis), MIT, 1955, (see Refs. [13,808]).

[1285] E.H. Taylor, S. Datz, Study of chemical reaction mechanisms with molecular beams: The reaction of K with HBr, J. Chem. Phys. 23 (1955) 1711–1718.

[1286] R.C.L. Bosworth, Contact potential difference as a tool in the study of adsorption, J. Proc. R. Soc. N. S. Wales 79 (1946) 53–62 (Chem. Abstr. 40 (1946) 4932₁).

[1287] J.-L. Desplat, Thermionic performance of rhenium emitters, AIP Conf. Proc. 746 (2005) 910–917 (Chem. Abstr. 143 (2005) 334640a).

[1288] E.M. Savitskii, I.V. Burov, L.N. Litvak, V.P. Polyakova, E.M. Khorlin, Thermionic emission properties of an iridium single crystal, in: 3rd Monokrist. Tugoplavkikh Redk. Metal., Mater. Vses. Soveshch., 1968, pp. 81–85 (Chem. Abstr. 75 (1971) 123785r).

[1289] J. Küppers, H. Michel, F. Nitschké, K. Wandelt, G. Ertl, Xenon adsorption as a tool for local surface structure determination at Ir(100) surfaces, Surf. Sci. 89 (1979) 361–369.

[1290] T. Hansson, J.B.C. Pettersson, L. Holmlid, Rate constants for cesium ion and atom desorption on iridium with graphite islands: Parallel processes studied by field reversal, Surf. Sci. 253 (1991) 345–352.

[1291] W. Sander, Thesis, Fritz–Haber Institute (see Ref. [429]).

[1292] S. Moré, W. Berndt, A.M. Bradshaw, R. Stumpf, Ordered phases of potassium on Pt{111}: Experiment and theory, Phys. Rev. B 57 (1998) 9246–9254.

[1293] P.J. Feibelman, Energetics of steps on Pt(111), Phys. Rev. B 52 (1995) 16845–16854.

[1294] J. Marien, Field emission study of hydrogen adsorption on (111), (110), (102) platinum surfaces, Bull. Soc. R. Sci. Liége 45 (1976) 103–116 (Chem. Abstr. 85 (1976) 149434g).

[1295] K. Möller, L. Holmlid, An electron emission study of a graphite covered platinum emitter for thermionic energy conversion: Dissolution of carbon into the bulk of the metal, Appl. Surf. Sci. 29 (1987) 474–478.

[1296] Y. Liang, J. Curless, C.J. Tracy, D.C. Gilmer, J.K. Schaeffer, D.H. Triyoso, P.J. Tobin, Interface dipole and effective work function of Re in Re/HfO₂/SiOₓ/n–Si gate stack, Appl. Phys. Lett. 88 (2006) 072907/1–3.

[1297] D. Pescia, F. Meier, Spin polarized photoemission from gold using circularly polarized light, Surf. Sci. 117 (1982) 302–309.

[1298] A. Siokou, V. Papaefthimiou, S. Kennou, A study of the conjugated Ooct–OPV5 oligomer/gold interface using photoelectron spectroscopy, Surf. Sci. 482–485 (2001) 1186–1191.

[1299] G.H. Kwei, J.A. Norris, D.R. Herschbach, Molecular beam kinetics: Reactions of K atoms with alkyl iodides, J. Chem. Phys. 52 (1970) 1317–1331.

[1300] J. Pelletier, C. Pomot, Work function of sintered lanthanum hexaboride, Appl. Phys. Lett. 34 (1979) 249–251.

[1301] H. Ahmed, A.N. Broers, Lanthanum hexaboride electron emitter, J. Appl. Phys. 43 (1972) 2185–2192.

[1302] G.A. Kudintseva, B.M. Tsarev, Emission properties of the hexaborides of certain rare earth metals, Radio Eng. Electr. Phys. 3 (1958) 182–185.

[1303] A.E. Bell, C.J. Bennette, R.W. Strayer, L.W. Swanson, Single Crystal Clean Work Functions and the Behavior of Various Adsorbates on Metal Surfaces, NASA–Lewis, Contract No. NAS 3–11820, 1970, 112 pp. (see Refs. [358,783]).

[1304] L.W. Swanson, L.C. Crouser, Total energy distribution of field emitted electrons and single crystal face work functions for Mo, in: 14th Field Emission Symp., Washington, 1967, 1 p (see Ref. [783]).

[1305] H. Arnolds, Ph.D. thesis, University of Marburg, 1996 (see Ref. [345]).

[1306] M. Deak, Activation of tantalum and platinum by thorium and thoria, Brown Boveri Rev. 53 (1966) 466–468 (Chem. Abstr. 66 (1967) 119792n).

[1307] L.W. Swanson, A.E. Bell, L.C. Crouser, Single–plane studies of oxygen adsorbed on tungsten by probe field–emission techniques, in: 27th Annu. Conf. Phys. Electron. Top. Conf. Amer. Phys. Soc., 1967, pp. 54–62, (Chem. Abstr. 70 (1969) 62273v).

[1308] L. Esaki, Electrical resistivity and thermionic emission of silicon, J. Phys. Soc. Japan 8 (1953) 347–349.

[1309] W. Mayerhof, Contact potential difference in silicon crystal rectifiers, Phys. Rev. 71 (1947) 727–735.

[1310] A.H. Smith, Temperature dependence of the work function of semiconductors, Phys. Rev. 75 (1949) 953–958.

[1311] H.P. Bonzel, Alkali–metal–affected adsorption of molecules on metal surfaces, Surf. Sci. Rep. 8 (1987) 43–125.

[1312] J. Hölzl, F.K. Schulte, Work function of metals, Springer Tracts Modern Phys. 85 (1979) 1–150.

[1313] H. Wagner, Physical and chemical properties of stepped surfaces, Springer Tracts Modern Phys. 85 (1979) 151–221.

[1314] G.N. Derry, P.N. Ross, High coverage states of oxygen adsorbed on Pt(100) and Pt(111) surfaces, Surf. Sci. 140 (1984) 165–180.

[1315] P.R. Norton, P.E. Bindner, K. Griffiths, The adsorption of oxygen on Pt(100)–(1×1) and hex surfaces at 123 K, J. Vac. Sci. Technol. A 2 (1984) 1028–1031.

[1316] C.R. Helms, H.P. Bonzel, S. Kelemen, The effect of the surface structure of Pt on its electronic properties and the adsorption of CO, O₂, and H₂: A comparison of Pt(100)–(5×20) and Pt(100)–(1×1), J. Chem. Phys. 65 (1976) 1773–1782.

[1317] W.H. Weinberg, D.R. Monroe, V. Lampton, R.P. Merrill, Interaction of H₂ and O₂ on platinum (111), J. Vac. Sci. Technol. 14 (1977) 444.

[1318] H. Niehus, G. Comsa, Surface and subsurface oxygen adsorbed on Pt(111), Surf. Sci. 93 (1980) L147–L150.

[1319] J. Topping, On the mutual potential energy of a plane network of doublets, Proc. R. Soc. Lond. Ser. A 114 (1927) 67–72.

[1320] J.D. Levine, E.P. Gyftopoulos, Adsorption physics of metallic surfaces partially covered by metallic particles. I. Atom and ion desorption energies, Surf. Sci. 1 (1964) 171–193.

[1321] J.E. White, Thermionic properties of tungsten in iodide vapors, Surf. Sci. 7 (1967) 93–108.

[1322] N. Sasaki, K. Kubo, M. Asano, S. Magari, Surface ionization and thermoelectronic property of uranium dioxide, Mass Spectrosc. 17 (1969) 745–753 (Chem. Abstr. 73 (1970) 71067v).

[1323] J.F. Garvey, A. Kuppermann, Total scattering, surface ionization, and photoionization of a beam of H₃ metastable molecules, J. Chem. Phys. 86 (1987) 6766–6781.

[1324] J.M. Schroeer, T.N. Rhodin, R.C. Bradley, A quantum–mechanical model for the ionization and excitation of atoms during sputtering, Surf. Sci. 34 (1973) 571–580.

[1325] P. Dyer, R.G.H. Robertson, A surface ionization source for beam energy calibration, Nucl. Instrum. Methods 189 (1981) 351–356.

[1326] M.L. Yu, N.D. Lang, Mechanisms of atomic ion emission during sputtering, Nucl. Instrum. Methods B 14 (1986) 403–413.

[1327] G.D. Alton, Ion sources for accelerators in materials research, Nucl. Instrum. Methods B 73 (1993) 221–288.

[1328] G.D. Alton, M.T. Johnson, G.D. Mills, A simple positive/negative surface ionization source, Nucl. Instrum. Methods A 328 (1993) 154–159.

[1329] P.U. Andersson, J.B.C. Pettersson, Ionization of water clusters by collisions with graphite surfaces, Z. Phys. D 41 (1997) 57–62.

[1330] E.K. Stefanakos, A.A. Fadl, R.F. Tinder, Desorption of Na and K from niobium, Surf. Sci. 28 (1971) 221–228.

[1331] R.V. Hill, E.K. Stefanakos, R.F. Tinder, Thermal desorption of Na and K from α iron, J. Appl. Phys. 43 (1972) 1976–1979.

[1332] R. Müller, H.-W. Wassmuth, Desorption kinetics of alkaline earth ad–particles on tungsten with variation of the oxygen surface coverage, Surf. Sci. 34 (1973) 249–267.

[1333] A. Latuszynski, V.I. Raiko, Studies of the ion source with surface–volume ionization, Nucl. Instrum. Methods 125 (1975) 61–66.

[1334] B. Rasser, M. Remy, Excitation partition functions for atomic and ionic uranium: Application to surface ionization, Int. J. Mass Spectrom. Ion Phys. 21 (1976) 159–163.

[1335] C.H. Wu, The formation of the LiH molecule on polycrystalline molybdenum, J. Chem. Phys. 66 (1977) 4400–4404.

[1336] J. Münzel, H. Wollnik, B. Pfeiffer, G. Jung, A high–temperature ion source for the on–line separator OSTIS, Nucl. Instrum. Methods 186 (1981) 343–347.

[1337] F. Touchard, J. Biderman, M. de Saint Simon, C. Thibault, G. Huber, M. Epherre, R. Klapisch, Production of ionic and atomic beams of alkaline elements, Nucl. Instrum. Methods 186 (1981) 329–334.

[1338] R.L. Gordon, Kinetics of the surface ionization of plutonium on carburized rhenium, Int. J. Mass Spectrom. Ion Processes 55 (1983/1984) 31–46.

[1339] N. Ikeda, Y. Shirakabe, J. Tanaka, T. Nomura, S. Ohkawa, S. Takaku, M. Oyaizu, H. Kawakami, I. Katayama, T. Shinozuka, Study of a thick target surface ionizer at INS, Nucl. Instrum. Methods B 70 (1992) 150–155.

[1340] T. Suzuki, H. Iwabuchi, K. Takahashi, M. Nomura, M. Okamoto, Y. Fujii, Chemical form effects on the surface ionization of lithium halides, Int. J. Mass Spectrom. Ion Processes 145 (1995) 131–137.

[1341] Y. Kawai, M. Nomura, H. Murata, T. Suzuki, Y. Fujii, Surface ionization of alkali–earth iodides in double–filament system, Int. J. Mass Spectrom. 206 (2001) 1–5.

[1342] M.L. Yu, N.D. Lang, Direct evidence of electron tunneling in the ionization of sputtered atoms, Phys. Rev. Lett. 50 (1983) 127–130.

[1343] M.J. Vasile, Velocity dependence of secondary–ion emission, Phys. Rev. B 29 (1984) 3785–3794.

[1344] H. Gnaser, Initial stages of cesium incorporation on keV–Cs^+–irradiated surfaces: Positive–ion emission and work–function changes, Phys. Rev. B 54 (1996) 17141–17146.

[1345] I.A. Wojciechowski, P. Bertrand, M.V. Medvedeva, V.Kh. Ferleger, The degree of positive ionization of sputtered metal clusters, Nucl. Instrum. Methods B 179 (2001) 32–36.

[1346] T. Wirtz, H.-N. Migeon, H. Scherrer, Useful yields of MCs_x^+ clusters: A cesium concentration–dependent study on the cation mass spectrometer (CMS), Int. J. Mass Spectrom. 225 (2003) 135–153.

[1347] T. Wirtz, H.-N. Migeon, Optimization of SIMS analyses performed in the MCs_x^+ mode by using an *in situ* deposition of neutral Cs, Surf. Sci. 557 (2004) 57–72.

[1348] P. Philipp, T. Wirtz, H.-N. Migeon, H. Scherrer, Cation mass spectrometer (CMS): Recent developments for quantitative analyses of positive and negative secondary ions, Appl. Surf. Sci. 231–232 (2004) 754–757.

[1349] V.Kh. Ferleger, Positive ionization probabilities of sputtered Ag and Ta clusters, Appl. Surf. Sci. 231–232 (2004) 94–96.

[1350] T. Wirtz, H.-N. Migeon, Optimization of SIMS analyses performed in the MCs_x^+ mode by using an *in situ* deposition of Cs, Appl. Surf. Sci. 231–232 (2004) 743–748.

[1351] H. Kawano, Effective work functions for ionic and electronic emissions from mono– and polycrystalline surfaces, Prog. Surf. Sci. 83 (2008) 1–165.

[1352] G.A. Haas, Work function and secondary emission, in: D.E. Gray (Ed.), American Institute of Physics Handbook, 3rd ed., McGraw–Hill, New York, 1972, pp. **9**–172/**9**–183.

[1353] R.C. Weast (Ed.), Electron work function of the elements, in: Handbook of Chemistry and Physics, 52nd ed., CRC Press, Boca Raton, 1971–1972, pp. **E**–69/**E**–71.

[1354] V.S. Fomenko, Emission Properties of Materials: Handbook, 4th ed., Naukova Dumka, Kiev, USSR, 1981, 339 pp.

[1355] H.B. Michaelson, Work function of the elements, J. Appl. Phys. 21 (1950) 536–540.

[1356] L.N. Dobretsov, T.L. Matskevich, Work function of metals, Sov. Phys. Tech. Phys. 11 (1967) 1081–1088.

[1357] G.S. Samsonov, Yu.B. Paderno, V.S. Fomenko, Sov. Phys. Tech Phys. 11 (1967) 1070–1080.

[1358] W.M. Haynes (Ed.), Electron work function of the elements, in: CRC Handbook of Chemistry and Physics, 97th ed., CRC Press, Boca Raton, 2016–2017, p. **12**–123.

[1359] D.R. Lide (Ed.), Electron work function of the elements, in: CRC Handbook of Chemistry and Physics, 82nd ed., CRC Press, Boca Raton, 2001–2002, p. **12**–130.

[1360] V.S. Fomenko, I.A. Podchernyaeva, Emission and Adsorption Properties of Substances and Materials: Handbook, Atomizdat, Moscow, 1975, 320 pp.

[1361] C. Agte, H. Alterthum, K. Becker, G. Hyne, K. Moers, Physical and chemical properties of rhenium, Z. Anorg. Allg. Chem. 196 (1931) 129–159.

[1362] I. Ameiser, Thermionic emission of metals in the neighborhood of their melting points, Z. Phys. 69 (1931) 111–140.

[1363] A.J. Ahearn, The effect of temperature on the emission of electron field currents from molybdenum and tungsten, Phys. Rev. 43 (1933) 1058.

[1364] H. Alterthum, K. Krebs, R. Rompe, The ionization of sodium and cesium vapor on glowing tungsten and rhenium surfaces, Z. Phys. 92 (1934) 1–18.

[1365] P.A. Anderson, The contact difference of potential between tungsten and barium: The external work function of barium, Phys. Rev. 47 (1935) 958–964.

[1366] P.A. Anderson, The contact difference of potential between tungsten and silver: The external work function of silver, Phys. Rev. 49 (1936) 320–323.

[1367] P.A. Anderson, The Volta potential between barium and magnesium: An experimental test of the relation between work functions and Volta potential, Phys. Rev. 52 (1937) 253.

[1368] P.A. Anderson, The contact difference of potential between barium and magnesium, Phys. Rev. 54 (1938) 753–757 (see Ref. [13]).

[1369] P.A. Anderson, The contact difference of potential between silver films on glass and on rocksalt, Phys. Rev. 56 (1939) 850.

[1370] P.A. Anderson, The contact difference of potential between barium and zinc: The external work function of zinc, Phys. Rev. 57 (1940) 122–127.

[1371] L. Apker, E. Taft, J. Dickey, Photoelectric emission and contact potentials of semiconductors, Phys. Rev. 74 (1948) 1462–1474.

[1372] T. Arizumi, On the thermionic constants of the polycrystalline metal (II), J. Phys. Soc. Japan 3 (1948) 186–190.

[1373] U. Arifov, A.Kh. Ayukhanov, V.M. Lovtsov, Determination of the absolute ionization coefficient on the surface of heated tungsten, Dokl. Akad. Nauk 68 (1949) 461–463.

[1374] P.A. Anderson, The work function of lithium, Phys. Rev. 75 (1949) 1205–1207.

[1375] L. Apker, E. Taft, J. Dikey, Some semimetallic characteristics of the photoelectric emission from As, Sb, and Bi, Phys. Rev. 76 (1949) 270–272.

[1376] L.L. Antes, N. Hackerman, Contact potential variations on freshly condensed metal films at low pressures, J. Appl. Phys. 22 (1951) 1395–1398.

[1377] I.S. Andreev, Investigation of electron emission from metal in the range of transition from cold emission to thermionic field emission, Zh. Tekh. Fiz. 22 (1952) 1428–1441.

[1378] I.S. Andreyev, Zh. Tekh. Fiz. 23 (1953) 849–852 (see Ref. [12]).

[1379] R. Asadullin, C.N. Shuppe, Work function of different faces of a nickel single crystal, Zh. Tekh. Fiz. 24 (1954) 205–215.

[1380] P.A. Anderson, Work function of cadmium, Phys. Rev. 98 (1955) 1739–1740 (see Ref. [349]).

[1381] P.A. Anderson, A.L. Hunt, Work function of lead, Phys. Rev. 102 (1956) 367–368.

[1382] F.G. Allen, A.B. Fowler, Variation of contact potential with crystal face for germanium, J. Phys. Chem. Solids 3 (1957) 107–114.

[1383] K. Albien, Diplomarbeit, Hannover, 1959 (see Ref. [3052]).

[1384] F.G. Allen, J. Eisinger, H.D. Hagstrum, J.T. Law, Cleaning of silicon surfaces by heating in high vacuum, J. Appl. Phys. 30 (1959) 1563–1571.

[1385] P.A. Anderson, A.L. Hunt, Effect of oxygen on the work function of barium, Phys. Rev. 115 (1959) 550–552.

[1386] J.S. Anderson, D.F. Klemperer, Photoelectric measurements on nickel and nickel oxide films, Proc. R. Soc. A 258 (1960) 350–376.

[1387] F.G. Allen, Field emission from silicon and germanium: Field desorption and surface migration, J. Phys. Chem. Solids 19 (1961) 87–99.

[1388] F.G. Allen, G.W. Gobeli, Work function and photoelectric threshold for atomically clean silicon, Bull. Am. Phys. Soc. 6 (1961) 421.

[1389] K. Albien, Unpublished (see Ref. [3052]).

[1390] R.L. Aamodt, L.J. Brown, B.D. Nichols, Thermionic emission from molybdenum in vapors of cesium and cesium fluoride, J. Appl. Phys. 33 (1962) 2080–2085 (see Ref. [2465]).

[1391] J.R. Arthur Jr., R.S. Hansen, Study of the adsorption of hydrogen, ethane, ethylene, and acetylene on iridium by field emission microscopy, J. Appl. Phys. 36 (1962) 2062–2071.

[1392] I. Ames, R.L. Christensen, Anomalous photoelectric emission from nickel, IBM J. Res. Dev. 7 (1963) 34–39 (Chem. Abstr. 58 (1963) 9725g).

[1393] S.G. Andresen, Surface ionization of lithium fluoride and thallium on tungsten, rhenium, and platinum surfaces (Ph.D. thesis), Univ. of Colorado, 1963, 67 pp.

[1394] J. Anderson, W.E. Danforth, Critical phenomena with thorium adsorbed on single crystal tungsten, J. Electrochem. Soc. 111 (1964) 1297–1298.

[1395] J.R. Arthur Jr., Surface structure and surface migration of germanium by field emission microscopy, J. Phys. Chem. Solids 25 (1964) 583–591.

[1396] F.G. Allen, G.W. Gobeli, Energy structure in photoelectric emission from Cs–covered silicon and germanium, Phys. Rev. 144 (1966) 558–575.

[1397] E.I. Adirovich, L.M. Gold'shtein, Determination of the work function and blackbody coefficient of boron and silicon by the intrinsic thermometer method, Sov. Phys.—Solid State 9 (1967) 984–985.

[1398] T. Alleau, A.M. Shroff, Work function distribution of thermo–emissive refractory layers, in: 27th Ann. Conf. Phys. Electron. Top. Conf. Amer. Phys. Soc., 1967, pp. 104–116 (Chem. Abstr. 70 (1969) 52038h).

[1399] S.D. Argade, The potential of zero charge (Ph.D. thesis), Univ. Pennsylvania, 1968, 408 pp. (Diss. Abstr. B 29 (1969) 3694–3695) (see Ref. [3264]).

[1400] U.A. Arifov, R.R. Rakhimov, Kh. Dzhurakulov, Potential and kinetic electron emission from the (110) and (111) faces of a Mo single crystal, Sov. Phys.—Solid State 10 (1968) 925–929.

[1401] T. Alleau, Electron emission of molybdenum–strontium surfaces, in: Round Table Conf. Surf. Phenom. Thermion. Emitters, 1969, pp. 54–56 (Chem. Abstr. 74 (1971) 17061w).

[1402] T. Alleau, Experimental Langmuir S–curves for tungsten(110)–cesium and molybdenum(110)–strontium, in: Rept. Thermion. Convers. Spec. Conf. Carmel, USA, 1969, pp. 9–17.

[1403] J.S. Anderson, E.A. Faulkner, D.F. Klemperer, Analysis of composite spectral–sensitivity functions, Austral. J. Phys. 12 (1969) 469–470.

[1404] J.R. Anderson, N. Thompson, Study of adsorption of titanium on tungsten and rhenium by field electron emission, Surf. Sci. 26 (1971) 397–414.

[1405] J.R. Anderson, N. Thompson, Adsorption of Cl_2 on titanium studied by field emission microscopy, Surf. Sci. 28 (1971) 84–94.

[1406] U.V. Azizov, T.A. Karabaev, Emission and adsorption properties of cesium films on the (110), (112), (100) and (111) faces of a large tantalum single crystal, Izv. Akad. Nauk Uzb.SSR, Ser. Fiz.-Mat. Nauk 16 (3) (1972) 78–79.

[1407] U.V. Azizov, T.A. Karabaev, Emission and adsorption properties of cesium films on the (110), (112), (100) and (111) faces of a large molybdenum single crystal, Izv. Akad. Nauk Uzb.SSR, Ser. Fiz.-Mat. Nauk 16 (2) (1972) 81–83.

[1408] J.A. Appelbaum, D.R. Hamann, Self–consistent electronic structure of solid surfaces, Phys. Rev. B 6 (1972) 2166–2177.

[1409] D. Azizova, U.V. Azizov, T.A. Karabaev, Sh.A. Nizamutdinova, Thermoemission and adsorption properties of cesium–barium films on the (110) face of molybdenum and niobium single crystals, in: Kratk. Soderzh. Dokl.-Vses. Konf. Emiss. Elektron., 15th (1973), Vol. 1, 1973, pp. 24–25 (Chem. Abstr. 83 (1975) 156512t).

[1410] H. Alder, M. Campagna, H.C. Siegmann, Spin polarization of photoelectrons from cesiated Fe, Co, and Ni, Phys. Rev. B 8 (1973) 2075–2082.

[1411] S. Andersson, W. Jostell, Monolayer K–films on Ni(100). I. Structure and work function, Solid State Commun. 13 (1973) 829–832.

[1412] P. Ascarelli, G. Missoni, Secondary electron emission and the determination of the vacuum level in ESCA, J. Electr. Spectrosc. Rel. Phenom. 5 (1974) 417–435.

[1413] S. Andersson, U. Jostell, Electron structure of Na and K adsorbed on Ni(100), Surf. Sci. 46 (1974) 625–640.

[1414] G.P. Alldredge, L. Kleinman, Self–consistent charge density and surface electronic states for the (001) face of lithium, Phys. Rev. B 10 (1974) 559–573.

[1415] A.N. Arsen'eva-Geil', A.A. Berezin, E.V. Mel'nikova, Photoelectric emission study of β–rhombohedral boron, Sov. Phys.—Solid State 17 (1975) 1624.

[1416] M. Abon, G. Bergeret, B. Tardy, Field emission study of ammonia adsorption and catalytic decomposition on individual molybdenum planes, Surf. Sci. 68 (1977) 305–311.

[1417] S. Andersson, J.B. Pendry, P.M. Echenique, Low energy electron diffraction from Na(110) and $Na_2O(111)$ surfaces, Surf. Sci. 65 (1977) 539–551.

[1418] L. Armand, J.L. Bouillot, L. Gaudart, Photoemission of thin and ultrathin films of calcium, Surf. Sci. 86 (1979) 75–82.

[1419] A. Kirkland, P.D. Brown (Eds.), The electron, in: Proc. Int. Centenn. Symp. Electron, IOM Communications Ltd., London, 1998.

[1420] U.V. Azizov, B.É. Égamberdiev, A. Kashetov, Temporal variations in the work function and adsorption of Cs atoms on the (110) face of Mo determined by Auger spectroscopy, Sov. Phys. Tech. Phys. 28 (1983) 98–99.

[1421] O.Z. Al-Rawi, I.P. Jones, A field emission study of silver on rhenium, Surf. Sci. 124 (1983) 220–240.

[1422] E.V. Albano, S. Daiser, G. Ertl, R. Miranda, K. Wandelt, N. Garcia, Nature of surface–enhanced–Raman scattering active sites on coldly condensed Ag films, Phys. Rev. Lett. 51 (1983) 2314–2317.

[1423] C. Argile, M.-G. Barthes-Labrousse, G.E. Rhead, Secondary electron emission changes due to metal monolayer adsorption, Surf. Sci. 138 (1984) 181–190.

[1424] H. Asonen, C. Barnes, A. Salokatve, A. Vuoristo, The growth mode of Cu overlayers on Pd(100), Appl. Surf. Sci. 22/23 (1985) 556–564.

[1425] M. Abon, J. Billy, J.C. Bertolini, B. Tardy, Carbon on Pt(111): Characterization and influence on the chemisorptive properties, Surf. Sci. 167 (1986) 1–17.

[1426] C. Argile, G.E. Rhead, The coadsorption of cesium and potassium on Ag(111): Characterization by Auger electron spectroscopy and work function changes; adsorption of oxygen, Surf. Sci. 203 (1988) 175–185.

[1427] C. Astaldi, K. Jacobi, Photoemission from xenon clusters on barium, Surf. Sci. 200 (1988) 15–25.

[1428] G.C. Aers, J.E. Inglesfield, Electric field and Ag(001) surface electronic structure, Surf. Sci. 217 (1989) 367–383.

[1429] M. Azizan, T.A. Nguyen Tan, R. Cinti, R. Baptist, G. Chauvet, Interface formation of W evaporated on Si(111)(7×7), Surf. Sci. 178 (1986) 17–26.

[1430] M. Azizan, T.A. Nguyen Tan, J.Y. Veuillen, First stage of the formation of refractory metal thin films on Si(111), Vacuum 41 (1990) 1132–1134.

[1431] C. Argile, G.E. Rhead, Adsorption of potassium on Cu(100) and coadsorption with oxygen, Surf. Sci. 279 (1992) 244–250.

[1432] I.A. Abrikosov, H.L. Skriver, Self–consistent linear–muffin–tin–orbitals coherent–potential technique for bulk and surface calculations: Co–Ni, Ag–Pd, and Au–Pt random alloys, Phys. Rev. B 47 (1993) 16532–16541.

[1433] T. Ando, K. Shinto, M. Wada, H. Tsuda, Work function measurements of alkali–metal adsorbed metal surfaces, Sci. Eng. Rev. Doshisha Univ. 35 (1994) 91–100.

[1434] M. Aldén, B. Johansson, H.L. Skriver, Surface shift of the occupied and unoccupied $4f$ levels of the rare–earth metals, Phys. Rev. B 51 (1995) 5386–5396.

[1435] S. Andersson, M. Persson, J. Harris, Physisorption energies: Influence of surface structure, Surf. Sci. 360 (1996) L499–L504.

[1436] P.H. Acioli, D.M. Ceperley, Diffusion Monte Carlo study of jellium surfaces: Electronic densities and pair correlation functions, Phys. Rev. B 54 (1996) 17199–17207.

[1437] D.J. Alberas-Sloan, J.M. White, Low–energy electron irradiation of methane on Pt(111), Surf. Sci. 365 (1996) 212–228.

[1438] H. Adachi, K. Ashihara, Y. Saito, H. Nakane, Reduction of work function on a W(100) field emitter due to co–adsorption of Si and Ti, J. Vac. Sci. Technol. B 16 (1998) 875–879.

[1439] C. Argile, Growth and structure of lead overlayers on nickel(100): Thermal stability of the adlayer, Surf. Sci. 398 (1998) 221–230.

[1440] A.A. Aliev, O.A. Makhmudov, Charge state of alkali atoms scattered by Mo and W surfaces, Vacuum 51 (1998) 393–396.

[1441] H. Ago, Th. Kugler, F. Cacialli, K. Petritsch, R.H. Friend, W.R. Salaneck, Y. Ono, T. Yamabe, K. Tanaka, Work function of purified and oxidized carbon nanotubes, Synth. Met. 103 (1999) 2494–2495.

[1442] V.V. Afanas'ev, M. Houssa, A. Stesmans, M.M. Heyns, Band alignments in metal–oxide–silicon structures with atomic–layer deposited Al_2O_3 and ZrO_2, J. Appl. Phys. 91 (2002) 3079–3084 (see Ref. [3519]).

[1443] J. Almanstötter, B. Eberhard, K. Günther, T. Hartmann, Sodium monolayers on thermionic cathodes, J. Phys. D 35 (2002) 1751–1756.

[1444] R. Arafune, K. Hayashi, S. Ueda, S. Ushioda, Energy loss of photoelectrons by interaction with image charge, Phys. Rev. Lett. 92 (2004) 247601/1–4.

[1445] B.B. Alchagirov, O.I. Kurshev, T.M. Taova, Kh.B. Khokonov, Electron work function in alloys from the tin–lead system, Tech. Phys. 51 (2006) 1624–1626.

[1446] R. Atta-Fynn, A.K. Ray, Ab initio full–potential fully relativistic study of atomic carbon, nitrogen, and oxygen chemisorption on the (111) surface of δ–Pu, Phys. Rev. B 75 (2007) 195112/1–13.

[1447] R. Atta-Fynn, A.K. Ray, Relaxation of the (111) surface of δ–Pu and effects on atomic adsorption: An *ab initio* study, Physica B 400 (2007) 307–316.

[1448] R. Atta-Fynn, A.K. Ray, Atomic adsorption on the (020) surface of α–Pu: A density functional study, Phys. Rev. B 77 (2008) 085105/1–11.

[1449] L.F.N. Ah Qune, H. Akiyama, T. Nagahiro, K. Tamada, A.T.S. Wee, Reversible work function changes induced by photoisomerization of asymmetric azobenzene dithiol self–assembled monolayers on gold, Appl. Phys. Lett. 93 (2008) 083109/1–3.

[1450] J.A. Becker, Thermionic and adsorption characteristics of caesium on tungsten and oxidized tungsten, Phys. Rev. 28 (1926) 341–361.

[1451] H. Bomke, Photoelectric properties of cadmium, especially the influence of gases, Ann. Phys. 10 (1931) 579–615.

[1452] J.J. Brady, The photoelectric properties of alkali metal films as a function of their thickness, Phys. Rev. 41 (1932) 613–626.

[1453] W.H. Brattain, J.A. Becker, Thermionic and adsorption characteristics of thorium on tungsten, Phys. Rev. 43 (1933) 428–450.

[1454] N.E. Bradbury, Energy distribution of photoelectrons from zinc surfaces, Phys. Rev. 43 (1933) 502.

[1455] A.K. Brewer, The effect of adsorbed oxygen on the photoelectric emissivity of silver, J. Am. Chem. Soc. 56 (1934) 1909–1913.

[1456] J.J. Brady, Energy distribution of photoelectrons as a function of the thickness of a potassium film, Phys. Rev. 46 (1934) 768–772.

[1457] J.J. Brady, V.P. Jacobsmeyer, Photoelectric properties of sodium films on aluminum, Phys. Rev. 49 (1936) 670–675.

[1458] J. Bardeen, Theory of the work function. II. The surface double layer, Phys. Rev. 49 (1936) 653–663.

[1459] R.C.L. Bosworth, E.K. Rideal, Studies in contact potentials: The condensation of potassium and sodium on tungsten, Proc. R. Soc. A 162 (1937) 1–31.

[1460] R.C.L. Bosworth, Contact potential of nickel, Trans. Faraday Soc. 35 (1939) 397–402.

[1461] A. Blanc-Lapierre, Determination of the photoelectric threshold of copper, C. R. Acad. Sci. Paris 215 (1942) 321–323.

[1462] A.S. Bhatnagar, Proc. Nat. Acad. Sci. India A 14 (1944) 5 (see Refs. [285,633]).

[1463] J. Becker, The use of the field emission electron microscope in adsorption studies of W on W and Ba on W, Bell Syst. Tech. J. 30 (1951) 907–932.

[1464] J.P. Barbour, W.W. Dolan, J.K. Trolan, E.E. Martin, W.P. Dyke, Space–charge effects in field emission, Phys. Rev. 92 (1953) 45–51.

[1465] V.G. Bol'shov, L.N. Dobretsov, Thermionic emission of copper at the melting point, Dokl. Akad. Nauk SSSR 98 (1954) 193–196.

[1466] V.G. Bol'shov, Thermionic emission at the solid–liquid transition point, Sov. Phys. Tech. Phys. 1 (1956) 1123–1133.

[1467] F. Baumann, The photoeffect in thin metal layers, Z. Phys. 158 (1960) 607–622.

[1468] V.G. Bol'shov, L.V. Vasil'eva, G.N. Pautova, Emission properties of silicon treated in cesium vapors, Sov. Phys.—Solid State 2 (1961) 1783–1785.

[1469] H. Busse, Dissertation, TU Hannover, 1962 (see Ref. [1153]).

[1470] Z.P. But, Photoelectron emission of Ge bombarded by electrons, Radiotekhn. Elektron. 8 (1963) 814–820.

[1471] B.E. Barnaby, T.E. Madey, A.A. Petrauskas, E.A. Coomes, Adsorption and migration of Sr on W, J. Appl. Phys. 35 (1964) 1759–1763.

[1472] N.G. Ban'kovskii, B.N. Formozov, Investigation of surface ionization of alkali metal atoms on the surface of silicon single crystals, Bull. Acad. Sci. USSR, Ser. Phys. 28 (1964) 1420–1423.

[1473] C.N. Berglund, W.E. Spicer, Photoemission studies of copper and silver: Experiment, Phys. Rev. 136 (1964) A1044–A1064.

[1474] G.-A. Boutry, R. Évrard, J.-C. Richard, Photoelectric properties of pure vacuum–prepared and –stored cesium, C. R. Acad. Sci. Paris 258 (1964) 143–146.

[1475] R. Bedos, Effect of the magnetic induction on the work functions of metals, C. R. Acad. Sci. Paris 259 (1964) 1695–1697.

[1476] B.H. Blott, B.J. Hopkins, Work function measurements on the sublimate from uranium carbide, Br. J. Appl. Phys. 16 (1965) 1215–1216.

[1477] P. Batzies, The workfunction–distribution of different surfaces of refractory metals, in: Int. Conf. Thermion. Electr. Power Generat. London, 1965, pp. 1–5.

[1478] G. Busch, A. Madjid, Emission of electrons from hot Si surfaces, Phys. Kondens. Mater. 4 (1965) 131–160.

[1479] B.V. Bondarenko, F.G. Tsukrov, The thermionic properties of the tungsten–hafnium system, Radiotekhn. Elekron. 10 (1965) 971–972.

[1480] B.H. Blott, B.J. Hopkins, T.J. Lee, The work function of caesium coated polycrystalline tungsten, Surf. Sci. 4 (1965) 493–496.

[1481] G.-A. Boutry, H. Dormont, R. Evrard, R. Perrin, Photoelectric properties of pure potassium, prepared and stored in ultrahigh vacuum, C. R. Acad. Sci. Paris 261 (1965) 383–386.

[1482] V.G. Bol'shov, Work function of carbides of refractory metals in cesium vapor, Sov. Phys. Tech. Phys. 11 (1966) 239–244.

[1483] A.J. Blodgett Jr., W.E. Spicer, The band structure of gadolinium: Photoemission and optical studies, in: Proc. Int. Conf. Optical Propert. and Electron. Struct. Metals and Alloys, Paris, 1965 (see Refs. [304,2943]).

[1484] D.E. Barry, B.J. Hopkins, A.J. Sargood, Some work functions of vapour deposited uranium on polycrystalline tungsten foil, Surf. Sci. 7 (1967) 365–379.

[1485] V.T. Bazanov, N.G. Ban'kovskii, O.M. Mul'tanovskaya, Thermionic emission of tungsten in a flux of barium and cesium atoms, Sov. Phys.—Solid State 10 (1968) 397–401.

[1486] N.G. Ban'kovskii, E.M. Stefanovskaya, V.P. Fedorinov, Investigation of the adsorption of potassium ions on the surface of molybdenum, Sov. Phys.—Solid State 10 (1968) 113–117.

[1487] M.E. Belyaeva, T.V. Kalish, R.Kh. Burshtein, Comparison of the differences in work functions and zero charge potentials of metals. II. Mercury–silver, Elektrokhim. 4 (1968) 862–864.

[1488] B.V. Bondarenko, V.I. Makhov, A.M. Kozlov, Structure and work function of chromium films on tungsten, Sov. Phys.—Solid State 11 (1970) 2991–2993.

[1489] G.-A. Boutry, H. Dormont, Some surface properties of pure alkali metals, Philips Tech. Rev. 30 (1969) 225–230 (Chem. Abstr. 73 (1970) 124762b).

[1490] B.H. Blott, T.J. Lee, A two frequency vibrating capacitor method for contact potential difference measurements, J. Phys. E 2 (1969) 785–788.

[1491] R.M. Broudy, Photoelectric emission from silicon, Phys. Rev. B 1 (1970) 3430–3438.

[1492] G. Bush, J. Wullschleger, Schottky effect on clean silicon surfaces, Phys. Kondens. Mater. 12 (1970) 47–71.

[1493] I. Buribaev, B.B. Shishkin, Field emission of electrons from tungsten in a magnetic field, Sov. Phys.—Solid State 12 (1971) 2678–2679.

[1494] B.V. Bondarenko, V.I. Makukha, The adsorption and electron emission of chromium films on a single tungsten crystal, Radio Eng. Electron. Phys. 15 (1970) 1280–1286.

[1495] R. Bouwman, W.M.H. Sachtler, Photoelectric study of adsorption of carbon monoxide and xenon by unordered and ordered ruthenium films, Ber. Bunsenges. Phys. Chem. 74 (1970) 1273–1277.

[1496] R.Z. Bakhtizin, I.L. Sokol'skaya, Adsorption of titanium on single crystals of p–type germanium, Sov. Phys.—Solid State 12 (1971) 2272–2276.

[1497] R. Bouwman, H.P. Van Keulen, W.M.H. Sachtler, Photoelectric studies of the adsorption of carbon monoxide on platinum films, Ber. Bunsenges. Phys. Chem. 74 (1970) 198–204.

[1498] R.J. Batt, C.H.B. Mee, A photoelectric technique for the study of adsorption: The aluminum–oxygen and aluminum–water systems, Appl. Opt. 9 (1970) 79–83.

[1499] V.Kh. Burkhanova, N.A. Gorbatyi, Thermoelectron parameters of (111) and (110) faces of tungsten single crystal coated with a germanium film, Izv. Akad. Nauk SSSR, Ser. Fiz. 35 (1971) 291–292.

[1500] L.C. Burton, A.H. Madjid, Reversible temperature induced inversion in the thermionic emission current anisotropy pattern emitted by atomically clean silicon cathodes, Phys. Chem. Solids 32 (1971) 2621–2629.

[1501] R.Z. Bakhtizin, N.V. Mileshkina, I.L. Sokol'skaya, Gold adsorption on atomically clean germanium surfaces, Sov. Phys.—Solid State 13 (1972) 3159–3161.

[1502] R.Z. Bakhtizin, N.V. Mileshkina, Effect of oxygen adsorption on the current–voltage characteristic of the field–emission current from p–Ge, Sov. Phys.—Solid State 13 (1972) 1727–1731.

[1503] A.J. Bennett, B. McCarroll, R.P. Messmer, Molecular orbital approach to chemisorption, II. Atomic H, C, N, O, and F on graphite, Phys. Rev. B 3 (1971) 1397–1406.

[1504] W.J. Baxter, Work function of tantalum carbide and the effects of adsorption and sputtering of cesium, J. Appl. Phys. 42 (1971) 2682–2688.

[1505] M.E. Belyaeva, T.V. Kalish, R.Kh. Burshtein, Effect of chemisorbed oxygen on the work function of silver, Elekrokhim. 7 (1971) 1711–1714.

[1506] G. Busch, M. Campagna, H.C. Siegmann, Spin–polarized photoelectrons from Fe, Co and Ni, Phys. Rev. B 4 (1971) 746–750.

[1507] J. Boggio, On the formation of very thin oxide films on metals: Contact potential measurements during the oxidation of different crystallographic faces of copper, J. Chem. Phys. 57 (1972) 4738–4742.

[1508] J.M. Baker, J.M. Blakely, A study of LEED intensities from cleaved beryllium and zinc surfaces, Surf. Sci. 32 (1972) 45–77.

[1509] R. Bouwman, G.J.M. Lippits, W.M.H. Sachtler, Photoelectric investigation of the surface composition of equilibrated Ag–Pd alloys in ultrahigh vacuum and in the presence of CO, J. Catalysis 25 (1972) 350–361.

[1510] V.F. Bibik, P.G. Borzyak, G.A. Zhykov, N.G. Nakhodkin, A.F. Yatsenko, Thermoelectric and ionic emission from silicon, in: 5th Czech. Conf. Electron. Vac. Phys., vol. 1, 1972, Ia–16, 2 pp. (Chem. Abstr. 83 (1975) 51762w).

[1511] M. Bacal, J.L. Desplat, T. Alleau, Adsorption of oxygen on the (100) plane of tungsten, J. Vac. Sci. Technol. 9 (1972) 851–856.

[1512] J. Bösenberg, Optical constants of lithium in the region of 2–3.8 eV determined by the excitation of surface plasma oscillations, Phys. Lett. 41 A (1972) 185–186.

[1513] B.G. Baker, B.B. Johnson, Surface potentials of xenon adsorbed on nickel, J. Vac. Sci. Technol. 9 (1972) 930–933.

[1514] G. Brodén, UV–photoemission measurements on erbium and samarium, Phys. Kondens. Mater. 15 (1972) 171–190.

[1515] B.V. Bondarenko, Emission properties of chromium and cathodes from it, in: 15th Vses. Konf. Emiss. Elektron., vol. 2, 1973, pp. 70–71 (Chem. Abstr. 83 (1975) 187054z).

[1516] M. Bujor, Work function variation across the surface of tungsten and vitreous carbon, Astrophys. Space Sci. Libr. 37 (1973) 323–330 (Chem. Abstr. 83 (1975) 36434x).

[1517] G.E. Becker, H.D. Hagstrum, Orbital energy spectra of CO and Hg adsorbed on Ni(100), J. Vac. Sci. Technol. 10 (1973) 31–34.

[1518] K. Bobev, V. Gaidarova, Total energy distribution of field emitted electrons from a molybdenum monocrystal covered with aluminum– and silicon oxide by means of a field emission microscope, Phys. Status Solidi (a) 23 (1974) K129–K133.

[1519] E. Bauer, H. Poppa, G. Todd, F. Bonczek, Adsorption and condensation of Cu on W single–crystal surfaces, J. Appl. Phys. 45 (1974) 5164–5175.

[1520] B.A. Boiko, D.A. Gorodetskii, A.A. Yas'ko, Structure of silicon and germanium films on the (110) face of tungsten, Sov. Phys.—Solid State 15 (1974) 2101–2106.

[1521] A. Baltog, I. Mustata, N. Betiu, A. Cormos, Emissive properties of chemical vapor deposited tungsten, Rev. Roum. Phys. 19 (1974) 713–729 (Chem. Abstr. 82 (1975) 10391k).

[1522] C.S. Bhatia, M.K. Sinha, Adsorption and surface diffusion of titanium on tungsten in a field emission microscope, Surf. Sci. 43 (1974) 369–384.

[1523] D. Briggs, Electron spectroscopic studies of the initial oxidation of zinc, Faraday Discuss. Chem. Soc. 60 (1975) 81–88.

[1524] E. Bechtold, L. Wiesberg, J.H. Block, Field electron microscopy of S_2– and H_2S–adsorption on tungsten, Z. Phys. Chem. 97 (1975) 97–112.

[1525] E. Bauer, H. Poppa, G. Todd, The early stages of condensation of lead on tungsten, Thin Solid Films 28 (1975) 19–36.

[1526] I.M. Bronshtein, I.L. Krainskii, Excitation of surface and bulk plasmons in magnesium, strontium, and copper, Sov. Phys.—Solid State 17 (1975) 778–779.

[1527] I. Buribaev, N. Talipov, Photoelectron emission of the molybdenum–cesium system in the 380–600 nm wavelength region, Nauchn. Tr., Tashk. Gos. Univ. 525 (1976) 24–26 (Chem. Abstr. 90 (1979) 160993n).

[1528] U. Bauder, K. Alex, E. Fromm, Photoelectric measurements on vapor–deposited tantalum films, Thin Solid Films 46 (1977) 229–237.

[1529] O.P. Burmistrova, G.G. Vladimirov, S.A. Shakirova, Adsorption of vanadium atoms on some tungsten faces, Sov. Phys.—Solid State 18 (1976) 1581–1583.

[1530] R.P. Bajpai, H. Kita, K. Azuma, Adsorption of water on Au and mercury on Au, Ag, Mo and Re: Measurements of the changes in work function, Japan. J. Appl. Phys. 15 (1976) 2083–2086.

[1531] C.F. Brucker, T.N. Rhodin, Oxygen chemisorption and reaction on α-Fe(100) using photoemission and low–energy electron diffraction, Surf. Sci. 57 (1976) 523–539.

[1532] G. Brodén, T.N. Rhodin, Chemisorption of CO on Ir(100) studied by photoemission, Solid State Commun. 18 (1976) 105–109.

[1533] G. Brodén, T.N. Rhodin, W. Capehart, Geometric and electronic effects in the chemisorption and reaction of acetylene, ethylene and benzene on the normal and reconstructed iridium(100) surface, Surf. Sci. 61 (1976) 143–176.

[1534] G. Brodén, T.N. Rhodin, Distortion and fragmentation of hydrocarbons chemisorbed on Ir(100), Chem. Phys. Lett. 40 (1976) 247–250.

[1535] D. Born, E. Linke, New investigation on the relation between electron emission and work function of aluminum in UHV, in: Proc. 5th Int. Symp. Exoelectr. Emiss. Dosim., 1976, pp. 265–269 (Chem. Abstr. 88 (1977) 114025j).

[1536] W. Brünger, M. Klein, Contact potential difference between Au and Ag measured by electron interferometry, Surf. Sci. 62 (1977) 317–320.

[1537] G.M. Bancroft, W. Gudat, D.E. Eastman, Photoemission studies of the outer core d level linewidths in Pb, In and Sn compounds using synchrotron radiation, J. Electron Spectrosc. Relat. Phenom. 10 (1977) 407–413.

[1538] E. Bauer, H. Poppa, G. Todd, P.R. Davis, The adsorption and early stages of condensation of Ag and Au on W single–crystal surfaces, J. Appl. Phys. 48 (1977) 3773–3787.

[1539] N.G. Ban'kovskii, K.G. Korotkov, Analysis of the change in the work function of a metal surface on simultaneous adsorption of atoms of two different elements, Sov. Phys.—Solid State 19 (1977) 1670–1671.

[1540] S.C. Barnes, K.E. Singer, A field–emission retarding–potential device for absolute work function measurements, J. Phys. E 10 (1977) 737–740.

[1541] G. Brodén, G. Gafner, H.P. Bonzel, A UPS and LEED/Auger study of adsorbates on Fe(110), Appl. Phys. 13 (1977) 333–342.

[1542] R.Kh. Burshtein, N.A. Shurmovskaya, T.V. Kalish, L.A. Larin, Effect of adsorbed gases on the surface properties of metals, Sov. Electrochem. 13 (1977) 677–681.

[1543] B.A. Boiko, D.A. Gorodetskii, Structure, electronic and dynamic properties of neodymium films on the (100) face of tungsten, Ukr. Fiz. Zh. 22 (1977) 1184–1190 (Chem. Abstr. 87 (1977) 144350h).

[1544] W. Braun, M. Neumann, M. Iwan, E.E. Koch, UPS measurements of CO chemisorbed and condensed on Rh(111) using synchrotron radiation, Phys. Status Solidi (b) 90 (1978) 525–533 (see Ref. [456]).

[1545] M.G. Burt, V. Heine, The theory of the work function of caesium suboxides and caesium films, J. Phys. C 11 (1978) 961–968.

[1546] G. Borstel, W. Braun, M. Neuman, G. Seitz, Band structure of rhodium and photoemission from its low index surfaces, Phys. Statuts Solidi (b) 95 (1979) 453–460 (see Refs. [456,1011]).

[1547] K.P. Bohnen, S.C. Ying, Electronic structure of K(100) surface by the density matrix method, Solid State Commun. 30 (1979) 301–304.

[1548] F. Bonczek, T. Engel, E. Bauer, The interaction of KCl with tungsten single crystal surfaces, Surf. Sci. 94 (1980) 57–72.

[1549] R. Błaszczyszyn, M. Błaszczyszyn, Work function of the adsorption system Ni/(100)W, Surf. Sci. 100 (1980) L499–L504.

[1550] G.I. Bigun, I.D. Nabitovich, Yu.S. Sukhorskii, Adsorption of potassium and sodium on the surface of a germanium single crystal, Sov. Phys.—Solid State 23 (1981) 1241–1244.

[1551] D. Bolmont, P. Chen, C.A. Sebenne, F. Proix, Structure and electronic properties of cleaved Si(111) upon room–temperature formation of an interface with Ag, Phys. Rev. B 24 (1981) 4552–4559.

[1552] D. Bolmont, P. Chen, C.A. Sebenne, Electronic properties of the annealed interface between Ag and 7×7 Si(111), J. Phys. C 14 (1981) 3313–3319.

[1553] S.N. Bezryadin, Yu.Kh Vekilov, V.D. Verner, M.B. Samsonova, Proc. 12th Annu. Int. Symp. Electron. Struct. Metals and Alloys, Dresden, 1982, pp. 129–132 (see Refs. [485,1557]).

[1554] C. Binns, C. Norris, Manganese overlayers on copper(100): A study by LEED, AES and UPS, Surf. Sci. 116 (1982) 338–350.

[1555] C. Binns, C. Norris, The epitaxial growth of thallium on copper(100): A study by EEED, AES, UPS and EELS, Surf. Sci. 115 (1982) 395–416.

[1556] K.-P. Bohnen, Lattice relaxation at Na(100) and Na(110) surfaces, Surf. Sci. 115 (1982) L96–L102.

[1557] S.N. Bezryadin, Yu.Kh Vekilov, V.D. Verner, M.B. Samsonova, Surface electron structure and work function of thin films of simple metals, Poverkhnost' (6) (1983) 24–32 (Chem. Abstr. 99 (1983) 59087f).

[1558] O.P. Burmistrova, M.A. Mittsev, A.M. Mukhuchev, Surface–coverage dependences of the heat of adsorption and lifetime of thulium atoms on tungsten surface, Sov. Phys.—Solid State 25 (1983) 25–29.

[1559] D.M. Bylander, L. Kleinman, Computational study of subsurface binding sites of oxygen on Al(111), Phys. Rev. B 28 (1983) 523–527.

[1560] M. Błaszczyszyn, R. Błaszczyszyn, R. Męclewski, A.J. Melmed, T.E. Madey, Interactions of sulfur with nickel surfaces: Adsorption, diffusion and desorption, Surf. Sci. 131 (1983) 433–447.

[1561] G. Binnig, N. Garcia, H. Rohrer, J.M. Soler, F. Flores, Electron–metal–surface interaction potential with vacuum tunneling: Observation of the image force, Phys. Rev. B 30 (1984) 4816–4818.

[1562] H. Burtscher, A. Schmidt-Ott, H.C. Siegmann, Photoelectron yield of small silver and gold particles suspended in gas up to a photon energy of 10 eV, Z. Phys. B 56 (1984) 197–199.

[1563] S.N. Bezryadin, V.D. Verner, T.I. Egorova, One–dimensional model of thin films: Study of aluminum surfaces, Poverkhnost' (6) (1984) 43–46.

[1564] J.C. Boettger, S.B. Trickey, Ground–state properties of a beryllium monolayer, J. Phys. F 14 (1984) L151–L153.

[1565] H.P. Bonzel, Alkali–promoted gas adsorption and surface reactions on metals, J. Vac. Sci. Technol. A 2 (1984) 866–872.

[1566] D. Bolmont, P. Chen, C.A. Sébenne, F. Proix, Room temperature adsorption and growth of Ga and In on cleaved Si(111), Surf. Sci 137 (1984) 280–292.

[1567] D. Brugniau, S.D. Parker, G.E. Rhead, Monolayers of platinum and iron on TiO$_2$(001): Characterization by Auger electron spectroscopy, secondary electron emission and work function, Thin Solid Films 121 (1984) 247–257.

[1568] I.P. Batra, Lattice relaxation in aluminum monolayers, J. Vac. Sci. Technol. A 3 (1985) 1603–1606.

[1569] J.C. Boettger, S.B. Trickey, Structure and properties of a beryllium dilayer, Phys. Rev. B 32 (1985) 1356–1358.

[1570] M. Błaszczyszyn, Influence of adsorbed sulfur on surface diffusion of potassium on nickel, Surf. Sci. 151 (1985) 351–360.

[1571] J.C. Boettger, S.B. Trickey, Structural optimization and properties of first row monolayers, J. Phys. F 16 (1986) 693–706.

[1572] C.J. Barnes, H. Asonen, A. Salokatve, M. Pessa, Growth mode and electronic structure of copper films on aluminum substrates, Surf. Sci. 184 (1987) 163–176.

[1573] I.P. Batra, N. García, H. Rohrer, H. Salemink, E. Stoll, S. Ciraci, A study of graphite surface with STM and electronic structure calculations, Surf. Sci. 181 (1987) 126–138.

[1574] A. Berkó, F. Solymosi, Structure and properties of potassium on Pd(100) surface, Surf. Sci. 187 (1987) 359–371.

[1575] X.-H. Bao, S.-Z. Dong, J.-F. Deng, Adsorption of oxygen on electrolytic silver by UPS and work function measurement, Surf. Sci. 199 (1988) 493–506.

[1576] G.A. Benesh, J.R. Hester, Na–Na interactions on Al(001), Surf. Sci. 194 (1988) 567–578.

[1577] J.C. Boettger, S.B. Trickey, Unpublished work on the basis of Ref. [2025] (see Refs. [2025,3366]).

[1578] J.C. Boettger, S.B. Trickey, First principles systematics of ordered metallic monolayers: I. Groups I and II through Sr, J. Phys.: Condens. Matter 1 (1989) 4323–4338.

[1579] P.M. Blass, X.-L. Zhou, J.M. White, Electron spectroscopy and temperature programmed desorption of potassium on Ag(111), Surf. Sci. 215 (1989) 74–90.

[1580] P.J. Berlowitz, N.D. Shinn, Growth and atomic structure of chromium over layers on W(110) and W(100), Surf. Sci. 209 (1989) 345–363.

[1581] A.V. Bulyga, V.K. Solonovich, The influence of temperature on the work function of W, LaB$_6$ and pseudo–alloys, Surf. Sci. 223 (1989) 578–584.

[1582] J.C. Boettger, S.B. Trickey, F. Müller-Plathe, G.H.F. Diercksen, Mono– and dilayer modifications of lithium lattice parameters, J. Phys.: Condens. Matter 2 (1990) 9589–9601.

[1583] A.S. Bhave, P.L. Kanitkar, Adsorption of La on W using probe–hole field emission microscopy, J. Phys. D 24 (1991) 454–457.

[1584] H.P. Bonzel, G. Pirug, C. Ritke, Adsorption of H$_2$O on alkali–metal–covered Pt(111) and Ru(001): A systematic comparison, Langmuir 7 (1991) 3006–3011.

[1585] G. Boishin, M. Tikhov, L. Surnev, Na–promoted oxidation of Si(111), Surf. Sci. 257 (1991) 190–198.

[1586] D.R. Baer, C.W. Hubbard, R.L. Gordon, Pd, Ni, and Cu overlayers on polycrystalline Re, J. Vac. Sci. Technol. A 10 (1992) 2391–2395.

[1587] G. Boishin, L. Surnev, Potassium adsorption and coadsorption with oxygen on a Si(111) surface, Surf. Sci. 273 (1992) 301–310.

[1588] A.V. Gostev, È.M. Reikhrudel', N.Ya. Rukhlyada, B.B. Shishkin, Universal instrument for the investigation of local and integral electron emission, Instrum. Exp. Tech. (4) (1978) 1053–1055.

[1589] G. Boishin, M. Tikhov, M. Kiskinova, L. Surnev, Interaction of oxygen with a Cs–covered Si(111)7×7 surface, Surf. Sci. 261 (1992) 224–232.

[1590] I.G. Batirev, A.N. Karavanov, J.A. Leiro, Surface segregation and catalytic properties of Pd–Ru alloys, Surf. Sci. 289 (1993) 357–362.

[1591] M. Błaszczyszynowa, R. Błaszczyszyn, A. Ciszewski, Ni adsorption on the principal faces of a tungsten crystal: Work function changes and adsorbate distribution, Surf. Sci. 304 (1994) 325–334.

[1592] J.C. Boettger, U. Birkenheuer, N. Rösch, S.B. Trickey, Quantum size effects in hexagonal aluminum films, Int. J. Quantum Chem. Quantum Chem. Symp. 28 (1994) 675–686.

[1593] A. Barbieri, M.A. Van Hove, G.A. Somorjai, Proc. 4th Int. Conf. Struct. Surf., 1994, p. 201 (see Ref. [1931]).

[1594] J.C. Boettger, U. Birkenheuer, S. Krüger, N. Rösch, S.B. Trickey, Theoretical investigation of Na on the Al(111) surface, Phys. Rev. B 52 (1995) 2025–2031.

[1595] U. Birkenheuer, J.C. Boettger, N. Rösch, A local density functional investigation of the clean and the hydrogen covered Li(001) surface, Surf. Sci. 341 (1995) 103–123.

[1596] H. Bross, M. Kauzmann, Electronic structure, surface states, surface energy, and work function of the Cu(100) surface, Phys. Rev. B 51 (1995) 17135–17150.

[1597] M. Böhmisch, F. Burmeister, J. Boneberg, P. Leiderer, Nanostructuring on WSe$_2$ with the atomic force microscope by a potential controlled electrochemical reaction, Appl. Phys. Lett. 69 (1996) 1882–1884.

[1598] A.G. Borisov, D. Teillet-Billy, J.P. Gauyacq, H. Winter, G. Dierkes, Phys. Rev. B 54 (1996) 17166–17174.

[1599] V.A. Bondzie, P. Kleban, D.J. Dwyer, XPS identification of the chemical state of subsurface oxygen in the O/Pd(110) system, Surf. Sci. 347 (1996) 319–328.

[1600] M. Böhmisch, F. Burmeister, A. Rettenberger, J. Zimmermann, J. Bonenberg, P. Leiderer, Atomic force microscope based Kelvin probe measurements: Application to an electrochemical reaction, J. Phys. Chem. B 101 (1997) 10162–10165.

[1601] C.J. Baddeley, A.W. Stephenson, C. Hardacre, M. Tikhov, R.M. Lambert, Structural and electronic properties of Ce overlayers and low–dimensional Pt–Ce alloys on Pt{111}, Phys. Rev. B 56 (1997) 12589–12598.

[1602] T.M. Bhave, S.V. Bhoraskar, Surface work function studies in porous silicon, J. Vac. Sci. Technol. B 16 (1998) 2073–2078.

[1603] A.K. Bhattacharya, D.R. Pyke, The interaction of ethylene, acetylene and butadiene with a clean tungsten(100) surface, J. Mol. Catal. A 129 (1998) 279–285.

[1604] I.A. Bönicke, F. Thieme, W. Kirstein, The interaction of carbon monoxide with the pure and potassium–promoted Cu(332) surface, Surf. Sci. 395 (1998) 138–147.

[1605] D.A. Buchanan, F.R. McFeely, J.J. Yurkas, Fabrication of midgap metal gates compatible with ultrathin dielectrics, Appl. Phys. Lett. 73 (1998) 1676–1678 (see Ref. [3519]).

[1606] A. Böttcher, H. Niehus, Oxygen adsorbed on oxidized Ru(0001), Phys. Rev. B 60 (1999) 14396–14404.

[1607] R. Bertacco, F. Ciccacci, Oxygen–induced enhancement of the spin–dependent effects in electron spectroscopies of Fe(001), Phys. Rev. B 59 (1999) 4207–4210.
[1608] P.B. Balbuena, P.A. Derosa, J.M. Seminario, Density functional theory study of copper clusters, J. Phys. Chem. B 103 (1999) 2830–2840.
[1609] C.S. Beleznai, D. Vouagner, J.P. Girardeau-Montaut, Work function variation during UV laser–induced oxide removal, Appl. Surf. Sci. 138–139 (1999) 6–11.
[1610] M. Brause, S. Skordas, V. Kempter, Study of the electronic structure of TiO$_2$(110) and Cs/TiO$_2$(110) with metastable impact electron spectroscopy and ultraviolet photoemission spectroscopy (HeI), Surf. Sci. 445 (2000) 224–234.
[1611] H.H. Busta, R.J. Espinosa, A.T. Rakhimov, N.V. Suetin, M.A. Timofeyev, P. Bressler, M. Schramme, J.R. Fields, M.E. Kordesch, A. Silzars, Performance of nanocrystalline graphite field emitters, Solid State Electron. 45 (2001) 1039–1047.
[1612] M. Brause, V. Kempter, Mg interaction with TiO$_2$(100): MIES and UPS(HeI) results, Surf. Sci. 490 (2001) 153–159.
[1613] M. Brajczewska, C. Henriques, C. Fiolhais, Dependence of metal surface properties on the valence–electron density in the stabilized model, Vacuum 63 (2001) 135–138.
[1614] A. Böttcher, B. Krenzer, H. Conrad, H. Niehus, Mesoscopic–scale growth of oxygen–rich films on Ru(0001) investigated by photoemission electron microscopy, Surf. Sci. 504 (2002) 42–58.
[1615] B.I. Birajdar, S.V. Shende, D.S. Joag, Adsorption studies of Cr on W(110) plane by probe hole field emission microscopy, Surf. Sci. 505 (2002) 285–288.
[1616] B.I. Birajdar, D.S. Joag, Unpublished work (see Ref. [1615]).
[1617] M.M.J. Bischoff, C. Konvicka, A.J. Quinn, M. Schmid, J. Redinger, R. Podloucky, P. Varga, H. van Kempen, Surf. Sci. 513 (2002) 9–25.
[1618] M. Breitholtz, T. Kihlgren, S.-Å. Lindgren, L. Walldén, Condensation of Na metal on graphite studied by photoemission, Phys. Rev. B 67 (2003) 235416/1–7.
[1619] P. Błoński, A. Kiejna, Calculation of surface properties of bcc iron, Vacuum 74 (2004) 179–183.
[1620] M. Breitholtz, J. Algdal, T. Kihlgren, S.-Å. Lindgren, L. Walldén, Alkali–metal–deposition–induced energy shifts of a secondary line in photoemission from graphite, Phys. Rev. B 70 (2004) 125108/1–7.
[1621] M.M. Beerbom, B. Lägel, A.J. Cascio, B.V. Doran, R. Schlaf, Direct comparison of photoemission spectroscopy and *in situ* Kelvin probe work function measurements on iridium tin oxide films, J. Electron Spectrosc. Relat. Phenom. 152 (2006) 12–17.
[1622] R. Błaszczyszyn, T. Biernat, Thermal desorption of dysprosium from tungsten microcrystal, Appl. Surf. Sci. 252 (2005) 1206–1210.
[1623] P. Błoński, A. Kiejna, J. Hafner, Theoretical study of oxygen adsorption at the Fe(110) and (100) surfaces, Surf. Sci. 590 (2005) 88–100.
[1624] A.M. Black-Schaffer, K. Cho, First–principles study of the work function of nitrogen doped molybdenum(110) surface, J. Appl. Phys. 100 (2006) 124902/1–4.
[1625] P. Błoński, A. Kiejna, Structural, electronic and magnetic properties of bcc iron surfaces, Surf. Sci. 601 (2007) 123–133.
[1626] A.V. Babich, V.V. Pogosov, Effect of dielectric coating on the electron work function and the surface stress of a metal, Surf. Sci. 603 (2009) 2393–2397.
[1627] H. Bentmann, J. Houser, A.A. Demkov, *Ab initio* study of early stages of III–V epitaxy on high–index surfaces of group–IV semiconductors: In adsorption on Si(112), Phys. Rev. B 80 (2009) 085311/1–10.
[1628] H.L. Cooke, O.W. Richardson, The absorption of heat produced by emission of ions from hot bodies, Phil. Mag. 25 (1913) 624–643.
[1629] H.L. Cooke, O.W. Richardson, The absorption of heat produced by emission of ions from hot bodies. II, Phil. Mag. 26 (1913) 472–476.
[1630] A.B. Cardwell, Photo–electric and thermionic properties of iron, Proc. Natl. Acad. Sci. 14 (1928) 439–445.
[1631] A.B. Cardwell, Effects of a crystallographic transformation on the photoelectric and thermionic emission from cobalt, Proc. Natl. Acad. Sci. 15 (1929) 544–551.
[1632] A.B. Cardwell, Photoelectric and thermionic emission from cobalt, Phys. Rev. 38 (1931) 2033–2040.
[1633] A.B. Cardwell, The photoelectric properties of tantalum, Phys. Rev. 38 (1931) 2041–2048.
[1634] H. Cassel, W.A. Schneider, Influence of the adsorption of atoms and molecules on the photoeffect of mercury, Naturwiss. 22 (1934) 464–465.
[1635] R.J. Cashman, W.S. Huxford, Photoelectric properties of pure and gas–contaminated magnesium, Phys. Rev. 48 (1935) 734–741.
[1636] A.B. Cardwell, The thermionic properties of tantalum, Phys. Rev. 47 (1935) 628–630.
[1637] R.J. Cashman, N.C. Jamison, Note on the analysis of photoelectric data, Phys. Rev. 50 (1936) 568–569.
[1638] R.J. Cashman, Effect of temperature on photoelectric emission, Phys. Rev. 52 (1937) 512–518.
[1639] R.J. Cashman, E. Bassoe, Experimental and theoretical photoelectric spectral sensitivity of strontium and magnesium, Phys. Rev. 53 (1938) 919.
[1640] R.J. Cashman, Comments concerning Anderson's paper on contact difference in potential between barium and magnesium, Phys. Rev. 54 (1938) 971.
[1641] R.J. Cashman, E. Bassoe, Surface and volume photoelectric emission from barium, Phys. Rev. 55 (1939) 63–69.
[1642] E.N. Carabateas, S.D. Pezaris, G.N. Hatsopoulos, Interpretation of experimental characteristics of cesium thermionic converters, J. Appl. Phys. 32 (1961) 352–358.
[1643] E.A. Coomes, W.L. Girard, Thermionic Specialist Conf. San Diego, Calf., 1965 (see Ref. [3691]).
[1644] P.E. Carroll, Photoelectric work function from analysis of emission in an accelerating field, Phys. Rev. 104 (1956) 660–661.
[1645] B. Conway, J.O'M. Bockris, Electrolytic hydrogen evolution kinetics and its relation to the electronic and adsorptive properties of the metal, J. Chem. Phys. 26 (1957) 532–541.
[1646] R. Culver, J. Pritchard, F.C. Tompkins, The dipole moment and nature of the chemisorption bond, Z. Elektrochem. 63 (1959) 741–745.
[1647] P.N. Chistyakov, R.A. Milovanova, The values of $V_{s.c.}$ and ϕ for a molybdenum cathode in argon, Sov. Phys. Tech. Phys. 6 (1961) 538–539.
[1648] G. Gaertner, D. den Engelsen, Hundred years anniversary of the oxide cathode: A historical review, Appl. Surf. Sci. 251 (2005) 24–30.
[1649] R.A. Chapman, Thermionic work function of thin–oxide–coated aluminum electrodes in vacuum and in cesium vapor, J. Appl. Phys. 35 (1964) 2832–2843.
[1650] E.A. Coomes, F.E. Girouard, The influence of patches on the average thermionic constants of tungsten and molybdenum emitters, in: Proc. Thermion. Convers. Spec. Conf., NASA Lewis Res. Cent., 1964, pp. 47–52 (see Refs. [325,2244]).
[1651] E.A. Coomes, Production and physics of single–crystal emitters, 1964, AD 602713, 32 pp. (Chem. Abstr. 61 (1964) 15475h).
[1652] P.N. Chistyakov, R.A. Milovanova, Proc. 7th Int. Conf. Phenom. Ionized Gases, Belgrade, 1, 1965, p. 216 (see Ref. [337]).
[1653] A.M. Cowley, S.M. Sze, Surface states and barrier height of metal–semiconductor systems, J. Appl. Phys. 36 (1965) 3212–3220 (see Ref. [1976]).
[1654] R.A. Collins, B.H. Blott, The field emission work function of uranium on tungsten, Surf. Sci. 9 (1968) 1–17.
[1655] R.A. Collins, B.H. Blott, Effects of hydrogen contamination on the work function of uranium on tungsten, Surf. Sci. 11 (1968) 149–152.
[1656] R.A. Collins, B.H. Blott, The adsorption and nucleation of zirconium on tungsten field emitters, Surf. Sci. 10 (1968) 349–368.
[1657] R.A. Collins, B.H. Blott, Multilayer adsorption of uranium on tungsten, Surf. Sci. 13 (1969) 401–413.
[1658] É.F. Chaikovskii, L.G. Mel'nik, G.M. Pyatigorskii, Monokrist. Tekh. (1) (1970) 129 (see Ref. [1354]).
[1659] E.F. Chaikovskii, Yu.F. Derkach, Monokrist. Tekh. (2) (1970) 119–125 (see Ref. [1354]).
[1660] É.F. Chaikovskii, L.I. Kaisheva, Thermionic emission and positive surface ionization of alkali metal atoms on germanium single crystals, Monokrist. Tekh. (3) (1970) 108–114.
[1661] J. Clerc, G. Giraud, J. Roussenq, Photoelectric effect of a copper single crystal, Compt. Rend. B 272 (1971) 1346–1349.
[1662] É.F. Chaikovskii, L.I. Kaisheva, M.L. Litvinenko, Thermionic emission from the (111) face of silicon single crystals, Monokrist. Tekh. (5) (1971) 101–106.
[1663] V.A. Chekina, N.A. Gorbatyi, Distribution of the velocities of thermionic electrons emitted by separate faces of tungsten single–crystal whiskers, in: Emiss. Elektron., Mater. Semin. Probl. Rab. Vykhoda Elektronov Adsorbtsii Met. Zavisimosti Kristallogr. Napravlenii, 2nd, 1971, pp. 85–92.
[1664] R.A. Collins, B.H. Blott, Adsorption of uranium on tungsten single crystal planes, J. Phys. D 4 (1971) 102–113.

[1665] R.A. Collins, B.H. Blott, Adsorption of zirconium on tungsten single crystal planes, J. Phys. D 4 (1971) 114–117.

[1666] J.M. Chen, C.A. Papageorgopoulos, Work function and LEED study of Na and O₂ covered surfaces of W(112), Surf. Sci. 26 (1971) 499–508.

[1667] J.M. Chen, C.A. Papageorgopoulos, Work function of alkali–covered W(100), Solid. State Comm. 11 (1972) 999–1002.

[1668] E. Chrzanowski, Symp. Met. Surf. Gotherburg, 1973, (see Ref. [2954]).

[1669] P. Cotti, H.-J. Güntherodt, P. Munz, P. Oelhafen, J. Wullschleger, Photoemission from liquid and solid mercury, Solid State Commun. 12 (1973) 635–638.

[1670] A. Cetronio, J.P. Jones, Reconstruction at a metallic interface studied by field ion and field emission microscopy, Surf. Sci. 40 (1973) 227–248.

[1671] R.A. Collins, Validity of the Fowler–Nordheim parameters measured for silicon adsorption on single crystal faces of tungsten, Surf. Sci. 40 (1973) 470–478.

[1672] J.M. Chen, Alkali–metal adsorption on metal surfaces, J. Franklin Inst. 298 (1974) 255–269.

[1673] A. Cetronio, J.P. Jones, A study by high field microscopy of the effect of substrate surface structure on the work function of layers of group 1b metals adsorbed on tungsten, Surf. Sci. 44 (1974) 109–128.

[1674] A. Cetronio, J.P. Jones, E.W. Roberts, A study of copper adsorption on (100) tungsten by high field microscopy, Surf. Sci. 52 (1975) 473–488.

[1675] R.A. Collins, C.A. Kiwanga, Field emission from silicon adsorbed on single crystal planes of molybdenum, Surf. Sci. 49 (1975) 349–355.

[1676] A. Cetronio, J.P. Jones, Thermal desorption of silver and gold from tungsten studied by field emission microscopy, Thin Solid Films 35 (1976) 113–126.

[1677] R.A. Collins, C.A. Kiwanga, Field emission studies of selenium adsorption on tungsten and molybdenum, Surf. Sci. 61 (1976) 491–503.

[1678] J.A. Connor, M. Considine, I.H. Hillier, Low energy photoelectron spectroscopy of solids aspects of experimental methodology concerning metals and insulators, J. Electron Spectrosc. Relat. Phenom. 12 (1977) 143–159.

[1679] J.R. Chelikowsky, Electronic structure of Al chemisorbed on the Si(111) surface, Phys. Rev. B 16 (1977) 3618–3627.

[1680] R.A. Collins, C.A. Kiwanga, Tellurium adsorption on tungsten and molybdenum field emitters, Surf. Sci. 64 (1977) 778–784.

[1681] K.-H. Chang, P.H.E. Meijer, Photoemission and LEED study of indium phosphide with a determination of minority carrier diffusion length, J. Vac. Sci. Technol. 14 (1977) 789–796.

[1682] R.A. Collins, C.A. Kiwanga, Tellurium adsorption on molybdenum and tungsten field emitters, Surf. Sci. 71 (1978) 185–190.

[1683] K. Christman, G. Ertl, H. Shimizu, The growth and structure of copper films on (0001) ruthenium surfaces, Thin Solid Films 57 (1979) 247–252.

[1684] B. Chatterjee, An anisotropic relation between work function and melting temperature, Phys. Lett. 69 A (1979) 429–430.

[1685] K. Christman, G. Ertl, H. Shimizu, Model studies on bimetallic Cu/Ru catalysts, J. Catalysis 61 (1980) 397–411.

[1686] M.H. Cobourne, W.T. Williams, Field emission of electrons from superconducting and normal electrodes, Physica B+C 104 (1981) 50–55.

[1687] V.I. Makukha, Adsorption of calcium on tungsten, Radiotekh. Elektron. 6 (1961) 339–341.

[1688] T.-C. Chiang, G. Kaindl, D.E. Eastman, Photoemission studies of Ar, Kr and Xe adsorbed on Al(111): Dipole moments, polarizabilities and spatial distributions, Solid State Commun. 41 (1982) 661–665.

[1689] Cr. Contescu, M.I. Vass, Field emission microscopy study of silver adsorption on tungsten single–crystal planes, Thin Solid Films 97 (1982) 245–257.

[1690] P.H. Citrin, G.K. Wertheim, Photoemission from surface–atom core levels, surface densities of states, and metal–atom clusters: A unified picture, Phys. Rev. B 27 (1983) 3176–3200.

[1691] M.P. Cox, J.S. Foord, R.M. Lambert, R.H. Prince, The halogen and alkali surface chemistry of group IIIA and IVA metals: Cl₂, Br₂, Na and Rb chemisorption and coadsorption on yttrium, titanium, zirconium and hafnium, Surf. Sci. 129 (1983) 375–398.

[1692] T.W. Capehart, R. Richter, J.G. Gray, J.R. Smith, J.C. Buchholz, F.J. Arlinghaus, Transition metal chemisorption on transition metals: Theoretical and experimental electronic structure for silver on palladium(100), J. Vac. Sci. Technol. A 1 (1983) 1214–1216.

[1693] M. Chelvayohan, Work function measurements on ion bombardment damaged (111) surface of silver by photoelectric and CPD methods, J. Phys. C 16 (1983) L323–L325.

[1694] P. Chen, D. Bolmont, C.A. Sebenne, Adsorption of Al on cleaved Si(111) at room temperature, J. Phys. C 17 (1984) 4897–4905.

[1695] T.-P. Chen, E.L. Wolf, A.L. Giorgi, Ultraviolet–photoemission and electron–energy–loss spectroscopic studies of ⁹⁹Tc, Phys. Rev. B 29 (1984) 6036–6042.

[1696] T.W. Capehart, Private communication (see Ref. [2981]).

[1697] J. Cousty, R. Riwan, P. Soukiassian, Adsorption of alkali metals on W(100): An EELS study, J. Physique 46 (1985) 1693–1698.

[1698] W. Kohn, Nobel lecture: Electronic structure of matter—Wave functions and density functionals, Rev. Modern Phys. 71 (1999) 1253–1266.

[1699] E.V. Chulkov, V.M. Silkin, *Ab initio* calculation of the surface electronic structure of Mg(0001), Solid State Commun. 58 (1986) 273–275.

[1700] E. Chrzanowski, E. Bauer, The adsorption of beryllium on the tungsten(211) surface, Surf. Sci. 173 (1986) 106–127.

[1701] M. Chelvayohan, R. Gomer, Temperature dependence of the work function of Cu layers on a W(110) plane, Surf. Sci. 172 (1986) 337–348.

[1702] S. Ciraci, I.P. Batra, Novel electronic properties of a potassium overlayers on Si(001)–(2×1), Phys. Rev. Lett. 56 (1986) 877–880.

[1703] V.T. Cherepin, A.A. Ostroukhov, V.N. Tomilenko, Calculation of the electronic structure of transition metal surfaces: Iron, lanthanum and thorium(100) and (110) monolayers in fcc and bcc phases, Poverkhnost' (2) (1987) 34–43.

[1704] E.V. Chulkov, V.M. Silkin, E.N. Shirykalov, Surface electronic structure of Be(0001) and Mg(0001), Surf. Sci. 188 (1987) 287–300.

[1705] S.R. Chubb, E. Wimmer, A.J. Freeman, J.R. Hiskes, A.M. Karo, All–electron local–density–functional theory of alkali–metal adsorption on transition metal surfaces: Cs on Mo(001), Phys. Rev. B 36 (1987) 4112–4122.

[1706] M. Chelvayohan, R. Gomer, Adsorption of CO on Cu layers adsorbed on a W(110) surface, Surf. Sci. 186 (1987) 412–446.

[1707] M.Y. Chou, J.R. Cherikowsky, Structural properties of the Ru(0001) surface, Phys. Rev. B 35 (1987) 2124–2127.

[1708] S.R. Chubb, W.E. Pickett, All–electron study of c (2×2) S chemisorbed above magnetic Fe(001), J. Appl. Phys. 63 (1988) 3493–3495.

[1709] S.D. Cameron, D.J. Dwyer, Charge transfer effects on CO bond cleavage: CO and potassium on Fe(100), Surf. Sci. 198 (1988) 315–330.

[1710] S.R. Chubb, W.E. Pickett, First–principles study of the electronic and magnetic structure of c(2×2) sulfur chemisorbed above Fe(100), Phys. Rev. B 38 (1988) 10227–10243.

[1711] E.V. Chulkov, V.M. Silkin, A.G. Lipnitskii, V.E. Panin, The first–principles calculations of the electronic structure of the surfaces of pure metals and layers adsorbed on their surfaces, Electrochim. Acta 34 (1989) 19–27.

[1712] E.V. Chulkov, Self–consistent semi–relativistic calculation of the electronic structure of strontium(001) and lead(001) surfaces, Poverkhnost' (12) (1989) 52–59 (Chem. Abstr. 112 (1990) 84867e).

[1713] T. Castro, Y.Z. Li, R. Reifenberger, E. Choi, S.B. Park, R.P. Andres, Studies of individual nanometer–sized metallic clusters using scanning tunneling microscopy, field emission, and field ion microscopy, J. Vac. Sci. Technol. A 7 (1989) 2845–2849.

[1714] E.V. Chulkov, V.M. Silkin, I.Yu. Sklyadneva, Surface electronic structure of metals, Surf. Sci. 231 (1990) 9–17.

[1715] G.R. Castro, P. Pervan, E.G. Michel, R. Miranda, K. Wandelt, Interaction of potassium with Si(100)2×1, Vacuum 41 (1990) 564–566.

[1716] J. Chrost, D. Fick, NMR experiments on Li adsorbed on a Si(111) surface, Surf. Sci. 251/252 (1991) 78–81.

[1717] R. Casanova, K. Prabhakaran, G. Thornton, Potassium adsorption on TiO₂(100), J. Phys.: Condens. Matter 3 (1991) S91–S95.

[1718] L.-J. Chen, N. Wang, E. Luo, *Ab initio* investigation of the Cs/Ir(001) system, J. Phys. D 26 (1993) 1316–1318.

[1719] S. Crampin, Fe on Au(001): Magnetism and band formation, J. Phys.: Condens. Matter 5 (1993) 4647–4664.

[1720] S. Crampin, Segregation and the wok function of a random alloy: PdAg(111), J. Phys.: Condens. Matter 5 (1993) L443–L448.

[1721] L.-J. Chen, N. Wang, E. Luo, Work function and charge transfer of overlayer–substrate system: Cs on Ir(001), Wuli Xuebao 42 (1993) 1149–1152 (Chem. Abstr. 120 (1994) 117673j).

[1722] S. Crampin, Unpublished and private communication (see Ref. [3369]).

[1723] S. Crampin, Partial–wave summations in atomic–sphere surface calculations, Phys. Rev. B 49 (1994) 14035–14038.

[1724] P.G. Collins, A. Zettl, A simple and robust electron beam source from carbon nanotubes, Appl. Phys. Lett. 69 (1996) 1969–1971.
[1725] D.V. Chakarov, L. Österlund, B. Hellsing, B. Kasemo, Photon induced desorption and intercalation of potassium atoms deposited on graphite(0001), Appl. Surf. Sci. 106 (1996) 186–192.
[1726] F.Y. Chuang, C.Y. Sun, H.F. Cheng, C.M. Huang, I.N. Lin, Enhancement of electron emission efficiency of Mo tips by diamondlike carbon coatings, Appl. Phys. Lett. 68 (1996) 1666–1668.
[1727] Y.-C. Chao, L.S.O. Johansson, R.I.G. Uhrberg, Adsorption of Na on Si(100)2×1 at room temperature studied with photoelectron spectroscopy, Phys. Rev. B 55 (1997) 7198–7205.
[1728] P.G. Collins, A. Zettl, Unique characteristics of cold cathode carbon–nanotube–matrix field emitters, Phys. Rev. B 55 (1997) 9391–9399.
[1729] Y.-C. Chao, L.S.O. Johansson, R.I.G. Uhrberg, Electronic structure of Rb–adsorbed Si(100) surfaces studied with angle–resolved photoemission, Phys. Rev. B 55 (1997) 7667–7672.
[1730] G.R. Condon, J.A. Panitz, Nanoscale imaging of the electronic tunneling barrier at a metal surface, J. Vac. Sci. Technol. B 16 (1998) 23–29.
[1731] A. Ciszewski, S.M. Zuber, Z. Szczudło, Interaction of hydrogen with ultrathin titanium layers on tungsten, Appl. Surf. Sci. 134 (1998) 234–242.
[1732] C.-P. Cheng, I.-H. Hong, T.-W. Pi, Synchrotron–radiation photoemission study of Ba on a Si(001)2×1 surface, Phys. Rev. B 58 (1998) 4066–4071.
[1733] J.B. Cui, J. Ristein, L. Ley, Electron affinity of the bare and hydrogen covered single crystal diamond(111) surface, Phys. Rev. Lett. 81 (1998) 429–432.
[1734] E.V. Chulkov, V.M. Silkin, P.M. Echenique, Image potential states on metal surfaces: Binding energies and wave functions, Surf. Sci. 437 (1999) 330–352.
[1735] P. Chen, X. Wu, X. Sun, J. Lin, W. Ji, K.L. Tan, Electronic structure and optical limiting behavior of carbon nanotubes, Phys. Rev. Lett. 82 (1999) 2548–2551 (see Refs. [291,3223]).
[1736] J.B. Cui, J. Ristein, L. Ley, Low–threshold electron emission from diamond, Phys. Rev. B 60 (1999) 16135–16142.
[1737] A. Ciszewski, Z. Szczudło, Y. Losovyi, Work function changes in Hf/W(011) and Hf/W(001) adsorption systems, Surf. Sci. 454–456 (2000) 122–126.
[1738] J.B. Cui, M. Stammler, J. Ristein, L. Ley, Role of hydrogen on field emission from chemical vapor deposited diamond and nanocrystalline diamond powder, J. Appl. Phys. 88 (2000) 3667–3673.
[1739] J.G. Che, C.T. Chan, Charge transfer, surface charging, and overlayer–induced faceting, Phys. Rev. B 67 (2003) 125411/1–8.
[1740] C.-W. Chen, M.-H. Lee, S.J. Clark, Gas molecule effects on field emission properties of single–walled carbon nanotubes, Dia. Rel. Mater. 13 (2004) 1306–1313.
[1741] J.-Q. Cai, X.-M. Tao, W.-B. Chen, X.-X. Zhao, M.-Q. Tan, Density functional theory study on the atomic structure and electronic states of Cu(100) ($\sqrt{2}$×2$\sqrt{2}$) R45°–O surface, Wuli Xuebao 54 (2005) 5350–5355 (Chem. Abstr. 144 (2006) 495959x).
[1742] J.-Q. Cai, X.-M. Tao, M.-Q. Tan, Atomic geometry and adsorption of Cu(100)/H surface, Wuli Huaxue Xuebao 23 (2007) 355–360 (Chem. Abstr. 148 (2008) 129114u).
[1743] C.E. Cordeiro, A. Delfino, T. Frederico, Theoretical study of work function of conducting single–walled carbon nanotubes by a non–relativistic field theory approach, Carbon 47 (2009) 690–695.
[1744] J. Chrzanowski, Yu.A. Kravtsov, Simple analytical expression for work function in the "nearest neighbour" approximation, Phys. Lett. A 375 (2011) 671–675.
[1745] J. Derieux, Photoelectric effects on mercury droplets, Phys. Rev. 11 (1918) 276–284.
[1746] C. Davisson, L.H. Germer, The thermionic work function of tungsten, Phys. Rev. 20 (1922) 300–330.
[1747] S. Dushman, Electron emission from metals as a function of temperature, Phys. Rev. 21 (1923) 623–636.
[1748] R. Döpel, The selective photoeffect of strontium, Z. Phys. 33 (1925) 237–245.
[1749] S. Dushman, J.W. Ewald, Electron emission from thoriated tungsten, Phys. Rev. 29 (1927) 857–870.
[1750] S. Dushman, D. Dennison, N.B. Reynolds, Electron emission and diffusion for tungsten filaments containing various oxides, Phys. Rev. 29 (1927) 903.
[1751] L.A. DuBridge, The photoelectric properties of thoroughly outgassed platinum, Phys. Rev. 29 (1927) 451–465.
[1752] H.K. Dunn, Changes in the photo–electric threshold of mercury, Phys. Rev. 29 (1927) 693–700.
[1753] L.A. DuBridge, The photoelectric and thermionic work functions of outgassed platinum, Phys. Rev. 31 (1928) 236–243.
[1754] L.A. DuBridge, The systematic variation of the constant A in thermionic emission, Phys. Rev. 31 (1928) 912–913.
[1755] P.H. Dowling, The contact potential between the solid and liquid phases of bismuth, Phys. Rev. 31 (1928) 244–250.
[1756] H. de Boer, J.D. Fast, Preparation of pure metals of the titanium group by thermal decomposition of the iodides. III. Hafnium, Z. Anorg. Allgem. Chem. 187 (1930) 193–208.
[1757] E.H. Dixon, Some photoelectric and thermionic properties of rhodium, Phys. Rev. 37 (1931) 60–69.
[1758] J.H. Dillon, Photoelectric properties of zinc single crystals, Phys. Rev. 38 (1931) 408–415.
[1759] S. Dushman, Thermionic emission, Rev. Modern Phys. 2 (1930) 381–476.
[1760] L.E. DuBridge, A further experimental test of Fowler's theory of photoelectric emission, Phys. Rev. 39 (1932) 108–118.
[1761] J.H. de Boer, Unpublished (see Ref. [2932]).
[1762] W. Distler, G. Mönch, Thermionic work function and atomic distance, Z. Phys. 84 (1933) 271–275.
[1763] C.F. DeVoe, The photoelectric properties of zinc, Phys. Rev. 50 (1936) 481–485.
[1764] W.P. Dyke, Ph.D. dissertation, Univ. of Washington, 1946 (see Refs. [179,963]).
[1765] J. Dickey, New aspects of the photoelectric emission from Na and K, Phys. Rev. 81 (1951) 612–616.
[1766] M. Drechsler, E.W. Müller, Field–electron emission and work function of separate crystal faces, Z. Phys. 134 (1953) 208–221.
[1767] W.P. Dyke, J.K. Trolan, W.W. Dolan, F.J. Grundhauser, Field emission current–density distribution, J. Appl. Phys. 25 (1954) 106–112.
[1768] J.A. Dillon Jr., H.E. Farnsworth, Work function of the (100) face of a germanium single crystal as a function of heat treatment and ion bombardment, Phys. Rev. 99 (1955) 1643.
[1769] J.A. Dillon Jr., Effects of oxygen adsorption on the work functions of clean germanium surfaces, Bull. Am. Phys. Soc. 1 (1956) 53.
[1770] J.A. Dillon Jr., H.E. Farnsworth, Work–function studies of germanium crystals cleaned by ion bombardment, J. Appl. Phys. 28 (1957) 174–184.
[1771] J.A. Dillon Jr., Work function studies of silicon single crystals, Bull. Am. Phys. Soc. 3 (1958) 31.
[1772] G.J. Daly, J.L. Gumnick, Experimental measurements of work function and richardson number relationships for rhenium, Bull. Am. Phys. Soc. 6 (1961) 421.
[1773] B.Ch. Dyubua, L.A. Stepanov, Thermionic emission of some metal–like compounds in barium vapor, Radiotekh. Elektron. 10 (1965) 2200–2204.
[1774] J.G. DeSteese, Thermionic emission characteristics of rhenium with low cesium coverage, Appl. Phys. Lett. 2 (1963) 25–27.
[1775] B.Ch. Dyubua, O.K. Kultashev, I.A. Tsyganova, The work function of Nb–Ta, Ti–Re and Ta–Re alloys, Radio Engin. Electr. Phys. 9 (1964) 1716–1720.
[1776] B.Ch. Dyubua, O.K. Kultashev, Surf. Phenom. in Metals and Solid Phases Occurring in Them, Kabard. Balkarskoye Publishing House, Nal'chik, 1965, pp. 433–437 (see Refs. [12,1354]).
[1777] B.Ch. Dyubua, O.K. Kultashev, L.V. Gorshkova, Work function of solid solutions of tungsten with molybdenum and tantalum, Sov. Phys.—Solid State 8 (1966) 882–885.
[1778] B.Ch. Dyubua, O.K. Kultashev, Work–function of the W–Hf, Ta–Hf, Nb–Hf, Re–Hf, Re–Zr, and W–Re alloys, Fiz. Metal. Metalloved. 21 (1966) 396–402 (Chem. Abstr. 65 (1966) 4771a).
[1779] A.V. Druzhinin, Emission and adsorption properties of binary systems of metal alloys, Radiotekh. Elektron. 12 (1967) 1265–1269.
[1780] A.V. Druzhinin, T.A. Kupriyanova, Investigation of the emission of binary metal alloys by the method of diffusion pairs, Radiotekh. Elektron. 12 (1967) 1261–1264.

[1781] P.J. Dobson, B.J. Hopkins, The structure of, and the contact potential difference between, polycrystalline tungsten foil and vapour–deposited films of tungsten on glass, J. Phys. D 1 (1968) 1241–1244.

[1782] R.D. Dixon, L.A. Lott, Work function of ultrahigh–vacuum–deposited beryllium films, J. Appl. Phys. 40 (1969) 4938–4939.

[1783] M. Drechsler, J.-M. Bermond, J.-P. Prulhière, Influence of temperature on the field electron emission by the (111) and (013) faces of tungsten at low current densities, C. R. Acad. Sci. Paris B 269 (1969) 1267–1270.

[1784] U. Decker, G. Möllenstedt, E. Wurster, Increase of the field emission of electrons from tungsten tips by evaporation of beryllium, Z. Phys. 229 (1969) 316–320.

[1785] R.J. D'Arcy, N.A. Surplice, Work function of titanium films, Surf. Sci. 36 (1973) 783–788.

[1786] N.D. Drandarov, Emission and adsorption properties of the tantalum–chromium system, in: Kratk. Soderzh. Dokl. Vses. Konf. Emiss. Elektron., 15th, 2, 1973, pp. 72–73 (Chem. Abstr. 83 (1975) 187055a).

[1787] J.L. Desplat, Variation of the work function of tungsten(100) by adsorption of oxygen and cesium and coadsorption of oxygen and cesium, Surf. Sci. 34 (1973) 588–596.

[1788] J.E. Demuth, D.W. Jepsen, P.M. Marcus, LEED spectra determination of the atomic location of tellurium adsorbed on Ni(001), J. Phys. C 6 (1973) L307–L310.

[1789] N.D. Drandarov, Emission and adsorption properties of the tantalum–chromium system, Izv. Akad. Nauk, Ser. Fiz. 38 (1974) 354–358.

[1790] J.E. Demuth, T.N. Rhodin, Chemisorption on (001), (110) and (111) nickel surfaces: A correlated study using LEED spectra, Auger spectra and work function change measurements, Surf. Sci. 45 (1974) 249–307.

[1791] J.E. Demuth, T.N. Rhodin, Elastic LEED intensity–energy studies of clean (001), (110) and (111) nickel surfaces, Surf. Sci. 42 (1974) 261–298.

[1792] J. David, J. Denisot, F. Floret, Work function variation of tungsten in strontium vapor, Japan. J. Appl. Phys. Suppl. 2 (Part 2) (1974) 745–748.

[1793] B.Ch. Dyubua, G.S. Solov'eva, V.M. Rozhdestvenskii, L.A. Kurakina, Electron work function of the (100), (111), and (110) faces of single crystals of alloys of tungsten with tantalum, Sov. Phys.—Solid State 17 (1975) 979–980.

[1794] J. Derrien, F.A. D'Avitaya, A. Glachant, LEED, AES and work function measurements on clean and cesium covered polar faces of GaP, Surf. Sci. 47 (1975) 162–166.

[1795] I.Ya. Dekhtyar, V.I. Silant'ev, N.A. Shevchenko, L.A. Narinskaya, Study of cesium adsorption on molybdenum and tungsten, Ukr. Fiz. Zh. 21 (1976) 500–505 (Chem. Abstr. 84 (1976) 185307f).

[1796] R. Dovesi, C. Pisani, F. Ricca, C. Roetti, Regular chemisorption of hydrogen on graphite in the crystalline orbital NDO approximation, J. Chem. Phys. 65 (1976) 3075–3084.

[1797] J.M. Derochette, J. Marien, Field emission study of hydrogen adsorbed on smooth and perfectly ordered iridium surfaces (111) and (100), Phys. Status Solidi (a) 39 (1977) 281–289.

[1798] Z. Dworecki, Growth of beryllium crystals on tungsten, Acta. Univ. Wratislav. Mat. Fiz. Astron. 29 (1977) 57–62 (Chem. Abstr. 89 (1978) 68731g).

[1799] J.E. Demuth, Chemisorption of C_2H_2 on Pd(111) and Pt(111): Formation of a thermally activated olefinic surface complex, Chem. Phys. Lett. 45 (1977) 12–17.

[1800] A. Dąbrowski, Field–electron–microscopy studies of potassium layers on rhenium: Average work function change, Acta Phys. Pol. A 52 (1977) 55–59.

[1801] D. Dayal, H. Geiger, P. Wissmann, Photoelectric measurements on pure and CO covered copper films, Z. Phys. Chem. (Wiesbaden) 110 (1978) 75–84.

[1802] J.M. Derochette, Adsorption of nitrogen on iridium: Influence of steps on the surface potential studied by field emission, Phys. Status Solidi (a) 45 (1978) 163–169 (see Ref. [2146]).

[1803] Z. Dworecki, Adsorption and growth of beryllium crystals on tungsten, Acta. Univ. Wratislav, Mat. Fiz. Astron. 31 (1977) 85–90 (Chem. Abstr. 91 (1979) 99996t).

[1804] E.I. Davydova, A.D. Karpenko, V.A. Shishkin, Stability of the field emission of fine–tip cathodes passivated by transition–metal films, Sov. Phys. Tech. Phys. 24 (1979) 1307–1309.

[1805] J.E. Demuth, The reaction of ethylene and acetylene with Pt(111) at room temperature: The formation of vinyl–like species, Surf. Sci. 80 (1979) 367–387.

[1806] P.R. Davis, The adsorption of Zr onto W(100) surfaces, Surf. Sci. 91 (1980) 385–399.

[1807] J.-L. Desplat, C.A. Papageorgopoulos, Interaction of cesium and oxygen on W(110). I. Cesium adsorption on oxygenated and oxidized W(110), Surf. Sci. 92 (1980) 97–118.

[1808] J.E. Demuth, The reaction of acetylene with Ni(100) and Ni(110) surfaces at room temperature, Surf. Sci. 93 (1980) 127–144.

[1809] S. Daiser, Diplome Thesis, Univ. of München, 1982 (see Ref. [3144]).

[1810] J.M. Derochette, Field emission thermal desorption spectroscopy: Desorption of hydrogen from Ir(100) and Ir(110), Surf. Sci. 118 (1982) 145–164.

[1811] E.I. Davydova, V.A. Shishkin, The stability of field emission of a W–Sc metal film cathode in an atmosphere of H_2, N_2, CH_4, and CO, Sov. Phys. Tech. Phys. 27 (1982) 1003–1007.

[1812] L.R. Danielson, Auger spectrum changes and work function of clean and contaminated zirconium, J. Vac. Sci. Technol. 20 (1982) 86–87.

[1813] E.B. Deblasi Bourdon, R.H. Prince, Chlorine and sodium chemisorption on scandium and yttrium, Surf. Sci. 144 (1984) 581–590.

[1814] E.B. Deblasi Bourdon, R.H. Prince, Electron and ion emission from zirconium, yttrium and scandium during chlorine and bromine adsorption, Surf. Sci. 144 (1984) 591–601.

[1815] R.A. dePaola, J. Hrbek, F.M. Hoffmann, Potassium promoted C–O bond weakening on Ru(001). I. Through–metal interaction at low potassium precoverage, J. Chem. Phys. 82 (1985) 2484–2498.

[1816] E. Döhl-Oelze, E.M. Stuve, J.K. Sass, Thermal activation of the cesium–induced reconstruction of Ag(110), Solid State Commun. 57 (1986) 323–327.

[1817] M. Domke, T. Mandel, C. Laubschat, M. Prietsch, G. Kaindl, Layer resolved photoemission study of the Cs/Si(111)2×1 interface, Surf. Sci. 189/190 (1987) 268–275.

[1818] R.A. de Paola, F.M. Hoffmann, D. Heskett, E.W. Plummer, The coadsorption of oxygen and potassium on Ru(001): Evidence for the formation of K–O compounds, J. Chem. Phys. 87 (1987) 1361–1366.

[1819] L.H. Dubois, B.R. Zegarski, H.S. Luftman, Complex CO–potassium interactions on Cu(100): An electron energy loss, thermal desorption, and work function study, J. Chem. Phys. 87 (1987) 1367–1375.

[1820] J. Derrien, F.A. d'Avitaya, Thin metallic silicide films epitaxially grown on Si(111) and their role in Si–metal–Si devices, J. Vac. Sci. Technol. A 5 (1987) 2111–2120.

[1821] O.I. Dubrovskii, S.I. Kurganskii, O.V. Farberovich, E.P. Domashevskaya, Self–consistent electronic structure of the aluminum(001) surface, Poverkhnost' (2) (1988) 28–34 (Chem. Abstr. 108 (1988) 210444x).

[1822] R. Duszak, R.H. Prince, Potassium adsorption on Ru(0001) at 450 K, Surf. Sci. 205 (1988) 143–152.

[1823] U.A. Ditzinger, Ch. Lunau, B. Schiewek, St. Tosch, H. Neddermeyer, M. Hanbücken, Photoemission from K/Si(111) 7×7 and Cs/Si(111) 7×7, Surf. Sci. 211/212 (1989) 707–715.

[1824] R. Duszak, R.H. Prince, Structure of Na overlayers on Ru(0001) at room temperature and above, Surf. Sci. 216 (1989) 14–22.

[1825] R. Dudde, K.H. Frank, B. Reihl, Unoccupied electronic band structure of an ordered potassium layer on copper: Cu(111)–(2×2)K, Phys. Rev. B 41 (1990) 4897–4900.

[1826] A. Domenicucci, R.W. Vook, Contact potential difference study of the growth of palladium on ⟨111⟩ fibre–textured aluminum thin films, Vacuum 41 (1990) 1422–1424.

[1827] R. Duszak, R.H. Prince, Anti–phase domain formation during cesium adsorption on Ru(0001), Surf. Sci. 226 (1990) 33–41.

[1828] A. Derraa, M.J.G. Lee, Configuration and electronic structure of silver overlayers on microscopic (110) facets of tungsten, Surf. Sci. 329 (1995) 1–13.

[1829] L. Diederich, O.M. Küttel, P. Aebi, E. Meillard-Schaller, R. Fasel, L. Schlapbach, Photoelectron emission from the negative electron affinity caesiated natural diamond(100) surface, Dia. Rel. Mater. 7 (1998) 660–665.

[1830] L. Diederich, O.M. Küttel, P. Aebi, L. Schlapbach, Electron affinity and work function of differently oriented and doped diamond surfaces determined by photoelectron spectroscopy, Surf. Sci. 418 (1998) 219–239.

[1831] L. Duò, R. Bertacco, G. Isella, F. Ciccacci, M. Richter, Electronic and magnetic properties of the Co/Fe(001) interface and the role of oxygen, Phys. Rev. B 61 (2000) 15294–15301.

[1832] I. Dontas, S. Kennou, The interfacial properties of erbium films on the two polar faces of 6H–SiC(0001), Dia. Rel. Mater. 10 (2001) 13–17.

[1833] T. Durakiewicz, A.J. Arko, J.J. Joyce, D.P. Moore, S. Halas, Electronic work function and its thermal shifts for polycrystalline metal surfaces, Bull. Am. Phys. Soc. 46 (2001) 1008.

[1834] J.L.F. Da Silva, C. Stampfl, M. Scheffler, Adsorption of Xe atoms on metal surfaces: New insights from first–principles calculations, Phys. Rev. Lett. 90 (2003) 066104/1–4.

[1835] S.K. Dey, J. Goswami, D. Gu, H. de Waard, S. Marcus, C. Werkhoven, Ruthenium films by digital chemical vapor deposition: Selectivity, nanostructure, and work function, Appl. Phys. Lett. 84 (2004) 1606–1608.

[1836] D.B. Dańko, M. Kuchowicz, J. Kołaczkiewicz, Adsorbate–induced surface rearrangement of the system Pd/Mo(111), Surf. Sci. 552 (2004) 111–122.

[1837] N. de Jonge, M. Allioux, M. Doytcheva, M. Kaiser, K.B.K. Teo, R.G. Lacerda, W.I. Milne, Characterization of the field emission properties of individual thin carbon nanotubes, Appl. Phys. Lett. 85 (2004) 1607–1609.

[1838] B. de Boer, A. Hadipour, M.M. Mandoc, P.W.M. Blom, Tuning of metal work function with self–assembled monolayers, in: Mater. Res. Soc. Symp. Proc. 871E, 2005 (Chem. Abstr. 149 (2008) 254941h). Avail. URL: http://www.mrs.org/s--mrs/bin.asp?CID=2734&DID=149198&DOC=FILE.PDF.

[1839] M. D'angelo, M. Konishi, I. Matsuda, C. Liu, S. Hasegawa, T. Okuda, T. Kinoshita, Alkali metal–induced Si(111)$\sqrt{21} \times \sqrt{21}$ structure: The Na case, Surf. Sci. 590 (2005) 162–172.

[1840] N. de Jonge, M. Allioux, J.T. Oostveen, K.B.K. Teo, W.I. Milne, Low noise and stable emission from carbon nanotube electron sources, Appl. Phys. Lett. 87 (2005) 133118/1–4.

[1841] T. Durakiewicz, Private communication (see Ref. [2070]).

[1842] D.B. Dańko, M. Kuchowicz, R. Szukiewicz, J. Kołaczkiewicz, Growth and thermal stability of ultra–thin Ag and Au layers on Mo(111) surface, Surf. Sci. 600 (2006) 2258–2267.

[1843] S.Yu. Davydov, Alkali metal adsorption on graphite: Calculation of a work function variation in the Anderson–Newns–Muscat model, Appl. Surf. Sci. 257 (2010) 1506–1510.

[1844] W. Espe, The Richardson constant of distillation cathodes, Z. Tech. Phys. 10 (1929) 489–495.

[1845] R.C. Evans, The surface ionization of potassium on molybdenum, Proc. Cambridge Philos. Soc. 29 (1933) 522–527.

[1846] A. Engelmann, Determination of the photoelectric long-wave limit for rhenium, Ann. Phys. 17 (1933) 185–208.

[1847] A. Ertel, Effect of impurities on thermionic emission from platinum, Phys. Rev. 78 (1950) 353–354.

[1848] J. Eisinger, Adsorption of CO on tungsten and its effect on the work function, J. Chem. Phys. 27 (1957) 1206–1207.

[1849] J. Eisinger, Electrical properties of nitrogen adsorbed on tungsten, J. Chem. Phys. 28 (1958) 165–166.

[1850] M.I. Elinson, V.A. Gor'kov, G.F. Vasil'ev, Field emission of rhenium, Radiotekh. Elektron. 3 (1958) 307–312.

[1851] J. Eisinger, Unpublished (see Ref. [1225]).

[1852] A. Eberhagen, The change of work function of a metal because of gas adsorption, Fortschr. Phys. 8 (1960) 245–294.

[1853] G. Ehrlih, F.G. Hudda, Low–temperature chemisorption. III. Studies in the field emission microscope, J. Chem. Phys. 35 (1961) 1421–1439.

[1854] P.J. Estrup, J. Anderson, W.E. Danforth, LEED studies of potassium adsorption on tungsten, Surf. Sci. 4 (1966) 286–298.

[1855] J. Ernst, About the Fowler–Nordheim plots of germanium field emitters, Phys. Status Solidi 24 (1967) 177–181.

[1856] W. Eckstein, K.F. George, W. Heiland, J. Kirschner, N. Müller, On the field emission from Ni, Gd, and EuS evaporated on to tungsten, Z. Naturforsch. 25 a (1970) 1981.

[1857] R.E. Ericson, An electrical, chemical, and structural study of the Ge(100)/Cs/O photosurface (Ph.D. thesis), Univ. of Minnesota, 1975, 166 pp. (Diss. Abstr. B 36 (1975) 1851) (see Ref. [1861]).

[1858] M.A. Eremeev, V.S. Neshpor, A.B. Novikov, E.M. Stefanovskaya, V.P. Fedorinov, Thermionic emission properties of zirconium, hafnium, and titanium nitrides in cesium vapor, Sov. Phys. Tech. Phys. 19 (1975) 1337–1341.

[1859] W.F. Egelhoff Jr., D.L. Perry, J.W. Linnett, The adsorption of mercury on tungsten(100) studied by ultra–violet photoelectron spectroscopy, Surf. Sci. 54 (1976) 670–674.

[1860] M. Caragiu, S. Finberg, Alkali metal adsorption on graphite: A review, J. Phys.: Condens. Matter 17 (2005) R995–R1024.

[1861] D. Edwards Jr., W.T. Peria, Thermal stability of the work function of NEA type surfaces, Appl. Surf. Sci. 1 (1978) 419–442.

[1862] G. Ebbinghaus, A. Simon, Electronic structure of Rb, Cs and some of their metallic oxides studied by photoelectron spectroscopy, Chem. Phys. 43 (1980) 117–133.

[1863] S.E. Efimovskii, G.A. Rump, O.P. Burmistrova, G.G. Vladimirov, Adsorption of titanium on the tungsten(011) surface, Sov. Phys. Tech. Phys. 26 (1981) 1400–1401.

[1864] M. El-Batanouny, M. Strongin, G.P. Williams, J. Colbert, Relationship between electronic structure and hydrogen–uptake kinetics, Phys. Rev. Lett. 46 (1981) 269–272.

[1865] G. Ertl, S.B. Lee, M. Weiss, Adsorption of nitrogen on potassium promoted Fe(111) and (100) surfaces, Surf. Sci. 114 (1982) 527–545.

[1866] W. Ekardt, Work function of small metal particles: Self–consistent spherical jellium–background model, Phys. Rev. B 29 (1984) 1558–1564.

[1867] K.G. Eyink, B.C. Lamartine, T.W. Haas, Measurement of work function in a cylindrical mirror electron spectrometer and application to characterization of thermionic electron emitters, Appl. Surf. Sci. 21 (1985) 29–36.

[1868] Y. Enta, T. Kinoshita, S. Suzuki, S. Kono, Angle–resolved photoelectron–spectroscopy study of the Si(001)2×1–K surface, Phys. Rev. B 36 (1987) 9801–9804.

[1869] Y. Enta, T. Kinoshita, S. Suzuki, S. Kono, Angle–resolved photoelectron–spectroscopic study of Si(001)2×1/K and Si(001)2×1/Cs surfaces, Phys. Rev. B 39 (1989) 1125–1133.

[1870] O. Eriksson, Y.G. Hao, B.R. Cooper, G.W. Fernando, L.E. Cox, J.W. Ward, A.M. Boring, Electronic structure of hydrogen and oxygen chemisorbed on plutonium: Theoretical studies, Phys. Rev. B 43 (1991) 4590–4597.

[1871] A.G. Eguiluz, M. Heinrichsmeier, A. Fleszar, W. Hanke, First–principles evaluation of the surface barrier for a Kohn–Sham electron at a metal surface, Phys. Rev. Lett. 68 (1992) 1359–1362.

[1872] U.A. Effner, D. Badt, J. Binder, T. Bertrams, A. Brodde, Ch. Lunau, H. Neddermeyer, M. Hanbücken, Photoemission and scanning tunneling microscopy on K/Si(100), Surf. Sci. 277 (1992) 207–219.

[1873] R. Eibler, H. Erschbaumer, C. Temnitschka, R. Podloucky, A.J. Freemann, *Ab–initio* calculation of the electronic structure and energetics of the unreconstructed Au(001) surface, Surf. Sci. 280 (1993) 398–414.

[1874] M. Eckhardt, H. Kleine, D. Fick, Influence of doping on the bulk diffusion of Li into Si(100), Surf. Sci. 319 (1994) 219–223.

[1875] H.D. Ebinger, H. Arnolds, C. Polenz, B. Polivka, W. Preyß, R. Veith, D. Fick, H.J. Jänsch, Adsorption and diffusion of Li on Ru(001) surface: An NMR study, Surf. Sci. 412/413 (1998) 586–615.

[1876] A. Ernst, J. Henk, M. Lüders, Z. Szotek, W.M. Temmerman, Quantum–size effects in ultrathin Ag films on V(001): Electronic structure and photoelectron spectroscopy, Phys. Rev. B 66 (2002) 165435/1–11.

[1877] C.J. Edgcombe, N. de Jonge, Deduction of work function of carbon nanotube field emitter by use of curved–surface theory, J. Phys. D 40 (2007) 4123–4128.

[1878] H. Freitag, F. Krüger, Electron emission from tungsten–molybdenum alloys, Ann. Phys. 21 (1934/1935) 697–742.

[1879] H.E. Farnsworth, Contact potential difference between different faces of silver single crystals, Phys. Rev. 51 (1937) 378.

[1880] G.M. Fleming, J.E. Henderson, A thermoelectric method for the determination of work functions, Phys. Rev. 56 (1939) 853.

[1881] H.E. Farnsworth, R.P. Winch, Work function of different faces of silver single crystals, Phys. Rev. 56 (1939) 1067.

[1882] G.M. Fleming, J.E. Henderson, The energy losses attending field current and thermionic emission of electrons from metals, Phys. Rev. 58 (1940) 887–894.

[1883] F. Fianda, E. Lange, The time curve of the electrical potential of several metals after abrasion in vacuum, Z. Elektrochem. 55 (1951) 237–244.

[1884] R.K. Fry, A.B. Cardwell, Photoelectric properties of natural uranium and changes occurring at crystallographic transformations, Phys. Rev. 125 (1962) 471–474.

[1885] A.N. Frumkin, Zero charge potentials of electrodes, Sven. Kem. Tidskr. 77 (1965) 300–322 (see Ref. [3264]).

[1886] D.L. Fehrs, R.E. Stikney, Contact–potential measurements of the adsorption of cesium and oxygen on (110) tantalum, in: Ann. Conf. Phys. Electron., 27th, Top. Conf. Amer. Phys. Soc., 1967, pp. 77–84 (Chem. Abstr. 70 (1969) 50856z).

[1887] D.L. Fehrs, T.J. Lee, R.E. Stickney, Measurements of the work function and desorption energy of cesium and potassium on (100) tungsten, in: Rep. 7th Ann. Thermion. Convers. Special. Conf., IEEE, 1968, pp. 10–17 (see Ref. [2481]).

[1888] D.L. Fehrs, R.E. Stickney, Contact–potential measurements of the adsorption of Cs, K, and Na on (110)Ta, Bull. Am. Phys. Soc. 13 (1968) 945.

[1889] T.E. Fischer, Surface properties of Si from photoelectric emission at room temperature and 80 °K, Surf. Sci. 10 (1968) 399–409.

[1890] L.A. Fokina, N.A. Shurmovskaya, R.Kh. Burshtein, Comparison of the differences in work functions and zero–charge potentials, Elektrokhim. 5 (1969) 225–227.

[1891] A.G. Fedorus, Yu.M. Konoplev, A.G. Naumovets, Electronic and adsorption properties of barium on the (100) face of tungsten, Sov. Phys.—Solid State 11 (1969) 160–162.

[1892] D.L. Fehrs, T.J. Lee, B.J. Hopkins, R.E. Stickney, Comments on "An electron diffraction study of cesium adsorption on tungsten", Surf. Sci. 21 (1970) 197–202.

[1893] R.R. Ford, J. Pritchard, Work function of gold and silver films, Trans. Faraday Soc. 67 (1971) 216–221.

[1894] B. Feuerbacher, B. Fitton, Experimental investigation of photoemission from satellite surface materials, J. Appl. Phys. 43 (1972) 1563–1572.

[1895] A.G. Fedorus, A.G. Naumovets, Yu.S. Vedula, Adsorbed barium films on tungsten and molybdenum (011) face, Phys. Status Solidi (a) 13 (1972) 445–456.

[1896] R.M. Finn, D.J. Nicholson, J.W. Trischka, Thermionic constants and electron reflection for Ta(100) by the Shelton retarding field method, Surf. Sci. 34 (1973) 522–546.

[1897] S.C. Fain Jr., J.M. McDavid, Work–function variation with alloy composition: Ag–Au, Phys. Rev. B 9 (1974) 5099–5107.

[1898] Y. Fukuda, W.T. Elam, R.L. Park, Absolute $2p_{3/2}$ core binding energies and work functions of $3d$ transition metal surfaces, Phys. Rev. B 16 (1977) 3322–3329.

[1899] P.J. Feibelman, J.A. Appelbaum, D.R. Hamann, Electronic structure of a Ti(0001) film, Phys. Rev. B 20 (1979) 1433–1443.

[1900] J.L. Freeouf, G.W. Rubloff, P.S. Ho, T.S. Kuan, Microscopic compound formation at the Pd–Si(111) interface, Phys. Rev. Lett. 43 (1979) 1836–1839.

[1901] K.W. Frese Jr., Simple method for estimating energy levels of solids, J. Vac. Sci. Technol. 16 (1979) 1042–1044.

[1902] P.J. Feibelman, F.J. Himpsel, Spectroscopy of a surface of known geometry: Ti(0001)–N(1×1), Phys. Rev. B 21 (1980) 1394–1399.

[1903] J.L. Freeouf, J.M. Woodall, Unpublished (see Ref. [1905]).

[1904] J.L. Freeouf, M. Aono, F.J. Himpsel, D.E. Eastman, A study of Schottky barrier formation for Ga/Si(111)–(2×1) and Sb/Si(111)–(2×1) interfaces, J. Vac. Sci. Technol. 19 (1981) 681–684.

[1905] J.L. Freeouf, J.M. Woodall, Schottky barriers: An effective work function model, Appl. Phys. Lett. 39 (1981) 727–729.

[1906] J.L. Freeouf, Silicide interface stoichiometry, J. Vac. Sci. Technol. 18 (1981) 910–916.

[1907] Å. Fäldt, The Ag(111)/K system studied with ellipsometry, LEED and EELS, Surf. Sci. 114 (1982) 311–319.

[1908] C.L. Fu, S. Ohnishi, E. Wimmer, A.J. Freeman, Energetics of surface multilayer relaxation on W(001): Evidence for short range screening, Phys. Rev. Lett. 53 (1984) 675–678.

[1909] P.J. Feibelman, D.R. Hamann, Electronic structure of a "poisoned" transition–metal surface, Phys. Rev. Lett. 52 (1984) 61–64.

[1910] J.S. Foord, A.E. Reynolds, Sulphur adsorption and sulphide growth on Rh(111), Surf. Sci. 164 (1985) 640–648.

[1911] C.L. Fu, A.J. Freeman, Structural, electronic, and magnetic properties of Au/Cr/Au(001) sandwiches: Theoretical total–energy studies, Phys. Rev. B 33 (1986) 1611–1620.

[1912] C.L. Fu, A.J. Freeman, Surface ferromagnetism of Cr(001), Phys. Rev. B 33 (1986) 1755–1761.

[1913] G.W. Fernando, Y.C. Lee, P.A. Montano, B.R. Cooper, E.R. Moog, H.M. Naik, S.D. Bader, Surface electronic behavior of face–centered–cubic iron on copper, J. Vac. Sci. Technol. A 5 (1987) 882–886.

[1914] C.L. Fu, A.J. Freeman, Electronic and magnetic properties of the fcc Fe(001) thin films: Fe/Cu(001) and Cu/Fe/Cu(001), Phys. Rev. B 35 (1987) 925–932.

[1915] B. Frick, K. Jacobi, Growth and electronic structure of ultrathin palladium films on Al(111) and their interaction with oxygen and carbon monoxide, Phys. Rev. B 37 (1988) 4408–4414.

[1916] G.W. Fernando, B.R. Cooper, Theory of electronic structure and magnetic behavior of fcc iron grown on Cu(001), Phys. Rev. B 38 (1988) 3016–3027.

[1917] Å. Fäldt, D.K. Kristensson, H.P. Myers, Valence of Sm adsorbed on Pd(001), Phys. Rev. B 37 (1988) 2682–2684.

[1918] C.L. Fu, A.J. Freeman, Covalent bonding of sulfur on Ni(001): S as a prototypical adsorbate catalytic poisoner, Phys. Rev. B 40 (1989) 5359–5362.

[1919] D. Fargues, J.J. Ehrhardt, Adsorption of xenon on oxidized Ni(100) and Ni(111) surfaces by LEED and photoemission, Surf. Sci. 209 (1989) 401–422.

[1920] N. Fischer, S. Schuppler, Th. Fauster, W. Steinmann, Intrinsic linewidths of image–potential states on Ni(111), Phys. Rev. B 42 (1990) 9717–9719.

[1921] F. Finocchi, C.M. Bertoni, S. Ossicini, Simple metal surfaces and image potential states, Vacuum 41 (1990) 535–537.

[1922] N. Fischer, S. Schuppler, R. Fischer, Th. Fauster, W. Steinmann, Electronic structure of a single layer of Na on Cu(111), Phys. Rev. B 43 (1991) 14722–14725.

[1923] J. Fusy, M. Alnot, H. Abouelaziz, J.J. Ehrhardt, Low temperature growth mechanism of cobalt on Pt(110)(1×2), Surf. Sci. 251/252 (1991) 573–578.

[1924] C. Fiolhais, J.P. Perdew, Energies of curved metallic surfaces from the stabilized–jellium model, Phys. Rev. B 45 (1992) 6207–6215.

[1925] P.J. Feibelman, First–principle calculation of the geometric and electronic structure of the Be(0001) surface, Phys. Rev. B 46 (1992) 2532–2539.

[1926] N. Fischer, S. Schuppler, R. Fischer, Th. Fauster, W. Steinmann, Image states and the proper work function for a single layer of Na and K on Cu(111), Co(0001), and Fe(110), Phys. Rev. B 47 (1993) 4705–4713.

[1927] P.J. Feibelman, Structure of H–covered Be(0001), Phys. Rev. B 48 (1993) 11270–11276.

[1928] V. Fiorentini, M. Methfessel, M. Scheffler, Reconstruction mechanism of fcc transition metal(001) surfaces, Phys. Rev. Lett. 71 (1993) 1051–1054.

[1929] W.C. Fan, A. Ignatiev, Reconstruction of the Si(111) surface induced by alkali metals, Surf. Sci. 296 (1993) 352–357.

[1930] A.G. Fedorus, E. Bauer, Atomic structure and thermal stability of metastable transition–metal clusters adsorbed by tungsten(011) surface, Bull. Russ. Acad. Sci. Phys. 58 (1994) 1641–1645.

[1931] P.J. Feibelman, Anisotropy of the stress of fcc(110) surfaces, Phys. Rev. B 51 (1995) 17867–17875.

[1932] V. Fiorentini, D. Fois, S. Oppo, Inhibited Al diffusion and growth roughening of Ga–coated Al(100), Phys. Rev. Lett. 77 (1996) 695–698.

[1933] A. Filippetti, V. Fiorentini, Reconstructions of Ir(110) and (100): An *ab initio* study, Surf. Sci. 377–379 (1997) 112–116.

[1934] L. Chen, X. Wang, S. Shi, Y. Cui, H. Luo, Y. Gao, Tuning the work function of VO$_2$(100) surface by Ag adsorption and incorporation: Insights from first–principles calculations, Appl. Surf. Sci. 367 (2016) 507–517.

[1935] C.J. Fall, N. Binggeli, A. Baldereschi, Deriving accurate work functions from thin–slab calculations, J. Phys.: Condens. Matter 11 (1999) 2689–2696.

[1936] C.J. Fall, N. Binggeli, A. Baldereschi, Local work function around sharp aluminum facets edges, Comput. Phys. Comm. 121–122 (1999) 631.

[1937] A. Fedorus, V. Koval, A. Naumovets, H. Pfnür, Metastable structures of Dy layers adsorbed on Mo(112) and their transformations, Eur. Phys. J. B 24 (2001) 395–403.

[1938] P.J. Feibelman, Surface–diffusion mechanism versus electric field: Pt/Pt(001), Phys. Rev. B 64 (2001) 125403/1–6.

[1939] Y.J. Feng, K.P. Bohnen, C.T. Chan, First–principles studies of Au(100)–hex reconstruction in an electrochemical environment, Phys. Rev. B 72 (2005) 125401/1–8.

[1940] H. Fukidome, M. Yoshimura, K. Ueda, Evaporation and thermionic emission processes of Pb/W(110) imaged *in situ* by emission electron microscopy, Japan. J. Appl. Phys. 45 (2006) 70–72.

[1941] C.B. Feng, Z.Q. Ma, Y.H. Li, F. Hong, Adsorption of Al on the Si(001) surface, Physica B 403 (2008) 2979–2986.

[1942] J.A. Farmer, N. Ruzycki, J.F. Zhu, C.T. Campbell, Lithium adsorption on MgO(100) and its defects: Charge transfer, structure, and energetics, Phys. Rev. B 80 (2009) 035418/1–8.

[1943] S.V. Faleev, O.N. Mryasov, T.R. Mattsson, Quasiparticle self–consistent GW calculation of the work functions of Al(111), Al(100), and Al(110), Phys. Rev. B 81 (2010) 205436/1–7.

[1944] A. Goetz, Studies on the electron emission from metals and its dependence upon the changes of state of the material of the cathode: II. The fusion diagrams of silver, gold and copper, Z. Phys. 43 (1927) 531–562.

[1945] A. Goetz, The photoelectric effect of molten tin and two of its allotropic modifications, Phys. Rev. 33 (1929) 373–385.

[1946] A. Goetz, Photoelectric effect of allotropic modification of tin, Z. Phys. 53 (1929) 494–525.

[1947] A. Goetz, The photoelectric effect of molten tin and two of its allotropic modifications, Phys. Rev. 33 (1929) 265.

[1948] E. Gaviola, J. Strong, Photoelectric effect of aluminum films evaporated in vacuum, Phys. Rev. 49 (1936) 441–443.

[1949] C.J. Gallagher, Adsorption of thorium on tantalum, Phys. Rev. 65 (1944) 46–50.

[1950] H. Kawano, H. Inouye, Time variation of ionic and neutral evaporation from alkali metal iodides on a platinum surface, J. Phys. Chem. 71 (1967) 712–717.

[1951] P. Gombás, The theory of metals, Hung. Acta Phys. 1 (1947) 1–33 (Chem. Abstr. 42 (1948) 6637d).

[1952] M.A. Gilleo, Photoemission from silver into AgCl, KBr, NaCl, and new bands of photosensitivity in AgCl, Phys. Rev. 91 (1953) 534–542.

[1953] J. Giner, E. Lange, Electron exit potentials of pure and oxygen–covered gold, platinum, and palladium from their Volta potentials against silver, Naturwiss. 40 (1953) 506.

[1954] V.M. Gavrilyuk, Influence of adsorbed atomic barium and polar molecular barium oxide films on the work function of tungsten, gold, and germanium, Izv. Akad. Nauk SSSR, Ser. Fiz. 20 (1956) 1071–1075 (Chem. Abstr. 51 (1957) 3272i).

[1955] W. Gordy, W.J.O. Thomas, Electronegativities of the elements, J. Chem. Phys. 24 (1956) 439–444.

[1956] K. Gschneidner, A compilation of the physical properties of the rare earth, scandium and yttrium metals, in: Symp. Rare Earth and Related Metals, Atom. Ener. Commiss., Chicago, 1959 (see Ref. [2750]).

[1957] J. Gerlach, Diss. Hannover, 1960 (see Ref. [3052]).

[1958] H. Gienapp, Electron work functions on macroscopic tungsten crystal faces, Z. Angew. Phys. 12 (1960) 254–257.

[1959] G.W. Gobeli, F.G. Allen, Surface measurements on freshly cleaved silicon *p–n* junctions, J. Phys. Chem. Solids 14 (1960) 23–26.

[1960] R. Garron, D. Testard, Evidence and measurement of an effect of temperature on the work function of potassium, Compt. Rend. 253 (1961) 1770–1771.

[1961] R. Garron, M. Liberman, D. Testard, Variation of the work function of potassium with temperature, Compt. Rend. 253 (1961) 2882–2883.

[1962] G. Gardner, R.L. Anthony, E.A. Coomes, Thermionic emission from single crystal molybdenum wire, Bull. Am. Phys. Soc. 6 (1961) 422.

[1963] V.M. Gavrilyuk, V.K. Medvedev, The adsorption of barium atoms and carbon monoxide molecules on the (113) face of a tungsten single crystal, Sov. Phys.—Solid State 4 (1963) 1737–1744.

[1964] I.I. Gofman, The electrostatic emission from tungsten in the region of weak fields, Dokl. Akad. Nauk Uzb.SSR 19 (6) (1962) 26–28.

[1965] I.I. Gofman, Investigation of electrostatic electron emission from tungsten in a broad current–density intervals, Sov. Phys.—Solid State 4 (1963) 1471–1477.

[1966] V.M. Gavrilyuk, A.G. Naumovets, Surface diffusion of adsorbed atoms in an electric field, Sov. Phys.—Solid State 5 (1964) 2043–2048.

[1967] F.E. Girouard, Average and monocrystallographic thermionic emission parameters for recrystallized molybdenum and tungsten filaments (Ph.D. Thesis), Univ. of Notre Dame, Indiana, 1964, 89 pp (see Ref. [3724]).

[1968] R. Garson, Photoelectric efficiency of thin films of Mg, Compt. Rend. 258 (1964) 1458–1460.

[1969] G.W. Obeli, F.G. Allen, Photoelectric properties and work function of cleaved germanium surfaces, Surf. Sci. 2 (1964) 402–408.

[1970] Yu.K. Gus'kov, V.P. Pashchenko, E.E. Sibir, Investigation of the operation of a thermoelectronic converter with different metal film cathodes, Izv. Akad. Nauk SSSR, Ser. Fiz. 28 (1964) 1537–1540.

[1971] G.W. Gobeli, F.G. Allen, Photoelectric properties of cleaved GaAs, GaSb, InAs, and InSb surfaces: Comparison with Si and Ge, Phys. Rev. 137 (1965) A245–254.

[1972] N.A. Gorbatyi, E.M. Ryabchenko, The behavior of adsorbed Cs films on single–crystal spikes of Ta and Ta$_2$C, Sov. Phys.—Solid State 7 (1965) 921–926.

[1973] R. Garron, Photosensitivity of thin metallic layers, Ann. Phys. (Paris) 10 (1965) 595–622.

[1974] V.M. Gavrilyuk, V.K. Medvedev, Investigation of the adsorption of lithium on the surface of a tungsten single crystal in a field–emission projector, Sov. Phys.—Solid State 8 (1966) 1439–1444.

[1975] A.V. Garnov, N.A. Gorbatyi, B.I. Karpachev, Adsorption–emission characteristics of rare earth metal films on faces of a tungsten single crystal, Izv. Akad. Nauk SSSR, Ser. Fiz. 35 (1971) 341–344.

[1976] D.V. Geppert, A.M. Cowley, B.V. Dore, Correlation of metal–semiconductor barrier height and metal work function: Effects of surface states, J. Appl. Phys. 37 (1966) 2458–2467.

[1977] V.M. Gavrilyuk, V.K. Medvedev, Adsorption of lithium on faces of a tungsten single crystal covered with an adsorbed oxygen film, Sov. Phys.—Solid State 9 (1967) 259–261.

[1978] V.M. Gavrilyuk, A.G. Naumovets, A.G. Fedorus, Investigation of adsorption of cesium on a tungsten single crystal, Sov. Phys.—JETP 24 (1967) 899–904.

[1979] A.A. Gugnin, O.Kh. Khamidov, The work function of the alloys of rhenium with scandium, Radiotech. Elektron. 12 (1967) 2270.

[1980] E.P. Gyftopoulos, Comments on work function theories, in: 2nd Int. Conf. Thermion. Electr. Power Generat., Stresa, Italy, 1968, pp. 1225–1248.

[1981] J.W. Gadzuk, Theory of metallic adsorption on real metal surfaces, in: G.A. Somoljai (Ed.), The Structure and Chemistry of Solid Surfaces, John Wiley, 1969, pp. 43/1–29.

[1982] D.A. Gorodetskii, A.A. Yas'ko, Investigation by low–energy electron diffraction of scandium films adsorbed on a (110) tungsten surface, Sov. Phys.—Solid State 10 (1969) 1812–1817.

[1983] R. Gerlach, T.N. Rhodin, Alkali atom adsorption on single crystal nickel surfaces: Surface structure and work function, in: Proc. Int. Mater. Symp., Berkley, 1968, pp. 55/1–25.

[1984] D.A. Gorodetskii, A.A. Yas'ko, Structure of lead films on a (110) face of tungsten, Sov. Phys.—Solid State 11 (1969) 640–641.

[1985] D.A. Gorodetskii, A.A. Yas'ko, Scandium and yttrium films on the (100) face of tungsten, Sov. Phys.—Solid State 11 (1970) 2028–2032.

[1986] D.A. Gorodetskii, A.A. Yas'ko, Structure of indium and yttrium films on a tungsten(110) face, Izv. Akad. Nauk SSSR, Ser. Fiz. 33 (1969) 467–472.

[1987] N.A. Gorbatyi, B.I. Karpachev, Emission and adsorption properties of gadolinium and yttrium films on a tungsten single crystal, Sov. Phys.—Solid State 11 (1969) 1144–1147.

[1988] R. Garron, L. Gaudart, R. Payan, Optical and photoelectric properties of thin films of sodium in relation to their electronic structure, Compt. Rend. B 268 (1969) 266–269.

[1989] L. Gaudart, Action of an electric field on the photoelectric effect of copper and silver thin films, Compt. Rend. B 269 (1969) 129–132.

[1990] Yu.Ya. Gurevich, Determination of the work function by electrochemical measurements, Sov. Phys.—Solid State 11 (1970) 2409–2412.

[1991] A.A. Galaev, Yu.N. Parkhomenko, A.P. Bliev, Interrelation between atomic structure and electron work function on cleaved (111) surface of germanium, Kristallografiya 25 (1980) 883–885.

[1992] R.L. Gerlach, T.N. Rhodin, Binding and charge transfer associated with alkali metal adsorption on single crystal nickel surfaces, Surf. Sci. 19 (1970) 403–426.

[1993] N.A. Gordienko, L.I. Antropov, Calculation of electron work function and null points, Ukr. Khim. Zh. 36 (1970) 1285–1286 (Chem. Abstr. 75 (1971) 11094h).

[1994] R.L. Gerlach, T.N. Rhodin, Unpublished (see Ref. [519]).

[1995] D.A. Gorodetskii, A.A. Yas'ko, Structure and work function of antimony films on a tungsten(100) surface, Sov. Phys.—Solid State 13 (1972) 2928–2929.

[1996] D.A. Gorodetskii, A.A. Yas'ko, S.A. Shevlyakov, Structure of lanthanum films on the (110) and (100) faces of tungsten, Izv. Akad. Nauk SSSR, Ser. Fiz. 35 (1971) 585–590.

[1997] L. Gaudart, R. Rivoira, Photoelectric properties of calcium thin films, Appl. Opt. 10 (1971) 2336–2343.

[1998] L. Gaudart, R. Rivoira, Photoelectric properties of calcium thin films in relation to their structure, Compt. Rend. B 272 (1971) 855–858.

[1999] L. Gaudart, R. Payan, Photoelectric properties of sodium thin films in the immediate vicinity of the photoelectric threshold, Thin Solid Films 7 (1971) R13–R16.

[2000] I.G. Gverdtsiteli, A.G. Kudziev, R.Ya. Kucherov, L.M. Tsakadze, V.K. Tskhakaya, Investigation of the collector material work function influence on the electrical characteristics of thermionic converters in an arc mode, in: Proc. 3rd Int. Conf. Thermion. Electr. Power Generat., Jülich, 1972, pp. 1117–1126 (see Ref. [2016]).

[2001] T.F. Gesell, E.T. Arakawa, Work function changes during oxygen chemisorption on fresh magnesium surfaces, Surf. Sci. 33 (1972) 419–421.

[2002] D.A. Gorodetskii, A.A. Yas'ko, Structure of lead films on a tungsten(100) surface, Sov. Phys.—Solid State 14 (1972) 636–638.

[2003] L. Gaudart, R. Rivoira, Photoelectric properties of calcium thin films subjected to an electric field perpendicular to their surface, Compt. Rend. B 275 (1972) 509–512.

[2004] M. Nekovee, J.M. Pitarke, Recent progress in the computational many–body theory of metal surfaces, Comput. Phys. Commun. 137 (2001) 123–142.

[2005] N.A. Gordienko, Potential barrier at the interphase boundary, electrode potential, and some possibilities for regulating electrode processes, Ukr. Respub. Konf. Elektrokhim. First, Kiev 1 (1973) 61–67.

[2006] P.O. Gartland, S. Berge, B.J. Slagsvold, Photoemission study of the anisotropic work function of a clean copper single crystal, Phys. Norv. 7 (1973) 39–49 (Chem. Abstr. 80 (1974) 42011m).

[2007] W.A. Gordon, G.B. Chapman: II. Determination of work functions near melting points of refractory metals by using a direct–current arc, Surf. Sci. 39 (1973) 121–135.

[2008] L. Gaudart, R. Rivoira, Action of an electric field on the photoelectric properties of thin films of calcium, Appl. Opt. 12 (1973) 1897–1903.

[2009] T. Gustafsson, G. Brodén, P.-O. Nilsson, Photoelectric properties of evaporated Be films, J. Phys. F 4 (1974) 2351–2358.

[2010] R. Garron, L. Gaudart, D. Testard, Action of an electrostatic field on photoelectric effect of thin films of iron, J. Appl. Phys. 45 (1974) 1701–1706.

[2011] N.A. Gorbatyi, A.V. Garnov, B.I. Karpachev, L.V. Reshetnikova, R.F. Gazizov, Emission–adsorption characteristics of rare earth metal films on a tungsten single–crystal surface, Izv. Akad. Nauk SSSR, Ser. Fiz. 38 (1974) 260–264.

[2012] N.A. Gorbatyi, V.A. Chekina, Distribution of the velocities of thermoelectrons emitted by individual faces of a tungsten single–crystal whisker, Izv. Akad. Nauk SSSR, Ser. Fiz. 38 (1974) 230–233.

[2013] N.M. Garifullin, Yu.V. Zubenko, Influence of adsorption of silicon atoms on work function of Ba deposited on (001) face of W, Sov. Phys.—Solid State 17 (1976) 2370–2371.

[2014] L. Gaudart, P. Renucci, R. Rivoira, Photoemission of thin films of strontium, Compt. Rend. B 281 (1975) 281–284.

[2015] P.E. Gregory, P. Chye, H. Sunami, W.E. Spicer, The oxidation of Cs–UV photoemission studies, J. Appl. Phys. 46 (1975) 3525–3529.

[2016] I.G. Gverdtsiteli, I.L. Korobova, R.Ya. Kucherov, B.Ya. Moizhes, L.M. Tsakadze, V.K. Tskhakaya, Effect of collector material on the characteristics of a thermionic converter, Sov. Phys. Tech. Phys. 21 (1976) 312–316.

[2017] D.A. Gorodetskiĭ, A.D. Gortinskiĭ, V.I. Maksimenko, Yu.P. Mel'nik, Concentration dependence of the characteristic loss spectrum of a monatomic barium film, Sov. Phys. Sold State 18 (1976) 691–692.

[2018] N.M. Garifullin, Yu.V. Zubenko, V.M. Yagodkin, Determination of the work function of bismuth and bismuth sulfide by a field–emission method, Radio Eng. Elect. Phys. 21 (1976) 145–146.

[2019] G.M. Guichar, C.A. Sébenne, G.A. Garry, M. Balkanski, Structure dependent oxidation of clean Si(111) surfaces, Surf. Sci. 58 (1976) 374–378.

[2020] M.S. Gupalo, V.K. Medvedev, T.P. Smereka, G.V. Babkin, B.M. Palyukh, Adsorption of lanthanum on the (100) face of a tungsten single crystal, Sov. Phys.—Solid State 19 (1977) 1731–1733.

[2021] L. Gaudart, P. Renucci, R. Rivoira, Photoemission from very thin films of strontium: Action of an electric field, Phys. Rev. B 15 (1977) 3078–3086.

[2022] D.A. Gorodetsky, Yu.P. Melnik, Barium on (110) tungsten, Surf. Sci. 62 (1977) 647–661.

[2023] G.M. Guichar, Electronic properties of tetrahedral coordination semiconductor surfaces (Ph.D. thesis), Univ. Pierre et Marie Curie, 1978, 52 pp. (see Ref. [2029]).

[2024] L. Gaudart, P. Renucci, R. Rivoira, Work functions and structures of alkaline–earth thin films, J. Appl. Phys. 49 (1978) 4105–4110.

[2025] A.K. Green, E. Bauer, Work function and purity of the beryllium(0001) surface, Surf. Sci. 74 (1978) 676–681.

[2026] F. Greuter, P. Oelhafen, Conduction electrons in solid and liquid gallium, Z. Phys. B 34 (1979) 123–128.

[2027] M.S. Gupalo, V.K. Medvedev, B.M. Palyukh, T.P. Smereka, Adsorption of lithium on the (112) face of a molybdenum crystal, Sov. Phys.—Solid State 21 (1979) 568–573.

[2028] S.K. Gupta, A.K. Kapil, C.M. Singal, V.K. Srivastava, Measurement of the work function of some metals using internal voltage in MIM (metal/insulator/metal) structures, J. Appl. Phys. 50 (1979) 2852–2855.

[2029] G.M. Guichar, G.A. Garry, C.A. Sébenne, Photoemission yield spectroscopy of electronic surface states on germanium(111) surfaces, Surf. Sci. 85 (1979) 326–334.

[2030] M.S. Gupalo, V.K. Medvedev, B.M. Palyukh, T.P. Smereka, Structure, work function, and thermal stability of sodium films on a (112) face of molybdenum, Sov. Phys.—Solid State 22 (1980) 1873–1876.

[2031] M.S. Gupalo, Adsorption of potassium on (112) face of molybdenum crystals, Sov. Phys.—Solid State 22 (1980) 1345–1347.

[2032] M.S. Gupalo, V.K. Medvedev, B.M. Palyukh, T.P. Smereka, Adsorption of cesium on a (112) face of a molybdenum crystal, Sov. Phys.—Solid State 23 (1981) 1211–1214.

[2033] H.S. Greenside, D.R. Hamann, Cl chemisorption on the Pd(001) surface: A self–consistent LCAO calculation of electronic structure, Solid State Commun. 39 (1981) 1129–1132.

[2034] M.S. Gupalo, T.P. Smereka, G.V. Babkin, B.M. Palyukh, Adsorption of lithium–lanthanum films on the tungsten(100) surface, Sov. Phys.—Solid State 24 (1982) 990–993.

[2035] T.M. Gardiner, The structure of ultrathin iron films on tungsten single–crystal surfaces, Thin Solid Films 105 (1983) 213–225.

[2036] F. Greuter, D. Heskett, E.W. Plummer, H.-J. Freund, Chemisorption of CO on Co(0001): Structure and electronic properties, Phys. Rev. B 27 (1983) 7117–7135.

[2037] N.A. Gorbatyi, L.V. Reshetnikova, Simultaneous adsorption of lutetium and barium on the surface of a tungsten point single crystal, Bull. Acad. Sci. USSR, Phys. Ser. 49 (9) (1985) 63–65.

[2038] E.L. Garfunkel, X. Ding, G. Dong, S. Yang, X. Hou, X. Wang, The coadsorption of sodium and oxygen on Ag(100): An XPS, UPS and HREELS study, Surf. Sci. 164 (1985) 511–525.

[2039] G.W. Graham, Electronic structure of palladium films on tungsten surfaces, J. Vac. Sci. Technol. A 4 (1986) 760.

[2040] F. Greuter, I. Strathy, E.W. Plummer, W. Eberhardt, Photoemission from H adsorbed on Ni(111) and Pd(111) surfaces, Phys. Rev. B 33 (1986) 736–746.

[2041] G.W. Graham, Carbon monoxide chemisorption on Cu(100)–c(2×2)Pd, Surf. Sci. 171 (1986) L432–L440.

[2042] J. Garbe, D. Venus, S. Suga, C. Schneider, J. Kirschner, Spin–polarized angle–resolved photoemission from the (110) surface of platinum, Surf. Sci. 178 (1986) 342–348.

[2043] F.M. Gonchar, V.K. Medvedev, T.P. Smereka, Ya.B. Lozovyi, G.V. Babkin, Adsorption of gadolinium and dysprosium on the (112) face of a tungsten single crystal, Sov. Phys.—Solid State 29 (1987) 1629–1630.

[2044] G.A. Gaudin, M.J.G. Lee, Emission parameters of low–index surfaces by a combined field and photofield emission method, Surf. Sci. 185 (1987) 283–298.

[2045] Y.M. Gong, R. Gomer, Thermal roughening on stepped tungsten surfaces. I. The zone (011)–(112), J. Chem. Phys. 88 (1988) 1359–1369.

[2046] F.M. Gonchar, T.P. Smereka, S.I. Stepanovskii, G.V. Babkin, Adsorption of terbium and gadolinium on a (111) face of a tungsten crystal, Sov. Phys.—Solid State 30 (1988) 2035–2037.

[2047] P. Giesert, Investigation of alkali adsorption and diffusion on Ni(100), as well as N_2–coadsorption using a new measurement method (Thesis), Univ. of Kassel, 1989 (see Ref. [915]).

[2048] A. Goldmann, G. Rosina, E. Bertel, F.P. Netzer, The electronic structure of rhodium: Angle–resolved studies of photoelectron and secondary electron emission, Z. Phys. B 73 (1989) 479–487.

[2049] F.M. Gonchar, V.K. Medvedev, T.P. Smereka, V.V. Savichev, Adsorption of holmium on the (112) face of a tungsten single crystal, Sov. Phys.—Solid State 31 (1989) 1056–1057.

[2050] G.H.M. Gubbels, L.R. Wolff, R. Metselaar, A WF_6–CVD tungsten film as an emitter for a thermionic energy converter. II. Electron and Cs^+– ion emission from WF_6–CVD tungsten films, Appl. Surf. Sci. 40 (1989) 201–207.

[2051] N.R. Gall', E.V. Rut'kov, A.Ya. Tontegode, Interaction of silicon atoms with the $(10\bar{1}0)$ surface of rhenium: Adsorption, desorption, and silicide formation, Sov. Phys. Tech. Phys. 35 (1990) 475–478.

[2052] F.M. Gonchar, V.K. Medvedev, T.P. Smereka, G.V. Babkin, Adsorption of dysprosium on the (112) face of a molybdenum crystal, Sov. Phys.—Solid State 32 (1990) 1092–1093.

[2053] H. Göhlich, T. Lange, T. Bergmann, U. Näher, T.P. Martin, Ionization energies of sodium clusters containing up to 22000 atoms, Chem. Phys. Lett. 187 (1991) 67–72.

[2054] G.A. Gaudin, M.J.G. Lee, Aggregates of chemisorbed copper on the (110) and (100) surfaces of tungsten, Surf. Sci. 280 (1993) 91–105.

[2055] D.A. Gorodetsky, Yu.P. Melnik, V.K. Sklyar, Coadsorption of barium and oxygen on W(100), Bull. Russ. Acad. Sci. Phys. Ser. 58 (1994) 1701–1704.

[2056] J. Giergiel, J. Kirschner, J. Landgraf, J. Shen, J. Woltersdorf, Stages of structural transformation in iron thin film growth on copper(100), Surf. Sci. 310 (1994) 1–15.

[2057] T.M. Grehk, L.S.O. Johansson, S.M. Gray, M. Johansson, A.S. Flodström, Adsorption of Li on the Si(100)2×1 surface studied with high–resolution core–level spectroscopy, Phys. Rev. B 52 (1995) 16593–16601.

[2058] N.R. Gall', E.V. Rut'kov, A.Ya. Tontegode, M.M. Usufov, Surface sulfide on (100)W: Formation, stability, absolute concentration of sulfur, Appl. Surf. Sci. 93 (1996) 353–358.

[2059] J. Günster, Th. Mayer, V. Kempter, Study of the electronic structure of Si(100)2×1 and Cs/Si(100)2×1 with MIES and UPS (HeI), Surf. Sci. 359 (1996) 155–162.

[2060] O. Gröning, O.M. Küttel, P. Gröning, L. Schlapbach, Field emitted electron energy distribution from nitrogen–containing diamondlike carbon, Appl. Phys. Lett. 71 (1997) 2253–2255.

[2061] P. García-González, J.E. Alvarellos, E. Chacón, Nonlocal symmetrized kinetic–energy density functional: Application to simple surfaces, Phys. Rev. B 57 (1998) 4857–4862.

[2062] S.Yu. Davydov, Effect of adsorption of group VI atoms on the silicon work function, Phys. Solid State 47 (2005) 1779–1783.

[2063] P.A. Gravil, H. Toulhoat, Ethylene, sulfur, and chlorine coadsorption on Pd(111): A theoretical study of poisoning and promotion, Surf. Sci. 430 (1999) 192–198.

[2064] A. Goldoni, G. Paolucci, The interaction of C_{60} with Ag(100): Strong predominantly ionic bonding, Surf. Sci. 437 (1999) 353–361.

[2065] Y. Gohda, S. Watanabe, Total energy distribution of field–emitted electrons from Al(100) surface with single–atom terminated protrusion, Phys. Rev. Lett. 87 (2001) 177601/1–4.

[2066] O. Gröning, L.-O. Nilsson, P. Gröning, L. Schlapbach, Properties and characterization of chemical vapor deposition diamond field emitters, Solid-State Electron. 45 (2001) 929–944.

[2067] Y. Gohda, S. Watanabe, *Ab initio* calculations of field emission from ultrathin Si(100) films, J. Vac. Sci. Technol. B 21 (2003) 2461–2465.

[2068] M. Gajdoš, A. Eichler, J. Hafner, CO adsorption on close–packed transition and noble metal surfaces: Trends from *ab initio* calculations, J. Phys.: Condens. Matter 16 (2004) 1141–1164.

[2069] H.R. Gong, A.K. Ray, A first–principles study of the (001), (111) and (110) surface of δ–Pu, in: Mater. Res. Soc. Symp. Proc., 2006, p. 45 (Chem. Abstr. 145 (2006) 34644r).

[2070] H.R. Gong, A.K. Ray, A fully–relativistic full–potential–linearized–augmented–plane–wave study of the (111) surface of δ–Pu, Surf. Sci. 600 (2006) 2231–2241.

[2071] D. Gao, A.K. Ray, On the convergence of the electronic structure properties of the fcc americium(001) surface, Surf. Sci. 600 (2006) 4941–4952.

[2072] Y. Gotoh, K. Mukai, Y. Kawamura, H. Tsuji, J. Ishikawa, Work function of low index crystal facet of tungsten evaluated by the seppen–katamuki analysis, J. Vac. Sci. Technol. B 25 (2007) 508–512.

[2073] H.R. Gong, Y. Nishi, K. Cho, Effects of strain and interface on work function of a Nb–W metal gate system, Appl. Phys. Lett. 91 (2007) 242105/1–3.

[2074] H.R. Gong, K. Cho, Electronic structure and work function of metal gate Mo–W system, Appl. Phys. Lett. 91 (2007) 092106/1–3.

[2075] D. Gao, A.K. Ray, Quantum size effects on the (0001) surface of double hexagonal close packed americium, Eur. Phys. J. B 55 (2007) 13–22.

[2076] D. Gao, A.K. Ray, A first–principles electronic structure study of the high–symmetry surfaces of fcc americium, J. Alloy. Comp. 444–445 (2007) 184–190.

[2077] S. García-Gil, A. García, N. Lorente, P. Ordejón, Optimal strictly localized basis sets for noble metal surfaces, Phys. Rev. B 79 (2009) 075441/1–9.

[2078] W. Hüttemann, Emissions of electrons and positive ions from glowing filaments, Ann. Phys. 52 (1917) 816–848.
[2079] R. Hamer, The limiting frequency of the photo–electric effect, Phys. Rev. 20 (1922) 198.
[2080] R. Hamer, Photoelectric thresholds of elements under ordinary conditions, J. Opt. Soc. Amer. 9 (1924) 251–258.
[2081] B. Hales, Critical photoelectric potential of clean mercury and the influence of gases and of the circulation of the mercury upon it, Phys. Rev. 32 (1928) 950–960.
[2082] J.E. Henderson, R.E. Badgley, The work required to remove a field electron, Phys. Rev. 38 (1931) 590.
[2083] C.L. Henshaw, Normal energy distribution of photoelectrons from thin potassium films as a function of temperature, Phys. Rev. 52 (1937) 854–865.
[2084] W. Heinze, The relation of contact potential with the work of emission, Z. Phys. 109 (1938) 459–471.
[2085] W.L. Hole, R.W. Wright, Emissive and thermionic characteristics of uranium, Phys. Rev. 56 (1939) 785–787.
[2086] A.E. Hennings, W.H. Kadesh, The relations of the photo–potentials assumed by different metals when stimulated by light of a given frequency, Phys. Rev. 8 (1916) 209–220.
[2087] R. Hirschberg, E. Lange, Electron–exit potentials of cadmium, copper, tin, and zinc on the basis of their potentials against silver, Naturwiss. 39 (1952) 131.
[2088] G.A. Haas, Dr. thesis, Univ. of Notre Dame, 1953 (see Ref. [134]).
[2089] H.D. Hagstrum, Instrumentation and experimental procedure for studies of electron ejection by ions and ionization by electron impact, Rev. Sci. Instrum. 24 (1953) 1122–1142.
[2090] H.E. Hintergger, Photoelectric emission in the extreme ultraviolet, Phys. Rev. 96 (1954) 538–539.
[2091] H.D. Hagstrum, Auger ejection of electrons from molybdenum by noble gas ions, Phys. Rev. 104 (1956) 672–683.
[2092] H.D. Hagstrum, Thermionic constants and sorption properties of hafnium, J. Appl. Phys. 28 (1957) 323–328.
[2093] D. Haneman, Photoelectric emission and work functions of InSb, GaAs, Bi_2Te_3 and germanium, J. Phys. Chem. Sol. 11 (1959) 205–214.
[2094] F.L. Hughes, H. Levinstein, R. Kaplan, Surface properties of etched tungsten single crystals, Phys. Rev. Lett. 2 (1959) 133.
[2095] A. Handorff, Diss. Hannover, 1960 (see Ref. [3052]).
[2096] A. Hermann, Diss. Hannover, 1960 (see Ref. [3052]).
[2097] P. Handler, Energy level diagrams for germanium and silicon surfaces, J. Phys. Chem. Sol. 14 (1960) 1–8.
[2098] G.A. Haas, J.T. Jensen Jr., Thermionic studies of various uranium compounds, J. Appl. Phys. 34 (1963) 3451–3457.
[2099] J.M. Houston, Thermion. Special. Conf., San Diego, 1965 (see Ref. [794]).
[2100] E.E. Huber Jr., C.T. Kirk Jr., Work function changes due to the chemisorption of water and oxygen on aluminum, Surf. Sci 5 (1966) 447–465.
[2101] J.M. Houston, High–work–function coatings on barium dispenser cathodes, in: 27th Ann. Conf. Phys. Electr., Top. Conf. Am. Phys. Soc., 1967, pp. 95–103 (Chem. Abstr. 70 (1969) 51879w).
[2102] B.J. Hopkins, K.R. Pender, Comments on "The adsorption of hydrogen on (100) tungsten single crystal surfaces" by R. A. Armstrong, Surf. Sci. 6 (1967) 479–480.
[2103] B.J. Hopkins, A.J. Sargood, Some properties of vapour–deposited uranium films in ultra–high vacuum and in hydrogen, Nuovo Cimento, Suppl. 5 (1967) 459–465.
[2104] B.J. Hopkins, B.J. Smith, Direct comparison of the Kelvin and the electron–beam methods of contact–potential–difference measurement, J. Appl. Phys. 39 (1968) 213–216.
[2105] J.M. Houston, Thermionic energy conversion, U.S. Clearinghouse Fed. Sci. Tech. Inform. AD (AD 669106) (1968) 158 pp (see Ref. [4362]).
[2106] B.J. Hopkins, S. Usami, Nitrogen adsorption on the (110) and (112) planes of tungsten single crystals, J. Appl. Phys. 39 (1968) 3500–3501.
[2107] D. Hillecke, Absolute measurements of the ionization coefficients of alkali atoms on metal surfaces. III. Rubidium atoms on tungsten and platinum surfaces, Z. Phys. 215 (1968) 343–349.
[2108] B.J. Hopkins, B.J. Smith, Adsorption of barium onto oriented tungsten surfaces, J. Chem. Phys. 49 (1968) 2136–2140.
[2109] D. Hillecke, Absolute measurements of the ionization coefficients of alkali atoms on metal surfaces. IV. Cesium atoms on tungsten and platinum surfaces, Z. Phys. 225 (1969) 76–78.
[2110] B.J. Hopkins, S. Usami, The surface potential of hydrogen on tungsten (100), (110) and (112) single crystal surfaces, Surf. Sci. 23 (1970) 423–426.
[2111] P. Jean, Photoelectric effect in liquid indium, C. R. Acad. Sci. Paris 260 (1965) 2465–2467.
[2112] B.J. Hopkins, C.B. Williams, P.C. Wilmer, Chemical and physical adsorption of oxygen on the (110) plane of tungsten, Surf. Sci. 25 (1971) 633–642.
[2113] G.K. Hall, C.H.B. Mee, The work function of α–iron, α–cobalt, and α–manganese, Phys. Status Solidi (a) 5 (1971) 389–395.
[2114] G.K. Hall, C.H.B. Mee, The adsorption of carbon monoxide on iron, cobalt, and manganese, Phys. Status Solidi (a) 12 (1972) 509–515.
[2115] C.R. Helms, W.E. Spicer, Comparison of the oxidation process in strontium and cerium by ultraviolet photoelectron spectroscopy, Appl. Phys. Lett. 21 (1972) 237–239.
[2116] C.R. Helms, W.E. Spicer, Photoemission studies of the oxidation of strontium, Phys. Rev. Lett. 28 (1972) 565–569.
[2117] G. Haufler, H. Goretski, J. Jucker, Electron work function change of interstitial compounds of the 4a and 5a metals in dependence on the nonmetal content, in: Proc. 3rd Int. Conf. Thermion. Electr. Power Generat., vol. 3, Jülich, 1972, pp. 1423–1433.
[2118] C. Haque, J. Fritz, Work function changes on contact materials, in: Proc. 19th Ann. Holm Semi. Electr. Cont. Phenom. Chicago, 1973, pp. 111–117.
[2119] T.W. Hall, C.H.B. Mee, The work function of rubidium, Phys. Status Solidi (a) 21 (1974) 109–113.
[2120] T.W. Hall, C.H.B. Mee, A photoelectric study of the adsorption of rubidium on tungsten, in: Proc. 2nd Int. Conf. Solid Surf., Tokyo, Japan. J. Appl. Phys. Suppl. 2 (Pt. 2) (1974) 741–744.
[2121] H. Hojo, K. Nakayama, Coated emitters of transition metal carbides, Shinku (J. Vac. Soc. Japan) 19 (1976) 312–317.
[2122] J.R. Hiskes, A. Karo, M. Gardner, Mechanism for negative–ion–production in the surface–plasma negative–hydrogen–ion source, J. Appl. Phys. 47 (1976) 3888–3896.
[2123] G.A. Haas, Surface analysis using complementary electronic and chemical measurements, J. Vac. Sci. Technol. 13 (1976) 479–486.
[2124] B.J. Hopkins, A.R. Jones, R.I. Winton, An AES, LEED and work function study of CO_2 adsorption on W(100), Surf. Sci. 57 (1976) 266–278.
[2125] Y. Hirai, Mean residence time and ionization efficiency measurements of potassium on platinum surface, Surf. Sci. 66 (1977) 361–364.
[2126] G.A. Haas, A. Shih, R.E. Thomas, Electronic and chemical behavior of oxygen in BaO films on Ir(100), Appl. Surf. Sci. 1 (1977) 59–80.
[2127] J.M. Heras, L. Viscido, V. Amorebieta, Decomposition of water molecule on pure cobalt surfaces, Z. Phys. Chem. 111 (1978) 257–260.
[2128] G.V. Hansson, S.A. Flodström, Angular–resolved photoemission from low–index crystal faces of silver—bulk and surface contributions, Phys. Rev. B 17 (1978) 473–483 (see Ref. [971,1261]).
[2129] G.N. Hatsopoulos, E.P. Gyftopoulos, Thermion. Ener. Conv., Vol. 2, Theory, Technology and Application, MIT Press, Cambridge, 1979, (see Ref. [3724]).
[2130] F.J. Himpsel, D.E. Eastman, Photoemission studies of intrinsic surface states on Si(100), J. Vac. Sci. Technol. 16 (1979) 1297–1299.
[2131] F.J. Himpsel, J.A. Knapp, J.A. Van Vechten, D.E. Eastman, Quantun photoyield of diamond(111) — A stable negative–affinity emitter, Phys. Rev. B 20 (1979) 624–627.
[2132] J.M. Heras, E.V. Albano, Adsorption and decomposition of water on metal films, in: Suppl., Proc. 4th Int. Conf. Solid Surf., Cannes, Vide Couches Minces 201 (1980) 291–294.
[2133] J.M. Heras, L. Viscido, Work function changes upon water contamination of metal surfaces, Appl. Surf. Sci. 4 (1980) 238–241.
[2134] G.A. Haas, A. Shih, Study of high work function materials needed for close–spaced grid applications, Appl. Surf. Sci. 4 (1980) 104–126.
[2135] B.E. Hayden, E. Schweizer, R. Kötz, A.M. Bradshaw, The early stages of oxidation of magnesium single crystal surfaces, Surf. Sci. 111 (1981) 26–38.

[2136] J.M. Heras, E.V. Albano, Work function changes of cobalt films at 77 K upon water adsorption, Appl. Surf. Sci. 7 (1981) 332–346.

[2137] F.J. Himpsel, D.E. Eastman, E.E. Koch, Free–electron–like bulk and surface states for Zn(0001), Phys. Rev. B 24 (1981) 1687–1690.

[2138] F.J. Himpsel, K. Christmann, P. Heimann, D.E. Eastman, Experimental energy–band dispersions and lifetimes for ruthenium, Phys. Rev. B 23 (1981) 2548–2552.

[2139] J.R. Hiskes, P.J. Schneider, Formation of H$^-$ and D$^-$ ions by hydrogen and deuterium particle backscattering from alkali–metal surfaces, Phys. Rev. B 23 (1981) 949–956.

[2140] K. Horn, C. Mariani, L. Cramer, Krypton and argon on Cu(110): Geometric and electronic structure, Surf. Sci. 117 (1982) 376–386.

[2141] J.M. Heras, H. Papp, W. Spiess, Face specificity of the H_2O adsorption and decomposition on Co surfaces — A LEED, UPS, sp and TPD study, Surf. Sci. 117 (1982) 590–604.

[2142] Y.-p. Hsu, K. Yacobi, H.H. Rotermund, Adsorption on N_2, Co and O_2 on Ni(110) at 20 K, Surf. Sci. 117 (1982) 581–589.

[2143] K. Horn, C. Mariani, L. Cramer, Krypton and argon on Cu(110): Geometric and electronic structure, Surf. Sci. 117 (1982) 376–386.

[2144] B.E. Hayden, K.C. Prince, P.J. Davie, G. Paolucci, A.M. Bradshaw, Alkali metal–induced reconstruction of Ag(110), Solid State Commun. 48 (1983) 325–327.

[2145] G.A. Haas, R.E. Thomas, A. Shih, C.R.K. Marrian, Work function measurements and their relation to modern surface analysis techniques, Ultramicrosc. 11 (1983) 199–206.

[2146] H.A.C.M. Hendrickx, A. Hoek, B.E. Nieuwenhuys, Influence of the surface structure on the adsorption of nitrogen on rhodium: Comparison with Pt, Ir, Pd and Ni, Surf. Sci. 135 (1983) 81–92.

[2147] J.M. Heras, E.V. Albano, Photoelectric work function and electrical resistance measurements on iron, cobalt and nickel films annealed at temperatures between 77 and 478 K, Thin Solid Films 106 (1983) 275–284.

[2148] F.J. Himpsel, B. Reihl, Experimental energy bands of a rare–earth metal: Gd(0001), Phys. Rev. B 28 (1983) 574–578.

[2149] G.A. Haas, A. Shih, C.R.K. Marrian, Interatomic Auger analysis of the oxidation of thin Ba films. II. Applications to impregnated cathodes, Appl. Surf. Sci. 16 (1983) 139–162.

[2150] G. Hollinger, F.J. Himpsel, Oxygen chemisorption and oxide formation on Si(111) and Si(100) surfaces, J. Vac. Sci. Technol. A 1 (1983) 640–645.

[2151] F.J. Himpsel, G. Hollinger, R.A. Pollak, Determination of the Fermi–level pinning position at Si(111) surfaces, Phys. Rev. B 28 (1983) 7014–7018.

[2152] J. Hrbek, Adsorption of cesium on Ru(001), Surf. Sci. 164 (1985) 139–148.

[2153] E.P. Gyftopoulos, G.N. Hatsopoulos, Quantum thermodynamic meaning of electronegativity and work function, in: Proc. 2nd Int. Conf. Thermion. Electric. Power Generat. Stresa, Italy, 1968, pp. 1249–1265 (Chem. Abstr. (1970) 71955n).

[2154] A. Hohlfeld, The adsorption of alkali atoms on Al(111) and Mg(0001) single crystal surfaces (Ph.D. thesis), Freie Universität Berlin, 1986, (see Ref. [2168]).

[2155] J.M. Heras, Private comm. (see Ref. [2649]).

[2156] Z.P. Hu, N.J. Wu, A. Ignatiev, Cs induced work function changes on the graphite (0001) surface, Surf. Sci. 177 (1986) L956–L962.

[2157] H. Huang, J. Hermanson, Electronic structure and magnetism of a Pd monolayer on Fe(100), Surf. Sci. 172 (1986) 363–371.

[2158] H. Höchst, E. Colavita, The interaction of CO, NO, and O_2 with sodium–promoted Rh(100) surfaces, J. Vac. Sci. Technol. A 4 (1986) 1442–1445.

[2159] J.E. Houston, C.H.F. Peden, D.S. Blair, D.W. Goodman, Monolayer and multilayer growth of Cu on the Ru(0001) surface, Surf. Sci. 167 (1986) 427–436.

[2160] M. Komai, M. Sasaki, R. Ozawa, S. Yamamoto, Microscopical analysis of structure and work function of Ba–covered Si(111)–(7×7) surface, Appl. Surf. Sci. 146 (1999) 158–161.

[2161] K. Harrison, R.M. Lambert, R.H. Prince, Structure and energetics of potassium overlayers on ruthenium(10$\bar{1}$0), Surf. Sci. 176 (1986) 530–546.

[2162] A. Hohlfeld, M. Sunjic, K. Horn, Electronic structure of cesium adsorbed on Al(111), J. Vac. Sci. Technol. A 5 (1987) 679–683.

[2163] H.A.C.M. Hendrickx, Adsorption and reactions of simple gases on Pd and Rh surfaces: A FEM and IR study (Ph.D. thesis), Rijksuniversiteit Leiden, 1988, (see Ref. [853,2068]).

[2164] H. Hinzert, K.K. Kleinherbers, E. Janssen, A. Goldmann, Chemisorption of halogens on silver: A critical comparison of results from photoemission and thermal desorption spectroscopy, Appl. Phys. A 49 (1989) 313–320.

[2165] Y.G. Hao, G.W. Fernand, B.R. Cooper, Surface electronic behavior of actinides metals, J. Vac. Sci. Technol. A 7 (1989) 2065–2069.

[2166] S.C. Hong, A.J. Freeman, C.L. Fu, Structural, electronic, and magnetic properties of a Ni monolayer on Ag(001): Ni adsorption versus Ag surface segregation, Phys. Rev. B 39 (1989) 5719–5725.

[2167] K.M. Ho, C.T. Chan, K.P. Bohnen, Model for the c(2×2) structure induced by K on Au(110), Phys. Rev. B 40 (1989) 9978–9981.

[2168] D. Heskett, T. Maeda Wong, A.J. Smith, W.R. Graham, N.J. DiNardo, E.W. Plummer, Correlation of alkali metal–induced work function changes on semiconductor and metal surfaces, J. Vac. Sci. Technol. B 7 (1989) 915–918.

[2169] L. Haderbache, P. Wetzel, C. Pirri, J.C. Peruchetti, D. Bolmont, G. Gewinner, Probing the Co coordination at the Si/CoSi$_2$(111) interface by photoemission, Phys. Rev. B 39 (1989) 12704–12707.

[2170] R.W.J. Hollering, D. Dijkkamp, H.W.L. Lindelauf, P.A.M. van der Heide, M.P.C.M. Krijn, Optical second–harmonic generation study of barium deposition on Si(001), J. Vac. Sci. Technol. A 8 (1990) 3997–4000.

[2171] E.C. Honea, M.L. Homer, J.L. Persson, R.L. Whetten, Generation and photoionization of cold Na$_n$ clusters: n to 200, Chem. Phys. Lett. 171 (1990) 147–154.

[2172] Y.G. Hao, O. Eriksson, G.W. Fernando, B.R. Cooper, Electronic structure of the (111) and (100) surfaces of δ–Pu, Phys. Rev. B 43 (1991) 9467–9474.

[2173] F.J. Himpsel, Image states at ferromagnetic surfaces: Fe(110), (100), (111) and Co(0001), Phys. Rev. B 43 (1991) 13394–13400.

[2174] A. Hamawi, L. Walldén, Overlayer states for Na on Si(100), Solid State Commun. 79 (1991) 101–104.

[2175] F.J. Himpsel, Exchange splitting of epitaxial fcc Fe/Cu(100) versus bcc Fe/Ag(100), Phys. Rev. Lett. 67 (1991) 2363–2366.

[2176] J. Hrbek, T.K. Sham, M.-L. Shek, G.-Q. Xu, Potassium–oxygen interactions on a Ru(001) surface, Langmuir 8 (1992) 2461–2472.

[2177] D. Heskett, D. Tang, X. Shi, K.-D. Tsuei, Coadsobate–induced undepolarization of alkali overlayers, Chem. Phys. Lett. 199 (1992) 138–143.

[2178] A. Hamawi, L. Walldén, Monolayer coverage dependence for the surface photovoltage of Si(100)/Na, J. Vac. Sci. Technol. B 10 (1992) 1914–1917.

[2179] M. Höfer, H. Stolz, H.-W. Wassmuth, Interaction of SO$_2$ with clean and Cs–precovered Ag(100), Surf. Sci. 272 (1992) 342–346.

[2180] Y.G. Hao, O. Eriksson, G.W. Fernando, B.R. Cooper, Surface electronic structure of γ–uranium, Phys. Rev. B 47 (1993) 6680–6684.

[2181] S.C. Hong, J.I. Lee, Electronic structure of the molybdenum(001) surface: Local density study, Internat. J. Modern Phys. B 7 (1993) 524–527.

[2182] Th. Härtel, U. Strüber, J. Küppers, Growth and properties of thin Ag films on Pt(111) surfaces, Thin Solid Films 229 (1993) 163–170.

[2183] D. Heskett, D. Tang, X. Shi, K.-D. Tsuei, Work function investigations of alkali–coadsorbate systems, J. Phys.: Condens. Matter 5 (1993) 4601–4610.

[2184] A. Hamawi, L. Walldén, Quantum size effect for Na films on Si(100), Surf. Sci. 285 (1993) 93–101.

[2185] K.M. Hock, R.E. Palmer, Temperature dependent behaviour in the adsorption of submonolayer potassium on graphite, Surf. Sci. 284 (1993) 349–360.

[2186] W.N. Hansen, K.B. Johnson, Work function measurements in gas ambient, Surf. Sci. 316 (1994) 373–382.

[2187] C.H. Hinrichs, W.A. Mackie, I. Cohen, D. Alin, D. Schnitzler, I. Noel, Work function measurements using an improved thermionic projection microscope, Rev. Sci. Instrum. 65 (1994) 3689–3696.

[2188] T. Hertel, H. Over, H. Bludau, M. Gierer, G. Ertl, Na adsorption on Ru(0001): A low–energy electron–diffraction analysis of three ordered phases, Surf. Sci. 301 (1994) 1–10.

[2189] K.I. Hashim, J.P. Jones, A study of group 1b metal adsorption on iridium, Thin Solid Films 245 (1994) 64–73.

[2190] A. Hamawi, Metallization, surface photovoltage, and quantum–well–type resonance for K–covered Si(100) observed via valence–band photoemission, Phys. Rev. B 50 (1994) 10910–10914.

[2191] S. Hadenfeldt, C. Benndorf, Coadsorption of K and CO on Cu(111) surfaces, Surf. Sci. 331–333 (1995) 110–115.

[2192] R. Heise, R. Courths, A photoemission investigation of the adsorption of potassium on perfect and defective TiO$_2$(110) surfaces, Surf. Sci. 331–333 (1995) 1460–1466.

[2193] B. Hellsing, D.V. Chakarov, L. Österlund, V.P. Zhdanov, B. Kasemo, Photoinduced desorption of potassium atoms from a two dimensional overlayer on graphite, J. Chem. Phys. 106 (1997) 982–1002.

[2194] P. Hądzel, T. Radoń, Photofield emission from clean and titanium covered (111) plane of tungsten, Vacuum 48 (1997) 337–340.

[2195] H. Ishida, Theory of the alkali–metal chemisorption on metal surfaces. II, Phys. Rev. B 42 (1990) 10899–10911.

[2196] P. Hądzel, T. Radoń, M.J.G. Lee, J.C.L. Chow, Surface density of states on the (0001) face of titanium, Surf. Sci. 442 (1999) 36–46.

[2197] M.Z. Hossain, T. Kubo, T. Aruga, N. Takagi, T. Tsuno, N. Fujimori, M. Nishijima, Adsorbed states of K on the diamond(100)(2×1) surface, Dia. Rel. Mater. 9 (2000) 162–169.

[2198] N. Hayashi, H. Ishii, Y. Ouchi, K. Seki, Examination of band bending at buckminsterfullerene (C$_{60}$)/metal interfaces by the Kelvin probe method, J. Appl. Phys. 92 (2002) 3784–3793.

[2199] M.A. Hoffmann, G. Wrigge, B.v. Issendorff, Photoelectron spectroscopy of Al$_{32000}^-$: Observation of a "Coulomb staircase" in a free cluster, Phys. Rev. B 66 (2000) 041404(R)/1–3.

[2200] R. Haight, G. Sirinakis, M. Reuter, Photoelectron spectroscopy of individual nanowires of Si and Ge, Appl. Phys. Lett. 91 (2007) 233116/1–3.

[2201] B. Ha, C.J. Lee, Electronic structure and field emission properties of *in situ* potassium–doped single–walled carbon nanotubes, Appl. Phys. Lett. 90 (2007) 023108/1–3.

[2202] M. Hasan, H. Park, H. Yang, H. Hwang, H.-S. Jung, J.-H. Lee, Ultralow work function of scandium metal gate with tantalum nitride interface layer for *n*–channel metal oxide semiconductor application, Appl. Phys. Lett. 90 (2007) 103510/1–3.

[2203] W. Huang, W. Lai, D. Xie, A DFT investigation of sulfur adsorption on Ir(100), J. Theor. Comput. Chem. 6 (2007) 177–185.

[2204] S. Hałas, T. Pieńkos, M. Czarnacki, T. Durakiewicz, Determination of work function of metals and alloys using diode with spiral anode, Vacuum 82 (2008) 1094–1098.

[2205] S. Hałas, T. Durakiewicz, Is work function a surface or a bulk property? Vacuum 85 (2010) 486–488.

[2206] H.E. Ives, A.R. Olpin, Maximum excursion of the photoelectric long wave limit of the alkali metals, Phys. Rev. 34 (1929) 117–128.

[2207] R. Ito, Pressure dependence of sensitivity of photoelectron counters, J. Phys. Soc. Japan 6 (1951) 188–191.

[2208] N.I. Ionov, The surface ionization of molecules of potassium chloride and cesium chloride in an electric field, Sov. Phys. Tech. Phys. 1 (1956) 2134–2137.

[2209] N.G. Imangulova, E.P. Sytaya, Konf. Elektr. Tekhn., (7) Emiss. Elektron., 1970, pp. 81–90 (see Ref. [1354]).

[2210] N.G. Imangulova, E.P. Sytaya, Determination of thermionic emission parameters of molybdenum single–crystal faces, Izv. Akad. Nauk Uzb.SSR, Ser. Fiz.-Mat. Nauk 17 (1973) 70–71.

[2211] T. Ishida, M. Sato, K. Fukui, K. Ueda, Studies of Ca$^+$ implanted Mo foil by means of work–function measurements and AES, Appl. Phys. Lett. 31 (1977) 813–815.

[2212] N.G. Imangulova, E.P. Sytaya, Effect of structural distortions on the thermoemission parameters of the boundaries of a large molybdenum single crystal, Nauch. Tr. Tashkent Gos. Univ. 525 (1976) 8–11.

[2213] J. Ihm, S.G. Louie, M.L. Cohen, Self–consistent pseudopotential calculations for Ge and diamond (111) surfaces, Phys. Rev. B 17 (1978) 769–775.

[2214] N.G. Imangulova, E.P. Sytaya, Study of the effect of structural imperfections on the emission properties of refractory metal single crystal faces, Nauchn. Tr., Tashkent Gos. Univ. 550 (1978) 49–53 (Chem. Abstr. 90 (1979) 213898u).

[2215] M. Isaacson, R. Gomer, Extended range field emission spectroscopy, Appl. Phys. 15 (1978) 253–256.

[2216] V.A. Ilatovskii, T.B. Dmitriev, G.G. Komissarov, Effect of the work function of the substrate on the photovoltaic activity of thin layers of phthalocyanine, Russ. J. Phys. Chem. 52 (1978) 1469–1470.

[2217] N.G. Imangulova, E.P. Sytaya, 17th Vses. Konf. Emiss. Electron., 1978, p. 144 (see Ref. [1354]).

[2218] M. Izuchi, K. Yamada, M. Wada, O. Nishikawa, Field ion microscopy of Ga–W and Ga–Mo interfaces. (I) Structures of Ga and field emission current, Shinku (J. Vac. Soc. Japan) 23 (1980) 289–296.

[2219] J. Ihm, M.L. Cohen, J.R. Chelikowsky, Electronic structure of a Pd monolayer on an Si(111) surface, Phys. Rev. B 22 (1980) 4610–4619.

[2220] V.A. Ivanov, T.S. Kirsanova, T.A. Tumareva, Field emission spectroscopy of tungsten covered by layers of barium and barium oxide, Sov. Phys.—Solid State 23 (1981) 377–379.

[2221] J.E. Inglesfirld, The screening of an electronic field at an Al(001) surface, Surf. Sci. 188 (1987) L701–L707.

[2222] H. Ishida, Theory of the alkali–metal chemisorption on metal surfaces, Phys. Rev. B 38 (1988) 8006–8021.

[2223] H. Ishida, Formation of free–electron–like resonant bands for alkali–metal overlayers on simple metals, Phys. Rev. B 40 (1989) 1341–1344.

[2224] H. Ishida, K. Terakura, Coverage dependence of the electronic structure of potassium adatoms on the Si(001)–(2×1) surface, Phys. Rev. B 40 (1989) 11519–11535.

[2225] J. Ishikawa, H. Tsuji, K. Inoue, M. Nagao, T. Sasaki, T. Kaneko, Y. Gotoh, Estimation of metal–deposited field emitters for the micro vacuum tube, Japan. J. Appl. Phys. 32 (1993) L342–L345.

[2226] H. Ishii, D. Yoshimura, K. Sugiyama, S. Narioka, Y. Hamatani, I. Kawamoto, T. Miyazaki, Y. Ouchi, K. Seki, Electronic structure of 8–hydroxyquinoline aluminum (Alq$_3$)/metal interfaces studied by UV photoemission, Synth. Metals 85 (1997) 1389–1390.

[2227] R. Ishii, K. Matsumura, A. Sasaki, T. Sakata, Work function of binary alloys, Appl. Surf. Sci. 169–170 (2001) 658–661.

[2228] T. Irawan, D. Boecker, F. Ghaleh, C. Yin, B. von Issendorff, H. Hövel, Metal clusters on rare gas layers — Growth and spectroscopy, Appl. Phys. A 82 (2006) 81–86.

[2229] Y. Ikuno, K. Kusakabe, A determination method of the work function using the slab model with a first–principles electronic structure calculation, *e–J*, Surf. Sci. Nanotech. 6 (2008) 103–106 (Avail. URL: http://www.jstage.jst.go.jp/article/ejssnt/6/0/103/-pdf) (Chem. Abstr. 149 (2008) 116374z).

[2230] T. Iwata, T. Yoshimoto, H. Yoshida, Y. Morita, S. Mikami, N. Mayama, M. Owari, Electron emission properties of simple field emitter covered with diamond–like carbon (DLC) film prepared by electro–deposition in methanol, Shinku (J. Vac. Soc. Japan) 52 (2009) 176–178 (Chem. Abstr. 151 (2009) 46630v).

[2231] H.E. Ives, The variation with temperature of the photoelectric effect in potassium photoelectric cell, J. Opt. Soc. Amer. 8 (1924) 551–580.

[2232] N.C. Jamison, R.J. Cashman, Photoelectric properties of barium and calcium, Phys. Rev. 50 (1936) 624–631.

[2233] M.C. Johnson, F.A. Vick, Modification of apparent thermionic constants for oxygenated tungsten by the temperature variation of adsorptive equilibrium, Proc. Roy. Soc. A 158 (1937) 55–68.

[2234] H. Jupnik, Photoelectric properties of bismuth, Phys. Rev. 60 (1941) 884–889.

[2235] E.F. Chaikovskii, Yu.F. Derkach, E.D. Kovtun, Study of emission and adsorption properties of tantalum and molybdenum, Izv. Akad. Nauk SSSR, Ser. Fiz. 40 (1976) 2450–2452.

[2236] S.C. Jain, K.S. Krishnan, Thermionic constants of metals and semiconductors. III. Monovalent metals, Proc. Roy. Soc. A 217 (1953) 451–461.

[2237] R.J. Jaccodine, Dr. thesis, Univ. of Notre Dame, 1957 (see Ref. [134]).

[2238] J.P. Jones, The adsorption of copper on tungsten, Proc. Roy. Soc. A 284 (1965) 469–487.

[2239] J.P. Jones, Arrangement of atoms in the first monolayer of nickel on tungsten, Nature 211 (1966) 479–481.

[2240] J.P. Jones, Adsorption of Gold on Tungsten, in: SCI (Soc. Chem. Ind., London) Monogr., No. 28, 1968, pp. 263–290 (Chem. Abstr. 70 (1969) 41042d).
[2241] R.C. Jerner, C.B. Magee, Effect of surface oxidation on the thermionic work function of beryllium, Oxid. Metals 2 (1970) 1–9.
[2242] M.R. Jeans, W.M. Mularie, U.S. Army Res. Develop., Final Rep. KAAKO 2–69–C–0155, 1970, (see Ref. [2483]).
[2243] S. Yamamoto, Fundamental physics of vacuum electron sources, Rep. Progr. Phys. 69 (2006) 181–232.
[2244] D.L. Jacobson, A.E. Campbell, Molybdenum work function determined by electron emission microscopy, Metall. Trans. 2 (1971) 3063–3066.
[2245] J.P. Jones, Adsorption of silver on tungsten, Surf. Sci. 32 (1972) 29–44.
[2246] M. Jałochowski, P. Mikołajczak, M. Subotowicz, Measurements of the work function and the Fermi level in thin tellurium films, Phys. Status Solidi (a) 14 (1972) K135–K137.
[2247] D.L. Jacobson, Emission characteristics of some dilute tungsten alloys, Metall. Trans. 3 (1972) 1263–1268.
[2248] A.P. Janssen, J.P. Jones, A study of the growth of germanium, and silicon, on tungsten, by field emission and field–ion microscopy, Surf. Sci. 41 (1974) 257–276.
[2249] J.P. Jones, A.D. Martin, High field microscopy of nickel on tungsten, Surf. Sci. 41 (1974) 559–580.
[2250] J.S. Jen, T.D. Thomas, X–ray photoemission from mercury in vapor and condensed phases, Phys. Rev. B 13 (1976) 5284–5294.
[2251] J.P. Jones, N.T. Jones, Field emission microscopy of gold on single–crystal planes of tungsten, Thin Solid Films 35 (1976) 83–97.
[2252] W. Jaschinski, R. Niedermayer, Work function changes induced by Ag adsorption on Mo(100), Thin Solid Films 32 (1976) 181–183.
[2253] J.P. Jones, E.W. Roberts, Adsorption of copper on single crystal planes of tungsten, Surf. Sci. 69 (1977) 185–204.
[2254] J.P. Jones, E.W. Roberts, Adsorption of lead on low–index planes of tungsten, Surf. Sci. 62 (1977) 415–430.
[2255] J.P. Jones, E.W. Roberts, Field emission energy distributions from layer and crystal structures of copper on W(100), Surf. Sci. 64 (1977) 355–361.
[2256] J.P. Jones, E.W. Roberts, Field emission microscopy of gold on (110), (100) and (211) tungsten surfaces, Thin Solid Films 48 (1978) 215–228.
[2257] J.P. Jones, E.W. Roberts, Some studies of lead and iron adsorption on the W(100) surface by field emission microscopy, Surf. Sci. 78 (1978) 37–57.
[2258] B.T. Jonker, J.F. Morar, R.L. Park, Surface states and oxygen chemisorption on Ti(0001), Phys. Rev. B 24 (1981) 2951–2957.
[2259] K. Jacobi, H.H. Rotermund, UV photoemission from physisorbed atoms and molecules: Electron binding energies of valence levels in mono– and multilayers, Surf. Sci. 116 (1982) 435–455.
[2260] J.P. Jones, Field emission spectroscopy of bismuth adsorbed on the W(100) surface, Surf. Sci. 121 (1982) 487–503.
[2261] H.J.F. Jansen, A.J. Freeman, M. Weinert, E. Wimmer, Phase trnsitions in a mercury monolayer, Phys. Rev. B 28 (1983) 593–597.
[2262] B.T. Jonker, N.C. Bartelt, R.L. Park, Quantum size effect in electron transmission through Cu and Ag films on W(110), Surf. Sci. 127 (1983) 183–199.
[2263] D.S. Joag, J.P. Jones, The effect of substrate temperature on the behavior of gold and silver on the 100 tungsten plane, J. Physique 45 (1984) C9–59/C9–64.
[2264] K. Jacobi, G. Zwicker, A. Gutmann, Work function, electron affinity and band bending of zinc oxide surfaces, Surf. Sci. 141 (1984) 109–125.
[2265] R.O. Jones, P.J. Jennings, O. Jepsen, Surface barrier in metals: A new model with application to W(001), Phys. Rev. B 29 (1984) 6474–6480.
[2266] A. Jablonski, S. Eder, K. Wandelt, Adsorbed xenon atoms as local surface structure problems: The initial growth of thin Ag films on Ru(001), Appl. Surf. Sci. 22/23 (1985) 309–324.
[2267] K. Jacobi, Work–function changes and photoemission final–state relaxation of Ne, Ar, Kr, Xe, H_2 and N_2 on gallium, Surf. Sci. 192 (1987) 499–506.
[2268] K. Jacobi, Photoemission from Ar, Kr and Xe on Pb(111), Phys. Rev. B 38 (1988) 5869–5877.
[2269] K. Jacobi, Field–state screening in photoemission from adsorbed xenon layers, Phys. Rev. B 38 (1988) 6291–6294.
[2270] B.G. Johnson, P.J. Berlowitz, D.W. Goodman, C.H. Bartholomew, The structural and chemisorptive properties of ultrathin cobalt overlayers on W(110) and W(100), Surf. Sci. 217 (1989) 13–37.
[2271] L.Q. Jiang, M.W. Ruckman, M. Strongin, Experimental evidence for room–temperature intermetallic compound formation at the Pd/Al interface, Phys. Rev. B 39 (1989) 1564–1568.
[2272] D.M. Jaffey, A.J. Gellman, R.M. Lambert, Overlayer and intermetallic compound surface phases in the samarium/Cu(111) system, Surf. Sci. 214 (1989) 407–435.
[2273] S.K. Jo, J.M. White, Correlation of photoelectron yields and photodissociation rates of CH_3Cl on Pt(111) and carbon–covered Pt(111), J. Phys. Chem. 94 (1990) 6852–6854.
[2274] L.S.O. Johansson, B. Reihl, Empty surface states on the Si(100)2×1–K surface: Evidence for overlayer metallization, Phys. Rev. Lett. 67 (1991) 2191–2194.
[2275] S.K. Jo, X.-Y. Zhu, D. Lennon, J.M. White, The role of photoelectrons in photodissociation of CH_3Cl on Pt(111) and C–covered Pt(111), Surf. Sci. 241 (1991) 231–243.
[2276] L.S.O. Johansson, B. Reihl, Empty surface–state band structure of the alkali–metal adsorbed single–domain Si(100)–(2×1) surface, Appl. Surf. Sci. 56–58 (1992) 486–492.
[2277] L.S.O. Johansson, B. Reihl, Electronic structure of the Na–adsorbed Si(100)2×1 surface studied by inverse and direct angle–resolved photoemission, Phys. Rev. B 47 (1993) 1401–1406.
[2278] L.S.O. Johansson, B. Reihl, Alkali metals on Si(100)2×1: Comparative study of the surface electronic structures for Li, Na and K adsorption, Surf. Sci. 287/288 (1993) 524–528.
[2279] J.P. Jones, Adsorption of gold and silver on the tungsten(110) surface studied by field emission microscopy, J. Solid State Chem. 104 (1993) 149–159.
[2280] T.V.W. Janssens, G.R. Kastro, K. Wandelt, J.W. Niemantsverdriet, Surface potential around potassium promoter atoms on Rh(111) measured with photoemission of adsorbed Xe, Kr, and Ar, Phys. Rev. B 49 (1994) 14599–14609.
[2281] M.G. Helander, M.T. Greiner, Z.B. Wang, Z.H. Lu, Pitfalls in measuring work function using photoelectron spectroscopy, Appl. Surf. Sci. 256 (2010) 2602–2605.
[2282] L.Q. Jiang, B.E. Koel, Superfulleride formation and electronic properties of C_{60} on K/Rh(111) surfaces, Chem. Phys. Lett. 223 (1994) 69–75.
[2283] M.K.-J. Johansson, S.M. Gray, L.S.O. Johansson, Low coverages of lithium on Si(001) studied with STM and ARUPS, Phys. Rev. B 53 (1996) 1362–1367.
[2284] J.F. Jia, Y. Hasegawa, K. Inoue, W.S. Yang, T. Sakurai, Steps on the Au/Cu(111) surface studied by local work function measurement with STM, Appl. Phys. A 66 (1998) S1125–S1128.
[2285] H.J. Jänsch, C. Polenz, C. Bromberger, M. Detje, H.D. Ebinger, B. Polivka, W. Preyß, R. Veith, D. Fick, The interaction of CO and Li at a Ru(001) surface — A thermal desorption study, Surf. Sci. 495 (2001) 120–128.
[2286] Y. Jia, B. Wu, H.H. Weitering, Z. Zhang, Quantum size effects in Pb films from first principles: The role of the substrate, Phys. Rev. B 74 (2006) 035433/1–10.
[2287] M. Juel, B.T. Samuelsen, M. Kildemo, S. Raaen, Surface alloy formation after deposition of Ce on Rh(110), Surf. Sci. 601 (2007) 2917–2923.
[2288] F. Jin, Y. Liu, C.M. Day, S.A. Little, Enhanced field emission from carbon nanotubes with a thin layer of low work function barium strontium oxide surface coating, J. Vac. Sci. Technol. B 25 (2007) 1785–1788.
[2289] O. Koppius, A comparison of the thermionic and photoelectric work function from platinum, Phys. Rev. 17 (1921) 395–397.
[2290] C.B. Kazda, Accurate measurements of the energy content of extreme ultra–violet mercury lines and the precise determination of the photoelectric long wave–length limit of a clean surface of mercury, Phys. Rev. 22 (1923) 523.
[2291] C.B. Kazda, The photo–electric threshold for mercury, Phys. Rev. 26 (1925) 643–654.
[2292] T.J. Killian, Thermionic phenomena caused by vapors of rubidium and potassium, Phys. Rev. 27 (1926) 578–587.
[2293] K.H. Besocke, Work function change of tungsten(110) planes as function of Mo coverage, in: Proc. 3rd Int. Conf. Thermion. Electric. Power Generat. Jülich, vol. 3, 1972, pp. 1385–1396.

[2294] H. Kösters, Measurements of potential difference between pure metals, Z. Phys. 66 (1930) 807–826.

[2295] C. Kenty, Variation of photoelectric efficiency with work function in the extreme ultraviolet, Phys. Rev. 43 (1933) 776.

[2296] F. Krüger, G. Stabenow, Measurement of the heat of vaporization and the temperature coefficients of the thermionic emission from molybdenum, tungsten and tantalum, Ann. Phys. 22 (1935) 713–734.

[2297] O. Klein, E. Lange, Work of electron emission in metals, Z. Elektrochem. 44 (1938) 542–562.

[2298] W. Kluge, H. Steyskal, Electronics of natural cleavage planes in single metallic crystals. I. Formation in high vacuum of cleavage planes in single crystals of zinc and preliminary photoelectric measurements, Z. Phys. 116 (1940) 415–427.

[2299] K. Kondo, On the relation between thermionic constant and work function, J. Phys. Soc. Japan 2 (1947) 32–35.

[2300] K. Kondo, The thermionic constant of platinum, Rept. Inst. Sci. Tech., Tokyo Univ. 1 (1947) 24–26 (Chem. Abstr. 45 (1951) 3235c).

[2301] M.D. Kruglova, I.L. Sokol'skaya, Thermoelectronic emission of tungsten covered with platinum, Zh. Tekh. Fiz. 19 (1949) 1292–1300.

[2302] E. Kelly, H.E. Farnsworth, E.N. Clarke, The photoelectric work function of a silver film on the (100) face of a silver crystal, Phys. Rev. 78 (1950) 316.

[2303] K.S. Krishnan, S.C. Jain, Thermionic constants of graphite, Nature 169 (1952) 702–703.

[2304] K.S. Krishnan, S.C. Jain, Thermionic constants of the iron group of metals, Nature 170 (1952) 759.

[2305] K.-B. Kim, I.L. Sokol'skaya, Surface ionization of sodium on platinized tungsten, Vestnik Leningrad. Univ., Ser. Mat., Fiz. Khim. 7 (1952) 67–79 (Chem.Abstr. 49 (1955) 2178b).

[2306] Kh.Kh. Khadzhimukhamedov, G.N. Shuppe, Local work function of polycrystalline tungsten, molybdenum and tantalum surfaces, Izv. Akad. Nauk Uzb.SSR, Ser. Fiz.-Mat. Nauk 2 (1957) 55–63 (Chem. Abstr. 53 (1959) 14697i).

[2307] G. Krüger, Diss. Hannover, 1960 (see Ref. [3052]).

[2308] A.P. Komar, V.P. Savchenko, V.N. Shrednik, Adsorption, migration and evaporation of Be deposited on W monocrystals, Radiotekh. Elektron. 5 (1960) 1211–1217.

[2309] G.A. Katrich, O.G. Sarbei, Photoelectron emission from gold and chromium, Sov. Phys. Solid State 3 (1961) 1181–1187.

[2310] D. Kern, Unpublished (see Ref. [3052]).

[2311] M. Kruel, Unpublished (see Ref. [3052]).

[2312] T.S. Kirsanova, A.R. Shul'man, Nature of the dependence of the work function of barium oxide–metal systems on the surface coverage, Sov. Phys.—Solid State 6 (1964) 225–230.

[2313] P. Köhler, E. Menzel, Light–electric exit potentials on spherical Cu crystals with an untouched surface, Z. Naturfor. 20 a (1965) 1223–1225.

[2314] D.R. Koenig, Surface ionization of cesium and thermionic emission from planar single crystals of tungsten (Ph.D. thesis), Univ. of Calif, Berkeley, 1966, 300 pp (Diss. Abstr. B 27 (1967) 3627).

[2315] D.R. Koenig, Surface Ionization of Cesium and Thermionic Emission from Planar Single Crystals of Tungsten, Rept. UCRL–11857, 305 pp (Chem. Abstr. 66 (1967) 69968b).

[2316] D.R. Koenig, T.H. Pigford, Work function and cesium desorption energies for planar tungsten single crystals, Bull. Amer. Phys. Soc. 11 (1966) 636.

[2317] P. Köhler, Work function of spherical copper single crystals with an untouched surface, Z. Angew. Phys. 21 (1966) 191–196.

[2318] V.A. Kuznetsov, B.M. Tsarev, Adsorption and electron emission of molybdenum films on a tungsten single crystal, Sov. Phys.—Solid State 9 (1968) 1987–1991.

[2319] T. Kuroda, S. Nakamura, Field emission microscope studies of coadsorption of oxygen and cesium on tungsten and rhenium, Shinku (J. Vac. Soc. Japan) 10 (1967) 289–297 (Chem. Abstr. 68 (1968) 62946a).

[2320] N.D. Konovalov, V.I. Makukha, Adsorption and electron emission of cesium films on iridium, Sov. Phys.—Solid State 9 (1968) 2108–2113.

[2321] R. Koyama, W.E. Spicer, N.W. Ashcroft, W.E. Lawrence, Photoemission and the density of states in indium, Phys. Rev. Lett. 19 (1967) 1284–1286.

[2322] O.K. Kultashev, A.P. Makarov, Rept. 13th Vses. Konf. Emiss. Elektron., 1968, p. 15 (see Ref. [12]).

[2323] E.V. Klimenko, V.K. Medvedev, Investigation of sodium adsorption on the surface of a tungsten single crystal in a field–emission microscope, Sov. Phys.—Solid State 10 (1969) 1526–1565.

[2324] T. Kuroda, H. Yagi, S. Nakamura, Field emission microscopy studies of cesium layers on refractory metals: Work function change, Mem. Inst. Sci. & Ind. Res. Osaka Univ. 26 (1969) 87–100 (Chem. Abstr. 71 (1969) 74502c).

[2325] A. Kashetov, N.A. Gorbatyi, Thermionic parameters of the faces of a rhenium crystal, Sov. Phys. J. 12 (1969) 856–859.

[2326] A. Kashetov, N.A. Gorbatyi, Correlation between the work functions and surface energies of the faces of metal crystals, Sov. Phys. J. 12 (1969) 860–863.

[2327] O.K. Kultashev, A.P. Makarov, Electron work function in titanium alloys with ruthenium, Fiz. Metal. Metalloved. 30 (1970) 924–928 (Chem. Abstr. 74 (1971) 58355p).

[2328] K.A. Kress, G.J. Lapeyre, Photoemission and optical investigation of the electronic structure of ruthenium, Phys. Rev. B 2 (1970) 2532–2537.

[2329] T.A. Karabaev, Thermionic emission properties of the (112) and (111) faces of a niobium single crystal in a stream of cesium atoms, Nauchn. Tr., Tashk. Gos. Univ. 379 (1970) 79–84 (Chem. Abstr. 81 (1974) 128376s).

[2330] O.K. Kultashev, A.P. Makarov, Coadsorption of yttrium and oxygen atoms on faces of a tungsten crystal, Sov. Phys.—Solid State 12 (1971) 1850–1853.

[2331] R.Ya. Kamilova, E.P. Sytaya, Emission and adsorption properties of the main faces of a tantalum single crystal in a flow of cesium atoms, Izv. Akad. Nauk Uzb.SSR, Ser. Fiz.-Mat. Nauk 15 (1971) 34–39 (Chem. Abstr. 75 (1971) 41929b).

[2332] K.A. Kress, G.J. Lapeyre, Photoemission measurement of the d–band energies in calcium, Solid State Commun. 9 (1971) 827–830.

[2333] H. Köster, W. Schütt, Field emission study of selenium and tellurium thin films on a tungsten surface, Phys. Status Solidi (a) 4 (1971) 265–269.

[2334] T.V. Kalish, R.Kh. Burshtein, Comparison of differences in the work functions and zero–charge potentials of metals. V. Mercury–lead, Elektrokhim. 7 (1971) 115–116.

[2335] V.A. Kuznetsov, Effect of the state of a tungsten surface on the emission of thin films in the W–Cs system, Sov. Phys.—Solid State 13 (1971) 1434–1440.

[2336] R.Y. Koyama, W.E. Spicer, Photoemission studies of indium, Phys. Rev. B 4 (1971) 4318–4329.

[2337] O.K. Kultashev, A.P. Makarov, Co–adsorption of scandium and oxygen atoms on (110), (100), and (111) faces of a tungsten crystal, Izv. Akad. Nauk SSSR, Ser. Fiz. 35 (1971) 351–354.

[2338] O.K. Kultashev, A.P. Makarov, Simultaneous adsorption of yttrium and rhodium on the (110), (100), and (111) faces of tungsten, in: Proc. 2nd Emiss. Elektron., Mater. Semin. Probl. Rab. Vykhoda Elektronov Adsorbtsii Met. Zavisimosti Kristallogr. Napravlenii, 1971, pp. 146–153 (Chem. Abstr. 85 (1976) 149487b).

[2339] V.A. Kuznetsov, I.P. Zasorin, Yu.S. Belomytsev, L.V. Bulgak, G.I. Zheleznov, V.D. Kapustin, Yu.I. Moskalev, A.N. Moskaleva, A.I. Nakonetchnikov, I.N. Prilezhaeva, L.V. Pavlinov, V.I. Rubtzov, N.Ya. Rukhljada, L.N. Saratovskii, A.A. Smirnov, Studies of physical–mechanical properties of monocrystal molybdenum and tungsten and electrical characteristics of TIC (thermionic converter), in: Proc. 3rd Int. Conf. Thermion. Electric. Power Generat. Jülich, vol. 2, 1972, pp. 797–818.

[2340] B. Krahl-Urban, H. Wagner, Work function dependence on crystal orientation for W with special emphasis to the variation near the [110] orientation, in: Proc. 3rd Int. Conf. Thermion. Electric. Power Generat. Jülich, vol. 3, 1972, pp. 1375–1384.

[2341] N.D. Konovalov, V.A. Kuznetsov, Emission properties of cesium films on the VR–27 alloy, Radiotekh. Elektron. 17 (1972) 216.

[2342] H.P. Bonzel, Kinetic processes on well–characterized metal surfaces, in: Proc. 7th Int. Vac. Congr. & 3rd Int. Conf. Solid Surf. Vienna, 1977, pp. 691–702.

[2343] B. Krahl-Urban, H. Wagner, Work function dependence on crystal orientation for tungsten, Dtsch. Luft–Raumfahrt, Mitt. (1973) DRL–Mitt. 73–29, pp. 25–34 (Chem. Abstr. 82 (1975) 37794f).

[2344] E.V. Klimenko, A.G. Naumovets, Adsorption of strontium on the (110) face of tungsten, Sov. Phys.—Solid State 15 (1974) 2181–2184.

[2345] Kh.B. Khokonov, S.N. Zadumkin, B.B. Alchagirov, Work function, surface tension, and density of the gallium/indium system, Dokl. Akad. Nauk SSSR 210 (1973) 899–902.

[2346] G.M. Kornacheva, R.Kh. Burshtein, N.A. Schurmovskaya, Adsorption of water vapor on iron, Elekrokhim. 9 (1973) 81–83.

[2347] O.V. Kanash, A.G. Naumovets, A.G. Fedorus, Phase transitions in submonolayer strontium films adsorbed on the (011) face of tungsten, Sov. Phys.—JETP 40 (1975) 903–907.

[2348] K. Kraemer, D. Menzel, Adsorption of gases on ruthenium field emitters. I. Carbon monoxide and oxygen, Ber. Bunsenges. Phys. Chem. 78 (1974) 591–598.

[2349] Kh.B. Khokonov, S.N. Zadumkin, B.B. Alchagirov, Electronic work function and surface tension of the binary systems gallium–indium, Sov. Electrochem. 10 (1974) 865–870.

[2350] C.A. Kiwanga, R.A. Collins, Silicon adsorption on single–crystal faces of tungsten, Phys. Status Solidi (a) 23 (1974) 209–214.

[2351] O.K. Kultashev, A.P. Makarov, Effect of the adsorption of oxygen on the electron and adsorption properties of barium atom on the (100), (110), and (111) faces of tungsten, Izv. Akad. Nauk SSSR, Ser. Fiz. 38 (1974) 317–321.

[2352] T.F. Kerr, C.H.B. Mee, Program for calculating work functions from photoelectric data, Comput. Phys. Comm. 7 (1974) 419–427.

[2353] Kh.B. Khokonov, S.N. Zadumkin, Work function of an electron of gallium–indium and gallium–bismuth alloys, Izv. Akad. Nauk SSSR, Met. (2) (1975) 189–191 (Chem. Abstr. 83 (1975) 89492w).

[2354] V.A. Kuznetsov, E.P. Sheshin, The energy spectrum of the field–emitted electrons from microprojections on a tungsten tip, Radiotekh. Elekron. 20 (1975) 1550–1553.

[2355] S. Kar, Determination of Si–metal work function differences by MOS capacitance technique, Solid State Electron. 18 (1975) 169–181.

[2356] V.A. Kuz'tin, V.S. Kucherov, D.S. Li, 16th Vses. Konf. Emiss. Elektron., vol. 1, 1976, pp. 156–157 (see Ref. [1354]).

[2357] B. Krahl-Urban, Electron work function of stepped tungsten surfaces, in: Ber. Kernforshungsanlage Jülich, No. 1276, 1976, 91 pp (Chem. Abstr. 86 (1977) 99643x).

[2358] R.L. Kautz, B.B. Schwartz, Surface of a spin–polarized electron gas, Phys. Rev. B 14 (1976) 2017–2031.

[2359] O.K. Kultashev, A.P. Makarov, S.E. Rozhkov, Effect of oxygen on the work function of electropositive metal films adsorbed on 4d and 5d transition metals, Izv. Akad. Nauk SSSR, Ser. Fiz. 40 (1976) 2478–2483.

[2360] E. Kikuchi, T. Ino, N. Ito, Y. Morita, Synthesis of gaseous hydrocarbons from carbon monoxide and hydrogen over transition metal catalysts. Part 1. The activity and selectivity of graphite–supported metal catalysts, Bull. Japan Petroleum Inst. 18 (1976) 139–145 (see Ref. [1425]).

[2361] V.A. Korol'kov, Yu.I. Malov, A.A. Markov, Electron work functions of alloys in the binary systems of bismuth–antimony, cadmium–bismuth, and tin–lead, Sov. Electrochem. 12 (1976) 570–571.

[2362] Kh.N. Kokov, S.N. Zadumkin, Kh.B. Khokonov, Study of the relation between the surface tension and electron work function of binary metallic systems, Fiz. Mezhfaznykh Yavlenii 2 (1977) 44–48 (see Ref. [1445]).

[2363] J. Kolaczkiewicz, Z. Sidorski, Adsorption of silver on (001), (011) and (111) oriented tungsten single crystals, Surf. Sic. 63 (1977) 501–506.

[2364] B.S. Karasik, Secondary electron emission of zinc in the primary electron low–energy region, in: 30th Fiz. Elektron. Nauchn. Dokl. Gertsenovskie Chteniya, 1977, pp. 16–17 (Chem. Abstr. 90 (1979) 32665v).

[2365] V.V. Kolesnikov, E.V. Polozhentsev, V.P. Sachenko, A.P. Kovtun, Size fluctuations of the work function in small metallic clusters, Sov. Phys.—Solid State 19 (1977) 883–884.

[2366] N.G. Krishnan, W.N. Delgass, W.D. Robertson, Electron binding energies of core levels in caesium adsorbed on a nickel(100) surface, J. Phys. F 7 (1977) 2623–2635.

[2367] Yu.I. Kostikov, N.V. Volkov, Yu.K. Gus'kov, Z.N. Kononova, Field emission of tungsten covered with tellurium and cesium films, Sov. Phys. Tech. Phys. 22 (1977) 375–377.

[2368] T.V. Kalish, M.E. Belyaeva, Effect of the chemisorption of oxygen and hydrogen on the work function of rhodium, Elektrokhim. 13 (1977) 1843–1846.

[2369] H. Kim, T. Sasaki, K. Okuno, Adsorption of iron on tungsten, Shinku (J. Vac. Soc. Japan) 21 (1978) 127–129 (Chem. Abstr. 89 (1978) 186400w).

[2370] D. Kohl, H. Moorman, G. Heiland, Correlated behaviour of hall mobility and work function in the case of accumulation layers on ZnO crystals, Surf. Sci. 73 (1978) 160–162.

[2371] Kh.O. Kuchkarov, G.G. Vladimirov, Simultaneous adsorption of Ba and Cu atoms on certain tungsten faces, Sov. Phys. Tech. Phys. 24 (1979) 953–954.

[2372] Kh.O. Kuchkarov, G.G. Vladimirov, Joint adsorption of barium and titanium atoms on certain tungsten faces, Sov. Phys. Tech. Phys. 24 (1979) 1313–1314.

[2373] J. Kołaczkiewicz, Investigation of the temperature dependent changes of work function induced by adsorption of Ag on W(011), Surf. Sci. 84 (1979) 475–481.

[2374] S.R. Kelemen, T.E. Fischer, Interaction of H_2S with the Ru(001) surface, Surf. Sci. 87 (1979) 53–68.

[2375] O.S. Koroleva, V.M. Silkin, E.V. Chulkov, Self–consistent electronic structures of Zn(0001), Cd(0001), and In(001) surfaces, Poverkhnost' (6) (1990) 72–79.

[2376] H. Kim, K. Okuno, T. Sasaki, Coadsorption of lanthanum and boron on a tungsten surface, Oyo Butsuri 49 (1980) 1082–1088 (Chem. Abstr. 94 (1981) 130910y).

[2377] L. Kleinman, K. Mednick, Self–consistent calculations of oxygen monolayers on Al(111) film, Phys. Rev. B 23 (1981) 4960–4964.

[2378] K. Kandasamy, N.A. Surplice, The predominance of a surface plane of high work function on Ti films, J. Phys. C 14 (1981) L61–L63.

[2379] G. Kaindl, T.-C. Chiang, D.E. Eastman, F.J. Himpsel, Private comm. (see Ref. [2498]).

[2380] E.V. Klimenko, Adsorption of oxygen and cesium on epitaxial chromium films grown on the (110) face of tungsten, Ukr. Fiz. Zh. 27 (1982) 221–226.

[2381] E.V. Klimenko, Coadsorption of oxygen and cesium on the niobium(110) face: Work function and thermal stability of cesium films, Ukr. Fiz. Zh. 27 (1982) 1087–1093 (Chem. Abstr. 97 (1982) 99024y).

[2382] Kh.B. Khokonov, P.M. Digilov, Yu.A. Orkvasov, B.G. Asadov, Electron theory of the size effect on surface energy and electron work function in metal films, Poverkhnost' (11) (1982) 37–44 (Chem. Abstr. 98 (1983) 149808a).

[2383] E. Schuhmacher, M. Kappes, K. Marti, P. Radi, M. Schär, B. Schmidhalter, Metal–clusters: Preparation, properties, theory, Ber. Bunsenges. Phys. Chem. 88 (1984) 220–228.

[2384] J. Kołaczkiewicz, E. Bauer, Temperature dependence of the work function of adsorbate–covered metal surfaces: A new method for the study of two–dimensional phase transitions, Phys. Rev. Lett. 53 (1984) 485–488.

[2385] J. Kołaczkiewicz, E. Bauer, The adsorption of Ag and Au on W(211) surfaces, Surf. Sci. 144 (1984) 477–494.

[2386] J. Kołaczkiewicz, E. Bauer, The adsorption of nickel on tungsten (110) and (211) surfaces, Surf. Sci. 144 (1984) 495–511.

[2387] O.V. Kanash, A.G. Fedorus, Atomic structure and work function of metal–film system lithium + (011) face of tungsten or molybdenum, Sov. Phys.—JETP 59 (1984) 126–131.

[2388] J. Kołaczkiewicz, E. Bauer, The dipole moments of noble and transition metal atoms adsorbed on W(110) and W(211) surfaces, Surf. Sci. 160 (1985) 1–11.

[2389] J. Kołaczkiewicz, E. Bauer, The adsorption of europium and terbium on the tungsten(211) surface, Surf. Sci. 154 (1985) 357–370.

[2390] S. Kennou, S. Ladas, C. Papageorgopoulos, The behavior of Cs on MoS_2, Surf. Sci. 152/153 (1985) 1213–1221.

[2391] M. Kiskinova, G. Rangelov, L. Surnev, Coadsorption of oxygen and sodium on Ru(001), Surf. Sci. 150 (1985) 339–350.

[2392] S. Kohiki, S. Ikeda, Photoemission from small palladium clusters supported on various substrates, Phys. Rev. B 34 (1986) 3786–3797.

[2393] J. Kołaczkiewicz, E. Bauer, The adsorption of Eu, Gd and Tb on the W(110) surface, Surf. Sci. 175 (1986) 487–507.

[2394] H. Kim, K. Okuno, T. Sakurai, Metal–semiconductor interface (Al–Si), J. Physique 48 (1987) C6–469/C6–472.

[2395] J.H. Kaiser, J.E. Ingelsfield, G.C. Aers, Interpretation of photoemission from Na(110), Solid State Commun. 63 (1987) 689–691.

[2396] T.V. Kalish, M.E. Belyaeva, S.I. Sergeev, Specific features of hydrogen and oxygen adsorption on the surfaces of rhodium (111) and (100) faces, Elektrokhim. 23 (1987) 126–129.

[2397] G. Kozlowski, S. Surma, Study of lanthanum on tungsten field emitter. II, J. Physique 48 (1987) C6–27/C6–31.

[2398] G.A. Katrich, V.V. Klimov, I.N. Yakovkin, Photoelectron investigation of strontium submonolayers on molybdenum(112), Izv. Akad. Nauk SSSR, Ser. Fiz. 52 (1988) 1544–1548.

[2399] T. Kato, K. Ohtomi, M. Nakayama, Coverage dependence of density of states and work function of a random adsorbate–surface system: Application to alkali–metal/Si(001)2×1 surface, Surf. Sci. 209 (1989) 131–150.

[2400] A. Kiejna, Work function of K and Rb submonolayers adsorbed on Al(111) and Mg(0001), Vacuum 41 (1990) 580–582.

[2401] S. Kennou, M. Kamaratos, C.A. Papageorgopoulos, Potassium adsorption on NiO(100), Vacuum 41 (1990) 22–24.

[2402] A. Kiejna, Image potential matched self–consistently to an effective potential for simple–metal surfaces, Phys. Rev. B 43 (1991) 14695–14698.

[2403] J. Kołaczkiewicz, M. Hochół, S. Zuber, LEED, AES, $\Delta\phi$ and EELS study of Al on Mo(110), Surf. Sci. 247 (1991) 284–293.

[2404] G.A. Katrich, V.V. Klimov, I.N. Yakovkin, Electronic structure of magnesium films on molybdenum crystal, Ukr. Fiz. Zh. 36 (1991) 929–933.

[2405] J. Kudrnovský, I. Turek, V. Drchal, P. Weinberger, N.E. Christensen, S.K. Bose, Self–consistent Green's–function method for random overlayers, Phys. Rev. B 46 (1992) 4222–4228.

[2406] K. Kobayashi, Y. Morikawa, K. Terakura, S. Blügel, Optimized structures and electronic properties of alkali–metal (Na, K)–adsorbed Si(001) surfaces, Phys. Rev. B 45 (1992) 3469–3484.

[2407] G.A. Katrich, V.V. Klimov, I.N. Yakovkin, Interrelation between atomic and electronic structures of the films of alkali–earth metals on molybdenum(112) and rhenium(10$\bar{1}$0) faces, Ukr. Fiz. Zh. 37 (1992) 429–437.

[2408] J. Kołaczkiewicz, E. Bauer, Ultrathin films of Rh, Ir and Pt on tungsten(110), Surf. Sci. 314 (1994) 221–242.

[2409] G.A. Katrich, V.V. Klimov, I.N. Yakovkin, Interrelation between atomic and electronic structures of alkaline–earth adlayers on Mo(112) and Re(10$\bar{1}$0), J. Electr. Spectrosc. Rel. Phenom. 68 (1994) 369–375.

[2410] J. Kollár, L. Vitos, H.L. Skriver, Surface energy and work function of the light actinides, Phys. Rev. B 49 (1994) 11288–11292.

[2411] H. Kawano, Compact positive/negative ion sources of electron–stimulation/thermal desorption types, in: Proc. Joint Japan–Philippines Workshop on Plasma Production and Industrial Applications, Univ. of the Philippines, Quezon City, 1995, pp. 63–77.

[2412] C.Y. Kim, K.S. Shin, K.D. Lee, J.W. Chung, Lithium–induced reconstructions of the Si(001) surface, Surf. Sci. 324 (1995) 8–16.

[2413] Y.-J. Ko, K.J. Chang, J.-Y. Yi, Atomic structure of Na–adsorbed Si(100) surfaces, Phys. Rev. B 51 (1995) 4329–4335.

[2414] H. Kleine, M. Eckhardt, H.J. Jänsch, D. Fick, Adsorption of Li on a Si(100)–2×1 surface, Surf. Sci. 323 (1995) 51–56.

[2415] E. Knoesel, T. Hertel, M. Wolf, G. Ertl, Femtosecond dynamics of electronic excitations of adsorbates studied by two–photon photoemission pulse correlation: CO/Cu(111), Chem. Phys. Lett. 240 (1995) 409–416.

[2416] M. Katoh, R. Fukuda, T. Igarashi, Thermionic properties and thermal stability of emitter with a (0001) oriented rhenium layers and graded structure, in: Proc. 4th Int. Symp. Funct. Graded Mater., 1996, pp. 655–660 (Chem. Abstr. 128 (1998) 50677h).

[2417] E. Kopatzki, H.-G. Keck, I.D. Baikie, J.A. Meyer, R.J. Behm, Combined work function and STM study on growth, alloying and oxidation of epitaxial aluminum films on Rh(0001), Surf. Sci. 345 (1996) L11–L18.

[2418] K. Kokko, P.T. Salo, R. Laihia, K. Mansikka, First–principles calculations for work function and surface energy of thin lithium films, Surf. Sci. 348 (1996) 168–174.

[2419] A. Kiejna, V.V. Pogosov, On the temperature dependence of the ionization potential of self–compressed solid– and liquid–metallic clusters, J. Phys.: Condens. Matter 8 (1996) 4245–4257.

[2420] J. Kołaczkiewicz, E. Bauer, Behaviour of Rh, Pd, Ir and Pt on the W(110) face above room temperature, Surf. Sci. 366 (1996) 71–84.

[2421] J.W. Kim, J.M. Seo, S. Kim, Surface electronic properties of Na/Ge(111)–3×1, Surf. Sci. 351 (1996) L239–L244.

[2422] H. Kawano, Ion desorption from solid surfaces: Fundamental research and its applications, in: Proc. 18th Int. Symp. Phys. Ionized Gases (18th SPIG), Kotor, Yugoslavia, 1997, pp. 169–183.

[2423] D.J. Klinke II, S. Wilke, L.J. Broadbelt, The theoretical study of carbon chemisorption on Ni(111) and Co(0001) surfaces, J. Catal. 178 (1998) 540–554.

[2424] S. Kitami, T. Nakane, A. Sakai, T. Sakata, The work function of the Cu–deposited Ti emitter, Ultramicrosc. 73 (1998) 37–42.

[2425] O.M. Küttel, O. Groening, C. Emmenegger, L. Schlapbach, Electron field emission from phase pure nanotube films grown in a methane/hydrogen plasma, Appl. Phys. Lett. 73 (1998) 2113–2115.

[2426] N. Kitano, N. Matuda, T. Azami, H. Matuura, Secondary electron emission from copper surface, Shinku (J. Vac. Soc. Japan) 41 (1998) 239–241 (Chem. Abstr. 129 (1998) 116617t).

[2427] A. Kiejna, Stabilized jellium — Simple model for simple–metal surfaces, Prog. Surf. Sci. 61 (1999) 85–125.

[2428] M. Kralj, P. Pervan, M. Milun, Growth, structure and properties of ultra–thin copper films on a V(110) surface, Surf. Sci. 423 (1999) 24–31.

[2429] J. Kołaczkiewicz, E. Bauer, Growth and thermal stability of Fe, Ni, Rh and Pd layers on the (111)W crystal face, Surf. Sci. 420 (1999) 157–173.

[2430] J. Kołaczkiewicz, E. Bauer, V and Fe on the W(110) face, Surf. Sci. 450 (2000) 106–116.

[2431] D. Kolthoff, H. Pfnür, Geometrical evidence for long-range coupling in strongly anisotropic adsorbate systems: Sr and Li on Mo(211), Surf. Sci. 459 (2000) 265–276.

[2432] A. Kiejna, V.V. Pogosov, Simple theory of elastically deformed metals: Surface energy, stress and work function, Phys. Rev. B 62 (2000) 10445–10450.

[2433] T. Kan, K. Mitsukawa, T. Ueyama, M. Takada, T. Yasue, T. Koshikawa, Secondary ion emission processes of sputtered alkali ions from alkali/Si(100) and Si(111), Surf. Sic. 460 (2000) 214–222.

[2434] T. Kondo, H. Kozakai, T. Sasaki, S. Yamamoto, Dynamics and thermal stability of Cs superstructures on a Pt(111) surface, J. Vac. Sci. Technol. A 19 (2001) 2866–2869.

[2435] N. Kiwa, Y. Gotoh, H. Tsuji, J. Ishikawa, Relationship between composition and work function of gold–samarium alloy thin films, Vacuum 66 (2002) 517–521.

[2436] D.-H. Kim, H.-R. Lee, M.-W. Lee, J.-H. Lee, Y.-H. Song, J.-G. Jee, S.-Y. Lee, Effect of the *in situ* Cs treatment on field emission of a multi–walled carbon nanotube, Chem. Phys. Lett. 355 (2002) 53–58.

[2437] M. Kralj, P. Pervan, M. Milum, P. Lazić, Ž. Crljen, R. Brako, Tetragonal silver film on V(100): Experimental and *ab initio* studies, Phys. Rev. B 68 (2003) 195402/1–8.

[2438] A. Kiejna, T. Ossowski, E. Wachowicz, Alkali metals adsorption on the Mg(0001) surface, Surf. Sci. 548 (2004) 22–28.

[2439] V.P. Kurbatsky, V.V. Pogosov, Analytical model for the Fermi energy and work function of thin metallic films, Vacuum 74 (2004) 185–189.

[2440] J. Kołaczkiewicz, M. Kuchowicz, R. Szukiewicz, Thermal stability of the Ta(111) surface covered with chemisorbed metal layer. Part I: Au, Surf. Sci. 548 (2004) 246–258.

[2441] J. Kołaczkiewicz, M. Kuchowicz, R. Szukiewicz, Thermal stability of the Ta(111) surface covered with chemisorbed metal layer. Part II: Ag, Surf. Sci. 548 (2004) 259–268.

[2442] A. Kokalj, T. Matsushima, A density–functional theory study of the interaction of N_2O with Rh(110), J. Chem. Phys. 122 (2005) 034708/1–10.

[2443] N.N. Kulkarni, J. Bae, C.-K. Shih, S.K. Stanley, S.S. Coffee, J.G. Ekerdt, Low–threshold field emission from cesiated silicon nanowires, Appl. Phys. Lett. 87 (2005) 213115/1–3.

[2444] S. Kajita, T. Nakayama, J. Yamauchi, Density functional calculation of work function using charged slab systems, J. Phys.: Conf. Ser. 29 (2006) 120–123.

[2445] P.S. Kirchmann, M. Wolf, J.H. Dil, K. Horn, U. Bovensiepen, Quantum size effects in Pb/Si(111) investigated by laser–induced photoemission, Phys. Rev. B 76 (2007) 075406/1–5.

[2446] K.K. Kim, J.J. Bae, H.K. Park, S.M. Kim, H.-Z. Geng, K.A. Park, H.-J. Shin, S.-M. Yoon, A. Benayad, J.-Y. Choi, Y.H. Lee, Fermi level engineering of single–walled carbon nanotubes by AuCl$_3$ doping, J. Am. Chem. Soc. 130 (2008) 12757–12761.

[2447] K. Kusakabe, Y. Ikuno, H. Nagara, Determination of the work function by the density functional theory, Hyomen Kagaku (Surf. Sci.) 29 (2008) 321–324 (Chem. Abstr. 150 (2009) 11269m).

[2448] T. Kim, T. Kawae, N. Ikegami, S. Yamada, Y. Yonezawa, K. Takahashi, A. Morimoto, M. Kumeda, Effect of microstructure and crystalline orientation of Pt single– or Pt/Ru bilayer–electrode on the work function and leakage current of SrTiO$_3$ capacitors, Japan. J. Appl. Phys. 47 (2008) 6374–6379.

[2449] M. Kuchowicz, R. Szukiewicz, S. Stepanovsky, J. Kołaczkiewicz, Adsorption of Sm and Gd on the Mo(111) face, Surf. Sci. 602 (2008) 3043–3050.

[2450] M. Kuchowicz, J. Kołaczkiewicz, Valence changes of Sm atoms adsorbed on Mo(211) surfaces, Surf. Sci. 602 (2008) 3721–3727.

[2451] M. Kutschera, T. Groth, C. Kentsch, I.L. Shumay, M. Weinelt, Th. Fauster, Electronic structure of CoS$_2$ films on Si(111) studied using time–resolved two–photon photoemission, J. Phys.: Condens. Matter 21 (2009) 134006/1–9.

[2452] M. Kuchowicz, J. Kołaczkiewicz, Gd adsorption on the Mo(211) surface, Surf. Sci. 603 (2009) 1018–1025.

[2453] H. Kawano, Quantitative relation between the thermionic contrast of metal surfaces and their degree of monocrystallization, Appl. Surf. Sci. 257 (2011) 4344–4349.

[2454] I. Langmuir, The effect of space charge and residual gases on thermionic currents in high vacuum, Phys. Rev. 2 (1913) 450–486.

[2455] I. Langmuir, Phys. Z. 15 (1914) 516–526 (see Ref. [2296]).

[2456] I. Langmuir, The relation between contact potential and electrochemical action, Trans. Am. Electrochem. Soc. 29 (1916) 125–182.

[2457] H. Lester, Phil. Mag. 31 (1916) 197 (see Ref. [633]).

[2458] L.L. Lockrow, The effect of oxygen and hydrogen on the emission of electrons from hot platinum, Phys. Rev. 19 (1922) 97–113.

[2459] I. Langmuir, K.H. Kingdon, Thermionic phenomena due to alkali vapors. Part II. Theoretical, Phys. Rev. 21 (1923) 381.

[2460] P. Lukirskii, S. Prilezaev, The normal photoelectric effect, Z. Phys. 49 (1928) 236–258.

[2461] R.Ya. Kamilova, M.A. Vakhabova, Thermoemission properties of faces of tungsten crystals coated with titanium, Izv. Akad. Nauk Uzb.SSR, Ser. Fiz. Mathem. (2) (1990) 79–82.

[2462] I. Langmuir, K.H. Kingdon, Contact potential measurements with adsorbed films, Phys. Rev. 34 (1929) 129–135.

[2463] I. Liben, The energy distribution of photoelectrons emitted by calcium and calcium oxide, Phys. Rev. 51 (1937) 642–647.

[2464] D.H. Loughridge, N.K. Olsen, Photoelectric long wave–length limit of magnetized iron, Phys. Rev. 54 (1938) 239.

[2465] J.D. Levine, E.P. Gyftopoulos, Adsorption physics of metals partially covered with metallic particles. Part III: Equations of state and electron emission S–curves, Surf. Sci. 1 (1964) 349–360.

[2466] E.M. Logothetis, P.L. Hartman, Three–photon photoelectric effect in gold, Phys. Rev. Lett. 18 (1967) 581–583.

[2467] C. Lea, C.H.B. Mee, The photoelectric work function of monolayer films of uranium on polycrystalline tungsten, Surf. Sci. 8 (1967) 417–425.

[2468] H.M. Love, J.R. Wilson, Work function of tungsten single crystals, Canad. J. Phys. 45 (1967) 225–227.

[2469] K.P. Lobanova, S.D. Levina, Electron work function of systems consisting of metals coated with thin phthalocyanine films, Elektrokhim. 3 (1967) 1233–1236.

[2470] V.B. Lazarev, Yu.I. Malov, External photoeffect in liquid potassium, rubidium and mercury, Fiz. Metal. Metalloved. 24 (1967) 565–566 (Chem. Abstr. 68 (1968) 44522e).

[2471] C. Lea, C.H.B. Mee, Work–function measurements on monolayer films of uranium on (100), (110), and (113) oriented faces of tungsten single crystals by photoelectric and contact potential difference techniques, J. Appl. Phys. 39 (1968) 5890–5896.

[2472] G.J. Lapeyre, K.A. Kress, Photoemission investigation of the electronic structure of chromium, Phys. Rev. 166 (1968) 589–598.

[2473] R.P.W. Lawson, G. Carter, Inert gas ion bombardment induced work function changes in polycrystalline tungsten and gold ribbon, Vacuum 18 (1968) 205–211.

[2474] N.D. Lang, Self–consistent properties of the electron distribution at a metal surface, Solid State Commun. 7 (1969) 1047–1059.

[2475] E.M. Logothetis, P.L. Hartman, Laser–induced electron emission from solids: Many–photon photoelectric effects and thermionic emission, Phys. Rev. 187 (1969) 460–474.

[2476] O. Lapp, K. Neumann, Photoelectric behavior of potassium in the solid and molten states, Z. Naturforsch. 24 a (1969) 596–601.

[2477] J.J. Lander, J. Morrison, Cesium plasma spectra in the system W(100)–Cs, Surf. Sci. 14 (1969) 465–472.

[2478] C. Lea, B.H. Blott, C.H.B. Mee, Computation of photoelectric work functions using the Fowler analysis, Appl. Opt. 8 (1969) 203–204.

[2479] A.G. Leiga, Photoemission from amorphous selenium, J. Appl. Phys. 41 (1970) 3227–3229.

[2480] G.J. Lapeyre, T. Huen, F. Wooten, Temperature and polarization dependence of photoemission from bismuth single crystals, Solid State Commun. 8 (1970) 1233–1236.

[2481] T.J. Lee, B.H. Blott, B.J. Hopkins, The work function variation during caesium deposition on the (100) and (110) single crystal surfaces of tungsten, J. Phys. F 1 (1971) 309–319.

[2482] L.D. Laude, B. Fitton, M. Anderegg, High–resolution photoemission study of the band structure of tellurium, Phys. Rev. Lett. 26 (1971) 637–640.

[2483] J.D. Levine, Structual and electronic model of negative electron affinity on the Si/Cs/O surface, Surf. Sci. 34 (1973) 90–107.

[2484] M.J.G. Lee, Field emission of hot electrons from tungsten, Phys. Rev. Lett. 30 (1973) 1193–1196.

[2485] M. Laguës, Band bending effect on the thermal dependence of photoemission from Li activated Si, Surf. Sci. 45 (1974) 432–440.

[2486] N.R. Avery, LEED, Auger and work function study of iodine adsorbed on W(110), Surf. Sci. 43 (1974) 101–122.

[2487] L.A. Larin, G.F. Voronina, T.V. Kalish, Work function of platinum and effect on its chemisorved oxygen and hydrogen, in: Tezisy Dokl.-Vses. Soveshch. Elektrokhim., 5th, 1, 1975, pp. 225–226 (Chem. Abstr. 83 (1975) 209678k).

[2488] R. Liu, G. Ehrlich, Adsorption of nitrogen on perfect Re(0001) planes, J. Vac. Sci. Technol. 13 (1976) 310–313.

[2489] M.V. Loginov, M.A. Mittsev, Concentration dependences of the lifetime and heat of adsorption of samarium atoms on a tungsten surface, Sov. Phys.—Solid State 20 (1978) 1603–1606.

[2490] Kh.I. Lakh, Z.V. Stasyuk, Electron–adsorption properties of potassium films on the (10$\bar{1}$0) surface of rhenium, Sov. Phys.—Solid State 20 (1978) 1149–1150.

[2491] S.Å. Lindgren, L. Walldén, Structure and electronic properties of Cs adsorbed on Cu(111), Solid State Commun. 25 (1978) 13–15.

[2492] M.J.G. Lee, R. Reifenberger, Periodic field–dependent photocurrent from a tungsten field emitter, Surf. Sci. 70 (1978) 114–130.

[2493] R.C. Lee, N.C. McGill, Variational calculation of the electron density and potential in a thin metal film, Surf. Sci. 84 (1979) 121–128.

[2494] M.V. Loginov, M.A. Mittsev, Investigation of the concentration dependences of the lifetime of europium atoms adsorbed on tungsten by flux modulation, Sov. Phys.—Solid State 22 (1980) 992–995.

[2495] S.Å. Lindgren, L. Walldén, Photoemission of electrons at the Cu(111)/Na interface, Solid State Commun. 34 (1980) 671–673.

[2496] S.Å. Lindgren, L. Walldén, Electronic structure of clean and oxygen–exposed Na and Cs monolayers on Cu(111), Phys. Rev. B 22 (1980) 5967–5979.

[2497] S.B. Lee, M. Weiss, G. Ertl, Adsorption of potassium on iron, Surf. Sci. 108 (1981) 357–367.

[2498] N.D. Lang, A.R. Williams, Theory of local–work function determination by photoemission from rare–gas adsorbates, Phys. Rev. B 25 (1982) 2940–2942.

[2499] R. Liu, G. Ehrlich, Chemisorption on densely packed metal surfaces: Mo, W, Re, and Ir, Surf. Sci. 119 (1982) 207–233.

[2500] A.T. Loburets, A.G. Naumovets, Yu.S. Vedula, Surface diffusion of lithium on (011) face of tungsten, Surf. Sci. 120 (1982) 347–366.

[2501] Kh.I. Lakh, Z.V. Stasyuk, Electronic properties of barium films on the surface $(10\bar{1}0)$ of a rhenium single crystal, Ukr. Fiz. Zh. 27 (1982) 146–147.

[2502] Ya.B. Lozovyĭ, V.K. Medvedev, T.P. Smereka, B.M. Palyukh, G.V. Babkin, Adsorption of lanthanum on a (112) face of a molybdenum crystal, Sov. Phys.—Solid State 24 (1982) 1213–1216.

[2503] Ya.B. Lozovyĭ, Structure of potassium films on the $(10\bar{1}0)$ face of rhenium, Sov. Phys.—Solid State 24 (1982) 1505–1506.

[2504] N.D. Lang, A.R. Williams, F.J. Himpsel, B. Reihl, D.E. Eastman, Absence of a charge–transfer instability for rare–gas atoms adsorbed on metals, Phys. Rev. B 26 (1982) 1728–1737.

[2505] H.S. Luftman, Y.-M. Sun, J.M. White, Coadsorption of CO and K on Ni(100). II. XPS, UPS, $\Delta\phi$ and ELS studies, Surf. Sci. 141 (1984) 82–100.

[2506] Ya.B. Lozovyĭ, V.K. Medvedev, T.P. Smereka, G.V. Babkin, B.M. Palyukh, Structure of submonolayer lanthanum films on a $(10\bar{1}0)$ face on rhenium, Sov. Phys.—Solid State 26 (1984) 738–739.

[2507] Ya.B. Lozovyĭ, V.K. Medvedev, T.P. Smereka, G.V. Babkin, B.M. Palyukh, O.S. Vasil'chishin, Adsorption of barium and lanthanum on the tungsten crystal (111) face, Sov. Phys.—Solid State 28 (1986) 2080–2083.

[2508] A.R. Law, M.T. Johnson, H.P. Hughes, Synchrotron–radiation–excited angle–resolved photoemission from single–crystal graphite, Phys. Rev. B 34 (1986) 4289–4297.

[2509] S.Å. Lindgren, L. Walldén, Discrete valence–electron states in thin metal overlayers on a metal, Phys. Rev. Lett. 59 (1987) 3003–3006.

[2510] C. Li, A.J. Freeman, C.L. Fu, Electronic structure and surface magnetism of fcc Co(001), J. Magn. Magn. Mater. 75 (1988) 53–60.

[2511] X.Q.D. Li, R. Vanselow, Adsorption of CO on kinked surface areas of Pt and Rh: The relation between work function change upon saturated adsorption and the work function of the corresponding clean adsorbent area, Surf. Sci. 236 (1990) L369–L371.

[2512] S.Å. Lindgren, L. Walldén, Layer–by–atomic–layer deposition of Cs from Cu(111)/Cs observed via photoemission, J. Phys.: Condens. Matter 2 (1990) 5929–5932.

[2513] J.C. Lin, N. Shamir, R. Gomer, Adsorption of Pd on O/W(110) and CO/W(110), Surf. Sci. 226 (1990) 26–32.

[2514] T.-S. Lin, H.-J. Lu, R. Gomer, Diffusion of CO on Ni(111) and Ni(115), Surf. Sci. 234 (1990) 251–261.

[2515] S.Å. Lindgren, L. Walldén, Ba adsorption on Cu(111) studied by photoemission, Surf. Sci. 257 (1991) L619–L622.

[2516] E.P.M. Leiva, Contribution of the metal to the capacitance of the double layer: A self–consistent calculation including pseudopotentials, Chem. Phys. Lett. 187 (1991) 143–148.

[2517] H.-Y. Li, L. Zhu, Y.B. Xu, L.Z. Cai, Work function study of CO and K coadsorption on Cu(111) surface, Acta. Phys. Sinica 40 (1991) 625–629.

[2518] A. Lamouri, I.L. Krainsky, Angle–resolved inverse photoemission from one monolayer of Ba on W(001), Surf. Sci. 278 (1992) 286–290.

[2519] J.I. Lee, S.K. Hwang, S.C. Hong, A.J. Freeman, All–electron local–density determination of the electronic structure and surface energy of Zr(0001), Internat. J. Modern Phys. B 7 (1993) 520–523.

[2520] M.E. Lin, R.T. Andres, R. Reifenberger, D.R. Huffman, Electron emission from an individual, supported C_{60} molecule, Phys. Rev. B 47 (1993) 7546–7553.

[2521] G. Li, Y.-C. Chang, Planar–basis pseudopotential calculations of the Si(001)2×1 surface with and without hydrogen passivation, Phys. Rev. B 48 (1993) 12032–12036.

[2522] D. Li, J. Zhang, P.A. Dowben, M. Onellion, Altering the Gd(0001) surface electronic structure with hydrogen adsorption, Phys. Rev. B 48 (1993) 5612–5620.

[2523] E. Leiva, W. Schmickler, Second harmonic generation at single crystal surfaces of metals in the vacuum and in a solution, Surf. Sci. 291 (1993) 226–232.

[2524] Z. Li, S. Gao, Band–theory calculation of image states on a metal surface, Phys. Rev. B 50 (1994) 15349–15352.

[2525] G. Li, Y.-C. Chang, Electronic structures of As/Si(001)2×1 and Sb/Si(001)2×1 surfaces, Phys. Rev. B 50 (1994) 8675–8680.

[2526] S.C. Lee, Y. Irokawa, M. Inoue, R. Shimizu, Behavior of zirconium in the Zr–O/W(100) system at high temperature, studied by ISS, AES and work–function measurements, Surf. Sci. 330 (1995) 289–296.

[2527] J. Liu, V.V. Zhirnov, A.F. Myers, G.J. Wojak, W.B. Choi, J.J. Hren, S.D. Wolter, M.T. McClure, B.R. Stoner, J.T. Glass, Field emission characteristics of diamond coated silicon field emitters, J. Vac. Sci. Technol. B 13 (1995) 422–426.

[2528] A. Lamouri, I.L. Krainsky, A.G. Petukhov, W.R.L. Lambrecht, B. Segall, Unoccupied electronic resonances of Sc adsorbed on W(001) by k–resolved inverse photoemission, Phys. Rev. B 51 (1995) 1803–1808.

[2529] J. Lehmann, P. Roos, E. Bertel, Incorporation of alkali metals on Pt(111), Phys. Rev. B 54 (1996) R2347–R2350.

[2530] E. Leiva, Recent developments in the theory of metal *upd* (underpotential deposition), Electrochim. Acta 41 (1996) 2185–2206.

[2531] Q.B. Lu, R. Souda, D.J. O'Connor, B.V. King, Interaction of oxygen with a Cs–monolayer–covered Si(100) surface, Phys. Rev. B 54 (1996) R17347–R17350.

[2532] Q.B. Lu, D.J. O'Connor, B.V. King, R.J. MacDonald, Local electrostatic potential determination of Cs/Cu(111) surfaces by negative ion spectroscopy, Surf. Sci. 347 (1996) L61–L65.

[2533] Ya.B. Losovyj, Adsorption of gadolinium on the Mo(112) crystal face, Vacuum 48 (1997) 195–198.

[2534] R. Löber, D. Hennig, Interaction of hydrogen with transition metal fcc(111) surfaces, Phys. Rev. B 55 (1997) 4761–4765.

[2535] Ya.B. Losovyj, N.T. Dubyk, F.M. Gonchar, Effect of initial stages of oxidation of W(111) and Mo(112) on the adsorption of Dy, Nd and Li, Vacuum 50 (1998) 85–87.

[2536] Z.-Y. Lu, G.L. Chiarotti, S. Scandolo, E. Tosatti, Atomic and electronic structure of ideal and reconstructed α–Sn(100) surfaces, Phys. Rev. B 58 (1998) 13698–13711.

[2537] J. Lahtinen, J. Vaari, K. Kauraala, Adsorption and structure dependent desorption of CO on Co(0001), Surf. Sci. 418 (1998) 502–510.

[2538] J. Lee II, I.G. Kim, Y.-R. Jang, S.C. Hong, First–principles study of surface electronic structures of half– and full–monolayer Na on Ta(110) surface, J. Korean Phys. Soc. 37 (2000) 99–103 (Chem. Abstr. 134 (2001) 11840k).

[2539] V.V. Levitin, O.L. Garin, V.K. Yatsenko, S.V. Loskutov, On structural sensibility of work function, Vacuum 63 (2001) 367–370.

[2540] M. Lüders, A. Ernst, W.M. Temmerman, Z. Szotek, P.J. Durham, *Ab initio* angle–resolved photoemission in multiple–scattering formulation, J. Phys.: Condens. Matter 13 (2001) 8587–8606.

[2541] W.-X. Li, C. Stampfl, M. Scheffler, Oxygen adsorption on Ag(111): A density–functional theory investigation, Phys. Rev. B 65 (2002) 075407/1–19.

[2542] A. Lohani, V. Bhattacharyya, Work function changes of W(110) with temperature and Sm adsorption using electron beam retarding potential technique, J. Electron Spectrosc. Relat. Phenom. 122 (2002) 79–84.

[2543] A.Y. Lozovoi, A. Alavi, Reconstruction of charged surfaces: General trends and a case study of Pt(110) and Au(110), Phys. Rev. B 68 (2003) 245416/1–18.

[2544] Y. Li, D.Y. Li, Experimental studies on relationships between the electron work function, adhesion, and friction for $3d$ transition metals, J. Appl. Phys. 95 (2004) 7961–7965.

[2545] H.-N. Li, X.-X. Wang, S.-L. He, H.-J. Zhang, H.-Y. Li, S.N. Bao, Electronic structure of Yb/H–Si(111) interface, Chin. J. Phys 13 (2004) 1941–1946.

[2546] S.C. Lim, H.J. Jeong, K.S. Kim, I.B. Lee, D.J. Bae, Y.H. Lee, Extracting independently the work function and field enhancement factor from thermal–field emission of multi–walled carbon nanotube tips, Carbon 43 (2005) 2801–2807.

[2547] W. Li, D.Y. Li, Variations of work function and corrosion behaviors of deformed copper surfaces, Appl. Surf. Sci. 240 (2005) 388–395.

[2548] S.V. Loskutov, Work function for the deformed metal surface, Surf. Sci. 585 (2005) L166–L170.

[2549] G. Li, X.-C. Lai, Y. Sun, An all–electron FLAPW study of property of the (001) surface of δ–Pu, Yuanzi Yu Fenzi Wuli Xuebao 22 (2005) 365–370 (Chem. Abstr. 144 (2006) 261455c).

[2550] W. Li, D.Y. Li, *In situ* measurements of simultaneous electronic behavior of Cu and Al induced mechanical deformation, Appl. Phys. 99 (2006) 073502/1–8.

[2551] E.P.M. Leiva, C.G. Sánchez, P. Vélez, W. Schmickler, Theory of electrochemical monatomic nanowires, Phys. Rev. B 74 (2006) 035422/1–7.

[2552] X.-G. Li, P. Zhang, C.K. Chan, First–principles calculation of Mg(0001) thin films: Quantum size effect and adsorption of atomic hydrogen, Physica B 390 (2007) 225–230.

[2553] S.-Y. Liu, F.-H. Wang, Y.-S. Zhou, J.-X. Shang, *Ab initio* study of oxygen adsorption on the Ti(0001) surface, J. Phys.: Condens. Matter 19 (2007) 226004/1–12.

[2554] Y. Lu, Q. Sun, Y. Jia, P. He, Adsorption and diffusion of adatoms on Ru(0001): A first–principles study, Surf. Sci. 602 (2008) 2502–2507.

[2555] P. Liu, Q. Sun, F. Zhu, K. Liu, K. Jiang, L. Liu, Q. Li, S. Fan, Measuring the work function of carbon nanotubes with thermionic method, Nano Lett. 8 (2008) 647–651.

[2556] Y. Li, P. Zhang, B. Sun, Y. Yang, Y. Wei, Atomic hydrogen adsorption and incipient hydrogenation of the Mg(0001) surface: A density–functional theory study, J. Chem. Phys. 131 (2009) 034706/1–10.

[2557] Y.-T. Li, T.-C. Chen, Field emission properties and electronic structures of ultra small diameter carbon nanotubes, Carbon 47 (2009) 1165–1170.

[2558] M.J. Mrtin, The photoelectric and thermionic properties of molybdenum, Phys. Rev. 33 (1929) 991–997.

[2559] E. Meyer, Electronic and positive–ionic emission from tungsten, molybdenum and tantalum filaments heated in potassium vapor, Ann. Phys. 4 (1930) 357–386.

[2560] L.W. Morris, Certain photoelectric properties of gold, Phys. Rev. 37 (1931) 1263–1268.

[2561] M.M. Mann Jr., L.A. DuBridge, The absolute photoelectric yields of Mg, Be and Na, Phys. Rev. 51 (1937) 120–124.

[2562] H. Mayer, The photoelectric properties of atomic films of potassium on platinum. I, Ann. Phys. 29 (1937) 129–159.

[2563] V. Middel, Photoelectric measurements upon metallic antimony, Z. Phys. 105 (1937) 358–377.

[2564] R.J. Maurer, The photoelectric and optical properties of sodium and barium, Phys. Rev. 57 (1940) 653–658.

[2565] E. Müller, Velocity distribution of electrons for field emission, Z. Phys. 120 (1943) 261–269.

[2566] R.J. Munick, W.B. LaBerge, E.A. Coomes, Periodic deviations in the Schottky effect for tantalum, Phys. Rev. 80 (1950) 887–891.

[2567] G.E. Moore, H.W. Allison, Thermionic emission of thin films of alkaline earth oxide deposited by evaporation, Phys. Rev. 77 (1950) 246–257.

[2568] S.B.L. Mathur, A new method for obtaining thermionic constants. II. The thermionic work function of iron, Proc. Natl. Inst. Sci. India 19 (1953) 165–168 (Chem. Abstr. 47 (1953) 11958i).

[2569] S.B.L. Mathur, A new method for obtaining thermionic constants. III. The thermionic work function of graphite, Proc. Natl. Inst. Sci. India 19 (1953) 169–171 (Chem. Abstr. 47 (1953) 11958i).

[2570] H.P. Myers, The simple varying capacitor method for the measurement of contact potential difference in high vacuum, Proc. Phys. Soc. B 66 (1953) 493–499.

[2571] H. Malamud, A.D. Krumbein, Measurement of the effect of chlorine treatment on the work function of titanium and zirconium, J. Appl. Phys. 25 (1954) 591–592.

[2572] G.E. Moore, H.W. Allison, Adsorption of strontium and of barium on tungsten, J. Chem. Phys. 23 (1955) 1609–1621.

[2573] J.C.P. Mignolet, Studies in contact potentials. I. Determination of the surface potential of some films on tungsten and mercury by the condenser method and a new form of the thermionic method, Rec. Trav. Chim. 74 (1955) 685–700.

[2574] E.W. Müller, Field desorption, Phys. Rev. 102 (1956) 618–624.

[2575] P.M. Marchuk, Evaporation of barium from the surface of some metals, Radiotekh. Elektron. 2 (1957) 1479–1490.

[2576] S. Methfessel, Outer photoelectric effect of alkali metals. III. Energy distribution for potassium and cesium, Z. Phys. 147 (1957) 442–464.

[2577] N.D. Morgulis, Variation of the work function of an electron from a metal under the influence of an adsorbed layer of molecules of barium oxide, Sov. Phys.—Solid State 1 (1959) 1029–1035.

[2578] V.I. Makukha, Adsorption of strontium on tungsten, Radiotekh. Elektron. 6 (1961) 342–343.

[2579] H. Mayer, W. Schroen, Absolute determination of the ionization yield by potassium atoms on metal surfaces, Naturwiss. 49 (1962) 202–203.

[2580] N.V. Mileshkina, I.L. Sokol'skaya, Energy distribution of electrons in field emission from germanium films on tungsten, Sov. Phys.—Solid State 5 (1964) 1826–1832.

[2581] G. Montet, M. Hoch, G. Hennig, Field Emission from Single Crystals of Graphite, U.S. At. Energy Comm. ANL–6804, 1964, 15 pp. (Chem. Abstr. 61 (1964) 7829f).

[2582] T.L. Matskevich, T.V. Krachino, A.P. Kazantsev, L.S. Markova, Thermoemission properties of some high–melting metal coatings on metal substrates, Sov. Phys. Tech. Phys. 9 (1965) 1554–1559.

[2583] D. Matthews, The mechanism of the hydrogen evolution reaction: A quantum mechanical study (Ph. D. thesis), Univ. of Pennsylvania, 1965, 608 pp. (Diss. Abstr. B 26 (1965) 3061) (see Ref. [3264]).

[2584] N.V. Mileshkina, I.L. Sokol'skaya, Experimental investigation of the energy spectrum and emission properties of thin germanium films on tungsten, Sov. Phys.—Solid State 7 (1965) 838–843.

[2585] T.E. Madey, A.A. Petrauskas, E.A. Coomes, Thermal desorption of Sr from W, J. Chem. Phys. 42 (1965) 479–485.

[2586] A.J. Melmed, Adsorption and surface diffusion of copper on tungsten, J. Chem. Phys. 43 (1965) 3057–3062.

[2587] V.I. Makukha, B.M. Tsarev, Adsorption and electron emission of alkaline–earth metal films on tungsten, iridium, and rhodium, Sov. Phys. Solid State 8 (1966) 1130–1138.

[2588] N.V. Mileshkina, I.L. Sokol'skaya, L.B. Kis, Study of the emission properties of germanium on various faces of a tungsten single crystal, Sov. Phys.—Solid State 8 (1966) 1110–1113.

[2589] H. Merdy, Optical and photoelectric properties of Te in the fundamental absorption range, Ann. Phys. (Paris) 1 (1966) 289–325.

[2590] V.I. Makukha, Investigation of the adsorption and electron emission of cesium films on a tungsten single crystal, Sov. Phys.—Solid State 9 (1967) 111–116.

[2591] L.P. Mosteller Jr., Optical Properties and Electronic Band Structure of Zinc: Reflectance and Photoemission Studies, U.S. At. Energy Comm. UCRL–50307, 1967, 101 pp. (Chem. Abstr. 69 (1968) 39986a).

[2592] T.E. Madey, J.T. Yates Jr., Work function studies: Chemisorption of diatomic molecules on single–crystal tungsten, Nuovo Ciment, Suppl. 5 (1967) 483–505.

[2593] E.V. Mikheeva, O.D. Protopopov, B.N. Sheinberg, G.N. Shuppe, Thermal emission parameters of rhenium single crystal faces, Tr. Konf. Elektr. Tekh. (4) (1968) 181–195.

[2594] H. Mayer, A. Rahn, Absolute measurements of the ionization coefficients of alkali atoms on metal surfaces. II. Sodium atoms on platinum and tungsten surfaces, Z. Phys. 212 (1968) 408–414.

[2595] V.K. Medvedev, Adsorption of barium on the (110) face of a tungsten single crystal, Sov. Phys.—Solid State 10 (1969) 2752–2753.

[2596] N.V. Mileshkina, L.L. Sokol'skaya, Stabilization of the emission characteristics of metal surfaces, Sov. Phys. Tech. Phys. 13 (1969) 1593–1595.

[2597] N.S. Mirolyubova, N.A. Shurmovskaya, R.Kh. Burshtein, Comparison of the differences in work functions and zero charge potentials of metals. I. Effect of water vapor on the work function of mercury, Elektrokhim. 4 (1968) 844–847.

[2598] A.R.L. Moss, B.H. Blott, The epitaxial growth of copper on the (110) surface of a tungsten single crystal studied by LEED, Auger electron, and work function techniques, Surf. Sci. 17 (1969) 240–261.

[2599] A.U. MacRae, K. Müller, J.J. Lander, J. Morrison, J.C. Phillips, Electronic and lattice structure of cesium films adsorbed on tungsten, Phys. Rev. Lett. 22 (1969) 1048–1051.

[2600] A.U. MacRae, K. Müller, J.J. Lander, J. Morrison, An electron diffraction study of cesium adsorption on tungsten, Surf. Sci. 15 (1969) 483–497.

[2601] L.P. Mosteller, T. Huen, F. Wooten, Photoelectric emission from Zn, Phys. Rev. 184 (1969) 364–366.

[2602] Ts.S. Marinova, Yu.V. Zubenko, Adsorption and work function of ytterbium and neodymium on tungsten, Sov. Phys.—Solid State 12 (1970) 398–400.

[2603] V.I. Makhov, B.V. Bondarenko, Structure and work function of lutetium films on the (110) face of a molybdenum single crystal, Sov. Phys.—Solid State 12 (1971) 2986–2987.

[2604] G. Maire, J.R. Anderson, B.B. Johnson, The adsorption of CH_4, C_2H_6 and neo-C_5H_{12} on (111), (100) and (111) faces of nickel observed by LEED and by photoelectric work function measurement, Proc. Roy. Soc. A 320 (1970) 227–250.

[2605] H. Mayer, D.L. Blanaru, H. Steffen, Photoelectric and optical properties of thin alkali metal films, Thin Solid Films 5 (1970) 389–406.

[2606] J.C. Mitchinson, R.D. Pringle, Work function of a gold film measured during the nucleation of silver overlayer, Appl. Phys. Lett. 17 (1970) 326–327.

[2607] L.D. Matthews, Radiotracer and photoemission studies of CO chemisorption on Mo(100), Surf. Sci. 24 (1971) 248–254.

[2608] T.L. Matskevich, D.S. Popov, Thermoemission properties of iron–sulfur alloys, Izv. Akad. Nauk SSSR, Ser. Metal. 6 (1971) 213–216.

[2609] E. Maier, G. Fröhlich, R. Mayer, I—V–characteristics of a plane parallel cesium diode with tantalum and tungsten emitter, in: Proc. 3rd Int. Conf. Thermion. Electr. Power Generat. Uülich, Vol. 3, 1972, pp. 1289–1299.

[2610] E.E. Mola, Thesis, Univ. Nacion. La Plata, Buenos Aires, 1973 (see Ref. [2649]).

[2611] V.K. Medvedev, T.P. Smereka, Adsorption of sodium on the (112) face of tungsten, Sov. Phys.—Solid State 15 (1973) 1106–1110.

[2612] Yu.I. Malov, M.D. Shebzukhov, Study of the photoemission of binary sodium–rubidium, sodium–cesium, rubidium–potassium, and potassium–cesium alloys, Elektrokhim. 9 (1973) 815–817.

[2613] Yu.I. Malov, M.D. Shebzukhov, V.B. Lazarev, Work functions of binary alloy systems with different kinds of phase diagrams, Surf. Sci. 44 (1974) 21–28.

[2614] Yu.I. Malov, M.D. Shebzukhov, Photoelectric properties of alloys of potassium with mercury and thallium, Elektrokhim. 10 (1974) 95–97.

[2615] J. Monin, G.-A. Boutry, Optical and photoelectric properties of alkali metals, Phys. Rev. B 9 (1974) 1309–1327.

[2616] A.J. Melmed, J.J. Carroll, R. Męclewski, Dependence of work function on coverage for aluminum/tungsten in the field electron microscope, Surf. Sci. 45 (1974) 649–656.

[2617] C.B. Magee, Quart. Rept. No. 7 (DRI-2395), Denver Res. Inst., Univ. Denver, Colorado, 1967 (see Ref. [1785]).

[2618] Z.D. Mireva, K.S. Bobev, Surface diffusion of chromium on tungsten studied with a field emission microscope, Ukr. Fiz. Zh. 20 (1975) 426–430 (Chem. Abstr. 83 (1975) 69948w).

[2619] V.K. Medvedev, A.I. Yakivchuk, Structure and electron–adsorption properties of cesium films on the (111) face of a tungsten single crystal, Sov. Phys.—Solid State 17 (1975) 7–11.

[2620] T. Murotani, K. Fujiwara, M. Nishijima, Photoemission measurements of surface states for cleaved and annealed Ge(111) surfaces, Phys. Rev. B 12 (1975) 2424–2426.

[2621] A.L. Musatov, V.L. Korotkikh, A.D. Korinfskii, Reflection of slow electrons from a gallium arsenide surface with a negative electron affinity, Izv. Akad. Nauk SSSR, Ser. Fiz. 40 (1976) 2523–2527.

[2622] O. Milton, Dr. Dissert., Brown Univ., 1963 (see Ref. [304]).

[2623] G. Margaritondo, J.E. Rowe, S.B. Christman, Surface spectroscopy of Schottky–barrier formation on Si(111) 7×7: Photoemission studies of filled surface states and band bending, Phys. Rev. B 14 (1976) 5396–5403.

[2624] Yu.I. Malov, A.A. Markov, V.A. Korol'kov, Electron work function of alloys of antimony with tin, indium, and zinc, Elektrokhim. 12 (1976) 1740–1742.

[2625] G. Margaritondo, S.B. Christman, J.E. Rowe, Chemisorption and Schottky barrier formation of Ga on Si(111)7×7, J. Vac. Sci. Technol. 13 (1976) 329–332.

[2626] Yu.I. Malov, V.A. Korol'kov, A.A. Markov, Electron work function of alloys of copper–antimony, copper–indium, and copper–cadmium binary systems, Elektrokhim. 13 (1977) 1243–1245.

[2627] N.S. Mirolyubova, I.I. Astakhov, N.A. Shurmovskaya, V.V. Surikov, The work function of electrolytic copper, Elektrokhim. 14 (1978) 306–308.

[2628] Yu.I. Malov, V.A. Korol'kov, A.A. Markov, Electron work functions of binary alloy systems, Electrokhim. 14 (1976) 1616 (VINITI, No. 2047–78, Moscow, June 20, 1978) (see Ref. [1445]).

[2629] R. Mehrotra, J. Mahanty, Free electron contribution to the work function of metals, J. Phys. C 11 (1978) 2061–2064.

[2630] J.E. McLean, J.J. Dillon, C.M. Talbert, UF_6^- Production from Surface Reactions of Uranium and Fluorine, Rept. ORNL/MIT–279, 1978, 18 pp. (Chem. Abstr. 91 (1979) 114182v).

[2631] V.K. Medvedev, I.N. Yakovkin, Adsorption of strontium on (112) face of molybdenum crystal, Sov. Phys.—Solid State 21 (1979) 187–190.

[2632] J. Massies, P. Devoldere, N.T. Linh, Work function measurements on MBE GaAs(001) layers, J. Vac. Sci. Technol. 16 (1979) 1244–1247.

[2633] H. Moormann, D. Kohl, G. Heiland, Work function and band bending on clean cleaved zinc oxide surfaces, Surf. Sci. 80 (1979) 261–264.

[2634] Yu.I. Malov, A.V. Onishchenko, Electron work function of copper alloys with certain rare–earth metals, Elektrokhim. 15 (1979) 732–733.

[2635] V.K. Medvedev, V.N. Pogorelyi, Adsorption of magnesium on the (112) face of a tungsten crystal, Ukr. Fiz. Zh. 25 (1980) 1524–1532.

[2636] K. Mednick, L. Kleinman, Preprint (see Ref. [1001]).

[2637] V.K. Medvedev, I.N. Yakovkin, Adsorption of barium on Mo(112) and Re(10$\bar{1}$0), Sov. Phys.—Solid State 23 (1981) 379–384.

[2638] F. Meier, D. Pescia, T. Schriber, Oxygen–induced magnetism of the nonreconstructed chromium(100) surface, Phys. Rev. Lett. 48 (1982) 645–648.

[2639] J.W. Mintmire, J.R. Sabin, S.B. Trickey, Local–density–functional methods in two–dimensionally periodic systems: Hydrogen and beryllium monolayers, Phys. Rev. B 26 (1982) 1743–1753.

[2640] M.G. Mason, Private comm. (see Ref. [1690]).

[2641] C.Q. Ma, M.V. Ramana, B.R. Cooper, Theory of electronic structure of copper overlayers on transition metal substrates, J. Vac. Sci. Technol. A 1 (1983) 1095–1098.

[2642] T. Mandel, G. Kaindl, K. Horn, M. Iwan, H.U. Middelmann, C. Mariani, Layer–dependent shifts in ionization potential and Auger energies for Kr/Cu(110), Solid State Commun. 46 (1983) 713–716.

[2643] A.J. Melmed, V. Maurice, O. Frank, J.H. Block, Rare–earth crystal growth from the vapor: Eu/Re and Eu/W, J. Physique 45 (1984) C9–47/C9–52.

[2644] W. McLean, H.-L. Chen, The thermionic emission and wok function of U and UO_2, J. Appl. Phys. 58 (1985) 4679–4684.

[2645] T. Maeda, S. Saito, Work function and dipole barrier of sputter–cleaned Fe–Ni alloy surfaces, Japan. J. Appl. Phys. 25 (1986) 1623–1627.

[2646] C.-Q. Ma, M.V. Ramana, B.R. Cooper, Practical implementation and remaining problems for the film linearized muffin–tin orbital calculation of surface electronic structure, Phys. Rev. B 34 (1986) 3854–3867.

[2647] S. Mróz, E. Bauer, The interaction of gold with the surface of a cylindrical tungsten single crystal, Surf. Sci. 169 (1986) 394–404.

[2648] L.F. Magaña, M.A. Ocampo, Extension of the Lang–Kohn work function calculation to the density of metallic hydrogen, Phys. Rev. B 33 (1986) 7294–7296.

[2649] E.E. Mola, J.L. Vicente, Self–consistent theory of water adsorption on metal surfaces, Surf. Sci. 172 (1986) 533–543.

[2650] P.A. Montano, G.W. Fernando, B.R. Cooper, E.R. Moog, H.M. Naik, S.D. Bader, Y.C. Lee, Y.N. Darici, H. Min, J. Marcano, Two magnetically different, closely lying states of fcc iron grown on copper(100), Phys. Rev. Lett. 59 (1987) 1041–1044.

[2651] K. Markert, P. Dolle, J.W. Niemantsverdriet, K. Wandelt, Mechanism of two–dimensional AgAu alloy formation on Ru(001), J. Vac. Sci. Technol. A5 (1987) 2849–2853.

[2652] K. Markert, Characterization of silver and gold films on Ru(001)– and Si(111)–7×7 surfaces (Ph.D. thesis), Freie Univ. Berlin, 1988 (see Ref. [2417]).

[2653] F. Maeda, T. Takahashi, H. Ohsawa, S. Suzuki, Unoccupied–electronic–band structure of graphite studied by angle–resolved secondary–electron emission and inverse photoemission, Phys. Rev. B 37 (1988) 4482–4488.

[2654] J.M. Mundenar, R. Murphy, K.D. Tsuei, E.W. Plummer, An experimental study of hydrogen adsorption on simple metals: Al and Na, Chem. Phys. Lett. 143 (1988) 593–598.

[2655] T.T. Magkoev, G.G. Vladimirov, G.A. Rump, Formation and emissivity of insulator–metal film systems on (011) Mo surfaces, Bull. Acad. Sci. USSR, Phys. Ser. 52 (8) (1988) 17–20.

[2656] M. Mundschau, E. Bauer, W. Święch, Photoemission microscopy and atomic steps on Mo{011}, Surf. Sci. 203 (1988) 412–422.

[2657] M.M. Marino, W.C. Ermler, G.S. Tompa, M. Seidl, Effects of hydrogen and of cesium adsorption on a beryllium surface: A theoretical and experimental study, Surf. Sci. 208 (1989) 189–204.

[2658] W. Maus-Friedrichs, H. Hoermann, V. Kempter, Alkali–metal–affected adsorption of oxygen on W(110), Surf. Sci. 224 (1989) 112–120.

[2659] K.O. Magnusson, B. Reihl, Destabilization of the Si(111) π–bonded chain structure upon Cs adsorption, Phys. Rev. B 39 (1989) 10456–10459.

[2660] K. Markert, P. Pervan, W. Heichler, K. Wandelt, Structural and electronic properties of Ag/Si(111) and Au/Si(111) surfaces, J. Vac. Sci. Technol. A 7 (1989) 2873–2878.

[2661] C. Marliere, Quantum size effect detected by work function measurements during indium deposition on polycrystalline, texturized gold substrate, Vacuum 41 (1990) 1192–1194.

[2662] V.K. Medvedev, T.P. Smereka, I.M. Ubogii, Ya.B. Lozovyi, G.V. Babkin, Structure and electronic adsorption properties of lithium films on tantalum(112) crystal faces, Ukr. Fiz. Zh. 35 (1990) 1848–1853.

[2663] K.O. Magnusson, S. Wiklund, R. Dudde, B. Reihl, Adsorption of Cs on Si(111)7×7: Studies of photoemission from surface states and core levels, Phys. Rev. B 44 (1991) 5657–5663.

[2664] V.K. Medvedev, T.P. Smereka, S.I. Stepanovskiĭ, F.M. Gonchar, R.R. Kamenetskiĭ, Adsorption of terbium and gadolinium on a (100) face of a tungsten crystal, Sov. Phys.—Solid State 33 (1991) 2028–2029.

[2665] N. Memmel, G. Rangelov, E. Bertel, V. Dose, Modification of surface states by alkali–metal adsorption and surface reconstruction: An inverse–photoemission study of Na/Ni(110), Phys. Rev. B 43 (1991) 6938–6945.

[2666] M.M. Marino, W.C. Ermler, *Ab initio* study of the effects of cesium, hydrogen and oxygen adsorption on the work function of beryllium, Chem. Phys. Lett. 176 (1991) 36–40.

[2667] U. Müller, M. Ammann, H. Burtscher, A. Schmidt-Ott, Photoemission from clean and oxygen–covered ultrafine nickel particles, Phys. Rev. B 44 (1991) 8284–8287.

[2668] E.G. Michel, P. Pervan, G.R. Castro, R. Miranda, K. Wandelt, Structural and electronic properties of K/Si(100)2×1, Phys. Rev. B 45 (1992) 11811–11821.

[2669] D.R. Mullins, P.F. Lyman, S.H. Overbury, Interaction of S with W(001), Surf. Sci. 277 (1992) 64–76.

[2670] M. Mazina-Ngokoudi, C. Argile, Adsorption and coadsorption of lead and 1,3–butadiene on platinum(111): An AES, LEED and $\Delta\phi$ study, Surf. Sci. 262 (1992) 307–317.

[2671] V.K. Medvedev, T.P. Smereka, S.I. Stepanovskiĭ, F.M. Gonchar, Terbium and samarium adsorption on the tungsten crystal face (112), Ukr. Fiz. Zh. 37 (1992) 1053–1057 (Chem. Abstr. 117 (1992) 240262q).

[2672] G.G. Magera, P.R. Davis, Interaction of cesium and barium on partially oxygen covered Nb(110), J. Vac. Sci. Technol. A 11 (1993) 2336–2341.

[2673] G.J. Mankey, R.F. Willis, F.J. Himpsel, Band structure of the magnetic fcc pseudomorphs: Ni(100), Co(100), and Fe(100), Phys. Rev. B 48 (1993) 10284–10291.

[2674] M.S. Mousa, Investigations of *in situ* carbon coating on field–emitter arrays, Vacuum 45 (1994) 241–244.

[2675] S.C. Meepagala, M.C. Baykul, Ballistic–electron emission into vacuum from a scanning–tunneling–microscope tip through free–standing gold films, Phys. Rev. B 50 (1994) 13786–13788.

[2676] G.G. Magera, P.R. Davis, The coadsorption of Cs and Ba onto the (110) surface of Mo, AIP Conf. Proc. 301 (1994) 1153–1157 (Chem. Abstr. 123 (1995) 322842s).

[2677] J.A. Martin-Gago, M.C. Asensio, F. Soria, P. Aebi, R. Fasel, D. Naumovic, J. Osterwalder, Direct evidence of occupied states near the Fermi level on the Si(100)2×1–K interface, Surf. Sci. 307–309 (1994) 995–1000.

[2678] S. Mizuno, H. Tochihara, T. Kawamura, Alkali–metal adsorption on dissimilar alkali–metal monolayers preadsorbed on Cu(001): Li on Na and Na on Li, Phys. Rev. B 50 (1994) 17540–17546.

[2679] P.J. Møller, S.A. Komolov, E.F. Lazneva, Influence of atomic Cu–layer epitaxy on CO_2 and CO photoinduced desorption from ZnO(0001), Appl. Surf. Sci. 82/83 (1994) 569–575.

[2680] Y. Morikawa, Further lowering of work function by oxygen adsorption on the K/Si(001) surface, Phys. Rev. B 51 (1995) 14802–14805.

[2681] A.J. Maxwll, Ph.D. Dissertation, Upsala Univ., 1996 (see Ref. [316]).

[2682] W.A. Mackie, J.E. Plumlee, A.E. Bell, Work function measurements of diamond film surfaces, J. Vac. Sci. Technol. B 14 (1996) 2041–2045.

[2683] A.J. Maxwell, P.A. Brühwiler, D. Arvanitis, J. Hasselström, N. Mårtensson, C 1s ionization potential and energy referencing for solid C_{60} films on metal surfaces, Chem. Phys. Lett. 260 (1996) 71–77.

[2684] T. Munakata, T. Sakashita, M. Tsukakoshi, J. Nakamura, Fine structure of the two–photon photoemission from benzene adsorbed on Cu(111), Chem. Phys. Lett. 271 (1997) 377–380.

[2685] M.V. Mamonova, V.V. Prudnikov, Calculation of the electron work function at metal surfaces by a density functional method, Russian Phys. J. 41 (1998) 1174–1179.

[2686] T. Munakata, T. Sakashita, K. Shudo, Two–photon photoemission from benzene adsorbed on Cu(111), J. Elect. Spectrosc. Rel. Phenom. 88–91 (1998) 591–595.

[2687] T. Munakata, K. Shudo, Two–photon photoemission from the adsorption–induced electronic states of benzene/Cu(111), Surf. Sci. 433–435 (1999) 184–187.

[2688] M. Murayama, T. Nakayama, A. Natori, Electronic structures of $\sqrt{3}\times\sqrt{3}$–Au/Si(111) surface, Surf. Sci. 493 (2001) 626–632.

[2689] V. Misra, G.P. Heuss, H. Zhong, Use of metal–oxide–semiconductor capacitors to detect interactions of Hf and Zr gate electrodes with SiO_2 and ZrO_2, Appl. Phys. Lett. 78 (2001) 4166–4168 (see Ref. [3519]).

[2690] P. Ma, A.J. Slavin, Adsorption of antimony on Au(111) at room temperature, J. Vac. Sci. Technol. A 11 (1993) 2003–2007.

[2691] A. Michaelides, P. Hu, M.-H. Lee, A. Alavi, D.A. King, Resolution of an ancient surface science anomaly: Work function change induced by N adsorption on W{100}, Phys. Rev. Lett. 90 (2003) 246103/1–4.

[2692] S. Mróz, B. Stachnik, Very thin silver layer growth on the Cu(111) face at different temperatures, Acta Phys. Pol. A 81 (1992) 233–238.

[2693] G.E. Becker, H.D. Hagstrum, Adsorption of tellurium on Ni(100), J. Vac. Sci. Technol. 12 (1975) 234–236.

[2694] A. Montoya, A. Schlunke, B.S. Haynes, Reaction of hydrogen with Ag(111): Binding states, minimum energy paths, and kinetics, J. Phys. Chem. B 110 (2006) 17145–17154.

[2695] R.R. Mulyukov, Influence of nanocrystalline structure on work function of tungsten, J. Vac. Sci. Technol. B 24 (2006) 1061–1066.

[2696] S.H. Ma, X.T. Zu, H.Y. Xiao, J.L. Nie, Adsorption of S on Ir(100) surface from first–principles calculations, Chem. Phys. Lett. 441 (2007) 53–57.

[2697] A.J. Morris, M. Stankovski, K.T. Delaney, P. Rinke, P. García-González, R.W. Godby, Vertex corrections in localized and extended systems, Phys. Rev. B 76 (2007) 155106/1–9.

[2698] T.T. Magkoev, A.M. Turiev, N.I. Tsidaeva, D.G. Panteleev, G.G. Vladimirov, G.A. Rump, Adsorption of boron on a Mo(110) surface, J. Phys.: Condens. Matter 20 (2008) 485007/1–5.

[2699] M. May, S. Gonzalez, F. Illas, A systematic density functional study of ordered sulfur overlayers on Cu(111) and Ag(111): Influence of the adsorbate coverage, Surf. Sci. 602 (2008) 906–913.

[2700] T.T. Magkoev, G.G. Vladimirov, G.A. Rump, Coadsorption of lanthanum with boron and gadolinium with boron on Mo(110), Surf. Sci. 602 (2008) 1705–1711.

[2701] M. Mrovec, J.-M. Albina, B. Meyer, C. Elsässer, Schottky barriers at transition–metal/SrTi$_3$(001) interfaces, Phys. Rev. B 79 (2009) 245121/1–18.

[2702] F. Mehmood, A. Kara, T.S. Rahman, C.R. Henry, Comparative study of CO adsorption on flat, stepped, and kinked Au surfaces using density functional theory, Phys. Rev. B 79 (2009) 075422/1–6.

[2703] A. Nitzsche, The relation of maximum velocity and work of expulsion of photoelectrons from the fracture planes of zinc single crystals to the orientation of the planes, Ann. Phys. 14 (1932) 463–480.

[2704] J.E. Nyrop, The surface–electrons, Phys. Rev. 39 (1932) 967–976.

[2705] W.B. Nottingham, Thermionic emission from tungsten with weak accelerating fields, Phys. Rev. 47 (1935) 806.

[2706] M.H. Nichols, Thermionic constants of tungsten for various crystallographic directions, Phys. Rev. 55 (1939) 1144 (see Ref. [149]).

[2707] M.H. Nichols, Average thermionic constants for single crystal tungsten wire, Phys. Rev. 59 (1941) 944.

[2708] G. Nadzhakov, V. Vasiley, St. Balabanov, Work function of gold and aluminum during vacuum–air transition, Compt. Rend. Acad. Bulgare Sci. 11 (1958) 461–464 (Chem. Abstr. 53 (1959) 21180c).

[2709] A.G. Naumovets, Desorption of potassium from tungsten in an electric field, Sov. Phys.—Solid State 5 (1964) 1668–1674.

[2710] R.L. Nemchenko, A.R. Shul'man, V.S. Grishin, Adsorption of barium on a polycrystalline gold substrate, Sov. Phys.—Solid State 5 (1964) 2602–2604.

[2711] A.G. Naumovets, The growth in an electrical field of lithium crystals from a film deposited on tungsten, Sov. Phys.—Solid State 6 (1965) 1647–1650.

[2712] H. Neumann, Adsorption of silicon on tungsten, Ann. Phys. 18 (1966) 145–158.

[2713] H. Neumann, Field emission by thin semiconductive layers on metals, Ann. Phys. 19 (1967) 270–285.

[2714] J. Nikliborc, Z. Dworecki, Work function of xenon on individual crystal faces of tungsten, Acta. Phys. Pol. 32 (1967) 1023–1024.

[2715] H. Neumann, Aluminum adsorption on tungsten in the field electron microscope, Ann. Phys. 21 (1968) 414–416.

[2716] R.L. Nemchenko, S.E. Strakovskaya, A.I. Titenskii, Energy distribution of photoelectrons of gadolinium and terbium, Sov. Phys.—Solid State 11 (1970) 2181–2182.

[2717] P.O. Nilsson, C. Norris, L. Walldén, Evidence for direct transitions from the d–band of gold, Solid State Commun. 7 (1969) 1705–1707.

[2718] C. Norris, L. Walldén, Photoemission from Pb, J. Phys. F 2 (1972) 180–188.

[2719] B.E. Nieuwenhuys, O.G. van Aardenne, W.M.H. Sachtler, Photoelectric determination of the changes in work function of nickel, rhodium and platinum films by nitrogen adsorption, Thin Solid Films 17 (1973) S7–S11.

[2720] P. Nielsen, Photoemission studies of sulfur, Phys. Rev. B 10 (1974) 1673–1682.

[2721] R. Nathan, B.J. Hopkins, An AC retarding potential technique for the continuous measurement of changes in work function, J. Phys. E 7 (1974) 851–854.

[2722] B.E. Nieuwenhuys, O.G. van Aardenne, W.M.H. Sachtler, Adsorption of xenon on group VIII and IB metals studied by photoelectric work function measurements, Chem. Phys. 5 (1974) 418–428.

[2723] B.E. Nieuwenhuys, Comments on "Anisotropy of the work function change in physical adsorption" by J. Müller, Surf. Sci. 49 (1975) 363–365.

[2724] P.R. Norton, An investigation of the adsorption of oxygen and oxygen containing species on platinum by photoelectron spectroscopy, Surf. Sci. 47 (1975) 98–114.

[2725] O. Nishikawa, A.R. Saadat, Field emission and field ion microscopy study of Ga, In and Sn on W: Structure, work function, diffusion and binding energy, Surf. Sci. 60 (1976) 301–324.

[2726] C. Norris, J.T.M. Wotherspoon, The optical density of states of liquid gallium, J. Phys. F 7 (1977) 1599–1606.

[2727] O. Nishikawa, A.R. Saadat, Field ion image qualities of Ga, In and Sn on W and work functions, Surf. Sci. 70 (1978) 292–301.

[2728] B.E. Nieuwenhuys, Applications of thin films to adsorption and catalysis, Thin Solid Films 50 (1978) 257–267.

[2729] M. Nilges, J.H. Freed, Photoelectric determination of work function via CREMSEE enhancement: Photo–CREMSEE (cyclotron resonance from microwave induced secondary electron emission), Chem. Phys. Lett. 85 (1982) 499–504.

[2730] S. Nakanishi, T. Horiguchi, The adsorption study of tellurium on iron(001) surface by means of LEED, AES and $\Delta\phi$, Surf. Sci. 125 (1983) 635–652.

[2731] J.E. Northrup, Surface states and dipoles on Si(111)1×1: Na, J. Vac. Sci. Technol. A 4 (1986) 1404–1406.

[2732] S. Nishigaki, T. Komatsu, M. Arimoto, M. Sugihara, Initial stage of Pd adsorption on Si(111)7 ×7 surface studied by AES and EELS, Surf. Sci. 167 (1986) 27–38.

[2733] T.A. Nguyen Tan, M. Azizan, J. Derrien, Interfacial reaction between Ta ultrathin films and Si(111) substrate, Surf. Sci. 189/190 (1987) 339–345.

[2734] R.M. Nix, R.M. Lambert, Surface crystallography and growth modes of rare earth metals and alloys on single crystal copper: Nd on Cu(100), Surf. Sci. 186 (1987) 163–183.

[2735] R.M. Nix, R.W. Judd, R.M. Lambert, Structure and properties of rare earth overlayers and ultra–thin alloy films on single crystal copper: Nd on Cu(111), Surf. Sci. 203 (1988) 307–322.

[2736] S. Nishigaki, M. Ohara, A. Murakami, S. Fukui, S. Matsuda, Adlayer formation and its local charge states of Li on Si(111)7×7 surface studied by $\Delta\phi$, MDS and AES, Appl. Surf. Sci. 35 (1988–1989) 121–136.

[2737] B.A. Nesterenko, Si(110) + Ni system: Structural, vibrational and electronic properties, Appl. Surf. Sci. 33/34 (1988) 21–30.

[2738] A.G. Naumovets, V.V. Poplavsky, Yu.S. Vedula, Diffusion and phase transitions in barium monolayers on the (011) plane of tungsten, Surf. Sci. 200 (1988) 321–334.

[2739] R.M. Nix, R.W. Judd, R.M. Lambert, Oxidation of neodymium overlayers and Nd/Cu alloy thin films on Cu(100): Properties of the NdO$_x$–Cu(100) interface, Surf. Sci. 205 (1988) 59–81.

[2740] H.B. Nielsen, U. Burghaus, G. Broström, E. Matthias, Electronic structure of K on Ag(100), Vacuum 41 (1990) 558–560.

[2741] S. Nishigaki, S. Matsuda, T. Sasaki, N. Kawanishi, H. Takeda, A. Kawase, Potassium and oxygen adsorption on Si(100): Local charge states probed with helium metastables, Vacuum 41 (1990) 632–634.

[2742] K. Nakamae, H. Fujioka, K. Ura, Measurement of surface vacuum potential from the energy spectrum on the secondary electron in the scanning electron microscope, Japan. J. Appl. Phys. 30 (1991) 875–881.

[2743] K. Nishimori, K. Tanaka, Y. Inoue, Characterization of lubricated systems on carbon coated media by low energy photoelectron spectroscopy method in ambient atmosphere, J. Appl. Phys. 69 (1991) 8042–8046.

[2744] C.L. Nicklin, C. Binns, C. Norris, P. McCluskey, M.-G. Barthés-Labrousse, Structural study of Tm on Mo(110), Surf. Sci. 269/270 (1992) 700–706.

[2745] M. Nekovee, S. Crampin, J.E. Ingelsfield, Magnetic splitting of image states at Fe(110), Phys. Rev. Lett. 70 (1993) 3099–3102.

[2746] A. Neumann, S.L.M. Schroeder, K. Christmann, Adsorption of sodium and potassium on a gold(100) surface: An example of alkali–metal–induced deconstruction, Phys. Rev. B 51 (1995) 17007–17022.

[2747] M. Nohlen, M. Schmidt, K. Wandelt, On the influence of adsorbates on heteroepitaxy: Work function oscillations during deposition of copper on platinum(111), Surf. Sci. 331–333 (1995) 902–907.

[2748] T. Nagao, Y. Iizuka, M. Umeuchi, T. Shimazaki, C. Oshima, Vibrations of alkali metal atoms chemisorbed on the Al(111) surface, Surf. Sci. 329 (1995) 269–275.

[2749] M.K. Naparty, J. Skonieczny, The study of epitaxial growth of thin Cu and Ag layers on Ag(110) and Cu(110) using total current spectroscopy, AES and work function measurement, Vacuum 46 (1995) 189–194.

[2750] M.V. Nikolić, S.M. Radić, V. Minić, M.M. Ristić, The dependence of the work function of rare earth metals on their electron structure, Microelectron. J. 27 (1996) 93–96.

[2751] C. Nützenadel, O.M. Küttel, O. Gröning, L. Slapbach, Electron field emission from diamond tips prepared by ion sputtering, Appl. Phys. Lett. 69 (1996) 2662–2664.

[2752] S. Nagashima, T. Tsunekawa, N. Shiroguchi, H. Zenba, M. Uda, Double cylindrical open counter of pocket size, Nucl. Instrum. Methods A 373 (1996) 148–152.

[2753] B. Naydenov, L. Surnev, Sodium adsorption on a Ge(100)–(2×1) surface, Surf. Sci. 370 (1997) 155–165.

[2754] T.-U. Nahm, R. Gomer, The conversion of Fe on W(110) from the low temperature to the high temperature form, Surf. Sci. 380 (1997) 52–60.

[2755] T.-U. Nahm, R. Gomer, The adsorption of Fe on W(110) and of O and H on Fe–covered W(110), Surf. Sci. 373 (1997) 237–256.

[2756] H. Nakane, S. Satoh, H. Adachi, Reduction of the work function on Mo(100) surface covered with ZrO_2, in: Tech. Dig. 17th Int. Vac. Nanoelectn. Conf. Cambridge, MA, 2004, pp. 136–137 (Chem. Abstr. 143 (2005) 17711b).

[2757] H. Nakane, S. Satoh, H. Adachi, Reduction of the work function on Mo(100) surface covered with ZrO_2, J. Vac. Sci. Technol. B 23 (2005) 769–771.

[2758] J.L. Nie, H.Y. Xiao, X.T. Zu, F. Gao, Atomic and electronic structures of the Rb–C(100) chemisorption system, Physica B 383 (2006) 219–225.

[2759] J.L. Nie, H.Y. Xiao, X.T. Zu, F. Gao, First principles calculations on Na and K–adsorbed diamond(100) surface, Chem. Phys. 326 (2006) 308–314.

[2760] C. Ouellet, E.K. Rideal, An investigation of adsorbed films by means of a photoelectric counter, J. Chem. Phys. 3 (1935) 150–158.

[2761] C.W. Oatley, The measurement of contact potential difference, Proc. Roy. Soc. A 155 (1936) 218–234.

[2762] C.W. Oatley, The adsorption of oxygen and hydrogen on platinum and the removal of these gasses by positive ion bombardment, Proc. Phys. Soc. 51 (1939) 318–328.

[2763] H. Ober, Diss. Hannover, 1959 (see Ref. [3052]).

[2764] R.M. Oman, Work function and adsorption properties of niobium and photoelectric and adsorption properties of gallium antimonide (Ph.D. thesis), Brown Univ., 1963, 85 pp. (Diss. Abstr. B 24 (1964) 3808).

[2765] R.M. Oman, Work function of lead sulfide, J. Appl. Phys. 36 (1965) 2091–2092.

[2766] A.P. Ovchinnikov, Adsorption and electron emission of potassium film on faces of a tungsten single crystal, Sov. Phys.—Solid State 9 (1967) 483–487.

[2767] E.V. Osipova, N.A. Shurmovskaya, R.Kh. Burshtein, Comparison of the differences in work functions and zero charge potentials of metals. IV. Gallium, Elektrokhim. 5 (1969) 1139–1141.

[2768] A.P. Ovchinnikov, B.M. Tsarev, Adsorption and electronic emission of double films of barium and cesium fluoride on tungsten, Radio Eng. Electron. Phys. 15 (1970) 753–755.

[2769] C. Oshima, S. Horiuchi, S. Kawai, Thin film cathodes of lanthanum hexaboride (LaB_6), Jpn. J. Appl. Phys. Suppl. 21 (Pt. 1) (1974) 281–284.

[2770] P. Oelhafen, Photoemission studies on liquid metals, (Ph.D. thesis), ETH Zürich, 1976 (Chem. Abstr. 89 (1978) 172445c), and also Private comm. (see Ref. [1312]).

[2771] P. Oelhafen, E. Gisler, F. Greuter, U. Gubler, H.P. Preiswerk, Private comm. (see Refs. [1312,2770]).

[2772] K. Okuno, T. Sasaki, H. Kim, T. Inoue, E. Sugata, Coadsorption of lanthanum and boron on tungsten, Japan. J. Appl. Phys. 17 (1978) 710–719.

[2773] E.G. Overbosch, B. Rasser, A.D. Tenner, J. Los, The ionization of hyperthermal sodium atoms on W(110) as a function of temperature, Surf. Sci. 92 (1980) 310–324.

[2774] E.G. Overbosch, J. Los, Positive surface ionization of hyperthermal sodium atoms on metal surfaces, Surf. Sci. 108 (1981) 99–116.

[2775] E.G. Overbosch, J. Los, Formation of negative sodium ions by hyperthermal beam scattering from surfaces, Surf. Sci. 108 (1981) 117–123.

[2776] K. Oura, T. Taminaga, T. Hanawa, Electronic properties and atomic arrangement of the Ag/Si(111) interface, Solid State Commun. 37 (1981) 523–526.

[2777] S. Ohnishi, A.J. Freeman, M. Weinert, Self–consistent FLAPW determination of surface magnetism: Fe(001), J. Magn. Magn. Mater. 31–34 (1983) 889–890.

[2778] R. Opila, R. Gomer, Photoemission of Xe and Kr adsorbed on the W(110) plane, Surf. Sci. 127 (1983) 569–597.

[2779] K. Okuno, H. Kim, A study of Pd adlayer on W surface, Oyo Butsuri 53 (1984) 1095–1102 (Chem. Abstr. 102 (1985) 33193t).

[2780] K. Okuno, H. Kim, Coadsorption of palladium and hydrogen on tungsten surface, Nagasaki Sogo Kagaku Daigaku Kiyo 21 (1980) 145–148 (Chem. Abstr. 96 (1982) 58293w).

[2781] E.M. Oelling, R. Miranda, New experimental studies on the adsorption of K on Si(100) and Si(111), Surf. Sci. 177 (1986) L947–L955.

[2782] N. Okuyama, M. Yamazaki, K. Tomita, H. Yasunaga, Electronic properties of Cs–covered surfaces of graphite(0001), Japan. J. Appl. Phys. 25 (1986) 178–182.

[2783] E.M. Oelling, R. Miranda, On the geometric and electronic structure of K on Si(100)2×1, J. Vac. Sci. Technol. A 5 (1987) 653–654.

[2784] H. Ohsawa, T. Takahashi, T. Kinoshita, Y. Enta, H. Ishii, T. Sagawa, Unoccupied electronic band structure of graphite studied by angle–resolved inverse photoemission, Solid State Commun. 61 (1987) 347–350.

[2785] E.M. Oelling, E.G. Michel, M.C. Asensio, R. Miranda, J.C. Durán, A. Muñoz, F. Flores, K/Si(100)2×1: A case study for the transfer of charge between alkali metals and semiconductor surfaces, Europhys. Lett. 5 (1988) 727–732.

[2786] A. Ortykov, R.R. Rakhimov, Ion–electron emission from cesium films on the (110) and (111) faces of molybdenum crystals, Radiotekh. Elektron. 33 (1988) 363–370.

[2787] H. Onishi, T. Aruga, C. Egawa, Y. Iwasawa, Modification of surface electronic structure on TiO_2(110) and TiO_2(441) by Na deposition, Surf. Sci. 199 (1988) 54–66.

[2788] H. Onishi, T. Aruga, C. Egawa, Y. Iwasawa, Photoelectron spectroscopic study of clean and CO adsorbed Ni/TiO_2(110) interfaces, Surf. Sci. 233 (1990) 261–268.

[2789] Y. Okabe, M. Sasao, H. Yamaoka, M. Wada, J. Fujita, Dependence of $Au^−$ production upon the target work function in a plasma–sputter type negative ion source, Japan. J. Appl. Phys. 30 (1991) 1307–1312.

[2790] M. Okada, H. Tochihara, Y. Murata, Temperature dependence of potassium adsorption on Au(001), Surf. Sci. 245 (1991) 380–388.

[2791] A.A. Ostroukhov, V.N. Tomilenko, Self consistent electronic structure of the (100) and (110) surfaces of tantalum in the non–MT approximation, Metallofiz. 13 (3) (1991) 70–75.

[2792] M. Okada, H. Iwai, R. Klauser, Y. Murata, Potassium–induced restructuring of the Au(001) surface, J. Phys.: Condens. Matter 4 (1992) L593–L600.

[2793] J.E. Ortega, R. Miranda, Growth of K, Rb and Cs on GaAs(110), Appl. Surf. Sci. 56–58 (1992) 211–217.

[2794] T.R. Ohno, G.H. Kroll, J.H. Weaver, L.P.F. Chibante, R.E. Smalley, C_{60} matrix–isolated in Xe: Plasmon shifts and polarization effects, Surf. Sci. 294 (1993) L964–L968.

[2795] T. Okuda, H. Shigeoka, H. Daimon, S. Suga, T. Kinoshita, A. Kakizaki, Surface and bulk core level shifts of the Si(111)3×1–Na and Si(111)δ7×7–Na surfaces, Surf. Sci. 321 (1994) 105–110.

[2796] K. Ozawa, T. Anazawa, S. Tokumitsu, R. Sekine, E. Miyazaki, K. Edamoto, S. Tanaka, S. Otani, Adsorption of K on NbC(100): Photoemission and thermal desorption study, Surf. Sci. 336 (1995) 93–100.

[2797] K. Ozawa, S. Tokumitsu, R. Sekine, E. Miyazaki, K. Edamoto, H. Kato, S. Otani, Potassium adsorption on the polar NbC(111) surface: Core–level photoemission study, Surf. Sci. 357–358 (1996) 350–354.

[2798] K. Ozawa, T. Iwasaki, K. Edamoto, S. Tanaka, S. Otani, Na adsorption process on a ZrC(100) surface, Appl. Surf. Sci. 121–122 (1997) 142–145.

[2799] K. Ozawa, S. Ishikawa, K. Edamoto, H. Kato, S. Otani, Na adsorption on the polar NbC(111) surface, Surf. Sci. 419 (1999) 226–235.

[2800] K. Ozawa, T. Noda, T. Nakane, K. Edamoto, S. Tanaka, Interaction of oxygen with potassium covered ZrC(111) surface: Photoemission spectroscopy study, Surf. Sci. 438 (1999) 223–230.

[2801] L. Österlund, D.V. Chakarov, B. Kasemo, Potassium adsorption on graphite(0001), Surf. Sci. 420 (1999) 174–189.

[2802] A.N. Obraztsov, A.P. Volkov, K.S. Nagovitsyn, K. Nishimura, K. Morisawa, Y. Nakano, A. Hiraki, CVD growth and field emission properties of nanostructured carbon films, J. Phys. D 35 (2002) 357–362.

[2803] T. Ohwaki, H. Ishida, A. Liebsch, First–principles calculation of field emission from metal surfaces, Phys. Rev. B 68 (2003) 155422/1–4.

[2804] T. Ohwaki, D. Wortmann, H. Ishida, S. Brügel, K. Terakura, Spin–polarized field emission from Ni(001) and Ni(111) surfaces, Phys. Rev. B 73 (2006) 235424/1–4.

[2805] T. Ossowski, A. Kiejna, Density functional study of surface properties of chromium, Surf. Sci. 602 (2008) 517–524.

[2806] R. Pohl, P. Pringsheim, The selective photoelectric effect of non–alkali metals, Ber. Phys. Ges. 13 (1911) 474–481.

[2807] T.J. Parmley, Photo–electric threshold of single bismuth crystals, Phys. Rev. 30 (1927) 656–663.

[2808] E. Patal, A method for the determination of contact potentials, Z. Phys. 59 (1930) 697–699.

[2809] R.L. Park, H.E. Farnsworth, Interaction of oxygen with (110) nickel, J. Appl. Phys. 35 (1964) 2220–2226.

[2810] D. Parker, Ph.D. Thesis, Univ. of Southampton, 1966 (see Ref. [13]).

[2811] N.B. Smirnova, G.N. Shuppe, O.L. Babushkin, Work function for the (111) and (110) faces of W alloyed with 1 % Os, Sov. Phys. J. 14 (1971) 1724–1725.

[2812] P.W. Palmberg, Secondary emission studies on Ge and Na–covered Ge, J. Appl. Phys. 38 (1967) 2137–2147.

[2813] P.W. Palmberg, W.T. Peria, Low energy electron diffraction studies on Ge and Na–covered Ge, Surf. Sci. 6 (1967) 57–97.

[2814] P.S. Popov, A.N. Makhotenko, Photoelectric emission of indium, Sov. Phys. J. 11 (1968) 99–100.

[2815] R. Perrin, Photoelectric properties of pure rubidium prepared and stored in ultravacua, C. R. Acad. Sci. Paris, B 267 (1968) 58–60.

[2816] B.M. Palyukh, L.L. Sivers, The effect of a field on the equilibrium concentration of yttrium atoms adsorbed on a tungsten point, Sov. Phys.—Solid State 10 (1969) 2962–2964.

[2817] B.M. Palyukh, L.L. Sivers, Adsorption, migration, and evaporation of yttrium on a tungsten single crystal, Sov. Phys.—Solid State 10 (1969) 1585–1588.

[2818] I.A. Podchernyaeva, G.V. Samsonov, V.S. Fomenko, Differences in emission parameters and adsorption properties of single–crystal faces, Sov. Phys. J. 12 (1969) 721–725.

[2819] B.M. Palyukh, L.L. Sivers, Desorption of yttrium from tungsten in a strong electric field, Sov. Phys.—Solid State 11 (1969) 814–816.

[2820] J. Psarouthakis, Work function variation of tungsten in barium plus cesium and strontium plus cesium vapor environments, Surf. Sci. 17 (1969) 316–332.

[2821] R.L. Park, Private comm. (see Ref. [2604]).

[2822] C.W. Peterson, J.H. Dinan, T.E. Fischer, Photoemission from amorphous silicon, Phys. Rev. Lett. 25 (1970) 861–864.

[2823] E.W. Plummer, R.D. Young, Field–emission studies of electronic energy levels of adsorbed atoms, Phys. Rev. B 1 (1970) 2088–2109.

[2824] J. Psarouthakis, J.D. Long, R.D. Huntington, Thermionic work function of Ru emitters, Bull. Am. Phys. Soc. 11 (1966) 636.

[2825] J.H. Pollard, A correlation of Auger emission spectroscopy, LEED and work function measurements for the epitaxial growth of thorium on a W(100) substrate, Surf. Sci. 20 (1970) 269–284.

[2826] B.M. Palyukh, T.P. Smereka, Study of cesium adsorption on a tungsten single crystal in a field emission microscope, Sov. Phys.—Solid State 13 (1971) 640–643.

[2827] B.M. Palyukh, A.I. Yakivchuk, Field–emission microscopy of some alloys in the lanthanum tungsten system, Sov. Phys.—Solid State 13 (1971) 149–152.

[2828] E.W. Plummer, A.E. Bell, Field emission energy distributions of hydrogen and deuterium on the (100) and (110) planes of tungsten, J. Vac. Sci. Technol. 9 (1972) 583–590.

[2829] C.A. Papageorgopoulos, J.M. Chen, LEED and work function study of Cs and O adsorption on W(112), J. Vac. Sci. Technol. 9 (1972) 570–574.

[2830] C.A. Papageorgopoulos, J.M. Chen, Cesium enhanced oxidation of Ni(100), Solid State Commun. 13 (1973) 1455–1457.

[2831] J. Polański, Z. Sidorski, Adsorption of copper on tungsten: Measurements on single crystal planes, Surf. Sci. 40 (1973) 282–294.

[2832] R.S. Polizzotti, Structure–sensitive chemisorption: Hydrogen and nitrogen on single crystal planes of tungsten and rhodium (Ph.D. thesis), Univ. of Illinois at Urbana–Champaign, 1974, 180 pp. (Diss. Abstr. B 35 (1974) 3351–3352) (see Ref. [853]).

[2833] J.O. Porteus, Sodium adsorption on aluminum (100) and (111) surfaces: ELEED, Auger, and contact potential measurements, Surf. Sci. 41 (1974) 515–532.

[2834] E.W. Plummer, B.J. Waclawski, T.V. Vorburger, Photoelectron spectra of the decomposition of ethylene on (110) tungsten, Chem. Phys. Lett. 28 (1974) 510–515.

[2835] M.M. Pant, M.P. Das, Work functions of alkali metals, J. Phys. F 5 (1975) 1301–1306.

[2836] V.A. Panteleev, V.V. Chernyakhovskii, S.N. Ershov, E.F. Volkov, Effect of ion bombardment on the silicon work function, Sov. Phys.—Solid State 17 (1975) 1006–1007.

[2837] J. Polański, Z. Sidorski, S. Zuber, Adsorption of beryllium on tungsten: Measurements on single–crystal planes, Acta Phys. Pol. A 49 (1976) 299–305.

[2838] R.A. Powell, W.E. Spicer, Photoemission study of oxygen chemisorption on tin, Surf. Sci. 55 (1976) 681–689.

[2839] R. Pantel, M. Bujor, J. Bardolle, Continuous measurement of surface potential variations during oxygen adsorption on the (100), (110) and (111) faces of niobium using mirror electron microscope, Surf. Sci. 62 (1977) 589–609.

[2840] P.G. Pallmer Jr., The electron work function of rhenium with dissolved carbon and graphitic surface layers (Ph.D. thesis), Washington State Univ., 1978, 128 pp. (Diss. Abstr. B 39 (1979) 3904) (Chem. Abstr. 90 (1979) 144796v).

[2841] L. Peralta, Y. Berthier, J. Oudar, Correlation between adsorption layer structure and work function of copper, Vide (Numero Spec.) (1978) 83–102 (Chem. Abstr. 90 (1979) 210517h).

[2842] C.A. Papageorgopoulos, The influence of coadsorbed oxygen on the work function of Cs on Cu(100), Solid State Commun. 27 (1978) 1069–1072.

[2843] C.A. Papageorgopoulos, Adsorption of Cs and O on MoS$_2$, Surf. Sci. 75 (1978) 17–28.

[2844] J.P. Perdew, R. Monnier, Physics of lattice relaxation at aluminum surfaces, J. Phys. F 10 (1980) L287–L291.

[2845] B.V. Paranjape, G.C. Aers, A note on the electron density profile at the surface of metals, Surf. Sci. 105 (1981) L245–L248.

[2846] J.P. Perdew, A. Zunger, Self–interaction correction to density–functional approximations for many–electron systems, Phys. Rev. B 23 (1981) 5048–5079 (see Refs. [351,1201]).

[2847] S. Prigge, H. Roux, E. Bauer, Pd layers on a W(100) surface, Surf. Sci. 107 (1981) 101–112.

[2848] A.W. Potts, P.J. Brigden, D.S. Law, E.P.F. Lee, Photoelectron spectroscopy of solids using gas–phase spectrometers, J. Electr. Spectros. Rel. Phenom. 24 (1981) 267–281.

[2849] G.D. Pettit, Private comm. (see Ref. [1904]).

[2850] C.A. Papageorgopoulos, Studies of separate adsorption and coadsorption of Cs and O$_2$ on Cu(100), Phys. Rev. B 25 (1982) 3740–3749.

[2851] J.P. Perdew, Physics of lattice relaxation at surfaces of simple metals, Phys. Rev. B 25 (1982) 6291–6299.

[2852] Ch. Park, H.M. Kramer, E. Bauer, The adsorption of selenium on a W(100) surface, Surf. Sci. 115 (1982) 1–14.

[2853] C. Park, H.M. Kramer, E. Bauer, Distinct binding states in adsorption on a homogeneous surface: Te on W(100), Surf. Sci. 116 (1982) 456–466.

[2854] C. Park, H.M. Kramer, E. Bauer, The chemisorption of sulphur on W(100), Surf. Sci. 116 (1982) 467–487.

[2855] Ch. Park, E. Bauer, H.M. Kramer, Multiple commensurate–incommensurate transitions in adsorbed layers: Te on W(110), Surf. Sci. 119 (1982) 251–265.

[2856] G. Popov, E. Bauer, The adsorption of sulfur on the tungsten(110) surface, Surf. Sci. 122 (1982) 433–446.

[2857] D. Prigge, W. Schlenk, E. Bauer, The adsorption of CO and O$_2$ on ultrathin Pd layers, Surf. Sci. 123 (1982) L698–L702.

[2858] J. Polański, Z. Sidorski, S. Zuber, Adsorption of gold on (110), (100) and (211) tungsten planes: Work function changes and loss spectra of backscattered electrons, Acta Phys. Pol. A 64 (1983) 377–392.

[2859] H.C. Peebles, J.M. White, Unpublished (see Refs. [1017,1909]).

[2860] W.J. Plieth, The work function of small metal particles and its relation to electrochemical properties, Surf. Sci. 156 (1985) 530–535.

[2861] Ch. Park, E. Bauer, H. Poppa, Growth and alloying of Pd films on Mo(110) surfaces, Surf. Sci. 154 (1985) 371–393.

[2862] M.T. Paffett, C.T. Campbell, T.N. Taylor, S. Srinivasan, Cu adsorption on Pt(111) and its effects on chmisorption: A comparison with electrochemistry, Surf. Sci. 154 (1985) 284–302.

[2863] G. Pirug, A. Winkler, H.P. Bonzel, Multilayer growth of potassium on a Pt(111) surface, Surf. Sci. 163 (1985) 153–171.

[2864] A. Pavlovska, M. Paunov, E. Bauer, The initial growth of gold on a clean Mo(100) surface, Thin Solid Films 126 (1985) 129–141.

[2865] C. Pirri, J.C. Peruchetti, G. Gewinner, J. Derrien, Early stages of epitaxial $CoSi_2$ formation on Si(111) surface as investigated by ARUPS, XPS, LEED and work function variation, Surf. Sci. 152/153 (1985) 1106–1112.

[2866] S.D. Parker, Lithium adsorption on Ag(111): Characterization by AES and work function changes, Surf. Sci. 157 (1985) 261–272.

[2867] S.D. Parker, P.J. Dobson, Monitoring alkali metal adsorption by secondary electron emission current measurements, Surf. Sci. 171 (1986) 267–278.

[2868] M.T. Paffett, C.T. Campbell, T.N. Taylor, Adsorption and growth modes of Bi on Pt(111), J. Chem. Phys. 85 (1986) 6176–6185.

[2869] M.T. Paffett, C.T. Campbell, T.N. Taylor, Surface chemical properties of silver/platinum(111): Comparisons between electrochemistry and surface science, Langmuir 1 (1985) 741–747.

[2870] J.C. Peruchetti, C. Pirri, D. Bolmont, G. Gewinner, Evidence for two oxygen chemisorption sites on the Cr(100) surface at room temperature, Solid State Commun. 59 (1986) 517–519.

[2871] A. Pavlovska, E. Bauer, Thin film formation on chemically modified surfaces: Au on Mo(110), Surf. Sci. 175 (1986) 369–384.

[2872] C. Pirri, J.C. Peruchetti, D. Bolmont, G. Gewinner, Surface structure of epitaxial $CoSi_2$ crystals grown on Si(111), Phys. Rev. B 33 (1986) 4108–4113.

[2873] S.D. Parker, G.E. Rhead, Oxidation of lithium monolayers on silver(111): A study by AES, work function and secondary emission changes, Surf. Sci. 167 (1986) 271–284.

[2874] X.-h. Pan, M.W. Ruckman, M. Strongin, Electronic structure and chemical properties of Pt overlayers on Nb(110), Phys. Rev. B 35 (1987) 3734–3739.

[2875] J. Paul, Alkali overlayers on aluminum, alumina, and aluminum carbide, J. Vac. Sci. Technol. A 5 (1987) 664–670.

[2876] C. Park, E. Bauer, H. Poppa, A re–examination of the Cu/Ru(0001) system, Surf. Sci. 187 (1987) 86–97.

[2877] C.H. Patterson, R.M. Lambert, Structure and properties of the palladium/sulphur interface: S_2 chemisorption on Pd(111), Surf. Sci. 187 (1987) 339–358.

[2878] D. Pescia, M. Stampanoni, G.L. Bona, A. Vaterlaus, R.F. Willis, F. Meier, Magnetism of epitaxial fcc iron films on Cu(001) investigated by spin–polarized photoelectron emission, Phys. Rev. Lett. 58 (1987) 2126–2129.

[2879] D. Pescia, G. Zampieri, M. Stampanoni, G.L. Bona, R.F. Willis, F. Meier, Ferromagnetism of thin epitaxial fcc cobalt films on Cu(001) observed by spin–polarized photoemission, Phys. Rev. Lett. 58 (1987) 933–936.

[2880] C. Park, Growth of Ag, Au and Pd on Ru(0001) and CO chemisorption, Surf. Sci. 203 (1988) 395–441.

[2881] C.A. Papageorgopoulos, Adsorption of Cs on H–precovered W(110) surfaces, Phys. Rev. B 40 (1989) 1546–1554.

[2882] P. Pervan, E. Michel, G.R. Castro, R. Miranda, K. Wandelt, Properties of potassium adsorbed on Si(100)2 ×1, J. Vac. Sci. Technol. A 7 (1989) 1885–1888.

[2883] C.A. Papageorgopoulos, M. Kamaratos, Adsorption of Cs and its effects on the oxidation of Ar^+ sputtered Si(100)2×1 substrate, Surf. Sci. 221 (1989) 263–276.

[2884] W.E. Pickett, S.C. Erwin, Electronic structure of an ideal diamond–nickel (001) interface, Phys. Rev. B 41 (1990) 9756–9765.

[2885] C.A. Papageorgopoulos, M. Kamaratos, Adsorption of K on clean and hydrogenated Si(100)2 ×1, Vacuum 41 (1990) 567–570.

[2886] G. Pirug, C. Ritke, H.P. Bonzel, Adsorption of H_2O on Ru(001): II. Effect of H_2O on Ru(001), Surf. Sci. 257 (1991) 50–62.

[2887] V.V. Pogosov, On some tenzoemission effects of the small metal particles, Solid State Commun. 81 (1992) 129–133.

[2888] G. Polanski, J.P. Toennies, The growth mode of aluminium on silver(111), Surf. Sci. 260 (1992) 250–256.

[2889] C.A. Papageorgopoulos, M. Kamaratos, Adsorption of elemental S on Ni(100) surfaces, Surf. Sci. 338 (1995) 77–82.

[2890] A. Papageorgopoulos, M. Kamaratos, Adsorption of elemental S on Si(100)–2×1 surfaces, Surf. Sci. 352–354 (1996) 364–368.

[2891] A. Papageorgopoulos, A. Corner, M. Kamaratos, C.A. Papageorgopoulos, Adsorption of elemental S on Si(100)2×1: Surface restoration, Phys. Rev. B 55 (1997) 4435–4441.

[2892] A. Papageorgopoulos, Deposition of sulfur on Si(100) 2×1: Surface restoration, Solid State Commun. 101 (1997) 383–387.

[2893] P. Pervan, K. Markert, K. Wandelt, Photoemission of Xe adsorbed on Si(111)7×7, Ag/Si(111), Au/Si(111) and O/Si(111) surfaces, Appl. Surf. Sci. 108 (1997) 307–317.

[2894] J.J. Paggel, G. Neuhold, H. Haak, K. Horn, Growth morphology and electronic structure of Na films on Si(111)–(7×7) and Si(111)–Na(3×1), Surf. Sci. 414 (1998) 221–235.

[2895] C.A. Papageorgopoulos, M. Kamaratos, A.C. Papageorgopoulos, Coadsorption of cesium and elemental sulfur on Ni(100) surfaces, Surf. Sci. 433–435 (1999) 806–810.

[2896] A.C. Papageorgopoulos, M. Kamaratos, Adsorption and desorption of Se on Si(100)2×1: Surface restoration, Surf. Sci. 466 (2000) 173–182.

[2897] R. Pentcheva, M. Scheffler, Stable and metastable structures of Co on Cu(001): An *ab initio* study, Phys. Rev. B 61 (2000) 2211–2220.

[2898] H. Petek, M.J. Weida, H. Nagano, S. Ogawa, Electronic relaxation of alkali metal atoms on the Cu(111) surface, Surf. Sci. 451 (2000) 22–30.

[2899] I. Polishchuk, P. Ranade, T.-J. King, C. Hu, Dual work function metal gate CMOS technology using metal interdiffusion, IEEE Electr. Dev. Lett. 22 (2001) 444–446.

[2900] O.A. Panchenko, S.V. Sologub, B.V. Stetsenko, A.I. Shchurenko, Electronic states of dysprosium submonolayer films adsorbed on the W(100) surface, Phys. Solid State 44 (2002) 793–795.

[2901] J.J. Paggel, C.M. Wei, M.Y. Chou, D.-A. Luh, T. Miller, T.-C. Chiang, Atomic–layer–resolved quantum oscillations in the work function: Theory and experiment for Ag/Fe(100), Phys. Rev. B 66 (2002) 233403/1–4.

[2902] S. Piccinin, A. Selloni, S. Scandolo, R. Car, G. Scoles, Electronic properties of metal–molecule–metal systems at zero bias: A periodic density functional study, J. Chem. Phys. 119 (2003) 6729–6735.

[2903] M.D.v. Przychowski, G.K.L. Marx, G.H. Fecher, G. Schönhense, A spatially resolved investigation of oxygen adsorption on polycrystalline copper and titanium by means of photoemission electron microscopy, Surf. Sci. 549 (2004) 37–51.

[2904] S.A. Pshenichnyuk, Yu.M. Yumaguzin, Field emission energy distributions of electrons from tungsten tip emitters coated with diamond–like film prepared by ion–beam deposition, Dia. Rel. Mater. 13 (2004) 125–132.

[2905] S. Park, L. Colombo, Y. Nishi, K. Cho, *Ab initio* study of metal gate electrode work function, Appl. Phys. Lett. 86 (2005) 073118/1–3.

[2906] K.J. Park, J.M. Doub, T. Gougousi, G.N. Parsons, Microcontact patterning of ruthenium gate electrodes by selective area atomic layer deposition, Appl. Phys. Lett. 86 (2005) 051903/1–3.

[2907] E. Pedersoli, F. Banfi, B. Ressel, S. Pagliara, C. Giannetti, G. Galimberti, S. Lidia, J. Corlett, G. Ferrini, F. Parmigiani, Evidence of vectorial photoelectric effect on copper, Appl. Phys. Lett. 87 (2005) 081112/1–3.

[2908] K.J. Park, G.N. Parsons, Selective area atomic layer deposition of rhodium and effective work function characterization in capacitor structures, Appl. Phys. Lett. 89 (2006) 043111/1–3.

[2909] H.-C. Ploigt, C. Brun, M. Pivetta, F. Patthey, W.-D. Schneider, Local work function changes determined by field emission resonances: NaCl/Ag(100), Phys. Rev. B 76 (2007) 195404/1–5.

[2910] Š. Pick, Density–functional study of the CO adsorption on ferromagnetic Co(0001) and Co(111) surfaces, Surf. Sci. 601 (2007) 5571–5575.

[2911] Š. Pick, P. Légaré, C. Demangeat, Density–functional study of the chemisorption of N on and below Fe(110) and Fe(001) surfaces, Phys. Rev. B 75 (2007) 195446/1–10.

[2912] C. Popa, A.P. van Bavel, R.A. van Santen, C.F.J. Flipse, A.P.J. Jansen, Density functional theory study of NO on the Rh(100) surface, Surf. Sci. 602 (2008) 2189–2196.

[2913] Š. Pick, Tailoring the surface reactivity: Comparison of Pd/Nb(110) and Rh/Nb(110), Coll. Czech. Chem. Comm. 73 (2008) 745–754.

[2914] V.V. Pogosov, A.V. Babich, On the effect of deformation and dielectric coating on the electron work function in a metal, Tech. Phys. 53 (2008) 1074–1082.

[2915] E. Pedersoli, C.M.R. Greaves, W. Wan, C. Coleman-Smith, H.A. Padmore, S. Pagliara, A. Cartella, F. Lamarca, G. Ferrini, G. Galimberti, M. Montagnese, S. dal Conte, F. Parmigiani, Surface and bulk contribution to Cu(111) quantum efficiency, Appl. Phys. Lett. 93 (2008) 183505/1–3.

[2916] Š. Pick, Density–functional study of the CO chemisorption on bimetallic Pd–Sn(110) surfaces, Surf. Sci. 603 (2009) 2652–2657.

[2917] Š. Pick, Density–functional study of the methoxy intermediates at Cu(111), Cu(110) and Cu(001) surfaces, J. Phys.: Condens. Matter 22 (2010) 395002/1–7.

[2918] L. Qiao, C. Wang, C.Q. Qu, Y. Zeng, S.S. Yu, X.Y. Hu, W.T. Zheng, Q. Jiang, First–principles investigation on the field emission properties of B–doped carbon nanotubes, Dia. Rel. Mater. 18 (2009) 657–661.

[2919] S. Roy, On the total photo–electric emission of electrons from metals as a function of temperature of the exciting radiation, Proc. Roy. Soc. A 112 (1926) 599–629.

[2920] D. Roller, The photoelectric behavior of solid and liquid mercury, Phys. Rev. 36 (1930) 738–742.

[2921] D. Roller, W.H. Jordan, C.S. Woodward, Some photoelectric properties of mercury films, Phys. Rev. 38 (1931) 396–400.

[2922] H.C. Rentschler, D.E. Henry, K.O. Smith, Photoelectric emission from different metals, Rev. Sci. Instrum. 3 (1932) 794–802.

[2923] B.A. Rose, Measurements on contact potential difference between different faces of copper single crystals, Phys. Rev. 44 (1933) 585–588.

[2924] H.C. Rentschler, D.E. Henry, Effect of oxygen upon the photoelectric thresholds of metals, J. Opt. Soc. Amer. 26 (1936) 30–34.

[2925] A.L. Reimann, The temperature variation of the work function of clean and of thoriated tungsten, Proc. Roy. Soc. A 163 (1937) 499–510.

[2926] A.L. Reimann, The evaporation of atoms, ions and electrons from tungsten, Phil. Mag. 25 (1938) 834–848.

[2927] H.C. Rentschler, D.E. Henry, Lowering of the photoelectric work function of zirconium, titanium, thorium and similar metals by dissolved gases, Trans. Electrochem. Soc. 87 (1945) 289–298.

[2928] E.S. Rittner, R.H. Ahlert, W.C. Rutledge, Studies on the mechanism of operation of the *L* cathodes. I, J. Appl. Phys. 28 (1957) 156–166.

[2929] U. Richter, Unpublished (see Ref. [3052]).

[2930] E.G. Raugh, Argonne Natl. Lab. Rep. ANL–5534 (see Refs. [232,1884]).

[2931] G. Reusmann, Unpublished (see Ref. [3052]).

[2932] J.C. Rivière, The work function of thorium, Proc. Phys. Soc. 80 (1962) 124–129.

[2933] J.C. Rivière, The work function of uranium, Proc. Phys. Soc. 80 (1962) 116–123.

[2934] U. Richter, Dissertation, TU Hannover, 1963 (see Refs. [1153,2929]).

[2935] J.C. Rivière, Unpublished (see Ref. [349]).

[2936] N.S. Rasor, C. Warner, Correlation of emission processes for adsorbed alkali films on metal surfaces, J. Appl. Phys. 35 (1964) 2589–2600.

[2937] B.S. Rump, B.L. Gehman, Work function measurements of nickel, molybdenum, and tungsten in a cesium–hydrogen atmosphere, J. Appl. Phys. 36 (1965) 2347–2352.

[2938] J.C. Rivière, The surface potential of oxygen on thorium, Br. J. Appl. Phys. 16 (1965) 1507–1511.

[2939] J.C. Rivière, Comment on a letter by B.H. Blott and B.J. Hopkins, "Work function measurements on the sublimate from uranium carbide", Brit. J. Appl. Phys. 16 (1965) 1926.

[2940] J.C. Rivière, The surface potential of hydrogen on uranium, Nuo. Cime. Suppl. 5 (1967) 466–471.

[2941] J. Roussenq, Photoelectric effect of thin gold layers deposited on a silver foil, C. R. Acad. Sci. Paris B 267 (1968) 966–969.

[2942] Z.A. Rotenberg, S.D. Levina, Determination of the contact potential difference between gallium and mercury on the basis of space charge limited currents in phthalocyanines, Elektrokhim. 5 (1969) 1141–1143.

[2943] R.L. Ramey, S.J. Katzberg, Surface work function of gadolinium, J. Chem. Phys. 53 (1970) 1347–1348.

[2944] M. Remy, R. Haug, A lithium ion source using the surface ionization process, Rev. Sci. Instrum. 41 (1970) 650–652.

[2945] J.C. Richard, P. Saget, G.-A. Boutry, Photoelectric properties of pure sodium prepared and maintained under ultrahigh vacuum, C. R. Acad. Sci. Paris B 271 (1970) 1098–1100.

[2946] J.C. Richard, P. Saget, Slow electron diffraction by the alkali metals, J. de Phys. 31 (1970) C1–155/C1–158.

[2947] P.K. Rawlings, H. Reiss, Work functions and surface double layer potentials of monovalent metals from a network model, Surf. Sci 36 (1973) 580–593.

[2948] G.E. Riach, W.T. Peria, Photoemission studies of the alkali–covered Ge(111) surface, Surf. Sci. 40 (1973) 479–498.

[2949] B.F. Rzyanin, Application of the Thomas–Fermi statistical method to calculate the work function of metals, Teplofiz. Vysok. Temp. 11 (1973) 34–38.

[2950] C. Raisin, J. Robin, Photoelectric emission of amorphous arsenic, C. R. Acad. Sci. Paris B 276 (1973) 195–198.

[2951] J.E. Rowe, H. Ibach, Surface and bulk contributions to ultraviolet photoemission spectra of silicon, Phys. Rev. Lett. 32 (1974) 421–424.

[2952] C. Raisin, R. Pinchaux, Photoelectric properties of crystalline arsenic between 7 and 11.4 eV, Solid State Commun. 16 (1975) 941–944.

[2953] B. Rasser, M. Remy, Experiments on a new surface ionization ion source with lithium, Rev. Sci. Instrum. 46 (1975) 325–326.

[2954] R. Riwan, C. Guillot, J. Paigne, Oxygen adsorption on clean Mo(100) surfaces, Surf. Sci. 47 (1975) 183–190.

[2955] T.T. Rozova, V.G. Ivanov, G.N. Fursei, Influence of a strong electric field on the adsorption of oxygen on germanium, Sov. Phys.—Solid State 17 (1975) 35–36.

[2956] L. Richter, R. Gomer, Field emission spectroscopy of gold on the (110) and (211) planes of tungsten, Surf. Sci. 59 (1976) 575–580.

[2957] B. Robrieux, R. Faure, R. Rivoira, Work function of thin calcium films as a function of their thickness, measured under high vacuum by the Kelvin method, C. R. Acad. Sci. Paris B 282 (1976) 463–466.

[2958] B. Robrieux, R. Faure, G. Desrousseaux, Study of the nucleation of silver on carbon by measuring the contact potential difference and by electron microscopy, Thin Solid Films 31 (1976) 311–319.

[2959] L. Richter, R. Gomer, Effect of Au adsorption on the tungsten(100) surface state, Phys. Rev. Lett. 37 (1976) 763–765.

[2960] T. Radoń, Ch. Kleint, Photo field–emission spectroscopy of optical transitions in the band structure of tungsten, Surf. Sci. 60 (1976) 540–560.

[2961] T.N. Rhodin, G. Brodén, Preparation and chemisorptive properties of the clean normal and reconstructed surfaces of Ir(100) — Role of multiplets, Surf. Sci. 60 (1976) 466–484.

[2962] G.W. Rubloff, J.E. Demuth, Ultraviolet photoemission and flash–desorption studies of the chemisorption and decomposition of methanol on Ni(111), J. Vac. Sci. Technol. 14 (1977) 419–423.

[2963] N.Ya. Rukhlyada, A.V. Gostev, B.B. Shishkin, Modification of a high–vacuum electron emission microscope for the simultaneous measurement of local and integral emission characteristics of electron emitters, Izv. Akad. Nauk SSSR, Ser. Fiz. 41 (1977) 1055–1058.

[2964] H. Roux, A. Piquet, G. Pralong, R. Uzan, Adsorption, diffusion and self–diffusion on tungsten surfaces with adsorbed palladium, Surf. Sci. 71 (1978) 375–386.

[2965] L. Richter, R. Gomer, The effect of metallic adsorbates on the surface resonances of the tungsten and molybdenum (100) planes, Surf. Sci. 83 (1979) 93–116.

[2966] T. Radoń, Z. Sidorski, Adsorption and condensation of bismuth on tungsten, J. Cryst. Growth 47 (1979) 115–120.

[2967] N.Ya. Rukhlyada, A.G. Trefilov, B.B. Shishkin, Thermionic emission and structure of hafnium, Bull. Acad. Sci. USSR, Phys. Ser. 43 (9) (1979) 42–46.

[2968] J.D. Riley, L. Ley, J. Azoulay, K. Terakura, Partial densities in amorphous $Pd_{0.81}Si_{0.19}$, Phys. Rev. B 20 (1979) 776–783.

[2969] L.V. Reshetnikova, M.Kh. Yuldasheva, Field–emission electron investigation of adsorption of dysprosium, holmium, and erbium on the surface of a point single crystal of tungsten, Bull. Acad. Sci. USSR, Phys. Ser. 43 (3) (1979) 74–77.

[2970] B. Rasser, D.I.C. Pearson, M. Remy, Surface ionization source for heavy ions, Rev. Sci. Instrum. 51 (1980) 474–477.

[2971] S. Romanowski, Work function at the interface: Copper monocrystal–electrolyte solution, in: Proc. 4th Int. Semin. on Energy Transfer in Cond. Matt., Prague, 1981, pp. 243–247.

[2972] G.W. Rubloff, P.S. Ho, J.F. Freeouf, J.E. Lews, Chemical bonding and reactions at the Pd/Si interface, Phys. Rev. B 23 (1981) 4183–4196.

[2973] L.A. Rudnitskiĭ, E.N. Martynyuk, A.I. Reznik, Electron work function of a nonideal metal surface. III. Size dependence of the work function of small particles, Sov. Phys. Tech. Phys. 27 (1982) 711–715.

[2974] H.H. Rotermund, K. Jacobi, The influence of dipoles in intermediate layers on the electronic levels of physisorbed species studied by UPS, Solid State Commun. 44 (1982) 493–496.

[2975] L.A. Rudnitskii, Electron work function and donor–acceptor properties of nonideal or adparticle–covered metal surfaces, Bull. Acad. Sci. USSR, Phys. Ser. 46 (7) (1982) 20–26.

[2976] R. Richter, J.W. Wilkins, Self–consistent surface electronic band structure calculations: Changes upon chemisorption, J. Vac. Sci. Technol. A 1 (1983) 1089–1094.

[2977] H.H. Rotermund, K. Jacobi, Physisorption on a low work function metal: ARUPS from xenon on cesium, Surf. Sci. 126 (1983) 32–40.

[2978] L.A. Rudnitskii, Donor–acceptor characteristics of a non–ideal metal surface or a metal surface covered by adsorbed metal species, Russ. J. Phys. Chem. 57 (1983) 739–742.

[2979] R. Richter, J.W. Wilkins, Overlayer screening of transition metal surfaces: p(1×1) H on W{100}, Surf. Sci. 128 (1983) L190–L196.

[2980] J. Rogozik, J. Küppers, V. Dose, 2π levels of CO and NO adsorbed at Pd(100) surfaces, Surf. Sci. 148 (1984) L653–L658.

[2981] R. Richter, J.G. Gay, J.R. Smith, An iron monolayer on silver{100}: Spin–polarized electronic structure, J. Vac. Sci. Technol. A 3 (1985) 1498–1501.

[2982] V. Russier, Private comm. (see Ref. [3590]).

[2983] V. Russier, J.P. Badiali, M.L. Rosinberg, To be published (see Refs. [947,3363]).

[2984] G. Rangelov, L. Surnev, Alkali metal adsorption on Ru(001), Surf. Sci. 185 (1987) 457–468.

[2985] S. Raaen, O.-M. Nes, Growth of gold monolayers on polycrystalline tantalum, Solid State Commun. 65 (1988) 1605–1608.

[2986] M.W. Ruckman, L.-Q. Jiang, Growth and thermal stability of Ag or Au films on Nb(110), Phys. Rev. B 38 (1988) 2959–2966.

[2987] H.H. Rotermund, S. Jakubith, A. von Oertzen, G. Ertl, Imaging of spatial pattern formation in an oscillatory surface reaction by scanning photoemission microscopy, J. Chem. Phys. 91 (1989) 4942–4948.

[2988] B. Roop, P.M. Blass, X.-L. Zhou, J.M. White, Interactions of CO and surface K: Neglisible CO adsorption on K/Ag(111), J. Chem. Phys. 90 (1989) 608–609.

[2989] S.-J. Romanowski, Phonon effects in the electron work function and surface charge: ECPA calculations for Cu single crystals, Z. Phys. Chem. 270 (1989) 876–886.

[2990] V. Russier, D.R. Salahub, C. Mijoule, Theoretical determination of work functions and adsorption energies of atoms on metal surfaces from small–cluster calculations: A local–spin–density approach, Phys. Rev. B 42 (1990) 5046–5056.

[2991] B. Reihl, K.O. Magnusson, Surface electronic structure of K on Si(111)2 ×1 as a function of potassium coverage, Phys. Rev. B 42 (1990) 11839–11844.

[2992] C. Rehren, M. Muhler, X. Bao, R. Schlögl, G. Ertl, The interaction of silver with oxygen: An investigation with thermal desorption and photoelectron spectroscopy, Z. Phys. Chem. 174 (1991) 11–52.

[2993] S. Lu, Z. Qin, Q. Guo, G. Cao, Work function mediated by deposition of ultrathin polar FeO on Pt(111), Appl. Surf. Sci. 392 (2017) 849–853.

[2994] D.M. Riffe, G.K. Wertheim, J.E. Rowe, P.H. Citrin, Coverage dependence of K adsorption on Si(100)2 ×1 by core–level photoemission: Structure, charge transfer, and metallization, Phys. Rev. B 45 (1992) 3532–3537.

[2995] P.N. Ross, A.T. D'Agostino, The effect of surface reconstruction on the capacitance of Au(100) surfaces, Electrochim. Acta 37 (1992) 615–623.

[2996] H.H. Rotermund, J. Lauterbach, G. Haas, The formation of subsurface oxygen on Pt(100), Appl. Phys. A 57 (1993) 507–511.

[2997] P. Rudolf, C. Astaldi, A. Bianco, S. Modesti, Ca chemisorption on Cu(100) in the submonolayer regime: Metastable and stable adsorption phases, Phys. Rev. B 47 (1993) 4123–4126.

[2998] K.B. Ray, X. Pan, E.W. Plummer, The interaction of H with Be(0001): A photoemission investigation, Surf. Sci. 285 (1993) 66–74.

[2999] C. Reuß, W. Wallauer, Th. Fauster, Image states of Ag on Au(111), Surf. Rev. Lett. 3 (1996) 1547–1554.

[3000] G.M. Roe, C.M.C. de Castilho, R.M. Lambert, Structure and properties of samarium overlayers and Sm/Ni surface alloys on Ni(111), Surf. Sci. 301 (1994) 39–51.

[3001] L.A. Rudnitsky, Analysis of the structure of two–dimensional layers of metal atoms adsorbed on the W(110) face based on electron work function experimental data, Appl. Surf. Sci. 75 (1994) 115–120.

[3002] P. Rudolf, S. Cerasari, S. Modesti, Unpublished (see Refs. [316,2683]).

[3003] T.H. Rho, S.C. Hong, M.S. Seo, J.I. Lee, LSDA study of the electronic and magnetic properties of Fe/Al(001), Sae. Mulli. 37 (1997) 38–44 (Chem. Abstr. 127 (1997) 140808k).

[3004] L. Reinaudi, M. Del Popolo, E. Leiva, Work function calculation for thick metal slabs with local pseudopotentials, Surf. Sci. 372 (1997) L309–L314.

[3005] O. Rader, W. Gudat, C. Carbone, E. Vescovo, S. Brügel, R. Kläsges, W. Eberhardt, M. Wuttig, J. Redinger, F.J. Himpsel, Electronic structure of two–dimensional magnetic alloys: $c(2 \times 2)$ Mn on Cu(100) and Ni(100), Phys. Rev. B 55 (1997) 5404–5415.

[3006] P. Rudolf, Private comm. (see Refs. [458,3002]).

[3007] Ch. Ross, B. Shirmer, M. Wuttig, Y. Gauthier, G. Bihlmayer, S. Brügel, Structure, growth, and magnetism of Mn on Cu(110), Phys. Rev. B 57 (1998) 2607–2620.

[3008] R. Ramprasad, P. von Allmen, L.R.C. Fonseca, Contributions to the work function: A density–functional study of adsorbates at graphene ribbon edges, Phys. Rev. B 60 (1999) 6023–6027.

[3009] A. Ramstad, S. Raaen, Formation of and CO adsorption on an inert La–Pt(111) alloy, Phys. Rev. B 59 (1999) 15935–15941.

[3010] T.H. Rho, Y.S. Kwon, S.C. Hong, J.I. Lee, Electronic and magnetic properties of 1Cr/1Fe/Cr(110), J. Korean Phys. Soc. 36 (2000) 408–411 (Chem. Abstr. 133 (2000) 328640c).

[3011] K. Reuter, M.V. Ganduglia-Pirovano, C. Stampfl, M. Scheffler, Metastable precursors during the oxidation of the Ru(0001) surface, Phys. Rev. B 65 (2002) 165403/1–10.

[3012] A.K. Ray, J.C. Boettger, A First Principles Electronic Structure Study of Quantum Size Effects in (111) Films of δ–Plutonium, Los Alamos Natl. Lab., 2004, arXiv:cond-mat/0401297 (Chem. Abstr.140 (2004) 100084h) (http://xxx.ianl.gov/pdf/cond-mat/0401297).

[3013] A.K. Ray, J.C. Boettger, First–principles electronic structure study of the quantum size effects in (111) films of δ–plutonium, Phys. Rev. B 70 (2004) 085418/1–6.

[3014] B. Rezek, C.E. Nebel, M. Stutzmann, Hydrogenated diamond surfaces studied by atomic and Kelvin force microscopy, Diam. Relat. Mater. 13 (2004) 740–745.
[3015] V.S. Robinson, Y. Show, G.M. Swain, R.G. Reifenberger, T.S. Fisher, Thermionic emission from surface–terminated nanocrystalline diamond, Diam. Relat. Mater. 15 (2006) 1601–1608.
[3016] J.A. Rothschild, M. Eizenberg, Work function calculation of solid solution alloys using the image force model, Phys. Rev. B 81 (2010) 224201/1–8.
[3017] E. Stoekle, Thermionic currents from molybdenum, Phys. Rev. 8 (1916) 534–560.
[3018] O. Stuhlman Jr., On the photoelectric long wave–length limit of platinum and silver, Phys. Rev. 15 (1920) 549–550.
[3019] R. Suhrmann, The influence of the gas content on the thermal and photoelectric emission of platinum and tantalum, Z. Phys. 13 (1923) 17–34.
[3020] H.J. Spanner, Thermionic emission of electrically charged particles, Ann. Phys. 75 (1924) 609–633.
[3021] R. Suhrmann, Red limit and work of escape of photoelectric electrons, Z. Phys. 33 (1925) 63–84.
[3022] E.E. Schumacher, J.E. Harris, Investigation of the thermionic properties of the rare–earth elements, J. Am. Chem. Soc. 48 (1926) 3108–3114.
[3023] R. Suhrmann, The change in the electrical condition of the surface of a metal after charging with hydrogen ions and bombarding with electrons, Z. Elektrochem. 35 (1929) 681–686.
[3024] G. Siljeholm, Investigation of the thermionic emission of iron, Ann. Phys. 10 (1931) 178–222.
[3025] R. Suhrmann, A. Schallamach, The origin of the spectral selectivity of the photoelectric effect of thin films of alkali metal, Z. Phys. 79 (1932) 153–160.
[3026] R. Suhrmann, R. Deponte, Photoelectric investigation of the temperature dependence of the work function for electrons from a nickel surface covered with atomic barium, Z. Phys. 86 (1933) 615–634.
[3027] R. Schulze, Experiments on the photoelectric effect. I. Systematic investigation of the external photoelectric effect in the elements of the periodic system, Z. Phys. 92 (1934) 212–227.
[3028] R. Suhrmann, A. Schallamach, Temperature dependence of photoelectric effect of pure and contaminated metal surfaces at low temperatures, Z. Phys. 91 (1934) 775–791.
[3029] R. Suhrmann, H. Csesch, Electric polarization of hydrogen adsorbed on pure metallic surfaces and its effect on the recombination of hydrogen atoms, Z. Phys. Chem. B 28 (1935) 215–235.
[3030] D. Schieber, Quasi–classical estimation of the work function of metals, Arch. Elektrotech. 67 (1984) 387–390.
[3031] R. Suhrmann, J. Pietrzyk, Change in photoelectric emission during the transition of pure zinc, cadmium, and aluminum layers from the disordered to the ordered state, and the effect of temperature on the sensitivity of these metals, Z. Phys. 122 (1944) 600–613.
[3032] W. Sachtler, Dissertation, Technische Hochschule Braunschweig, 1952 (see Ref. [1066]).
[3033] B.G. Smirnov, G.N. Shuppe, Work function of the electrons at some of the faces of a tungsten monocrystal, Zh. Tekh. Fiz. 22 (1952) 973–980.
[3034] V.K. Nevolin, V.A. Osadkin, T.D. Shermergor, Electron work function and electron affinity of intrinsic semiconductors, Sov. Phys. J. 28 (1985) 1008–1011.
[3035] A.R. Shul'man, A.P. Rumyantsev, Thermoemissive properties of thin films of thorium oxide, and of thorium on metallic carriers, Zh. Tekh. Fiz. 25 (1955) 1898–1909.
[3036] W.M.H. Sachtler, G.J.H. Dorgleo, The polarity of the chemisorptive bonding: Measure of the potential of the surface and of the conductivity on evaporated metallic films, J. Chim. Phys. 54 (1957) 27–36.
[3037] G.N. Shuppe, E.P. Sytaya, R.M. Kadyrov, Positive surface ionization of sodium and potassium and the process of output of a monocrystal of tungsten, Trudy Sredneaz. Gos. Univ. 91 (1957) 5–15 (Nucl. Sci. Abstr. 14 (1957) 370) (see Ref. [145]).
[3038] R. Suhrmann, G. Wedler, E.-A. Dierk, Temperature dependence of the spectral photoelectric electron emission of semiconducting bismuth films, Z. Phys. 153 (1958) 96–105.
[3039] V.N. Shrednik, Zirconium and barium adsorption on tungsten and the electronic work function, Izv. Akad. Nauk SSSR, Ser. Fiz. 22 (1958) 594–604.
[3040] R. Suhrmann, G. Wedler, E.-A. Dierk, Photoelectric investigation of the chemisorption state of oxygen on bismuth films degassed in high vacuum, Z. Phys. Chem. 18 (1958) 255–264.
[3041] M.I. Smorodinova, E.P. Sytaya, Variation of thermionic properties of cathodes of rheniated tungsten, Trudy Sredn. Gos. Univ. Lenina, Fiz. Mat. Nauk 148 (20) (1959) 9–22 (Chem. Abstr. 55 (1961) 6142h).
[3042] V.N. Shrednik, The problem of the interpretation of field emission patterns of metal–film cathodes, Sov. Phys.—Solid State 1 (1960) 1037–1042.
[3043] R.E. Simon, Contact potential difference measurements on (111) silicon surfaces prepared by cleavage in high vacuum, Bull. Am. Phys. Soc. 4 (1959) 410.
[3044] R.E. Simon, The work function of the (100) plane of iron produced by cleavage in high vacuum, Bull. Am. Phys. Soc. 4 (1959) 264.
[3045] R. Suhrmann, G. Wedler, Electronic interaction as a preliminary to chemical reaction between metals and chemisorbed gases, Z. Elektrochem. 63 (1959) 748–756.
[3046] R. Suhrmann, H. Ober, G. Wedler, Influence on work function and electric resistance of vapor–deposited films of Fe, Ni, Cu, Zn, and Ga by adsorption of carbon monoxide at 90 °K and 293 °K, Z. Phys. Chem. 29 (1961) 305–316.
[3047] I.L. Sokol'skaya, Adsorption, migration and evaporation of cadmium on tungsten, Sov. Phys.—Solid State 3 (1961) 574–579.
[3048] R. Suhrmann, G. Krüger, G. Wedler, Alteration of the work function and the electrical resistance of vapor–deposited films of Fe, Ni, Cu, Zn, Pd, Ag by adsorption of benzene at 90 °K, Z. Phys. Chem. 30 (1961) 1–16.
[3049] R. Suhrmann, A. Mata Arjona, G. Wedler, Electron exchange between carbon monoxide and vaporized tungsten films, Z. Elektrochem. 65 (1961) 786–788.
[3050] E. Sugata, H. Kim, Adsorption of Th on tungsten surface — Its field emission microscope study, Oyo Butsuri 30 (1961) 345–352.
[3051] G. Schwandt, Unpublished (see Ref. [3052]).
[3052] R. Suhrmann, G. Wedler, Newer measurements of electronic work functions from disordered and ordered metal films, Z. Angew. Phys. 14 (1962) 70–74.
[3053] R. Suhrmann, A. Hermann, G. Wedler, Regularities in the electronic interaction between hydrogen and vapor–deposited films of 3d–metals, Z. Phys. Chem. 35 (1962) 155–178.
[3054] W.G. Spitzer, C. Mead, Barrier height studies on metal–semiconductor systems, J. Appl. Phys. 34 (1963) 3061–3069.
[3055] W. Schroen, Absolute measurement of the ionization efficiency of alkali atoms on metal surfaces. I. Potassium atoms on tungsten and platinum surfaces, Z. Phys. 176 (1963) 237–252.
[3056] R. Suhrmann, M. Kruel, G. Wedler, Electrical resistance and work function of pure germanium layers evaporated in ultrahigh vacuum, Z. Phys. 173 (1963) 71–77.
[3057] J.G. Simmons, Intrinsic fields in thin insulating films between dissimilar electrodes, Phys. Rev. Lett. 10 (1963) 10–12 (see Ref. [13]).
[3058] R. Suhrmann, D. Kern, G. Wedler, Influence of the state of order of vapor–deposited nickel films on the electronic interaction between formic acid and metal, Z. Phys. Chem. 36 (1963) 165–178.
[3059] R. Suhrmann, M. Kruel, G. Wedler, Mutual electronic exchange between evaporated germanium films and oxygen, Z. Naturforsch. 18 a (1963) 119–125.
[3060] R. Suhrmann, M. Kruel, G. Wedler, Electronic interaction between CO and evaporated Ge films with clean or oxygen–adsorbed surfaces, Z. Naturforsch. 18 a (1963) 633–638.
[3061] M. Shiraishi, M. Ata, Work function of carbon nanotubes, Mat. Res. Soc. Symp. 633 (2001) A 4.4.1–4.4.6.
[3062] V.N. Shrednik, E.V. Snezhko, Field emission microscopy of Na on W under migration equilibrium conditions, Sov. Phys.—Solid State 6 (1965) 2727–2737.
[3063] I.L. Sokol'skaya, N.V. Mileshkina, Field emission and surface migration of germanium on tungsten, Sov. Phys.—Solid State 6 (1964) 1401–1410.
[3064] V.M. Sultanov, G.N. Shuppe, Work function and heat of adsorption of Ba on W single crystals at various crystal faces, Izv. Akad. Nauk Uzb.SSR, Ser. Fiz.-Mat. Nauk 9 (5) (1965) 49–53 (Chem. Abstr. 64 (1966) 1447a).

[3065] L.D. Schmidt, R. Gomer, Coadsorption of hydrogen and potassium on tungsten: Adsorption of hydrogen on potassium, J. Chem. Phys. 43 (1965) 95–102.

[3066] M.L. Shaw, N.P. Carleton, Chemisorption of electronegative gases on refractory metals, J. Chem. Phys. 44 (1966) 3387–3392.

[3067] D. Steiner, E.P. Gyftopoulos, Equation for the prediction of bare work functions, Bull. Am. Phys. Soc. 12 (1967) 982.

[3068] R.K. Swank, Surface properties of II–VI compounds, Phys. Rev. 153 (1967) 844–849.

[3069] I.L. Sokol'skaya, V.G. Ivanov, G.N. Fursey, Study of barium adsorption on germanium by field–emission microscopy, Phys. Status Solidi 21 (1967) 789–795.

[3070] J.J. Scheer, J. van Laar, Fermi level stabilization at cesiated semiconductor surfaces, Solid State Commun. 5 (1967) 303–306.

[3071] E.M. Savitskii, V.F. Terekhova, E.V. Maslova, Thermionic emission of yttrium, scandium and erbium, Radiotekh. Elektron. 12 (1967) 1320–1321.

[3072] E. Sugata, H. Kim, Cleaning of silicon surface by high field and heating, Tech. Rep. Osaka Univ. 17 (1967) 237–247.

[3073] A.J. Sargood, Private comm. (see Ref. [1656]).

[3074] L.W. Swanson, R.W. Strayer, L.E. Davis, Desorption, mobility and work function change of mercury on tungsten and molybdenum substrates, Surf. Sci. 9 (1968) 165–186.

[3075] R. Suhrmann, J.M. Heras, L. Viscido de Heras, G. Wedler, Chemisorption and decomposition of water molecules on pure iron and copper surfaces at low temperatures, Ber. Bunsenges. Phys. Chem. 72 (1968) 854–863.

[3076] A.J. Sargood, The adsorption of monolayer films of uranium and zirconium on tungsten (Ph.D. thesis), Univ. of Southampton, 1969 (see Refs. [1664,1665,2251]).

[3077] E. Sugata, H.-W. Kim, K.-S. Chang, An adsorption study of O_2 and H_2 on Mo by field emission retarding potential analyser, Japan. J. Appl. Phys. 8 (1969) 127–128.

[3078] E.N. Sloth, Effect of anionic constituents on the surface ionization of lithium salts (Ph.D. thesis), Illinois Inst. of Technol., 1969, 235 pp. (see Ref. [54]).

[3079] Z. Sidorski, I. Pelly, R. Gomer, Adsorption of Cs on tungsten: Measurements on single–crystal planes, J. Chem. Phys. 50 (1969) 2382–2391.

[3080] T. Schneider, The work function in simple metals, Phys. Status Solidi 32 (1969) 323–329.

[3081] N.V. Smith, W.E. Spicer, Photoemission studies of the alkali metals. I. Sodium and potassium, Phys. Rev. 188 (1969) 593–605.

[3082] L.L. Sivers, Investigation of adsorption of yttrium on individual faces of a tungsten single crystal using an electron field emission projector, Sov. Phys.—Solid State 11 (1969) 843–844.

[3083] N. Sasaki, K. Kubo, M. Asano, Heats of vaporization and work functions of atoms and cations of rhenium, tantalum, and tungsten, Bull. Engine's Res. Inst. Kyoto Univ. 38 (1970) 38 (Chem. Abstr. 78 (1973) 8589e).

[3084] N.B. Smirnova, Tr. Konf. Elektron. Tekhn., No. 7, Emiss. Elektrn., 1970, pp. 55–58 (see Ref. [1354]).

[3085] E.M. Savitskii, I.V. Burov, L.N. Litvak, V.P. Polyakova, G.D. Shnyrev, 14th Vses. Konf. Emiss. Elektron. Tashkent, 2, 1970, p. 21 (see Refs. [1354,3087]).

[3086] N.B. Smirnova, B.G. Smirnov, S.M. Mikhailov, G.N. Shuppe, Thermoemissive properties of (100) faces of single crystals of solid solutions of iridium, osmium, and rhenium in tungsten, Sov. Phys. Tech. Phys. 12 (1970) 1001–1002.

[3087] E.M. Savitskii, L.N. Litvak, I.V. Burov, V.P. Polyakova, G.D. Shnyrev, Anisotropy of the work function of a ruthenium single crystal, Sov. Phys. Dokl. 15 (1970) 602–604.

[3088] A.J. Sargood, C.W. Jowett, B.J. Hopkins, A relationship between surface potential and electronegativity for adsorption on tungsten single crystals, Surf. Sci. 22 (1970) 343–356.

[3089] E. Sugata, K. Takeda, Adsorption and nucleation of silver on tungsten, Phys. Status Solidi 38 (1970) 549–557.

[3090] A.R. Shul'man, R.L. Nemchenok, S.Ye. Strakovskaya, Energy distribution of the photoelectrons from barium films of different thickness, Radio. Eng. Electr. Phys. 15 (1970) 1929–1931.

[3091] N.V. Smith, G.B. Fisher, Photoemission studies of the alkali metals. II. Rubidium and cesium, Phys. Rev. B 3 (1971) 3662–3670.

[3092] R.W. Strayer, L.W. Swanson, Private comm. (see Ref. [2828]).

[3093] K. Shimada, Out–of–core evaluations of uranium nitride–fueled converters, in: Proc. 3rd Int. Conf. Thermion. Electr. Power Generat. Jülich, Vol. 3, 1972, pp. 1269–1277.

[3094] O.F. Swenson, M.K. Sinha, Field emission study of silicon on tungsten, J. Vac. Sci. Technol. 9 (1972) 942–946.

[3095] I.L. Sokol'skaya, N.V. Mileshkina, R.Z. Bakhtizin, Gold adsorption on clean germanium field emitters, Phys. Status Solidi (a) 14 (1972) 417–422.

[3096] E.M. Savitskii, Single crystals of high–melting and rare metals, Vestn. Akad. Nauk SSSR (1) (1973) 68–76.

[3097] W.B. Shepherd, W.T. Peria, Observation of surface–state emission in the energy distribution of electrons field–emitted from (100) oriented Ge, Surf. Sci. 38 (1973) 461–498.

[3098] H.T. Spath, K. Mayer, K. Torkar, Photoelectric work functions of silver catalysts and silver catalysts modified by addition of alkaline earth compounds, J. Catalysis 35 (1974) 100–114.

[3099] S.T. Sabirov, Sh. Nizamutdinova, Thermoemission and adsorption properties of Cs and Ba on the (110) face of molybdenum, Nauchn. Tr., Tashk. Gos. Univ. 459 (1974) 52–55.

[3100] B. Seroczyńska-Wojas, Photoemission from beta–rhombohedral boron, Phys. Status Solidi (a) 30 (1975) K73–K76.

[3101] L.W. Swanson, Comparative study of the zirconiated and built–up W thermal–field cathode, J. Vac. Sci. Technol. 12 (1975) 1228–1233.

[3102] L.W. Swanson, N.A. Martin, Field electron cathode stability studies: Zirconium/tungsten thermal–field cathode, J. Appl. Phys. 46 (1975) 2029–2050.

[3103] E.P. Sytaya, N.G. Imangulova, K.Zh. Zanabergenov, Behavior of sodium and lithium atoms on the basal faces of tungsten, molybdenum, and tantalum single crystals, in: 15th Vses. Konf. Emiss. Elektron. Kiev, vol. 1, 1973, pp. 25–27.

[3104] K.A.G. Schultes, M.F. Ebel, Absolute determination of the work function of palladium with an X–ray photoelectron spectrometer, J. Electron Spectrosc. Relat. Phenom. 8 (1976) 449–458.

[3105] E.M. Savitskii, V.F. Terakhova, I.V. Burov, L.N. Litvak, O.D. Chistyakov, Work function of an yttrium single crystal, Izv. Akad Nauk SSSR, Ser. Fiz. 40 (1976) 1726–1727.

[3106] N.A. Shurmovskaya, E.M. Egorova, G.M. Kornacheva, Electron work function of gallium, Elektrokhim. 12 (1976) 590–591.

[3107] Kh. Sattarov, T. Mikhailova, T.A. Karabaev, Behavior of cesium on an oxidized molybdenum surface, Nauchn. Tr., Tashkent. Gos. Univ. 525 (1976) 20–23.

[3108] V.A. Sobyanin, V.V. Gorodetskii, N.N. Bulgakov, Oxygen adsorption on silver–gold alloy, React. Kin. Catal. Lett. 7 (1977) 285–290.

[3109] C.A. Sebenne, High–resolution photoemission yield and surface states in semiconductors, Nuo. Cimento 39 B (1977) 768–780.

[3110] A.L. Suvorov, Field emission microscopy and emission properties of uranium, Atomnaya Energiya 42 (1977) 280–285 (Chem. Abstr. 87 (1977) 32169z).

[3111] A. Simon, G. Ebbinghaus, Private comm. (see Ref. [1545]).

[3112] E.M. Savitskii, I.V. Burov, L.N. Litvak, 17th Vses. Konf. Emiss. Elektron., 1978, pp. 206–207 (see Ref. [1354]).

[3113] L.V. Sumin, Formation of Na_2Cl^+ ions in exposure of hot tungsten and rhenium surfaces to a sodium chloride beam, Sov. Phys. Tech. Phys. 23 (1978) 967–969.

[3114] L.W. Swanson, Current fluctuations from various crystal faces of a clean tungsten field emitter, Surf. Sci. 70 (1978) 165–180.

[3115] Z. Stepien, W. Lenkow, Effect of the size of the analyzed region on the value of the local work function of the (011) plane of tungsten, Mater. Semin. Nauk. Wydz. Mat.-Przyr. Wyzsza Szk. Pedagog. Czestochowie 3 (1979) 30–32 (Chem. Abstr. 96 (1982) 78516z).

[3116] Z. Sidorski, T. Szelwicki, Z. Dworecki, Effect of substrate temperature on the relation between the work function and the coverage for silver layers adsorbed on tungsten, Thin Solid Films 61 (1979) 203–215.

[3117] Z. Sidorski, S. Zuber, J. Polanski, Adsorption of beryllium on (211) oriented tungsten single crystal: Work function changes and energy losses of scattered electrons, Surf. Sci. 80 (1979) 626–636.

[3118] K. Schwaha, N.D. Spencer, R.M. Lambert, A single crystal study of the initial stages of silver sulphidation: The chemisorption and reactivity of molecular sulphur (S_2) on Ag(111), Surf. Sci. 81 (1979) 273–284.

[3119] D. Schmeisser, K. Jacobi, Photoelectron spectroscopy of nickel on zinc oxide in the monolayer and submonolayer range, Surf. Sci. 88 (1979) 138–152.

[3120] W.D. Schneider, C. Laubschat, Binding energies and work–function changes in $Eu_xLa_{1-x}Al_2$ compounds studied by X–ray photoelectron spectroscopy, Phys. Rev. B 20 (1979) 4416–4422.

[3121] F. Soria, H. Poppa, Comparison of the early stages of condensation of Cu and Ag on Mo(100) with Cu and Ag on W(100), J. Vac. Sci. Technol. 17 (1980) 449–452.

[3122] W. Schlenk, E. Bauer, Beryllium films on the tungsten {110} surface, Surf. Sci. 94 (1980) 528–546.

[3123] W. Schlenk, E. Bauer, Properties of ultrathin layers of palladium on a tungsten {110} surface, Surf. Sci. 93 (1980) 9–32 (see Ref. [2857]).

[3124] W.D. Schneider, C. Laubschat, Binding energies, work–function Changes, and saturation moments in the compounds UPt and UPt_2, Physica 102 B (1980) 111–113.

[3125] S.I. Sergeev, M.E. Beryaeva, N.A. Shurmovskaya, G.M. Kornacheva, T.V. Kalish, Study of oxygen and hydrogen adsorption on rhodium by the method of Auger spectroscopy and external photoeffect, Elektrokhim. 16 (1980) 175–179.

[3126] J.R. Smith, J.G. Gay, F.J. Arlinghaus, Pd(100) surface electronic structure, Bull. Am. Phys. Soc. 25 (1980) 236.

[3127] A. Schmidt-Ott, P. Schurtenberger, H.C. Siegmann, Enormous yield of photoelectrons from small particles, Phys. Rev. Lett. 45 (1980) 1284–1287.

[3128] P.J. Schneider, K.H. Berkner, W.G. Graham, R.V. Pyle, J.W. Stearns, H^- and D^- production by backscattering from alkali–metal targets, Phys. Rev. B 23 (1981) 941–948.

[3129] Z. Sidorski, T. Szelwicki, Z. Dworecki, Adsorption of copper on tungsten low index planes at various substrate temperatures: A field emission microscopy study, Thin Solid Films 75 (1981) 87–104.

[3130] D. Schmeisser, K. Jacobi, Reaction of oxygen with gallium surfaces, Surf. Sci. 108 (1981) 421–434.

[3131] S. Saito, T. Maeda, Work function of ferromagnetic metals and alloys. I. Work function of Fe–Ni alloy system, Shinku (J. Vac. Soc. Jpn.) 24 (1981) 220–222 (Chem. Abstr. 95 (1981) 89651v).

[3132] W.-D. Schneider, C. Laubschat, Actinide–noble metal systems: An X–ray–photoelectron–spectroscopy study of thorium–platinum, uranium–platinum, and uranium–gold intermetallics, Phys. Rev. B 23 (1981) 997–1005.

[3133] G.C. Smith, C. Norris, C. Binns, H.A. Padmore, A photoemission study of ultra–thin palladium overlayers on low–index faces of silver, J. Phys. C 15 (1982) 6481–6496.

[3134] G.C. Smith, H.A. Padmore, C. Norris, The growth of Fe overlayers on Ag(100), Surf. Sci. 119 (1982) L287–L291.

[3135] A. Shih, G.A. Haas, C.R.K. Marrian, Preparation and oxidation of a thin Ba film, Appl. Surf. Sci. 16 (1983) 93–105.

[3136] M. Salmerón, S. Ferrer, M. Jazzar, G.A. Somorjai, Core– and valence–band energy–level shifts in small two–dimensional islands of gold deposited on Pt(100): The effect of step–edge, surface, and bulk atoms, Phys. Rev. B 28 (1983) 1158–1160.

[3137] X. Sun, M. Farjam, C.-W. Woo, Correlated–basis–functions theory of metal surfaces, Phys. Rev. B 28 (1983) 5599–5627.

[3138] M.L. Shek, P.M. Stefan, I. Lindau, W.E. Spicer, Photoemission study of the adsorption of Cu on Pt(111), Phys. Rev. B 27 (1983) 7277–7287.

[3139] Y.-M. Sun, H.S. Luftman, J.M. White, Potassium and coadsorbed potassium and deuterium on Ni(100), Surf. Sci. 139 (1984) 379–395.

[3140] X. Shen, D.J. Frankel, J.C. Hermanson, G.J. Lapeyre, R.J. Smith, Photoemission studies of ordered Pd overlayers on Au(111): Implications for CO chemisorption, Phys. Rev. B 32 (1985) 2120–2125.

[3141] D. Straub, et al., Unpublished (see Ref. [1124]).

[3142] S. Sendecki, Photoelectric and AES studies of the KCl vapour interaction with Ag(111), Surf. Sci. 165 (1986) 402–412.

[3143] J.M. Saleh, Field–emission studies of the adsorption of mercury on tungsten at 295 K, J. Physique 47 (1986) C7–111/C7–115.

[3144] I.T. Steinberger, K. Wandelt, Ionization energies of valence levels in physisorbed rare–gas multilayers, Phys. Rev. Lett. 58 (1987) 2494–2497.

[3145] M. Stampanoni, A. Vaterlaus, M. Aeschlimann, F. Meier, Magnetism of epitaxial bcc iron on Ag(001) observed by spin–polarized photoemission, Phys. Rev. Lett. 59 (1987) 2483–2485.

[3146] A. Stenborg, E. Bauer, Two–dimensional Yb on a Mo(110) surface, Phys. Rev. B 36 (1987) 5840–5847.

[3147] A. Stenborg, E. Bauer, The adsorption of Sm on a Mo(110) surface, Surf. Sci. 185 (1987) 394–412.

[3148] A. Stenborg, E. Bauer, Ordered structures of Yb and Sm on a Mo(110) surface, Surf. Sci. 189/190 (1987) 570–577.

[3149] V.M. Silkin, M.N. Zargar'yants, E.V. Chulkov, Electronic structure and the work function of thin films Al(001) and Al(001) + c(2×2)Na, Poverkhnost' (9) (1987) 59–64.

[3150] V.M. Silkin, E.V. Chulkov, Electronic structure of the Be(0001) surface, Poverkhnost' (4) (1987) 126–131.

[3151] M.B. Samsonova, V.G. Shnol, Electronic properties of (111) surfaces of silicon and germanium with one and three dangling bonds, Poverkhnost' (7) (1987) 145–149.

[3152] T.K. Sham, J. Hrbek, Electronic structure of Cs multilayer and monolayer adsorbed on Ru(001): A photoemission study, J. Chem. Phys. 89 (1988) 1188–1194.

[3153] S. Saito, T. Maeda, T. Soumura, K. Takeda, Temperature variation of the work function of sputter cleaned polycrystalline cobalt, Appl. Surf. Sci. 33/34 (1988) 1088–1093.

[3154] M. Stampanoni, A. Vaterlaus, D. Pescia, M. Aeschlimann, F. Meier, W. Dürr, S. Blügel, Lack of evidence for ferromagnetism in the vanadium monolayer on Ag(001), Phys. Rev. B 37 (1988) 10380–10382.

[3155] M. Surman, K.C. Prince, L. Sorba, A.M. Bradshaw, The influence of coadsorbed K on the electronic energy levels of chemisorbed CO, Surf. Sci. 206 (1988) L864–L870.

[3156] V.M. Silkin, I.Yu. Sklyadneva, E.V. Chulkov, Surface and subsurface electronic states of Al with adsorbed layers of H and Na, Poverkhnost' (1) (1989) 93–99.

[3157] M.A. Shevchenko, A.S. Shakirova, Emission characteristics of terbium and lutetium films on various faces of a tungsten single crystal, Sov. Phys.—Solid State 31 (1990) 1854–1855.

[3158] L.-A. Salmi, M. Persson, Electron resonances in alkali–metal overlayers on metals, Phys. Rev. B 39 (1989) 6249–6252.

[3159] J. Schott, Vibration spectroscopic investigations on metal–adsorbate systems with model relevance for electrochemistry (Ph.D. thesis), Techn. Univ. Berlin, 1990 (see Ref. [3172]).

[3160] M. Skottke-Klein, The semiconductor CsAu structure and electronic properties of thin films on Ru(001) (Ph.D. thesis), Freie Univ. Berlin, 1990 (see Ref. [2417]).

[3161] P. Shiller, A.B. Anderson, Effect of chemisorbed and substitutional 0, I, and II Ge, Sn, and Pb on CO adsorption on Pt(111): Molecular orbital theory, Surf. Sci. 236 (1990) 225–232.

[3162] S.A. Shakirova, M.A. Shevchenko, Adsorption of holmium atoms on the surfaces of a tungsten single crystal, Sov. Phys.—Solid State 32 (1990) 405–408.

[3163] S.A. Shakirova, V.A. Pleshkov, G.A. Rump, Adsorption of erbium atoms on the (110) faces of a single molybdenum crystal, Poverkhnost' (11) (1990) 40–45.

[3164] J.S. Suchorski, Surface diffusion of potassium on (100) and (111) germanium planes, Surf. Sci. 231 (1990) 130–134.

[3165] N.K. Singh, R.G. Jones, Mercury adsorption on Ni(111). I. Adsorption at room temperature and above, Surf. Sci. 232 (1990) 229–242.

[3166] N.K. Singh, R.G. Jones, Mercury adsorption on Ni(111). II. Adsorption at low temperatures, Surf. Sci. 232 (1990) 243–258.

[3167] I.Yu. Sklyadneva, E.V. Chulkov, Self–consistent calculation of the electronic structure of hafnium bulk and surface by the nonlinear pseudopotential method, Metallofiz. 12 (4) (1990) 38–43.

[3168] W. Schmickler, A model for the adsorption of metal ions on single crystal surfaces, Chem. Phys. 141 (1990) 95–104.

[3169] S. Sendecki, Temperature dependence of the photoemission threshold of the KCl–Ag system, Surf. Sci. 247 (1991) 294–298.

[3170] Yu. Sukhorski, Field desorption and surface diffusion of sodium on germanium (100) and (111) planes, Surf. Sci. 247 (1991) 346–351.

[3171] I.Yu. Sklyadneva, E.V. Chulkov, Self–consistent calculation of the electronic structure of hafnium(001) and tantalum(001) surfaces, Poverkhnost' (6) (1991) 29–35.

[3172] J.K. Sass, D. Lackey, J. Schott, B. Straehler, Electrochemical double layer simulations by halogen, alkali and hydrogen coadsorption with water on metal surfaces, Surf. Sci. 247 (1991) 239–247.

[3173] T. Solomun, H. Baumgärtel, K. Christmann, The interaction of nitriles with a potassium promoted gold(100) surface, J. Phys. Chem. 95 (1991) 10041–10049.

[3174] P.T. Sprunger, E.W. Plummer, An experimental study of the interaction of hydrogen with the Mg(0001) surface, Chem. Phys. Lett. 187 (1991) 559–564.

[3175] P.A. Serena, N. García, Studies of adsorption of alkali atoms on Al(111) as a function of coverage, Surf. Sci. 251/252 (1991) 866–871.

[3176] F. Solymosi, J. Kiss, K. Révész, Surface photochemistry: Adsorption and dissociation of CH_3Cl on clean and K–promoted Pd(100) surfaces, J. Chem. Phys. 94 (1991) 8510–8519.

[3177] R. Souda, W. Hayami, T. Aizawa, S. Otani, Y. Ishizawa, Charge state of potassium on metal and semiconductor surfaces studied by low–energy D^+ scattering, Phys. Rev. Lett. 69 (1992) 192–195.

[3178] N. Sato, Y. Saito, H. Shinohara, Threshold ionization energy of C_{60} in the solid state, Chem. Phys. 162 (1992) 433–438.

[3179] H.L. Skriver, N.M. Rosengaard, *Ab initio* work function of elemental metals, Phys. Rev. B 45 (1992) 9410–9412.

[3180] S. Schuppler, N. Fischer, Th. Fauster, W. Steinmann, Lifetime of image–potential states on metal surfaces, Phys. Rev. B 46 (1992) 13539–13547.

[3181] S.A. Shakirova, V.A. Pleshkov, G.A. Rump, Adsorption of rare–earth metals (Tb, Dy, Er) on a Mo(110) surface, Surf. Sci. 279 (1992) 113–118.

[3182] C. Su, X. Shi, D. Tang, D. Heskett, K.-D. Tsuei, Core–level photoemission and work–function investigation of Na on Cu(110), Phys. Rev. B 48 (1993) 12146–12150.

[3183] X. Shi, D. Tang, D. Heskett, K.-D. Tsuei, H. Ishida, Y. Morikawa, K. Terakura, Coverage–dependent core–level binding–energy shifts of alkali–metal atoms on metal surfaces, Phys. Rev. B 47 (1993) 4014–4017.

[3184] N. Safta, J.-P. Lacharme, C.A. Sébenne, Clean Si(110): A surface with intrinsic or extrinsic defects ? Surf. Sci. 287/288 (1993) 312–316.

[3185] X. Shi, D. Tang, D. Heskett, K.-D. Tsuei, H. Ishida, Y. Morikawa, Coverage–dependent core level photoemission investigations of Na/Cu(111) and Na/Ni(111), Surf. Sci. 290 (1993) 69–79.

[3186] H. Stolz, M. Höfer, H.-W. Wassmuth, TPD, AES, $\Delta\phi$ and LEED investigations of cesium adsorbed on Ag(100), Surf. Sci. 287/288 (1993) 564–567.

[3187] R. Souda, W. Hayami, T. Aizawa, Y. Ishizawa, Chemical analysis of alkali–metal adatoms using low–energy D^+ scattering, Phys. Rev. B 48 (1993) 17255–17261.

[3188] R. Souda, W. Hayami, T. Aizawa, Y. Ishizawa, Low–energy D^+ scattering from clean and alkalated $TiO_2(110)$ surfaces, Surf. Sci. 285 (1993) 265–274.

[3189] R. Souda, W. Hayami, T. Aizawa, Y. Ishizawa, Low–energy D^+ scattering from Cs and CsCl adsorbed on the Si(100)2×1 surface, Surf. Sci. 290 (1993) 245–254.

[3190] B. Schleicher, H. Burtscher, H.C. Siegmann, Photoelectric quantum yield of nanometer metal particles, Appl. Phys. Lett. 63 (1993) 1191–1193.

[3191] R. Souda, W. Hayami, T. Aizawa, S. Otani, Y. Ishizawa, Potassium adsorption on metal and semiconductor surfaces studied by low–energy D^+ scattering, Phys. Rev. B 47 (1993) 6651–6660.

[3192] S. Saito, K. Takeda, T. Soumura, M. Ohki, T. Tani, T. Maeda, Hysteresis of the work function of Co(0001) surface resulting from an allotropic transformation, J. Appl. Phys. 71 (1992) 5500–5503.

[3193] S. Saito, K. Takeda, T. Soumura, T. Tani, T. Maeda, Effects of surface roughness and patches on the work function of cobalt, Phys. Status Solidi (a) 142 (1994) K29–K32.

[3194] L. Szunyogh, B. Újfalussy, P. Weinberger, J. Kollár, The self–consistent fully relativistic SKKR Green function method: Application to the (100), (110) and (111) surfaces of Au and Pt, J. Phys. Cond. Matt. 6 (1994) 3301–3306.

[3195] Z. Szczudło, K. Sendecka, W. Gubernator, A. Ciszewski, Adsorption and nucleation of hafnium on facets and stepped surface areas of tungsten, Vacuum 45 (1994) 263–266.

[3196] K. Sakamoto, T. Okuda, H. Nishimoto, H. Daimon, S. Suga, T. Kinoshita, A. Kakizaki, Photoemission study of the Si(111)3×1–K surface, Phys. Rev. B 50 (1994) 1725–1732.

[3197] U. Schneider, H. Busse, R. Linke, G.R. Castro, K. Wandelt, Interaction properties of molecules with binary alloy surfaces, J. Vac. Sci. Technol. A 12 (1994) 2069–2073.

[3198] M. Schmidt, H. Wolter, M. Nohlen, K. Wandelt, Work–function oscillations during Cu film growth on an oxygen precovered Ru(0001) surface: A basically old technique as a powerful film growth monitor, J. Vac. Sci. Technol. A 12 (1994) 1818–1824.

[3199] A. Siokou, S. Kennou, S. Ladas, An XPS and WF study of the Er/Si(100) interface formation, Surf. Sci. 331–333 (1995) 580–584.

[3200] R. Stumpf, P.J. Feibelman, Interaction of hydrogen with the Be(0001) surface, Phys. Rev. B 51 (1995) 13748–13759.

[3201] T.P. Smereka, S.I. Stepanovskii, R.R. Kamenetskii, The common adsorption of rare–earth elements and oxygen on certain faces of tungsten crystal, Vacuum 46 (1995) 425–427.

[3202] S.L.M. Schroeder, A. Neumann, T. Solomun, P. Lenz-Solomun, K. Christmann, Potassium–induced reconstructive phase transitions on Au(100), Surf. Sci. 337 (1995) 285–293.

[3203] R. Stumpf, M. Scheffler, *Ab initio* calculations of energies and self–diffusion on flat and stepped surfaces of Al and their implications on crystal growth, Phys. Rev. B 53 (1996) 4958–4973.

[3204] R. Shimizu, S. Lee, A new development in high–temperature surface materials: Thermal field emitter of Zr–O/W(100), Oyo Buturi 65 (1996) 251–255.

[3205] T. Sumi, Y. Sakai, E. Miyoshi, Molecular–orbital study of Li and LiOH adsorption on a Cu(001) surface. II. Cluster–model calculations with image charges, Phys. Rev. B 55 (1997) 4755–4760.

[3206] Y.G. Shen, D.J. O'Connor, R.J. MacDonald, Combined ion scattering, electron diffraction and work function change study on growth, alloying and initial oxygen adsorption of ultrathin Al films in Pd(001), J. Phys. Cond. Matt. 9 (1997) 9459–9467.

[3207] R. Steinke, M. Hoffmann, M. Böhmisch, J. Eisenmenger, K. Dransfeld, P. Leiderer, Potentiometry with the acoustic near field microscope: A new method for microscopy of surface potentials, Appl. Phys. A 64 (1997) 19–27.

[3208] M. Seidl, J.P. Perdew, M. Brajczewska, C. Fiolhais, Ionization energy and electron affinity of a metal cluster in the stabilized jellium model: Size effect and charging limit, J. Chem. Phys. 108 (1998) 8182–8189.

[3209] Y.G. Shen, D.J. O'Connor, J. Yao, The adsorption of Al on Pd(001) and of O and CO on an interfacial Al–alloyed Pd(001) surface, Appl. Surf. Sci. 125 (1998) 300–312.

[3210] S. Stepanowskyi, I. Ubogyi, J. Kołaczkiewicz, Ultrathin films of Pd and Pt on the molybdenum(211) face, Surf. Sci. 411 (1998) 176–185.

[3211] R. Saradha, M.V. Sangaranarayanan, Crystal face specificity of electronic and electrochemical properties of a neutral interface: Analysis using density functional theory and the Bethe approximation, J. Phys. Chem. B 102 (1998) 5099–5106.

[3212] R. Schlaf, B.A. Parkinson, P.A. Lee, K.W. Nebesny, G. Jabbour, B. Kippelen, N. Peyghambarian, N.R. Armstrong, Photoemission spectroscopy of LiF coated Al and Pt electrodes, J. Appl. Phys. 84 (1998) 6729–6736.

[3213] R.B. Sharma, P.W. Yawalkar, N. Pradeep, D.S. Joag, Adsorption of nickel on tungsten: A probe–hole field emission microscopy study, Ultramicroscopy 73 (1998) 99–106.

[3214] C.G. Sánchez, M.G. Del Pópolo, E.M.P. Leiva, An embedded atom approach to underpotential deposition phenomena, Surf. Sci. 421 (1999) 59–72.

[3215] Ch. Sommerhalter, Th.W. Matthes, Th. Glatzel, A. Jäger-Waldau, M.Ch. Lux-Steiner, High–sensitivity quantitative Kelvin probe microscopy by noncontact ultra–high–vacuum atomic force microscopy, Appl. Phys. Lett. 75 (1999) 286–288.

[3216] S. Suzuki, F. Maeda, Y. Watanabe, T. Ohno, Work function changes of GaAr surfaces induced by Se treatment, Japan. J. Appl. Phys. 38 (1999) 5847–5850.

[3217] C. Sánchez, E.M.P. Leiva, Cu underpotential deposition on Au(111) and Au(100). Can this be explained in terms of the energetics of the Cu/Au system ? Electrochim. Acta 45 (1999) 691–697.

[3218] R. Schletti, P. Wurz, T. Fröhlich, Metallic work function measurement in the range 2—2.33 eV using a blue light–emitting diode source, Rev. Sci. Instrum. 71 (2000) 499–503.

[3219] V. Saltas, C.A. Papageorgopoulos, Adsorption of Li on Ni(110) surfaces at low and room temperature, Surf. Sic. 461 (2000) 219–230.

[3220] I. Sarria, C. Henriques, C. Fiolhais, J.M. Pitarke, Slabs of stabilized jellium: Quantum–size and self–compression effects, Phys. Rev. B 62 (2000) 1699–1705.

[3221] C. Shen, A. Kahn, Electronic structure, diffusion, and *p*–doping at the Au/F$_{16}$CuPc interface, J. Appl. Phys. 90 (2001) 4549–4554.

[3222] Z. Szczudło, A. Ciszewski, Y.B. Losovyj, Field electron emission study of Ti and Hf adsorption layers on W, Appl. Surf. Sci. 174 (2001) 138–147.

[3223] S. Suzuki, Y. Watanabe, T. Kiyokura, K.G. Nath, T. Ogino, S. Heun, W. Zhu, C. Bower, O. Zhou, Electronic structure at carbon nanotube tips studied by photoemission spectroscopy, Phys. Rev. B 63 (2001) 245418/1–7.

[3224] S.A. Surma, Correlation of electron work function and surface–atomic structure of some d transition metals, Phys. Status Solidi (a) 183 (2001) 307–322.

[3225] S. Suzuki, Y. Watanabe, T. Kiyokura, K.G. Nath, T. Ogino, S. Heun, W. Zhu, C. Bower, O. Zhou, Effects of air exposure and Cs deposition on the electronic structure of multiwalled carbon nanotubes, Surf. Rev. Lett. 9 (2002) 431–435.

[3226] M.J.S. Spencer, A. Hung, I.K. Snook, I. Yarovsky, Sulfur adsorption on Fe(110): A DFT study, Surf. Sci. 540 (2003) 420–430.

[3227] T. Sakata, M. Masutani, A. Sakai, The work function reduction of the Pt field emitter, Surf. Sci. 542 (2003) 205–210.

[3228] M. Shiraisi, K. Shibata, R. Maruyama, M. Ata, Electronic structures of fullerenes and metallofullerenes studied by surface potential analysis, Phys. Rev. B 68 (2003) 235414/1–5.

[3229] S. Suzuki, F. Maeda, Y. Watanabe, T. Ogino, Electronic structure of single–walled carbon nanotubes encapsulating potassium, Phys. Rev. B 67 (2003) 115418/1–6.

[3230] A. Sinsarp, Y. Yamada, M. Sasaki, S. Yamamoto, Microscopic study on the work function reduction induced by Cs–adsorption, Japan. J. Appl. Phys. 42 (2003) 4882–4886.

[3231] S. Satoh, H. Nakane, H. Adachi, Predominant field emission from Mo(100) due to surface modification with ZrO$_2$, Shinku (J. Vac. Soc. Jpn.) 47 (2004) 143–146.

[3232] R. Szukiewicz, J. Kołaczkiewicz, Thermal stability of the Ta(111) surface covered with Pd, Vacuum 74 (2004) 55–68.

[3233] S. Suzuki, Y. Watanabe, T. Ogino, Y. Homma, D. Takagi, S. Heum, L. Gregoratti, A. Barinov, M. Kiskinova, Observation of single–walled carbon nanotubes by photoemission microscopy, Carbon 42 (2004) 559–563.

[3234] E. Schröder, R. Fasel, A. Kiejna, O adsorption and incipient oxidation of the Mg(0001) surface, Phys. Rev. B 69 (2004) 115431/1–8.

[3235] J.K. Schaeffer, L.R.C. Fonseca, S.B. Samavedam, Y. Liang, P.J. Tobin, B.E. White, Contributions to the effective work function of platinum on hafnium dioxide, Appl. Phys. Lett. 85 (2004) 1826–1828.

[3236] M.J.S. Spencer, I.K. Snook, I. Yarovsky, Coverage–dependent adsorption of atomic sulfur on Fe(110): A DFT study, J. Phys. Chem. B 109 (2005) 9604–9612.

[3237] S.A. Shakirova, E.V. Serova, Production of the two–dimensional submonolayer Gd silicides on the W(001) plane: A field emission study, Surf. Sci. 600 (2006) 4365–4368.

[3238] S. Schramm, S. Dantscher, C. Schramm, O. Autzen, C. Wesenberg, E. Hasselbrink, W. Pfeiffer, Photoinduced interface charging in multiphoton photoemission from ultrathin Ag films on Si(100), Appl. Phys. A 88 (2007) 459–464.

[3239] W.S. Su, T.C. Leung, B. Li, C.T. Chan, Work function of small radius carbon nanotubes and their bundles, Appl. Phys. Lett. 90 (2007) 163103/1–3.

[3240] W.S. Su, T.C. Leung, C.T. Chan, Work function of single–walled and multiwalled carbon nanotubes: First–principles study, Phys. Rev. B 76 (2007) 235413/1–8.

[3241] S.J. Sferco, P. Blaha, K. Schwarz, Deep multilayer relaxations on the Al(001) surface: *Ab initio* all–electron calculations, Phys. Rev. B 76 (2007) 075428/1–15.

[3242] H.-Z. Song, P. Zhang, X.-G. Zhao, First–principles calculation of Be(0001) thin films: Quantum size effect and adsorption of atomic hydrogen, Acta Phys. Sin. 56 (2007) 465–472.

[3243] H. Sa'adi, B. Hamad, First–principles investigations of iridium low index surfaces, J. Phys. Chem. Solids 69 (2008) 2457–2464.

[3244] G. Santarossa, A. Vargas, M. Iannuzzi, C.A. Pignedoli, D. Passerone, A. Baiker, Modeling bulk and surface Pt using the "Gaussian and plane wave" density functional theory formalism: Validation and comparison to *k*–point plane wave calculations, J. Chem. Phys. 129 (2008) 234703/1–12.

[3245] F. Saad, M. Zemirli, M. Benakki, S. Bouarab, *Ab–initio* study of the coadsorption of Li and H on Pt(001), Pt(110) and Pt(111) surfaces, Physica B 407 (2012) 698–704.

[3246] E.J. Spadafora, K. Saint-Aubin, C. Celle, R. Demadrille, B. Grévin, J.-P. Simonato, Work function tuning for flexible transparent electrodes based on functionalized metallic single walled carbon nanotubes, Carbon 50 (2012) 3459–3464.

[3247] S. Taubes, Determination of the photoelectric long wave limit of mercury, Ann. Phys. 76 (1925) 629–721.

[3248] J.B. Taylor, I. Langmuir, Evaporation of atoms, ions and electrons from caesium films on tungsten, Phys. Rev. 44 (1933) 423–458.

[3249] L.P. Thein, Photoelectric sensitization of aluminum, Phys. Rev. 52 (1937) 245.

[3250] L.P. Thein, The photoelectric sensitization of aluminum, Phys. Rev. 53 (1938) 287–292.

[3251] E. Taft, L. Apker, Photoelectric determination of the Fermi level at surfaces of amorphous arsenic, Phys. Rev. 75 (1949) 344.

[3252] E. Taft, L. Apker, Photoelectric determination of the Fermi level at amorphous arsenic surfaces, Phys. Rev. 75 (1949) 1181–1182.

[3253] E. Taft, Private comm. (see Ref. [1765]).

[3254] E. Taft, L. Apker, Photoemission from cesium and rubidium tellurides, J. Opt. Soc. Amer. 43 (1953) 81–83.

[3255] E. Taft, L. Apker, Fermi level in amorphous antimony films, Phys. Rev. 96 (1954) 1496–1497.

[3256] B.M. Tsarev, Kontaktnaya Raznost' Potentsialov (Contact Potential Difference) GITTL, Moscow, 1955 (see Refs. [1354,3543]).

[3257] B.M. Tsarev, Proc. Conf. SHF Electronics, 1959, p. 236 (see Refs. [12,190]).

[3258] M.C. Teich, J.M. Schroeer, G.J. Wolga, Double quantum photoelectric emission from sodium metal, Phys. Rev. Lett. 13 (1964) 611–614.

[3259] E.A. Tishin, B.M. Tsarev, Problem of the existence of a work–function minimum for film cathodes, Sov. Phys.—Solid State 8 (1967) 2547–2551.

[3260] M.C. Teich, G.J. Wolga, Work–function estimation with a single yield measurement, J. Opt. Soc. Amer. 57 (1967) 542–543.

[3261] E.A. Tishin, B.M. Tsarev, Contact potential difference of double–layer Ba and Au films on Nb, Sov. Phys.—Solid State 10 (1969) 1719–1720.

[3262] M.J. Turner, E.H. Rhoderick, Metal–silicon Schottky barriers, Solid State Electronics 11 (1968) 291–300.

[3263] E.A. Tishin, B.M. Tsarev, Contact potential of double layers, Sov. Phys.—Solid State 11 (1969) 931–934.

[3264] S. Trasatti, Work function, electronegativity, and electrochemical behaviour of metals. II. Potentials of zero charge and "electrochemical" work functions, J. Electroanal. Chem. Interfacial Electrochem. 33 (1971) 351–378.

[3265] S. Trasatti, Work function, electronegativity, and electrochemical behaviour of metals. I. Selection of experimental values for the work function, Chim. Ind. (Milan) 53 (1971) 559–564 (Chem. Abstr. 75 (1971) 92260j) (see Ref. [3264]).

[3266] R.E. Thomas, G.A. Haas, Diffusion measurements in thin films utilizing work function changes: Cr into Au, J. Appl. Phys. 43 (1972) 4900–4907.

[3267] S. Trasatti, Electronegativity, work function, and heat of adsorption of hydrogen on metals, J. Chem. Soc. Faraday Trans. I 68 (1972) 229–236.

[3268] S. Trasatti, Oparative (electrochemical) work function of gold, Electroanal. Chem. Interf. Electrochem. 54 (1974) 19–24.

[3269] Y. Teisseyre, R. Coelho, R. Haug, Photo–stimulated field emission of barium–coated tungsten, Surf. Sci. 52 (1975) 120–124.

[3270] A. Thanailakis, A. Rasul, Transition–metal contacts to atomically clean silicon, J. Phys. C 9 (1976) 337–343.

[3271] E.A. Tishin, Temperature dependence of the work function of a W–Th film, Sov. Phys. Tech. Phys. 21 (1976) 619–621.

[3272] N. Tallaj, M. Buyle-Bodin, Work function measurements on germanium by thermionic emission, Surf. Sci. 69 (1977) 428–436.

[3273] C. Tejedor, Theoretical analysis of (100) and (111) faces of copper, J. Phys. F 7 (1977) 991–997.

[3274] N. Tallaj, Gas effect on surface states and work function of germanium by thermionic emission and longitudinal conduction method, Ned. Tijdschr. Vacuumtech. 16 (1978) 244–245 (Chem. Abstr. 89 (1978) 98448n).

[3275] R.E. Thomas, T. Pankey, J.W. Gibson, G.A. Haas, Thermionic properties of BaO on iridium, Appl. Surf. Sci. 2 (1979) 187–212.

[3276] K. Takayanagi, D.M. Kolb, K. Kambe, G. Lehmpfuhl, Deposition of monolayer and bulk lead on Ag(111) studied in vacuum and in electrochemical cell, Surf. Sci. 100 (1980) 407–422.

[3277] A.Ya. Tontegode, N.A. Kholin, Auger electron spectroscopy and thermoemission study of high–temperature adsorption of carbon and benzene on (111) and (100) faces of iridium, Poverkhnost' (1) (1983) 41–50.

[3278] H. Tochihara, Electronic excitations in K monolayer adsorbed on Si(100)2×1, Surf. Sci. 126 (1983) 523–528.

[3279] A. Taleb-Ibrahimi, C.A. Sébenne, D. Bolmont, P. Chen, Electronic properties of cleaved Si(111) upon room–temperature deposition of Au, Surf. Sci. 146 (1984) 229–240.

[3280] S. Trasatti, Prediction of double layer parameters: The case of silver, J. Electroanal. Chem. 172 (1984) 27–48.

[3281] A. Taleb-Ibrahimi, C.A. Sébenne, F. Proix, P. Maigne, Adsorption of Sn on cleaved Si(111) surfaces, Surf. Sci. 163 (1985) 478–488.

[3282] A. Taleb-Ibrahimi, V. Mercier, C.A. Sébenne, D. Bolmont, P. Chen, Effect of Cu deposition on structural and electronic properties of cleaved Si(111) surfaces, Surf. Sci. 152/153 (1985) 1228–1238.

[3283] G.S. Tompa, W.E. Carr, M. Seidl, Cesium coverage on molybdenum due to cesium ion bombardment, Appl. Phys. Lett. 48 (1986) 1048–1050.

[3284] D. Tománek, S.G. Louie, C.-T. Chan, *Ab initio* calculation of coverage–dependent adsorption properties of H on Pd(001), Phys. Rev. Lett. 57 (1986) 2594–2597.

[3285] A. Taleb-Ibrahimi, C.A. Sébenne, Effect of valency in metal adsorption on Si(111): The case of Sb on the cleaved surface, Surf. Sci. 168 (1986) 114–121.

[3286] G.S. Tompa, M. Seidl, W.C. Ermler, W.E. Carr, Work function of cesium–covered polycrystalline beryllium, Surf. Sci. 185 (1987) L453– L458.

[3287] M. Tikhov, M. Stolzenberg, E. Bauer, New type of two–dimensional phase transition, Phys. Rev. B 36 (1987) 8719–8724.

[3288] M. Tikhov, E. Bauer, Unpublished (see Ref. [2656]).

[3289] G.S. Tompa, W.E. Carr, M. Seidl, Work function of metallic surfaces bombarded with cesium ions, Surf. Sci. 198 (1988) 431–448.

[3290] M. Tikhov, E. Bauer, The interaction of Pb and Sn with the Mo(110) surface, Surf. Sci. 203 (1988) 423–448.

[3291] A. Dal Corso, Clean Ir(111) and Pt(111) electronic surfaces states: A first–principle fully relativistic investigation, Surf. Sci. 637–638 (2015) 106–115.

[3292] A.Ya. Tontegode, Mechanism for interaction of graphite islands on metal surfaces, Sov. Tech. Phys. Lett. 15 (1989) 271–272.

[3293] M. Tikhov, E. Bauer, Growth, structure and energetics of ultrathin ferromagnetic single crystal films on Mo(110), Surf. Sci. 232 (1990) 73–91.

[3294] M. Tikhov, G. Boishin, L. Surnev, Sodium adsorption on a Si(001)–(2×1) surface, Surf. Sci. 241 (1991) 103–110.

[3295] D. Tang, D. McIlroy, X. Shi, C. Su, D. Heskett, The structure of Na overlayers on Cu(111) at room temperature, Surf. Sci. 255 (1991) L497–L503.

[3296] K.-D. Tsuei, D. Heskett, A.P. Baddorf, E.W. Plummer, Electron loss spectra from thin alkali films on Al(111), J. Vac. Sci. Technol. A 9 (1991) 1761–1768.

[3297] H. Tochihara, S. Mizuno, A coverage–dependent reaction of Li adatoms on Cu(001) with H$_2$O, Chem. Phys. Lett. 194 (1992) 51–56.

[3298] H. Tochihara, S. Mizuno, Observation of anomalous LEED patterns from Li adsorbed Cu(001): 2×1, 3×3 and 4×4, Surf. Sci. 279 (1992) 89–98.

[3299] T. Tachibana, B.E. Williams, J.T. Glass, Correlation of the electrical properties of metal contacts on diamond films with the chemical nature of the metal–diamond interface. II. Titanium contacts: A carbide–forming metal, Phys. Rev. B 45 (1992) 11975–11981.

[3300] R.T. Howe, J.K. Nørskov, P.A. Pianetta, Using first–principles simulations to discover materials with ultra–low work functions for energy conversion applications, Prog. Rep. (2012) 10 pp.

[3301] C. Tomas, J.P. Giardeau-Montaut, M. Afif, M. Romand, M. Charbonnier, C. Giardeau-Montaut, Photoemission monitored cleaning of pure and implanted tungsten photocathodes by picosecond UV laser, Appl. Surf. Sci. 109/110 (1997) 509–513.

[3302] C. Tomas, T. Ossowski, J. Kołaczkiewicz, Growth and thermal stability of Fe and Ni adsorption layers on the (111) Ta crystal face, Surf. Sci. 494 (2001) 183–196.

[3303] O.M.N.D. Teodoro, J. Los, A.M.C. Moutinho, Anomalos growth of Ba on Ag(111), J. Vac. Sci. Technol. A 20 (2002) 1379–1383.

[3304] Q.-L. Tang, Z.-X. Chen, Density functional slab model studies of water adsorption on flat and stepped Cu surfaces, Surf. Sci. 601 (2007) 954–964.

[3305] Y.-F. Tzeng, Y.-C. Lee, C.-Y. Lee, I.-N. Lin, H.-T. Chiu, On the enhancement of field emission performance of ultrananocrystalline diamond coated nanoemitters, Appl. Phys. Lett. 91 (2007) 063117/1–3.

[3306] H. Tollefsen, L.J. Berstad, S. Raaen, Characterization of Ce–Pd(111) and Ce–Pd(110) surface alloys, J. Vac. Sci. Technol. A 25 (2007) 1433–1437.

[3307] C. Tomas, S. Stepanovski, Sz. Klein, J. Śliwiński, J. Kołaczkiewicz, The adsorption of Ni on the Mo(111) crystal face, Vacuum 83 (2009) 1368–1375.

[3308] N. Underwood, The photoelectric properties of the (100) and (111) faces of a single copper crystal, Phys. Rev. 47 (1935) 502–505.

[3309] S. Usami, The surface potential of carbon monoxide on the single crystal surfaces of tungsten, J. Phys. Soc. Japan 30 (1971) 1076–1082.

[3310] K. Ueda, R. Shimizu, An apparatus for simultaneous LEED and photoelectric work function measurements, Technol. Rep. Osaka Univ. 22 (1972) 419–427.

[3311] K. Ueda, R. Shimizu, Initial oxidation studies on Fe(100) by means of photoelectric work function measurements combined with Auger electron spectroscopy, Surf. Sci. 43 (1974) 77–87.

[3312] C.A. Utreras-Diaz, Metallic surfaces in the Thomas–Fermi–von Weizsäcker approach: Self–consistent solution, Phys. Rev. B 36 (1987) 1785–1788.

[3313] M. Uda, A. Nakamura, T. Yamamoto, Y. Fujimoto, Work function of polycrystalline Ag, Au and Al, J. Electron Spectrosc. Relat. Phenom. 88–91 (1998) 643–648.

[3314] I. Ubogyi, J. Kołaczkiewicz, Growth and thermal stability of Pd and Pt adsorption layers on the Ta(211) face, Vacuum 49 (1998) 145–151.

[3315] M. Uda, Y. Nakagawa, T. Yamamoto, M. Kawasaki, A. Nakamura, T. Saito, K. Hirose, Successive change in work function of Al exposed to air, J. Electron Spectrosc. Relat. Phenom. 88–91 (1998) 767–771.

[3316] I. Ubogyi, S. Stepanovskyi, J. Kołaczkiewicz, Yb adsorption on the (211) faces of molybdenum and tantalum, Phys. Rev. B 61 (2000) 11097–11104.

[3317] Y. Umeno, C. Elsässer, B. Meyer, P. Gumbsch, M. Nothacker, J. Weissmüller, F. Evers, *Ab initio* study of surface stress response to charging, Europhys. Lett. 78 (2007) 13001/1–5.

[3318] R.M. Vasenin, The work of electron emission, Nauch. Tr. Moskov. Tekhnol. Inst. Legkoĭ Prom. (11) (1958) 208–228 (Chem. Abstr. 55 (1961) 15140c).

[3319] J. van Laar, J.J. Scheer, Photoelectric determination of the electron work function of indium, Philips Res. Repts. 15 (1960) 1–6.

[3320] Yu.S. Vedula, V.M. Gavrilyuk, V.K. Medvedev, Concerning the effect of electron bombardment on the adsorption properties of tungsten surfaces, Sov. Phys.—Solid State 4 (1963) 1870–1872.

[3321] I.M. Vesel'nitskii, A vacuum photocell with a tellurium cathode for ultraviolet radiation, Prib. Tekh. Eksp. 10 (6) (1965) 157–159 (Chem. Abstr. 64 (1966) 15193a).

[3322] G.J.M. van der Velden, Private comm. (see Ref. [3536]).

[3323] V.B. Voronin, Work function of the adsorption system scandium–tungsten, Sov. Phys.—Solid State 9 (1968) 1758–1761.

[3324] P. Vernier, E. Coquet, E. Boursey, Variations in the work function of gold with the crystallographic face, C. R. Acad. Sci. Paris B 264 (1967) 986–989.

[3325] R.C. Vehse, J.L. Stanford, E.T. Arakawa, Discrete energy losses by photoexcited electrons in silver and palladium, Phys. Rev. Lett. 19 (1967) 1041–1044.

[3326] I. Vacz, The work functions of tungsten wires made with various ingredients, Acta. Tech. Acad. Sci. Hung. 59 (1967) 311–324 (Chem. Abstr. 68 (1968) 117897t).

[3327] G.G. Vladimirov, Desorption of titanium from tungsten in a strong electric field, Sov. Phys.—Solid State 10 (1968) 957–962.

[3328] P. Vernier, E. Coquet, E. Boursey, Photoelectric emission of thin films, J. Physique 29 (1968) C2–53/C2–58.

[3329] V.B. Voronin, A.G. Naumovets, Electron and adsorption properties of the scandium films on the (110) face of tungsten, Ukr. Fiz. Zh. 13 (1968) 1389–1393 (Chem. Abstr. 69 (1968) 99788x).

[3330] P. Vernier, E. Coquet, E. Boursey, New data on photoelectric emission obtained with the Lallemand electronic camera, Czech. J. Phys. B 19 (1969) 918–922 (Chem. Abstr. 71 (1969) 34357c).

[3331] M.A. Vakhabova, Thermoelectronic emission from (110) and (111) faces of a large single crystal of Mo, Nauch. Tr. Bukh. Ped. Inst. 18 (1969) 302–309 (see Refs. [1354,3348]).

[3332] P. Vernier, M. Pauty, F. Pauty, A new method for measuring energy distribution of photoelectrons: Application to complex Au–Cs films, J. Vac. Sci. Technol. 6 (1969) 743–745.

[3333] J. van Laar, J.J. Scheer, Influence of band bending on photoelectric emission from silicon single crystals, Philips Res. Rep. 17 (1962) 101–124.

[3334] G.G. Vladimirov, B.K. Medvedev, I.L. Sokol'skaya, Migration of Ti on tungsten in strong electric fields, Sov. Phys.—Solid State 12 (1970) 413–416.

[3335] V.B. Voronin, A.G. Naumovets, Adsorption of yttrium atoms on a tungsten single crystal, Izv. Akad. Nauk SSSR, Ser. Fiz. 35 (1971) 355–358.

[3336] Th.G.J. van Oirschot, W.M.H. Sachtler, Photoelectric emission from vapour quenched and annealed sodium films, Surf. Sci. 27 (1971) 611–624.

[3337] Th.G.J. van Oirschot, M. van der Brink, W.M.H. Sachtler, Phtoelectric emission and phase transitions of evaporated metastable sodium, potassium and sodium–potassium alloy films, Surf. Sci. 29 (1972) 189–202.

[3338] M. von Bradke, Work function measurements at simulated collector conditions of thermionic diodes, in: Proc. 3rd Int. Conf. Thermion. Electr. Power Generat. Jülich, Vol. 3, 1972, pp. 1435–1444.

[3339] U. von Barth, L. Hedin, A local exchange–correlation potential for the spin polarized case: I, J. Phys. C 5 (1972) 1629–1642 (see Refs. [719,1201]).

[3340] V.B. Voronin, A.G. Naumovets, A.G. Fedorus, Connection between the work function and the thickness of a cesium film adsorbed on the (100) face of tungsten, JETP Lett. 15 (1972) 370–371.

[3341] Yu.S. Vedula, Yu.M. Konoplev, V.K. Medvedev, A.G. Naumovets, T.P. Smereka, A.G. Fedorus, Work function, thermal stability and atomic structure of electropositive films adsorbed on metallic monocrystals, in: Proc. 3rd. Int. Conf. Thermion. Electr. Power Generat. Jülich, Vol. 3 (1972), pp. 1351–1360.

[3342] N.V. Volkov, Yu.K. Gus'kov, Z.N. Kononova, Yu.I. Kostikov, Field emission of tungsten coated with a selenium film, in: Kratk. Soderzh. Dokl.-Vses. Konf. Emiss. Elektron, 15th, vol. 1, 1973, p. 84 (Chem. Abstr. 83 (1975) 187041t).

[3343] G. Venkatachalam, M.K. Sinha, Adsorption of silicon on molybdenum in a field emission microscope, Surf. Sci. 44 (1974) 157–169.

[3344] M.A. Vakhabova, R.Ya. Kamilova, Thermionic emission from an etched surface of (110), (100) and (111) faces of a large molybdenum crystal, Izv. Akad. Nauk Uzb.SSR, Ser. Fiz.-Mat. Nauk 19 (5) (1975) 57–59.

[3345] M.I. Vass, Cr. Contescu, FEM study of silver layers adsorbed on tungsten: I. Work function and surface migration, Rev. Roum. Chim. 20 (1975) 1253–1265 (see Ref. [3280]).

[3346] G.G. Vladimirov, Yu.V. Zubenko, Kh.O. Kuchkarov, Adsorption of iron and cobalt atoms on tungsten, Vestn. Leningr. Univ. Fiz. Khim. (3) (1976) 87–91 (Chem. Abstr. 85 (1976) 182822e).

[3347] M.A. Vakhabova, E.P. Sytaya, Study of changes in electronic emission and structure of the surface of (110) faces of Ta and Nb single crystals during different heat treatments, Nauchn. Tr., Tashk. Gos. Univ. 499 (1976) 48–50.

[3348] M.A. Vakhabova, E.P. Sytaya, Change in the electron emission of molybdenum single crystal faces during different heat treatments, Izv. Akad. Nauk Uzb.SSR, Ser. Fiz.-Mat. Nauk (6) (1976) 49–52.

[3349] B.P. Varaksin, A.S. Titkov, Arc regime of a thermionic converter with different tungsten emitters, Sov. Phys. Tech. Phys. 21 (1976) 957–960.

[3350] Yu.S. Vedula, V.V. Gonchar, A.G. Naumovets, A.G. Fedorus, Influence of the electron structure of the substrate on the properties of metal film systems, Sov. Phys.—Solid State 19 (1977) 1505–1509.

[3351] Yu.S. Vedula, Influence of oxygen on emission–adsorption properties of lanthanum metal systems, Sov. Tech. Phys. Lett. 3 (1977) 47–48.

[3352] V.M. Volkov, The electron work functions and surface potentials of metals, Russ. J. Phys. Chem. 52 (1978) 1394–1396.

[3353] M.A. Vakhabova, Z.L. Fedorenko, Study of the electron emission properties and surface structures of the principal faces of refractory metals during different heat treatments, Nauchn. Tr., Tashk. Gos. Univ. 550 (1978) 64–67 (Chem. Abstr. 90 (1979) 213899v).

[3354] G.F. Voronina, L. Larin, T.V. Kalish, Effect of chemisorbed hydrogen on the electron work function of a platinum, Elektokhim. 14 (1978) 297–299.

[3355] M.A. van Hove, Surface crystallography and bonding, in: T.N. Rhodin, G. Ertl (Eds.), The Nature of the Surface Chemical Bond, Elsevier, Amsterdam, 1979, pp. 275–311 (see Ref. [1909]).

[3356] S.H. Vosko, L. Wilk, M. Nusair, Accurate spin–dependent electron liquid correlation energies for local spin density calculations: A critical analysis, Canad. J. Phys. 58 (1980) 1200–1211 (see Refs. [1086,1201,3452]).

[3357] M.A. Vakhabova, E.P. Sytaya, Study of thermoemission properties and structure of the surface of (111) and (110) faces of tungsten, molybdenum, and niobium in heat treatment by alternating and direct currents in a variable vacuum, Izv. Akad. Nauk Uzb.SSR, Ser. Fiz.-Mat. Nauk (5) (1980) 52–54 (Chem. Abstr. 94 (1981) 40126t).

[3358] G. Valette, Hydrophilicity of metal surfaces: Silver, gold and copper electrodes, J. Electroanal. Chem. 139 (1982) 285–301.

[3359] J.C. Vickerman, K. Christmann, G. Ertl, P. Heimann, F.J. Himpsel, D.E. Eastman, Geometric structure and electronic states of copper films on a ruthenium(0001) surface, Surf. Sci. 134 (1983) 367–388.

[3360] M.A. Vakhabova, E.P. Sytaya, Heterogeneous emissions from a tantalum(111) crystal face, Izv. Akad. Nauk Uzb.SSR, Ser. Fiz.-Mat. Nauk (1) (1986) 71 (Chem. Abstr. 104 (1986) 198209g).

[3361] Yu.S. Vedula, V.V. Poplavskiĭ, Layer–by–layer growth of lithium films on tungsten and molybdenum (011) faces: Manifestations in the work function, JETP Lett. 46 (1987) 230–233.

[3362] Yu.Kh. Vekilov, G.R. Umarov, A.A. Firsanov, Influence of cesium on the electronic spectrum of the surface and the work function of silicon, Sov. Phys. Tech. Phys. 32 (1987) 237.

[3363] G. Valette, Silver–water interactions: Part I. Model of the inner layer at the metal/water interface, J. Electroanal. Chem. 230 (1987) 189–204 (see Ref. [2983]).

[3364] R.W. Vook, T.J. Swirbel, J.V. Bucci, The dependence of work function on overgrowth thickness in epitaxial Cu–Pd systems, J. Vac. Sci. Technol. A 6 (1988) 1710–1711.

[3365] Yu.S. Vedula, A.G. Naumovets, V.V. Poplavskiĭ, Lanthanum diffusion on the (011) face of tungsten, Ukr. Fiz. Zh. 33 (1988) 934–939.

[3366] J.L. Vicente, A. Paola, A. Razzitte, E.E. Mola, S.B. Trickey, Static quantum size effects in ultra–thin beryllium films, Phys. Status Solidi (b) 155 (1989) K93–K98.

[3367] J. Vancea, G. Reiss, D. Butz, H. Hoffmann, Thickness–dependent effects in the work function of polycrystalline Cu–films, Europhys. Lett. 9 (1989) 379–384.
[3368] T. Valla, M. Milun, Properties of ultra thin silver films on a V(100) surface in a wide temperature range, Surf. Sci. 315 (1994) 81–92.
[3369] L. Vitos, J. Kollár, H.L. Skriver, Full charge–density calculation of the surface energy of metals, Phys. Rev. B 49 (1994) 16694–16701.
[3370] D. Vlachos, M. Kamaratos, C. Papageorgopoulos, Ba deposition on Si(100)2×1, Solid State Commun. 90 (1994) 175–181.
[3371] T. Valla, P. Pervan, M. Milun, Photoelectron spectroscopy characterization of the V(100) surface, Surf. Sci. 307–309 (1994) 843–847.
[3372] T. Valla, P. Pervan, M. Milun, Photoelectron spectroscopy of gold and silver ultra–thin films on V(100), Surf. Sci. 307–309 (1994) 576–581.
[3373] J. Vaari, J. Lahtinen, P. Hautojärvi, Reactive and thermal properties of CO on potassium–covered polycrystalline cobalt, Appl. Surf. Sci. 78 (1994) 255–267.
[3374] T. Valla, P. Pervan, M. Milun, Characterization of the 1 and 2 ML silver films on the V(100) surface, Vacuum 46 (1995) 1223–1226.
[3375] T. Valla, P. Pervan, M. Milun, Interaction of oxygen and silver on the V(100) surface, Appl. Surf. Sci. 89 (1995) 375–381.
[3376] D. Vlachos, S.D. Foulias, S. Kennou, C. Pappas, C. Papageorgopoulos, Ba deposition on Ni(110), Surf. Sci. 331–333 (1995) 673–678.
[3377] P. van Gelderen, S. Crampin, J.E. Ingelsfield, Quantum–well states in Cu/Co overlayers and sandwiches, Phys. Rev. B 53 (1996) 9115–9122.
[3378] R.W. Verhoef, W. Zhao, M. Asscher, Repulsive interactions of potassium on Re(001), J. Chem. Phys. 106 (1997) 9353–9361.
[3379] A. Voskoboinikov, I. Osadchi, Surface properties of alkali metals within the modulated jellium model, Surf. Sci. 375 (1997) 120–128.
[3380] T. Valla, P. Pervan, M. Milun, K. Wandelt, Growth modes and electronic properties of copper ultra–thin films on a V(100) surface, Surf. Sci. 374 (1997) 51–60.
[3381] T. Vaara, J. Vaari, J. Lahtinen, Adsorption of potassium on Co(0001), Surf. Sci. 395 (1998) 88–97.
[3382] D. Vogtenhuber, Ab–initio study of the adsorption of Cu on Pt(100), Phil. Mag. B 79 (1999) 269–279.
[3383] S.C. Veenstra, A. Heeres, G. Hadziioannou, G.A. Sawatzky, H.T. Jonkman, On interface dipole layers between C_{60} and Ag or Au, Appl. Phys. A 75 (2002) 661–666.
[3384] A.E. Woodruff, The variation in the photo–electric emission from platinum, Phys. Rev. 26 (1925) 655–670.
[3385] A. Wehnelt, S. Seiliger, Emission of electrons and positive ions by metals at the melting point, Z. Phys. 38 (1926) 443–464.
[3386] A. Warner, A comparison of the thermionic and photoelectric work functions for clean tungsten, Proc. Natl. Acad. Sci. 13 (1927) 56–60.
[3387] G.B. Welch, Photoelectric threshold for germanium, J. Opt. Soc. Amer. 14 (1927) 233.
[3388] G.B. Welch, Photo–electric thresholds and fatigue for iron, cobalt, and nickel, Phys. Rev. 31 (1928) 709.
[3389] G.B. Welch, Photo–electric thresholds and fatigue, Phys. Rev. 32 (1928) 657–666.
[3390] A.H. Warner, Variation of the photoelectric effect with temperature and determination of the long wave–length limit for tungsten, Phys. Rev. 33 (1929) 815–818.
[3391] R.P. Winch, The photoelectric properties of silver, Phys. Rev. 37 (1931) 1269–1275.
[3392] A.H. Warner, The determination of the photoelectric threshold for tungsten by Fowler's method, Phys. Rev. 38 (1931) 1871–1875.
[3393] R.P. Winch, Photoelectric properties of thin unbacked gold films, Phys. Rev. 38 (1931) 321–324.
[3394] G.B. Welch, Additional experimental verification of Fowler's photoelectric theory, Phys. Rev. 40 (1932) 470–471.
[3395] A.H. Weber, Some photoelectric properties of evaporated bismuth films, Phys. Rev. 53 (1938) 895–899.
[3396] H.B. Wahlin, L.V. Whitney, Temperature scale and thermionic emission from rhodium, J. Chem. Phys. 6 (1938) 594–597.
[3397] A.H. Weber, L.J. Eisele, Photoelectric and electric properties of thin bismuth films of measured thickness, Phys. Rev. 59 (1941) 473.
[3398] A.H. Weber, L.J. Eisele, Note on the photoelectric threshold of bismuth films of measured thickness, Phys. Rev. 60 (1941) 570–573.
[3399] G.L. Weissler, R.W. Kotter, Workfunctions of a gas–coated surface, Phys. Rev. 73 (1948) 538–539.
[3400] H.B. Wahlin, The thermionic properties of chromium, Phys. Rev. 73 (1948) 1458–1459.
[3401] H.B. Wahlin, L.O. Sordahl, The emission of electricity from columbium (niobium), Phys. Rev. 45 (1934) 764.
[3402] D.A. Wright, Rare metals in electron tubes, J. Brit. Inst. Radio Engrs. 11 (1951) 381–392 (Chem. Abstr. 46 (1952) 3389e).
[3403] D.C. West, The photoelectric constants of iodine, Canad. J. Phys. 31 (1953) 691–701.
[3404] D.A. Wright, Proc. IRE 100 (1953) 125 (see Ref. [12]).
[3405] G.L. Weissler, T.N. Wilson, Work functions of gas–coated tungsten and silver surfaces, J. Appl. Phys. 24 (1953) 472–475.
[3406] M.K. Wilkinson, Crystallographic variations of field emission from tungsten, J. Appl. Phys. 24 (1953) 1203–1209.
[3407] H.F. Weber, Work function of the (110) plane of tantalum as a function of cesium coverage, in: Rep. Thermion. Convert. Specialist Conf. Schnectady, 1963, pp. 187–191 (see Ref. [683]).
[3408] W. Weiershausen, Thermal ionization of Cu, Ag, and Ti on pure and covered polycrystalline W and Re surfaces, Ann. Phys. 15 (1965) 30–48.
[3409] W. Weiershausen, Study of oxygen adsorption on polycrystalline tungsten and rhenium by surface ionization of copper and silver, Ann. Phys. 15 (1965) 150–161.
[3410] R.G. Wilson, Electron and ion emission from cesiated and vacuum surfaces, Bull. Am. Phys. Soc. 10 (1965) 432.
[3411] W.F. Wei, Photoelectric emission and work function of semiconducting diamonds (Ph.D. thesis), Oklahoma State Univ., 1965, 87 pp. (Diss. Abstr. B 27 (1966) 281) (Chem. Abstr. 65 (1966) 19438e).
[3412] R.G. Wilson, Correlation of cesiated surface–emission data with surface–adsorption theory, Bull. Am. Phys. Soc. 11 (1966) 637.
[3413] R.G. Wilson, Electron and ion emission from polycrystalline surfaces of Be, Ti, Cr, Ni, Cu, Pt, and Type–304 stainless steel in cesium vapor, J. Appl. Phys. 37 (1966) 3161–3169.
[3414] R.G. Wilson, Electron and ion emission from polycrystalline surfaces of Nb, Mo, Ta, W, Re, Os, and Ir in cesium vapor, J. Appl. Phys. 37 (1966) 4125–4131.
[3415] R. Wichner, Work functions of monocrystalline and polycrystalline rhenium, in: Proc. Thermion. Conv. Specialist Conf. Houston, 1966, pp. 405–412 (see Ref. [1287]).
[3416] R. Wichner, Work functions of monocrystalline and polycrystalline rhenium (Ph.D. thesis), Univ. of Calif., Berkeley, 1966, 108 pp. (Diss. Abstr. B 27 (1967) 4064) (Chem. Abstr. 67 (1967) 94705s).
[3417] Y. Hasegawa, J.-f. Jia, K. Inoue, A. Sakai, T. Sakurai, Spatial variation of local work function of the Au/Cu(111) and Pd/Cu(111) systems, Sci. Rep. RITU, A 44 (1997) 109–112.
[3418] J.L. Desplat, LEED, Auger, work–function study of oxygen/cesium adsorption and coadsorption on (100) tungsten, Japan. J. Appl. Phys. Suppl. 2 (Pt. 2) (1974) 177–180.
[3419] R.G. Wilson, Electron and ion emission from a copper surface in the presence of oxygen, cesium, and oxygen plus cesium, Surf. Sci. 7 (1967) 157–174.
[3420] C.B. Williams, Ph.D. thesis, Univ. of Southampton, 1969 (see Ref. [777]).
[3421] A.H. Weber, T.H. Zepf, Photoelectric and thermionic Schottky deviations for molybdenum single crystals, Surf. Sci. 14 (1969) 247–265.
[3422] R.E. Weber, A.L. Johnson, Determination of surface structures using LEED and energy analysis of scattered electrons, J. Appl. Phys. 40 (1969) 314–318.
[3423] R.E. Weber, W.T. Peria, Work function and structural studies of alkali–covered semiconductors, Surf. Sci. 14 (1969) 13–38.
[3424] R.J. Whitefield, J.J. Brady, New value for work function of sodium and the observation of surface–plasmon effects, Phys. Rev. Lett. 26 (1971) 380–383.
[3425] R.G. Wilson, Surface ionization hysteresis phenomena, Surf. Sci. 25 (1971) 385–393.
[3426] J. Wysocki, The evaluation of the parameters of the tip in field electron microscope: Measurements on single faces, Acta Phys. Pol. A 39 (1971) 153–159.
[3427] J. Wysocki, Thermal–field emission from single crystal planes of tungsten, Acta Phys. Pol. A 42 (1972) 129–145.

[3428] R.G. Wilson, Surface ionization of indium and aluminum on iridium, J. Appl. Phys. 44 (1973) 2130–2132.
[3429] R.H. Williams, J.I. Polanco, The electronic structure of chalcogenide solids: A photoemission study of ordered and disordered selenium and tellurium, J. Phys. C 7 (1974) 2745–2759.
[3430] W. Wüstner, D. Menzel, A field emission investigation of adsorption and nucleation of silver on tungsten, and of the interaction of the deposits with oxygen, Thin Solid Films 24 (1974) 211–228.
[3431] E.G. Wolff, Thermionic emission of boron– and lanthanum–coated boron filaments, J. Appl. Phys. 45 (1974) 3840–3843.
[3432] B.J. Waclawski, J.F. Herbst, Photoemission for Xe physisorbed on W(100): Evidence for surface crystal–field effects, Phys. Rev. Lett. 35 (1975) 1594–1596.
[3433] P. Weightman, P.T. Andrews, L.A. Hisscott, Relaxation processes accompanying photoemission from solid cadmium, J. Phys. F 5 (1975) L220–L224.
[3434] W.F. Wei, W.J. Leivo, Photoelectric emission and work function of semiconducting diamonds, Carbon 13 (1975) 425–427.
[3435] C.-S. Wang, High photoemission efficiency of submonolayer cesium–covered surfaces, J. Appl. Phys. 48 (1977) 1477–1479.
[3436] S.-L. Weng, E.W. Plummer, T. Gustafsson, Experimental and theoretical study of the surface resonances on the (100) faces of W and Mo, Phys. Rev. B 18 (1978) 1718–1740.
[3437] J.T.M. Wotherspoon, D.C. Rodway, C. Norris, A photoemission study of liquid and solid thallium, lead and bismuth, Phil. Mag. B 40 (1979) 51–70.
[3438] M. Wohlmuth, E. Bechtold, Adsorption of sulfur on a tungsten field emitter, Appl. Surf. Sci. 5 (1980) 243–257.
[3439] S.-L. Weng, M. El-Batanouny, Photoemission observation of the formation of Pd(111) surface states (surface resonances) and resonant *d* levels for Pd overlayers on Nb, Phys. Rev. Lett. 44 (1980) 612–615.
[3440] J.K. Wysocki, Use of the thermal–field emission characteristics for the evaluation of work function and electric field strength in FEM, Surf. Sci. 104 (1981) 463–477.
[3441] D.-s. Wang, A.J. Freeman, H. Krakauer, Self–consistent electronic structure and chemisorption bonding of oxygen on Al(111) surfaces, Phys. Rev. B 24 (1981) 3092–3103.
[3442] D.M. Wood, Classical size dependence of the work function of small metallic spheres, Phys. Rev. Lett. 46 (1981) 749.
[3443] S.-L. Weng, Photoemission and electron–stimulated desorption studies of H on W(110): Single–versus two–binding–site models, Phys. Rev. B 25 (1982) 6188–6194.
[3444] K. Wandelt, Photoemission studies of adsorbed oxygen and oxide layers, Surf. Sci. Rep. 2 (1982) 1–121.
[3445] R.J. Wilson, A.P. Mills Jr., Electron and positron work functions of chromium(100), in: Proc. 6th Int. Conf. Positron Annihilation, 1982, pp. 156–158 (Chem. Abstr. 98 (1983) 61406g).
[3446] R.J. Wilson, A.P. Mills Jr., Electron and positron work functions of Cr(100), Surf. Sci. 128 (1983) 70–80.
[3447] M. Wada, K.H. Berkner, R.V. Pyle, J.W. Stearns, Photoelectric work function measurement of a cesiated metal surface and its correlation with the surface–produced H⁻ ion flux, J. Vac. Sci. Technol. A 1 (1983) 981–984.
[3448] S.-L. Weng, Formation of WSi₂ at the Si–W(110) interface, Phys. Rev. B 29 (1984) 2363–2365.
[3449] K. Wandelt, B. Gumhalter, Face specificity of the Xe/Pd bond and the s–resonance model, Surf. Sci. 140 (1984) 355–376.
[3450] B. Woratschek, W. Sesselmann, J. Küppers, G. Ertl, H. Haberland, Singlet to triplet conversion of metastable He atoms during deexcitation at a Cs covered surface, Phys. Rev. Lett. 55 (1985) 611–614.
[3451] L. Walldén, Surface photoelectric effect for thin metal overlayers, Phys. Rev. Lett. 54 (1985) 943–946.
[3452] M. Weinert, A.J. Freeman, S. Ohnishi, H and the W(100) surface reconstructions: Local bonding to surface states, Phys. Rev. Lett. 56 (1986) 2295–2298.
[3453] B. Woratschek, W. Sesselmann, J. Küppers, G. Ertl, H. Haberland, The interaction of cesium with oxygen, J. Chem. Phys. 86 (1987) 2411–2422.
[3454] B. Woratschek, W. Sesselmann, J. Küppers, G. Ertl, H. Haberland, Electron spectroscopy of alkali metal surfaces by deexcitation of metastable He atoms, Surf. Sci. 180 (1987) 187–202.
[3455] R.G. Windham, M.E. Bartram, B.E. Koel, Coadsorption of ethylene and potassium on Pt(111): I. Formation of a π–bonded state of ethylene, J. Phys. Chem. 92 (1988) 2862–2870.
[3456] L.J. Whitman, W. Ho, The kinetics and mechanisms of alkali metal–promoted dissociation: A time resolved study of NO adsorption and reaction on potassium–precovered Rh(100), J. Chem. Phys. 89 (1988) 7621–7645.
[3457] X.W. Wang, S.G. Louie, First principles studies of S/Mo(001) surfaces, Surf. Sci. 226 (1990) 257–262.
[3458] J.Z. Wu, S.B. Trickey, J.C. Boettger, Beryllium–hydrogen ultrathin films. II. Ground–state properties of the dilayer, Phys. Rev. B 42 (1990) 1668–1673.
[3459] G. Wang, H.-Y. Li, Y.-B. Xu, The work–function change of K/Cu(111), Acta Phys. Sin. 39 (1990) 1989–1992.
[3460] R.M. Wolf, J.W. Bakker, B.E. Nieuwenhuys, Design and performance of a scanning probe–hole field emission microscope, Surf. Sci. 246 (1991) 420–427.
[3461] P. Wetzel, L. Haderbache, C. Pirri, J.C. Peruchetti, D. Bolmont, G. Gewinner, Room–temperature growth of Er films on Si(111): A photoelectron spectroscopy investigation, Phys. Rev. B 43 (1991) 6620–6626.
[3462] R. Wu, C. Li, A.J. Freeman, C.L. Fu, Structural, electronic, and magnetic properties of rare–earth metal surfaces: hcp Gd(0001), Phys. Rev. B 44 (1991) 9400–9409.
[3463] T.N. Wittberg, Barium adsorption on nickel: Auger electron spectroscopy and work–function measurements, J. Vac. Sci. Technol. A 9 (1991) 2400–2401.
[3464] H.H. Weitering, J. Chen, N.J. DiNardo, E.W. Plummer, Electron correlation, metallization, and Fermi–level pinning at ultrathin K/Si(111) interfaces, Phys. Rev. B 48 (1993) 8119–8135.
[3465] H.H. Weitering, J. Chen, N.J. DiNardo, E.W. Plummer, Electronic structure of K/Si(111) interfaces, J. Vac. Sci. Technol. A 11 (1993) 2049–2053.
[3466] W.J. Wytenburg, R.M. Ormerod, R.M. Lambert, Growth and stability of ultra–thin alminium films on Ag(110) and Ag(111), Surf. Sci. 282 (1993) 205–215.
[3467] K.F. Wojciechowski, H. Bogdanów, Work function of simple metals: Relation between theory and experiment, Acta. Phys. Pol. A 85 (1994) 875–890.
[3468] J.E. Whitten, R. Gomer, Deposition of Ni monolayers on O/W(110), H/W(110) and CO/W(110): Search for metallicity, Surf. Sci. 316 (1994) 36–46.
[3469] J.E. Whitten, R. Gomer, Interaction of oxygen and Ni on W(110), Surf. Sci. 316 (1994) 1–22.
[3470] H.H. Weitering, J. Chen, R. Pérez-Sandoz, N.J. DiNardo, Electron localization and the nonmetal–to–metal transition at ultrathin alkali–metal/Si(111) interfaces, Surf. Sci. 307–309 (1994) 978–983.
[3471] H.H. Weitering, N.J. DiNardo, R. Pérez-Sandoz, J. Chen, E.J. Mele, Structural model for metal–induced Si(111)3×1 reconstruction, Phys. Rev. B 49 (1994) 16837–16840.
[3472] J.E. Whitten, R. Gomer, Adsorption of Ni and Ag on benzene covered W(110): Search for metallicity, J. Phys. Chem. 99 (1995) 2826–2832.
[3473] R. Wu, A.J. Freeman, Bonding mechanism at bimetallic interfaces: Pd overlayer on various substrates, Phys. Rev. B 52 (1995) 12419–12425.
[3474] R. Wu, The bonding mechanism at bimetallic interface: Pd/Ta(110), Chem. Phys. Lett. 238 (1995) 99–103.
[3475] W. Wallauer, Th. Fauster, Exchange splitting of image states on Fe/Cu(100) and Co/Cu(100), Phys. Rev. B 54 (1996) 5086–5091.
[3476] K.F. Wojciechowski, Work function of transition metals calculated from Brodie's expression (corrected values), Vacuum 48 (1997) 891–892.
[3477] K.F. Wojciechowski, Application of Brodie's concept of the work function to simple metals, Europhys. Lett. 38 (1997) 135–140.
[3478] K.F. Wojciechowski, H. Bogdanów, Quantum size effects of ultrathin simple metal layers on the example of lithium, Surf. Sci. 397 (1998) 53–57.
[3479] K.F. Wojciechowski, Ionization energy and electron affinity of small alkali–metal clusters, J. Chem. Phys. 108 (1998) 816–817.
[3480] Y. Wang, Q. Sun, K. Fan, J. Deng, Interaction of halogen atom with Ag(110): *Ab initio* pseudopotential density functional study, Chem. Phys. Lett. 334 (2001) 411–418.
[3481] E. Wachowicz, A. Kiejna, Bulk and surface properties of hexagonal–close–packed Be and Mg, J. Phys.: Condens. Matter 13 (2001) 10767–10776.

[3482] K. Wong, V. Kasperovich, G. Tikhonov, V.V. Kresin, Photo–ionization efficiency curves of alkali nanoclusters in a beam and determination of metal work functions, Appl. Phys. B 73 (2001) 407–410.

[3483] C.M. Wei, M.Y. Chou, Theory of quantum size effects in thin Pb(111) films, Phys. Rev. B 66 (2002) 233408/1–4.

[3484] K. Wu, Y. Fujikawa, T. Nagao, Y. Hasegawa, K.S. Nakayama, Q.K. Xue, E.G. Wang, T. Briere, V. Kumar, Y. Kawazoe, S.B. Zhang, T. Sakurai, Na adsorption on the Si(111)–(7×7) surface: From two–dimensional gas to nanocluster array, Phys. Rev. Lett. 91 (2003) 126101/1–4.

[3485] S. Watanabe, Y. Gohda, K. Watanabe, K. Tada, M. Araidai, First–principles calculations of field electron emission, Kotai Buturi (Solid State Phys.) 38 (2003) 537–543 (Chem. Abstr. 139 (2003) 252850x).

[3486] L.-L. Wang, H.-P. Cheng, Rotation, translation, charge transfer, and electronic structure of C_{60} on Cu(111) surface, Phys. Rev. B 69 (2004) 045404/1–7.

[3487] C. Weindel, H.J. Jänsch, G. Kirchner, H. Kleine, J.J. Paggel, J. Roth, H. Winnefeld, D. Fick, Phys. Rev. B 71 (2005) 115318/1–7.

[3488] X. Wu, A.K. Ray, Full–potential LAPW electronic structure study of δ–plutonium and the (001) surface, Phys. Rev. B 72 (2005) 045115/1–9.

[3489] D.G. Walker, C.T. Harris, T.S. Fisher, J.L. Davidson, Estimation of parameters in thermal–field emission from diamond, Diam. Relat. Mater. 14 (2005) 113–120.

[3490] H. Wen, M. Neurock, H.N.G. Wadley, Influence of oxygen on the interfacial stability of Cu on Co(0001) thin films, Phys. Rev. B 75 (2007) 085403/1–17.

[3491] L.-L. Wang, H.-P. Cheng, Embedding atom–jellium model for metal surface, Eur. Phys. J. D 43 (2007) 247–250.

[3492] C.M. Wei, M.Y. Chou, Quantum size effect in Pb(100) films: Critical role of crystal band structure, Phys. Rev. B 75 (2007) 195417/1–4.

[3493] F.-H. Wang, S.-Y. Liu, J.-X. Shang, Y.-S. Zhou, Z. Li, J. Yang, Oxygen adsorption on Zr(0001) surface: Density functional calculations and a multiple–layer adsorption model, Surf. Sci. 602 (2008) 2212–2216.

[3494] J.-G. Wang, E. Prodan, R. Car, A. Selloni, Band alignment in molecular devices: Influence of anchoring group and metal work function, Phys. Rev. B 77 (2008) 245443/1–8.

[3495] M. Xu, R.J. Smith, Electronic structure of Pd thin films on the Al(110) surface, J. Vac. Sci. Technol. A 6 (1988) 739–742.

[3496] F. Xu, G. Manicò, F. Ascione, A. Bonanno, A. Oliva, Evidence of charge transfer from Na adatoms to the Cs substrate: A collisionally excited autoionization electron–emission study, Phys. Rev. B 54 (1996) 10401–10404.

[3497] Y. Xue, S. Datta, M.A. Ratner, Charge transfer and "band lineup" in molecular electronic devices: A chemical and numerical interpretation, J. Chem. Phys. 115 (2001) 4292–4299.

[3498] H.Y. Xiao, X.T. Zu, Y.F. Zhang, L. Yang, First–principles study of the adsorption of cesium on Si(001)(2×1) surface, J. Chem. Phys. 122 (2005) 174704/1–9.

[3499] H.Y. Xiao, X.T. Zu, Adsorption of Na on Ge(001)(2×1) surface, Physica B 371 (2006) 50–55.

[3500] H.Y. Xiao, X.T. Zu, Y.F. Zhang, F. Gao, Adsorption of alkali metals on Ge(001)(2×1) surface, Chem. Phys. Lett. 417 (2006) 6–10.

[3501] H.Y. Xiao, X.T. Zu, Y.F. Zhang, F. Gao, Atomic and electronic structures of rubidium adsorption on Si(001)(2×1) surface: Comparison with Cs/Si(001) surface, Chem. Phys. 323 (2006) 383–390.

[3502] C.F. Ying, H.E. Farnsworth, Changes in work function of vacuum distilled gold films, Phys. Rev. 85 (1952) 485–486.

[3503] R.D. Young, ASTIA Document No. 94853, 1956 (see Ref. [913]).

[3504] R.D. Young, E.W. Müller, Experimental measurement of the total–energy distribution of field–emitted electrons, Phys. Rev. 113 (1959) 115–120.

[3505] A.Y.-C. Yu, Stanford Electro. Lab. Tech. Rep. No. 5215–1, 1967 (see Ref. [304]).

[3506] A.Y.-C. Yu, W.E. Spicer, Photoemission studies of the electronic structure of cobalt, Phys. Rev. 167 (1968) 674–686.

[3507] V.D. Yagodovskiĭ, Yu.A. Zubarev, G.N. Denisov, Photoelectric and conductometric determinations of the polarization of molecules adsorbed on granular films of metals, Zh. Fiz. Khim. 47 (1973) 3077–3080.

[3508] P.L. Young, R. Gomer, Energy distributions of field emitted electrons from tungsten in the presence of adsorbed CO, J. Chem. Phys. 61 (1974) 4955–4972.

[3509] P.L. Young, R. Gomer, Field emission spectroscopy of gold on tungsten, Surf. Sci. 44 (1974) 268–274.

[3510] H. Yasunaga, Calibrated source of atomic cesium beams, Rev. Sci. Instrum. 47 (1976) 726–729.

[3511] K.Y. Yu, C.R. Helms, W.E. Spicer, P.W. Chye, Photoemission studies of the surface and bulk electronic structure of the Cu–Ni alloy, Phys. Rev. B 15 (1977) 1629–1639.

[3512] S. Yamamoto, K. Susa, U. Kawabe, H. Okano, Work functions of binary compounds (Adsorption model), Japan. J. Appl. Phys. Suppl. 2 (Pt. 2) (1974) 209–212.

[3513] D.-Q. Yang, E.-G. Chen, A new method of measuring the work function of materials, Acta Phys. Sin. 37 (1988) 2017–2022.

[3514] R. Yu, P.K. Lam, First–principles total–energy study of hydrogen adsorption on Be(0001), Phys. Rev. B 39 (1989) 5035–5040.

[3515] D.-Q. Yang, A new method of calculating atomic radius and work function of metals, Acta Phys. Sin. 43 (1994) 1507–1516 (Chem. Abstr. 122 (1995) 197549c).

[3516] M. Yamamoto, C.T. Chan, K.M. Ho, S. Naito, First–principles calculation of oxygen adsorption on Zr(0001) surface: Possible site occupation between the second and the third layer, Phys. Rev. B 54 (1996) 14111–14120.

[3517] Y.-C. Yeo, Q. Lu, P. Ranade, H. Takeuchi, K.J. Yang, I. Polishchuk, T.-J. King, C. Hu, S.C. Song, H.F. Luan, D.-L. Kwong, Dual–metal gate CMOS technology with ultrathin silicon nitride gate dielectric, IEEE Electr. Dev. Lett. 22 (2001) 227–229.

[3518] Y. Yamada, A. Sinsarp, M. Sasaki, S. Yamamoto, Scanning tunneling microscopy (STM)/local tunneling barrier height (LBH) studies on Cs adsorption on a Pt(111) surface, Japan. J. Appl. Phys. 41 (2002) 5003–5007.

[3519] Y.-C. Yeo, T.-J. King, C. Hu, Metal–dielectric band alignment and its implications for metal gate complementary metal–oxide–semiconductor technology, J. Appl. Phys. 92 (2002) 7266–7271.

[3520] Y.-C. Yeo, P. Ranade, T.-J. King, C. Hu, Effects of high–κ gate dielectric materials on metal and silicon gate workfunctions, IEEE Electr. Dev. Lett. 23 (2002) 342–344.

[3521] D. Yu, M. Scheffler, First–principles study of low–index surfaces of lead, Phys. Rev. B 70 (2004) 155417/1–8.

[3522] M. Yoshitake, Principle and practical tips of work function measurement using UPS, XPS and AES instruments, Hyomen Kagaku (Surf. Sci.) 28 (2007) 397–401 (Chem. Abstr. 147 (2007) 375054p).

[3523] C. Zwikker, Physical properties of tungsten at high temperatures, Physica 5 (1925) 249–260.

[3524] C. Zwikker, Thermionic emission of tungsten, molybdenum, thorium, zirconium and hafnium, Proc. Roy. Acad. Amsterdam 29 (1926) 792–802 (Chem. Abstr. 21 (1927) 1230).

[3525] C. Zwikker, Thermal emission of electrons from metallic tungsten, molybdenum, thorium, zirconium and hafnium, Verslag Akad. Wetenschappen Amsterdam 35 (1926) 336–346 (Chem. Abstr. 20 (1926) 2785).

[3526] C. Zwikker, Physical properties of molybdenum at high temperatures, Physica 7 (1927) 71–74.

[3527] C. Zwikker, The influence of surface layers on the thermionic emission of metals, Phys. Z. 30 (1929) 578–580.

[3528] Ya.P. Zingerman, V.A. Ishchuk, V.A. Morozovskiĭ, Electronic and adsorptive properties of films of barium atoms on tungsten, Sov. Phys.—Solid State 2 (1960) 2030–2038.

[3529] Yu.V. Zubenko, I.L. Sokol'skaya, Field emission of tungsten carbide and thoriated tungsten carbide, Radio Engin. Electr. Phys. 5 (1960) 201–208.

[3530] Ya.P. Zingerman, V.A. Ishchuk, V.A. Morozovskiĭ, Adsorption of atoms of the alkali earth group by polycrystalline tungsten, Sov. Phys.—Solid State 3 (1961) 760–766.

[3531] Yu.V. Zubenko, Adsorption, migration, and evaporation of barium on tungsten carbide, Sov. Phys.—Solid State 3 (1961) 387–391.

[3532] Ya.P. Zingerman, V.A. Ishchuk, The problem of the adsorption of barium atoms on tungsten, Sov. Phys.—Solid State 4 (1963) 1618–1619.

[3533] Yu.V. Zubenko, I.L. Sokol'skaya, Work function of tungsten carbide, Sov. Phys. Tech. Phys. 7 (1962) 270–272.

[3534] R.J. Zollweg, Electron reflection from cesium–coated polycrystalline metals at low primary energy, J. Appl. Phys. 34 (1963) 2590–2598.

[3535] Yu.V. Zubenko, Adsorption and evaporation of barium on a rhenium single crystal, Sov. Phys.—Solid State 6 (1964) 98–103.

[3536] P. Zalm, A.J.A. van Stratum, Osmium dispenser cathodes, Philips Tech. Rev. 27 (1966) 69–75.

[3537] É.Ya. Zandberg, A.Ya. Tontegode, Surface ionization of alkali–halide molecules on platinum–group metals, Sov. Phys. Tech. Phys. 12 (1968) 1548–1549.

[3538] É.Ya. Zandberg, U.Kh. Rasulev, Surface ionization of the $C_4H_{10}N$ radical, Sov. Phys. Dokl. 13 (1968) 35–37.

[3539] G. Zuther, H. Köster, G. Becherer, Electron field emission from germanium single–crystal surfaces, Ann. Phys. 26 (1971) 193–200.

[3540] G.A. Zykov, N.G. Nakhodkin, Thermionic emission and emission of alkali metal ions from the (111) face of a silicon single crystal, Izv. Akad. Nauk SSSR, Ser. Fiz. 35 (1971) 1070–1074.

[3541] K.Zh. Zhanabergenov, E.P. Sytaya, Effect of heterogeneities in the structure of (110) and (111) faces of a tungsten single crystal on their thermionic emission characteristics, Nauch. Tr., Tashk. Gos. Univ. (393) (1971) 237–246 (Chem. Abstr. 78 (1973) 89933n).

[3542] K.Zh. Zhanabergenov, E.P. Sytaya, Surface ionization of lithium on the (110) and (111) faces of a tungsten single crystal, Nauch. Tr. Tashk. Gos. Univ. (393) (1971) 247–253 (Chem. Abstr. 78 (1973) 89946u).

[3543] Yu.V. Zubenko, Adsorption of barium on platinum, Sov. Phys.—Solid State 14 (1972) 377–379.

[3544] J. Żebrowski, Field emission from Ge–W and Ge–Mo adsorption systems, Acta. Phys. Pol. A 44 (1973) 201–209.

[3545] J. Żebrowski, G.G. Vladimirov, Emission properties of the system germanium (monolayer coating)–titanium–tungsten, Sov. Phys.—Solid State 17 (1975) 962–963.

[3546] É.Ya. Zandberg, E.V. Rut'kov, A.Ya. Tontegode, Role of valence state of surface–layer atoms of a solid in phase transitions in submonolayer adsorbed films, Sov. Phys. Tech. Phys. Lett. 1 (1975) 324–325.

[3547] É.Ya. Zandberg, E.V. Rut'kov, A.Ya. Tontegode, Thermionic–emission study of the influence of valence saturation of atoms at the surface of a solid on the phase state of adsorbed particles: The systems Ir(111)–Ba and Ir(111)–C–Ba, Sov. Phys. Tech. Phys. 21 (1976) 1541–1545.

[3548] J. Żebrowski, Work function of the Pb/W adsorption system, Acta. Phys. Pol. A 50 (1976) 307–314.

[3549] H.I. Zhang, M. Schlüter, Studies of the Si(111) surface with various Al overlayers, Phys. Rev. B 18 (1978) 1923–1935.

[3550] S. Zuber, Z. Sidorski, J. Polański, Work function and loss spectra of beryllium layers adsorbed on tungsten single crystals with (110) and (100) orientations, Surf. Sci. 87 (1979) 375–388.

[3551] É.Ya. Zandberg, É.G. Nazarov, U.Kh. Rasulev, E.V. Rut'kov, Simple method for monitoring high–work–function regions on solid surfaces, Sov. Tech. Phys. Lett. 8 (1982) 471–472.

[3552] W.A. Saunders, K. Clemenger, W.A. de Heer, W.D. Knight, Photoionization and shell structure of potassium clusters, Phys. Rev. B 32 (1985) 1366–1368.

[3553] Yu.V. Zubchenko, M.B. Ishmukhametov, Adsorption and emission properties of the barium–germanium–tungsten system, Bull. Acad. Sci. USSR, Phys. Ser. 46 (12) (1982) 71–73.

[3554] Yu.V. Zubenko, M.B. Ishmukhametov, Field–electron emission from tungsten coated with germanium, Sov. Phys.—Solid State 25 (1983) 713–715.

[3555] Yu.V. Zubenko, M.B. Ishmukhametov, Adsorption of barium on germanium–coated tungsten, Sov. Phys.—Solid State 25 (1983) 98–99.

[3556] X.-y. Zhu, H. Huang, J. Hermanson, Electronic structure and magnetism of the Cu/Ni{100} interface: Self–consistent local orbital calculations, Phys. Rev. B 29 (1984) 3009–3014.

[3557] G. Zajac, S.D. Bader, R.J. Friddle, Epitaxy and electronic structure of p (1×1) Cr/Au(100), Phys. Rev. B 31 (1985) 4947–4953.

[3558] A.D. Zdetsis, Crystal and electronic structure of metallic lithium at low temperatures, Phys. Rev. B 34 (1986) 7666–7669.

[3559] É.Ya. Zandberg, N.M. Nasrullaev, E.V. Rut'kov, A.Ya. Tontegode, Increasing the sensitivity of surface–ionization detection of atomic fluxes by means of a substitution reaction on the surface of the ion emitter, Sov. Phys. Tech. Phys. 34 (1989) 1279–1281.

[3560] Y.B. Zhao, R. Gomer, Adsorption of CO on Pd_1/W(110), Surf. Sci. 239 (1990) 189–202.

[3561] Y. Zhang, A.J. Slavin, Adsorption of metallic tin on the Au(111) surface, J. Vac. Sci. Technol. A 9 (1991) 1784–1788.

[3562] Y.B. Zhao, R. Gomer, Adsorption of Hg on CO, O, and H adsorbed on W(110), Surf. Sci. 271 (1992) 85–102.

[3563] Y.B. Zhao, R. Gomer, Adsorption of Pd on H_1/W(110), Surf. Sci. 273 (1992) 285–290.

[3564] Z. Zhang, V.E. Henrich, Electronic interactions in the vanadium/TiO_2(110) and vanadia/TiO_2(110) model catalyst systems, Surf. Sci. 277 (1992) 263–272.

[3565] Y.B. Zhao, R. Gomer, The adsorption of Ag on CO, O and H covered W(110): II. Metallicity, Surf. Sci. 280 (1993) 138–144.

[3566] J. Zhang, D. Li, P.A. Dowben, Electronic properties of metallic Hg monolayers on W(110), J. Phys.: Condens. Matter 6 (1994) 33–54.

[3567] J. Zhang, P.A. Dowben, D. Li, M. Onellion, Angle–resolved photoemission study of oxygen chemisorption on Gd(0001), Surf. Sci. 329 (1995) 177–183.

[3568] V.V. Zhirnov, W.B. Choi, J.J. Cuomo, J.J. Hren, Diamond coated Si and Mo field emitters: Diamond thickness effect, Appl. Surf. Sci. 94/95 (1996) 123–128.

[3569] V. Zhukov, K.D. Rendulic, A. Winkler, Coadsorption of hydrogen and potassium on silver single crystal surfaces, Vacuum 47 (1996) 5–11.

[3570] G. Zhou, W. Duan, B. Gu, Electronic structure and field–emission characteristics of open–ended single–walled carbon nanotubes, Phys. Rev. Lett. 87 (2001) 095504/1–4.

[3571] Q. Zhong, C. Gahl, M. Wolf, Two–photon photoemission spectroscopy of pyridine adsorbed on Cu(111), Surf. Sci. 496 (2002) 21–32.

[3572] G. Zhao, Q. Zhang, H. Zhang, G. Yang, O. Zhou, L.-C. Qin, J. Tang, Field emission of electrons from a Cs–doped single carbon nanotube of known chiral indices, Appl. Phys. Lett. 89 (2006) 263113/1–3.

[3573] Y.G. Zhou, X.T. Zu, J.L. Nie, H.Y. Xiao, First–principles study of sulfur adsorption on Mo(110), Chem. Phys. 353 (2008) 109–114.

[3574] Y.G. Zhou, X.T. Zu, J.L. Nie, H.Y. Xiao, Adsorption of Li on Cu(110): Density–functional calculations, Chem. Phys. 355 (2009) 135–140.

[3575] P.A. Anderson, Continuous measurement of changes in the electronic work function during the fusion of tin, Phys. Rev. 50 (1936) 386–387.

[3576] L. Apker, E. Taft, J. Dickey, On the photoelectric emission and energy structure of BaO, Phys. Rev. 84 (1951) 508–511.

[3577] A.N. Arsen'eva-Geĭl, The energy distribution of electrons at the external photoelectric effect of germanium containing impurities, Zh. Tekh. Fiz. 25 (1955) 1544–1546.

[3578] R.L. Anthony, G. Gardner, E.A. Coomes, Thermionic emission from single crystal tungsten wire with [110] inclined to wire axis, Bull. Am. Phys. Soc. 6 (1961) 422.

[3579] F.G. Allen, G.W. Gobeli, Rept. of the Int. Conf. on the Phys. of Semiconductors, IOP, 1962, p. 818 (see Ref. [3624]).

[3580] A.N. Arkhipov, G.A. Ivanov, V.L. Naletov, Determination of the position of the chemical potential level in bismuth–antimony alloys doped with tin and tellurium, in: G.A. Ivanov (Ed.), Poluprovodn. Dielekt., Leningrad, 1974, pp. 34–38.

[3581] M.S. Avedillo, J.L. De Segovia, Determination of the work function of tungsten (110), (111), (223), (121), (100), (012) and (223) using the "sound orifice" method in a field emission microscope, Electron. Fis. Apl. 19 (1976) 39–40 (Chem. Abstr. 86 (1977) 82382p).

[3582] U.V. Azizov, D. Azizova, T.A. Karabaev, Study of the thermoemission properties of spherical polycrystalline rhenium in a stream of barium and cesium atoms, Nauchn. Tr., Tashk. Gos. Univ. 525 (1976) 31–35 (Chem. Abstr. 90 (1979) 160896h).

[3583] R.M. Abdullaev, A.Ya. Tontegode, F.K. Yusifov, Adsorption and condensation of samarium on iridium, Sov. Phys.—Solid State 20 (1978) 1352–1359.

[3584] G.C. Allen, P.M. Tucker, B.E. Hayden, D.F. Klemperer, Early stages in the oxidation of magnesium, aluminium and magnesium/alminium alloys. I. Exoelectron emission and long wavelength photoemission, Surf. Sci. 102 (1981) 207–226.

[3585] A.K. Brewer, The photoelectric and thermionic properties of platinum coated glass filaments, Phys. Rev. 35 (1930) 1360–1366.

[3586] A.J. Becker, W.H. Brattain, The thermionic work function and the slope and intercept of Richardson plots, Phys. Rev. 45 (1934) 694–705.

[3587] H.P. Bonzel, G. Pirug, Photoelectron spectroscopy of NO adsorbed on Pt(100), Surf. Sci. 62 (1977) 45–60.

[3588] E. Bauer, Adsorbed metal layers: Structure, work function and bonding, J. Physiq. 38 (1977) C4–146/C4–154.

[3589] D. Bolmont, C. Sébenne, C. Ping, Effect of Ag impurities on the electronic properties of the Si(111) surface, in: Suppl. 4th Int. Conf. Solid Surf., vol. 2, Vide 201 (1980) 963–966.

[3590] J.P. Badiali, Contribution of the metal to the differential capacitance of the ideally polarizable electrode, Electrochim. Acta 31 (1986) 149–154.

[3591] P.J. Berlowitz, J.E. Houston, J.M. White, D.W. Goodman, Properties of monolayer and multilayer Ni films on the Ru(0001) surface, Surf. Sci. 205 (1988) 1–11.

[3592] G. Bachmann, W. Berthold, H. Oechsner, Work function spectroscopy as a tool for thin film analysis, Thin Solid Films 174 (1989) 149–154.

[3593] M. Bockstedte, A. Kley, J. Neugebauer, M. Scheffler, Density–functional theory calculations for poly–atomic systems: Electronic structure, static and elastic properties and *ab initio* molecular dynamics, Comput. Phys. Commun. 107 (1997) 187–222 (see Ref. [3486]).

[3594] H.E. Clark, Electronic properties of a thin germanium layer adsorbed on a tungsten surface (Ph.D. thesis), The American Univ. Washington DC, 1971, 94 pp. (see Ref. [3544]).

[3595] D.M. Ceperley, B.J. Alder, Ground state of the electron gas by a stochastic method, Phys. Rev. Lett. 45 (1980) 566–569 (see Ref. [719]).

[3596] B.M. Carev, Kontaktnaya Raznost Potencialov, Gotstchizdat, Moscow, 1991 (see Ref. [2750]).

[3597] J.B. Cui, R. Graupner, J. Ristein, L. Ley, Electron affinity and band bending of single crystal diamond(111) surface, Diam. Rel. Mater. 8 (1999) 748–753.

[3598] J.B. Cui, J. Ristein, L. Ley, Dehydrogenation and the surface phase transition on diamond(111): Kinetics and electronic structure, Phys. Rev. B 59 (1999) 5847–5856.

[3599] F. Deininger, The emission of negative ions from glowing metals and calcium oxide, Ann. Phys. 25 (1908) 285–308 (see Ref. [114]).

[3600] J.L. Desplat, W(100) work function change during adsorption of oxygen, cesium, and oxygen–cesium co–adsorption, in: Proc. 3rd Int. Conf. Thermion. Electric. Power Generat., Jülich, vol. 3, 1972, pp. 1397–1407.

[3601] N. de Jonge, M. Allioux, J.T. Oostveen, K.B.K. Teo, W.I. Milne, Optical performance of carbon–nanotube electron sources, Phys. Rev. Lett. 94 (2005) 186807/1–4.

[3602] G. Eng, H.K.A. Kan, Scanning Auger and work–function measurements applied to dispenser cathodes, Appl. Surf. Sci. 8 (1981) 81–94.

[3603] S. Eder, K. Markert, A. Jablonski, K. Wandelt, Substrate dependence of the 2D gas–solid phase transition in adsorbed xenon layers, Ber. Bunsenges. Phys. Chem. 90 (1986) 225–228.

[3604] H. Engelhard, J. Hölzl, Thermionic emission from polycrystalline cobalt: Temperature dependence at T_c, J. Magn. Magn. Mater. 79 (1989) 154–156.

[3605] Y. Enta, S. Suzuki, S. Kono, T. Sakamoto, Electronic structures of the single–domain Si(001)2×1 and 2×8 surfaces, J. Phys. Soc. Japan 59 (1990) 657–661.

[3606] H.D. Ebinger, H.J. Jänsch, C. Polenz, B. Polivka, W. Preyss, V. Saier, R. Veith, D. Fick, NMR Observation of diffusion barriers for lithium adsorbed on Ru(001), Phys. Rev. Lett. 76 (1996) 656–659.

[3607] C.J. Edgcombe, U. Valdrè, The enhancement factor and the characterization of amorphous carbon field emitters, Solid-State Electron. 45 (2001) 857–863.

[3608] G.W. Fox, R.M. Bowie, A new method for determining the thermionic work functions of metals and its application to nickel, Phys. Rev. 44 (1933) 345–348.

[3609] S.M. Fainshtein, A cascade electron multiplier for photometric purposes, Zavodskaya Lab. 14 (1948) 64–67.

[3610] H.E. Farnsworth, Comments on the paper by J.C Revière: "Contact potential difference measurements by the Kelvin method", Proc. Phys. Soc. 71 (1958) 703–704.

[3611] A.B. Fowler, Contact potential measurements on cleaned germanium surfaces, J. Appl. Phys. 30 (1959) 556–558.

[3612] D.L. Fehrs, R.E. Stickney, Unpublished (see Refs. [1892,1981]).

[3613] E.G. Fedorova, N.N. Vyatkin, V.A. Ivchenko, N.N. Syutkin, Field emission of an iridium–cerium alloy, Izv. Akad. Nauk SSSR, Ser. Fiz. 40 (1976) 1595–1598.

[3614] A.J. Freeman, Electronic structure and magnetism of surfaces and interfaces, J. Magn. Magn. Mater. 35 (1983) 31–36.

[3615] C.L. Fu, S. Ohnishi, H.J.F. Jansen, A.J. Freeman, All–electron local–density determination of the surface energy of transition metals: W(001) and V(001), Phys. Rev. B 31 (1985) 1168–1171.

[3616] A.G. Fedorus, A.A. Mitryaev, M.A. Mukhtarov, H. Pfnür, Yu.S. Vedula, A.G. Naumovets, The processes of ordering and formation of two–dimensional glasses at metal surfaces, Surf. Sci. 600 (2006) 1566–1573.

[3617] D.A. Gorodetskii, A.V. Martynyuk, Studies in the processes of scandium oxidation by the methods of electron spectroscopy, Ukr. Fiz. Zh. 31 (1986) 1054–1059.

[3618] R. Gomer, Private comm. (see Ref. [3144]).

[3619] Y. Gotoh, M. Nagao, M. Matsubara, K. Inoue, H. Tsuji, J. Ishikawa, Relationship between effective work functions and noise powers of emission currents in nickel–deposited field emitters, Japan. J. Appl. Phys. 35 (1996) L1297–L1300.

[3620] O. Gröning, O.M. Küttel, P. Gröning, L. Schlapbach, Field emission properties of nanocrystalline chemically vapor deposited–diamond films, J. Vac. Sci. Technol. B 17 (1999) 1970–1986.

[3621] A.E. Hennings, A study of contact potentials and photoelectric properties of metals in vacuo: and the mutual relation between these phenomena, Phys. Rev. 4 (1914) 228–246.

[3622] J. Hubbard, The description of collective motions in terms of many body perturbation theory, Proc. R. Soc. A 243 (1957) 336–352 (see Ref. [2835]).

[3623] E.B. Hensley, Thermionic emission constants and their interpretation, J. Appl. Phys. 32 (1961) 301–308.

[3624] V. Heine, Theory of surface states, Phys. Rev. 138 (1965) A1689–A1696.

[3625] T.W. Hall, R.M. Eastment, C.H.B. Mee, Photoelectric properties of amorphous and crystalline films of antimony, Phys. Status Solidi (a) 2 (1970) 327–334.

[3626] H. Kawano, Thermal negative ion emission from binary cesium halide mixtures on a niobium surface, J. Phys. Chem. 75 (1971) 3741–3745.

[3627] D.M. Hanson, R. Stockbauer, T.E. Madey, Photon–stimulated desorption and other spectroscopic studies of the interaction of oxygen with a titanium(001) surface, Phys. Rev. B 24 (1981) 5513–5521.

[3628] S.N. Zadumkin, Kh.B. Khokonov, Surface energy and work function of electron escape from metal, Fiz. Met. Metallov. 23 (1967) 565–568.

[3629] K. Horn, A. Hohlfeld, J. Somers, Th. Lindner, P. Hollins, A.M. Bradshaw, Identification of the *s*–derived valence–electron level in photoemission from alkali–metal adlayers on aluminum, Phys. Rev. Lett. 61 (1988) 2488–2491.

[3630] M.B. Hugenschmidt, P. Dolle, J. Jupille, A. Cassuto, Ethylene π species on bare and cesiated Pt(111) surfaces, J. Vac. Sci. Technol. A 7 (1989) 3312–3316.

[3631] T. Hertel, E. Knoesel, E. Hasselbrink, M. Wolf, G. Ertl, Unoccupied adsorbate states of CO/Cu(111) analyzed with two–photon photoemission, Surf. Sci. 317 (1994) L1147–L1151.

[3632] T. Hertel, M. Wolf, G. Ertl, UV Photostimulated desorption of ammonia from Cu(111), J. Chem. Phys. 102 (1995) 3414–3430.

[3633] K.M.E. Habelmehl-Ćwirzeń, J. Katainen, P. Hautojärvi, An experimental study on adsorption of benzene on Co(0001), Surf. Sci. 507–510 (2002) 57–61.

[3634] C.G. Hwang, N.D. Kim, G. Lee, S.Y. Shin, S.H. Uhm, H.S. Kim, J.S. Kim, J.W. Chung, Origin of unusual work function change upon forming Tl nanoclusters on Si(111)–7×7 surface, Appl. Phys. A 89 (2007) 431–435.

[3635] J.F. Janak, V.L. Moruzzi, A.R. Williams, Ground–state thermochemical properties of some cubic elements in the local–density formalism, Phys. Rev. B 12 (1975) 1257–1261 (see Ref. [1201]).

[3636] K. Jacobi, Private comm. (see Ref. [3144]).

[3637] K.L. Jensen, Exchange–correlation, dipole, and image charge potentials for electron sources: Temperature and field variation of the barrier height, J. Appl. Phys. 85 (1999) 2667–2680.

[3638] W. Kohn, L.J. Sham, Self–consistent equations including exchange and correlation effects, Phys. Rev. 140 (1965) A1133–A1138 (see Ref. [719]).

[3639] W.F. Krolikowski, Stanford Electron. Lab. Rept. No. 5218–1, 1967 (see Ref. [304]).

[3640] K.A. Kress, G.J. Lapeyre, Proc. Electron. Density of States Symp, NBS, Gaithersburg, Md, 1969 (see Ref. [304]).

[3641] S.A. Komolov, L.T. Chadderton, Interaction of slow electrons with surfaces: I. Desorption and adsorption of gas on {100} vanadium, Radiat. Eff. 31 (1976) 1–6.

[3642] G. Kozlowski, A. Ciszewski, Adsorption of antimony on the surface of a tungsten FEM emitter tip, Acta Univ. Wratislav., Mat., Fiz., Astron. 40 (1980) 63–68 (Chem. Abtr. 95 (1981) 210212h).

[3643] H. Kawano, F.M. Page, G. Younes, The determination of electron affinities by surface ionization, Adv. Mass Spectrom. 8 B (1980) 1794–1797.

[3644] S. Kennou, An X–ray photoelectron spectroscopy and work–function study of the Er/α–SiC(0001) interface, J. Appl. Phys. 78 (1995) 587–589.

[3645] J.-S. Kang, D.W. Hwang, J.H. Hong, J.I. Jeong, H.K. An, Y.P. Lee, J.J. Lee, K.H. Kim, Angle–resolved photoemission study of Pd(111) and Co/Pd(111), J. Magn. Magn. Mater. 150 (1995) 323–328.

[3646] S. Kennou, A. Siokou, I. Dontas, S. Ladas, An interface study of vapor–deposited rhenium with the two (0001) polar faces of single crystal 6H–SiC, Diam. Rel. Mater. 6 (1997) 1424–1427.

[3647] Y.-J. Ko, K.J. Chang, J.-Y. Yi, Atomic and electronic structure of Li–adsorbed Si(100) surfaces, Phys. Rev. B 56 (1997) 9575–9582.

[3648] J.W. Kim, S. Kim, J.M. Seo, S. Tanaka, M. Kamada, Photoemission studies of the Na/Ge(111)–3×1 surface, J. Phys.: Condens. Matter 10 (1998) 3731–3741.

[3649] O.M. Küttel, O. Gröning, Ch. Emmenegger, L. Nilsson, E. Maillard, L. Diederich, L. Schlapbach, Field emission from diamond, diamond–like and nanostructured carbon films, Carbon 37 (1999) 745–752.

[3650] T. Kondo, S. Yagyu, T. Hiraoka, T. Ikeuchi, S. Yamamoto, Work function of Pt(111) modified by hyperthermal CH_4 molecular beam, Shinku (J. Vac. Soc. Japan) 43 (2000) 745–749 (Chem. Abstr. 134 (2001) 21807u).

[3651] L. Kang, B.H. Lee, W.-J. Qi, Y. Jeon, R. Nieh, S. Gopalan, K. Onishi, J.C. Lee, Electrical characteristics of highly reliable ultrathin hafnium oxide gate dielectric, IEEE Electr. Dev. Lett. 21 (2000) 181–183.

[3652] H.J. Lemmens, M.J. Jansen, R. Loosjes, A new thermionic cathode for heavy loads, Philips Techn. Rev. 11 (1950) 341–372.

[3653] L. Ley, G.P. Kerker, N. Mårtensson, Surface electronic structure of calcium, strontium, and barium, Phys. Rev. B 23 (1981) 2710–2717.

[3654] C. Li, A.J. Freeman, C.L. Fu, Electronic structure and magnetism of surfaces and interfaces: Selected examples, J. Magn. Magn. Mater. 83 (1990) 51–56.

[3655] G.A. Rump, G.G. Vladimirov, T.T. Magkoev, Adsorption of B on Mo(011), Poverkhnost' (4) (1987) 33–36.

[3656] Q. Lu, R. Lin, P. Ranade, Y.C. Yeo, X. Meng, H. Takeuchi, T.-J. King, C. Hu, H. Luan, S. Lee, W. Bai, C.-H. Lee, D.-L. Kwoung, X. Guo, X. Wang, T.-P. Ma, Tech. Dig. Int. Electron Devices Meet., 2000, p. 641 (see Ref. [3519]).

[3657] W. Lai, D. Xie, First–principles study of K and Cs adsorbed on Pd(111), J. Phys. Chem. B 110 (2006) 23904–23910.

[3658] E.W.J. Mitchell, J.W. Mitchell, Work function of germanium, in: Proc. Conf. Univ. Reading, Engl., Semiconducting Materials, 1951, pp. 148–150 (Chem. Abstr. 48 (1954) 5683a).

[3659] J. Mort, A.I. Lakatos, Int. Conf. Liquid Amorphous Semicond, Cambridge, Engl., 1969 (see Ref. [2479]).

[3660] V. Maurice, L. Peralta, Y. Berthier, J. Oudar, Adsorption of sulphur on the (100) face of molybdenum: A complete crystallographic discussion, Surf. Sci. 148 (1984) 623–634.

[3661] T. Mandel, Location–dependent photo– and Auger–electron spectroscopy on physisorbed noble gases (Ph.D. thesis), Freie Univ. Berlin, 1986 (see Ref. [3144]).

[3662] D.R. Mullins, J.M. White, H.S. Luftman, Probing potassium on Ni(100) with adsorbed rare gas atoms, Surf. Sci. 167 (1986) 39–56.

[3663] J.P. Muscat, I.P. Batra, Coverage dependence of the work function of metals upon alkali–metal adsorption, Phys. Rev. B 34 (1986) 2889–2892.

[3664] W.A. Mackie, C.H. Hinrichs, I.M. Cohen, J.S. Alin, D.T. Schnitzler, P. Carleson, R. Ginn, P. Krueger, C.G. Vetter, Effective thermionic work function measurements of zirconium carbide using a computer–processed image of a thermionic projection microscope pattern, J. Vac. Sci. Technol. A 8 (1990) 2333–2337.

[3665] Y. Morikawa, K. Kobayashi, K. Terakura, S. Blügel, Theoretical support to the double–layer model for potassium adsorption on the Si(001) surface, Phys. Rev. B 44 (1991) 3459–3462.

[3666] G. Moos, C. Gahl, R. Fasel, M. Wolf, T. Hertel, Anisotropy of quasiparticle lifetimes and the role of disorder in graphite from ultrafast time–resolved photoemission spectroscopy, Phys. Rev. Lett. 87 (2001) 267402/1–4.

[3667] W.B. Nottingham, Influence of accelerating fields on the photoelectric and thermionic work function of composite surfaces, Phys. Rev. 35 (1930) 1128.

[3668] W.B. Nottingham, Photoelectric and thermionic emission from composite surfaces, Phys. Rev. 41 (1932) 793–812.

[3669] É.L. Nagaev, Small metal particles, Sov. Phys. Usp. 35 (1992) 747–782.

[3670] T. Oguri, Studies on chemisorption of nitrogen on tungsten with the field emission microscope, J. Phys. Soc. Japan 19 (1964) 83–91.

[3671] S. Ohnishi, C.L. Fu, A.J. Freeman, Local spin density total energy study of surface magnetism: V(100), J. Magn. Magn. Mater. 50 (1985) 161–168.

[3672] J. Peisner, P. Roboz, P.B. Barna, Thickness dependence of the quantum yield and attenuation length of photoelectrons in thin indium films, Phys. Status Solidi (a) 4 (1971) K187–K191.

[3673] M.M. Pant, A.K. Rajagopal, Theory of inhomogeneous magnetic electron gas, Solid State Commun. 10 (1972) 1157–1160.

[3674] C.A. Papageorgopoulos, J.M. Chen, Coadsorption of cesium and oxygen on Ni(100). II. Cesium enhanced chemisorption and oxidation, Surf. Sci. 52 (1975) 53–61.

[3675] L.G. Petersson, S.-E. Karlsson, Clean and oxygen exposed potassium studied by photoelectron spectroscopy, Phys. Scr. 16 (1977) 425–431.

[3676] J. Polański, Z. Sidorski, S. Zuber, Effect of temperature on the adsorption of gold on the (110) tungsten single crystal plane, in: Suppl., Proc. Int. Conf. Solid Surf., 4th, vol. 1, Vide 201 (1980) 233–236.

[3677] A. Pargellis, M. Seidl, Formation of H^- ions by backscattering thermal hydrogen atoms from a cesium surface, Phys. Rev. B 25 (1982) 4356–4361.

[3678] E. Puckrin, A.J. Slavin, Adsorption of bismuth onto the Au(111) surface, Phys. Rev. B 41 (1990) 4970–4975.

[3679] G.G. Vladimirov, T.T. Magkoev, G.A. Rump, Adsorption of Ti, Cr and Cu atoms on a Mo(011) surface, Poverkhnost' (5) (1990) 20–25.

[3680] N. Pradeep, R.B. Sharma, D.S. Joag, Field emission from a nickel adsorbed tungsten tip: Temperature dependent growth and its effects on current stability, Ultramicrosc. 73 (1998) 59–66.

[3681] W.-J. Qi, R. Nieh, B.H. Lee, L. Kang, Y. Jeon, J.C. Lee, Electrical and reliability characteristics of ZrO_2 deposited directly on Si for gate dielectric application, Appl. Phys. Lett. 77 (2000) 3269–3271.

[3682] L. Qiao, W.T. Zheng, H. Xu, L. Zhang, Q. Jiang, Field emission properties of N–doped capped single–walled carbon nanotubes: A first–principles density–functional study, J. Chem. Phys. 126 (2007) 164702/1–7.

[3683] O.W. Richardson, K.T. Compton, LIII. The photoelectric effect, Phil. Mag. 24 (1912) 575–594.

[3684] H. Roux, A. Piquet, R. Uzan, M. Drechsler, A determination of the surface self–diffusion coefficient in the presence of an adsorption layer by using field emission points (nickel on tungsten), Surf. Sci. 59 (1976) 97–114.

[3685] B. Reihl, R. Dudde, L.S.O. Johansson, K.O. Magnusson, The electronic structure of alkali–metal layers on semiconductor surfaces, Appl. Phys. A 55 (1992) 449–460.

[3686] N.Ya. Roukhlyada, S.G. Samoilov, Anomalies in the temperature dependence of the work function of ruthenium faces (11$\bar{2}$2) and (11$\bar{2}$5), Phys. Scr. 62 (2000) 341–343.

[3687] P. Ranade, Y.C. Yeo, Q. Lu, H. Takeuchi, T.-J. King, C. Hu, Molybdenum as a gate electrode for deep sub–micron CMOS technology, Mater. Res. Soc. Symp. Proc. (611) (2001) C3.2.1.–C3.2.6.

[3688] A.R. Shul'man, A.N. Pisarevskiĭ, The change with temperature of the work function at n– and p–germanium, Zh. Tekh. Fiz. 25 (1955) 1547–1555.

[3689] Yu.G. Shishkin, I.L. Sokol'skaya, Work function and properties of the surface in the copper–barium system, Fiz. Tverd. Tela, Akad. Nauk SSSR, Sbornik Statei 2 (1959) 273–275 (Chem. Abstr. 56 (1962) 3001b).

[3690] M.D. Scheer, J. Fine, Work function of the (110) plane of tungsten as determined by the surface ionization of NaCl, Bull. Am. Phys. Soc. 10 (1965) 69.

[3691] L.W. Swanson, A.E. Bell, L.C. Crouser, B.E. Evans, R.W. Strayer, Investigations of Electron Emission Characteristics of Low Work Function Surfaces, Final Rept. Contract NASw–1516, 1967, 105 pp.

[3692] K.S. Singwi, M.P. Tosi, R.H. Land, Electron correlations at metallic densities, Phys. Rev. 176 (1968) 589–599 (see Ref. [2835]).

[3693] K.S. Singwi, A. Sjölander, M.P. Tosi, R.H. Land, Electron correlations at metallic densities. IV, Phys. Rev. B 1 (1970) 1044–1053 (see Ref. [2835]).

[3694] P.P. Shatillo, Investigation of the photoelectron emission of a barium getter, Elektrovak. Tekh. 52 (1971) 18.

[3695] N.B. Smirnova, B.G. Smirnov, R.G. Masagutova, A.M. Shmakov, G.N. Shuppe, Thermionic parameters of the basic faces of a vanadium single crystal, in: Emiss. Elektron., Mater. Semin. Probl. Rab. Vykhoda Elektronov Adsorbtsii Met. Zavisimosti Kristallogr. Napravlenii, 2nd, 1971, pp. 103–104 (Chem. Abstr. 85 (1976) 135513v).

[3696] J.A. Dillon Jr., Private comm. (see Ref. [903]).

[3697] F.K. Schulte, A theory of thin metal films: Electron density, potentials and work function, Surf. Sci. 55 (1976) 427–444 (see Ref. [2512]).

[3698] P.J. Schneider, K.H. Berkner, W.G. Graham, R.V. Pyle, J.W. Stearns, D^- production by backscattering from clean alkali–metal surfaces, in: Proc. Symp. Produc. Neutraliz. of Negative Hydrogen Ions and Beams, 1977, pp. 63–69 (Brookhaven Natl. Lab. BNL–Rept. 50727 (1977)).

[3699] C. Sébenne, D. Bolmont, G. Guichar, M. Balkanski, Surface states from photoemission threshold on silicon(111) face, Japan. J. Appl. Phys. Suppl. 2 (Pt. 2) (1974) 405–408.

[3700] V.I. Spitsyn, M.P. Glazunov, B.F. Gulev, V.I. Makarenkov, O.A. Balakhovskiĭ, Experimental determination of technetium thermionic work function, Dokl. Akad. Nauk SSSR, Ser. Fiz. Khim. 267 (1982) 416–418.

[3701] A. Shih, C.R.K. Marrian, G.A. Haas, Reaction products and subsequent thermal decomposition of Ba films exposed to CO, CO_2 and O_2, Appl. Surf. Sci. 16 (1983) 106–124.

[3702] E. Schweizer, Ph.D. thesis, Freie Univ. Berlin, 1986 (see Ref. [2529]).

[3703] R.W. Schoenlein, J.G. Fujimoto, G.L. Eesley, T.W. Capehart, Femtosecond studies of image–potential dynamics in metals, Phys. Rev. Lett. 61 (1988) 2596–2599.

[3704] S.A. Shakirova, M.A. Shevchenko, Adsorption of heavy rare–earth atoms on (011) and (111) W, J. Phys. Colloq. 50 (1989) C8–129/C8–131.

[3705] M. Schmidt, H. Wolter, M. Schick, K. Kalki, K. Wandelt, Compression phases in copper/oxygen coadsorption layers on a Ru(0001) surface, Surf. Sci. 287/288 (1993) 983–987.

[3706] M. Schmidt, H. Wolter, K. Wandelt, Work–function oscillations during the surfactant induced layer–by–layer growth of copper on oxygen precovered Ru(0001), Surf. Sci. 307–309 (1994) 507–515.

[3707] C.A. Schmuttenmaer, M. Aeschlimann, H.E. Elsayed-Ali, R.J.D. Miller, D.A. Mantell, J. Cao, Y. Gao, Time–resolved two–photon photoemission from Cu(100): Energy dependence of electron relaxation, Phys. Rev. B 50 (1994) 8957–8960.

[3708] A. Sioku, S. Kennou, S. Ladas, T.A. Nguyen Tan, J.-Y. Veuillen, Growth and characterization of the Re/Si(111) interface, Surf. Sci. 352–354 (1996) 628–633.

[3709] P. Segovia, G.R. Castro, A. Mascaraque, P. Prieto, H.J. Kim, E.G. Michel, Origin of the surface metallization in single–domain K/Si(100)2×1, Phys. Rev. B 54 (1996) R14277–R14280.

[3710] J. Schneider, A. Rosenhahn, K. Wandelt, STM measurements on alloy formation during submonolayer growth of Mn on Cu(111), Appl. Surf. Sci. 142 (1999) 68–74.

[3711] R. Schlaf, H. Murata, Z.H. Kafafi, Work function measurements on indium tin oxide films, J. Electron Spectrosc. Relat. Phenom. 120 (2001) 149–154.

[3712] T. Toya, Lattice vibration and thermal expansion of universal metals, J. Res. Inst. Catal., Hokkaido Univ. 8 (1961) 178–210 (see Ref. [2835]).

[3713] F. Toigo, T.O. Woodruff, Calculation of the dielectric function for a degenerate electron gas with interactions. I. Static limit, Phys. Rev. B 2 (1970) 3958–3966 (see Ref. [2835]).

[3714] M. Tabe, M. Takahashi, Y. Sakakibara, Oxygen–doped Si epitaxial film (OXSEF), Japan. J. Appl. Phys. 26 (1987) 1830–1837.

[3715] V.M. Tapilin, D.Y. Zemlyanov, M.Y. Smirnov, V.V. Gorodetskii, Angle resolved photoemission study and calculation of the electronic structure of the Pt(111) surface, Surf. Sci. 310 (1994) 155–162.

[3716] T. Takahashi, T. Kawamukai, S. Ono, T. Noda, H. Sakaki, Kelvin probe force microscopy on InAs thin films on (110)GaAs substrates, Japan. J. Appl. Phys. 39 (2000) 3721–3723.

[3717] T.A. Tumareva, G.G. Sominskiĭ, A.A. Veselov, Potassium–induced activation of field emitters with fullerene coating, Tech. Phys. 49 (2004) 916–919.

[3718] H. Tollefsen, E.O. Laastad, S. Raaen, Surface alloying and mixed valence in thin layers of Ce and Pd on Ru(0001), Surf. Sci. 603 (2009) 197–202.

[3719] J. van Laar, J.J. Scheer, Proc. Int. Conf. Phys. Semiconductors, Exeter, 1962 (see Ref. [1229]).

[3720] G. Valette, A. Hameline, Structure and properties of the double electrochemical layer at the silver/sodium fluoride aqueous solution interface, J. Electroanal. Chem. 45 (1973) 301–319 (see Ref. [3280]).

[3721] J.N.M. van Wunnik, J.J.C. Geerlings, J. Los, The velocity dependence of the negatively charged fraction of hydrogen scattered from cesiated tungsten surfaces, Surf. Sci. 131 (1983) 1–16.

[3722] J.N.M. van Wunnik, J.J.C. Geerlings, E.H.A. Granneman, J. Los, The scattering of hydrogen from a cesiated tungsten surface, Surf. Sci. 131 (1983) 17–33.

[3723] P.W. van Amersfoort, J.J.C. Geerlings, L.F.Tz. Kwakman, A. Hershcovitch, E.H.A. Granneman, J. Los, Formation of negative hydrogen ions on a cesiated W(110) surface: The influence of hydrogen implantation, J. Appl. Phys. 58 (1985) 3566–3572.

[3724] R. Vanselow, Compensation effects in thermionic electron emission, Surf. Sci. 149 (1985) 381–393.

[3725] E. Wigner, J. Bardeen, Theory of the work functions of monovalent metals, Phys. Rev. 48 (1935) 84–87.

[3726] H. Washimi, Field emission studies of sodium iodide and mercury on tungsten, Japan. J. Appl. Phys. 12 (1973) 1446–1454.

[3727] R.E. Watson, M.L. Perlman, J.F. Herbst, Core level shifts in the $3d$ transition metals and tin, Phys. Rev. B 13 (1976) 2358–2365.

[3728] K.F. Wojciechowski, Electronic properties of alkali submonolayers on a metal substrate, Surf. Sci. 55 (1976) 246–258.

[3729] E. Wimmer, All–electron local density functional study of metallic monolayers. II: Alkali–earth metals, J. Phys. F 14 (1984) 681–690.

[3730] S. Wriedt, L. Holmlid, Work function measurements on rhenium foils in a directed cesium flux: Thermionic converter applications, Appl. Surf. Sci. 31 (1988) 197–210.

[3731] H. Wolter, M. Schmidt, K. Wandelt, Surfactant induced layer–by–layer growth of Cu on Ru(0001), Surf. Sci. 298 (1993) 173–186.

[3732] J.E. Whitten, R. Gomer, Interaction of hydrogen and Ni on W(110), Surf. Sci. 316 (1994) 23–35.

[3733] A. Wachter, K.P. Bohnen, K.M. Ho, Structure and dynamics at the Pt(100)–surface, Ann. Phys. 5 (1996) 215–223.

[3734] L. Xu, H.Y. Xiao, X.T. Zu, Hydrogen adsorption on Ru(001) surface from density–functional periodic calculations, Chem. Phys. 315 (2005) 155–160.

[3735] L. Yang, R. Hudson, Effect of preferred crystal orientation and surface treatment on the work function of vapor deposited tungsten, in: IEEE Conf. Record of Thermion. Convers. Special. Conf., Houston, Texas, 1966, p. 395.

[3736] M.L. Yu, Work–function dependence of negative–ion production during sputtering, Phys. Rev. Lett. 40 (1978) 574–577.

[3737] I.T. Yakubov, A.G. Khrapak, V.V. Pogosov, S.A. Trigger, Thermodynamic characteristics of liquid metal droplets, Phys. Status Solidi (b) 145 (1988) 455–466.

[3738] Yu.V. Zubenko, Field emission from titanium films on tungsten and tungsten carbide, Radiotekh. Elektron. 8 (1963) 1239–1245.

[3739] Yu.V. Zubenko, The effect of electronegative adsorbates on the work function of the barium–tungsten system, Radio Eng. Electron. Phys. 14 (1969) 1978–1980.

[3740] H.I. Zhang, M. Schlüter, A theoretical study of Al overlayers on Si(111), J. Vac. Sci. Technol. 15 (1978) 1384–1388.

[3741] J. Żebrowski, Effect of temperature on the work function of tin, Acta Phys. Polon. A 61 (1982) 459–461.

[3742] V.V. Zhirnov, On the cold emission mechanism of diamond coated tips, in: Proc. 43rd IFES, J. Phys. IV 6 (C5) (1996) C5–107/C5–112.

[3743] A. Biedermann, R. Tscheließnig, M. Schmid, P. Varga, Crystallographic structure of ultrathin Fe films on Cu(100), Phys. Rev. Lett. 87 (2001) 086103/1–4.

[3744] H.E. Farnsworth, Preparation, structural characterization, and properties of atomically clean surfaces, J. Vac. Sci, Technol. 20 (1982) 271–280.

[3745] W. Zhang, W.S. Zhao, D.X. Li, M.L. Sui, Martensitic transformation from α–Ti to β–Ti on rappid heating, Appl. Phys. Lett. 84 (2004) 4872–4875.

[3746] R.C.L. Bosworth, Studies in contact potentials: The evaporation of sodium films, Proc. R. Soc. A 162 (1937) 32–49.

[3747] G.M. Pyatigorskii, Surface ionization of molecules of alkali halide salts, Sov. Phys. Tech. Phys. 10 (1965) 867–870.

[3748] M.J. Copley, R.W. Spence, The contact potential of an iodine film on tungsten, J. Am. Chem. Soc. 61 (1939) 3027–3030.

[3749] T. Nakane, S. Kitami, A. Sakai, M. Sakata, Mezo Zairyo Kenkyu Senta Kenkyu Seika Hokokusho 5 (1996) 67–75 (Chem. Abstr. 128 (1998) 264806y) (see Ref. [2424]).

[3750] D.A. Gorodetsky, A.N. Knysh, The study of structure and work function of barium oxide films and the Ba–O double system on the (0001) face on rhenium: II. Double Ba–O–Re(0001) system, Surf. Sci. 40 (1973) 651–668.

[3751] A.Ya. Tontegode, É.Ya. Zandberg, Effect of impurity adsorption on surface ionization of CsCl on iridium, Sov. Phys. Tech. Phys. 15 (1970) 483–486.

[3752] S.Ya. Levedev, Yu.Ya. Stavisskii, Surface ionization of cesium in diffusion of cesium vapor through porous nickel, Sov. Phys. Tech. Phys. 8 (1963) 1094–1095.

[3753] A.Ya. Tontegode, R.M. Abdullaev, F.K. Yusifov, Interstitial atomic diffusion between the surface and the interior of a solid: Carbon diffusion in rhenium, Sov. Phys. Tech. Phys. 21 (1976) 1201–1207.

[3754] W.G. Graham, Negative–hydrogen–ion production by low energy hydrogen atom bombardment of surfaces, Preprint LBL–9511, US Department of Energy W–7405–ENG–48, 1979, 20 pp.

[3755] T.V. Krachino, M.V. Kuz'min, M.V. Loginov, M.A. Mittsev, Yb and Sm adsorption and silicide formation on Si(111) surface, Phys. Low-Dim. Struct. 9/10 (1999) 95–106.

[3756] M. Takahashi, Work function change of Cs–Mo surface by hydrogen adsorption (Master's thesis), Doshisha Univ., 1991, 63 pp.

[3757] T.V. Krachino, M.V. Kuz'min, M.V. Loginov, M.A. Mittsev, Adsorption stage of the Eu–Si(111) interface formation, Appl. Surf. Sci. 182 (2001) 115–132.

[3758] T.V. Krachino, M.V. Kuz'min, M.V. Loginov, M.A. Mittsev, Effect of temperature and surface coverage on the samarium interaction with Si(111), Phys. Solid. State 40 (1998) 1758–1764.

[3759] B.E. Evans, L.W. Swanson, A.E. Bell, Adsorption of cesium fluoride on tungsten, Surf. Sci. 11 (1968) 1–18.

[3760] R.G. Jones, D.L. Perry, Halogen adsorption on Fe(100): II. The adsorption of I_2 studied by AES, LEED, thermal desorption and work function change, Surf. Sci. 88 (1979) 331–347.

[3761] P. Cremaschi, H. Yang, J.L. Whitten, *Ab initio* chemisorption studies of H on Fe(110), Surf. Sci. 330 (1995) 255–264.

[3762] O.K. Husmann, A comparison of the contact ionization of cesium on tungsten with that of molybdenum, tantalum, and rhenium surfaces, in: AIAA Electric Propulsion Conf., Colorado Springs, 1963, 27 pp.

[3763] O.K. Husmann, Experimental evaluation of porous materials for surface ionization of cesium and potassium, Progr. Astronaut. Rocketry 9 (1963) 195–217.

[3764] S.I. Kim, M. Seidl, A new solid–state cesium ion source, J. Appl. Phys. 67 (1990) 2704–2710.

[3765] J.G. Alessi, A. Hershcovitch, Th. Sluyters, Cesiated porous molybdenum converter for intense negative ion sources, Rev. Sci. Instrum. 55 (1984) 8–11.

[3766] T. Nagata, Surface ionization of sodium and potassium atoms on heated tungsten, Res. Bull. Meisei Univ., Phys. Sci. Eng. 17 (1981) 45–52 (Chem. Abstr. 95 (1981) 121347p).

[3767] P.D. Rack, J. Li, P. Ostdiek, J.J. Peterson, L. Li, T. Rogelstad, Materials development and current transport in vacuum microelectronic devices, in: Proc. 14th Bienn. Univ./Gov./Indus. Microelectron. Symp. Richmond, 2001, pp. 140–143 (Chem. Abstr. 136 (2002) 192289x).

[3768] E.G. Overbosch, Positive and negative surface ionization of hyperthermal sodium atoms (Thesis), FOM Inst. for Atomic and Molecular Phys., Amsterdam, 1980.

[3769] J. Loss, E.A. Overbosch, J. van Wunnik, Positive and negative ionization by scattering from surfaces, in: Proc. 2nd Int. Symp. Produc. and Neutraliz. Negat. Hydrogen Ions and Beams, BNL–51304, 1980, pp. 23–32.

[3770] W.G. Graham, Negative hydrogen ion production by low energy hydrogen atom bombardment of surfaces, Phys. Lett. 73 A (1979) 186–188.

[3771] A. Danon, A. Amirav, Surface–molecule electron transfer: I_2–diamond scattering at 1–12 eV, Phys. Rev. Lett. 61 (1988) 2961–2964.

[3772] A. Bekkerman, B. Tsipinyuk, S. Verkoturov, E. Kolodney, Negative ion formation in near grazing surface scattering of hyperthermal neutral C_{60}: Image charge effects, J. Chem. Phys. 109 (1998) 8652–8658.

[3773] A. Bekkerman, B. Tsipinyuk, E. Kolodney, Charge transfer in hyperthermal surface collisions of C_{60}^0 and C_{60}^-: Experiment and model calculations, J. Chem. Phys. 116 (2002) 10447–10457.

[3774] J.N.M. van Wunnik, J. Los, Resonant charge transfer in atom–metal surface reactions, Phys. Scrip. T 6 (1983) 27–34.

[3775] A. Bekkerman, B. Tsipinyuk, E. Kolodney, Relative yield of C_{60}^- in hyperthermal surface scattering of neutral C_{60}: Outgoing velocity dependence, Phys. Rev. B 61 (2000) 10463–10470.

[3776] V.N. Ageev, S.M. Solov'ev, Electron–stimulated desorption of lithium ions from silicided tantalum surfaces, Surf. Sci. 451 (2000) 53–58.

[3777] D. Menzel, R. Gomer, Desorption from metal surfaces by low–energy electrons, J. Chem. Phys. 41 (1964) 3311–3328.

[3778] V.N. Ageev, Yu.A. Kuznetsov, N.D. Potekhina, Electron–stimulated desorption of alkali metal and barium atoms from an oxidized tungsten surface, Surf. Sci. 367 (1996) 113–127.

[3779] J. Behm, C.R. Brundle, K. Wandelt, To be published (See Ref. [914]).

[3780] W.G. Graham, Properties of alkali metals adsorbed onto metal surfaces, in: Proc. 2nd Int. Symp. Prod. Neutralizat. Negat. Hydrogen Ions and Beams, 1980, pp. 126–136 (Chem. Abstr. 95 (1981) 158118r).

[3781] R. Forman, Surface studies of barium and barium oxide on tungsten and its applications to understanding the mechanism of operation of an impregnated tungsten cathode, J. Appl. Phys. 47 (1976) 5272–5279.

[3782] M. Rogozia, H. Niehus, A. Böttcher, Formation of Cs–H surface compounds, Surf. Sci. 519 (2002) 101–114.

[3783] É.Ya. Zandberg, É.G. Nazarov, U.Kh. Rasulev, E.V. Rut'kov, Simple method for monitoring high–work–function regions on solid surfaces, Sov. Tech. Phys. Lett. 8 (1982) 471–472.

[3784] É.Ya. Zandberg, N.D. Potekhina, E.V. Rut'kov, A.Ya. Tontegode, Migration of Cs and Ba on an iridium surface and on a graphite monolayer on an iridium substrate, Sov. Phys. Tech. Phys. 27 (1982) 1478–1482.

[3785] A.R. Olpin, Unpublished (see Refs. [1374,3725]).

[3786] K.H. Kingdon, Comparison of thermal electron emission from a pool of caesium and from adsorbed films, Phys. Rev. 25 (1925) 892.

[3787] X. Shao, D. Li, J. Cai, H. Luo, C. Dong, First–principles study of structural and work function properties for nitrogen–doped single–walled carbon nanotubes, Appl. Surf. Sci. 368 (2016) 477–482.

[3788] M. Akbi, A. Bouchou, N. Zouache, Effects of vacuum heat treatment on the photoelectric work function and surface morphology of multilayered silver–metal electrical contacts, Appl. Surf. Sci. 303 (2014) 131–139.

[3789] G. Zampieri, R. Baragiola, Ion–induced Auger emission from solids: Correlation between Auger energies and work function, Phys. Rev. B 29 (1984) 1480–1482.

[3790] M.M. Marino, W.C. Ermler, *Ab initio* study of hydrogen adsorption on Be(0001), J. Chem. Phys. 94 (1991) 8021–8028.

[3791] L.A. Rudnitskii, Non–uniformity of the heat of adsorption of ions on non–planar and non–ideal metallic surfaces. II. Distribution of the surface potential step over a non–ideal metal surface and characterization of the donor properties of the surface, Russ. J. Phys. Chem. 55 (1981) 1172–1175.

[3792] Ts.S. Marinova, Yu.V. Zubenko, Adsorption and desorption of ytterbium on carbonized tungsten, Sov. Phys.—Solid State 13 (1971) 635–636.

[3793] N.I. Ionov, Ts.S. Marinova, Desorption of ytterbium and neodymium from tungsten by an electric field, Sov. Phys.—Solid State 13 (1971) 557–563.

[3794] R.C. Evans, The atomic work function of tungsten for potassium, Proc. R. Soc. A 145 (1934) 135–144.

[3795] M.-S. Jung, T.-L. Choi, W.-J. Joo, J.-Y. Kim, I.-T. Han, J.M. Kim, Transparent conductive thin films based on chemically assembled single–walled carbon nanotubes, Synth. Met. 157 (2007) 997–1003.

[3796] R.Z. Bakhtizin, A.L. Suvorov, R.F. Zaripov, Field emission study of germanium thin films on a niobium surface, Acta Phys. Pol. A 81 (1992) 247–255.

[3797] E.O. Lawrence, L.B. Linford, The effect of intense electric fields on the photoelectric properties of metals, Phys. Rev. 36 (1930) 482–497.

[3798] J.M. Houston, Thermionic emission of refractory metals in cesium vapors, Bull. Am. Phys. Soc. 6 (1961) 358.

[3799] J.M. Houston, H.F. Webster, Thermionic energy conversion, Adv. Electr. Erectr. Phys. 17 (1962) 125–206.

[3800] H.Y. Fan, Thermionic emission from sintered cathode of thoria and tungsten mixture, J. Appl. Phys. 20 (1949) 682–690.

[3801] I. Langmuir, Thoriated tungsten filaments, J. Franklin Inst. 217 (1934) 543–569 (see Ref. [3271]).

[3802] B. Krahl-Urban, Thesis, Univ. Köln (1976) (see Refs. [147,1312]).

[3803] Y.-C. Chao, L.S.O. Johansson, R.I.G. Uhrberg, Adsorption of Rb on Si(100)2×1 at room temperature studied with photoelectron spectroscopy, Appl. Surf. Sci. 123/124 (1998) 76–81.

[3804] L.S.O. Johansson, T. Dütemeyer, L. Duda, B. Reihl, Electronic structure of the Rb–adsorbed Si(100)2×1 surface studied by direct and inverse angle–resolved photoemission, Phys. Rev. B 58 (1998) 5001–5006.

[3805] M.-L. Ernst-Vidalis, M. Kamaratos, C. Papageorgopoulos, The effects of Cs on the adsorption of H_2 on Mo(110), Surf. Sci. 189/190 (1987) 276–284.

[3806] B. Nieber, C. Benndorf, Ethylene oxide adsorption of K–promoted Ni(111), Surf. Sci. 235 (1990) 129–141.

[3807] C.A. Papageorgopoulos, M. Kamaratos, A. Papageorgopoulos, Coadsorption of Na and elemental S on Ni(100), Surf. Sci. 402–404 (1998) 120–124.

[3808] P.W. Kidd, Effect of cesium vapor on the emission characteristics of uranium carbide at elevated pressures, J. Appl. Phys. 36 (1965) 14–17.

[3809] Y. Nakayama, H. Kondoh, T. Ohta, Nanometer–scale mapping of local work function with a photon–assisted STM technique, Appl. Surf. Sci. 241 (2005) 18–22.

[3810] B.N.J. Persson, L.H. Dubois, Work function, optical absorption, and second–harmonic generation from alkali–metal atoms adsorbed on metal surfaces, Phys. Rev. B 39 (1989) 8220–8235.

[3811] A.K. Sotiropoulos, M. Kamaratos, A study of Cs adsorption on Se–covered Si(100)2×1 surfaces, Appl. Surf. Sci. 229 (2004) 161–166.

[3812] G.S. Tompa, W.E. Carr, M. Seidl, Work function reduction of a tungsten surface due to cesium ion bombardment, Appl. Phys. Lett. 49 (1986) 1511–1513.

[3813] J.A. Becker, Study of surfaces by using new tools, Solid State Phys. 7 (1958) 379–424.

[3814] R.M. Digilov, V.F. Sozaev, Kh.B. Khokonov, Anisotropy of the surface energy and the electron work function of simple metals, Poverkhnost' (1) (1987) 13–18.

[3815] W. Carr, M. Seidl, G.S. Tompa, A. Souzis, Composite thin–film production by ion bombardment, J. Vac. Sci. Technol. A 5 (1987) 1250–1253.

[3816] E. Sugata, T. Kuroda, Adsorption of cesium on a tungsten surface, in: Abstr. 13th Ann. Meet. Appl. Phys. Soc. Japan, vol. 3, 1966, p. 17.

[3817] M. Šnábl, M. Ondřejček, V. Cháb, Z. Chvoj, W. Stenzel, H. Conrad, A.M. Bradshaw, Surface diffusion of K on Pd{111}: Coverage dependence of the diffusion coefficient determined with the Boltzmann–Matano method, J. Chem. Phys. 108 (1998) 4212–4218.

[3818] R. Gomer, Chemisorption on metals, Solid State Phys. 30 (1975) 93–225.

[3819] G.M. Guichar, M. Balkanski, C.A. Sébenne, Semiconductor surface state spectroscopy, Surf. Sci. 86 (1979) 874–887.

[3820] Z.T. Stott, H.P. Hughes, Chlorine and iodine adsorption on the Ta(100) and Ta(110) surfaces, Surf. Sci. 126 (1983) 455–462.

[3821] R.I. Hegde, J. Tobin, J.M. White, Surface chemistry of phosphorus–containing molecules: I. Interaction of phosphine with rhodium(100) and the effect of preadsorbed phosphorus, J. Vac. Sci. Technol. A 3 (1985) 339–345.

[3822] W. Ermrich, Influence of slow–electron impact upon gases adsorbed on tungsten, investigated by means of a field electron microscope, Philips Res. Repts. 20 (1965) 94–105.

[3823] P. Philipp, T. Wirtz, H.-N. Migeon, H. Scherrer, Cation mass spectrometer (CMS): Recent developments for quantitative analyses of positive and negative secondary ions, Appl. Surf. Sci. 231–232 (2004) 754–757.

[3824] G.R. Hertel, Surface ionization: I. Desorption of U+ ions from W and Re surfaces, J. Chem. Phys. 47 (1967) 133–137.

[3825] R. Kirchner, On the thermoionization in hot cavities, Nucl. Instrum. Moth. A 292 (1990) 203–208.

[3826] Y. Kawai, M. Nomura, Y. Fujii, T. Suzuki, Calcium ion generation from calcium iodide by surface ionization in mass spectrometry, Int. J. Mass Spectrom. 193 (1999) 29–34.

[3827] T. Suzuki, H. Iwabuchi, K. Takahashi, M. Nomura, M. Okamoto, Y. Fujii, Chemical form effects on the surface ionization of lithium halides, Int. J. Mass Spectrom. Ion Processes 145 (1995) 131–137.

[3828] B.H. Wolf, Characterization of ion sources, in: B. Wolf (Ed.), Handbook of Ion Sources, CRC Press, Boca Raton, 1995, pp. 313–331.

[3829] H. Zhang, Ion Sources, Science Press, Beijing/Springer, Berlin, 1999, pp. 13–16.

[3830] T.J. Lee, B.J. Hopkins, B.H. Blott, Effect of temperature on the work–function minimum of cesiated tungsten surfaces, J. Appl. Phys. 40 (1969) 3825–3827.

[3831] T.J. Lee, B.H. Blott, B.J. Hopkins, Contact potential difference measurements between polycrystalline tungsten surfaces in caesium vapor, in: Proc. 1st Int. Conf. Thermion. Generat. Electr. Power, London, 1965, pp. 1–6.

[3832] R.J. Zollweg, Electron and ion emission from cesium–coated refractory metals in electric field, Appl. Phys. Lett. 2 (1963) 27–29.

[3833] S.Yu. Davydov, I.V. Noskov, Effect of adsorption of alkali metal atoms on the work function of rutile, Tech. Phys. 47 (2002) 1481–1483.

[3834] G.A. Morosov, Surface ionization of barium on tungsten, Zh. Tekh. Fiz. 17 (1947) 1143–1146.

[3835] I.V. Chernyshev, L.L. Shanin, Surface ionization of lead on oxidized tungsten, Dokl. Phys. Chem. 188 (1969) 704–707.

[3836] R. Mueller, H.-W. Wassmuth, Discrimination of nuclear reaction–produced isobars by means of positive and negative surface ionization, Nucl. Instrum. Meth. 127 (1975) 225–236.

[3837] L. Dobrezow, Ionization of alkali metal atoms on tungsten, molybdenum and thoriated tungsten, Z. Phys. 90 (1934) 788–801.

[3838] A. Latuszynski, V.I. Raiko, Studies of the ion source with surface–volume ionization, Nucl. Instrum. Meth. 125 (1975) 61–66.

[3839] N.D. Morgulis, Thermal ionization of sodium vapors on the surface of incandescent tungsten, Zh. Fiz. Khim. 5 (1934) 236–239.

[3840] R.L. Aamodt, Private comm. (see Ref. [3841]).

[3841] C. Warner III, Statistical mechanical treatment of surface ionization, Atomics Int. Rept. AI–6799 (1961) 85–110.

[3842] F. Yerzley, An investigation of irregularities in thermionic emission from tungsten, Phys. Rev. 50 (1936) 610–616.

[3843] D.G. Worden, The effects of surface structure and adsorption on the ionization efficiency of a surface ionization, Prog. Astronaut. Rocketry 5 (1961) 141–160 (Chem. Abstr. 55 (1961) 25471b).

[3844] H. Kawano, Unpublished.

[3845] K. Christmann, J.E. Demuth, The adsorption and reaction of methanol on Pd(100). I. Chemisorption and condensation, J. Chem. Phys. 76 (1982) 6308–6317.

[3846] D.L. Fehrs, Ph.D. thesis, MIT, 1968 (see Ref. [1981]).

[3847] J.A. Becker, R.G. Brandes, On the adsorption of oxygen on tungsten as revealed in the field emission electron microscope, J. Chem. Phys. 23 (1955) 1323–1330.

[3848] E.P. Gyftopoulos, Work function in the system thorium–rhenium, J. Appl. Phys. 35 (1964) 464.

[3849] M. Huang, Y. Liu, A. Masuda, Accurate measurement of ruthenium isotopes by negative thermal ionization mass spectrometry, Anal. Chem. 68 (1996) 841–844.

[3850] A. Piotrowski, T. Kozłowski, M. Laskus, Study of negative ion emission from the tubular ionizer, Nucl. Instrum. Methods Phys. Res. B 129 (1997) 410–413.

[3851] R. Kirchner, Progress in ion source development for on–line separators, Nucl. Instrum. Methods 186 (1981) 275–293.

[3852] H. Ebinghaus, U. Holm, H.V. Klapdor, H. Neuert, A source for polarized lithium nuclei, Z. Phys. 199 (1967) 68–81.

[3853] D.M. Jamba, Surface ionization source for ion implantation, Rev. Sci. Instrum. 40 (1969) 1072–1074.

[3854] G.D. Alton, M.T. Johnson, G.D. Mills, A simple positive/negative surface ionization source, Nucl. Instrum. Methods A 328 (1993) 154–159.

[3855] M.L. Yu, Work function dependence and isotope effect in the production of negative hydrogen ions during sputtering of adsorbed hydrogen on Cs covered Mo(100) surfaces, in: Symp. Produc. Neutraliz. Negat. Hydrog. Ions and Beams, 1977, pp. 48–52.

[3856] L.H. Germer, The distribution of initial velocities among thermionic electrons, Phys. Rev. 25 (1925) 795–807.

[3857] E.H.A. Granneman, J.J.C. Geerlings, J.N.M. van Wunnik, P.J. van Bommel, H.J. Hopman, J. Los, H⁻ and Li⁻ formation by scattering H⁺, H₂⁺ and Li⁺ from cesiated tungsten surfaces, in: AIP Conf. Proc. No.111: 3rd Int. Symp. Product. Neutraliz. Neg. Ions and Beams, Upton, USA, 1983, pp. 206–218.

[3858] N.I. Ionov, Shift of retarding–potential curves due to electrode coverage by two–dimensional condensation, Sov. Phys. Tech. Phys. 18 (1973) 102–105.

[3859] Ch. Kleint, R. Męclewski, Flicker noise and surface migration during potassium–deposition on tungsten emitters in a field emission microscope, Acta. Phys. Polon. 33 (1968) 887–897.

[3860] J.M. Palau, A. Ismail, E. Testemale, L. Lassabatère, Calculation of the work function of a substrate thin–film heterojunction, Thin Solid Films 78 (1981) 177–186.

[3861] J.J. Stoffels, Spectrometer for on–line analysis of radionuclides (SOLAR), Nucl. Instrum. Meth. 119 (1974) 251–254.

[3862] T.H. George, P.M. Stier, Chemisorption of oxygen on ordered tungsten surfaces, J. Chem. Phys. 37 (1962) 1935–1946.

[3863] J.G. Korsgren, J.B.C. Pettersson, Collision dynamics and decomposition of NaCl nanometer particles on hot platinum surfaces, J. Phys. Chem. B 103 (1999) 10425–10432.

[3864] T. Kuroda, S. Nakamura, Field emission microscope studies of coadsorption of oxygen and cesium on refractory metals, Mem. Inst. Sci. & Ind. Res. Osaka Univ. 25 (1968) 49–61.

[3865] S. Nakamura, T. Kuroda, Field emission microscope studies of coadsorption of oxygen and cesium on tungsten, Mem. Inst. Sci. & Ind. Res. Osaka Univ. 24 (1967) 83–90.

[3866] B. Lägel, I.D. Baikie, K. Dirscherl, U. Petermann, A novel approach for true work function determination of electron–emissive materials by combined Kelvin probe and photoelectric effect measurements, Mat. Res. Soc. Symp. Proc. 621 (2000) R 3.5/1–7.

[3867] I.D. Baikie, P.J. Estrup, Low cost PC based scanning Kelvin prove, Rev. Sci. Instrum. 69 (1998) 3902–3907.

[3868] U. Petermann, I.D. Baikie, B. Lägel, K.M. Dirscherl, Work function study for the search of efficient target materials for use in hyperthermal surface ionization using a scanning Kelvin prove, Mat. Res. Soc. Symp. Proc. 623 (2000) 37–42.

[3869] L.P. Smith, The emission of positive ions from tungsten and molybdenum, Phys. Rev. 35 (1930) 381–497.

[3870] L.P. Smith, Positive ion emission from tungsten and molybdenum, Phys. Rev. 34 (1929) 1496–1497.

[3871] L.L. Barnes, The temperature variation of the positive ion emission from molybdenum, Phys. Rev. 42 (1932) 492–497.

[3872] R.E. Honig, Mass spectrometric study of the molecular sublimation of graphite, J. Chem. Phys. 22 (1954) 126–131.

[3873] G. Glockler, J.W. Sausville, The electron affinity of the carbon atom, Trans. Electrochem. Soc. 95 (1949) 282–291.

[3874] L.L. Barnes, The emission of positive ions from heated metals, Phys. Rev. 40 (1932) 1044.

[3875] L.L. Barnes, The emission of positive ions from heated metals, Phys. Rev. 42 (1932) 487–491.

[3876] G.A. Jarvis, Positive ion emission from nickel, Phys. Rev. 57 (1940) 335.

[3877] H.B. Wahlin, The emission of positive ions from metals, Phys. Rev. 37 (1931) 467–468.

[3878] F.A. White, T.L. Collins, F.M. Rourke, Search for possible naturally occurring isotopes of low abundance, Phys. Rev. 101 (1956) 1786–1791.

[3879] H.B. Wahlin, The emission of positive ions from metals, Phys. Rev. 34 (1929) 164.

[3880] H.B. Wahlin, The emission of positive ions from metals, Nature 123 (1929) 912.

[3881] F.A. White, T.L. Collins Jr., F.M. Rourke, New naturally occurring isotope of tantalum, Phys. Rev. 97 (1955) 566–567.

[3882] M. Asano, Surface ionization, Bull. Instr. Atom. Ener. Kyoto Univ. 43 (1973) 1–16 (Chem. Abstr. 79 (1973) 149418f).

[3883] J. Cesario, Y. Boulin, B. Landeau, An improved surface ionization ion source, Int. J. Mass Spectrom. Ion Phys. 46 (1983) 35–38.

[3884] H.J. Grover, The positive ion work function of molybdenum, Phys. Rev. 49 (1936) 878.

[3885] W.A. Jenkins, On the emission of positive ions from hot tungsten, Phil. Mag. 47 (1924) 1025–1047.

[3886] N.P. Katrich, V.N. Kanishchev, Study of the positive thermionic emission of refractory metals, Prib. Tekh. Eksp. (5) (1980) 176–179.

[3887] G.H. Palmer, The thermal–emission ion source in solid–source mass spectrometry, J. Nucl. Ener. 7 (1958) 1–12.

[3888] G.H. Palmer, High sensitivity solid source mass spectrometry, Adv. Mass Spectrom. 1 (1959) 89–102.

[3889] L.P. Smith, The emission of positive ions from tungsten at high temperatures, Phys. Rev. 33 (1929) 279.

[3890] L.P. Smith, On the emission of positive ions from hot tungsten, Phys. Rev. 33 (1929) 1082.

[3891] B. Toubes, G.K. Rollefson, The nature of ions emitted by heated filaments and salts, J. Chem. Phys. 8 (1940) 495–496.

[3892] J.A. Becker, Thermionic electron emission and adsorption. Part I. Thermionic emission, Rev. Modern Phys. 7 (1935) 95–128.

[3893] A.L. Reimann, Thermionic Emission, Chapman & Hall, London, 1934.

[3894] L.W. Swanson, P.R. Davis, Work function measurements, Meth. Exper. Phys. 22 (1985) 1–22.

[3895] N.D. Lang, The density–functional formalism and the electronic structure of metal surfaces, Solid State Phys. 28 (1973) 225–300.

[3896] É.Ya. Zandberg, Recent developments in surface ionization (Review), Sov. Phys. Tech. Phys. 19 (1975) 1133–1144.

[3897] F.I. Itskovich, Effective work functions of different types of electron emission from metals, Sov. Phys.—JETP 24 (1967) 202–206.

[3898] N.A. Surplice, R.J. D'Arcy, A critique of the Kelvin method of measuring work functions, J. Phys. E 3 (1970) 477–482.

[3899] J. Baczyński, L. Wojtczak, Dependence of work function on surface magnetization, Acta Phys. Pol. A 80 (1991) 707–716.

[3900] P.J. Godowski, J. Onsgaard, Work function of vicinal copper surfaces, Acta Phys. Pol. A 123 (2013) 115–117.

[3901] A. Kiejna, K.F. Wojciechowski, Work function (pp. 123–130), Work function of simple metals: Relation between theory and experiment (pp. 131–140), and Adsorption of alkali atoms on metal surface (pp. 223–243), in: Metal Surface Electron Physics, 1st ed., Pergamon, 1996, 303 pp.

[3902] A.G. Knapp, Surface potentials and their measurement by the diode method, Surf. Sci. 34 (1973) 289–316.

[3903] Yu.V. Zubenko, M.B. Ishmukhametov, Effect of germanium on the adsorption bond of barium with tungsten, Poverkhnost' (8) (1983) 68–72.

[3904] C.M. Horowitz, C.R. Proetto, J.M. Pitarke, Exact–exchange Kohn–Sham potential, surface energy, and work function of jellium slabs, Phys. Rev. B 78 (2008) 085126/1–12.

[3905] H. Luo, W. Hackbush, H.-J. Flad, D. Kolb, Fully self–consistent Hartree–Fock calculation of jellium slabs: Exact treatment of the exchange operator, Phys. Rev. B 78 (2008) 035136/1–12.

[3906] R. Gomer, Field Emission and Field Ionization, Harvard Univ. Press, 1961, 195 pp.

[3907] E.W. Müller, Field ionization and field ion microscopy, Adv. Electr. Electr. Phys. 13 (1960) 83–179.

[3908] Ya.S. Umanskii, Yu.A. Skakov, Physics of Metals: Atomic structure of metals and alloys, Atomizdat (1978) 352 pp. (see Ref. [2967]).

[3909] V.N. Ageev, A.I. Gubanov, S.T. Dzhalilov, L.F. Ivantsov, Oxygen–tantalum interaction due to electron–stimulated desorption, Sov. Phys. Tech. Phys. 21 (1976) 1535–1540.

[3910] E.G. Brock, Field emission microscopy of an allotropic transformation: α–β titanium, Phys. Rev. 100 (1955) 1619–1626.

[3911] D.P. Pappas, K.-P. Kämper, H. Hopster, Reversible transition between perpendicular and in–plane magnetization in ultrathin films, Phys. Rev. Lett. 64 (1990) 3179–3182.

[3912] J. Thomassen, F. May, B. Feldmann, M. Wuttig, H. Ibach, Magnetic live surface layers in Fe/Cu(100), Phys. Rev. Lett. 69 (1992) 3831–3834.

[3913] P. Schmailzl, K. Schmidt, P. Bayer, R. Döll, K. Heinz, The structure of thin epitaxial Fe films on Cu(100) in the transition range fcc→bcc, Surf. Sci. 312 (1994) 73–81.

[3914] B.W. Lee, R. Alsenz, A. Ignatiev, M.A. Van Hove, Surface structures of the two allotropic phases of cobalt, Phys. Rev. B 17 (1978) 1510–1520.

[3915] M.E. Bridge, C.M. Comrie, R.M. Rambert, Chemisorption studies on cobalt single crystal surfaces. I. Carbon monoxide on Co(0001), Surf. Sci. 67 (1977) 393–404.

[3916] H. Masumoto, A new transformation of cobalt and the equilibrium diagrams of nickel–cobalt and iron–cobalt, Sci. Rept. Tohoku Univ. Ser. 1: Math. Phys. Chem. 15 (1926) 449–477.

[3917] Z. Nishiyama, Mechanism of transformation of face–centered cubic into hexagonal close–packed lattice, Sci. Rept. Tohoku Univ. Ser. 1: Math. Phys. Chem. 25 (1936) 79–93.

[3918] A.P. Komar, V.N. Shrednik, Investigation of the allotropic transformation $\alpha \rightleftarrows \beta$ Zr with the aid of an electronic projector, Sov. Phys.—JETP 5 (1957) 127–128.

[3919] V.I. Emel'yanov, O.Ya. Maslennikov, P.N. Roukhlyada, Determination of the latent heat of phase transitions in ruthenium by means of a thermionic microscope, Appl. Surf. Sci. 215 (2003) 96–100.

[3920] N.Ya. Rukhlyada, I.P. Li, V.Ya. Pliskovski, Change in work function during a phase transition in a single crystal of (0001) terbium, in: Proc. 19th All–Union Conf. Emiss. Elect. Tashkent, 1984, p. 156 (see Ref. [4146]).

[3921] N.Ya. Rukhlyada, A.G. Trefilov, B.B. Shishkin, Polymorphic transformation in a single crystal of hafnium, Moscow Univ. Bull. Ser. 3: Fiz. Astron. 20 (1979) 70–72 (Chem. Abstr. 91 (1979) 47578p).

[3922] L.N. Dobretsov, M.V. Gomoyunova, Emission Electronics, Nauka, Moscow, 1966 (see Ref. [2349]).

[3923] J. de Miguel, A. Ceboladda, J.M. Gallego, R. Miranda, C.M. Schneider, P. Schuster, J. Kirshner, Influence of the growth conditions on the magnetic properties of fcc cobalt films: From monolayers to superlattices, J. Mag. Magn. Mater. 93 (1991) 1–9.

[3924] T. Maeda, S. Saito, Variation of the work function of Gd caused by the polarization of conduction electrons, J. Magn. Magn. Mater. 196–197 (1999) 694–695.

[3925] H. Schade, Work functions and sublimation entropies of the elements, Appl. Phys. 18 (1979) 339–344.

[3926] J. Frenkel, Elementary theory of the magnetic and electrical properties of the metals at absolute zero temperature, Z. Phys. 49 (1928) 31–45.

[3927] Ig. Tamm, D. Blochinzev, The work function for electrons in metals, Z. Phys. 77 (1932) 774–777.

[3928] F. Rother, H. Bomke, Calculation of emission potentials from simple metal constants, Z. Phys. 86 (1933) 231–240.

[3929] F. Rother, H. Bomke, Evaluation of the outer work of electron removal, W_a, Z. Phys. 87 (1934) 806–809.

[3930] E.H.B. Bartelink, Approximate method for calculating the work function of metals, Physica 3 (1936) 193–204.

[3931] J. Chittum, An approach to an explanation of the surface work functions of pure metals, J. Phys. Chem. 38 (1934) 79–84.

[3932] R.M. Vasenin, The possibility of calculating the potentials of zero charge, Zh. Fiz. Khim. 27 (1953) 878–888.

[3933] R.M. Vasenin, Dependence of the overvoltage on the electrode material, Zh. Fiz. Khim. 30 (1956) 629–638.

[3934] Z. Berkes, Photoelectric studies of thin alkali–meta layers, Mathem. Fiz. Lapok. Budapest 41 (1934) 131–161.

[3935] L.S.O. Johansson, T.M. Grehk, S.M. Gray, M. Johansson, A.S. Flodström, High resolution core–level spectroscopy study of low–coverage lithium adsorption on the Si(100)2×1 surface, Nucl. Instrum. Methods Phys. Res. B 97 (1995) 364–367.

[3936] G.I. Bigun, I.D. Nabitovich, Yu.S. Sukhorskii, Adsorption of lithium on the surface of germanium single crystal, Izv. Akad. Nauk SSSR, Ser. Fiz. 46 (1982) 1256–1259.

[3937] Yu.V. Zubenko, Ts.S. Marinova, Adsorption of beryllium on tungsten, Uch. Zap. Leningrad Gos. Univ., Ser. Fiz. Geol. Nauk 12 (354) (1970) 3–7 (Chem. Abstr. 74 (1971) 131764c).

[3938] Y. Namba, Attempt to grow diamond phase carbon films from an organic solution, J. Vac. Sci. Technol. A 10 (1992) 3368–3370.

[3939] J. Nakamura, I. Toyoshima, K. Tanaka, Formation of carbidic and graphitic carbon from CO on polycrystalline cobalt, Surf. Sci. 201 (1988) 185–194.

[3940] J. Wu, Z.-X. Shen, D.S. Dessau, R. Cao, D.S. Marshall, P. Pianetta, I. Lindau, X. Yang, J. Terry, D.M. King, B.O. Wells, D. Elloway, H.R. Wendt, C.A. Brown, H. Hunziker, M.S. de Vries, Electronic structure of single crystal C_{60}, Physica C 197 (1992) 251–260.

[3941] D. Chen, D. Sarid, Temperature effects of adsorption of C_{60} molecules on Si(111)–(7×7) surfaces, Rhys. Rev. B 49 (1994) 7612–7619.

[3942] G.L. Martin, P.R. Schwoebel, Field electron emission images of multi–walled carbon nanotubes, Surf. Sci. 601 (2007) 1521–1528.

[3943] O. Gröning, O.M. Küttel, Ch. Emmenegger, P. Gröning, L. Schlapbach, Unpublished (see Ref. [2425]).

[3944] E. Jensen, E.W. Plummer, Experimental band structure of Na, Phys. Rev. Lett. 55 (1985) 1912–1915.

[3945] S. Andersson, B. Kasemo, Low–energy electron diffraction intensities from the clean nickel(001) surface, Surf. Sci. 25 (1971) 273–288.

[3946] W. Cao, Adsorption of surface active elements on the iron(100) surface: A study based on *ab initio* calculations (Licentiate thesis), Roy. Inst. Tech., Sweden, 2009, 40 pp.

[3947] D. Jeon, T. Hashizume, T. Sakurai, R.F. Willis, Structural and electronic properties of ordered single and multiple layers of Na on the Si(111) surface, Phys. Rev. Lett. 69 (1992) 1419–1422.

[3948] S.K. Gupta, C.M. Singal, V.K. Srivastava, Thickness dependence of internal voltage in metal–insulator–metal structure with dissimilar electrodes, J. Appl. Phys. 48 (1977) 2583–2586.

[3949] I.P. Batra, F. Herman, Electronic states of ideal Ge–Al interfaces, J. Vac. Sci. Technol. A 1 (1983) 1080–1084.

[3950] R.M. Broudy, Vectorial photoelectric effect, Phys. Rev. B 3 (1971) 3641–3651.

[3951] M.C. Hanf, C. Pirri, J.C. Peruchetti, D. Bolmont, G. Gewinner, Formation of an interfacial alloy and epitaxial bcc Cr layers on Au(100), Phys. Rev. B 39 (1989) 1546–1556.

[3952] J.A. Becker, Adsorption on metal surfaces and its bearing on catalysis, Adv. Catal. 7 (1955) 135–211.

[3953] J.A. Becker, The life history of adsorbed atoms, ions, and molecules, Ann. New York Acad. Sci. 58 (1954) 723–740.

[3954] S.M. Dunaevskii, Model of the surface of a ferromagnetic jellium, Sov. Phys.—Solid State 23 (1981) 1495–1497 (see Ref. [503]).

[3955] K. Christmann, Private comm. (see Ref. [2876]).

[3956] H. Kawano, Unpublished (see Footnote 205 for Ag in Table 1).

[3957] C.S. Feigerle, R.R. Corderman, S.V. Bobashev, W.C. Lineberger, Binding energies and structure of transition metal negative ions, J. Chem. Phys. 74 (1981) 1580–1598 (see Footnote 297 for W in Table 1).

[3958] D.G. Leopold, J. Ho, W.C. Lineberger, Photoelectron spectroscopy of mass–selected metal cluster anions, J. Chem. Phys. 86 (1987) 1715–1726.

[3959] J.M. Bermond, B. Felts, M. Drechsler, A field emission measurement of the isosteric heat of adsorption of metallic adatoms on single crystal faces of a metal (Pb/W), Surf. Sci. 49 (1975) 207–220.

[3960] K. Ishikawa, H. Tobuse, AES Observation of thoriated tungsten cathodes, Japan. J. Appl. Phys. 15 (1976) 1571–1572.

[3961] W.L. Hole, R.W. Wright, Emissive and thermionic characteristics of uranium, Phys. Rev. 56 (1939) 785–787.

[3962] S.Yu. Davydov, Adsorption of sodium atoms on the (111) germanium surface, Semiconductors 43 (2009) 833–836.

[3963] I.V. Tvauri, S.A. Khubezhov, A.T. Nakusov, G.S. Grigorkina, Z.S. Demeev, A.P. Bliev, V.A. Sozaev, O.G. Ashkhotov, T.T. Magkoev, Probing the lanthanum–boron double film by carbon monoxide adsorption, Vacuum 120 (2015) 121–123.

[3964] R.A. Collins, B.H. Blott, Hydrogen adsorption of the (110), (112), (100), and (111) tungsten single–crystal faces, J. Appl. Phys. 40 (1969) 5390–5392.

[3965] G.H.M. Gubbels, L.R. Wolff, R. Metselaar, WF$_6$–CVD tungsten film as an emitter for a thermionic energy converter. I. Production, texture and morphology of WF$_6$–CVD tungsten films, Appl. Surf. Sci. 40 (1989) 193–199.

[3966] F.H. Spedding, Properties of rare earth metals, in: R.C. Weast (Ed.), CRC Handbook of Chemistry and Physics, 52nd ed., CRC Press, Boca Raton, 1971/1972, p. B–234.

[3967] P. Duwez, The effect of the rate of cooling on the allotropic transformation temperatures of uranium, J. Appl. Phys. 24 (1953) 152–156.

[3968] J. Wintterlin, M.-L. Bocquet, Graphene on metal surfaces, Surf. Sci. 603 (2009) 1841–1852.

[3969] J.-M. Bonard, H. Kind, T. Stöckli, L.-O. Nilsson, Field emission from carbon nanotubes: The first five years, Solid-State Electron. 45 (2001) 893–914.

[3970] A.G. Knapp, Surface potentials and their measurement by the diode method, Surf. Sci. 34 (1973) 289–316.

[3971] D.T. Pierce, W.E. Spicer, Photoemission studies of ferromagnetic and paramagnetic nickel, Phys. Rev. Lett. 25 (1970) 581–584.

[3972] N.B. Reynolds, Schottky effect and contact potential measurements on thoriated tungsten filaments, Phys. Rev. 35 (1930) 158–171.

[3973] P. Massmann, H.J. Hopman, J. Los, Negative surface ionization of hydrogen and its application to plasma diagnostics, Nucl. Instrum. Methods 165 (1979) 531–535.

[3974] H.O. Pritchard, H.A. Skinner, The concept of electronegativity, Chem. Rev. 55 (1955) 745–786.

[3975] S. Yamamoto, K. Susa, U. Kawabe, Work function of binary compounds, J. Chem. Phys. 60 (1974) 4076–4080.

[3976] M.S. Gupalo, T.P. Smereka, G.V. Babkin, B.M. Palyukh, Combined adsorption of lithium and oxygen on (100) faces of tungsten, Sov. Phys. Tech. Phys. 26 (1981) 233–236.

[3977] A.G. Burlakova, A.V. Ivanov, S.P. Shilkin, Electron work function of intermetallic compounds in the cerium–cobalt system, Tech. Phys. 56 (2011) 1216–1218.

[3978] S. Halas, T. Durakiewicz, P. Mckiewicz, Temperature–dependent work function shifts of hydrogenated/deuteriated palladium: A new theoretical explanation, Surf. Sci. 555 (2004) 43–50.

[3979] R. Dus, E. Nowicka, Segregation of deuterium and hydrogen on surfaces of palladium deuteride and hydride at low temperatures, Langmuir 16 (2000) 584–591.

[3980] B. Tamamushi, et al. (Eds.), Dictionsry of Physics and Chemistry, 3rd ed., Iwanami, Tokyo, 1976, p. 1447.

[3981] Z. Dworecki, Coadsorption of beryllium and potassium on a (001) tungsten plane, Acta Phys. Pol. A 81 (1992) 125–129.

[3982] H. Wagner, Work function of bare and coated metal surfaces, in: Proc. 3rd Int. Conf. Thermion. Electric. Power Generat., Jülich, vol. 3, 1972, pp. 1301–1321.

[3983] N. Shamir, J.C. Lin, R. Gomer, Cu overlayers on oxygen and on carbon monoxide adsorbed on tungsten(110), J. Chem. Phys. 90 (1989) 5135–5145.

[3984] S.Y. Davydov, On the specific features of work function coverage dependence for Na adatoms on the Cs substrate, Appl. Surf. Sci. 140 (1999) 52–57.

[3985] D.A. Gorodetskii, Yu.P. Mel'nik, Correlation between the work function and structure of monomolecular films, Sov. Phys.—Solid State 16 (1975) 1805.

[3986] É.Ya. Zandberg, E.V. Rut'kov, A.Ya. Tontegode, N.D. Potekhina, Initial stages of the growth of a barium film on the (111) face of iridium covered with a carbon monolayer with graphite structure, Sov. Phys.—Solid State 19 (1977) 972–975.

[3987] J.A. Becker, C.D. Hartman, Field emission microscope and flash filament techniques for the study of structure and adsorption on metal surfaces, J. Phys. Chem. 57 (1953) 153–159.

[3988] T.N. Rhodin, C.F. Brucker, A.B. Anderson, Structure and bonding of acetylene and ethylene on α–iron surfaces at low temperatures, J. Phys. Chem. 82 (1978) 894–898.

[3989] M. Kudo, E.L. Garfunkel, G.A. Somorjai, An ultraviolet photoelectron spectroscopic study of the interaction of potassium with carbon monoxide and benzene on the Pt(111) surface, J. Phys. Chem. 89 (1985) 3207–3211.

[3990] W.M. Tong, D.A.A. Ohlberg, H.K. You, R.S. Williams, S.J. Anz, M.M. Alvarez, R.L. Whetten, Y. Rubin, F.N. Diederich, X–ray diffraction and electron spectroscopy of epitaxial molecular C$_{60}$ films, J. Phys. Chem. 95 (1991) 4709–4712.

[3991] M. Todorova, K. Reuter, M. Scheffler, Oxygen overlayers on Pd(111) studied by density functional theory, J. Phys. Chem. B 108 (2004) 14477–14483.

[3992] M. Schenk, M. Krüger, P. Hommelhoff, Strong–field above–threshold photoemission from sharp metal tips, Phys. Rev. Lett. 105 (2010) 257601/1–4.

[3993] S. Saraf, A. Rothschild, Defect chemical modeling of Pd/ZnO Schottky junctions, Solid State Ion. 233 (2013) 80–86.

[3994] S.Yu. Luchkin, H.-Y. Amanieu, D. Rosato, A.L. Kholkin, Li distribution in graphite anodes: A Kelvin probe force microscopy, J. Power Sources 268 (2014) 887–894.

[3995] R.T. Howe, J.K. Nørskov, P.A. Pianetta, I. Bargatin, F. Abild-Pedersen, J. Voss, A. Vojvodic, S. Chou, H. Yuan, Using first principles simulations to discover materials with ultra–low work functions for energy conversion applications, in: Global Climate and Energy Project Annual Report, 2013, 15 pp.

[3996] K. Gajewski, W. Szymański, P. Niedzielski, T. Gotszalk, Kelvin probe force microscopy investigations of high strength metallurgical graphene transferred on low–density polyethylene, Microelectron. Eng. 157 (2016) 71–77.

[3997] K. Gajewski, S. Goniszewski, A. Szmska, M. Moczała, P. Kunicki, J. Gallop, N. Klein, L. Hao, T. Gotszalk, Raman spectroscopy and Kelvin probe force microscopy characteristics of the CVD suspended graphene, Diam. Relat. Mater. 64 (2016) 27–33.

[3998] N. Gozlan, U. Tisch, H. Haick, Tailoring the work function of gold surface by controlling coverage and disorder of polar molecular monolayers, J. Phys. Chem. C 112 (2008) 12988–12992.

[3999] Y. Ge, T. Weidner, H. Ahn, J.E. Whitten, M. Zharnikov, Energy level pinning in self–assembled alkanethiol monolayers, J. Phys. Chem. C 113 (2009) 4575–4583.

[4000] K. Heister, M. Zharnikov, M. Grunze, L.S.O. Johansson, Adsorption of alkanethiols and biphenylthiols on Au and Ag substrates: A high–resolution X–ray photoelectron spectroscopy study, J. Phys. Chem. B 105 (2001) 4058–4061.

[4001] B. Jaeckel, J. Sambur, B.A. Parkinson, A photoemission study of the morphology and barrier heights of the interface between chyrsene and inert substrates, J. Phys. Chem. C 113 (2009) 1837–1849.

[4002] M.E. Vaida, T. Gleitsmann, R. Tchitnga, T.M. Bernhardt, Femtosecond–laser photoemission spectroscopy of Mo(100) covered by ultrathin MgO(100) films of variable thickness, J. Phys. Chem. C 113 (2009) 10264–10268.

[4003] J.D. Wiggins-Camacho, K.J. Stevenson, Effect of nitrogen concentration on capacitance, density of states, electronic conductivity, and morphology of N–doped carbon nanotube electrodes, J. Phys. Chem. C 113 (2009) 19082–19090.

[4004] D.-P. Ji, Q. Zhu, S.-Q. Wang, Detailed first–principles studies on surface energy and work function of hexagonal metals, Surf. Sci. 651 (2016) 137–146.

[4005] T. Li, B.L. Rickman, W.A. Schroeder, Density functional theory analysis of hexagonal close–packed elemental metal photocathodes, Phys. Rev. Spec. Top.-Accel. & Beams 18 (2015) 073401/1–11.

[4006] W. Gordy, A new method of determining electronegativity from other atomic properties, Phys. Rev. 69 (1946) 604–607.

[4007] P. Zeller, S. Dänhardt, S. Gsell, M. Schreck, J. Wintterlin, Scalable synthesis of graphene on single crystal Ir(111) films, Surf. Sci. 606 (2012) 1475–1480.

[4008] H. Xiao, D. Xie, Density functional study of the adsorption of Na and K on Rh(111), Surf. Sci. 553 (2004) 13–22.

[4009] H.W. Hugosson, W. Cao, S. Seetharaman, A. Delin, Sulfur– and oxygen–induced alterations of the iron(001) surface magnetism and work function: A theoretical study, J. Phys. Chem. C 117 (2013) 6161–6171.

[4010] R.J. Cashman, W.S. Huxford, Photoelectric sensitivity of magnesium, Phys. Rev. 43 (1933) 811–818.

[4011] D.A. Gorodetskii, S.A. Shevlyakov, Structures of scandium on the (112) surface of tungsten, Sov. Phys. Crystallogr. 25 (1980) 377–378.

[4012] D.V. Buturovich, M.V. Kuz'min, M.V. Loginov, M.A. Mittsev, Friedel oscillations in Ytterbium films deposited on the Si(111)7×7 surface, Phys. Solid State 48 (2006) 2205–2208.

[4013] M.V. Kuz'min, M.V. Loginov, M.A. Mittsev, Nonmonotonic dependence of the work function of ytterbium nanofilms deposited on the Si(111)7×7 surface at room temperature on the film thickness, Phys. Solid State 50 (2008) 369–373.

[4014] C.J. Workowski, Field emission microscopy of titanium films on tungsten: Adsorption and epitaxial growth, Acta Phys. Pol. A 49 (1976) 699–707.

[4015] T. Radoń, Adsorption of silicon and carbon on tungsten, Acta Phys. Pol. A 43 (1973) 699–704.

[4016] Ch. Kleint, S.M. Abd El-Halim, Reflection electron energy loss spectroscopy of alkali metals on silicon, Acta Phys. Pol. A 81 (1992) 47–65.

[4017] R. Błaszczyszyn, M. Błaszczyszynowa, W. Gubernator, Thermal desorption of potassium from clean and sulfur covered nickel, Acta Phys. Pol. A 88 (1995) 1151–1160.

[4018] R. Błaszczyszyn, E. Wachowicz, M. Błaszczyszynowa, Interaction of hydrogen with vanadium layers preadsorbed on tungsten field emitter tip, Acta Phys. Pol. A 93 (1998) 763–773.

[4019] S.G. Nelson, M.J.S. Spencer, I.K. Snook, I. Yarovsky, Effect of S contamination on properties of Fe(100) surfaces, Surf. Sci. 590 (2005) 63–75.

[4020] A. Böttcher, A. Morgante, R. Grobecker, T. Greber, G. Ertl, Singlet–to–triplet conversion of metastable He atoms at alkali–metal overlayers, Phys. Rev. B 49 (1994) 10607–10612.

[4021] W. Steurer, Crystal structures of the elements, in: K.H.J. Buchow (Ed.), Encyclopedia of Materials: Science and Technology, Elsevier, Amsterdam, 2001, pp. 1880–1897.

[4022] H.L. Skriver, Crystal structure from one–electron theory, Phys. Rev. B 31 (1985) 1909–1923.

[4023] J.I. Lee, C.L. Fu, A.J. Freeman, Electronic structure and magnetism of metastable bcc Co(001), J. Magn. Magn. Mater. 62 (1986) 93–100.

[4024] R. Wu, C. Li, A.J. Freeman, Structural, electronic and magnetic properties of Co/Pd(111) and Co/Pt(111), J. Magn. Magn. Mater. 99 (1991) 71–80.

[4025] D. Velic, E. Knoesel, M. Wolf, Observation of a direct transition in the sp–band of Cu(111) and ($\sqrt{3}\times\sqrt{3}$)R30°–CO/Cu(111) in one– and two–photon photoemission, Surf. Sci. 424 (1999) 1–6.

[4026] G.W. Fernando, J.W. Wilkins, Systematics in bonding of simple adsorbates on a transition–metal surface, Phys. Rev. B 35 (1987) 2995–2998.

[4027] P. Zoccali, A. Bonano, M. Camarca, A. Oliva, F. Xu, Projectile and target autoionization electron emission in 700–eV Ne$^+$–Na/M (M = Cr, Cu, Mo, and Pt) collisions, Phys. Rev. B 50 (1994) 9767–9773.

[4028] G.A. Prinz, Stabilization of bcc Co via epitaxial growth on GaAs, Phys. Rev. Lett. 54 (1985) 1051–1054.

[4029] A.V. Babich, V.V. Pogosov, P.V. Vakula, Self–consistent calculations of work function, Shottky barrier heights and surface energy of metal nanofilms in dielectric confinement, Radiophys. (1) (2013) 7–20.

[4030] H. Dai, Carbon nanotubes: Opportunities and challenges, Surf. Sci. 500 (2002) 218–241.

[4031] M.V. Mamonova, V.V. Prudnikov, Development of a technique for calculating work functions of metal surfaces, Phys. Met. Metallogr. 86 (1998) 129–133.

[4032] N.I. Medvedeva, D.P. Frikkel', M.V. Kuznetsov, A.L. Ivanovskii, Electron structure and properties of Ti(0001) surface, Phys. Met. Metallogr. 86 (1998) 232–236.

[4033] D. Velic, A. Hotzel, M. Wolf, G. Ertl, Electronic states of the C_6H_6/Cu{111} system: Energetics, femtosecond dynamics, and adsorption morphology, J. Chem. Phys. 109 (1998) 9155–9165.

[4034] W. Cao, S. Liang, X. Zhang, X. Wang, X. Yang, Effect of Mo addition on microstructure and vacuum arc characteristics of CuCr50 alloy, Vacuum 85 (2011) 943–948.

[4035] J.P. Perdew, Simple theories for simple metals: Face–dependent surface energies and work functions, Prog. Surf. Sci. 48 (1995) 245–259.

[4036] P. Ziesche, J.P. Perdew, C. Fiolhais, Spherical voids in the stabilized jellium model: Rigorous theorems and Padé representation of the void–formation energy, Phys. Rev. B 49 (1994) 7916–7928.

[4037] J.-M. Themlin, S. Bouzidi, F. Colleti, J.-M. Debever, G. Gensterblum, L.-M. Yu, J.-J. Pireaux, P.A. Thiry, One–dimensional commensurability and conduction-band dispersion in heteroepitaxial C_{60} on GeS, Phys. Rev. B 46 (1992) 15602–15605.

[4038] S. Fölsch, T. Maruno, A. Yamashita, T. Hayashi, Epitaxial C_{60} films on CaF_2(111) grown by molecular beam deposition, Appl. Phys. Lett. 62 (1993) 2643–2645.

[4039] K. Tanigaki, S. Kuroshima, J. Fujita, T.W. Ebbesen, Crystal growth of C_{60} thin films on layered substrates, Appl. Phys. Lett. 63 (1993) 2351–2353.

[4040] A. Fartash, Growth and interfacial evolution of oriented C_{60} overlayers on Au(111), Appl. Phys. Lett. 67 (1995) 3901–3903.

[4041] A. Fartash, Interfacially ordered C_{60} films on Cu(111) substrates, J. Appl. Phys. 79 (1996) 742–749.

[4042] G. Bigun, Yu. Suchorski, Electron density near clean and alkali covered semiconductor surfaces, Surf. Sci. 247 (1991) 111–114.

[4043] L.J. Sham, W. Kohn, One–particle properties of an inhomogeneous interacting electron gas, Phys. Rev. 145 (1966) 561–567.

[4044] P. Hohenberg, W. Kohn, Inhomogeneous electron gas, Phys. Rev. 136 (1964) B864–B871.

[4045] N.D. Lang, W. Kohn, Surface–dipole barriers in simple metals, Phys. Rev. B 8 (1973) 6010–6012.

[4046] Y.G. Zhou, X.T. Zu, J.L. Nie, H.Y. Xiao, Adsorption of Li on Mo(110) surface: A first–principles study, Surf. Rev. Lett. 16 (2009) 589–597.

[4047] E.P. Gyftopoulos, J.D. Levine, Work function variation of metals coated by metallic films, J. Appl. Phys. 33 (1962) 67–73.

[4048] A.R. Miedema, F.R. de Boer, P.F. de Chatel, Empirical description of the role of electronegativity in alloy formation, J. Phys. F 3 (1973) 1558–1576.

[4049] I.N. Stranski, R. Suhrmann, Electron emission from crystalline metal surfaces and its relation to the crystal structure. I. Pure metal surfaces, Ann. Phys. 1 (1947) 153–168.

[4050] S.A. Komolov, Total Current Spectroscopy of Surfaces, pp. 132–133 and 231–234, Gordon and Breach, Philadelphia, 1992, 257 pp.

[4051] H. Shade, Work functions and sublimation entropies of the elements, in: Proc. 7th Int. Vac. Congr. and 3rd Int. Conf. Solid Surfaces, Vienna, 1977, pp. 437–439 (see Ref. [1312,3925]).

[4052] N.V. Volkov, Yu.K. Gus'kov, Z.N. Kononova, Yu.I. Kostikov, Effect of selenium and sulfur on the work function of tungsten, in: 15th Vses. Konf. Emiss. Elektron. 1, 1973, pp. 84–85.

[4053] N.A. Gordienko, Correlation between electron work function and the ionization potential of an atom, Ukr. Khim. Zh. 36 (1970) 1287–1288 (Chem. Abstr. 74 (1971) 131620c).

[4054] A.I. Reznik, N.V. Rudenko, Relation between internal and external functions of metals, Izv. Akad. Nauk SSSR, Ser. Fiz. 43 (1979) 1823–1829.

[4055] G. Zampieri, F. Meier, R. Baragiola, Formation of autoionizing states of Ne in collisions with surfaces, Phys. Rev. A 29 (1984) 116–122.

[4056] H. Yang, J.L. Whitten, Chemisorption of hydrogen on the nickel(111) surface, J. Chem. Phys. 89 (1988) 5329–5334.

[4057] L.T. Kong, B.X. Liu, Orientation and composition dependences of the surface energy and work function observed by first–principles calculation for the Mo–Hf system, J. Phys. Soc. Japan 74 (2005) 1766–1771.

[4058] S. Halas, 100 years of work function, Mater. Sci.-Poland 24 (2006) 951–966 (Chem. Abstr. 146 (2007) 344806k).

[4059] P.R. Abbott, The effect of average grain size on the work function of polycrystalline diamond films (Ph.D. thesis), Univ. of North Texas, 2002, 134 pp. (Diss. Abstr. Int. B 65 (2004) 260).

[4060] J.-L. Desplat, Evaluation of oxygen dispensing collectors for thermionics, AIP Conf. Proc. 458 (1999) 1452–1457.

[4061] M. Methfessel, D. Hennig, M. Scheffler, Calculated surface energies of the 4*d* transition metals: A study of bond–cutting models, Appl. Phys. A 55 (1992) 442–448.

[4062] B. Chatterjee, Anisotropy of melting for cubic metals, Nature 275 (1978) 203.

[4063] A. Chattopadhyay, H. Yang, J.L. Witten, Adsorption of ammonia on Ni(111), J. Phys. Chem. 94 (1990) 6379–6383.

[4064] S.M. Foiles, M.I. Baskes, M.S. Daw, Embedded–atom–method functions for the fcc metals Cu, Ag, Au, Ni, Pd, Pt, and their alloys, Phys. Rev. B 33 (1986) 7983–7991.

[4065] S. Saito, T. Soumura, T. Maeda, Improvements of the piezoelectric driven Kelvin probe, J. Vac. Sci. Technol. A 2 (1984) 1389–1391.

[4066] Yu.I. Malov, A.V. Onishchenko, L.I. Mironkova, Work function of rare–earth metals, Phys. Met. Metallogr. 47 (4) (1979) 195–197.

[4067] W. Sesselmann, B. Woratschek, G. Ertl, J. Küppers, H. Haberland, Low temperature formation of benzene from acetylene on a Pd(111) surface, Surf. Sci. 130 (1983) 245–258.

[4068] S.Yu. Davydov, A.V. Pavlyk, Calculation of the variation in the work function caused by adsorption of metal atoms on semiconductors, Semicond. 35 (2001) 796–799.

[4069] K.N. Khanna, Work function in alkali and noble metals, Phys. Status Solidi (b) 100 (1980) 315–319.

[4070] J.R. Smith, A. Banerjea, New approach to calculation of total energies of solids with defects: Surface energy anisotropies, Phys. Rev. Lett. 59 (1987) 2451–2454.

[4071] J.-M. Zhang, F. Ma, K.-W. Xu, Calculation of the surface energy of bcc metals by using the modified embedded–atom method, Surf. Interface Anal. 35 (2003) 662–666.

[4072] W.R. Tyson, Estimation of surface energies from phonon frequencies for bcc and fcc metals, J. Appl. Phys. 47 (1976) 459–465.

[4073] S.Yu. Davydov, On the description of the coadsorption of cesium and selenium atoms on the silicon surface, Phys. Solid State 51 (2009) 849–853.

[4074] S.Yu. Davydov, A.V. Pavlyk, Adsorption of vanadium on rutile: A change in the electron work function, Tech. Phys. Lett. 29 (2003) 500–501.

[4075] S.Yu. Davydov, Adsorption of barium and rare–earth metals on silicon, Phys. Solid State 46 (2004) 1141–1144.

[4076] S.Yu. Davydov, A.V. Pavlyk, Rare–earth metal adsorption on silicon: Variation of the work function, Phys. Solid State 45 (2003) 1388–1391.

[4077] L. Vitos, A.V. Ruban, H.L. Skriver, J. Kollár, The surface energy of metals, Surf. Sci. 411 (1998) 186–202.

[4078] S.N. Zadumkin, I.G. Shebuhkhova, B.B. Al'chagirov, Surface energy and work function of the smooth facets of metallic single crystal, Phys. Met. Methallogr. 30 (1970) 195–198.

[4079] M. Legesse, F. El Mellouhi, El T. Bentria, M.E. Madjet, T.S. Fisher, S. Kais, F.H. Alharbi, Reduced work function of graphene by metal adatoms, Appl. Surf. Sci. 394 (2017) 98–107.

[4080] B. Bröker, R.-P. Blum, J. Frisch, A. Vollmer, O.T. Hofmann, R. Rieger, K. Müllen, J.P. Rabe, E. Zojer, N. Koch, Gold work function reduction by 2.2 eV with an air–stable molecular donor layer, Appl. Phys. Lett. 93 (2008) 243303/1–3.

[4081] Yu. Suchorski, Field stimulated surface diffusion of lithium on germanium (100) and (111) planes, Acta Phys. Pol. A 81 (1992) 295–302.

[4082] M. Akbi, A. Bouchou, M. Ferhat-Taleb, Effects of surface treatments on photoelectric work function of silver–nickel alloys, Vacuum 101 (2014) 257–266.

[4083] V.A. Korol'kov, Yu.I. Malov, A.A. Markov, Electron work function of binary systems of indium–bismuth and indium–lead, Phys. Met. Metallogr. 40 (6) (1975) 176–178.

[4084] S.N. Zadumkin, V.G. Yegiyev, Work function and surface energy of metals, Phys. Met. Metallogr. 22 (1) (1966) 123–125.

[4085] S.N. Zadumkin, I.G. Shebzukhova, Approximate determination of the orientation dependence of the surface energy and surface tension of metal crystals, Phys. Met. Metallogr. 28 (3) (1969) 50–56.

[4086] N.I. Medvedeva, M.V. Kuznetsov, A.L. Ivanovskii, Theoretical study of nitrogen adsorption on the Ti(0001) surface, Phys. Met. Metallogr. 88 (2) (1999) 122–130.

[4087] N.E. Singh-Miller, N. Marzari, Surface energies, work functions, and surface relaxations of low–index metallic surfaces from first principles, Phys. Rev. B 80 (2009) 235407/1–9.

[4088] G.N. Derry, M.E. Kern, E.H. Worth, Recommended values of clean metal surface work functions, J. Vac. Sci. Technol. A 33 (2015) 060801/1–9.

[4089] V. Heine, C.H. Hodges, Theory of the surface dipole on nontransition metals, J. Phys. C 5 (1972) 225–230.

[4090] M.C. Richter, J.-M. Mariot, M.A. Gafoor, L. Nicolaï, O. Heckmann, U. Djukic, W. Ndiaye, I. Vobornik, J. Fujii, N. Barrett, V. Feyer, C.M. Schneider, K. Hricovini, Bi atoms mobility-driven circular domains at Bi/InAs(111) interface, Surf. Sci. 651 (2016) 147–153.

[4091] J. Wang, S.-Q. Wang, Surface energy and work function of fcc and bcc crystals: Density functional study, Surf. Sci. 630 (2014) 216–224.

[4092] A. Böttcher, R. Imbeck, A. Mogante, G. Ertl, Nonadiabatic surface reaction: Mechanism of electron emission in the Cs + O$_2$ system, Phys. Rev. Lett. 65 (1990) 2035–2037.

[4093] A. Böttcher, R. Grobecker, R. Imbeck, A. Mogante, G. Ertl, Exoelectron emission during oxidation of Cs films, J. Chem. Phys. 95 (1991) 3756–3766.

[4094] T. Greber, R. Grobecker, A. Morgante, A. Böttcher, G. Ertl, O$^-$ escape during the oxidation of cesium, Phys. Rev. Lett. 70 (1993) 1331–1334.

[4095] G.A. Prinz, G.T. Rado, J.J. Krebs, Magnetic properties of single–crystal {110} iron films grown on GaAs by molecular beam epitaxy, J. Appl. Phys. 53 (1982) 2087–2091.

[4096] J.J. Krebs, B.T. Jonker, G.A. Prinz, Properties of Fe single–crystal films grown on (100)GaAs by molecular–beam epitaxy, J. Appl. Phys. 61 (1987) 2596–2599.

[4097] G.A. Prinz, J.J. Krebs, Molecular beam epitaxial growth of single–crystal Fe films on GaAs, Appl. Phys. Lett. 39 (1981) 397–399.

[4098] G.A. Prinz, J.M. Ferrari, Molecular beam epitaxial growth of single crystal Al films on GaAs(110), Appl. Phys. Lett. 40 (1982) 155–157.

[4099] S. Yamamoto, Electron emission and work function — Past, present and future, Appl. Surf. Sci. 251 (2005) 4–13.

[4100] L.A. Rudnitskii, Electron work function of microscopic metal granules, Sov. Phys. Dokl. 24 (1979) 467–468.

[4101] J.P. Perdew, Energetics of charged metallic particles: From atom to bulk solid, Phys. Rev. B 37 (1988) 6175–6180.

[4102] G. Popov, E. Bauer, The adsorption of Se on a W(110) surface, Surf. Sci. 123 (1982) 165–172.

[4103] J.-H. Kim, J.H. Hwang, J. Suh, S. Tongay, S. Kwon, C.C. Hwang, J. Wu, J.Y. Park, Work function engineering of single layer graphene by irradiation–induced defects, Appl. Phys. Lett. 103 (2013) 171604/1–5.

[4104] K.P. Loh, Q. Bao, P.K. Ang, J. Yang, The chemistry of graphene, J. Mater. Chem. 20 (2010) 2277–2289.

[4105] S.-M. Choi, S.-H. Jhi, Y.-W. Son, Effects of strain on electronic properties of graphene, Phys. Rev. B 81 (2010) 081407(R)/1–4.

[4106] X. Chen, L. Zhang, S. Chen, Large area CVD growth of graphene, Synth. Met. 210 (2015) 95–108.

[4107] R. Gomer, Metallicity of ultrathin metal layers, Acc. Chem. Res. 29 (1996) 284–291.

[4108] S. De Waele, K. Lejaeghere, M. Sluydts, S. Cottenier, Error estimates for density functional theory predictions of surface energy and work function, Phys. Rev. B 94 (2016) 235418/1–13 (see Ref. [4460]).

[4109] T.V. Krachino, M.V. Kuz'min, M.V. Loginov, M.A. Mittsev, Thermally activated reconstruction in Yb–Si(111) thin–film structures, Phys. Solid State 39 (1997) 1493–1497.

[4110] M.V. Kuz'min, N.V. Mikhaïlov, M.A. Mittsev, Formation and properties of a binary adsorbed layer in a two–component adsorption system (Sm + Yb)–Si(111), Phys. Solid State 45 (2003) 579–585.

[4111] T.V. Krachino, M.V. Kuz'min, M.V. Loginov, M.A. Mittsev, Adsorption stage in the formation of Eu–Si(111) thin–film structures, Phys. Solid State 42 (2000) 566–576.

[4112] T.V. Krachino, M.V. Kuz'min, M.V. Loginov, M.A. Mittsev, Growth of an Eu–Si(111) thin film structure: The stage of silicide formation, Phys. Solid State 46 (2004) 563–568.

[4113] C. Awada, G. Barbillon, F. Charra, L. Douillard, J.-J. Greffet, Experimental study of hot spots in gold/glass nanocomposite films by photoemission electron microscopy, Phys. Rev. B 85 (2012) 045438/1–6.

[4114] M. Akbi, A method for measuring the photoelectric work function of contact materials versus temperature, IEEE Trans. Compon. Pack. Manuf. Technol. 4 (2014) 1293–1302.

[4115] Yu.V. Zubenko, N.L. Sokol'skaya, Adsorption and surface diffusion of platinum on tungsten, Bull. Acad. Sci. USSR, Phys. Ser. 30 (1966) 936–939.

[4116] V.S. Fomenko, Work function for polycrystals modeled by a film or cluster, Metallofizika 14 (6) (1992) 81–87 (Chem. Abstr. 118 (1993) 202610q).

[4117] I. Brodie, S.H. Chou, H. Yuan, A general phenomenological model for work function, Surf. Sci. 625 (2014) 112–118.

[4118] K. Wittmaak, Unravelling the secrets of Cs controlled secondary ion formation: Evidence of the dominance of site specific surface chemistry, alloying and ionic bonding, Surf. Sci. Rep. 68 (2013) 108–230.

[4119] A. Novikov, Experimental measurement of work function in doped silicon surfaces, Solid–State Electron. 54 (2010) 8–13.

[4120] T. Ossowski, A. Kiejna, Oxygen adsorption on Fe(110) surface revisited, Surf. Sci. 637–638 (2015) 35–41.

[4121] X. Tan, J. Zhou, Y. Peng, First–principles study of oxygen adsorption on Fe(110) surface, Appl. Surf. Sci. 258 (2012) 8484–8491.

[4122] L.C. Burton, Temperature dependence of the silicon work function by means of a retarding potential technique, J. Appl. Phys. 47 (1976) 1189–1191.

[4123] J. Żebrowski, The effect of temperature on the field emission from lead, Acta Phys. Pol. A 57 (1980) 369–376.

[4124] M.J.S. Spencer, A. Hung, I.K. Snook, I. Yarovsky, Density functional theory study of the relaxation and energy of iron surfaces, Surf. Sci. 513 (2002) 389–398.

[4125] J.P. Lacharme, N. Benazzi, C.A. Sébenne, Compositional and electronic properties of Si(001)2×1 upon diatomic sulfur interaction, Surf. Sci. 433–435 (1999) 415–419.

[4126] K.T. Chan, J.B. Neaton, M.L. Cohen, First–principles study of metal adatom adsorption on graphene, Phys. Rev. B 77 (2008) 235430/1–12.

[4127] K.-H. Jin, S.-M. Choi, S.-H. Jhi, Crossover in the adsorption properties of alkali metals on graphene, Phys. Rev. B 82 (2010) 033414/1–4.

[4128] Y.-J. Yu, Y. Zhao, S. Ryu, L.E. Brus, K.S. Kim, P. Kim, Tuning the graphene work function by electric field effect, Nano Lett. 9 (2009) 3430–3434.

[4129] R. Yan, Q. Zhang, W. Li, I. Calizo, T. Shen, C.A. Richter, A.R. High-Walker, X. Liang, A. Seabaugh, D. Jena, H.G. Xing, D.J. Gundlach, N.V. Nguyen, Determination of graphene work function and graphene–insulator–semiconductor band alignment by internal photoemission spectroscopy, Appl. Phys. Lett. 101 (2012) 022105/1–4.

[4130] D.E. Jiang, E.A. Carter, Adsorption and diffusion energetics of hydrogen atoms on Fe(110) from first principles, Surf. Sci. 547 (2003) 85–98.

[4131] A.F. Takács, F. Witt, S. Schmaus, T. Balashov, M. Bowen, E. Beaurepaire, W. Wulfhekel, Electron transport through single phthalocyanine molecules studied using scanning tunneling microscopy, Phys. Rev. B 78 (2008) 233404/1–4.

[4132] M. Akbi, On the temperature dependence of the photoelectric work function of contact materials, in: 27th Int. Conf. Electr. Contacts, Dresden, 2014, pp. 463–467.

[4133] M. Akbi, Effect of arcing in air on the photoelectric work function of silver–based contacts, IEEE Trans. Plasma Sci. 43 (2015) 637–642.

[4134] M. Akbi, Effects of arcing in air on the microstructure and morphology of silver–based contact materials in correlation with their electron emission properties, IEEE Trans. Plas. Sci. 44 (2016) 1847–1857.

[4135] B. Sun, P. Zhang, S. Duan, X.-G. Zhao, Q.-K. Xue, First–principles calculations of Cs adsorbed on Cu(001): Quantum size effect in surface energetics and surface chemical reactivities, Phys. Rev. B 75 (2007) 245422/1–11.

[4136] B.Ya. Moizhes, V.A. Nemchinskii, A simple formula for the electron work function of metals, Sov. Phys. Tech. Phys. 27 (1982) 1298–1300.

[4137] D.R. Lide (Ed.), Electron work function of the elements, in: CRC Handbook of Chemistry and Physics, 77th ed., CRC Press, Boca Raton, 1996–1997, pp. **12**–122/**12**–123.

[4138] J. Jortner, Cluster size effects, Z. Phys. D 24 (1992) 247–275.

[4139] Kh.I. Ibragimov, V.A. Korol'kov, Temperature dependence of the work function of metals and binary alloys, Inorg. Mater. 37 (2001) 567–572.

[4140] H.K. Kim, A.S. Hyla, P. Winget, H. Li, C.M. Wyss, A.J. Larrain, J.P. Sadighi, C. Fuentes-Hernandez, B. Kippelen, J.-L. Brédas, S. Barlow, S.R. Marder, Reduction of work function of gold by N-heterocyclic carbenes, Chem. Mater. 29 (2017) 3403–3411.

[4141] A.B. Alchagirov, B.B. Alchagirov, T.A. Sizlfazhev, Kh.B. Khokonov, M.A. Yaganov, Work function of sodium–rubidium alloys, Russ. J. Electrochem. 40 (2004) 102–104.

[4142] R.Kh. Khisamov, I.M. Safarov, R.R. Mulyukov, Yu.M. Yumaguzin, Effect of grain boundaries on the electron work function of nanocrystalline nickel, Phys. Solid State 55 (2013) 1–4.

[4143] S. Karkare, J. Feng, X. Chen, W. Wan, F.J. Palomares, T.-C. Chiang, H.A. Padmore, Reduction of intrinsic electron emittance from photocathodes using ordered crystalline surfaces, Phys. Rev. Lett. 118 (2017) 164802/1–5.

[4144] B.B. Alchagirov, R.Kh. Arkhestov, F.F. Dyshekova, Electron work function in alloys with alkali metals, Tech. Phys. 57 (2012) 1541–1546.

[4145] B.A. Boiko, Structure, electronic and dynamic properties of thin films of some substances on the surface of a tungsten single crystal, Ph.D., Kiev Gos. Univ., 1978, (see Ref. [4146]).

[4146] V.S. Fomenko, Work function of yttrium and lanthanide single crystals, Powd. Metallur. Met. Ceram. 33 (1994) 85–90.

[4147] G. Rosina, E. Bertel, F.P. Netzer, Angle–resolved UV photoemission of cerium, J. Less–Common Met. 111 (1985) 285–290.

[4148] M.M. Kappes, M. Schär, P. Radi, E. Schumacher, On the manifestation of electronic structure effects in metal clusters, J. Chem. Phys. 84 (1986) 1863–1875.

[4149] K. Randemann, B. Kaiser, U. Even, F. Hensel, Size dependence of the gradual transition to metallic properties in isolated mercury clusters, Phys. Rev. Lett. 59 (1987) 2319–2321.

[4150] H. Bogdanów, K.F. Wojciechowski, Electronic surface properties of alkali–metal alloys, J. Phys. D 29 (1996) 1310–1315.

[4151] G. Heimel, L. Romaner, J.-L. Brédas, E. Zojer, Organic/metal interfaces in self–assembled monolayers of conjugated thiols: A first–principles benchmark study, Surf. Sci. 600 (2006) 4548–4562.

[4152] H. Li, Y. Duan, V. Coropceanu, J.-L. Brédas, Electronic structure of the pentacene–gold interface: A density–functional theory study, Org. Electr. 10 (2009) 1571–1578.

[4153] H. Li, Y. Duan, P. Paramonov, V. Coropceanu, J.-L. Brédas, Electronic structure of self–assembled (fluoro)methylthiol monolayers on the Au(111) surface: Impact of fluorination and coverage density, J. Electron Spectrosc. Relat. Phenom. 174 (2009) 70–77.

[4154] D. Cornil, J. Cornil, Work–function modification of the (111) gold surface upon deposition of self–assembled monolayers based on alkanethiol, J. Electron Spectrosc. Relat. Phenom. 189 (2013) 32–38.

[4155] O. Fenwick, C. Van Dyck, K. Murugavel, D. Colnil, F. Reinders, S. Haar, M. Mayor, J. Cornil, P. Samori, Modulating the charge injection in organic field–effect transistors: Fluorinated oligophenyl self–assembled monolayers for high work function electrodes, J. Mater. Chem. C 3 (2015) 3007–3015.

[4156] V. De Renzi, R. Rousseau, D. Marchetto, R. Biagi, S. Scandolo, U. del Pennino, Metal work–function changes induced by organic adsorbates: A combined experimental and theoretical study, Phys. Rev. Lett. 95 (2005) 046804/1–4.

[4157] P.C. Rusu, G. Brocks, Surface dipoles and work functions of alkylthiolates and fluorinated alkylthiolates on Au(111), J. Phys. Chem. B 110 (2006) 22628–22634.

[4158] Cumulative list of authors citing Michaelson's review (Ref. [1045]) (http://aip.scitation.org/doi/citedby/10.1063/1.323539).

[4159] N.D. Orf, I.D. Baikie, O. Shapira, Y. Fink, Work function engineering in low–temperature metals, Appl. Phys. Lett. 94 (2009) 113504/1–3.

[4160] A.C. Papageorgopoulos, M. Kamaratos, Interactions between Se, Cs and Si upon Se adsorption on Cs/Si(111)–7×7 surfaces, J. Phys.: Condens. Matter 14 (2002) 5255–5270.

[4161] C. Bréchignac, Ph. Cahuzac, F. Carlier, J. Leygnier, Photoionization of mass–selected K_n^+ ions: A test for the ionization scaling law, Phys. Rev. Lett. 63 (1989) 1368–1371.

[4162] C. Bréchignac, M. Broyer, Ph. Cahuzac, G. Delacretaz, P. Labastie, J.P. Wolf, L. Wöste, Probing the transition from van der Waals to metallic mercury clusters, Phys. Rev. Lett. 60 (1988) 275–278.

[4163] W.G. Burgers, On the process of transition of the cubic–body–centered modification into the hexagonal–close–packed modification of zirconium, Physica 1 (1934) 561–568.

[4164] J.B. Newkirk, A.H. Geisler, Crystallographic aspects of the beta to alpha transformation in titanium, Acta Metall. 1 (1953) 370–374.

[4165] A.J. Williams, R.W. Cahn, C.S. Barrett, The crystallography of the β–α transformation in titanium, Acta Metall. 2 (1954) 117–128.

[4166] G.G.E. Seward, S. Celotto, D.J. Prior, J. Wheeler, R.C. Pond, *In situ* SEM–EBSD observations of the hcp to bcc phase transformation in commercially pure titanium, Acta Mater. 52 (2004) 821–832.

[4167] S.R. Nishitani, H. Kawabe, M. Aoki, First–principles calculations on bcc–hcp transition of titanium, Mater. Sci. Eng. A 312 (2001) 77–83.

[4168] D. Bhattacharyya, G.B. Viswanathan, R. Denkenberger, D. Furrer, H.L. Fraser, The role of crystallographic and geometrical relationships between α and β phases in an α/β titanium alloy, Acta Mater. 51 (2003) 4679–4691.

[4169] N. Gey, M. Humbert, Characterization of the variant selection occurring during the $\alpha \to \beta \to \alpha$ phase transformations of a cold rolled titanium sheet, Acta Mater. 50 (2002) 277–287.

[4170] W.G. Burgers, J.J.A. Ploos van Amstel, Electronoptical observation of metal surfaces: III. Crystal growth and allotropic transition in zirconium, Physica 5 (1938) 305–312.

[4171] H.-R. Wenk, I. Lonardelli, D. Williams, Texture changes in the hcp $\to$ bcc $\to$ hcp transformation of zirconium studied *in situ* by neutron diffraction, Acta Mater. 52 (2004) 1899–1907.

[4172] T. Karthikeyan, S. Saroja, M. Vijayalakshmi, Evaluation of misorientation angle axis–set between variants during transformation of bcc to hcp phase obeying Burgers orientation relation, Scr. Mater. 55 (2006) 771–774.

[4173] C. Soldano, A. Mahmood, E. Dujardin, Production, properties and potential of graphene, Carbon 48 (2010) 2127–2150.

[4174] G. Giovannetti, P.A. Khomyakov, G. Brocks, V.M. Karpan, J. van den Brink, P.J. Kelly, Doping graphene with metal contacts, Phys. Rev. Lett. 101 (2008) 026803/1–4.

[4175] J. Duch, P. Kubisiak, K.H. Adolfsson, M. Hakkarainen, M. Golda-Cepa, A. Kotarba, Work function modifications of graphite surface via oxygen plasma treatment, Appl. Surf. Sci. 419 (2017) 439–446.

[4176] E. Czerwosz, P. Dłużewski, T. Kutner, T. Stacewicz, Photoelectric work function studies of carbonaceous films containing Ni nanocrystals, Thin Solid Films 423 (2003) 161–168.

[4177] S.A. Komolov, T.O. Artamonova, I.V. Baryshev, É.F. Lazneva, I.N. Fedorov, Laser cleaning of a silicon surface: Monitoring by electron spectroscopy and laser desorption, Sov. Tech. Phys. Lett. 14 (1988) 868–870.

[4178] V.V. Pogosov, D.P. Kotlyarov, A. Kiejna, K.F. Wojciechowski, Energetics of finite metallic nanowires, Surf. Sci. 472 (2001) 172–178.

[4179] Y.-S. Lin, K.-W. Huang, H.-C. Lin, M.-J. Chen, Effective work function modulation of the bilayer metal gate stacks by the Hf–doped thin TiN interlayer prepared by the *in–situ* atomic layer doping technique, Solid State Commun. 258 (2017) 49–53.

[4180] M. Jankowski, E. van Vroonhoven, H. Wormeester, H.J.W. Zandvliet, B. Poelsema, Alloying, dealloying, and reentrant alloying in (sub)monolayer growth of Ag on Pt(111), J. Phys. Chem. C 121 (2017) 8353–8363.

[4181] A. Bilić, J.R. Reimers, N.S. Hush, J. Hafner, Adsorption of ammonia on the gold(111) surface, J. Chem. Phys. 116 (2002) 8981–8987.

[4182] T. Pabisiak, A. Kiejna, Stability of gold nanostructures on rutile TiO_2(110) surface, Surf. Sci. 605 (2011) 668–684.

[4183] S.M. Tadayyon, H.M. Grandin, K. Griffiths, L.L. Coatsworth, P.R. Norton, H. Aziz, Z.D. Popovic, Reliable and reproducible determination of work function and ionization potentials of layers and surfaces relevant to organic light emitting diodes, Organ. Electron. 5 (2004) 199–205.

[4184] S.A. Komolov, L.T. Chadderton, Total current spectroscopy, Surf. Sci. 90 (1979) 359–380.

[4185] B. Ghosh, Work function engineering and its applications in ohmic contact fabrication to II–VI semiconductors, Appl. Surf. Sci. 254 (2008) 4908–4911.

[4186] M. Ťapajna, K. Hušeková, J.P. Espinos, L. Harmatha, K. Fröhlich, Precise determination of metal effective work function and fixed oxide charge in MOS capacitors with high–κ dielectric, Mater. Sci. Semicond. Process. 9 (2006) 969–974.

[4187] Y. Du, B. Chang, X. Wang, J. Zhang, B. Li, M. Wang, Theoretical study of Cs adsorption on GaN(0001) surface, Appl. Surf. Sci. 258 (2012) 7425–7429.

[4188] M. Márquez-Mijares, B. Lepetit, D. Lemoine, Carbon adsorption on tungsten and electronic field emission, Surf. Sci. 645 (2016) 56–62.

[4189] X. Wei, D. Yu, Z. Sun, Z. Yang, X. Song, B. Ding, Arc characteristics and microstructure evolution of W–Cu contacts during the vacuum breakdown, Vacuum 107 (2014) 83–89.

[4190] L.B. Jones, T.S. Beaver, S. Mistry, B.L. Militsyn, T.C.Q. Noakes, R. Valizadeh, Energy distribution and work function measurements for metal photocathodes with measured levels of surface roughness, in: Proc. IPAC 2017, Copenhagen, Denmark, pp. 1580–1583.

[4191] D.R. Lide (Ed.), Electron work function of the elements, in: CRC Handbook of Chemistry and Physics, 79th ed., CRC Press, Boca Raton, 1998–1999, p. **12**–124.

[4192] A. Halder, V.V. Kresin, Nanocluster ionization energies and work function of aluminum, and their temperature dependence, J. Chem. Phys. 143 (2015) 164313/1–4.

[4193] V.V. Pogosov, V.I. Reva, Work function of electrons of metal and ionization potential of the metal cluster containing vacancies, Metallofiz. Noveish. Tekhnol. 39 (2017) 285–308.

[4194] K.H. Meiwes-Broer, Work functions of metal clusters, Hyperfine Interact. 89 (1994) 263–269.

[4195] B. Quiniou, V. Bulović, R.M. Osgood Jr., Observation of image–potential–induced resonances on Cu(110) using the two–photon photoemission technique, Phys. Rev. B 47 (1993) 15890–15895.

[4196] K.E. Schriver, J.L. Persson, E.C. Honea, R.L. Whetten, Electronic shell structure of group–IIIA metal atomic clusters, Phys. Rev. Lett. 64 (1990) 2539–2542.

[4197] M. Seidl, K.-H. Meiwes-Broer, M. Brak, Finite–size effects in ionization potentials and electron affinities of metal clusters, J. Chem. Phys. 95 (1991) 1295–1303.

[4198] G. Makov, A. Nitzan, L.E. Brus, On the ionization potential of small metal and dielectric particles, J. Chem. Phys. 88 (1988) 5076–5085.

[4199] H. Tollefsen, E.O. Laastad, X. Yu, S. Raaen, Initial oxidation of the Ce–Ru(0001) interface, Phil. Mag. 88 (2008) 665–675.

[4200] A. Herrmann, E. Schumacher, L. Wöste, Preparation and photoionization potentials of molecules of sodium, potassium, and mixed atoms, J. Chem. Phys. 68 (1978) 2327–2336.

[4201] Y.A. Wu, Y. Fan, S. Speller, G.L. Creeth, J.T. Sadowski, K. He, A.W. Robertson, C.S. Allen, J.H. Warner, Large single crystals of graphene on melted copper using chemical vapor deposition, ACS Nano 6 (2012) 5010–5017.

[4202] A.L. Dadlani, P. Schindler, M. Logar, S.P. Walch, F.B. Prinz, Energy states of ligand capped Ag nanoparticles: Relating surface plasmon resonance to work function, J. Phys. Chem. C 118 (2014) 24827–24832.

[4203] Y.C. Zhou, J.X. Tang, Z.T. Liu, C.S. Lee, S.T. Lee, Slope parameters at metal organic interfaces, Appl. Phys. Lett. 93 (2008) 093502/1–3.

[4204] N. Koch, J. Ghijsen, R. Ruiz, J. Pflaum, R.L. Johnson, J.-J. Pireaux, J. Schwartz, A. Kahn, Interaction and energy level alignment at interfaces between pentacene and low work function metals, in: Mat. Res. Soc. Symp. Proc., vol. 708, 2002, pp. 9–14.

[4205] A.Y. Liu, D.J. Singh, bcc cobalt: Metastable phase or forced structure? J. Appl. Phys. 73 (1993) 6189–6191.

[4206] V.B. Lazarev, Yu.I. Malov, Relationship between the surface and photoelectric properties of metallic alloys. III. Photoelectric properties of alloys in the system lead–sodium, Sov. Electrochem. 4 (1968) 587–589.

[4207] V.B. Lazarev, Yu.I. Malov, G.A. Sharpataya, Relation between the surface and photoelectric properties of metallic alloys. IV. The photoelectric and surface properties of concentrated cesium amalgams, Sov. Electrochem. 6 (1970) 794–797.

[4208] Yu.I. Malov, V.B. Lazarev, A.V. Salov, Electronic work function of some alkali metals and their alloys, Bull. Acad. Sci. USSR, Div. Chem. Sci. (9) (1970) 1996–1997.

[4209] Yu.I. Malov, A.V. Salov, V.B. Lazarev, Electron work function of alloys of Hg–Rb–Cs system, Bull. Acad. Sci. USSR, Div. Chem. Sci. (6) (1971) 1261–1263.

[4210] O. Renault, R. Brochier, A. Roule, P.-H. Haumesser, B. Krömker, D. Funnemann, Work–function imaging of oriented copper grains by photoemission, Surf. Interface Anal. 38 (2006) 375–377.

[4211] S.Yu. Davydov, Adsorption of potassium on graphite: Work function calculations, Tech. Phys. Lett. 35 (2009) 847–849.

[4212] Y. Ge, J.E. Whitten, Interfacial electronic properties of thiophene and sexithiophene adsorbed on a fluorinated alkanethiol monolayer, J. Phys. Chem. C 112 (2008) 1174–1182.

[4213] P. Borghetti, A. El-Sayed, E. Goiri, C. Rogero, J. Lobo-Checa, L. Floreano, J.E. Ortega, D.G. de Oteyza, Spectroscopic fingerprints of work–function–controlled phthalocyanine charging on metal surfaces, ACS Nano 8 (2014) 12786–12795.

[4214] L.A. Gonzalez, M. Angelucci, R. Larciprete, R. Cimino, The secondary electron yield of noble metal surfaces, AIP Adv. 7 (2017) 115203/1–6.

[4215] P.C. Rusu, G. Giovannetti, C. Weijtens, R. Coehoorn, G. Brocks, Work function pinning at metal–organic interfaces, J. Phys. Chem. C 113 (2009) 9974–9977.

[4216] S.H. Chou, J. Voss, I. Bargatin, A. Vojvodic, R.T. Howe, F. Abild-Pedersen, Orbital–overlap model for minimal work functions of cesiated metal surfaces, J. Phys.: Condens. Matter 24 (2012) 445007/1–7.

[4217] N. Koch, E. Zojer, A. Rajagopal, J. Ghjisen, R.L. Johnson, G. Leising, J.-J. Pireaux, Electronic properties of the interfaces between the wide bandgap organic semiconductor *para*–sexiphenyl and samarium, Adv. Funct. Mater. 11 (2001) 51–58.

[4218] K.-Q. Tang, K.-H. Zhong, Y.-M. Cheng, Z.-G. Huang, Effect of Gd doping on the magnetism and work function of $Fe_{1-x}Gd_x$/Fe(001), Chin. Phys. B 23 (2014) 056301/1–6.

[4219] N. Srivastava, Q. Gao, M. Widom, R.M. Feenstra, S. Nie, K.F. McCarty, I.V. Vlassiouk, Low–energy electron reflectivity of graphene on copper and other substrates, Phys. Rev. B 87 (2013) 245414/1–19.

[4220] P.J. Møller, S.A. Komolov, E.F. Lazneva, A.S. Komolov, Unoccupied states evolution with oxidation of ultrathin Mg, Zn and Cd layers on $SrTiO_3$(100) surfaces, Appl. Surf. Sci. 175–176 (2001) 663–669.

[4221] B.Ch. Dyubua, L.A. Stepanov, The thermionic emission of metal–like compounds in barium vapors, Radio Eng. Electron. Phys. 10 (1965) 1878–1881.

[4222] T. Kurihara, Evaluation of metal work functions by a first–principles electronic structure study and comparison with experimental data (B.S. thesis), Kouchi Institute of Technology, 2002, 45 pp.

[4223] V.B. Lazarev, Yu.I. Malov, Photoelectric phenomena in dilute alkali metal amalgams, Dokl. Akad. Nauk SSSR 164 (1965) 846–848.

[4224] V.B. Lazarev, Yu.I. Malov, G.A. Sharpataya, Electronic work function and surface tension of concentrated cesium amalgams, Dokl. Akad. Nauk SSSR 178 (1968) 355–357.

[4225] V.B. Lazarev, Yu.I. Malov, Association between the surface and photoelectric properties of an alloy: I. Photoelectric phenomena in dilute liquid and solid amalgams of alkali metals, Élektrokhimiya 3 (1967) 294–299.

[4226] Yu.I. Malov, A.A. Markov, V.A. Korol'kov, The electron work functions of cadmium–zinc–antimony alloys, Russ. J. Phys. Chem. 51 (1977) 888–889.

[4227] K. Wong, V.V. Kresin, Photoionization threshold shapes of metal clusters, J. Chem. Phys. 118 (2003) 7141–7143.

[4228] A. Filippetti, V. Fiorentini, K. Stokbro, R. Valente, S. Baroni, Formation energy, stress, and relaxations of low–index Rh surfaces, in: Mater. Res. Soc. Symp. Proc., vol. 408 (Mater. Theory, Simulations, etc.), 1996, pp. 457–460.

[4229] G. Xu, Q. Wu, Z. Chen, Z. Huang, R. Wu, Y.P. Feng, Disorder and surface effects on work function of Ni–Pt metal gates, Phys. Rev. B 78 (2008) 115420/1–6.

[4230] R.H. Prince, R. Persaud, Contribution of broadening effects to chemisorptive emission, Surf. Sci. 207 (1988) 207–214.

[4231] Yu.S. Veluda, A.G. Naumovets, Barium adsorption on single–crystal films of copper, silver, and iron, Ukr. Fiz. Zh. 18 (1973) 1000–1006.

[4232] A.V. Onishchenko, Yu.I. Malov, V.I. Lazareva, Work function of binary metallic alloys with sodium, Fiz. Metal. Metalloved. 51 (1981) 659–661.

[4233] L. Gao, J. Souto-Casares, J.R. Chelikowsky, A.A. Demkov, Orientation dependence of the work function for metal nanocrystals, J. Chem. Phys. 147 (2017) 214301/1–8.

[4234] E.V. Klimenko, A.G. Naumovets, Effect of substrate nature on emission properties and thermal stability of cesium–oxygen film–metal adsorption systems, Ukr. Fiz. Zh. 27 (1982) 1674–1679.

[4235] V.K. Medvedev, T.P. Smereka, S.I. Stepanovskii, G.V. Babkin, Coadsorption of terbium and oxygen on tungsten crystal face (111), Ukr. Fiz. Zh. 35 (1990) 251–255.

[4236] P.A. Milovanova, P.N. Chistyakov, Work function of metals in inert gases, Fiz. Elektron. (3) (1966) 44–50.

[4237] S.A. Shakirova, R.A. Kinzin, Titanium adsorption on tungsten single planes, Poverkhnost' (3) (1984) 96–99.

[4238] G.G. Vladimirov, G.A. Rump, Emission–adsorption properties of the gadolinium–molybdenum(001) system, Poverkhnost' (10) (1986) 61–64.

[4239] S.E. Rozhkov, O.K. Kultashev, L.I. Dashevskaya, Work function of the alloys of iridium with lanthanum, cerium, praseodymium, neodymium, and samarium, Radiotekh. Elektron. 14 (1969) 936–937.

[4240] S.E. Rozhkov, O.K. Kultashev, Work function of the alloys of rhenium with rare–earth metals of yttrium and gadolinium groups, Radiotekh. Elektron. 13 (1968) 570–571.

[4241] B.B. Alchagirov, Kh.B. Khokonov, R.Kh. Arkhestov, Temperature dependence of the work functions for the alkali metals, Dokl. Akad. Nauk 326 (1992) 121–125.

[4242] N.T. Khoa, S.W. Kim, D.-H. Yoo, E.J. Kim, S.H. Hahn, Size dependent work function and catalytic performance of gold nanoparticles decorated graphene oxide sheets, Appl. Catal. A 469 (2014) 159–164.

[4243] K.C. Kwon, K.S. Choi, B.J. Kim, J.-L. Lee, S.Y. Kim, Work–function decrease of graphene sheet using alkali metal carbonates, J. Phys. Chem. C 116 (2012) 26586–26591.

[4244] A. Prem, V.V. Kresin, Photoionization profiles of metal clusters and the Fowler formula, Phys. Rev. A 85 (2012) 025201/1–4.

[4245] K.C. Kwon, K.S. Choi, S.Y. Kim, Increased work function in few–layer graphene sheets via metal chloride doping, Adv. Funct. Mater. 22 (2012) 4724–4731.

[4246] L.P. Aref'eva, I.G. Shebzukhova, Electron work function and surface energy of body–centered and face–centered cubic modifications of $4d$– and $5d$–metals, Phys. Solid State 58 (2016) 1289–1294.

[4247] L.D. Laude, B. Fitton, B. Kramer, K. Maschke, Direct evidence for disorder effects on the electronic structure of selenium, Phys. Rev. Lett. 27 (1971) 1053–1057.

[4248] L.D. Laude, R.F. Willis, B. Fitton, Localized states in amorphous tellurium, Phys. Rev. Lett. 29 (1972) 472–475.

[4249] B.B. Alchagirov, Kh.Kh. Kalazhokov, Kh.B. Khokonov, Study of electron work function of In–Pb, In–Sn and Sn–Pb binary systems, Poverkhnost' (7) (1982) 49–55.

[4250] G.G. Vladimirov, B.S. Lidzhiev, Work function variations with chromium atoms adsorption on single tungsten planes, Poverkhnost' (3) (1987) 139–141.

[4251] Yu.I. Malov, A.V. Onishchenko, V.A. Korol'kov, Electron work function of rare–earth intermetallic compounds, Élektrokhim. 16 (1980) 421–423.

[4252] B.Ch. Dyubua, L.A. Yermolayev, O.K. Kultashev, Emission properties of Pt–Th, Ir–Th, Os–Th and Re–Th alloys, Radiotekh. Elektron. 11 (1966) 1149–1150.

[4253] A.V. Onishchenko, Yu.I. Malov, Concerning the influence of chemical composition on the value of the work function of intermetallides, Fiz. Met. Metalloved. 54 (1982) 94–96.

[4254] M. Seidl, M.E. Spina, M. Brack, Semiclassical variational calculation of liquid–drop model coefficients for metal clusters, Z. Phys. D 19 (1991) 101–103.

[4255] V.V. Pogosov, A.V. Babich, P.V. Vakula, On the influence of the band structure of insulators and image forces on the spectral characteristics of metal–insulator film systems, Phys. Solid State 55 (2013) 2120–2123.

[4256] K. Wong, G. Tikhonov, V.V. Kresin, Temperature–dependent work functions of free–alkali metal nanoparticles, Phys. Rev. B 66 (2002) 125401/1–5.

[4257] T. Andreev, I. Barke, H. Hövel, Adsorbed rare–gas layers on Au(111): Shift of the Shockley surface state studied with ultraviolet photoelectron spectroscopy and scanning tunneling spectroscopy, Phys. Rev. B 70 (2004) 205426/1–13.

[4258] V. Vlahos, J.H. Booske, D. Morgan, *Ab initio* investigation of barium–scandium–oxygen coatings on tungsten for electron emitting cathodes, Phys. Rev. B 81 (2010) 054207/1–15.

[4259] I.G. Shebzukhova, L.P. Aref'eva, Anisotropy in the electronic work function of crystals of 3d metals, Bull. Russ. Acad. Sci. Phys. 79 (2015) 811–814.

[4260] E.L. Leshchinskaya, A.G. Fedorus, Interaction of chromium with the (011) faces of tungsten and niobium, Poverkhnost' (5) (1982) 89–100.

[4261] M. Svanqvist, K. Hansen, Non–jellium scaling of metal cluster ionization energies and electron affinities, Eur. Phys. J. D 56 (2010) 199–203.

[4262] M.K. Harbola, Theoretical study of the size dependence of ionization potential and electron affinity of metallic clusters, J. Chem. Phys. 97 (1992) 2578–2582.

[4263] G.M. Koretsky, M.B. Knickelbein, The evolution of electronic structure in lanthanide metal clusters: Threshold photoionization spectra of Ce_n and Pr_n, Eur. Phys. J. D 2 (1998) 273–278.

[4264] G.M. Koretsky, M.B. Knickelbein, Photoionization studies of manganese clusters: Ionization potentials for Mn_7 and Mn_{64}, J. Chem. Phys. 106 (1997) 9810–9814.

[4265] V.A. Korol'kov, Yu.I. Malov, A.A. Markov, Study of surface layers of metallic alloys by the contact potential difference method, Fiz. Khim. Granits Razdela Kontakt. Faz (1976) 128–130.

[4266] H. Batey, Determination of the work function of platinum alloyed with alkaline earth metals, Proc. Inst. Elec. Engrs. London 108 (Pt. B) (1961) 468–469.

[4267] E.M. Gullikson, A.P. Mills Jr., Positron deformation potential and the temperature dependence of the electron and positron work functions, Phys. Rev. B 35 (1987) 8759–8762.

[4268] F. Schulz, R. Drost, S.K. Hämäläinen, T. Demonchaux, A.P. Seitsonen, P. Liljeroth, Experimental hexagonal boron nitride on Ir(111): A work function template, Phys. Rev. B 89 (2014) 235429/1–8.

[4269] M. Brack, The physics of simple metal clusters: Self–consistent jellium model and semiclassical approaches, Rev. Modern Phys. 65 (1993) 677–732.

[4270] T.J. Drummond, Work Functions of the Transition Metals and Metal Silicides, Sandia Natl. Lab. Rept. SAND 99–0391J, 1999, 30 pp.

[4271] G.A. Rump, G.G. Vladimirov, T.T. Magkoev, Coadsorption of lanthanum and gadolinium with boron on the (011) Mo face, Poverkhnost' (3) (1988) 54–58.

[4272] V.A. Pleshkov, S.A. Shakirova, G.A. Rump, Adsorption of Dy atoms on a Mo(110) surface, Poverkhnost' (10) (1990) 16–23.

[4273] V.A. Pleshkov, S.A. Shakirova, G.A. Rump, Adsorption of terbium atoms on molybdenum(110) surfaces, Poverkhnost' (4) (1991) 34–43.

[4274] V.K. Medvedev, T.P. Smereka, S.I. Stepanovskii, Adsorption of samarium and oxygen on the (112) face of a tungsten crystal, Ukr. Fiz. Zh. 40 (1995) 849–855.

[4275] V.K. Medvedev, I.N. Yakovkin, Interaction of adsorbed magnesium and strontium atoms on the $(10\bar{1}0)$ face of a rhenium crystal, Poverkhnost' (5) (1982) 112–118.

[4276] V.V. Gonchar, O.V. Kanash, A.G. Fedorus, Atomic structure and electronic properties of lanthanum films adsorbed on the (011) face of chromium, Poverkhnost' (6) (1983) 39–46.

[4277] S.V. Loskutov, V.V. Levitin, V.V. Pogosov, On measuring the work function by the vibrating capacitor technique, Poverkhnost' (8) (1992) 121–123.

[4278] I.D. Baikie, A.C. Grain, J. Sutherland, J. Law, Ambient pressure photoemission spectroscopy of metal surfaces, Appl. Surf. Sci. 323 (2014) 45–53.

[4279] T.C. Back, A.K. Schmid, S.B. Fairchild, J.J. Boeckl, M. Cahay, F. Derkink, G. Chen, A. Sayir, Work function characterization of directionally solidified LaB_6–VB_2 eutectic, Ultramicroscopy 183 (2017) 67–71.

[4280] A. Sherehiy, S. Dumpala, A. Safir, D. Mudd, I. Arnold, R.W. Cohn, M.K. Sunkara, G.U. Sumanasekera, Thermionic emission properties and the work function determination of arrays of conical carbon nanotubes, Diam. Relat. Mater. 34 (2013) 1–8.

[4281] M. Uda, Open counter for low energy electron detection, Japan. J. Appl. Phys. 24 (Suppl. 24–4) (1985) 284–288.

[4282] Y. Murata, E. Starodub, B.B. Kappes, C.V. Ciobanu, N.C. Bartelt, K.F. McCarty, S. Kodambaka, Orientation–dependent work function of graphene on Pd(111), Appl. Phys. Lett. 97 (2010) 143114/1–3.

[4283] S. Misra, M. Upadhyay, S.K. Mishra, Thermionic emission from monolayer graphene, sheath formation and its feasibility towards thermionic converters, J. Appl. Phys. 121 (2017) 065102/1–10.

[4284] P.A. Khomyakov, G. Giovannetti, P.C. Rusu, G. Brocks, J. van den Brink, P.J. Kelly, First–principles study of the interaction and charge transfer between graphene and metals, Phys. Rev. B 79 (2009) 195425/1–12.

[4285] H. Yuan, S. Chang, I. Bargatin, N.C. Wang, D.C. Riley, H. Wang, J.W. Schwede, J. Provine, E. Pop, Z.-X. Shen, P.A. Pianetta, N.A. Melosh, R.T. Howe, Engineering ultra–low work function of graphene, Nano Lett. 15 (2015) 6475–6480.

[4286] A. Sherehiy, Thermionic emission properties of novel carbon nanostructures (Ph.D.), Univ. Louisville, 2014, 135 pp.

[4287] A. Sherehiy, S. Dumpala, M.K. Sunkara, J.R. Jasinski, R.W. Cohn, G.U. Sumanasekera, Thermionic emission from phosphorus (P) doped diamond nanocrystals supported by conical carbon nanotubes and ultraviolet photoelectron spectroscopy of P–doped diamond films, Diam. Relat. Mater. 50 (2014) 66–76.

[4288] R.C. Mani, X. Li, M.K. Sunkara, K. Rajan, Carbon nanopipettes, Nano Lett. 3 (2003) 671–673.

[4289] S. Dumpala, J.B. Jasinski, G.U. Sumanasekera, M.K. Sunkara, Large area synthesis of conical carbon nanotube arrays on graphite and tungsten foil substrates, Carbon 49 (2011) 2725–2734.

[4290] S. Dumpala, A. Safir, D. Mudd, R.W. Cohn, M.K. Sunkara, G.U. Sumanasekera, Controlled synthesis and enhanced field emission characteristics of conical carbon nanotubular arrays, Diam. Relat. Mater. 18 (2009) 1262–1266.

[4291] Y. Chen, L. Guo, S. Patel, D.T. Shaw, Aligned conical carbon nanotubes, J. Mater. Sci. 35 (2000) 5517–5521.

[4292] Z. Lou, C. Chen, Q. Chen, Growth of conical carbon nanotubes by chemical reduction of $MgCO_3$, J. Phys. Chem. B 109 (2005) 10557–10560.

[4293] B. Chernomordik, S. Dumpala, Z.Q. Chen, M.K. Sunkara, Nanodiamond tipped and coated conical carbon tubular structures, Chem. Vapor Depos. 14 (2008) 256–262.

[4294] S.K. Srivastava, V.D. Vankar, V. Kumar, Excellent field emission properties of short conical carbon nanotubes prepared by microwave plasma enhanced CVD process, Nanoscale Res. Lett. 3 (2008) 25–30.

[4295] S. Kamarian, M. Salim, R. Dimitri, F. Tornabene, Free vibration analysis of conical shells reinforced with agglomerated carbon nanotubes, Int. J. Mech. Sci. 108–109 (2016) 157–165.

[4296] H. Yanagisawa, C. Hafner, P. Doná, M. Klöckner, D. Leuenberger, T. Greber, J. Osterwalder, M. Hengsberger, Laser–induced field emission from a tungsten tip: Optical control of emission sites and the emission process, Phys. Rev. B 81 (2010) 115429/1–10.

[4297] B.B. Alchagirov, B.S. Karamurzov, T.A. Sizhazhev, T.M. Taova, R.Kh. Arkhestov, Electron work function of Rb–Cs alloys, Tech. Phys. 51 (2006) 1627–1629.

[4298] B.B. Alchagirov, L.Kh. Afaunova, F.F. Dyshekova, R.Kh. Arkhestov, Lithium electron work function: State of the art, Tech. Phys. 60 (2015) 292–299.

[4299] B.B. Alchagirov, L.Kh. Afaunova, F.F. Dyshekova, T.M. Taova, R.Kh. Arkhestov, A.G. Mozgovoi, Z.A. Kokov, An instrument for measuring thermal characteristics of metals and alloys, Prib. Tekh. Eksp. (3) (2009) 148–151.

[4300] R.Kh. Arkhestov, B.B. Alchagirov, Z.A. Kegadueva, Electron work function of sodium: The current state of researches, in: Proc. 10th Int. Vac. Electr. Sour. Conf. (IVESC 2014) No. 22, 2pp.

[4301] M.M. Kappes, Experimental studies of gas–phase main group metal clusters, Chem. Rev. 88 (1988) 369–389.

[4302] W.A. de Heer, The physics of simple metal clusters: Experimental aspects and simple models, Rev. Modern Phys. 65 (1993) 611–676.

[4303] K. Yamanouchi, T. Kondow, Chemistry initiated by cluster beams, Bunkou Kenkyuu 35 (1986) 445–464.

[4304] J. Tiggesbäumker, F. Stienkemeier, Formation and properties of metal clusters isolated in helium droplets, Phys. Chem. Chem. Phys. 9 (2007) 4748–4770.

[4305] V.B. Lazarev, Yu.I. Malov, Relationship between the photoelectric and surface properties of lead–sodium alloys, Izv. Akad. Nauk SSSR, Ser. Khim. (9) (1967) 2091–2093.

[4306] Y. Wei, K. Jiang, X. Feng, P. Liu, L. Liu, S. Fan, Comparative studies of multiwalled carbon nanotube sheets before and after shrinking, Phys. Rev. B 76 (2007) 045423/1–7.

[4307] X. Wei, S. Wang, Q. Chen, L. Peng, Breakdown of Richardson's law in electron emission from individual self–Joule–heated carbon nanotubes, Sci. Rep. 4 (2014) 5102/1–5.

[4308] Y. Murata, S. Nie, A. Ebnonnasir, E. Starodub, B.B. Kappes, K.F. McCarty, C.V. Ciobanu, S. Kodambaka, Growth structure and work function of bilayer graphene on Pd(111), Phys. Rev. B 85 (2012) 205443/1–6.

[4309] A.A.B. Padama, K. Oka, W.A. Diño, H. Kasai, Analysis of the changes in electronic structures and work function variation in alkali metal–metal surface systems, J. Vac. Soc. Jpn. 57 (2014) 27–31.

[4310] A.V. Babich, V.V. Pogosov, V.I. Reva, Estimation of the vacancy contribution to the work functions of electrons and positrons released from metals, Tech. Phys. Lett. 42 (2016) 1027–1030.

[4311] J. Kim, S. Qin, W. Yao, Q. Niu, M.Y. Chou, C.-K. Shih, Quantum size effects on the work function of metallic thin film nanostructures, Proc. Natl. Acad. Sci. USA 107 (2010) 12761–12765.

[4312] A. Patra, J.E. Bates, J. Sun, J.P. Perdew, Properties of real metallic surfaces: Effects of density functional semilocality and van der Waals nonlocality, Proc. Natl. Acad. Sci. USA 114 (2017) E9188–E9196.

[4313] M.J.S. Spencer, A. Hung, I.K. Snook, I. Yarovsky, Sulfur adsorption on Fe(110): A DFT study, Surf. Sci. 540 (2003) 420–430.

[4314] B.B. Alchagirov, R.Kh. Arkhestov, Kh.B. Khokonov, Temperature dependence of the electron work function of solid and liquid sodium, Zh. Fiz. Khim. 67 (1993) 1892–1895.

[4315] B.B. Alchagirov, L.Kh. Afaunova, F.F. Dyshekova, R.Kh. Arkhestov, T.M. Taova, Electron work function of lithium: The current state of researches, in: Proc. 10th Int. Vac. Electr. Sour. Conf. (IVESC 2014), No. 7, 2 pp.

[4316] A.A. Ramanathan, A DFT calculation of Nb and Ta(001) surface properties, J. Mod. Phys. 4 (2013) 432–437.

[4317] Y.M. Choi, C. Compson, M.C. Lin, M. Liu, *Ab initio* analysis of sulfur tolerance of Ni, Cu, and Ni–Cu alloys for solid oxide fuel cells, J. Alloy. Compd. 427 (2007) 25–29.

[4318] D.R. Lide (Ed.), Electron work function of the elements, in: CRC Handbook of Chemistry and Physics, 78th, 1997–1998, p. **12**–124.

[4319] S.A. Shakirova, I. Bayo, Work function dynamics in a Cu/W(112) adsorption system, Tech. Phys. Lett. 33 (2007) 567–570.

[4320] Kh.O. Kuchkarov, Dissertation, Leningrad, 1979 (see Ref. [4319]).

[4321] E. Engel, J.P. Perdew, Theory of metallic clusters: Asymptotic size dependence of electronic properties, Phys. Rev. B 43 (1991) 1331–1337.

[4322] K.I. Peterson, P.D. Dao, R.W. Farley, A.W. Castleman Jr., Photoionization of sodium clusters, J. Chem. Phys. 80 (1984) 1780–1785.

[4323] W.A. de Heer, P. Milani, Comment on "photoionization of mass–selected K_n^+ ions: A test for the ionization scaling law", Phys. Rev. Lett. 65 (1990) 3356 (see Ref. [4161]).

[4324] S. Nakanishi, K. Sasaki, Adsorption of sulfur on the iron(001) surface, Surf. Sci. 194 (1988) 245–256.

[4325] N. Spiridis, T. Ślęzak, M. Zając, J. Korecki, Ultrathin epitaxial bcc–Co films stabilized on Au(001)–*hex*, Surf. Sci. 566–568 (2004) 272–277.

[4326] M. Dubecký, F. Dubecký, The work function of Au/Mg decorated Au(100), Mg(001), and AuMg alloy surfaces: A theoretical study, J. Chem. Phys. 141 (2014) 094705/1–6.

[4327] S. Nakanishi, T. Horiguchi, Adsorption study of selenium on Fe(001) surfaces by means of LEED, AES and work–function measurements, Surf. Sci. 133 (1983) 605–617.

[4328] B.B. Alchagirov, Kh.Kh. Kalazhokov, Kh.B. Khokonov, Modern methods of measuring fast changes in the electron work function, Bull. Acad. Sci. USSR, Phys. Ser. 55 (12) (1991) 164–168.

[4329] J. Wang, G. Wang, J. Zhao, Nonmetal–metal transition in Zn_n ($n = 2$–20) clusters, Phys. Rev. A 68 (2003) 013201/1–6.

[4330] D. Gu, S.K. Dey, P. Majhi, Effective work function of Pt, Pd, and Re on atomic layer deposited HfO_2, Appl. Phys. Lett. 89 (2006) 082907/1–3.

[4331] Y. Cheng, Y. Zheng, X. Huang, K. Zhong, Z. Chen, Z. Huang, Magnetism and work function of Ni–Cu alloys as metal gates, Rare Metals 31 (2012) 130–134.

[4332] N. Yang, D. Yang, L. Chen, D. Liu, M. Cai, X. Fan, Design and adjustment of the graphene work function via size, modification, defects, and doping: A first–principle theory study, Nanoscale Res. Lett. 12 (2017) 642/1–8.

[4333] D.L.S. Nieskens, D.C. Ferré, J.W. Niemantsverdriet, The influence of promoters and poisons on carbon monoxide adsorption on Rh(100): A DFT study, ChemPhysChem. 6 (2005) 1293–1298.

[4334] B. Caglar, A.C. Kizilkaya, J.W. Niemantsverdriet, C.J. Weststrate, Application of work function measurements in the study of surface catalyzed reactions on Rh(100), Catal. Struct. React. 4 (2018) 1–11.

[4335] P. Tegeder, M. Danckwerts, S. Hagen, A. Hotzel, M. Wolf, Structural transition in cyclooctatetraene adsorbed on Ru(001) probed by thermal deposition and two–photon photoemission spectroscopy, Surf. Sci. 585 (2005) 177–190.

[4336] T. Nishizawa, K. Ishida, The Co (cobalt) system, Bull. Alloy Phase Diagr. 4 (1983) 387–390.

[4337] W. Cao, A. Delin, T. Matsushita, S. Seetharaman, Theoretical investigation of sulfur adsorption on Fe(100), in: Suppl. Proc. 138th TMS Ann. Meet. 3, 2009, pp. 523–528 (Chem. Abstr. 151 (2009) 83145m).

[4338] R.C. Reuel, C.H. Bartholomew, The stoichiometries of H_2 and CO adsorptions on cobalt: Effects of support and preparation, J. Catalysis 85 (1984) 63–77.

[4339] A.D. Pandey, G. Müller, D. Reschke, X. Singer, Field emission from crystalline niobium, Phys. Rev. Spec. Topics 12 (2009) 023501/1–8.

[4340] J.L. LaRue, J.D. White, N.H. Nahler, Z. Liu, Y. Sun, P.A. Pianetta, D.J. Auerbach, A.M. Wodtke, The work function of submonolayer cesium–covered gold: A photoelectron spectroscopy study, J. Chem. Phys. 129 (2008) 024709/1–6.

[4341] T.U. Kampen, A. Das, S. Park, W. Hoyer, D.R.T. Zahn, Relation between morphology and work function of metals deposited on organic substrates, Appl. Surf. Sci. 234 (2004) 333–340.

[4342] Y. Luo, R. Qin, Surface energy and its anisotropy of hexagonal close–packed metals, Surf. Sci. 630 (2014) 195–201.

[4343] P. Batzies, J. Demny, H.-E. Schmid, Preparation and investigation of tungsten surfaces with preferred orientations, in: 2nd Int. Conf. Therm. Elect. Power Generat., Stresa, Italy, 1968, pp. 1303–1312.

[4344] T.A. Flaim, Surface reactions of boron with clean tungsten substrates (Dr. Dissertat), Missouri Univ. of Sci. and Technol., 1971, 107 pp. (see Ref. [913]).

[4345] D.P. Pappas, K.-P. Kämper, B.P. Miller, H. Hopster, D.E. Fowler, A.C. Luntz, C.R. Brundle, Z.-X. Shen, Magnetism of ultrathin films of Fe on Cu(100), J. Appl. Phys. 69 (1991) 5209–5211.

[4346] D.P. Pappas, C.R. Brundle, H. Hopster, Reduction of macroscopic moment in ultrathin Fe films as the magnetic orientation changes, Phys. Rev. B 45 (1992) 8169–8172.

[4347] R. Allenspach, A. Bishof, Magnetization direction switching in Fe/Cu(100) epitaxial films: Temperature and thickness dependence, Phys. Rev. Lett. 69 (1992) 3385–3388.

[4348] B. Heinrich, J.F. Cochran, A.S. Arrott, S.T. Purcell, K.B. Urquhart, J.R. Dutcher, W.F. Egelhoff Jr., Appl. Phys. A 49 (1989) 473–490.

[4349] T.L. Jones, D Venus, Structural and magnetic characterization of thin iron films on a tungsten(001) substrate, Surf. Sci. 302 (1994) 126–140.

[4350] M. Donath, Magnetic order and electronic structure in thin films, J. Phys.: Condens. Matter 11 (1999) 9421–9436.

[4351] W. Dürr, M. Taborelli, O. Paul, R. Germar, W. Gudat, D. Pescia, M. Landolt, Magnetic phase transition in two–dimensional ultrathin Fe films on Au(100), Phys. Rev. Lett. 62 (1989) 206–209.

[4352] S.D. Bader, E.R. Moog, Magnetic properties of novel epitaxial films, J. Appl. Phys. 61 (1987) 3729–3737.

[4353] C. Liu, E.R. Moog, S.D. Bader, Polar Kerr–effect observation of perpendicular surface anisotropy for ultrathin ferromagnetic films: fcc Fe/Cu(100), J. Appl. Phys. 64 (1988) 5325–5327.

[4354] P.J. Jensen, H. Dreyssé, K.H. Bennemann, Thickness dependence of the magnetization and the Curie temperature of ferromagnetic thin films, Surf. Sci. 269/270 (1992) 627–631.

[4355] F. Huang, M.T. Kief, G.J. Mankey, R.F. Willis, Magnetism in the few–monolayers limit: A surface magneto–optic Kerr–effect study of the magnetic behavior of ultrathin films of Co, Ni, and Co–Ni alloys on Cu(100) and Cu(111), Phys. Rev. B 49 (1994) 3962–3971.

[4356] N.Ya. Roukhlyada, Phase transitions and emission properties of allotropic metals, Phys. Scr. 81 (2010) 045701/1–6.

[4357] S.N. Bezryadin, Yu.Kh. Vekilov, V.D. Verner, M.B. Samsonova, Electron structure of metal surfaces, Izv. Akad. Nauk SSSR, Ser. Fiz. 46 (1982) 1230–1234.

[4358] B. Zheng, H.-t. Yu, Y. Xie, Y.-f. Lian, Engineering the work function of buckled boron α–sheet by lithium adsorption: A first–principles investigation, Appl. Mater. Interfaces 6 (2014) 19690–19701.

[4359] V. Bezugly, J. Kunstmann, B. Grundkötter-Stock, T. Frauenheim, T. Niehaus, G. Cuniberti, Highly conductive boron nanotubes: Transport properties, work functions, and structural stabilities, ACS Nano 5 (2011) 4997–5005.

[4360] D.G. Kvashnin, P.B. Sorokin, J.W. Brüning, L.A. Chernozatonskii, The impact of edges and dopants on the work function of graphene nanostructures: The way to high electronic emission from pure carbon medium, Appl. Phys. Lett. 102 (2013) 183112/1–5.

[4361] S.S.A. Razee, J.B. Staunton, L. Szunyogh, B.L. Gyorffy, Onset of magnetic order in fcc–Fe films on Cu(100), Phys. Rev. Lett. 88 (2002) 147201/1–4.

[4362] J.R. Smith, A.L. Smith, A Simple Empirical Formulation of Electron Emission from Cesiated Metal Surfaces, NASA TM X–52716, 1969, 6 pp.

[4363] W.G. Burgers, L.J. Groen, Mechanism and kinetics of the allotropic transformation of tin, Discuss. Faraday Soc. 23 (1957) 183–195.

[4364] F.H. Spedding, Properties of rare earth metals, in: R.C. Weast (Ed.), CRC Handbook of Chemistry and Physics, 52nd ed., 1971–1972, p. B–234.

[4365] S. Westermeyr, R. Müller, J. Scholtes, H. Oechsner, Temperature dependence of the electron energy gap of high T_c superconductors studied by work function spectroscopy, Appl. Phys. Lett. 64 (1994) 1726–1728.

[4366] S. Gestermann, M. Nohlen, M. Schmidt, K. Wandelt, Growth investigations of ultrathin Ag films on Pt(111) using STM and dynamical work function measurements, Surf. Rev. Lett. 4 (1997) 1179–1183.

[4367] Y. Kudriavtsev, R. Asomoza, Work function change caused by alkali ion sputtering of a sample surface, Appl. Surf. Sci. 167 (2000) 12–17.

[4368] Y. Zhang, O. Pluchery, L. Caillard, A.-F. Lamic-Humblot, S. Casale, Y.J. Chabal, M. Salmeron, Sensing the charge state of single gold nanoparticles via work function measurements, Nano Lett. 15 (2015) 51–55.

[4369] W. Pfeiffer, C. Kennerknecht, M. Merschdorf, Electron dynamics in supported metal nanoparticles: Relaxation and charge transfer studied by time–resolved photoemission, Appl. Phys. A 78 (2004) 1011–1028.

[4370] A. Gloskovskii, D.A. Valdaitsev, M. Cinchetti, S.A. Nepijko, J. Lange, M. Aeschlimann, M. Bauer, M. Klimenkov, L.V. Viduta, P.M. Tomchuk, G. Schönhense, Electron emission from films of Ag and Au nanoparticles excited by a femtosecond pump–probe laser, Phys. Rev. B 77 (2008) 195427/1–11.

[4371] H. Kato, D. Takeuchi, M. Ogura, T. Yamada, M. Kataoka, Y. Kimura, S. Sobue, C.E. Nebel, S. Yamasaki, Heavily phosphorus–doped nano–crystalline diamond electrode for thermionic emission application, Diam. Relat. Mater. 63 (2016) 165–168.

[4372] G.S. Bocharov, A.V. Eletskii, Theory of carbon nanotube (CNT)–based electron field emitters, Nanomaterials 3 (2013) 393–442.

[4373] T.L. Westover, A.D. Franklin, B.A. Cola, T.S. Fisher, R.G. Reifenberger, Photo– and thermionic emission from potassium–intercalated carbon nanotube arrays, J. Vac. Sci. Technol. B 28 (2010) 423–434.

[4374] D. Wiśnios, A. Kiejna, J. Korecki, First–principles study of the adsorption of MgO molecules on a clean Fe(001) surface, Phys. Rev. B 92 (2015) 155425/1–8.

[4375] S.K. Ravi, W. Sun, D.K. Nandakumar, Y. Zhang, S.C. Tan, Optical manipulation of work function contrasts on metal thin films, Sci. Adv. 4 (2018) eaao 6050/1–8.

[4376] J.T. Robinson, J. Culbertson, M. Berg, T. Ohta, Work function variations in twisted graphene layers, Sci. Rep. 8 (2018) 2006/1–9.

[4377] M. Stampanoni, Magnetic properties of thin epitaxial films investigated by spin–polarized photoemission, Appl. Phys. A 49 (1989) 449–458.

[4378] P.O. Nilsson, D.E. Eastman, Photoemission anisotropy studies for Ag(111) and Ag(100) single crystal films, Phys. Scripta 8 (1973) 113–118.

[4379] K. Christmann, G. Ertl, Surface studies with epitaxially grown metal films, Thin Solid Films 28 (1975) 3–18.

[4380] E.I. Altman, R.J. Colton, The interaction of C_{60} with noble metal surfaces, Surf. Sci. 295 (1993) 13–33.

[4381] E.I. Altman, R.J. Colton, Interaction of C_{60} with the Au(111) $23 \times \sqrt{3}$ reconstruction, J. Vac. Sci. Technol. B 12 (1994) 1906–1909.

[4382] H.W. King, Temperature–dependent allotropic structures of the elements, Bull. Alloy Phase Diagr. 3 (1982) 276.

[4383] C.N. Singman, Atomic volume and allotropy of the elements, J. Chem. Educ. 61 (1984) 137–142.

[4384] S.D. Barrett, Angle–resolved photoemission and LEED from rare–earth metals, Surf. Sci. Rep. 14 (1992) 271–354.

[4385] https://en.wikipedia.org/wiki/Allotropy.

[4386] G.W. Fernando, Y.C. Lee, P.A. Montano, B.R. Cooper, E.R. Moog, H.M. Naik, S.D. Bader, Surface electronic behavior of face–centered–cubic iron on copper, J. Vac. Sci. Technol. A 5 (1987) 882–886.

[4387] J.J. De Miguel, A. Cebollada, J.M. Gallego, S. Ferrer, R. Miranda, C.M. Schneider, P. Bressler, J. Garbe, K. Bethke, J. Kirschner, Characterization of the growth processes and magnetic properties of thin ferromagnetic cobalt films on Cu(100), Surf. Sci. 211/212 (1989) 732–739.

[4388] A. Clarke, P.J. Rous, M. Amott, G. Jennings, R.F. Willis, Thickness dependent relaxation in γ fcc Fe films on Cu(001): A LEED structural study, Surf. Sci. 192 (1987) L843–L848.

[4389] M. Farle, Ferromagnetic resonance of ultrathin metallic layers, Rep. Progr. Phys. 61 (1998) 755–826.

[4390] C.A.F. Vaz, J.A.C. Bland, G. Lauhoff, Magnetism in ultrathin film structures, Rep. Progr. Phys. 71 (2008) 056501/1–78.

[4391] C.M. Schneider, P. Bressler, P. Schuster, J. Kirschner, J.J. de Miguel, R. Miranda, Curie temperature of ultrathin films of fcc cobalt epitaxially grown on atomically flat Cu(001) surfaces, Phys. Rev. Lett. 64 (1990) 1059–1062.

[4392] C.M. Schneider, P. Bressler, P. Schuster, J. Kirschner, J.J. de Miguel, R. Miranda, S. Ferrer, Epitaxy and magnetic properties of fcc cobalt films on Cu(100), Vacuum 41 (1990) 503–505.

[4393] A. Schatz, S. Dunkhorst, S. Lingnau, U. von Hörsten, W. Keune, RHEED intensity oscillations during epitaxial growth of fcc Fe on Cu(001), Surf. Sci. 310 (1994) L595–L600.

[4394] C.C. Kuo, C.L. Chiu, W.C. Lin, M.-T. Lin, Drastic depression of Curie temperature for magnetic Co/Cu(100) ultrathin films upon deposition at elevated temperature, Surf. Sci. 520 (2002) 121–127.

[4395] L.J. Sham, Walter Kohn (1923–2016), Nature 534 (2) (2016) 38.

[4396] P.C. Hohenberg, J.S. Langer, Walter. Kohn, Phys. Today 69 (8) (2016) 64.

[4397] https://en.wikipedia.org/wiki/Walter_Kohn.

[4398] C. Fall, *Ab initio* study of the work functions of elemental metal crystals (Thesis), École Polytech. Lausanne (EPFL), 1999, 139 pp.

[4399] Y. Yang, Z. Sroubek, J.A. Yarmoff, Internal electronic structure of adatoms on Fe(110) and Fe(100) surfaces. A low–energy Li$^+$ scattering study, Phys. Rev. B 69 (2004) 045420/1–9.

[4400] Y. Qi, X. Ma, P. Jiang, S. Ji, Y. Fu, J.-F. Jia, Q.-K. Xue, S.B. Zhang, Atomic–layer–resolved local work functions of Pb thin films and their dependence on quantum well states, Appl. Phys. Lett. 90 (2007) 013109/1–3.

[4401] S. Zhang, C.M. Tan, S. Cheng, T. Deng, F. He, H. Su, *Ab initio* simulation of electronic and mechanical properties of alminium for fatigue early feature investigation, Int. J. Nanotechnol. 11 (2014) 373–385.

[4402] B. Cook, A. Russakoff, K. Varga, Coverage dependent work function of graphene on a Cu(111) substrate with intercalated alkali metals, Appl. Phys. Lett. 106 (2015) 211601/1–5.

[4403] Y. Fujimoto, First–principles theoretical investigation of graphene layers for sensor applications: A review, Nanomater. Nanotechnol. 7 (2017) 1–7.

[4404] H.Z. Jooya, K.S. McKay, E. Kim, P.F. Weck, D.P. Pappas, D.A. Hite, H.R. Sadeghpour, Mechanisms for carbon adsorption on Au(110)–(2×1): A work function analysis, Surf. Sci. 677 (2018) 232–238.

[4405] S.A. Surma, J. Brona, A. Ciszewski, Electron work functions of (hkl)–surfaces, Mater. Sci.–Poland 36 (2018) 225–234.

[4406] H. Kawano, Theoretical study of the mechanism how the effective work functions are governed by patchy surface components, to be published.

[4407] L. Giordano, M. Baistrocchi, G. Pacchioni, Bonding of Pd, Ag, and Au atoms on MgO(100) surfaces and MgO/Mo(100) ultra–thin films: A comparative DFT study, Phys. Rev. B 72 (2005) 115403/1–11.

[4408] G. Heimel, L. Romaner, J.-L. Brédas, E. Zojer, Interface energetics and level alignment at covalent metal–molecule junctions: π–conjugated thiols on gold, Phys. Rev. Lett. 96 (2006) 196806/1–4.

[4409] A. Mattausch, O. Pankratov, *Ab initio* study of graphene on SiC, Phys. Rev. Lett. 99 (2007) 076802/1–4.

[4410] N.E. Singh-Miller, Molecular–scale devices from first principles (Ph.D. thesis), MIT, 2009, 167 pp.

[4411] F. Liu, C. Shen, Z. Su, X. Ding, S. Deng, J. Chen, N. Xu, H. Gao, Metal–like single crystalline boron nanotubes: Synthesis and *in situ* study on electric transport and field emission properties, J. Mater. Chem. 20 (2010) 2197–2205.

[4412] A.A. Ramanathan, Surface structural properties of the V, Nb and Ta(001) surfaces, Suppl. Proc. Mater. Process. Prop. 1 (2010) 779–784.

[4413] D. Otálvaro, T. Veening, G. Brocks, Self–assembled monolayer induced Au(111) and Ag(111) reconstructions: Work functions and interface dipole formation, J. Phys. Chem. C 116 (2012) 7826–7837.

[4414] X. Lin, A. Groß, First–principles study of the water structure on flat and stepped gold surfaces, Surf. Sci. 606 (2012) 886–891.

[4415] R. Ruffieux, O. Gröning, M. Bielmann, P. Mauron, L. Schlapbach, P. Gröning, Phys. Rev. B 66 (2002) 245416/1–8.

[4416] N. Bonnet, N. Marzari, First–principles prediction of the equilibrium shape of nanoparticles under realistic electrochemical conditions, Phys. Rev. Lett. 110 (2013) 086104/1–5.

[4417] D. Ji, S. Wang, Study of surface energy and work function of hex metals by first–principles calculation, Acta Metall. Sin. 51 (2015) 597–602.

[4418] J. Kaur, R. Kant, Curvature–induced anomalous enhancement in the work function of nanostructures, J. Phys. Chem. Lett. 6 (2015) 2870–2874.

[4419] F.R. Fazylov, Macroscopic theory of the electron work function in solids, Phil. Magaz. 94 (2014) 1956–1966.

[4420] J. Kaur, R. Kant, Theory of Work function and potential of zero charge for metal nanostructured and rough electrodes, J. Phys. Chem. C 121 (2017) 13059–13069.

[4421] S. Smidstrup, D. Stradi, J. Wellendorff, P.A. Khomyakov, U.G. Vej-Hansen, M.-E. Lee, T. Ghosh, E. Jónsson, H. Jónsson, K. Stokbro, First–principles Green's–function method for surface calculations: A pseudopotential localized basis set approach, Phys. Rev. B 96 (2017) 195309/1–17.

[4422] P.A. Fernández Garrillo, B. Grévin, N. Chevalier, Ł. Borowik, Calibrated work function mapping by Kelvin probe force microscopy, Rev. Sci. Instrum. 89 (2018) 043702/1–7.

[4423] Y.-K. Park, D.-Y. Kim, J.-S. Kim, Y.-S. Nam, M.-H. Park, H.-C. Choi, B.-C. Min, S.-B. Choe, Experimental observation of the correlation between the interfacial Dzyaloshinskii–Moriya interaction and work function in metallic magnetic trilayers, NPG Asia Mater. 10 (2018) 995–1001.

[4424] M. Bercx, B. Partoens, D. Lamoen, Quantitative modeling of secondary electron emission from slow–ion bombardment on semiconductors, Phys. Rev. B 99 (2019) 085413/1–8.

[4425] S. De Waele, et al., Private comm. (see Ref. [4424]).

[4426] M. Yortanli, E. Mete, Common surface structures of graphene and Au(111): The effect of rotational angle on adsorption and electronic properties, J. Chem. Phys. 151 (2019) 214701/1–8.

[4427] P. Zhang, H. Z.-Song, First–Principles Calculation of Be(0001) Thin Films: Quantum Size Effect and Adsorption of Atomic Hydrogen, Los Alamos Natl. Lab., Prep. Archive, Condens. Matt./ 0703331, 2007, 6 pp. (Chinese Ed.: Acta Physica Sinica 56 (2007), No.1).

[4428] O.R. Jolayemi, J.O. Idiodi, Electronic and surface properties of molybdenum: A first principle study, J. Niger. Assoc. Math. Phys. 39 (2017) 291–296.

[4429] V. Chang, T.C.Q. Noakes, N.M. Harrison, Work function and quantum efficiency study of metal oxide thin films on Ag(100), Phys. Rev. B 97 (2018) 155436/1–8.

[4430] K. Akada, S. Obata, K. Saiki, Work function lowering of graphite by sequential surface modifications: Nitrogen and hydrogen plasma treatment, ACS Omega 4 (2019) 16531–16535.

[4431] V.V. Pogosov, More on the effect of vacancies on metal characteristics: Work function and surface energy, Phys. Solid State 61 (2019) 84–89.

[4432] L. Gao, W. Guo, A. Posadas, A.A. Demkov, Electron accumulation and charge neutrality level at the Eu/EuO interface, Phys. Rev. Mater. 3 (2019) 094403/1–9.

[4433] K. Kobayashi, A distance between first–principles calculations and experiments, Hyoumen Kagaku (Surf. Sci.) 28 (2007) 129–134.

[4434] S. Prada, U. Martinez, G. Pacchioni, Phys. Rev. B 78 (2008) 235423/1–8.

[4435] H. Hibino, H. Kageshima, F. Maeda, F.-Z. Guo, Y. Watanabe, Dependence of electronic properties of epitaxial few–layer graphene on the number of layers investigated by photoelectron emission microscopy, Phys. Rev. B 79 (2009) 125437/1–7.

[4436] H. Hibino, H. Kageshima, M. Nagase, Experimental few–layer graphene: Towards single crystal growth, J. Phys. D 43 (2010) 374005/1–14.

[4437] K. Akada, T. Terasawa, G. Imamura, S. Obata, K. Saiki, Control of work function of graphene by plasma assisted nitrogen doping, Appl. Phys. Lett. 104 (2014) 131602/1–4.

[4438] B. Eren, U. Gysin, L. Marot, Th. Glatzel, R. Steiner, E. Meyer, Work function of few layer graphene covered nickel thin films measured with Kelvin probe force microscopy, Appl. Phys. Lett. 108 (2016) 041602/1–3.

[4439] T. Yi, B. Zheng, H. Yu, Y. Xie, Structure, stabilities and work functions of alkali–metal–adsorbed boron α_1–sheets, Chem. Res. Chin. Univ. 33 (2017) 631–637.

[4440] Z. Tian, X. Zhou, G. Song, First–principles calculation of Li thin films: Quantum size effects and adsorption of atomic hydrogen, Chin. J. Comput. Phys. 35 (2018) 729–736.

[4441] M.I. Nikitin, N.S. Chilingarov, E.L. Osima, S.B. Osin, Thermodynamic calculation of the characteristics of metal thermionic emission, High Temp. 56 (2018) 532–537.

[4442] P. Zhang, H.Z. Song, First–Principles Calculation of Atomic Hydrogen Adsorption on Be(10$\bar{1}$0) Thin Films, Los Alamos Natl. Lab., Prepr. Archive, Cond. Matt. 0703332, 2007, 5 pp.

[4443] V. Panchal, R. Pearce, R. Yakimova, A. Tzalenchuk, O. Kazakova, Standardization of surface potential measurements of graphene domains, Sci. Rep. 3 (2013) 2597/1–8.

[4444] S.H. Ma, X.T. Zu, First–principle study of sulfur adsorption on Ir(100) surface, Mater. Sci. Forum 561–565 (2007) 2435–2438.

[4445] L. de Knoop, F. Houdellier, C. Gatel, A. Masseboeuf, Determining the work function of a carbon–cone cold–field emitter by *in situ* electron holography, Micron 63 (2014) 2–8.

[4446] C.-W. Chen, M.-H. Lee, *Ab initio* calculations of dimensional and adsorbate effects on the work function of single–walled carbon nanotube, Diam. Relat. Mater. 12 (2003) 565–571.

[4447] D.A. Gorodetskii, A.V. Martinyuk, Oxidation of scandium thin films on the surface of tungsten, Poverkhnost' (10) (1988) 98–100.

[4448] B. He, G. Tian, J. Gou, B. Liu, K. Shen, Q. Tian, Z. Yu, F. Song, H. Xie, Y. Gao, Y. Lu, K. Wu, L. Chen, H. Huang, Structural and electronic properties of atomically thin bismuth on Au(111), Surf. Sci. 679 (2019) 147–153.

[4449] U. Zerweck, Ch. Loppacher, T. Otto, S. Grafström, L.M. Eng, Kelvin probe force microscopy of C_{60} on metal substrates: Towards molecular resolution, Nanotechnology 18 (2007) 084006/1–5.

[4450] A.G. Fedorus, A.A. Mityraev, A.G. Naumovets, Beryllium overlayers on Mo(112) and Mo(011) surfaces, Surf. Sci. 606 (2012) 580–589.

[4451] O. Leenaerts, B. Partoens, F.M. Peeters, A. Volodin, C. Van Haesendonck, The work function of few–layer graphene, J. Phys.: Condens. Matter 29 (2017) 035003/1–8.

[4452] R. Friedl, U. Fantz, Influence of H_2 and D_2 plasmas on the work function of caesiated materials, J. Appl. Phys. 122 (2017) 083304/1–7.

[4453] M. Duan, C. Tian, Y. Hu, A. Mei, Y. Rong, Y. Xiong, M. Xu, Y. Sheng, P. Jiang, X. Hou, X. Zhu, F. Qin, H. Han, Boron–doped graphite for high work function carbon electrode in printable hole–conductor–free mesoscopic perovskite solar cells, Appl. Mater. Interfaces 9 (2017) 31721–31727.

[4454] X.-F. Sun, H.-T. Wang, E.-H. Han, Effect of Cr doping on the surface characteristics of Ni metal studied with first–principles calculation, Acta Metall. Sin. 32 (2019) 461–467.

[4455] A.E. Curtin, M.S. Fuhre, J.L. Tedesco, R.L. Myers-Ward, C.R. Eddy Jr., D.K. Gaskill, Kelvin probe microscopy and electronic transport in graphene on SiC(0001) in the minimum conductivity regime, Appl. Phys. Lett. 98 (2011) 243111/1–3.

[4456] T. Filleter, K.V. Emtsev, Th. Seyller, R. Bennewitz, Local work function measurements of epitaxial graphene, Appl. Phys. Lett. 93 (2008) 133117/1–3.

[4457] K.V. Emtsev, A. Bostwick, K. Horn, J. Jobst, G.L. Kellogg, L. Ley, J.L. McChesney, T. Ohta, S.A. Reshanov, J. Röhrl, E. Rotenberg, A.K. Schmid, D. Waldmann, H.B. Weber, T. Seyller, Towards wafer–size graphene layers by atmospheric pressure graphitization of silicon carbide, Nat. Mater. 8 (2009) 203–207.

[4458] E.V. Rut'kov, E.Y. Afanas'eva, N.R. Gall, Graphene and graphite work function depending on layer number on Re, Diam. Relat. Mater. 101 (2020) 107576/1–5.

[4459] I.G. Shebzukhova, L.P. Sref'eva, Anisotropy of the surface energy and work function of IIB metals, Tech. Phys. 64 (2019) 274–277.

[4460] S. De Waele, Error estimates for *ab initio* prediction of surface energy and work function (Master's dissertation), Univ. Gent, 2015, 88 pp.

[4461] R. Tran, X.-G. Li, J.H. Montoya, D. Winston, K.A. Persson, S.P. Ong, Anisotropic work function of elemental crystals, Surf. Sci. 687 (2019) 48–55.

Biography
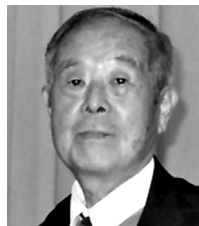
H. Kawano was born in Shimonoseki in 1934. After graduation from Hikoshima Junior High School and Shimonoseki West High School, he attained the B.Sc., M.Sc. and D.Sc. degrees at Kyoto University, Japan. He was Assistant Professor at Research Institute for Scientific Measurements, Tohoku University, Sendai, from 1962 to 1970, and was Associate Professor or Professor at Ehime University, Matsuyama until 2000, and now Professor Emeritus. He has authored or coauthored more than 200 original papers and review articles in the areas of physical chemistry and surface science, especially focused on the experimental and theoretical studies about the mechanism and processes of surface reactions emitting ions and electrons together with neutral atoms and molecules from various solid surfaces heated or electron-stimulated in vacua.